Number 1 Volume 21 1957

PI

BULLETIN

of the

Academy of Sciences of the USSR

- Physical Series -

(Izvestiia Akademii Nauk SSSR)
(Seriia fizicheskaia)

Reproduction rights reserved

by

Columbia Technical Translations
5 Vermont Avenue
White Plains, New York

Single Issues

$20

Annual Subscription

$215

Lithoprinted in U.S.A.
EDWARDS BROTHERS, INC.
Ann Arbor, Michigan

Transactions of the Eighth All-Union Conference

on

SEMICONDUCTORS

(Continued from Volume 20, No. 12 b)

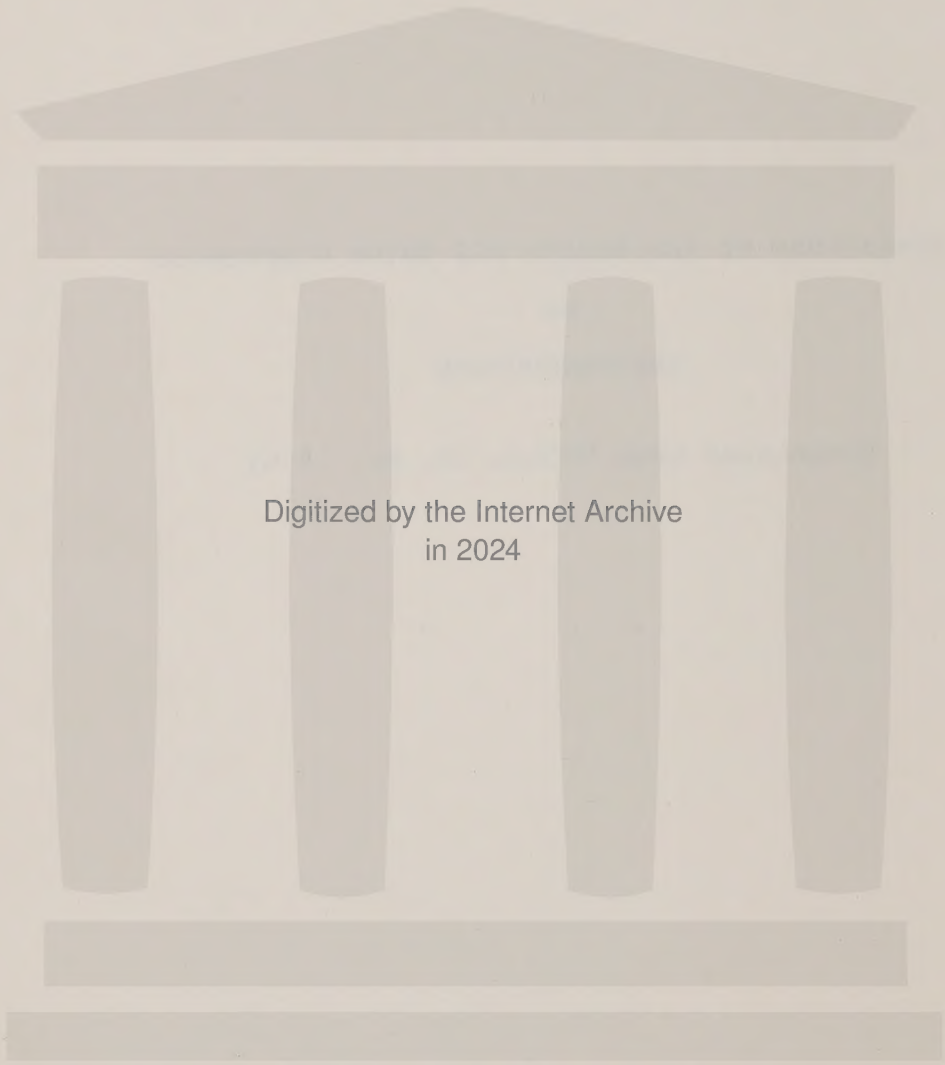

Digitized by the Internet Archive
in 2024

https://archive.org/details/russian-academy-of-sciences-physics-bulletin_1957_21

Section on the Theory of Semiconductors

THE METHOD OF TRACES FOR CONDUCTION ELECTRONS IN SEMICONDUCTORS
Part I. WEAK INTERACTION BETWEEN ELECTRONS AND VIBRATIONS

- M.A.Krivoglaz & S.I.Pekar

The quantum states of conduction electrons interacting with crystal lattice vibrations have been investigated by many authors. In all of these works the applicability of the methods used was restricted to relatively low temperatures. In the strong-coupling theory of the polaron, this temperature restriction is expressed by the inequality (see Eqs.(16) and (42) of Ref.1)

$$|J_0| \gg \left(\bar{n} + \frac{1}{2}\right)\hbar\omega. \qquad (1)$$

Here ω is the frequency of the longitudinal polarization vibrations, $\bar{n}$ is the mean Planck value of the oscillator quantum number corresponding to these vibrations and J_0 is the ground state energy of the polaron. For ionic crystals with strong coupling, for instance, for certain alkali halides, inequality (1) means that $\bar{n}$ can have a value of several units, i.e., that the temperature can be relatively high.

The situation is much worse where published works employing the weak-coupling method are concerned, for in all the variants proposed so far it is required that

$$\bar{n} \ll 1 \qquad (2)$$

(cf. Refs. 2-6), which holds true in real crystals only far below room temperature.

It will be shown below that the weak-coupling method (expansion in powers of the coupling constant between the conduction electron and the lattice vibrations) requires no restriction to low temperatures, and that for ionic crystals better results are, in fact, obtained at high temperatures. As the temperature is increased the weak-coupling expansion converges more strongly, and the region of applicability of this theory is extended to include crystals with intermediate coupling. Thus the temperature restriction of Eq.(2) is not required in the weak-coupling method per se, but is necessary only in the particular variants of this method that have been used so far.

In a number of theoretical investigations, the polaron calculations are performed by means of a direct variational method[2,4,5,7,8 & 9]; this method allows of evaluating only the lowest part of the energy spectrum of the system and this, in turn, makes it difficult to calculate the sum-over-states of the current carriers through which all the thermodynamic functions of the conduction electrons are determined. The method suggested below makes it possible to calculate the sum-over-states of the conduction electrons at arbitrarily high temperatures.

For the sake of brevity we shall term the method used below "the method of traces". It consists of constructing an operator whose trace has the property that either it, its limiting values or the coefficients of its power series expansion equal the desired physical quantities. As is well known, the trace of an operator is invariant under unitary transformations, i.e., its values calculated in terms of different complete sets of orthonormal functions

are identical. It may therefore be calculated in terms of any arbitrary complete set of orthogonal functions, so that it is not necessary to solve any wave equation or find the eigenfunctions of any of the operators entering into the problem. Herein lies the advantage of the method of traces over other methods of quantum mechanics.

For instance, if the desired physical quantity is the sum-over-states Z of a system, it can be found as the trace of the operator $e^{-\lambda H}$, where $\lambda = 1/kT$, and H is the energy operator of the system. The mean thermodynamic energy of the system $\bar{E}$, as is well known, is given in terms of Z by the equation

$$\bar{E} = -\frac{d}{d\lambda} \ln Z. \tag{3}$$

The lowest energy level of the system is obtained as the limiting value of (3) as $T \to 0$, i.e., as $\lambda \to \infty$. Thus the ground state energy of the system can be calculated without solving any wave equation.

The motion of a conduction electron interacting with lattice vibrations is described by an energy operator of the form

$$H = -\frac{\hbar^2}{2\mu}\Delta + \sum_{\vec{\varkappa}} \hbar\omega_{\vec{\varkappa}} a^{+}_{\vec{\varkappa}} a_{\vec{\varkappa}} + \sum_{\vec{\varkappa}} (V_{\vec{\varkappa}} a_{\vec{\varkappa}} e^{i\vec{\varkappa}\vec{r}} + V^{*}_{\vec{\varkappa}} a^{+}_{\vec{\varkappa}} e^{-i\vec{\varkappa}\vec{r}}). \tag{4}$$

Here r is the coordinate of the conduction electron, μ is its effective mass (in the case of fixed atoms), $\omega_{\vec{\varkappa}}$ are the inherent frequencies of the lattice vibrations, $a^{+}_{\vec{\varkappa}}$ and $a_{\vec{\varkappa}}$ are the phonon creation and annihilation operators, respectively, and $V_{\vec{\varkappa}}$ is the coupling coefficient between the electron and the normal vibrations denoted by the index $\vec{\varkappa}$. The form of the $V_{\vec{\varkappa}}$ coefficients will later be specified explicitly for various types of crystals.

The procedures developed below can also be applied in solving other problems with Hamiltonians of the type of Eq.(4), such as the problem of a nucleon interacting with a meson field.

In the case of weak coupling, the term

$$H_1 = H - H_0 = \sum_{\vec{\varkappa}} (V_{\vec{\varkappa}} a_{\vec{\varkappa}} e^{i\vec{\varkappa}\vec{r}} + V^{*}_{\vec{\varkappa}} a^{+}_{\vec{\varkappa}} e^{-i\vec{\varkappa}\vec{r}}) \tag{5}$$

of the Hamiltonian is treated as a small perturbation. The calculation of Z in this case can be performed by using Schwinger's[10] equation which gives the expansion of the operator $e^{-\lambda(H_0+H_1)}$ in powers of the coupling coefficient, which appears as a factor in H_1:

$$\begin{aligned} Z = Z^{(0)} + Z^{(1)} + Z^{(2)} + \ldots + Z^{(p)} + \ldots = \operatorname{sp} e^{-\lambda H_0} + (-\lambda) \operatorname{sp} H_1 e^{-\lambda H_0} + \\ + \frac{(-\lambda)^2}{2} \int_0^1 du_1 \operatorname{sp} H_1 e^{-\lambda H_0 (1-u_1)} H_1 e^{-\lambda H_0 u_1} + \ldots + \\ + \ldots + \frac{(-\lambda)^p}{p} \int_0^1 u_1^{p-2} du_1 \int_0^1 u_2^{p-3} du_2 \ldots \int_0^1 du_{p-1} \operatorname{sp} H_1 e^{-\lambda H_0 (1-u_1)} \times \\ \times H_1 e^{-\lambda H_0 u_1 (1-u_2)} H_1 e^{-\lambda H_0 u_1 u_2 (1-u_3)} \ldots \\ \ldots H_1 e^{-\lambda H_0 u_1 u_2 \ldots u_{p-2}(1-u_{p-1})} H_1 e^{-\lambda H_0 u_1 u_2 u_3 \ldots u_p} + \ldots \end{aligned} \tag{6}$$

Let us consider the general term of this expansion. If $Z^{(p)}$ is written as a sum of single terms containing factors $\ldots a^{+}_{\vec{\varkappa}} \ldots a_{\vec{\varkappa}'} \ldots$ in various orders, the trace will be nonzero only in those terms that have equal numbers of annihilation and creation operators for a given $\vec{\varkappa}$. This can readily be shown by calculating the trace in terms of a set of orthogonal functions of the form

$$\psi_{kn} = \frac{1}{V\bar{V}} e^{ikr} \prod_{\vec{\varkappa}} \Phi_{n_{\vec{\varkappa}}}, \tag{7}$$

where $\Phi_{n_{\vec{\varkappa}}}$ are eigenfunctions of the operators $\hat{n}_{\vec{\varkappa}} = a^+_{\vec{\varkappa}} a_{\vec{\varkappa}}$, $\hat{n}_{\vec{\varkappa}} \Phi_{n_{\vec{\varkappa}}} = n_{\vec{\varkappa}} \Phi_{n_{\vec{\varkappa}}}$, and V is the volume of the base region of the crystal. It follows from this that $Z^{(p)}$ is nonzero only for even values of p.

It also follows that if a nonvanishing term contains the operator $a_{\vec{\varkappa}}$ as a factor, it must also contain the operator $a^+_{\vec{\varkappa}}$ with the same index $\vec{\varkappa}$. Therefore after multiplying out the p operators in H_1, the expression for $Z^{(p)}$ contains not a p-fold sum over $\vec{\varkappa}$, but a $p/2$-fold sum. Thus $Z^{(p)}$ can be written

$$Z^{(2m)} = \frac{(\lambda)^{2m}}{2m} \int_0^1 u_1^{2m-2} du_1 \int_0^1 u_2^{2m-3} du_2 \ldots \int_0^1 du_{2m-1} \sum_{\vec{\varkappa}_1, \vec{\varkappa}_2 \ldots \vec{\varkappa}_m} Q |V_{\varkappa_1}|^2 |V_{\varkappa_2}|^2 \ldots$$

$$\ldots |V_{\vec{\varkappa}_m}|^2 \mathrm{sp} e^{-\lambda H_0 (1-u_1)} a^+_{\vec{\varkappa}} e^{-i\vec{\varkappa}_1 r} \ldots e^{-\lambda H_0 u_1 u_2 \ldots u_{m-1}(1-u_m)} \times$$

$$\times a^+_{\vec{\varkappa}_m} e^{-i\vec{\varkappa}_m r} e^{-\lambda H_0 u_1 \ldots u_m (1-u_{m+1})} a_{\vec{\varkappa}_1} e^{i\vec{\varkappa}_1 r} \ldots e^{-\lambda H_0 u_1 \ldots u_{2m-2}(1-u_{2m-1})} \times$$

$$\times a_{\vec{\varkappa}_{2m-1}} e^{i\vec{\varkappa}_{2m-1} r} e^{-\lambda H_0 u_1 \ldots u_{2m-1}} a_{\vec{\varkappa}_m} e^{i\vec{\varkappa}_m r}. \tag{8}$$

Here Q denotes the sum of all possible permutations of the operators $a_{\vec{\varkappa}_i} e^{i\vec{\varkappa}_i r}$ and $a_{\vec{\varkappa}_j} e^{i\vec{\varkappa}_j r}$, as well as $a^+_{\vec{\varkappa}_l} e^{-i\vec{\varkappa}_l r}$, except that the creation operators are ordered so that $a^+_{\vec{\varkappa}_1} e^{-i\vec{\varkappa}_1 r}$ is on the left of $a^+_{\vec{\varkappa}_2} e^{-i\vec{\varkappa}_2 r}$, which in turn is on the left of $a^+_{\vec{\varkappa}_3} e^{-i\vec{\varkappa}_3 r}$, etc. Thus the $a^+_{\vec{\varkappa}_i} e^{-i\vec{\varkappa}_i r}$ are ordered according to the index i (the order of the $a_{\vec{\varkappa}_i} e^{i\vec{\varkappa}_i r}$ is not restricted in this way).

If the trace in Eq.(8) is calculated in the orthogonal set of Eqs.(7), then after integrating over k and summing over $n_{\vec{\varkappa}}$ and the two possible electron spins, we obtain

$$Z^{(2m)} = \frac{(\lambda)^{2m}}{2m} Z^{(0)} \int_0^1 u_1^{2m-2} du_1 \ldots \int_0^1 du_{2m-1} \sum_{\vec{\varkappa}_1, \vec{\varkappa}_2 \ldots \vec{\varkappa}_m} \bar{Q} |V_{\vec{\varkappa}_1}|^2 |V_{\vec{\varkappa}_2}|^2 \ldots$$

$$\ldots |V_{\vec{\varkappa}_m}|^2 \left[\begin{matrix} \bar{n}_{\vec{\varkappa}_1} \\ \bar{n}_{\vec{\varkappa}_1} + 1 \end{matrix} \right] \ldots \left[\begin{matrix} \bar{n}_{\vec{\varkappa}_m} \\ \bar{n}_{\vec{\varkappa}_m} + 1 \end{matrix} \right] \exp\left\{ \lambda \left[\frac{1}{2\mu} (u_1 g'_{2m} + u_1 u_2 g'_{2m-1} + \ldots \right. \right.$$

$$\ldots + u_1 \ldots u_{2m-1} g'_2)^2 + u_1 \left(\frac{g'_{2m}}{2\mu} (g_{2m} + g_{2m-1}) + \delta_{2m} \right) + \ldots$$

$$\left. \left. \ldots + u_1 \ldots u_{2m-1} \left(\frac{g'_2}{2\mu} (g_2 + g_1) + \delta_2 \right) \right] \right\}, \tag{9}$$

where

$$\bar{n}_{\vec{\varkappa}} = \frac{1}{e^{\lambda \hbar \omega_{\vec{\varkappa}}} - 1} \quad \text{and} \quad Z^{(0)} = 2V \left(\frac{\mu}{2\pi\hbar^2 \lambda} \right)^{3/2} \prod_{\vec{\varkappa}} \frac{1}{1 - e^{-\lambda \hbar \omega_{\vec{\varkappa}}}}. \tag{10}$$

Here $\bar{Q}$ denotes summation over all the above mentioned permutations of the operators $a^+_{\vec{\varkappa}} e^{-i\vec{\varkappa} r}$ and $a_{\vec{\varkappa}'} e^{i\vec{\varkappa}' r}$ in Eq.(8). In the brackets in Eq.(9) the upper values should be taken if the relevant term contains $a_{\vec{\varkappa}}$ on the right of

$a^+_{\vec{\varkappa}}$ and the lower values if the opposite order obtains. Let us number the positions occupied by the operators $a^+_{\vec{\varkappa}}$ and $a_{\vec{\varkappa}}$ in any of the terms in Eq. (8) from right to left. Then with the ν-th position we associate the phonon momentum change g'_ν due to creation or annihilation of a phonon: in the case of creation ($a^+_{\vec{\varkappa}}$ is in the ν-th position) $g'_\nu = \hbar\vec{\varkappa}$; in the case of annihilation ($a_{\vec{\varkappa}}$ is in the ν-th position) $g'_\nu = -\hbar\vec{\varkappa}$.

$$g_\nu = \sum_{\nu_1=1}^{\nu} g'_{\nu_1}.$$

$$\delta_\nu = \begin{cases} +\hbar\omega_{\vec{\varkappa}} \text{ if } a^+_{\vec{\varkappa}} \text{ is in the } \nu\text{-th position} \\ -\hbar\omega_{\vec{\varkappa}} \text{ if } a_{\vec{\varkappa}} \text{ is in the } \nu\text{-th position.} \end{cases}$$

Thus, for instance, in calculating $Z^{(6)}$, if the order of the operators is

$$a^+_{\vec{\varkappa}_1} \ldots a_{\vec{\varkappa}_3} \ldots a_{\vec{\varkappa}_2} \ldots a^+_{\vec{\varkappa}_2} \ldots a^+_{\vec{\varkappa}_3} \ldots a_{\vec{\varkappa}_1},$$

then

$$g'_4 = -\hbar\vec{\varkappa}_2, \quad g_4 = \hbar(\vec{\varkappa}_3 - \vec{\varkappa}_1), \quad \delta_4 = -\hbar\omega_{\vec{\varkappa}_2}.$$

If $V_{\vec{\varkappa}}$ is a homogeneous function of $\vec{\varkappa}$ of degree s (that is $V_{\vec{\varkappa}} \sim \varkappa^s$) and $\omega_{\vec{\varkappa}}$ is a homogeneous function of $\vec{\varkappa}$ of degree t (that is $\omega_{\vec{\varkappa}} \sim \varkappa^t$), then for the limiting case of extremely high temperatures ($kT = 1/\lambda \gg \hbar\omega_{\vec{\varkappa}}$) we can find the temperature dependence of $Z^{(2m)}$. To do this, we transform from the variables $\vec{\varkappa}$ in Eq. (9) to the new variables $\vec{\varkappa}' = \sqrt{\lambda}\vec{\varkappa}$, and then allow λ to approach zero, which corresponds to extremely high temperatures. In so doing the terms $\lambda\delta_\nu$ vanish in the exponential, and since all other terms are quadratic in $\vec{\varkappa}$, in the new variables they will not contain λ.

Since at high temperatures

$$\left[\begin{matrix} \bar{n}_{\vec{\varkappa}} \\ \bar{n}_{\vec{\varkappa}} + 1 \end{matrix}\right] \to \frac{1}{\lambda\hbar\omega_{\vec{\varkappa}}} \sim \frac{1}{\lambda\varkappa^t}$$

is also a homogeneous function of $\vec{\varkappa}$, after performing the replacement of variables, all factors λ can be taken out from under the integral sign, so that the integral is no longer λ-dependent. We thus obtain

$$Z^{(2m)} = A^{(2m)}(b^2\lambda^{\frac{t}{2}-s-\frac{1}{2}})^m Z^{(0)}(\lambda), \tag{11}$$

where b is the coupling constant and enters as a factor in all the $V_{\vec{\varkappa}}$, and $A^{(2m)}$ is a constant independent of both the coupling constant and the temperature. Thus the expansion is actually in powers of

$$b^2\lambda^{\frac{t}{2}-s-\frac{1}{2}} \tag{12}$$

and if

$$\frac{t}{2} - s - \frac{1}{2} > 0,$$

its convergence becomes stronger as the temperature increases.

In the above investigation of the temperature-dependence of $Z^{(2m)}$, it was assumed that the integrand decreases sufficiently rapidly as we increase the variables $\vec{\varkappa}_1 \ldots \vec{\varkappa}_m$. It is for this reason that we could perform the integration over infinite $\vec{\varkappa}$-space. If the integrand does not decrease sufficiently rapidly, the integration over $\vec{\varkappa}$-space should be carried to some maximum value $\vec{\varkappa}_{max}$ corresponding to the shortest possible wavelength of the vibrations of the lattice atoms. Then on going over to the new variables $\vec{\varkappa}' = \sqrt{\lambda}\vec{\varkappa}$, the limit of integration in $\vec{\varkappa}'$-space becomes λ-dependent, and $A^{(2m)}$ in Eq. (11) becomes temperature

dependent.

The term $Z^{(0)}$ is given simply by Eq.(10). Let us now go on to a more detailed calculation of the next term $Z^{(2)}$.

In this case Eq.(9) becomes

$$Z^{(2)} = \frac{\lambda^2}{2} Z^{(0)} \int_0^1 du \sum_{\vec{\varkappa}} |V_{\vec{\varkappa}}|^2 \exp\left\{-\lambda \frac{\hbar^2 \varkappa^2}{2\mu}(1-u)u\right\} \times \left[\bar{n}_{\vec{\varkappa}} e^{\lambda\hbar\omega_{\vec{\varkappa}} u} + (\bar{n}_{\vec{\varkappa}} + 1) e^{-\lambda\hbar\omega_{\vec{\varkappa}} u}\right]. \quad (13)$$

Performing the substitution

$$u = \frac{1+v}{2},$$

we arrive at

$$Z^{(2)} = \frac{\lambda^2}{2} Z^{(0)} \int_0^1 dv \sum_{\vec{\varkappa}} |V_{\vec{\varkappa}}|^2 \exp\left\{-\lambda \frac{\hbar^2 \vec{\varkappa}^2}{8\mu}(1-v^2)\right\} \frac{\operatorname{ch} \frac{1}{2}\lambda\hbar\omega_{\vec{\varkappa}} v}{\operatorname{sh} \frac{1}{2}\lambda\hbar\omega_{\vec{\varkappa}}}. \quad (14)$$

Further calculations necessitate explicit expressions for $V_{\vec{\varkappa}}$ and $\omega_{\vec{\varkappa}}$ as functions of $\vec{\varkappa}$, corresponding to the various types of interaction between the electron and lattice vibrations and to the different dispersion laws for the natural frequencies of lattice vibrations.

Ionic crystals. In this case the conduction electron interacts most strongly with longitudinal polarization vibrations. Let us first consider the case in which the electron interacts significantly only with one mode of the vibrations in a cubic crystal. The calculations presented below can be used to show that the electron interacts primarily with long-wavelength vibrations which have only a weak frequency dispersion. We shall therefore set $\omega_{\vec{\varkappa}}$ equal to the limiting value of the vibration frequency ω. In this case

$$V_{\vec{\varkappa}} = \frac{e}{|\vec{\varkappa}|} \sqrt{\frac{2\pi\hbar\omega c}{V}}, \quad c = \frac{1}{n^2} - \frac{1}{\varepsilon}, \quad (15)$$

where ε is the dielectric constant, and n is the index of refraction. Inserting this into Eq.(14), going over from the summation to the integral

$$\frac{V}{2\pi^2} \int_0^\infty \varkappa^2 d\varkappa \{\ldots\}$$

and bearing in mind that[11]

$$\int_0^1 \frac{\operatorname{ch} \frac{1}{2}\lambda\hbar\omega v}{\sqrt{1-v^2}} dv = \frac{\pi}{2} I_0\left(\frac{1}{2}\lambda\hbar\omega\right) \quad (16)$$

(I_0 is the zero-order Bessel function of an imaginary argument, $I_0(z) = j_0(iz)$), we obtain

$$Z^{(2)} = Z^{(0)} \frac{\sqrt{\pi} e^2 \omega c \sqrt{\mu} \lambda^{3/2}}{2\sqrt{2} \operatorname{sh}\left(\frac{1}{2}\lambda\hbar\omega\right)} I_0\left(\frac{1}{2}\lambda\hbar\omega\right) = Z^{(0)} \frac{\sqrt{\pi}}{2} (\lambda\hbar\omega)^{3/2} \frac{I_0\left(\frac{1}{2}\lambda\hbar\omega\right)}{\operatorname{sh}\left(\frac{1}{2}\lambda\hbar\omega\right)} \alpha. \quad (17)$$

Here

$$\alpha = \frac{ce^2}{2\hbar} \sqrt{\frac{2\mu}{\hbar\omega}} \quad (18)$$

is the square of the dimensionless coupling constant used in many investigations devoted to weak-coupling theory.

Up to terms of order α inclusive, we have

$$\ln Z = \ln (Z^{(0)} + Z^{(2)} + \ldots) = \ln Z^{(0)} + \frac{\sqrt{\pi}}{2} (\lambda\hbar\omega)^{3/2} \frac{I_0\left(\frac{1}{2}\lambda\hbar\omega\right)}{\operatorname{sh}\left(\frac{1}{2}\lambda\hbar\omega\right)} \alpha + \ldots \quad (19)$$

We can now use Eq.(3) to calculate the mean thermodynamic energy of the system:

$$\bar{E} = \bar{E}^{(0)} - \frac{\sqrt{\pi}}{4} \frac{\lambda^{1/2}(\hbar\omega)^{3/2}}{\operatorname{sh}\left(\frac{1}{2}\lambda\hbar\omega\right)} \left\{3I_0\left(\frac{1}{2}\lambda\hbar\omega\right) - \lambda\hbar\omega\left[I_0\left(\frac{1}{2}\lambda\hbar\omega\right)\operatorname{cth}\left(\frac{1}{2}\lambda\hbar\omega\right) - I_1\left(\frac{1}{2}\lambda\hbar\omega\right)\right]\right\}\alpha, \quad (20)$$

where $\bar{E}^{(0)}$ is the mean energy of the system in the absence of electron-lattice vibration interaction.

By using Eq.(19) for $\ln Z$, it is not difficult to calculate, in addition, all the other thermodynamic functions of the system.

The formulas may be simplified in the limiting cases of the extreme of high and low temperatures. For high temperatures, when $kT \gg \hbar\omega$, i.e., $\lambda\hbar\omega \ll 1$,

$$I_0\left(\frac{1}{2}\lambda\hbar\omega\right) \approx 1, \quad I_1\left(\frac{1}{2}\lambda\hbar\omega\right) \approx \frac{1}{4}\lambda\hbar\omega,$$

$$\ln Z = \ln Z^{(0)} + \sqrt{\pi}(\lambda\hbar\omega)^{1/2}\alpha, \quad (21)$$

$$\bar{E} = \bar{E}^{(0)} - \frac{\sqrt{\pi}}{2}\left(\frac{\hbar\omega}{\lambda}\right)^{1/2}\alpha. \quad (22)$$

In the case of ionic crystals, the parameters of Eq.(12) have the following values: s = -1, t = 0. Therefore, in this case the expansion is in powers of

$$\frac{b^2}{\sqrt{T}} \sim \frac{\alpha}{\sqrt{T}}. \quad (23)$$

Thus the convergence becomes stronger as the temperature is increased, and the region of applicability of weak-coupling theory is extended.

In the case of low temperatures, when $kT \ll \hbar\omega$, i.e., $\lambda\hbar\omega \gg 1$,

$$I_0\left(\frac{\lambda}{2}\hbar\omega\right) = \frac{e^{\frac{\lambda}{2}\hbar\omega}}{\sqrt{\pi\lambda\hbar\omega}}\left\{1 + \frac{1}{4\lambda\hbar\omega} + \ldots + \frac{[(2k-1)!!]^2}{k!\,(4\lambda\hbar\omega)^k} + \ldots\right\}, \quad (24)$$

$$Z = Z^{(0)}\left\{1 + \alpha\lambda\hbar\omega + \frac{\alpha}{4} + \ldots + \frac{\alpha}{4}\frac{[(2k-1)!!]^2}{k!\,(4\lambda\hbar\omega)^{k-1}} + \ldots\right\}, \quad (25)$$

$$\bar{E} = \bar{E}^{(0)} - \alpha\hbar\omega + \frac{9}{32}\frac{\alpha}{\hbar\omega\lambda^2} + \ldots \quad (26)$$

As $T \to 0$, the value of $\bar{E}$ given by Eq.(26) approaches the energy E_0 of the ground state of the system.

The method of traces developed above allows of calculating not only the sum-over-states and ground-state energy, but also the dependence of the energy on the total momentum of the system at absolute zero. To do this, we must bear in mind that the interaction of the electron with the lattice vibrations, since it is a small perturbation, should not change the type of energy spectrum. As in the case of no interaction, the total momentum $\vec{P}$ of the system should be the only continuous quantum number (the total momentum $\vec{P}$ is also an exact integral of the motion in the presence of interaction). The momentum-dependence of the energy in isotropically polarizable crystals should be of the form

$$E(P, l) = \mathcal{E}_0(l) + P^2\mathcal{E}_2(l) + P^4\mathcal{E}_4(l) + \cdots \quad (27)$$

Here the l's are the discrete quantum numbers of the system.

Let us now calculate the sum-over-states of a system whose energy spectrum is given by Eq.(27). In summing over l we need consider only the first term, which corresponds to the lowest energy for a given momentum, since the remaining terms are of exponentially lower orders at low temperatures. Hereinafter $\mathcal{E}_0, \mathcal{E}_2, \mathcal{E}_4, \ldots$ shall denote the expansion coefficients in (27) for this value of l. Noting that $\mathcal{E}_0$ equals the energy of the ground state of the system, which according to Eq.(26) is given by

$$E_0 = E_0^{(0)} - \alpha\hbar\omega, \quad (28)$$

where $E_0^{(0)}$ is the ground level of the system in the absence of interaction, we obtain the following expression for the sum-over-states of the system whose energy spectrum is described by (27):

$$Z = \frac{Z^{(0)}}{(2\mathscr{E}_2\mu)^{3/2}}\left\{1 + \lambda\hbar\omega\alpha - \frac{1\cdot3\cdot5}{2^2}\frac{\mathscr{E}_4}{\mathscr{E}_2^2\lambda} - \frac{1\cdot3\cdot5\cdot7}{2^3}\frac{\mathscr{E}_6}{\mathscr{E}_2^3\lambda^3} - \ldots - \frac{(2n+1)!!}{2^n}\frac{\mathscr{E}_{2n}}{\mathscr{E}_2^n\lambda^{n-1}} - \ldots\right\}. \quad (29)$$

In this expression we have dropped terms of order α^2 and higher. Comparing (29) and (25), and equating coefficients of equal powers of λ, we obtain

$$\mathscr{E}_2 = \left[2\mu\left(1 + \frac{\alpha}{6}\right)\right]^{-1};$$
$$\mathscr{E}_{2n} = -\frac{(2n-1)!!\,\alpha}{4n!\,(2n+1)\,\mu^n\,(4\hbar\omega)^{n-1}} \text{ with } n \geqslant 2. \quad (30)$$

For small values of P we can restrict ourselved to the first two terms of the expansion (27) and introduce the effective mass of the current carrier,

$$M = \frac{1}{2\mathscr{E}_2} = \mu\left(1 + \frac{\alpha}{6}\right). \quad (31)$$

Then, if $\frac{P^2}{2\mu\hbar\omega} < 1$, (27) can be summed using the coefficients (30); we arrive at

$$E(P) = E_0^{(0)} + \frac{P^2}{2\mu} - \alpha\hbar\omega\frac{\arcsin\sqrt{\frac{P^2}{2\mu\hbar\omega}}}{\sqrt{\frac{P^2}{2\mu\hbar\omega}}}. \quad (32)$$

The ground state energy given by Eq.(28) was first obtained by Fröhlich, Pelzer and Zienau[2] using ordinary perturbation theory methods. The effective mass given by (31) was also obtained by several authors.[3-6] Equ.(32) can be derived from Eq.(29) of Lee, Low and Pines[5], by noting that in their equation η is of order α and by considering terms only up to first order in α.

The advantage of our method of traces lies in the fact that it makes it possible to calculate the sum-over-states of the system (Eqs.(10) and (17)), as well as all other thermodynamic functions, at any temperature. In particular, it may be used at high temperatures, where the region of applicability of the weak-coupling approximation is extended and comprises the case of real crystals. In this way all the thermodynamic functions are obtained without recourse to the approximation that the energy depends quadratically on the momentum.

Let us now generalize the result obtained to the case of cubic crystals with several branches of dispersion of the longitudinal polarization vibrations. It can be shown that in this case the energy operator of the system is of the form

$$H = -\frac{\hbar^2}{2\mu}\Delta + \sum_{\vec{x}j}\hbar\omega_j\, a^+_{\vec{x}j}\, a_{\vec{x}j} + \sum_{\vec{x}j}(V_{\vec{x}j}\, a_{\vec{x}j}\, e^{i\vec{x}\vec{r}} + V^*_{\vec{x}j}\, a^+_{\vec{x}j}\, e^{-i\vec{x}\vec{r}}); \quad (33)$$

where

$$V_{\vec{x}j} = \frac{e}{|\vec{x}|}\sqrt{\frac{2\pi\hbar\omega_j c_j}{V}}, \quad (34)$$

j is the number of the dispersion branch (band) and ω_j is the frequency of the limiting extreme polarization vibrations of this branch. We shall neglect, as previously, the dependence of the natural frequencies on $\vec{x}$, since the electron interacts primarily with long-wavelength vibrations. It is expedient to express the constants c_j and ω_j, pertaining to longitudinal polarization vibrations, in terms of parameters of the transverse vibrations, according to

the method given by one of the present authors[14], since these parameters are easily determined experimentally by measurements of the dispersion of infrared light in the crystal. This requires that the experimentally determined dependence of ε on the frequency ω' of the light, be approximated by the formula

$$\frac{\varepsilon(\omega')}{n^2} = 1 + \sum_j \frac{a_j}{\omega_{\perp j}^2 - \omega'^2}. \tag{35}$$

This will also determine the limiting frequencies $\omega_{\perp j}$ of the transverse vibrations and the coefficients a_j. Further, according to Ref.14, the limiting frequencies ω_j of the longitudinal vibrations can be determined as the roots of the equation obtained by setting the right side of Eq.(35) equal to zero. Then identifying (35) with

$$\frac{\varepsilon(\omega')}{n^2} = \left(1 - \sum_j \frac{b_j}{\omega_j^2 - \omega'^2}\right)^{-1} \tag{36}$$

defines the coefficients b_j ; the coefficients c_j are given in terms of these by the equation

$$c_j = \frac{b_j}{n^2 \omega_j^2}. \tag{37}$$

Eq.(14) shows that in general $Z^{(2)}/Z^{(0)}$ is a sum of the terms corresponding to electron interactions with different normal vibrations of the crystal (perturbations due to the different normal vibrations do not "interfere" with each other in the approximation being considered). Hence in the case of several modes of polarization vibrations, the results of interaction with each of the modes should be summed separately. Thus, instead of (17), we obtain

$$Z^{(2)} = Z^{(0)} \sum_j \frac{\sqrt{\pi}}{2} (\lambda \hbar\omega_j)^{3/2} \frac{I_0\left(\frac{\lambda}{2}\hbar\omega_j\right)}{\mathrm{sh}\left(\frac{\lambda}{2}\hbar\omega_j\right)} \alpha_j, \tag{38}$$

where

$$\alpha_j = \frac{c_j e^2}{2\hbar} \sqrt{\frac{2\mu}{\hbar\omega_j}}. \tag{39}$$

Instead of Eq.(20), we obtain

$$\overline{E} = \overline{E}^{(0)} - \sum_j \frac{\sqrt{\pi}}{4} \frac{\lambda^{1/2} (\hbar\omega_j)^{3/2}}{\mathrm{sh}\left(\frac{\lambda}{2}\hbar\omega_j\right)} \left\{3 I_0\left(\frac{\lambda}{2}\hbar\omega_j\right) - \lambda\hbar\omega_j \left[I_0\left(\frac{\lambda}{2}\hbar\omega_j\right) \mathrm{cth}\left(\frac{\lambda}{2}\hbar\omega_j\right) - I_1\left(\frac{\lambda}{2}\hbar\omega_j\right)\right]\right\} \alpha_j. \tag{40}$$

In the high-temperature case, Eqs.(21) and (22) are replaced, respectively, by

$$\ln Z = \ln Z^{(0)} + \sum_j \sqrt{\pi} (\lambda\hbar\omega_j)^{1/2} \alpha_j, \tag{41}$$

and

$$\overline{E} = \overline{E}^{(0)} - \sum_j \frac{\sqrt{\pi}}{2} \left(\frac{\hbar\omega_j}{\lambda}\right)^{1/2} \alpha_j. \tag{42}$$

In the low-temperature case Eqs.(25), (26), (28) and (31) are replaced, respectively, by

$$Z = Z^{(0)} \left[1 + \sum_j \left(\lambda\hbar\omega_j \alpha_j + \frac{\alpha_j}{4}\right) + \ldots\right], \tag{43}$$

$$\overline{E} = \overline{E}^{(0)} - \left(\sum_j \hbar\omega_j \alpha_j - \frac{9}{32} \frac{\alpha j}{\hbar\omega j \lambda^2} + \ldots\right), \tag{44}$$

$$E_0 = E_0^{(0)} - \sum_j \alpha_j \hbar\omega_j; \tag{45}$$

$$M = \mu\left[1 + \frac{1}{6}\sum_j \alpha_j\right]. \tag{46}$$

Homeopolar crystals. Let us consider for simplicity a solid body with isotropic elastic properties, in which the effective mass of the conduction electrons is the same in all directions. Let $\mathbf{u}(\mathbf{r})$ be the displacement of a point of the body incident to its acoustical vibrations. Then in the approximation of the macroscopic theory of elasticity, the potential energy of deformation of the body can be written

$$U = \frac{1}{2}\left(K + \frac{4}{3}\mu'\right)\int (\operatorname{div}\mathbf{u})^2\, d\tau + \frac{\mu'}{2}\int (\operatorname{rot}\mathbf{u})^2\, d\tau, \tag{47}$$

where K is the bulk modulus of compressibility and μ' is the sheer modulus.

The kinetic energy of the vibrating body is

$$\frac{\rho}{2}\int \dot{\mathbf{u}}^2\, d\tau, \tag{48}$$

where ρ is its density. The interaction potential of a conduction electron with the vibrations will be taken in the form

$$H_1 = b \operatorname{div}\mathbf{u}(\mathbf{r}), \tag{49}$$

where b is a constant and r is the coordinate of the electron. Equation (49) was proposed by Bardeen and Shockley[15] and independently by one of the authors in collaboration with Deigen[16].

For longitudinal acoustical vibrations, $\operatorname{rot}\mathbf{u} = 0$, and $\operatorname{div}\mathbf{u} \neq 0$; for transverse acoustical vibrations, on the contrary, $\operatorname{rot}\mathbf{u} \neq 0$, and $\operatorname{div}\mathbf{u} = 0$. The last means that transverse acoustical vibrations do not interact with conduction electrons. We shall, therefore, consider them to be a conservative closed system and ignore them in what follows. Expanding the irrotational part of the vector u in a Fourier series

$$\mathbf{u} = \sum_{\vec{\varkappa}} \mathbf{u}_{\vec{\varkappa}}\chi_{\vec{\varkappa}}(\mathbf{r}); \quad \chi_{\vec{\varkappa}}(\mathbf{r}) = \sqrt{\frac{2}{V}}\begin{cases}\cos \vec{\varkappa}\mathbf{r} & \varkappa_x < 0\\ \sin \vec{\varkappa}\mathbf{r} & \varkappa_x \geqslant 0\end{cases} \tag{50}$$

and picking the dimensionless normal coordinates

$$q_{\vec{\varkappa}} = u_{\vec{\varkappa}}\sqrt{\frac{\rho\omega_{\vec{\varkappa}}}{\hbar}}, \tag{51}$$

whose canonical conjugate momenta are

$$g_{\vec{\varkappa}} = \dot{u}\sqrt{\frac{\rho}{\hbar\omega_{\vec{\varkappa}}}}, \tag{52}$$

we can write the Hamiltonian of the electron and the longitudinal acoustical vibrations in the form

$$H = -\frac{\hbar^2}{2\mu}\Delta + \frac{1}{2}\sum_{\vec{\varkappa}}\hbar\omega_{\vec{\varkappa}}\left[q_{\vec{\varkappa}}^2 + g_{\vec{\varkappa}}^2\right] + b\sum_{\vec{\varkappa}}\sqrt{\frac{\hbar}{\rho\omega_{\vec{\varkappa}}}}\, q_{\vec{\varkappa}}\,|\vec{\varkappa}|\,\chi_{-\vec{\varkappa}}(\mathbf{r});$$
$$[q_{\vec{\varkappa}}q_{\vec{\varkappa}'}] = [g_{\vec{\varkappa}}g_{\vec{\varkappa}'}] = 0; \quad [q_{\vec{\varkappa}}g_{\vec{\varkappa}'}] = i\delta_{\vec{\varkappa}\vec{\varkappa}'}. \tag{53}$$

Here $\omega_{\vec{\varkappa}}$ are the frequencies of the longitudinal acoustical vibrations; they are given by

$$\omega_{\vec{\varkappa}} = w|\vec{\varkappa}|, \tag{54}$$

where $w = \sqrt{\frac{K + \frac{4}{3}\mu'}{\rho}}$ is the velocity of longitudinal sound in the body.

Introducing the new variables

$$\alpha_{\vec{\varkappa}}^{+}=\frac{1}{2}(q_{\vec{\varkappa}}-iq_{-\vec{\varkappa}}+ig_{\vec{\varkappa}}+g_{-\vec{\varkappa}}); \qquad a_{\vec{\varkappa}}^{+}=\frac{1}{2}(q_{\vec{\varkappa}}+iq_{-\vec{\varkappa}}-ig_{\vec{\varkappa}}+g_{-\vec{\varkappa}})$$

$$a_{-\vec{\varkappa}}=\frac{1}{2}(q_{\vec{\varkappa}}+iq_{-\vec{\varkappa}}+ig_{\vec{\varkappa}}-g_{-\vec{\varkappa}}); \quad a_{-\vec{\varkappa}}^{+}=\frac{1}{2}(q_{\vec{\varkappa}}-iq_{-\vec{\varkappa}}-ig_{\vec{\varkappa}}-g_{-\vec{\varkappa}}) \text{ for } \vec{\varkappa}_x>0;$$

$$[a_{\vec{\varkappa}'}a_{\vec{\varkappa}''}]=[a_{\vec{\varkappa}'}^{+}a_{\vec{\varkappa}''}^{+}]=0; \quad [a_{\vec{\varkappa}'}a_{\vec{\varkappa}''}^{+}]=[a_{-\vec{\varkappa}'}, \ a_{-\vec{\varkappa}''}]=\delta_{\vec{\varkappa}'\vec{\varkappa}''}, \tag{55}$$

we finally obtain a Hamiltonian of the form of equation (4), in which

$$V_{\vec{\varkappa}}=b\sqrt{\frac{\hbar}{2V\rho w}}\cdot\sqrt{|\vec{\varkappa}|}. \tag{56}$$

Equations (47)-(49) are valid only for long-wavelength vibrations. It will be seen later, however, that in a homeopolar crystal the short-wavelength vibrations also interact strongly with the electron. The Hamiltonian will still retain the form of Eq.(4), but $V_{\vec{\varkappa}}$ for large $\varkappa$ will differ somewhat from the form given by Eq.(56), and the velocity of sound w in Eq.(54) should be considered dependent on $\varkappa$ for large $\varkappa$. The deviation of $V_{\vec{\varkappa}}$ from equation (56) for large values of $\varkappa$ will be taken into account by considering b a function of $\varkappa$. As $\vec{\varkappa}\to 0$, we have $b_{\vec{\varkappa}}\to b$ and $w_{\vec{\varkappa}}\to w$.

Let us now go on to a calculation of $Z^{(2)}$ according to Eq.(14). Inserting (54) and (56) into (14), we obtain

$$Z^{(2)}=\frac{\lambda^2}{8\pi^2}Z^{(0)}\frac{\hbar}{\rho}\int_0^1 dv\int_0^{\varkappa_m}\frac{d\varkappa\, b_{\vec{\varkappa}}^2\varkappa^3}{w_{\vec{\varkappa}}}\frac{\operatorname{ch}\frac{\lambda}{2}\hbar\omega_{\vec{\varkappa}}v}{\operatorname{sh}\frac{\lambda}{2}\hbar\omega_{\vec{\varkappa}}}\exp\left\{-\lambda\frac{\hbar^2\varkappa^2}{8\mu}(1-v^2)\right\}. \tag{57}$$

If the integral over $\varkappa$ is taken from zero to infinity, it diverges. Actually, however, a crystal cannot vibrate with an arbitrarily large $\varkappa$. The maximum value $(\varkappa_m)$ of $\varkappa$ is given by the condition that the number of vibrations with $\varkappa\leqslant\varkappa_m$ must equal one third the number of vibrational degrees of freedom of the system, i.e., the number N of atoms in the crystal:

$$\varkappa_m=\left(\frac{6\pi^2N}{V}\right)^{1/3}. \tag{58}$$

The rest of the calculation of $Z^{(2)}$ depends on the assumption

$$p\equiv\frac{\hbar\varkappa_m^2}{8\mu}\lambda\gg 1. \tag{59}$$

This inequality is usually satisfied in reality, since p is of the order of magnitude of the ratio of the conduction band width to kT. In Eq.(57) we perform the substitution $v=1-x$, and the whole x-dependent part of the integrand is written in the form of an exponential whose argument is expanded in powers of x. Further, it follows from (59) that the main contribution to the integral comes from the region of small x. We can therefore handle the exponential as follows: we keep all terms linear in x in the exponential, and treat those quadratic and of higher order in x as small corrections and expand the exponential as a series in these corrections. Then in performing the term-by-term integration over x, we can use the limits 0 to ∞, rather than 0 to 1. We thus obtain

$$Z^{(2)}=\frac{\lambda^2}{8\pi^2}Z^{(0)}\frac{\hbar}{\rho}\int_0^{\varkappa_m}\frac{d\varkappa\, b_{\vec{\varkappa}}^2\varkappa^3}{w_{\vec{\varkappa}}}\frac{\operatorname{cth}\frac{\lambda}{2}\hbar\omega_{\vec{\varkappa}}}{\frac{\hbar^2\varkappa^2}{4\mu}\lambda+\frac{\lambda}{2}\hbar\omega_{\vec{\varkappa}}\operatorname{th}\frac{\lambda}{2}\hbar\omega_{\vec{\varkappa}}}\times$$

$$\times\left[1+\frac{\frac{\hbar^2\varkappa^2}{4\mu}\lambda+\left(\frac{\lambda}{2}\hbar\omega_{\vec{\varkappa}}\right)^2\left(\operatorname{ch}\frac{\lambda}{2}\hbar\omega_{\vec{\varkappa}}\right)^{-2}}{\left(\frac{\hbar^2\varkappa^2}{4\mu}\lambda+\frac{\lambda}{2}\hbar\omega_{\vec{\varkappa}}\operatorname{th}\frac{\lambda}{2}\hbar\omega_{\vec{\varkappa}}\right)^2}+\ldots\right]. \tag{60}$$

In the extremely low-temperature case, when $kT \ll \hbar\omega_{\varkappa_m}$, Eq.(60) becomes

$$Z^{(2)} = Z^{(0)} \frac{\lambda}{2\pi^2} \frac{\mu}{\hbar\rho} \int_0^{\varkappa_m} \frac{d\varkappa b_\varkappa^2 \varkappa^2}{w_\varkappa \left(\varkappa + \frac{2\mu w_\varkappa}{\hbar}\right)} \left[1 + \frac{1}{\frac{\lambda\hbar^2}{4\mu}\left(\varkappa + \frac{2\mu w_\varkappa}{\hbar}\right)^2}\right]. \tag{61}$$

From this we obtain the ground-state energy of the system

$$E_0 = E_0^{(0)} - \frac{1}{2\pi^2} \frac{\mu}{\hbar\rho} \int_0^{\varkappa_m} \frac{d\varkappa b_\varkappa^2 \varkappa^2}{w_\varkappa \left(\varkappa + \frac{2\mu w_\varkappa}{\hbar}\right)} \tag{62}$$

and the effective mass of the current carriers

$$\frac{M}{\mu} = 1 + \frac{4}{3\pi^2} \frac{\mu^2}{\hbar^3\rho} \int_0^{\varkappa_m} \frac{d\varkappa b_\varkappa^2 \varkappa^2}{w_\varkappa \left(\varkappa + \frac{2\mu w_\varkappa}{\hbar}\right)^3}. \tag{63}$$

The values of E_0 and M correspond to the case $T \to 0$, when $p \to \infty$ and errors associated with the inequality (59) vanish.

If $b_\varkappa$ and $w_\varkappa$ are independent of $\varkappa$, the integrals in Eqs.(61)-(63) can be calculated by elementary quadrature.

In the extreme high-temperature case, when $kT \gg \hbar\omega_{\varkappa_m}$, in view of the inequality (59), from Eq.(57), we obtain the approximation

$$Z^{(2)} = Z^{(0)} \frac{\mu}{\pi^2\hbar^2\rho} \int_0^{\varkappa_m} \frac{b_\varkappa^2 d\varkappa}{w_\varkappa^2}. \tag{64}$$

Thus when taking account of interactions, the high-temperature sum-over-states is given a temperature-independent correction factor. Hence in the approximation being used the correction to the mean thermodynamic energy of the system is zero.

Eqs.(62)-(64) show that the results depend strongly on $\varkappa_m$. This means that the electron interacts to a significant extent with short-wavelength acoustical vibrations as well. In treating such an interaction, it is not rigorously correct to use the effective-mass method. Therefore, the results obtained above for homeopolar crystals are not evaluative in character.

The results here obtained, in particular, the equations for the sum-over-states, will be used in a following article to deduce new expressions for the thermal electron emission, the temperature dependence of the current carrier concentration in a semiconductor, and the heat capacity.

The authors take this opportunity to correct an error discovered in one of their previous works[17] by K.B.Tolpygo. On the right side of Eq.(132) of Ref.17, the homogeneous function of k should be of degree -1/2, rather than 1. It then follows that the factor $(\omega - \omega^0_{\varkappa_s z})^3$ in Eq.(134) vanishes. This leads to a correction in Ref.18, where the term αT^7 in Eq.(78) should be replaced by αT^4. All other results in these articles remain valid.

Institute of Physics and
Institute of Metal Physics of the
Ukrainian SSR Academy of Sciences

References

1. S.I.Pekar, Issledovania po elektronnoi teorii kristallov (Studies in the electron theory of crystals), M. 1951.
2. H.Fröhlich, H.Pelzer & S.Zienau, Phil.Mag., 41, 221 (1950).
3. S.B.Tiablikov, Zhur.eksp.i teor.fiz., 22, 513 (1952).
4. M.Gurary, Phil.Mag., 44, 329 (1953).
5. T.D.Lee, F.E.Low & D.Pines, Phys.Rev., 90, 297 (1953).
6. E.Haga, Progr.Theor.Phys.(japan), 11, 449 (1954).
7. T.D.Lee & D.Pines, Phys.Rev., 92, 883 (1953).
8. G.Höhler, ZS.f.Phys.,140, 192 (1955), Nuovo Climento, 11, 691 (1955).
9. R.P.Feynman, Phys.Rev., 97, 660 (1955).
10. J.Schwinger, Phys.Rev., 82, 664 (1951).
11. I.M.Ryzhik & I.S.Gradshtein, Tablitsy integralov, summ, riadov i proizvedenii (Tables of integrals, sums, series and products), M. 1951.
12. S.I.Pekar, Zhur.eksp.i teor.fiz., 16, 341 (1946).
13. S.I.Pekar, Zhur.eksp.i teor.fiz., 19, 796 (1949).
14. M.A.Krivoglaz & S.I.Pekar, Zhur.eksp.i teor.fiz., 31, 343 (1956).
15. J.Bardeen & W.Shockley, Phys.Rev., 80, 72 (1951).
16. M.F.Deigen & S.I.Pekar, Zhur.eksp.i teor.fiz., 21, 803 (1951).
17. M.A.Krivoglaz & S.I.Pekar, Trudy (Transactions), Inst. of Phys., Ukrainian SSR Ac. of Sci., No.4, 37 (1953).
18. M.A.Krivoglaz, Zhur.eksp.i teor.fiz., 25, 191 (1953).

THE METHOD OF TRACES FOR CONDUCTION ELECTRONS IN SEMICONDUCTORS
Part II. VARIATIONAL METHOD

- M.A.Krivoglaz and S.I.Pekar

In the preceding article[1] (hereinafter referred to as Part I) we considered a system consisting of a crystal and a conduction electron, described by the Hamiltonian

$$H = -\frac{\hbar^2}{2\mu}\Delta + \sum_{\vec{x}} \hbar\omega_{\vec{x}} a^+_{\vec{x}} a_{\vec{x}} + \sum_{\vec{x}} (V_{\vec{x}} a_{\vec{x}} e^{i\vec{x}\vec{r}} + V^*_{\vec{x}} a^+_{\vec{x}} e^{i\vec{x}\vec{r}}). \tag{1}$$

It was shown that many of the quantities characterizing the states of current carriers in a semiconductor can be described in terms of the traces of various operators. The trace of the operator $e^{-\lambda H}$, which gives the sum-over-states when $\lambda = 1/kT$, was examined in detail. In order to calculate the trace of this operator, the electron-lattice vibration interaction energy (the last term in Eq.(1)) was considered a small perturbation.

In this part we shall calculate the trace of $e^{-\lambda H}$ without assuming weak coupling between the electron and the lattice vibrations. To do this we shall develop a direct variational method, in which the original energy operator will be approximated by a simpler one containing parameters which will be varied. The idea of this method was inspired by a recent publication of Feynman[2], in which the Lagrangian formulation is used to find an approximate solution of the time-dependent Schroedinger equation for a system whose Hamiltonian is given by (1). In the solution obtained, the time t is replaced by the imaginary quantity $i\tau$, so that the time-dependent exponentials multiplying the stationary eigenfunctions have real arguments, and we can write

$$\Psi = \sum_n c_n \psi_n e^{-iE_n t/\hbar} = \sum_n c_n \psi_n e^{-E_n \tau/\hbar}. \tag{2}$$

As $\tau \to \infty$, the term in Eq.(2) pertaining to the ground state begins to dominate (since the other exponentials decay more rapidly). The ground state energy E_0 is found by investigating the behavior of Ψ as $\tau \to \infty$.

The method of traces used herein, the substance of which was described in Part I, also allows of finding the ground state energy of the system. In fact, if Feynman's approximations are made, the method can be used to obtain all of his results. Moreover, this method makes it possible to calculate the sum-over-states and other thermodynamic functions at any arbitrary temperature, as well as the dependence of the energy of the system on the total momentum.

1. Elimination of the Vibrational Degrees of Freedom of the System

Herein we shall use the following method of ordering the operators. Non-commuting operators are given indices which indicate the order in which they act: operators with lower indices act before those with higher ones. When these indices are used, as has been shown by Feynman[3], we may ignore the fact that the operators do not commute, and treat functions of operators as we would functions of ordinary c-numbers. This considerably simplifies transformation of the operator expressions. After all the mathematical manipulations have been performed, the final expression must be "disentangled"; all operator factors must be written out with their indices in increasing order, and the indices can then be dropped since the order of operation now corresponds to the order of the operators. Using this method and Feynman's results[3], the operator $e^{-\lambda H}$ can be brought to the form

$$e^{-\lambda H} = G(\mathbf{r}) \exp\left(-\int_0^{\lambda} \mathfrak{R}_{r\lambda_1} d\lambda_1\right) \exp(-\lambda H) \exp\left(-\sum_{\vec{x}} \beta^*_{\vec{x}} a^+_{\vec{x}}\right) \exp\left(-\sum_{\vec{x}} \beta_{\vec{x}} a_{\vec{x}}\right), \tag{3}$$

where

$$G(\mathbf{r}) = \exp\left(\sum_{\vec{x}} |V_{\vec{x}}|^2 \int_0^{\lambda} e^{i\vec{x}\vec{r}_{\lambda_1} - \hbar\omega_{\vec{x}}\lambda_1} d\lambda_1 \int_0^{\lambda_1} e^{-i\vec{x}\vec{r}_{\lambda_2} + \hbar\omega_{\vec{x}}\lambda_2} d\lambda_2\right), \tag{4}$$

$$H_r = -\frac{\hbar^2}{2\mu}\Delta, \tag{5}$$

$$\mathfrak{R} = \sum_{\vec{x}} \hbar\omega_{\vec{x}} a^+_{\vec{x}} a_{\vec{x}}, \tag{6}$$

$$\beta_{\vec{x}} = V_{\vec{x}} \int_0^{\lambda} e^{i\vec{x}\vec{r}_{\lambda_1} - \hbar\omega_{\vec{x}}\lambda_1} d\lambda_1; \quad \beta^*_{\vec{x}} = V^*_{\vec{x}} \int_0^{\lambda} e^{-i\vec{x}\vec{r}_{\lambda_1} + \hbar\omega_{\vec{x}}\lambda_1} d\lambda_1. \tag{7}$$

The vibrational degrees of freedom in expressions (3) and (4) are "disentangled", since $a_{\vec{x}}$, $a^+_{\vec{x}}$ and $\mathfrak{R}$ already contain no ordering indices and act, as usual, in the order in which they appear. Operators depending on the electron coordinate r are not "disentangled", λ_1 and λ_2 are continuous indices determining the order in which they act. Expressions of the form

$$\exp\left[\int_0^{\lambda} A_{\lambda_1} d\lambda_1 + \int_0^{\lambda} B_{\lambda_2} d\lambda_2\right],$$

where A and B are noncommuting operators should be thought of as infinite products of factors such as

$$e^{A_{\lambda_1} d\lambda_1} \text{ and } e^{B_{\lambda_2} d\lambda_2},$$

which differ by an infinitesimal quantity from unity and which act in order given by the increasing order of the indices at A and B.

Let us now turn to a calculation of the trace of the operator of (3) in terms of the complete set of orthogonal functions of the form

$$\Psi_{ln} = \chi_l(\mathbf{r})\,\Phi_n, \quad \Phi_n = \prod_{\vec{x}} \Phi_{n_{\vec{x}}}, \tag{8}$$

where $\Phi_{n_{\vec{x}}}$ are one-dimensional harmonic oscillator wave functions, i.e., eigenfunctions of operators $a^+_{\vec{x}} a_{\vec{x}}$ and $\chi_l(\mathbf{r})$ is any complete set of orthogonal functions of r.

We shall calculate the trace of expression (3) in two steps: we shall first find the diagonal matrix elements for the Φ_n functions and sum over n. We thus obtain an operator $L(\mathbf{r})$ which depends only on r; we shall then find the trace of L in terms of the $\chi_l(\mathbf{r})$.

Proceeding to the first stage of the calculation, we note that only the last three exponentials of Eq. (3) act on the vibrational degrees of freedom, and these can be written as the product $\prod_{\vec{x}}$ of operators such as

$$R = \exp(-\lambda\hbar\omega a^+ a) \exp(-\beta^* a^+) \exp(-\beta a). \tag{9}$$

Expanding $e^{-\beta^* a^+}$ and $e^{-\beta a}$ into power series, we obtain

$$\mathrm{sp}\, R = \sum_{m=0}^{\infty} \langle \Phi_m, R\Phi_m \rangle = \sum_{m=0}^{\infty} e^{-\lambda\hbar\omega m} \sum_{i=0}^{\infty} \frac{(\beta^*\beta)^i}{(i!)^2} m(m-1)\ldots(m-i+1). \tag{10}$$

Introducing the notation $\alpha = e^{-\lambda\hbar\omega}$, we can rewrite Eq. (10) as

$$\mathrm{sp}\,R=\sum_{i=0}^{\infty}\frac{(\beta^{*}\beta)^{i}}{(i!)^{2}}\alpha^{i}\frac{d^{i}}{(d\alpha)^{i}}\sum_{m=0}^{\infty}\alpha^{m}=\sum_{i}\frac{(\beta^{*}\beta)^{i}}{i!}\frac{\alpha^{i}}{(1-\alpha)^{i+1}}=(1-e^{-\lambda\hbar\omega})^{-1}\exp\frac{\beta^{*}\beta}{e^{\lambda\hbar\omega}-1}. \tag{11}$$

If $\lambda = 1/kT$, then the expression

$$\bar{n}=(e^{\lambda\hbar\omega}-1)^{-1} \tag{12}$$

gives the mean Planck value of the oscillator quantum number. Then Eq.(11) can be written in the form

$$\mathrm{sp}R=(\bar{n}+1)\exp(\bar{n}\beta^{*}\beta). \tag{13}$$

According to (3), (9) and (13),

$$L(\mathbf{r})=XL(\mathbf{r}), \tag{14}$$

where

$$L(\mathbf{r})=L(\mathbf{r})\exp\left(-\int_{0}^{\lambda}H_{\mathbf{r}\lambda_1}d\lambda_1\right)\exp\left(\sum_{\vec{\varkappa}}\bar{n}_{\vec{\varkappa}}\beta^{*}_{\vec{\varkappa}}\beta_{\vec{\varkappa}}\right), \tag{15}$$

$$X=\prod_{\vec{\varkappa}}(1-e^{-\lambda\hbar\omega_{\vec{\varkappa}}})^{-1}. \tag{15a}$$

If $\lambda = 1/kT$, then X is the sum-over-states of the lattice vibrations in the absence of the conduction electron.

Thus in order to calculate the trace of $e^{-\lambda H}$, we now need only calculate the trace of the ordered operator $L(\mathbf{r})$, which no longer contains the vibrational degrees of freedom.

2. Approximate Method

The difficulty in calculating the trace of the ordered operator $L(\mathbf{r})$ stems from the fact that it is not "disentangled". It can be "disentangled", for example, after it is expanded in a series in powers of the coupling constant $V_{\vec{\varkappa}}$.

We then obtain the results of Part I, which are valid for cases of weak coupling. In the present part we shall not restrict the strength of the interaction and shall calculate sp L by an approximate method based on the variational principle for ordered operators. To do this, we must first prove an auxiliary theorem.

Let

$$I=\mathrm{sp}\exp\left[\int_{0}^{\lambda}A_{\lambda_1}d\lambda_1+s\int_{0}^{\lambda}B_{\lambda_1}d\lambda_1\right], \tag{16}$$

where A and B are self-conjugate operators, λ_1 is an ordering index and s is an arbitrary parameter. If we disentangle the factor $e^{A\lambda}$ in Eq.(16), by using Eqs.(16)-(18) of Feynman[3], we obtain

$$I=\mathrm{sp}\,e^{\lambda A_\lambda}e^{s\int_{0}^{\lambda}B'_{\lambda_1}d\lambda_1}\equiv\mathrm{sp}\,e^{P}e^{sQ}, \tag{17}$$

where

$$B'_{\lambda_1}=e^{-\lambda_1 A_{\lambda_1}}B_{\lambda_1}e^{\lambda_1 A_{\lambda_1}};\quad 0\leqslant\lambda_1\leqslant\lambda;\quad P=\lambda A;\quad Q=\int_{0}^{\lambda}B'_{\lambda_1}d\lambda_1. \tag{18}$$

Let us now introduce a certain average $\bar{B}$, defined by

$$\lambda\overline{B} = \frac{\operatorname{sp}\left\{\int_0^\lambda B_{\lambda_1} d\lambda_1 \exp \int_0^\lambda A_{\lambda_1} d\lambda_1\right\}}{\operatorname{sp} \exp \int_0^\lambda A_{\lambda_1} d\lambda_1} = \frac{\operatorname{sp}\left\{e^{\lambda A_\lambda} \int_0^\lambda B'_{\lambda_1} d\lambda_1\right\}}{\operatorname{sp} \lambda A} = \frac{\operatorname{sp}\{e^P Q\}}{\operatorname{sp} e^P} \equiv \overline{Q}. \tag{19}$$

Let

$$I_1 = \operatorname{sp}\, e^{\lambda A} e^{s\lambda \overline{B}} = \operatorname{sp} e^P e^{s\overline{Q}}. \tag{20}$$

The theorem states:

$$I \geqslant I_1. \tag{21}$$

To prove this inequality, we note that

$$\frac{d}{ds}\left(\frac{I}{I_1}\right) \frac{\operatorname{sp}\{e^P (Q - \overline{Q})\, e^{s(Q-\overline{Q})}\}}{\operatorname{sp} e^P}. \tag{22}$$

The sign of this expression is always the same as that of s. Indeed, let us calculate the trace in Eq.(22) in terms of the eigenfunctions of Q. When $s = 0$, expression (22) equals zero in view of (19). If, for instance, $s > 0$, then all positive eigenvalues of the operator $Q - \bar{Q} - Q_n - \bar{Q}$ are multiplied by the factors $e^{s(Q_n - \bar{Q})}$, which are greater than unity, while the negative eigenvalues of $Q_{n'} - \bar{Q}$ are multiplied by similar factors smaller than unity. Thus for $s > 0$, the value of (22) is greater than for $s = 0$, i.e., is positive. Since for $s = 0$

$$\frac{I}{I_1} = 1,$$

by taking account of the sign of the derivative of expression (22), we obtain $I/I_1 \geqslant 1$, which proves (21).

The proposed approximation method consists of the following. The trace of $L(r)$

$$I = \operatorname{sp} L = \operatorname{sp} \exp\left\{\sum_{\vec{\varkappa}} |V_{\vec{\varkappa}}|^2 \left[\int_0^\lambda d\lambda_1 \int_0^{\lambda_1} d\lambda_2 e^{i\vec{\varkappa}(r_{\lambda_1} - r_{\lambda_2}) - \hbar\omega_{\vec{\varkappa}}(\lambda_1 - \lambda_2)} + \right.\right.$$
$$\left.\left. + \bar{n}_{\vec{\varkappa}} \int_0^\lambda d\lambda_1 \int_0^\lambda d\lambda_2 e^{i\vec{\varkappa}(r_{\lambda_1} - r_{\lambda_2}) - \hbar\omega_{\vec{\varkappa}}(\lambda_1 - \lambda_2)}\right] - \int_0^\lambda H_{r_{\lambda_1}} d\lambda_1\right\} \tag{23}$$

is regarded as the I in the above theorem. The argument of the exponential in Eq.(23) is approximated by another operator which depends on certain parameters. This operator is then A of Eq.(16). Then the operator $\int_0^\lambda B_{\lambda_1} d_{\lambda_1}$ in Eq. (16) is the difference between this approximation and the exact operator in expression (23). The approximation consists of replacing B by $\overline{B}$, so that I goes over into I_1, i.e., decreases. Then the parameters of the approximating operator A are varied, and finally chosen so that I_1 is maximal. If the approximating operator is chosen in a sufficiently general way, then variation of the parameters can give an extremely close approximation to the exact operator. In this way I_1 could be made arbitrarily close to I. This method is analogous to the usual variational method of quantum mechanics, except for the important difference that we are here approximating not a wave function, but an operator.

The form of A must be chosen simple enough for the values of Eqs.(19) and (20) to be calculable. In doing this we must take account of the fact that the field of a conduction electron causes a local distortion in the crystal (a persistent dielectric polarization in ionic crystals, or a persistent density increase in homeopolar crystals); this distortion attracts the electron and moves together with it through the whole volume of the crystal. Feynman[2] has described these characteristics of the electron motion by the following simple model. The local distortion of the crystal and its influence

on the electron is treated as a second particle which attracts the electron. The attractive potential is chosen proportional to the square of the distance between the particles. These interacting particles can freely move through the volume of the crystal. Thus the effect of atomic vibrations on the electron is approximated by the attraction of a second particle. In accord with this approximation, let us write the Hamiltonian of the two particles in the form

$$H' = -\frac{\hbar^2}{2\mu}\Delta - \frac{\hbar^2}{2\mu_2}\Delta_2 + \frac{C}{2}(\mathbf{r} - \mathbf{r}_2)^2. \tag{24}$$

Here the mass μ_2 of the second particle and the elastic coupling coefficient C are the parameters which we shall later vary.

In order to obtain an expression for I_1 which will approximate (23) in the model described above, we must first eliminate the coordinates $\mathbf{r}_2$ of the second particle from $e^{-\lambda H'}$, leaving the one variable r, just as prior to calculating I, we eliminated the vibrational degrees of freedom from $e^{-\lambda H}$ and left only the variable r.

The operator $e^{-\lambda H'}$ is written in the ordered form $e^{-\int_0^\lambda H'_{\lambda_1} d\lambda_1}$. We then disentangle all factors containing the variable $\mathbf{r}_2$ in this ordered operator; in doing this we again use Feynman's[3] Eq.(18). We then calculate the trace of the operator thus obtained in terms of the eigenfunctions of the operator

$$-\frac{\hbar^2}{2\mu_2}\Delta_2 + \frac{C}{2}\mathbf{r}_2, \tag{25}$$

noting that these eigenfunctions depend only on $\mathbf{r}_2$. Hence the trace obtained depends only on r. It is of the form

$$L'(\mathbf{r}) = \exp\left\{-\int_0^\lambda H_{\mathbf{r}\lambda_1} d\lambda_1 + U'\right\},$$

$$U' = -\frac{C}{2}\int_0^\lambda \mathbf{r}_{\lambda_1}^2 d\lambda + \frac{\hbar\omega_2 C}{2}\int_0^\lambda\int_0^{\lambda_1} (\mathbf{r}_{\lambda_1}, \mathbf{r}_{\lambda_2})\, e^{\hbar\omega_2(\lambda_2 - \lambda_1)} d\lambda_1 d\lambda_2 +$$

$$+ \bar{n}_2 \frac{\hbar\omega_2 C}{2}\int_0^\lambda\int_0^\lambda (\mathbf{r}_{\lambda_1}, \mathbf{r}_{\lambda_2})\, e^{\hbar\omega_2(\lambda_2 - \lambda_1)} d\lambda_1 d\lambda_2 - 3\ln\left(2\,\mathrm{sh}\,\frac{\hbar\omega_2\lambda}{2}\right), \tag{26}$$

where

$$\omega_2 = \sqrt{\frac{C}{\mu_2}},\quad \bar{n}_2 = \frac{1}{e^{\lambda\hbar\omega_2} - 1}. \tag{27}$$

The operator $L'(\mathbf{r})$ is an approximation to the exact operator $L(\mathbf{r})$ (cf. Eqs.(15) and (23)) in the simplified model described above.

Let us denote the argument of the exponential in (23) by $-\int_0^\lambda H_{\mathbf{r}\lambda_1} d\lambda_1 + U$. Writing (23) in the form

$$I = \mathrm{sp}\exp\left\{-\int_0^\lambda H_{\mathbf{r}\lambda_1} d\lambda_1 + U' + (U - U')\right\} \tag{28}$$

and treating $-\int_0^\lambda H_{\mathbf{r}\lambda_1} d\lambda_1 + U'$ as the operator $\int_0^\lambda A_{\lambda_1} d\lambda_1$ of Eq.(16), and $U - U'$ as

the operator $\int_0^\lambda B_{\lambda_1} d\lambda_1$, we go on to a calculation of I_1, as defined by Eqs.(19)-(20).

The expression $\mathrm{sp}\, e^{\lambda A} = \mathrm{sp}\, L'(\mathbf{r}) = \mathrm{sp}\, e^{\left[-\int_0^\lambda H_{\mathbf{r}\lambda_1} d\lambda_1 + U'\right]} \equiv Z'$ of (19)-(20) is most easily calculated as the trace of the original operator $e^{-\lambda H'}$. Invoking Eq.(24), it is easily shown that

$$Z' = \mathrm{sp}\, e^{-\lambda H'} = V\left(\frac{M'}{2\pi\hbar^2\lambda}\right)^{3/2}\left(2\,\mathrm{sh}\,\frac{\lambda}{2}\,\hbar\sqrt{\frac{C}{\mu'}}\right)^{-3}, \tag{29}$$

where $\mu' = \frac{\mu\mu_2}{\mu+\mu_2}$ is the reduced mass of the two particles, and $M' = \mu + \mu_2$.

Further, according to Eq.(19)

$$\overline{U'} = \mathrm{sp}\left[U' \exp\left(-\int_0^\lambda H_{r\lambda_1} d\lambda_1 + U'\right)\right] \Big/ Z'. \tag{30}$$

This expression is most easily calculated by noting that according to (26) all the terms except the last, constant one in U' contain C linearly; therefore the mean values of these terms can be obtained by differentiating Z' with respect to C, multiplying the result by C, and dividing by Z'. We then arrive at

$$\overline{U'} = -3\ln\left(2\,\mathrm{sh}\,\frac{\lambda}{2}\,\hbar\omega_2\right) + \frac{C}{Z'}\left(\frac{\partial Z'}{\partial C}\right)_{\omega_2 = \mathrm{const}}. \tag{31}$$

Let us now calculate the mean value of the ordered operator

$$U = \sum_{\vec{\varkappa}} |V_{\vec{\varkappa}}|^2 \left[\int_0^\lambda\int_0^{\lambda_1} e^{i\vec{\varkappa}(\mathbf{r}_{\lambda_1} - \mathbf{r}_{\lambda_2}) - \hbar\omega_{\vec{\varkappa}}(\lambda_1 - \lambda_2)}\, d\lambda_1 d\lambda_2 + \right.$$
$$\left. + \bar{n}_{\vec{\varkappa}} \int_0^\lambda\int_0^\lambda e^{i\vec{\varkappa}(\mathbf{r}_{\lambda_1} - \mathbf{r}_{\lambda_2}) \quad \hbar\omega_{\vec{\varkappa}}(\lambda_1 - \lambda_2)}\, d\lambda_1 d\lambda_2\right] \equiv \sum_{\vec{\varkappa}} U_{\vec{\varkappa}}. \tag{32}$$

In taking an average according to Eq.(19), the average of a sum is equal to the sum of the averages. Therefore we shall first calculate $\overline{U}_{\vec{\varkappa}}$ and then sum the result over $\vec{\varkappa}$. We calculate $\overline{U}_{\vec{\varkappa}}$ in the following artificial way. We construct the Hamiltonian

$$H'' = H' - \frac{\hbar^2}{2\mu}\frac{\partial^2}{\partial x_3^2} + \frac{\mu\omega_{\vec{\varkappa}}^2}{2} x_3^2 + V_{\vec{\varkappa}} a_3 e^{i\vec{\varkappa}\mathbf{r}} + V_{\vec{\varkappa}}^* a_3^+ e^{-i\vec{\varkappa}\mathbf{r}}, \tag{33}$$

where H' is given by Eq.(24). The transition from the Hamiltonian of (24) to that of (33) can be thought of as equivalent to the addition of a third particle undergoing one-dimensional harmonic oscillations of frequency $\omega_{\vec{\varkappa}}$ about a fixed equilibrium position and having an infinitesimally weak interaction with the first particle (since $V_{\vec{\varkappa}}$ is inversely proportional to the square root of the volume of the base region, i.e., may be arbitrarily small); a_3 and a_3^+ are annihilation and creation operators for the oscillation quanta of this third particle.

If we disentangle the coordinates of the second and third particle in $e^{-\int_0^\lambda H''_{\lambda_1} d\lambda_1}$, using a method similar to that used above, and if we then calculate the trace of this operator in terms of a complete set of orthogonal functions of $\mathbf{r}_2$ and x_3, we obtain an operator $\tilde{L}$, which now depends only on r:

$$\widetilde{L}(\mathbf{r})\,2\,\mathrm{sh}\,\frac{\lambda}{2}\hbar\omega_{\vec{\varkappa}} \equiv L''(\mathbf{r}) = \exp\left\{-\int_0^{\lambda} H_{\mathbf{r}\lambda_1}\,d\lambda_1 - \frac{C}{2}\int_0^{\lambda}\mathbf{r}_{\lambda_1}^2\,d\lambda_1 + \right.$$

$$+\frac{C}{2}\hbar\omega_2\int_0^{\lambda}\int_0^{\lambda_1}(\mathbf{r}_{\lambda_1},\ \mathbf{r}_{\lambda_2})\,e^{\hbar\omega_2(\lambda_2-\lambda_1)}d\lambda_1 d\lambda_2 + \bar{n}_2\frac{C}{2}\hbar\omega_2\int_0^{\lambda}\int_0^{\lambda}(\mathbf{r}_{\lambda_1},\ \mathbf{r}_{\lambda_2})\,e^{\hbar\omega_2(\lambda_2-\lambda_1)}d\lambda_1 d\lambda_2 +$$

$$\left. + U_{\vec{\varkappa}} - 3\ln\left(2\,\mathrm{sh}\,\frac{\lambda}{2}\hbar\omega_2\right)\right\} = L'(\mathbf{r})\,e^{U_{\vec{\varkappa}}}. \tag{34}$$

Let us denote the trace of $L''(\mathbf{r})$ calculated in terms of the set of orthogonal functions of $\mathbf{r}$ by Z'', so that

$$Z'' = \mathrm{sp}\,L''(\mathbf{r}) = \left(2\,\mathrm{sh}\,\hbar\omega_{\vec{\varkappa}}\right)\mathrm{sp}\,e^{-\lambda H''}. \tag{35}$$

If we now go to the limit $|V_{\vec{\varkappa}}|^2 \to 0$, i.e., $U_{\vec{\varkappa}} \to 0$ in Eq.(34), then $L''(\mathbf{r})$ becomes $L'(\mathbf{r})$, and Z'' becomes Z'.

According to Eqs.(32) and (19), the quantity

$$\overline{U}_{\vec{\varkappa}} = \frac{|V_{\vec{\varkappa}}|^2}{Z'}\left(\frac{dZ''}{d\,|V_{\vec{\varkappa}}|^2}\right)_{|V_{\vec{\varkappa}}|^2=0}, \tag{36}$$

is the desired mean value of $U_{\vec{\varkappa}}$.

The above ordering of $e^{-\lambda H''_{\vec{\varkappa}}}$ and the subsequent disentanglement of the variables $\mathbf{r}_2$ and x_3 were necessary in order to obtain Eq.(36). It is simpler, however, to calculate Z'' itself by using the original expression (33) for H''. Then because the interaction term with the oscillations (proportional to $V_{\vec{\varkappa}}$) is infinitesimally small, we can use the method of small perturbations developed by Schwinger (cf. Eq.(6) of Part I). We thus obtain

$$Z'' = Z' + \lambda^2\,\mathrm{sh}\,\frac{\lambda}{2}\hbar\omega_{\vec{\varkappa}}\int_0^1 du\,\mathrm{sp}\left[e^{-(1-u)\lambda H_0}H_1 e^{-u\lambda H_0}H_1\right], \tag{37}$$

where

$$H_1 = V_{\vec{\varkappa}}a_3 e^{i\vec{\varkappa}\mathbf{r}} + V^*_{\vec{\varkappa}}\,a_3^+ e^{-i\vec{\varkappa}\mathbf{r}}, \quad H_0 = H'' - H_1. \tag{38}$$

In Eq.(37) we have dropped terms of higher order in $|V_{\vec{\varkappa}}|^2$, since when (37) is inserted into (36) these terms vanish identically in the limit $|V_{\vec{\varkappa}}|^2 \to 0$.

The trace in Eq.(37) is calculated in terms of the eigenfunctions of H_0, which can be written

$$\frac{1}{\sqrt{V}}e^{i\mathbf{k}\mathbf{R}}\prod_{j=1}^{3}\Phi_{m_j}\left(r'_j\sqrt{\frac{\omega'\mu'}{\hbar}}\right)\Phi_{n_3}\left(x_3\sqrt{\frac{\omega_{\vec{\varkappa}}\mu}{\hbar}}\right). \tag{39}$$

Here

$$\left.\begin{aligned} R &= \frac{1}{M'}(\mu\mathbf{r}+\mu_2\mathbf{r}_2);\ \ \omega' = \sqrt{\frac{C}{\mu'}};\\ r'_1 &= x - x_2;\quad r'_2 = y - y_2;\\ r'_3 &= z_1 - z_2. \end{aligned}\right\} \tag{40}$$

The last factor in (39) is an eigenfunction of $-\frac{\hbar^2}{2\mu}\cdot\frac{\partial^2}{\partial x_3^2} + \frac{\mu\omega_{\vec{\varkappa}}^2}{2}x_3^2$, and the rest of the factors make up an eigenfunction of the operator H'; the functions Φ_{m_j} and Φ_{n_3} are simple harmonic oscillator wave functions.

Since

$$H_1 e^{ikR}\Phi_{n_3} = V_{\vec{x}} e^{i\left[(k+\vec{x})R+\frac{\mu_2}{M'}(\vec{x},\,r')\right]}\sqrt{n_3}\,\Phi_{n_3-1} + V_{\vec{x}}^{*}\sqrt{n_3+1}\,e^{i\left[(k-\vec{x})R-\frac{\mu_2}{M'}(\vec{x},\,r')\right]}\Phi_{n_3+1}, \quad (41)$$

after summing in (37) over n_3 and k, (analogously to the calculations in Part I), we obtain

$$Z'' = Z'\left\{1+\frac{1}{2}\lambda^2\left(2\,\mathrm{sh}\,\frac{\lambda}{2}\hbar\omega'\right)^3 |V_{\vec{x}}|^2\int_0^1 du\,[\bar{n}_{\vec{x}}\,e^{u\lambda\hbar\omega_{\vec{x}}} + \right.$$

$$\left. + (\bar{n}_{\vec{x}}+1)\,e^{-u\lambda\hbar\omega_{\vec{x}}}]\times e^{-\lambda\frac{\hbar^2\varkappa^2}{2M'}u(1-u)}\prod_{j=1}^{3}\sum_{m_j=0}^{\infty} e^{-(1-u)\lambda\hbar\omega'\left(m_j+\frac{1}{2}\right)}\times$$

$$\times\left\langle\Phi_{m_j}(\xi_j),\ e^{-i\sqrt{\frac{\mu_2\hbar}{\mu M'\omega'}}\varkappa_j\xi_j}\exp\left[-u\lambda\frac{\hbar\omega'}{2}\left(-\frac{\partial^2}{\partial\xi_j^2}+\xi_j^2\right)\right]e^{i\sqrt{\frac{\mu_2\hbar}{\mu M'\omega'}}\varkappa_j\xi_j}\Phi_{m_j}(\xi_j)\right\rangle,$$

$$\xi_j = r_j'\sqrt{\frac{\omega'\mu'}{\hbar}}. \quad (42)$$

In order to calculate the diagonal matrix elements $\langle\Phi_m\ldots\Phi_m\rangle$ in Eq. (42), let us expand the functions of ξ_j in terms of the orthogonal functions $\Phi_p(\xi_j)$. This gives

$$e^{i\sqrt{\frac{\mu_2\hbar}{\mu M'\omega'}}\varkappa\xi}\Phi_m(\xi) = \sum_{p=0}^{\infty} a_{mp}\,\Phi_p(\xi), \quad (43)$$

$$a_{mp} = \int_{-\infty}^{\infty}\Phi_p(\xi)\,\Phi_m(\xi)\,e^{i\sqrt{\frac{\mu_2\hbar}{\mu M'\omega'}}\varkappa\xi}\,d\xi. \quad (44)$$

We finally arrive at

$$\langle\Phi_m\ldots\Phi_m\rangle = \sum_{p=0}^{\infty}|a_{mp}|^2\exp\left[-u\lambda\hbar\omega'\left(p+\frac{1}{2}\right)\right]. \quad (45)$$

By using (44) and (45), the sum over m in Eq. (42) can be rewritten

$$\sum_{m=0}^{\infty} e^{-(1-u)\lambda\hbar\omega'\left(m+\frac{1}{2}\right)}\langle\Phi_m\ldots\Phi_m\rangle = \sum_{m,\,p=0}^{\infty}\exp\left\{-\lambda\hbar\omega'\left[(1-u)\left(m+\frac{1}{2}\right)+\right.\right.$$

$$\left.\left.+u\left(p+\frac{1}{2}\right)\right]\right\}\iint_{-\infty}^{\infty}\Phi_p(\xi)\,\Phi_m(\xi)\,\Phi_p(\xi')\,\Phi_m(\xi')\,e^{i\sqrt{\frac{\mu_2\hbar}{\mu M'\omega'}}\varkappa(\xi-\xi')}d\xi d\xi'. \quad (46)$$

The summation over m and p is easily performed by using the expression for Slater's sum

$$\sum_{m=0}^{\infty}\Phi_m(\xi)\,\Phi_m(\xi')\,e^{-\gamma\left(m+\frac{1}{2}\right)} = (2\pi\,\mathrm{sh}\,\gamma)^{-1/2}\exp\left[-\frac{1}{4}(\xi+\xi')^2\,\mathrm{th}\,\frac{\gamma}{2}-\frac{1}{4}(\xi-\xi')^2\,\mathrm{cth}\,\frac{\gamma}{2}\right]. \quad (47)$$

It is then simple to perform the integration over ξ and ξ'. Inserting the results into (42) and performing some elementary operations, we obtain

$$Z'' = Z'\left\{1+\frac{\lambda^2}{2}|V_{\vec{x}}|^2\int_0^1 du\,[\bar{n}_{\vec{x}}\,e^{u\lambda\hbar\omega_{\vec{x}}}+(\bar{n}_{\vec{x}}+1)\,e^{-u\lambda\hbar\omega_{\vec{x}}}]\,e^{-\lambda\frac{\hbar^2\varkappa^2}{2M'}u(1-u)}\times\right.$$

$$\times \exp\left[-\left(\frac{\mu_2}{M'}\right)^2 \frac{x^2}{\operatorname{cth}\frac{\lambda}{2}\hbar\omega' u + \operatorname{cth}\frac{\lambda}{2}\hbar\omega'(1-u)}\right]\Bigg\}. \tag{48}$$

From Eq.(36) it is now simple to obtain

$$\overline{U} = \sum_{\vec{x}} \overline{U}_{\vec{x}} = \frac{\lambda^2}{2} \sum_{\vec{x}} |V_{\vec{x}}|^2 \int_0^1 dv e^{-\lambda \frac{\hbar^2 x^2}{8M'}(1-v^2)} \frac{\operatorname{ch}\frac{\lambda}{2}\hbar\omega_{\vec{x}} v}{\operatorname{sh}\frac{\lambda}{2}\hbar\omega_{\vec{x}}} \times$$

$$\times \exp\left\{-\frac{1}{2}\frac{\mu_2 \hbar x^2}{M'\mu\omega'}\left(\operatorname{cth}\frac{\lambda}{2}\hbar\omega' - \frac{\operatorname{ch}\frac{\lambda}{2}\hbar\omega' v}{\operatorname{sh}\frac{\lambda}{2}\hbar\omega'}\right)\right\}. \tag{49}$$

Let us now return to the fundamental problem of the present article, that is to the calculation of the trace of $e^{-\lambda H}$. This trace, as has been shown in Part I, is equal to the trace of $L(r)$, defined by Eqs. (14)-(15a). We have further replaced $I = \operatorname{sp} L(r)$, in accord with Eq.(21), by the approximate minimizing expression

$$I_1 = Z' e^{\overline{U} - \overline{U}'}. \tag{50}$$

Thus, according to (14)-(15a), (29), (31) and (49),

$$Z = \operatorname{sp} e^{-\lambda H} \geqslant Z_1 = Z^{(0)} \frac{\nu^3 \left(\operatorname{sh}\frac{\lambda}{2}\hbar\omega_2\right)^3}{\left(\operatorname{sh}\frac{\lambda}{2}\hbar\omega_2\nu\right)^3} \times \exp\left\{\frac{3}{4}\lambda\hbar\omega_2 \frac{\nu^2-1}{\nu} \operatorname{cth}\frac{\lambda}{2}\hbar\omega_2\nu - \frac{3}{2}\cdot\frac{\nu^2-1}{\nu^2} + \overline{U}\right\}, \tag{51}$$

where

$$Z^{(0)} = 2VX\left(\frac{\mu}{2\pi\hbar^2\lambda}\right)^{3/2} \tag{52}$$

(we have here included the spin factor 2, which was previously omitted for simplicity),

$$\nu = \sqrt{1 + \frac{\mu_2}{\mu}}. \tag{53}$$

We have introduced the parameters ν and ω_2 in place of the previous parameters μ_2 and C; these parameters must be chosen so that the right side of Eq.(51), namely, Z_1, is maximal, i.e., so as to obtain the best approximation to the desired value of Z. The above method of approximation is applicable to any problem with a Hamiltonian such as given by Eq.(1). In order to proceed further with the calculations it is necessary to specify the system under consideration, i.e., to specify the coefficients $V_{\vec{x}}$ and frequencies $\omega_{\vec{x}}$ in the Hamiltonian.

3. Electron in an Ionic Crystal

As in Part I, let us assume that the conduction electron interacts only with longitudinal polarization vibrations. Let us restrict ourselves to the case in which there exists only one mode of such vibrations with the limiting frequency ω. Then in the approximation of a dielectric continuum, we have

$$\omega_{\vec{x}} = \omega; \quad V_{\vec{x}} = \frac{e}{|\vec{x}|}\sqrt{\frac{2\pi\hbar\omega c}{V}}; \quad c = \frac{1}{n^2} - \frac{1}{\varepsilon}. \tag{54}$$

Inserting these values into Eq.(49), carrying out summation (integration)

over $\vec{x}$ and introducing the notation

$$\alpha = \frac{ce^2}{2\hbar}\sqrt{\frac{2\mu}{\hbar\omega}}; \quad \beta = \frac{\lambda}{2}\hbar\omega = \frac{\hbar\omega}{2kT}; \quad \rho = \frac{\omega_2}{\omega}, \tag{55}$$

we arrive at

$$\ln Z_1 = \ln Z^{(0)} + 3\ln\nu - 3\ln\operatorname{sh}\beta\nu\rho + 3\ln\operatorname{sh}\beta\rho - \frac{3}{2} + \frac{3}{2\nu^2} +$$

$$+ \frac{3}{2}\cdot\frac{\nu^2-1}{\nu}\beta\rho\operatorname{cth}\beta\nu\rho + \sqrt{\frac{8}{\pi}}\frac{\beta^{3/2}}{\operatorname{sh}\beta}\alpha\nu\int_0^1 \frac{\operatorname{ch}\beta\, v dv}{\sqrt{1-v^2+\frac{2(\nu^2-1)}{\beta\nu\rho}\left[\operatorname{cth}\beta\nu\rho - \frac{\operatorname{ch} 3\,\nu\rho v}{\operatorname{sh}\beta\nu\rho}\right]}}. \tag{56}$$

We must now vary ν and ρ to obtain the maximum value of this expression. Eq.(56) can be simplified in the limiting cases of low and high temperatures.

Low temperatures

If $T \to 0$, then $\beta \to \infty$ and Eq.(56) becomes

$$\ln Z_1 = \ln Z^{(0)} + 3\ln\nu - \frac{3}{2}\frac{\beta\rho}{\nu}(\nu-1)^2 - \frac{3}{2} + \frac{3}{2\nu^2} +$$

$$+ \frac{2}{\sqrt{\pi}}\beta\alpha\nu\int_0^\infty e^{-v'}dv'\left[\frac{(\nu^2-1)}{\rho\nu}(1-e^{-\rho\nu v'}) + v'\left(1-\frac{v'}{2\beta}\right)\right]^{-1/2}, \tag{57}$$

where $v' = \beta(1-v)$. Expanding the above integral in powers of $1/\beta$, we obtain

$$\ln Z_1 = \ln Z^{(0)} + \beta\left(f_0 + \frac{f_1}{\beta} + \frac{f_2}{\beta^2} + \cdots\right), \tag{57a}$$

where

$$f_0 = -\frac{3}{2}\frac{\rho}{\nu}(\nu-1)^2 + \frac{2\alpha\nu}{\sqrt{\pi}}\int_0^\infty e^{-v'}\left[\frac{\nu^2-1}{\rho\nu}(1-e^{-\rho\nu v'}) + v'\right]^{-1/2}dv'; \tag{58}$$

$$f_1 = 3\ln\nu - \frac{3}{2} + \frac{3}{2\nu^2} + \frac{\alpha\nu}{2\sqrt{\pi}}\int_0^\infty v'^2 e^{-v'}\left[\frac{\nu^2-1}{\rho\nu}(1-e^{-\rho\nu v'}) + v'\right]^{-3/2}dv'; \tag{59}$$

$$f_2 = \frac{3\alpha\nu}{16\sqrt{\pi}}\int_0^\infty v'^4 e^{-v'}\left[\frac{\nu^2-1}{\rho\nu}(1-e^{-\rho\nu v'}) + v'\right]^{-5/2}dv'. \tag{60}$$

We can now calculate the ground state energy of the system as the limit of the mean thermodynamic energy,

$$\bar{E} = -\frac{d\ln Z_1}{d\lambda}, \tag{61}$$

as $T \to 0$, i.e., as $\lambda \to \infty$ and $\beta \to \infty$. We arrive at

$$E_0 = E_0^{(0)} + \frac{3}{4}\hbar\omega\frac{(\nu_0-1)^2}{\nu_0}\rho_0 - \hbar\omega\frac{\nu_0\alpha}{\sqrt{\pi}}\int_0^\infty e^{-v'}\left[\frac{\nu_0^2-1}{\rho_0\nu_0}(1-e^{-\rho_0\nu_0 v'}) + v'\right]^{-1/2}dv'. \tag{62}$$

Here the parameters ν_0 and ρ_0 are essentially the values of ν and ρ corresponding to the maximum of Z_1 as $T \to 0$, i.e., to the minimum ground state energy of Eq.(62). This expression is in exact agreement with the ground state energy obtained by Feynman (Eqs.(33) and (31) in Ref.2).

As in Part I, let us assume that the energy distribution of the system can be characterized by

$$E(P, l) = \mathcal{E}_0(l) + P^2\mathcal{E}_2(l) + P^4\mathcal{E}_4(l) + \cdots, \tag{63}$$

where the total momentum P of the system is the only continuous quantum number, while all other quantum numbers l are discrete. Then for the extreme low temperatures, the sum-over-states of the system, whose energy spectrum is given by Eq.(63), can be calculated by considering only the first term in the summation over l, this term corresponding to the lowest energy for a given (sufficiently low) momentum; this is true because the following terms decrease exponentially compared to the first term.

Hereinafter we shall use $\mathcal{E}_0, \mathcal{E}_2, \mathcal{E}_4, \ldots$ to denote the coefficients in the expansion (63) for this value of l. Introducing the effective polaron mass $M = (2\mathcal{E}_2)^{-1}$ and expanding the sum-over-states of the system whose spectrum is given by Eq.(63) in powers of the temperature, we obtain

$$\ln Z = \ln Z^{(0)} - \lambda(\mathcal{E}_0 - E_0^{(0)}) + \frac{3}{2}\ln\frac{M}{\mu} - 15M^2\mathcal{E}_4\frac{1}{\lambda} + \cdots \qquad (64)$$

If we now also expand expression (57) in powers of the temperature and identify this expansion with Eq.(64), then by equating the coefficients of equal powers of $1/\lambda$ we can determine $\mathcal{E}_0, \mathcal{E}_2, \mathcal{E}_4, \ldots$.

In order to expand (57) in powers of $1/\beta$, we must bear in mind that the extremum values of ν and ρ depend on the temperature. These parameters can be expanded in powers of $1/\beta$ if the extremum equations

$$\frac{\partial \ln Z_1}{\partial \nu} = 0 \quad \text{and} \quad \frac{\partial \ln Z_1}{\partial \rho} = 0,$$

are solved by successive approximation, considering the quantity $\frac{1}{\beta}f_1 + \frac{1}{\beta^2}f_2 + \cdots$ small and taking ν_0 and ρ_0 as the zeroth approximation. The resulting expansion of expression (57) in powers of $1/\beta$ is of the form

$$\ln Z_1 = \ln Z^{(0)} + \beta f_0 + f_1 + \frac{f_2}{\beta} + \\ + \frac{1}{2\beta}\left[\frac{\partial^2 f_0}{\partial\rho^2}\cdot\frac{\partial^2 f_0}{\partial\nu^2} - \left(\frac{\partial^2 f_0}{\partial\rho\,\partial\nu}\right)^2\right]^{-1}\left[2\frac{\partial^2 f}{\partial\rho\,\partial\nu}\cdot\frac{\partial f_1}{\partial\rho}\cdot\frac{\partial f_1}{\partial\nu} - \frac{\partial^2 f_0}{\partial\rho^2}\left(\frac{\partial f_1}{\partial\nu}\right)^2 - \frac{\partial^2 f_0}{\partial\nu^2}\left(\frac{\partial f_1}{\partial\rho}\right)^2\right]. \qquad (65)$$

In this expression the functions f_i and their derivatives are evaluated at the point ν_0, ρ_0 and are therefore temperature independent.

Equating (65) and (64), we obtain

$$\mathcal{E}_0 = E_0;$$

$$\frac{M}{\mu} = \exp\frac{2}{3}f_1(\nu_0\rho_0) = \nu_0^2\exp\left\{\frac{1}{\nu_0^2} - 1 + \frac{\alpha\nu}{3\sqrt{\pi}}\int_0^\infty v'^2 e^{-v'}\left[\frac{\nu_0^2-1}{\rho_0\nu_0}(1-e^{-\rho_0\nu_0 v'}) + v'\right]^{-3/2}dv'\right\}; \qquad (66)$$

$$\mathcal{E}_4 = -\frac{2}{15M^2\hbar\omega}\left\{f_2 + \frac{1}{2}\left[\frac{\partial^2 f_0}{\partial\rho^2}\frac{\partial^2 f_0}{\partial\nu^2} - \left(\frac{\partial^2 f_0}{\partial\rho\,\partial\nu}\right)^2\right]^{-1}\times\left[2\frac{\partial^2 f_0}{\partial\rho\,\partial\nu}\cdot\frac{\partial f_1}{\partial\rho}\cdot\frac{\partial f_1}{\partial\nu} - \frac{\partial^2 f_0}{\partial\rho^2}\left(\frac{\partial f_1}{\partial\nu}\right)^2 - \frac{\partial^2 f_0}{\partial\nu^2}\left(\frac{\partial f_1}{\partial\rho}\right)^2\right]\right\}. \qquad (67)$$

For comparison we present the polaron effective mass as obtained by Feynman (Eq.(45) of Ref.2), namely,

$$\frac{M_F}{\mu} = 1 + \frac{\alpha\nu_0^3}{3\sqrt{\pi}}\int_0^\infty v'^2 e^{-v'}\left[\frac{\nu_0^2-1}{\rho_0\nu_0}(1-e^{-\rho_0\nu_0 v'}) + v'\right]^{-3/2}dv'. \qquad (68)$$

The relation between our value of the effective mass M, and Feynman's value M_F is

$$\frac{M}{\mu\nu_0^2} = \exp\left(\frac{M_F}{\mu\nu_0^2} - 1\right). \qquad (69)$$

We note that $M \geqslant M_F$.

Since Eq.(64) is derived on the basis of (63) and does not involve the approximations used in the present article, it can be used to calculate the sum-over-states Z_F in Feynman's case for extreme low temperatures when the term with $\mathcal{E}_4$ may be dropped. Since the ground state energy E_0 is the same according to Feynman's method and ours, Eq.(64) gives

$$\frac{Z_1}{Z_F} = \left(\frac{M}{M_F}\right)^{3/2}, \text{ i.e., } Z_1 \geqslant Z_F. \tag{70}$$

Since Z_1 is obtained by the direct variational method, it is an underestimate (cf. Eq.(21)) and, therefore Z_F is even more under-valued. Thus, although the ground state energy obtained by both methods is the same, our method gives a somewhat more accurate value for the polaron effective mass. The difference between M and M_F, however, is very small and vanishes entirely in the limiting cases of weak and strong coupling, as shall be shown below.

Case of weak coupling and arbitrary temperatures

The last term involving the integral in Eq.(56) becomes small when α becomes small. In this case Z_1 is maximum when ν is close to unity. Let us set

$$\nu = 1 + \varepsilon, \quad \varepsilon \ll 1.$$

It is easy to see that ε is of order α. Therefore on expanding Z_1 in powers of ε, we shall restrict ourselves to terms proportional to ε^2 and $\alpha\varepsilon$. We then obtain

$$\ln Z_1 = \ln Z^{(0)} + \sqrt{2\pi}\,\frac{\beta^{3/2} I_0(\beta)}{\operatorname{sh}\beta}\alpha + \sqrt{2\pi}\,\frac{\beta^{3/2}}{\operatorname{sh}\beta}\Big\{I_0(\beta) - \frac{1}{\gamma \operatorname{sh}\beta}\left[(\gamma+\beta)\, I_1(\beta+\gamma) + (\beta-\gamma) I_1(\beta-\gamma) - 2\beta I_1(\beta)\operatorname{ch}\gamma\right]\Big\}\alpha\varepsilon + 3\left[1 - \frac{1}{2}\gamma \operatorname{cth}\gamma - \frac{1}{2}\frac{\gamma^2}{\operatorname{sh}^2\gamma}\right]\varepsilon^2. \tag{71}$$

Here $\gamma = \beta\rho$, and I_0 and I_1 are Bessel functions of an imaginary argument of order zero and one, respectively. The maximum of expression (71) as ε is varied is

$$\ln Z_1 = \ln Z^{(0)} + \sqrt{2\pi}\,\frac{\beta^{3/2} I_0(\beta)}{\operatorname{sh}\beta}\alpha + \frac{\pi}{3}\,\frac{\beta^3}{\operatorname{sh}^2\beta}\,\frac{\left[\gamma I_0(\beta)\operatorname{sh}\gamma - (\beta+\gamma) I_1(\beta+\gamma) - (\beta-\gamma) I_1(\beta-\gamma) + 2\beta I_1(\beta)\operatorname{ch}\gamma\right]^2}{\gamma^2\left[\frac{\gamma}{2}\operatorname{sh}2\gamma - \operatorname{ch}2\gamma + 1 + \gamma^2\right]}\alpha^2. \tag{72}$$

Here the term proportional to α is in exact agreement with the result of weak-coupling theory (cf. Part I). We have yet to find the maximum of expression (72) for variation of ρ, i.e., of γ. This can be done simply in the limiting cases of extreme low and high temperatures.

At low temperatures, when $kT \ll \hbar\omega$, using the asymptotic expression for I_0 and I_1, we obtain $\rho_0 = 3$. Then

$$\ln Z_1 = \ln Z^{(0)} + \lambda\hbar\omega\alpha\left[1 + \frac{1}{4\lambda\hbar\omega} + \frac{9}{32(\lambda\hbar\omega)^2}\right] + \frac{\lambda\hbar\omega\alpha^2}{81}\left[1 + \frac{4}{3\lambda\hbar\omega} + \frac{2{,}034}{(\lambda\hbar\omega)^2}\right], \tag{73}$$

$$E_0 = E_0^{(0)} - \hbar\omega\left(\alpha + \frac{\alpha^2}{81}\right), \tag{74}$$

$$\frac{M}{\mu} = 1 + \frac{\alpha}{6} + 0{,}0249\alpha^2, \tag{75}$$

$$\mathcal{E}_4 = -\frac{1}{\mu^2\hbar\omega}(0{,}01875\alpha - 0{,}004576\alpha^2). \tag{76}$$

The difference between M and M_F in the weak-coupling cases is insignificant:

$$\frac{M - M_F}{M} = 1{,}71 \cdot 10^{-4}\alpha^2.$$

In the high-temperature case, when $kT \gg \hbar\omega$, i.e., $\beta \ll 1$, expansion of (72) in powers of β makes it possible to find the maximum of this expression for variation of γ. Numerical solution of the transcendental equation gives $\gamma = 3.25$ and the maximum of $\ln Z_1$ for variation of γ is

$$\ln Z_1 = \ln Z^{(0)} + \sqrt{\pi}\,(\lambda\hbar\omega)^{1/2}\left[1 + \frac{1}{48}(\lambda\hbar\omega)^2\right]\alpha + \frac{\pi}{12}\lambda\hbar\omega\,[0{,}0804 - 0{,}00132\,(\lambda\hbar\omega)^2]\,\alpha^2. \quad (77)$$

The corresponding mean thermodynamic energy of the system, as defined by Eq.(61), is

$$\overline{E} = \overline{E}^{(0)} - \frac{\sqrt{\pi}\hbar\omega}{2(\lambda\hbar\omega)^{1/2}}\,[\alpha + 0{,}024\,(\lambda\hbar\omega)^{1/2}\alpha^2]. \quad (78)$$

Case of high temperatures and arbitrary coupling

For small values of β the integral term in Eq.(56) can again be treated as a small perturbation, since it is proportional to $\alpha\sqrt{\beta}$. As a result, the value of ν at the extremum, as in the previous case, is close to unity, so that Eqs.(77) and (78) are valid in this case. The region of applicability of these formulas depends on the smallness of $\alpha\sqrt{\beta}$. Therefore, the higher the temperature, the stronger the coupling permissible. This is fully consistent with the results obtained in Part I.

Case of strong coupling and arbitrary temperatures

Let us assume that

$$\beta\nu\rho \gg 1; \quad \nu \gg 1. \quad (79)$$

Then in expression (56) we may set

$$\ln \operatorname{sh} \beta\nu\rho = \beta\nu\rho - \ln 2,$$

$$\operatorname{cth} \beta\nu\rho = 1, \quad \frac{\operatorname{ch} \beta\nu\rho v}{\operatorname{sh} \beta\nu\rho} = e^{-\beta\nu\rho(1-v)},$$

and the integral term may be expanded in powers of the first expression under the radical sign (i.e., $1 - v^2$).

As a result, we obtain

$$\ln Z_1 = \ln Z^{(0)} + 3\ln\nu - \frac{3}{2}\beta\rho\left(\nu + \frac{1}{\nu}\right) + 3\ln 2 + 3\ln\operatorname{sh}\beta\rho - \frac{3}{2} + \\ + \frac{3}{2\nu^2} + \frac{2}{\sqrt{\pi}}\beta\,(\rho\nu)^{1/2}\left[1 + \frac{2\ln 2\operatorname{cth}\beta}{\rho\nu} - \frac{\rho}{2\beta\nu}(\beta\operatorname{cth}\beta - 1)\right]\alpha. \quad (80)$$

We now find the extremum of $\ln Z_1$ with respect to the parameters ρ and ν; we obtain a set of two equations which can be solved approximately by expanding in inverse powers of ν, which is reasonable because of (79). It is then found that $\ln Z_1$ is maximum for

$$\rho = 1 + \cdots, \quad \nu = \frac{4}{9\pi}\alpha^2 + \cdots \quad (81)$$

Inserting these values into (80), we obtain the maximum value

$$\ln Z_1 = \ln Z^{(0)} + 3 \ln \frac{4\alpha^2}{9\pi} + \frac{2\alpha^2}{3\pi}\beta + 6\beta\left(\ln 2 + \frac{1}{4}\right) + \varphi(\beta), \tag{82}$$

where

$$\varphi(\beta) = 3\ln(2\,\mathrm{sh}\,\beta) - \frac{3}{2}\beta(\mathrm{cth}\,\beta + 1) + 6\ln 2(\mathrm{cth}\,\beta - 1)\beta. \tag{83}$$

As T → 0, when $\beta \to \infty$ we have $\varphi(\beta) \to 0$ and $\frac{\partial\varphi}{\partial\beta} \to 0$. The mean thermodynamic energy of the system can be found from Eq.(61):

$$\overline{E} = \overline{E}^{(0)} - \frac{\alpha^2}{3\pi}\hbar\omega - 3\hbar\omega\left(\ln 2 + \frac{1}{4}\right)\mathrm{cth}\,\beta + 3\hbar\omega\left(\ln 2 - \frac{1}{4}\right)\frac{\beta}{\mathrm{sh}^2\beta}. \tag{84}$$

The ground state energy is obtained if we go to the limit $\beta \to \infty$ in Eq. (84):

$$E_0 = E_0^{(0)} - \frac{\alpha^2\hbar\omega}{3\pi} - 3\hbar\omega\left(\ln 2 + \frac{1}{4}\right). \tag{85}$$

We shall use Eq.(66) to calculate the polaron effective mass M, replacing ρ_0 and ν_0 by ρ and ν from (81). Then, invoking the inequality $\nu \gg 1$, we readily obtain

$$\frac{M}{\mu} = \nu^2 = \frac{16}{81\pi^2}\alpha^4 = 2{,}00 \cdot 10^{-2}\alpha^4. \tag{86}$$

The ground state energy given by Eq.(85) and the polaron effective mass given by Eq.(86) are in exact agreement with the results of Feynman[2]. The same value of M was obtained in previously published papers on strong-coupling polaron theory[4,5] if the electron wave function is approximated by $\psi = Ae^{-ar^2}$.

If the more accurate approximation

$$\psi = A(1 + ar + br^2)e^{-ar}$$

is used in Refs. 4 & 5, we obtain

$$\frac{M}{\mu} = 20{,}8 \cdot 10^{-3}\alpha^4. \tag{87}$$

This more accurate value for the effective mass, deduced in the adiabatic approximation, is some 4% greater than that of (86).

In the limit $\alpha \to \infty$, the ground state energy given by (85), as has already been pointed out by Feynman, agrees exactly with the previous results of one of the present authors[5,6], obtained using the approximation

$$\psi = Ae^{-ar^2}.$$

If the more accurate approximation $\psi = A(1+ar+br^2)e^{-ar}$ is used in Refs.5 & 6, the energy $E_0 - E_0^{(0)}$ obtained is 3% lower than that of (85).

For large α the coefficient $\mathcal{O}_4$ defined by Eq.(67) is proportional to α^{-10}. In general as α increases, the quadratic approximation of the momentum-dependence of the system's energy becomes valid for larger values of the momentum.

For higher temperatures, when $kT \gg \hbar\omega$, i.e., when $\beta \ll 1$, while inequalities (79) are still fulfilled, Eqs.(82)-(83) lead to

$$Z_1 = Z^{(0)}\left(\frac{M}{\mu}\right)^{3/2} e^{\frac{2\alpha^2}{3\pi}\beta}\left(\frac{8\beta}{\sqrt{e}}\right)^3, \tag{88}$$

where M is given by (86), and e is the natural logarithm base.

When $\beta \ll 1$, Eq.(84) leads to

$$\overline{E} = \overline{E}^{(0)} - \frac{\alpha^2}{3\pi}\hbar\omega - 3kT. \tag{89}$$

The frequency ω does not appear in Eqs.(88)-(89), which might have been expected in view of Eq.(55) for α.

The strong-coupling criteria are given by (79). These inequalities, in turn, reduce to

$$|E_0 - E_0^{(0)}| \gg kT, \quad \text{i.e.,} \quad \frac{\alpha^2}{3\pi} \gg \frac{kT}{\hbar\omega}; \tag{90}$$

$$|E_0 - E_0^{(0)}| \gg \hbar\omega, \quad \text{i.e.,} \quad \frac{\alpha^2}{3\pi} \gg 1. \tag{91}$$

Both of these coincide with Eqs. (16) and (42) of Ref.5.

If the temperature is so high that inequality (90) is replaced by its opposite, we have the previously considered limiting case of extreme high temperatures, when Eqs.(77) and (78) are valid.

Conclusions

We have calculated the sum-over-states of a system (consisting of a particle interacting with a field) whose Hamiltonian is given by Eq.(1), as the trace of the operator $e^{-\lambda H}$ (where $\lambda = 1/kT$). The coupling strength (coefficients $V_{\vec{k}}$) is arbitrary. In calculating the trace, we first eliminate the vibrational degrees of freedom of the field from the operator $e^{-\lambda H}$ by using Feynman's[3] ordering parameters. As a result we obtain an operator depending only on the particle coordinate r (see Section I); its trace is calculated approximately by using a special variational method in which the energy operator rather than the wave function is varied (see Section 2). We thus obtain an underestimated value for the sum-over-states, which is equal to the maximum value obtained for the right side of Eq.(51) by varying the parameters v and ω_2.

We then consider a particular problem: a conduction electron in an ionic crystal, when $V_{\vec{k}}$ is given by Eq.(54). In this case the logarithm of the sum-over-states is found by maximizing expression (56) by varying the parameters v and ρ (also see Eq.(55)). Whereas in all previous works on polaron theory only the limiting case of extreme low temperatures was considered, in the present article we determine the sum-over-states and, consequently, all the other thermodynamic functions of the system at any arbitrary temperature.

The mean thermodynamic energy of the system can be calculated from (61). As $T \to 0$, it goes to the ground state energy of the system given by (62). In contrast to previous methods, the present approach allows of calculating the dependence of the energy on the total system momentum for any coupling, without restricting the treatment to the quadratic approximation (in the case of low temperatures) (see Eqs.(63)-(67)).

The results are simplified for various limiting values of the coupling constant α and the temperature. The regions of α and $kT/\hbar\omega$ in which the various limiting formulas are applicable are shown in the accompanying figure.

In the region of low temperatures ($\beta \gg 1$) and arbitrary coupling, i.e., the region denoted by I in the diagram, the results are described by Eqs.(57)-(67). The ground state energy as given by (62) is in exact agreement with that deduced by Feynman[2]. The relation between our value M for the polaron effective mass and Feynman's value M_F is given by Eq.(69). Our value of M is somewhat higher and, therefore, presumably somewhat more accurate than M_F. The actual difference between M and M_F is insignificant and in the limiting cases of weak and strong coupling it vanishes.

In the case of weak coupling or for arbitrary coupling and extreme high temperatures, when $\alpha < 3$ or $\alpha\sqrt{\hbar\omega/kT} < 5$, that is, in region II in the diagram

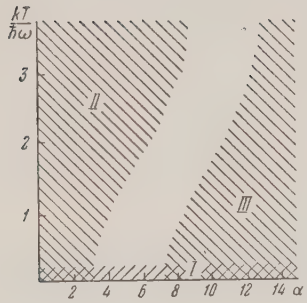

the result is given by Eq.(72). Eqs.(73)-(78) give consequences of (72) for various special cases. If in these formulas we retain only the terms linear with respect to α they agree with the results of weak coupling theory given in Part 1. In Eqs.(77)-(78) the expansion is carried out in powers of $\alpha\sqrt{\hbar\omega/kT}$. Therefore, the higher the temperature, the more rapidly the series converge, and the larger the coupling constant α permissible. This is consistent with the deductions of Part I.

For strong coupling, i.e., in the region III in the figure, when the binding energy of the polaron is greater than kT and $\hbar\omega$ (criteria (90) and (91)), the results are given by Eqs.(82)-(84). For low temperatures, when $kT \ll \hbar\omega$, these equations lead to the ground state energy of Eq.(65) and the polaron effective mass of Eq.(86). These are in agreement with the respective values obtained by Feynman[2] and differ by only 3-4% from the more accurate values obtained by one of the authors in the adiabatic approximation[4,5,6]. At higher temperatures, when $kT \gg \hbar\omega$, but inequality (90) is still fulfilled, the results are given by Eqs.(88)-(89). The mean energy (89) can also be obtained by the method of Ref.5, if the electron wave function is approximated by

As for the sum-over-states given by (88), it cannot be calculated using the method of Ref.5, for (although the error in Ref.5 as regards the energy is relatively low) at high energies it is of the order of kT which may lead to a large error in the sum-over-states.

Thus the variational method developed gives results which agree with the exact results of perturbation theory (Part I) in the limiting case of weak coupling or of arbitrary coupling and high temperature. For strong coupling and low temperatures the results are within 3-4% of those given by the adiabatic approximation, which is accurate in this region. For extreme low temperatures and arbitrary coupling, Feynman's results[2] are obtained: the energy values agree exactly while the effective masses differ insignificantly. We may, therefore, assume that the solution obtained is a good interpolation in the general case as well.

Institute of Physics and
Institute of Metal Physics of the
Ukrainian SSR Academy of Sciences

References

1. M.A.Krivoglaz & S.I.Pekar, Present issue of the Bulletin, p.1.
2. R.P.Feynman, Phys.Rev., 97, 660 (1955).
3. R.P.Feynman, Phys.Rev., 84, 108 (1951).
4. L.D.Landau & S.I.Pekar, Zhur.eksp.i teor.fiz., 18, 419 (1948).
5. S.I.Pekar, Issledovaniia po elektronnoi teorii kristallov (Studies in the electron theory of crystals), M. 1951.
6. S.I.Pekar, Zhur.eksp.i teor.fiz., 16, 335 (1946).

INFLUENCE OF THE POLARON EFFECT ON THE THERMODYNAMICS OF CONDUCTION ELECTRONS IN SEMICONDUCTORS (Part III)

- M.A.Krivoglaz and S.I.Pekar

In the two preceding articles[1,2] (hereinafter referred to as Parts I and II, respectively), we calculated the sum-over-states Z of a crystal with a single conduction electron. The result in all cases can be written in the form

$$Z = Z^{(0)}\chi,$$

where $Z^{(0)}$ is the sum-over-states of the system in the absence of interaction between the electron and lattice vibrations and χ is a correction factor due to the interaction.

The results of Parts I and II lead to a determination of χ for any arbitrary temperatures and coupling strengths. In particular, for instance, for an ionic crystal with weak coupling Eqs.(10, (17) and (19) of Part I give

$$\chi = 1 + \frac{\sqrt{\pi}}{2}\left(\frac{\hbar\omega}{kT}\right)^{3/2} \frac{I_0\left(\frac{\hbar\omega}{2kT}\right)}{\operatorname{sh}\frac{\hbar\omega}{2kT}}\,\alpha. \qquad (1)$$

The condition of weak coupling is equivalent to saying that χ cannot differ greatly from 1 in this case. The notation is the same as in Parts I and II.

In the case of strong coupling with $kT \ll \hbar\omega$, Eqs.(64) and (85) of Part II lead to

$$\chi = \left(\frac{M}{\mu}\right)^{3/2} \exp\left\{\left[\frac{\alpha^2}{3\pi} + 3\left(\ln 2 + \frac{1}{4}\right)\right]\frac{\hbar\omega}{kT}\right\}. \qquad (2)$$

In this case χ may be much greater than 1. For instance, when $\alpha = 7$, according to Eq.(86) of Part II,

$$\frac{M}{\mu} = 48 \quad \text{and} \quad \chi = 333\exp\frac{8{,}02\,\hbar\omega}{kT}.$$

If the temperature is such that $\hbar\omega/kT = 3$, we obtain $\chi = 10^{13}$.

In the case of strong coupling, with $kT \gg \hbar\omega$, Eq.(88) of Part II leads to

$$\chi = \left(\frac{M}{\mu}\right)^{3/2}\left(\frac{4}{\sqrt{e}}\cdot\frac{\hbar\omega}{kT}\right)^3 e^{\frac{\alpha^2}{3\pi}\cdot\frac{\hbar\omega}{kT}}. \qquad (3)$$

Here e is the base for natural logarithms. In this case χ may also be much greater than 1.

If the concentration of conduction electrons is not too great, so that we may neglect interaction between them, the preceding results are easily generalized to the case of N conduction electrons in the crystal:

$$Z_N = Z_N^{(0)}\chi^N; \quad Z_N^{(0)} = \frac{X}{N!}\left[2V\left(\frac{\mu kT}{2\pi\hbar^2}\right)^{3/2}\right]^N. \qquad (4)$$

Here $Z_N^{(0)}$ is the sum-over-states for a system in which there is assumed to be no interaction between the conduction electrons and the lattice vibrations, Z_N is the sum-over-states for the system, taking this interaction into account and X is the sum-over-states of the crystal alone, in the absence of conduction electrons.

Equilibrium Concentration of Conduction Electrons

As an example, let us consider the simplest case of a semiconductor containing only one kind of monovalent impurity centers (electron donors). Let the number of such centers be N_0. We also assume that at absolute zero temperature there is one electron at each center and that there are no electrons in the conduction band. The sum-over-states for such a system, calculated for a given N, is

$$\zeta(N) = \frac{N_0!\, 2^{N_0-N}}{(N_0-N)!\, N!}\, e^{(N_0-N)\frac{W}{kT}}\, Z_N. \tag{5}$$

Here W is the electron thermal dissociation energy associated with transition from a donor to the bottom of the conduction band. The factor 2^{N_0-N} is related to the electron spin.

For thermal equilibrium ζ, as a function of N, must have a maximum. This extremum (maximum) condition gives us the equilibrium concentration of conduction electrons, namely,

$$\frac{N}{\sqrt{N_0-N}} = \left(\frac{\mu kT}{2\pi\hbar^2}\right)^{3/4} \sqrt{V}\,\sqrt{\chi}\, e^{-\frac{W}{2kT}}. \tag{6}$$

We thus see that in the case of interaction between the conduction electrons and lattice vibrations, we obtain a factor $\sqrt{\chi}$ which does not appear in the noninteraction case.

Thermionic Emission

We shall not deal with a Maxwell velocity distribution for the conduction electrons, which is valid only if there is no interaction of the electrons with the lattice vibrations, but shall calculate the thermionic emission current by considering thermodynamic equilibrium between the conduction electron gas and an ideal free electron gas in the vacuum at the surface of a semiconductor. The equilibrium conditions can be written

$$\frac{\partial F}{\partial N} = \frac{\partial F_1}{\partial N_1}, \tag{7}$$

where F and F_1 are the free energies of the conduction electron gas (interacting with the lattice) and the free electron gas in vacuum, respectively. There are N and N_1 electrons in these gases. For the free electron gas

$$F_1 = N_1 u - kT\left\{N_1 \ln\left[2V_1\left(\frac{mkT}{2\pi\hbar^2}\right)^{3/2}\right] - N_1(\ln N_1 - 1)\right\}, \tag{8}$$

where m is the mass of a free electron, u is the work function for raising an electron from the bottom of the Bloch conduction band to the vacuum and V_1 is the volume of the electron gas in vacuum. For the conduction electron gas, $F = -kT \ln Z_N$, where Z_N is given by Eq.(4). Then Eq.(7) becomes

$$\frac{N_1/V_1}{N/V} = \left(\frac{m}{\mu}\right)^{3/2} e^{-\frac{u}{kT}} \frac{1}{\chi}. \tag{9}$$

Thus for a given conduction electron concentration, the electron concentration in vacuum is found to be χ times less than when the interaction between the conduction electrons and the lattice vibrations is disregarded. The emission current from a semiconductor, as is well known, can be evaluated as the electron current from the vacuum into the semiconductor. The latter is

$$I = eD\frac{N_1}{V_1}\sqrt{\frac{kT}{2\pi m}} = eD\left(\frac{m}{\mu}\right)^{3/2}\frac{N}{V}\sqrt{\frac{kT}{2\pi m}}\,e^{-\frac{u}{kT}}\frac{1}{\chi}, \tag{10}$$

where D is the mean coefficient of transfer of thermal electrons from the vacuum into the semiconductor. Thus for a given conduction electron concentration N/V, the emission current will be smaller by a factor of χ than when the interaction is neglected. Eq.(10) can be verified experimentally by simultaneous measurement of the emission current and the Hall effect.

In order to express the emission current in terms of the donor concentration, rather than in terms of N/V, we need an explicit expression for N/V as a function of the donor concentration and the temperature. In the special case in which Eq.(6) is valid and when $N \ll N_0$, we obtain

$$I = D\sqrt{\frac{N_0}{V}}\frac{em}{\mu^{3/4}\hbar^{3/2}}\left(\frac{kT}{2\pi}\right)^{3/4}e^{-\frac{u+\frac{W}{2}}{kT}}\frac{1}{\sqrt{\chi}}. \tag{11}$$

Thus for a given donor concentration N_0/V, the emission current proves to be $\sqrt{\chi}$ times less than when the interactions is neglected.

In the case of strong coupling and low temperatures, χ in Eq.(11) is given by Eq.(2), and the value of the emission current so obtained is almost exactly the same as that obtained by Morgulis and Tolpygo[3], who examined the influence of the polaron effect on thermionic emission in the adiabatic approximation of polaron theory[4]. In other limiting cases when χ is given by (1) or (3), as well as in the general case of arbitrary temperatures and coupling strengths, when χ is given by Eq.(56) of Part II, Eq.(11) yields new expressions for the emission current.

Let us now analyze the errors stemming from the earlier practice of experimenters of processing their data according to formulas not taking into account the polaron effect, i.e., formulas with 1 instead of χ. Inasmuch as the exponents in Eqs.(6) and (11) are usually measured experimentally, rather than calculated theoretically, in cases, such as those characterized by (2) and (3), when $\sqrt{\chi}$ also contains an exponential, we can simply reinterpret the measured value of the exponents, that is, consider that they also contain the exponential factor of $\sqrt{\chi}$. The matter is not so simple in the case of the factors multiplying the exponentials in (6) and (11), since these have often been calculated theoretically. This means that there was always an error, in that the factor multiplying the exponential in the expressions for $\sqrt{\chi}$ was neglected and, although it hardly differs from unity in homeopolar crystals, in ionic crystals it is of the order of ten to a hundred. In Eqs. (2) and (3), for instance, these factors are

$$\left(\frac{M}{\mu}\right)^{3/4} \text{ and } \left(\frac{M}{\mu}\right)^{3/4}\left(\frac{4}{\sqrt{e}}\frac{\hbar\omega}{kT}\right)^{3/2}. \tag{12}$$

It is therefore desirable to re-evaluate the results of earlier studies.

Specific Heat of Conduction Electrons

Let us consider, as above, the simplest case of a semiconductor containing N_0 monovalent donors of only one kind. Let us choose the zero energy as the energy of the system when all N_0 electrons from the donors are at the bottom of the Bloch conduction band, and the lattice is undergoing only zero-point vibrations. Then the mean thermodynamic energy of the system is

$$\overline{E} = \overline{E}_{\text{lat}} + N\left[\frac{3}{2}kT + kT^2\frac{d}{dT}\ln\chi\right] - (N_0 - N)W. \tag{13}$$

Here the first term is the mean energy of the lattice vibrations, the second is the energy of the N conduction electrons taking into account their interactions with the lattice vibrations and the third is the energy of the N_o - N electrons located on impurity levels.

The specific heat of the semiconductor is defined as the temperature derivative of the mean energy given by Eq.(13), namely,

$$c = c_{\text{lat}} + N\left[\frac{3}{2}k + k\frac{d}{dT}T^2\frac{d}{dT}\ln\chi\right] + \frac{dN}{dT}\left(\frac{3}{2}kT + kT^2\frac{d}{dT}\ln\chi + W\right). \qquad (14)$$

Here the first term is the specific heat of the crystal lattice, the second is the specific heat of the conduction electrons, and the third is associated with the thermal excitation of new conduction electrons. The derivative dN/dT can be calculated by Eq.(6) or obtained directly from experiment. The value of χ appropriate to the given case must be inserted into Eq.(14).

For strong coupling and high temperatures, for instance, when χ is given by Eq.(3), we have

$$c = c_{\text{lat}} - \frac{3}{2}kN + \frac{dN}{dT}\left(W - \frac{3}{2}kT - \frac{\alpha^2}{3\pi}\hbar\omega\right). \qquad (15)$$

Thus by taking account of the interaction between the conduction electrons and lattice vibrations, we have introduced a correction equal to $-3kT - \frac{\alpha^2}{3\pi}\hbar\omega$ into the mean electron energy and a correction equal to $-3k$ into the electron specific heat. Hence, as can be seen from Eq.(15), the specific heat of the conduction electrons, oddly enough proves to be $-3kN/2$, i.e., is of the opposite sign. This result is in agreement with that obtained in the adiabatic polaron theory[4], where the production of each conduction electron is associated with a decrease of 3 in the number of vibrational degrees of freedom of the lattice.

Institute of Physics and
Institute of Metal Physics of the
Ukrainian SSR Academy of Sciences

References

1. M.A.Krivoglaz & S.I.Pekar, Present issue of the Bulletin, p.1.
2. M.A.Krivoglaz & S.I.Pekar, Present issue of the Bulletin, p. 13.
3. N.D.Morgulis & K.B.Toplygo, Zhur.eksp.i teor.fiz., 25, 718 (1953).
4. S.I.Pekar, Issledovaniia po elektronnoi teorii kristallov (Studies in the electron theory of crystals), M. 1951.

INTERACTION OF EXCITONS WITH A MOLECULAR LATTICE

- E.I.Rashba

Introduction

In recent years the list of substances classed as semiconductors has expanded considerably due to the inclusion of many organic molecular crystals. There have been many experimental papers on their electric and photoelectric properties so that by now there is a whole literature on the subject.

The semiconductor effects in all these organic substances are extremely weak; the quantum yield of the internal photoeffect is usually about 10^{-4}, while the dark conductivity at room temperature is about 10^{-16}-10^{-18} mho/cm. Since, at present the self-absorption of light is undergoing the most thorough theoretical treatment specifically where molecular crystals are concerned, there is reason to hope that study of these crystals will lead to better understanding of electronic processes in other semiconductors as well. This is true primarily with regard to the role of excitons in electric, photoelectric and thermal phenomena.

The theory of excitons in molecular crystals, as developed by Davydov[1], has made possible satisfactory interpretation of the experimental data on the splitting of nondegenerate molecular terms in crystals into multiplets consisting of several strongly polarized narrow lines. Davydov suggests that when there is a strong resonance interaction between the molecules, the exciton-phonon interaction may be considered weak. Some experiments, however, indicate that at very low temperatures there is wide-band adsorption whose integral intensity would appear to be (there are no absolute measurements at low temperatures) much greater than the intensity of the narrow lines associated with free excitons. Therefore in spite of the successes of the free exciton theory, it may be useful to consider various aspects of the theory with strong exciton-phonon coupling. Such analysis is facilitated by application of the methods developed by Pekar[2] in his polaron theory.

1. Classification of Excited Crystal States

Since the intermolecular interaction energies in molecular crystals are much lower than the intramolecular binding energies, the wave functions of the crystal in the ground state and the first few excited states may be constructed by the Heitler-London method and an exciton may be regarded as an intramolecular excitation moving from site to site in the crystal[1,3]. The nature of the energy spectrum and excited state wave functions depend strongly on the ratio between the width $\Delta\varepsilon$ of the exciton band in a crystal with a nondeformed lattice and the mean energy $\hbar\omega$ of the phonons which interact most strongly with an exciton. Depending on whether

$$\Delta\varepsilon \gg \frac{\hbar\omega}{2} \quad \text{(a) or} \quad \Delta\varepsilon \ll \frac{\hbar\omega}{2} \quad \text{(b)} \tag{1}$$

we may speak of the formation of "light" or "heavy" excitons in the crystal.

In the first case the exciton is a fast subsystem, whereas the molecules are a slow one; the effective mass of a band exciton is small and the mean rate at which the excitation moves from one lattice site to a neighboring one is much less than the vibration period of the molecules. In the second case, on the contrary, the exciton is the slow subsystem, and moves from site to site in a time large compared with a molecular vibration. The formation of "light" excitons is facilitated by greater strength of optical transition oscillators.

The character of the excited crystal states in which "light" excitons are produced is determined by the shape of the energy surface, i.e., by the dependence of the energy of the whole system on the coordinates of the molecules provided the exciton always remains in a given quantum state and the molecules are at rest. In the Heitler-London approximation, the wave function of the excited crystal with the molecules fixed in displaced positions is

$$\Phi^f = \sum_{n\alpha} a_{n\alpha} \chi^f_{n\alpha}. \tag{2}$$

Here $\chi^f_{n\alpha}$ is the antisymmetrized electron wave function of the crystal, when the molecule $n\alpha$ is excited and all other molecules are in the ground state; the index n gives the number of the unit cell, and α ($\alpha = 1, 2, \ldots, \sigma$) is the number of the molecule within the cell. We shall call the coefficients $a_{n\alpha}$ the excitation amplitudes and the set $a = \{a_{n\alpha}\}$, the exciton wave function; this wave function must satisfy the normalization condition

$$\sum_{n\alpha} |a_{n\alpha}|^2 = 1.$$

In this same approximation the energy of the excited crystal is

$$E^f[R, a] = E^0[R] + \Delta e^f + \sum_{n\alpha} |a_{n\alpha}|^2 D^f_{n\alpha}(R) + \sum_{\substack{n\alpha,\ m\beta \\ n\alpha \neq m\beta}} a^*_{n\alpha} M^f_{n\alpha,\ m\beta}(R_{n\alpha}, R_{m\beta})\, a_{m\beta}. \tag{3}$$

Here $D^f_{n\alpha}$ is the change that occurs in the interaction energy of the $n\alpha$-th molecule with all the others when it is excited, $M^f_{n\alpha,\ m\beta}(R_{n\alpha}, R_{m\beta})$ the energy of resonance interaction between molecules $n\alpha$ and $m\beta$, Δe^f is the energy of excitation of an isolated molecule, and $E^0[R]$ is the energy of the nonexcited crystal with the same deformation; $R = \{R^j_{n\alpha}\}$ denotes the set of molecule coordinates, $j = 1, 2, 3$ pertaining to translations and $j = 4, 5, 6$ to rotations.

If the right side of Eq.(3) is expanded in a series of powers of the displacements, retaining terms through the quadratic in the first term and only the linear ones in the last two, and if we transform to normal coordinates according to

$$R^i_{n\alpha} = (\sigma N)^{-1/2} \sum_{qs} R_{qs} \frac{\zeta^i_{\alpha s}(q)}{\sqrt{m_i}}\, e^{iqr_\alpha(n)}, \tag{4}$$

where $\zeta^i_{\alpha s}(q)$ are the amplitudes of the normal modes (q is the wave vector, s is the index of the frequency mode ($s = 1, 2, \ldots, 6\sigma$)), and m_i is the mass of the molecule for $i = 1, 2, 3$ and is one of its principal moments of inertia for $i = 4, 5, 6$, then Eq.(3) becomes

$$E^f[\{R_{qs}\},\ a] = E^f_0 + \frac{1}{2}\sum_{qs} \omega^2_{qs} R^*_{qs} R_{qs} + \sum_{\substack{n\alpha,\ m\beta \\ n\alpha \neq m\beta}} a^*_{n\alpha} M^f_{n\alpha,\ m\beta}\, a_{m\beta} + \sum_{n\alpha,\ m\beta} \sum_{qs} a^*_{n\alpha} G^{fqs}_{n\alpha,\ m\beta} R_{qs}\, a_{m\beta}; \tag{5}$$

Here $E^f_0 = E^0 + \Delta e^f + D^f$, E^0 is the energy of the nondeformed nonexcited crystal, ω_{qs} are the normal mode frequencies, and

$$G^{fqs}_{n\alpha,\ n\alpha} = (\sigma N)^{-1/2} \sum_{m\beta j} \frac{1}{\sqrt{m_j}} \left(\frac{\partial D^f_{n\alpha}}{\partial R^j_{m\beta}}\right) \zeta^i_{\beta s}(q)\, e^{iqr_\beta(m)}, \tag{6}$$

$$G^{fqs}_{n\alpha,\ m\beta} = (\sigma N)^{-1/2} \sum_j \frac{1}{\sqrt{m_j}} \left(\frac{\partial M^f_{n\alpha,\ m\beta}}{\partial R^j_{n\alpha}}\right) \zeta^j_{\alpha s}(q)\, e^{iqr_\alpha(n)} +$$

$$+ (\sigma N)^{-1/2} \sum_j \frac{1}{\sqrt{m_j}} \left(\frac{\partial M^f_{n\alpha,\ m\beta}}{\partial R^i_{m\beta}}\right) \zeta^j_{\beta s}(q)\, e^{iqr_\beta(m)} \quad (n\alpha \neq m\beta). \tag{7}$$

For each given deformation R, the exciton wave function is found by minimizing Eq.(5) with respect to all the $a_{n\alpha}$. The resulting infinite set of equations cannot, of course, be solved in general. This is not necessary, however, in order to classify the excited states. Just as in polaron theory[2], particular importance is attached to self-consistent states corresponding to the minima of the energy surfaces. If we minimize $E^f[\{R_{qs}\}, a]$ with respect to the R_{qs}, we find at the extremum

$$E^f[a] = E_0^f + \sum_{\substack{n\alpha,\ m\beta \\ n\alpha \neq m\beta}} a_{n\alpha}^* M^f_{n\alpha, m\beta} a_{m\beta} - \frac{1}{2}\sum_{qs} \frac{\left| \sum_{n\alpha,\ m\beta} a_{n\alpha}^* G^{fqs}_{n\alpha, m\beta} a_{m\beta} \right|^2}{\omega_{qs}^2}. \qquad (8)$$

Minimization of (8) with respect to the excitation amplitudes leads to a nonlinear set of equations for the self-consistent exciton wave functions, namely,

$$\sum_{\substack{m\beta \\ m\beta \neq n\alpha}} M^f_{n\alpha, m\beta} a_{m\beta} - \sum_{qs} \frac{1}{\omega_{qs}^2} \sum_{l\gamma,\ p\delta} a^*_{l\gamma} G^{*fqs}_{l\gamma,\ p\delta} a_{p\delta} \sum_{m\beta} G^{fqs}_{n\beta, m\beta} a_{m\beta} = \Lambda^f a_{n\alpha}. \qquad (9)$$

One set of exact solutions can be found immediately: by dropping the nonlinear term, we arrive at the set of equations previously obtained by Davydov[1] in free-exciton theory. Its solutions are the plane waves

$$a_{n\alpha} = (\sigma N)^{-1/2} B^{\mu}_{\alpha}(k)\, e^{ikr_{\alpha}(n)}; \qquad (10)$$

the energy values corresponding to which are $\varepsilon^f_{\mu}(k)$. In Eq.(10), $B^{\mu}_{\alpha}(k)$ (where $\mu = 1, 2, \ldots, \sigma$) are coefficients which give the phase difference of the wave function between two lattice sites of a given unit cell, and μ is the number of the exciton band.

Let us now return to Eq.(9) and first assume that the exciton bands (in a crystal with a nondeformed lattice) do not overlap. Let us consider the states near the bottom of the μ-th exciton band located at the point k_0.* Then by expanding the exciton wave function in a series in terms of the plane waves pertaining to the μ-th band and considering terms only through the quadratic in $k - k_0$ in the expansion of the exciton "kinetic" energy, we can greatly simplify the first term in Eq.(9). Then Eq.(9) becomes

$$(\Delta_{n\alpha} + \Lambda^f) b_{n\alpha} = \sum_{m\beta,\ l\gamma,\ p\delta} b^*_{l\gamma} G^{l\gamma,\ p\delta}_{n\alpha,\ m\beta} e^{ik(r_{\beta}(m) - r_{\alpha}(n) + r_{\delta}(p) - r_{\gamma}(l))} b_{p\delta} b_{m\beta}, \qquad (11)$$

where

$$G^{l\gamma,\ p\delta}_{n\alpha,\ m\beta} = \sum_{qs} \frac{G^{*fqs}_{l\gamma,\ p\delta} G^{fqs}_{n\alpha,\ m\beta}}{\omega_{qs}^2} \quad (a), \qquad b_{n\alpha} = e^{-ik_0 r_{\alpha}(n)} a_{n\alpha} \quad (b), \qquad (12)$$

and $\Delta_{n\alpha}$ denotes formal differentiation with respect to the coordinates of the $n\alpha$-th lattice site expressed in $X = \frac{\sqrt{2m_{\mu x}}}{\hbar} x$ units (with similar expressions for the other coordinates); here $m_{\mu x}$, $m_{\mu y}$ and $m_{\mu z}$ are the principal values of the effective mass tensor of a band exciton.

Inasmuch as the states being considered have a radius considerably greater

*The case of several equal minima on the $\varepsilon^+_{\mu}(k)$ surface can be treated in a similar way.

than the lattice constant, the formal differentiation with respect to the discrete argument $n\alpha$ in Eq.(11) may be replaced by differentiation with respect to the continuum. Then Eq.(11) becomes a special case of the more general equation

$$(\Delta + \lambda)\psi(\mathbf{r}) = -U\psi(\mathbf{r}), \tag{13}$$

within the base region having a volume $V = L^3$. In Eq.(13), U is a nonlinear integral operator with kernel $K(\mathbf{r}, \{\xi_l\}\{\eta_j\})$; it is given by

$$U\psi(\mathbf{r}) = \int K(\mathbf{r}, \{\xi_l\}\{\eta_j\}) \prod_{l=1}^{p} \prod_{j=1}^{q} \psi^*(\vec{\xi}_l)\psi(\vec{\eta}_j)\, d\vec{\xi}_l\, d\vec{\eta}_j. \tag{14}$$

$$(l = 1, 2, \ldots, p,\ j = 1, 2, \ldots, q,\ s = p + q).$$

We shall assume that with a sufficiently large volume V the inequality

$$\frac{1}{V^{s/2}} \int |K(\mathbf{r}, \{\vec{\xi}_l\}\{\vec{\eta}_j\})| \prod_{lj} d\vec{\xi}_l\, d\vec{\eta}_j \leqslant CV^{-\alpha - \frac{1}{2}}. \tag{15}$$

is fulfilled. Then the following assertion can be proved.

If $\alpha > 2/3$, then in the limit $V \to \infty$ the solutions of Eq.(13) tend to approach the plane waves $\psi_k^{(0)} = e^{ikr}/\sqrt{V}$.

From (6), (7), and (12a) it follows that the series

$$\sum_{m\beta,\ l\gamma,\ p\delta} |G_{n\alpha,\ m\beta}^{l\gamma,\ p\delta}|$$

diverges at most logarithmically as $L \to \infty$ so that Eq.(11) pertains to the case $\alpha > 1-\eta$ (where η is an arbitrary positive number). Therefore plane waves are solutions of Eq.(11). This result can be generalized to the case of overlapping exciton bands and arbitrary values of k. In addition, it can be shown that the extrema on the energy surfaces which correspond to free excitons are actually minima.

Thus in molecular crystals, the plane waves of Eq.(10) which describe free excitons becomes exact solutions of Eq.(9) as $V \to \infty$ and correspond to minima in the energy surfaces.

This result is equally valid for other systems with short-range forces, such as condensons and excitons in ionic crystals. It should be noted, on the other hand, that even for $\alpha > 0$ the right side of Eq.(13) evaluated for plane waves as $V \to \infty$ becomes infinitesimally small at each point, compared to the individual terms on the left side. Nevertheless, for $0 < \alpha \leqslant 2/3$, there do not, in general, exist the self-consistent solutions whose norm approaches that of plane waves as $V \to \infty$ and the bottom of the band breaks up even for states with an arbitrarily low lattice deformation energy. This occurs in systems with long-range forces, in particular, in the polaron problem, which corresponds to $\alpha = 1/3$.

In the case of small local deformations of the crystal lattice, the exciton remains in a band state and the energy of the system rises. As the lattice deformation energy increases, however, the potential well due to the deformation may become so deep that there will appear in it a discrete-spectrum energy level; in this case the exciton may move from the exciton band to this discrete level. If with further increase in deformation the energy of the system begins to decrease, there may appear, on the energy-surface "sheet" splitting off the bottom of the exciton band, an additional minimum, corresponding to a self-consistent state with a deformed lattice and exciton moving in a bounded region. We shall call this occurence a deforming excitation.

Since the solution of Eq.(9) is equivalent to minimization of the functional of Eq.(8), in order to prove the existence of deforming excitation levels, lying below the bottom of the lowest (μ_0-th) exciton band it is sufficient to find at least one normalized set of excitation amplitudes for which $E^f[a] < \varepsilon^f_{\mu_0}(\mathbf{k}_0)$. If we use the approximation of infinitesimally small radii and set $a_{n\alpha} = \delta_{nn_0}\delta_{\alpha\alpha_0}$, this criterion can be written

$$\frac{1}{2}\sum_{qs}\frac{\left|G^{fqs}_{n_0\alpha_0,\ n_0\alpha_0}\right|^2}{\omega^2_{qs}} > -\varepsilon^f_{\mu_0}(\mathbf{k}_0). \tag{16}$$

We note that $\varepsilon^f_{\mu_0}(\mathbf{k}_0)$ is always negative, and therefore deforming excitations can occur only when the exciton-phonon interaction is sufficiently strong. If the exciton interacts with modes whose dispersion may be neglected and which can be assigned a mean frequency ω, (16) is simplified to

$$\frac{1}{2\omega^2}\sum_{m\beta j}\frac{1}{m_j}\left(\frac{\partial D^f_{n\alpha}}{\partial R'_{m\beta}}\right)^2 > -\varepsilon^f_{\mu_0}(\mathbf{k}_0). \tag{17}$$

Criterion (17) can be generalized to the case in which translational and rotational vibrations of the lattice can be separated, while the dispersion is low for both rotational and translational vibrations that interact strongly with the exciton. For typical molecular crystal parameters, the left side of (17) proves to be of the same order or greater than the right side. Therefore conditions in molecular crystals are favorable for deforming excitations.

It is possible to derive the criterion for the occurrence of deforming excitations from the point of view of the large-radius approximation. Specifically, if we seek the exciton wave function in the form

$$a_{n\alpha} = \sigma^{-1/2}B^{\mu_0}_{\alpha}(\mathbf{k}_0)\,e^{i\mathbf{k}_0\mathbf{r}_{\alpha}(n)}\varphi(\mathbf{n}), \tag{18}$$

where $\varphi(\mathbf{n})$ is a continuous lattice function of constant sign which decays exponentially at infinity, then instead of Eq.(8) we obtain

$$E^f[\varphi] = E^f_0 + \varepsilon^f_{\mu_0}(\mathbf{k}_0) - \frac{\hbar^2}{2}\sum_{\mathbf{n}}\varphi^*(\mathbf{n})\left[\frac{1}{m_{\mu_0 x}}\frac{\partial^2}{\partial x^2_{\mathbf{n}}} + \frac{1}{m_{\mu_0 y}}\cdot\frac{\partial^2}{\partial y^2_{\mathbf{n}}} + \frac{1}{m_{\mu_0 z}}\cdot\frac{\partial^2}{\partial z^2_{\mathbf{n}}}\right]\varphi(\mathbf{n}) - \frac{g^f_0}{2}\sum_{\mathbf{n}}|\varphi(\mathbf{n})|^4; \tag{19}$$

Here g^f_0 is a constant depending on $B^{\mu_0}_{\alpha}(\mathbf{k}_0)$ and the coefficients of Eqs.(6) and (7). In our particular case of radii of states $1/p$, much greater than the lattice constant d, Eq.(19) reduces to

$$E^f(p) = E^f_0 + \varepsilon^f_{\mu_0}(\mathbf{k}_0) + \gamma_1\frac{\hbar^2p^2}{2m^*_{\mu_0}} - \frac{\gamma_2}{50}\,g^f_0d^3p^3. \tag{20}$$

Here $m^*_{\mu_0}$ is the mean effective mass and the coefficients $\gamma_1, \gamma_2 \sim 1$ are determined by the particular choice of $\varphi(\mathbf{n})$.

If the inequality $E^f(p) < E^f_0 + \varepsilon^f_{\mu_0}(\mathbf{k}_0)$ begins to be fulfilled in the region in which the macroscopic approximation is applicable, i.e., when $pd \ll 1$, then, as indicated by Deigen and Pekar[4] this is a sufficient condition for the production of deforming excitations. Where the lowest band is concerned, this criterion is of an order of magnitude more severe than (16). It has, however, the advantage that it can be generalized to the production of deforming excitations at the bottom of any non-overlapping exciton band. Since $E^f(p)$ decreases monotonically after passing through a maximum at large p the ground state of a deforming excitation does not lie in the region of applicability of the large-radius approximation, and the radius of this state may not be greater than of the order of the lattice constant.

Thus in three-dimensional molecular crystals there is no competition between the production of free excitons and deforming excitations, and in the case of strong exciton-phonon interaction the energy surfaces are devoid of minima corresponding to both free excitons and deforming excitations.

2. Deforming Excitons in Molecular Chains

It may be considered established at present that the absorption of light by molecular chains is of an exciton character[5,6]. This pertains both to long chain molecules consisting of weakly coupled links and to linear polymers consisting of millions of organic molecules.

The spectra of self-consistent states in molecular crystals and in chains differ greatly. In chains, states corresponding to the bottom of the exciton band are not self-consistent, and $E^f(p)$ for small values of p is given by

$$E^f(p) = E_0^f + \varepsilon^f_{\mu_0}(\mathbf{k}_0) + \gamma_1 \frac{\hbar^2 p^2}{2m_{\mu_0}} - \frac{\gamma_2}{4} g_0^f dp. \tag{21}$$

It follows from (21) that the transition of an exciton to a deforming state occurs with monotonically decreasing energy and does not require temperature fluctuation. The equation for chains which can be analogously derived from (19) by minimization with respect to φ^*, always has a single normalized solution when $pd \ll 1$ and this solution belongs to the discrete spectrum:

$$\varphi = \frac{1}{2}\sqrt{\frac{b}{2}} \Big/ \operatorname{ch}\left(\frac{bx}{4}\right), \quad b = \frac{2m_{\mu_0} g_0^f d}{\hbar^2}. \tag{22}$$

This result is valid for all non-overlapping exciton bands.

3. Band Structure of the Spectra of Deforming Exciton and Localized Excitations

In Section 1 we considered the energy of the system when the molecules are at rest. Hereinafter we shall assume that the crystal lattice deformation energy at an energy surface minimum corresponding to a deforming excitation is much greater than the mean energy of the phonons that interact strongly with the exciton. Then if the center of the deforming excitation is close to the $n\alpha$ site, in the zeroth approximation the wave function of the system can be written as

$$\psi^f_{\{n_{qs}, m_{qs}\}}(n\alpha) = \Phi^f(\{R_{qs}\}) \prod_{qs}{}' R_{n_{qs}m_{qs}}(\rho_{qs}(n\alpha))\, \Phi_{m_{qs}}(\varphi_{qs}(n\alpha)). \tag{23}$$

Here $\Phi^f(\{R_{qs}\})$ is the electron wave function of the system, which depends parametrically on the molecule coordinates

$$R_{qs} = \sqrt{\frac{\hbar}{2\omega_{qs}}}\, \rho_{qs} e^{-i\varphi_{qs}}$$

and adiabatically follows changes therein; a prime on the product indicates that q runs through half the cell of the reciprocal lattice;

$$R_{nm} = \frac{\rho^{|m|} e^{-\frac{\rho^2}{2}}}{\sqrt{\frac{1}{2}\left(\frac{n-m}{2}\right)!\left(\frac{n+m}{2}\right)!}} Q^{|m|}_{\frac{n-|m|}{2}}(\rho^2), \quad \Phi_m(\varphi) = \frac{e^{im\varphi}}{\sqrt{2\pi}}, \tag{24}$$

where $Q^s_p(x)$ is a Laguerre polynomial. The index $n\alpha$ in parentheses next to ρ_{qs} and φ_{qs} in Eq.(23) indicates that these are reckoned from the displaced equilibrium positions corresponding to localization of the center of the deforming excitation at the $n\alpha$ site. Because of the equivalence of all the lattice sites,

the proper functions for the zeroth approximation will be the linear combinations (with T ≈ 0)

$$\Psi^f_{k\{n_{qs}m_{qs}\}} = (\sigma N)^{-1/2} \sum_{n\alpha} A_\alpha(\mathbf{k})\, e^{i\mathbf{k}\mathbf{r}_\alpha(n)} \psi^f_{\{n_{qs}m_{qs}\}}(n\alpha), \tag{25}$$

which are simultaneously eigenfunctions of the momentum operator. Determination of the coefficients $A_\alpha(\mathbf{k})$ and the energy values reduces, in the first approximation, to finding the eigenvalues and eigenvectors for a set of σ linear equations whose coefficients depend on k. This defines σ deforming excitation bands. Analysis of the set of equations leads to the conclusion that the width of the individual bands is as a rule greater than the separation between them. The width decreases exponentially as the exciton-phonon interaction energy increases and as the radius of the a-cloud decreases; at the same time the effective mass of the deforming excitations increases exponentially. Evaluations show that in molecular crystals the width of the deforming excitation bands should be of the order of 0.1-1 $\hbar\omega$, which corresponds to effective masses of the deforming excitations of the order of hundreds and thousands of electron masses (the evaluations were made for a lattice deformation energy of $\sim 5\hbar\omega$).

In the formation of "heavy"excitons, when lattice deformation follows the slow movement of an intramolecular excitation, the crystal wave function in the zeroth approximation can also be written in the form of a linear combination such as (25), except that $\Phi^f(\{R_{qs}\})$ should be replaced by $\chi^f_{n\alpha}$. The effective mass of the whole "formation", including the "heavy" exciton and the accompanying lattice deformation ("localized" excitation) also increases exponentially as the exciton-phonon interaction energy increases, but the numerical values of the effective masses prove to be much greater. For instance, for a lattice deformation energy associated with a "heavy" exciton of $\sim 5\hbar\omega$, the effective mass of the "localized" excitation is found to be $\sim 10^5\, m_e$.

4. Optical Transitions in Molecular Crystals

If a light wave propagates through an absorbing crystal, the operator of the perturbation caused by the wave is of the form

$$V(t) = Ve^{-i\omega t} + \overset{*}{V}e^{i\omega t} = \frac{e}{m\omega i}\sum_l \mathbf{p}_l \varkappa \left[\mathbf{E}_0 e^{i(\vec{\eta}\mathbf{r}_l - \omega t)} + \mathbf{E}_0^* e^{-i(\overset{*}{\vec{\eta}}\mathbf{r}_l - \omega t)}\right]. \tag{26}$$

Here $\varkappa = \|\varkappa_{ij}\|$ is the effective field tensor, $\mathbf{E}_0$ and $\vec{\eta}$ are the complex amplitude and wave vector of the light wave, and $\mathbf{p}_l$ and $\mathbf{r}_l$ are the momentum and coordinate of the l-th electron; the sum is taken over all electrons in the crystal. The perturbed crystal wave function is given by

$$\Psi(t) = \Psi_0 e^{-i\frac{E_0}{\hbar}t} + \int_{\perp} \frac{V_{\nu_0}\Psi_\nu}{E_0 - E_\nu + \hbar\omega}\, d\nu\, e^{-\frac{i}{\hbar}(E_0+\hbar\omega)t} + \int \frac{\overset{*}{V}_{\nu_0}\Psi_\nu}{E_0 - E_\nu - \hbar\omega}\, d\nu\, e^{-\frac{i}{\hbar}(E_0-\hbar\omega)t}. \tag{27}$$

In Eq.(27) the first integral is taken along a contour which passes below the singular point $E_\nu = E_0 + \hbar\omega$ in the complex plane of E_ν; ν is an index numbering the excited state of the system. Using the ordinary semiclassical method of subdividing the crystal into cells in each of which the amplitude and phase of the light wave might be considered constant, and calculating the complex dipole moment of each cell separately, we obtain the following formulas for the polarizability $\alpha_{ij}(\omega)$ and conductivity $\sigma_{ij}(\omega)$ tensors:

$$\alpha_{ij}(\omega) = \frac{1}{vN}\oint d\nu \left(e\sum_l r_{l\varkappa}\right)^i_{\nu 0} \left(e\sum_l \mathbf{r}_{l\varkappa}\right)^j_{0\nu} \frac{2(E_\nu - E_0)}{(E_\nu - E_0)^2 - (\hbar\omega)^2}, \tag{28}$$

$$\sigma_{ij}(\omega) = \frac{\pi\omega}{vN} \int d\nu \left(e \sum_l \mathbf{r}_l \varkappa \right)^i_{\nu 0} \left(e \sum_l \mathbf{r}_l \varkappa \right)^j_{0\nu} \delta(E_0 + \hbar\omega - E_\nu). \tag{29}$$

In (28), we take the principal part of the integral; v is the volume of the unit cell. Comparison of (28) and (29) leads to the first universal integral relation between $\alpha_{ij}(\omega)$ and $\sigma_{ij}(\omega)$ (Ref.7):

$$\alpha_{ij}(\omega) = \frac{2}{\pi} \int_0^\infty \frac{\sigma_{ij}(\omega')}{(\omega')^2 - \omega^2} d\omega'. \tag{30}$$

Eq.(30) can be treated as a singular integral equation for $\sigma_{ij}(\omega)$; solving it, we obtain the second integral relation

$$\sigma_{ij}(\omega) = \frac{2\omega^2}{\pi} \int_0^\infty \frac{\alpha_{ij}(\omega')}{\omega^2 - (\omega')^2} d\omega' + \sigma_{ij}(0). \tag{31}$$

Eqs.(30) and (31) relate the conductivity and polarizability tensors and where the frequency dependence of one is known, enable us to establish the other.

If we remain within the framework of the Heitler-London method, then without any additional assumptions concerning the exciton-lattice coupling or the form of the excited state wave functions, provided $\vec{\varkappa}_{ij}$ may be considered frequency independent, Eq.(29) leads to

$$\frac{\hbar}{\pi} \int \sigma_{ij}(\omega) \frac{d\omega}{\omega} = \frac{1}{v} \sum_\alpha (e\mathbf{r}_\alpha \varkappa)^i (e\mathbf{r}_\alpha \varkappa)^j. \tag{32}$$

Here $\mathbf{r}_\alpha$ is the matrix element of the coordinate of the α-th molecule calculated between the ground state and the f-th excited state; the integration is extended into the region of the spectrum in which the absorption is due to transitions to states arising from the f-th intramolecular level. If $\mathbf{r}_\alpha$ does not change when a molecule is inserted into the crystal, which is true for the first transitions when their intensity is not too weak, then if we have $\mathbf{r}_\alpha$ from independent measurements we can find the components of the effective field tensor $\vec{\varkappa}_{ij}$ by means of Eq.(32).

The frequency dependence of σ_{ij} and α_{ij} can be found only if the excited state wave functions are sufficiently well known. Where the "localized" excitations are concerned, invoking the functions of (25), which take account of degeneracy due to the equivalence of all the molecules of the crystal, and making use of the narrowness of the "localized" excitation bands compared with $\hbar\omega$, one can show that the absorption due to these "localized" excitations will have all the attributes of impurity absorption[8]; Eq.(30) can be used to find the shape of the dispersion curve. For instance, in the case of strong exciton-lattice interaction

$$\sigma_{ij}(\omega) = \frac{\sqrt{\pi} e^2 \omega}{v\hbar g} \sum_\alpha (\mathbf{r}_\alpha \varkappa)^i (\mathbf{r}_\alpha \varkappa)^j \left[1 + \frac{1}{3g^3} \sum_{qs} \omega^3_{qs} \rho^2_{qs0} \Omega^3_- \right] e^{-\Omega^2_-}, \tag{33}$$

and

$$\alpha_{ij} = -\frac{2e^2}{v\hbar g} \sum_\alpha (\mathbf{r}_\alpha \vec{\varkappa})^i (\mathbf{r}_\alpha \vec{\varkappa})^i \times$$

$$\times \left\{ w(\Omega_-) - w(\Omega_+) - \frac{1}{3g^3} \sum_{qs} \omega^3_{qs} \rho^2_{qs0} \left[\frac{\Omega^2_- + \Omega^2_+}{2} - \Omega^2_- w(\Omega_-) - \Omega^3_+ w(\Omega_+) + \frac{1}{2} \right] \right\}, \tag{34}$$

where

$$w(x) = e^{-x^2} \int_0^x e^{s^2} ds, \quad g = \left[\frac{1}{2} \sum_{qs} \omega^2_{qs} (n_{qs} + 1) \rho^2_{qs0} \right]^{1/2}, \quad \Omega_\pm = \frac{1}{g} \left(\omega \pm \frac{E^f_0}{\hbar} \right), \tag{35}$$

and ρ_{qs0} is the displacement of the oscillator equilibrium positions incident to excitation of the crystal and $\bar{n}_{qs}$ are the average values of the quantum numbers equal to twice the values given by the Planck distribution for a linear oscillator of the same frequency.

If deforming excitations are produced in the crystal, the absorption spectrum will be more complicated and will consist of a superposition of a narrow free exciton band on the wide-band absorption due to the deforming excitations. The intensity of the wide-band absorption will increase rapidly with temperature, especially at the long-wave edge. If the bottom of the free exciton band corresponds to the state with k = 0 and the exciton-phonon interaction is so strong that there are no discrete-spectrum levels in the potential well at the minimum in the energy surface corresponding to the nondeformed lattice, the narrow free-exciton band will be smeared out and all of the absorption will be of the wide-band type, even when T = 0.

The luminescence spectrum will also be a superposition of free exciton spectra and deforming excitation spectra. The spectral dependence of the wide-band luminescence associated with the deforming excitations is similar to the spectral dependence of the impurity luminescence and its polarization is determined by the orientation of the vectors

$$\vec{\mathfrak{R}}_\alpha = \sum_{m\beta} a_{m\beta}(n\alpha)\, r_{\beta\varkappa}.$$

The direction of $\vec{\mathfrak{R}}_\varkappa$ is the same as that of $r_{\alpha\varkappa}$ which, according to (32), determine the relation between the integral absorption intensities of the different components only for deforming excitations of extremely small radius. There is no mirror correspondence between the deforming excitation absorption and luminescence spectra.

Let us consider "light" excitons in molecular chains. Since the edge of the exciton band breaks down in these chains, in the case of a strong exciton-phonon interaction the narrow free-exciton line should vanish; all the persisting absorption will be of the wide-band type. Due to the complex configuration of the energy surface, for any information on the shape of the absorption curve, we must turn to statistical theory[9], according to which one may expect an asymmetric bell-shaped curve.

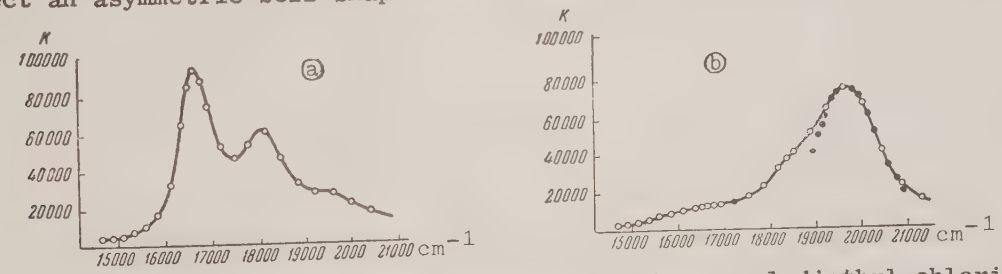

Absorption bands of aqueous solutions of pinacyanol-diethyl-chloride at 20°: a) concentration of $3.2\cdot10^{-6}$ mole/liter; b) concentration of $1.8\cdot10^{-3}$ mole/liter. The circles denote experimental points; the solid dots indicate the Gaussian approximation.

Ecker[10] has described the absorption spectrum of an aqueous solution of pinacyanol-diethylchloride dye (see Figure).

Diagram a shows the absorption spectrum of a dilute water solution, where the monomer (16,680 cm^{-1}) and dimer (18,300 cm^{-1}) bands are clearly discernable. In contrast, in the spectrum of a concentrated solution (diagram b) the predominant absorption is in the wide band at 19,600 cm^{-1} that

is associated with the high-polymer form. The exciton band width in the non-deformed polymer chain is, as evaluated from the oscillator strength (f = 0.7), about 1500 cm^{-1}; since the frequencies of lattice vibrations are of an order of magnitude lower, the excitons are "light" ones. Since the interaction with the solvent is already manifest in some widening of the monomer band and since incident to polymerization the interaction can only become weaker due to delocalization of excitations, the experimentally observed large widening of the polymer band as compared with the monomer band (particularly noticeable near the absorption maximum) can be explained only by the appreciable deformation of the polymer chain about the exciton, i.e., by deforming excitations. It is interesting to note that approximation by means of a Gaussian is futile for the monomer band, whereas it gives good results for the polymer band. Similar spectra were observed for benzocarbocyanine and a number of other dyes of the same series[11]; in addition to such absorption, wide-band luminescence has been observed in monobenzothiazol[12]. Unfortunately, there are no quantitative data on these spectra in the literature. It is still impossible to carry out a comparison of theory and experiment for three-dimensional crystals due to the complete absence of quantitative measurements at low temperatures.

Davydov and author[13] have previously examined absorption and dispersion in molecular crystals, as well as in one- and two-dimensional molecular structures in the case of weak exciton-phonon coupling. The shape of the absorption curves can be investigated when one can restrict the consideration to interactions with one of the modes of crystal vibration. When "light" excitons are formed, as has been noted in Ref.1, there may appear low-frequency satellites at the spectral series lines due to interactions with the lattice; these satellites persist even at the lowest temperatures. As the dimensionality of the crystal structure is increased, the contours of these satellite lines become smoother. The distance between the maxima of the background (satellites) and the main lines of the series depends on the structure of the exciton band and mode of oscillation. In three-dimensional crystals even for "heavy" excitons these distances are in all cases different from the limiting frequencies, i.e., correspond to certain intermediate values of the vibrational frequencies, and should not be matched with the frequencies determined from infrared absorption. These deductions are substantiated by the analysis of experimental data[14] on the absorption by naphthalene[13] at 20°K.

Institute of Physics of the
Ukrainian SSR Academy of Sciences

References

1. A.S.Davydov, Teoriia pogloshcheniia sveta v molekuliarnykh kristallakh (Theory of light absorption in molecular crystals), Ukrainian SSR Ac. of Sci., 1951.

2. S.E.Pekar, Issledovaniia po elektronnoi teorii kristallov (Studies in the electron theory of crystals.) M. 1951.

3. Ia.I.Frenkel', Phys.Rev., 37, 17, 1276 (1931); Zhur.eksp.i teor.fiz., 6, 647 (1936).

4. M.F.Deigen & S.I.Pekar, Zhur.eksp.i teor.fiz., 21, 803 (1951).

5. J.Franck & E.Teller, J.Chem.Phys., 6, 861 (1938).

6. A.S.Davydov, Zhur.eksp.i teor.fiz., 18, 515 (1948).

7. H.A.Kramers, Atti cong.intern.fisici., Commo, 2, 545 (1927).

8. S.I.Pekar, Usp.fiz.nauk., 50, 197 (1953); A.S.Davydov, Zhur.eksp.i teor.fiz., 24, 197 (1953); M.Lax, J.Chem.Phys., 20, 1752 (1952).

9. V.M.Agranovich & A.S.Davydov, Uchenye zapiski (Scientific Notes) Kiev State Univ., No.7, 1953.

10. H.Ecker, Kolloid,Z., 92, 35 (1940).

11. G.Scheibe, Kolloid.Z., 82, 1 (1938).

12. G.Scheive, ZS.Elektorechem., 47, 73 (1941).

13. A.S.Davydov, E.I.Rashba, Ukrainian Physics Journal, 2,3 (1957).

14. A.F.Prikhot'ko, Zhur.eksp.i teor.fiz., 19, 383 (1949).

INVESTIGATIONS IN THE MICROSCOPIC THEORY OF CRYSTALS

- K.B.Tolpygo

The development of the theory of the solid state and, in particular, of semiconductors is necessarily based on a number of conceptual models. As experimental data are accumulated, every model sooner or later is found to be inadequate and has to be replaced by a more comprehensive one capable of describing more facts. From the quantum mechanical point of view the choice of model determines the Hamiltonian of the problem to be solved. In the electronic theory of semiconductors we have seen the successive use of the Hamiltonians of a free-electron, of an electron in a periodic field weakly perturbed by atomic vibrations, and of an electron interacting strongly with phonons in an inertially polarizable continuum.

A very wide range of phenomena of solid state physics can be described by nonrelativistic quantum mechanics based on the now known properties of electrons and nuclei. Attempts are currently being made to treat many solid state effects on the basis of the exact Hamiltonian of the problem (the sum of the kinetic energies and the interaction energies of all electrons and nuclei). The advantage of this approach is the possibility of encompassing a large number of phenomena from a unified standpoint. In some cases it becomes feasible to establish relations between different properties, relations that may not be immediately evident when using special models.

The present article is a review of attempts in this direction made by the author and his students.

1. Elements of the Microtheory of Ideal Ionic Lattices

The properties of ideal crystal lattices which are most important from the point of view of the electronic theory of semiconductors and insulators are their inherent vibration spectra and the form of the interaction of these vibrations with external fields and conduction electrons or impurity centers. In Refs. 1 and 2 the inherent frequencies of NaCl and KCl were found using the Born approximation of point ions. In this way it is not possible, for instance, to give a correct description of the interaction between the vibrations and a conduction electron, since the entire polarization is found to be inertial. Actually, part of the polarization, that due to the deformation of the electron shells, noninertially (i.e., immediately) follows the electron motion and simply makes a certain contribution to the periodic potential of the crystal.

One can obtain equations describing vibrations of the ions (classical or quantum), with their accompanying deformation taken into account, by solving the general problem of electronic and nuclear motion in the adiabatic approximation. The initial electron energy U is found for arbitrary values of the nuclear coordinates. This will play the role of the potential energy in nuclear motion. It is usually sufficient to know the energy for nuclear positions close to the equilibrium ones. Then in the harmonic approximation U subdivides into a sum of terms each of which depends on the displacement of no more than two nuclei. These terms will no longer, however, be the pair interactions of Born theory[3].

It is convenient to try to find U, as well as the electron wave function, by the variational method in two stages: we first obtain the best solution with the auxiliary conditions $P_s^l = \text{const}$, where P_s^l is the dipole moment of the electron shell of the s-th ion of the l-th cell, and then minimize U by varying all the P_s^l. If the crystal is in an external field, which is approxi-

mately homogeneous within the region of each ion, and if the potential of this field is $v(\mathrm{r})$, then

$$U = U^0(\ldots \mathbf{R}_s^l \ldots \mathbf{P}_s^l \ldots) + \sum_{sl} e_s v(\mathbf{R}_s^l) - \sum_{sl} \mathbf{P}_s^l \cdot \mathbf{E}^0(R_s^l). \tag{1}$$

Here the $\mathbf{R}_s^l$ are the coordinates of the nuclei, and e_s are the ionic charges. The quantities $\mathbf{P}_s^l$ are found from the equations $\frac{\partial}{\partial \mathbf{P}_s^l} U = 0$. The classical equations for ionic vibrations are conveniently written in a symmetric form with respect to the two sets of variables $\mathbf{u}_s^l = \mathbf{R}_s^l - \mathbf{r}_s^l$ (the displacements of the nuclei) and $\mathbf{P}_s^l$ (the dipole moments):

$$m_s \ddot{\mathbf{u}}_s^l = -\frac{\partial U}{\partial \mathbf{u}_s^l}; \quad 0 = -\frac{\partial U^0}{\partial \mathbf{P}_s^l} + \mathbf{E}^0(\mathbf{R}_s^l), \tag{2}$$

where $\mathbf{r}_s^l$ are the coordinates of the lattice sites and m_s are the ion masses.

For sufficiently symmetric crystals, we attempt to find the electron wave function Ψ in the form of the antisymmetrized product of functions ψ_s^l for the separate ions, each of which is sought in the form of the series

$$\psi_s^l = \sum_{i=0}^{\infty} C_{si}^l \psi_{si}, \quad \text{where} \quad |C_{si}^l|^2 \ll 1 \text{ with } i \geqslant 1, \tag{3}$$

where ψ_{si} pertains to the excited states of the s-th ion.

After minimizing the average Hamiltonian obtained with this Ψ function over all C_{si}^l with $i \geqslant 1$, we obtain

$$U^0 = \sum_{sl} \left\{ \frac{(P_s^l)^2}{2\alpha_s} + \sum_{s'l'}^{(n)} \mathbf{P}_s^l \cdot \beta_{ss'}(\mathbf{R}_{ss'}^{ll'}) + u(\ldots \mathbf{R}_{ss'}^{ll'} \ldots) \right\} + U_{\text{cou}}, \tag{4}$$

where α_s is the polarizability of the s-th ion in the crystal and U_{cou} is the Coulomb interaction energy of all the charges and dipoles $\beta_{ss'}$ and $u(\ldots \mathbf{R}_{ss'}^{ll'} \ldots)$ is a function of the distance $\mathbf{R}_{ss'}^{ll'} = \mathbf{R}_s^l - \mathbf{R}_{s'}^{l'}$ of the s^l ion from its nearest neighbors, the number of which is given by n. The difference between Eq.(4) and Born theory[3] lies not only in the dependence of U_{cou} on the $\mathbf{P}_s^l$, but also in the dependence of the exchange integrals (second term in (4)) on these dipole moments. In addition, $u(\ldots \mathbf{R}_{ss'}^{ll'} \ldots)$ contains small corrections which cannot be broken up into a sum of pair interactions. These corrections are of order $|C_{si}^l|^2$.

2. Inherent Frequencies and Specific Heats of NaCl, KCl, and KBr

Solutions of the inherent frequency equations (2) have been found for NaCl, KCl, and KBr, neglecting the corrections mentioned at the end of Section 1 above. These solutions are in the form of plane waves

$$\mathbf{u}_s^l = \mathbf{u}_s^{\alpha \mathbf{K}} e^{i\mathbf{K}\cdot\mathbf{r}_s^l - i\omega_{\alpha \mathbf{K}} t}; \quad P_s^l = P_s^{\alpha \mathbf{K}} e^{i\mathbf{K}\cdot\mathbf{r}_s^l - i\omega_{\alpha \mathbf{K}} t}, \tag{5}$$

where $\mathbf{K}$ is the wave vector, and $\alpha = 1, 2, \ldots, 6$ enumerates the vibration modes.

The inherent frequencies and normalized amplitudes $\mathbf{u}_s^{\alpha \mathbf{K}} \mathbf{P}_s^{\alpha \mathbf{K}}$ have been found for 28 values of the wave vector $\mathbf{K}$. This is sufficient to know them for a network of 729 points homogeneously distributed through a cell of the reciprocal lattice at distances of 1/8 the length of its edge. The summation of the electromagnetic forces acting on one ion from directions of all other ions was found using the method of Ewals, taking into account retardation. Since the solutions of Eqs.(2) in the long-wavelength region where $a\mathbf{K} \ll 1$ (here a

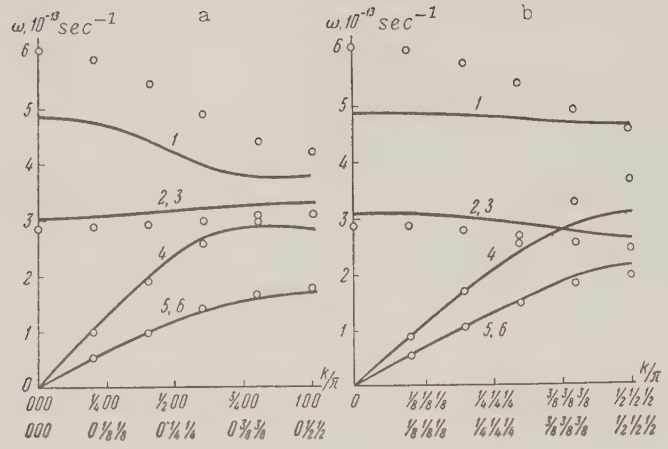

Fig.1. Dependence of the inherent frequencies of the NaCl lattice on the wave vector, when this vector is directed a) along the edge, b) along the diagonal of the cube and passes through the origin. The circles give Kellerman's results.

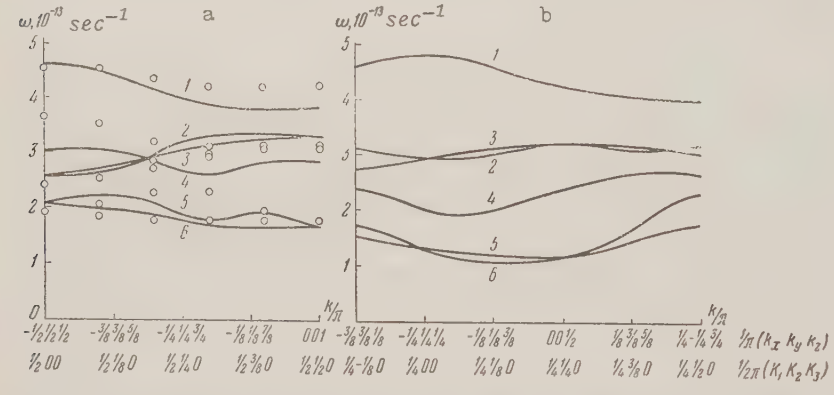

Fig.2. Frequencies $\omega_{\varkappa K}$ for NaCl when K varies a) along the edge of the cube and b) parallel to the edge of the cube.

is the lattice constant) describe the propagation of light, the parameters of the theory[4] were obtained by comparison with the experimental value of the index of refraction cK/ω. In addition, use was made of the values of the dielectric constant ϵ, the infrared absorption frequency, the positive ion polarizability (which is little dependent on the surrounding medium) and the pressure dependence of ϵ and n_0^2 (n_0 is the optical index of refraction).

The frequencies $\omega_{\varkappa K}$ for NaCl, obtained in Ref. 5, are shown in Figs.1 and 2. Curves 1, 2 and 3 represent one longitudinal and two transverse optical modes, while curves 4, 5 and 6 pertain to acoustical modes. The circle points give Kellerman's results[1]. Rigorous separation of the longitudinal and transverse vibrations obtains only when K is directed along the diagonal of the cube or the diagonal of a face. Otherwise the amplitudes $u_s^{\alpha K}$ may deviate up to 25° from the direction of K or perpendiculars to the vector.

The dipole moment $P_2^{\alpha K}$ of the electron shell of a negative ion is found to be of the same order of magnitude as the moment due to the displacement of the nucleus $p_2^{\alpha K} = e_2 u_2^{\alpha K}$. However, $P_1^{\varkappa K}$ is much smaller than $p_1^{\varkappa K}$. Kellerman's value of ω_{1K} is an overestimate because the polarizability of the ions was not taken into account. Calculations[6] of the temperature dependence of the NaCl specific heat yielded fairly satisfactory agreement with experiment (Fig.3).

A calculation of the frequencies and amplitudes for KCl was performed by the author together with Zaslavskaia[7] for a network over 1/4 the edge of the reciprocal cell (seven values of K for a network of 125 points); another calculation was made by Kucher[8] for a network twice as dense (28 values of K).

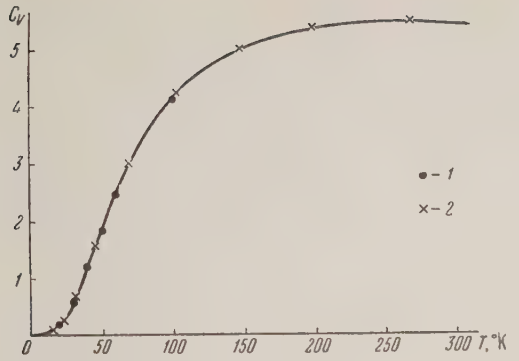

Fig.3. Temperature dependence of the specific heat of NaCl: 1) Kellermann's results, 2) Zaslavskaia's results. Solid line - experimental data.

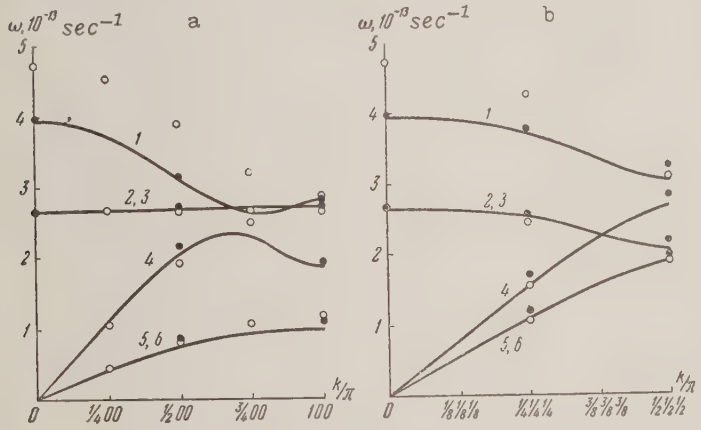

Fig.4. Frequencies $\omega_{\alpha K}$ for KCl: ○ - results of Jona, • - results of Tolpygo & Zaslavskaia; solid lines - results of Kucher. The directions of the wave vector - same as in Fig.1.

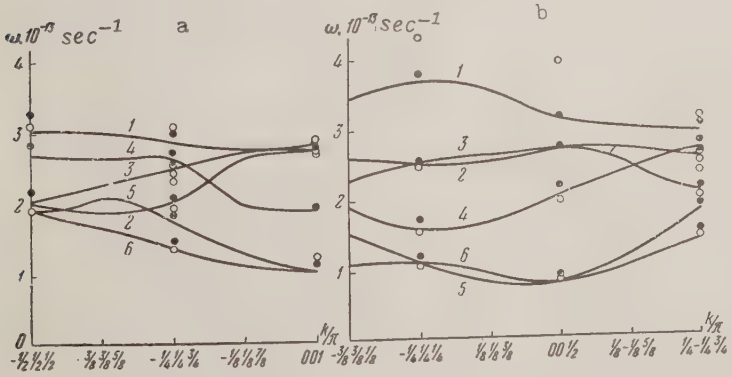

Fig.5. Frequencies $\omega_{\alpha K}$ for KCl. Notation as in Fig.2; wave vector directions as in Fig.2.

The results are shown in Figs.4 and 5, together with frequency data obtained by Jona[2] (circles). His values for ω_{1K} are overestimates for the same reason as are Kellermann's. The minor difference between Kucher's values and ours stems from the different crystal parameters used. The agreement with experiment of the temperature dependence of the specific heat obtained by Kycher[9] is somewhat worse than that found by Jona[2] (see Fig.6). The dependence of $\omega_{\sigma K}$ on K is stronger in this case than for NaCl (the ion masses are about equal) and a more important part here is played by the dipole moment P_1^l of the positive ion (which has a large polarizability α_1).

The calculations of $\omega_{\alpha K}$ and $u_s^{\alpha K}$, $P_s^{\alpha K}$ for KBr were first performed by the author in collaboration with Demidenko, student at the Kiev State University. The results are shown in Figs. 7 & 8. Fig.9 shows the theoretical and experimental temperature dependences of the specific heat. The experimental data were taken in all cases from Clusins et al[10].

Analysis of Figs.3,6 and 9 shows no advantage of the present treatment of a crystal as compared with the Born method where the theoretical specific heat is concerned. This might have been expected, since $C_V(T)$ is relatively insensitive to the detail of the frequency distribution. The merit of our method lies in the fact that it enables us to treat a

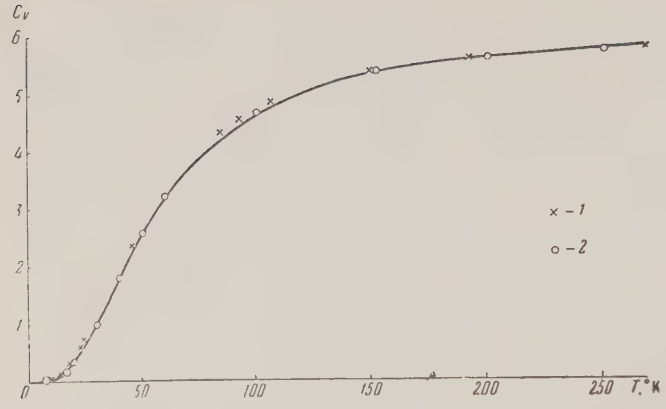

Fig.6. Temperature dependence of the specific heat of KCl: 1) results of Kucher, 2) results of Jona. Solid line - experimental data.

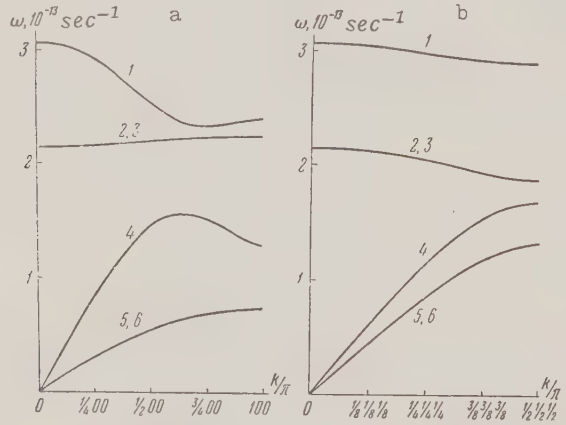

Fig.7. Frequencies $\omega_{\alpha K}$ for KBr. The directions of the wave vector as in Fig.1.

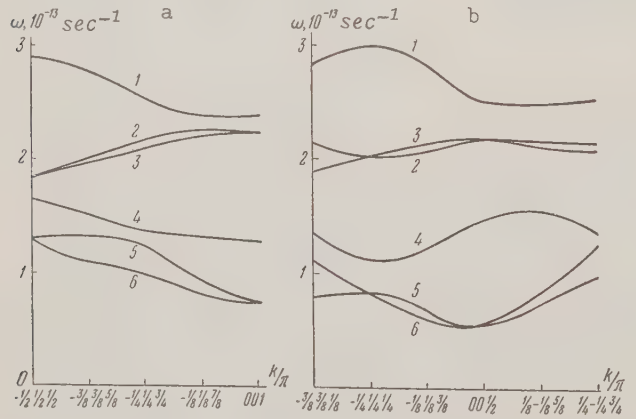

Fig.8. Frequencies $\omega_{\alpha K}$ for KBr. The directions of the wave vector as in Fig.2.

wider range of phenomena, namely, the optical, electrical, elastic and thermal properties of crystals, from a unified standpoint. In particular, our method can be used to obtain a more accurate expression for the generalized force $Q_{\alpha K}$, acting on the normal coordinate $q_{\alpha K}$ of the crystal as a result of the external field. If $q_{\alpha K}$ is defined by the expansion

$$\mathbf{p}_s^l = \sum_{\alpha K} \mathbf{p}_s^{\alpha K} q_{\alpha K} e^{iK \cdot r_s^l},$$ then the generalized force is given by

$$Q_{\alpha K} = \frac{e^2}{\mu} \sum_s E_s^{0K} \cdot (\mathbf{p}_s^{\alpha K} + \mathbf{P}_s^{\alpha K}), \quad (6)$$

where E_s^{0K} is the Fourier component of the external field and μ is the reduced mass of a pair of ions. The equation of motion for the coordinate $q_{\alpha K}$ is then[11]

$$\ddot{q}_{\alpha K} + \omega_{\alpha K}^2 q_{\alpha K} = Q_{\alpha K}. \quad (7)$$

Since for many values of K the quantities $\mathbf{p}_s^{\alpha K}$ and $\mathbf{P}_s^{\alpha K}$ are of the same order of magnitude, neglecting the ion polarizability would lead to large errors in determining the generalized "driving" force (i.e., the force forcing the vibrations). In the literature[12] the correct expression for $Q_{\alpha K}$ has been given only for the limiting case of extreme long wavelengths.

Calculations of the ion displacements under the influence of the "driving" force (utilizing the frequency data of Ref.7) have been carried out by Dykman[13] for the purpose of finding the half-width of the exciton absorption band in KCl

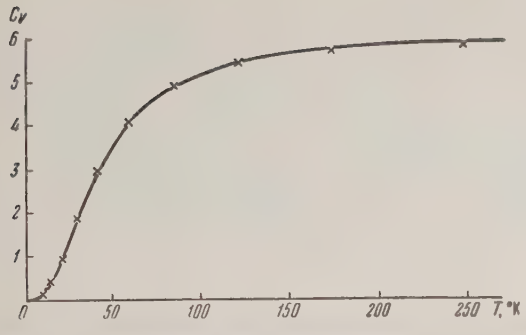

Fig.9. Temperature dependence of the specific heat of KBr: X - theoretical values; solid line - experimental values.

and by Dykman, Kaplunova & Tolpygo[14] to determine the exciton effective mass in KCl and NaCl. The effective mass value obtained was of the order of 10^4 m_e.

3. Theory of Homeopolar Crystals

A dependence of the exchange integrals on the dipole moments P_s^l, leading to an interdependence between these and the displacements u_s^l, should obviously also obtain in homeopolar crystals. In particular, in this case we will have interaction between the external electric field producing the polarization and the displacements of neutral atoms. Apparently, this is the interaction that is primarily responsible for infrared absorption by the lattice, as well as for the interaction of conduction electrons with the optical vibrations of homeopolar crystals.

Lax and Burstein[15] based their theory of infrared absorption in diamond, Si and Ge on the dependence of the dipole moment, produced by an external field, on the displacements of the atoms without specifying this dependence in any concrete way. A treatment similar to that of Section 1 leads to an expression equivalent to Eq.(4) in which U_{cou} contains only the interactions of different dipoles P_s^l (the atoms are neutral). In addition, the quantities $\beta_{ss'}$ and $u\,(\ldots R_{ss'}^{ll'}\ldots)$ have somewhat different properties.

As opposed to what happens in ionic crystals, when atoms are bound in a homeopolar crystal their electron shells undergo an appreciable deformation in connection with the formation of σ-bonds. Together with Mashkevich[16] the author carried out a calculation of U^0 for diamond type crystals. It was assumed that in the expansion (3) the first four states ψ_{si} correspond to the same principal quantum number for the valence electrons, so that the energy differences $E_{si}-E_{s1}$ are comparable with the interaction energy of the atoms. Accordingly, the first four coefficients C_{s1}^l are of order unity and are much greater than all the others. For simplicity, $C_{s1}^l \ldots C_{s4}^l$ were assumed to be independent of the displacement. From symmetry considerations, we deduced that the expansions of $\beta_{ss'}$ and $u\,(\ldots R_{ss'}^{ll'}\ldots)$ in powers of the displacements are of the form

$$\vec{\beta}_{ss'} = \vec{\beta}^0_{ss'} + b\,(\mathbf{u}_s^l - \mathbf{u}_{s'}^{l'}) + c\,\frac{(\mathbf{u}_s^l - \mathbf{u}_{s'}^{l'})\cdot \mathbf{r}_{ss'}^{ll'}}{|\,\mathbf{r}_{ss'}^{ll'}\,|^2}\,\mathbf{r}_{ss'}^{ll'},$$

$$u\,(\cdots \mathbf{R}_{ss'}^{ll'}\cdots) = u_0 + \frac{1}{2}\sum_{s'l'}^{(n)}\left\{g\,(\mathbf{u}_s^l - \mathbf{u}_{s'}^{l'})^2 + d\cdot\frac{[(\mathbf{u}_s^l - \mathbf{u}_{s'}^{l'})\cdot \mathbf{r}_{ss'}^{ll'}]^2}{|\,\mathbf{r}_{ss'}^{ll'}\,|^2}\right\}, \qquad (8)$$

where b, c, g and d are independent theoretical parameters. Like the polarizability coefficient α, they can be determined from the optical index of refraction n_0, the elastic constants C_{11}, C_{12} & C_{44} and the Raman frequency ω_0, which coincides with the limiting optical mode frequency.

Mashkevich has determined these parameters for diamond, silicon and germanium[17] and has studied the inherent vibration spectrum of these crystals at the limit of extreme long wavelengths (up to terms in a^2K^2 inclusive), taking retardation into account. In addition to three optical and three acoustical modes, there are also two so-called light modes for which almost

everywhere the $u_s^{(l)}$ are small and $\omega \approx cK/n_0$. In the region of the limiting frequency $\omega \approx \omega_0$, however, u_s^l is comparable with P_s^l and the function $\omega(K)$ is more complicated. In this case double refraction should obtain. The connection between displacements and dipole moments found in Ref.16 has been interpreted by Mashkevich[18] as the reason for light absorption in crystals as well as for scattering of conduction electrons by lattice vibrations. The absorption coefficient and electron mobility deduced by Mashkevich were of the right order of magnitude and the temperature dependence of the latter was given correctly.

4. Theory of Not Fully Polar Crystals

A careful comparison of theory with experiment[4] showed that the assumption that LiF, NaCl, KCl and KBr are entirely heteropolar crystals is justified. This is also true for CsCl, CrBr, TlCl, TlBr, AgCl, AgBr, and MgO. One may suppose that these crystals, in addition to their basic ion bonds, have a covalent bonds as was suggested by Eucken and Büchner[19]. In accord with the general statement of the problem, one may expect such crystals to be characterized by a general electron ψ-function[4] where the charges of the different atoms are fractional and a pure heteropolar compound simply represents an extreme limiting case.

Such a charge distribution can be described by the antisymmetrized product of the wave functions for a positive ψ_1^l- and a negative Φ_2^l-ion. We shall seek the latter in the form

$$\Phi_2^l = \delta^l \psi_2^l + \sum_{l'}^{(n)} \delta^{ll'} A \cdot C \cdot \psi_3^l \psi_4^{l'}, \tag{9}$$

where the ψ_2^l are the functions for an isolated negative ion, ψ_3^l is the function for this ion when it has lost an electron and $\psi_4^{l'}$ is the function of the electron which has passed from a negative to a positive ion. Close to the nucleus, this function is nearly identical with the function of a valence electron, but it falls off more rapidly with distance due to the denser packing of atoms in ionic crystals as compared with metals. The symbol A·C indicates the antisymmetrized product $\psi_3\,\psi_4$; the δ^l, $\delta^{ll'}$ are parameters to be determined from the variational principle. In most cases $|\delta^{ll'}| \ll 1$, since one of the configurations (ionic or atomic) has a lower mean energy. For weakly polar crystals, on the contrary, ψ_2^l is an atomic, and ψ_3^l an ionic (cation) state. The functions ψ_1, ψ_2 and ψ_3 are sought in the form of expansions such as Eq.(3); as for the last electron, it is more correct to consider ψ_4 fixed and to describe its polarization by changes in the coefficients δ^l and $\delta^{ll'}$. For binary crystals

$$U = \sum_l \left\{ \frac{(\dot{\mathbf{P}}_1^l)^2}{2\alpha_1} + \frac{(\mathbf{P}_2^l)^2}{2\bar{\alpha}_2} + \sum_{l'}^{(n)} (\vec{\beta}_{12} \cdot \mathbf{P}_1^l + \vec{\beta}_{21} \mathbf{P}_2^l) + \right.$$
$$\left. + u(\ldots \mathbf{R}_{ss'}^{ll'} \ldots) \right\} + U_{\text{cou}} + \sum_{sl} \bar{e}_s v(\mathbf{R}_s^l) - \sum_{sl} \mathbf{P}_s^l \cdot \mathbf{E}^0(\mathbf{R}_s^l), \tag{10}$$

$$\bar{\alpha}_2 = \alpha_2 - n(\alpha_2 - \alpha_3) |\delta^{ll'}|^2; \quad \bar{e}_s = e_s + (-1)^s en |\delta^{ll'}|^2, \tag{11}$$

where $\bar{\alpha}_2$ is the effective polarizability of the negative ion, α_3 is its polarizability in the state described by ψ_3, and $\bar{e}_s$ is the effective charge of the s-th ion. With some approximation, we may write

$$\delta^{ll'} = \frac{I_0 - R_0}{E_3 + E_4 - E_2 + \frac{2ll_1}{a}\,\alpha_M + e(\mathbf{r}_s^l) - v(\mathbf{r}_{s'}^{l'})}, \tag{12}$$

where α_M is the Madelung constant, E_2, E_3 and E_4 are the mean energies of the

ions in the states described by ψ_{20}, ψ_{30} and ψ_4, and R_o and I_o are the Coulomb and exchange integrals for transition of the electron from ion 2 to ion 1. For heteropolar crystals $E_3 + E_4 - E_2$ and $I_o - R_o$ are much less than the Madelung energy, and $|\delta^{ll'}| \ll 1$.

Eqs.(11) and (12) describe the experimentally observed difference between the polarizabilities of negative ions in different compounds (cf. Ref.20) and the pressure dependence of the polarizability (Ref.21). Furthermore, Eq.(12) indicates the additional polarizability of the crystal associated with alteration of the charges $\bar{e}_s$:

$$\Delta\alpha = \frac{a^3}{\alpha_M} \frac{e}{e_1} |\delta^{ll'}|^2. \tag{13}$$

Further development and verification of the theory require the knowledge of many parameters, for which the experimental data are insufficient.

5. Multiple-Electron Treatment of the Motion of an Excess Electron (Hole) in an Ionic Crystal

The motion of an excess electron introduced into the crystal, as has been shown by Pekar[12], is conveniently treated in the adiabatic approximation, when the state and energy of the internal electrons are functions of the coordinate r of the excess electron. This energy will be a periodic function $V_p(r)$ and can be eliminated by the effective-mass method. This treatment, however, is not practical for calculating states with small radii, when the effective-mass method is not applicable because $V_p(r)$ is not known. Furthermore, it is not useful in treating the motion of a hole, whose coordinate cannot be specified with an uncertainty less than a. It should also be noted that the motion of the excess electron within the region occupied by each ion takes place at practically the same rate as that of the internal electrons of this ion. Thus the conditions for the adiabatic approximation are not fulfilled.

One can, however, modify the adiabatic approximation and consider that only the electron motion from one ion to another is slow, while movement of the electron in the neighborhood of each nucleus is the same as in an isolated ion. The state of this ion will be described by antisymmetrized products $\psi_1^l \psi_4^l$ or $\psi_2^l \psi_5^l$, where ψ_1, ψ_2 and ψ_4 have the same meaning as in the previous sections, and ψ_5 is a function characterizing the motion of the excess electron in the neighborhood of a negative ion. In order to describe the adiabatic succession of the electron states as a function of the position of the excess electron, we introduce the subsidiary function

$$\Psi_s^l = A \cdot C \cdot \prod_{s'l'} \psi_{s'}^{l'} \cdot \psi_{4,5}^l(\rho) \tag{14}$$

and determine the form of all the $\psi_{s'}^{l'}$ from the condition that the mean Hamiltonian $\bar{H}$ satisfied by the Ψ_s^l of Eq.(14) be a minimum. Analogously, we can describe the state of a crystal with a hole at the l_s ion. In doing this, one of the ψ_s^l functions in the product $\Pi\psi_{s'}^{l'}$ should be replaced by the function $\bar{\psi}_s^l$ of an ion that lost an electron.

The calculation of $\bar{H}$ is performed the same way as in Section 1, using the expansion of Eq.(3). The equations for the dipole moments P_s^l are again of the form of Eq.(2), except that we must add both the field due to the excess charge (electron or hole) and that due to the crystal defect to the external field E^0. The P_s^l are found by Fourier expansion of (2). After finding $\psi_{s'}^{l'}$, the state of the electrons in the crystal should be sought in the form of the superposition

$$\Psi = \sum_{sl} b_s^l \Psi_s^l. \tag{15}$$

The coefficients b_s^l can be found from the variational principle by minimizing $\overline{H}$ with respect to the functions of Eq.(15). If the excess charge is in a band state, $b_s^l = b_s e^{iK \cdot r_s^l}$. For a local state of small radius, only a few of the b_s^l are nonzero and some of them are equal to each other due to symmetry.

Together with Kucher[22] the author found $\overline{H}$ for the case when one of the ions is absent and neutrality is assured by the presence of an additional electron or hole. In order to find the ground state of an electron or hole F-center of small radius, we determined the equilibrium displacements of the ions and expressed $\overline{H}$ in the form of a fourth order polynomial in one of the b_s^l coefficients. Further minimization of $\overline{H}$ with respect to b_s^l is feasible by numerical methods for one of the crystals whose inherent frequencies and amplitudes are known (see Section 2).

6. Motion of a Hole in a Homeopolar Crystal

Whereas in ionic crystals the removal of a single electron gives rise to a field acting on the remaining ions, in a homeopolar crystal the removal of one of the valence electrons destroys the interatomic bond. This leads to the appearance of a directed force between two neighboring atoms, and therefore to a distinctive kind of interaction between the hole and optical vibrations. It is thus necessary to reconsider the theory of hole mobility, which has so far been constructed in the same way as that for electrons. In the theory of Shockley and Bardeen, the role of the perturbation causing the interaction with long-wavelength acoustical phonons is played by the so-called deformation potential. But this approach cannot be used to account in turn for the interaction with optical vibrations. This interaction is usually considered weak, but if it is considered negligibly weak one cannot explain the observed deviation of the temperature dependence[23] of the mobility in Ge from the theoretical $T^{-3/2}$ dependence.

In collaboration with Fedorchenko[24] the author undertook a multiple-electron treatment of a hole in a crystal of the diamond type, without recourse to the "almost filled band" concept. The electron wave function was written in the form of the antisymmetrized product of functions of separate σ-bonds, as in Section 3 and Ref.16:

$$\psi_{ab}(\mathbf{r}_1\mathbf{r}_2\sigma_1\sigma_2) = [\psi_a(\mathbf{r}_1)\psi_b(\mathbf{r}_2) + \psi_a(\mathbf{r}_2)\psi_b(\mathbf{r}_1)]\chi_a(\sigma_1\sigma_2), \tag{16}$$

where a and b are the indices of the atoms, and $\mathbf{r}_1$, $\mathbf{r}_2$ are the coordinates and σ_1, σ_2 are the spins of the two electrons responsible for the σ-bond. If there is a hole localized on atom a with the indices l_s and bonds ab with number α, then in this product one of the ψ_{ab} functions should be replaced by $\psi_b(\mathbf{r}_2)[\alpha_b(\sigma_2) + \beta_b(\sigma_2)]$, where $\alpha(\sigma)$ and $\beta(\sigma)$ are elementary spin functions. We shall denote the corresponding auxiliary function of all the electrons by $\Psi_{ls\alpha}$ and set

$$\Psi = \sum_{ls\alpha} A_{ls\alpha} \Psi_{ls\alpha}, \tag{17}$$

where the $A_{ls\alpha}$ are coefficients to be determined. If all the atoms are at rest at the lattice sites, then

$$A_{ls\alpha} = A_{s\alpha} e^{iK \cdot r_s^l}.$$

where K is the sole wave vector that can be called the wave vector of the hole. Minimization of the mean Hamiltonian written in terms of the functions of Eq.(17) gives a set of eight equations for the coefficients A_{sx}. When we take account only of those exchange integrals which describe transition of the hole from one atom to another along a single bond or from one bond to another in the same atom, the atomic levels partially split into four bands and two double levels. The edges of the upper two bands contact each other, as do those of the lower pair of bands (Fig.10), and the two double levels coincide with the edges of the first and third bands. Close to the free edges of the bands the energy varies as K^2, and the hole can be assigned a single, unique effective mass. Thus the theory does not explain the more complex, experimentally observed[25] structure of the hole band; this may be due to failure to take into account the longer-range exchange integrals.

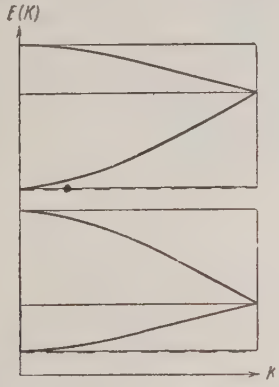

Fig.10. The distribution of hole bands in a diamond type crystal. The dash line indicates the position of the energy levels that do not split into bands.

In his dissertation Fedorchenko investigated the possibility of forming a self-consistent local state of a hole similar to a polar state by taking into account the dependence of the exchange integrals on displacement. He found that for reasonable values of the exchange integrals and the effective mass of a hole, such states with large radii are energetically improbable. This has also been shown[24] for states of small radius. This is related to the fact that in view of the short effective range of covalent forces, a hole can interact only with a small number of atoms at a time and the energy gain due to their displacement cannot come up to the kinetic energy increase associated with localization of the hole.

Finally, the interaction of a hole with atomic displacements was treated by perturbation theory. Separate calculations of acoustical and optical mode scattering of the band states of Eq.(17) gave the following temperature dependences of the mobility: in the first case (scattering by acoustical vibrations) $u \approx T^{-3/2}$ and in the second case (optical vibrations) $u \approx e^{\hbar\omega_0/kT}-1)$ or $u \approx T^{-5/2}$ (for low and high temperatures, i.e., $kT \ll \hbar\omega_0$ and $kT \gg \hbar\omega_0$, respectively). This should lead to an overall temperature variation of the mobility more rapid than $T^{-3/2}$. At low temperatures, scattering by acoustical vibrations predominates and the mean free path of a hole is not velocity dependent. At high temperatures scattering by optical vibrations is also significant and the mean free path is inversely proportional to the square of the velocity. This should lead to some change in the temperature dependence of such parameters as the thermo-emf and the Nernst-Ettingshausen coefficient, which, for a relation of the form $l \simeq v^n$ between the mean free path and the velocity, are characterized by[26]

$$\alpha = \frac{k}{e}\left\{\frac{n}{2}+2+\ln\frac{2(2\pi m^* kT)^{3/2}}{\hbar^3 N}\right\};\quad V_n = \frac{n-1}{2}\frac{kT}{e}\sigma RH\frac{dT}{dx}. \qquad (18)$$

As T increases, n changes from n = 0 to n = -2.

7. Generation of Lattice Vibrations by a Fast-Moving Polaron

As we have shown elsewhere[27], when one takes account of the finite wavelength of the vibrations, not only the longitudinal optical, but also the transverse optical and the acoustical vibrations possess longitudinal dipole moments

(of the order of a^2K^2 for alkali halide crystals). They will therefore interact with an electron in the polaron state. For a stationary polaron this should lead to a certain correction to its energy. For a fast-moving polaron, resonance between the "driving force" and the natural oscillations will occur earlier for transverse optical and acoustical vibrations, whose frequencies are 1.5-2 times lower than the limiting frequency of the longitudinal vibrations. This will involve energy transfer from the polaron to the lattice vibrations.

A quantitative investigation of this effect has been carried out by the author and Uritskii[28], using the following approximation. The polaron is assumed to have a large radius, so that its state is determined primarily by its interaction with longitudinal optical vibrations. The polaron velocity V is restricted by the condition that for most of the Fourier components in the expansion of the polaron field D(r), namely, in the expansion

$$\mathbf{D}(\mathbf{r}) = \sum_{\mathbf{K}} \mathbf{D}(\mathbf{K})\, e^{i\mathbf{K}\cdot\mathbf{r}} \tag{19}$$

the resonance condition $\omega_{\alpha K} = \mathbf{K}\cdot\mathbf{V}$ does not obtain. Thus the energy transfer to lattice vibrations realized due to the "tail" of the Fourier expansion (19) at large K and the polaron ψ-function may be considered velocity independent.

Since for a moving polaron $\psi(\mathbf{r}) \to \psi(\mathbf{r}-\mathbf{vt})$, as $\mathbf{D}(\mathbf{r}) \to \mathbf{D}(\mathbf{r}-\mathbf{vt})$,

$$\mathbf{D}(\mathbf{K}) \to \mathbf{D}(\mathbf{K})\, e^{-i\mathbf{K}\cdot\mathbf{v}t}.$$

The force acting on the normal coordinates $q_{\alpha K}$, according to Eq.(6), becomes

$$Q_{\alpha K} = \frac{e^2}{\mu} \sum_s \mathbf{D}(\mathbf{K}) \cdot (\mathbf{p}_s^{\alpha K} + \mathbf{P}_s^{\alpha K})\, e^{-i\mathbf{K}\cdot\mathbf{v}t} = Q_{\alpha K}^0 e^{-i\mathbf{K}\cdot\mathbf{v}t}. \tag{20}$$

The solution of Eq.(7) for forced vibrations is then

$$q_{\alpha K} = \frac{Q_{\alpha K}^0}{\omega_{\alpha K} - (\mathbf{K}\cdot\mathbf{v})^2} \{\cos \mathbf{K}\cdot\mathbf{v}\, t - \cos \omega_{\alpha K} t - i \sin \mathbf{K}\cdot\mathbf{v}t + b_{\alpha K} \sin(\omega_{\alpha K} t + \beta_{\alpha K})\}. \tag{21}$$

According to Eq.(21), the work done by the polaron on the crystal per unit time, as $t \to \infty$, is the sum of the work for each mode:

$$A_\alpha = \frac{N^2 \mu \Delta}{8\pi e^2} \frac{1}{v} \int |\, Q_{\alpha K}^0(K, \vartheta_\alpha)\,|^2 K\, dK, \tag{22}$$

where ϑ_α is the resonance value of the angle given by $\cos\vartheta_\alpha = \frac{\omega_{\alpha K}}{Kv}$ or $\frac{C_\alpha}{v}$ for the optical and acoustical modes, respectively, where C_α is the velocity of sound for the α-th mode. For the acoustical modes, Eq.(22) gives the basic velocity dependence, namely,

$$A_\alpha = \frac{A_\alpha^0 C_\alpha}{v} \quad \text{when} \quad v > C_\alpha \quad \text{and} \quad A_\alpha = 0 \quad \text{when} \quad v < C_\alpha.$$

The results of calculations for NaCl, KCl and KBr, based on a Gaussian polaron function $\psi(r) \approx e^{-\alpha r^2}$, are shown in Fig.11. For a more exact polaron function such as $\psi(r) \approx (1 + \alpha r + \beta r^2)\, e^{-\alpha r}$ obtained by Pekar[12], the polaron energy loss was calculated by A.M.Nosar, student at the Kiev State University. The results obtained are shown in Fig.12.

As can be seen from the figures, at low polaron velocities ($v \leqslant 2\text{-}4 \cdot 10^5$ cm/sec) primarily acoustical and transverse optical vibrations are generated. At velocities over $5\text{-}10 \cdot 10^5$ cm/sec the generation of longitudinal optical

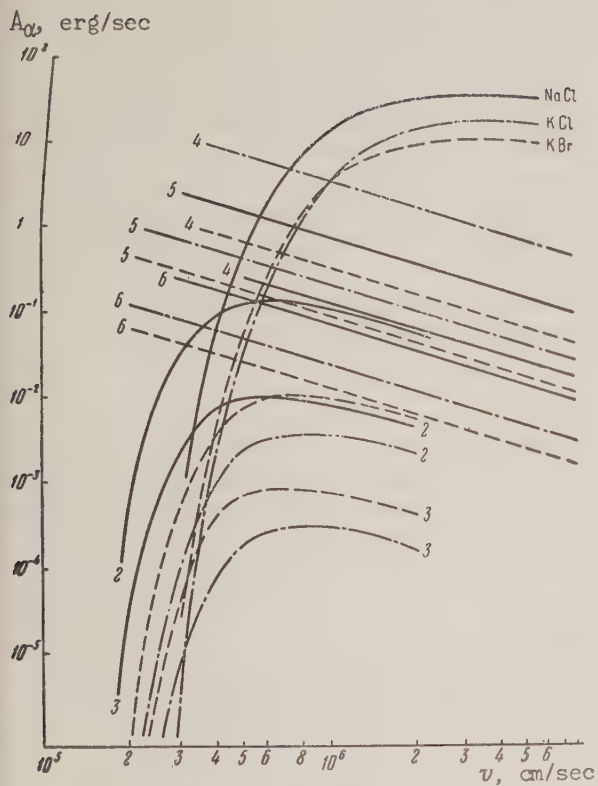

Fig.11. Energy loss per unit time by a moving polaron in NaCl, KCl and KBr assuming a Gaussian polaron function.

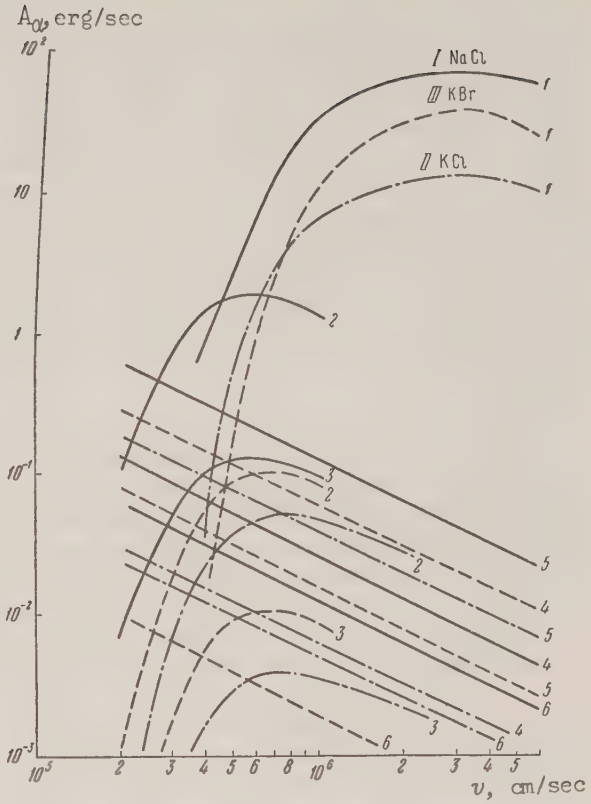

Fig.12. Energy loss by a moving polaron whose ψ-function is that given by Pekar[12].

vibrations predominates. In this case, for the more exact polaron function A_α decreases more slowly with decreasing v.

These results, particularly if first refined by taking account of the velocity dependence of the polaron ψ-function, should prove useful for formulating a polaron theory of breakthrough of ionic dielectrics.

8. Forbidden Band Widths in Polaron Theory

Tiablikov[29,30] has suggested that the polaron spectrum should have a band-like character with allowed band widths some two-three orders of magnitude smaller than the usual Brillouin zones. According to Tiablikov's choice of wave functions[30] (translation of a small-radius polaron function from site to site, together with crystal polarization), the forbidden band width should be of the order of the separation between the levels of a hydrogen-like atom. Tiablikov gives no more precise quantitative calculations. One cannot, however, agree with his assertions, since his treatment[30] of the polaron is not consistent. Actually the polarization radius of a polaron amounts to no less than 2-3 lattice constants and, as has been noted by Pekar, the polaron center may occupy any position in the lattice, i.e., need not coincide with lattice site as implied by Tiablikov. Consequently, in view of translational symmetry (with arbitrary translation vector) there is obtained from a single electron level not one, but an infinite number of narrow close-

lying bands. If the widths of the forbidden bands are $\ll kT$, the presence of such bands will lead to no attributes distinctive from those associated with a continuous spectrum. There is, therefore, no justification for Tiablikov's[31] earlier treatment of thermionic emission from semiconductors based on taking account of only one polaron band.

Together with Gitterman[32], the author performed a quantitative investigation of polaron bands for the case of a polaron of sufficiently large radius, when the wave function in the zeroth approximation can be found by the effective mass method and the energy in the first approximation is defined as the mean (expectation) value of the exact Hamiltonian (including the periodic potential) for the zeroth approximation wave functions.

According to the effective-mass method, the electron wave function in a crystal with a periodic potential $V_p(r)$, perturbed by a smooth potential $W(r)$, can be written

$$\psi(\mathbf{r}) = \sum_K a_K \psi_K(r), \tag{23}$$

where $\psi_K = e^{-iK\cdot r} u_K(\mathbf{r})$ is a Bloch function, and the a_K are the plane-wave expansion coefficients of the sybsidiary function $\varphi(r)$, which is a solution of the Schroedinger equation with effective mass m^*:

$$-\frac{\hbar^2}{2m^*}\Delta\varphi + W(\mathbf{r})\varphi = \varepsilon_0\varphi. \tag{24}$$

In the first approximation the energy is

$$\varepsilon_1 = \int \psi^* \left[-\frac{\hbar^2}{2m}\Delta + V_p(\mathbf{r}) + W(\mathbf{r})\right]\psi\, d\tau = \sum_K |a_K|^2 E_K + \\ + \sum_{KK'} a^*_{K'} a_K \int e^{-i(K'-K)\cdot r} u^*_{K'}(\mathbf{r})\, W(\mathbf{r})\, u_{K'}(r)\, d\tau, \tag{25}$$

where E_K are the energy eigenvalues corresponding to the states ψ_K.

If the polaron center is at a point ξ, then

$$\varphi(\mathbf{r}) = \varphi_0(\mathbf{r} - \xi) \quad \text{and} \quad a_K = a^0_K e^{-iK\vec{\xi}}, \tag{26}$$

where $\varphi_0(\mathbf{r})$ is the function of a polaron at rest at the origin. Eqs.(25) and (26) give the dependence of the polaron energy on the position $\vec{\xi}$ of its center (periodic). The further investigation of the polaron motion can be performed in the adiabatic approximation[12], when $\varepsilon_1(\vec{\xi})$ plays the role of potential energy. The motion is then described by the equation

$$\left[-\frac{\hbar^2}{2M}\Delta_\xi + \varepsilon_1(\vec{\xi})\right]\Phi = E\Phi, \tag{27}$$

where M is the effective mass of the polaron. In Pekar's theory[12] $\varepsilon_1(\vec{\xi})$ was neglected and the solution of Eq.(27) was written in the form of plane waves

$$\Phi \approx e^{iK\cdot\vec{\xi}} \quad \text{and} \quad E = \frac{\hbar^2}{2M}K^2. \tag{28}$$

If in the expansion $\varepsilon_1(\xi) = \sum_g \varepsilon_g e^{ig\cdot\xi}$, where g is a reciprocal lattice vector, all the ε_g with $g \neq 0$ are considered small, then in the weak electron coupling approximation, the forbidden band widths are $2|\varepsilon_g|$. A specific calculation of ε_g was performed on the assumption that

$$u_{\mathbf{K}}(\mathbf{r}) = \sum_{l} e^{-i\mathbf{K}\cdot\mathbf{r}_1^l}\psi_\alpha(\mathbf{r} - \mathbf{r}_1^l), \tag{29}$$

where the ψ_a are the atomic functions at positive sites whose coordinates are given by $\mathbf{r}_1^l$. The function $W(\mathbf{r})$, which is a polarization potential, was calculated on the assumption that the electron charge density is $|\psi|^2$, rather than $|\varphi(\mathbf{r})|^2$, as commonly approximated in the macroscopic theory[12]. Neglecting the dispersion of the inherent frequencies of the crystal, we obtained

$$\varepsilon_g = -\frac{8\pi^2 e^2 N^3 e^2}{\omega^2 \mu} \sum_{ss'} \vec{\pi}_{s-\vec{\varkappa}} \vec{\pi}_{s'\vec{\varkappa}} \sum_{\mathbf{K}\mathbf{K}'\vec{\varkappa}} \sum_{\mathbf{q}\mathbf{q}'\mathbf{p}\mathbf{p}'\mathbf{p}''} a^0_{\mathbf{K}} a^0_{\mathbf{K}'} a^{0*}_{\mathbf{K}'+\vec{\varkappa}+\mathbf{p}-\mathbf{p}'+\mathbf{p}''} \times$$

$$\times\, a^{0*}_{\mathbf{K}-\vec{\varkappa}-\mathbf{p}+\mathbf{p}'-\mathbf{p}''+\mathbf{g}} \cdot \psi_{\mathbf{K}+\mathbf{q}} \psi_{\mathbf{K}'+\mathbf{p}} \psi^*_{\mathbf{K}'+\vec{\varkappa}+\mathbf{p}+\mathbf{p}''} \psi^*_{\mathbf{K}-\vec{\varkappa}-\mathbf{p}-\mathbf{p}'-\mathbf{p}''+\mathbf{q}'+\mathbf{g}} \times$$

$$\times \frac{(\mathbf{p}''+\vec{\varkappa})\cdot(\mathbf{p}''+\mathbf{p}+\mathbf{q}-\mathbf{p}'-\mathbf{q}'-\mathbf{g}+\vec{\varkappa})}{(\mathbf{p}''+\vec{\varkappa})^2(\mathbf{p}''+\mathbf{p}+\mathbf{q}-\mathbf{p}'-\mathbf{q}'-\mathbf{g}+\vec{\varkappa})^2} e^{-i\mathbf{p}''\cdot\mathbf{r}_{s'}+i(\mathbf{p}''+\mathbf{q}+\mathbf{p}-\mathbf{p}'-\mathbf{q}'-\mathbf{g})\mathbf{r}_s}, \tag{30}$$

where $\mathbf{q}, \mathbf{q}', \mathbf{p}, \mathbf{p}', \mathbf{p}''$ and $\mathbf{g}$ are reciprocal lattice vectors, the $\psi_{\mathbf{K}+\mathbf{q}}$ are the Fourier components of the expansion of the atomic function $\psi_a(\mathbf{r})$, ω is the limiting frequency of the longitudinal optical vibrations of the lattice, the $\vec{\pi}_{s\vec{\varkappa}}$ are the amplitudes of the natural vibrations of ions of the s-th kind belonging to the $\vec{\varkappa}$-th wave vector, and N is the number of cells in the base region. The computations of ε_g were carried out for NaCl, KCl, KBr and KI, using the functions for Na and K obtained by Fock and Petraschen[33] and Hartree and Hartree[34]. The polaron function was approximated by a Gaussian. On retaining only the main terms in the sum of Eq.(30), the values obtained for the first forbidden band were ε_g = 0.00627, -0.000101, -0.0000386 and -0.0000427 ev, respectively.

Thus with the exception of NaCl, the forbidden band width $2|\varepsilon_g|$ proves to be much smaller than both the minimum $\frac{3\hbar^2\pi^2}{2Ma^2}$ and the maximum $\frac{5\hbar^2\pi^2}{2Ma^2}$ width of the allowed band. Therefore the first and second allowed bands must overlap. All the other successive forbidden bands should be even narrower.

Thus for crystals with polarons of relatively large radii, Eq.(28) of the macroscopic theory is virtually correct. For polarons of smaller radius (in NaCl and in particular in LiF and BaO) the approximation of quasi-free electrons becomes inapplicable, since the oscillations of $\varepsilon_1(\xi)$ are comparable with the kinetic energy. Here reliable data on the structure of the polaron spectrum can be obtained only after the development of a small-radius polaron theory. For a stationary polaron this can be done using the methods of Section 5. The problem of the motion of a small-radius polaron is more complicated.

Institute of Physics of the
Ukrainian SSR Academy of Sciences

References

1. E.W.Kellerman, Phil.Trans.Roy.Soc., A 238,513 (1940); Proc.Roy.Soc., A 178, 17 (1941).
2. M.Jona, Phys.Rev., 60, 822 (1941).
3. M.Born & M.Geppert-Mayer, Theory of Solids (in Russian trans. M.1938).
4. K.B.Tolpygo and others, Trudy (Transactions) Inst. of Phys., Ukrainian SSR Ac. of Sci., No.5, 28 (1954).
5. K.B.Tolpygo & I.G.Zaslavskaia, Ukr.fiz.zhurn. (Ukrainian Physical Journal) 1, 226 (1956).
6. I.G.Zaslavskaia, Ukr.fiz.zhurn.(Ukrainian Physical Journal) 1, 366 (1956).
7. K.B.Tolpygo & I.G.Zaslavskaia, Trudy (Transactions) Inst. of Phys., Ukrainian SSR Ac. of Sci., No.4, 71 (1953).
8. T.I.Kucher, Zhur.eksp.i teor.fiz., 32, 152 (1957).
9. T.I.Kucher & K.B.Tolpygo, Zhur.eksp.i teor.fiz., 31, 1002 (1956).
10. K.Clusins, J.Goldmann & A.Perlick, ZS.f.Naturforsch, 4a, H, 6, 424 (1949).
11. K.B.Tolpygo, Trudy (Transactions) Kiev State Univ.Math.Collection, No.5, 99 (1951).
12. S.I.Pekar, Issledovaniia po elektronnoi elektronnoi teorii kristallov (Studies in the electron theory of crystals), M.-L., 1951.
13. I.M.Dykman, Trudy (Transactions) Inst. of Phys. Ukrainian SSR Ac. of Sci., No.5, 48 (1954).
14. I.M.Dykman, E.I.Kaplunova & K.B.Tolpygo, Zhur.tekh.fiz., 26, 2459 (1956).
15. M.Lax & E.Burstein, Phys.Rev., 97, 1, 39 (1955).
16. V.S.Mashkevich & K.B.Tolpygo, Doklady AN SSSR, 111, 575 (1956).
17. V.S.Mashkevich, Zhur.eksp.i teor.fiz., 32, 4 (1957).
18. V.S.Mashkevich, Optika i spektroskopiia (Optics & Spectroscopy) (1957).
19. A.Euken & A.Buchner, ZS.f.Phys.Chem., 27, 231 (1934).
20. K.B.Tolpygo, Zhur.eksp.i teor.fiz., 20, 497 (1950).
21. E.Burstein & P.L.Smith, Phys.Rev., 74, 229 (1948).
22. T.I.Kucher & K.B.Tolpygo, Zhur.eksp.i teor.fiz., 31, 1002 (1956).
23. W.C.Dunlap, Phys.Rev., 79, 286 (1950).
24. K.B.Tolpygo & A.M.Fedorchenko, Zhur.eksp.i teor.fiz., 31, 845 (1956).
25. F.G.Morin, Phys.Rev., 93, 1, 62 (1954).
26. K.B.Tolpygo, Trudy (Transactions) Inst.of Phys.Ukrainian Ac. of Sci., No.3, 52 (1952).
27. K.B.Tolpygo, Trudy (Transactions) Inst. of Phys. Ukrainian Ac. of Sci., No.6, 102 (1955).
28. K.B.Tolpygo & Z.I.Uritskii, Zhur.eksp.i teor.fiz., 30, 929 (1956).
29. S.V.Tiablikov, Zhur.eksp.i teor.fiz., 21, 337 (1951).
30. S.V.Tiablikov, Zhur.eksp.i teor.fiz., 23, 381 (1952).
31. Soveshchanie po teorii poluprovodnikov (Conference on semiconductor theory), Zhur.eksp.i teor.fiz., 25, 2381 (1955).
32. M.S.Gitterman & K.B.Tolpygo, Zhur.eksp.i teor.fiz., 32, 4 (1957).
33. W.A.Fock & M.Petraschen, Phys.ZS.d.Sow.Un., 6, 368 (1934).
34. D.R.Artree & W.Hartree, Proc.Cambr.Phil.Soc., 34, 550 (1938).

DISCUSSION

V.S.Mashkevich. We investigated the equations of motion corresponding to the crystal energies whose determination was discussed in the report we just heard. The equations were solved by a method of successive approximation for long wavelengths. The principal results are the following.

The vibration spectrum consists of eight branches or modes: three acoustical, three optical, and two which we have called light modes. For the optical modes, in the zeroth approximation the displacements and dipole moments of the atoms are nonzero, but the dipole moment of the unit cell vanishes. The light modes characterize the propagation of infrared light in the crystal: the displacements are equal to zero, but the dipole moment of the cell is nonzero. In a certain wavelength region the optical and light modes go over into one another. Here both the atomic displacements and the dipole moment of the cell are nonzero. This fact makes it possible to explain the experimentally observed absorption of light by lattice vibrations in diamond, silicon and germanium. The mechanism of light absorption by lattice vibrations in homeopolar crystals differs substantially from that in ionic crystals. The amount of absorption is determined not by the anharmonicity, as in ionic crystals, but by the transformation of the energy of the dipole moments to that of atomic vibrations. Numerical calculations yield agreement with experiment at least as regards order of magnitude.

Pleochroism should be observed. In particular, if the light propagates along the diagonal of a face of the lattice cube, the component whose electric vector lies in the plane of this face should undergo no absorption at all.

There should be appreciable double refraction in the infrared region of the spectrum, and the crystal proves to be heptaxial.

Thus in the infrared absorption region, diamond, Si, and Ge should exhibit strong optical anisotropy. We have seen no experimental studies of this anisotropy. This may be due to the fact that cubic crystals are commonly considered to be optically isotropic. In order to test the deduction regarding optical anisotropy, we used the methods of group theory to investigate the most general equations of motion. We obtained the same qualitative results. Thus if it is assumed that the state of a diamond type crystal is described by the displacements and dipole moments of the atoms (which would appear to be correct for infrared optics) then from general considerations we are led - with no specific restrictions - to absorption of light by lattice vibrations, strong pleochroism, and double refraction. It would be interesting to subject these theoretical deductions to experimental tests.

We also investigated the lattice vibration scattering of conduction electrons, associated with the longitudinal component of the dipole moment. Scattering by acoustical vibrations gives the usual 3/2-law for the temperature dependence of the mobility. An exponential dependence is obtained for optical mode scattering. Numerical calculations yield good agreement with experiment.

THEORY OF EXCITONS IN IONIC CRYSTALS

- I.M.Dykman

1. The investigations of E.F.Gross and a number of other authors have by now furnished ample proof of the existence of excitons, which were first examined theoretically by Ia.I.Frenkel' in 1931. If as a result of the absorption of a photon the orbit radius of an optical electron becomes larger than the lattice constant, this electron can be treated as a conduction electron localized in the Coulomb field of the ionic residue (the hole). The relative motion of the electron and hole can be characterized by a hydrogen-like Hamiltonian.

In the bound state the electron and hole are not current carriers. Therefore the absorption of light associated with the formation of excitons should not be accompanied by photoconductivity. The absence of photoconductivity in pure crystals in the case of exciton type absorptions has, in fact, been substantiated experimentally. Often, however, instead of the discrete lines, which should appear in the case of light absorption by hydrogen-like particles, rather wide bands are observed. This broadening of the spectral lines may be attributed to ionic vibrations.

In Ref. 1 S.I.Pekar and the writer solved the problem of the interaction of an exciton with lattice vibrations for an ionic crystal. It was assumed that the radius of the orbit of the electron and the hole is so large that the interaction may be treated as an interaction between two opposite point charges in a continuous medium. The problem was solved by the direct variational method by finding the extrema of the energy functional.

It was found that two types of excitons may be formed in crystals, depending on the values of $k = \mu_2/\mu_1$ and n^2c (where μ_1 and μ_2 are the effective masses of the electron and hole, n is the index of refraction of the crystal and c is a constant from polaron theory). Excitons of one type do not polarize the crystal on the average and their motion through the crystal is not related to ion inertia. Such excitons have a hydrogen-like atom type absorption spectrum consisting of narrow lines. They were called nonpolarizing excitons.

Excitons of the other type - called polarizing excitons - interact strongly with the ions of the lattice. The self-consistent inertial polarization which results in the crystal represents a potential well for the exciton, a well in which it can be localized.

Polarizing excitons are formed only when their energy level lies below the corresponding level of a nonpolarizing exciton. When $k < 8$, formation of polarizing excitons in the 1s-state is generally impossible. The conditions for formation of polarizing excitons in more highly excited states are less rigorous. It follows that in some crystals nonpolarizing excitons are formed in the lower energy states and polarizing excitons are produced in higher lying ones. The absorption spectrum in such cases will consist of narrow lines at the red end and, at the violet end, of bands associated with the absorption by polarizing excitons interacting strongly with lattice vibrations.

2. When the effective radius of the electron and hole is less than the lattice constant, the macroscopic method of calculation is no longer applicable. In this case the crystal polarization must be determined by a detailed calculation taking into account the microscopic structure of the crystal. This pertains, in particular, to excitons in alkali halide crystals.

The writer[2] has given an exciton model for alkali halide crystals in which the exciton is represented as a positive point charge +e at the site of a halide ion and six negative charges of -(1/6)e at the six closest metal ions.

Calculation led to a half-width for the exciton absorption band in KCl crystal of the order of tenths of an electronvolt, which, in so far as one can judge, is in agreement with the experimental data[3]. Such a large half-width is evidence of strong interaction between excitons and lattice vibrations in alkali halide crystals. Calculations indicate that as the temperature is reduced the half-width decreases and at T = 0 is about $1/\sqrt{3}$ that at room temperature.

3. It can be shown that when they do form polarizing excitons can be localized at arbitrary points in the crystal. The exciton problem here is characterized by translational degeneracy, i.e., the exciton may move through the crystal together with the local inertial polarization which it creates. This type of motion is wholly analogous to the motion of polarons and, as in polaron theory, the effective mass of the exciton in the macroscopic treatment can be written

$$M = \frac{c}{4\pi\omega^2}\int\left(\frac{\partial D}{\partial x'}\right)^2 d\tau' \qquad (1)$$

(where ω is the inherent frequency, and D is the field induction vector).

Simple calculations performed on the basis of Eq.(1) give the following expression for the exciton effective mass in terms of the quantities x_0, y_0 introduced in Ref.1:

$$M = \frac{4k^2e^2}{\pi^2n^8\omega^2(1+k)}\left(\frac{\mu_1 e^2}{\hbar^2}\right)^3 x_0^2 y_0^2. \qquad (2)$$

Eq.(2) holds only when the macroscopic method of calculation is applicable. Applied to alkali halide crystals (2) yields $M \approx 10^6\ m_e$. This value is probably much too high since, as has already been mentioned, the macroscopic method is not really valid for these crystals.

Let us try to evaluate the order of magnitude of the exciton effective mass in alkali halide crystals using the model mentioned above. We assume that, as in the case of polaron motion, the exciton effective mass is determined primarily by ion inertia, rather than by the electron transition. Then treating ion motion classically, it can be shown that the variation with time of the generalized force $Q_{\alpha\varkappa}$ is given by

$$Q_{\alpha\vec{\varkappa}}(t) = e^{-i\vec{\varkappa}\vec{v}t}Q_{\alpha\vec{\varkappa}}, \qquad (3)$$

where v is the exciton velocity and $Q_{\alpha\vec{\varkappa}}$ is the generalized force for an exciton at rest, previously calculated by the author in Ref.2. Here α is the number of the vibration mode, and $\vec{\varkappa}$ is the wave vector.

The inertial part of the energy of a crystal (consisting of N pairs of ions) including the exciton-ion interaction energy is given by

$$H = -\frac{N}{2}\sum_{\alpha,\vec{\varkappa}}\frac{Q^*_{\alpha\vec{\varkappa}}q_{\alpha\vec{\varkappa}}\omega^2_{\alpha\vec{\varkappa}}}{[\omega^2_{\alpha\vec{\varkappa}} - (\vec{\varkappa}\vec{v})^2]^2}[\omega^2_{\alpha\vec{\varkappa}} - 3(\vec{\varkappa}\vec{v})^2]. \qquad (4)$$

If the velocity is low, H may be expanded in powers of v. Equating the term proportional to v^2 to the kinetic energy $Mv^2/2$, we obtain the following formula for the exciton effective mass:

$$M = \frac{N}{3}\sum_{\alpha\vec{\varkappa}} Q^*_{\alpha\vec{\varkappa}}q_{\alpha\vec{\varkappa}}\frac{\varkappa^2}{\omega^2_{\alpha\vec{\varkappa}}}. \qquad (5)$$

Eq.(5) gives exciton effective masses of $1.0 \cdot 10^4$ and $0.9 \cdot 10^4$ m_e in KCl and NaCl crystals, respectively. The exact value of the effective mass can be obtained by quantum mechanical calculation taking into account the electron eigenfunction.

Institute of Physics of the
Ukrainian SSR Academy of Sciences

References

1. L.M.Dykman & S.I.Pekar, Trudy (Transactions) Institute of Physics, Ukrainian SSR Ac. of Sci., 3, 92 (1952).
2. I.M.Dykman, Zhur.eksp.i teor.fiz., 26, 307 (1954).
3. R.Hilsch & R.W.Pohl, ZS.f.Phys., 59, 812 (1930).

INTERACTION OF LOCALIZED ELECTRONS WITH ACOUSTICAL VIBRATIONS IN HOMEOPOLAR CRYSTALS (Abstract)

- M.F.Deigen

Investigations of the energy distribution of electrons localized in the vicinity of a defect in a homeopolar crystal have usually been restricted to the solution of the hydrogen-like problem. If one does not take account of electron-lattice vibration interaction, however, it is impossible to evaluate the absorption band width of local centers, the difference between the thermal dissociation or photodissociation energies, etc.

In the present report we consider the interaction of localized electrons with the acoustical vibrations of the lattice on the basis of the "condenson" mechanism[1], which can be described as follows: let there be a region of enhanced density due to local elastic deformation in the crystal. In view of the increased density the region will also be characterized by an elevated dielectric constant. According to macroscopic electrostatics, electrons will be pulled into this region. Hence the high density region will act as a potential well for the electron, for it will not follow the electron motion due to the inertia of the atoms.

The Hamiltonian of such a system can be written

$$H = -\frac{\hbar^2}{2\mu}\Delta + Q(r) + v(r) + \hat{H}_{ac}.$$

Here we have used the effective-mass method[2].

In the above equation $Q(r)$ is the energy of the electron in the defect field, $\hat{H}_{ac}$ is the Hamiltonian of acoustical lattice vibrations, and $v(r)$ is the interaction energy between the electron and the deformed region of the crystal (condenson interaction energy).

A solution of the Schrödinger equation corresponding to the above Hamiltonian determines the energy levels and wave functions of the system.

We have found the parameters of the $1s$- and $2p$-states, as well as the thermal dissociation energy of a localized electron.

It was found that for homeopolar crystals (as for ionic) the photodissociation energy has a larger absolute value than the thermal dissociation energy. The results of Pekar and Krivoglaz[3] can be used to obtain the parameters of the band associated with light absorption by impurity atoms. Calculations show that the half-width of the absorption curve due to the condenson interaction may be appreciable even at absolute zero.

Institute of Physics of the
Ukrainian SSR Academy of Sciences

References

1. M.F.Deigen, Zhur.eksp.i teor.fiz., 31, 24 (1956).
2. S.I.Pekar, Zhur.eksp.i teor.fiz., 16, 993 (1946).
3. S.I.Pekar, M.A.Krivoglaz, Trudy (Transactions), Institute of Physics, Ukrainian SSR Ac. of Sci., 4, 37 (1953).

STATE OF AN IMPURITY-CENTER ELECTRON IN AN ANISOTROPIC CRYSTAL
(Abstract - Complete report in Zhur. eksp. i teor. fiz., 25, 2044 (1955))
- A.I.Ansel'm & L.I.Korovin

The stationary states of an electron in an impurity center of an atomic semiconductor are considered taking into account the tensor character of both the electron effective mass and the dielectric constant.

The energy levels and wave functions of the ground and excited states are calculated by the direct variational method.

* * * * * *

CONTRIBUTION TO THE THEORY OF RECOMBINATION OF ELECTRONS WITH IMPURITY CENTERS IN IONIC CRYSTALS (Abstract)
- Iu.E.Perlin

The highly excited states of an impurity center are treated as the motion of a polaron in the Coulomb field of a defect. The single-quantum scattering operator raises a polaron having an energy less than $\hbar\omega$ from the continuous spectrum state to high-lying levels of the discrete spectrum.

The probability of capture is evaluated and the temperature dependence of the polaron lifetime is determined. The applicability of the diffusion recombination theory to trapping by Coulomb impurity centers is discussed.

Department of Theoretical Physics,
Kishenevsk State University

* * * * * *

THERMOMAGNETIC AND GALVANOMAGNETIC EFFECTS IN SEMICONDUCTORS TAKING INTO ACCOUNT VARIATIONS IN THE CURRENT CARRIER CONCENTRATION
(Abstract - Complete report in Zhur. tekh. fiz., 26, 22 & 36 (1956)
- G.E.Pikus

Thermo- and galvanomagnetic effects in semiconductors with current carriers of both types are considered. Account is taken of changes in the concentration of electron-hole pairs both in weak fields when the pair concentration differs little from the equilibrium one and in strong magnetic fields when $uH/C \gg 1$ (u is the mobility and H is the magnetic field intensity).

The influence of deviations from the equilibrium concentration in the electron and exciton thermal conductivities is also investigated.

* * * * * *

RECOMBINATION IN SEMICONDUCTORS INCIDENT TO COLLISION OF CURRENT CARRIERS

- L.Sosnowski

An exact knowledge of recombination processes is very important for an understanding of the phenomena related to deviations from thermodynamic equilibrium of the current carrier concentrations in semiconductors. Among such processes are, for instance, photoconductivity and contact effects associated with the motion of the minority carriers in crystal diodes and transistors. The most decisive role here is played by lifetimes of the electrons in the conduction band and of the holes in the valence band.

Recombination processes have for a long time been the subject of many investigations, both experimental and theoretical; serious difficulties have been encountered in such studies from their very beginning. Many problems still remain unsolved.

Recombination process can essentially be divided into two classes: a) those associated with radiative transitions, and b) those associated with nonradiative transitions.

Radiative transitions, in which the electron's energy is emitted in the form of a photon, are of fundamental importance in phosphors. Phosphors, however, are an exceptional and not very numerous class of substances; the principal recombination mechanism in typical semiconductors involves nonradiative transitions. This is connected with the relatively low probability for radiative transitions, which correspond to excited-state lifetimes of the order of 10^{-7}-10^{-8}sec in the visible and infrared regions.

The discovery, within the last few years, of electroluminescence and photoluminescence in the infrared region indicates that the radiative recombination mechanism does make some contribution even in typical semiconductors. Nevertheless it is certainly not the predominant mechanism.

The interaction of an electron with the crystal lattice is considered the basic process in nonradiative recombination. In this process the electron energy is transferred to the crystal lattice, exciting its vibration. Thus, nonradiative recombination is related to the emission of phonons.

Since the maximum phonon energy is of the order of $k\theta$, i.e., several hundredths of an electronvolt, whereas the energy liberated incident to recombination is of the order of an electronvolt, the recombination process must involve the simultaneous generation of a large number of phonons.

In the present paper we shall discuss certain experimental and theoretical data relating to a new recombination mechanism which may play an important role in semiconductors.

This mechanism involves recombination through the interaction of three particles, an electron and two holes or two electrons and one hole, the process being such that the recombination energy is transferred to the other electron (or hole). This process is the inverse of impact ionization. The excitation energy in an ionizing collision derives from the kinetic energy of the colliding electron; in the recombination in question, which we shall henceforth call impact recombination, the excitation energy is transferred to the other electron in the form of kinetic energy. Let τ be the electron lifetime in a conduction band; then $1/\tau$ is the probability of recombination (in a unit time). We shall speak of the probabilities for radiative ($1/\tau_1$), phonon ($1/\tau_2$), and impact ($1/\tau_3$) recombination. Then

$$\frac{1}{\tau} = \frac{1}{\tau_1} + \frac{1}{\tau_2} + \frac{1}{\tau_3}.$$

Let the number of electrons which can recombine with a given center be n (or p, if we are considering holes); then the probabilities for radiative and phonon recombination will be proportional to n (or p), whereas the probability for impact recombination, which requires a pair of electrons (or holes), will be proportional to n^2 (or p^2) for a given center. When the probability for one of the recombination mechanisms predominates, we may neglect the other two terms in Eq.(1). When the dominant mechanism is impact recombination, we have

$$\frac{1}{\tau} \approx \frac{1}{\tau_3} \approx n^2 \text{ (or } p^2)$$

If we plot a graph of the logarithm of τ as a function of the logarithm of n or of p, we obtain a straight line of slope -2. Until now all experimental proofs of the existence of impact recombination are based on substantiating this dependence.

The earliest data on impact recombination were obtained by T.S.Moss[1] in England in 1953, and then at the Physical Institute of the Polish Academy of Sciences in Warsaw by the author in collaboration with Ostrowski[2]. In recent years there have appeared the experimental investigations of Hornbeck & Haynes[3] and the first attempts at a theoretical treatment of this effect by Pincherle[4] in England and Sclar & Burstein[5] in the U.S.A.

Moss[1] investigated natural PbS; direct lifetime measurements were performed only for times exceeding 1 microsec. Shorter times were determined on the basis of photoconductivity and the photoelectromagnetic effect. These lifetime evaluations involved many assumptions. Thus Moss assumes that the quantum yield is the same and equal to unity for all his specimens and that the electron and hole mobilities are constant and approximately equal to each other. With these assumptions Moss determines $\tau = j(\sigma)$ which is tantamount to determining $\tau = f(n)$. The experimental points do really fit a straight line. If, on the other hand, it is assumed that a relation of the form $1/\tau = An^{\alpha}$ obtains, then the straight line corresponding to $\alpha = 2$ agrees fairly well with the experimental data.

An entirely different method was chosen by the author and Ostrowski[2]. The specimens investigated were thin polycrystalline films of p-type Tl_2S, which has a high photoconductivity. The hole concentration in the specimen was first controlled by illuminating it at a constant intensity. Onto this constant illumination background we then applied square-wave pulses of low-intensity light and measured the relaxation time τ and the sensitivity $S = d\sigma/\sigma dI$. From the fact that $S\sigma/\tau$ was constant, we concluded that the conductivity is proportional to the concentration p of current carriers. In addition, we made a more accurate verification of the dependence of τ on p, assuming that $1/\tau = ap^2$ and using the relation

$$\frac{dp}{dt} = \gamma I + ap_0^3 - ap^3,$$

where I is the light intensity. From this we obtain $\sigma = j(I)$. The agreement between theory and experiment was excellent.

Hornbeck & Haynes[3] worked with silicon. They showed that in the case of p-type silicon there are two types of traps, shallow and deep, lying 0.57 and 0.79 ev, respectively, below the bottom of the conductions band. Injection of electrons results in partial filling of the traps, from which the electrons can either return to the conduction band due to thermal excitation or recombine with holes in the valence band.

Electrons can also be generated in the conduction band by illumination of the crystal. The decay of the photoconductivity is a complicated process in view of multiple trapping. The purpose of Hornbeck & Haynes was to study the kinetics of these effects. Where our present argument is concerned only the recombination of electrons from the deep traps is of interest. We again find the $\frac{1}{\tau} \approx p^2$ law. Hornbeck & Haynes do not attempt to interpret this result and offer no explanation of the recombination mechanism.

Similar relations hold true also for n-type silicon for which a $1/\tau \approx n^2$ relation has been established. The above-mentioned data, as far as we know, virtually exhaust the experimental results published on the question. The first attempt at a theoretical examination was given by Pincherle[4].

Pincherle attempts to establish an analogy between impact recombination and the Auger effect, using the familiar theory of this phenomenon.

The transition probability is given by the expression

$$W = \frac{1}{\tau} = \frac{2\pi}{h} \rho(E) |V_{12}|^2,$$

where V_{12} is the matrix element of the interaction potential of the electrons, namely,

$$V_{12} = \int \Psi_1^*(\mathbf{r}_1) \Psi_1^*(\mathbf{r}_2) \frac{e^2}{|\mathbf{r}_2 - \mathbf{r}_1|} \Psi_2(\mathbf{r}_1) \Psi_2(\mathbf{r}_2) \, d\mathbf{r}_1 \, d\mathbf{r}_2,$$

where Ψ_1 and Ψ_2 pertain to the initial and final states, respectively.

Assuming that the recombination energy E is large compared with kT, we may take the electron energy after collision to be E. Then

$$\rho(E) = \frac{4\pi V (2m)^{3/2}}{h^3} E^{1/2}.$$

In order to obtain a numerical value for τ, Pincherle introduces the concept of a radius of action R; then $\rho V = \frac{4}{3} \pi R^3$.

Considering the initial-state wave functions to be plane waves, and those for the final state of the bound electron to be spherically symmetrical and restricted to within a region of radius R, we obtain the following expression for the probability of recombination:

$$\frac{1}{\tau} = C \frac{m^{3/2} e^4 E^{1/2} R^7}{h^3} p^2,$$

where the constant C depends on the choice of the wave function (it is of the order of 100 for the S-state). Pincherle takes R to be equal to usual ionic radii, i.e., about 1 Å. Assuming the numerical values corresponding to the case investigated by Hornbeck & Haynes, we obtain

$$10^{29} < \tau p^2 < 10^{33} \text{ cm} \cdot \text{sec}^6,$$

while the experimental values are 10^{32} for n-type silicon and 10^{34} for p-type silicon. In view of the rough character of the evaluations, the agreement is quite satisfactory.

Before concluding, I would like to mention the work of Sclar & Burstein[5] who refer to experimental studies of the photoconductivity of germanium and silicon at liquid helium temperatures and attempt to explain the high recombination coefficient observed in this case. According to not very accurate data, the lifetimes are of the order of 10^{-9}–10^{-11} sec. Such short lifetimes cannot be explained with the aid of known recombination mechanisms. This impelled the authors to evaluate the probability of impact recombination. They

calculate the coefficient of impact ionization, using the Born approximation and the functions for a hydrogen-like recombination center; the influence of the surrounding medium is taken into account by introducing the dielectric constant. The calculations lead to the carrier concentration n^* at which the probability for impact recombination becomes equal to that for phonon recombination. At higher concentrations, obviously, impact recombination will predominate. The values of n^* deduced by Sclar & Burstein lie between $1 \cdot 10^9$ and $1.6 \cdot 10^{11}$ cm^{-3}, i.e., are much lower than the concentrations we usually encounter in semiconductors.

The absolute values of the calculated recombination coefficients, however, are too small to explain the observed short lifetimes, so that the authors come to the conclusion that it is necessary to seek yet other recombination mechanisms.

Without going into the reliability of the absolute values of the recombination coefficients as calculated by Sclar & Burstein, we can safely assert, on the basis of their work, that impact recombination can play an important role even at relatively low carrier concentrations.

We feel that the material presented is convincing proof of the fact that impact recombination can be the dominating mechanism in a number of different cases, and that this process is common and often important in semiconductor physics. There is still very little experimental data on the subject and the few attempts at theoretical interpretation can only be regarded as the first steps towards the development of a consistent theory. We undoubtedly have here an interesting field for further experimental and theoretical work.

Institute of Physics of the
Polish Academy of Sciences

References

1. T.S.Moss, Proc. Phys. Soc., B.66, 993 (1953).
2. J.Ostrowski & L.Sosnowski, Buill. Pol. Ac. Sc., 3, 2, 392 (1954).
3. J.A.Hornbeck & J.R.Haynes, Phys. Rev., 97, 311 (1955).
4. L.Pincherle, Proc. Phys. Soc., B.68 (1955).
5. N.Sclar & E.Burstein, Phys. Rev., 98, 1757 (1955).

EXCITED STATES OF TWO-ELECTRON COLOR CENTERS IN IONIC CRYSTALS AND THE α AND β ABSORPTION BANDS.

- O.F.Tomasevich

In 1951 S.I.Pekar and the author[1,2] presented a theory for the ground state of F'-centers. The model used for the F'-center was that suggested by Pick[3], i.e., an F-center with an electron bound to it.

Through calculation of the ground state it is possible to determine only one quantity that could be compared with experiment, namely, the thermal dissociation energy of an F'-center.

We felt it would be of interest to develop the theory further to the point where it would be feasible to determine the frequency absorbed by the F'-center and the shape of the F'-band.

Initially limiting ourselves to a classical treatment of ion motion and assuming that the phototransition occurs with the ions stationary (Franck-Condon principle), we calculated the excitation of the so-called nonself-consistent state of the F'-center when the Hamiltonian

$$H = \frac{\mu e^4}{\hbar^2 \varepsilon^2}\left\{-\frac{1}{2}(\Delta_1+\Delta_2) - Z\left(\frac{1}{r_1}+\frac{1}{r_2}\right) + \frac{\varepsilon}{n^2}\frac{1}{r_{12}} - \varepsilon\int_J P_0 \cdot \left(\nabla\frac{1}{|r_1-r|} - \nabla\frac{1}{|r_2-r|}\right)d\tau \right. \qquad (1)$$

contains the polarization P_0 corresponding to the initial ground state of both electrons of the F'-center.

Using a direct variational method, we sought an excited-state function which is symmetric in the coordinates, assuming that one of the electrons is in the 1s-state and the other in the 2p-state. The calculations were performed for a vacancy with charges Z = 1 and Z = 2. It was found impossible to obtain a general solution for the equations characterizing the trial parameters (radii of the 1s- and 2p-electrons) as a function of Z and ε/n^2.

Computations were carried for a monovalent center (Z = 1) in NaCl, CKl and KBr crystals. Since Pekar[4] has already found the effective mass of the electron for these crystals from the theory of F-centers, there remained no free parameter which could be used for "fitting" the theory to experiment in the present work.

Crystal	$h\nu_{theo}$, ev	$h\nu_{exp}$, ev (F'-band peak)
NaCl	1.1	2.4
KCl	0.8	1.7
KBr	0.65	1.4

Our results are compared with the experimental values in the accompanying table.

Although the agreement cannot be considered satisfactory, the divergence should not be attributed to a fundamental defect of the theory. The thing is that use of the Franck-Condon principle yields only one absorption line, which for monovalent crystals must be compared with a very wide experimental F'-band extending from 1 to 2.5-3 ev.

In the same approximation, calculation should give a better result if Z = 2 (for instance in bivalent crystals), since in that case one may expect the F' band to be narrower.

This case is also of interest because if a vacancy forms in a crystal composed of bivalent ions (for instance in BaO), then, in view of the net neutrality of the crystal, obviously two electrons should be localized at the vacancy. Thus the two-electron center should be the principal type of impurity center in such crystals.

In 1951 Kane[5] presented the absorption curve of BaO containing Ba as an impurity. The additional bell-shaped band having a peak at 2.3-2.4 ev can be assigned to F'-centers, present in such barium oxide. This is verified by

investigations[6] of the thermionic emission, which increases when the cathode is illuminated by 500 μ light ($h\nu$ = 2.48 ev) (the radiation may ionize or excite F'-centers and thus facilitate thermionic emission).

In addition, the activation of the cold oxide with $h\nu \geq 3.7$ ev light leads to the appearance of a maximum in the photocurrent curve at h = 2.5 ev (Ref.7).

The theory developed for Z = 2 enabled us to calculate the energies of the ground state J_g and the nonself-consistent excited state J_e of an F'-center in BaO. Both these quantities, and therefore $h\nu_{F'} = J_e - J_g$, contain the effective mass μ as a parameter which could be determined from a comparison of $h\nu_{exp}$ and $h\nu_{theo}$. The value of ε of BaO, necessary for the theoretical calculations, was determined experimentally by Beyer & Sproull[8], as 34; however, this value is doubtful, since for MgO, CaO, and SrO the dielectric constant is 8.2, 11.8 and 13.3, respectively. Therefore we took ε = 14 for BaO in analogy with these compounds.

The effective mass found for BaO was μ/m = 5.85.

The thermal dissociation energy W_T for an F'-center is then 1.6 ev, while from the experimental investigations of the temperature dependence of conductivity in BaO crystals[9], it would appear that W_T lies between 1.2 and 1.7 ev. It should be noted that the use of the macroscopic theory is here not entirely rigorous, since the radius of the F'-center is small (the polarization radius of the state is about 5Å.

We were also able to evaluate the effective mass M and mobility u of a polaron in BaO using the above μ/m value. The calculated polaron mobility proved to be in good agreement with experiment:

$$M_{pol} = 740\ m_e;$$

at T = 700°K

$$u = 2\ cm^2/volt \cdot sec.$$

The experimental value[10] is u ≈ 3-9 cm^2 volt sec.

We may thus consider that our theory of the F'-center is in satisfactory agreement for BaO.

The classical treatment of ion motion and the nonself-consistent excited state of the center cannot, however, be used to calculate the width of the absorption band.

A general theory which gives an absorption band rather than a line and makes it possible to calculate the width of this band was developed by Pekar[4] for any kind of impurity centers. In order to apply this theory to an F'-center, however, in lieu of the nonself-consistent state, it is necessary to use the so-called self-consistent excited state in which the polarization is defined in terms of the electron wave function in this state. Then P_o in Eq.(1) should be replaced by

$$P = \int \frac{|\psi'(r)|^2 (r - r')}{|r - r'|^3} d\tau.$$

The same direct variational method was used to calculate the self-consistent excited state for Z = 1 and Z = 2.

The following results were obtained: for crystals with Z = 1 we plotted the energy curve of a crystal with an F'-center in a self-consistent excited state, as well as the energy curve for a crystal containing an F'-center dissociated into an F-center and a polaron. It was found that for all values of ε/n^2 the excited state has a higher energy than the dissociated one, which lies in the continuous spectrum. Thus the assumption that the excited state

lies in the discrete spectrum is incorrect, and an F'-center with Z = 1 has a single discrete level - the ground state one - while its excited state lies in the continuous spectrum. Seitz[11] had previously come to the same conclusion on the basis of the analogy between an F'-center with Z = 1 and a hydrogen H^- ion. Thus our calculations support his deduction.

Calculations of the self-consistent excited states of an F'-center with Z = 2 showed that they occur in crystals in which $\varepsilon/n^2 < 3.2$ and do not occur when $\varepsilon/n^2 > 3.2$.

The band width theory was applied to crystals with Z = 2 wherein $\varepsilon/n^2 < 3.2$ (i.e., when an excited self-consistent state exists). We calculated the photo-transition matrix elements for such cases.

Unfortunately, in BaO, however,

$$\varepsilon / n^2 = \frac{14}{3,8} > 3,2$$

and quantum theory could not be applied. An attempt was made to apply it to one of the absorption bands in MgO, which might be considered an F' absorption band, but the experimental determination of this band width[12] is very unreliable and the radius of the F'-center state was furthermore found to be very small.

Thus there is as yet no experimental substantiation of the F'-band-width theory.

Using developed concepts and the theory of F- and F'-centers, we made an attempt to calculate the positions of the so-called Greek-letter bands (designated α and β) which were first observed in KI by Delbecq et al[13]. These bands appear close to the edge of the self-absorption band and are presumably associated with electron transitions from the ground state to a vacancy level with the formation of an F-center (α-band) and to the F-center level with the formation of an F'-center (β-band).

In both cases the final state of the system is known - it is either an F-center or an F'-center - but the initial state energy, when the electron is the host material, is not known. Thus a calculation of the transition frequencies for the α and β bands separately is impossible. Assuming, however, that in both transitions the electron has the same initial energy, we can calculate the frequency difference $\Delta\nu$ between the α and β bands, as well as the band widths δ_α and δ_β.

Difficulties were encountered in view of the fact that it is necessary to take into account the presence of a hole close to the F- or F'-center formed as a consequence of the phototransition.

In the first attempt at calculation, it was assumed that the hole leaves the point at which the electron is located. This variant of the theory seemed attractive, for in this case the calculations do not contain a single extraneous parameter (the effective mass is known from F-center theory), and all three quantities $\Delta\nu$, δ_α and δ_β could be compared with experiment. This variant led, however, to a value for $\Delta\nu_{theo}$ four times greater than the experimental one.

In the more refined variant the influence of the hole was allowed for only in the β transition where the final product is a negatively charged F'-center. In the α transition the F-center formed is neutral, and if the hole should come close to this center it would be repelled by the concentrated positive charge of the vacancy.

It was, therefore, necessary to calculate the state of a system consisting of two electrons and a hole localized close to a Coulomb center. The effective mass of the hole was introduced, and the Hamiltonian of the system contained

the ratio of the hole and electron effective masses, namely, μ_h/μ_e.

The wave functions of the electron and hole were assumed to be of the form

$$\Psi_e = A(1+\alpha r)e^{-\alpha r} \quad \text{and} \quad \Psi_h = Bre^{-\beta r}, \quad \text{where} \quad \frac{\beta}{\alpha} = \gamma$$

and the direct variational method was used to find the parameters α and γ of these states as a function of μ_h/μ_e.

In order to calculate the frequencies corresponding to the α and β absorption band peaks it is necessary to find the quantities

$$a = \frac{c}{4\pi\hbar\omega}\int (D_{in} - D_{fi})^2 d\tau,$$

of Pekar's theory, where D_{in} and D_{fi} are the electric inductions in the initial and final states of the system and $c = \frac{1}{n^2} - \frac{1}{\varepsilon}$.

We calculated $h\Delta\nu = \nu_\beta - \nu_\alpha$, δ_α and δ_β. They were found to depend on μ_h/μ_e. This parameter of the theory was found by comparing the calculated value of $h\Delta\nu$ with the experimental one. In spite of the incompleteness of the theory and the approximate nature of the calculations, we obtained the correct order of magnitude for $\Delta\nu$($h\Delta\nu_{theo}$ = 0.4 ev as against $h\Delta\nu_{exp} \approx$ 0.3 ev) on the assumption of a reasonable value of ~4.5 Å for the radius of the hole, i.e., in the case when the hole moves over the negative ions closest to the vacancy. The values δ_α = 0.3 ev and δ_β = 0.13 ev found on the basis of the computed parameters are in satisfactory agreement with the corresponding experimental values: ~0.4 ev and ~0.22 ev, respectively.

Thus the interpretation of the α- and β-bands suggested by previous investigators is apparently correct, but in calculating the β-band one must not neglect the presence of the hole.

A deficiency of the theory is the fact that a value of 2.7 is obtained for the ratio μ_e/μ_h so that μ_h cannot really be called the effective mass of the hole. The true value of μ_h should, of course, be greater than the electron effective mass.

"T.G.Shevchenko" Kiev State University

References

1. S.I.Pekar & O.F.Tomasevich, Zhur.eksp.i teor.fiz., 21, 1218 (1951).
2. O.F.Tomasevich, Zhur.eksp.i teor.fiz., 21, 1223 (1951).
3. H.Pick, Ann. d. Physik, 31, 365 (1938).
4. S.I.Pekar, Issledovanniia po elektronnoi teorii kristalov (Studies in the electron theory of crystals), M.-L. 1951.
5. E.O.Kane, J. of Appl. Phys., 22, 1214 (1951).
6. T.Hibi & K.Ishikawa, Phys. Rev., 83, 805 (1951).
7. H.De-Vore & J.Dewdney, Phys. Rev., 83, 805 (1951).
8. S.Beyer & R.Sproull, Phys.Rev., 83, 801 (1951).
9. Semiconducting Materials, p. 122. - London.
10. E.M.Pell, Phys.Rev., 87, 457 (1952).
11. F.Seitz, Rev.Mod.Phys., 18, 384 (1946).
12. H.Weber, ZS. f. Phys., 130, 392 (1951).
13. C.J.Delbecq, P.Pringsheim & P.Jouster, J. of Chem.Phys., 19, 574 (1951).

ON THE EXCITON ENERGY SPECTRUM IN AN IONIC CRYSTAL

- I.P.Ipatova

The experimental investigations of E.F.Gross and his co-workers[1], as well as the work of a number of foreign authors[2], have made further theoretical examination of the behavior of excitons in ionic crystals timely.

The question of the energy spectrum of an exciton, taking into account strong interaction with polarization lattice vibrations has been treated by Dykman and Pekar[3]. Their calculations were based on the adiabatic method previously used by Pekar in polaron theory[4]. The solution is essentially the zeroth approximation, i.e., does not take into account the oscillation of ions about the new displaced (due to polarization) equilibrium positions. This treatment is valid in the case of strong coupling between the exciton and lattice vibrations.

We felt it would be of interest to compare the results already obtained with the results of calculation of the exciton energy spectrum, taking into account the oscillations of the ions about the displaced equilibrium positions. This can be done by using the direct variational method - also known as the "intermediate coupling" method introduced by Tomonaga[5] - which, however, breaks down for high values of the coupling constant. This method has recently been successfully employed by Lee, Low and Pines[6,7] for calculation of the polaron ground state. There is even more justification for applying it to the exciton case since due to the presence of opposite charges the polarization effects are partially compensated so that the coupling constant is reduced.

1. Hamiltonian of the system

We shall adopt a Hamiltonian consisting of three parts describing, respectively, the exciton, the lattice vibrations and the interaction between them.

1. To describe the exciton we use Mott's[8] hydrogen-like model:

$$\hat{H}_{ex} = -\frac{\hbar^2}{2m_1}\Delta_{r_1} - \frac{\hbar^2}{2m_2}\Delta_{r_2} - \frac{e^2}{n^2 r_{1,2}}. \tag{1}$$

Here r_1 and r_2 are the radii-vectors of the electron and hole, $r_{1,2}$ is the distance between them, n is the refraction index of the medium and m_1 and m_2 are the effective masses of the electron and hole, respectively.

2. If we agree to approximate the crystal by a continuous medium, the interaction can be written by means of the potential of the polarized medium[3,4] in the form

$$\hat{H}_{int} = e\int \frac{\operatorname{div} P(r')}{|r_1 - r'|}(dr') - e\int \frac{\operatorname{div} P(r')}{(r_2 - r')}(dr'), \tag{2}$$

where $-e$ is the electron charge.

With this choice of interaction, only the longitudinal component $P_{\parallel}(r)$ of the polarization is of any importance. After requantization of the scalar field of longitudinal polarization lattice vibrations, the Hamiltonians for the interaction and for the lattice vibrations become

$$\hat{H}_{int} = \sum_{(k)} A_k \alpha_k \{e^{ikr_1} - e^{-ikr_2}\} - \sum_{(k)} A_k^* \alpha_k^+ \{e^{-ikr_1} - e^{ikr_2}\},$$

and (3)

$$\hat{H}_{osc} = \frac{1}{2}\sum_{(k)} \hbar\omega(\alpha_k^+\alpha_k + \alpha_k\alpha_k^+).$$

Here k is the wave vector of the field quanta (phonons), α_k^+ and α_k are the creation and annihilation operators for phonons satisfying the commutation rules

$$[\alpha_k, \alpha_{k'}^+] = \delta_{kk'};$$

and A_k has the meaning

$$A_k = -ie\sqrt{\frac{2\pi\hbar\omega c}{V}} \cdot \frac{1}{k}, \quad c = \frac{1}{n^2} - \frac{1}{\varepsilon}, \tag{4}$$

where ω is the frequency of longitudinal optical vibrations, V is the volume of the crystal, n is the refraction index of the medium, and ε is the static dielectric constant.

Transforming to the coordinates of the center of mass of the electron-hole system according to the equations

$$\mathbf{r}_1 = \mathbf{R} + \frac{m_2}{m_1+m_2}\mathbf{r}, \quad \text{and} \quad \mathbf{r}_2 = \mathbf{R} - \frac{m_1}{m_1+m_2}\mathbf{r},$$

we write the total Hamiltonian of the system in the form

$$\hat{H} = -\frac{\hbar^2}{2M}\Delta_R - \frac{\hbar^2}{2\mu}\Delta_r - \frac{e^2}{n^2 r} + \sum_{(k)}\hbar\omega\alpha_k^+\alpha_k +$$

$$+\sum_{(k)} A_k\alpha_k e^{i\mathbf{kR}}\left\{e^{i\frac{m_2}{m_1+m_2}\mathbf{kr}} - e^{-i\frac{m_1}{m_1+m_2}\mathbf{kr}}\right\} + \sum_{(k)} A_k^*\alpha_k^+ e^{-i\mathbf{kR}}\left\{e^{-i\frac{m_2}{m_1+m_2}\mathbf{kr}} - e^{i\frac{m_1}{m_1+m_2}\mathbf{kr}}\right\}. \tag{5}$$

Here $M = m_1 + m_2$, $\mu = \frac{m_1 m_2}{m_1+m_2}$.

Since the total momentum

$$\hat{\mathbf{P}} = -i\hbar\frac{\partial}{\partial \mathbf{R}} + \sum_{(k)}\hbar\,\mathbf{k}\,\alpha_k^+\alpha_k$$

of the system is conserved, i.e., since $[\hat{P}, \hat{H}] = 0$, it is convenient to seek our solution in the representation in which the total momentum is diagonal. The transition to this "total momentum representation" is accomplished by the canonical transformation

$$S = e^{i/\hbar\left(\mathbf{P} - \sum_{(k)}\hbar k\alpha_k^+\alpha_k,\ \mathbf{R}\right)}, \tag{6}$$

which transforms the operator $\hat{\mathbf{P}}$ into the appropriate "c" number P.

The transformed Hamiltonian is

$$\hat{H} = S^{-1}\hat{H}S = \frac{\left(\mathbf{P} - \sum_{(k)}\hbar\,k\alpha_k^+\alpha_k\right)^2}{2M} - \frac{\hbar^2}{2\mu}\Delta_r - \frac{e^2}{n^2 r} +$$

$$+\sum_{(r)}\hbar\omega\alpha_k^+\alpha_k + \sum_{(k)} A_k\alpha_k\left\{e^{i\frac{m_2}{m_1+m_2}\mathbf{kr}} - e^{-i\frac{m_1}{m_1+m_2}\mathbf{kr}}\right\} + \sum_{(k)} A_k^*\alpha_k^+\left\{e^{-i\frac{m_2}{m_1+m_2}\mathbf{kr}} - e^{i\frac{m_1}{m_1+m_2}\mathbf{kr}}\right\}. \tag{7}$$

We note that (7) no longer contains the coordinate R, and that the total momentum of the system appears in it as a "c" number. A transformation such as (6) has been used previously[6,9,10,11].

The state of the system whose Hamiltonian is given by Eq.(7) is conveniently described in terms of the Fock[9] functionals Ω. For a discrete spectrum, an expansion of Ω in a series of eigenfunctionals Ω_N of the number-of-phonons operator

$$\hat{N} = \sum_{(k)}\alpha_k^+\alpha_k$$

is of the form

$$\Omega = \sum_{N=0}^{\infty} \Omega_N, \tag{8}$$

where

$$\Omega_N = \sum_{n_1 n_2 \ldots} f(\mathbf{r}; n_1 n_2 \ldots)(\alpha_1^+)^{n_1}(\alpha_2^+)^{n_2}\ldots|0\rangle. \tag{9}$$

Here $N = n_1 + n_2 + \ldots$, where n_i is the number of phonons in state i; as before, α_i^+ and α_i are the creation and annihilation operators for field quanta, so that

$$\alpha_i \Omega = \frac{\delta}{\delta \alpha_i^+} \Omega,$$

$$f(\mathbf{r}, n_1, n_2 \ldots) = \sqrt{\frac{N!}{n_1! n_2! \ldots}}\, \Psi(\mathbf{r}; \mathbf{k}_1 \mathbf{k}_2 \ldots \mathbf{k}_N), \tag{10}$$

where $\Psi(\mathbf{r}, \mathbf{k}_1 \mathbf{k}_2 \ldots \mathbf{k}_N)$ is a symmetric wave function describing a system of N quanta with wave vectors $k_1 k_2 \ldots k_N$ and a particle (exciton) with coordinate r, and $|0\rangle$ is the functional which describes the vacuum state, defined by the condition

$$\alpha_i |0\rangle \equiv 0.$$

As has already been mentioned, the "intermediate coupling" method of Tomonaga shall be used to find the energy eigenvalues of the system described by the Hamiltonian (7). The expectation value

$$E = \langle \Omega | \hat{H} | \Omega \rangle \tag{11}$$

of this Hamiltonian is minimized with the subsidiary condition

$$\langle \Omega | \Omega \rangle = 1. \tag{12}$$

2. Choice of the trial functions

Let us calculate the expectation value of the energy in a coordinate system bound to the center of mass of the system, which means that we set $\mathbf{P} = 0$ in (7). We can then use the commutation relations $[\alpha_k, \alpha_{k'}] = \delta_{kk'}$ to rewrite the Hamiltonian in the form

$$\hat{H} = -\frac{\hbar^2}{2\mu}\Delta_r - \frac{e^2}{\varepsilon r} + \sum_{(k)}\left(\hbar\omega + \frac{\hbar^2 k^2}{2M}\right)\alpha_k^+\alpha_k + \sum_{(k)} A_k \alpha_k \left\{e^{i\frac{m_2}{m_1+m_2}\mathbf{kr}} - e^{-i\frac{m_1}{m_1+m_2}\mathbf{kr}}\right\} +$$

$$+ \sum_{(k)} A_k^* \alpha_k^+ \left\{e^{-i\frac{m_2}{m_1+m_2}\mathbf{kr}} - e^{i\frac{m_1}{m_1+m_2}\mathbf{kr}}\right\} + \frac{\hbar^2}{2M}\sum_{(k)(k')}(\mathbf{k}, \mathbf{k}')\,\alpha_k^+\alpha_{k'}^+\alpha_k\alpha_{k'}. \tag{13}$$

The last term in Eq.(13) depends on the angle between the two wave vectors k, and k' of the field quanta and describes the angular correlation of the emitted phonons. The rest of the terms depend only on the modulus $|k|$.

In order to solve the variational problem we must first specify the form of the wave function of Eq.(10). If $\Psi(\mathbf{r}, \mathbf{k}_1 \mathbf{k}_2 \ldots \mathbf{k}_N)$ is chosen to depend only on the modulus $|k|$, the expectation value of the angular correlation term as calculated with such functions will always be zero. In order to take account of the angular correlation, the trial function must be chosen dependent on the vector k itself. The "intermediate coupling" method makes it possible to account for the symmetry properties of the system being considered in a consistent way.

The essence of this method is that the wave function of Eq.(10) is written

in the form of a product of the individual wave functions of the separate field quanta. The field quanta, differing as regards angular momentum l and its projection m are described by different individual functions: quanta in states with $l = 0$ and $m = 0$ are described by spherically symmetrical functions $f(k)$, those in states with $l = -1, m = -1$ are described by functions $g_1(\mathbf{k})$, those in states with $l = 1, m = 0$ are described by functions $g_2(\mathbf{k})$, and those with $l = 1, m = 1$ are described by functions $g_3(\mathbf{k})$. Hereinafter, for the sake of brevity, we shall refer to them as s, p, d, etc. quanta, respectively.

If we take account only of s and p quanta in the field, then according to the "intermediate coupling" method the wave function of Eq.(10) should be taken in the form

$$\Psi(\mathbf{r}, \mathbf{k}_1, \mathbf{k}_2 \ldots \mathbf{k}_N) = \sqrt{\frac{n!\, m_1!\, m_2!\, m_3!}{N!}}\, \chi(\mathbf{r})\, C_{nm_1m_2m_3} \times$$

$$\times S \prod_{i=0}^{n} f(k_i) \prod_{j_1=n+1}^{n+m_1} g_1(\mathbf{k}_{j_1}) \prod_{j_2=n+m_1+1}^{n+m_1+m_2} g_2(\mathbf{k}_{j_2}) \prod_{j_3=n+m_1+m_2}^{N} g_3(\mathbf{k}_{j_3}), \qquad (14)$$

where $N = n + m_1 + m_2 + m_3$ is the total number of particles in the field, n, m_1, m_2 and m_3 being the numbers of phonons in the states with $l = 0, m = 0$ and $l = 1, m = 0, \pm 1$; the function $\chi(\mathbf{r})$ is one which approximates the dependence on the relative coordinate r and S is the symmetrization operator for all field quanta.

The coefficients $C_{n; m_1; m_2; m_3}$, the individual wave functions $f(k)$ and $g_1(\mathbf{k})$, with $i = 1, 2, 3$, as well as the parameters entering the function $\chi(\mathbf{r})$ are found by the variational problem.

If we restrict our consideration to only the s quanta in the field and thus maintain only the spherically symmetric functions $f(k)$, in Eq.(14), then in calculating the expectation value of the energy the contribution from the angular correlation term vanishes; if, however, we include p quanta and pick the wave function in the form of Eq.(14), the angular correlation term gives a nonzero contribution to the energy. If we were to consider also quanta in states with higher angular momenta, the correlation terms corresponding to these quanta would yield additional corrections to the energy. This increase in the number of field quanta being considered and the corresponding inclusion of a large number of different individual wave functions in the trial function is analagous to increasing the number of parameters in the variational problem and leads to greater "flexibility" of the trial function.

Lee and Pines[6] have discussed in detail the question of accounting for quanta with higher angular momenta in the case of the polaron problem. They showed that for coupling constant values that are not too high (~ 5-6) it is sufficient to take into account only the s quanta since taking into account the p quanta as well reduces the energy only by 6%. Lee and Pines attribute this weak influence of the correlation term to the fact that the number of quanta with high angular momenta is relatively small.

The description of the properties of the quantum field in the exciton problem is analogous to that in polaron theory. Therefore we may expect that the influence of correlation in this case, too, will not be great. In fact, we carried out an evaluation[12] which showed that in the cases being considered herein correlation terms can make a contribution of not over 2.5% referred to the energy calculated without taking correlation into account. The evaluation mentioned was performed with the aid of the second approximation of perturbation theory, in which the zeroth approximation was taken as the solution without correlation.

In view of the above, we shall seek the stationary states of an exciton with a trial function such as that given by Eq.(10), but containing only the products of the spherically symmetrical individual wave functions $f(k)$.

3. Calculation of the 2p-state of the exciton without taking correlation into account

Using Eq.(10), we can write the functional of (8) for the case in which (10) is chosen as the product of the spherically symmetric individual functions of the s quanta; we obtain

$$\Omega = \chi(\mathbf{r}) \sum_{N=0}^{\infty} C_N \frac{1}{\sqrt{N!}} \Big(\sum_{(\mathbf{k})} f(k)\, \alpha_k^+ \Big)^N |0\rangle. \tag{15}$$

With the interaction we have chosen, the coefficients C_N can always be taken in the form[14] (also, see Ref.13)

$$C_N = e^{-\frac{1}{2}U^2} \frac{U^N}{\sqrt{N!}}.$$

Then Eq.(15) becomes

$$\Omega = e^{-\frac{1}{2}U^2} \chi(\mathbf{r}) \sum_{N=0}^{\infty} \frac{U^N}{N!} \Big(\sum_{(\mathbf{k})} f(k)\, \alpha_{\mathbf{k}}^+ \Big)^N |0\rangle = e^{-\frac{1}{2}U^2} \chi(\mathbf{r})\, e^{U \sum_{(k)} f(k) \alpha_{\mathbf{k}}^+} |0\rangle. \tag{16}$$

Now instead of an infinite number of coefficients C_N, we have the single parameter U of the variational problem. With the aid of the relation

$$e^{f(k)\alpha_{\mathbf{k}} + f^*(k)\alpha_{\mathbf{k}}^+} = e^{\frac{1}{2}|f(k)|^2}\, e^{f(k)\alpha_{\mathbf{k}}}\, e^{f^*(k)\alpha_{\mathbf{k}}^+}$$

if can be shown that the field part of the functional of (16) is the same as that of Lee, Low & Pines[7].

It can readily be shown that

$$\alpha_k \Omega = U f(k)\, \Omega. \tag{17}$$

In view of (17), the mean value of the Hamiltonian (13) becomes

$$E = \langle \Omega | \hat{H} | \Omega \rangle = -\frac{\hbar^2}{2\mu} \langle \chi | \Delta_{\mathbf{r}} | r \rangle - \frac{e^2}{n^2} \langle \chi \Big| \frac{1}{r} \Big| \chi \rangle + U^2 \sum_{(\mathbf{k})} \Big(\hbar\omega + \frac{\hbar^2 k^2}{2M} \Big) |f(k)|^2 +$$

$$+ 2U \sum_{(\mathbf{k})} A_k f(k) \Big\langle \chi \Big| \Big\{ e^{i \frac{m_2}{m_1+m_2} \mathbf{kr}} - e^{-i \frac{m_1}{m_1+m_2} \mathbf{kr}} \Big\} \Big| \chi \Big\rangle. \tag{18}$$

From the condition $\partial E / \partial U = 0$, we arrive at

$$U = \frac{\sum_{(\mathbf{k})} A_k f(k) \Big\langle \chi \Big| \Big\{ e^{i \frac{m_2}{m_1+m_2} \mathbf{kr}} - e^{-i \frac{m_1}{m_1+m_2} \mathbf{kr}} \Big\} \Big| \chi \Big\rangle}{\sum_{(\mathbf{k})} \Big(\hbar\omega + \frac{\hbar^2 k^2}{2M} \Big) |f(k)|^2}. \tag{19}$$

Inserting (19) into (18), we have

$$E = -\frac{\hbar^2}{2\mu} \Big\langle \chi | \Delta_{\mathbf{r}} | \psi \Big\rangle - \frac{e^2}{n^2} \Big\langle \chi \Big| \frac{1}{r} \Big| \chi \Big\rangle - \frac{\Big[\sum_{(\mathbf{k})} A_k f(k) \Big\langle \chi \Big| \Big\{ e^{i \frac{m_2}{m_1+m_2} \mathbf{kr}} - e^{-i \frac{m_1}{m_1+m_2} \mathbf{kr}} \Big\} \Big| \chi \Big\rangle \Big]^2}{\sum_{(\mathbf{k})} \Big(\hbar\omega + \frac{\hbar^2 k^2}{2M} \Big) |f(k)|^2}. \tag{18a}$$

From the functional variation of $f(k)$ in (18a), and making use of the relation

$$\frac{\partial E}{\partial f} = 0,$$

we obtain

$$f(k) = \frac{N_1 A_k^*}{\left(\hbar\omega + \frac{\hbar^2 k^2}{2M}\right)} \left\langle \chi \left| \left\{ e^{-i\frac{m_2}{m_1+m_2}\mathbf{kr}} - e^{i\frac{m_1}{m_1+m_2}\mathbf{kr}} \right\} \right| \chi \right\rangle. \tag{20}$$

The normalizing constant N_1 is given by the condition

$$\sum_{(k)} |f(k)|^2 = 1.$$

Inserting (20) into (18a), introducing dimensionless parameters in which k is measured in units of $\frac{1}{a_0} = \frac{\mu e^2}{\hbar^2 n^2}$ and E in units of $\mu e^4/\hbar^2 n^4$, and going over from summation to integration according to the rule

$$\sum_{(\mathbf{k})} \cdots \to \frac{V}{(2\pi)^3} \int (d\mathbf{k}) \ldots,$$

we obtain

$$E = -\frac{1}{2}\left\langle \chi | \Delta_{\mathbf{r}} | \chi \right\rangle - \left\langle \chi \left| \frac{1}{r} \right| \chi \right\rangle - \frac{n^2 c}{\pi} \int \frac{\left\langle \chi \left| \left\{ e^{i\frac{m_2}{m_1+m_2}\mathbf{kr}} - e^{-i\frac{m_1}{m_1+m_2}\mathbf{kr}} \right\} \right| \chi \right\rangle^2}{(1+\zeta k^2)} dk, \tag{21}$$

where

$$\zeta = \frac{\mu}{2M} \frac{1}{\hbar\omega} \cdot \frac{\mu e^4}{\hbar^2 n^4}. \tag{22}$$

The integral here is taken from zero to some value v_0 determined by the reciprocal lattice constant.

Further calculations require an analytic expression for $\chi(\mathbf{r})$. In order to be specific, let us calculate the 2p-state of the exciton. Accordingly, $\chi(\mathbf{r})$ must fulfill the following requirements: 1) it must be normalized, 2) it should have one node, 3) it must be orthogonal to the spherically symmetric ground state function, and 4) in the limit

$$c = \left(\frac{1}{n^2} - \frac{1}{\varepsilon}\right) \to 0,$$

it must describe the appropriate hydrogen-like state.

The function most readily satisfying these requirements is

$$\chi(\mathbf{r}) = Are^{-\delta r}\cos\vartheta, \tag{23}$$

where δ is a dimensionless variation parameter, and $A = \frac{1}{\sqrt{\pi}}\delta^{5/2}$ is determined from the normalization condition.

As the author has shown previously[12], however, calculation with this function is extremely difficult. It is therefore more reasonable to choose $\chi(\mathbf{r})$ in the form

$$\chi(\mathbf{r}) = Are^{-\delta r^2}\cos\vartheta, \tag{24}$$

where $A = 2\left(\frac{2}{\pi}\right)^{3/4}\delta^{5/4}$ is found by normalization.

This function clearly satisfies the first three requirements mentioned above. It can be shown that the fourth requirement is fulfilled approximately.

In fact solving the direct variational problem for a hydrogen-like atom (the case when $c \to 0$) with the function of Eq.(24) leads to the energy value

$$E = -0{,}111 \frac{\mu e^4}{\hbar^2 n^4}, \tag{25}$$

which differs little from the energy

$$E = -0{,}125 \frac{\mu e^4}{\hbar^2 n^4}. \tag{26}$$

obtained by solution with the exact hydrogen-like function of Eq.(23).

Calculating the matrix elements entering into Eq.(21), we obtain

$$E = \frac{5}{2\zeta}\xi - \frac{4\sqrt{2}}{3\sqrt{\pi}}\frac{1}{\sqrt{\zeta}}\xi^{1/2} - \frac{n^2 c}{\pi\sqrt{\zeta}}\left\{\sqrt{\pi}\left[\left(\frac{\beta_1^2+\beta_2^2}{2}\right)^{1/2} - \frac{\beta_1^2\beta_2^2}{\sqrt{2}(\beta_1^2+\beta_2^2)^{1/2}} - \frac{3}{8}\right]\xi^{-1/2} + \right.$$

$$+\sqrt{\pi}\left[\frac{1}{4\sqrt{2}}\frac{\beta_1^2\beta_2^2}{(\beta_1^2+\beta_2^2)^{1/2}} - \frac{1}{16}(\beta_1^3+\beta_2^3)\right]\xi^{-3/2} + \left[1+\frac{\beta_1^2}{4\xi}\right]^2\int_0^\infty \frac{e^{-\frac{(\beta_1 t)^2}{4\xi}}}{(1+t^2)}\,dt + \left[1+\frac{\beta_2^2}{4\xi}\right]\int_0^\infty \frac{e^{-\frac{(\beta_2 t)^2}{4\xi}}}{(1+t^2)}\,dt -$$

$$\left. -\left[1+\frac{\beta_1^2}{4\xi}\right]\left[1+\frac{\beta_2^2}{4\xi}\right]\int_0^\infty \frac{e^{-\frac{(\beta_1^2+\beta_2^2)t^2}{8\xi}}}{(1+t^2)}\,dt\right\}. \tag{27}$$

Here for convenience we have introduced the new variable of integration

the new dimensionless parameter

$$\xi = \delta\zeta, \tag{28}$$

and the notation

$$\beta_1 = \frac{m_2}{m_1+m_2}, \quad \text{and} \quad \beta_2 = \frac{m_1}{m_1+m_2}.$$

In addition, the integration everywhere is taken from 0 to ∞, since from the form of the integrand one may conclude that the region of large k does not contribute measurably to the integral.

We used a graphical method for minimizing E with respect to ξ. By using the formula

$$W(a) = \frac{2}{\pi}\int_0^\infty \frac{e^{-a^2t^2}}{(1+t^2)}\,dt = e^{a^2}\left(1 - \frac{2}{\pi}\int_0^a e^{-u^2}\,du\right)$$

the integrals that enter into E are easily reduced to probability integrals.

The values of these integrals were taken from the tables of Faddeeva & Terent'ev[13]. The calculations were carried out for a Cu_2O crystal. The appropriate values of the index of refraction and dielectric constant are taken from Pekar[4], namely,

$$n^2 = 4, \quad \text{and} \quad \varepsilon = 9.$$

We distinguish between two cases depending on the values of m_1 and m_2

1. $m_1 = m_2$. In this case, as is easily shown, the polarizing action of the exciton on the crystal lattice vanishes. Therefore the energy of the 2p-state for this nonpolarizing exciton will be the energy corresponding to the hydrogen-like level of Eq.(25). This conclusion, however, should not be regarded as a result of the theory, since it follows directly from the choice of the interaction.

2. $m_1 \neq m_2$. In this case the polarizing action of the exciton differs from zero. The energy level of such an exciton always lies below the corresponding hydrogen-like level. The results of the calculation of the energy of the 2p-state for different values of m_1 and m_2 are given below in units of $\mu e^4/\hbar^2 n^4$.

m_1	$m_2 = 2m_1$	$m_2 = 9m_1$
$0{,}5m$	$-0{,}139$	$-0{,}225$
m	$-0{,}135$	$-0{,}200$
$2m$	$-0{,}131$	$-0{,}185$

Here m is the free electron mass.

4. Discussion

1. It is important to note that for $m_1 \neq m_2$ the energy E has a single minimum, which corresponds to the presence of a polarizing exciton in the Cu_2O crystal. A nonpolarizing exciton occurs only when $m_1 = m_2$.

This conclusion differs qualitatively from the 2p-state exciton calculation of Dykman and Pekar[3], where the energy expectation value has two minima corresponding, respectively, to a nonpolarizing and a polarizing exciton.

According to the theory of the direct variational method, physical meaning should be assigned only to the absolute minimum. From the 2p-state exciton data of Dykman and Pekar, when $1/3 < m_1/m_2 < 3$, the lowest minimum is the first one, corresponding to the nonpolarizing exciton. For all other effective-mass ratios it is the second minimum which is the lowest, i.e., a polarizing exciton is present in the crystal.

Our calculations give only a single minimum for $m_1 = 2m_2$; this corresponds to a polarizing exciton in the crystal, whereas for the same condition Dykman and Pekar obtained a nonpolarizing exciton.

2. From the cited results it will be apparent that the 2p-state energy of a polarizing electron depends not only on the effective mass ratio, but also on the mass values per se.

This deduction is also at variance with the results of Dykman and Pekar, where the energy in atomic units depends only on the effective-mass ratio.

3. It also follows from the values listed in the table that for a given m_1 increasing the mass ratio leads to a gradual increase in the polarizing action of the exciton on the lattice and to a continuous lowering of the 2p-exciton level with respect to the corresponding hydrogen-like level.

According to Dykman and Pekar, on the other hand, the transition from the nonpolarizing exciton to the polarizing one occurs in the form of a sudden jump when the mass ratio takes on a certain value, which is constant for a given energy level.

There is reason to assume that this appreciable qualitative difference between our results and those of Dykman & Pekar stems from the fact that we did not use the adiabatic approximation, which is valid for strong coupling.

4. In the present work we have calculated only one exciton energy level. It would nevertheless seem possible to arrive at certain conclusions with respect to the spectrum as a whole. Except for the case $m_1 = m_2$, the exciton spectrum will differ from the hydrogen-like one in two ways: first, in the location of the levels, since the various hydrogen-like levels will be depressed by unequal amounts due to the polarization; second, in the number of levels, since the interaction of the exciton with the phonon field removes the "accidental" degeneracy in the orbital quantum number. This means, for instance, that the 2p- and 2s-levels of the exciton should differ, whereas in the case of a hydrogen-like atom they coincide.

5. The entire theory has been constructed on the assumption that the exciton wave function is so "smeared out" that the crystal may be treated as a

continuous medium. The amount of "smearing out" of the wave function is given by the variation parameter δ. On transforming to parameters which are not dimensionless, we must compare $1/\delta_{dim}$ with the square of the lattice constant.

In a Cu_2O crystal the lattice constant is of the order of 4 Å. In all cases investigated, $(1/\delta_{dim})/a^2$ is much greater than unity ($\sim 10^3$) and, therefore, the wave function is smeared out over a large number of unit cells (~ 30). Therefore the continuum approximation may be considered acceptable.

Leningrad Physical-Technical Institute

References

1. E.F.Gross & N.A.Karryev, Doklady AN SSSR, 84, 261, 471 (1952); E.F.Gross & B.P.Zakharchenia, Doklady AN SSSR, 90, 745 (1953); E.F.Gross, B.P.Zakharchenia & N.M.Reinov, Doklady AN SSSR, 92, 265, (1953); 97, 57, 221 (1954); 99, 231, 527 (1954).

2. S.Nikitine, M.Sieskind & G.Perny, C.R., 238, 67, 1987 (1954); M.Hyashi & K.Katsuki, J.Phys.Soc.Japan, 7, 599 (1952).

3. I.M.Dykman & S.I.Pekar, Doklady AN SSSR, 96, 1137 (1954); Trudy (Transactions) Inst. of Phys., Ukrainian Ac. of Sci., No.s, 92 (1952).

4. S.I.Pekar, Issledovaniia po elektronnoi teorii kristallov (Studies in the electron theory of crystals) M. 1951.

5. S.Tomonaga, Progr. Theor. Phys., 2, 6 (1947).

6. T.D.Lee & D.Pines, Phys.Rev., 90, 382 (1953).

7. T.D.Lee, F.E.Low & D.Pines, Phys.Rev., 90, 297 (1953).

8. N.F.Mott, Proc.Roy.Soc., 167, 384 (1938).

9. W.A.Fock, Sow.Phys., 6, 425 (1934).

10. N.N.Bogoliubov, Ukr.matem.zhurnal (Ukrainian Math.Journal) 2,3 (1950).

11. Iu.V.Novozhilov, Vestnik (Review), Leningrad State Univer., No.11, (1954).

12. I.P.Ipatova, Dissertation, Leningrad State Univ., 1955.

13. V.N.Faddeeva & N.M.Terent'ev, Tablitsy znachenii integrala veroiatnostei (Tables of probability integrals), Moscow, 1954.

14. P.S.Mattews & A.Salam, Phys.Rev., 86, 715 (1952).

ON A CURRENT CARRIER RECOMBINATION MECHANISM IN STRONGLY ALLOYED SEMICONDUCTORS

- V.L.Bonch-Bruevich

Introduction

The problem of nonradiative electron transitions in crystals cannot yet be considered definitively solved, despite the significant advances made in this direction during the past few years[1-3]. Yet the problem is an important and timely one, for upon its solution hinge such other problems as, for example, determining the cross section for recombination of current carriers in semiconductors. A fundamental difficulty in theoretical treatments of the problem is clarification of the mechanism by which energy liberated in recombination is carried off (the law of the conservation of quasimomentum leads to no difficulties whenever the recombination takes place in the field of some structural defect or recombination center). It is usually assumed that the evolved energy is transferred directly to the lattice, so that one must consider the complex problem of interactions between the electrons and the lattice, taking into account large deformations of the latter.

Without in any sense discounting the importance of the direct interaction between current carriers and the lattice, we would like to point out that there may well exist another mechanism for removing the energy, a mechanism which does not involve its immediate transfer to the lattice. Actually, for recombination it is necessary only to transfer some of the current carrier energy to any elementary excitations without charge (or with only a very small effective charge). For example, a pure electron system, considered in the approximation of the equilibrium lattice, possesses such neutral excitations. We are referring here to excitons* of some type or plasma vibrations of the electron-hole gas (in ferromagnetic semiconductors we must also add spin waves). In the present article we shall consider recombination with energy transfer to plasma oscillations.

1. Plasma oscillations of the electron-hole gas in semiconductors

As has previously been shown[6], the many-electron problem in semiconductors can be systematically reduced to the simpler problem of the behavior of a set of elementary excitations, namely, the "excess" electrons (which we shall henceforth refer to simply as electrons) and holes. As has been emphasized in Ref.6 the matter of taking into account the interaction between these is a separate problem, which can be most readily solved by the method of "collective variables," developed by D.N.Zubarev[7]. We shall, however, have to generalize and extend the method to the case of the presence of an external field and of two "kinds" of interacting particles.

The equation for the system of electrons and holes can be written in configuration space in the form of the usual Schrödinger equation with a Hamiltonian:

---

*The inverse process, an exciton breaking up into current carriers in the field of a defect, has already been treated by Lashkarev[4] and Zhuze & S.M.Ryvkin[5] in connection with photoconductivity studies.

$$H = \sum_i -\frac{\hbar^2}{2m}\nabla_i^2 + \sum_a -\frac{\hbar^2}{2m}\nabla_a^2 + \frac{1}{2}\sum_{i\neq j} u(\mathbf{r}_i - \mathbf{r}_j) +$$

$$+ \frac{1}{2}\sum_{a\neq b} u(\mathbf{r}_a - \mathbf{r}_b) + \sum_{i\neq a} u(\mathbf{r}_i - \mathbf{r}_a) + \sum_i u_1(r_i) + \sum_a u_2(\mathbf{r}_a). \qquad (1)$$

Here i, j and a, b are indices numbering the electrons and holes, respectively, $\mathbf{r}_i$ and $\mathbf{r}_a$ are the corresponding coordinate vectors, and $u(\mathbf{r}_i - \mathbf{r}_j)$, $u(\mathbf{r}_a - \mathbf{r}_b)$ and $u(\mathbf{r}_i - \mathbf{r}_a)$ are the potential energies of interaction, respectively, of the electrons with each other, holes with each other, and electrons with holes; u_1 and u_2 are the effective potential energies of an electron and a hole in the external field (for instance, the field of the crystal lattice or of defects in the lattice) and m is the true mass of the electron (in this description the true electron mass also appears in the kinetic energy of a hole; see also Heisenberg[8]).

Let us write the potential energies in the form (V is the normalizing volume)

$$u(\mathbf{r}_i - \mathbf{r}_j) = \sum_k \frac{v_1(\mathbf{k})}{V} e^{i(\mathbf{k}, \mathbf{r}_i - \mathbf{r}_j)}, \qquad (2)$$

$$u(\mathbf{r}_a - \mathbf{r}_b) = \sum_k \frac{v_2(\mathbf{k})}{V} e^{i(\mathbf{k}, \mathbf{r}_a - \mathbf{r}_b)}, \qquad (3)$$

$$u(\mathbf{r}_i - \mathbf{r}_a) = \sum_k \frac{v(\mathbf{k})}{V} e^{i(\mathbf{k}, \mathbf{r}_i - \mathbf{r}_a)}, \qquad (4)$$

$$u_1(\mathbf{r}_i) = \sum_k \frac{b_1(\mathbf{k})}{V} e^{-i\mathbf{k}\mathbf{r}_i}, \qquad (5)$$

$$u_2(\mathbf{r}_a) = \sum_k \frac{b_2(\mathbf{k})}{V} e^{-i\mathbf{k}\mathbf{r}_a}, \qquad (6)$$

and, following Zubapev[7], introduce the collective variables

$$\rho_1(\mathbf{k}) = \frac{1}{\sqrt{N_1}} \sum_{i=1}^{N_1} e^{-i\mathbf{k}\mathbf{r}_i}; \quad \mathbf{k} \neq 0. \qquad (7)$$

$$\rho_2(\mathbf{k}) = \frac{1}{\sqrt{N_2}} \sum_{a=1}^{N_2} e^{-i\mathbf{k}\mathbf{r}_a}; \quad \mathbf{k} \neq 0. \qquad (8)$$

Here N_1 and N_2 are the numbers of electrons and holes. It is assumed in Eqs.(7), (8) that $k < k_0$, where k_0 has yet to be evaluated. In distinction from Ref. 7, we have here two types of collective variables, corresponding to the two kinds of particles. The Hamiltonian in the "mixed" representation, when the wave function depends on the individual variables $\mathbf{r}_i$, $\mathbf{r}_a$ and on the collective ones ρ_1, ρ_2, is easily written by analogy with the development in Ref.7. We have

$$\sum_{i\neq a} u(\mathbf{r}_i - \mathbf{r}_a) = \sum_{i\neq a}\sum_k \frac{v(\mathbf{k})}{V} e^{i(\mathbf{k}, \mathbf{r}_i - \mathbf{r}_a)} = \sum_{i\neq a}\sum_{k>k_0} \frac{v(k)}{V} e^{i(\mathbf{k}, \mathbf{r}_i - \mathbf{r}_a)} +$$

$$+ \frac{\sqrt{N_1 N_2}}{V} \sum_{\substack{k\neq 0 \\ k<k_0}} v(\mathbf{k})\rho_1(-\mathbf{k})\rho_2(\mathbf{k}) + \frac{N_1 N_2}{V} v(0) - \frac{\min\{N_1, N_2\}}{V} \sum_{\substack{k\neq 0 \\ k<k_0}} v(\mathbf{k}). \qquad (9)$$

$$\sum_i V_i(\mathbf{r}_i) = \sum_{\substack{k\neq 0 \\ k<k_0}} \frac{\sqrt{N_1}}{V} b_1(\mathbf{k})\rho_1(\mathbf{k}) + \sum_{\substack{k,\, i \\ k>k_0}} \frac{b_1(\mathbf{k})}{V} e^{-i\,\mathbf{k}\mathbf{r}_i} + \frac{N_1}{V} b_1(0). \qquad (10)$$

$$\sum_a V_2(\mathbf{r}_a) = \sum_{\substack{k\neq 0\\ k<k_0}} \frac{\sqrt{N_2}}{V} b_2(k)\rho_2(\mathbf{k}) + \sum_{\substack{k,\ a\\ k>k_0}} \frac{b_2(\mathbf{k})}{V} e^{-i\,\mathbf{k}\mathbf{r}_a} + \frac{N_2}{V} b_2(0). \tag{11}$$

The remaining terms are calculated in exactly the same way as in Ref.7. Let us write the wave function ψ in the form

$$\psi = e^{\frac{1}{4}\sum\limits_{k<k_0}\sum\limits_{i=1,2} \rho_i(\mathbf{k})\rho_i(-\mathbf{k}) + \frac{i}{\hbar}\varepsilon_0 t}\Phi, \tag{12}$$

where ε_0 is a constant defined by

$$\varepsilon_0 = \frac{1}{2}\frac{N_1^2}{V}\nu_1(0) + \frac{1}{2}\frac{N_2^2}{V}\nu_2(0) + \frac{N_1N_2}{V}\nu(0) + \frac{N_1}{V}b_1(0) + \frac{N_2}{V}b_2(0) +$$

$$+\frac{1}{2}\sum_{\substack{k\neq 0\\ k<k_0}}\left\{E_1(k) + E_2(k) - \frac{\hbar^2k^2}{m} - \frac{N_1}{V}\nu_1(k) - \frac{N_2}{V}\nu_2(k) - 2\frac{\min\{N_1, N_2\}}{V}\nu(k)\right\}, \tag{13}$$

$$E_i^2(k) = \sqrt{\frac{N_i}{V}\cdot\frac{\hbar^2k^2}{m}\nu_i(k) + \left(\frac{\hbar^2k^2}{2m}\right)^2} \quad (i = 1, 2). \tag{14}$$

(In the case of Coulomb interaction the terms in the first line of Eq.(13) make no contribution, for, owing to the electrical neutrality of the system, when added to the appropriate Fourier coefficient of the interaction energy for stationary charges they vanish.)

Then according to Ref.7, after second quantization we obtain a wave equation for Φ whose Hamiltonian is

$$H = H_1 + H_2 + H' + H'' + H'''.$$

$$H_1 = \sum_{f,\sigma,i}\left\{\frac{\hbar^2f^2}{2m}a^*_{f,i,\sigma}a_{f,i,\sigma} + \sum_{k>k_0}\frac{b_i(k)}{V}a^*_{k-f,i,\sigma}a_{f,i,\sigma}\right\}. \tag{15}$$

$$H_2 = \sum_{\substack{k\neq 0\\ k<k_0}}\left\{\sum_{i=1,2}E_i(k)\xi_i^*(\mathbf{k})\xi_i(\mathbf{k}) + \frac{\sqrt{N_1N_2}}{V}\nu(k)\lambda_1(-\mathbf{k})\lambda_2(\mathbf{k})\times\right.$$

$$\left.\times[\xi_1(-\mathbf{k}) + \xi_1^*(\mathbf{k})][\xi_2(\mathbf{k}) + \xi_2^*(-\mathbf{k})] + \sum_{i=1,2}\frac{\sqrt{N_i}}{V}\lambda_i(\mathbf{k})b_i(\mathbf{k})[\xi_i(\mathbf{k}) + \xi_i^*(-\mathbf{k})]\right\}. \tag{16}$$

$$H' = -\sum_{i=1,2}\frac{1}{\sqrt{N_i}}\sum_{f,\sigma}\sum_{\substack{k\neq 0\\ k<k_0}}\frac{\hbar^2(\mathbf{k},\mathbf{f})}{2m\lambda_i(\mathbf{k})}\{[1+\lambda_i^2(\mathbf{k})]\xi_i(-\mathbf{k}) +$$

$$+[\lambda_i^2(\mathbf{k}) - 1]\cdot\xi_i^*(\mathbf{k})\}a^*_{\mathbf{f}-\mathbf{k},\,i,\sigma}a_{\mathbf{f},i,\sigma}. \tag{17}$$

$$H'' = \frac{1}{2}\sum_{\substack{f,f'\\ \sigma,\sigma'}}\sum_{k>k_0}\left\{\sum_{i=1,2}\frac{\nu_i(k)}{V}a^*_{\mathbf{f},i,\sigma}a^*_{\mathbf{f}',i,\sigma'}a_{\mathbf{f}'+k,i,\sigma'}a_{\mathbf{f}-\mathbf{k},i,\sigma} +\right.$$

$$\left.+2\frac{\nu(k)}{V}a^*_{\mathbf{f},1,\sigma}a^*_{\mathbf{f}',2,\sigma'}a_{\mathbf{f}'+\mathbf{k},2,\sigma'}a_{\mathbf{f}-\mathbf{k},1,\sigma}\right\}. \tag{18}$$

Translation editor's note: While we normally try to repair minor misprints in the process of stripping in the equations, this article has so many "typos" that we had to give up the attempt. C.T.T.

$$H''' = \sum_{i=1,2} \frac{1}{\sqrt{N_i}} \sum_{\substack{k,\ k'<k_0 \\ k+k'\neq 0}} \frac{\hbar^2(\mathbf{k},\mathbf{k}')}{8m} \frac{\lambda_i(\mathbf{k}+\mathbf{k}_i)}{\lambda_i(\mathbf{k})\lambda_i(\mathbf{k}')} \{\xi_i(\mathbf{k}+\mathbf{k}') + \xi_i^*(-\mathbf{k}-\mathbf{k}')\} \times$$

$$\times \{[1+\lambda_i^2(\mathbf{k})]\,\xi_i(-\mathbf{k}) + [\lambda_i^2(\mathbf{k})-1]\,\xi_i^*(\mathbf{k})\}\{[1+\lambda_i^2(\mathbf{k}')]\,\xi_i(-\mathbf{k}') +$$

$$+ [\lambda_i^2(\mathbf{k}')-1]\,\xi_i^*(\mathbf{k}')\}. \tag{19}$$

Here $a^*_{\mathbf{f},i,\sigma}$ and $a_{\mathbf{f},i,\sigma}$ are the creation and annihilation operators for fermions with momentum $\mathbf{f}$ and spin σ; these excitations correspond to electrons ($i=1$) and holes ($i=2$) of the standard theory; $\xi_i(\mathbf{k})$ and $\xi_i^*(\mathbf{k})$ are Bose operators describing the plasma vibrations, and the $\lambda_i(\mathbf{k})$ are given by the relations (i = 1, 2):

$$\lambda_i^4(\mathbf{k})\left[\frac{N_i}{V}\nu_i(\mathbf{k}) + \frac{\hbar^2k^2}{4m}\right] = \frac{\hbar^2k^2}{4m}. \tag{20}$$

The operators H_1 and H_2, respectively, describe the behavior of non-interacting fermions and bosons in an external field, and make up the main part of the Hamiltonian. The rest of the terms in H are treated as perturbations. The validity of this approximation is discussed in Ref.7. In our case Eq.(33) of Ref.7 remains valid, so that hereinafter we will consider $\lambda_i^4(\mathbf{k}) \ll 1$, neglecting $\lambda_i^2(\mathbf{k})$ with respect to unity. The condition for weakness of the interaction between fermions and phonons differs from that deduced in Ref.7, since in the system we are considering, the Fermi gas is, in general, not degenerate. From what follows it will be evident that the concept of bands (conduction and hole) is applicable to our Fermi excitations (hence, for the sake of brevity, we will hereinafter refer to them simply as electrons and holes).

Clearly the matrix elements of H' are small whenever the energy of most of the electrons (holes) in the band is less than the minimum energy of the plasma phonons. The latter is defined as the first eigenvalue of H_2 (see below; with Coulomb interaction and only one kind of particle present, it is given by $\sqrt{\frac{4\pi Ne^2\hbar^2}{mV}}$).

We shall see later that in the case which concerns us this condition is actually fulfilled.

Eq.(15) generalizes the results of Ref.7 to the case of an external field and two kinds of particles. In the present case, however, the main part of the Hamiltonian is not diagonal and we must therefore first consider its diagonalization.

Let us first perform the canonical transformation (cf. Ref.9).

$$\xi_i(\mathbf{k}) = \sum_{\mu=1,2} \{u_\mu(i,\mathbf{k})\,\eta_\mu(\mathbf{k}) + \overline{v_\mu}(i,\mathbf{k})\,\eta_\mu^*(\mathbf{k})\}, \tag{21}$$

where $\eta_\mu^*(\mathbf{k})$ and $\eta_\mu(\mathbf{k})$ are new Bose operators, and the functions $u_\mu(i,\mathbf{k})$ and $v_\mu(i,\mathbf{k})$ are defined by

$$\left.\begin{aligned} \sum_i \{[E_i(k)\,\delta_{ij} + n_{ij}(\mathbf{k})]\,v_\mu(i,\mathbf{k}) + n_{ij}(\mathbf{k})\,u_\mu(i,\mathbf{k})\} &= -W_\mu v_\mu(j,\mathbf{k}), \\ \sum_j \{[E_j(k)\,\delta_{ij} + n_{ii}(\mathbf{k})]\,u_\mu(j,\mathbf{k}) + n_{ij}(\mathbf{k})\,v_\mu(j,\mathbf{k})\} &= W_\mu u_\mu(i,\mathbf{k}). \end{aligned}\right\} \tag{22}$$

Here W_μ are the eigenvalues of Eqs.(22), and we have introduced the notation

$$n_{ij}(\mathbf{k}) = \frac{\sqrt{N_1 N_2}}{V} \nu(\mathbf{k}) \lambda_i(-\mathbf{k}) \lambda_j(\mathbf{k}), \quad i \neq j; \quad n_{ij}(\mathbf{k}) = 0, \quad i = j. \tag{23}$$

We note that for a Coulomb interaction, all the quantities entering into these expressions are even functions of k, and the functions u and v are real.

In terms of the new operators, the Hamiltonian H_2 of the Bose field becomes (for the case of a Coulomb interaction, when $\nu_1 = \nu_2 = \frac{4\pi e^2}{k^2}$ and $\nu = -\frac{4\pi e^2}{k^2}$)

$$H_2 = -\sum_\mu \sum_i \sum_{\substack{k \neq 0 \\ k < k_0}} \left\{ W_\mu(k) |v_\mu(i,k)|^2 + \sqrt{\frac{N_i}{V}} \lambda_i(k) b_i(\mathbf{k}) [u_\mu(i,k) \eta_{|\mu}(\mathbf{k}) + \right.$$

$$\left. + \bar{v}_\mu(i,k) \eta^*_{|\mu}(-\mathbf{k}) + \bar{u}_\mu(i,k) \eta^*_{|\mu}(\mathbf{k}) + v_\mu(i,k) \eta_{|\mu}(-\mathbf{k})] \right\} + \sum_\mu \sum_k W_\mu(\mathbf{k}) \eta^*_{|\mu}(\mathbf{k}) \eta^*_{|\mu}(\mathbf{k}). \tag{24}$$

The eigenvalues $W_\mu(k)$ are found to be

$$W_{1,2}(k) = \left\{ \frac{\frac{4\pi e^2 \hbar^2}{m}(n_1 + n_2) + \left(\frac{\hbar^2 k^2}{2m}\right)^2}{2} \pm \sqrt{\frac{\left[\frac{4\pi e^2 \hbar}{m}(n_1 - n_2) + \left(\frac{\hbar^2 k^2}{2m}\right)^2\right]^2}{4} + \left(\frac{4\pi e^2 \hbar^2}{m}\right)^2 n_1 n_2} \right\}^{1/2}, \tag{25}$$

where $n_i = \frac{N_i}{V}$ are the concentrations of electrons and holes.*

Now setting

$$\eta_\mu(\mathbf{k}) = B_\mu(\mathbf{k}) + \varphi_\mu(\mathbf{k}), \tag{26}$$

where $B_\mu(\mathbf{k})$ are Bose operators, and φ_μ is the "c" number given by the equation

$$\varphi_\mu(\mathbf{k}) = -\frac{1}{V\sqrt{V}} \sum_i \frac{V n_i \lambda_i(k)}{W_\mu(k)} \{\bar{v}_\mu(i,k) b_i(\mathbf{k}) + \bar{u}_\mu(i,k) b_i(-\mathbf{k})\}, \tag{27}$$

we finally obtain

$$H_2 = -\sum_{\substack{\mu, k \neq 0 \\ k < k_0}} \left\{ \sum_i |w_\mu(i,k)|^2 + |\varphi_\mu(\mathbf{k})|^2 - B^*_\mu(\mathbf{k}) B_\mu(\mathbf{k}) \right\} W_\mu(k).$$

We note that there now appear terms without Bose operators in H'. These may reasonably be included in H_1 in the zeroth approximation. Thus we now have (neglecting $\lambda_i^2(\mathbf{k})$ as compared with unity)

$$H_1 = \sum_{f,\sigma,i} \left\{ \frac{\hbar^2 f^2}{2m} a^*_{\mathbf{f},i,\sigma} a_{\mathbf{f},i,\sigma} + \sum_{k > k_0} \frac{b_i(\mathbf{k})}{V} a^*_{\mathbf{k}-\mathbf{f},i,\sigma} a_{\mathbf{f},i,\sigma} \right\} +$$

$$+ \frac{i}{V} \frac{\hbar}{2m} \sum_{i,j,\mu} \sum_{\substack{k \neq 0 \\ k < k_0}} \frac{(\mathbf{k},\mathbf{f})}{W_\mu(k)} u_\mu(i,k) \bar{v}_\mu(j,k) \left\{ [b_j(-\mathbf{k}) + \right.$$

$$\left. + b_j(\mathbf{k})] \sqrt{\frac{n_j}{n_i}} \frac{\lambda_j(k)}{\lambda_i(k)} a^*_{\mathbf{f}-\mathbf{k},i,\sigma} a_{\mathbf{f},i,\sigma} + [b_i(-\mathbf{k}) + b_i(\mathbf{k})] \sqrt{\frac{n_i}{n_j}} \cdot \frac{\lambda_i(k)}{\lambda_j(k)} a^*_{\mathbf{f}-\mathbf{k},j,\sigma} a_{\mathbf{f},j,\sigma} \right\}. \tag{28}$$

---

*The author has now found a more accurate expression for the spectrum: m^{-1} in Eq.(25) should actually be replaced by the average reciprocal effective mass multiplied by the number of minima (the dielectric susceptibility of the substance is added to the denominator). These changes, however, do not significantly alter the evaluation of Eq.(40)(in the case of Ge and Si).

(If there exist particles of only one kind - i.e., electrons or holes - then either $u = 0$ or $v = 0$ and the last term in Eq.(28) is absent).

In order to diagonalize H_1 let us perform the following canonical transformation on the Fermi operators,

$$a_{\mathbf{f},i,\sigma} = \sum_r \varphi_r(\mathbf{f})\, A_{r,i,\sigma}, \tag{29}$$

where the $A_{r,i,\sigma}$ are new Fermi operators and the functions $\varphi_r(\mathbf{f})$ are the orthonormal solutions of the equation

$$\frac{\hbar^2 f^2}{2m}\varphi_r(\mathbf{f}) + \sum_{\mathbf{k}>k_0}\frac{b_i(-\mathbf{k})}{V}\varphi_r(\mathbf{k}-\mathbf{f}) + \frac{\hbar^2}{2mV}\sum_{j,\mu}\sum_{\substack{k\neq 0\\ k<k_0}}\frac{b_j(-\mathbf{k})+b_j(\mathbf{k})}{2W_\mu(k)}(\mathbf{k},f)\sqrt{\frac{n_j}{n_i}\frac{\lambda_j(\mathbf{k})}{\lambda_i(k)}}\left[u_\mu(i,k)\,\bar{v}_\mu(j,k) + \right.$$

$$\left. + u_\mu(j,k)\,\bar{v}_\mu(i,k)\right]\varphi_r(\mathbf{f}-\mathbf{k}) = E_{r,i}\varphi_r(\mathbf{f}). \tag{30}$$

Then

$$H_1 = \sum_{r,i,\sigma} E_{r,i}\, A^*_{r,i,\sigma}\, A_{r,i,\sigma}. \tag{31}$$

We note that the operators A and A* describe the equivalent here of electrons and holes in ordinary semiconductor theory. Eq.(30) is nothing other than the wave equation for an electron (hole) in the momentum representation, with the effective field acting on the fermions modified due to screening.* The index r which numbers the eigenvalues of Eq.(30) is actually a set of indices, indicating, for instance, the band number (electron or hole) and quasimomentum, or the set of quantum numbers (except the spin) characterizing the possible local levels.

The perturbing terms in Eq.(15) play no significant role in the calculation of the energy spectrum of the system in our approximation. The operator H', however, is extermely important in considering nonequilibrium processes in semiconductors, since it describes the energy exchange between fermions and bosons and provides, in particular, for the possibility of current carrier recombination under given conditions. (The role of current carriers, naturally, is played by the Fermi excitations since the effective charge of the plasma phonons is zero.) In terms of the new operators A and B, the operator H' becomes

$$H' = -\sum_{i,\mu}\sum_{\sigma}\sum_{r,r'}\sum_{\substack{k\neq 0\\ k<k_0}}\frac{\hbar^2}{2mV\sqrt{N_i}}A^*_{r,i,\sigma}A_{r',i,\sigma}\{[u_\mu(i,k)\times$$

$$\times F^{(i)}_{r,r'}(-\mathbf{k}) - v_\mu(i,k)\,F^{(i)}_{rr'}(\mathbf{k})]\,B_\mu(\mathbf{k}) + [v_\mu(i,k)\,F^{(i)}_{rr'}(-\mathbf{k}) - u_\mu(i,k)\,F^{i}_{rr'}(\mathbf{k})]\,B^*_\mu(\mathbf{k})\}. \tag{32}$$

where we have introduced the notation

$$F^{(i)}_{rr'}(\mathbf{k}) = \sum_{\mathbf{f}}\frac{(\mathbf{k},f)}{\lambda_i(k)}\bar{\varphi}_r(\mathbf{f}-\mathbf{k})\,\varphi_{r'}(\mathbf{f}). \tag{33}$$

The operator H' is not Hermitian, but as is made clear in Ref.7, in the

---

*It is clear from Eq.(30) that the periodicity of the potential, as one may have expected, is retained in this approximation.

present case this situation requires no further analysis.*

2. Electron-hole recombination with energy transfer to plasma vibrations.

The operator H' which takes into account the interaction of the current carriers with plasma type vibrations, describes, in particular, the processes of localization of carriers on impurity levels** with the simultaneous creation of Bose excitations. For sufficiently high energies of the latter (that is for sufficiently large electron or hole concentrations) these processes are possible even in the first approximation of perturbation theory and hence should not be ignored.

To be specific, we shall consider an n-type semiconductor, assuming that it contains two types of defects (as appears to be the actual case in a number of instances): those of one type are ordinary donors that determine the type of conductivity; those of the other are located deeper below the bottom of the conduction band and, as will be shown below, are capable of acting as traps (the generalization to several types of traps leads to trivial results). It will be evident from what follows that the entire calculation is of interest only for a sufficiently high donor concentration n_d. We shall therefore assume this concentration to be significantly greater than the trap concentration n_t, which makes it possible to neglect the contribution of the traps to the equilibrium conditions in determining the electron concentration n_1 in the conduction band. For conditions of complete depletion*** of the donors, n_1 may be considered temperature independent (for equilibrium we would have $n_1 = n_d$; we shall not, however, use this equation, for we wish to consider, for instance, the possibility of high injection).

The hole concentration n_2 in the given case is small compared with n_1; assuming $n_1 \ll \sqrt{n_1 n_2} \ll n_2$ and bearing in mind the normalization conditions for u and v, Eq.(22) leads to

$$u_1(1, k) \approx 1; \quad u_1(2, k) \approx \frac{n_{12}}{W_1};$$
$$v_i(1, k) \approx 0; \quad v_1(2, k) \approx -\frac{n_{12}}{W_1}; \tag{34}$$

$$W_1(k) \approx \sqrt{\frac{4\pi n_1 e^2 \hbar^2}{m} + \left(\frac{\hbar^2 k^2}{2m}\right)^2}. \tag{35}$$

The second solution of Eqs.(22) vanishes in this approximation (i.e., the plasma oscillations are due only to electrons; strictly speaking, there is also a "hole" mode, but the corresponding quanta are too small and are of no interest where our problem is concerned). We can accordingly drop the index μ of the Bose operators, since it now takes on only one value.

Eq.(32) for H' becomes

$$H' = H_1' + H_2',$$

---

*It would be more correct to say that the operator H' is Hermitian with respect to a certain weighted inner product which takes into account the coupling between $\rho_i(k)$ and r_i, r_a.

**We shall call such defects traps without specifying for the time being whether they are recombination centers in the strict sense or simply give rise to "sticking levels".

***At the donor concentrations with which we shall deal, complete depletion does in fact occur at room temperatures.

where

$$H_1' = -\sum_{\sigma}\sum_{r,\,r'}\sum_{\substack{k\neq 0\\ k<k_0}} \frac{\hbar^2}{2m\sqrt{N_1}} A^*_{r,\,1,\,\sigma} A_{r',\,1,\,\sigma} \{F^{(1)}_{rr'}(-\mathbf{k})\, B(\mathbf{k}) - F^{(1)}_{rr'}(\mathbf{k})\, B^*(\mathbf{k})\}, \qquad (36)$$

and

$$H_2' = -\sum_{\sigma}\sum_{r,\,r'}\sum_{\substack{k\neq 0\\ k<k_0}} \frac{\hbar^2}{2m\sqrt{N_2}} A^*_{r,\,2,\,\sigma} A_{r',\,2,\,\sigma} \frac{n_{12}(k)}{W_1(k)} \times$$

$$\times \{[F^{(2)}_{rr'}(-\mathbf{k}) + F^{(2)}_{rr'}(\mathbf{k})]\, B(\mathbf{k}) - [F^{(2)}_{rr'}(-\mathbf{k}) + F^{(2)}_{rr'}(\mathbf{k})]\, B^*(\mathbf{k})\}. \qquad (37)$$

The operators H_1' and H_2' describe the processes of recombination of majority and minority carriers, respectively, with the emission of plasma quanta (as well as the inverse processes). The indices r and r' take on the following values:

a) In H_1': $r = r_1$ is the number of the local electron level, $r' = \mathbf{p}$ is the quasi-wave vector of the conduction electron (the corresponding energy is $E_1(\mathbf{p})$).

b) In H_2': $r = r_2$ is the number of the local hole level, $r' = \mathbf{p}$ is the quasi-wave vector of the hole in a hole zone (the corresponding energy is $E_2(\mathbf{p})$).

Obviously, for the processes under consideration to be possible, the following energy conditions must be satisfied:

$$E_i(\mathbf{p}) - E_{r_i} = W_1(k) \quad (i = 1 \text{ or } 2), \qquad (38)$$

and the value of k obtained from this condition (let us denote it by $\varkappa$) should be no greater than k_0, that is,

$$\varkappa \leqslant k_0. \qquad (39)$$

Bearing in mind[7] that $k_0 \leqslant 2\left(\frac{\pi n_1}{a_0}\right)^{1/4}$, where $a_0 = \frac{\hbar^2}{me^2}$, Eq. (38) and Eq. (39) lead to

$$n_1 \geqslant 4\cdot 10^{20}\varkappa^2 \text{cm}^{-3} \qquad (40)$$

Here $\varkappa$ is the difference $E_i(\mathbf{p}) - E_{r_i}$ in electronvolts.

The meaning of this condition is clear: the plasma vibration quanta must be sufficiently large. It is clear from Eq. (40) that the recombination mechanism suggested here can operate only in strongly alloyed specimens (or for a very high injection level); for $E_i(\mathbf{p}) - E_{r_i} \approx 0.1$ ev, for instance, n_1 is found to be about 10^{18} cm^{-3}. Therefore what has been said herein should not be interpreted as a complete negation of the direct role of the lattice in recombination processes. In those cases, however, when the plasma mechanism is possible, it can apparently be extremely important, since the cross sections for it may be quite large, as we shall now show.

In order to calculate the transition probabilities due to the operator H', we must know $F^{(i)}_{rr'}(\mathbf{k})$ (see Eq. (33)). Approximating the electron and hole wave functions in their respective zones by plane waves, we obtain

$$F^{(i)}_{rr'}(\mathbf{k}) = \frac{(\mathbf{k}, \mathbf{p})}{\lambda_i(k)}\, \varphi_{r_i}(\mathbf{p} - \mathbf{k}), \qquad (41)$$

where $\varphi_{r_i}(\mathbf{p}-\mathbf{k})$ is the Fourier coefficient of the electron (hole) wave function for a local level.

Then the recombination cross sections for majority (σ_1) and minority (σ_2) carriers are given by

$$\sigma_1 = g(r_1)\,\frac{mm_1 p}{2\pi n_1 \hbar^4 \varkappa}(E_1(\mathbf{p}) - E_{r_1})^2 \int_0^{\pi} \sin\theta\cos^2\theta\,|\varphi_{r_1}(\mathbf{p}-\mathbf{k})|^2\,d\theta, \tag{42}$$

$$\sigma_2 = g(r_2)\,\frac{2\pi m_2 n_1 e^4 p}{m\,[E_2(\mathbf{p}) - E_{r_2}]^2} \int_0^{\pi} \sin\theta\cos^2\theta\,|\varphi_{r_2}(\mathbf{p}-\mathbf{k}) - \varphi_{r_2}(\mathbf{p}+\mathbf{k})|^2\,d\theta. \tag{43}$$

Here θ is the angle between the vectors $\mathbf{p}$ and $\mathbf{k}$; m_1 and m_2 are the effective masses of electrons and holes, respectively,* and $g(r_1)$ and $g(r_2)$ are the statistical weights of the electron and hole local states. It is assumed that the functions φ_{r_i} are normalized to a unit volume.

The dependence of σ on the depth of the local level, which appears explicitly in Eqs.(42) and (43), is not final, since the wave functions φ_{r_i} also depend on E_{r_i}. This dependence cannot be found in general (since actually the functions φ_{r_i} depend on the specific nature of the defect). Since the defects most active in the recombination process are obviously charged ones (of the appropriate sign), let us calculate the cross sections of Eq.(42) and (43) for the special case in which the functions φ_{r_i} have the Coulomb interaction form**

$$\varphi_{r_i}(\mathbf{p}-\mathbf{k}) = \frac{8\alpha_i^{5/2}\sqrt{\pi}}{[\alpha_i^2 + (\mathbf{p}-\mathbf{k})]^2}, \tag{44}$$

and

$$E_{r_i} = -\frac{\alpha_i e^2}{2} \tag{45}$$

(we reckon the energy from the lower edge of the corresponding band).

Bearing in mind that $\alpha \gg \tilde{p}$ when $E_{r_i} \approx 0.1$ ev (here $\tilde{p}$ is the statistical average of the quasi-wave vector in the nondegenerate gas), Eqs.(42)-(45) lead to

$$\sigma_1 \approx g(r_1)\,\frac{64\alpha_1^5 mm_1}{p\hbar^4 n_1 \varkappa^7}\,[E_1(\mathbf{p}) - E_{r_1}]^2 \approx 2\cdot 10^3 g(r_1)\,\frac{mm_1(\Delta W_1)^6}{p\hbar^4 e^{10} n_1 \varkappa^7}, \tag{46}$$

$$\sigma_2 \approx 8\cdot 10^6 g(r_2)\,\frac{m_2 n_1 p^3 (\Delta W_2)^3}{e^6 \varkappa^{11}}, \tag{47}$$

where ΔW_1 and ΔW_2 denote the energies liberated when a current carrier is captured.

As regards order of magnitude, in both cases we obtain (with $m_1, m_2 \approx m$, $\tilde{p} \approx 10^{-6}\,\mathrm{cm}^{-1}$, $\Delta W = 0.1$ ev, $g = 1$): $\sigma_1 = \sigma_2 \approx 10^{-14} - 10^{-15}\ \mathrm{cm}^2$, which means that if it is possible at all, this recombination mechanism must play an extremely important role. We note the strong dependence of the cross sections (Eqs.(46) and (47)) on the depth of the local level. Shallow lying levels are completely ineffective from the point of view of recombination by this mechanism.

The dependence of the cross sections on the majority carrier concentrations may be of experimental interest. In view of Eqs.(40) and (42), σ_1 should

---

*If the isoenergetic surfaces are not spherical, m_1 and m_2 are actually some combinations of the effective masses; for a rough evaluation, however, their exact form is not important.

**We do not, of course, mean that the wave functions are of the form given by Eq.(44) simultaneously for both electrons and holes.

increase rapidly from zero to the value given by Eq.(42) when n_1 becomes sufficiently large, after which it should decay hyperbolically as n_1 increases further. On the other hand, the capture cross section σ_2 for minority carriers, after the same sudden rise, should increase linearly as with n_1.

In conclusion we note that the recombination mechanism considered herein is not necessarily peculiar to germanium (or silicon). Similar processes are possible, for instance, in compounds of the InSb type, where, in fact, they may be even more important, since in these compounds it is easier to realize the necessary conduction electron concentration. It should be borne in mind, however, that in these substances the interaction of electrons with the lattice vibrations may be quite strong (rather than weak, as we assumed in the present article), which may necessitate some change in the calculational procedure employed in the present article.

"M.V.Lomonosov" Moscow State University

References

1. A.E.Adirovich, Nekotorye voprosy teorii liuminestsentsii kristallov (Some problems pertaining to the theory of the luminescence of crystals), M. 1951.

2. K.Huang & A.Rhys, Proc.Roy.Soc., A204, 406 (1950).

3. M.A.Krivoglaz, Zhur.eksp.i teor.fiz., 25, 191 (1953).

4. V.I.Lashkerev in Sbornik pamiati S.I.Vavilova (Symposium in memory of S.I.Vavilov), p. 324, M. 1952.

5. V.P.Zhuze & S.M.Ryvkin, Doklady AN SSSR, 77, 241 (1951).

6. V.L.Bonch-Bruevich, Fizicheskii sbornik (Collected physics articles) Lvov State University, Vol. 1, No. 6, (1955).

7. D.N.Zubarev, Zhur. eksp. i teor. fiz., 25, 548 (1953).

8. W.Heisenberg, Ann. d. Phys., 10, 888 (1931).

9. M.M.Bogoliubov, Lektsii z kvantovoi ststistiki (Lectures on quantum statistics), Kiev 1949.

SOME ASPECTS OF THE THERMODYNAMICS OF ELECTRON AND PHONON GAS IN SOLIDS

- Iu.N.Obraztsov

The purpose of the present report is to call attention to certain distinctive features of the thermodynamics of electron and phonon gas in solids. It can readily be shown that the application of the usual thermodynamic relations to this case, which may at first seem valid, leads to several paradoxes.

Let us consider, for example, the temperature dependence of the chemical potential of the electrons in an electronic semiconductor at temperatures close to absolute zero. In this case the chemical potential μ, as is well known, is given by

$$\mu = -\frac{\Delta E}{2} - \frac{1}{2} kT \ln \frac{2(2\pi mkT)^{3/2}}{n_d h^3}. \tag{1}$$

Here n_d is the density of donor levels, and ΔE is their distance from the lower edge of the conduction band, which we shall take as the zero energy datum.

Let us find the temperature derivative of the chemical potential at constant pressure p.

In doing this one should in principle take into account the fact that ΔE and the effective mass m depend on the volume and, consequently, at constant pressure on the temperature. According to the Nernst theorem, however, the coefficient of thermal expansion approaches zero as the temperature approaches zero, and hence in our particular case we may consider these quantities to be constant.

Differentiating Eq.(1) with respect to the temperature, we obtain

$$\left(\frac{\partial \mu}{\partial T}\right)_p = -\frac{1}{2} k \ln \frac{2(2\pi mkT)^{3/2}}{n_d h^3} - \frac{3}{4} k. \tag{2}$$

On the other hand, from thermodynamics, we have

$$\left(\frac{\partial \mu}{\partial T}\right)_p = -s, \tag{3}$$

where s is the entropy per particle.

We note that in deducing Eq.(2) we considered the external pressure constant; in view of the fact that we are neglecting thermal motion of the nuclei ($T \to 0^\circ$), this is equivalent to considering the pressure exerted by all the electrons (not just by the conduction band electrons) constant; therefore s must be understood as the total entropy S divided by the number of electrons in the crystal.

In view of the Nernst theorem s approaches zero as $T \to 0^\circ$, whereas $-\left(\frac{\partial \mu}{\partial T}\right)_p$, according to Eq.(2), tends to infinity. It can be easily shown that a similar contradiction is obtained for an intrinsic semiconductor.

Furthermore, it follows from the familiar thermodynamic relation

$$\mu N = E + pV - ST, \tag{4}$$

where E is the internal energy, V is the volume, S is the entropy, and N is the number of particles, that at T = 0

$$p = -\frac{E + \mu N}{V}. \tag{5}$$

For the above case of an electronic semiconductor, Eq.(1) gives

$$\mu = -\frac{\Delta E}{2}$$

at T = 0. If, however, there is even an arbitrarily small number of electrons in the conduction band at this temperature, $\mu = 0$. It thus follows from Eq.(5) that the appearance of even one electron in the conduction band changes the pressure by a finite amount.

To these contradictions we may add the following. According to kinetic theory, the differential thermo-emf of an electronic semiconductor is

$$\alpha = \frac{\mu - \varepsilon_T}{eT}, \tag{6}$$

where ε_T is the mean energy transferred by an electron. As the temperature approaches absolute zero, ε_T also approaches zero regardless of the scattering mechanism, and therefore according to Eqs.(6) and (1) the differential thermo-emf tends to infinity. On the other hand, in view of the Nernst theorem, the thermo-emf should approach zero, as is actually the case in a metal.

Similar paradoxes are encountered when we turn to the thermodynamics of phonon gas. In this case, $\mu = 0$, and it follows from Eq.(4) that the pressure of the phonon gas is

$$p = \frac{ST - E}{V} = -\frac{F}{V}. \tag{7}$$

At low temperatures, the free energy of the phonon gas, as we know, is

$$F = -\frac{\pi^2}{30} \cdot \frac{(kT)^4}{(\hbar u)^3} V, \tag{8}$$

where u is the mean velocity of sound.

Inserting (8) into (7), we obtain an obviously incorrect expression for the phonon gas pressure.

This is evident, for instance, from the fact that according to this expression the pressure depends, aside from the temperature, only on the velocity of sound, i.e., on the elastic constants. Yet, as is well known, it depends on the coefficients of anharmonicity and goes to zero in the case of quasi-elastic forces.

We note that, except for a numerical factor of 2/3 which is associated with the fact that electromagnetic waves have no longitudinal component, the free energy expression for black-body radiation differs from Eq.(7) only in that the velocity of sound is replaced by the velocity of light. From this standpoint it is incomprehensible why, despite the fact that the free energy values for a phonon gas and a photon gas are given by similar expressions, the pressure in the two cases is determined by entirely different quantities.

It can readily be shown that the above paradoxes are the result of improper application of expressions (3) and (4), which assume the additivity of thermodynamic functions, to systems in which this additivity condition is not fulfilled (the paradox connected with the behavior of the thermo-emf of a semiconductor at absolute zero involves other factors as well).

If a thermodynamic function, for example, the free energy F, is additive, its dependence on the volume V and the number of particles N is of the form

$$F = Vf\left(\frac{V}{N}, T\right). \tag{9}$$

In the case of the phonon or electron gas in a crystal, however, the expression for the free energy is

$$F = Vf\left(\frac{V}{N},\ \frac{V}{N_a},\ T\right), \tag{10}$$

wherein the number of nuclei N_a appears in the role of a parameter (in the case of a phonon gas $\frac{\partial F}{\partial N} = \mu_{\text{ph}} = 0$).

Here by the free energy of the electron gas we mean the free energy of the solid body minus the free energy corresponding to motion of the nuclei and their potential energy in the equilibrium position, i.e., we are here considering a one-component system consisting of the electron gas in the given periodic field of the nuclei.

Similarly, the free energy of the phonon gas is defined as the free energy of the solid body minus the potential energy of the atoms in their equilibrium positions, the zero-point energy, and the energy of electronic excitations.

As is evident from Eq.(10), the free energy considered as a function of V and (in the case of an electron gas) N, is not an additive quantity.

The reason for this is obvious. In the case of a free electron gas, a change in volume leads to a proportional change in the number of levels within a given energy interval, so that the level density (number of levels divided by the volume) remains constant. Hence if the concentration and temperature remain constant, a volume change leads to a similar system. In the case of an electron gas in a solid body, however, a volume change with the number of atoms remaining constant leads to a change in the interatomic distances. Consequently, the electron energy spectrum changes; in particular, changes occur in the electron effective mass, in the widths of the allowed and forbidden bands, and in the number of levels per unit volume in the bands. This last change is the significant factor where the above-examined examples are concerned.

An analogous argument can obviously be made for the case of the phonon gas.

Applying Euler's theorem for homogeneous functions to Eq.(10) and bearing in mind that

$$\left(\frac{\partial F}{\partial N}\right)_{V,T,N_a} = \mu \quad \text{and} \quad \left(\frac{\partial F}{\partial V}\right)_{T,N,N_a} = -p,$$

we obtain

$$F = \mu N - pV + N_a\left(\frac{\partial F}{\partial N_a}\right)_{V,T,N}, \tag{11}$$

whence it follows that Eq.(4), which is valid only for additive systems, should be replaced by

$$\mu N = E + pV - ST - N_a\left(\frac{\partial F}{\partial N_a}\right)_{N,V,T}. \tag{12}$$

On the other hand, in the general case of a nonadditive system, in lieu of Eq.(3), we have

$$\left(\frac{\partial \mu}{\partial T}\right)_{p,N} = -\left(\frac{\partial S}{\partial N}\right)_{p,T} = -s - N\left(\frac{\partial s}{\partial N}\right)_{p,T}, \tag{13}$$

where the last term on the right side is due to the nonadditivity of the entropy of the system.

It should be emphasized that in the above formulas the pressure p, the

free energy F and other thermodynamic parameters are understood to be quantities pertaining to the phonon or electron gas treated as independent systems. A solid body regarded as a many-component system consisting of electrons and nuclei is, of course, an additive system. The additivity condition is characterized by Eq.(10) if F is understood to be the free energy of the body and N_a, the number of nuclei, is regarded as a thermodynamic quantity. Then the derivative $\left(\frac{\partial F}{\partial N_a}\right)_{V,T,N}$, entering into Eq.(11) and Eq.(12), acquires the sense of the chemical potential of the nuclei. If in these formulas we segregate the terms pertaining to the electron or the phonon gas we obtain expressions of the same form pertaining to each of these gases separately.

In the case of a phonon gas $\mu = 0$ and according to (11),

$$p = -\frac{F}{V} + \frac{N_a}{V}\left(\frac{\partial F}{\partial N_a}\right)_{V,T} = -\left(\frac{\partial F}{\partial V}\right)_{T,N_a}. \tag{14}$$

Thus the nonadditivity of the free energy leads to an additional term in the expression for the pressure, a term associated with the dependence of the inherent frequencies on the atomic separations. It now becomes clear why, in spite of the similarity of the expressions for the free energy of the photon and phonon gases, different results are obtained for the pressure.

In calculating the pressure in terms of the volume derivative of the free energy, the difference between photon and a phonon gas is explained by the fact that the velocity of light is a constant, whereas the velocity of sound u depends on the density, i.e., for a given number of atoms, on the volume.

In particular, when there is no anharmonicity, the forces involved are linear functions of the atomic displacements and the interatomic distances do not enter into the equations of motion. Consequently, for a given number of atoms, $u/V^{1/3}$, whence it follows in accordance with (14) and (8) that $p = 0$.

It is not difficult to show that Eq.(13) is actually satisfied in the above case of an electronic semiconductor near absolute zero, i.e., that the right side of this equation is equal to the derivative of the chemical potential as given by Eq.(2).

Actually, as has already been noted, in the limit $T \to 0$ derivatives taken at constant pressure can be replaced by derivatives for constant volume, so that

$$\left(\frac{\partial S}{\partial N}\right)_{p,T} = \left(\frac{\partial S}{\partial N}\right)_{V,T} = \left(\frac{\partial S}{\partial N}\right)_{E,V} + \left(\frac{\partial S}{\partial E}\right)_{V,N}\left(\frac{\partial E}{\partial N}\right)_{V,T} = \frac{\left(\frac{\partial E}{\partial N}\right)_{V,T} - \mu}{T}. \tag{15}$$

Thus the problem reduces to calculating

$$\left(\frac{\partial E}{\partial N}\right)_{V,T} = \left(\frac{\partial \varepsilon}{\partial n}\right)_{V,T},$$

where ε is the energy per unit volume and n is the electron concentration. To do this we must consider the virtual states for which the electron concentration n differs from the normal concentration n_0 in a neutral semiconductor by an amount $\Delta n = n - n_0$. The energy of such states is

$$\varepsilon = \varepsilon_0 + n_d' \Delta E + \frac{3}{2} n kT, \tag{16}$$

where ε_0 is the energy of the electrons filling all levels lying below the conduction band, i.e., the energy of the electrons in a neutral semiconductor

at T = 0°, n_- is the electron concentration in the conduction band and n'_d is the concentration of free donor levels, which is related to n_- by the equation

$$n_- = n'_d + \Delta n. \tag{17}$$

Therefore

$$\left(\frac{\partial \varepsilon}{\partial n}\right)_{V,T} = \frac{3}{2} kT \frac{\partial n_-}{\partial n} + \Delta E \frac{\partial n'_d}{\partial n}. \tag{18}$$

In order to calculate $\partial n_-/\partial n$ and $\partial n'_d/\partial n$ we must evaluate the chemical potential. This is easily done by using Eq.(17), which in this case replaces the neutrality condition.

Knowing the chemical potential, we can readily find

$$\frac{\partial n_-}{\partial n} = \frac{\partial n_-}{\partial \mu} \cdot \frac{\partial \mu}{\partial n} \text{ and } \frac{\partial n'_d}{\partial n} = \frac{\partial n'_d}{\partial \mu} \cdot \frac{\partial \mu}{\partial n}.$$

Simple calculations give $\frac{\partial n_-}{\partial n} = \frac{1}{2}$ and $\frac{\partial n'_d}{\partial n} = -\frac{1}{2}$ for $\Delta n = 0$ and as T → 0.

Inserting these values into (18) and (15), and making use of (1), we obtain the same expression for $(\partial \mu/\partial T)_p$ as that given by Eq.(2).

It may seem that our result contradicts the Nernst theorem which requires that the entropy be independent of any parameters at absolute zero and therefore, presumably, the vanishing of the derivative $\left(\frac{\partial S}{\partial N}\right)_{p,T}$.

It can be shown, however, that there is no contradiction. Indeed, close to absolute zero, the derivative $\left(\frac{\partial S}{\partial N}\right)_{p,T}$ differs from zero in the interval $\Delta N \approx \frac{2V}{h^3}(2\pi mkT)^{3/2}$ about $N = N_0$, which corresponds to all levels below the conduction band being filled at absolute zero (since outside this interval, degeneracy occurs). Therefore, with any finite change in the number N of electrons, the entropy change, equal to $\int \frac{\partial S}{\partial N} dN$, is proportional to $T^{3/2} \ln T$, and approaches zero as the temperature approaches zero.

Thus, as T → 0, the entropy approaches a value independent of N, and the Nernst theorem is satisfied.

It can be shown that the above-mentioned distinctive dependence of the entropy on the number of electrons at absolute zero leads to the result that in semiconductors (in contrast to metals) it is not a necessary consequence of the Nernst theorem that the differential thermo-emf must go to zero.

However, analysis of this problem, which involves recourse to certain concepts of kinetics and irreversible thermodynamics, lies outside the proper scope of this article and will be given elsewhere. We note only that one can arrive at the same conclusion through a different line of reasoning: it follows from the Nernst theorem that at absolute zero the entropy flux density $S = \Pi i/T$ must be zero; here Π is the Peltier coefficient, and i is the current density. For a metal in an electric field of finite intensity, $i \neq 0$ and, therefore, the differential thermo-emf should go to zero. In the case of a semiconductor the current density is proportional to the electron concentration in the conduction band and it, therefore, tends to zero as T → 0; thus in this case the thermo-emf should not go to zero.

Semiconductor Institute of the
Academy of Sciences of the USSR

Note Added in Proof

When the present article was already in print, the author became acquainted with the contribution of M.Kohler (Abh. Braunschw. Wiss. Ges. B3, 49 (1951)), where a treatment similar to the present is given for the behavior of the thermo-emf close to absolute zero. I take this occasion to express my deep gratitude to Ia. Tauts for calling my attention to Kohler's article and sending me a photostat of it.

MEAN FREE PATH OF ELECTRONS IN LIQUID AND AMORPHOUS CONDUCTORS

- A.I.Gubanov

By solving the Schrödinger equation in a coordinate system deformed so that the self-consistent field for the electrons in a liquid is approximately periodic, the writer was able to show[1] that the electron energy spectrum has a band-like structure, as in the case of a crystal. The electrons are described by Bloch wave functions in the deformed system of coordinates, i.e., are quasi-free.

The disturbance of long-range order in a liquid, however, leads to a specific type of "liquid" electron scattering. In order to calculate this scattering, it was shown that the quasi-Bloch functions of the form

$$\psi = u(\xi)\, e^{i\mathbf{k}\mathbf{r}}, \tag{1}$$

where u is a periodic function of the deformed coordinate ξ satisfy an equation which differs from the Schrödinger equation by small terms of order ϵ, where ϵ is of the order of magnitude of the small deformation of the unit cells when a crystal melts. Using the function of Eq.(1) as the zeroth approximation, and treating the small terms as perturbations, the writer calculated the electron mean free path l_{li} for liquid scattering.

If the functions of Eq.(1) are used, electron scattering by thermal phonons in the liquid can be calculated in the same way as for a crystal, but the calculation has certain distinctive features. In particular, due to the absence of long-range order in liquids, the momentum of the electron-phonon system need not be conserved. This leads to the presence of phonon-liquid scattering in addition to the usual scattering by phonons. The mean free path $l_{ph\text{-}li}$ of electrons for this type of scattering was calculated for metals and atomic and ionic semiconductors. It was found that for metals $l_{ph\text{-}li}$ is comparable with l_{ph} (ordinary scattering by phonons), while for semiconductors $l_{ph\text{-}li} \gg l_{ph}$. Finally, the mean free path l_d for scattering by defects and deviations from ideal periodicity in the coordinate system was computed.

The resultant mean free path is given by

$$\frac{1}{l} = \frac{1}{l_{li}} + \frac{1}{l_{ph}} + \frac{1}{l_{ph\text{-}li}} + \frac{1}{l_d} \tag{2}$$

The writer also analyzed the dependence of l on the electron energy u and the temperature T for metals and atomic and ionic semiconductors. In the case of atomic semiconductors, for example, the energy dependence of the mean free path is characterized by

$$\frac{1}{l} = A + Bu$$

where A and B are functions of the temperature.

The results of the investigation are given more fully in the articles listed under Ref.2.

Leningrad Physical-Technical Institute of the
Academy of Sciences of the USSR

References

1. A.I.Gubanov, Zhur.eksp.i teor.fiz., 26, 139 (1954); 28, 401 (1955).
2. A.I.Gubanov, Zhur.eksp.i teor.fiz., 30, 862 (1956); 31, 462 (1956); Zhur.tekh.fiz., 26, 1651 (1956).

INTERACTION OF SEMICONDUCTOR ELECTRONS WITH LATTICE VIBRATIONS AT ULTRALOW TEMPERATURES

- L.E.Gurevich

Introduction

At temperatures satisfying the condition

$$T \ll mc^2,\ v \ll c, \tag{1}$$

where T is the temperature in energy units (i.e., the temperature in degrees multiplied by Boltzmann's constant), m is the electron mass, v is the mean velocity of its thermal motion and c is the velocity of sound. An electron cannot interact with lattice vibrations by emitting or absorbing a single phonon, for from energy and momentum conservation

$$\frac{\hbar^2 k^2}{2m} = \frac{\hbar^2 (\mathbf{k} \mp \mathbf{q})^2}{2m} \pm \hbar c q,$$

(where k and q are the wave vectors of the electron and phonon, and the upper signs pertain to emission and the lower to absorption of a phonon by the electron) it follows that

$$q \mp 2k \cos(\mathbf{k}, \mathbf{q}) \mp 2k_0 = 0, \tag{2}$$

where $k_0 = \frac{mc}{\hbar}$.

When $T \ll mc^2$ for an electron having a mean momentum $\bar{k}$

$$\frac{\bar{k}}{k_0} = \sqrt{\frac{T}{mc^2}} = \frac{v}{c} \ll 1, \tag{3}$$

while for a phonon with a mean momentum $\bar{q}$

$$\frac{\bar{q}}{k_0} = \frac{T}{\hbar c k_0} = \frac{T}{mc^2} \ll 1 \tag{4}$$

and therefore an average electron can neither emit nor absorb phonons. Consequently, when there is little scattering by lattice defects, the mobility at $T \ll mc^2$ should increase with decreasing temperature according to the

$$u \approx e^{\frac{mc^2}{T}},$$

law, for this is the law characterizing the temperature dependence of the number of electrons capable of emitting and absorbing phonons.

The situation here is analogous to the one in which a free electron moving at a velocity greater than that of light can emit and absorb photons, while one moving at a "sub-light" speed can do neither. Actually, however, we shall see that the mobility increases about as T^{-8}, since it is restricted by second order processes. Such processes include, in particular, simultaneous emission of one phonon and absorption of another, which is an analog of the Compton effect (the simultaneous emission of two phonons, like the inverse process of simultaneous absorption, remains impossible and hence immaterial to our discussion).

If a phonon of momentum q is emitted and one of momentum q′ is absorbed, the conservation of energy and momentum law becomes

$$\Delta q^2 + 2k\Delta q - 2k_0 q_1 = 0, \tag{5}$$

where

$$\Delta q = q' - q,\ q_1 = q' - q,\ k_0 = \frac{mc}{\hbar}. \tag{6}$$

We shall find the small parameter

$$\sqrt{\frac{T}{mc^2}} \tag{7}$$

to be of importance and we shall expand all quantities in powers of this parameter. We shall not, however, exhibit this parameter explicitly in the expanded quantities, but shall denote their degree of smallness by a factor λ whose exponent will serve to indicate this degree. For instance, according to Eqs.(3) and (4), we shall write $\lambda k/k_0$ and $\lambda^2 q/k_0$ instead of k/k_0 and q/k_0. In the final formulas we shall set $\lambda = 1$. To find q_1 from Eq.(5), we set

$$\mathbf{q} = q\mathbf{n} \quad \text{and} \quad \mathbf{q}' = (q + q_1)\,\mathbf{n}' = q\,(1 + x)\,\mathbf{n}'. \tag{8}$$

Inserting this into (5) and solving for $\frac{q_1}{q} = x$, we obtain

$$x = \frac{q_1}{q} = \frac{(\mathbf{k} + q\mathbf{n}')\,\Delta\mathbf{n}}{k_0 - (\mathbf{k} + q\Delta\mathbf{n})\,\mathbf{n}' - \frac{1}{2}\,q_1}, \tag{9}$$

where $\Delta\mathbf{n} = \mathbf{n}' - \mathbf{n}$.

It will be seen that $\frac{q_1}{q}$ is of the same order as $\frac{k}{k_0}$, i.e., λ; hence in dropping q_1 in the denominator we will be neglecting a term of the order $\frac{q_1}{k_0} \approx \lambda^3$. Therefore we can write

$$x = \frac{q_1}{q} = \frac{(\mathbf{k} + \lambda q\mathbf{n}')\,\Delta\mathbf{n}}{k_0\left[1 - \lambda\,\frac{\mathbf{k}\mathbf{n}'}{k_0} - \lambda^2\,\frac{q}{k_0}\,\mathbf{n}'\Delta\mathbf{n}\right]},$$

or expanding in a series up to terms in λ^3,

$$x = \lambda x_1 + \lambda^2 x_2 + \lambda^3 x_3 + \cdots, \tag{10}$$

where

$$\left.\begin{aligned} x_1 &= \frac{\mathbf{k}\Delta\mathbf{n}}{k_0}, \\ x_2 &= \frac{q}{k_0}\,(\mathbf{n}'\Delta\mathbf{n}) + \frac{1}{k_0^2}\,(\mathbf{k}\mathbf{n}')\,(\mathbf{k}\Delta\mathbf{n}), \\ x_3 &= \frac{q}{k_0^2}\,(\mathbf{k}\Delta\mathbf{n})\,(\mathbf{n}'\Delta\mathbf{n}) + \frac{1}{k_0^3}\,(\mathbf{k}\Delta\mathbf{n})\,(\mathbf{k}\mathbf{n}')^2 + \frac{q}{k_0^2}\,(\mathbf{k}\mathbf{n}')\,(\mathbf{n}'\Delta\mathbf{n}). \end{aligned}\right\} \tag{11}$$

Thus the interaction of an electron with the vibrations of the lattice is almost elastic. The phonons absorbed and emitted have almost the same energy. Nevertheless, the energy difference between these phonons cannot be neglected, since if it is, the mobility obtained is not finite.

1. Transition probability

The double processes in question can take place in the second approximation of perturbation theory under the influence of a perturbation which for long-wave lattice vibrations can be written

$$V(\mathbf{r}) = E_0 \operatorname{div} \mathbf{s}, \tag{12}$$

where s is the lattice displacement vector, and E_0 is a constant with the dimensions of energy and of the order of 1 ev. Eq.(12) is not the most general expression for the interaction energy. In the general case of an arbitrary lattice, we may have

$$V(\mathbf{r}) = \sum E_{ik} s_{ik},$$

where s_{ik} is the strain tensor, and E_{ik} is a function of the coordinates and has the periodicity and symmetry of the crystal. For a cubic lattice with no mass anisotropy, however, Eq.(12) is adequate to our purposes.

Double processes in a cubic lattice can take place in the first approximation of perturbation theory due to the interaction

$$V^{(2)}(\mathbf{r}) = E_1 (\operatorname{div} \mathbf{s})^2 + E_2 \sum s_{ik}^2. \qquad (13)$$

It can be easily shown, however, that Eq.(13) gives a probability for double processes which is much lower than that given by Eq.(12), and we shall therefore not take it into account.

Setting $\mathbf{s} = \Sigma \mathbf{e}_q s_q e^{i\mathbf{qr}}$ and noting that in the approximation of Eq.(12) the electron interacts only with longitudinal waves, we obtain the modulus of the matrix element corresponding to the transition $\mathbf{k} \to \mathbf{k} - \mathbf{q}$ associated with the emission of a phonon of momentum q, namely,

$$|V_{\mathbf{k},\mathbf{k}-\mathbf{q}}| = E_0 q s_q \begin{Bmatrix} \sqrt{N_q} \\ \sqrt{N_q + 1} \end{Bmatrix}.$$

For both transition variants corresponding to the alternate sequences of the emission of phonon q and absorption of phonon q′, $|V_{1a}V_{a2}| = |V_{1b}V_{b2}|$ (where 1 and 2 are the initial and final states and a and b are the intermediate states), since both are given by

$$|V_{1a}V_{a2}| = |V_{1b}V_{b2}| = E_0^2 q q' s_q s_{q'} \sqrt{(N_q + 1) N_{q'}} = \frac{E_0^2 \hbar}{2NMc} \sqrt{qq'} \sqrt{(N_q + 1) N_{q'}},$$

where N_q is the number of q phonons, M is the mass of the unit crystal cell, N is the number of cells, and $\omega = cq$, where we consider the velocity c independent of the direction. The vectors q and q′ are arbitrary and the restriction imposed upon them by the conservation laws is taken account of by the δ-function which enters into the expression for the transition probability. Thus the second order matrix elements are of the form

$$|V_{1a}V_{a2}| \left(\frac{1}{E_1 - E_a} + \frac{1}{E_1 - E_B} \right).$$

Here

$$E_1 - E_a = \frac{\hbar^2 k^2}{2m} - \frac{\hbar^2 (\mathbf{k} - \mathbf{q})^2}{2m} - \hbar\omega = \frac{\hbar^2}{2m} (-\lambda^4 q^2 + 2\mathbf{kq}\lambda^3 - 2k_0 q \lambda^2),$$

$$E_1 - E_b = \frac{\hbar^2 k^2}{2m} + \hbar\omega' - \frac{\hbar^2 (\mathbf{k} + \mathbf{q}')^2}{2m} = \frac{\hbar^2}{2m} (q'^2 - 2\mathbf{kq}' + 2k_0 q'),$$

where the power of λ gives the order of magnitude (smallness) of the quantities with respect to k_0.

If we made the substitution $q' = q + q_1 = \lambda^2 q (1 + \lambda x_1 + \lambda^2 x_2 + \lambda^3 x_3 + \cdots)$, we would find that $-(E_1 - E_a)$ differs from $E_1 - E_b$, starting with the terms of order λ^3, so that we must calculate these with an accuracy up to λ^4. This is so because the terms of order λ^3, as we shall see, do not yield a finite mobility. After somewhat cumbersome calculations, we obtain

$$\left(\frac{1}{E_1 - E_a} + \frac{1}{E_1 - E_b} \right)^2 = \frac{(\mathbf{nn}')^2}{(mc^2)^2} \left[1 + 2\lambda \frac{\mathbf{k}(\mathbf{n} + \mathbf{n}')}{k_0} \right].$$

Let us now write the transition probability

$$w = \frac{2\pi}{\hbar} |V_{1a}V_{a2}|^2 \left(\frac{1}{E_1 - E_a} + \frac{1}{E_1 - E_b}\right)^2 \delta(E_{12}) =$$
$$= \frac{\pi}{2} \frac{E_0^4 \hbar (\mathbf{nn}')^2}{N^2 (Mc)^2 (mc^2)^2} qq' \left[1 + 2\lambda \frac{\mathbf{k}(\mathbf{n}+\mathbf{n}')}{k_0}\right] \delta(E_{12}). \qquad (14)$$

But

$$E_{12} = \frac{\hbar^2 (\mathbf{k}+\Delta\mathbf{q})^2}{2m} - \frac{\hbar^2 k^2}{2m} + hc(q' - q) = \frac{\hbar^2}{2m}(\Delta q^2 + 2\mathbf{k}\Delta\mathbf{q}) + \hbar c q_1.$$

Multiplying (14) by

$$\frac{V^2}{(2\pi)^6} q^2 dq dO q'^2 dq' dO' = \frac{V^2}{(2\pi)^6} q^2 dq dO q'^2 dq_1' dO'$$

and integrating the δ-function over q_1 with an accuracy up to λ, we obtain the following expression for the transition probability in the interval of states $dqdOdO'$

$$\frac{1}{4(2\pi)^5}\left(\frac{E_0}{Mc^2}\right)^4 \left(\frac{M}{m}\right)^2 ca^6 qq' \left(1 - \lambda \frac{\mathbf{kn}'}{k_0}\right)\left[1 + 2\lambda \frac{\mathbf{k}(\mathbf{n}+\mathbf{n}')}{k_0}\right] \times (N_q + 1) N_{q'} q^2 q'^2 dq dO dO'. \qquad (15)$$

2. Integral equation

Let us assume that the number of electrons per unit quasi-momentum interval is given by

$$n_k = n_k^0 + n_k^{(\prime)} = n_k^0 \{1 + \varphi(E)(\mathbf{kb}) + \cdots\} = n_k^0 \{1 + \varphi(E) k \cos(\mathbf{k}, \mathbf{b}) + \cdots\}, \qquad (16)$$

where n_k^0 is the equilibrium distribution, and $\mathbf{b}$ is a unit vector in some fixed direction, which in our case we shall take to be the direction of the external electric field. The terms that are not written out contain spherical functions of higher order. We shall see that an expansion in spherical functions up to a given order is the same as the expansion in the parameter λ of Eq.(7) in the sense that the terms discarded in Eq.(15) are of higher order in this parameter.

Since

$$n_{k+\Delta q}^0 N_q^0 (N_{q'}^0 + 1) = n_k^0 (N_q^0 + 1) N_{q'}^0,$$

we may write the kinetic equation of an electron, if we assume an equilibrium phonon distribution, in the form

$$\frac{dn_k}{dt} = A \int (qq')^3 n_k^0 (N+1) N' \left(1 - \lambda \frac{\mathbf{kn}'}{k_0}\right)\left[1 + 2\lambda \frac{\mathbf{k}(\mathbf{n}+\mathbf{n}')}{k_0}\right] \times$$
$$\times \{\varphi(E + \Delta E)[(\mathbf{k}+\Delta\mathbf{q})\mathbf{b}] - \varphi(E)(\mathbf{kb})\} dO dO' dq. \qquad (17)$$

where we have replaced N_q and $N_{q'}$ by N and N'.

But the change in the energy of the electron is

$$\frac{\Delta E}{E} = \frac{\hbar c q_1}{E} \approx \frac{q_1}{q} \ll 1,$$

and we may therefore set

$$\varphi(E + \Delta E) \approx \varphi(E) + \hbar\omega x \varphi'(E). \qquad (18)$$

Setting $n_k = n_k^0$ on the left side of Eq.(16), we obtain

$$\frac{1}{n_0}\frac{dn_{\mathbf{k}}^0}{dt} = A\int (qq')^3\left[1+2\lambda\frac{\mathbf{k}(\mathbf{n}+\mathbf{n}')}{k_0}\right]\left(1-\lambda\frac{\mathbf{kn}'}{k_0}\right)\times\{\varphi(E)(\mathbf{b}\Delta\mathbf{q})+\hbar\omega x\varphi'(E)(\mathbf{kb})\}\,dOdO'dq, \quad (19)$$

where

$$A = \frac{1}{4(2\pi)^5}\left(\frac{E_0}{Mc^2}\right)^4\left(\frac{M}{m}\right)^2 ca^6. \quad (20)$$

If we use Eq.(8) to express q and q', we may write

$$\mathbf{b}\Delta\mathbf{q} = q[(\mathbf{b}\Delta\mathbf{n})+x(\mathbf{bn}')]. \quad (21)$$

If we now neglect terms of order λ and higher, i.e., set $q=q'$ and $x=0$, then the integrand in Eq.(19) is antisymmetric with respect to the vectors $\mathbf{n}$ and $\mathbf{n}'$ due to the factor $\mathbf{b}\Delta\mathbf{n} = \mathbf{b}(\mathbf{n}'-\mathbf{n})$ and therefore integration over the angles $dOdO'$ will yield zero. We therefore set

$$q'^3N' = q^3N + qx(q^3N)',$$

where the prime denotes differentiation with respect to q.

We insert this expression and Eq.(21) into (19), make use of expressions (10) and (11) for and retain only terms containing λ in the lowest order. We then obtain

$$\frac{1}{n_{\mathbf{k}}^0}\frac{dn_{\mathbf{k}}^0}{dt} = A\int q^7N(N+1)\left[1+2\lambda\frac{\mathbf{k}(\mathbf{n}+\mathbf{n}')}{k_0}\right]\left(1-\lambda\frac{\mathbf{kn}'}{k_0}\right)\times$$
$$\times\left[1+xq\frac{(q^3N)'}{q^3N}\right]\left\{\varphi(E)(\mathbf{b}\Delta\mathbf{n})+x\left[\varphi(E)(\mathbf{bn}')+mc^2\frac{(\mathbf{kb})}{k_0}\varphi'(E)\right]\right\}dOdO'dq =$$
$$= A\int q^7N(N+1)\,dq\int dOdO'\left\{\varphi(E)(\mathbf{b}\Delta\mathbf{n})+\right.$$
$$+\lambda\left[2\frac{\mathbf{k}(\mathbf{n}+\mathbf{n}')}{k_0}\varphi(E)(\mathbf{b}\Delta\mathbf{n})-\frac{(\mathbf{kn}')}{k_0}\varphi(E)(\mathbf{b}\Delta\mathbf{n})+\right.$$
$$\left.\left.+x_1q\frac{(q^3N)'}{q^3N}\varphi(E)(\mathbf{b}\Delta\mathbf{n})+x_1\varphi(E)(\mathbf{bn}')+x_1mc^2\frac{(\mathbf{kb})}{k_0}\varphi'E)\right]\right\}. \quad (22)$$

The λ-independent term and the first and last terms proportional to λ are antisymmetric with respect to $\mathbf{n}$ and $\mathbf{n}'$ (since according to Eq.(11), x_1 is antisymmetric in these vectors), and hence in integration over the angles of both phonons give zero. Therefore the term containing $\varphi'(E)$ drops out; if this were not true, the expression would not agree with the form of the distribution function as assumed in Eq.(16). In higher approximations, which include higher powers of λ, this assumption is no longer correct, and the distribution function must contain spherical functions of higher order.

Let us now drop these terms from Eq.(22), make the substitution

$$\frac{\hbar cq}{T} = \frac{\hbar\omega}{T} = \xi,$$

and invoke Eq.(20) for A.

Finally, we rewrite the integral of the second and fourth terms in the square brackets of Eq.(22) as follows:

$$\int\left\{x_1(\mathbf{bn}')-\frac{1}{k_0}(\mathbf{kn}')(\mathbf{b}\Delta\mathbf{n})\right\}dOdO' = \int[\mathbf{k}(\mathbf{n}'-\mathbf{n})](\mathbf{bn}')-$$
$$-(\mathbf{kn}')[\mathbf{b}(\mathbf{n}'-\mathbf{n})]\,dOdO' = \int\{(\mathbf{kn}')(\mathbf{bn})-(\mathbf{kn})(\mathbf{bn}')\}\,dOdO' = 0$$

which follows from antisymmetry with respect to $\mathbf{n}$ and $\mathbf{n}'$.

After these operations we finally obtain the right side of Eq.(21) in the form

$$\frac{1}{4(2\pi)^5}\left(\frac{E_0}{Mc^2}\right)\left(\frac{M}{m}\right)^2\frac{c}{a^2}\left(\frac{T}{\theta}\right)^8\varphi(E)\times\int\xi^8N(N+1)\frac{(\xi^3N)'}{\xi^3N}d\xi\int\frac{1}{k_0}(\mathbf{k}\Delta\mathbf{n})(\mathbf{b}\Delta\mathbf{n})\,dOdO',$$

where $\theta=\hbar\omega_m=\frac{\hbar c}{a}$ is the characteristic (Debye) temperature, and a is the lattice constant.

The integral over angles is

$$\frac{32\pi}{3}\frac{k}{k_0}\cos(\mathbf{k},\mathbf{b})=\frac{32\pi}{3}\frac{v}{c}\cos(\mathbf{v},\mathbf{E}),$$

and the integral over ξ is (-5·7!). Therefore the right side of Eq.(22) is

$$\sim 11\left(\frac{E_0}{Mc^2}\right)^4\left(\frac{M}{m}\right)^2\frac{v}{a^2}\left(\frac{T}{\theta}\right)^8\varphi(E)\cos(\mathbf{v},\mathbf{E}).$$

Since the left side of (22) is

$$\frac{1}{n_{\mathbf{k}}^{\circ}}\frac{dn_{\mathbf{k}}^{\circ}}{dt}=-\frac{eEv\cos(\mathbf{v},\mathbf{b})}{T}=-\frac{mv}{\hbar\tau}\varphi(E)\cos(\mathbf{v},\mathbf{b}),$$

where τ is the mean time between phonon events for an electron with velocity v, we have

$$\tau\approx 0{,}09\left(\frac{Mc^2}{E_0}\right)^4\left(\frac{m}{M}\right)^2\frac{ma^2}{\hbar}\left(\frac{\theta}{T}\right)^8.$$

Setting

$$\frac{ma^2}{\hbar}=\frac{m}{M}\frac{Ma^2}{\hbar}=\frac{m}{M}\frac{Mc^2}{\theta}\frac{1}{\omega_m},$$

we may write

$$\tau\approx 0{,}09\left(\frac{Mc^2}{E_0}\right)^4\left(\frac{m}{M}\right)^2\frac{mc^2}{\theta}\left(\frac{\theta}{T}\right)^8\frac{1}{\omega_m}. \qquad (23)$$

Thus τ is independent of v. If

$$E_0\approx Mc^2,$$

and the molecular weight of a unit cell is 100, so that

$$\frac{m}{M}\approx 5\cdot10^{-6},\quad \omega_m\approx 10^{13},\quad c\approx 3\cdot10^5,$$

we arrive at

$$\tau\approx 1{,}8\cdot10^{-27}\left(\frac{\theta}{T}\right)^8.$$

It can be seen from Eq.(22) that $\varphi(E)$ is independent of the energy in our approximation, so that $\varphi'(E)$ is actually a small quantity of first or higher order in λ and the deviation from the electron distribution of Eq.(16), which contains only the first Legendre polynomial, is of order λ^2 or higher.

At the limit of applicability of the theory, i.e., when $T\approx mc^2$, we may compare the mean free times τ_1 and τ_2 associated with first order and second order processes. Since with the interaction of Eq.(12) and with $T\ll\theta$

$$\tau_1=8\pi\frac{Mc^2}{E_0}\frac{\theta}{E_0}\frac{\theta}{mc^2}\frac{c}{v}\frac{\theta}{T}\frac{1}{\omega_m}, \qquad (24)$$

according to Eq.(22), for $T\approx mc^2$ we have

$$\frac{\tau_2}{\tau_1}\approx 4{,}4\cdot10^{-3}\left(\frac{Mc^2}{E_0}\right)^3\left(\frac{m}{M}\right)^2\left(\frac{mc^2}{\theta}\right)^2\frac{E_0}{\theta}\frac{v}{c}\left(\frac{\theta}{T}\right)^7. \qquad (25)$$

These two times may be comparable. If, however, $\tau_2\ll\tau_1$ second order processes may begin to play a significant role even when T is somewhat larger than mc^2. A separate calculation is necessary in order to evaluate this effect.

We can calculate the thermo-emf α and the Peltier coefficient Π in the region where second order processes are important. According to the general formula

$$-e\Pi = E_F + \left(\frac{5}{2} + r\right)T,$$

where E_F is the separation between the Fermi level and the lower edge of the conduction band, e is the electron charge and r is the exponent of the expression giving the mean time as a function of the electron energy. In our case $r = 0$ and

$$-e\Pi = E_F + \frac{5}{2}T,$$

whence the thermo-emf is given by

$$\alpha = \frac{\Pi}{T} = -\frac{1}{e}\left(\frac{5}{2} + \frac{E_F}{T}\right).$$

It has sometimes been said that as a result of the Nernst theorem the thermo-emf must approach zero as the temperature is reduced to $0^{\circ}K$. This is a misapprehension. From the Nernst theorem it follows only that the total electron energy flux

$$w = \Pi j,$$

where j is the current density, must be zero, since it is related to the transfer of entropy, which approaches zero. As for the Peltier coefficient or more accurately the quantity $e\Pi$, it represents the energy flux per free electron. This energy flux per electron obviously tends to the finite value E_F if there is no degeneracy of the electrons in the conduction band, i.e., if the energy gap remains finite to absolute zero. Clearly this is not in contradiction with the statement that the total entropy flux, which is related to the quantity Πj, approaches zero.

Leningrad Physical-Technical Institute of the
Academy of Sciences of the USSR

CONCERNING CERTAIN ELECTROACOUSTICAL EFFECTS

- L.E.Gurevich

1. Entrainment of current carriers by ultrasonic phonons

Parmenter[1] recently established that there should exist an "acousto-electric" effect in metals and semiconductors. This effect consists of "trapping" and entrainment of current carriers by an acoustic wave, accompanied by the development of a potential gradient in the direction of propagation of the wave. The effect must have a maximum value (corresponding to the equilibrium number of current carriers trapped by the wave) at the acoustic frequencies for which an average electron moving at a velocity v remains in each potential trough or well produced by the wave for a time appreciably greater than the relaxation time τ. Inasmuch as at ordinary temperatures $v \gg c$, where c is the velocity of sound, the above condition leads to the requirement that $\lambda/v \gg \tau$ or

$$\omega\tau \ll \frac{c}{v} \ll 1. \tag{1}$$

In this case the trapping equilibrium assumed by Parmenter can be attained and the effect should occur.

In the other limiting case

$$\omega\tau \gg 1 \tag{2}$$

the Parmenter effect disappears; we shall see, however, that there exists another electroacoustical effect, which is weak when condition (1) is fulfilled but should become measurable under condition (2). This effect is analagous to the entrainment of electrons and holes by lattice vibrations whose frequency satisfies[2] Eq.(2). This electro-acoustical effect is produced by electrons whose energy is greater than the depth of the potential well and which are therefore not captured by the sound wave but are only scattered by it in the direction of propagation in a manner differing from the scattering in the opposite direction.

Since the electric conductivity is

$$\sigma = \frac{e^2 n\tau}{m^*} = \frac{enu}{300\, m^*}, \tag{3}$$

where n is the number of carriers per unit volume, e is their charge, m^* their effective mass and u their mobility, Eq.(2) may be written

$$\omega > \omega_1 = \frac{ne^2}{m^*\sigma} = \frac{300\, e}{m^* u}. \tag{4}$$

Ultrasonic frequencies as high as $2\pi \cdot 1.3 \cdot 10^9 \approx 10^{10}$ have already been realized within the past decade.[3]

As for the lowest actually obtainable values of ω_1, we note that for the semiconductor InSb at room temperatures $u \approx 8 \cdot 10^4$ cm^2/volt sec or even higher. Taking $u_0 = 10^5$, we obtain

$$\frac{\omega_1}{\omega_m} = 1{,}8 \cdot \frac{u_0}{u} \frac{m}{m^*},$$

where m is the free electron mass.

McDonald and Mendelssohn[5] have obtained samples of sodium for which the ratio of the electric conductivities at 273° and 4.2°K was $3.8 \cdot 10^{-4}$. Since

at 273°K, $\sigma_{Na} = 2.26 \cdot 10^5$ mho/cm, at 4.2°K we should have $\sigma_{Na} = 0.54 \cdot 10^{21}$ abs. units. Taking the lattice constant[6] to be $a = 5.34 \cdot 10^{-8}$ cm and assuming that each of the four atoms of the unit cell has one free electron, we obtain $n = 2.65 \cdot 10^{22}$, and therefore

$$\frac{\omega_1}{\omega} = 1{,}26 \frac{m}{m^*}.$$

Thus the now attainable value of ω_1/ω_m is close to unity both for conductors and semiconductors, and hence there is good reason to investigate the possible entrainment of current carriers by ultrasonic phonons.

It is well known[7] that the damping of ultrasonic waves in a dielectric may be regarded as the result of the interaction between ultrasonic phonons and thermal phonons, if the uncertainty $\hbar/\tau_{ph}$ in the thermal phonon energy (where τ_{ph} is the mean free time of a thermal phonon) is less than the energy $\hbar\omega$ of an ultrasonic phonon.

Similarly, the damping of ultrasonic frequencies in metals can be regarded as the result of the interaction of the ultrasonic phonons with electrons, if the uncertainty $\hbar/\tau_2$ in the electron energy (where τ_2 is the mean free time of an electron) is less than the energy $\hbar\omega$ of an ultrasonic phonon[8]. Therefore Eq.(2) defines the condition for quantum treatment of the interaction between ultrasonic vibrations and electrons, i.e., simple quantum mechanical treatment in which the first approximation of perturbation theory can be applied since Eq.(2) means that this interaction is weak.

On the other hand, electron motion caused by ultrasonic waves can be treated classically if

$$\frac{\hbar}{mv} \ll \lambda = \frac{c}{\omega}, \qquad (5)$$

where c is the velocity of sound and v is the electron velocity. This condition is satisfied up to the highest ultrasonic frequencies and almost to the lowest temperatures attainable. Thus both the classical method and the quantum mechanical one in the first approximation of perturbation theory are equally applicable in this case.

The quantum approach is considerably simpler, since the classical solution requires averaging over all positions of the electron along the extent of the ultrasonic wave, whereas in the quantum treatment this is automatically included in the calculation of the interaction matrix element.

The situation here is to some extent analogous to that obtaining in the theory of the anomalous skin effect, wherein both conditions (2) and (5) are also satisfied. The electromagnetic field, however, is strongly attenuated at a distance much shorter than its wavelength for reasons having only an indirect bearing on the magnitude of τ_e, so that the effective field attenuation distance may be much shorter than the mean free path of the electrons (this is what occurs in the case of the anomalous skin effect).[9] Consequently, the quantum treatment of the effect actually becomes more complicated than the classical one.

Since at present an order-of-magnitude evaluation of the entrainment of electrons by ultrasound must suffice (a precise calculation is scarcely worth attempting at this stage), we shall limit our examination here to the case where $\omega \gg \omega_1$, when the quantum mechanical calculation in the first approximation of perturbation theory is possible. The case $\omega \ll \omega_1$, which requires classical treatment of the ultrasonic field, will be considered at another time.

Case 1. Entrainment of electrons by ultrasonic phonons in metals

The probability of an electron transition from a state close to a Fermi surface to a neighboring state as a result of interaction with the lattice vibrations is almost independent of the vibration frequency[2]; after averaging over all the angles, the probability is found to be approximately

$$w \approx \frac{\omega_m}{N}\left(N_{\mathbf{k}} + 1\right), \tag{6}$$

where ω_m is the maximum frequency of lattice vibrations, $N_{\mathbf{k}}$ is the quantum number of the vibration with which the electron interacts, $\mathbf{k}$ is the wave vector of the vibration, N is the number of atoms per unit volume, c is the velocity of sound, and v is the velocity of electrons with the limiting energy ε_0.

In view of energy conservation, we have

$$\varepsilon_{\mathbf{p}} - \varepsilon_{\mathbf{p}-\mathbf{k}} = \hbar\omega_{\mathbf{k}},$$

where

$$\hbar\omega_{\mathbf{k}} = \hbar ck,$$

and p is the electron quasimomentum. Now writing

$$\varepsilon_{\mathbf{p}} - \varepsilon_{\mathbf{p}-\mathbf{k}} = \mathbf{k}\nabla_{\mathbf{p}}\varepsilon = \hbar\,\mathbf{kv} = \hbar kv\cos\vartheta,$$

we obtain

$$\cos\vartheta = \frac{c}{v}, \tag{7}$$

where ϑ is the angle between the phonon wave vector and the velocity of the electron entrained by it.

The equation of motion of an electron in the presence of an ultrasonic wave of high frequency can be written

$$n' = \int \tau w \left(n^0_{\varepsilon+\hbar\omega_{\mathbf{k}}} - n^0_{\varepsilon}\right) N'_{\mathbf{k}}\,(dk),$$

where n^0_{ε} is the equilibrium electron distribution function and n' is the deviation from it, and N'_k is the additional number of phonons associated with the presence of the ultrasonic wave.

Inserting Eq.(6) into this expression and expanding into the series

$$n^0_{\varepsilon+\hbar\omega_{\mathbf{k}}} - n^0_{\varepsilon} = \hbar\omega_{\mathbf{k}}\frac{dn^0_{\varepsilon}}{d\varepsilon},$$

we obtain

$$n' \approx \frac{\tau\omega_m}{N}\frac{dn^0_{\varepsilon}}{d\varepsilon}\int \hbar\omega_{\mathbf{k}} N'_{\mathbf{k}}\,(dk) = \frac{\tau\omega_m}{N}\frac{dn^0_{\varepsilon}}{d\varepsilon}W, \tag{8}$$

where W is the energy density of the ultrasonic wave.

The electron current density in the direction of the phonon flux (the x direction) is

$$i = -\int en' v_x \Delta d\varepsilon dO = -\int en' v\cos\vartheta\,\Delta d\varepsilon dO, \tag{9}$$

where Δ is the electron level density, and dO is the solid angle element.

Inserting (7) and (8) into (9), and bearing in mind that

$$\int \frac{dn^0_{\varepsilon}}{d\varepsilon}\,d\varepsilon = -1,$$

we obtain

$$i = \mp e \int n' v \cos\vartheta \, (dp),$$

where Δ_0 is the density of states in the neighborhood of the Fermi level and S is the intensity of the ultrasound. Setting

$$i = \sigma \mathcal{E},$$

where $\mathcal{E}$ is the resulting longitudinal electric field, and bearing in mind Eq.(3) and the order-of-magnitude relation

$$4\pi\Delta_0 \approx \frac{\pi}{\varepsilon_0},$$

where ε_0 is the limiting energy, we obtain

$$\mathcal{E} = \frac{2\omega_m}{Nev^2} S. \tag{10}$$

On the basis of the above we arrive at the following conclusions:

1. When Eq.(2) is satisfied, the ratio $\mathcal{E}/S$ is temperature independent.

2. For good semiconductors ($N \approx 3 \cdot 10^{22}$, $\omega_m \approx 10^{13}$ and $v \approx 10^8$), the ratio $\mathcal{E}/S \approx 10^{16}$, so that if S = 0.1 W/cm^2, we obtain $\mathcal{E} \approx$ μv/cm, which is measurable.

The question now arises whether phonons satisfying Eq.(2) can actually propagate in a metal.

In order to answer this question, let us write the equation of motion for these phonons, namely,

$$\frac{dN_k}{dt} = -N_k \int w \left(n_\varepsilon^0 - n_{\varepsilon\mp\hbar\omega_k}^0\right) \Delta d\varepsilon \, dO = -N_k \hbar\omega_k \int \omega \frac{dn_\varepsilon^0}{d\varepsilon} \Delta d\varepsilon \, dO,$$

or, according to Eq.(6),

$$-\frac{1}{N_k}\frac{dN_k}{dt} = \frac{4\pi\hbar\omega_k\omega_m\Delta_0}{N}.$$

From this we obtain the time in which a phonon is absorbed, namely

$$t_\omega \approx \frac{N}{4\pi\Delta_0\hbar\omega_m\omega}$$

and

$$\omega t_\omega \approx \frac{N}{4\pi\Delta_0\hbar\omega_m} \approx \frac{N}{\pi}\cdot\frac{\varepsilon_0}{k\theta}, \tag{11}$$

where θ is the characteristic Debye temperature, and k is Boltzmann's constant. It follows that

$$\text{a)}\ t_\omega \approx \frac{1}{\omega},$$

$$\text{b)}\ \omega t_\omega \gg 1,$$

which means that such phonons can propagate. In and article[8] published some years ago a calculational error led to the incorrect deduction that $\omega t_\omega \ll 1$.

Case 2. Entrainment of electrons (and holes) by ultrasonic phonons in semiconductors

As previously, the current density is

$$i = \mp e \int n' v \cos\vartheta \, (dp),$$

where

$$n' = \tau \int w \, (n^0_{\varepsilon+\hbar\omega} - n^0_\varepsilon) \, N' \, (dk),$$

and - and + signs correspond to electrons and holes.

Since

$$n^0_{\varepsilon+\hbar} - n^0 = \hbar\omega \frac{dn^0_\varepsilon}{d\varepsilon} = -\frac{\hbar\omega}{kT} n^0_\varepsilon$$

and $\cos\vartheta = \frac{c}{v}$, we have

$$i = \mp \frac{ec}{kT} \int \tau n^0_\varepsilon (dp) \int wh\omega N' (dk). \qquad (12)$$

The interaction of electrons with (longitudinal) lattice vibrations can be taken in the form

$$V(\mathrm{r}) = E_0 dw\, \mathrm{s} = iE_0 \sum k s_k e^{i\mathbf{kr}},$$

where s is the displacement at point r, and E_0 is a characteristic energy having an order of magnitude of an electronvolt.

The transition probability is

$$w = \frac{2\pi}{\hbar} \left| V_{12} \right|^2 \delta (E_{12}) = \frac{2\pi}{\hbar} \left(E_0 \sqrt{\frac{\hbar}{2NMc}} k \right)^2 \delta \left[\hbar k \, (v\cos\vartheta - c) \right] = \frac{\pi E_0^2}{NMc} \delta \left[\hbar k \, (v\cos\vartheta - c) \right], \qquad (13)$$

where M is the mass of a unit cell of the crystal and N is the number of such cells per unit volume. Inserting (13) into (12) and averaging over ϑ, we obtain (using the properties of the δ-function)

$$i = \mp \frac{\pi}{2} \frac{E_0^2 eS}{NMc\hbar kT} \int \frac{\tau}{v} n^0_\varepsilon (dp) \approx \mp \frac{\pi E_0^2 en\tau}{NMkT\hbar vc} S, \qquad (14)$$

where

$$S = c \int \hbar\omega N' (dk)$$

is the ultrasonic intensity, and the mean values of τ and v are taken out from under the integral sign.

Setting Eq. (14) equal to $\sigma\mathcal{E} = \frac{ne^2\tau}{m}\mathcal{E}$, we obtain

$$\mathcal{E} = \mp \frac{\pi}{2} \frac{E_0^2}{c\hbar e\rho} \left(\frac{m}{kT} \right)^{3/2} S, \qquad (15)$$

where ρ is the density of the semiconductor.

For $T = 10^2$, $S = 0.1$ w/cm^2, $\rho = 10$, $E_0 = 1$ ev, and $c = 3\cdot 10^5$, the electroacoustical field $\mathcal{E} \approx 6$ μv/cm.

In order to find the attenuation time of ultrasonic waves satisfying Eq. (2), let us again write the equation of motion of the phonons, namely

$$\frac{dN_k}{dt} = -N_k \int w \, (n^0_\varepsilon - n^0_{\varepsilon+\hbar\omega}) \, (dp) = -N_k \frac{\hbar\omega}{kT} \int w n^0_\varepsilon (dp).$$

Inserting (13) and averaging over ϑ, we obtain

$$-\frac{1}{N_k} \frac{dN_k}{dt} = \frac{\hbar\omega}{kT} \frac{\pi E_0^2}{NMc} \frac{n}{\hbar v},$$

whence

$$\omega t_\omega = \frac{1}{\pi}\left(\frac{M}{m}\right)^{\frac{1}{2}}\left(\frac{Mc^2}{E_0}\right)^{\frac{1}{2}}\left(\frac{kT}{E_0}\right)^{1/2}\frac{N}{n}. \qquad (16)$$

If

$$\frac{Mc^2}{E_0} \approx 1,\ \frac{M}{m} \approx 10^5,\ \frac{E_0}{kT} \approx 10^2,\ \frac{n}{N} \approx 10^{-5},$$

we have $\omega t_\omega \approx 10^4$, i.e., ultrasound of such frequencies can propagate, for it will be damped out only after many periods.

2. Piezoelectric effect

When sound propagates in a conducting body or when there is a pressure gradient in it, an electric field parallel to the pressure gradient is produced in the body. In the presence of a magnetic field, in addition, there appears a transverse potential difference. In metals, sound waves may give rise to longitudinal alternating potential differences of up to 10^{-8} volts.

In 1937 Haalck[10] suggested that the magnetic field of the Earth may be due to "squeezing out" of electrons by hydrostatic pressure. Haalck's concepts of electrons in conductors, however, are in conflict with the basic premises of modern physics and, therefore, his theoretical development is unconvincing. Actually this effect would be too weak to explain the Earth's magnetic field, as will be seen from what follows.

Let us denote the chemical potential of the electrons by φ and their electrical potential by V. At equilibrium, the total potential should be a constant,

$$\varphi - eV = \text{const},$$

whence the electric potential difference can be written

$$\delta V = \frac{1}{e}\delta\varphi = \frac{1}{e}\frac{d\varphi}{dp}\delta p,$$

where δp is the pressure difference. In metals

$$\frac{d\varphi}{dp} = \frac{d\varepsilon_0}{dp} = \frac{d\varepsilon_0}{d\rho}\frac{d\rho}{dp} \approx \frac{\varepsilon_0}{\rho c^2},$$

where ε_0 is the Fermi energy ρ is the density, and c is the velocity of propagation of longitudinal sound waves.

Therefore

$$\delta V = \frac{\alpha\varepsilon_0}{e\rho c^2}\delta p, \qquad (17)$$

where α is a factor of order unity. When $\delta p = 10^3$, $\varepsilon_0 = 5$ ev, $\rho = 5$ and $c = 2\cdot10^5$, we have $\delta V \approx 2\cdot10^{-8}$.

The hydrostatic pressure of the upper layers of the Earth on the lower ones "squeezes out" the electrons towards the surface and produces a radial potential drop between the center and the surface of about 40 volts (assuming the Earth to be a conductor).

The electric current density is proportional to the chemical potential gradient

$$\mathrm{i} = \beta\nabla(\varphi - eV) = \beta\nabla\varphi + \beta e\mathcal{E},$$

whence $\beta e = \sigma$ is the electric conductivity. In the presence of a magnetic field, we must add the Hall current, so that

$$\mathbf{i} = \sigma\left(\mathcal{E} + \frac{1}{e}\nabla\varphi\right) = \sigma'\mathcal{E} \times H, \tag{18}$$

where σ' is the Hall coefficient. We then have

$$\frac{\sigma'}{\sigma} = H_0 \approx \frac{mC}{e\tau}, \tag{19}$$

where C is the velocity of light, and H_0 is a quantity having the dimensions of the magnetic field. At ordinary temperatures, $H_0 \approx 10^6$ oersted, while at low temperatures this may drop to hundreds of oersteds.

In the stationary state, i = 0, and

$$\vec{\mathcal{E}} + \vec{\mathcal{E}} \times \mathbf{h} = -\frac{1}{e}\nabla\varphi = -\frac{1}{e}\frac{d\varphi}{dp}\nabla p,$$

where $\mathrm{h} = \frac{\mathrm{H}}{H_0}$. Then from (17) we have

$$\vec{\mathcal{E}} = -\frac{\alpha\varepsilon_0}{e\rho c^2}\frac{1}{1+h^2}[\nabla p + h \times \nabla p + h\,(h\nabla p)]. \tag{20}$$

Let us evaluate the alternating current in a metal through which sound waves are propagating. We have

$$\frac{\partial}{\partial t}\nabla^2 V = -\frac{\partial}{\partial t}\operatorname{div}\vec{\mathcal{E}} = 4\pi\frac{\partial}{\partial t}(en) = 4\pi\operatorname{div}\mathbf{i},$$

whence, according to (17),

$$\mathbf{i} = \frac{1}{4\pi}\frac{\partial\vec{\mathcal{E}}}{\partial t} = \frac{\alpha\varepsilon_0}{4\pi e\rho c^2}\frac{\partial}{\partial t}\nabla p. \tag{21}$$

Setting

$$p = p_0 + \delta p = p_0 + \delta p_0 e^{i(kx-\omega t)},$$

we obtain

$$i_0 = \frac{\alpha\varepsilon_0\omega^2}{4\pi e\rho c^3}\delta p_0 = \frac{\omega^2}{4\pi c}\delta V_0. \tag{22}$$

If $\omega = 10^9$ in the above example, $i_0 \approx 10^8$ amp/cm^2.

The semiconductors, variations of the chemical potential are determined by variations of the forbidden band width for intrinsic conductivity and by variations of the ionization potential of impurity centers with extrinsic conductivity. If for one of these quantities we set

$$\frac{\delta E}{E} = \alpha\beta\delta p, \tag{23}$$

where β is the compressibility, α is a factor of order ± 1, and $\delta E = \alpha\beta E\delta p \ll kT$, then when

$$\varphi = -\frac{\Delta E}{2} + \frac{kT}{2}\ln\left[n_0\left(\frac{2\pi\hbar^2}{mkT}\right)^{3/2}\right],$$

where n_0 is the number of impurity centers per unit volume, we have

$$\delta\varphi = \frac{1}{2}\left(-\delta E + kT\frac{\delta n_0}{n_0}\right) = \frac{1}{2}(-\delta E + kT\beta\delta p).$$

Inserting (23) into this expression, we obtain the piezoelectric chemical-potential difference

$$\delta\varphi = \frac{1}{2}(-\alpha E + kT)\beta\delta p,$$

whence the electric potential difference is

$$\delta V = \frac{1}{2}(-\alpha E + kT)\frac{\beta}{e}\delta p \approx (-\alpha E + kT)\frac{\delta p}{2e\rho c^2}, \qquad (24)$$

i.e., an effect of the same order of magnitude as that given by Eq.(17) for metals but decidedly temperature dependent.

Leningrad Physical-Technical Institute of the
Academy of Sciences of the USSR

References

1. R.H.Parmenter, Phys.Rev., 89, 990 (1953).
2. L.E.Gurevich, Zhur.eksp.i teor.fiz., 16, 193 (1953).
3. S.Ia.Sokolov, Usp.fiz.nauk, 40, 3 (1950).
4. B.Seraphin, ZS. Naturforsch, 9A, 5, 450 (1954).
5. D.K.C.Mcdonald & K.Mendelssohn, Proc.Roy.Soc., 202A, 103 (1950).
6. G.B.Bokii, Vvedenie v kristallokhimiiu (Introduction to crystal chemistry) M. 1954.
7. L.Landau & O.Rumer, Phys. ZS. Sowjetun, 11, H.1, 18 (1937).
8. L.E.Gurevich, Zhur.eksp. i teor.fiz., 14, 202 (1944).
9. G.Reuter & E.Sondheimer, Proc. Roy. Soc., 195A, 336 (1948).
10. H.Haalck, ZS. f. Phys., 105, 81 (1937).

Section on the

Chemistry of Semiconductors

SOME ASPECTS OF THE CRYSTAL CHEMISTRY OF COMPOUNDS WITH THE ZINCBLENDE STRUCTURE

- N.A.Goriunova

Introduction

One of the most important activities of chemists working in the field of semiconductors is the quest for new materials capable of meeting the requirements of present-day semiconductor engineering. This search for new materials should be based on the theory relating the electric properties of matter with its structure and the character of the electronic binding between its atoms.

Extant solid state theory is not sufficiently advanced to permit of qualitative evaluation of the electric properties of substances on the basis of the geometric arrangement of atoms and the type of bonds between them. There are actually only a few semiconductors for which the theory satisfactorily agrees with experiment. These are elements of the IVB subgroup of the periodic system - principally silicon and germanium[1].

Some of the predictions of theory are also validated for indium antimonide (a compound of the $A^{III}B^{V}$ type), as was noted by Nasledova earlier at this Conference[2]. In general, however, it must be admitted that the theory as it now stands cannot serve as a scientific basis in the search for semiconductors with requisite properties. At present, therefore, we must be guided in our search for new materials by qualitative considerations and empirical relationships.

As the point of departure in our search for new semiconductor materials (principally substitutional solid solutions), we chose compounds with zincblende structure and elements in the IVB column of the periodic table. This choice was dictated by the fact that this group of substances comprises semiconductors with properties that can be extremely valuable in engineering and technological applications.

In the present report we set forth certain considerations of a qualitative character based on the position of the component elements in the Mendeleev periodic system. These considerations served us as working hypotheses both in orienting the research and classifying the materials as to their crystallochemical attributes and in the experimental part of the work, as a guide in selecting materials for determining the possibility of formation of substitutional solid solutions.

The results, where the last point is concerned, will only be given briefly since detailed reports on this part of the work have already been published or are in press. We shall also express some views regarding the place occupied by compounds with the sphalerite structure among other compounds with semiconductor attributes and make some observations regarding use of the electronic lattice as a model for interpreting the properties of compounds with covalent bonds.

1. History of compounds with the zincblende structure as semiconductors.

In the course of an investigation of gray tin undertaken at the suggestion of Academician A.F.Ioffe, the writer[3] in 1950 came to the conclusion that compounds with the zincblende structure formed according to the Grimm-Sommerfeld rule[4] are not only structural analogs of elements of the IVB subgroup but that there exists between them a more profound resemblance based on the near identity of the chemical bonds between the atoms. A substantiating experimental fact was the transformation of the white tin to gray tin, stable under the same low temperature conditions, by "seeding" the former with indium antimonide and cadmium telluride.[3]

In 1951 the writer suggested that these substances with the structure of zincblende belong in the class of semiconductors; this idea was substantiated by exploratory experiments[5].

In the same year Regel' & Blum[6] at the Leningrad Physical Institute showed for the first time that in at least one substance with the zincblende structure - specifically, in mercury selenide - the mobility of current carriers appreciably exceeds the mobility in germanium. Later, it was definitively established at the Institute that the crystallochemical analog of gray tin, indium antimonide, belongs in the class of semiconductors[7].

In 1952 Welker[8] published his classical work in which he described a group of semiconductors of the indium antimonide or $A^{III}B^{V}$ type; the following years saw many other publications on the subject.

Thus in the period from 1950 to 1952 there were accumulated experimental data justifying inclusion of semiconductors with the zincblende structure into the same group with diamond, silicon, germanium and gray tin and at present these different substances may be treated from the same unified view point.

2. Group of binary compounds with the zincblende structure and elements of the IVB subgroup.

The need for separating semiconductor substances in separate groups on the basis of their crystallographic attributes will be clear in view of the following considerations.

1. In such groups, where the substances are arranged according to their structure and the position of their elements in the periodic table, it is easier to follow the regularities in the variation of their properties.

2. On the basis of these regularities, comparing the properties of already studied compounds, one can at least tentatively evaluate the properties of as yet uninvestigated substances of the same group.

The results of the numerous experimental investigations published over the last three years have made it possible to determine the principal common attributes of compounds with the zincblende structure and elements of the IVB subgroup of the periodic table, crystallizing with the structure of diamond. It may be considered established that the far-reaching qualitative resemblance in the properties of these substances is based on their crystallochemical similarity. Both the former and the latter are characterized by a tetrahedral arrangement of the atoms and tetrahedrally directed covalent bonds.

To this group of semiconductors, formed with elements symmetrically arranged with respect to the fourth column of the periodic table, one may join gallium chalcogenide and indium telluride[9] which are formed of asymmetrically located elements. These substances also crystallize with the structure of zincblende, but differ from our main group in that in them the gallium or

indium atoms occupy only two-thirds of the sites normally "reserved" for the corresponding components.[10] They may, by analogy with $A^{III}B^{V}$ type compounds, be called $A_2^{III}B_3^{VI}$ substances. On the basis of the structural similarity and from considerations of isomorphism (see below), the writer predicted some years ago that certain parameters of the substances in this group, for example, the width of the forbidden band, must have values intermediate between those common to compounds of the $A^{II}B^{VI}$ and $A^{III}B^{V}$ types.[9] This prediction was subsequently fully verified in connection with an investigation of the photoelectric properties of these compounds.[11]

On the other hand, the distinguishing characteristic of the group of compounds of the $A_2^{III}B_3^{VI}$ type, namely, the statistical distribution of vacancies in the structure, is evinced in the low carrier mobility exhibited by these substances.[12]

Table 1

Type designation	Binary compounds with the zincblende structure or elements with the diamond structure		
A^{IV}	C(diamond)	Si,Ge	α-Sn
$A^{III}B^{V}$	AlP*	AlAs*	AlSb
	GaP	GaAs	GaSb
	InP	InAs	InSb
$A_2^{III}B_3^{VI}$	Ga_2S_3*	Ga_2Se_3	Ga_2Te_3 In_2Te_3
$A_2^{I}B^{VI}$		Cu_2Se*	
$A^{II}B^{VI}$	BeS*	BeSe*	BeTe*
	ZnS	ZnSe	ZnTe
	CdS	CdSe	CdTe
	HgS	HgSe	HgTe
$A^{I}B^{VII}$**	CuCl	CuBr	CuI AgI

*The electric properties of these compounds have not yet been studied.

**The $A^{I}B^{VII}$ compounds are not typical semiconductors and are included in the table to demonstrate the transition to substances with an appreciable fraction of ionic bonds within the range of the same type of structure. The existence of CuF is open to question.

Another substance that should apparently be classified with the binary semiconductor compounds with the structure of zincblende is the high temperature modification of copper selenide (Cu_2Se).[13]

Thus the entire group of binary compounds with the zincblende structure and semiconductor properties can be arranged in the form shown in Table 1.

Closely allied to our group of semiconductors with the zincblende structure are compounds with the structure of wurzite and ternary compounds of the chalcopyrite type[14,15] as well as quadruple and more complex compounds based on these substances.

On the basis of its crystallochemical similarity to the above, it may be assumed that the ternary compound CuZnAs described by Ormont[13], which is a simulacre of GaAs, will also exhibit semiconductor characteristics.

3. Variation of the type of bonds in the group of compounds with the zincblende structure and elements of the IVB subgroup.

The group of substances listed in Table 1 are characterized not only by a structural likeness but also by crystallochemical similarity. This similarity is based on the regular change in the type of bonds in the various compounds in accord with the position of the component elements in the periodic table. The physical and physicochemical properties of the substances in this group change with changes in the type of bonds. There are a number of general considerations regarding the character of these changes on the basis of which one can predict some of the properties of as yet uninvestigated substances. Attempts along this line have been made by Welker[8], the writer[5,9] and other authors.

It may be worthwhile at this point to recall a number of elementary

concepts, lack of clear understanding of which, as will be shown below, often leads to confusion.

With increasing atomic weight of the first component elements - the analogs of C (diamond), Si, Ge or α-Sn - there is superposed on the principal type of bond (covalent) in these substances a "metallic" binding due to increasing nuclear screening. This "metallization" of the bonds results in narrowing of the forbidden band and increase in the carrier mobility.

If the compounds with the structure of zincblende are arranged in order of increasing atomic weight. It will be found that the changes in their electric properties will parallel their arrangement in the series C(diamond)—Ge —Si—α-Sn, as may be seen from Table 2, which was compiled on the basis of the data in the literature.

Table 2

A^{IV}	ΔE, eV, 0°K	μ_n, $cm^2/v \cdot sec$	$A^{III}B^{V}$	ΔE, eV, 0°K	μ_n, $cm^2/v \cdot sec$	$A^{III}B^{VI}$	ΔE, eV, 0°K	μ_n $cm^2/v \cdot sec$
C(diamond)	5,3	900	GaP	2,4		ZnS	3,6	
Si	1,15	1700	GaAs	1,5	4 000	ZnSe	2,8	
Ge	0,78	3600	GaSb	0,78	5 000	CdTe	1,5	600
α-Sn	0,08	3000	InSb	0,27	80 000	HgTe	0,09	10 000

It follows from the theory of the electric conductivity of crystals that the carrier mobility should increase with increasing atomic weight (other conditions being equal). This is connected with the fact that the amplitude of the harmonic vibrations of the atoms with a given interatomic binding decreases with increasing mass and hence the electron scattering is reduced. The observed narrowing of the energy gap is due to strengthening of the metallic binding, which within the limits of such series may be regarded as a certain weakening of the binding between the electrons in the covalent "bridges".

In all probability other groups of semiconductor substances, i.e., substances grouped on the basis of their crystallochemical resemblance (for example, semiconductors with the antifluorite structure) will be characterized by an analogous variation of the electric properties with increasing atomic weight. An apparent exception to this rule may be formed by substances which are difficult to obtain in the form of single crystals or prone to decomposition, etc.

Different regularities as regard changes in the type of bond are observed in so-called isoelectronic series of compounds with the zincblende structure and elements of the IVB subgroup[9] (see Table 3).

In each of these series, characterized by close periods of identity and an equal number of electrons in the inner atomic shells, the electron interaction is also comprised of two components: covalent or covalent-"metallic" interaction (depending on the series) which may be regarded as the principal interaction for the series and ionic interaction which, naturally, increases as we move further from the central column of the Mendeleev table. The combination of these two interaction components leads to a monotonic broadening of the forbidden band with the appearance of a maximum mobility at the optimum ratio of the two forms of electron interaction. The energy gap widens due to increasing difference between the maximum potentials in the periodic field of the crystal lattice. The mobility can have a maximum value in compounds of $A^{III}B^{V}$ type by virtue of the appreciable decrease in electron scattering by thermal vibrations of the lattice. The ionic bonds act to strengthen the structure thereby reducing the thermal vibrations. This effect is appreci-

ably stronger than the increase in optical mode scattering associated with the appearance of polarity (due to the ionic component).

Table 3

Isoelectronic series					Number of inner electrons	Period of unit cell, kX (Ref. 16)
$A^{I}B^{VII}$	$A^{II}B^{VI}$ ($A_2^{I}B^{VI}$)	$A_2^{III}B_3^{VI}$	$A^{III}B^{V}$	A^{IV}		
			AlP	C Si	2 10; 10	3,56 5,42; 5,42
CuCl	ZnS	Ga_2S_3	AlAs GaP	Ge + Si*	28; 10	5,406: 5,412 5,181; 5,62; 5,436
CuBr	(Cu_2Se) ZnSe	Ga_2Se_3	GaAs	Ge	28; 28	5,681; 5,659; 5,65; 5,429; 5,635; 5,65;
	[HgS]** CdS		AlSb InP	Ge	46; 10 (78; 10)	[5,84]; 5,82; 6,13 5,861; 5,65
CuI	ZnTe	Ga_2Te_3	GaSb	Ge + α-Sn*	28; 46	6,043; 6,07; 5,886; 6,118;
	[HgSe]** CdSe		InAs	Ge + α-Sn*	46; 28 (78; 28)	[6,07]; 6,04; 6,036
AgI	[HgTe]** CdTe	In_2Te_3	InSb	α-Sn	46; 46 (78; 46)	6,473; [6,36]; 6,41; 6,158; 6,461

*These formulas stand for hypothetical compounds.

**The mercury compounds shown in brackets have an "extra" 32-electron shell compared with their analogs.

In the isoelectronic series beginning with Ge + α-Sn (see Table 3) the mobility maximum occurs in the $A^{III}B^{V}$ type compounds (see Table 2). We feel, however, that the problem of the relative current carrier mobilities in $A^{III}B^{V}$ type compounds and the isoelectronic elements of the IV column is not as simple as made out by Welker[8]. Despite the fact that all the now available data on carrier mobilities indicate that the mobility is generally greater in $A^{III}B^{V}$ compounds than in isoeletronic A^{IV} elements, we doubt that the mobility in the as yet uninvestigated compound AlP will be greater than in Ge. We think the opposite will be true for the following reasons.

In a short isoelectronic series, for example, in the two-member Si-AlP series, the increase in the ionic character of the bonds occurs much more rapidly than in long series, for example, in the Ge-GaAs-Ga_2Se_2-ZnSe-CuBr series, due to the greater difference in the electronegativities in AlP as compared with GaAs. As a result the following, third member of the short series (in our case MgS) no longer crystallizes in the zincblende structure due to the highly ionic character of the bonds. As regards a number of physical properties, for example, color, AlP differs a great deal more from Si than GaAs differs from Ge; this is undoubtedly due to the stronger shift from covalent to ionic bonds. Hence one can hardly expect the mobility in AlP to be greater than in silicon despite the general statements in Ref.8 regarding the greater mobility in $A^{III}B^{V}$ substances as compared with A^{IV} elements.

Similar arguments can be put forth in favor of the assumption that the mobility in gallium arsenide, even the purest, will not differ greatly from the mobility in germanium (in practice this is observed in the parallel case of indium antimonide and gray tin).

As Zhuze[17] showed there is in general a definite correlation between the current carrier mobility and the heat of formation of many compounds including compounds with the zincblende structure. Unfortunately, the heats of formation of most $A^{III}B^{V}$ type compounds are as yet unknown.

Investigation and comparison of the physical properties of compounds in the different isoelectronic series[18] are of undoubted interest. However, as may be seen from the contribution of Goodman & Douglas[14] in which some of the suggestions advanced by Welker[8] are criticized, there may arise some misunderstandings and differences of opinion here. Thus Welker's suggestion regarding the low mobility and large widths of the energy gap in compounds of the $A^{II}B^{VI}$ type, which Goodman & Douglas disagree with, should, of course, be understood in application only to isoelectronic compounds of the $A^{III}B^{V}$ type.* As far as we know Welker's deduction actually does hold in all the cases investigated so far. The mobility in mercury selenide should be compared not with the mobility in any $A^{III}B^{V}$ compound but only with that in the corresponding isoelectronic substance. If mercury selenide had an electronic analog of the $A^{III}B^{V}$ type, i.e., if there existed a modification of thallium arsenide with the zincblende structure, presumably this would have a greater mobility and a narrower energy gap than mercury selenide. Another such compound might be gallium bismuthide if it crystallized with the zincblende structure. Welker's deductions cannot be taken without reference to the isoelectronic series, as Goodman & Douglas have done, for otherwise the effect of the increasing ionic character of the bonds may be compensated for or masked by enhancement of the "metallic" bonds.

Thus, in order to draw qualitative conclusions regarding the electric properties of compounds with the zincblende structure, one must bear in mind the existence of the mixed type of electronic interaction and its regular variation in the isoelectronic series and in series of compounds formed by analog-elements.

4. Isomorphism** of compounds with the zincblende structure

Highly interesting materials for investigation from the viewpoint of determining the character of changes in the electric properties incident to changes in the ratio between the different types of bonds may be substances allowing of isomorphic replacement over a wide range.

There are, in general, few investigations devoted to the electric properties of solid solutions of substances with semiconductor properties; in fact we know of only two studies in this category where substances with the zincblende structure are concerned: Refs.20 & 21.*** Serious comprehensive studies of the interrelated properties of substitutional solid solutions of this type must be preceded by separate thorough investigation of the limits

---

*As noted above, in our opinion Welker's deduction which is valid for all hitherto investigated compounds, may prove to be inapplicable in case of compounds of higher-lying isoelectronic series.

**Note added in proof. Another contribution on the subject has recently appeared, "On the electric properties of mixed crystals of the As_yP_{1-y} type" by H.Weiss.[37]

***By isomorphism here we understand the ability of substances to form mutual substitutional solid solutions as well as to serve as inoculants ("seeds") in crystallization under appropriate conditions.[9]

and conditions of isomorphic replacement. Below we shall comment briefly on studies of this type.

It has been established that isomorphic replacements, analogous to the formation of substitutional solid solutions, are possible when the identity periods of the structure and the character of the interatomic bonds are close in the compounds involved.[22]

The specific laws of isomorphism applying to a given compound are affected by the character of the predominant bonds. Determination of the distinctive features of isomorphism of compounds with pronounced covalent binding is of interest from the point of view of obtaining additional information on the nature of covalent bonds. In addition, investigation of isomorphic series or substitutional solid solutions is of practical interest from the viewpoint of semiconductor technology.

It is known that the statistical character of substitution in solid solutions leads, in the general case, to gradual continuous variation of all the properties with gradual changes in the parameters and character of the electronic interaction. This fact in itself may, in some cases, prove useful in selecting substances with the requisite combination of attributes. Where some characteristics, for example, the current carrier mobility, are concerned, however, the variation may pass through a maximum (or a minimum) value and then reverse its trend.

Thus, the maximum current carrier mobility may obtain when a certain optimal electron density distribution in the solid solution series is attained, i.e., when an optimal ratio between the different types of bonds is reached, as occurs, for example, in the isoelectronic series Ge-GaAs-ZnSe-CuBr, etc. In addition, a mobility maximum may also be obtained as a result of strengthening of the structure, as has been shown by Nikol'skaia & Regel[20], or apparently as the result of ordering. In the formation of substitutional solid solutions by a compound with the zincblende structure and a compound with a different but similar structure, it may be assumed that the current carrier mobility in a solid solution of substances with a sphalerite structure will be greater than in the initial binary compound with a different structure (for example, see case cited in Ref.23).

We carried out a series of experimental studies aimed at investigating the possibility of formation of substitutional solid solutions of compounds with the zincblende structure. The principal results obtained were the following.

In view of the considerations set forth above regarding the variation in the character of the bonds in series of compounds formed by analog-elements and in isoelectronic series, the experiments on the formation of substitutional solid solutions were carried out along these two lines. This approach makes it possible to evaluate the influence of different changes in the type of bonds on the isomorphism. First we investigated solid solutions of compounds formed by analog-elements.

In systems based on compounds of the $A^{II}B^{VI}$ type, the formation of substitutional solid solutions is possible in a wide range of concentrations not only when both binary components have an identical structure[19] but also when the components are characterized by a similar spatial arrangement of the structural units.[23] Data reported by other investigators substantiate this (Refs.20 & 24).

Substitutional solid solutions were found to form in a wide range of concentrations in systems based on compounds of the $A_2^{III}B_3^{VI}$ type[25]. Analogous experiments on determining the possibility of formation of substitutional solid

solutions in systems based on $A^{III}B^{V}$ compounds led us to conclude that the processes involved in the formation of such solutions are hindered for compounds of elements of the lower part of the periodic table[26]. This observation pertains to the arsenides and antimonides of gallium and indium in which "cationic" isomorphism is realized through a series of intermediate metastable states, while "anionic" isomorphism is not observed at all. In this connection it must be noted that the compounds InAs, GaAs, InSb and GaSb do not obey the law of isomorphism holding for compounds with metallic bonds. In accordance with this law, the analogous compounds NiAs and NiSb form substitutional solid solutions over the full range of concentrations[27]. It must be noted, also, that our data for the InSb-GaSb system do not agree with the results reported by Köster & Thoma[28]. We feel that the reason for this disagreement lies in the distinctive features of the crystallization of substitutional solid solutions of compounds with covalent bonds[29], features which possibly were not taken into account by Köster & Thoma.

In a recently published work Folberth[21] demonstrates the existence of substitutional solid solutions over the entire range of concentrations in the InAs-InP and GaAs-GaP systems, which is in agreement with our data.

Next we investigated the formation of substitutional solid solutions in the isoelectronic series. Solid solutions were found to form in a wide range of concentrations in the $ZnSe-Ga_2Se_3$ and $ZnTe-Ga_2Te_3$ systems[30] and, what is particularly interesting, in the Ga_2Se_3-GaAs system[25]. Preliminary experiments carried out by the writer in collaboration with Fedorova yielded for the middle point of the Ga_2S_3-GaP system one group of lines corresponding to the zincblende structure with identity periods midway between their values for the initial binary components.

Thus, the experiments showed that $A_2^{III}B^{V}$ compounds as regards the nature of their bonds are close to $A^{II}B^{VI}$ and $A^{III}B^{V}$ compounds, i.e., that in spite of their defective structure the character of the electron density distribution in these compounds is the same as in the non-defective $A^{II}B^{VI}$ and $A^{III}B^{V}$ compounds. It is difficult, however, to imagine the existence of tetrahedrally directed bonds extending from vacant sites. Apparently, the usual graphic representations are very rough compared with the actual electron density distribution. Inasmuch as $A_2^{III}B_3^{VI}$ compounds can be isomorphic also with $A^{II}B^{VI}$ compounds, we felt it reasonable to assume that as regards certain physical characteristics, for example, hardness and the width of the energy gap, $A_2^{III}B_3^{VI}$ compounds may occupy an intermediate position between the corresponding isoelectronic $A^{II}B^{VI}$ and $A^{III}B^{V}$ compounds. Later experiments showed that this assumption was correct where the width of the forbidden band is concerned (Ref. 11).

As was noted above the current carrier mobility in $A_2^{III}B_3^{VI}$ compounds proved to be low due to the disordered distribution of vacancies[3]. We assume, however, that on condition of ordering of the structure the carrier mobility in these compounds will also be intermediate between the mobilities in the isoelectronic $A^{II}B^{VI}$ and $A^{III}B^{V}$ compounds.

Experiments aimed at finding ways and means of realizing such ordering have given promising results. It was found that the compound In_2Se_3 of the same $A_2^{III}B_3^{VI}$ group, but crystallizing by itself in a structure different from the sphalerite one, yields ordered solid solutions of the zincblende type with cadmium selenide[23]. The fact that in our experiments, on the one hand, it was impossible to replace the arsenic with antimony in gallium arsenide, while on the other hand, the arsenic could readily be replaced by selenium in the same compound, gives reason to assume that the difference in the

character in the bonds between GaAs and GaSb is greater than between Ga_2Se_3 and GaAs. It is possible that a significant role is played here by the closeness of the atomic tetrahedral radius of selenium to the atomic tetrahedral radius of arsenic (1.14 for Se and 1.18 for As, but 1.36 for Sb, according to Pauling).

In view of the results obtained in these experiments, Fedorova and the writer decided to go further and attempt to realize isomorphic substitution in the same isoelectronic series in the GaAs-Zn-Se system[31]. X-ray analysis data for this four-component system give reason to assert that there are formed in it substitutional solid solutions in a wide range of concentrations. More detailed investigation of this system, including investigation of its electric properties, should, we feel, be of great interest, for it should make it possible to obtain variations of properties over an extensive range. The results of these experiments may be compared with our earlier data on the seeding of white tin both with indium antimonide and cadmium telluride, substances belonging in the same isoelectronic series[3]. Experiments on detecting isomorphism of Ge and compounds with the zincblende structure are now under way.

It may be concluded, therefore, that replacement in isoelectronic series of compounds with the structure of zincblende proceeds more easily than in series of compounds formed by analog-elements. We feel that this is indicative of the great qualitative changes that "metallization" introduces into the general character of the electron density distribution in compounds with the sphalerite structure and is evidence of much greater distortion of the density distribution in the case of replacement by analog-elements as compared with the distortion in case of replacement by elements in the same row of the Mendeleev table, on condition of charge compensation.

Summarizing the results of our experimental work, it may be said that among the compounds with the zincblende structure there exists a large number of substitutional solid solution systems, including systems based on semiconductors with a high carrier mobility (for example, the InSb-GaSb system). The different series of substitutional solid solutions obtained can readily be utilized for observing the regularities in the variation of electric properties with changes in the character of the electronic interaction (bonds). The question of whether any of these substances can be of practical value can be decided only by all around investigation of the systems including their electric properties. There can be no doubt, however, that the study of the different solid solutions obtained should make it possible to vary the properties of the corresponding semiconductors over an appreciable range.

5. Position occupied by compounds with the zincblende structure among other inorganic compounds.

The possession of typical semiconductor properties, for example, a high current carrier mobility, is connected primarily with the covalent bonds characteristic of certain inorganic compounds (see Refs. 12 & 32). Nevertheless, typical inorganic semiconductor compounds of the $A^{III}B^{V}$, $A^{II}B^{VI}$, $A_2^{II}B^{IV}$ and similar types are often called intermetallic compounds*. One cannot agree with this if only because some of these compounds are formed by

---

*Note added in proof. Thus after presentation of this report there appeared the article listed under Ref. 38, entitled "Semiconductor and intermetallic compounds", in which the authors describe substances of the $A^{III}B^{V}$ type.

typical nonmetals (for example, phosphorous and arsenic which differ in principle from metals in that they have a forbidden band and should therefore be classed as semiconductors).

In many recent chemical textbooks a sharp distinction is made between intermetallic and inorganic compounds (see, for example, Ref.16). The latter in most cases conform to the conventional rules of valence. A high degree of ordering and the predominance of covalent or ionic bonds sharply differentiate inorganic compounds from intermetallic ones.

As we learn more about the nature of different compounds, it becomes necessary to shift some of them from one class to another. This applies, for example, to the compounds Mg_2Si, Mg_2Ge, Mg_2Sn and Mg_2Pb which in the light of present knowledge can no longer be considered intermetallic compounds with mixed ionic-metallic bonds, but must rather be classed as inorganic or normally valent compounds with pronounced or predominantly covalent bonds[12].

Krebs[32] and Zhuze[17], in refutation of earlier concepts, argue in favor of the existence of covalent bonds in semiconductors of the PbS type. Apparently in classifying the different compounds, particularly compounds with intermediate properties, as intermetallic or normal-valence compounds an important factor to consider is the width of the homogeneity region which can be comparatively narrow for the latter.[33]

Examining the known semiconductors from this general standpoint, we feel it would be useful to represent the position of the group of compounds with the zincblende structure in the series of inorganic compounds formed under condition of equality (or a multiple of eight) of the sum of the outer valence electrons as shown in Table 4. It is known that this condition is satisfied with a formal realization of the maximal valence with respect to hydrogen for nonmetals and with respect to oxygen for metals. In more extended form the table would appear as shown in Table 5.

Table 4

	IV	V	VI	VII
IV	A^{IV}	$A_3^{IV}B_4^{V}$	$A^{IV}B_2^{VI}$	$A^{IV}B_4^{VII}$
III	$A_4^{III}B_3^{IV}$	$A^{III}B^{V}$	$A_2^{III}B_3^{IV}$	$A^{III}B_3^{VII}$
II	$A_2^{II}B^{IV}$	$A_3^{II}B_2^{V}$	$A^{II}B^{VI}$	$A^{II}B_2^{VII}$
I	$A_4^{I}B^{IV}$	$A_3^{I}B^{V}$	$A_2^{I}B^{VI}$	$A^{I}B^{VII}$

The elements of the side subgroups of the higher periods in Mendeleev's system are not included in our table since the filling of the d-shells complicates the picture and leads to special regularities in the variations of the structures and types of bonds.

In Tables 4 & 5 we have distinguished (heavy lines) the groups comprising compounds with semiconductor properties. As may be seen the compounds with the zincblende structure occupy a central "diagonal" position and as regards structure are the simplest ones. They are characterized by a 1:1 ratio of the component element atoms.

As the structure becomes more complex in connection with changes with valence of the component elements, in most cases the compounds in the boxes neighboring the diagonal in Table 5 still retain cubic symmetry and the typical tetrahedral surrounding arrangement where at least one of the types of atoms involved is concerned. For example, in the cubic structure of cuprous oxide and silver oxide each oxygen atom is surrounded by four copper or silver atoms.

In the pseudocubical structures of Zn_3P_2, Zn_3As_2, Cd_3P_2 and Cd_3As_2 each zinc or cadmium atom is situated inside a slightly distorted tetrahedron of phosphorus or arsenic atoms; actually there also exist truly cubical modifications of these compounds[13]. In the tetragonal cell of HgI_2 each mercury atom

Table 5

		IV					V					VI					VII				
		C	Si	Ge	Sn	Pb	N	P	As	Sb	Bi	O	S	Se	Te	Po	F	Cl	Br	J	
IV	C	**C**										CO_2	CS_2				CF_4	CCl_4	CBr_4	CJ_4	
	Si	**SiC**	**Si**				Si_3N_4					SiO_2	SiS_2				SiF_4	$SiCl_4$		SiJ_4	
	Ge			**Ge**			Ge_3N_4					GeO_2	GeS_2				GeF_4	$GeCl_4$	$GeBr_4$	GeJ_4	
	Sn				**Sn**			Sn_3P_4				SnO_2	SnS_2	$SnSe_2$				$SnCl_4$		SnJ_4	
	Pb					**Pb**						PbO_2									
III	B						**BN**					B_2O_3					BF_3	BCl_3	BBr_3		
	Al	Al_4C_3					**AlN**	**AlP**	**AlAs**	**AlSb**		Al_2O_3					AlF_3	$AlCl_3$		AlJ_3	
	Ga						**GaN**	**GaP**	**GaAs**	**GaSb**		Ga_2O_3	Ga_2S_3	Ga_2Se_3	Ga_2Te_3						
	In						**InN**	**InP**	**InAs**	**InSb**	**InBi**	In_2O_3	In_2S_3		In_2Te_3						
	Tl									**TlSb**	**TlBi**	Tl_2O_3									
II	Be	Be_2C					Be_3N_2	Be_3P_2				**BeO**	**BeS**	**BeSe**	**BeTe**		BeF_2				
	Mg		Mg_2Si	Mg_2Ge	Mg_2Sn	Mg_2Pb	Mg_3N_2	Mg_3P_2	Mg_3As_2	Mg_3Sb_2	Mg_3Bi_2	**MgO**	**MgS**	**MgSe**	**MgTe**		MgF_2	$MgCl_2$	$MgBr_2$	MgJ_2	
	Zn						Zn_3N_2	Zn_3P_2	Zn_3A_2	Zn_3Sb_2		**ZnO**	**ZnS**	**ZnSe**	**ZnTe**		ZnF_2	$ZnCl_2$			
	Cd						Cd_3N_2	Cd_3P_2		Cd_3Sb_2		**CdO**	**CdS**	**CdSe**	**CdTe**		CdF_2	$CdCl_2$	$CdBr_2$	CdJ_2	
	Hg											**HgO**	**HgS**	**HgSe**	**HgTe**		HgF_2	$HgCl_2$	$HgBr_2$	HgJ_2	
I	Li						Li_3N	Li_3P	Li_3As	Li_3Sb	Li_3Bi	Li_2O	Li_2S	Li_2Se	Li_2Te		**LiF**	**LiCl**	**LiBr**	**LiJ**	
	Na							Na_3P	Na_3As	Na_3Sb	Na_3Bi	Na_2O	Na_2S	Na_2Se	Na_2Te		**NaF**	**NaCl**	**NaBr**	**NaJ**	
	Cu				Cu_4Sn		Cu_3N	Cu_3P	Cu_3As	Cu_3Sb		Cu_2O	Cu_2S	Cu_2Se	Cu_2Te		**CuF?**	**CuCl**	**CuBr**	CuJ	
	Ag				Ag_4Sn					Ag_3Sb		Ag_2O	Ag_2S	Ag_2Se	Ag_2Te		**AgF**	**AgCl**	**AgBr**	**AgJ**	
	Au																				

is surrounded by four iodine atoms arranged in a tetragonal tetrahedron[13].

It might be thought that many of the chemical compounds in Table 5 in which the tetrahedral arrangement is retained (with the exception of those which like substances of the $A^{I}B^{VII}$ type occupy occupy a boundary position as regards a number of attributes) will be characterized by pronounced covalent binding and typical semiconductor properties.

The relative positions of the semiconductor compounds formed by elements with stable s^2-groups, for example, Tl_2S, Tl_2Se, PbS, PbSe, PbTe, Bi_2S_3, Bi_2Se_3, Bi_2Te_3 (stable $6s^2$-group), Sb_2S_3, Sb_2Se_3 and Sb_2Te_3 (stable $5s^2$-group) among the compounds formed by elements of columns VI, V, IV and III of the periodic table, exhibiting incomplete valences, can be represented schematically in an analogous fashion. Such schematic arrangements, we feel, may prove very useful as a guide in exploratory research.

In concluding we would like to make a number of general observations.

1. Taking the results of our experiments on isomorphism[25,30] in conjunction with the data in the literature on the existence of such compound with the zincblende structure as Cu_2Se, CuZnAs, Ag_2HgI_4 and Cu_2HgI_4 (Refs.13 & 34), we come to the conclusion that the stability limits of the sphalerite structure are determined not so much by the number of atoms as by the concentration of electrons in the unit cell. Thus, despite the absence of a third or a fourth of the "cations" in the compounds Ga_2Se_3 and Ag_2HgI_4, respectively, their structure is of the zincblende type. In isomorphic substitution, when the number of vacancies as a whole changes continuously, the basic structure is retained.

The opposite situation - i.e., a greater than "necessary" number of atoms in the structure of such compounds as Cu_2Se and CuZnAs - apparently need not necessarily lead to transition to the antifluorite structure, but can yield the zincblende structure under certain conditions. In contrast, a deviation one way or another from the given concentration of electrons per unit cell inevitably leads to formation of new structures despite retention of the original ratio of different atoms.

Thus one can imagine a series of substances with a varying concentration of electrons in the unit cell and with related but not identical structures (Table 6).

Table 6

Substance	ZnSb CdSb	InSb & others	GaSe
Number of electrons per"formular unit" (Ref.16)	2+5 = 7	3+5 = 8	3+6 = 9
Number of electrons in a unit cell	28	32	36

Apparently, the character of the bonds in compounds such as ZnSb, CdSb and GaSe will be predominantly covalent and distortions of the structure with conservation of the general crystallochemical similarity* may lead to interesting consequences from the point of view of semiconductor attributes.

We feel that it is essential to investigate and compare the physical, chemical and electrical properties of compounds in such series since this is virtually

*The similarity of the structures GaSe and diamond have been demonstrated by Schubert et al[35]. Schubert also puts forward the concept of an "electronic lattice" more or less analogous to the one discussed in the present report.

the only way to observe changes in the physical parameters with distortions of the structure associated with changes of the electron concentration in the unit cells.

The fact that there exist compounds with the zincblende structure with an excess or deficiency of atoms and, particularly, the possibility of isomorphism between defect containing and ordinary compounds of the ZnS type leads to the idea that there exists in compounds of both these types a lattice consisting of rigid directed covalent bonds. Such an "electronic lattice" may serve as the basis of the structure of these substances and be responsible for determining their properties. Possibly the "electronic lattice" model may be helpful in theoretical interpretation of the physical phenomena occurring in substances with pronounced covalent bonds, both those with the zincblende structure and those with closely related structures (GaSe, CdSb, ZnSb, Mg_2Sn, etc.).

The concept of the "electronic lattice" has also been advanced as the basis for a quantum chemical model of the bonds in germanium by Tovstiukh in a report presented at this conference.

In conclusion, we would like to say that the experimental data on isomorphism and the interpretations and considerations set forth in the present report can serve only as the first step in the overall investigation of chemical systems, investigations which should make it possible to develop scientific criteria for efficient selection of semiconductor materials having desired or requisite properties.

Leningrad Physical-Technical Institute of the
Academy of Sciences of the USSR

References

1. A.F.Ioffe, Poluprovodniki v sovremennoi fizike (Semiconductors in modern physics), M. 1954.
2. D.M.Masledov, Zhur.tekh.fiz., 26, 6 (1956).
3. N.A.Goriunova, Doklady AN SSSR, 75, 51 (1950).
4. H.G.Grimm & A.Sommerfeld, ZS.f.Phys., 36, 36 (1926).
5. N.A.Goriunova, Dissertation, L., 1951.
6. A.R.Regel' & A.I.Blum, Zhur.tekh.fiz., 21, 316 (1951).
7. A.R.Regel' & N.P.Mokrovskii, Zhur.tekh.fiz., 22, 1281 (1952).
8. H.Welker, ZS.f.Naturf. 7a, 744 (1953).
9. N.A.Goriunova, Materially soveshchaniia po poluprovodnikam v Institute metallurgii (Transactions of the conference on semiconductors held at the Institute of Metallurgy), Pub. AN SSSR, 1954.
10. H.Hahn & W.Klinger, ZS.f.anogr.Chem., 259, 135 (1949).
11. N.A.Goriunova, V.S.Grigor'eva, B.M.Konovalenko & S.M.Ryvkin, Zhur. tekh.fiz., 25, 1675 (1955).
12. H.Welker, Physica, 20, 893 (1954).
13. B.F.Ormont, Struktury neorganicheskikh veshchestv (Structures of inorganic substances), 1950.
14. C.H.Goodman & R.W.Douglas, Physica, 20, 1107 (1954).
15. V.P.Zhuze, V.M.Sergeeva & E.L.Shtrum, Zhur.tekh.fiz., (1957).
16. G.B.Bokii, Vvedenie v kristallokhimiiu (Introduction to crystal chemistry), M. 1954.
17. V.P.Zhuze, Zhur.tekh.fiz., 25, 2079 (1955).

18. B.Seraphin, ZS.f.Naturf., 9a, 450 (1954).
19. N.A.Goriunova & N.N.Fedorova, Doklady AN SSSR, 90, 6, 1039 (1953).
20. E.I.Nikol'skaia & A.R.Regel', Zhur.tekh.fiz, 25, No.8, 1347 (1955).
21. O.G.Folberth, ZS.f.Naturf., 10a, H.6, 502 (1955).
22. B.A.Nikitin, Usp.khim., 13, 435 (1944).
23. N.A.Goriunova, V.A.Kotovich & V.A.Frank-Kamenetskii, Zhur.tekh.fiz., 25, 2419 (1955).
24. A.V.Moskvin, Katodoliuminestsentsiia (Cathode luminescence), M.,1949.
25. N.A.Goriunova & V.S.Grigor'eva, Zhur.tekh.fiz., 26, 2157 (1956).
26. N.A.Goriunova & N.N.Fedorova, Zhur.tekh.fiz., 25, No.7, 1339 (1955).
27. I.I.Kornilov, Doklady AN SSSR, 81, 4 (1951).
28. W.Köster & B.Thoma, ZS.f.Metallkunde, 46, 293 (1955).
29. D.A.Petrov, Zhur.fiz.khim., 21, No.12, 1449 (1947).
30. N.A.Goriunova, V.A.Kotovich & V.A.Frank-Kamenetskii, Doklady AN SSSR, 103, 4, 659 (1955).
31. N.A.Goriunova & N.N.Fedorova, Zhur.tekh.fiz.(1957).
32. H.Krebs, Physica, 20, 11, 1125 (1954).
33. B.F.Ormont, N.A.Goriunova, I.N.Ageeva & N.N.Fedorova, Present issue of the Bulletin, p. 128.
34. J.A.Ketelaar, ZS.Krist. 87, 435 (1935).
35. K.Schubert, E.Dörre & M.Kluge, ZS.f.Metallkunde, 46, 216 (1955).
36. K.Schubert, ZS.f.Naturf., 8a, 30 (1953).
37. H.Weiss, ZS.f.Naturf., 11a, 430 (1956).
38. G.Pincherle & J.M.Radcliff, Adv. in Phys. (1956).

CONTRIBUTION TO THE THEORY OF PHASES OF VARIABLE COMPOSITION WITH THE ZINCBLENDE STRUCTURE (ON THE POSSIBLE REGION OF HOMOGENEITY OF $A^{III}B^{V}$ TYPE COMPOUNDS)

- B.F.Ormont, N.A.Goriunova, I.N.Ageeva & N.N.Fedorova

1. The modern theory of phases of variable composition owes its development to N.S.Kurnakov[1] and his school. In their investigations a distinction is made between two kinds of variable-composition phases: Daltonides and Bertholletides. In the former case the base compound appears (in the form of a Dalton point) within the phase homogeneity region; in the latter, it lies outside this region.

In 1944 Mikheeva[2] showed that the elements forming Bertholletides as defined by Kurnokov are Sb, Pb, Bi, Tl and, to a lesser extent also Sn, Hg, Cd, Zn, Cu, Ni, Co and Fe.

In 1947 B.F.Ormont[3] drew attention to the fact that many compounds until then regarded as forming phases of constant composition (oxides, nitrides, carbides, etc.) are actually phases of variable composition, not having singular points, particularly, within the boundaries of the homogeneity region. Ormont suggested that such phases, which are formed by almost all elements and particularly by ds-elements*, be termed Bertholletides in the broad sense of the word. Whereas until then the fundamental experimental problem in the field was assumed to be that of identifying and separating out the few phases of variable composition from among the numerous phases of presumably constant composition, now, according to Ormont[3], even in investigating so-called "typically chemical compounds", the problem is to seek out the relatively small number of phases of virtually constant composition from among the multiplicity of phases that are actually of variable composition.

2. During the past twenty years many authors, here and abroad, have shown that, for example, most of the substances crystallizing with the structure of rock salt - oxides, nitrides, carbides and the like - are actually phases of variable composition. For example, in the series CaO, TiO, TiN, and TiC, the last three compounds exist in the form of phases of variable composition with a very wide region of homogeneity. Thus, according to the data of Ehrlich and others, the "TiO"-phase (the quotation marks are ours) is characterized by a range of compositions from $TiO_{0.7}$ to $TiO_{1.25}$, while the "TiC"-phase covers the gamut from $TiC_{0.4}$ to TiC_1.

In view of the somewhat incorrect use of x-ray phase analysis for establishing phase homogeneity boundaries[4] in some cases the homogeneity boundaries of phases with variable composition now given in the literature are of doubtful accuracy and require refinement.

However, for such carbide phases as, for example, tantalum carbide, it has been clearly established[5] that the γ-phase (cubic tantalum carbide) has a homogeneity region extending from $TaC_{0.58}$ to $TaC_{0.91}$ and probably actually to TaC_1, while the homogeneity interval of the β-phase (hexagonal tantalum carbide) is $TaC_{0.38}$ to $TaC_{0.50}$, i.e., the phase exists even when 25 to 40% of the carbon atoms are absent from their sites in the lattice.

As is known, even in the case of narrow phase homogeneity regions, the physical properties of the material may vary very appreciably within the limits of the homogeneity region. This applies particularly to electric properties. Thus, as follows from Ref.6 and Ehrlich's data, in the case of the

---

*Elements in which the d- and s-electrons are valence electrons. Term originated by Ormont.

"TiO_2"-phase the change in composition from TiO_2 to $TiO_{1.92}$ is accompanied by a 10^{10}-fold decrease in resistivity. Obviously, no chemical analysis can characterize the variations in oxygen concentration in the phase as sensitively as measurements of the electric resistance.

3. In recent years physicists have shown an increasing interest in compounds of the $A^{III}B^{V}$ type with the zincblende (sphalerite) structure. The distinctive physical attributes of some of these compounds (a high current-carrier mobility, the ability to form p-n junctions, etc.) are undoubtedly connected with their specific crystal structure and the character of the chemical bonds in these materials.

Substances with the structure of zincblende (hereinafter - S) are not, structurally speaking, an isolated or unique type. Forming as a result of replacement in the diamond cubic lattice in turn of one atom by zinc (in the general case an A atom) and of the next by sulfur (in the general case a B atom), they are characterized by tetrahedral configuration of the coordination sphere. A similar configuration is characteristic of substances with the structure of wurzite (hereinafter - W) which differ from the former only as regards the orientation of the tetrahedrons in the successive alternating layers.

In most AB substances crystallizing in both forms - $(AB)_S$ and $(AB)_W$ - the inter-atomic distances in the tetrahedrons are very close: for example, in $(ZnS)_S$ d = 2.35 kX, while in $(ZnS)_W$, d = 2.36 kX (Ref.7).

Obviously with equal coordination numbers and almost equal interatomic distances A—B, the enthalpy and the free energy of the phase transition from the sphalerite to the wurzite modification, i.e., $(AB)_S \rightleftarrows (AB)_W$ must be small. Nevertheless, while there are a few substances crystallizing with the tetrahedral coordination that are known to undergo such phase transitions, many others are still known only in one modification. Incidentally, an analogous situation obtains in the case of other structures, including those of many simple substances[8].

In 1940 Zhuze and Hahn[9] assembled and correlated the then available data on sphalerite-wurzite structures. Their table, supplemented by us as regards $A^{I}B^{VII}$ and other compounds (data in parentheses), is given below.

Table 1

Element	F	Cl	Br	J	Element	O	S	Se	Te	Element	N	P	As	Sb
Li	(NaCl)	(NaCl)	(NaCl)	(NaCl)	Be	*W*	*S*	*S*	*S*	B	*BN*	—	—	—
Na	(NaCl)	(NaCl)	(NaCl)	(NaCl)	Mg	(NaCl)	(NaCl)	NaCl	*W*	Al	*W*	*S*	*S*	*S*
Cu	(*S*)	(*S*)	(*S*)	(*S*)	Zn	*W*	*W,S*	*S*	*S*	Ga	*W*	*S*	*S*	*S*
Ag	(NaCl)	(NaCl)	(NaCl)	(*W,S*)	Cd	(NaCl)	*W,S*	*W,S*	*S*	In	*W*	(*S*)	(*S*)	*S*
					Hg	HgO	HgS,*S*	*S*	*S*	Tl	—	—	—	CsCl

4. The question of the formations of phases of variable compositions in substances with sphalerite and wurzite structures has not yet been examined in its general form. Some authors assume that the formation of the tetrahedral coordination sphere, for example, due to sp^3-hybridization of the orbits, necessarily indicates the presence of predominantly covalent bonds, which preclude the formation of phases of variable composition. These ideas have been advanced with particular emphasis where $A^{III}B^{V}$ compounds are concerned.

Commonly in the literature these compounds are assumed to have rigorously stoichiometric proportions and are therefore treated as phases of constant composition. In fact, some authors assert that compounds of $A^{III}B^{V}$ type are

suitable for industrial use only because there is no appreciable solubility of the components in the compounds in the solid state[10]; there are, however, some investigators who doubt or contradict this assertion[11]. Actually, to date, no one has attempted an exhaustive investigation of this problem.

General conclusions of this kind regarding structures with the coordination number 4 are not only extremely vulnerable from the theoretical standpoint but in many cases fail to stand up under experimental checks. In this connection we need only point to the researches of Wagner, Strock and others (Ref. 12 & 13) who nearly 20 years ago studied the equilibrium, structure and properties of different phases in the ZnO and AgI systems and contrast them with the more recent investigations of Maurer[14] and others in which it was clearly demonstrated that such compounds do form phases of variable composition.

We feel that the data of Table 1 should be interpreted in the following manner.

Let us examine compounds of the $A^{I}B^{VII}$ type. With increasing polarization from Na^{+} to Ag^{+}, there is first formed the NaCl structure, then the W (wurzite) and finally the S (sphalerite) structure*. Naturally, in CuX compounds the polarization is much stronger than in AgX ones. This is evinced in the formation of the S-structure by all CuX compounds, whereas in the case of silver all the halides except AgI have the NaCl structure and only AgI exhibits the W- and S-structures (forming phases of variable composition). Inasmuch as the NaCl structure in the case of bonds of mixed character is tolerant of the formation of phases of variable composition it may be assumed that the W-structure, which is intermediate between the NaCl- and the S-structures allows of the formation of phases of variable composition more readily than the S-structure.

Let us now turn to $A^{II}B^{VI}$ and $A^{III}B^{V}$ compounds. Here, too, with increasing polarization of the anion, the initial NaCl-structure disappears in favor of the W-structure. It may be noted in passing that ZnO (W-structure), for example, is a phase of variable composition. Obviously, deviation from purely ionic or purely covalent bonds to mixed bonds more or less ionic in character is sufficient in this group of compounds for the formation of phases of variable composition despite the 4-coordination. The important point is that in the given case this coordination is energetically more advantageous than, for example, 6-coordination where violation of the Mangus-Goldschmidt-Bragg rule is concerned[8].

As present in connection with the use of compounds of the $A^{III}B^{V}$ type in semiconductor devices there has developed a demand for the production of such materials with reproducible parameters. Consequently, the question of the possible deviation of such compounds from stoichiometric proportions has acquired practical significance. We shall discuss this question from the theoretical standpoint below in Section 6.

5. The experimental part of our work involved primarily the compounds GaAs, InAs and InSb. Consequently, we shall speak here of the methods of synthesis of only these compounds.

There is not much in the literature on the preparation of these compounds which were first synthesized by Goldschmidt[15] in 1927. Initially Goldschmidt obtained GaAs by the indirect method from the oxide. Next, we have the work of Kochnev[16] and Gans and his collaborators[11] who developed methods of synthesis of the arsenides in a heterogeneous medium. Wolf, Keck & Broder[17] describe a general procedure for obtaining compounds of the $A^{III}B^{V}$ type,

---

*This was first noted by V.M.Goldschmidt; also see Ref.9.

consisting of growing single crystals from a solution of the nonmetal in the metal. In some recent investigations of the electric properties of $A^{III}B^{V}$ compounds, the authors report preparing their samples, both antimonides and arsenides, by melting in evacuated sealed quartz ampoules (see, for example, Refs. 18 & 19). After synthesis the samples are generally purified by the zonal melting procedure or by drawing from the melt by the Kyropoulus or Chokhral'ski technique.

To judge from the most recent publications there is a tendency to combine the final purification procedure with the synthesis[20].

Goldschmidt established that the $A^{III}B^{V}$ compounds have the zincblende structure and determined their identity period. Jandelli[21] carried out separate syntheses of these compound for the same purpose. The lattice constants have also been determined by a number of other investigators[18,19]. Phase diagrams of the systems have been investigated by Köster & Thoma[23], Liu & Peretti[24] and Pogodin & Dubinskii[25]. The heat of formation of one of these compounds has been determined by Kleppa[26].

The admittedly scanty data in the literature on the structure and thermochemical characteristics of GaAs, InAs and InSb are summarized in Table 2.

Table 2

Compound	Melting point	Heat of formation	Lattice constant	
			kX	Å
GaAs	1238° (23)	--	5.64 (19) 5.637 (22)* 5.635 (15)	
InAs	942° (24b)	--	6.055 (22)*	6.058 (24)
InSb	525° (24a)	18 kJ = 4300 cal (26)**	6.465 (22)* 6.452 (15)	6.4782 (18) 6.4760 (24)

The numbers in () indicate the References.

*In Ref.22 the lattice constants of GaAs, InAs and InSb are erroneously given in A instead of kX.

**In Ref.26 ΔH_f was determined at 450° by dissolving in molten tin.

In all the cited investigations the identity periods of the prepared substances were determined without allowing for the possible deviation of the composition from the stoichiometric (deviations due to errors in weighing or to kinetic or thermodynamic factors). This is particularly disappointing in the case of the investigation of Ref.18 which was carried out with an accuracy to 0.0001 kX. So high an accuracy could help clarify whether or not a homogeneity region exists; the authors of Ref.18, however, remain silent on this point and in fact do not even raise the question of the possible existence of phases of variable composition.

Thus even the data on the lattice constants of compounds listed in Table 2 do not correspond to any proved, i.e., definitely known, composition. One might say that calorimetrically and, in general, thermodynamically investigation of these systems is in the embryonic stage.

The data on the melting points listed in Table 2 are apparently reliable within the limits corresponding to the accuracy of thermal analysis.

6. As may be concluded from the above (section 5) to date (1955) the question of the possible formation of phases of variable composition in the case of $A^{III}B^{V}$ compounds has virtually not been discussed in the literature.

Theoretically, in the $A^{I}B^{VII}$, $A^{II}B^{VI}$ and $A^{III}B^{V}$ series, such as the series CuBr, ZnSe and GaAs, within the limits of the same period, the ionic character of the bonds must weaken if only due to increasing closeness of the properties of the elements and, in particular, of the values of the ionization potential I of the A and B atoms (for example, I equals 7.67 v for Cu, 11.82 v for Br, 9.37 v for Zn and 9.75 v for Se).

To the extent to which the character of the bonds approaches the covalent, naturally the formation of phases of variable composition will be hindered, particularly in the case of $A^{III}B^{V}$ compounds such as GaAs. But as we go over to the succeeding periods the binding will be increasingly metallic. Consequently, in the series GaAs-InSb-(TlBi) the probability of formation of phases of variable composition should increase. Incidentally the components of the TlBi system are typical of compounds forming the Bertholletides of Kurnakov (see Ref.2). TlBi, however, although it is isoelectronic with lead which has a face-centered cubic lattice, crystallizes in the CsCl structure, i.e., falls outside the class of substances of interest to us here.

Investigation of the influence of the character of the chemical bonds on the formation of phases of variable composition by compounds with a tetrahedral coordination sphere is not only an interesting crystallochemical problem but is also important from the viewpoint of the theory and practical development of $A^{III}B^{V}$ type semiconductors with the given type of structure.

Another incidental problem is the influence of admixtures of ds-elements on the properties of structures with tetrahedral coordination (broadening of the homogeneity region, changes in the electric conductivity, etc.), as well as the possibility of phase transitions of the $[AB_xM_y]_S \leftrightarrows [AB_xM_y]_W$ type, where M is an impurity atom and x and y are the fractional stoichiometric coefficients, and then of $[AB_xM_y]_W \rightleftarrows [AB_xM_y]_{NaCl}$ transitions.

A third problem may be formulated as evaluation of the relative tendency of sphalerite and wurzite structures to form phases of variable composition.

Finally, a fourth problem consists of establishing the role of substituent elements, including the sp-elements, in the formation of sharing or partition structures which, as is known, occur also in the case of lattices with the coordination number 4. Thus as Ketelaar[27] and Strock[13] (also, see Refs.28, 29 & 30) have shown, as we go from AgI to Ag_2HgI_4 (and, also to Cu_2HgI_4) three atoms (2Ag + Hg) occupy four positions in a unit cell with a statistically uniform distribution. A common condition here is the saturation of valence which makes the unit cell as a whole electrically neutral. Goriunova[31] has pointed to the existence of analogous compounds - Ga_2S_3, Ga_2Se_3, Ga_2Te_3, In_2Te_3, and Cu_2Se - within the range of sphalerite structures. Goriunova and her co-workers have obtained substitutional solid solutions on the basis of such compounds[32].

Obviously, through appropriate selection of the impurity and variation of its concentration one can attempt to obtain partition structures on the base of a sphalerite or wurzite modification with different numbers of occupied sites in the unit cell and different characteristics of the replacing and replaced atoms in the lattice as a whole[32].

Investigations in this field have been carried out in the laboratory of D.N.Nasledov in the Physical-Technical Institute of the USSR Academy of

Sciences and in the laboratory of B.F.Ormont in the "L.Ia.Karpov" Physical Chemistry Institute; their results may present some interest where both the general theory and practical development of semiconductors are concerned. We shall describe the preliminary results of these studies in the following section.

7. Experiments on the synthesis of $A^{III}B^{V}$ compounds were carried out in the laboratory of the Physical-Technical Institute. Except for the arsenic, materials of two degrees of purity were used. The arsenic in all the experiments was of the same quality - purified by distillation - and contained traces of bismuth and antimony.

According to the supply-plant laboratory the impurity content of the gallium and indium was the following (percent):

Element	C	Al	K	Ca	Mg	Na	Si+P
Ga 99,8	0,03	0,01	0,05	0,05	0,001	0,01	0,05
In 99,9	0,01	0,01	0,02	0,002	0,001	0,01	0,05

The other synthesis experiments were made with specially purified gallium and indium containing less than 0.0001% impurities according to spectroscopic analysis. The antimony was also obtained by special purification and according to spectroanalysis contained only traces of copper. For preparing the samples the initial elements were melted in evacuated quartz ampoules, which is a convenient procedure for obtaining samples with desired deviations from the stoichiometric proportions. The initial components were weighed with an accuracy of 10^{-4} gram.

In determining upon the synthesis procedure it is necessary to take into account the fact that ZnAs, GaAs and InSb do not yield homogeneous specimens at temperatures below their melting points. Preliminary experiments carried out at temperatures equal to 2/3 the absolute melting-point temperature showed that despite the fact that the diffusion process at this temperature should be rather intense the combining reaction did not go to completion in the case of our compounds. Under the microscope one could readily distinguish the unreacted initial elements. In the literature there is no information on the kinetics of the formation of $A^{III}B^{V}$ type compounds, but in view of the test results it may be assumed that diffusion in a solid state in the case of the investigated substances is hindered by the presence of covalent bonds (also see Refs. 30,31 & 33).

Hence the synthesis procedure had perforce to comprise heating of the components to relatively high temperatures.

In the case of GaAs and InAs the ampoules containing the mixture were heated to the melting point of the more refractory component at a rate not exceeding 150° per hour. The melt was held at this temperature over an hour and then the temperature was raised at the rate of 200° per hour to $30\text{-}50^{\circ}$ above the melting point of the given compound. The alloy was held at this temperature for about 30 minutes and then cooled at a rate not exceeding 100° per hour to $1000\text{-}1500^{\circ}$ for GaAs and to $850\text{-}800^{\circ}$ for InAs. At this point the furnace was switched off and the sample allowed to cool with the furnace. The cooling rate over the initial temperature range was approximately $200\text{-}250^{\circ}$ per hour. After cooling to room temperature the ampoule was opened and the alloy and sublimate (an appreciable amount of sublimate was present only in case of a large excess of arsenic) was separated from the quartz and ground to a powder.

Somewhat different synthesis conditions were employed in the case of InSb in view of the fact that the melting point of indium is lower than that of antimony; homogenization of the alloy (the second stage of the synthesis) was carried out at a temperature of about 800°; in other respects the procedure was the same as for GaAs and InAs.

The syntheses were carried out in a vertical electric crucible furnace; the temperatures were measured by means of chromel-alumel thermocouples calibrated with reference to the melting points of the appropriate metals.

In addition to the stoichiometric compositions, alloys whose components were taken in the ratios of the A:B components equal to 2:1, 1.5:1, 1:1, 1:1.5 and 1:2 were synthesized.

The various alloy specimens were subjected to x-ray analysis.

In the present report we shall only briefly describe some of the results obtained for the gallium-arsenic system.

8. The x-ray patterns were recorded in a 143 mm diameter camera with asymmetric placement of film and also by the method of back reflection in KROS and Sachs cameras; the specimen to film distance was 65 mm. Radiation from copper was employed, the wavelengths[34] being $CuK\alpha_1$ = 1.54050 Å = 1.537395 kX and $CuK\alpha_2$ = 1.54434 Å = 1.541232 kX. The values of the precision angle were 76°40' for $K\alpha_1$ and 77°20' for $K\alpha_2$.

The lattice period found for GaAs was 5.6533 ± 0.001 Å, i.e., differed appreciably from the data in the literature (Table 1). There was observed an appreciable variation of the period (exceeding the experimental error) for samples of different composition. However, until the accuracy of determination is increased to the point where the uncertainty is less than ± 0.0002 Å the question of the existence of a region of homogeneity where GaAs is concerned must be regarded as open.

Similar work on the above-named and other compounds will be continued in the near future in the Physical-Technical Institute and in the "Karpov" Institute; the program includes plans to use a camera with high resolving power equipped with a thermostat.

In order to establish the extent of the homogeneity region, it is necessary also to know the composition of the phase corresponding to a given changes in the lattice constant. There are known[5] to be phases in which rather appreciable changes in the chemical composition within the bounds of the homogeneity region, for example, the β-phase of the tantalum-carbon system in the range from $TaC_{0.38}$ to $TaC_{0.50}$, leads to a change in the order of only 0.001 Å in the lattice distance. In the case of GaAs and of $A^{III}B^{V}$ compounds in general the variations in the chemical composition will probably be appreciably smaller than the Ta-C and similar systems.

Thus, where phases in $A^{III}B^{V}$ systems are concerned determination of the width of the homogeneity regions will require the use of precision x-ray and chemical phase analysis. It is planned to continue research along these lines. We also intend to investigate the different factors (see Section 6) that theoretically may exert an influence on the homogeneity regions.

"L. Ia.Karpov" Physical Chemistry Institute and
Leningrad Physical-Technical Institute of the
Academy of Sciences of the USSR

References

1. N.S.Kurnakov, Vvedenie v fiziko-khimicheskii analiz (Introduction to physico-chemical analysis), M. 1940.

2. V.I.Mikheeva, Izv. AN SSSR, Otd.Khim.nauk., No.6, 396 (1944).

3. B.F.Ormont, Zhur.fiz.khim., 22, 1406 (1948); Zhur.ob.khim., 19, 210 (1949).

4. B.F.Ormont & V.I.Smirnova, Zhur.fiz.khim., 30, 2588 (1956). B.F.Ormont, Report at the Third All-Union Conference on Physico-Chemical Analysis, 2 June 1955, Pub. AN SSSR; Zhur.neorg.khim (Journal of Inorganic Chemistry), 1, 1457 (1956).

5. V.I.Smirnova & B.F.Ormont, Doklady AN SSSR, 96, 557, 1017 (1954); Doklady AN SSSR, 100, 127 (1955).

6. Scott & Mayer, Semiconductor Materials (in Russian trans.).

7. Strukturbericht, p. 76-79.

8. B.F.Ormont, Struktury neorganicheskikh veshchestv (Structures of inorganic substances), M. 1950.

9. B.Juza & H.Hahn, ZS.f.anorg.Chem., 244, 146 (1940).

10. H.Welker, Physica, 20, 893 (1954); ZS.f.Naturf., 7a, 744 (1952); Ibid., 248 (1953).

11. F.Gans, J.Lagrenaudie & P.Seguin, C.R., 237 (4), 310 (1953).

12. C.Wagner, Trans.Farad.Soc., 34, 851 (1938).

13. A.Strock, ZS.Phys.Chem., (B), 25, 441 (1934).

14. J.J.Maurèr, Chem.Soc., 13, 321 (1945).

15. V.M.Goldschmidt, Scriften Norske Vid. A.R.Mat. u Nat., 8, (1927).

16. M.I.Kochnev, Zhur.prikl.khim., 23, 561 (1950).

17. G.Wolff, P.H.Keck & J.Broder, Phys.Rev., 94, 753 (1954).

18. R.G.Brackenridge, R.F.Blunt, W.R.Holser, H.R.P.Frederikse, J.H.Becker, & W.Oshinsky, Phys.Rev., 96, 571 (1954).

19. R.Barrie, F.A.Cunnel, J.T.Edmond & J.M.Ross, Physica, 20, 1087 (1954).

20. O.G.Folbert & H.Weiss, ZS.f.Naturf., 10a, 8 (1955).

21. A.Jandelli, Gaz. chim. Italiana, 71, 58 (1941).

22. N.A.Goriunova & N.N.Fedorova, Zhur.tekh.fiz., 25, 1339 (1955).

23. W.Köster & B.Thoma, ZS.f.Metallk., 46(4), 291 (1955).

24. T.S.Liu & E.A.Peretti, Trans.Am.Soc.Met., 44, 539 (1953); 45, 667 (1953).

25. S.A.Pogodin & S.A.Dubinskii, Izv. (Bulletin) SFKhA, 17, 204 (1949).

26. O.J.Kleppa, J.Am.Chem.Soc., 77(4), 897 (1955).

27. Z.Ketelaar, Krist., 87, 436 (1934). Trans.Far.Soc., 34, 874 (1938); ZS.f.Phys.Chem., (b), 26, 327 (1934).

28. Laves, Usp.khim., 7, 574 (1938).

29. A.Kh.Breger, Usp.khim., 9, 165 (1940).

30. B.F.Ormont, Usp.fiz.nauk., 1036, 38 (1936); Zhur.fiz.khim., Supplementary Volume, p.8 (1947).

31. N.A.Goriunova, Present issue of the Bulletin, p. 114.

32. N.A.Goriunova, Materialy soveshchaniia po poluprovodnikam v Institute metallurgii (Transactions of the conference on semiconductors held at the Institute of Metallurgy), Pub.AN SSSR, 1954.

33. D.A.Petrov, Zhur.fiz.khim., 21, 12, 1449 (1947).

34. W.Bragg, Phys.Rev., 72, 436 (1947); E.Armstrong-Wood, Phys.Rev., 72, 436 (1947).

PHYSICO-CHEMICAL ANALYSIS OF SOME SEMICONDUCTOR SYSTEMS

- N.Kh.Abrikosov

Investigations of semiconductor systems and particularly of such systems comprised of chemical compounds offer great potentialities as regards obtaining new semiconductor materials with diverse properties. Furthermore, such investigations provide the experimental data necessary for a more profound understanding of the regularities governing the formation of chemical compounds of the semiconductor type.

The present report is devoted to a summary of the results of a series of investigations by the methods of physico-chemical analysis of four systems: Cr-Sb, Co-Sb, Fe-Si and Bi-Te. These systems have been studied by a number of investigators in the early years of this century. The phase diagrams obtained then, almost half a century ago, are still in use now with little change. Analysis of these early studies shows, however, that most of the investigators did not pay due attention to attainment of equilibrium and hence in a number of cases overlooked slowly proceeding phase transformations, which incidentally are characteristic of semiconductor systems. Moreover, the electric properties of the alloys in the region of possible semiconductor compounds were investigated only partially or in the case of some systems not at all.

In the present investigations particular attention was paid to attainment of equilibrium in the alloys; this was checked by various methods: examination of the microstructure, x-ray analysis and measurement of the indicative properties. The systems were studied in a wide range of concentrations and after different heat treatments of the alloys.

The investigation of the Cr-Sb system was carried out by V.F.Bankina, that of the Co-Sb system by L.D.Dudkin, and that of the Bi-Te system by V.F. Bankina and G.A.Fedorova. Detailed reports on the results obtained for each system will be published by the respective investigators in the form of separate articles.

Cr-Sb System

The Cr-Sb system comprises two chemical compounds: CrSb and $CrSb_2$. The former crystallizes directly from the liquid phase at 1100°; the latter forms by the peritectic reaction at 676°.

Our studies[1] showed that the compound $CrSb_2$ has metallic properties. Equilibrium in alloys having the composition of $CrSb_2$ is attained with great difficulty due to the low rate of the peritectic reaction. The properties exhibited by equilibrium alloys having the composition of $CrSb_2$ indicate that this compound has the attributes of a semiconductor.

Fig.1 shows the variation of the logarithm of the electric conductivity for $CrSb_2$ with the reciprocal of the absolute temperature. It will be seen that the plot comprises two rectilinear sections: the first in the temperature interval from 40 to 350°, the second in the region above 350°. The forbidden band widths corresponding to these straight line sections are 0.16 ev and 0.32 ev. It is possible that one of these values corresponds to the valence bonds between the antimony atoms and the other to the bonds between the chromium and antimony atoms.

Co-Sb System

The Co-Sb system, in addition to the two compounds - CoSb and $CoSb_2$ -

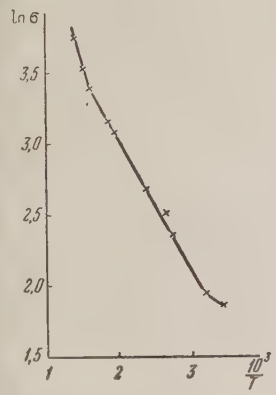

Fig. 1. Temperature dependence of the conductivity of $CrSb_2$.

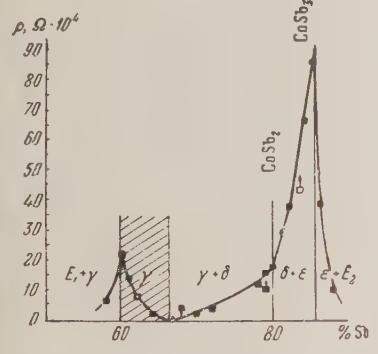

Fig.3. Resistivity isotherm of the Co-Sb system.

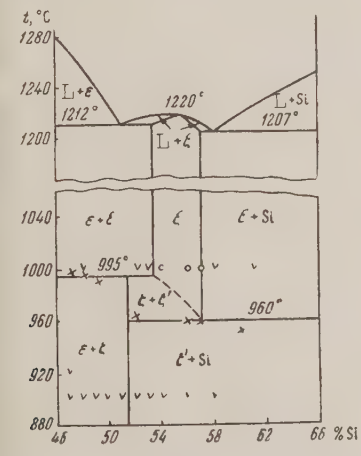

Fig.4. Phase diagram for the Fe-Si system in the region of the compound $FeSi_2$.

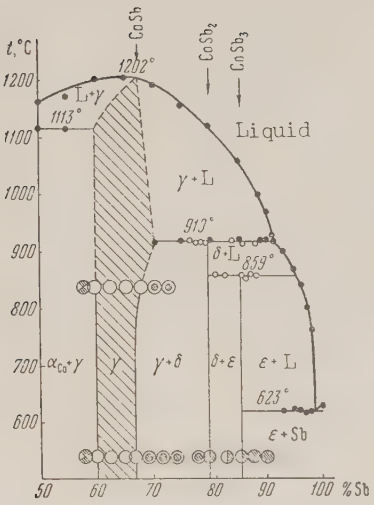

Fig.2. Phase diagram for the Co-Sb system in the region of cobalt antimonides based on the data of thermal analysis: ● - simple; ○ - differential.

described in the literature, comprises yet another chemical compound, namely, $CoSb_3$. This compound[2] forms by the peritectic reaction at 859° (Fig.2). The maximum in the conductivity isotherm corresponds to this compound (Fig.3). X-ray analysis showed that the compound $CoSb_3$ has the structure of scutterudite ($CoAs_3$).

The compound CoSb has metallic properties, while the compounds $CoSb_2$ and $CoSb_3$ are compounds of the semiconductor type with energy gaps of 0.2 and 0.5 ev, respectively[2].

The strength of the valence bonds of the chemical compounds in the Co-Sb system increases with increasing content of the electronegative element; at the same time the melting point goes down. The Co-Sb system is a typical representative of the group of systems in which the melting point of the chemical compounds does not characterize the strength of the valence bonds.

Fe-Si System

Kurnakov and Urazov[3] established that the Fe-Si system includes a phase of variable composition, containing from 55.2 to 61.5% Si, that crystallizes from the liquid. They named this phase Lebeauite in honor of the French scientist P.Lebeau famed for his investigation of alloys of iron with silicon. The Lebeauite phase crystallizes in a tetragonal lattice with three atoms per unit cell and consists of a solid solution of silicon in the compound $FeSi_2$ (50.1% Si).[4]

According to our data[5], at 960° the Lebeauite phase undergoes eutectoid decomposition to a new phase and silicon. The new phase has a composition close to that corresponding to the stoichiometric formula $FeSi_2$ and is therefore a low-temperature modification of this compound (Fig.4). In

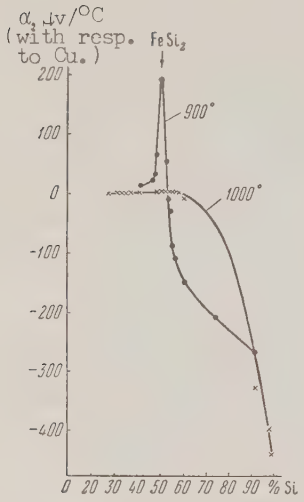

Fig.5. Thermo-emf isotherm for the Fe-Si system in the region of the compound $FeSi_2$.

contrast to the case of the Lebeauite phase, no region of solid solutions on the base of the low-temperature modification of the compound $FeSi_2$ was found in our investigations. The low-temperature modification of $FeSi_2$ crystallizes with a lattice differing from that of the Lebeauite phase.

Measurements of the thermo-emf coefficient of alloys annealed for a prolonged period at a temperature below that of the eutectoid decomposition of the Lebeauite phase showed that there is a pronounced maximum in the thermo-emf isotherm at the point corresponding to the composition $FeSi_2$ (Fig.5).

The high value of the thermo-emf coefficient for the compound $FeSi_2$ (almost 200 μv/°C) justifies classifying this compound as a compound of the semiconductor type.

Three of the investigated systems - Cr-Sb, Co-Sb and Fe-Si - comprise semiconductor compounds of the AB_2 type where B is the electronegative element. The Co-Sb system also has a semiconductor compound of the AB_3 type ($CoSb_3$). The character of the chemical bonds in these compounds has not been determined; it may be assumed, however, that the covalent bonds between the atoms of the electronegative element are at least partially retained. This assumption is supported by the small distances between these atoms in the crystal lattice; these distances are approximately equal to the interatomic separation corresponding to covalent bonds.

Bi-Te System

According to data in the literature[6] the Bi-Te system comprises the compound Bi_2Te_3 which melts with an open maximum at 586°. Semiletov[7] investigated thin films of bismuth-tellurium alloys, obtained by condensation of the vapor on glass supports, by the electron diffraction method. He established the existence of a phase pertaining, in his opinion, to the compound BiTe and crystallizing in the NaCl lattice. The minerals hadleyite and wehrlite exist in nature; the former is ascribed[8] the formula $Bi_{14}Te_6$, the latter has tentatively been identified[9] as Bi_3Te_2.

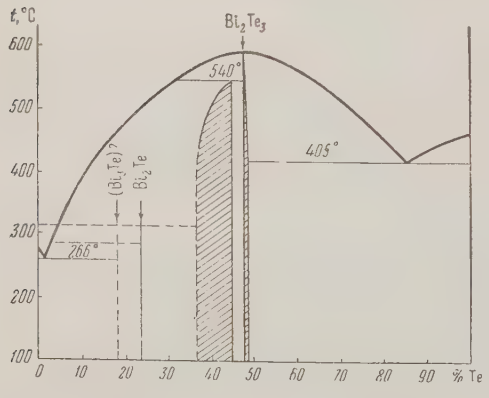

Fig.6. Phase diagram of the Bi-Te system.

We proved that there exist in the Bi-Te system, in addition to the compound Bi_2Te_3, two other phases: the compound Bi_2Te and a phase extending from a 43% Te content to the side of higher bismuth concentrations and having a homogeneity region of over 6%. This phase forms by the peritectic reaction at 540°. In addition investigation of

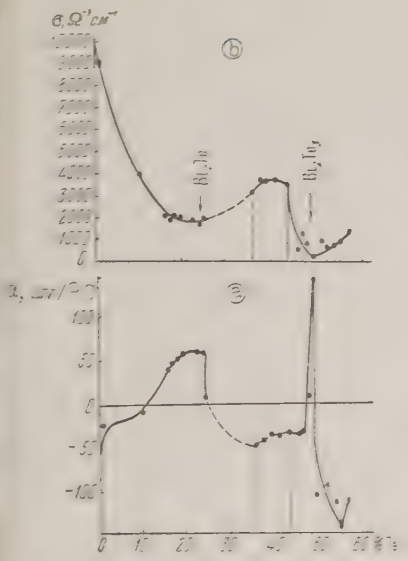

Fig.7. Isotherms for a) the thermo-emf and b) the conductivity of the BiTe system after prolonged (final) annealing.

the microstructure of the alloys gave reason to assume the possible existence of a compound having a composition close to Bi_3Te (Fig.6).

The existence of a wide region of solid solutions with the compound Bi_2Te_3 as the base, suggested by some investigators, was not substantiated: the solubility of tellurium in the compound Bi_2Te_3 is less than 1%, while the solubility of bismuth was found to be virtually nil.

Prolonged annealing led to a sharp change in the properties of the alloys in the region of existence of intermediate phases (Fig.7).

An excess of tellurium above the stoichiometric proportions for Bi_2Te_3 leads, according to the data in the literature[10], to an increase in the conductivity and a change in the sign of the thermo-emf from positive to negative.

The observed change in the properties of these alloys may be explained by replacement of the bismuth with tellurium in the crystal lattice of the compound Bi_2Te_3, which is entirely possible inasmuch as bismuth and tellurium are located in neighboring columns of the periodic table. In replacing the bismuth in the Bi_2Te_3 lattice the tellurium acquires a positive valence proper to bismuth in this compound. The most stable compounds of tellurium are those with a positive valence of 4 (for example, TeO_2 and TeS_2). Having a positive valence greater than the valence of bismuth in the compound Bi_2Te_3, the tellurium gives up its "excess" electrons to the conduction band.

"A.A.Baikov" Institute of Metallurgy of the
Academy of Sciences of the USSR

References

1. N.Kh.Abrikosov & V.F.Bankina, Doklady AN SSSR, 108, 4, 627 (1956).
2. L.D.Dudkin & N.Kh.Abrikosov, Zhur.neorg.khim. (Journal of inorganic chemistry), 1, 2096 (1956).
3. N.S.Kurnakov, Izbrannye raboty (Selected works) Vol.2, M.-L., 1939.
4. G.Phragmen, J.Iron Steel Inst., 114, 397 (1926).
5. N.Kh.Abrikosov, ISFKhA AN SSSR, 27, 157 (1956).
6. M.Hansen, Structure of binary alloys (In Russian trans. M.1941).
7. S.A.Semiletov, Trudy Instituta kristallografii (Transactions of the Institute of Crystallography), No.10, p.76-83, 1954.
8. N.Abrikosov, Chemical Abstracts, 39, 5212 (1945).
9. J.D.Dana, System of Mineralogy (In Russian trans. M. 1951).
10. R.Mvlasova & L.S.Stil'bans, Zhur.tekh.fiz., 25, 4, 569 (1955).

GROWTH OF SINGLE-CRYSTAL LAYERS OF SILICON AND GERMANIUM FROM THE VAPOR PHASE*

- N.N.Sheftal', N.P.Kokorish & A.V.Krasilov

The greater part of all semiconductor materials and, in fact, virtually all the silicon and germanium now produced are obtained by crystallization from a melt. Crystallization from the vapor phase is used primarily for preparing polycrystalline silicon films for detectors and obtaining small crystals (for example, cadmium and lead sulfide and selenide) for photoelectric applications.

Crystallization from the vapor phase is the least studied and least frequently employed procedure where preparation of industrial crystals is concerned. The great shortcoming of this method is the slow rate of growth due to the low concentration of the crystallized substance in the vapor. In the laboratory, however, the growth from a vapor procedure (principally by means of an appropriate chemical reaction) has been used for over a hundred years in view of the fact that it allows of using lower crystallization temperatures. For example, Durocher[1] used this procedure in 1851 to obtain the first artificially grown CdS crystals.

Admittedly in view of the low rate of growth this method is not promising for the preparation of large single crystals. Our research shows, however, that it has tremendous advantages where slow growth is a desirable rather than an undesirable feature, i.e., where the problem is to obtain minute crystals and very thin layers from a fraction of a micron to 100-200 microns thick. In the case of slow crystallization one can differentiate the process and control the individual stages and details. Moreover, in the case of crystallization from the vapor phase it becomes relatively simple to introduce various impurities into the growing crystals.

Generally speaking, monocrystalline layers have the most valuable and reproducible properties. Such layers, characterized by an appreciable strength, can be obtained on single-crystal plates cut from crystals grown from a melt. The composition of the accretion layer continuing the lattice of the massive single crystal can virtually be "constructed" to meet the specific requirements of the experimentor. This makes it possible to obtain monocrystalline layers with desired electric properties and, in particular, makes it possible to obtain p-n junctions.

The substrate on which the oriented monocrystalline layer is grown does not necessarily have to be a crystal of the identical material. This follows from the results of numerous studies of epitaxy following the original work of Frankenheim[2]. For epitaxy (oriented growth) it is sufficient for the substrate to have the requisite dimensional and energetic similarity with the crystallizing substance or even for its surface to have metric and energetic correspondence with at least one principal face of the crystallizing material. The kinetics and regularities of such superficial growth have been investigated in detail by Dankov[3] who formulated the principles of crystallochemical correspondence.

In the present report we shall describe the results of our work on crystallization on single-crystal substrates only where the crystallization of substances identical with the substrate is concerned, i.e., specifically crystallization of silicon on silicon and germanium on germanium.

---

*The first results of practical importance in this investigation were obtained in 1954.

In 1922 Koref[4] demonstrated the possibility of supplementary growth of single-crystal tungsten wire by accretion of material from the vapor phase. In a number of Koref's experiments the grown tungsten layer had a spongy dendritic structure, i.e., in some cases Koref did not succeed in obtaining true monocrystalline growth.

The theoretical considerations involved are the following. The single-crystal plate introduced into the supersaturated vapor phase should act as an inoculant or seed. If the degree of supersaturation is low and no crystallization nuclei are present, the introduction of the seed plate eliminates the necessity of overcoming the potential barrier in the form of the work (A_k) of formation of a crystallization nucleus:

$$A_k = \frac{1}{3}\sum \sigma F_i,$$

where σ is the surface energy and F_i is the area of the i^{th} face. Crystallization on the face should begin in this case even with weak supersaturation. The situation is somewhat more complicated when there is a high degree of supersaturation of the crystallizing substance in the vapor phase.

In this connection Dankov[3] notes that "at high degrees of supersaturation of the vapor, in view of the low value of the work of formation of nuclei, orientation of the crystallites will not obtain despite the favorable relationship between the parameters of the initial and newly forming crystals". He adds that this observation pertains as well to the case of crystallization from the vapor of substances identical with the support.

In other words, if the nuclei form readily they will appear independently, so to say without utilizing the orienting influence of the substrate, and oriented superficial growth will not occur inasmuch as the substrate orients individual atoms rather than entire crystals.

The behavior of real crystals, however, does not conform with these commonly accepted theoretical concepts. In reality oriented growth of even whole small crystals may occur provided the crystallization is not too rapid. This is evinced by a quartz crystal grown by one of the authors, the surface of which is covered with a growth of minute crystals (Fig.1). That these fine crystals are oriented is substantiated by the fact that with further growth the top faces of neighboring crystals join, forming triangles. The crystals are parallel to each other and parallel to the surface of the (1011) face of the quartz rhombohedron on which they grew. Shubnikov[5], too, also mentions the possibility of growth of the supporting crystal at the expense of the minute crystals on its surface.

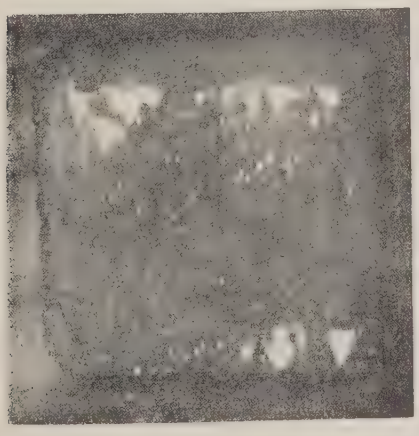

Fig.1. Oriented growth of an artificial quartz crystal at the expense of minute surface crystals, Magnification: 2X.

The orientation of such minute crystals is due to the influence of van der Waals' forces. Hence, other conditions being equal, the orientation is more strongly manifest in the case of small formations inasmuch as the van der Waals' forces attracting the crystals to the substrate increase more slowly than their mass. Consequently, the first necessary condition for good oriented growth is a degree of supersaturation low

enough to insure that the crystallization proceeds slowly and that the size of the crystals, if any are present, is small. Under such conditions there should not develop spongy dendritic formations of the type described by Koref[4].

The quality of the crystal growth depends also on the crystallographic orientation of the substrate. The planes parallel to the densest faces, for example, the (111), (110) and (100) planes, have the strongest orienting effect. The binding forces acting along the normal to these faces and determining the rate of growth are minimal because of the distance between the dense networks. In contrast, the forces acting in the planes of these faces and tending to orient the particles properly are particularly strong.

Hence the orientation of the atoms in the case of tangential growth along the densest planes occurs with a minimal number of "misalignments". The densest faces grow most slowly and most uniformly.

The degree of perfection or quality of the growth also depends on the temperature of the substrate. Up to a point, a higher temperature enhances the influence of the substrate on the crystallization: the higher the temperature, the more uniform the growth, the closer the matching of the growing layer with the substrate lattice and the more nearly perfect the growing lattice.

Thus, Neuhaus[6] in his experiments on the growth of NaCl and LiF crystal under vacuum and from the vapor phase on supports of the same materials established that oriented growth for NaCl begins only at 250° and for LiF only at 315°. Or, more precisely, for oriented accretion on the (111) face of a LiF crystal it must be heated to 380°, while for oriented growth on the denser (100) face heating to 315° is sufficient (at the same time the quality of the growth is better). Without sufficient activation of the substrate by heating, the growth upon it from the vapor phase is chaotic.

Finally, the surface of single crystals being prepared for use as the substrate must be etched or otherwise cleansed to insure complete removal of all impurities that might affect the electric properties of the crystals.

By way of crystallization procedure we chose the method of Krasilov, Maklakov and Mel'nikov, developed by them in 1951 and since then used for preparing thin silicon layers for detectors. The basic set-up is shown in Fig.2. The flow of hydrogen, passing over the surface of the $SiCl_4$ (liquid), takes up the $SiCl_4$ vapor and carries it to the quartz crystallization tube which is heated to 1100° in the furnace. The reaction of the $SiCl_4$ with the hydrogen yields free silicon and hydrogen chloride. The last, together with the small amount of undecomposed silicon tetrachloride and a fraction of the suspended silicon particles is exhausted into the atmosphere. The major fraction of the silicon, however, is deposited on the walls of a short (about 10 cm) section of the quartz tube comprising the crystallization zone. Objects - specifically, the substrate plates - in this zone become covered with a coating of polycrystalline silicon.

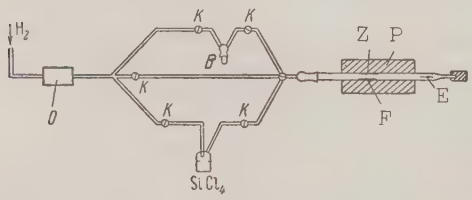

Fig.2. Diagram of set-up for the crystallization of silicon and germanium by the hydrogen method: O) hydrogen purifier, K) valves, F) furnace, P) plates on which growth occurs, Z) crystallization zone, E) outlet for waste gases, B) cylinder containing the chloride of the desired impurity element.

With all the valves open, the hydrogen flows through all three lines: the bottom one (in Fig.2) opening into the $SiCl_4$ container, the middle one leading directly to the crystallization tube and the top one connecting to the cylinder containing the chloride of the element it is desired to introduce as the impurity. Any of the lines can be closed off at will; this one can send pure hydrogen through the crystallization chamber to drive off all traces of the impurity or hydrogen plus $SiCl_4$ vapor in order to crystallize pure silicon. The identical set-up is used for crystallizing germanium except that the $SiCl_4$ is replaced by $GeCl_4$.

With the described procedure the substrate single crystal builds up through the accretion not only of single atoms but also groups of atoms and microscopic crystals of different size. This is evident from the following.

The structure of the polycrystalline film is not homogeneous along its length. At the beginning, i.e., near the entrance, it consists of a mass of very small almost amorphous particles and is relatively thin (2 to 10μ). As we go further into the crystallization zone, the size of the crystals and thickness of the film increase. From about 4 centimeters in, the film consists of a fairly continuous single layer of crystals. Towards the end of the tube, the coating is made up of intermittently distributed individual crystals up to 200 μ in diameter. The crystals at the same distance from the beginning of the film are of approximately the same size. This indicates that at the beginning of the film we have a very high rate of formation of crystallization nuclei and a very low linear rate of crystallization, whereas towards the end, on the contrary, the rate of crystallization is high while the rate of formation of nuclei is low. In view of the structure of the film we can distinguish two stages in the process of its formation: an initial stage and a second or main stage.

In the initial stage numerous crystallization centers form at the beginning of the crystallization zone and are then scattered throughout the zone by the gas stream.

During the second stage new crystallization centers continue to form the beginning section of the tube. Part of them settle there, but many are carried along by the gas stream, which moves at the rate of about 5 cm/sec, and, beginning with the point where the crystals are arranged in a single layer, no longer give rise to new crystals but adhere to the crystals already present. This reasoning is substantiated by analysis of the mechanism of growth of the individual crystals towards the end of the tube. It may be assumed that these grow about a few of the larger centers carried along by the gas stream and that they continue to grow during their journey from the beginning of crystallization to the point of deposit. The fact that the crystals at the same distance from the beginning of the tube are of more or less the same size and the absence of minute crystals between them indicate that new centers brought by the gas stream to that section of the tube do not give rise to new crystals but rather adhere to those already present.

It was noted that in the case of germanium there appears on the inner surface of the quartz tube in the zone of crystallization a crystal-free rim or band up to 5 mm wide around the substrate plate. This shows that the growing single crystal, attracting the material in its immediate vicinity, gives rise to a region of reduced concentration or a so-called "crystallization yard" similar to that forming about crystals growing from solution. The presence of such a "crystal yard" around the germanium single-crystal plates shows that the plates grow not only at the expense of individual atoms of groups of atoms but also through the accretion of submicroscopic particles carried

past by the flow of gas, thereby eliminating the possibility of such particles settling and forming the centers of new growth in the given area.

Description of the Experiments

Our experiments on the etching and growth of non-oriented and oriented silicon and germanium crystals yielded interesting information on their structure and the mechanism of their growth.

The flat surfaces of plates cut from silicon single crystals, grown from a melt and having a random orientation, were etched for 4-5 minutes in a boiling 30% solution of NaOH in water. Microscopic examination of the surfaces (Fig.3) shows that etching brings out a laminar structure of the crystal when the plane of the cut is not parallel to the laminae. The dissolving by the etchant proceeds not so much in the direction normal to the plane of the cut as in the direction of the fronts of the laminae along which the growth occurred. This shows that there exist between the neighboring laminae surfaces of separation due to minute inclusions of impurities and mismatching of the adjacent lattices. Thick layers appear to be made up of thinner parallel laminae, more weakly but still distinctly brought out by the etching and, consequently, also interlaid with impurities. Differently oriented, arbitrary cuts of silicon single crystals inevitably show such laminae, although their appearance varies for different cuts.

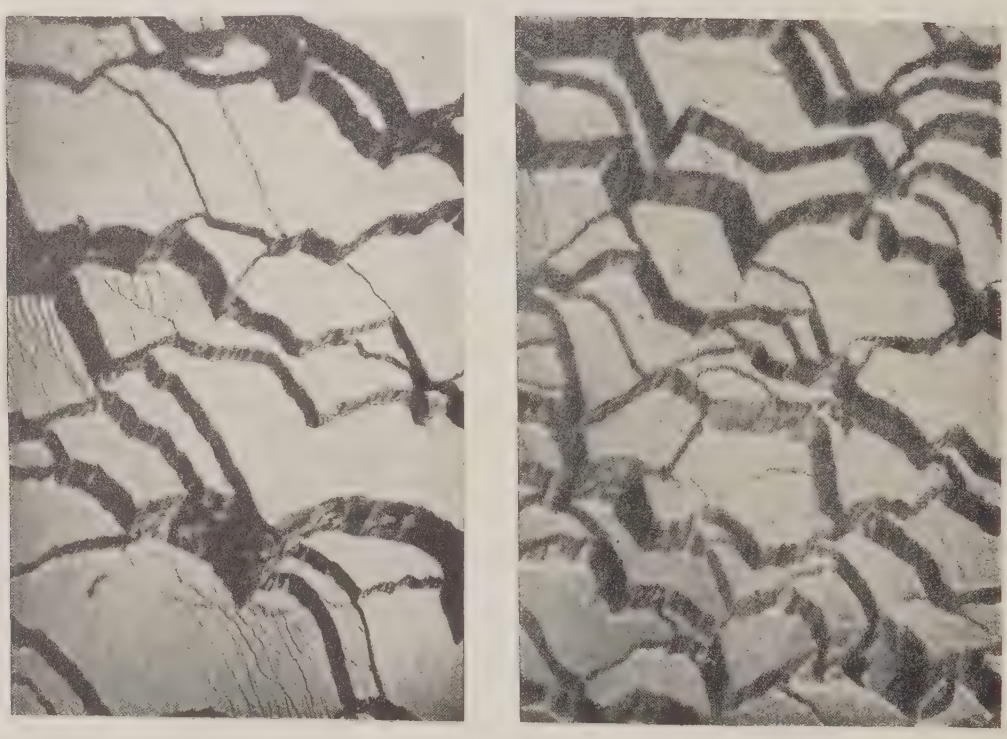

a b

Fig.3. Laminar structure of silicon single crystal brought out by etching. Magnification 450 X. (Microphotograph made by S.Kh.Mukhonkin & V.M.Soboleva.)

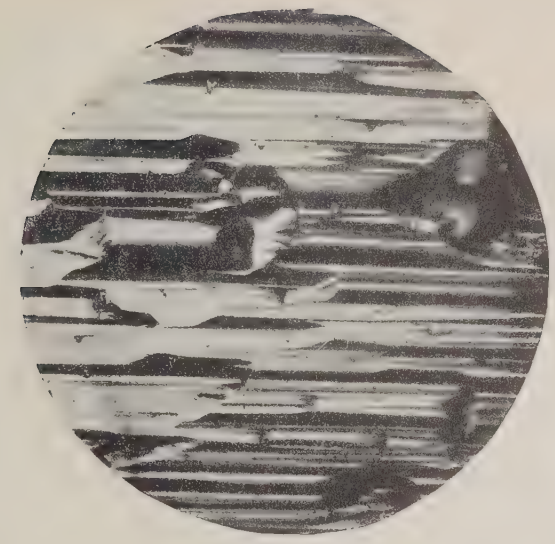

a

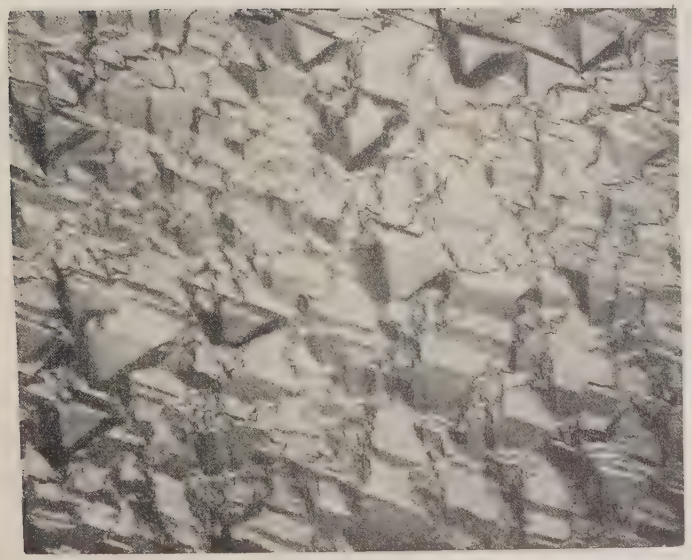

b

Fig.4. Crystal growth on surface of a silicon single crystal having an initially random orientation. Layer ~30μ thick. The growth is monocrystalline in character. Magnification: a) 383 X; b) 450 X.

After crystal growth upon them, such surfaces, characterized by an initial random orientation, appear as shown in Fig.4. It will be seen that the growth is predominantly monocrystalline. This is evinced by the parallelism of the subindividual crystals covering the exposed surface and bounded by the principal crystal faces. Through the accretion of these subindividual crystals the original random, non-oriented surface of the substrate crystal is replaced by the principal, i.e., densest, crystal face closest to it (Fig.5).

Electron diffraction patterns recorded after crystal growth substantiate the monocrystalline character of the layer.

Single-crystal plates of arbitrary orientation cut from germanium crystals, when etched in boiling perhydrol exhibit a less pronounced but highly distinctive laminar structure. The surface of the exposed layers is not smooth as in the case of silicon, but pitted (Fig.6). Plates cut parallel to the (100), (110) or (111) face of the germanium single crystal, after some 14 minutes etching in boiling perhydrol show etch figures having a diffuse, somewhat rounded shape. The figures exhibit, albeit indistinctly, the symmetry elements perpendicular to the etched planes of the crystal. Thus the etch figures on the (111) face of a plate have L^3 3P symmetry (Fig.7).

When germanium plates cut parallel to the (100), (110) and (111) planes are etched for 2 min in the strong solvent SS-4 (Russian: CP-4) (a mixture of HNO_3, HF, CH_3COOH and Br) there is obtained a rather even surface with discernible steps of laminae weakly reflecting the crystallographic character-

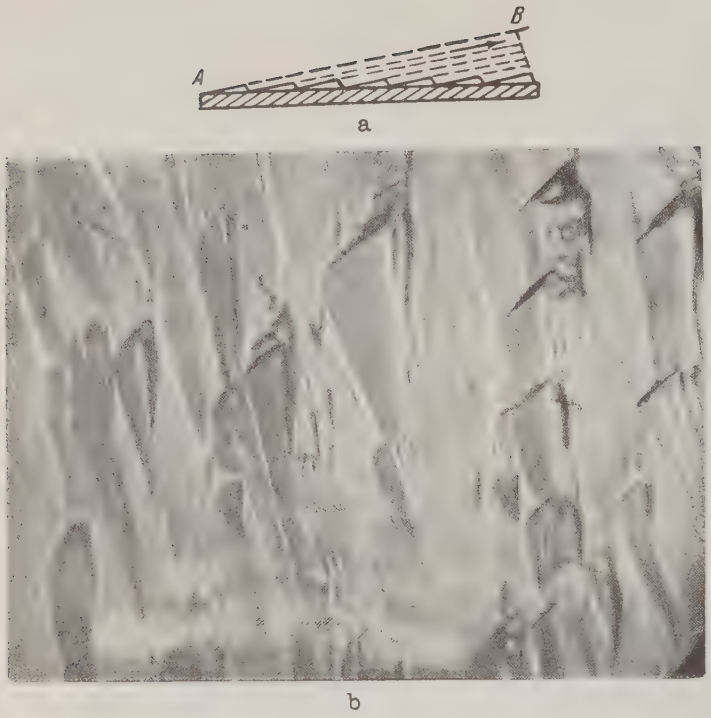

Fig.5. Replacement of a random non-crystallographic single crystal by the surface of the dense face closest to it: a) idealized diagram and b) picture of similar actual growth. Magnification: 450 X.

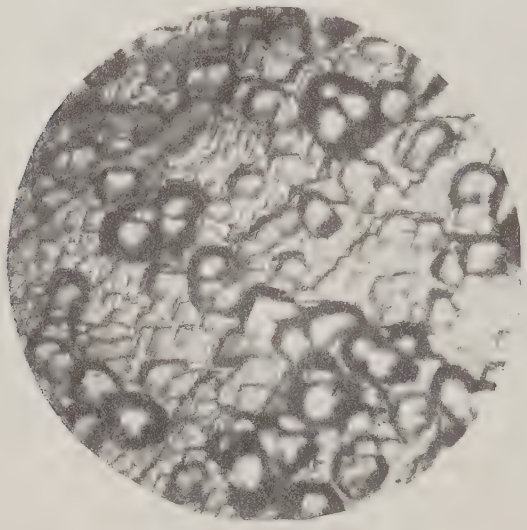

Fig.6. Laminar structure of germanium crystal brought out by etching. Magnification 383 X.

istics of the corresponding plane. Such surfaces are more convenient for crystal growth experiments since they may be assumed to be more nearly true planes than the distinctly stepped surfaces with a random non-crystallographic orientation. The best etched surfaces were obtained in the case of cuts parallel to the (110) plane.

In the case of crystal growth on a germanium plate of random orientation, the plate becomes covered with subindividual formations with a rounded surface from the appearance of which it is difficult to know to what extent the growth is oriented. Electron diffraction patterns with Kikouchi lines, which are virtually identical with the electron diffraction patterns of the initial substrate, substantiate the monocrystalline character of such growths. Monocrystalline growths on oriented germanium surfaces parallel to the (100), (110) and (111) planes shows that the most even accretion is obtained on plates oriented along the (110) plane (Fig.8).

In the case of germanium, the minimum temperature at which there is obtained a stably orientated growth and the decomposition of $GeCl_4$ proceeds satisfactorily is about 700°. Very good growth is obtained at 850°. Good growth of silicon at 1150° is observed only when the rate of growth does not exceed ~1 μ per minute. Under conditions

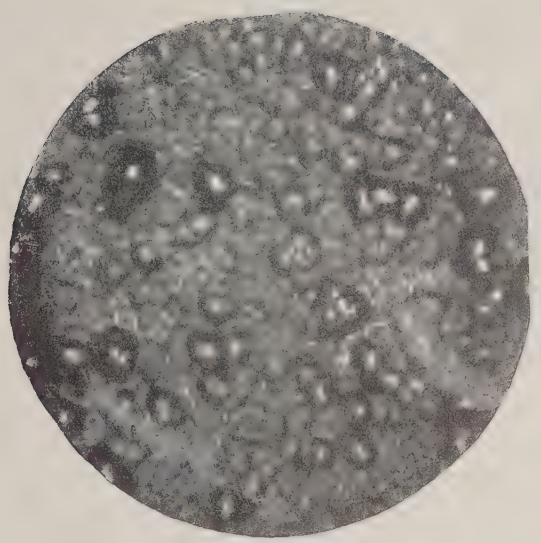

Fig. 7.

differing greatly from the optimal, the growth of both germanium and silicon is polycrystalline.

The thickness of the monocrystalline layers obtained on silicon and germanium single crystals varies from a fraction of a micron to 200 microns. The area

---

Fig.7. Surface of germanium crystal parallel to the (111) plane etched with a weak solvent. Magnification 383 X.

Fig.8. Crystal growths on germanium single-crystal surfaces parallel to the a - (111), b - (100) and c - (110) planes; surfaces etched before crystal growth with a strong solvent (a mixture of HNO_3, HF, CH_3COOH and Br). Layer 20-25 μ thick. Magnification 200 X.

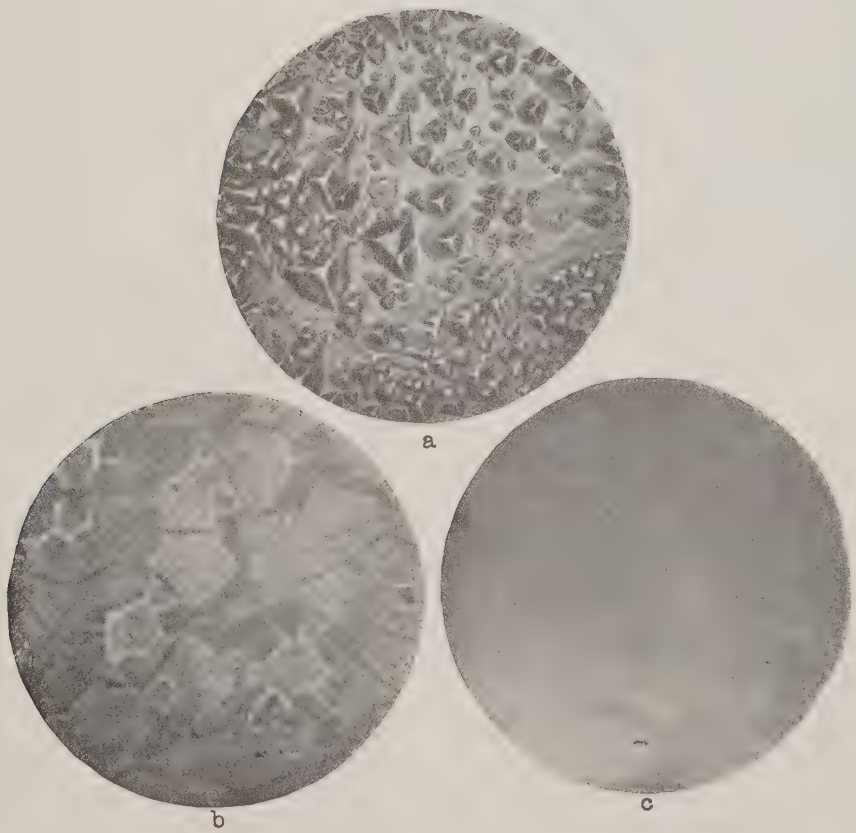

Fig. 8.

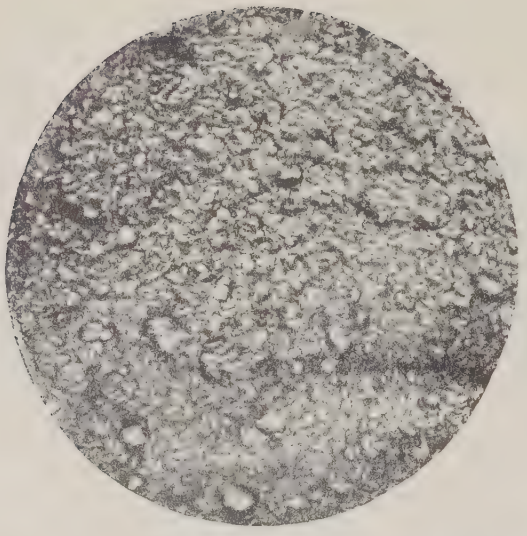

a

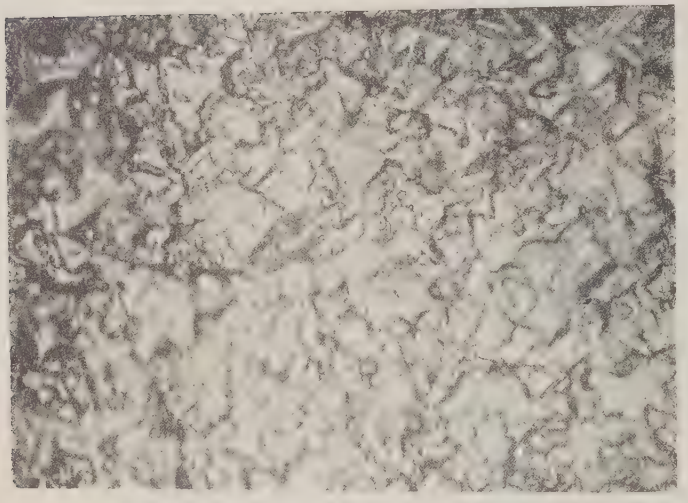

b

Fig.9. Polycrystalline growths on single crystals: a) germanium (Magnification: 383 X) and b) silicon (Magnification 450 X).

of growth in our experiments attained 2.5 cm^2, but can undoubtedly be appreciably increased by suitable modification of the equipment.

The introduction of impurities into the crystallizing material, for example, phosphorus and arsenic into germanium, does not affect the monocrystalline character of the growth.

We investigated some of the electric properties of the materials prepared in the above described manner. Silicon layers are characterized by a reverse breakthrough voltage of 80 to 220 v and n-type conductivity. We also succeeded in obtaining grown germanium layers n-type conductivity. Measurements of the resistivity of germanium showed that ρ varies from 1 to 4 ohm-cm if no impurities are introduced during the growth. When impurities are introduced the resistivity drops to a few percent of the above values. The diffusion length in germanium specimens into which no impurities were especially introduced was found to be from 0.2 to 0.7 mm.

The described procedure was also used for preparing germanium junction triodes of the p-n-i-p (or n-p-i-n) type, described by Early[7]. In the fabrication of such triodes one of the most important operations is preparation of germanium plates with intrinsic conductivity (30-40 ohm) and having a surface layer of n-type germanium with a resistivity of 0.1-1 ohm-cm and a thickness from 7 to 12 μ.

According to Early such triodes must be prepared by fusing a lead-arsenic or lead-antimony mixture onto a plate cut from a germanium crystal with intrinsic conductivity and subsequent diffusion of arsenic or antimony from the depth of the plate.

We prepared the plates by growing a thin layer of n-type germanium by crystallization from the vapor phase with an impurity onto a plate cut from a crystal with intrinsic conductivity. This procedure proved to be much

easier than the diffusion method. It yields a plane boundary between the substrate and the surface layer that is much sharper than can readily be obtained by simple diffusion.

Concurrently with part of our work, I.P.Lukasheva carried out experiments on obtaining monocrystalline layers from germanium by sputtering under vacuum. In this procedure the material arrives at the substrate in the form of single atoms. It proved impossible under comparable conditions to obtain technically acceptable crystals, indicating that the lattices formed in this procedure are less perfect. It is possible that with appreciable supercooling under conditions of low mobility of the particles it is more difficult to obtain an adequately perfect lattice from single atoms as compared with a mixture of individual atoms, groups and blocks.

Conclusions

1. Crystallization from the vapor phase can be used in practice for producing monocrystalline layers, having a desired constant or variable composition, on single-crystal plates cut from crystals obtained from a melt. In particular this method can be used for making p-n junctions.

2. At present the most suitable crystal growth method as regards both quality of the product and simplicity of the equipment is the method of crystallization of silicon and germanium at atmospheric pressure in a flow-through tube with decomposition of $SiCl_4$ or $GeCl_4$ at a high temperature in a stream of hydrogen (the method of Krasilov, Maklakov and Mel'nikov).

3. We established the optimum conditions for high quality growth of germanium and to an extent silicon (preparation of the surface, orientation, temperature, etc.). We obtained monocrystalline growth layers of germanium from a fraction of a micron to 200 microns thick on areas up to 2.5 cm^2.

4. The practical utility of the method was demonstrated by successful preparation of plates with a grown layer, suitable for the fabrication of p-n-i-p triodes analogous to those described by Early[7].

5. In the case of crystallization from the vapor phase at atmospheric pressure the growth occurs not only through the accretion of individual atoms and the groups of atoms but also at the expense of small crystals. Nevertheless, as the result of such growth there is obtained a crystal lattice with a sufficiently high degree of perfection for technical applications. On the other hand, in experiments with crystallization by vacuum sputtering, where the growth occurs primarily through the accretion of single atoms, it proved impossible to obtain layers possessing electric properties suitable for engineering use. This leads us to ask:

1) Does crystallization through incorporation of individual atoms have any advantages over crystallization through accretion of atomic complexes where obtaining a nearly perfect lattice is concerned?

2) Does not normal crystallization of a real crystal, even at low degrees of supersaturation, always proceed at the expense of submicroscopic crystals and groups of atoms, which may or may not include individual atoms?

A positive answer to the latter question is suggested by the experimentally substantiated work of Mayer[8], Band[9], Frenkel'[10] and Vukalovich & Novikov[11] on the theory of a real gas.

If we accept this proposition, then it must be assumed that crystallization and solution of real crystals, in particular, in the vapor phase, even under conditions of low supersaturation does not conform to the concepts developed in the molecular-kinetic theory of Kossel[12] and Stranski[13] which

theory is based on the assumption that the growth of crystals occurs by the addition of single atoms and molecules. Furthermore, it would follow where crystalline semiconductor materials are concerned that the electric properties of grown crystals must depend on the degree of supersaturation or supercooling under which they are grown inasmuch as this determines the mean size of the aggregations or crystals from which the real crystal is built up and this should obviously influence its physical properties.

Institute of Crystallography of the
Academy of Sciences of the USSR

References

1. J.Durocher, C.R., 32, 823 (1951).
2. L.M.Frankenheim, Poggend. Ann., 37, 516 (1836).
3. P.D.Dankov, Trudy 2-i Konferentsii po korrozii metallov (Transactions of the second conference on the corrosion of metals), 2, 120 (1943).
4. F.Koref, ZS.f.Elektrochem., 28, 511 (1922).
5. A.V.Shubnikov, Kak rastut kristally (How crystals grow), M. 1935.
6. A.Neuhaus, ZS. Elektrochem., 56, 453 (1952).
7. I.M.Early, The Bell Syst. Techn. J., 33, 517 (1954).
8. I. Mayer, J. Chem. Phys., 5, 67 (1937).
9. W.Band, J. Chem. Phys., 7, 324, 927 (1939).
10. Ia.I.Frenkel', Zhur.eksp.i teor.fiz., 9, 199 (1939).
11. M.P.Vukalovich & I.I.Novikov, Doklady AN SSSR, 23, 8, 767 (1939); Uravnenie real'nogo gaza (Equations of a real gas), 1948.
12. W.Kossel, Nachr. Ges. Wiss. Götting. Math.-phys. Kl., 135 (1927).
13. I.Stranski, ZS. f. Physik. Chem., 136, 259 (1928).

PREPARATION OF SINGLE-CRYSTAL SPECIMENS OF CUPROUS OXIDE

- Iu.I.Gritsenko

Introduction

Most studies devoted to the investigation of the semiconductor properties of cuprous oxide have been carried out on polycrystalline specimens. Individual measurements performed on artificial single crystals[1] have not been systematic and did not disclose any appreciable difference where the electric conductivity of monocrystalline as against polycrystalline specimens is concerned.

Recently it has been shown that there is a difference between the conductivity of Cu_2O crystalline grains and the intercrystalline laminae[2]. It has also been suggested that the intercrystalline laminae may influence not only the magnitude of the conductivity of cuprous oxide[3] but also the temperature dependence of the conductivity[4].

The problem of the influence of intercrystalline strata on the different semiconductor properties of cuprous oxide can be solved only through systematic investigation of these properties in single crystals and comparison with the corresponding properties of polycrystalline specimens. Until now, however, as far as we know, there has not been developed any reasonably simple and satisfactory method for obtaining single crystals of cuprous oxide.

The procedures proposed hitherto involve prolonged high-temperature annealing (for hundreds of hours) of either copper single crystals[1] or polycrystalline copper[5]. In the latter case, as the authors in question themselves note, large single crystals ($\sim$100 mm^2) were obtained only by chance.

Hence we felt it would be of value to determine the different conditions and factors influencing the dimensions of crystal grains of Cu_2O obtained by oxidizing copper and to explore the possibilities of obtaining single crystals of this semiconductor material. The specific purpose of the present investigation was to study the influence of the properties of the initial material, namely, its purity and crystal structure, on the grain size of the oxide.

1. Influence of the properties of the initial copper on the Cu_2O grain size

The cuprous oxide was prepared by oxidation of copper plates in an electric furnace in an atmosphere of air at a temperature of $\sim 1050^{\circ}$. According to the phase diagram this temperature at a partial pressure of oxygen equal to the pressure of oxygen in atmospheric air corresponds to the region of stability of cuprous oxide.

In investigating the influence of the purity of the initial copper we used electrolytic copper of three kinds: No.1 - with a 99.95% copper content, No.2 - with a 99.99% copper content and No.3 - copper subjected to repeated careful refining and analyzing 99.998% pure*. The impurity content of copper No.3 as determined by analysis is shown in the table on the next page.

In the course of multiply repeated experiments we detected no noticeable difference in the grain size obtained with these three different sorts of copper.

One can judge of the grain size from Fig.1 which shows a photograph of

---

*Copper samples Nos.2 & 3 with the corresponding analyses were kindly put at our disposal by D.P.Zosimovich of the Institute of General and Inorganic Chemistry of the Ukrainian SSR Academy of Sciences. We take this occasion to thank him.

Analysis of copper No. 3 (values in %)

Sb	Bi	Fe	Mo	Pb	Zn	As	Mn
0,00016	0,00001	0,0014	0,0000	0,0002	0,0003	0,00001	0,0000

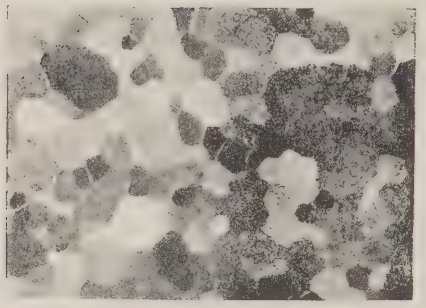

Fig.1. Surface of cuprous oxide obtained by oxidation of a 1 mm thick plate of 99.99% pure copper. (Magnification 5 X).

the surface of the cuprous oxide obtained by oxidizing copper No.2 at 1050° for 6 hours. As noted, the same grain size was obtained from the other two sorts of copper.

It may therefore be concluded that the purity of the initial copper (within the investigated range, i.e., with less than 0.05% impurities) does not have an appreciable influence on the grain size of the cuprous oxide obtained by oxidation.

In investigating the influence of the crystal structure of the initial copper we used plates both with a fine-crystal and a coarse-crystal structure. To obtain the coarse-crystal structure plates, we made use of the effect of recrystallization when the metal is heated after plastic deformation.

It is known that the heat treatment conditions as well as the optimal plastic deformation before recrystallization depend on the properties of the copper and must be found experimentally. Tests showed that in the case of our copper rather large grains were obtained through the following treatment. First, in order to relieve stresses, the copper plates were annealed under vacuum at ~1000° for two hours with subsequent slow cooling. Then they were subjected to 1-2% plastic deformation in tension in an appropriate testing machine. Next, these plates were annealed under vacuum for ~36 hours while the temperature was slowly raised from 500 to 1000°. The resultant plates had individual grains of up to 1 cm^2 in area interspersed, however, with fine crystals.

In Fig.2 we reproduce photographs of the surface of recrystallized copper plates 1 mm thick (a and b) and photographs of the surface of the cuprous oxide (c and d) obtained by oxidizing these plates for 6 hours at ~1050°. In order to bring out the grain boundaries both the copper and cuprous oxide plates were etched in dilute nitric acid.

It will be seen from the photographs of Fig.2 that the more coarse-crystal cuprous oxide was formed from the more coarse-grained copper. However, it is difficult to establish from these photographs any clear relationship between the grains of the initial copper and the cuprous oxide. It was not clear to us why in general there is no definite correlation between the size and shape of the copper grains and those of the cuprous oxide, even though, as is evident from the photographs, the crystal structure of the initial copper does have a definite influence on the grain size of the Cu_2O.

In order to clarify the character of the Cu_2O grains at the first stages of oxidation we carried out the following experiments. The recrystallized copper plates before oxidation were photographed and then placed in a furnace for 1 to 5 minutes to induce the formation of a thin layer of Cu_2O. This, after chemical removal of the cupric oxide film that develops during cooling

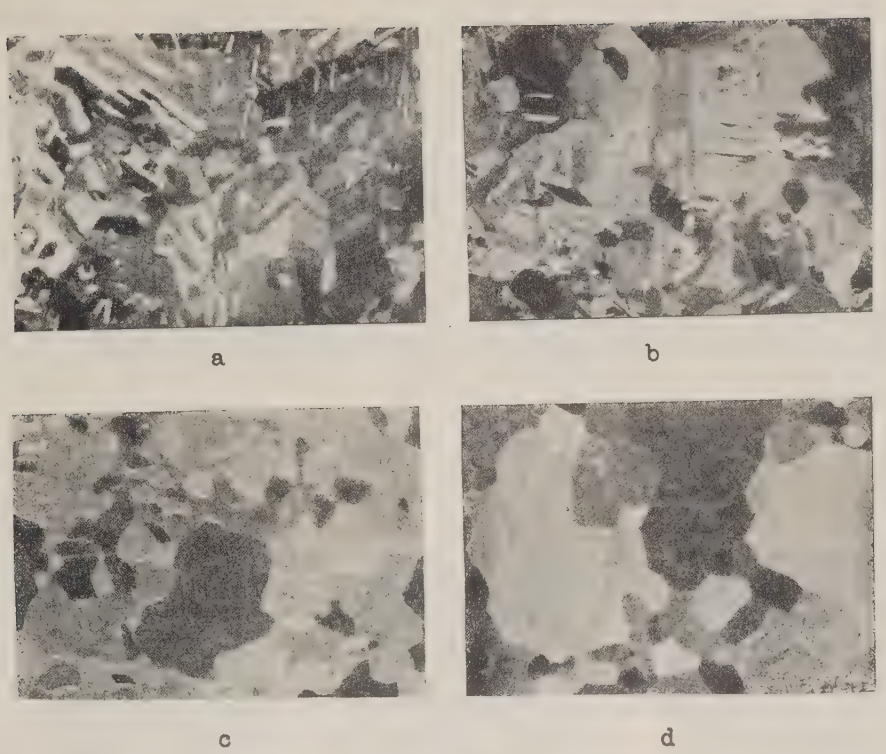

Fig.2. a & b) Surface of recrystallized copper plates (a - annealed 6 hours; b - annealed 34 hours). c & d) Surface of cuprous oxide obtained by oxidation of these plates for 6 hours at 1050°. (Magnification 3.5 X).

in air, was also photographed. It was established that the size of the grains in the thin layer of Cu_2O obtained in this manner depends both on the rate of its formation (rate of oxidation) and on the state of the surface of the initial copper. Thus, if the surface of the copper plates is cleaned (for example, by etching with dilute nitric acid) immediately before placing them in the furnace heated to 1050°, there is always obtained a fine grained Cu_2O layer. On the other hand, if after surface cleansing the copper plates are stored for 12-24 hours in dry air and then oxidized at 1050°, the cuprous oxide layer formed in the course of 1-5 minutes usually exhibits grains nearly identical in shape and size with the grains of the initial copper.

Further, if the oxidation is carried out at a reduced temperature (850-880°) there is always obtained a Cu_2O layer with grains of the same size and shape as those of the initial copper regardless of whether the chemical cleansing is carried out immediately or long before oxidation. In this case, in order to remain within the region of stability of the cuprous oxide, it was necessary to reduce the partial pressure of oxygen to 10 mm Hg.

Fig.3 shows photographs of the surface of a recrystallized copper plate (a) and the surface of the cuprous oxide layer (b) formed on this plate in the course of 5 minutes at 880° (partial oxygen pressure p_O = 10 mm Hg). It will readily be noted that the grains of the Cu_2O layer have the same shape as those in the initial copper.

The reasons for the effect of cleaning the surface of recrystallized copper plates on the grain size are apparently the following.

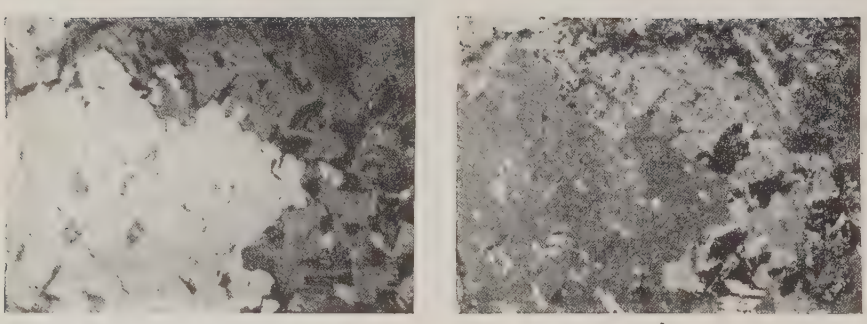

a b

Fig.3. a) surface of a recrystallized copper plate; b) surface of cuprous oxide layer formed on this plate by 5 minutes oxidation at 880°. (Magnification 3.5 X).

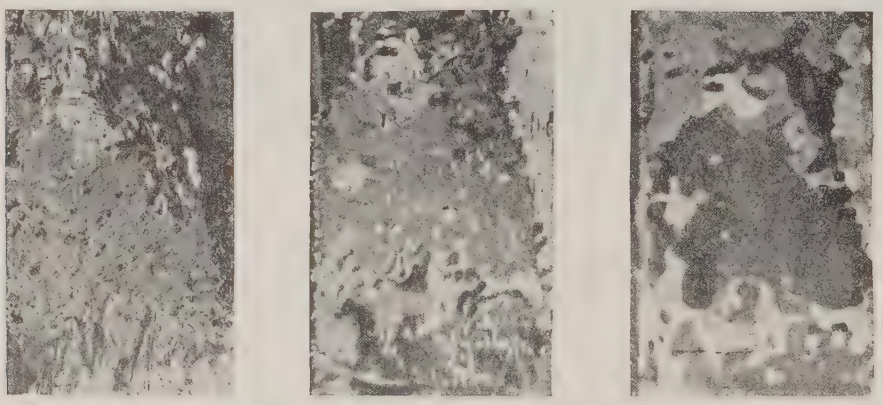

a b c

Fig.4. a) recrystallized copper plate; b) cuprous oxide formed on this plate during 10 hours at 880°; c) same cuprous oxide after repeat annealing at 1050°. (Magnification 2.5 X).

It is known that under ordinary conditions copper is always covered with an oxide film[6]; this film is always monocrystalline on single crystals and polycrystalline on polycrystalline copper. Consequently, it may be assumed that our coarse grained recrystallized copper after some hours storage at room temperature became covered with a layer of coarse-crystal cuprous oxide, i.e., a film formed under conditions of low intensity oxidation. If this film is removed (for example, by etching), then at a high rate of oxidation (i.e., in the furnace) there rapidly develop many crystallization centers and, consequently, a Cu_2O layer with a fine-grained structure is formed.

It may be asserted, therefore, that the crystalline structure of cuprous oxide forming at low rates of oxidation is determined by the crystalline structure of the copper substrate.

If a sufficiently thick (several hundredths of a millimeter) Cu_2O layer is allowed to form at a low rate of oxidation and then the temperature and oxygen pressure are brought up to the usual value ($T \approx 1050°$ and $p_O \approx 170$ mm Hg),

then with further oxidation the grains change as regards both size and shape.

This is illustrated in Fig.4 in which we reproduce a photograph of the surface of the initial recrystallized copper plate (a), a photograph of the cuprous oxide formed on this plate over a period of 10 hours at $\sim 880^{\circ}$ and p_O = 10 mm Hg (b) and a photograph of the same specimen reheated in the furnace for 10 hours at $\sim 1050^{\circ}$ and atmospheric oxygen pressure (c). It will be evident from these photographs that the longer the specimen remains in an oxidizing atmosphere, the fainter the similarity between the grains of the cuprous oxide formed and the grains of the initial copper. The fact that one and the same specimen contains both large grains (cross section area of the order of tens of square millimeters) and very fine grains indicates that, in the case of the described process of oxidation of coarse-crystal copper, the increase in the grain size of Cu_2O occurs through "absorption" of small grains by large ones.

Thus there are two features worth noting in connection with the grain formation process in the case of the described procedure for oxidizing coarse-crystal copper: 1) at the very beginning of oxidation there are formed large Cu_2O grains of a size and shape corresponding to the grains of the initial copper, and 2) during the oxidation and then as long as the specimen remains in an oxidizing atmosphere after complete oxidation of the copper, the size of the grains continues to change through "absorption" of small grains by large ones.

This mechanism of the formation of cuprous oxide differs from the mechanism described by Andrievskii & Mishchenko[7], which apparently operates only in the case of oxidation of fine-crystal copper.

2. Procedure for obtaining monocrystalline Cu_2O

On the basis of our experiments we developed a procedure for obtaining coarse-crystal cuprous oxide with subsequent separation of Cu_2O single crystals. Briefly, the procedure is the following. Prior to oxidation, the crystal structure of the copper plates is made coarser by recrystallization; the initial stage of oxidation is carried out at a slow rate which is realized by reducing the temperature of the furnace and the partial pressure of the oxygen.

One hour after the beginning of oxidation the temperature of the furnace is raised to about 1050° and then the oxygen pressure is raised to that of atmospheric oxygen.

The copper plates used in our experiments had a thickness of 1-1.5 mm. From 6 to 14 hours (depending on the thickness of the plate) were required for complete oxidation of such plates at a temperature of 1050° in air. In order to obtain larger crystals, we usually kept the plates in an oxidizing atmosphere somewhat longer (12-20 hours).

The cuprous oxide plates prepared in this manner had a coarse crystal structure with individual single crystals measuring up to 1 cm^2 in area. The thickness of such single crystals is determined by the thickness of the initial copper plate and may be varied within reasonable limits.

If the cuprous oxide is cooled in air by simply withdrawing it from the furnace its mechanical strength is sufficiently high to permit cutting out many of the individual single crystals.

Fig.5,a is a photograph of a plate of coarse-crystal cuprous oxide obtained by oxidation for 26 hours at a temperature of 1050°. Fig.5,b shows photographs of single crystal specimens of Cu_2O extracted from such a plate

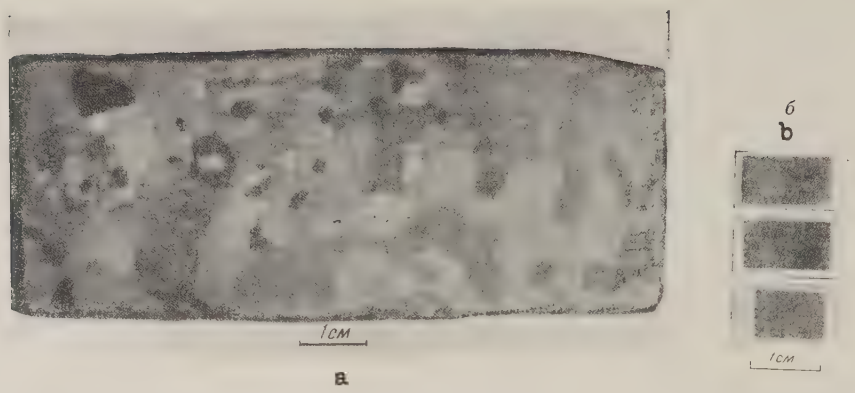

Fig.5 a) plate of coarse-crystal cuprous oxide; b) individual single crystal specimens obtained from such a plate.

of coarse-crystal cuprous oxide. X-ray diffraction patterns (Laue photographs) showed that these were true single crystals.

In conclusion it must be noted that our preliminary investigation of the electric, thermoelectric and photoelectric properties showed no appreciable difference between single crystals and coarse-grained polycrystalline specimens of cuprous oxide. Further studies along this line are under way.

Conclusions

1. The purity of the initial copper, provided the amount of impurities in it does not exceed 0.05%, has no appreciable effect on the grain size of the Cu_2O obtained by our oxidation procedure.

2. The crystal structure of the initial copper has a strong influence on the size of the Cu_2O grains.

3. The process of formation of Cu_2O grains in the case of oxidation of coarse-grained copper differs from the process of formation of Cu_2O grains obtaining in the case of oxidation of fine-grained copper.

4. We have developed a procedure for obtaining coarse-crystal cuprous oxide for subsequent mechanical extraction of individual Cu_2O single crystals having a cross section area of 30 mm^2 on the average and up to 120 mm^2 in individual cases.

The writer desires to express his deep gratitude to V.E.Lashkarev for suggesting the subject and guiding the work. I.A.Ivanchenko of Kiev State University participated in the work.

"T.G.Shevchenko" Kiev State University

References

1. E.Engelhard, Ann.d.Phys., 17, 501 (1933).
2. A.I.Andrievskii, V.I.Voloshchenko & M.T.Mishchenko, Doklady AN SSSR, 90, 521 (1953).
3. P.Schmidt, Ann.d.Phys., 14, 265 (1952).
4. J.S.Anderson & N.N.Greenwood, Proc.Roy.Soc., A. 215, 353 (1952).
5. G.Blankenburg, K.Kassel, Ann.d.Phys., 10, 201 (1952).
6. Z.G.Pinsker, Diffraktsiia elektronov (Electron diffraction), M.1949.
7. A.I.Andrievskii & M.T.Mishchenko, Zhur.tekh.fiz., 22, 1713 (1952).

INVESTIGATION OF THE COEFFICIENTS OF SELF-DIFFUSION OF I & K IONS IN X-RAY IRRADIATED ALKALI HALIDE CRYSTALS

- V.V.Mumladze

It has become clear as the result of investigations performed during the past few years that defects of the crystal lattice play a significant role in determining many physical properties of solids.

Thus, for example, diffusion of ions in alkali halide crystals can occur only when there are unoccupied points, called vacant sites, in the crystal lattice. Inasmuch as the crystal as a whole is neutral it must comprise vacancies of both polarities in equal number. It has been established that positive ion vacancies have a higher mobility than negative ion vacancies. In view of the fact that the vacancies have opposite effective charges they attract each other and form a neutral pair. Such pairs, as Mott & Gurney have shown, have a much higher mobility than an isolated negative ion vacancy and the density of such pairs even at a temperature of 560° is comparable with the density of isolated, single ion vacancies. Such pairs, together with isolated vacancies, may participate in the diffusion process[1].

In addition to vacant sites, there exist in real crystals defects of yet another type, namely, dislocation type defects.[2,3 & 4] If we assume that the process of diffusion in alkali halide crystals is due to the motion of the diffused substance over the vacant sites, obviously an increase in the number of vacant sites must lead to an increase in the rate of diffusion.

A number of investigators[2,5 & 6] have shown that in the process of x-ray irradiation of alkali halide crystals there may be produced an additional number of positive and negative vacant sites. These additional vacancies originate from Taylor-Orovan type dislocations. Hence, in view of the additional number of vacancies present one may expect to observe an increase in the rate of diffusion in irradiated specimens.

On the other hand, in the process of diffusion annealing the additional isolated vacancies, generated as a result of irradiation, tend rather readily to form pairs and more complex groupings (clusters), which may lead to the appearance of new dislocations. Furthermore, the diffusing vacancies may be captured by already existing dislocations[7]. This will reduce the number of isolated vacancies and pairs. A high annealing temperature will no doubt favor the capture process, i.e., the combining of isolated vacancies with extant dislocations, in view of which one should expect a decrease in the rate of diffusion.

The present work was devoted to this problem. We investigated potassium iodide crystals irradiated with x-rays and compared the coefficients of diffusion of crystals treated in this manner with the coefficients for non-irradiated specimens. The coefficients of diffusion were determined by the method of radioactive tracers. The active substances were I^{131} and K^{42}.

Potassium iodide single crystals grown from a melt were split into pieces; selected pieces were then ground to plates measuring 0.8 x 0.8 x 0.02 cm, and then irradiated. Next a radioactive layer of NaI^{131} or $K^{42}Cl$ was applied by vacuum evaporation to one of the surfaces, following which the plates were annealed at temperatures of 350, 400 and 500°. The annealing time varied from 10 to 40 hours. The actual measurements of the diffusion coefficient were carried out by the thin layer method developed by Kriukov & Zhukhovitskii[8]. This method is essentially a modification of the adsorption method and reduces to measuring the β-activity of the surfaces on opposite sides of the plate. Kriukov & Zhukhovitskii proposed the following formula for the diffusion coefficient:

$$\log \frac{J_1 - J_2}{J_1 + J_2} = \log K - \frac{\pi^2 D}{d^2} t,$$

where J_1 and J_2 are the intensities of the radioactivity on the opposite sides of the specimen, d is the thickness of the specimen, D is the diffusion coefficient, t is the annealing time and K is a constant.

According to our evaluation, the error in determining D did not exceed 30%.

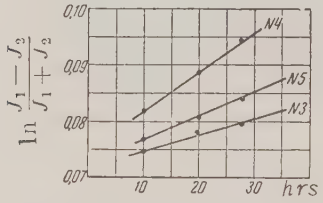

Fig.1. Dependence of $\ln(J_1-J_2)/(J_1+J_2)$ on the annealing time for the case of diffusion of I^{131} in KI crystals. The straight line plot No.4 was obtained for a non-irradiated crystal, plots 5 & 3 were obtained for crystals x-rayed for 30 to 60 min, respectively. Annealing temperature t = 450°.

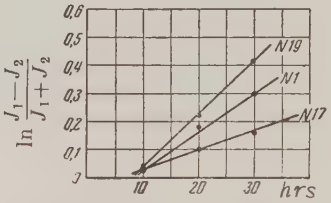

Fig.2. Dependence of $\log(J_1-J_2)/(J_1+J_2)$ on the annealing time for the case of diffusion of K^{42} in KI crystals. Plot No.19 was obtained for a non-irradiated crystal; plots 1 & 17 were obtained for crystals irradiated for 30 and 60 min, respectively; t = 500°.

It was found that the coefficient of diffusion of both the metal and halide ions decreases in the investigated temperature range (Figs.1 & 2).

Thus irradiation of alkali halide crystals with x-rays followed by annealing leads to a reduction in the total number of isolated vacant sites and pairs, which either form new structure dislocations or combine with already present dislocations and thereby hinder the diffusing process.

Institute of Physics of the
Georgian SSR Academy of Sciences

References

1. F.Seitz, Rev.Mod.Phys., 18, 384 (1946).
2. F.Seitz, Phys.Rev., 80, 239 (1950).
3. F.Seitz, Rev.Mod.Phys., 23, 328 (1951).
4. O.Kotrel', Usp.fiz.nauk., 46, 179 (1952).
5. I.Esterman, W.J.Leivo & O.Stern, Phys.Rev., 75, 627 (1949).
6. N.P.Kalabukhov, Zhur.eksp.i teor.fiz., 27, 347 (1954).
7. R.Fletcher & W.Brown, Phys.Rev., 92, 585 (1953).
8. S.I.Kriukov & A.A.Zhukhovitskii, Doklady AN SSSR, 90, 379 (1953).

BULLETIN of the Academy of Sciences of the USSR - Physical Series
Vol.21, No.1, 1957 - Transactions of the Eighth All-Union Conference on Semiconductors (Continued from Vol.20, No.12 b)

TABLE OF CONTENTS

	Page Orig.	Trans.
Section on the Theory of Semiconductors		
The method of traces for conduction electrons in semiconductors. Part I. Weak interaction between electrons and vibrations - M.A.Krivoglaz & S.I.Pekar	3	1
The method of traces for conduction electrons in semiconductors. Part II. Variational method - M.A.Krivoglaz & S.I.Pekar	16	13
Influence of the polaron effect on the thermodynamics of conduction electrons in semiconductors (Part III) - M.A.Krivoglaz & S.I.Pekar	33	29
Interaction of excitons with a molecular lattice - E.I.Rashba	37	33
Investigations in the microscopic theory of crystals - K.B.Tolpygo	48	44
Theory of excitons in ionic crystals - I.M.Dykman	65	60
Interaction of localized electrons with acoustical vibrations in homeopolar crystals (Abstract) - M.F.Deigen	68	63
State of an impurity-center electron in an anisotropic crystal (Abstract) - A.I.Ansel'm & L.I.Korovin	69	64
Contribution to the theory of recombination of electrons with impurity centers in ionic crystals (Abstract) - Iu.E.Perlin	69	64
Thermomagnetic and galvanomagnetic effects in semiconductors taking into account variations in the current carrier concentration (Abstract) - G.E.Pikus	103	64
Recombination in semiconductors incident to collision of current carriers - L.Sosnowski	70	65
Excited states of two-electron color centers in ionic crystals and the α and β absorption bands - O.F.Tomasevich	74	69
On the exciton energy spectrum in an ionic crystal - I.P.Ipatova	78	73

On a current carrier recombination mechanism in strongly alloyed semiconductors - V.L.Bonch-Bruevich 87 82

Some aspects of the thermodynamics of electron and phonon gas in solids - Iu.N.Obraztsov 97 92

Mean free path of electrons in liquid and amorphous conductors - A.I.Gubanov 104 98

Interaction of semiconductor electrons with lattice vibrations at ultralow temperatures - L.E.Gurevich 105 99

Concerning certain electroacoustical effects - L.E.Gurevich 112 106

Section on the Chemistry of Semiconductors

Some aspects of the crystal chemistry of compounds with the zincblende structure - N.A.Goriunova 120 114

Contribution to the theory of phases of variable composition with the zincblende structure (On the possible region of homogeneity of $A^{III}B^{V}$ type compounds) - B.F.Ormont, N.A.Goriunova, I.N.Ageeva & N.N.Fedorova 133 128

Physico-chemical analysis of some semiconductor systems - N.Kh.Abrikosov 141 136

Growth of single-crystal layers of silicon and germanium from the vapor phase - N.N.Sheftal', N.P.Kokorish & A.V.Krasilov 146 140

Preparation of single-crystal specimens of cuprous oxide - Iu.I.Gritsenko 153 151

Investigation of the coefficients of self-diffusion of I & K ions in x-ray irradiated alkali halide crystals - V.V.Mumladze 158 157

Translated in 1958 by
Columbia Technical Translations
5 Vermont Ave., White Plains, N.Y.

TRANSACTIONS OF THE EIGHTH ALL-UNION CONFERENCE ON SEMICONDUCTORS

(Continued from Vol. 20, No. 12 b and Vol. 21, No. 1)

Section on Semiconductor Catalysis

The All-Union Conference on Semiconductors, which was held in Leningrad in November 1955, comprised a special section on the catalytic action of semiconductors. The same subject is dealt with in a report by S.Z.Roginskii and two commentaries by F.F. Vol'kenshtein which were delivered at the plenary meetings of the Conference and which are published below. S.Z.Roginskii's report is printed in summarized form, but it contains some new material which has appeared during the year and a half that have elapsed since the Conference.

The Section on Semiconductor Catalysis held two meetings, at which nine reports were presented. Owing to lack of space, however, some of these reports are not included herein.

With the authors' consent, we have omitted the report "Radiochemical Investigation of the Capture of Microimpurities by Semiconductor Catalysts" by E.S.Dokukina, G.M.Zhabrova and V.I.Rzhishcheva and the report "On the Influence of Heat Treatment on the Structure and Catalytic Properties of Zinc Oxide" by A.V.Shekhter.

S.Z.Roginskii's report on electronic processes accompanying the chemical transformations of solids has likewise been omitted, since it will be published in the Bulletin (Izvestiia) of the USSR Academy of Sciences, Chemical Sciences Section.

We have also omitted F.F.Vol'kenshtein's report "On the Mechanism of the Catalytic Action of Semiconductors", since the material contained in it was incorporated in two reports presented by the author at the International Congress on Catalysis held in Philadelphia, U.S.A., in September 1956. These two reports ("On Different Types of Bonds in Chemosorption on Semiconductors" and "On the Mechanism of the Catalytic Action of Semiconductors") will also appear in the Bulletin (Izvestiia) of the USSR Academy of Sciences, Chemical Sciences Section.

Lastly, lack of space has made it impossible to give the discussions following the reports.

SOME PROBLEMS IN THE FIELD OF SEMICONDUCTOR CATALYSIS

- S.Z.Roginskii

1. Semiconductor catalysis

Many of the chemical processes that have played a fundamental role in determining the scope and development of our present-day chemical and petroleum industry are based on the use of catalysts. Most catalysts are semiconductors. Thus, vanadic and ferric oxide, manganese dioxide and cuprous oxide are used as catalysts in industrial oxidation with molecular oxygen; the sulfides of tungsten, molybdenum and zinc and the oxides of chromium and molybdenum are used to accelerate hydrogenation; aluminum oxide, thorium dioxide and tungsten trioxide are employed to control reactions involving hydration or dehydration. In the ideal case the catalyst is not consumed in the process but is capable of promoting the interaction of an infinitely large amount of the reagents. To the class of obvious semiconductor catalysts one must add solids of other electronic types covered with a semiconductor coating. As we noted some years ago[1] and as has recently been proved by emission microscope [2,3] and electron diffraction experiments[4], metals used as catalytic agents often become covered with a virtually invisible superficial coating consisting of a binary compound, i.e., the corresponding oxide, hydride or nitride. Often in the case of dielectric catalysts there occurs a chemical change of the surface layer accompanied by the appearance of semiconductor characteristics. Inasmuch as only the surface of a solid catalyst participates in the reaction, catalysis on metals and dielectrics is frequently actually masked catalysis on a semiconductor. We feel it is important to show that the characteristic electronic properties of semiconductors bear a direct relationship to their catalytic effect in chemical reactions.

Analysis of the empirical data accumulated in chemistry on the selection of catalytic agents may help throw some light on the question. There are extensive classes of chemical reactions for which the only good solid catalysts are semiconductors and metals[5,6], that is, conventional semiconductors and semiconductors in the form of thin coatings jacketing a metal core. Very often semiconductors with a narrow energy gap and degenerate semiconductors are particularly effective. Using the classification of defective structures proposed by Reese[7] we find that the most active catalysts are a) nonstoichiometric compounds with unbalanced valences, b) nonstoichiometric mixtures with semiconduction dependent on the valence and c) semiconductors with dual valence.

There are also secondary regularities characterizing the particular catalytic properties of semiconductors with different specific types of structure and defects. Thus, where certain kinds of specific reaction are concerned outstanding catalytic properties are exhibited by oxide compounds with the spinel structure[8] familiar to the physicists as ferromagnetic materials. As a rule the best contact catalysts show intensive color in the visible and near-ultraviolet regions of the spectrum. Such properties are typical of catalysts accelerating the oxidation of inorganic and organic compounds with molecular oxygen and of catalysts hastening combination with, removal of and redistribution of hydrogen and other oxidation-reduction type reactions. These, it must be noted, are precisely the reactions which in essence amount to a transition of electrons from one type of molecules or ions to another.

In addition there are certain groups or classes of reactions with respect to which typical semiconductor catalysts behave exactly as dielectrics or poor

semiconductors with similar chemical properties. It is natural to assume that in the former case catalysis depends on some sort of microscopic processes peculiar to semiconductors, while in the latter case these particular processes play no part and hence the given compounds having an electronic structure typical of semiconductors is no actual advantage. If this assumption is correct then we can say that we have distinctive semiconductor catalysis only in reactions of the former type and that not every catalytic process involving semiconductors necessarily belongs in this category. In other words, there may exist specifically semiconductor catalyses and processes in which semiconductors can serve as catalysts as well as other substances.

Until recently we have had virtually no information on the character of the action of semiconductors as catalysts or on the possible connection between the physical properties of semiconductors and their catalytic activity.

2. Catalytic properties of semiconductors not containing transition elements

It has long been assumed that in the case of many reactions it was important for at least one of the elements entering into the composition of the solid catalyst to have an unfilled d-shell[9,10]. However, recent developments in semiconductor physics have shown that there exists a large class of semiconductors that do not contain transition elements but still have much in common, as regards the character of their solid state electron spectrum, with semiconductors containing transition elements.

We felt it would be of interest to determine whether this similarity extends to semiconductor catalysis, whether there do not exist, among the new types of semiconductors, substances capable of catalyzing oxidation-reduction processes despite the absence of transition elements in their crystal lattice. To this end we investigated the properties of "metallic" germanium having the atomic structure of diamond without vacancies in the d-shell. In collaboration with O.V.Krylov and V.M.Frolov we investigated the influence of Ge in the form of a crystalline powder on a number of catalytic processes. The $CO + O_2$ and $H_2 + O_2$ reactions proved to be unsuitable due to the strong affinity of germanium for oxygen. In both cases, the Ge rapidly absorbs oxygen with resulting cessation of the catalyzed reaction. Positive results were obtained, however, with the decomposition of alcohols. Methanol noticeably decomposes in the presence of deoxidized crystalline germanium powder according to the formula $CH_3OH = CO + 2H_2$, beginning at 400°, i.e., at a temperature some 350° lower than that necessary for a noticeable reaction to occur in the absence of Ge (also see Ref.11). The catalytic action of Ge is even stronger in the case of dehydrogenation of isopropyl alcohol to acetone[12]: $CH_3CHOHCH_3 = CH_3COCH_3 + H_2$. In the presence of crystalline Ge powder with a relatively small active surface about 50% of the isopropyl alcohol is decomposed within half an hour at 170° (Fig.1).

The observed activation energy for the reaction is insignificant (4-5 Kcal). The chemosorption of even a small amount of oxygen, however, noticeably slows down the reaction. Germanium dioxide is appreciably less active than crystalline germanium and primarily promotes dehydration. This shows that the catalyzer for the above two reactions of the oxidizing type is actually germanium in the elementary form.* Consequently, despite the absence

---

*Since the conference we have found that germanium in the form of condensed films is capable of catalyzing a number of other reactions as well.[53].

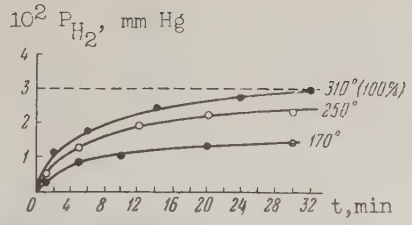

Fig.1. Decomposition of isopropyl alcohol ($CH_3CHOHCH_3$ -- -- H_2 + CH_3COCH_3) in the presence of Ge at an initial pressure of $3 \cdot 10^{-2}$ mm Hg.

of d-electrons germanium proves to be an active catalyst for certain oxidation-reduction reactions. Germanium also actively promotes such topochemical processes as the decomposition of the hydrides of arsenic, germanium and antimony; we have not yet determined, however, whether the same type of catalysis obtains here as in the above-mentioned reactions[13]. One of the obvious advantages of using germanium in investigating the correlation between the catalytic and electronic properties of materials lies in the fact that its physical attributes and structure have been thoroughly studied.

The closest isoelectronic analogs of germanium and silicon are binary $A^{III}B^{V}$ and $A^{II}B^{VI}$ type compounds, for example, GaAs or CdTe, in which the average number of electrons per atom is the same as in germanium and silicon and the crystal structure of which has much in common with that of silicon[14,15]. As a rule these compounds do not contain transition elements and hence investigation of their catalytic properties is of great theoretical interest. So far we have had occasion to study only zinc sulfide, selenide and telluride.* All three compounds are of the $A^{II}B^{VI}$ type and have the zincblende structure. They all proved to be effective dehydrogenating catalyzers for isopropyl alcohol; their activity increased sharply with increasing atomic weight of the metal (Fig.2). The increase is accompanied by a decrease in their chemical stability under the reaction conditions. Zinc telluride activates the reaction even at room temperature.

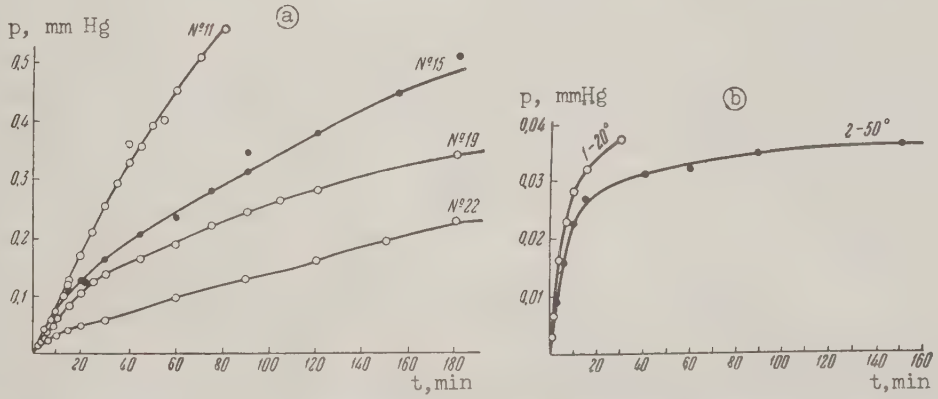

Fig.2. Decomposition of isopropyl alcohol in the presence of a) ZnSe and b) ZnTe.

Thus the presence of unfilled d-electron shells in the atoms of the binary $A^{II}B^{VI}$ compounds is not indispensable for semiconductor catalysis. It does not necessarily follow, however, that there are no special effects due

---

*The zinc selenide in a highly dispersed state, prepared by precipitation from solutions, was put at our disposal by M.S.Belen'ki (Azerbaidzhan Polytechnic Institute); the zinc telluride was obtained in the form of a crystalline powder from the melt by N.A.Goliunova (Leningrad Physical-Technical Institute). We take this occasion to thank them.

to d-electrons in chemosorption and catalysis. In view of the results obtained by Dauden[16] and others for metals and our[8] results for oxides, the importance of these electrons in certain cases may be considered definitely established; it may also be considered an established fact that as regards electric conductivity binary semiconductors containing transition elements have certain distinctive characteristics which led Schottky and others[17] to introduce the concept of "semiconductors with an open band". In view of this it is highly probable that semiconductors of this type do have catalytic attributes not encountered in semiconductors of other types. At the same time the presence of vacancies in the d-shell is one of the factors facilitating the realization of semiconductors with a narrow energy gap together with a crystal lattice of high strength.

3. Catalysis on n- and p-type semiconductors

One cannot predict on the basis of what is now known regarding semiconductor catalysis in just which cases one can expect marked qualitative differences in the catalytic action of n- as against p-semiconductors. We also cannot tell whether semiconductors with mixed n-p conductivity should exhibit specific catalytic properties or whether homogeneous or heterogeneous distribution of centers with n- and p-conductivity and the character of the atomic and ionic lattice defects have any significance where any catalytic properties are concerned. Until we have the results of a series of experiments (planned for the near future) involving tests with semiconductors having different types of conduction and different distributions of n- and p-centers, we must necessarily base our speculations on qualitative comparisons. Some authors, comparing the catalytic action of different oxides on the basis of data in the literature, have come to the conclusion that semiconductors with different types of current carriers are not catalytically equivalent. Thus, it has been asserted that as regards decomposition of N_2O into N_2 and O_2 and oxidation of CO by molecular oxygen p-semiconductors are superior to n-semiconductors, while for hydrogenation and isotopic hydrogen exchange, n-semiconductors have the advantage over p-semiconductors[18]. In view of the great sensitivity of semiconductor catalysts to the method of preparation, the presence of impurities and the influence of the catalytic reaction itself, the results of such comparisons based on disparate data from the literature are unconvincing.

4. Modified nickel monoxide and zinc oxide

Clearer indications regarding the effect of the type of conductivity on the catalytic behavior can be obtained from comparative analysis of the influence of additives on the catalytic activity in the same reaction of semiconductors with conductivities of different types[19,20].

Most investigators in the field have used nickel monoxide as the p-semiconductor and zinc oxide as the n-semiconductor catalyst in the oxidation of carbon monoxide. Both these oxides interact and form solid solutions with a number of oxides of different valence. As has been described in detail in Ref.21, the addition of bivalent oxides (MgO and ZnO) has only a weak effect on the catalytic activity and conductivity of nickel monoxide. The oxide of monovalent lithium (Li_2O) produces a strong increase in the electric conductivity and a very pronounced decrease in the low-temperature catalytic activity, while the oxide of trivalent iron has the opposite effect. While the results of different authors are not in complete agreement as regards the influence of the same additives, all report the antagonistic influence of

monovalent-metal as against trivalent-metal oxides and the fact that large changes in the conductivity are accompanied by significant changes in the catalytic activity. In cases when solid solutions of n-conducting zinc oxide and p-conducting nickel monoxide were studied under similar conditions all investigators report that the same additives produce opposite effects where the catalytic behavior of these two materials was concerned. In the case of the isotopic exchange reaction $H_2 + D_2 = 2HD$ in the presence of zinc oxide the addition of an Me^+ oxide has the opposite effect to that produced by the addition of an Me^{3+} oxide, but in this case the influence of the additives on n-conducting zinc oxide[22] is analogous to their influence on p-conducting NiO and contrary to their effect on ZnO as a catalytic agent in the oxidation of CO and the decomposition of N_2O.

The pronounced influence of purposely or accidentally introduced impurities on the catalytic activity is characteristic of semiconductor catalysts. One can only compare the magnitude of these effects with the magnitude of the influence of impurities on the electric properties of semiconductors; hence the opposite effect of the same additives on the catalytic properties of n- as against p-type semiconductors, established in a number of investigations, gives reason to expect systematic and substantial differences between the catalytic properties of semiconductors of these two types.

Nearly 20 years ago, on the basis of experimental results on the influence of impurities on the catalytic activity of certain substances, the writer and his co-workers proposed a microchemical conception of the activity of catalysts in which the dominant role in the formation of an active surface on various substances was ascribed to impurities trapped by the solid and to deviations from stiochiometric proportions[23].

As a rule, an impurity when present in a low concentration (γ) activates the catalyst. As the concentration is increased, the effect after passing through a maximum at a certain optimal γ begins to fall off rapidly. Such impurities act primarily to change the activation energy for the process. This is paralleled by a change in the logarithm of the factor k_o in the equation for the rate constant: $k = k_o \exp(-E/RT)$; $\log k_o$ and E bear a linear relationship, i.e.,

$$\log k_o = \text{const} + \text{Œ}E,$$

which leads to a number of characteristic effects.

The above described influence of impurities is characteristic of modifying additives that change the rate of the principal stages of the catalytic process and the relation between them[24]. The mechanism of the influence of such impurities, which control the activity and selective action of the catalyzers, has until now remained obscure. The effect of different additives on NiO and ZnO shows that their catalytic activity is substantially influenced only by substances that also produce a strong change in the electric conductivity of the initial material, i.e., that evince properties of typical modifying additives. These data and particularly evidence of effective compensation in the case of simultaneous introduction of contrarily acting oxides (for example, Li_2O and Fe_2O_3 - Ref.21) makes it probable that the electric conductivity and the catalytic activity are related to the same structures.*

---

*The idea of such a relationship has already been utilized by Vol'kenshtein for explaining the phenomenon of modification[54].

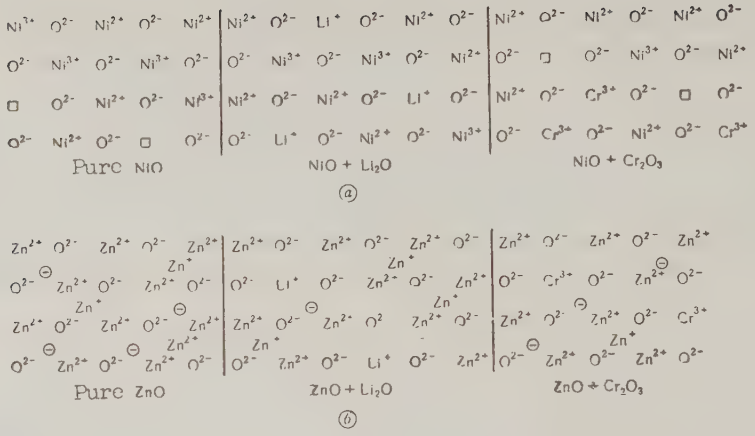

Fig.3. Structure of a) NiO and b) ZnO according to Hauffe[25].

For the specific cases of nickel monoxide and zinc oxide the probable variants of such structures are shown in Fig.3. In the former case groupings of the $Me^{3+}O^{2-}Ni^{2+}\square$* or $Me^{3+}O^{2-}Li^{+}O^{2-}$ type are important. Where zinc oxide is concerned, as Moshkovski & Shekter[26] have noted, the activity may be connected with interstital zinc. In the band model the presence of extraneous (impurity) cations of a different valence leads to the appearance of additional impurity levels (Fig.4).

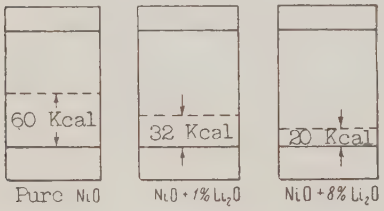

Fig.4. Influence of admixtures of Li_2O on NiO (band diagram).

Through comparison of the electric conductivity with the catalytic activity of NiO and ZnO, we were able to ascertain the nature of the structures determining the modification. It is worth noting that the character of the effect produced by an impurity is determined primarily by the charge of the cations of the introduced oxide and not by the size of these cations or other parameters that are commonly considered in similar cases in the theory of catalysis.

5. Character of the relation between the conductivity of semiconductors and their catalytic activity

In recent years there have been published the results of a number of experimental measurements of the electric conductivity of related catalysts characterized by different activities. In view of the resistance of intercrystalline contacts and other complications such measurements do not yield the absolute values of the number of current carriers and their mobility. In many such investigations there was no attempt to determine the nature of the carriers. Moreover, given different degrees of dispersion of the initial particles, the observed relative values of the conductivity and activation energy may actually be closer to either the volume or surface values. Hence

---

*□ denotes a vacancy in the lattice.

one cannot hope to obtain an entirely consistent picture from the data in the literature. The most extensive parallelism between the conductivity and the catalytic activity was found by Charman, Griffith & Marsh[27] in a study involving comparison of the electric conductivity of mixed catalysts of chromium and aluminum oxide with their catalytic activity with respect to the transformation of heptane to toluene (aromatization). In the case of this reaction, which is of the oxidation-reduction type, these investigators observed complete similarity in the shape of rather complex peaking curves characterizing the dependence of the catalytic activity and the conductivity on the composition. They obtained quantitative coincidence of the activation energy for the catalytic process and for the electric conductivity. This is most readily explained by fortuitous coincidence of the stages determining the conductivity and the catalysis. As may be seen from Fig.5, where the oxidation of CO in the presence of NiO is concerned, the variation of the two values of E differs; the two values coincide only for one particular composition.

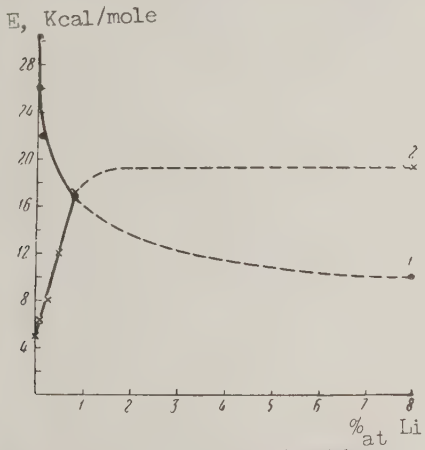

Fig.5. Relative activation energies for 1) conductivity and 2) catalysis of solid solutions of Li_2O in NiO (reaction: oxidation of CO).

A more quantitative but still clear parallelism between the initial conductivity of zinc oxide and its catalytic activity in the $D_2 + H_2 = 2HD$ exchange reaction was observed by Heckelsberger, Clark & Baily[28] for specimens subjected to different treatments. A like parallelism in the dehydrogenation of isopropyl alcohol to acetone is reported by Miasnikov & Pshezhetskii[29] in the case of ZnO specimens treated with oxygen. Further in the same category, we have the observations of Matveev & Boreskov[30] on the parallel variations of the conductivity σ and the activity of ZnO as a catalyst in the decomposition of methanol. An appreciably more complex correlation between σ and the catalytic activity A is evinced in the investigation of Belianskii, Deren' & Gaber[31] who worked with the mixed catalysts MgO & Cr_2O_3 and ZnO & Fe_2O_3.

Thus even in cases when the character of changes in the intercrystalline contact is less obvious a clear correlation between σ and the activity, tending often to parallelism, appears to be widespread in semiconductor catalysis. This suggests that conductivity measurements might be used for quality and production control of semiconductor catalysts of a given type and for improving present catalytic agents. This approach, however, is not promising when it comes to comparing semiconductors differing appreciably as regards electronic type and chemical structure, for the close correlation or parallelism holds only within a given type compound.

Many organic substances with pronounced semiconductor characteristics are known. In many of them the activation energy for conductivity is of the same order of magnitude as in typical inorganic semiconductor catalysts. Although we know of no systematic investigations of the catalytic properties of organic semiconductors, we see no reason to doubt that organic semiconductors with similar electric characteristics may prove to be at least equal to inorganic semiconductors as regards catalytic activity[32].* (Footnote on following page.) The opposite is true of metals in which σ is many order of magnitude higher than in inorganic semiconductors, while the specific activity A

is frequently of the same order of magnitude. This cannot in all cases be explained by the blocking influence of the semiconductor coating on the metal surface, since in the case of the more noble metals this coating has a thickness of only one to three monolayers.

So great a divergence between the results of comparisons of σ and A in substances of the same or different electron-chemical types is inexplicable in the framework of the rough approximations accepted in most works on the electronic theory of chemosorption and catalysis[34,35]. However, aside from the number of current carriers, which is determined by the width of the forbidden band and the polarization of the surface layer, the character of the chemosorption and, in particular, its activation energy and the energy of the surface bonds formed are determined by the magnitude of the exchange integrals of the interaction between the adsorbed molecules (atoms) and the atoms of the surface to which these become attached.

The role played by nearest atoms is the greater, the greater the covalent component of the surface chemical bonds. As work function measurements show, this component may be very appreciable: it may exceed 70% even in the case of chemosorption of gases on metals. The possibility of formation of covalent bonds and their strength are determined by the structure of the electronic shells of the atoms linked by the chemical bonds. In view of this it is clear that a metal covered with a monatomic layer of oxygen or a di- or triatomic layer of oxide must as regards chemosorption be close to the bulk oxide of the same metal; analogously a metal covered with a layer of nitrogen atoms or a coating of the nitride will be close to the bulk nitride and so on, i.e., will be very similar to a semiconductor in this respect. In the same way a semiconducting organic compound may, as regards its properties as a chemosorbent, approach solid saturated hydrocarbons if the carbon or carbon-nitrogen molecular skeleton is surrounded homeopolarly by bound hydrogen atoms. For the same reason the presence of two or more high-charge metal (particularly transition) ions in an organic molecule may bring the given substance close to inorganic semiconductors as regards chemosorption and catalytic attributes; possibly this factor plays a certain part in the activity of such substances as biocatalysts. In view of this it will not be surprising if there are found among the less common organic semiconductors catalysts able to promote gaseous oxidation-reduction reactions.

6. On the mechanism of semiconductor catalysis

In general the catalytic process is comprised of a number of distinct stages. In heterogeneous catalysis one of the important stages is more or less complete chemical adsorption. There are numerous observations of the variation in the conductivity of semiconductors incident to such adsorption. Such data, however, must be treated with caution, first, because of possible surposition of yet stronger effects associated with reduction or oxidation of the solid either in depth or on the surface and, second, because of similar effects during physical adsorption which has no direct connection with the catalytic process.

---

*(From p.169) Recently Tsigler showed that the precipitates formed by triethylaluminum with metal halides show an exceptional catalytic activity as regards the polymerization of ethylene to polythene[33]. Very probably this precipitate is a semiconductor and it is not impossible that its action in this case is connected with semiconductivity.

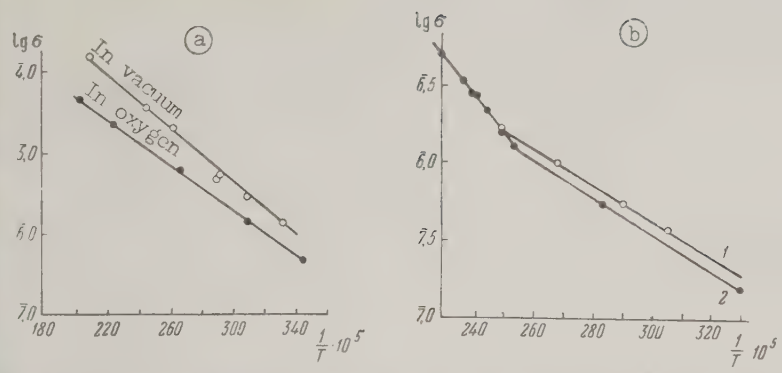

Fig.6. Temperature dependence of the electric conductivity of a) V_2O_5 and b) Cu_2O annealed at 1000°; the oxygen content in sample 1 was higher than in sample 2.

Apparently the character of the change in σ incident to the adsorption of the same substances is different for extrinsic n- and p-type semiconductors (Fig.6). The electron donor and acceptor molecules act in opposite ways on the conductivity of semiconductors of the two types. This antagonistic effect must be absent in the case of semiconductors with intrinsic conductivity. The observed variation of σ indicates that the current carriers - both electrons and holes - may participate in the adsorption in the manner suggested by Vol'kenshtein[36], Germain[37] and Hauffe[25]. The probable types of surface bonds forming in such cases have been considered in a recent publication[38].

As the admittedly few determinations of the influence of adsorption on the work function indicate, adsorption is accompanied by the formation of a double electric layer with a negative (rarely a positive) charge on the adsorbed molecules. It may be assumed that in the specific case of catalytic oxidation with molecular oxygen, the process begins with adsorption involving the transfer of an electron to the oxygen and that further the adsorbed oxygen ion-radical reacts with the CO, H_2, ethylene or other oxidized material with intermediate formation of peroxide forms. During one of these later stages the electron returns to the semiconductor, reestablishing electric neutrality.

For example:

$$Cat^{\oplus} + O_2 \rightarrow Cat^{\oplus} \ldots O_2^{\ominus} \xrightarrow{+C_2H_4} Cat^{\oplus} \ldots [O_2C_2H_4]^{\ominus} \rightarrow Cat^{\oplus\ominus} + 2CH_2O$$

or

$$O_2^{\ominus} \ldots Cat^{\oplus} + CO \rightarrow O_2^{\ominus} \ldots Cat^{\oplus} \ldots CO^{\ominus} \rightarrow Cat^{\oplus} \ldots CO_3^{\ominus} \rightarrow$$
$$\rightarrow Cat^{\oplus} \ldots O^{\ominus} + CO_2 \xrightarrow{CO} CO_2 + Cat^{\oplus\ominus}.$$

Where processes of this type are concerned n- and p-semiconductors may not be equally effective. In some cases the process may be facilitated by the presence of separate donor and acceptor sections or areas on the surface of the semiconductor; these perform different functions and the charges are equalized by the flow of electrons through the solid phase as shown in Fig.7 for the case of decomposition of hydrogen peroxide[39]. The rate of the catalytic process may be controlled by one of the chemosorption stages (for example, by the chemosorption of O_2 on the donor sections or chemosorption of CO on the areas covered with O_2^-). The absolute rate of such a process may well depend on whether absorption occurs only where there happens to be a free electron (or hole) at a given instant or anywhere upon impact by the reacting molecules with extraction of the requisite electron (or hole) from the lattice. In cases when the chemosorption steric factor[40] is excessively small the first alternative is more probable.

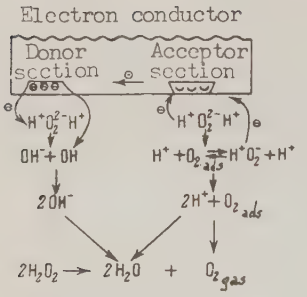

Fig.7. Decomposition of H_2O_2 in the presence of donor and acceptor sections.

When adsorption on electrons and holes does not require an activation energy, the observed energy of activation of chemosorption and catalysis will coincide with the energy of activation of conductivity (it will equal the full or half-width of the forbidden band). In the presence of an additional barrier for electron transitions between the lattice and the molecule, we will have $E_{cat} = E_{chemos.} > E_{conduct.}$.

Hauffe & Engel'[41] and Weisz[42] have shown that the surface electron levels must necessarily be distorted in the case of adsorption with the participation of the electrons and holes of the semiconductor and simultaneous change in the width of the forbidden band. This at the same time leads to a change in the number of free current carriers and in the activation energy for conductivity. A change in the latter may, in turn, change the energy of activation of the adsorption processes and the catalysis dependent upon them.

Assuming the change Δn_{ee} in the number of electrons in the surface layer to be equal to the number of adsorbed molecules q and the change ΔE in the activation energy to be proportional to Δn_{ee}, we obtain:

$$dq/dt = \text{const} \cdot \exp\left[-\frac{E_0 - \beta q}{RT}\right] = k \exp(-\alpha q)$$

or

$$q = \alpha^{-1} \ln(t + t_0) + C,$$

wherein $t_0 = 1/C$.

This is a new explanation of the logarithmic kinetic isotherm, characteristic for chemosorption, that was discovered by Zel'dovich and the author and that has recently been the subject of theoretical discussion[44,45]. Another, equally common parabolic kinetic isotherm $q = at^{1/n}$ (the Benheim isotherm) is obtained in the case of logarithmic variation of the chemosorption activation energy with the number of reacted electrons (holes):

$$E_q \approx (n-1) RT \ln q.$$

From the participation of the semiconductor electrons and holes in chemosorption with charging of the surface there follows the possibility of changes in the specific chemosorption and catalytic activity in case of a sufficiently pronounced change in the degree of dispersion. The size of the crystal grains at which this effect should become evident depends on the concentration of free current carriers in the solid and on the length of their free path. The presence of electron-hole equilibrium and the charging of the semiconductor surface give real physical meaning to the frequently postulated non-Coulomb repulsion of adsorbed molecules that are not in direct contact.

With the initial assumptions commonly accepted, theoretical analysis of this problem is possible only for degrees of covering of the surface close to the lower limit of conventional measurements. There is sense in applying the statistical and kinetic isotherms of electron adsorption only to very low degrees of covering. The changes observed in this case are too great for Coulomb repulsion. Part of these changes can probably be explained by interaction of the above mentioned type, but the stronger effects are due to biographic inhomogeneity. A number of effective isotopic methods[46] have recently

been developed for determining whether the inhomogeneity or the interaction makes a greater contribution, as well as for evaluating the magnitude of the interaction and the character of the inhomogeneity. These methods may be of value also in studying other, purely physical properties of semiconductors since the effect of biographic inhomogeneity and interaction can be observed in solids in connection with diverse phenomena.

7. On new effects and the problems of theory

In the case of the electronic mechanism, the molecules of the initial substances and the chemical reaction products, chemosorbed on the semiconductor, participate as donor and acceptor purities in the electron-hole equilibrium and in the formation of a charged boundary layer. In cases when the associated effects are appreciable, the basic concepts of Langmuirian kinetics of catalytic processes are inapplicable in principle while the applicability of the equations following from the theory of processes on widely-inhomogeneous surfaces is limited. Characteristic here is the possibility, in addition to repulsion, of mutual attraction of the adsorbed molecules accompanied by an increase in Q and a decrease in E; further the equality of the influence on Q and E of equivalent amounts of different substances with similar distributions disappears. In the adsorption of extraneous substances, in addition to a retarding action amounting to blocking by a homogeneous or inhomogeneous surface, there must obtain activation and modification and the character of the effect should primarily be determined by the acceptor-donor properties of the molecules of the adsorbent.

The participation of electrons and holes in chemosorption and catalysis on semiconductors raises a new aspect of the question of the active forms and chains in catalysis. The transition of an electron or hole produces charged surface ion-radicals analogous to the intermediate formations in oxidizing-reducing processes in solutions. Such formations, rather than the non-charged free atoms and radicals and saturated neutral molecules of gas kinetics, should predominate in semiconductor catalysis[47].

Inasmuch as the active forms of heterogeneous semiconductor catalysis differ substantially from the active forms typical of homogeneous gas reactions, their different specific mechanism must involve plane chains, the probable role of which in catalysis was first suggested by Semenov & Voevodskii[48]. The actual existence of these chains cannot be doubted in the light of recent work[49] on the mechanism of the synthesis of hydrocarbons from CO and H_2 and the distribution of deuterium in isotopic heterogeneous exchange and catalysis[50]. Electric surface factors must undoubtedly exert a certain influence on the probability of formation, development and breaking off of the plane chains and, possibly, on the transition of these chains into the ambient gas.

Conclusions

Our survey of the problems in the field of semiconductor analysis is not exhaustive, not only for lack of space but also owing to the newness of the field. Chemists beginning to study semiconductor analysis find themselves in the situation of Moliere's famous character who, having grown rich in his old age, learned to his amazement that he had been speaking in prose all his life. Undoubtedly his prose was not on a level with the best samples of contemporary French belles-lettres. In a way, the same thing may be said of the semiconductor "prose" of our chemists. The difference is that whereas the Bourgeois

Gentil'homme was free to write neither prose nor poetry, our chemists are compelled by the advance of science to proceed in all haste with the development of the theory of semiconductor analysis. As investigations proceed, present problems will be solved but new ones will arise and very likely the reformation of our present concepts and methods will go much further than we can now imagine. In particular, there may very well be developed a new kinetic theory of catalytic reactions, a theory dispensing with Langmuirian concepts and dealing directly with electronic processes in the boundary layer.

However, before we can radically reform kinetic theory or even solve the problem of selecting suitable semiconductor catalysts on a purely scientific basis, we must first accumulate much more dependable experimental data. This in turn is predicated upon the development of reliable methods and procedures for investigating the semiconductor properties of catalysts in the form and state commonly employed in catalysis. In this field the domains of physics and chemistry overlap and success depends on the realization of a program of properly integrated complex investigations carried out with the collaboration of chemists and physicists.

Undoubtedly the present lack of systematic reliable experimental data will soon be made up and only then will we begin to feel the serious shortcomings and deficiencies of present day theory, regarding which we have already heard from a number of speakers at this conference. In theoretical investigations of catalysis we must abandon the one-sided approximations based on taking into account only electron-hole equilibrium and the presence of bands in the crystal or only variations of surface charge and distortion of energy bands incident to adsorption, in favor of an approach taking account simultaneously of all the first order factors.

Where the influence of adsorption on the electric conductivity and work function is concerned the first successful attempt in this direction has been made by Sandomirskii[51]. Promising, too, is the attempt made by Koutecki[52] to apply to chemosorption and catalysis, together with band theory, the method of molecular orbits which makes it possible to take into account the detailed electronic structure of the molecules better than has hitherto been feasible; this approach in effect erects a bridge between the electron theory of semiconductors and quantum chemistry of molecules. We must not hesitate to make simultaneous use of the band theory of semiconductors, the theory of the boundary layer and the method of molecular orbits for solving our basic problems and striving to arrive at new broad concepts.

Among the many lacunae in the general theory of catalysis, the ones that appear to be most serious at the moment are 1) the insufficient clarity of the theoretical concepts regarding the surface properties of semiconductors, in particular, highly dispersed ones, 2) the primitive state of the theory as regards the volume and surface characteristics of semiconductors containing atoms of transition elements and 3) the impossibility of deducing the properties of a semiconductor from the electronic characteristics and mass of the atoms forming the semiconductor lattice.

Institute of Physical Chemistry of the
USSR Academy of Sciences

References

1. S.Z.Roginskii, in Sb. Problemy kinetiki i kataliza (Symposium: Problems of kinetics and catalysis), 4, 187 (1937); Acta Physicochim., 9, 475 (1938).

2. E.W.Müller, Ergebnisse der exakten Naturwissenschaften. Berlin, 1953.

3. S.Z.Roginskii & I.I.Tret'iakov, Doklady AN SSSR, 105, 112 (1955); I.I.Tret'iakov & S.Z.Roginskii, Doklady AN SSSR, 107, 857 (1956).

4. R.E.Schlier & H.E.Farnsworth, J.Appl.Phys., 25, 1333 (1954); Bull. Am.Phys.Soc., 29, 35 (1954).

5. S.Z.Roginskii, in Sb.Problemy kinetiki i kataliza (see Ref.1), 6, 9 (1949).

6. T.Germain, Bull.Union Phys., 49, 385 (1955).

7. A.Reese, Chemistry of crystals with defects (In Russian trans.)M.1956.

8. S.Iu.Elovich, G.M.Zhabrova, L.Ia.Margolis & S.Z.Roginskii, Doklady AN SSSR, 52, 421 (1946).

9. L.V.Pisarzhevskii & M.A.Rozenberg, Elektron v khimii rastvorov i elektrokhimii (The electron in the chemistry of solutions and electrochemistry), Kiev, 1956.

10. S.Z.Roginskii, Zhur.fiz.khim., 6, 334 (1935).

11. H.Taylor, Can.J.Chem., 33, 838 (1955).

12. O.V.Krylov, V.M.Frolov & S.Z.Roginskii, Doklady AN SSSR, 111, 623 (1956).

13. K.Tamaru, M.Boudart & H.Taylor, J.Phys.Chem., 59, 801 (1955).

14. S.E.Volz & S.W.Weller, J.Phys.Chem., 59, 569 (1955).

15. N.A.Goriunova, in Sb. Voprocy issledovaniia poluprovodnikov i protsessov poluprovodnikovoi metallurgii (Symposium: Questions connected with the investigation of semiconductors and the processes of semiconductor metallurgy), M. 1955; N.A.Goriunova & B.T.Kolomiets, Zhur.tekh.fiz., 25, 984 (1955).

16. D.A.Dauden, J.Chem.Soc., 242, (1950); Ind.Eng.Chem., 44, 977 (1952).

17. H.Krebs & W.Schottky, Halbleiterprobleme, 1, 25 (1954); G.Parravano, J.Chem.Phys., 23, 5 (1955).

18. F.S.Stone, Chemistry of the solid state, Ed: W.E.Garner, p.367. London, 1955; H.I.Engell, Halbleiterprobleme, 1, 249 (1954).

19. G.M.Schwab & J.Block, Z. phys. Chem., 1, 92 (1955); Z.Electrochem., 58, 756 (1954).

20. G.Parravano, J.Am.Chem.Soc., 75, 1448, 1482 (1953); G.Parravano & M.Boudart, Advances in catalysis, 7, 50 (1955).

21. N.P.Keier, S.Z.Roginskii & I.S.Sazonova, Doklady AN SSSR, 105, 859 (1956).

22. A.Cimino, E.Cipollini & E.Molinari, Naturwiss., 43, 3, 58 (1956).

23. S.Z.Roginskii, Zhur.fiz.khim., 15, 1 (1940); B.V.Makarov, B.A.Rodin & N.M.Emanuel', Kinetika khimicheskikh reaktsii. (Kinetics of chemical reactions), Lithographed course of instructions based on lectures by Prof.M.Z.Roginskii, L.1939.

24. S.Z.Roginskii, Doklady AN SSSR, 87, 1013 (1952); in Sb.Geterogennyi kataliz v khimicheskoi promyshlennosti (Symposium: Heterogeneous catalysis in industrial chemistry), M.1955.

25. K.Hauffe, Reaktionen an und in festen Stoggen. Springer, Berlin, 1954.

26. A.B.Shekhter & Iu.Sh.Moshkovskii, Doklady AN SSSR, 89, 1075 (1953).

27. R.P.Charman, R.H.Griffith & J.D.F.Marsh, Proc. Roy. Soc., 224, 419 (1954).

28. L.F.Heckelsberger, A.Clark & G.S.Baily, J. Phys. Chem., 60, 559 (1956).

29. I.A.Miasnikov & S.L.Pshezhetskii, in Sb.Problemy kinetiki i kataliza (see Ref.1), 8, 34 (1955).

30. K.I.Matveev & G.K.Boreskov, in Sb. Problemy kinetiki i kataliza (See Ref.1), 8, 165 (1955).

31. A.Belianskii, I.Deren' & I.Gaber, Bulletin, Polish Academy of Sciences, Section 3, 3, 221 (1955).

32. M.Calvin, E.G.Cockbain & M.Polanyi, Trans. Faraday Soc., 32, 1443 (1936); M.Polanyi, Ibid. 34, 1191 (1938).

33. A.V.Topchiev & B.A.Krentsel', Usp. khimi, 25, 921 (1956).

34. F.F.Vol'kenshtein, Zhur.fiz.khim., 27, 159, 167 (1953); in Sb.Geterogennyi kataliz v khimicheskoi promyshlennosti (See Ref.24), M. 1955.

35. P.Aigrain & C.Dugas, Z.Electrochem., 56, 363 (1952).

36. F.F.Vol'kenshtein & V.B.Sandomirskii, Sb.Problemy kinetiki i kataliza (See Ref.1), 8, 189 (1955).

37. I.E.Germain & C.R.Acad.sci., 238, 236, 345 (1954); J.Chim.Phys., 51, 263 (1954).

38. F.F.Vol'kenshtein & S.Z.Roginskii, Zhur.fiz.khim., 29, 485 (1955).

39. S.Z.Roginskii, in Sb.Problemy kinetiki i kataliza (See Ref.1), 8, 110 (1955).

40. S.Z.Roginskii, in Sb.Problemy kinetiki i kataliza (See Ref.1), 3, 356 (1935); O.I.Leipunskii, Doklady AN SSSR, 1, 31 (1935); Acta Physicochim., II, 737 (1935).

41. K.Hauffe, Z.angew.Chem., 67, 189 (1955).

42. P.B.Weisz, J.Chem.Phys., 20, 1483 (1952); 21, 1531 (1953).

43. S.Z.Roginskii, Ia.B.Zel'dovich, Acta Physiocochim., 1, 554, 595 (1934); Ia.B.Zel'dovich, Zhur.eksp.i teor.fiz., 5, 22 (1935); S.Z.Roginskii, Nature, 134, 935 (1934).

44. P.T.Landsberg, J.Chem.Phys., 23, 1079 (1955).

45. H.Taylor & N.Thon, J.Am.Chem.Soc., 74, 4169 (1952); 75, 2747 (1953).

46. S.Z.Roginskii, in Sb.Problemy kinetiki i kataliza (See Ref.1), 9 (1957).

47. O.V.Krylov & S.Z.Roginskii, Izv.AN SSSR, Otd. Khim. nauk. 2, 145 (1956).

48. N.N.Semenov & V.V.Voevodskii, in Sb.Geterogennyi kataliz v khimicheskoi promyshlennosti (See Ref.24), M. 1955.

49. O.A.Golovina, S.Z.Roginskii, M.M.Sakharov & Ia.T.Eidus, Doklady AN SSSR, 108, 3 (1956).

50. S.Z.Roginskii, Teoreticheskie osnovy izotopnykh metodov izucheniia khimicheskikh reaktsii (Theoretical bases of isotopic methods of investigating chemical reactions), M.1956.

51. B.V.Sandomirskii, Dissertation, Institute of Physical Chemistry, USSR Ac. of Sci., 1956.

52. J.Koutecki, Doklady AN SSSR, 101, 119 (1955); Chem.listy, 50, 677 (1956).

53. S.Z.Roginskii, Khim. nauka i prom. (Chemical science and industry), 2, 137 (1957).

54. F.F.Vol'kenshtein, Zhur.fiz.khim, 25, 1244 (1951).

ON PROBLEMS ARISING IN THE THEORY OF SEMICONDUCTORS AS CATALYTIC AGENTS
(Remarks on the reports of S.I.Pekar and A.I.Ansel'm made at a plenary meeting of the Conference)

- F.F.Vol'kenshtein

S.I.Pekar and A.I.Ansel'm in their reports formulated a number of the problems arising in the theory of semiconductors. I would like to add to their list yet another group of problems which until recently have remained outside the field of view of theoreticians. These are the problems that arise when we transfer our attention from the bulk of the semiconductor to its surface.

Among other interesting properties the surface of the semiconductor has the ability of catalyzing many chemical reactions. For example, if a mixture of gases that tend to react chemically is brought into contact with a semiconductor surface the rate of the reaction is often substantially increased. That is, the conductor appears in the role of a catalyst.

In essence the molecules of the reacting gases are adsorbed on the surface of the semiconductor and then, while adsorbed, react with each other; finally the reaction product is desorbed. Thus the reaction is transferred from the gas phase to the surface of the semiconductor. There is good reason to ask: why does this lead to a substantial acceleration of the reaction (sometimes by a factor of thousands or tens of thousands)?

It might appear that the problem of the catalytic action of the semiconductors is a chemical problem rather than one in the physics of semiconductors. Actually, however, the semiconductor serves here not as an inert substrate upon which the chemical process occurs, but rather appears in the role of an active participant in the process. It participates in the intermediate stages of the reaction as one of the components but upon completion of the process is fully regenerated, that is, ends up in its initial state. The catalytic effectiveness of a semiconductor surface depends on the nature of the semiconductor and is closely related (as experimental facts show) with the electronic processes occurring in the semiconductor.

The mechanism of the catalytic action of semiconductors is hidden inside the material. The problem is to discover the nature of this mechanism. It is one of the more important problems in the theory of semiconductors. Let us list some of the questions encountered by the theoretical physicist or chemist exploring this field.

Every catalytic process on the surface of a semiconductor always begins with adsorption. The adsorption we have to deal with here is not the ordinary so-called "physical" adsorption due to van der Waals' forces, the forces of electrostatic polarization or electric repulsion. The adsorption involved in catalysis is "chemical" adsorption or so-called chemosorption, i.e., adsorption due to forces of a chemical nature (forces of the exchange type). This type of adsorption amounts to a chemical union of the gas molecules with the solid.

From the theoretical standpoint the two types of adsorption, "physical" and "chemical", require entirely different approaches. Whereas in "physical" adsorption the adsorbent and adsorbate are essentially two independent systems and the action of the adsorbent on the adsorbate may be regarded as a weak perturbation, in the case of "chemical" adsorption the semiconductor crystal and the gas molecule adsorbed on its surface comprise a single quantum mechanical system and must be considered as a whole.

What is the mechanism of chemical adsorption, i.e., the mechanism of formation of a chemical bond between the crystal and the gas molecule? This is the first problem facing the theoretician. So far it has received scant at-

tention.

Chemical adsorption as a rule requires a certain activation energy. In theoretical interpretations this activation energy is commonly associated with a potential barrier on the adsorption curve, i.e., on the curve characterizing the energy of the system as a function of the distance between the adsorbed molecule and the solid. Essentially the potential barrier acts to prevent access to the surface of all molecules whose kinetic energy is below a certain level.

What is the origin of the potential barrier on the adsorption curve, i.e., the origin of the activation energy necessary for chemical adsorption to occur? This is the second problem encountered by theoreticians.

Dissociation of the molecules often occurs in chemical adsorption: each molecule breaks up into two parts. In other words, the bond linking the two atoms or two groups of atoms comprising the molecule is ruptured as a result of adsorption. This may be regarded as an experimentally established fact. The adsorbed particles on the surface are not entire molecules but molecular fragments. What is the mechanism of this dissociation occurring at the instant of adsorption? Elucidation of this mechanism is the third problem awaiting theoretical analysis.

We know that the catalytic activity of a semiconductor depends to an appreciable extent on the nature and concentration of impurities contained therein. Some impurities, even when present in minute amounts, suppress the catalytic activity of the semiconductor (so-called "poisons"), while other impurities, on the contrary, intensify its activity (so-called "promoters"). It is interesting to note that the same impurity can be a promoter where one reaction is concerned and a poison with regard to another. In fact the same impurity can serve as a promoter or a poison for the same reaction, depending on its concentration and the ambient temperature.

In what way (that is, through what mechanism) can impurities introduced into the crystal exert such an appreciable effect on chemical processes occurring on its surface?

The transfer of the reaction from the gas phase to the surface of the catalyst (and this is essentially the effect of the catalyst) leads, as we have noted, to an acceleration of the reaction. This means that in the adsorbed state the molecules acquire an enhanced ability to react. What is this due to? In what manner is the reactive power of the molecules increased as the result of adsorption? Why is this effect of semiconductors connected, as experimental evidence indicates, with the concentration of free electrons and holes in it?

Here we have yet another (possibly the central) problem requiring solution.

We have enumerated only a few of the problems that must be solved in developing the theory of semiconductors from the standpoint of their behavior as catalysts.

These are the problems that have been under theoretical investigation in the Catalysis Laboratory of the Institute of Physical Chemistry of the Academy of Sciences. Some matters have been clarified, but much still remains obscure.

Some of the questions I have touched upon will be discussed in the reports to be presented to the Section on Semiconductor Catalysis at the present Conference.

This is the first time that a section on semiconductor catalysis has been

included in the agenda of a conference on semiconductors. This does not mean that catalysis on semiconductors has not been studied hitherto. Chemists have been working on catalysis for decades, but they have not been aware until now (and some perhaps are still not aware) that their catalysts are semiconductors; likewise, physicists dealing with semiconductors often do not know that their semiconductors' catalytic properties exist and have been used for years in the chemical industry as catalytic agents.

The inclusion of the subject of semiconductor catalysis in the agenda of our conference means that the problem of catalysis is at last being viewed from the standpoint of the physics of semiconductors. And this problem does become a problem of the physics of semiconductors (and even of the theory of semiconductors) as soon as we raise the question of the physical mechanism of the phenomenon.

ON SOME QUESTIONS OF SEMICONDUCTOR ANALYSIS

(Remarks on the report of S.Z.Roginskii made at a plenary meeting)

- F.F.Vol'kenshtein

I would like to say a few words in connection with the report of S.Z. Roginskii. I will not speak now in regard to theoretical questions; these will be considered in my report to be presented later. At the moment I would like to recall certain experimental facts, facts which I believe are indicative of the close relationship between the electronic properties of semiconductors and their catalytic and adsorptive attributes.

Every catalytic process on the surface of the semiconductor begins with chemosorption. The adsorbed molecule in this case forms a chemical compound with the solid (semiconductor). Consequently, the wave functions of the molecule and the lattice overlap so that the crystal and the molecule chemosorbed on its surface form a single quantum mechanical system and must be considered as a whole.

The chemosorbed molecules, therefore, play the role of an impurity on the surface of the semiconductor. Their appearance signifies the appearance of local surface levels which may be of either the acceptor or donor type depending on the nature of the adsorbed molecules.

With establishment of electron equilibrium in the system these levels become filled to a greater or lesser extent by electrons (in the case of acceptor levels) or by holes (in the case of donor levels), as a result of which the surface becomes charged relative to the volume. Thus chemosorption always leads to charging of the surface.

It is immediately apparent what must happen. The energy bands become distorted near the surface and, consequently, the work function of the semiconductor changes; at the same time its electric conductivity may also change. The last occurs, of course, only in the case of sufficiently small crystals when the change in conductivity in the surface layer of the semiconductor due to deformation of the energy bands can affect its conductivity as a whole (its bulk conductivity). Such changes in the work function and the conductivity under the influence of adsorption have actually been observed by V.I. Liashenko and I.I.Stepko as well as by a number of other investigators.

Thus a chemosorbed molecule, as any impurity center, may be in a neutral or a charged state. It is interesting to note that the strength of its binding with the lattice in these two states differs. In the case of localization of an electron or hole on a neutral molecule its binding with the surface is strengthened. This is accompanied by a change in its reactivity, i.e., its ability to enter into a chemical compound with other adsorbed molecules or molecules impinging from the vapor phase.

The probability that a given chemosorbed molecule will be in a neutral or a charged state on the surface (or, in other words, the probability that it will be more or less strongly bound with the surface or, put another way, the probability that it will be more or less prone to react) will depend on the level of the chemical potential. In other words, this probability is directly related with the concentration of free electrons or holes in the crystal.

This is evinced, for example, by the experiments of J.Hedvall who investigated the adsorptive power of mercury sulfide as a function of its stoichiometric composition (we note that the adsorptive power characterizes the strength of the binding between the adsorbed molecules and the surface of the adsorbent). Hedvall found that the greater the deviation from stiochiometric proportions inside the crystal and, consequently, the greater its con-

ductivity, the greater is the adsorptive power of the surface, i.e., the greater the number of molecules retained on the surface in equilibrium with the gas phase (other conditions - pressure and temperature - being equal).

This is further substantiated by experiments on the influence of illumination on the adsorptive power. Hedvall and other investigators observed a sharp increase in the adsorptive ability of surfaces under the influence of light. It is noteworthy that this effect of illumination occurs not at all frequencies but only at photoelectrically active frequencies that give rise to an internal photoeffect in the crystal.

In fact, in some cases, illumination leads to the opposite effect: to a decrease rather than an increase in the adsorptive power. I have in mind here the experiments of A.N.Terenin and his colleagues as well as the last experiments of I.A.Miasnikov, who observed photodesorption of oxygen from zinc oxide crystals. In these experiments photodesorption occurred when the crystal was illuminated with light of frequencies corresponding to the absorption band of the material. I think that we have here the same exciton mechanism as that encountered by V.E.Lashkarev and by V.P.Zhuze & S.M.Ryvkin in investigating photoconductivity in cuprous oxide. As a result of interaction with an exciton, the chemosorbed molecule is rid of the electron (or hole) localized on it; consequently, its binding with the surface is weakened and desorption is facilitated.

I have cited all these facts as evidence indicating that the electrons of the crystal lattice apparently participate directly in the mechanism of chemosorption. In chemosorption, which, it will be recalled, is the first stage of every catalytic process, the entire lattice of the adsorbent enters the ensuing chemical process as a whole.

Let us now turn to another matter. I would like to speak of the influence of impurities introduced into the semiconductor on its catalytic activity.

The catalytic activity of a given semiconductor with respect to a particular reaction is characterized by the rate constant K which usually obeys Arrhenius' rule:

$$K = K_o e^{-E/kT}.$$

We note that in log K vs 1/T coordinates Arrhenius' equation is represented by a straight line which, however, can exhibit breaks similar to those encountered in the rectilinear plots characterizing the electric conductivity. This is shown in Fig.1 which is taken from a report by Margolis & Todes who investigated the ethylene oxidation reaction in the presence of magnesium-Chromium and copper-chromium catalysts.

The introduction of impurities into the semiconductor leads to a change in the value of both the activation energy E and the factor K_o in Arrhenius' equation. Obviously, this results in a change in the rate constant K, that is, in a modification of the catalytic activity of the semiconductor with respect to the given reaction.

It is noteworthy that the rectilinear Arrhenius plots for samples of the same semiconductor differing as regards impurity content may intersect, as shown in Fig.2. This figure pertains to the oxidation of ethylene in the presence of $MgO \cdot Cr_2O_3$ catalysts with different amounts of Na_2SO_3, studied by O.V.Krylov & L.Ia.Margolis.

Let us look at curves 1 and 5 in this figure. Curve 5 pertains to the sample with the highest impurity content, while curve 1 pertains to the sample with the lowest Na_2SO_3 content. We see that in this case increase in the

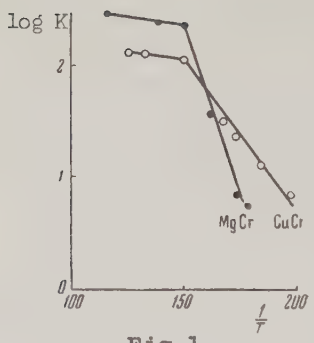

Fig.1.

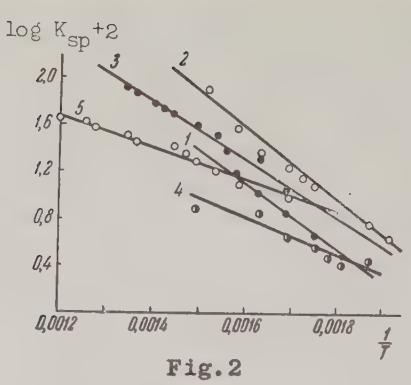

Fig.2

amount of impurity brings down the activation energy E and reduces the factor K_o. Consequently at low temperatures the activity of the catalyst is increased, while at high temperatures, on the contrary, it is reduced. Thus the same impurity introduced in the same amount acts as a promoter at low temperatures (accelerates the reaction) and as a poison at high temperatures (slows down the reaction).

It is remarkable, too, that at a given temperature the same impurity may have a promoting or poisoning effect depending on its concentration. This is evident from the same Fig.2, wherein the plots are numbered in order of increasing impurity content. This is even more clearly evident from Fig.3 (taken from G.M.Zhabrova & E.A.Fokina) which shows the variation of the activity of a catalyst (i.e., the rate constant K) as a function of the impurity concentration Z. The points on the several curves correspond to samples with different impurity contents. The figure pertains to the decomposition of hydrogen peroxide on MgO crystals containing different amounts of Sb_2O_3 as the impurity.

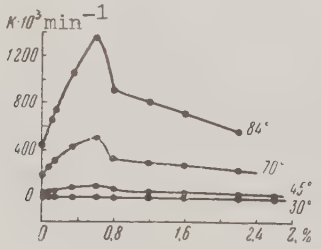

Fig.3.

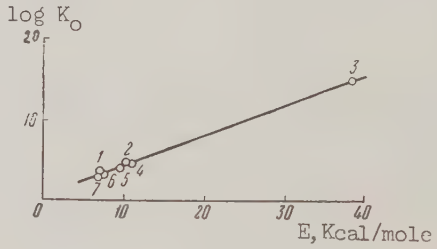

Fig.4.

Thus we see that the factor K_o and the activation energy E in Arrhenius' equation are functions of the impurity concentration Z. Both K_o and E change with Z. It appears, however, that there is a linear relation between ln K_o and E; this was established by Constable and has been substantiated by a number of investigators for different reactions on different catalysts. By way of illustration of the Constable law we have the curve of Fig.4 plotted on the basis of the data of Margolis and Todes who investigated the oxidation of isooctane on a magnesium-chromium catalyst modified by admixtures of H_3PO_4. The points in the figure are numbered in order of increasing impurity (H_3PO_4) content.

Constable's law $\ln K_o = a + bE$ recalls the empirical law of Meyer-Neldel for the electric conductivity. It is worth noting that the numerical value of the coefficient b in Constable's law (b = 0.2-0.5 mole/Kcal) agrees with the value of the corresponding coefficient in the Meyer-Neldel law. Thus according to the data of A.B.Shekhter & Iu.Sh.Moshkovskii the coefficient b in Constable's law has a value of 0.35 mole/Kcal for the decomposition of methanol on zinc oxide samples heated to different temperatures. The corresponding coefficient in the Meyer-Neldel law for the same zinc oxide has a value of 0.30 mole/Kcal.

How can an impurity introduced in a minute amount into the interior of a semiconductor exert so substantial an influence on the rate of chemical reactions occurring on its surface?

It seems to me that the explanation is that introduction of impurities changes the concentration of the electron and hole gas in the semiconductor and this in turn determines, as we have seen, the reactivity of the molecules adsorbed on the surface of the semiconductor and thereby its catalytic activity.

I do not want to go into extended theoretical considerations here. I only wanted to cite (in amplification of S.Z.Roginskii's report) some facts which, it seems to me, indicate that the electrons and holes of the crystal lattice are direct participants in and even regulators of the chemical processes developing on semiconductor surfaces.

If this is true (and the experimental evidence speaks in favor of this assertion) the theory of the catalytic action of semiconductors must develop in close contact with the theory of semiconductors in general and, in fact, must be regarded as a special section or chapter of the general theory of semiconductors.

This is what I have been leading up to. This was the purpose of my remarks.

In concluding, I would like to say a few words on the present situation in the theory of catalysis. There does not exist as yet a true physical theory of heterogeneous catalysis, a theory which would disclose the physical mechanism of catalytic processes. The theories now in vogue among chemists are essentially phenomenological.

Extant theories and the future as yet far from completely developed physical theory of catalysis (which we are only beginning to construct and which we call the electronic theory of catalysis) are approximately in the same relationship to each other as the theory of chemical bonds of the past century which operated with valence dashes (and had little in hand except those short lines on paper) and the modern quantum mechanical theory of chemical bonds which has given the valence dashes a physical content and thus furnishes an insight into the physical nature of chemical forces.

INVESTIGATION OF THE CATALYTIC PROPERTIES OF NiO BASE SOLID SOLUTIONS

- N.P.Keier, S.Z.Roginskii & I.S.Sazonova

There is much that still remains unclear regarding the correlation between the electronic and catalytic properties of semiconductors. In view of this there is undoubted interest in investigating solid solutions with non-volatile additives, the advantage of the latter being that they allow of close control of the electric conductivity and assure a known and stable impurity distribution. We know that most effective semiconductor catalysts are compounds of the transition elements with incomplete d-shells; particularly promising appear to be systems in which the basic substance is a binary compound (oxide, sulfide, selenide or the like) with the transition element as the cation. As a guide in working with these compounds one may well take the principle formulated by Verwey and his co-workers[1] in 1948 as a development of the basic idea of an earlier investigation by DeBoer and Verwey[2]. According to this principle, the electric conductivity of polar binary compounds of the transitions elements may be varied over a wide range by introducing into their lattice compounds composed of the same nonmetal and a different metal in a valence state differing from the valence state of the cation in the base (solvent) compound.

In the so-far most thoroughly investigated case of solid solutions of oxides of metals of different valence, prepared in the presence of oxygen, the introduction of cations with a lower valence (to conserve neutrality) should be accompanied by the appearance of new holes, while the introduction of cations with a higher valence should be accompanied by the appearance of excess electrons or the disappearance of part of the holes.

In such systems Schottky and Frenkel defects play a substantial role in contrast to the case of oxides with a nonstoichiometric composition. For such systems the relation between the conductivity and the nature of the impurity is particularly simple and hence the conductivity can readily be varied as desired over a wide range. As the specific subject of our investigation we selected catalytic oxidation of carbon monoxide in the presence of nickel monoxide. A number of previous investigations in our laboratory were devoted to this system[3,4]. These investigations brought out the various stages of the process and showed that the catalytic activity of nickel monoxide is sensitive to the conditions of preparation of the NiO in so far as they lead to the formation of structures deviating more or less from the stoichiometric.

The present investigation was concerned with determining the catalytic properties of solid solutions of nickel monoxide, differing as regards electronic characteristics[5]. In addition to the oxides of monovalent and trivalent metals, we dissolved the oxides of bivalent metals in the NiO. We also investigated ternary systems containing the oxides of both monovalent and trivalent metals. This enabled us to obtain a clearer idea of the correlation between the electric and catalytic properties of NiO base solid solutions.

1. Test procedure and Description of Specimens

A. Preparation of the solid solutions

The nickel monoxide and its solid solutions were obtained by sintering nickel carbonate and mixtures of this with the appropriate salts for two hours at 900° in air. The nickel carbonate was precipitated from a solution of nickel sulfate by means of sodium carbonate and was then washed with hot distilled water until sulfate tests yielded negative results.

For obtaining solid solutions with lithium oxide containing up to one atomic percent lithium cations with respect to the total number of cations (this is what hereinafter will be understood by atomic percent), the nickel carbonate was impregnated with an aqueous solution of lithium carbonate containing the appropriate amount of this compound. For obtaining solid solutions with a higher lithium cation content the nickel carbonate was mixed with the requisite amount of solid lithium carbonate. The mixture was then treated in the same way as nickel carbonate alone in the preparation of NiO without additives. The solid solutions with magnesium oxide were prepared by joint precipitation of the mixed carbonate from appropriately proportioned solutions of nickel and magnesium sulfates by means of an aqueous solution of soda. The composition of the solid solutions of magnesium oxide in nickel monoxide was determined analytically: the magnesium was determined by precipitation with 8-hydroxyquinoline; the nickel by precipitation with dimethylglyoxine. The solid solutions with zinc oxide were prepared by sintering the appropriate mixture of nickel carbonate and zinc oxide; the solutions with ferric oxide by sintering a mixture of nickel carbonate and ferric nitrate; the solutions with chromium trioxide by sintering a mixture of nickel carbonate with chromic oxide.

B. Structure of the NiO solid solutions

X-ray analyses carried out by M.Ia.Kushnerev showed that the prepared catalysts were true solid solutions. The addition of magnesium oxide increased the lattice constant of NiO; the addition of Li_2O decreased the constant.

C. Electric conductivity of NiO base solid solutions

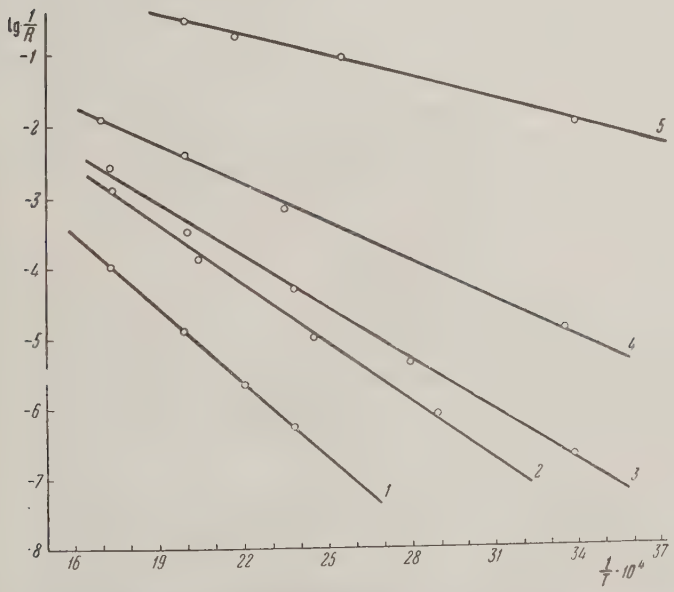

Fig.1. Temperature dependence of the conductivity of solid solutions of nickel monoxide with lithium oxide: 1) NiO, 2) NiO + 0.008%$_{at}Li^+$, 3) NiO + 0.08%$_{at}Li^+$, 4) NiO + 0.82%$_{at}Li^+$, 5) NiO + 8%$_{at}Li^+$.

We used the measured value of the electric conductivity as an index to changes in the electronic structure of the solid solutions.

For determining the conductivity we measured the resistance (by means of a dc bridge) of tablets compressed of the investigated oxides at a pressure of 400 atmospheres; in this range the resistance of tablets is independent of the forming pressure. It was established that the measured resistance of the different tablets varied in proportion to the length and weight of the tablets. This indicated that the measured resistance was the true resistance of the tablet and not of the contacts between the tablet and the metal holding clamps. We found the absolute value

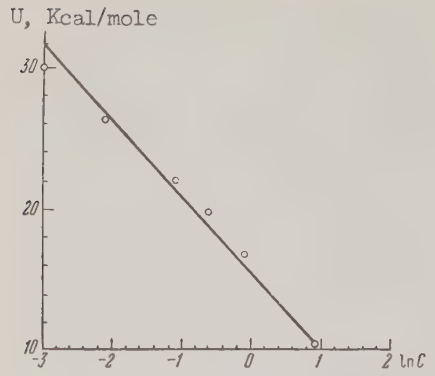

Fig.2. Variation of the activation energy for conductivity with the logarithm of the atomic concentration of lithium.

of the resistivity of nickel monoxide to be 10^5 ohm cm, which is about two orders of magnitude lower than the value given by Verwey; this is partially connected with the fact that our samples were sintered at 900° whereas Verwey sintered his specimens at 1200°. When lithium oxide is dissolved in the NiO the conductivity increases due to reduction of the activation energy. Fig.1 shows the temperature dependence of the conductivity of solid solutions of nickel monoxide with different Li_2O concentrations. The activation energy for conductivity varies linearly with the logarithm of the concentration (Fig.2). Dependence can be described by the empirical equation

$$U \approx (- 5.25 \ln C + 15.75) \text{ Kcal/mole} \quad (1)$$

The 10^{-3} value assumed for the concentration of impurities in the initial ("pure") NiO is plausible in view of the fact that the nickel carbonate was precipitated with sodium bicarbonate. The introduction of the oxides of bivalent metals into the NiO lattice has little effect on the resistivity. The increase in resistivity to 10^7 ohm cm in specimens containing 45%$_{at}$ magnesium is due to the screening influence of the magnesium cations. The activation energy for this specimen was 32 Kcal/mole, i.e., virtually did not change with introduction of the magnesium.

In contrast to the case of admixtures of oxides of monovalent and trivalent metals, solution of bivalent metal oxides produces a noticeable effect only when a large quantity of the additive is introduced. In the case of solution of ferric oxide, the activation energy remains close to the initial value (28 Kcal/mole). We note, however, that ferric oxide dissolves in NiO only in limited amounts. Lithium oxide increases the solubility of ferric oxide in NiO. In the case of solution of equivalent quantities of lithium and ferric oxide the resistivity and activation energy for conductivity remain the same as for "pure" nickel monoxide. If less ferric oxide than lithium oxide is used, the resistivity is reduced in accord with the uncompensated amount of lithium oxide.

D. Measurements of the catalytic activity

The catalytic activity with respect to the oxidation of CO was investigated in a vacuum set-up. The principal measurements were made with a stoichiometric mixture ($2CO + O_2$) under static conditions and pressures under 2 mm Hg with freezing out of the CO_2; prior to each experiment the catalyzer was degassed at 450°.

The oxidation rate on nickel monoxide and the investigated solid solutions in the temperature range from room temperature to 350° up to the point of 90% of transformation was found to be proportional to the pressure. The half-transformation time τ when the reaction is carried out in a constant volume is proportional to the initial pressure. An analogous pressure dependence was found for the oxidation of CO in the presence of NiO by Winter[6]. This dependence and the other kinetic regularities will be analyzed in a separate report.

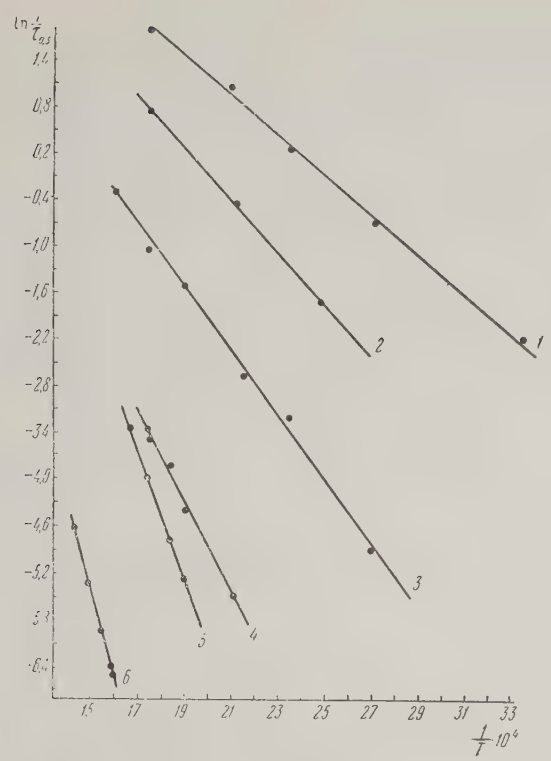

Fig.3. Temperature dependence of the half-reaction time: 1) NiO, 2) NiO + + 0.08%$_{at}$Li$^+$, 3) NiO + 0.25%$_{at}$Li$^+$, 4) NiO + 0.45%$_{at}$Li$^+$, 5) NiO + 0.82%$_{at}$ Li$^+$, 6) NiO + 8%$_{at}$Li$^+$.

Here we will compare the catalytic activities of different specimens recalculated for 1 cm^2 catalyzer surface and an initial pressure of the mixture equal to 1 mm Hg.

The activation energy was found from the dependence of log $(1/\tau_{0.5})$ on 1/T.

The factor K_o in the expression for the rate constant per unit surface of the catalyst was calculated from the relation

$$K = K_0 e^{-E/RT}, \qquad (2)$$

while the constant K was found from the kinetic equation

$$\ln \frac{p}{p_0} = -\frac{K}{p_0} t. \qquad (3)$$

The values of the specific surfaces were determined from the isotherm for the adsorption of nitrogen at -195°. Solution of lithium oxide and ferric oxide reduces the magnitude of the specific surface; the maximum reduction did not exceed 70%. Magnesium oxide, on the contrary, increases the specific surface; at 45 atomic percent of magnesium, the specific surface increases by a factor of almost four.

2. Experimental Results

A. Investigation of the initial nickel monoxide and its solid solutions with lithium oxide

Table 1

Values of the activation energy and the constant K_o for solid solutions of lithium oxide in NiO

Composition of specimens	$K_{o\,spec.}$	E, Kcal/molc
NiO	$3{,}8\cdot10^2$	5,0
NiO + 0,08 %$_{at}$Li$^+$	$4{,}8\cdot10^2$	6,5
NiO + 0,25 %$_{at}$Li$^+$	$3{,}8\cdot10^2$	8,0
NiO + 0,45 %$_{at}$Li$^+$	$1{,}5\cdot10^3$	12,0
NiO + 0,82 %$_{at}$Li$^+$	$7{,}45\cdot10^4$	17,0
NiO + 8,00 %$_{at}$Li$^+$	$3{,}2\cdot10^4$	20,0

The activation energy of "pure" NiO remained constant (5.0±0.5 Kcal/mole) over the entire investigated temperature range. The reproducibility of the observed values was good.

With a view to determining the character of the influence of Li_2O, we investigated solutions of nickel monoxide containing from 0.08 to 8.0% of lithium cations*. (Footnote on next page.) Fig.3 shows the temperature dependence of the natural logarithm of the reciprocal of the time for oxidation

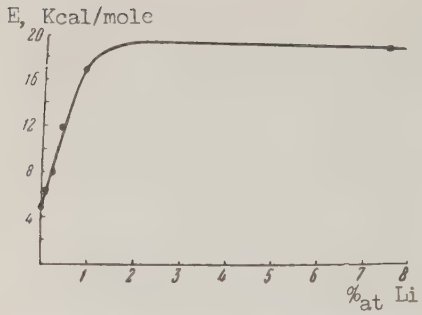

Fig.4. Variation of the energy of activation for oxidation of CO on NiO and its solid solutions with Li_2O.

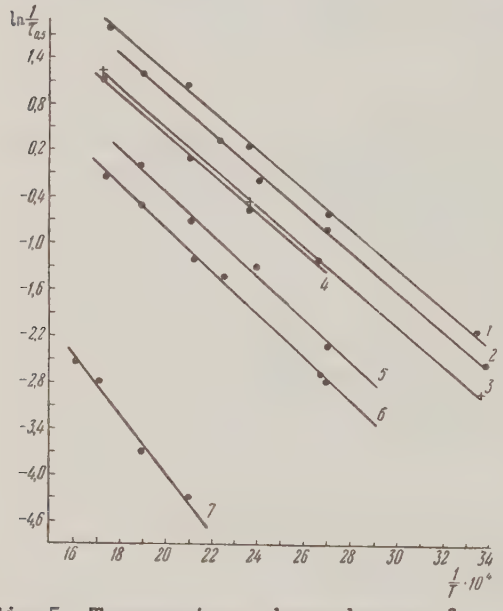

Fig.5. Temperature dependence of the half-reaction time:

1) NiO, 2) NiO + 1%$_{at}Zn^{2+}$,

3) NiO + 10%$_{at}Mg^{2+}$, 4) NiO +

+ 2%$_{at}Mg^{2+}$, 5) NiO + 45%$_{at}Mg^{2+}$,

6) NiO + 10%$_{at}Zn^{2+}$, 7) MgO.

of 50% of the CO at an initial pressure of the gas mixture equal to 1 mm Hg for different specimens. It will be seen from the figure that the rate of oxidation falls off sharply with increasing lithium oxide content, while the activation energy increases. The values of the activation energy and the factor K_o in the expression for the rate constant calculated on the basis of the experimental data are listed in Table 1.

With increasing lithium concentration in the NiO the activation energy increases linearly with the lithium content up to about 1%$_{at}$Li; above this concentration the rate of growth falls off sharply and the activation energy tends to a constant value (Fig.4). The factor K_o also increases with rising activation energy.

B. Investigation of solid solutions of bivalent metals in NiO

As is known, the oxides of magnesium and zinc form solid solutions with nickel monoxide over a wide range of concentrations. We investigated the catalytic properties of solid solutions containing up to 45%$_{at}$ Mg^{2+} and from 1 to 10% Zn^{2+} referred to the Ni. The dependence of log $(1/\tau_{0.5})$ on 1/T for the different specimens is shown in Fig.5.

As may be seen from Fig.5 and Table 2 the activation energy remains constant over a wide range of concentrations of the introduced bivalent metal oxides. The factor K_o, however, does change several-fold which explains the relatively moderate differences in the oxidation rate observed in the experiments. A small increase in the energy of activation (from 5.0 to 5.9 Kcal/mole) is observed at a Zn^{2+} concentration of 10%$_{at}$ referred to the Ni.

It will be seen from the cited data that the introduction of even ap-

---

*(From p. 187) According to the results of Verwey et al[1] the concentration of lithium in a solid NiO solution as determined analytically is close to the value calculated on the basis of the amount of lithium carbonate mixed with the nickel carbonate before sintering. Up to 10%$_{at}$Li the computed and analytically determined concentrations coincide. The concentrations given in the present report are computed values.

Table 2

Values of the activation energy and factor K_o for oxidation of CO on solid solutions of NiO with the oxides of bivalent metals

Composition of specimens	$K_{o\,spec.}$	E, Kcal/mole
NiO	$3{,}8 \cdot 10^2$	5,0
NiO + 2 $\%_{at}Mg^{2+}$	$1{,}9 \cdot 10^2$	5,0
NiO + 10 $\%_{at}Mg^{2+}$	$1{,}6 \cdot 10^2$	5,0
NiO + 45 $\%_{at}Mg^{2+}$	$3{,}2 \cdot 10^1$	5,4
NiO + 1 $\%_{at}Zn^{2+}$	$5{,}7 \cdot 10^2$	5,0
NiO + 10 $\%_{at}Zn^{2+}$	$2{,}6 \cdot 10^2$	5,9
MgO	1,8	10,0
ZnO	No catalysis in the given temperature range	

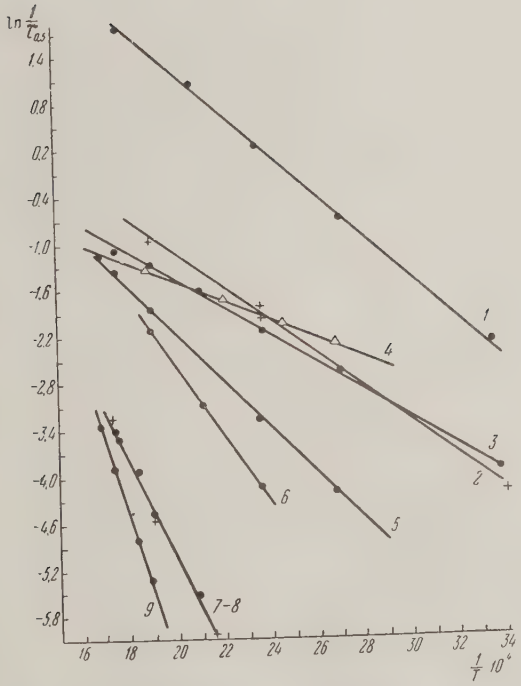

Fig.6. Temperature dependence of the half-reaction time: 1) NiO, 2) NiO + +0.82$\%_{at}Li^+$ + 1$\%_{at}Fe^{3+}$, 3) NiO + + 1$\%_{at}Fe^{3+}$, 4) NiO + 0.82$\%_{at}Li^+$ + + 2.7$\%_{at}Fe^{3+}$, 5) NiO + 1$\%_{at}Cr_2O_3$, 6) Fe_2O_3, 7) NiO + 0.45$\%_{at}Li^+$, 8) NiO + 0.82$\%_{at}Li^+$ + 0.5$\%_{at}Fe^{3+}$, 9) NiO + 0.82$\%_{at}Li^+$

preciable quantities of the oxides of bivalent metals has relatively little effect on the catalytic properties of nickel monoxide.

C. Investigation of solid solutions of trivalent metal oxides in NiO

We investigated the catalytic activity of solid solutions of NiO containing 1%at chromium and iron. The experimental results are summarized in Table 3 and Fig.6.

These data indicate that the oxide of trivalent chromium dissolved in the NiO slightly increases the activation energy for the investigated reaction and lowers the factor K_o by almost an order of magnitude. This leads to a reduction of the catalytic activity.

Introduction of ferric oxide into the NiO produces a small decrease in the energy of activation and a drop in the value of K_o that is about 59 times greater than the reduction in the specific surface. The retarding effect of trivalent metal oxides on the rate of oxidation of CO is due primarily to a decrease in the value of K_o.

Investigation of the catalytic properties of the ternary system $NiO-Li_2O-Fe_2O_3$ showed that the catalytic activity rises with increasing ferric oxide content (with the Li_2O concentration constant). For example, when 1$\%_{at}Fe^{3+}$ is introduced into the NiO solution containing 0.82$\%_{at}Li^+$ the activation energy is reduced from 17.0 to 4.2 Kcal/mole, while the factor K_o drops from $7.45 \cdot 10^4$ to 26. Further increase in the amount of iron cations leads to a reduction of K_o to 6 and of the activation energy to 2.4 Kcal/mole.

In the case of introduction of less iron than there is lithium present (in atomic percent) there is obtained only a partial reduction of the effect

Table 3

Values of the activation energy and factor K_o for oxidation for CO on solid solutions of NiO with trivalent metal oxides

Composition of specimens	$K_{o\,spec.}$	E, Kcal/mole
NiO	$3{,}8 \cdot 10^2$	5,0
NiO+1 $\%_{at}Cr^{3+}$	$4{,}5 \cdot 10$	6,5
NiO +1 $\%_{at}Fe^{3+}$	$1{,}1 \cdot 10$	3,5
NiO+—0,82 $\%_{at}Li^{+}$+0,5 $\%_{at}Fe^{3+}$	$\sim 1{,}5 \cdot 10^3$	~12,0
NiO +0,82 $\%_{at}Li^{+}$+1 $\%_{at}Fe^{3+}$	$2{,}6 \cdot 10$	4,20
NiO +0,82 $\%_{at}Li^{+}$+2,7 $\%_{at}Fe^{3+}$	6	2,40

of the latter. Thus when 0.5 $\%_{at}Fe^{3+}$ is introduced into a specimen containing 0.82 $\%_{at}Li^{+}$ there is obtained a specimen whose activation energy and catalytic activity are close to those of the solid solution of NiO containing 0.45 $\%_{at}Li^{+}$ (see Fig.6); in this case the activation energy is reduced from 17.5 to only 12.0 Kcal/mole.

3. Discussion of Results

Our investigation of catalysis on solid solutions of nickel monoxide containing the oxides of metals of different valence showed that the solution of lithium oxide has a particularly strong effect on the catalytic activity. Introduction of Li_2O leads to an appreciable growth of the activation energy and the factor K_o; up to a point the increases are proportional.

The dissolving of appreciable quantities of bivalent metal oxides (up to 45 $\%_{at}Mg^{2+}$) has no appreciable effect on the activation energy and reduces K_o by less than an order of magnitude. Dissolving Fe_2O_3 in NiO depresses the rate of oxidation of CO at room temperature by a factor of 2.5 and at 300° by a factor of 9. The observed reduction of the oxidation rate is due to a decrease of K_o by a factor of 35 with a simultaneous reduction of the activation energy by 1.5 Kcal/mole.

Introduction of 1 $\%_{at}Fe^{3+}$ into the solid solution of NiO containing 0.8 $\%_{at}$ Li^{+} results in a reduction of the activation energy by 13 Kcal/mole and a decrease in K_o by a factor of $3 \cdot 10^3$. As a result the effective oxidation rate is increased by a factor of about 100 (at 250°).

As regards both the materials employed and its purpose, the present investigation is close to those of Parravano[8] and Schwab[7], who obtained conflicting results. Parravano found that when 0.01 $\%_{mole}Li_2O$ is dissolved in the NiO, the activation energy is increased by 4.3 Kcal/mole. We investigated a series of three solutions of NiO in which the concentration of Li^{+} was varied from 0.08 to 8.0 $\%_{at}$. This made it possible to bring out the character of the dependence of the activation energy and rate constant on the lithium cation concentration. According to our data, a higher concentration of Li_2O than that mentioned by Parravano is required to obtain an increase of 4.3 Kcal/mole in the activation energy. Further, we did not observe two temperature regions differing as regards values of the activation energy. Even though the temperature range (23-350°) in our experiments was wider than that covered by Parravano, we found that the kinetic law and the activation energy remained constant over the entire investigated range. Accordingly, the observed influence of admixtures of Li_2O, Fe_2O_3 and the other oxides extends over the entire temperature range; according to Parravano[8], on the other hand, impurities do not affect the kinetics of oxidation at temperatures under 180°.

According to our data, the activation energy for the oxidation of CO on "pure" NiO is 5.0 Kcal/mole which agrees with the value published by Winter[6] but is some 8 Kcal/mole lower than the value given by Parravano. Schwab[7] does not give a specific value for the activation energy for the reaction on

pure NiO, but according to his curve it should be of the order of 16 Kcal/mole. Further, according to Parravano, introduction of oxides of trivalent metals produces a stronger effect than observed in our experiments; according to Parravano the activation energy is reduced from 13.7 to 5 Kcal/mole which is apparently connected with the higher value of the activation energy for his initial nickel monoxide. As we established in investigating ternary systems, introduction of trivalent metal oxides compensates the influence of monovalent metal oxides dissolved in the NiO. Parravano[9] notes that his initial NiO contained dissolved Na_2O, the presence of which, like that of lithium, increased the activation energy for oxidation of CO. It follows from our data that in this case (introduction of trivalent metal oxides) there should be observed a compensating effect leading to a reduction of the activation energy.

The reasons for the divergence between our results and those published by Schwab and his co-workers are obscure at present.

It should be noted, however, that although there are profound disagreements between certain particular results of the three investigations devoted to the influence of dissolved oxides on the catalytic activity of nickel monoxide, there is full agreement as regards two important points: 1) the strong and opposite influence of the oxides of monovalent and trivalent metals, and 2) the marked change in the activation energy for the catalyzed processes resulting from the addition of these metal oxides. Our data on the compensation of the effects produced by the introduction of monovalent and trivalent metal oxides and on the relative insensitivity of the catalytic activity of nickel monoxide to the solution in it of bivalent metal ions furnish additional proof of the decisive influence of the charge of the introduced cation on the character of its effect where catalytic activity is concerned. Inasmuch as a similar picture is observed where the influence of impurities on the electric conductivity is concerned, it may be asserted that our results tend to substantiate the hypotheses developed in our laboratory regarding the participation of the electrons and holes of the catalyst in the catalysis of oxidation reactions[10].

Institute of Physical Chemistry of the
Academy of Sciences of the USSR

References

1. E.J.Verwey, P.W.Haayman & F.C.Romein, Chem.Weekblad., 44, 705 (1948).
2. J.F.DeBoer & E.J.W.Verwey, Proc.Phys.Soc., London, 49, extra part, 5971 (1937).
3. S.Z.Roginskii & T.F.Tselinskaia, Zhur.fiz.khim., 18, 477 (1944).
4. N.P.Keier & S.Z.Roginskii, Zhur.fiz.khim., 21, 539 (1947).
5. N.P.Keier, S.Z.Roginskii & I.S.Sazonova, Doklady AN SSSR, 106, 859 (1956).
6. E.R.S.Winter, J.Chem.Soc., L., 2726 (1955).
7. G.M.Schwab & J.Block, Z.Elektrochem., 58, 756 (1954).
8. G.Parravano, J.Am.Chem.Soc., 74, 1194 (1954); 75, 1448, 1452 (1953).
9. G.Parravano, J.Chem.Phys., 23, 5 (1955).
10. S.Z.Roginskii & F.F.Vol'kenshtein, in Sb.Kataliz (Symposium: Catalysis), Kiev, 1950; F.F.Vol'kenshtein, Zhur.fiz.khim., 24, 1068 (1950); 25, 1214 (1951); in Sb. Problemy kinetiki i kataliza (Symposium: Problems of kinetics and catalysis), 8, 79 (1955); S.Z.Roginskii, Ibid., 8, 110 (1955).

RELATION BETWEEN THE CATALYTIC ACTIVITY AND ELECTRIC CONDUCTIVITY OF ZINC OXIDE AND THE INFLUENCE OF OPTICAL RADIATION ON THESE PROPERTIES

- I.A.Miasnikov

Our investigation was concerned with one aspect of the problem of transformation of high-energy radiation into chemical energy. Semiconductor materials are among the most suitable and interesting subjects for investigations of this kind. There have already been numerous studies showing that under the influence of radiation both n- and p-type semiconductors undergo a change in their conductivity and luminescence and emission properties, that is, the properties connected with the electron structure of the crystals.

We know that ZnO type semiconductors are capable of sensitizing certain chemical reactions in solutions[1]. Further, it is also known that the catalytic and electric attributes of semiconductors depend on their previous history and treatment and may be substantially changed by the introduction of minor amounts of impurities.

In the theoretical investigations of F.F.Vol'kenshtein and others, free electrons and holes are treated as free surface valences responsible for the activation of adsorption and catalysis. If this interpretation is valid there must be an intimate qualitative relationship between the catalytic activity of semiconductors and their electric conductivity.

For the purpose of determining the nature of this relationship we undertook an experimental investigation of the specific case of dehydrogenation of isopropyl alcohol on zinc oxide (an n-type semiconductor) in a stream of nitrogen in the presence of minute amounts of oxygen, the partial pressure of which amounted to some thousandths of a percent of the pressure of the alcohol vapor and nitrogen.

Upon being adsorbed on the surface of zinc oxide, oxygen changes the conductivity of this semiconductor. Hence we could control the conductivity of the catalyst over a wide range by varying the concentration of oxygen in the reaction zone. In our first experiments the ZnO catalyst was prepared in the form of a rod 3 cm long and 0.5 cm in diameter. The reaction was carried out in a flow-through set-up. As a result of these experiments it was found that the catalytic activity of zinc oxide varies symbatically with its conductivity[2]. With this set-up, however, we were unable to establish a quantitative relationship in view of the fact that the conductivity of the internal layers of the ZnO rod changed little in the presence of minor amounts of oxygen, while large amounts of oxygen tended to interfere with the course of the dehydrogenation reaction.

In investigating the same reaction on ZnO prepared in the form of a thin film on the inner surface of a quartz tube, we succeeded in establishing that the variation in the conductivity of such a film is linearly related with the change in its catalytic activity.

These experiments were carried out in the flow-through apparatus shown in Fig.1. The quartz tube with the ZnO film was mounted in the reaction vessel 2. The leads from the platinum contacts connected with the film were brought out through appropriate glass seals. The rate of the reaction was measured on the basis of the concentration of hydrogen as determined by means of an interferometer with a 1 mm thick cell (accuracy of measurement - 0.01% H_2 per scale division of the interferometer drum).

The temperature in the reaction vessel was maintained constant at 360°. The rate of gas flow was monitored by a glass membrane type flow meter and was 8 milliliters/min. The electric conductivity of the ZnO film was measured by the compensation method.

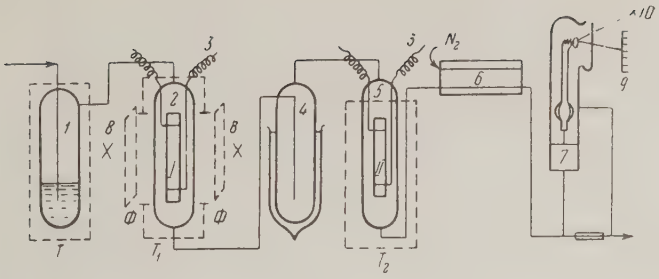

Fig.1. Diagram of flow-through apparatus: 1) evaporator, 2) reaction vessel with ZnO film (I), 3) platinum contacts, 4) trap in Dewar flask, 5) vessel with ZnO film (II), 6) interferometer, 7) membrane type flow meter, 8) quartz mercury tube, 9) scale, 10) light source; T, T_1 and T_2) thermostats, ϕ) filters.

The results of these measurements are shown in Table 1 and graphically in Fig.2 where the rate of the dehydrogenation reaction is plotted against the relative conductivity. It will be seen that the experimental points fall close to a straight line. The slope of the plots is close to unity.

Table 1

Sample No.	Reaction rate in N_2, q_o, mole/hr. ($\times 10^4$)	Reaction rate in N_2+O_2 q, mole/hr. ($\times 10^4$)	$\frac{\Delta q}{q_o} = A$	Conductivity of ZnO in N_2+alcohol, σ, Kilomho ($\times 10^4$)	Conductivity of ZnO in N_2+O_2+alcohol, σ Kmho ($\times 10^4$)	$\frac{\Delta\sigma}{\sigma_o} = B$	$\frac{A}{B}$
1	6,78	1,16	0,83	3,80	0,79	0,80	1,03
	6,78	2,43	0,64	3,66	1,54	0,58	1,10
	6,95	3,39	0,51	3,22	1,72	0,47	1,08
	6,78	4,07	0,40	3,32	2,04	0,39	1,04
2	13,0	5,06	0,62	6,05	0,60	0,91	0,68
	14,2	5,90	0,59	6,25	1,45	0,80	0,74
	12,2	7,00	0,43	6,05	2,00	0,67	0,64
	12,5	7,80	0,38	6,10	2,80	0,54	0,71
	13,0	8,20	0,37	6,55	2,90	0,56	0,66
	13,0	10,40	0,20	6,55	5,90	0,10	2,00

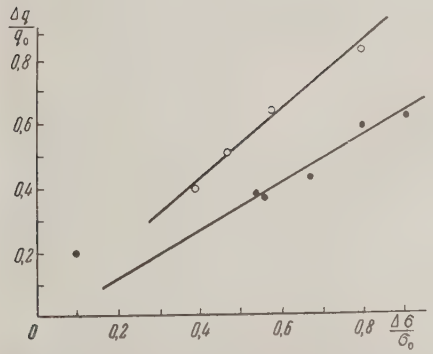

Fig.2. Relation between the catalytic activity and the conductivity of ZnO: Δq is the increment in catalytic activity, $\Delta\sigma$ is the increment in conductivity, q_o is the catalytic activity and σ_o the conductivity of ZnO in the absence of oxygen.

From the linearity of the observed relationship it is evident that the oxygen chemically adsorbed on the ZnO blocks the centers responsible for the catalytic activity and those responsible for the electric conductivity to an equal extent.

What is the mechanism of activated adsorption of oxygen on zinc oxide? The first step in activated adsorption on ZnO at moderate temperatures consists, apparently, of the formation on the surface of molecular O_2^- ions linked with the irregular singly charged Zn^+ ions. The formation of negative molecular ions is fully probable in view of the fact that the electron affinity of oxygen molecules, as is known, is of the order of 1 ev.

The possibility of formation of molecular oxygen ions on the ZnO surface was first suggested by Veselovskii[1] and used

by him in interpreting the sensitization of oxidation reactions in aqueous solutions by zinc oxide.

The activated adsorption of oxygen on ZnO under the conditions of our experiments is probably connected with the formation of a surface compound of oxygen and irregular (interstital) Zn^+ ions with the participation of a free lattice electron. The reduction in the electric conductivity of ZnO observed in the presence of oxygen is due, as is known, to the trapping of free electrons.

The reverse process (desorption) apparently consists in the decomposition of surface oxide with the evolution of oxygen and liberation of the trapped electron. This process is accompanied by an increase in the conductivity of ZnO. If the above assumptions are true, the equation for the direct and reverse reactions can be written as

$$Zn^+ + e + O_2 \rightleftarrows (Zn^+ O_2^-). \tag{1}$$

The law of mass action for this reaction can then be written as

$$\frac{[e]\,[Zn^+]\,[O_2]_S}{[Zn^+ O_2^-]} = k(t), \tag{2}$$

where $[e]$ is the equilibrium concentration of electrons, $[Zn^+]$ is the concentration of zinc ions and $[O_2]_S$ is the concentration of oxygen on the surface.

Assuming that 1) $[e] = [Zn^+]$, 2) $[Zn^+O_2^-] = [e]_0 - [e]$ and 3) $[O_2]_S = \alpha p_{O_2}$, we obtain

$$\frac{[e]^2 p_{O_2}}{[e]_0 - [e]} = \frac{k}{\alpha}, \tag{3}$$

where α is the distribution coefficient and $[e]_0$ is the concentration of electrons in the absence of oxygen.

The first and second assumptions are valid in the case of absence of extraneous impurities and a moderate temperature; the assumption holds for oxygen pressures in the region of applicability of Henry's law. If in the absence of oxygen the conductivity σ_0 is appreciably greater than the equilibrium conductivity σ, i.e., if $[e]_0 \gg [e]$, then with some approximation we can write

$$[e]^2 p_{O_2} = \frac{k\,[e]_0}{\alpha}, \tag{4}$$

whence

$$\sigma = \frac{k}{\sqrt{p_{O_2}}}, \tag{5}$$

where $k = \frac{k\sigma_0 ev}{\alpha}$, e is the electron charge, σ_0 is the conductivity in the absence of oxygen and v is the electron mobility.

As will be shown below, experiments substantiate this relationship.

Let us now turn to the kinetic equations for the forward and reverse reactions. Let us assume that the decrease of free electrons in the presence of oxygen will be proportional to $[e]$, $[Zn^+]$ and p_{O_2}, then

$$-\frac{d[e]}{dt} = k_1 [e]\,[Zn^+]\,p_{O_2}. \tag{6}$$

This expression is valid in the case when the occupied portion of the surface is small, i.e., when the reverse reaction can be neglected.

Assuming, as in the case of equilibrium, that $[e] = [Zn^+]$, we obtain for the case of constant oxygen pressure

$$\frac{1}{[e]} = k_1 p_{O_2} + a, \tag{7}$$

where a is an integration constant.

From the boundary condition $[e] = [e]_0$ with t = 0, we find that

$$a = \frac{1}{[e]_0}.$$

Substituting this value of a and $[e] = \frac{\sigma}{ev}$, where σ is the conductivity, e is the electron charge and v is the electron mobility, into (7) we obtain

$$\frac{1}{\sigma} = \frac{k_1 p_{O_2}}{ev} t + \frac{1}{\sigma_0} \tag{8}$$

or

$$\frac{\sigma_0}{\sigma} = k_1 t + 1, \tag{9}$$

where $k_1 = \frac{k_1 p_{O_2} \sigma_0}{e_0}$.

As will be shown below, this kinetic expression for the forward reaction is substantiated by experiment.

As a result of the reverse reaction the concentration of free electrons will, obviously, increase with time. Assuming that at the initial instant of the decomposition reaction the occupied surface is large, while the concentration of oxygen in the volume is small, we can write

$$-\frac{d[Zn^+ O_2^-]}{dt} = k_2 [Zn^+ O_2^-]. \tag{10}$$

In view of the fact that the decrease in the electric conductivity of ZnO in the presence of oxygen is due only to trapping of electrons by the oxygen, we can justifiably write

$$[Zn^+ O_2^-] = [e]_0 - [e]. \tag{11}$$

Substituting (11) into (10), we obtain

$$-\frac{d([e]_0 - [e])}{([e]_0 - [e])} = k_2 dt. \tag{12}$$

Integrating Eq.(12) and substituting $[e] = \frac{\sigma}{ev}$ and $[e]_0 = \frac{\sigma_0}{ev}$, we obtain

$$\ln(\sigma_0 - \sigma) = -k_2 t + \text{const}, \tag{13}$$

or

$$\ln\left(1 - \frac{\sigma}{\sigma_0}\right) = -k_2 t + \text{const}. \tag{14}$$

This expression which characterizes the change in electric conductivity during desorption of oxygen is also substantiated by experiment.

Our experiments aimed at investigating the electric conductivity of zinc oxide in the case of its equilibrium with oxygen and also the variation of the conductivity during adsorption and desorption of oxygen were carried out in the vacuum apparatus sketched in Fig.3.

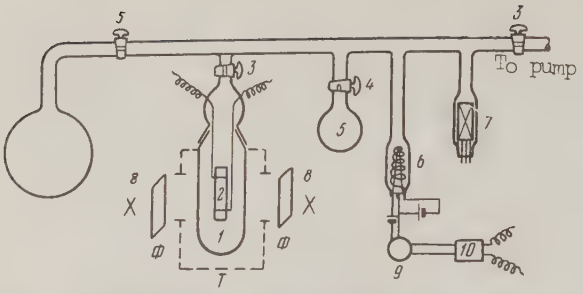

Fig.3. Diagram of apparatus used for investigating the equilibrium and the kinetics of adsorption and desorption of oxygen by ZnO on the basis of its electric conductivity: 1) reaction vessel, 2) ZnO film, 3) valve, 4) gage cock, 5) flask with oxygen, 6) ionization tube, 7) thermocouple tube, 8) quartz mercury tube, 9) relay, 10) loop oscillograph.

The zinc oxide was applied in the form of a thin film (1-10 μ) to a quartz tube 5 mm in diameter and 30 mm long. The quartz tube with its ZnO coating was mounted in the quartz reaction vessel which was maintained at the desired temperature by means of a thermostat. The leads from the platinum contacts to the Zn film were brought out through seals in the glass sleeve connecting the reaction vessel with the vacuum system. The oxygen from its storage flask was admitted to the reaction vessel by means of a metering gage cock. The oxygen pressure was measured by means of a thermocouple pressure gage. The electric conductivity in the state of equilibrium with the oxygen was measured by the compensation method; in investigating the kinetic processes, the conductivity was determined by the oscillographic method. In the experiments in which oxygen was admitted to the reaction vessel, the oscillograph recording was initiated automatically simultaneous with the beginning of the reaction by means of a relay coupled through an amplifier with an ionization tube (6 in Fig.3). In investigating desorption, which is a slower process (than adsorption), the recording was started manually simultaneously with opening the valve connecting the reaction vessel with the vacuum line. Typical oscillograms are reproduced in Figs. 4 & 5.

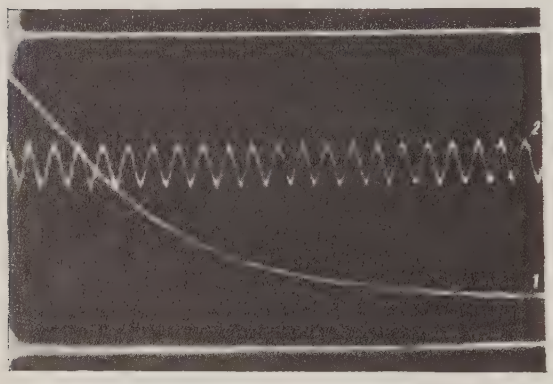

Fig.4. Oscillogram showing variation of electric conductivity during adsorption of oxygen: 1) variation of conductivity, 2) time scale.

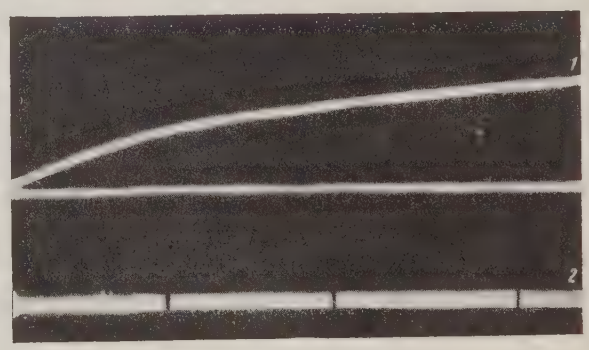

Fig.5. Oscillogram showing variation of conductivity during desorption of oxygen: 1) variation of conductivity, 2) time scale.

The experiments were carried out at temperatures from 250 to 600°. The results for the variation in conductivity as a function of the oxygen pressure are shown in Fig.6. The oxygen pressure was varied from 10^{-3} to 10^{-1} mm Hg.

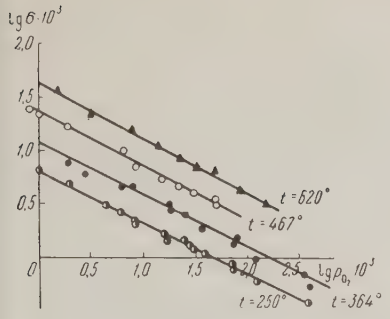

Fig.6. Dependence of the conductivity of ZnO on the equilibrium oxygen pressure at different temperatures.

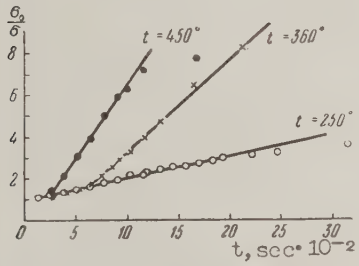

Fig.7. Kinetics of the conductivity of ZnO during adsorption of oxygen with p_{O_2} = 4 mm Hg at different temperatures.

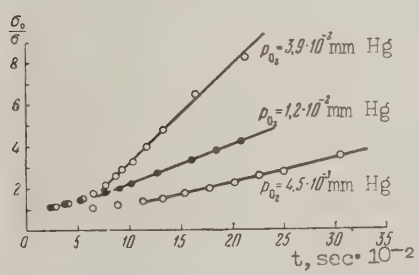

Fig.8. Kinetics of the conductivity of ZnO during adsorption of oxygen at different oxygen pressures and t = 360°.

It will be seen that in the temperature interval from 250-670°, log σ shows a linear variation with log p_{O_2}. The slope of these plots is about 1/2, i.e., the square of the conductivity of ZnO is inversely proportional to the oxygen pressure.

Thus the dependence of the conductivity on the oxygen pressure deduced above- Eq.(5) - is in agreement with experiment. Consequently, the hypothesis of the formation of O_2^- on the zinc oxide surface is upheld by experiment. If it is assumed that under the conditions of our experiments the oxygen oxidizes irregular zinc atoms to ZnO with the formation of a strong double chemical bond, then calculations show that in this case the conductivity must be inversely proportional to the fourth root of the oxygen pressure. An analogous expression was deduced by Wagner and his co-workers for high temperatures and oxygen pressures ($n = 4.3$). It is conceivable that under these conditions the oxygen dissociates on the ZnO surface and that the electrons are captured by atomic rather than molecular oxygen.

The results of our investigation of the kinetics of adsorption of oxygen on ZnO are shown in Fig.7. It will be seen that the experimental points satisfactorily fall on curves the type $\sigma_o/\sigma = k, t + 1$. There are, however, deviations from rectilinearity both for extended reaction times and near the origin of the coordinates. The former are connected with the reverse reaction; the latter are due to diffusion of oxygen from the gage cock to the ZnO film. On some oscillograms this diffusion picture is masked by virtue of the fact that the ionization tube triggered the recording with some delay.

The plots of Fig.8 show that the same kinetic equation holds for adsorption at constant temperature at different oxygen pressures.

Thus the experimental data on the kinetics of the electric conductivity of ZnO during adsorption of oxygen substantiate the formation of O_2^-.

The results of our measurements of the variation of the conductivity during desorption are shown in Fig.9. It will be seen that the experimental points for 405° fit a straight line, while at a higher temperature (460°) there is some deviation from a straight line towards the end of the experimental interval. This deviation is due to the influence of the reverse reaction.

Thus the data on the kinetics of desorption are also in agreement with the hypothesis regarding the formation of O_2^- on the surface of the zinc oxide.

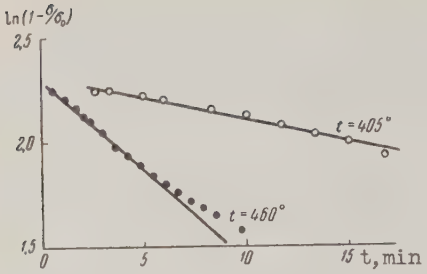

Fig.9. Kinetics of the conductivity of ZnO during desorption of oxygen.

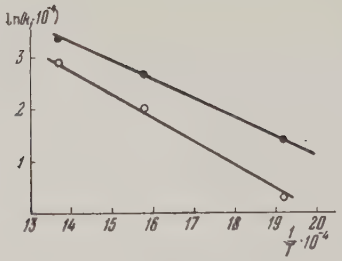

Fig.10. Arrhenius' plots based on the conductivity during adsorption of oxygen.

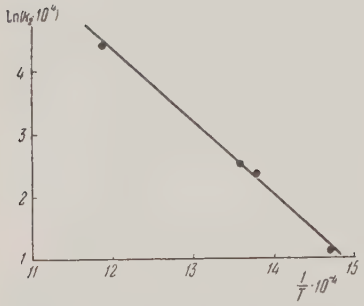

Fig.11. Arrhenius' plot based on the conductivity during desorption of oxygen.

The calculated values of the rate constants for the forward and reverse reactions at different temperatures are in satisfactory agreement with Arrhenius' equation (Figs.10 & 11):

$$k = k_0 e^{-E/RT}.$$

The calculated values of the energy of activation were E = 8 Kcal for adsorption and E = 23 Kcal for desorption. Hence the heat of the reaction Q = 15 Kcal.

The cited results substantiated our assumption regarding the formation of an unstable surface oxygen compound ($Zn^+O_2^-$) under the conditions of our experiments. At the same time, as was shown above, the catalytic activity of the zinc oxide decreases in proportion to the decrease in conductivity.

It follows from our results that this is connected with the fact that the oxygen, capturing electrons, blocks the Zn^+ ions which together with the free electrons can apparently be regarded as the active centers as regards catalysis and activated adsorption.

In general this picture is in qualitative agreement with that developed by Vol'kenshtein[3] for an ionic crystal wherein the free electrons of the lattice are assumed to play the part of adsorption centers.

In conclusion I would like to describe briefly the results of our experiments on the irradiation of zinc oxide with ultraviolet light (light in the region of absorption - 3600 Å) in the presence of oxygen and alcohol vapor.

As has been shown by Pshezhetskii and the writer[4] and by Putseiko and Terenin[5], when a zinc oxide film with oxygen adsorbed thereon is illuminated with light of a wavelength in the region of self-absorption, desorption of the oxygen occurs. In view of this we undertook an investigation aimed at determining the activity of the desorbed oxygen as regards oxidation reactions.

By way of a typical reaction we chose the oxidation of isopropyl alcohol in a stream of nitrogen in the presence of minor amounts of oxygen. The ZnO, as in the previous experiments, was in the form of a film applied to a quartz tube. The concentration of oxygen in the reaction vessel was monitored by the conductivity of the catalyst, while the concentration outside the reaction vessel was determined on the basis of the conductivity of another ZnO film mounted in a glass flask (5 in Fig.1). The leads from the platinum contacts were brought out through glass seals as usual. This second flask was located after

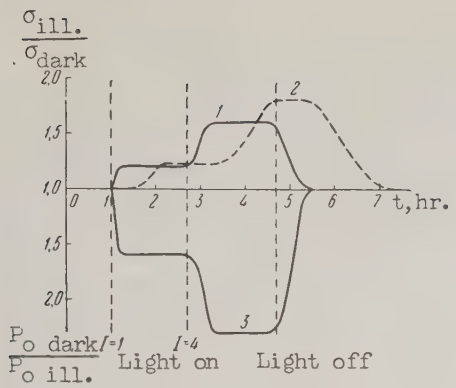

Fig.12. Variation of the electric conductivity of zinc oxide and the concentration of oxygen in the reaction vessel incident to illumination of the zinc oxide in the presence of alcohol vapor: 1) variation in the conductivity of the ZnO film (I), 2) variation of the zinc oxide film (II) (see Fig.1), 3) variation in the oxygen concentration as calculated on the basis of the conductivity; I - intensity of illumination in relative units.

the trap with liquid air. The temperature of this ZnO film was maintained constant at 230°. The reaction was investigated at temperatures from 250 to 320°. The partial pressure of the alcohol was about 200 mm Hg; the partial pressure of the oxygen was of the order of 10^{-2} mm Hg. The gas flow rate was 8 millimeters/min.

After allowing the conductivity of the ZnO to attain a stable value, the film in the quartz vessel was illuminated with light from two PRK-2 mercury tubes equipped with filters transmitting 3600 Å light. As a result the conductivity of the ZnO film in the reaction vessel increased, leveling off at a constant value corresponding to the intensity of the incident illumination. After some time the conductivity of the second film, which was not illuminated, also increased. This delay interval corresponded to the time necessary for the passage of the gas from the reaction vessel to the flask containing the second ZnO film. The change in the quilibrium pressure of oxygen was calculated from the conductivity of the zinc oxide according to the previously found dependence: $\sigma = K/\sqrt{p_{O_2}}$.

These experimental results can be explained if we assume that under illumination in the region of absorption of ZnO there is formed on its surface oxygen with an enhanced activity as regards the oxidation reaction. This enhanced activity of the oxygen leads to an increase in the rate of oxidation of the alcohol vapor and, consequently, to a reduction of the concentration of oxygen both in the reaction vessel and in the gas stream after it.

The enhanced activity of the oxygen can be interpreted as follows. The energy of the adsorbed light (3600 Å) is equivalent to 78 Kcal; the energy of activation for desorption of oxygen as found in our experiments is 23 Kcal. As is known, the activation energy in the case of optical excitation is greater than the thermal one, i.e., is of the order of 40 Kcal. Consequently, the O_2 molecule can be excited to the $1\Sigma_g^+$ state with an excitation energy 1.6 ev, i.e., 37 Kcal. This state is metastable with a lifetime of the order of 1 sec.

Thus zinc oxide illuminated with light in its absorption range sensitizes the oxidation of alcohol vapor.

These experimental results are in agreement with the findings of Putseiko & Terenin[5] regarding the irreversibility of the photo-emf of zinc oxide after prolonged illumination of the ZnO in the presence of oxygen and alcohol vapor.

It may be assumed that the mechanism responsible for the transfer of the light energy absorbed by the crystal lattice as a whole to the surface centers on which the oxygen is adsorbed is an exciton mechanism. In any case this mechanism is probably analogous to that obtaining in the production of photoelectrons in zinc oxide.

"L.Ia.Karpov" Physical-Chemical Institute

References

1. V.I.Veselovskii & D.M.Shub, Zhur.fiz.khim., 26, 509 (1952).
2. I.A.Miasnikov & S.Ia.Pshezhetskii, Doklady AN SSSR, 99, 277 (1954).
3. F.F.Vol'kenshtein, Zhur.fiz.khim., 27, 159 (1953).
4. I.A.Miasnikov & S.Ia.Pshezhetskii, Doklady AN SSSR, 99, 125 (1954).
5. E.K.Putseiko & A.N.Terenin, Doklady AN SSSR, 101, 645 (1955).

SUMMARY OF RESULTS OF INVESTIGATIONS OF THE RELATION BETWEEN THE ELECTRONIC SURFACE STATES IN A SEMICONDUCTOR AND CATALYTIC EFFECTS

- V.I.Liashenko & I.I.Stepko

1. Investigation of electronic surface states is not only of theoretical interest but also of practical value. One of the fields in which an understanding of the surface states may prove useful is catalysis. It is known that many semiconductors are good catalysts; it is also known that the catalytic activity is strongly dependent on the state of the surface of the catalyst and that there is a definite correlation between the catalytic effectiveness of a semiconductor and its electronic properties[1].

Some years ago Vol'kenshtein[2] published his theoretical investigations in which he examined the relation between the surface states & electric conductivity of a semiconductor and the rate of catalytic reactions on it. There have also been a number of experimental studies in which the catalytic properties of semiconductors were juxtaposed with their electric conductivity[3,4].

We feel, however, that it is more expedient to compare or correlate the catalytic activity of semiconductors not with the conductivity but with the electronic surface states, or more accurately speaking, with a parameter, such as the work function, that is directly dependent on the surface charge.

This suggestion is based on the results of our experiments[5] in which it was shown that adsorption of molecules on Cu_2O, CuO, CdO, ZnO and other semiconductors leads to a change in the work function as a result of a change in the filling of the surface levels (change in the surface charge). Our first experiments were concerned with the adsorption of vapors: alcohol, acetone and benzene. Subsequently, we investigated the adsorption of such gases as oxygen, carbon monoxide and carbon dioxide. We evaluated the change in the work function on the basis of the contact difference of potential which we measured by the capacitor method by means of a special instrument developed in our laboratory.

2. For the purpose of investigating the change in work function incident to the beginning of a catalytic reaction we employed the $2CO + O_2 \rightarrow CO_2$ reaction catalyzed by cuprous oxide at temperatures slightly above room temperature. We determined the variation with temperature of the work function of cuprous oxide in an atmosphere of oxygen, carbon monoxide and carbon dioxide. We found that the work function in vacuum remained constant in the temperature range from 20 to 150°; in the case of adsorption of oxygen or carbon monoxide the work function became somewhat greater but remained virtually constant over the indicated temperature range.

When, however, the specimen was placed in an atmosphere consisting of a mixture of oxygen and carbon monoxide the work function φ decreased sharply at the temperature marking the beginning of the catalytic oxidation reaction (Fig.1).

Simultaneously with the work function we also measured the conductivity. In vacuum or in an atmosphere of oxygen or carbon monoxide the plot of log σ (conductivity) vs 1/T is a straight line. In the case of a mixture of oxygen and carbon monoxide the rectilinear plot shows a break at the temperature corresponding to the sharp change in the work function and the appearance of the product of the catalytic reaction (CO_2).

It is known that catalytic oxidation of carbon monoxide also occurs on nickel monoxide. Experiments with NiO yielded analogous results. The temperature dependence of the contact potential difference V_c under conditions of the catalytic reaction $2CO + O_2 \rightarrow 2CO_2$ is shown in Fig.2. A distinctive

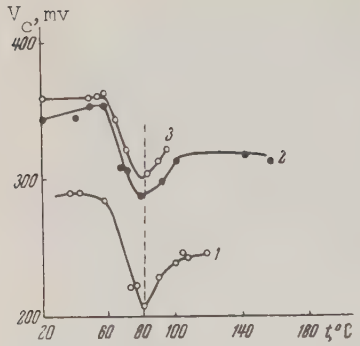

Fig.1. Temperature dependence of the contact potential of CuO during catalytic oxidation of CO. The numbered curves pertain to different cycles.

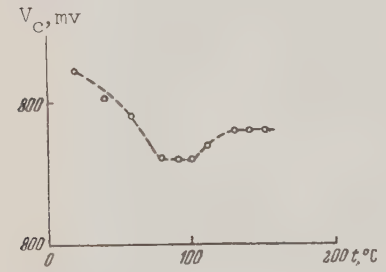

Fig.2. Temperature dependence of the contact potential of NiO during catalytic oxidation of CO.

feature of this curve is the flat minimum which extends from about 80 to 100° in the illustrated case. For other samples this flat section was even wider and began at a lower temperature. It is interesting to note that after the minimum there is a certain increase in the work function. Analysis of the gas mixture showed that in the given experiment no carbon dioxide was formed at temperatures below 70° and that measureable amounts were formed only at 80° and higher temperatures.

These experiments show that the variation of the work function with temperature is due to the catalytic process rather than to the inherent properties of the semiconductor per se.

3. We suggest the following as one of the possible interpretations of the results obtained in our experiments.

The oxygen is adsorbed on the surface levels occupied by electrons. This is in accord with our experiments, the theory of Vol'kenshtein[2] and the observations of Dell & Stone[6] who showed that the oxygen adsorbed from nickel oxide is in the form of ions even at room temperature. Consequently, the electrons in the surface level are drawn to and captured by the oxygen molecules and as a result the work function increases.

In the case of adsorption of carbon monoxide only a fraction of the CO molecules are able to capture an electron. The number of such molecules depends on the temperature and pressure, or more accurately speaking, on the position of the chemical potential level of the semiconductor[2]. As more molecules arrive at the surface the distortion of the bands due to adsorption of the molecules increases to the point where the work function φ becomes equal to V_i the ionization potential of the CO molecules.

As is known, as the temperature is increased above a certain point, the interatomic bond in CO is weakened and the carbon monoxide molecules begin to exchange atoms freely[7]. In the presence of iron this occurs at a temperature of about 120°. It may be assumed that the bonds in the oxygen molecule also weaken at an elevated temperature and, consequently, that the concentration of O^- ions increases with increasing temperature. Ionized $(CO)^+$ molecules capture O^- ions and form CO_2 which, being neutral, is only weakly retained at the surface and hence readily desorbs. At the same time the "macrodipole" formed by the electron from the surface level trapped by the oxygen atom and its screening hole breaks up. In consequence the work function decreases, the decrease being the greater, the greater the number of CO_2 molecules formed. This is consistent with results of our experiments. The fact that the observed decrease in the work function occurs in a rather narrow temperature interval gives reason to assume that the surface levels are located close to the chemical potential level and that consequently with decreasing work function the filling of these levels appreciably increases, which leads to an increase in the amount of oxygen ions and the number of $(CO)^+$ ions.

The catalytic oxidation reaction owes its intensity to the fact that there occur simultaneously three processes: 1) adsorption of oxygen with the formation of negative ions which tends to increase the work function, 2) adsorption of CO and 3) desorption of CO_2, both leading to a decrease in the work function. The opposed tendencies of these processes as regards change in work function leads to a small displacement of the surface energy system with respect to the position of the chemical potential level in the semiconductor.

It is possible that the effectiveness of a given semiconductor as a catalyst is predicated on its having an appropriate work function and a surface energy structure conducive to the simultaneous occurrence of these processes.

4. The catalytic activity of a semiconductor depends on the number of electrons and holes in its surface levels. This dependence has been demonstrated theoretically by Vol'kenshtein but has not been verified experimentally.

We attempted to establish the relationship between the number of electrons and holes in the surface levels and the catalytic activity by direct experiments. For the solution of this problem it was necessary to determine the change in the occupation of the surface levels during adsorption of a mixture of gases and the effect of this change on the rate of the catalytic reaction. At first we thought of using the same cupric oxide specimens as in the previous experiments. In view of the fact, however, that the oxidation of carbon monoxide occurred on the cupric oxide only at a relatively high temperature, when there could be appreciable diffusion, and the fact that even a small variation of temperature proved to have an appreciable effect on the results, we selected another semiconductor, namely, manganese dioxide on which this reaction occurs at room temperature.

The experiments were carried out with four different lots of manganese dioxide specimens. In order to obtain different electric properties the specimens were heated in vacuum at different temperatures from 200 to 300°. As a result there were obtained different deviations from stoichiometry and, consequently, different values of the electric conductivity and work function.

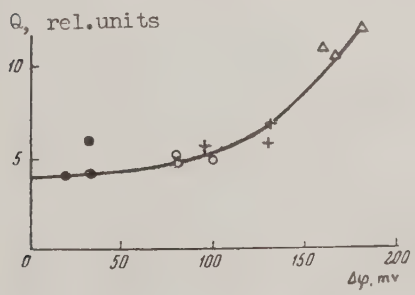

Fig.3. Dependence of the filling of the surface levels on the change in work function for four specimens of MnO_2.

The results of these experiments are shown in Fig.3. It will be seen that the specimens for which we observed the greatest change in work function $\Delta\varphi$ during adsorption of the gases and, consequently, the greatest change in the filling of the surface levels also showed the highest catalytic reaction rate. It is obvious that there is an intimate relationship between the rate of the catalytic reaction and the change in filling of the surface levels. This deduction is quantitative; we refrain from any qualitative conclusions in view of the narrow experimental range of $\Delta\varphi$.

Naturally, where the rate of a given catalytic reaction is concerned, not only the degree of filling of the surface levels but also their energetic depth is important.

The above described experiments all involved oxidation reactions. We felt it would be of interest to determine how the work function changes in the case of a catalytic decomposition reaction. For this purpose we selected one of the simplest reactions, namely, $2N_2O \rightarrow 2N_2 + O_2$.

It is known[6,8] that this reaction occurs on a number of semiconductor catalysts, including nickel monoxide. Specimens of NiO prepared by oxidation of metallic zinc evaporated under vacuum proved to be relatively inactive up

to 250-300°. On the other hand, specimens prepared by the decomposition of a mixture of nickel carbonate and nickel nitrate deposited on a glass support proved to be active. We observed noticeable decomposition of nickel monoxide on such specimens at temperatures of about 100°. The specimens prepared in this manner consisted of a powdery mass and crumbled readily, which obviously presented experimental difficulties. It was impossible to obtain reproducable results with these specimens. We could establish only the general character of the variation of the work function with the temperature of the specimen in the presence or absence of decomposition products. In all cases, regardless of whether the work function increased or decreased, we observed a minimum or plateau in the V_c vs T curve in the vicinity of 100° and following this an increase in the work function and the presence of nitrogen from decomposed N_2O. There was no noticeable decomposition of the nitrogen monoxide at lower temperatures, i.e., before the minimum or plateau.

It was obviously necessary to find another more suitable semiconductor catalyst.

It is known that the surface states in germanium play an important part in many processes. We therefore tried to realize the decomposition of N_2O on germanium.

The specimens were prepared in the form of thin layers (1 μ) by vacuum evaporation of high-resistance (50 ohm-cm) germanium and in the form of plates cut from single crystals. With both types of specimens we observed the decomposition of the nitrous oxide when the catalyst was heated to about 180°. The activity of the specimens, particularly the thin-layer ones, decreased slowly during the course of the reaction.

We investigated the temperature dependence of the change of work function of germanium under the conditions of this catalytic reaction. The results of some of these measurements are shown in Fig.4. Curve 1 pertains to the decomposition reaction on a freshly prepared surface. It will be seen that the curve has a minimum at 170°. After cooling, the work function of this specimen was equal to its initial value. Prior to this the reaction products were pumped out but the specimen was left undisturbed. Curve 2 was recorded on the following day. It will be seen that at first it nearly coincides with curve 1 but then deviates. The minimum is shifted to 180° and is less sharp than in curve 1. Curve 3 was recorded for the same specimen on the third day. It has no minimum but only a plateau.

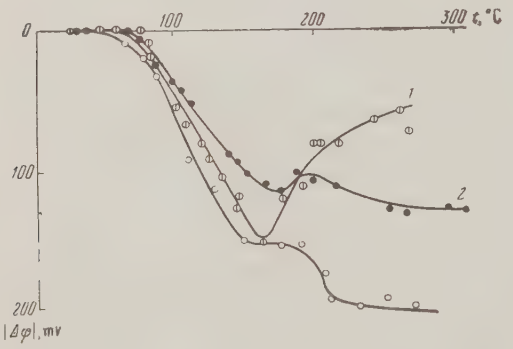

Fig.4. Temperature dependence of the work function of germanium during catalytic decomposition of N_2O. Curves recorded on successive days.

During the experiments the specimen was heated slowly at a uniform rate from one temperature of measurement to the next. The rate of heating in all three series of measurements was approximately the same.

The amount of reaction products formed was determined at the end of each series of measurements. It was found that the amount was somewhat smaller in the second cycle and much smaller in the third as compared with the first. This indicated that the catalyst was poisoned.

We also found that after such experiments the resistance of the thin-layer specimens was appreciably increased. It may safely be assumed that the oxygen liberated in the decomposition of N_2O oxidized the germanium surface and thereby affected the shape of the curves and the yield of the catalytic reaction.

Freshly prepared specimens always exhibited a minimum in the V_c vs T curve and an increase in the work function after this minimum (in this respect curve 1 is typical). It was established that adsorption of N_2O on germanium leads to a decrease of the work function. Hence we believe that the decrease in the work function to a minimum (such as that in curve 1) can be explained by a decrease in the surface charge due to adsorption of N_2O, which increases with increasing temperature. At temperatures above the temperature of the minimum, the nitrous oxide decomposes, the liberated oxygen oxidizes the surface of the germanium, while the nitrogen leaves the surface. In the case of a partially oxidized surface one can naturally expect the yield to be smaller and the minimum in the curve to be less pronounced. No decomposition occurs on a fully oxidized surface and no increase in the work function is observed.

In view of the described experimental results it may be concluded that there is an intimate relationship between the change in work function and the surface states in a semiconductor determining it, on the one hand, and the character of the catalytic reaction occurring on the semiconductor surface, on the other hand. The correlation obtains in the case of both oxidation and decomposition reactions. The fact that such a correlation exists opens new ways of investigating both surface states and catalysis on semiconductors.

The writers desire to thank V.E.Lashkarev for his interest in the work and valuable discussions.

Institute of Physics of the
Ukrainian SSR Academy of Sciences

References

1. S.Z.Roginskii, In "Elektronnye iavleniia v katalize i adsorbtsii," (Electronic phenomena in catalysis and adsorption), p.5, M., 1955.

2. F.F.Vol'kenshtein, Zhur.fiz.khim., 22, 30 (1948); 24, 1068 (1950); 25, 1214 (1951).

3. W.E.Garner & F.S.Stone, Proc.Roy.Soc., 197, 204 (1949); 212, 478 (1952).

4. E.K.Boreskov & K.I.Matveev, In "Elektronnye iavleniia v adsorbtsii i katalize," (see Ref.1), p. 615, M., 1955.

5. V.I.Liashenko & I.I.Stepko, Zhur.fiz.khim., 29, 401 (1955).

6. R.M.Dell & F.S.Stone, Trans.Faraday Soc., 50, 501 (1954).

7. R.P.Eischens & H.N.Webb, J.Chem.Phys., 20, 1048 (1952).

8. R.M.Dell, F.S.Stone & P.F.Tiley, Trans.Faraday Soc., 49, 195; 49,201 (1953).

INVESTIGATION OF ADSORPTION OF GASES ON MANGANESE DIOXIDE BY THE ELECTRIC CONDUCTIVITY METHOD

- S. Iu. Elovich & L. Ia. Margolis

The two distinctive features of heterogeneous catalysis are 1) the presence of a solid (the substance accelerating the chemical reaction) and 2) the concentration of the reacting molecules on the phase interface. Inasmuch as the primary cause of the crowding together of the molecules is adsorption, investigation of heterogeneous catalysis necessarily involves elucidation of the laws of adsorption and establishing the relative importance of different types of adsorption in the catalytic process.

There have been many investigations of the adsorption stages in catalytic processes for the purpose of establishing the character of the adsorption mechanism. At the same time, as a rule, the adsorption effects have been studied separately from the catalysis and the resultant data used to draw deductions regarding the interactions occurring on the catalyst surface during the chemical reaction. It is difficult, however, to form a clear idea of the changes in the degree of covering by the adsorbed substance during the time of the reaction and determine the types of adsorption obtaining when molecules of different types are being simultaneously adsorbed and when there may be both physical and chemical adsorption.

There are in general two methods of monitoring the state and number of molecules on the surface during heterogeneous catalysis. One, the more commonly employed, is based on determining the concentration of the molecules in the volume of the gas phase on the basis of study of the separate and joint adsorption of the molecules involved; from the changes in concentration one can indirectly judge of the effects occurring on the catalyst. The other method is based on observing changes in the properties of the catalyst under the influence of the adsorption or the reaction. Thus, for example, one can follow the changes in the concentration of hydrogen in the volume and on the surface of palladium during catalytic hydrogenation on the basis of the changes in the conductivity of the catalyst layers[1].

A few years ago Sokol'skii[2] developed a method for monitoring the hydrogen concentration on the surface of a metallic powder catalyst in the case of hydrogenation in a liquid medium on the basis of retarding potential (voltage vs emission current) curves. The limitations of these methods are obvious for it is clear that they are applicable only to adsorption of hydrogen on metals.

Recent advances in the field of semiconductors make it possible to utilize their electronic properties for the purpose of studying adsorption effects on their surface. The character of the coupling of the atoms and molecules with the semiconductor surface may differ. In the case when the coupling or binding is of a donor-acceptor character, the adsorption is accompanied by localization of a free current carrier (electron or hole) on the adsorpted molecule. This type of binding between the adsorbed particle and the semiconductor, which might be called chemical[3], leads to a change in the electronic state of the semiconductor with a consequent increase or decrease in its electric conductivity. This effect has been observed by a number of investigators[4].

Physical or van der Waals' adsorption which does not involve the donor-acceptor mechanism, obviously should not affect the conductivity of the semiconductor. Some authors (for example, Vol'kenshtein[3] and Vol'kenshtein & Roginskii[5]) come to the conclusion that there exist different types of chemical adsorption associated with strong or weak homeopolar and ionic bonds. Obviously, in the case of weak chemical bonds the conductivity of the semiconductor

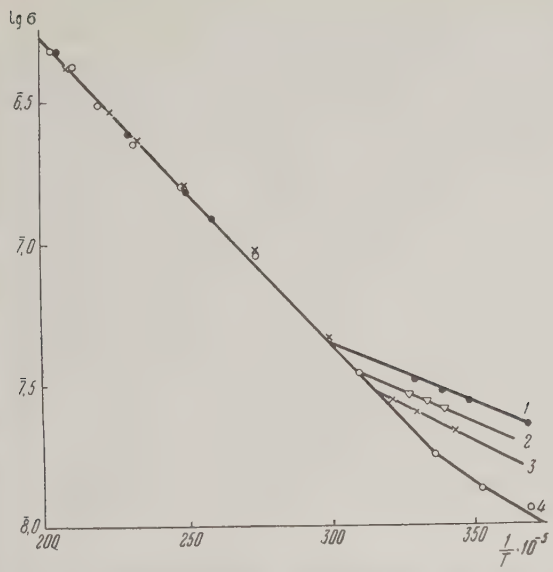

Fig.1. Temperature dependence of the conductivity of MnO_2.

should change much less than in the case of strong binding between the adsorbed atoms or molecules and the semiconductor. Experimental investigation of the different types of chemical adsorption on semiconductors is now only beginning.

In the present work we attempted to use the electric conductivity method for investigating the adsorption of O_2, CO, CO_2, H_2O, C_2H_6 and C_6H_6 on active manganese dioxide which, as is known, is a low-temperature catalyst for the oxidation of carbon monoxide.

The MnO_2 powder (grain size - 25 μ) was compressed at a pressure of about 1 atmosphere between two platinum wires which served as the electrodes. (Comparison of the temperature dependence of the conductivity of our specimen with a specimen obtained by compressing at a pressure of 120 atmospheres showed that in this respect they were identical). The electrodes were connected to a bridge circuit by means of which resistances from 10 to 10^7 ohms could be measured. The catalyst was mounted in a reaction vessel connected to a vacuum system capable of reducing the pressure in the vessel to 10^{-5} mm Hg. Prior to the experiments, the manganese dioxide was aged for 2-3 hours at 250°. Aging of MnO_2 specimens at higher temperatures leads to partial loss of the oxygen.

There are no data in the literature on the type of conduction in manganese dioxide.

The variation of the logarithm of the conductivity σ with the reciprocal of the temperature is shown in Fig.1. It will be seen that the plot is comprised of two straight lines intersecting in the temperature interval from 30 to 60°. The data shown in Fig.1 pertain to four specimens of MnO_2 differing as regards composition: specimens identified by higher numbers contain a greater excess of Mn ions.

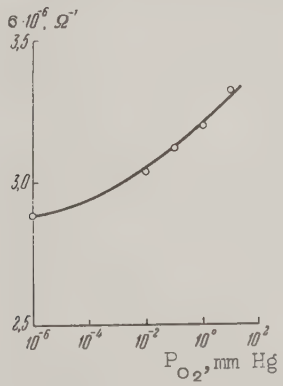

Fig.2. Variation of the conductivity of MnO_2 with the oxygen pressure at 20°.

The situation pictured in Fig.1 is analogous to that observed by Zhuze & Kurchatov[7] as regards the conductivity of Cu_2O as a function of the composition (metal ion content) and shows that manganese dioxide is a p-type semiconductor.

Passing carbon dioxide or carbon monoxide through the apparatus led to no change in the type of conductivity, such as was observed by Chapman et al[6] for Cr_2O_3.

We investigated the adsorption at -78°, -11°, 0° and 20°C. We recorded both the conductivity of the oxide and the variation in gas

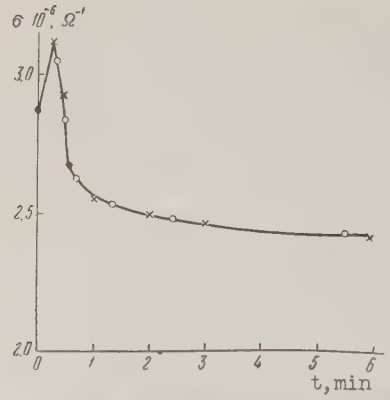

Fig.3. Variation of the conductivity of MnO_2 during adsorption of CO_2 at 20°: - adsorption, - desorption.

pressure simultaneously. The sorption of oxygen as measured at 20° is reversible and rapidly obtains equilibrium at a given pressure. The conductivity of the manganese dioxide increases continuously with increasing occupation of the adsorbent surface (Fig.2).

The adsorption of carbon dioxide as indicated by the conductivity is distinctive (Fig.3). At first the conductivity increases sharply and then slowly falls off. The reason for this is not entirely clear at present. It is possible that the initial rapid rise in conductivity is connected with the formation of strong bonds between the adsorbed molecules and the hydrated particles on the MnO_2 surface.

As Vainshtein & Turovskii[8] showed complete dehydration of manganese dioxide can be assured only by heating the material under vacuum to 550°. However, an appreciable part of the combined oxygen is also driven off under these conditions.

The decrease in conductivity after the maximum is presumably due to donor adsorption of the CO_2. This is substantiated by experiments on the desorption of CO_2. If the vacuum pump is started after adsorption of some carbon dioxide, during the evacuation the conductivity of the MnO_2 increases gradually to the value corresponding to the maximum point. Further evacuation at the temperature of the experiment does not lead to any significant change in conductivity. To obtain complete desorption of the CO_2 the temperature of the specimen must be increased to 100°. When this is done the conductivity returns to its initial value.

The variation of conductivity during adsorption of carbon monoxide (Fig. 4) yields a similar curve. Upon admission of CO the conductivity rises rapidly and then slowly falls off, yielding a maximum analogous to that observed before the adsorption of CO_2. If the gas is pumped out of the reaction vessel at some point in the region of increasing conductivity (i.e., some minutes after passage through the maximum), the conductivity gradually increases to the maximum value. If oxygen is admitted at this time, the conductivity again begins to decrease, approximately following the same curve in the reverse direction. At the same time carbon dioxide appears in the gas phase.

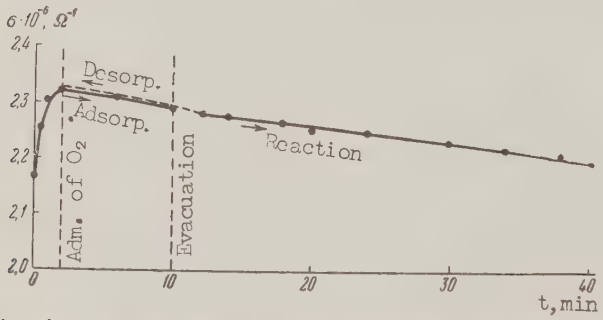

Fig.4. Variation of the electric conductivity of MnO_2 (20°). The experiment involved successive admission of CO (adsorption), evacuation (desorption) and admission of O_2.

Thus the experiment shows that the descending section of the conductivity curve during adsorption of carbon monoxide or dioxide is due specifically to adsorption of CO_2 molecules on the surface of the manganese dioxide.

In addition, it may be asserted that the CO molecules are very strongly adsorbed on the manganese dioxide and hence a very appreciable time passes between their adsorption and their interaction with the surface of the MnO_2. Our data show that a certain part of the adsorbed CO molecules reacts with oxygen as much as 60 min after their adsorption on the MnO_2 surface. Thus, although the curves obtained for the adsorption of carbon monoxide are similar in character to those obtained for the adsorption of carbon dioxide, they must be interpreted somewhat differently.

The first rapid increase in conductivity in the case of adsorption of CO is connected with acceptor adsorption. The subsequent decrease in conductivity is due to adsorption of CO_2 formed as a result of oxidation.

Our results show that the experimental procedure based on measuring the conductivity can be used for observing certain features of the interaction of molecules with the surface of an adsorbent, features that are not susceptible of investigation by other methods.

Adsorption of the other gases we investigated also influences the conductivity of manganese dioxide. Thus adsorption of water vapor leads to an increase in the conductivity of MnO_2. Such stable molecules as C_2H_6 (at $-10^{\circ}C$) and C_6H_6 (at 0°) are rapidly adsorbed on MnO_2; the adsorption of these substances results in a decrease in conductivity.

Our experiments show that in all cases adsorption leads to a change in the number of current carriers with a resultant decrease or increase in the conductivity of the specimens. Obviously, the molecules adsorbed on the semiconductor are localized on positive or negative surface ions thereby changing the electronic state of the MnO_2 and hence its conductivity.

The adsorption of carbon monoxide on manganese dioxide has been studied by many investigators[9]. Elovich & Kharakhorin established that at -78° very rapid reversible adsorption occurs. As the temperature is increased, in addition to the equilibrium adsorption which decreases with increasing temperature, there develops a more persistent kind of adsorption which requires an activation energy of the order of 6000 cal/mole; this latter kind of adsorption increases and proceeds at a more rapid rate with increasing temperature. The heat of the low-temperature adsorption has been found to be 2200-2300 cal/mole, which only slightly exceeds the heat of condensation of CO: 1414 cal/mole. This effect has been interpreted as physical adsorption of carbon monoxide on MnO_2.

We investigated the sorption of carbon monoxide at -78°, a temperature at which chemical adsorption of CO ceases entirely. At -78° the surface of the MnO_2 is covered to the extent of several percent even at the relatively low carbon monoxide pressures (20 mm Hg) used in our experiments. However, in this case we did not detect any change in the electric conductivity of our specimen.

It must, therefore, be concluded that physical adsorption which does not involve localization of the semiconductor electrons on the adsorbed molecules, does not alter the number of current carriers and thus does not affect the conductivity. Whether such adsorption also involves very weak chemical bonds, such as those postulated by Vol'kenshtein & Roginskii[5], it is difficult to decide at present since such chemical binding has not yet been identified experimentally.

Analogous effects were observed by Clarke[10] studying the adsorption of argon at $197^{\circ}K$ on germanium. Clarke, too, observed virtually no change in the conductivity of the specimen.

In one of his publications Low[11] expresses the opinion that physical adsorption should not influence the conductivity; however, he cites no experimental data on the subject.

Nevertheless, it may be assumed that investigation of the conductivity may yield valuable information on the character of adsorption and make it possible to distinguish between chemical adsorption and physical adsorption.

Conclusions

1. It has been shown that by measuring the electric conductivity of specimens of manganese dioxide during adsorption of O_2, CO, CO_2, H_2O, C_6H_6 at temperatures from -78° to 20°C one can deduce certain information regarding the character of the adsorption and the degree of covering of the catalyst-adsorbent surface.

2. An appreciable change in conductivity during adsorption presumably indicates chemical sorption leading to a change in the number of current carriers.

No change in the electric conductivity incident to appreciable adsorption (as observed in the case of CO at -78°) would indicate that the adsorption is primarily of the physical type.

Institute of Physical Chemistry of the
Academy of Sciences of the USSR

References

1. D.P.Dobychin & A.V.Frost, Zhur.fiz.khim., 5, 1031 (1934).
2. D.V.Sokol'skii, Vestnik (Review) Kazan SSR Ac. of Sci., 8, (113), 66 (1954).
3. F.F.Vol'kenshtein, Zhur.fiz.khim., 22, 311 (1948); 26, 1462 (1952); 28, 422 (1954).
4. V.I.Liashenko, Trudy (Transactions) Physical Institute, Ukrainian SSR Ac. of Sci., 4, 33 (1953); T.Grey, Semiconductor Materials (in Russian trans.), M. 1954.
5. F.F.Vol'kenshtein & S.Z.Roginskii, Zhur.fiz.khim., 29, 485 (1955).
6. P.R.Chapman, R.H.Griffith & J.D.Marsh, Proc.Roy.Soc., 224, 419 (1954).
7. V.P.Zhuze & I.V.Kurchatov, Sow.Phys., 2, 454 (1932).
8. F.V.Vainshtein & G.Ia.Turovskii, Doklady AN SSSR, 72, 207 (1950).
9. S.Z.Roginskii & Ia.B.Zel'dovich, Acta physicochim. USSR, 1,3-4,554 (1934); S.Iu.Elovich & F.F.Kharakhorin, Problemy kinetiki i kataliza (Problems in kinetics and catalysis), Vol. III, M. 1937.
10. E.N.Clarke, Annals of the New York Academy of Sciences, 58, Art.6 (1954).
11. C.Low, J.Phys.Chemistry, 59, 543 (1955).

INFLUENCE OF ADSORPTION ON THE CONDUCTIVITY AND WORK FUNCTION OF SEMICONDUCTORS

- V.B.Sandomirskii

Introduction

The results of numerous experimental studies indicate that adsorption of a gas on the surface of a semiconductor alters its electric properties, specifically, its conductivity and work function. On the other hand, it follows from a number of investigations of adsorption and catalysis on semiconductors that the state of the adsorbed and reacting gases is influenced by the electronic structure of the semiconductor, i.e., by the distribution of energy levels, the amount of impurities present, etc. It has also been found that experimental methods based on measuring the electric characteristics of semiconductors and their variation during adsorption and catalysis can yield valuable information on these processes. In view of this further theoretical treatment and analysis of the problems involved becomes important.

In recent years (since 1951) there have appeared abroad a number of contributions devoted to the development of the "theory of the boundary layer" in which attempts are made to examine theoretically the influence of adsorption on the electric properties of semiconductors and to relate their surface properties with the electronic structure of the bulk material or crystal. This undoubtedly constitutes an important advance.

Despite the successes scored by the boundary layer theory, however, the treatment of the problem in the above mentioned investigations is not always entirely correct and, in fact, involves certain specific errors. Hence we felt it desirable to undertake a critical analysis of these contributions and to re-examine the problem from the point of view of the theory of adsorption and catalysis developed by F.F.Vol'kenshtein.

1. Critique of the "boundary layer theory"

The basic premise of the "boundary layer theory" is that the particles chemosorbed on the surface of the semiconductor act as donor or acceptor impurities. There is no basic objection to this premise which in fact is taken from the work of Vol'kenshtein, as indicated, for example, by Engell[1] who is one of the proponents of the "boundary layer theory". It must be noted, however, that in this theory all the defects in the semiconductor, both in the volume and on the surface, are assumed to be fully ionized. From the standpoint of the electronic concepts developed by Vol'kenshtein this means that only the atoms (or molecules) that have formed "strong" homeopolar (or ionic) bonds with the semiconductor material are considered to be adsorbed, while particles in a state of "weak" homeopolar binding are neglected[2].

There is no justification for taking into account only one type of binding and doing so makes it impossible to consider the different states of the adsorbed particles on the surface, i.e., to raise the question of their different reactivities.

The assumption of complete ionization of the impurity atoms in the bulk of the semiconductor limits the treatment to the case when the Fermi level lies below the impurity level (in n-type semiconductors). This case, of course, does occur, but for most ionic semiconductors with a sufficiently high activation energy for conductivity it is realized either at a very high temperature or at a very low impurity concentration. Moreover, in this region of temperatures and impurity concentrations the current carrier concentration is independent of the temperature.

The principal quantity calculated in the "boundary layer theory" is the difference in potential (U_L) between the surface and the center of the crystal as a function of the occupation (covering) of the surface by adsorbed atoms and the concentration of impurities in the bulk of the crystal; this quantity is found from Poisson's equation assuming appropriate boundary conditions. Inasmuch as the case considered in the "boundary layer theory" is the one when the center of the crystal remains electrically neutral during adsorption, U_L is exactly equal to the change in work function occurring as the result of adsorption. Engell & Hauffe[3], however, include another term in the expression for the change in work function, namely, aN where a is the distance from the surface of the crystal to the center of gravity of the adsorbed molecule and N is the number of adsorbed molecules per unit surface. A number of deductions regarding the kinetics of catalytic processes are drawn on the basis of this incorrect result.

We note, also that the expression for U_L obtained in the "boundary layer theory" is limited to the case of sufficiently great covering of the surface ($U_L/kT \gg 1$); no specific deductions are made regarding the change in electric conductivity of a single crystal during adsorption.

The above are only some of the more obvious deficiencies of the "boundary layer theory".

2. Formulation of the problem

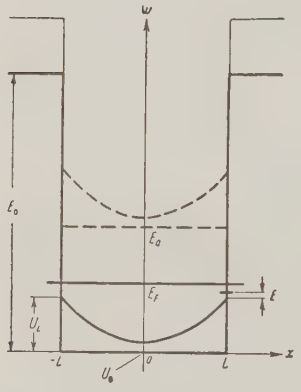

Fig.1. Energy level scheme for a p-type semiconductor. E_F - Fermi level, E_a - acceptor impurity level, E_O - height of barrier, E - surface acceptor level produced by the adsorbed particle.

For the sake of concreteness let us consider specifically the influence of adsorption of acceptor molecules on the electric properties of a p-type semiconductor.

The pertinent energy level diagram is shown in Fig.1. The light lines show the increase in the height of the barrier due to adsorption. The curved solid and dash lines, respectively, indicate the position of the normal band and the acceptor impurity level after adsorption. The energy is reckoned from the upper edge of the filled band prior to adsorption. The crystal is assumed to be a plate of infinite extent and of thickness 2L in the x direction. The adsorption occurs on the surface of this plate. Surface bands are assumed to be absent. This last assumption is made for the sake of simplifying the problem. Furthermore, it may be that taking account of the surface levels produced only by adsorbed atoms may yield information on character of the physical effects occurring during adsorption.

Let us further assume that the adsorbed atoms (molecules) may be present on the surface of the crystal in states of "weak" or "strong" homeopolar binding. We shall not take ionic binding into account. (Or it may be considered that ionic binding is taken into account and that the particles are in a neutral state, while atoms in the state of "strong" homeopolar binding are not taken into account). If there are N atoms adsorbed per unit surface, the number of atoms in the state of "strong" binding is

$$n_1 = \frac{N}{1 + e^{\frac{E+U_L-E_F}{kT}}}, \tag{1}$$

while the number of atoms in the "weakly" bound state is

$$N - n_1. \tag{2}$$

The atoms in the state of "strong" binding lead to the formation of a negative surface charge of density $-n_1 e$ (e is the absolute value of the electron charge). This in turn induces a volume charge of opposite polarity. Let us denote the potential energy of the electron in the field of this charge through $U(x)$. In other words, we have distortion of the bands (Fig.1): the bands are raised at each point a distance equal to $U(x)$. gives the change in work function of the semiconductor. In order to find the relative change in conductivity ($\Delta\sigma/\sigma_0$) we must know $U(0) = U_0$ and $dU/dx = f(x)$. These quantities can be found by solution of Poisson's equation with appropriate boundary conditions. It can be shown that integration of Poisson's equation leads to the following two expressions

$$\operatorname{ch}\frac{U_L}{kT} - \operatorname{ch}\frac{U_0}{kT} = \frac{1}{2}\left(\frac{n_1}{2l_0 p_0}\right)^2, \tag{3}$$

$$\int_{U_0}^{U_L} \frac{d\,(U/kT)}{\sqrt{\operatorname{ch} U/kT - \operatorname{ch} U_0/kT}} = \sqrt{2}\,\frac{L}{l_0}, \tag{4}$$

where $l_0 = \sqrt{\frac{\varepsilon kT}{8\pi e^2 p_0}}$, is the screening length,

and ε is the dielectric constant of the semiconductor, k is Boltzmann's constant, T is the temperature in °K and p_0 is the concentration of free holes in the normal zone prior to adsorption. It is assumed that the Fermi level does not intersect the normal band, i.e., that

$$U_L < E_F. \tag{5}$$

This requirement imposes a limitation on the degree of occupation of the surface. The set of equations (3) and (4) cannot be solved in the general case. However, we can examine two limiting cases when it is possible to obtain a solution. These are the cases of a "thick" and a "thin" crystal. In the case of a "thick" crystal we have $U_0 = 0$, while in the case of a "thin" crystal $U_0/kT \gg 1$.

Here we shall examine the case of a "thick" crystal inasmuch as it is the more important one. It can be shown that the condition for its realization is

$$\frac{L}{l_0} + \ln \frac{1 + {}^1/_2\left(\frac{N}{2l_0 p_0}\right)^2}{\frac{N}{2l_0 p_0}\sqrt{1 + {}^1/_4\left(\frac{N}{2l_0 p_0}\right)}} \gg 1. \tag{6}$$

It follows that this case obtains for a crystal of sufficiently great actual thickness or when the fraction of the surface covered by the adsorbed atoms is not excessively large. If $L \gg l_0$, (6) is fulfilled with all degrees of occupation of the surface inasmuch as the minimum value of the logarithm equals zero. (The term "thick" as applied here to crystals is used in a relative sense; inasmuch as l_0 is of the order of 10^{-6}-10^{-4} cm, the actual physical thickness of a "thick" crystal may be ~1 μ.)

In the case of a "thick" crystal Eq.(4) drops out and Eq.(3) assumes the form

$$\operatorname{sh}\frac{U_L}{2kT} = \frac{n_1}{2l_0 p_0}. \tag{7}$$

It can be shown that in this case the change in conductivity is given by

$$\frac{\Delta\sigma}{\sigma_0} = \frac{2l_0}{L}\left(e^{U_L/kT} - 1\right). \tag{8}$$

It follows from these expressions that in the given case the work function and conductivity increase by an amount dependent on U_L.

3. Approximate calculations neglecting "weak" binding

Let us find the change in the work function and conductivity neglecting the influence of "weak" binding. This is justifiable provided

$$e^{\frac{E+U_L-E_F}{kT}} \ll 1,$$

i.e., the surface levels are always below the Fermi level. This imposes a certain limitation on the degree of covering of the surface and imposes the requirement that the surface level must be located close to the top of the normal band.

As can readily be shown, in the given case we have

$$U_L = kT \ln\left\{{}^1\!/_2\left(\frac{N}{2l_0 p_0}\right)^2 + 1 + \sqrt{\left[1 + {}^1\!/_2\left(\frac{N}{2l_0 p_0}\right)^2\right]^2 - 1}\right\} \tag{9}$$

and

$$\frac{\Delta\sigma}{\sigma_0} = \frac{2l_0}{L}\left\{\left[{}^1\!/_2\left(\frac{N}{2l_0 p_0}\right)^2 + 1 + \left(\left[1 + {}^1\!/_2\left(\frac{N}{2l_0 p_0}\right)^2\right]^2 - 1\right)^{1/2}\right]^{1/2} - 1\right\}. \tag{10}$$

These expressions are complicated and difficult to manipulate; they are greatly simplified in the two limiting cases of "low" and "high" degrees of occupation of the surface. Thus, we have with ${}^1\!/_2\left(\frac{N}{2l_0 p_0}\right)^2 \ll 1$ (low degree of occupation)

$$U_L = kT\frac{N}{2l_0 p_0}; \tag{9a}$$

$$\frac{\Delta\sigma}{\sigma_0} = {}^1\!/_2\frac{N}{Lp_0}; \tag{10a}$$

or with ${}^1\!/_2\left(\frac{N}{2l_0 p_0}\right)^2 \gg 1$ (high degree of occupation)

$$U_L = 2kT\ln\frac{N}{2l_0 p_0}; \tag{9b}$$

$$\frac{\Delta\sigma}{\sigma_0} = \frac{N}{Lp_0}. \tag{10b}$$

It follows from Eq.(9) that the temperature dependence of the work function also changes incident to adsorption.

Figs. 2,3 & 4 show the dependences, calculated on the basis of Eq.(7) of U_L and $\Delta\sigma/\sigma_0$ on N, the number of adsorbed atoms per 1 cm^2 surface at a concentration of acceptor impurities in the bulk of the crystal $N_a = 10^{17}$ cm^{-3}.

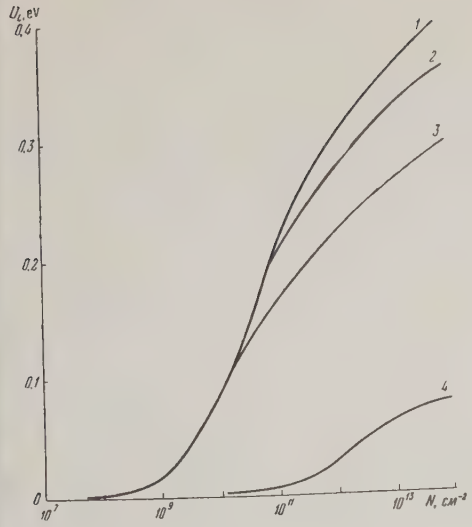

Fig.2. Curves of $U_L = f(N)$ calculated for T = 300°K and σ_o = $= 1.7 \cdot 10^{-4}$ mho/cm: 1) E = 0.05 ev, 2) E = 0.1 ev, 3) E = 0.2 ev, 4) E = 0.5 ev.

These curves show that U_L and $\Delta\sigma/\sigma_o$ can attain large values. The behavior of U_L as a function of T is interesting; this quantity at low degrees of occupation decreases with the temperature, while at high degrees of occupation it increases. As follows from the above equations, both U_L and $\Delta\sigma/\sigma_o$ decrease with increasing impurity concentration in the bulk of the crystal and with rising temperature.

Expression (10b) shows that if $\Delta\sigma/\sigma_o \gg 1$, the activation energy for conductivity becomes equal to zero. Actually it does fall off appreciably (as will be seen in the following section); its going to zero in this case is a consequence of neglecting "weak" binding. The decrease in the activation energy can be explained as follows: in this range of degrees of occupation of the surface the number of adsorbed atoms exceeds the number of current carriers in the bulk. Inasmuch as all the adsorbed atoms are assumed to be in the state of "strong" binding, the number of free holes produced by them exceeds the number of free holes previously present in the bulk and is independent of the temperature. The same situation obtains in the bulk of the crystal when the Fermi level is located somewhat above the impurity level in the volume of the crystal, but the conduction band does not yet participate in the transitions.

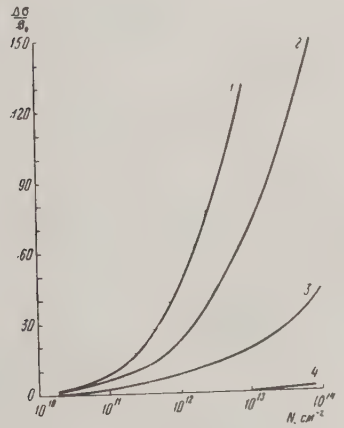

Fig.3. Curves of $\Delta\sigma/\sigma_o = f(N)$ calculated for T = 300°K and σ_o = $= 1.7 \cdot 10^{-4}$ mho/cm: 1) E = 0.05 ev, 2) E = 0.1 ev, 3) E = 0.2 ev, 4) E = 0.5 ev.

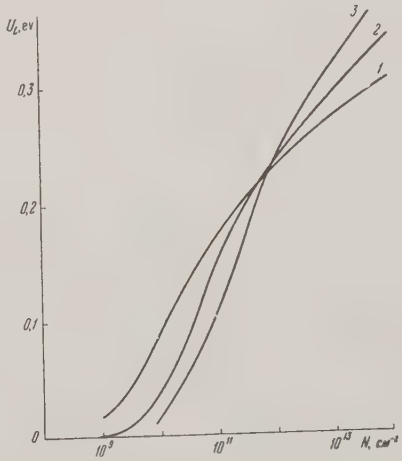

Fig.4. Curves of $U_L = f(N)$ for E = $= 0.2$ ev: 1) T = 300°K, σ_o = $= 1.7 \cdot 10^{-4}$ mho/cm, 2) T = 400°K, $\sigma_o = 4.53 \cdot 10^{-3}$ mho/cm, 3) T = 500°K, $\sigma_o = 3.56 \cdot 10^{-2}$ mho/cm.

4. Calculation taking "weak" binding into account

Let us now carry out calculations taking into account the adsorbed atoms in the state of "weak" binding. In this connection we can also raise the question of the reactivity of the adsrobed particles.

In the general case Eq.(7) cannot be solved for U_L. Hence let us consider two cases corresponding to two different positions of the surface acceptor level:

$$\frac{E-E_F}{kT} \gg 1 \tag{11a}$$

and

$$\frac{E_F-E}{kT} \gg 1. \tag{11b}$$

In the former case (11a) with the surface unoccupied (no adsorbed atoms) the surface level is located above the Fermi level. Inasmuch as incident to adsorption of acceptor atoms (or molecules) the bands are distorted or bent upward, the surface level in the process of adsorption moves even further from the Fermi level. Thus in this case the fraction of "weakly" bound atoms is great from the very beginning of adsorption and grows with increasing occupation of the surface. It follows, therefore, that the changes in work function and electric conductivity will be small, while the reactivity (fraction of "weakly" bound atoms) $\eta = 1 - n_1/N_0$ will be close to unity.

We note that in the case of adsorption of molecules the reactivity is determined by the value of 1 - η.

Assuming $U_1/kT \ll 1$, we obtain the approximate expression

$$\eta = 1 - \sqrt{\frac{N_v}{N_a}} e^{-\frac{E-E_a/2}{kT}}. \tag{12}$$

This expression shows that in the given case η is virtually independent of the degree of occupation of the surface and only weakly dependent on N_a. Since $E > E_a/2$, η decreases with increasing T. Inasmuch as U_L and $\Delta\sigma/\sigma_0$ are small here, their variation is of little practical interest.

Let us turn to the case of Eq.(11b). At the beginning of adsorption the surface level lies below the Fermi level. As the surface becomes covered with adsorbed atoms, the surface level approaches E_F and two cases are possible.

In the first case adsorption stops before the surface level crosses the Fermi level. In this case the fraction of "strongly" bound atoms is great and, consequently, the reactivity is low. To all intents and purposes we have here the case characterized above in Section 3.

The second case occurs when at high degrees of occupation of the surface the surface level rises above the Fermi level. Then in the range of degrees of occupation at which the surface level is still below the Fermi level, we have the preceding case (low reactivity), whereas when the surface level rises above the Fermi level the reactivity becomes high. It can readily be shown that the expression for η will be

$$\eta = 1 - \frac{1}{N^{1/3}} \left(\frac{N_v \varepsilon kT}{2\pi e^2}\right)^{1/3} \exp(-E/3kT). \tag{13}$$

This expression shows that at high degrees of occupation of the surface by adsorbed atoms η is virtually independent of the concentration of impurities in the bulk of the semiconductor.

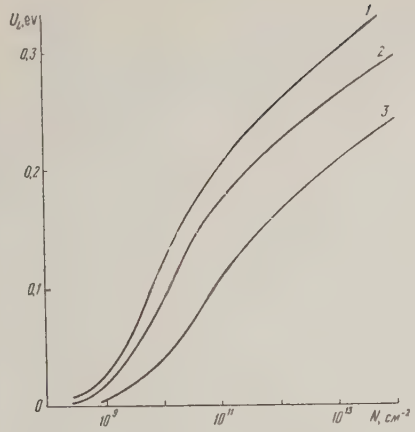

Fig.5. Curves of $U_L = f(N)$ with $E = 0.2$ ev: 1) $N_a = 10^{16}$ cm^{-3}, $\sigma_o = 5.26 \cdot 10^{-5}$ mho/cm, 2) $= 10^{17}$ cm^{-3}, $\sigma_o = 1.7 \cdot 10^{-4}$ mho/cm, 3) $= 10^{19}$ cm^{-3}, $\sigma_o = 1.78 \cdot 10^{-3}$ mho/cm.

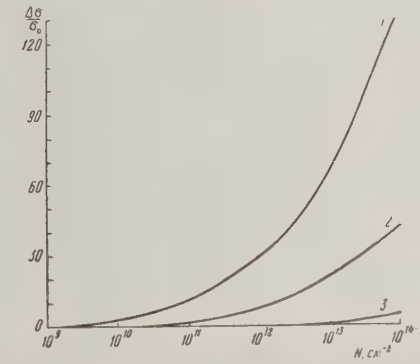

Fig.6. Curves of $\Delta\sigma/\sigma_o = f(N)$ with $E = 0.2$ ev. Designations same as in Fig.5.

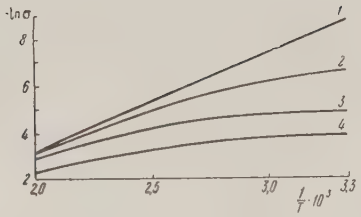

Fig.7. Curves characterizing the temperature dependence of the conductivity with $N_a = 10^{17}$ cm^{-3} and $E = 0.05$ ev: 1) $N = 0$, 2) $N = 10^{11}$, 3) $N = 10^{12}$, 4) $N = 10^{13}$ cm^{-2}.

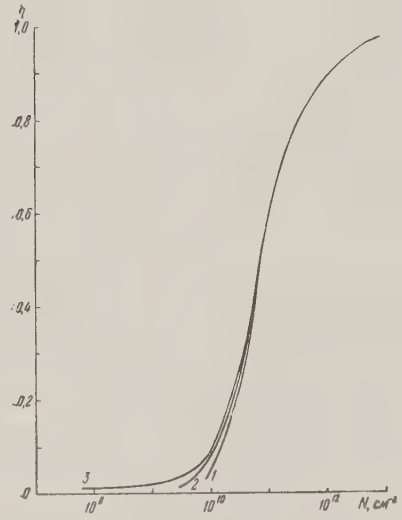

Fig.8. Curves of $\eta = f(N)$ with $E = 0.2$ ev. Designations as in Fig.5.

Figs.5 through 9 show the variation of the change in work function, electric conductivity and reactivity during adsorption as functions of the height of the surface acceptor level and the concentration of impurities in the bulk of the crystal. These curves were calculated on the basis of Eq.(7). In all cases the height of the internal impurity level was assumed to be 0.6 ev, the thickness $L = 10^{-3}$ and $T = 300^{\circ}$K (except, of course, in the case of Fig.7).

It follows from these curves that U_L and $\Delta\sigma/\sigma_o$ are strongly dependent on E, N_a and N, decreasing with increasing N_a and E and increasing with N. It also appears that the activation energy for conductivity may change greatly at large degrees of occupation and small values of E. The reactivity depends greatly on the position of the surface level and only weakly on the concentration of internal impurities; the latter is further weakened with increasing occupation of the surface.

Let us analyze the significance of the last deduction further. The derived expressions show that the fraction of adsorbed atoms in a given ("strongly"

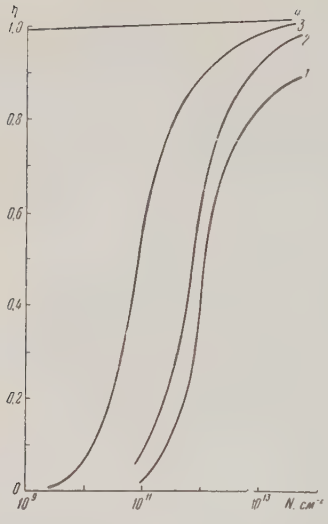

Fig.9. Curves of $\eta = f(N)$ with $N_a = 10^{17}$ cm^{-3} and $\sigma_o = 1.7 \cdot 10^{-4}$ mho/cm: 1) E = 0.05 ev, 2) E = 0.1 ev, 3) E = 0.2 ev, 4) E = 0.5 ev.

or "weakly" bound) state on the surface of the crystal is only weakly dependent on the concentration of impurities inside the semiconductor. This result may have been expected. Thus it can be shown that the fraction of "strongly" bound atoms is

$$\eta_1 = \frac{1}{1 + e^{\frac{E+U_L-E_F}{kT}}}. \qquad (14)$$

In this expression only U_L and E_F depend on the impurity concentration in the bulk of the semiconductor.

As was shown above, U_L decreases with increasing concentration of impurities in the semiconductor. At the same time the Fermi level is also lowered. Thus U_L and E_F simultaneously increase or decrease with variation of the impurity concentration in the bulk of the semiconductor. In view of this, in the range of low degrees of occupation of the surface the difference $(U_L - E_F)$ entering in Eq.(14) varies little and hence a change in the impurity concentration in the semiconductor has little influence on the state of the adsorbed molecules on the surface. At high degrees of surface occupation, this is a consequence of the smallness of the statistical factor. It follows that η_1 can be changed a) by varying only E_F (U_L = const), b) varying only U_L (E_F = const) or c) making E_F and U_L change in opposite directions. We are at a loss to indicate how (a) can be realized. U_L can be changed by introducing a small amount of an appropriate impurity onto the surface of the semiconductor. This can be done by effecting the adsorption of appropriate acceptor or donor atoms on the surface of the crystal.

It may be possible to realize the third alternative (c) by introducing an acceptor impurity with a large E_a into the bulk of the semiconductor.

Conclusions

1. The electric conductivity and work function of a semiconductor change incident to adsorption due to formation of a surface charge. We have shown that these changes are strongly dependent on the position of the surface level produced by the adsorbed particles, the concentration of impurities in the bulk of the semiconductor and the temperature. If the change in conductivity incident to adsorption is great, there also occurs an appreciable change in the activation energy for conductivity.

2. With increasing occupation of the surface there may occur a great change in the reactivity of the adsorbed atoms (or molecules). The reactivity is greatly dependent on the position of the surface level. On the other hand, the reactivity proves to be only weakly dependent on the initial concentration of impurities in the bulk of the semiconductor. The reactivity can be varied by introducing (adsorbing) an appropriate impurity onto the surface of the semiconductor. The reactivity can also be changed by the introduction into the bulk of the crystal of an extraneous impurity (an impurity of a different

character than that responsible for the initial conductivity of the semiconductor).

In conclusion we note that the method of calculation used in the present investigation is taken from the reports of Pikus[4] and Lashkarev[5]. The expression for the change in work function during adsorption was derived by Morgulis[6].

Institute of Physical Chemistry of the
Academy of Sciences of the USSR

References

1. H.J.Engell, Halbleiterprobleme, No.1, 249 (1954).
2. F.F.Vol'kenshtein & S.Z.Roginskii, Zhur.fiz.khim., 29, 485 (1955).
3. H.J.Engell & K.Hauffe, Z.Elektrochem., 57, 8, 762 (1953).
4. G.E.Pikus, Zhur.eksp.i teor.fiz., 21, 11, 1227 (1951).
5. V.E.Lashkarev, Izv.AN SSSR, Ser.fiz., 16, 203 (1952).
6. N.D.Morgulis, Zhur.eksp.i teor.fiz., 16, 959 (1946).

Section on the Optical Properties of Semiconductors

ABSORPTION OF LIGHT IN MERCURY HALIDE CRYSTALS

- E.F.Gross & A.A.Kaplianskii

Introduction

Excited states in solids are increasingly often taken into account in theoretical treatments of the diverse effects observed in dielectrics and semiconductors (internal and external photoeffects, luminescence, heat conduction, photochemical processes, etc.). Exciton states are evinced most directly in the absorption spectra of crystals in the form of a discrete structure of the long-wave absorption edge. Absorption edges with fine line structure have been reported for a number of crystals, for example, Cu_2O, CdS, PbI_2, CdI_2 and CuI (Refs.1-11).

On the one hand, no such fine structure is observed in many crystals. On the other hand, where present, it differs radically in different crystals. This means that some particular conditions that are not realized in all crystals must be present for the exciton-line structure to exist. In crystals where these conditions are fulfilled, the appearance of the fine structure is largely determined by the specific properties of the crystal itself.

Among the factors determining the existence and, when present, the character of exciton levels in a crystal, probably the most important is the structure of the crystal lattice.

It is known that the nature of the lattice structure has a great influence on many properties (electric, luminescent and others) of crystals. Hence the lattice structure may be expected to have a strong influence on the exciton levels of the crystal inasmuch as excitons are essentially lattice formations, the very existence of which is due to the regular crystal structure of matter. There are a number of ways in which the role of the lattice in determining the existence and characteristics of the exciton levels can be studied experimentally.

First, one can investigate and compare the absorption spectra of crystals of different chemical compounds having similar crystal lattices; if the crystal lattice does exert a strong influence on the exciton levels, the absorption spectra of such crystals must obviously exhibit definite similarities.

Second, one can study the absorption spectra of the crystals of different modifications of the same polymorphous substance; by this procedure one can eliminate the effect of chemical composition and bring out the influence of the crystal lattice per se on the exciton states.

In the present work we attempted to determine the influence of the lattice structure on the excitation levels in crystals by investigating absorption in a number of mercury halides. Specifically, we studied the absorption spectra of two crystal modifications of mercuric iodide HgI_2 and the absorption of crystals of mercurous iodide HgI and mercuric bromide $HgBr_2$.

1. Absorption spectra of tetragonal HgI_2

Two modifications of mercuric iodide are known: a red (tetragonal) and a yellow (rhombic). The yellow form is normally stable only above 130°, but it can be "frozen" by rapid cooling and studied at low temperatures. Our

observations with natural and polarized light were made on single crystals and polycrystalline specimens at the temperature of liquid nitrogen (77.3°K) and of liquid helium (4.2°K)* as well as at room temperature.

The absorption spectrum of single crystals of red HgI_2 at 77.3°K comprises a narrow line at 5330 Å, which is observed against the background of a step of the continuous absorption.** Investigation of the absorption spectrum of single crystals at 4.2°K showed that at this temperature this line is displaced to 5296 A and that in addition there appears a weak line at 5321 A; the continuous absorption step is shifted to 5260 Å and against it one can discern a weak line having a wavelength of 5238 Å. All these components of the structure are fully polarized with the electric vector being perpendicular to the optical axis of the crystal.

Investigation of the absorption spectra of polycrystalline layers of red HgI_2, having a fraction of the thickness of the investigated single crystal, made it possible to detect some other characteristics of the absorption in the short-wave region. In addition to the structure observed for single crystals, in the spectra of the polycrystalline layers we observed an intense absorption line located at λ = 4932 Å at 77.3°K;*** at 4.2°K this line is shifted to 4886 Å and the edge of a second continuum step becomes discernible at 4820 Å. Further, in the ultraviolet region in the absorption spectra of very thin polycrystalline layers there appear two wide absorption bands with peaks at 3960 Å and 3725 Å (at 77.3°K), the latter band being the more intense. It is interesting to note that whereas the lines observed near the absorption edge are very narrow and resemble atomic lines (at 4.2°K, for example, the lines in the spectrum of single crystals are comparable to the atomic lines in the standard reference spectrum of iron), the above mentioned bands in the region of characteristic absorption have an entirely different character. The band counters are very wide (100-150 Å, i.e., ~0.1 ev) bell-shaped peaks.****

Thus the absorption spectrum of crystals of red HgI_2 has a complex and diversified structure (lines, bands and steps of continuous absorption) extending over the spectral range from 5330 Å to 3725 Å (at 77.3°K). The equivalent energy width of this region is about 1 ev (see Fig.1,a).

According to the investigations of Dykman & Pekar[12] two types of excitons - nonpolarizing and polarizing - may be excited in ionic crystals. They indicate that there may be a case when low-lying excited states are nonpolarizing, while the high-lying states are polarizing. Optical excitation of nonpolarizing excitons leads to the formation of narrow lines, while the excitation of polarizing excitons leads to the appearance of wide (~0.1 ev) absorption bands. In view of these deductions of theory it would appear logical to associate the narrow lines in the absorption spectrum of red HgI_2 with the excitation of nonpolarizing excitons in the crystal lattice. The wide bands can then be attributed to the formation of polarizing excitons associated with

---

*We take this opportunity to thank N.M.Reinov, director of the Cryogenic Laboratory of the Leningrad Physical-Technical Institute, for his assistance in the work with liquid helium.

**A full report of our investigation of the absorption spectra of red HgI_2 was published earlier[6]. Absorption in crystals of red mercuric iodide has also been investigated by Nikitine and his coworkers[9,10].

***Judging by the reflection spectra for single crystals, this line is polarized with E ∥ C.

****A similar absorption spectrum with narrow lines at the edge and wide bands in the midst of the fundamental absorption region was also observed by us for superthin PbI_2 single crystals[6].

higher lying excitation levels in the red mercuric iodide crystal.

We felt that this interpretation of the observed structure of the spectrum of red HgI_2 as an exciton structure required experimental verification. It might be supposed that in addition to the ions of the HgI_2 crystal lattice, the absorption might be due to excess (sur-stoichiometric) Hg and I atoms or ions, different types of defects and extraneous impurities. If these "irregularities" are to be held responsible for the structure of the absorption spectrum, it must be assumed that they are present in a concentration comparable to that of the atoms of the HgI_2 lattice, that is, in a concentration capable of insuring the very high ($\sim 10^5$ cm^{-1}) absorption coefficient observed in the lines and bands of the structure. This consideration alone makes it impossible to attribute the observed structure to extraneous impurities and makes any such attribution at least improbable where irregularities of the lattice are concerned. Accordingly, we undertook a series of special experiments to investigate the absorption spectra of crystals of red HgI_2 containing a large excess of Hg. Our initial materials for preparing these crystals were a) mercurous oxide that had decomposed into HgI_2 and Hg and b) mercuric iodide comprising a large addition of metallic mercury. No significant difference between the spectra of these crystals and the spectra of crystals of ordinary HgI_2 crystals was observed. The introduction of excess iodine into the HgI_2 lattice, as Chepur[13] showed, leads to the appearance of an additional absorption band located at 5900 Å at room temperature, i.e., in an entirely different spectral region than occupied by the structure in question (the closest 5330 Å line referred to above is shifted at most to 5530 Å when the crystal is heated to 20°). Thus, we have proved experimentally that the observed structure is not due to stoichiometrically excess Hg or I atoms and ions.

Comparison of the absorption spectra of single crystals and polycrystalline layers shows that the absorption lines in the spectra of polycrystalline layers are somewhat less sharp and in some cases are displaced relative to the position of the corresponding lines in the spectra of single crystals. This may be explained by the fact that different defects frozen into the rapidly cooled layers distort and diffuse the energy levels existing in a perfect HgI_2 lattice; a certain minor displacement of the lines may also be due to stresses in the lattice. The defects themselves, however, are not evinced in the spectrum, at any rate in the case of thin layers, and, consequently, are not the cause of the observed absorption structure. Thus, although definitive proof that the structure is associated with excitons must be predicated on quantitative measurements of absorption coefficients, the results of the above described experiments and a number of other considerations are convincing evidence in favor of this hypothesis. Thus, it can safely be asserted that the discrete structure of the absorption spectrum is due to the excitation of excitons in the crystal lattice of the red modification of HgI_2.

2. Absorption spectra of crystals of rhombic HgI_2, $HgBr_2$ and HgI

We found no discrete structure in the absorption spectra of the yellow modification of mercuric iodide (Fig.1,b). Single crystals of yellow HgI_2 (obtained by sublimation; d = 50 μ) exhibit only a diffuse absorption edge located in the vicinity of 3990 A (at 77.3°K). With increasing thickness of the specimens this diffuse edge is displaced to the short-wave side. In the case of thin (d = 0.1 μ) fused polycrystalline layers this absorption edge appears at 3750 Å. This is indicative of a monotonic increase in the coefficient of absorption with decreasing wavelength and of the absence of any struc-

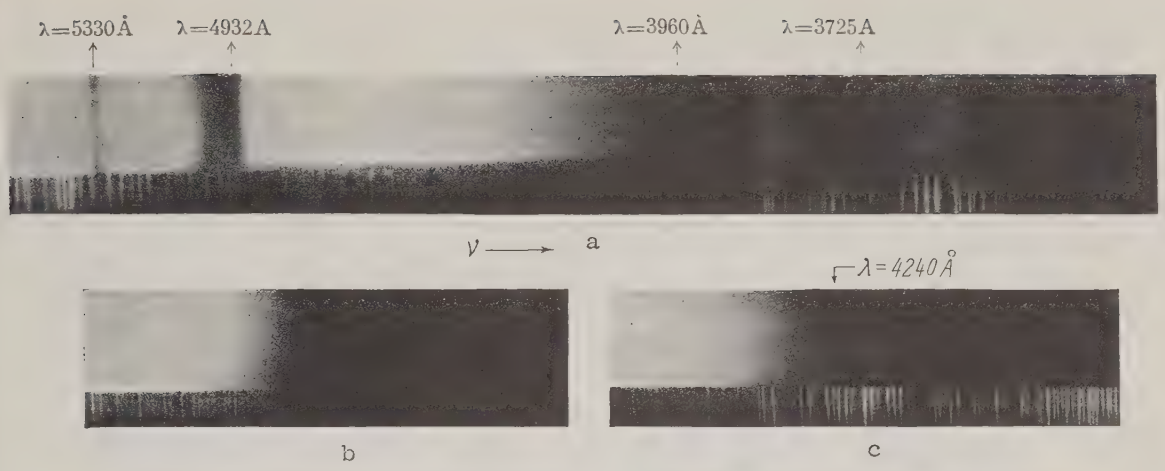

Fig.1. Absorption spectra of mercury iodide crystals at 77.3°K: a) red modification of HgI_2, b) yellow modification of HgI_2, and c) HgI.

ture near the absorption edge in the spectrum of crystals of yellow HgI_2. With the transition of the yellow form to the red, structure appears in the absorption spectra. The reverse transformation (for example, induced by heating) leads to disappearance of the structure.

In addition to the spectra of the yellow modification of HgI_2, we investigated the absorption spectra of $HgBr_2$. The rhombic lattice of mercuric bromide is fully isomorphic with the lattice of yellow HgI_2 and these two compounds yield an extensive continuous series of mixed crystals. The absorption spectrum of $HgBr_2$ crystals is entirely similar to the spectrum of yellow HgI_2. It is also devoid of structure and has only a diffuse absorption edge which shifts to the short-wave side with increasing thickness of the specimens. In the spectrum of $HgBr_2$ crystals (grown from an acetone solution; d = 50 μ) it is located at about 3050 Å (at 77.3°K), while in the spectrum of fused polycrystalline layers (d = 0.5 μ) it is observed at 2900 Å.

Thus, the results of our investigation of the absorption spectra of the crystals of two modifications of HgI_2 and of $HgBr_2$ all indicate that the structure of the lattice exerts a strong influence on the exciton levels in the crystals. Reconstruction of the lattice incident to the transformation from one modification to the other produces a radical change in the appearance of the absorption spectra. The complex structure clearly evident in the spectrum of the red modification of HgI_2 vanishes entirely when we go over to the yellow modification. Apparently, in this case, a necessary condition for the existence of a discrete structure in the absorption spectrum is a specific type of lattice.

In going over from one modification of HgI_2 to the other the ionic character of the bonds persists and the laminar structure typical of HgI_2 is retained; there is little change in the separation between particles and the transformation energy is very low. Consequently, the principal difference between the yellow and red modifications of HgI is in the lattice geometry. It would appear, therefore, that it is precisely the geometry of the crystal lattice that exerts so strong an influence on the exciton levels in HgI_2.

It is possible that an important role is played by the symmetry of the lattice (the red tetragonal form of HgI_2 belongs to the middle, while the yellow rhombic modification belongs to the lowest type of symmetry). It may be that a significant factor is the character of the first coordination spheres in the lattice. Thus, in the lattice of red HgI_2 each Hg ion is located at the center of a regular tetrahedron of four I ions. In the lattice of the yellow modification, on the other hand, each Hg ion is surrounded by six irregularly arranged I ions.

It is possible that both these structure elements - the lattice symmetry and the coordination spheres - jointly exert a strong influence on the excitation levels in the crystals. We investigated the absorption spectrum of crystals of mercurous iodide HgI which obviously differs HgI_2 as regards stoichiometric ratio of Hg to I. Like that of HgI_2, the lattice of HgI is tetragonal, but the coordination spheres in the HgI lattice are more complicated and irregular. We studied the absorption spectra of single crystals obtained by sublimation of the salt as well as of fused and "smoked on" polycrystalline layers. In the spectra of single crystals ($d \approx 50$ μ) at 77.3°K, we observed only the two close absorption edges associated with the ordinary and extraordinary rays (minor dichroism) at $\lambda = 4350$ A. No fine structure was observed in the spectra of single crystals. In the spectra of thin (0.5 μ) polycrystalline layers there appeared a wide band just below the continuous absorption (Fig.1,c). The center of the band is located at 4240 Å (at 77.3°K); its width is 100-150 Å (~0.1 ev). On the basis of its appearance, this band may be attributed to the excitation of polarizing excitons in the HgI lattice. This would indicate that the influence of the lattice structure may be different where the levels of the polarizing and nonpolarizing excitons are concerned.

Although our experiments show that the type of lattice undoubtedly has a considerable influence on the exciton levels in crystals, we cannot yet with any certainty identify the elements of the lattice structure predominantly responsible. Our investigation was devoted mainly to the Hg-I system and before any more definite conclusions can be drawn there must be a more extensive experimental study of the absorption spectra of the crystals of both polymorphous and isomorphous compounds.

3. Structure of the absorption spectra and the internal photoeffect in crystals of the two modifications of HgI_2

Our investigation of the two crystal modifications of HgI_2 has made it possible to substantiate the existence of a relationship between exciton absorption of light and photoconductivity. The hypothesis regarding the important part played by excitons in the internal photoeffect is based on certain characteristics of the photoconduction process[14] and on the fact that in the case of many substances the peak of the spectral sensitivity curve is located at the principal absorption edge of the crystal, i.e., at the wavelength where the exciton line-absorption appears[15]. It has also been noted[15] that there is a parallelism between the presence of line-absorption in crystals and their strong photosensitivity. In view of this, comparison of the photosensitivities of the two modifications of HgI_2 is of particular interest inasmuch as the absorption spectra of these modifications differ greatly from each other, while the compound involved is the same. The strong photosensitivity of the red modification of HgI_2 has been remarked on by a number of investigators[16, 17 & 18]. Our earlier measurements [18] of the photosensitivity of yellow HgI_2 showed that its photosensitivity is much lower than that of the

red modification.

Thus we find that the crystals of red mercuric iodide which have an exciton line structure at the absorption edge possess a high photosensitivity, while the crystals of the yellow modification, which are devoid of any structure at the absorption edge, show almost no photoeffect. This parallelism between the presence of an exciton line structure in the absorption and the photoconductivity exhibited by the crystals of two modifications of the same substance is convincing evidence of the important part played by excitons in the internal photoeffect.

Physical-Technical Institute of the
Academy of Sciences of the USSR

References

1. E.F.Gross & N.A.Karryev, Doklady AN SSSR, 84, 471 (1952).
2. E.F.Gross & B.P.Zakharchenia, Doklady AN SSSR, 90, 745 (1953).
3. M.Hayaski & K.Katsuki, J.Phys.Soc.Jap., 7, 599 (1952).
4. S.Nikitine, G.Perny & M.Sieskind, C.R., 238, 67 (1954).
5. E.F.Gross & M.A.Iakobson, Zhur.tekh.fiz., 25, 364 (1955); Doklady AN SSSR, 102, 485 (1955).
6. E.F.Gross & A.A.Kaplianskii, Zhur.tekh.fiz., 25, 2061 (1955).
7. S.Nikitine & G.Perny, C.R., 240, 64 (1955).
8. E.F.Gross & A.A.Kaplianskii, Zhur.tekh.fiz., 25, 1661 (1955).
9. S.Nikitine, M.Sieskind, L.Couture & G.Perny, C.R., 238, 1786 (1954).
10. S.Nikitine & M.Sieskind, C.R., 240, 1324 (1955).
11. S.Nikitine, C.R., 241, 629 (1955).
12. I.M.Dykman & S.I.Pekar, Doklady AN SSSR, 83, 825 (1952).
13. D.V.Chepur, Radiotekhnika i elektronika, 2, No.2 (1957).
14. V.P.Zhuze & S.M.Ryvkin, Doklady AN SSSR, 76, 241 (1951); Izv.AN SSSR, Ser.fiz., 16, 93 (1952).
15. E.F.Gross & M.L.Belle, Zhur.tekh.fiz., 25, 948 (1955).
16. L.Bergmann & J.Hänsler, ZS.f.Phys., 100, 50 (1936).
17. E.K.Putseiko, Izv.AN SSSR, Ser.fiz., 16, 34 (1952).
18. Kämpf, Ann.d.Phys., 66, 463 (1921); ZS.f.Phys., 38,104 (1926).

TRANSACTIONS OF THE FIFTH CONFERENCE

ON THE

APPLICATION OF X-RAYS TO THE INVESTIGATION OF MATERIALS

(Leningrad, 23-29 June 1955)

(Conclusion from Nos. 6 and 7 of Vol. 20)

EXPERIMENTAL VERIFICATION OF THE INFLUENCE OF ANISOTROPY OF THE CRYSTALLITES ON THE SHAPE OF THE DEBYE RING IN THE X-RAY PATTERN OF STRESSED SPECIMENS

- G. I. Aksenov & V. A. Moshchanskii

In 1929 one of the present authors[1] carried out a theoretical analysis of the conditions of reflection of monochromatic x-rays from the atomic planes in a linearly stressed polycrystalline aggregate and showed that elastic deformation must produce displacement of the Debye lines in the x-ray patterns. In 1934 this theoretical analysis was extended to take into account the anisotropy of the elastic properties of crystallites and it was shown that, in addition to displacement, the Debye lines must undergo some diffusion or broadening[2]. The fundamental equation for the displacement of the Debye lines deduced from the Bragg equation is

$$\Delta\theta = - 2\frac{d' - d}{d} \tan\frac{\theta}{2} ,$$

where θ is the Bragg glancing angle, d is the interplanar distance before deformation and d' is the distance after deformation. It will be seen from this equation that the displacement is directly proportional to the magnitude of the strain and to the glancing angle.

By going over to tensor concepts, one can transform this equation so that it will comprise the dependence of the displacement of the Debye line on the elastic constants of the material, the direction in which the displacement is measured, the angle of incidence of the x-rays and certain other factors.

The experimental results of the investigation of Ref.2 yielded a partial substantiation of the theoretical calculations but, as the author pointed out, in order to determine fully the mechanism of deformation of the individual crystallites, it is necessary to solve the two- and three-dimensional problem and carry out a systematic experimental verification of the theoretical deductions.

The present authors, utilizing the earlier procedure, carried out a theoretical calculation of the conditions of reflection of monochromatic x-rays taking into account the anisotropy of the elastic properties of crystallites for the (112) and (310) faces of iron and the (511) crystal face of aluminum.

This theoretical analysis showed the following:

a) deformation under tension (elongation) must produce a displacement of the Debye lines: instead of the circle obtained in the case of an unstressed specimen there must be observed an elipse with semiaxes $a < b$;

b) the displacement of the Debye lines for the same stress should differ for different faces; thus for the (511) face the displacement should be greater than for the (310) face; the lines associated with the (112) face should not shift to any extent;

c) the displacement of the Debye lines should increase with increasing stress;

d) the lines should also undergo diffusion or broadening under elastic strain; the diffusion of the lines associated with all the faces in question should be greater than their displacement;

e) the character of the diffusion should differ for different lines: for the (310) face the greatest broadening should occur along the diagonal directions of the quadrants; for the (112) face the greatest diffusion should occur along the vertical axis, while for the (511) face the greatest broadening should be observed along the horizontal axis.

The experimental verification of the theoretical deductions was carried out on a specially designed back-reflection camera incorporating an ionic

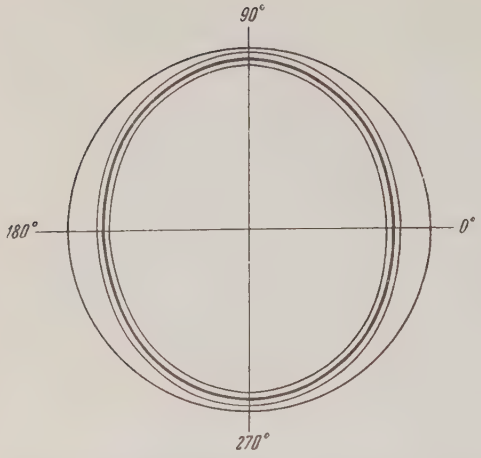

Fig.1. Displacement of the Debye lines under elastic deformation: circle - Debye ring prior to deformation of the specimen; elipse - after deformation.

x-ray tube. The camera had a special device for stressing the specimen in pure bending; the film holder in the form of a disc was designed to record the complete Debye ring pattern.

The stress in the specimen was measured by means of resistance sensing elements mounted on the specimen and connected to a Wheatstone bridge; the arrangement was calibrated with reference to a strain gage up to the elastic limit of the specimen.

The following x-ray patterns were recorded for each face: three for the initial unstressed state, three for each loading below the elastic limit, two for each loading beyond the elastic limit and one with the specimen unloaded.

Analysis of the x-ray patterns yielded the following results:

a) the Debye lines are displaced under elastic strain (Fig.1): the initial circle is deformed to an elipse;

b) the numerical values for the displacement (ΔS) of the Debye line at two values of the stress (σ) are listed in the accompanying table; it will be seen that there is close agreement between the experimental and theoretically calculated values; according to the calculations there should be virtually no displacement of the line associated with the (112) face and this was substantiated by the patterns of the reflections from this face (a nearly perfect circle is obtained for both the stressed and unstressed states);

c) the magnitude of the displacement for the (310) and (511) faces increases with increasing stress; the proportionality between the displacement and the stress breaks down near the elastic limit; whereas at stresses below the elastic limit the initial Debye ring is distorted to an elipse, above the elastic limit it degenerates into a line that is nearly circular.

The diffusion of the Debye lines was investigated by means of an MF-2 microphotometer. Preliminary measurements showed that although there is some angular anisotropy of the broadening it is very minor; consequently, in all cases the patterns were photometered only along the horizontal axis.

Figs.2, 3 & 4 show the results obtained for the x-ray patterns of the reflections from the (112), (310) and (511) faces of the specimens in the unstressed and the stressed states. It will be seen that the separations between the components of the doublet remain constant.

(310) face; σ=20 kg/mm²			(511) face; σ=10 kg/mm²		
Angle, degr.	ΔS, мм		Angle degr.	ΔS, мм	
	theo.	exp.		theo.	exp.
0	0,63	0,62	0	0,59	0,67
45	0,59	0,58	45	0,57	0,60
90	0,56	0,49	90	0,53	0,56

With increasing stress the peaks become lower, while the saddle between the peaks rises, which indicates increasing diffusion of the Debye lines. It must be noted that the broadening begins in the region of elastic deformation, which is in accord with the predictions of theory, and in some cases is very appreciable. Thus, for the (310)

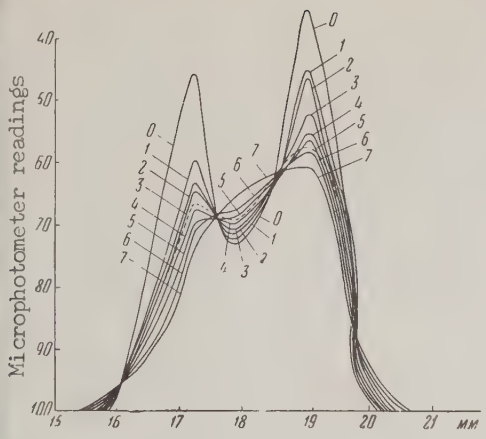

Fig.2. Results of photometric measurements of the x-ray patterns from the (112) face of a 60 S2 (60 C2) steel specimen under the following stresses: 0) 0, 1) 10, 2) 20, 3) 30, 4) 40, 5) 50, 6) 60, 7) 70 Kg/mm^2. Elastic limit $\sigma_S \approx 40$ kg/mm^2. Dash line - photometric curve obtained from the pattern for the unloaded specimen.

and (112) faces the broadening is so great that the doublet, which is still distinguishable close to the elastic limit, is completely diffused and indistinguishable as such beyond the elastic limit. In the case of the (511) face the diffusion is much weaker and the doublet remains discernible even beyond the elastic limit.

Photometric measurements for the unloaded specimen (the external stress was removed after straining beyond the elastic limit - see dash line curves in the figures) show that the diffusion of the lines is reduced but not entirely eliminated. The doublets in the patterns for the (310) and (112) faces, which are wholly diffused beyond the elastic limit, reappear in the unloaded specimen pattern. The width of the lines for the unloaded specimen is somewhat greater than for the specimen in the initial state. This shows that residual strains persist in the specimens stressed beyond the elastic limit.

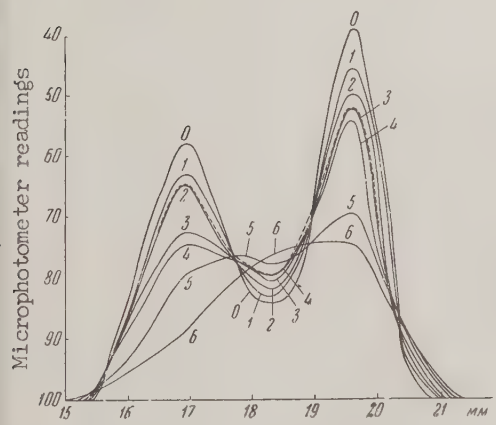

Fig.3. Results of photometric measurements of x-ray patterns from the (310) face of a 60 S2 steel specimen under the following stresses: 0) 0, 1) 10, 2) 20, 3) 30, 4) 40, 5) 50, 6) 60 kg/mm^2. Elastic limit $\sigma_S \approx 40$ kg/mm^2. Dash line - photometric curve obtained from the pattern for the unloaded specimen

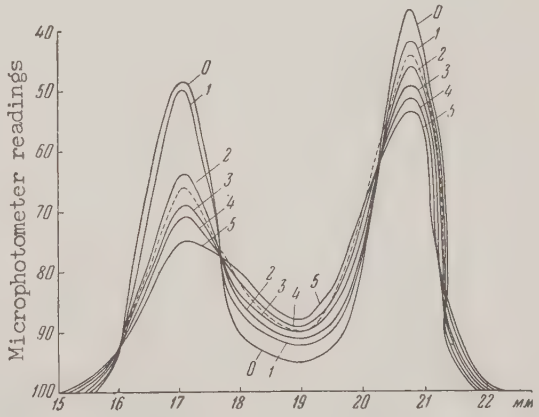

Fig.4. Results of photometric measurements of the x-ray patterns from the (511) face of a duraluminum specimen under the following stresses: 0) 0, 1) 5, 2) 10, 3) 15, 4) 20 5) 30 kg/mm^2. Elastic limit $\sigma_S \approx 18$-20 kg/mm^2. Dash line - photometric curve obtained from the pattern for the unloaded specimen.

Conclusions

1. The fact that the results of our theoretical analysis of the conditions of reflection of monochromatic x-rays from the atomic planes in a linearly stressed polycrystalline specimen taking into account the anisotropy of the crystallites are in very close agreement with the experimental results is, we feel, proof that the anisotropy of the crystallites influences the behavior of polycrystalline material under elastic deformation.

Under loads up to the elastic limit the stress field in a polycrystal is inhomogeneous. There are breaks or discontinuities in the force field in going from one crystallite to another when their crystallographic orientations are different. In view of this the shape of the Debye ring changes as the specimen is stressed.

2. We did not obtain complete agreement of the theoretical results with experiment; the minor divergence is due to the fact that in the theoretical calculations we assumed free anisotropic deformation of the crystallites without taking into account the interaction of the contacting crystallites or the possible influence of the intercrystalline material. Obviously, in a rigorous analysis these factors cannot be neglected inasmuch as the crystallites being in intimate contact with each other cannot but affect the character of the deformation of their neighbors and, consequently, of the polycrystalline specimen as a whole.

3. Kitaigorodskii[3], Rovinskii[4] and other investigators suggest that the x-ray criterion for the presence of stresses of the first kind is displacement of the lines on the patterns and that the principal criterion for presence of stresses of the second kind, which develop beyond the elastic limit, is diffusion or broadening of the lines.

Our theoretical calculations substantiated by experiment show, however, that diffusion of the lines begins in the region of elastic deformation far below the elastic limit. In view of this we must question the validity of the above mentioned criteria for stresses of the first and second kinds.

Our x-ray patterns showed that the diffusion of the lines occurring under the elastic limit are characterized by a residual diffusion. This shows that in this case residual strains persist in polycrystalline specimens.

4. In order to obtain the most accurate results in measuring stresses by the x-ray method it is essential to select the face and the azimuth on the Debye ring for which the displacement of the line will be maximal.

5. The modulus of elasticity determined by the x-ray method differed from the modulus determined by the mechanical method. The moduli differ from each other not only as regards numerical value but also in that the mechanical modulus is isotropic whereas the x-ray modulus of elasticity is anisotropic.

6. Beyond the elastic limit the mechanical interaction between the individual crystals becomes so appreciable and the deformation of the crystals attains such a magnitude that we have the advent of complete averaging of the individual anisotropic properties of the crystallites in consequence of which the polycrystalline specimen begins to behave as an isotropic entity.

Faculty of Metal Research of the
"A.A.Zhdanov" Gorki Polytechnic Institute

References

1. G.I.Aksenov, Zhur.tekh.fiz., 6, 3 (1929).
2. G.I.Aksenov, Zhur.eksp. i teor.fiz., 4, 627 (1934).
3. A.I.Kitaigorodskii, Rengenostrukturnyi analiz (X-Ray structural analysis), M.-L. 1950.
4. V.M.Rovinskii, Zhur.tekh.fiz., 18, 1273 (1948).

TRANSACTIONS OF THE FIRST CONFERENCE ON FERROELECTRICITY

(Leningrad, 19-24 June 1956)

SURVEY OF SOME OF THE RESULTS OF RECENT INVESTIGATIONS OF FERROELECTRIC MATERIALS

- G.A. Smolenskii

The problem of ferroelectricity is one of the most important problems in solid state physics. Investigation of ferroelectric effects yields direct information on the nature of crystals. At the same time such studies are of intrinsic interest particularly in view of the increasing application and use of ferroelectric materials in diverse engineering fields.

The principal distinctive characteristic of ferroelectrics is the presence of a phase transition of the first or second order from the disordered to the ordered polarized state. As a result of spontaneous polarization ferroelectrics exhibit more or less pronounced anomalies of their electric and other properties as compared with ordinary ionic crystals. Ferroelectrics are also characterized by spontaneous deformations and lower symmetry of the lattice at temperatures below the Curie point.

The presence of spontaneous polarization can be explained in the framework of classical electrostatic interaction inasmuch as the internal field is determined by the interaction of dipoles due to ionic displacements. Naturally, a significant part in the process is played not only by long range forces, i.e., dipole forces, but also by short range forces. Spontaneous polarization occurs only in the case when the elastic component of the restoring force arising due to displacement of the ions is weaker than the dipole forces.

In contrast to the case of ferroelectrics in which, at temperatures below the phase transition point, the ions of one type are all shifted in one direction, in antiferroelectrics the ions are displaced antiparallel and the net spontaneous polarization in such crystals equals zero. Ferro- and antiferroelectrics are in a sense electric analogs of ferro- and antiferromagnets. In certain crystals the ions of one type can be displaced either parallel or antiparallel to each other depending on the external conditions (temperature, pressure and electric field). There is no point in attempting to classify such crystals as ferroelectric or antiferroelectric; it is more expedient simply to indicate that under a given set of conditions they are in the ferroelectric state and under other conditions in the antiferroelectric state.

All the known ferroelectrics and antiferroelectrics may be divided into two principal groups: 1) ferroelectrics and antiferroelectrics containing hydrogen (Rochelle salt, the phosphates and arsenites of potassium and similar compounds) and 2) ferroelectric and antiferroelectrics not containing hydrogen (barium titanate, lead titanate, potassium niobate, etc.). The structure and properties of the materials in these two groups differ appreciably. All the ferroelectric and antiferroelectrics of the second group are characterized by an octahedral arrangement of the oxygen ions surrounding the comparatively smaller cation. Hence, hereinafter we shall refer to the latter as ferroelectrics and antiferroelectrics of the oxy-octahedral type. The basic physical theory of ferroelectric effects was developed by Kurchatov in the late thirties and early forties in connection with extensive investigations of Rochelle salt and isomorphous crystals[1]. At that time Kurchatov suggested that the appearance of spontaneous polarization in ferroelectrics is explicable in the framework of classical electrostatic interaction. The ferroelectrically active ion, i.e., the ion responsible for spontaneous polarization in Rochelle salt, potassium arsenites and phosphates and other crystals containing hydrogen is apparently the hydrogen proton. It is, however, difficult to determine the

location of the proton in the complicated structure of these crystals. Moreover, Rochelle salt is very brittle and decomposes at a relatively low temperature. In the arsenites and phosphates of potassium spontaneous polarization appears at low temperatures. These various factors hindered further investigation of ferroeletric materials and severely limited their practical application.

The discovery by Vul and Gol'dman[2] of a new ferroelectric, namely, barium titanate which crystallizes in the simple perovskite lattice, has a relatively high Curie point (120°) and is characterized by good mechanical strength and thermostability, played an important part in the development of our present understanding of ferroelectric effects. This discovery served as the point of departure for many investigations of ferroelectrics of the oxy-octahedral type and led to the creation of a new group of engineering materials.

The principal properties of polycrystalline barium titanate were first investigated in detail by Vul and his coworkers[3,4]. Their reports, however, covered only a few early studies of single crystals.

I. New Data on Barium Titanate Single Crystals

Single crystals of barium titanate came to be studied later than polycrystalline specimens. Investigation of single crystals is of considerable interest, for such investigations allow of studying the properties of the material in purer form, which is important for development of ferroelectric theory; moreover, in working with single crystals the domain structure can be observed.

The preparation of single crystals of barium titanate and other ferroelectrics is not only of scientific interest but also of practical value. Barium titanate single crystals are now being tested and used in various computers.

At first investigators found it difficult to grow single crystals more than a few millimeters in length, but later they succeeded in obtaining large single crystals with a rib length of several centimeters.

At present there are three basic procedures employed in growing barium titanate single crystals:

1) growth from the melt[5];

2) growth from a solution of its component compounds in fused barium chloride (the Blattner method[6]);

3) growth from a solution of barium titanate in a melt of potassium fluoride (the Remeika method[7]).

The first method consists of direct crystallization of barium titanate from the melt. The barium titanate with 1-2% strontium carbonate is heated in a platinum crucible in an inert atmosphere of nitrogen to the melting point of barium titanate ($\geq$ 1600°) and then slowly cooled. The barium titanate crystallizes in cooling. An important factor in the process is the temperature gradient in the furnace. At 1300° the nitrogen is replaced by oxygen. Barium titanate single crystals measuring several centimeters in length have been obtained by this procedure.

The second procedure does not require so high a temperature. It is based on heating a finely powdered mixture of barium chloride, barium carbonate and titanium dioxide in a corundum crucible to 1150-1300°. The barium chloride fuses at 962°; then the other two components begin to dissolve in it and interact. The mixture is held for some time at the maximum temperature to allow the solution to go to completion and then slowly cooled. The solubility

decreases with decreasing temperature and the barium titanate comes out of the solution, forming single crystals.

Different investigators recommend different proportions of the components. Better results are obtained if the amount of barium carbonate is taken somewhat in excess of the amount necessary for the formation of barium titanate. Commonly the initial materials are taken in the following proportions (in moles):

$$BaCl_2 : BaCO_3 : TiO_2 = (1\text{-}3.3) : (1.4\text{-}1.5) : 1.$$

Thin single crystal plates measuring several centimeters on edge have been grown by this procedure.

The third procedure consists of heating a finely powdered mixture of chemically pure barium titanate (30%) and chemically pure anhydrous potassium fluoride (70%) with a small amount of ferric oxide (0.2%) in a closed platinum crucible to 1150-1200°. The mixture is held for several hours at this temperature. The ferric oxide is added to improve the electric properties of the crystals.

After an appropriate period of heating the crucible is cooled at the rate of 30-70° per hour. At 850° the excess melt may be poured off. The single crystals formed remain in the crucible. By this method one can obtain thin single crystal plates measuring up to 1-2 cm with domains in which the spontaneous polarization is normal to the plane of the plate; this is a necessary condition for obtaining a rectangular hysteresis loop.

It is extremely difficult to determine the small displacements of the ions in barium titanate in the ferroelectric region. It has apparently been possible to do this more accurately by the neutron diffraction technique than was feasible by x-ray diffraction. The data reported by different investigators are listed in Table 1.

Table 1

Results of investigations of ionic displacements (δz, Å) in barium titanate by x-ray and neutron diffraction techniques

Ion*	X-ray studies			Neutron diffraction, Frazer et al
	Känzig	Evans I	Evans II	
O_I	−0,13	−0,10	−0,02	−0,04
Ti	+0,06	+0,05	+0,14	+0,12
Ba	0	0	+0,08	+0,06

*z for O_{II} is assumed to be $\frac{1}{2}c$ (a=3,986, c=4,026 Å). The oxygen ions are designated in the usual manner.

The temperature dependence of the dielectric constant and spontaneous polarization of single-domain barium titanate crystals has been investigated by Merz[9]. However, the first "single-domain" crystals obtained by Merz apparently had antiparallel domains. Later he prepared and made measurements on higher quality single crystals which were distinguished by a higher spontaneous polarization ($26 \cdot 10^{-6}$ Coulomb/cm^2 at room temperature), a lower dielectric constant along the ferroelectric axis (ϵ_c = 160) and a rectangular hysteresis loop[10].

The coercive force of ferroelectric materials depends to an appreciable extent on the quality of the specimens. It is not surprising therefore to find a considerable divergence between the results of different investigators[11,12]. Merz's "single-domain" crystals are characterized by a minimum value of the coercive force. Merz reports that as the temperature is reduced the coercive force increases from 250 v/cm at 180°K to 10,000 v/cm at 4.2°K.[11]

We have already noted that spontaneous polarization is accompanied by spontaneous deformation. Merz[9] showed that the relative change in the lattice constant in the tetragonal phase is approximately proportional to the square of the spontaneous polarization. The birefringence, in turn, proves to be proportional to the deformation.

The piezoelectric behavior of barium titanate single crystals in the tetragonal region has been studied in detail by Caspari and Merz[13-15]. The piezoelectric coefficient d_{31} at different temperatures was determined from the contraction of the crystal in an applied dc field. In order to eliminate the influence of strains due to rearrangement of the domains, the crystals were prepolarized in a strong field (10,000 v/cm applied for two days). The average value of d_{31} obtained from measurements on six crystals at room temperature was $-1.1 \cdot 10^{-6}$ cgse units (statcoul/dyne).

Interesting results were obtained by these investigators in studying the temperature dependence of the resonance frequency f_r and antiresonance frequency f_a of prepolarized crystals. It was found that in crystals with large internal strains (poor crystals) the resonance frequency f_r has a minimum at a temperature a few degrees below the transition point as determined from the dielectric constant peak; the frequency difference $\Delta f = f_a - f_r$ reaches a maximum value at this temperature. Such single crystals exhibit only a slight piezoelectric response above the Curie point. In single-domain crystals with a minimum of internal strain and no domains perpendicular to the thickness of the crystal plate (good crystals) the resonance frequency drops off rapidly near the Curie point and does not rise again. No piezoeffect is observed in these good crystals above the Curie point.

Observations of optical characteristics show that most prepolarized crystals, when heated, break up into domains somewhat below the Curie point. The minimum resonance frequency f_r and the maximum frequency difference $\Delta f = f_a - f_r$ are observed at the temperature at which the transformation from a single-domain to a multidomain crystal occurs. In poor crystals this fragmentation into domains occurs at lower temperatures as compared with good crystals. It may be assumed that due to the influence of internal strains, in poor crystals different parts of the crystal are transformed to the cubic structure at different temperatures as a result of which the transition is realized over a certain temperature range.

The above named investigators explain the minimum in the resonance frequency curve near the Curie point by the fact that the elastic coefficients are small in the region of the phase transition.

The absolute value of the piezoelectric coefficient d_{33} is 2.3 times greater than that of d_{31}.

Bond, Mason & McSkimin[16] determined the elastic and piezoelectric coefficients of large ($\sim$1 cm edge) barium titanate single crystals at room temperature by the dynamic method. In this case the piezoelectric coefficients were found to be appreciably larger than those reported by Caspari & Merz: $d_{31} = -3.1 \cdot 10^{-6}$ and $d_{33} = 9.5 \cdot 10^{-6}$ statcoulomb/dyne. The value of the electromechanical coupling coefficient ($k = 0.675$) found by these investigators for a single crystal is appreciably greater than the value of the coupling coefficient for polarized polycrystalline specimens. These authors give the following values for the elastic constants of barium titanate single crystals (for constant electric induction):

$$C_{11}^{D} = 2.06 \cdot 10^{12} \text{ dyne/cm}^2,$$

$$C_{12}^{D} = 1.40 \cdot 10^{12} \text{ dyne/cm}^2,$$

$$C_{44}^{D} = 1.26 \cdot 10^{12} \text{ dyne/cm}^2.$$

The specific heat anomaly of barium titanate single crystals in the vicinity of the Curie point has been investigated by Blattner & Merz[17]. The temperature dependence of the specific heat curve for barium titanate has a rather flat maximum in contrast to the case of KH_2PO_4 for which this curve exhibits a sharp peak[18]. The latent heat calculated from the specific heat jump proves to be small:

$$Q = \int \Delta C dT = 47 \text{ cal/mole}.$$

The effect of pressure on the Curie point of barium titanate single crystals has been studied by Merz[19]. Up to about 2500 atmospheres the transition temperature decreases linearly with increasing pressure ($\Delta t/\Delta p = 5.74 \cdot 10^{-9}$ degree/bar).

After publication of Megaw's[20] reports on the temperature dependence of the lattice parameters of barium titanate, many investigators assumed that the phase transition at 120° is of the second order. Later investigators, however, observed a sudden change in birefringence[21] and spontaneous polarization[10] as well as temperature hysteresis of certain properties[22,23] of barium titanate at the 120° transition point, effects that are characteristic of first order transitions. Apparently as Roi[23] first suggested, a first order phase transition occurs in barium titanate at about 120°.

Merz[24] and Little[25] have published reports on the variation of the domain structure of barium titanate single crystals under the influence of an electric field. Investigating the changes in the direction of spontaneous polarization in single crystals under the influence of an external magnetic field, Merz came to the conclusion that this process occurs in two stages: the first consists of nucleation of new domains and the second of linear growth of these domains through the crystal. In contrast to the case in ferromagnets, in barium titanate no sidewise motion of the domain walls is observed. Merz attributes the absence of sidewise motion of the domain walls to the fact that the specific wall energy is relatively high (about 7 erg/cm^2 according to his calculations), while the wall thickness is relatively small so that displacement of the walls through even a small distance requires an excessive energy expenditure. The growth of the domains in the direction of the field occurs at an average rate of about $0.5 \cdot 10^4$ cm/sec in an applied field of 14,000 v/cm. The rate of growth increases with increasing temperature and field strength.

Little[25] made an optical study of the changes in domain structure under the influence of electric fields. She showed that in a single-domain crystal the application of a field perpendicular to the polar axis leads to the appearance of domains with the polar axis parallel to the field. The critical value of the field for the formation of these domains is 2.4 kv/cm and decreases as the Curie point is approached. Little found that at low frequencies the 90° walls oscillate under the influence of even a weak alternating field. In contrast to the case of Merz's electrical measurements, Little observed a sidewise displacement of the 180° walls which she explains by successive reorientation of the dipole moments of the boundary unit cells. The sidewise motion of the domain walls, however, is a slower process than the growth of new domains. Little also investigated some of the regularities of the dynamics of the 90 and 180° domain walls under the influence of electric fields.

In this survey we will not describe the results of work on growing barium titanate and other ferroelectric single crystals and investigations of their properties carried out in the Institute of Crystallography of the USSR Academy of Sciences and in Rostov State University, for these results will be given in separate reports to be presented at this conference.

II. Review of Microscopic Theories of Ferroelectric Effects

The theory of ferroelectric effects has developed concurrently with the accumulation of experimental data on ferroelectric materials.

The thermodynamic theory of ferroelectric phenomena on the basis of the general phase transition theory of Landau has been largely developed by Ginzburg[26]. The thermodynamic theory has been further developed and extended to single-domain crystals characterized by cubic symmetry above the Curie point by Devonshire[27], Shirobokov & Kholodenko[28,29], Kittel[30] and Smolenskii with Kozlovskii and Pasynkov[31,32].

In recent years there has been marked development not only of the thermodynamic theory but also of microscopic theory of ferroelectric effects.

A number of molecular theories have been proposed for explaining the behavior of barium titanate; among these particularly worthy of mention are the theory based on the model of local minima, the theory employing the model of anharmonic oscillators and the so-called electronic theory.*

Mason & Matthias[33] base their theoretical interpretation on the model in which the titanium ion has six equally probable positions corresponding to local potential energy minima in the unit cell. The authors argue that in view of the fact that the titanium—oxygen bond is partly homeopolar the equilibrium position of the titanium ion is not at the center of the octahedron but somewhat nearer to one of the oxygen ions. As a result of thermal motion, the titanium ions jump from one equilibrium position to another. At a sufficiently high temperature ($T > \theta$) the thermal energy is sufficient to cause any one of the six positions to be equally probable and the average position of the titanium ion concides with the center of the octahedral. At temperatures below θ the thermal energy is no longer sufficient for this and the titanium ion is displaced towards one of the oxygen ions.

According to Mason & Matthias the dipole polarization P_d due to nonsymmetric distribution of the ions over the potential wells has the following form:

$$P_d = N\mu \frac{\mathrm{sh}\,(\mu F/kT)}{2 + \mathrm{ch}\,(\mu F/kT)}\,, \qquad (1)$$

where F is the intensity of the effective field, N is the number of unit cells per unit volume and μ is the dipole moment of a unit cell. It is assumed that the intensity of the effective field is described by

$$F = E + \beta P = \frac{E + \beta P_d}{1 - \beta\gamma}\,, \qquad (2)$$

where E is the intensity of the average macroscopic field, β is the Lorentz coefficient and γ is the polarizability due to all polarization mechanisms except that of the titanium ion displacement. Mason & Matthias do not compute the Lorentz factor but find it from optical data. Thus their theory is semi-empirical.

---

*We shall not describe the work of V.Kh.Kozlovskii on the molecular dynamic theory of ferroelectrics inasmuch as he is scheduled to present a report at this Conference.

Further these authors calculate the Curie temperature, the dielectric constant above and below the Curie point, the relaxation frequency, the coercive force and the specific heat anomaly.

According to Mason & Matthias the dielectric constant in a weak field above the Curie point is given by

$$\varepsilon = \varepsilon_0 + \frac{4\pi}{\beta(1-\beta\gamma)} \cdot \frac{\theta'}{T-\theta'}, \tag{3}$$

where ϵ_o is the dielectric constant at low temperatures.

The measurements of Roberts[34] and other investigators have shown, however, that the temperature dependence of the dielectric constant near the Curie point is described by a formula without a constant term, namely,

$$\varepsilon = \frac{C_W}{T-\theta'}. \tag{4}$$

In Eqs.(3) & (4) θ' is always lower than the transition temperature θ for barium titanate as well as for other ferroelectrics. An analogous relationship is observed for ferromagnetic materials.

The maximum spontaneous polarization at low temperatures is given by

$$\frac{P_0^2}{Nk\theta'} = \frac{3}{\beta(1-\beta\gamma)}. \tag{5}$$

The value of $\beta(1-\beta\gamma)$ can be determined from different experimental data. From the temperature dependence of the dielectric constant at $T > \theta'$ we obtain $\theta' = 380^oK$ and $C_W = (1.5 \cdot 10^5)^oK$. Then from (3) and (4), we find

$$\beta(1 - \beta\gamma) = 0.032.$$

If we take $P_o = 26 \cdot 10^{-6}$ Coulomb/cm^2, $N = 1.56 \cdot 10^{22}$ cm^{-3} and $\theta' = 380^oK$, then from (5) we obtain

$$\beta(1 - \beta\gamma) = 0.39.$$

It will be seen that the two values differ by a factor of 12 which cannot be attributed to experimental errors. Jaynes[35] was the first to attempt calculations of this type; unfortunately, he used incorrect values for the spontaneous polarization.

Another difficulty encountered by this theory is connected with the change in entropy in going through the Curie point[35]. Presumably at $T > \theta$ the titanium ion can occupy six equilibrium positions in the unit cell, while at a temperature a few degrees below the Curie point it can occupy only one position. Thus in going through the Curie point the entropy changes by K ln 6 = 1.79 k (per unit cell). This value is 90 times greater than the experimental one. Smolenskii & Rasnykov[31] were the first to call attention to the anomalously great specific heat at the transition point.

Later Mason[36] introduced certain changes in his treatment of the above-described model. However, in this case, too, Mason incorrectly evaluated the effective fields acting on the ions.

Mason & Matthias, although they assume that the crystal is partially homeopolar, use charge values typical of ionic crystals in their computations. Furthermore, the mathematical treatment employed by these authors is valid only in the case when $U_o \gg F\mu$ and $U_o \gg kT$, where U_o is the height of the potential barrier between local minima. Actually $U_o \approx F\mu$ and consequently the

approximation made by Mason and Matthias is extremely rough. Furthermore, in Ref.33 they do not take into account the fact that at $T < \theta$ all the ions rather than only the titanium ions are displaced to some extent.

This model has been developed further in the extensive investigations of Bogdanov[37] and Glauberman & Lubchenko[38] which are devoid of some of the listed shortcomings. However, as follows from what has been said above and from the experimental results of Smolenskii and Pasynkov[31], the model of deep potential minima cannot be utilized for explaining the properties of barium titanate. It should be noted that if the titanium ion had several potential minima in the unit cell, relaxation dielectric polarization should occur in the nonferroelectric region. Actually no such relaxation processes have been detected in investigations of barium titanate single crystals extending over a wide range of frequencies and an appreciable temperature interval above the Curie point.

Smolenskii & Pasynkov[31] analyzed the model of local minima in its general form (i.e., for any number of local minima per unit cell). In their treatment they assumed that the number of local minima in a unit cell does not change incident to low-temperature transitions. First, they calculated the effective field using Skanavi's method of structural internal field coefficients. Next, they found the components of the polarization along the axes along which the ions may be displaced. As a result, they obtained a set of equations which was investigated in the absence of an external field for both nonorthogonal and orthogonal axes. They found that in the first case (nonorthogonal axes), there can exist only a single Curie point. The second case is of greater interst. As a result of their analysis of this case, Smolenskii & Pasynkov came to the conclusion that the model of local minima in the form of rather deep potential wells with steep walls cannot be used for explaining the properties of barium titanate. This is evidenced, according to their calculations, by the absence of nonlinear effects in the vicinity of the Curie point, the fact that the specific heat tends to become infinite at $T = \theta$, the excessively sharp drop in the dielectric constant beyond the Curie point and the absence of low-temperature phase transitions.

In other investigations the ferroelectric properties of barium titanate have been explained on the basis of the assumption that it is essential to take into account the anharmonic part of the energy of oscillation of the titanium ions. The model of anharmonic oscillators was first proposed independently by Ginzburg[26] and Devonshire[27]. Thanks to the calculations carried out by Slater[39] this model has been better developed than the local minima model. In treatments based on this model, it is assumed that the central ions in the oxygen octahedra perform anharmonic oscillations. The potential energy U of the titanium ion in the absence of a field is described by

$$U = c(x^2 + y^2 + z^2) + b_1(x^4 + y^4 + z^4) + 2b_2(x^2y^2 + x^2z^2 + y^2z^2), \qquad (6)$$

where x, y, z are the coordinates of the ion (the origin is taken at the equilibrium position), c is the elastic coupling coefficient and b_1 and b_2 are the anharmonicity coefficients.

The instantaneous position of the point dipoles formed incident to the displacement of the titanium ions relative to the center of the cell are assumed to be independent of each other. The interaction of the dipoles is taken into account by introducing an averaged field, determined by the influence of all the other dipoles on the given dipole. To this end a term eFr is introduced into the expression for the potential energy (e is the charge of the central ion, F is the effective field acting on the ion and r is the

radius vector extending from the center of symmetry of the cell to the ion). Thus Slater considers the anharmonic oscillations of the ions relative to centers whose positions in the unit cell depend on the intensity of the effective field.

To solve the problem Slater finds the free energy represented in the form of a power series in terms of components of the effective field F. He deduces the statistical integral of the system in which the expression under the integral sign is expanded in a series in terms of the anharmonic components of the ion energy. From this Slater deduces expressions for the entropy, polarization, spontaneous polarization and the polarizability of the ionic displacement. It follows from his calculations that the polarizability of the ionic displacement in the region where $T > \theta$ decreases with increasing temperature.

Slater further determined a number of parameters for barium titanate on the basis of the model of anharmonic oscillators. He came to the conclusion that the internal field acting on the titanium ions is appreciably greater than the usual Lorentz field $(4\pi/3)P$, primarily because of the influence exerted on the Ti ions by the O_I ions located on the same Z axis with the titanium ions. It must be noted that this very interesting deduction was arrived at considerably earlier by Skanavi[40]. The contribution of the titanium ions to the total polarization, according to Slater's calculations, is 37% (31% due to ionic displacement and 6% due to electronic polarization), while the contribution of the O_I type ions attains 59%. In shifting, the titanium ions polarize the O_I type oxygen ions, which in turn act on the titanium ions; as a result there is formed a chain of dipoles directed in the same direction, which leads to spontaneous polarization below the Curie point.

A satisfactory value ($1.2 \cdot 10^5$ erg/cm^2) as regards order of magnitude is obtained for the electric coupling coefficient if it is assumed that the effective charge of a titanium ion equals the charge of an electron. Thus, Slater comes to the conclusion that barium titanate is not a typical ionic crystal.

This model, however, gives a "smoothed out" phase transition of the second order. In order to increase the rate of increase of the spontaneous polarization below the Curie point, Devonshire[27] introduces into the expression for the free energy terms proportional to the polarization to the first power and taking into account the electrostriction part of the thermodynamic potential. Devonshire took recourse to this somewhat arbitrary procedure in order to obtain better agreement with experiment. It must be noted, however, that Devonshire determined the effective fields acting on the ions in the lattice incorrectly and hence his calculations lose much of their value.

Slater's mathematical treatment of the model of anharmonic oscillators involves a number of simplifying approximations and assumptions and, moreover, fails to take into account deformation and the piezoelectric effect.

Jaynes[35] is of the opinion that according to the calculations of Slater the ferroelectric condition is attained too readily and that the value of the polarizability of ionic displacements referred to a titanium ion is anomalously low. Jaynes bases this assertion on the work of Devonshire[27] who, following Born, evaluated the restoring force acting on a titanium ion as $f = -94 \cdot 10^5 \cdot z$, where z is the displacement of the ion in centimeters. From this one can calculate the polarizability of the ionic displacement. It proves to be four times greater than the value deduced by Slater. One cannot, however, wholly agree with Jaynes inasmuch as the value of the polarizability of the ionic displacement is not anomalously low ($\alpha'_{Ti} = 0.927 \cdot 10^{-27}$ cm^3) and commensurate with the electronic polarizability of the ions. In general, one must proceed

with caution in using Devonshire's data inasmuch as he treats barium titanate as an ionic crystal.

One can, however, agree with other remarks made by Jaynes. He considers that in barium titanate as in other crystals the effective fields decrease due to overlapping of the electron shells of the ions and fluctuations of the neighboring dipoles. These factors were not taken into account by Slater. Furthermore, as Cohen[41] showed, Slater determined the effective fields at the original lattice points of the ions. One should, of course, determine the fields at the true, i.e., displaced positions, for otherwise large errors may result.

In another contribution Cohen[42] showed that if the local fields are determined at the displaced positions of the ions, the antiferroelectric state for barium titanate proves to be more probable than the ferroelectric state. In his treatment Cohen regards the barium titanate lattice as an array of dipoles formed by Ti and O_I ions and does not take into account the presence of the other oxygen ions and the barium ions. For such a model an antiparallel arrangement of the dipoles will always be favored. It does not follow, however, that this will necessarily hold for actual barium titanate.

The model of anharmonic oscillators has been further developed in a number of recent contributions[31,43-45]. Barret[43] attempted a quantum mechanical treatment of the model of anharmonic oscillators. Like Slater, he assumed that the titanium ions are weakly bound: their interaction with each other is taken into account only through the effective field. Barret treats the "anharmonic" part of the potential energy of the oscillators as a perturbation. It would appear that at low temperatures, i.e., where quantum effects play a significant role, there occurs a deviation from the Curie-Weiss law. In this case ($T < h\nu/k$), the dielectric constant at $T > \theta$ increases more slowly with the temperature than according to the Curie-Weiss law. As may have been expected, it follows from Barret's calculations that as absolute zero is approached, the dielectric constant becomes temperature independent inasmuch as any system having discrete energy states goes over to the ground state at absolute zero.

Schweinler[44] discussed ferroelectrics with the ilmenite (hexagonal) structure using the anharmonic oscillator model. He computed the local field strengths by Ewald's method[46] generalized to the case of a nonorthogonal lattice.

Smolenskii & Kozlovskii[45], using the virial theorem (Clausius' formula), determined the displacement of an anharmonic oscillator in a constant electric field. Then treating the crystal as a system of point ions oscillating independently of each other, they were able to investigate the fundamental properties of ferroelectrics and extend Slater's computation to the case of a spherically symmetric potential well. They obtained more accurate expressions characterizing the dependence of the displacement of the oscillators on the temperature and field intensity. They established the inequalities determining the applicability limits of Slater's approximations. Further, they determined the condition for the appearance of ferroelectricity which is that the strength of the dipole-dipole interaction must be greater than that of the restoring elastic force. They showed that the factors favoring spontaneous polarization are a large internal field constant, a high effective charge of the central ion and a small elastic coupling coefficient. They deduced an expression for the Curie point. They also examined the behavior of ferroelectrics in strong electric fields and calculated the critical field strength at which the domain structure in a crystal disappears. They investigated the

hysteresis loop for a single-domain crystal and found the value of the ionic polarizability in weak fields. Further, they carried out numerical calculations for a number of parameters characterizing barium titanate. In these calculations the effective charge of the central ion was taken equal to $5 \cdot 10^{-10}$ cgse units. In this choice of the effective charge, they were guarded by the considerations set forth by Slater. The calculated values of the displacement of the titanium ions and spontaneous polarization at very low temperatures proved to be close to the experimental values. The calculated coercive force, however, proved to be appreciably greater than that observed experimentally.

Above we have discussed the model of deep potential minima and the model of anharmonic oscillators. In real crystals, however, there may be a gradual transition from one model to the other. Furthermore, in some cases the potential minima may be very shallow. In such crystals the potential wells will virtually not be manifest at high temperatures. Obviously, in such crystals the character of the ionic displacement will change with changes in temperature.

We now come to the electronic theory of ferroelectric effects proposed by Jaynes & Wigner[35,47] who consider that barium titanate does not form typically ionic crystals. These authors refer to the work of van Santen and Shockley. Van Santen[48,49] notes that the high index of refraction of barium titanate and of crystals with oxygen-titanium octahedra in general is not consistent with the values of the electronic polarizability of their component ions, i.e., with the values which these ions exhibit in other crystals. Shockley[50] advanced the hypothesis that the polarizability of the oxygen ions in the presence of titanium ions is two times greater than in other oxides. The high polarizability of the oxygen ions in compounds of the barium titanate type can be explained by the appreciable overlapping of the electron shells of the titanium and oxygen ions. The question of taking into account the homeopolar character of the bonds in ferroelectric crystals is not new and has been discussed by many investigators. Until now, however, the determining factor in the rise of spontaneous polarization has been assumed to be the mechanism of ion transfer or the mechanism of ionic displacements. In their quantum mechanical theory these authors attempt to explain the ferroelectric properties of barium titanate as the result of the change of state of the electrons in the $BaTiO_3$ crystal.

Jaynes & Wigner consider each octahedron as a system having an internal electronic quantum state independent of the state of the neighboring unit cells. Thus, they assume the existence of strong interaction of the exchange type between the elements of the oxygen octahedron; this interaction determines the character of the chemical bonds. In the absence of an electric field the ground state of this electronic configuration is cubically symmetric and hence possesses no dipole moment. These authors then introduce another assumption, namely, that the interaction between neighboring octahedra must be appreciable if they are in states with approximately the same energy and of opposite parity. This interaction perturbs the ground state of the octahedron as a result of which the initial cubically symmetric wave function of the ground state is distorted. In this case the wave function of the octahedron may be represented in the form of a linear combination of the initial cubically symmetric functions and the electronic configuration has a dipole moment differing from zero.

The initially degenerate ground-state energy level splits in the presence of the perturbation so that the energy of the perturbed state proves to be lower (by a factor of several kT) than the energy of the ground state. This

determines the stability of the state with the nonzero dipole moment. Thus there arise an internal field and spontaneous polarization.

The effective fields in the work referred to above are described very inaccurately by the expression

$$F = E + \beta(P_e + P_d + P_i) = \frac{E + 3P_e}{1 - \beta\gamma}. \quad (7)$$

Here P_e is the polarization due to the displacement of the generalized electrons of the oxygen octahedron and P_d is the polarization resulting from the displacement of the ions. The polarization P_i is not accurately defined by the authors; it may be assumed that it is the electronic polarization due to the Ba ions.

For their mathematical treatment of the problem these authors use group theory. The energy spectrum of the system calculated in this manner makes it possible to apply statistics for taking account of the influence of temperature. The free energy and polarization are determined through the statistical sum in the usual manner. The authors also find the dielectric constant above the phase transition point. Using experimental data these authors find

$$\frac{1}{\beta(1-\beta\gamma)} = 8.3 \quad (8)$$

In view of this, in order to obtain a satisfactory value for γ, the Lorentz factor must not exceed 0.5.

Discussion of their results forced the authors to admit that in order to obtain quantitative agreement with experiment one must attribute half the total spontaneous polarization to the electronic component of the polarization of the octahedra (P_e). The other half of the polarization must be attributed to the displacement of the ions and displacement of the electron shells of the Ba ions.

It must be admitted that this electronic theory has a certain value as the first attempt to use quantum concepts for explaining the appearance of spontaneous polarization. At present, however, one cannot say the validity of the basic premises of this theory has been proved. In Jaynes' work no attempt is made to justify the treatment of the octahedron as a single electronic system. The strong exchange interaction between the oxygen ions is only assumed but is not evaluated. The electronic theory as it now stands is largely formal and has not been substantiated by experiment; its internal mechanism is still unclarified. The calculated Lorentz factor is anomalously small and the effective fields, as we noted, are only roughly approximated. Furthermore, no consideration is given to spontaneous deformations, the piezoeffect and the low-temperature phase transitions.

A theoretical investigation of a single-domain crystal of barium titanate at room temperature has also been carried out by Hagedorn[51]. Hagedorn calculates the effective fields, the spontaneous polarization and the dielectric constant on the basis of the x-ray data of Känzig[22]. It is assumed that the oscillation of the ions can be neglected and that the position of the ions in the lattice is completely defined by their mean (averaged in time) coordinates. In other words, Hagedorn is not interested in the temperature effect and without recourse to any specific model calculates the principal electric parameters characterizing the system in a state distant from the transition point. It may be noted that in Hagedorn's treatment 1) the ions are considered to be point charges, the effective values of which are taken into account by introducing appropriate parameters that are different for each type of ion, 2) the

ferroelectric effect is assumed to be due to the displacement of the titanium and O_I type oxygen ions initially aligned parallel to the spontaneous polarization axis and 3) the temperature is introduced indirectly together with the electrostriction by taking into account the axial ratio of the unit cell (c/a = 1.01).

Hagedorn uses the method of Madelung[52] to calculate the effective fields and polarizations for the displaced positions of the ions. However, the author determines only the periodic solution corresponding to the action of the ions inside the Lorentz sphere. He does not take into account the Lorentz correction ($4\pi P/3$) which is an error that casts doubt on the validity of his results and conclusions.

Upon substituting the values of the effective field, charges and polarizabilities, taken on the assumption that the crystal is a typically ionic one, into his deduced system of equations, Hagedorn arrives at results that are in sharp disagreement with experiment. In view of this Hagedorn concludes that the character of the bonds in barium titanate is partially homeopolar. He then calculates the effective ionic charges and the ionic and electronic polarizabilities which when substituted in the earlier deduced equations for the effective fields would yield the correct values for the spontaneous polarization and dielectric constant. In determining the effective charges and polarizabilities he makes the two following rather arbitrary assumptions: a) that the electronic polarizability of the ions is proportional to the cube of the radius, and b) that the radius of the ions is linearly dependent on the effective charge.

In view of the complex character of the equations involved in finding the effective charges Hagedorn has recourse to the method of successive approximations. The effective charges found as the result of the seventh approximation indicate that the bonds are highly homeopolar in character.

It will be seen from this brief examination of extant microscopic theories that some success in their development has been acheived in recent years. However this is only the beginning. The various theoretical investigations involve a number of more or less arbitrary assumptions and simplifications. This is largely due to the lack of a consistent quantum mechanical theory of condensed systems.

III. New Ferroelectrics and Antiferroelectrics of the Oxy-octahedral Type

For some time after the discovery of the ferroelectric properties of barium titanate it was assumed that $BaTiO_3$ is the only ferroelectric among crystals of the perovskite type inasmuch as the distance between the titanium and oxygen ions in the barium titanate lattice is greater than the sum of the radii. This characteristic should lead to a greater ionic polarizability incident to displacement of the titanium ions.

Subsequently, however, Smolenskii, Matthias, Roberts and other investigators showed that barium titanate is only one of many ferroelectrics of the oxy-octahedral type. At present we already know of an appreciable number of ferroelectrics and antiferroelectrics crystallizing with the structures of perovskite, ilmenite, rhenium trioxide and pyrochlore.

Let us review the principal characteristics of these new ferroelectrics and antiferroelectrics.

1. Strontium titanate

Strontium titanate crystallizes with a cubic structure of the perovskite type. Smolenskii[31] showed that polycrystalline specimens of strontium titanate obtained from technical grades of titanium dioxide possess ferroelectric properties at very low temperatures (20-30°K). At approximately the same time Hulm[54] published a communication in which he asserted the contrary.

This disagreement can readily be understood if we bear in mind that the temperature of the Curie point of ferroelectrics depends on the sintering and other heat treatment conditions and on the character of the impurities present in the specimen. Thus, for example, the Curie point for different specimens of $BaTiO_3$ varies over a temperature range from 70 to 130°. Inasmuch as the Curie point of strontium titanate is rather close to absolute zero, it is possible that spontaneous polarization does not arise at all in some specimens of $SrTiO_3$. It would be desirable to investigate the properties of pure polycrystalline specimens and single crystals of strontium titanate at low temperatures.

2. Lead titanate

Lead titanate crystallizes in the perovskite structure. At room temperature the lead titanate lattice is tetragonal; the ratio of the unit cell edges $c/a = 4.141/3.891 = 1.0635$ (Megaw[20]).

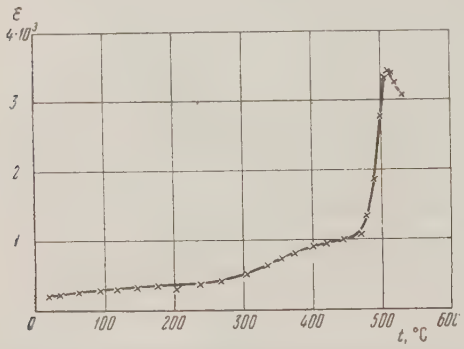

Fig.1. Temperature dependence of the initial dielectric constant of polycrystalline lead titanate (after Smolenskii).

The phase transition in lead titanate at 500° was discovered by Smolenskii[53] and Shirane, Hoshino & Suzuki[55] independently. The idea that lead titanate is a ferroelectric with a high Curie point was first suggested by Jonker & van Santen[56]. These investigators discovered that the phase transition temperature of $(Ba,Pb)TiO_3$ and $(Sr,Pb)TiO_3$ solid solutions increases with increasing $PbTiO_3$ content. From this they concluded that lead titanate itself has ferroelectric properties. They did not, however, investigate pure lead titanate or solid solutions with a high concentration of the compound.

The temperature dependences of the dielectric constant and the coefficient of linear expansion of polycrystalline lead titanate are shown in Figs.1 & 2.

The curve characterizing the temperature dependence of the linear expansion coefficient has a minimum at the transition point temperature. This minimum is explained by the fact that during heating the volume and linear dimensions of a ferroelectric material change both due to ordinary thermal expansion and due to deformations associated with the decrease in spontaneous polarization. With increasing temperature, the net volume may decrease due to decrease in spontaneous polarization (positive volume electrostriction) as in the case of lead titanate or it may increase (negative volume electrostriction).

It may be noted that in barium titanate the volume spontaneous electrostriction is also greater than zero (positive). The electrostriction in lead titanate, however, is much greater than in barium titanate. This has

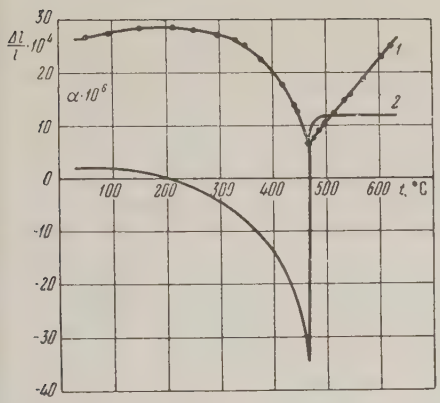

Fig.2. Temperature dependence of the relative change in length (1) and the coefficient of linear expansion (2) of a polycrystalline specimen of lead titanate (after Smolenskii).

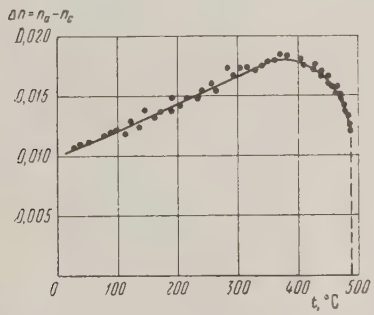

Fig.3. Birefringence of lead titanate as a function of temperature (after Shirane, Pepinsky & Frazer).

been directly substantiated by neutron diffraction studies[8] of the ionic displacements in the $PbTiO_3$ (Table 2).

Table 2

Results of neutron diffraction studies of ionic displacements in lead titanate.

Ion*	Displacement δz, Å
O_I	0
Ti	0.30
Pb	0.47

*$z_{O_{II}}$ is assumed to be equal to $^1/_2$ c; ($a = 3{,}904$; $c = 4{,}152$ Å).

X-ray diffraction studies[8,55] have shown that lead titanate has a cubic crystal structure above 500° and a tetragonal structure below this temperature. In lead titanate, as in barium titanate, one axis, the c axis, is elongated (and apparently becomes the polar axis, while the other two axes are shortened; the net volume of the unit cell is increased as a result.

The heat of the phase transition in lead titanate is appreciably greater than in barium titanate and equals about 1150 cal/mole[57].

In lead titanate the birefringence $\Delta\eta$ changes anomalously with the temperature (Fig.3). It is known that in barium titanate birefringence increases with decreasing temperature.

The temperature dependences of the dielectric constant and coefficient of linear expansion shown in Figs.1 & 2 were obtained with the specimens heated at the rate of one degree per minute. It will be seen from these figures that at this heating rate no low-temperature phase transitions were detected in lead titanate at temperatures under 195°. It is reported[57a], however, that if the specimen is heated very slowly a phase transition is observed at -100°.

It has proved impossible to obtain hysteresis loops with polycrystalline specimens of lead titanate. It would appear that at high temperatures the conductivity of the specimens is very high, while at temperatures far below the transition points the domains are no longer oriented in permissible fields.

Lead titanate single crystals have been grown and investigated by Beliaev & Khodakov[58]. Fesenko[59] succeeded in detecting a domain net in lead titanate single crystals. Fesenko also determined the index of refraction of $PbTiO_3$ ($\eta = 2.65$). Blokhin[60], investigating the influence of temperature on the x-ray K absorption spectrum, came to the conclusion that lead titanate is a typical electronic (p-type) semiconductor.

3. Cadmium titanate

In contrast to most of the known ferroelectrics which are characterized by the perovskite structure, cadmium titanate has a non-cubic structure in the paraelectric region. At room temperature the structure of this titanate is orthorhombic. This distinctive attribute of $CdTiO_3$ is explained by the small size of the cadmium ions which leads to a monoclinic shift of the axes in the nonferroelectric region. According to Naray-Szabo[61] a similar distortion of the structure obtains in calcium titanate.

Ferroelectricity in cadmium titanate was first discovered by Smolenskii[53]. The $\epsilon = f(t)$ curve exhibits a maximum at 50-60°K. The Curie-Weiss constants of cadmium titanate at $T > \theta$ proved to be appreciably smaller than for barium titanate and do not exceed 40,000-50,000°K. Hysteresis loops have been observed at temperatures below 50-60°. So far this ferroelectric has been studied very little.

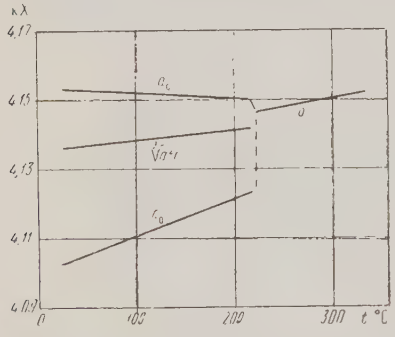

Fig.4. Variation of the $PbZrO_3$ subcell parameters with temperature (according to Sawaguchi).

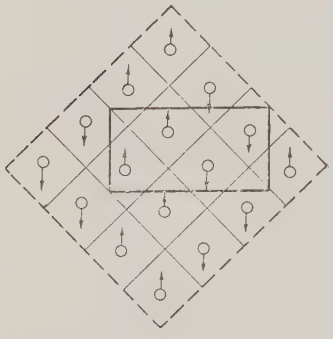

Fig.5. Projection on the (001) plane of the packet structure of lead zirconate: rhombic (heavy solid lines) and pseudotetragonal (dash lines) (after Sawaguchi, Maniwa & Hoshino).

4. Lead zirconate

The existence of a phase transition at 230° in lead zirconate was discovered independently by Smolenskii[53] and Roberts[62]. Lead zirconate crystallizes in the perovskite structure[63,61 &64].

Ueda & Shirane [65] and Sawaguchi[66], using x-ray procedures, determined the changes in the parameters of the lattice as a function of the temperature and confirmed the existence of the phase transition at 230° (Fig.4). At temperatures above the Curie point the unit cell is characterized by cubic symmetry of the perovskite type, while at temperatures below the Curie point there is formed a rhombic packet structure consisting of subcells with tetragonal symmetry. The parameters and volume of the unit cell change suddenly at the transition point; the volume of the cell increases by 0.29 Å^3 incident to the transition to the paraelectric state, whereas in $BaTiO_3$ the unit cell volume decreases incident to this transition.

Sawaguchi, Maniwa & Hoshino[67] synthesized minute single crystals of lead zirconate. On the basis of optical studies and x-ray analysis of a single-domain crystal these authors showed that lead zirconate crystallizes at room temperature with an orthorhombic packet structure. The orthorhombic unit cell has the parameters $a = a_0\sqrt{2} = 5.87$ Å, $b = a_0 2\sqrt{2} = 11.74$ Å and $c = 2c_0 = 8.20$ Å and contains eight $PbZrO_3$ "molecules". According to these authors the space group may be either $D_{2h}(9)$ or $C_{2v}(8)$.

The packet structure model corresponding to these space groups is shown in Fig.5 in the form of a projection on the (001) plane. In the case of the $D_{2h}(9)$ space group the authors

calculate that the Pb ions are displaced antiparallel 0.2 Å along the orthorhombic a axis, as shown in Fig.5. In case the symmetry is C_{2v} the authors consider that the lead ions are also slightly shifted parallel to each other along the c axis. Thus the authors associate the appearance of the superstructure spots in the x-ray diffraction patterns of $PbZrO_3$ with the antiparallel displacement of the lead ions. The small piezoelectric effect detected by Roberts[68] in a prepolarized polycrystalline specimen of $PbZrO_3$ indicates that the spatially non-centrosymmetric $C_{2v}(8)$ group is more probable than D_{2h}. However, as Venevtsev[69] points out we cannot yet be certain of the space group.

The superstructure of $PbZrO_3$ can also be approximately described by means of a pseudotetragonal packet structure with the parameters $4a_0 \times 4a_0 \times 2c_0$ or $4a_0 \times 4a_0 \times c_0$. The projection of such a cell model on the (001) plane is shown in Fig.5.

The temperature dependences of the dielectric constant and coefficient of linear expansion for polycrystalline lead zirconate are shown in Figs.6 & 7. The Curie-Weiss law, $\epsilon = 1.15 \cdot 10^5/T-228$, holds above the transition point.

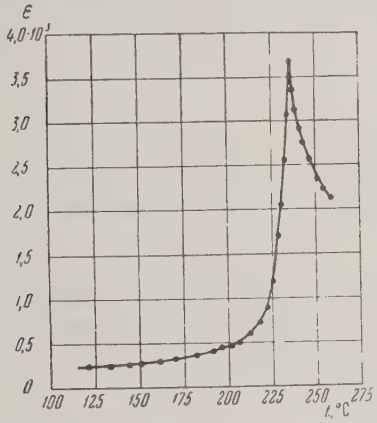

Fig.6. Temperature dependence of the initial dielectric constant of polycrystalline $PbZrO_3$ (after Smolenskii).

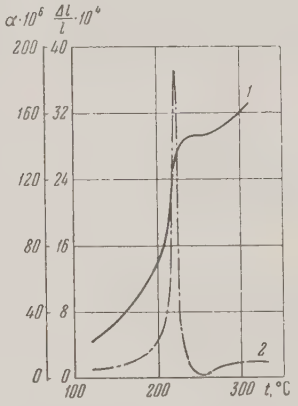

Fig.7. Temperature dependences of the relative change in length (1) and the coefficient of linear expansion (2) of a polycrystalline specimen of $PbZrO_3$ (after Smolenskii).

The phase transition in lead zirconate is accompanied by negative volume electrostriction. The abrupt change in the volume of the unit cell, the appreciable electrostriction, the comparatively large heat of the transition (440 cal/mole - Shirane[70]), the sudden change in dielectric constant and temperature hysteresis of the constant (+4°) at the transition point and the linear dependence of the polarization on the field strength above the Curie point, all indicate that the phase transition in $PbZrO_3$ at 230° is a first order transition.

Lead zirconate has a number of distinctive characteristics as compared with barium titanate: 1) it exhibits no hysteresis loop in fields below a certain critical value, 2) it has superstructure, 3) the volume of the crystal decreases with cooling near the Curie point (negative volume electrostriction), 4) the transition point is displaced to the side of low temperatures when a dc field is applied, 5) the reversible permittivity increases in the region of the phase transition with increasing strength of the biasing field, 6) anomalous (for ferroelectrics) hysteresis loops are observed in strong ac fields,

and 7) no discharge in current is observed during the heating of a specimen previously held in a dc field.

Shirane, Sawaguchi and Takagi[71], noting all these distinctive features, suggest that lead zirconate with a minimal impurity content is antiferroelectric. These authors are also of the opinion that in (Pb,Ba)ZrO_3 and Pb(Zr,Ti)O_3 solid solutions with decreasing temperature there first occurs a transition from the paraelectric to the ferroelectric state and then to the antiferroelectric state, while in (Pb,Sr)ZrO_3 solid solutions there is a direct transition from the paraelectric to the antiferroelectric state.

Hitherto in considering ferroelectrics and, in particular, barium titanate it has commonly been assumed that long range forces are primarily responsible for the phase transition from the disordered to the ordered, polarized state. In the case of crystals in which orientational melting occurs it is clear, however, that the phase transitions are due to short range forces. It is obvious that in some ferroelectric materials, too, short range forces may play an appreciable role and significantly affect the behavior of the ferroelectric in electric fields. It is not impossible that this holds for lead zirconate. Definitive determination of the nature of the phase transition in $PbZrO_3$ must await careful neutron diffraction and spectroscopic studies of single crystals of the material; possibly the procedures of nuclear resonance may also prove helpful.

5. Lead hafnate

Shirane & Pepinsky[72] observed two phase transitions - at 163 and 215° - in polycrystalline $PbHfO_3$ which has the perovskite type structure.

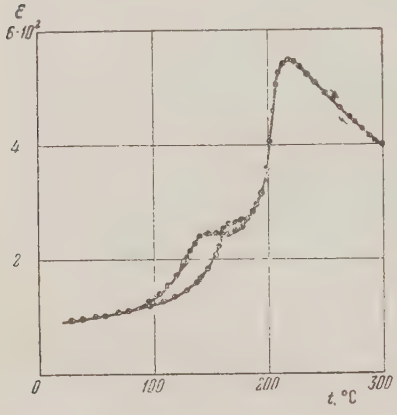

Fig.8. Temperature dependence of the initial dielectric constant of polycrystalline $PbHfO_3$ (according to Shirane & Pepinsky).

The temperature dependence of the dielectric constant of a polycrystalline specimen is shown in Fig.8. The polarization in the temperature range where $T < \theta$ is virtually independent of the field strength. At room temperature the unit cell is pseudotetragonal. These authors are unable to establish definitely the lattice symmetry (tetragonal with an axial ratio $c/a < 1$ or orthorhombic). In the temperature interval from 163 to 215° $PbHfO_3$ has a tetragonal lattice with $c/a = 0.997$; above 215° it has a cubic lattice. In heating the volume of the unit cell increases at the phase transition points, i.e., both transitions are characterized by negative volume electrostriction. Superstructure lines are discernible in x-ray patterns of $PbHfO_3$ obtained at temperatures below 215°. These investigators conclude that $PbHfO_3$ is antiferroelectric at temperatures below 215°.

6. (Ba,Pb)SnO_3 solid solutions

In contrast to lead zirconate and titanate, lead stannate does not exist as an independent chemical compound[69,73]. With a sufficiently high (at least 30%) concentration of barium stannate one can, however, obtain (Ba,Pb)SnO_3 solid solutions with the perovskite type structure. The lattice parameters of such solid solutions, according to the data of Kalinina, are listed in Table 3.

Table 3

Lattice parameters of $(Ba,Pb)SnO_3$ solid solutions

Composition, mole %		Lattice parameter Å
$BaSnO_3$	$PbSnO_3$	
100	0	4,1164
90	10	4,1130
75	25	4,1048
50	50	4,0991
30	70	4,0320

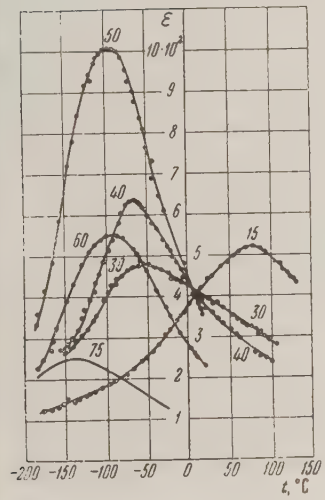

Fig.9. Temperature dependences of the initial dielectric constant of polycrystalline specimens of $(Ba,Pb)SnO_3$ solid solutions. The figures at the curves give the barium stannate content in mole percent (after Smolenskii & Agranovskaia).

The ferroelectric characteristics of these solid solutions were first detected by Smolenskii & Agranovskaia[74,75]. The temperature dependences of the dielectric constant of different solid solutions are shown in Fig.9. The temperature of the phase transitions, or more accurately the temperature of the dielectric constant peak, decreases with increasing concentration of barium stannate which, incidentally, is not ferroelectric.

Changes in the value of the coefficient of linear expansion are observed in the region of temperatures corresponding to the maximum values of the dielectric constant, which is evidence of the existence of a phase transition. True, here, as in a number of other solid solutions, this transition is "diffused".

The spontaneous polarization of the solid solution $(Ba_{0.3},Pb_{0.7})SnO_3$ attains $12.8 \cdot 10^{-6}$ Coulomb/cm^2 at -120°.

Smolenskii & Myl'nikov recently discovered that phase transitions are also observed in (Sr,Pb)--SnO_3 solid solutions.

7. Tungsten trioxide

The ferroelectric properties of WO_3 were discovered by Matthias[76] in 1949. Since then there have been many investigations devoted to its properties and structure[77-86]. Nevertheless we still do not have fully reliable data on the phase transitions in WO_3 and the arrangement of the ions in its lattice at different temperatures. This is partly explained by the high conductivity of WO_3 which hampers investigation of certain of its properties. Studies of WO_3 have been carried out on both single crystals and on polycrystalline specimens.

The structure of WO_3 is a somewhat deformed ReO_3 structure. This structure may be regarded as the perovskite structure with the calcium ions removed. At room temperature, the WO_3 unit cell is monoclinic and contains four "molecules". Some investigators (for example, Matthias[76]) are of the opinion that tungsten trioxide has ferroelectric properties at room temperature, while others[86] assert that it is antiferroelectric in the room temperature range.

At 740° there occurs a phase transition as a result of which the lattice goes over from the monoclinic to the tetragonal[77]. The volume of the unit cell decreases sharply in the process of heating in the vicinity of the phase transition point, i.e., there is positive volume electrostriction (Fig.10); the latent heat of the transition is about 450 cal/mole (Fig.11). Sawada et al[80] note that the domain structure disappears when the crystal is heated above 710°. On the basis of x-ray analysis Kehl, Hay & Wahl[84] conclude that in its tetragonal modification tungsten trioxide is antiferroelectric.

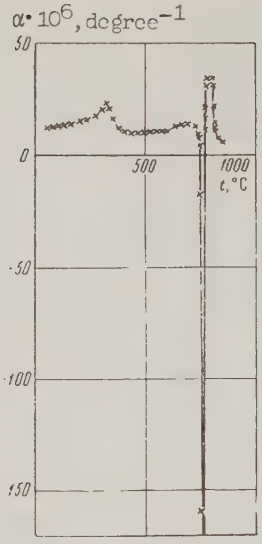

Fig.10. Temperature dependence of the coefficient of linear expansion of polycrystalline tungsten trioxide (according to Sawada, Ando, Hoshino & Nomura).

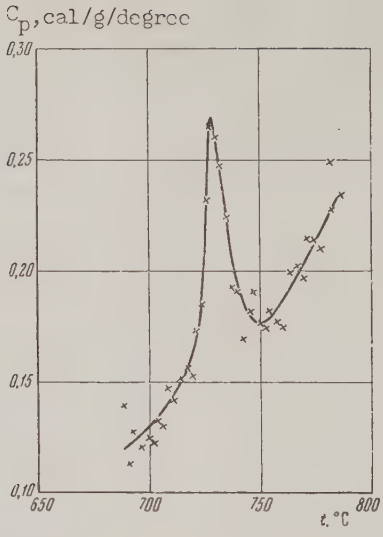

Fig.11. Temperature dependence of the true specific heat of polycrystalline tungsten trioxide (according to Sawada, Ando, Hoshino & Nomura).

According to Matthias & Wood[82], at -50° there also occurs a phase transition from the monoclinic to a more symmetric phase which is ferroelectric. The dielectric constant of single crystals at the temperature of liquid air attains 300 (Matthias[76]).

8. Lead metaniobate and metatantalate

In 1953 Goodman[87] showed that lead metaniobate ($PbNb_2O_6$) is a ferroelectric with a phase transition at 570°. On the basis of x-ray studies of minute single crystals this investigator asserts that the unit cell is orthorhombic, comprises 40 "molecules" and has the following parameters: a = 25, b = 25 and c = 7 Å.

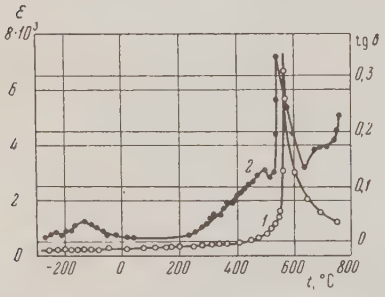

Fig.12. Temperature dependences of the dielectric constant (1) and loss tangent (2) of a polycrystalline specimen of lead metaniobate in weak fields (according to Goodman).

In all probability the niobium ions are octahedrally surrounded by oxygen ions, but the arrangement of the oxygen octahedra differs from that in perovskite.

The temperature dependences of the dielectric constant, the loss tangent and the relative change in length of a polycrystalline specimen of lead metaniobate are shown in Figs.12 & 13. At $T > \theta$ the dielectric constant varies with the temperature according to the Curie-Weiss law: $\epsilon = 2.95 \cdot 10^5/T-530$.

Lead metaniobate is characterized by positive spontaneous electrostriction. No low-temperature phase transitions have been detected in $PbNb_2O_6$ (down to -195°).

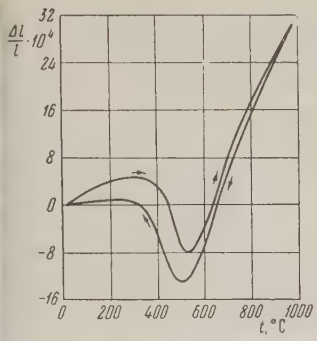

Fig.13. Temperature dependence of the relative change in length of a polycrystalline specimen of lead metaniobate (according to Goodman).

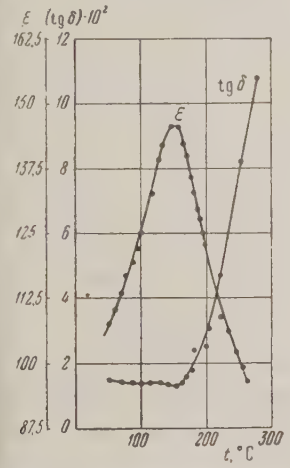

Fig.14. Temperature dependences of the dielectric constant and loss tangent of a polycrystalline specimen of lead metatantalate in weak fields (according to Smolenskii & Agranovskaia).

Goodman observed hysteresis loops but was unable to attain saturation of polarization. At room temperature and E = 60 kv/cm the residual polarization equals $0.6 \cdot 10^{-6}$ Coulomb/cm^2, while the coercive force is 17 kv/cm.

Lead metaniobate is distinguished by interesting properties from a technological standpoint. It can be used for preparing piezoelectric elements suitable for operation at elevated temperatures. Some of the outstanding properties of polycrystalline $PbNb_2O_6$ are compared with those of polycrystalline barium titanate in Table 4. The $PbNb_2O_6$ specimens studied by Goodman were polarized in a dc field of 20 kv/cm at 200-250° for half an hour.

Table 4

Comparison of the properties of polycrystalline lead niobate with those of barium titanate

Properties	$PbNb_2O_6$	$BaTiO_3$
Specific gravity, g/cm^3	6.33	5.7
Dielectric constant in weak fields at 25°	280	1700
Piezoelectric coefficient d_{33}, Coulomb/kg	$8.1 \cdot 10^{-10}$	$19.4 \cdot 10^{-10}$
Young's modulus, dyne/cm^2	$6.2 \cdot 10^{11}$	$9.4 \cdot 10^{11}$
Electromechanical coupling coefficient (thickness - shear vibrations)	0.26	0.21

After the discovery of ferroelectricity in lead metaniobate by Goodman, Smolenskii & Agranovskaia[76] showed that spontaneous polarization also arises in lead metatantalate ($PbTa_2O_6$). The temperature dependences of the dielectric constant and loss tangent in weak fields are shown in Fig.14. The transition from the nonpolarized to the polarized state occurs at 260°. The spontaneous polarization of lead metatantalate at room temperature equals $2.5 \cdot 10^{-6}$ Coulomb/cm^2. The crystal structure of this compound has not yet been determined.

9. Cadmium pyroniobate and strontium pyrotantalate

As a result of their investigation of the properties of a number of niobates and tantalates of bivalent metals, Wainer & Wentworth[88] established that polycrystalline cadmium pyroniobate ($Cd_2Nb_2O_7$) is characterized by a relatively high dielectric constant (about 500 at room temperature) with a large negative temperature coefficient. Later measurements by Cook & Jaffe (Ref.89,90) showed that cadmium pyroniobate is a ferroelectric with a phase

transition point at -90° (-103°). This compound crystallizes in the cubic $E8_1$ structure of pyrochlore ($NaCaNb_2O_6F$). This structure has a certain similarity with the structure of distorted fluorite. However, instead of the composition $(A,B)_4X_8$, which would correspond in fluorite to the proportion AX_2, the descriptive formula is $(A,B)_4X_7$ so that one of the eight anions in the fluorite type structure is omitted and the remaining oxygen ions are shifted appreciably. There are eight "molecules" per unit cell. The structural framework consists of three-dimensional chains of octahedra sharing corners. The seventh oxygen ion and the A ion occupy the holes between the octahedra. The configuration of the octahedra projected on the (110) plane is shown in Fig.15. In contrast to the case of perovskite, the O-B-O chains are arranged zig-zag fashion along the [111] direction. In pyrochlore structure the A ions and the seventh anions can be absent just as the A ions in the structure of perovskite, inasmuch as they are not essential for the stability of the network provided, of course, that electric neutrality obtains.

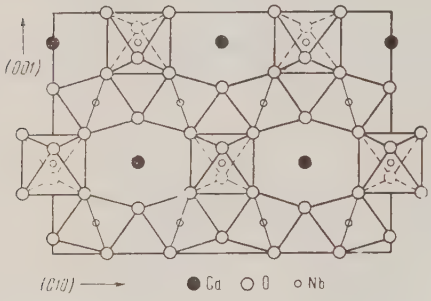

Fig.15. Configuration of the octahedra in cadmium pyroniobate, projected on the (110) plane (according to Jona, Shirane & Pepinsky).

Jona, Shirane & Pepinsky[91] carried out a detailed x-ray and optical investigation of cadmium pyroniobate and a number of solid solutions based on this compound. These investigators grew small single crystals (0.03 x 0.03 x 0.10 mm) from a melt of pure $Cd_2Nb_2O_7$. At room temperature the lattice constant of such crystals is the same as that measured for polycrystalline specimens, namely, a = 10.372 ± 0.001 A. The optical studies indicated that there is a phase transition from the cubic to a noncubic phase at about -90°. No distinct domains were observed below the Curie point. X-ray patterns from single crystals obtained at -150° show very slight distortion of the lattice, but it proved impossible to determine the structure in the ferroelectric region. The authors conclude that there must be a shift of the cadmium ions relative to the niobium ions.

Single crystals grown from a melt of $Cd_2Nb_2O_7$ with the addition of NaF as a flux are probably described by the formula $Cd_{1.6}Na_{0.4}Nb_2O_{6.6}F_{0.4}$. The phase transition point of such crystals is reduced to -120°. At -140° the lattice is tetragonal (a = 10.378 A and c/a = 1.0011).

The temperature dependence of the dielectric constant of a polycrystalline specimen of cadmium pyroniobate according to the data of Shirane & Pepinsky[92] is shown in Fig.16. A second phase transition is observed at -190°. Analogous results were obtained by Hulm[93]. The Curie-Weiss law $\epsilon = 4.6 \cdot 10^4/T-150$ is satisfied above the Curie point. At -173° and E = 25 kv/cm the spontaneous polarization of the crystal equals $1.8 \cdot 10^{-6}$ Coulomb/cm^2. This is approximately half the value reported by Cook & Jaffe.

The specific heat anomaly in the vicinity of the phase transition at -90° was investigated by Danner & Pepinsky[94]. The latent heat of the transition as determined from the $C_p = f(t)$ curve was found to be 18±2 cal/mole, which corresponds to an entropy change

$$\Delta S = \int \frac{\Delta C_p}{T} dt = 0.09 \pm 0.01 \text{ cal/mole degree.}$$

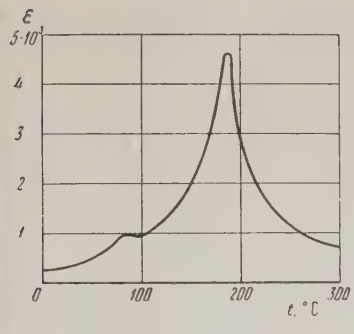

Fig.16. Temperature dependence of the initial dielectric constant of a polycrystalline specimen of cadmium pyroniobate (according to Hulm).

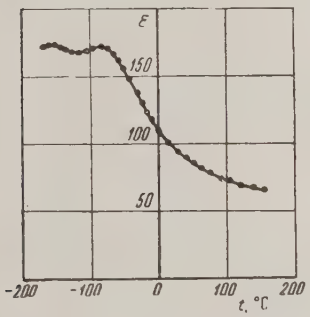

Fig.17. Temperature dependence of the initial dielectric constant of a polycrystalline specimen of strontium pyrotantalate (according to Smolenskii, Isupov & Agranovskaia).

Jona, Shirane & Pepinsky also studied a number of solid solutions with cadmium niobate. They found that a continuous series of solid solutions with the cubic structure forms in the $Cd_2Nb_2O_7$-$Cd_2Ta_2O_7$ system; in the $Cd_2Nb_2O_7$-$Pb_2Nb_2O_7$ system solid solutions apparently form with $Pb_2Nb_2O_7$ concentrations up to 90 mole %. $Ca_2Nb_2O_7$ dissolves in $Cd_2Nb_2O_7$ only up to 20 mole %.

Lead pyroniobate ($Pb_2Nb_2O_7$) also crystallizes with the perovskite structure. In contrast to $Cd_2Nb_2O_7$, lead niobate has a rhombohedral structure[91] at room temperature with a = 10.570 A and $\alpha = 89^{\circ}15'$.

A maximum at 14-15°K has been observed[92,93] in the temperature variation of the dielectric constant of polycrystalline specimens of $Pb_2Nb_2O_7$. No hysteresis loops were observed below this temperature at field strengths up to 10-15 kv/cm. According to these investigators the question of a phase transition from the non-polarized to the polarized state remains open.

Recently Smolenskii, Isupov & Agranovskaia[95] discovered that polycrystalline strontium pyrotantalate is ferroelectric. The presence of spontaneous polarization in strontium pyrotantalate is rather surprising inasmuch as Hulm[93] detected no evidence of ferroelectricity in $Cd_2Ta_2O_7$ and $Pb_2Ta_2O_7$. By analogy with the titanates one might expect the appearance of ferroelectric properties primarily in lead and cadmium titanates rather than in strontium titanate.

The variation of the dielectric constant of polycrystalline $Sr_2Ta_2O_7$ as a function of the temperature is shown in Fig.17. A second maximum in the curve for ϵ appears at -180°; this presumably corresponds to a low-temperature transition. Hysteresis loops are observed at temperatures below that of the first maximum. This ferroelectric is distinguished by its low dielectric constant. The structure of strontium pyrotantalate is not yet known.

10. Tantalates and niobates of alkali metals

The ferroelectric properties of lithium tantalate and niobate were discovered by Matthias & Remeika[96]. According to the authors these compounds crystallize with the ilmenite type structure (rhombohedral lattice). This structure can best be described as a slightly distorted dense hexagonal packing of oxygen ions. One third of the octahedral positions in lithium tantalate (niobate) is occupied by tantalum (niobium) ions, one third by lithium ions and the remaining third is vacant. There are two "molecules" in each unit cell. In the ilmenite structure the octahedra share not corners but edges and faces and the symmetry is lower than in perovskite.

The transition from the polarized to the nonpolarized state in these compounds occurs in the range of temperatures above 450°. In the temperature range from -100 to +450° the dielectric constant, the spontaneous polarization and the coercive force of lithium tantalate single crystals increase with rising temperature. The spontaneous polarization of lithium niobate varies analogously as a function of the temperature. This type of temperature dependence led Matthias[97] to postulate the existence of a low-temperature phase transition in these ferroelectrics.

Spontaneous polarization in the tantalates and niobates of sodium and potassium with the perovskite type structure was discovered by Matthias[98]. $KTaO_3$ and $NaTaO_3$ single crystals were grown from a melt of Ta_2O_5 with KOH and of Ta_2O_5 with NaOH by Vousden[99]. At room temperature the potassium tantalate lattice has cubic symmetry, while that of sodium tantalate has orthorhombic symmetry. The phase transition from the paraelectric to the ferroelectric state in $KTaO_3$ occurs at a very low temperature[100]. The dielectric constant of potassium tantalate single crystals attains a maximum value at 13.2°K. Hysteresis loops have been observed below this temperature. In the temperature range from 50 to 85°K the variation of the dielectric constant is given by the Curie-Weiss law: $\epsilon = (6\text{-}8)\cdot 10^4/T-\theta'$.

In $NaTaO_3$ the transition from the orthorhombic to the cubic structure occurs at 475° according to Matthias[101]. According to the data of Isupov, however, this transition is not associated with a transformation from the paraelectric to the antiferroelectric or ferroelectric state but is rather due to a change in the orientation of the octahedra. Analogous transitions have been observed in $(Ca,Sr)TiO_3$ solid solutions at a certain calcium titanate concentration. At high temperatures, the axes of the octahedra are directed parallel to each other and the crystal structure is cubic. As the temperature is reduced, the octahedra rotate slightly about the titanium ions, the symmetry of the crystal is lowered and there develops a Naray-Szabo type structure of monoclinic symmetry. In $NaTaO_3$ at 475° there occurs, apparently, an ordinary polymorphous transformation not leading to the appearance of an electric moment in the unit cell. At present the existence in $NaTaO_3$ of a phase transition below the temperature of which the unit cell acquires an electric moment cannot be regarded as definitively proved.

$KNbO_3$ single crystals have been grown[96,102,103] from melts of K_2CO_3 and Nb_2O_5 or KOH and Nb_2O_5. Investigations of the temperature dependences of ϵ and tan δ for $KNbO_3$ single crystals[96,102] and x-ray and optical studies of these crystals[103] indicate the existence of three phase transitions, occurring at 435, 225 and -10°. The structure of $KNbO_3$ in the process of cooling changes similarly to that of barium titanate: from the cubic to the tetragonal, from the tetragonal to the orthorhombic and finally from the orthorhombic to the rhombohedral. The lattice parameters according to Wood are the following: a = 4.024 A at 500°, a = 4.00 and c = 4.072 A at 260°, a = 4.045, b = 3.984, c = 4.045 A and β = 90°21' (monoclinic axes) or a = 5.702, b = 5.739 and c = 3.984 A (orthorhombic cell containing two "molecules") at 25°.

The values of the transition heat ΔQ and entropy change ΔS in the transitions of polycrystalline potassium niobate are compared with the corresponding quantities for barium titanate in Table 5 (Pavlovic & Pepinsky[102]).

Triebwasser & Halpern[104,105] showed that at $T > \theta$ the dielectric constant is characterized by the Curie-Weiss law: $\epsilon = 2.68\cdot 10^5/T-350$.

The spontaneous polarization near the transition equals $26\cdot 10^{-6}$ Coulomb/cm^2.

Table 5

Latent heat ΔQ (cal/mole) and entropy change ΔS (cal/mole degree) associated with the phase transitions in potassium niobate and barium titanate

Material	Quantity	Transition		
		Cubic to tetragonal	Tetragonal to orthorhombic	Orthorhombic to rhombohedral
$BaTiO_3$	ΔQ	47-50	16-26	8-14
	ΔS	0.12-0.13	0.06-0.09	0.04-0.07
$KNbO_3$	ΔQ	190±15	85±10	32±5
	ΔS	0.28	0.17	0.12

Cotts & Knight[106] studied the nuclear magnetic resonance and nuclear quadrupole resonance of Nb^{93} in a $KNbO_3$ single crystal in magnetic fields of up to 5250 oersted. The phase transition temperatures as determined by means of x-ray, optical and electric methods and by the nuclear resonance method are listed in Table 6.

Table 6

Phase transition temperatures (°C) in $KNbO_3$ according to the data of Cotts and Knight[106]

Method	Transition temperatures		
	Cubic to tetragonal	Tetragonal to orthorhombic	Orthorhombic to rhombohedral
X-ray & optical	435	225	--
Dielectric constant	410 to 435	210 to 220	-55 to -10
Nuclear resonance	426 to 431	207 to 222	-52 to -27

The transition temperatures listed in the table are for heating and cooling of the crystal. Cotts & Knight infer that the phase transitions in $KNbO_3$ are all first order transitions inasmuch as all are associated with abrupt changes in the quadrupole resonance frequency and, hence, of the quadrupole interaction. Furthermore, Cotts & Knight established that the quadrupole coupling is large, which is explained by the influence of covalent bonds. Cott & Knight note that the model of Mason & Matthias with six equilibrium positions for the central ion is not consistent with the large quadrupole coupling in the tetragonal phase and the single magnetic resonance line in the cubic phase.

Sodium niobate single crystals have been grown from a melt of Na_2CO_3 and Nb_2O_5 with sodium fluoride as the flux by Wood[103]. Gross & Nicholson [107], who used optical methods report observing four phase transitions in $NaNbO_3$ single crystals at approximately 360, 470, 518 and 640°. Below 360° the crystal structure is orthorhombic, above 640° it is cubic, while in the interval from 360-640° it is pseudo-tetragonal. Not all these phase transitions can be detected by x-ray studies. Additional superstructure lines appear in the x-ray diffraction patterns. The structure of sodium niobate has been studied in some detail by Vousden[108] who showed that at room temperature the niobium ions are displaced 0.11 A in opposite directions along the a axis.

Gross & Nicholson[107] investigated the variation of the dielectric constant in single crystals at the phase transition points: the dielectric

constant changes abruptly at 360°, while the changes observed at 518 and 640° are relatively minor. Earlier investigators were unable to detect hysteresis loops in $NaNbO_3$ and hence sodium niobate was classed as an antiferroelectric. Gross & Nicholson showed, however, that in fields of appropriate strength and direction one can observe in a certain temperature range both ordinary hysteresis loops and the double loops characteristic of antiferroelectrics. Thus sodium niobate can exhibit both ferroelectric and antiferroelectric properties. Despite the small distortions of the structure and the minor changes in ϵ at 518 and 640°, it may reasonably be assumed that sodium niobate becomes paraelectric above 360°. The transitions at 518 and 640° observed in $NaNbO_3$ are analogous to the transitions in $(Ca,Sr)TiO_3$ solid solutions and according to Krainik their specific character may be connected with the small dimension of the sodium ion.

The phase transition temperatures, structure and lattice parameters of some of the new ferroelectric and antiferroelectric materials are listed in Table 7.

Table 7

Structure, lattice parameters and phase transition temperatures of new ferroelectric and antiferroelectric materials

	Formula	Structure	Lattice parameters, A (at 20°C)	Transition points, °C
1	$SrTiO_3$	Perovskite	$a=3,897$	—250 (?)
2	$CdTiO_3$	»	$a=c=3,784$; $\beta=91°10'$ $b=3,800$	—210
3	$PbTiO_3$	»	$a=3,896$ $c/a=1,063$	500
4	$PbZrO_3$	»	$a=4,150$ $c/a=0,998$	235
5	$(Pb, Ba)SnO_3$	»	—	
6	$NaTaO_3$	»	$a=5,5239$ $b=3,8831$ $c=5,4778$	475 (?)
7	$KTaO_3$	»	$a=3,9885$	—260
8	$NaNbO_3$	»	$a=2\cdot3,921$ $b=4\cdot3,885$, $\beta=90°10'$ $c=2\cdot3,921$	640,518, 470,360
9	$KNbO_3$	»	$a=4,045$, $b=3,984$, $\beta=90°21'$ $c=4,045$	435,225,—10
10	$PbHfO_3$	»	$a=4,136$ $c/a=0,991$	215,163
11	$LiTaO_3$	Ilmenite	$a=5,49$, $\alpha=56°30'$	>450
12	$LiNbO_3$	»	$a=5,47$ $\alpha=55°43'$	>450
13	WO_3	Rhenium trioxide	$a=7,274$ $b=7,501$, $\beta=89°56'$ $c=3,824$	740,—50
14	$Cd_2Nb_2O_7$	Pyrochlore	—	—90,—190
15	$Sr_2Ta_2O_7$	—	—	—90,—190
16	$PbNb_2O_6$	—	—	570
17	$PbTa_2O_6$	—	—	260

IV. New Ferroelectrics and Antiferroelectrics with Hydrogen Bonds

Ferroelectric materials containing hydrogen have been less intensively investigated than ferroelectrics of the oxy-octahedral type. Nevertheless, ferroelectric and antiferroelectric properties have been detected in recent years in a number of compounds containing hydrogen bonds.

1. $NH_4H_2PO_4$ and $ND_4D_2PO_4$

Mason & Matthias[109] on the basis of their study of the piezoelectric, dielectric and elastic properties of ammonium dihydrogen phosphate and the deuterated compound inferred that both these compounds are antiferroelectrics. These crystals have the same tetragonal structure at room temperature and the orthorhombic structure at temperatures below their respective transition points. A sharp change in the properties of the crystals along the *a* axis occurs at the transition points (-125° for $NH_4H_2PO_4$ and -31° for $ND_4D_2PO_4$); the latent heat of the transitions is very appreciable; however, no hysteresis loops were observed at temperatures below the Curie point. The authors deduce that the antiferroelectric axis is aligned with one of the *a* crystallographic axes.

2. CsH_2AsO_4

Table 8

Temperatures of phase transitions in the dihydrogen phosphates and arsenates of alkali metals

Formula	Transition temp., °C
KH_2PO_4	—150
RbH_2PO_4	—125
KH_2AsO_4	—178
RbH_2AsO_4	—160
CsH_2AsO_4	—130

Physicists have known of the ferroelectric properties of the tetragonal modifications of all K, Rb and Cs di-H phosphates and arsenates (except CsH_2AsO_4) for some time.

In 1953 Frazer & Pepinsky[110] discovered that cesium dihydrogen arsenate is also a ferroelectric with a transition point at -130°. Typical hysteresis loops are observed at $T < \theta$.

From the available data on the properties of the known ferroelectric dihydrogen arsenates and phosphates we can conclude that in general the larger the alkali cation, the higher the transition point and the lower the dielectric constant. The phase transition temperatures in different di-H arsenates and phosphates are listed in Table 8.

3. $(NH_4)_2H_3IO_6$

According to Baertschi[111], a phase transition associated with a pronounced dielectric anomaly occurs in $(NH_4)_2H_3IO_6$ in the temperature interval between -20 and -30°. The latent heat of the transition is about 350 cal/mole. Inasmuch as no hysteresis loops at temperatures below the transition point have been observed, Busch, Känzig & Meier[112] have inferred that this compound is antiferroelectric. This assumption is substantiated by the fact that superstructure lines appear in x-ray patterns recorded at $T < \theta$. The lattice periods in the direction perpendicular to the trigonal axis are doubled in the transition.

4. $Ag_2H_3IO_6$

In a recent investigation Gränicher, Meier & Petter report that $Ag_2H_3IO_6$ is antiferroelectric[113].

5. $LiNH_4C_4H_4O_6.H_2O$ and $LiTlC_4H_4O_6.H_2O$

The fact that lithium-ammonium tartrate has ferroelectric properties has been reported by Merz[114] and by Matthias & Hulm[115]. This salt has the orthorhombic structure at about 20°. The dielectric constant at room temperature is small along all three axes. The dielectric constant along the a and c axes changes very little, while ϵ_b passes through a sharp maximum at -167°. The spontaneous polarization at low temperatures is $0.21 \cdot 10^{-6}$ Coulomb.cm^2. At room temperature the piezoelectric coefficient $d_{25} = 20 \cdot 10^{-8}$ cgse units, while at the transition point it rises to $(10{,}000\text{-}20{,}000) \cdot 10^{-8}$ units.

Lithium-ammonium tartrate has certain distinctive characteristics as compared with Rochelle salt: the spontaneous polarization in $LiNH_4C_4H_4O_6.H_2O$ is directed along the b axis, while in Rochelle salt it is aligned with the a axis. Only one phase transition has been observed in this ferroelectric. Instead of four water "molecules", as in Rochelle salt, lithium-ammonium tartrate has only one water "molecule" per unit cell.

The presence of spontaneous polarization in $LiTlC_4H_4O_6.H_2O$ at very low temperatures ($\sim$10°K) was discovered by Matthias & Hulm[115]. The spontaneous polarization in this crystal is directed along the a axis and at 1.3°K equals approximately $0.14 \cdot 10^{-6}$ Coulomb/cm^2.

6. $(CN_3H_6)Al(SO_4)_2.6H_2O$

A new class of ferroelectrics containing hydrogen bonds was recently discovered by Holden, Matthias, Merz & Remeika[116]. Guanidine aluminum sulfate hexahydrate is ferroelectric in a wide temperature range. This is the first ferroelectric with a hydrogen bond to be discovered that has a transition point in the region of high temperatures (200-300°). The authors, however, note that above 100° the crystal begins to lose its water of crystallization. The crystal structure is trigonal. The space group is reported as $C_{3v}(2)$-P3lm; the unit cell contains three "molecules". This ferroelectric is readily grown from aqueous solutions by the conventional procedure.

Table 9

Temperatures of phase transitions in some ferroelectrics and antiferroelectrics with hydrogen bonds

Chemical formula	Phase transition temp., °C
$NH_4H_2PO_4$	—125
$ND_4D_2PO_4$	—31
CsH_2AsO_4	—130
$(NH_4)_2H_3IO_6$	—20 ÷ —30
$Ag_2H_3IO_6$	—46
$LiNH_4C_4H_4O_6.H_2O$	—167
$LiTlC_4H_4O_6.H_2O$	—263
$(CN_3H_6)Al(SO_4)_2.6H_2O$	200 ÷ 300

At room temperature the saturation polarization is about $0.35 \cdot 10^{-6}$ Coulomb/cm^2 and the coercive force is 1200-1500 v/cm. Both these quantities increase with decreasing temperature. The hysteresis loops are symmetric and rectangular; hence the material will undoubtedly be of technological interest. The crystal is characterized by a small dielectric constant ($\epsilon_{\parallel} = 15$, and $\epsilon_{\perp} = 5$). The authors report that there can be obtained isomorphous substances in which the Al^{3+} is replaced by Cr^{3+} and Ga^{3+}, the $(SO_4)^{2-}$ by $(SeO_4)^{2-}$ and the H_2O by D_2O.

The phase transition temperatures of a number of the new ferroelectrics and antiferroelectrics with hydrogen bonds are listed in Table 9.

Space obviously does not allow of listing all the investigations devoted to ferroelectrics and antiferroelectrics in recent years. It will be obvious from this review, however, that the past decade has been marked by intensive study of ferroelectric effects with the result that our insight into the nature of ferroelectric and antiferroelectric phenomena has been broadened and deepened.

References

1. I.V.Kurchatov, Segnetoelektriki (Ferroelectrics), M.-L., 1933
2. B.M.Vul, I.M.Gol'dman, Doklady AN SSSR, 46, 154 (1945); 49, 179 (1945); 51, 21 (1946).
3. B.M.Vul, Elektrichestvo (Electricity), 3, 12 (1946).
4. A.V.Rzhanov, Usp.fiz.nauk, 38, 461 (1949).
5. H.F.Kay, Rep.Progr.Phys., 18, 230 (1955).
6. H.Blattner, B.Matthias & W.Merz, Helv.Phys.Acta, 20, 225 (1947).
7. J.P.Remeika, J.Am.Chem.Soc., 76, 940 (1954).
8. G.Shirane, R.Pepinsky & B.C.Frazer, Acta Cryst., 9, 131 (1956).
9. W.J.Merz, Phys.Rev., 76, 1221 (1949); 78, 52 (1950).
10. W.J.Merz, Phys.Rev., 91, 513 (1953).
11. W.J.Merz, Phys.Rev., 81, 1064 (1951).
12. J.K.Hulm, Proc.Phys.Soc.(London), 63A, 1884 (1950).
13. W.J.Merz, Phys.Rev., 78, 642 (1950).
14. M.E.Caspari, Phys.Rev., 78, 341 (1950).
15. M.E.Caspari & W.J.Merz, Phys.Rev., 80, 1082 (1950).
16. W.L.Bond, W.P.Mason & H.J.McSkimin, Phys.Rev., 82, 442 (1951).
17. H.Blattner & W.Merz, Helv.Phys.Acta. 21, 210 (1948).
18. A.Hippel, Rev.Mod.Phys., 22, 221 (1950).
19. W.J.Merz, Phys.Rev., 78, 52 (1950).
20. H.D.Megaw, Trans.Farad.Soc., 42A, 224 (1946); Proc.Roy.Soc.,A189,261 (1947).
21. H.F.Kay & P.Vousden, Phil.Mag., 40, 1019 (1949).
22. W.Känzig, Helv.Phys.Acta., 24, 175 (1951).
23. N.A.Roi, Doklady AN SSSR, 81, 545 (1951).
24. W.J.Merz, Phys.Rev., 95, 690 (1954).
25. E.A.Little, Phys.Rev., 98, 978 (1955).
26. V.L.Ginzberg, Zhur.eksp.i teor.fiz., 15, 739 (1945); 19, 36 (1949).
27. A.F.Devonshire, Phil.Mag., 40, 1040 (1949); 42, 1065 (1951).
28. M.Ia.Shirobokov & L.P.Kholodenko, Zhur.eksp.i teor.fiz., 21, 1239 (1951).
29. L.P.Kholodenko & M.Ia.Shirobokov, Zhur.eksp.i teor.fiz., 21, 1250 (1951).
30. C.Kittel, Phys.Rev., 82, 729 (1951).
31. G.A.Smolenskii & R.E.Pasynkov, Doklady AN SSSR, 79, 431 (1951); Zhur. eksp.i teor.fiz., 24, 70; 25, 57 (1953).
32. G.A.Smolenskii & V.Kh.Kozlovskii, Zhur.eksp.i teor.fiz., 26, 684 (1954).
33. W.P.Mason & B.T.Matthias, Phys.Rev., 74, 1622 (1948).
34. S.Roberts, Phys.Rev., 75, 989 (1949).
35. E.T.Jaynes, Ferroelectricity. Princeton, 1953.

36. W.P.Mason, Piezoelectric crystals and their application in ultrasonics (In Russ. translation, M.1952).
37. S.V.Bogdanov, Dissertation, Physics Institute USSR Ac. of Sci., 1950.
38. A.E.Glauberman & A.F.Lubchenko, Zhur.eksp.i teor.fiz., 23, 188 (1952).
39. J.C.Slater, Phys.Rev., 78, 748 (1950).
40. G.I.Skanavi, Fizika dielektrikov (Physics of dielectrics), M.-L., 1948.
41. M.H.Cohen, Phys.Rev., 84, 368 (1951).
42. M.H.Cohen, Phys.Rev., 84, 369 (1951).
43. J.H.Barret, Phys.Rev., 86, 118 (1952).
44. H.C.Schweinler, Phys.Rev., 87, 5 (1952).
45. G.A.Smolenskii & V.Kh.Kozlovskii, Zhur.tekh.fiz., 23, 445 (1953).
46. P.P.Ewald, Ann.Phys., 64, 253 (1921).
47. E.T.Jaynes & E.P.Wigner, Phys.Rev., 79, 213 (1950).
48. J.H.VanSanten, F.deBoer, Nature, 163, 957 (1949).
49. J.H.VanSanten & G.H.Jonker, Philips.Res.Rep., 3, 371 (1949).
50. W.Shockley, Phys.Rev., 70, 105 (A) (1946); 73, 1273 (1948).
51. C.R.Hagedorn, ZS.Phys., 133, 394 (1952).
52. E.Madelung, Phys.ZS., 19, 524 (1918).
53. G.A.Smolenskii, Doklady AN SSSR, 70, 405 (1950); 85, 985 (1952); Zhur. tekh.fiz., 20, 137 (1950); 21, 1045 (1951).
54. J.K.Hulm, Proc.Phys.Soc., 63, 1184 (1950).
55. G.Shirane, S.Hoshino & K.Suzuki, Phys.Rev., 80, 1105 (1950).
56. G.H.Jonker & J.VanSanten, Chemisch Weekbld, 43, 672 (1947).
57. G.Shirane & E.Sawaguchi, Phys.Rev., 81, 458 (1951).
57a. J.Kobayashi & R.Ueda, Phys.Rev., 99, 1900 (1955).
58. I.N.Beliaev & A.L.Khodakov, Zhur.eksp.i teor.fiz., 22, 376 (1952).
59. E.G.Fesenko, Doklady AN SSSR, 88, 785 (1953).
60. M.A.Blokhin, Doklady AN SSSR, 95, 1165 (1954).
61. J.Naray-Szabo, Naturwiss, 31, 202 (1943).
62. S.J.Roberts, J.Amer.Cer.Soc., 33, 63 (1950).
63. A.Hoffman, ZS.Phys.Chem., 1328, 65 (1935).
64. H.D.Megaw, Proc. Phys. Soc., 58, 133 (1946).
65. R.Ueda & G.Shirane, Phys.Soc. Japan, 6, 3, 209 (1951).
66. E.Sawaguchi, J.Phys.Soc.Japan, 7, 110 (1952); 8, 615 (1953).
67. E.Sawaguchi, H.Maniwa & S.Hoshino, Phys.Rev., 83, 1078 (1951).
68. S.Roberts, Phys.Rev., 83, 1078 (1951).
69. Iu.N.Venevtsev, Dissertation, Moscow Phys. & Eng.Inst., 1955.
70. G.Shirane, Phys.Rev., 84, 854 (1951); 86, 219 (1952).
71. G.Shirane, E.Sawaguchi & Y.Takagi, Phys.Rev., 84, 476 (1951).
72. G.Shirane & R.Pepinsky, Phys.Rev., 91, 812 (1953).
73. G.G.Urazov, E.I.Speranskaia & Z.F.Gulianitskaia, in Abstracts of Reports presented at the Third All-Union Conference on Physico-Chemical Analysis, Pub. AN SSSR, M., 1955.
74. G.A.Smolenskii & A.I.Agranovskaia, Doklady AN SSSR, 97, 237 (1954).
75. G.A.Smolenskii, A.I.Agranovskaia, A.M.Kalinina & G.M.Fedotova, Zhur.tekh. fiz., 25, 2134 (1955).
76. B.T.Matthias, Phys.Rev., 76, 430 (1949).
77. R.Ueda & T.Ichinokawi, Phys.Rev., 80, 1106 (1950).
78. R.Ueda & T.Ichinokawi, Phys.Rev., 82, 563 (1951).
79. R.Ueda & T.Ichinokawi, Phys.Soc.Japan, 6, 122 (1951).
80. S.Sawada, R.Ando & S.Nomura, Phys.Rev., 82, 952 (1951).
81. S.Sawada, R.Ando & S.Nomura, Phys.Rev., 84, 1054 (1951).
82. B.T.Matthias & E.A.Wood, Phys.Rev., 84, 1255 (1951).

83. R.G.Rhodes, Nature, 170, 369 (1952).
84. W.L.Kehl & R.G.Hay & D.Wahl, J.Appl.Phys., 23, 282 (1952).
85. H.D.Megaw, Acta Cryst., 5, 739 (1952).
86. R.Ueda & J.Kobayashi, Phys.Rev., 91, 1565 (1953).
87. G.Goodman, J.Amer.Cer.Soc., 30, 368 (1953).
88. E.Wainer & C.Wentworth, J.Amer.Cer.Soc., 35, 207 (1952).
89. W.R.Cook & H.Jaffe, Phys.Rev., 88, 1426 (1952).
90. W.R.Cook & H.Jaffe, Phys.Rev., 89, 1297 (1953).
91. F.Jona, G.Shirane & R.Pepinsky, Phys.Rev., 98, 903 (1955).
92. G.Shirane & R.Pepinsky, Phys.Rev., 92, 504 (1953).
93. J.K.Hulm, Phys.Rev., 92, 504 (1953).
94. H.Danner & R.Pepinsky, Phys.Rev., 99, 1215 (1955).
95. G.A.Smolenskii, V.A.Isupov & A.I.Agranovskaia, Doklady AN SSSR, 108, 232 (1956).
96. B.T.Matthias & J.P.Remeika, Phys.Rev., 76, 1886 (1949).
97. B.T.Matthias, Science, 113, 591 (1951).
98. B.T.Matthias, Phys.Rev., 75, 117 (1949).
99. P.Vousden, Acta Cryst., 4, 373 (1951).
100. J.K.Hulm, B.T.Matthias & E.A.Long, Phys.Rev., 79, 885 (1950).
101. B.T.Matthias, Phys.Rev., 75, 1771 (1949).
102. A.Pavlovic & R.Pepinsky, Phys.Rev., 93, 672 (1954).
103. E.A.Wood, Acta Cryst., 4, 353 (1951).
104. S.Triebwasser & T.Halpern, Phys.Rev., 98, 1562 (1955).
105. S.Triebwasser, Phys. Rev., 101, 993 (1956).
106. R.M.Cotts & W.D.Knight, Phys.Rev., 96, 1285 (1954).
107. L.E.Gross & B.J.Nicholson, Phil. Mag., 46, 453 (1955).
108. P.Vousden, Acta Cryst., 4, 545 (1951).
109. W.P.Mason,& B.T.Matthias, Phys.Rev., 88, 477 (1952).
110. B.C.Frazer & R.Pepinsky, Phys.Rev., 91, 212 (1953).
111. P.Baertschi, Helv. Phys. Acta., 18, 267 (1945).
112. G.Busch, W.Känzig & W.M.Meier, Helv.Phys.Acta, 26, 385 (1953).
113. H.Gränicher, W.M.Meier & W.Petter, Helv.Phys.Acta., 27, 216 (1954).
114. W.J.Merz, Phys.Rev., 82, 562 (1951).
115. B.T.Matthias & J.K.Hulm, Phys. Rev., 82, 1, 108 (1951).
116. A.N.Holden, B.T.Matthias, W.J.Merz & J.P.Remeika, Phys.Rev., 98, 546 (1955).

ORIENTATION OF THE DOMAINS AND MACROSYMMETRY OF THE PROPERTIES OF FERROELECTRIC SINGLE CRYSTALS

- I.S.Zheludev & L.A.Shuvalov

Introduction

A characteristic common to all ferroelectric crystals is the presence of a specific temperature interval limited from above and below (the lower bound may be absolute zero), commonly known as the ferroelectric region. The boundary of this region, the so-called Curie point, is the phase transition temperature at which the crystal undergoes a polymorphic transformation and changes its symmetry, i.e., becomes ferroelectric on "entering" this region. Distinctive features of a crystal in the ferroelectric state are the presence of spontaneous internal polarization and the breaking up of the single crystal into domains: regions within which the spontaneous polarization of all the unit cells has the same direction.

The breaking up or fragmentation of a single crystal into domains can readily be interpreted qualitatively on the basis of energy considerations. A single crystal, becoming spontaneously polarized, acquires a certain energy of the electrostatic field produced by this polarization. Any decrease of this electrostatic energy, naturally, reduces the energy of the crystal as a whole. Fragmentation of the crystal into domains serves to reduce this external field and its electrostatic energy, bringing the crystal into an energetically more advantageous state. Fragmentation into domains is accompanied by the formation of domain boundaries (walls) which calls for the expenditure of a certain energy; when the domains are not very small this energy is much lower than the energy released by the decrease of the external field. The energy of the external field produced by volume polarization is proportional to the cube of the linear dimensions of the domains, while the energy of the domain walls is proportional to the square of the linear dimensions. Hence the fragmentation continues to the point where the domain dimensions become so small that the energy expended on the formation of the domain walls becomes equal to the energy liberated by the reduction of the external field. This then is the critical size of the domain corresponding to the minimum free energy of the crystal. In the process the net (macroscopic) polarization of the crystal proves statistically equal to zero.

In the above interpretation we have not mentioned the fact that in the process of breaking up into domains frequently part of the energy is also expended on deformation (twin rotations, shifts, displacements, etc.). This does not alter the process in principle, but of course it may affect the critical size of the domains. This "secondary" expenditure of energy may serve to explain, for example, why the 180° domains in $BaTiO_3$ are smaller than the 90° domains, which themselves often break up into 180° domains. The formation of the 180° domains does not involve any deformation of the crystal, while the formation of the 90° domains is accompanied by shear strains.

It should be noted that in the case of ferroelectrics in the breaking up of the crystal into domains there need not necessarily appear "closing regions" as in ferromagnets. In the case of ferroelectrics free charges settling from the surrounding medium can compensate (neutralize) small microfields on the surface of a multidomain crystal. The availability of this compensation explains why large single-domain blocks are much more frequently encountered in ferroelectric crystals as compared with ferromagnetic ones.

The net (macroscopic) polarization of a single crystal could be statistically equal to zero even with a disordered arrangement of the domains in all directions similar to the arrangement of crystallites in a polycrystal. Actually, however, orientation of the domains in ferroelectric crystals, despite the great diversity of the known and fairly well studied domain structures, is subject to certain rigorous regularities which although they differ in detail for crystals of different types have certain traits in common.

Let us try to formulate the general regularities governing the orientation of domains in all ferroelectric crystals.

Two types of ferroelectric crystals and the dependence of the orientation of the domains on the symmetry of the initial nonferroelectric phase

First we must note that the character of the domain structure and the orientation of the domains depend on the number of axes of spontaneous polarization in the crystal. (The axis of spontaneous polarization or so-called ferroelectric axis is the crystallographic line along which the spontaneous polarizations of the unit cells arise in the ferroelectric phase, generally in opposite directions, but in the case of the polar axis in the same direction.) The number of such axes differs in different crystals. Thus in Rochelle salt and KH_2PO_4 there is one such axis (the x or z axis, respectively); in perovskite-type ferroelectrics ($BaTiO_3$, $KNbO_3$ and the like) in the tetragonal modification there are three axes, in the rhombic modification six axes and in the rhombohedral modification four axes. Accordingly, by analogy with ferromagnets, all ferroelectric crystals can be divided into two groups: electrically uniaxial and electrically multiaxial.

This subdivision is not purely formal. First, in this manner we separate the crystals (uniaxial crystals) in which there can exist only the simplest - antiparallel - arrangement of the domains and only 180° walls, from crystals in which in view of the availability of several directions of spontaneous polarization there is a tendency towards complicated twinning of the domains and in which therefore the domains may be oriented in a more diverse fashion, the domain structure can be appreciably more complex and 90° the other walls may exist in addition to the 180° walls (multiaxial crystals).

Second, this subdivision has a profound significance as regards other important properties of ferroelectric crystals, primarily as regards the character of polarization curves. In electrically uniaxial crystals there obtains only "longitudinal inversion" (to borrow from the terminology of ferromagnetism), i.e., displacement of only the 180° walls. In multiaxial crystals, in addition to longitudinal inversion, there may occur transverse inversion; in fact, in some types of multiaxial crystals, for example, in rhombic and rhombohedral perovskite-type ferroelectrics, there must obtain several different transverse inversions (as well as longitudinal ones)*. Just as in ferromagnets, in multiaxial (for example, perovskite) ferroelectrics, the displacement of the 180° walls (longitudinal inversion) proceeds with a considerably lower expenditure of energy than displacement of the 90° walls and other forms of transverse inversion, inasmuch as the last are accompanied by deformations of the lattice. (We note that in the uniaxial crystals of Rochelle salt and KH_2PO_4 displacement of the 180° walls occurs - in contrast to the analogous process in $BaTiO_3$ - with deformation of the lattice and hence must require a comparatively large amount of energy.) Hence in weak fields

---

*The analogous case for the rhombohedral ferromagnetic Ni has recently been examined by Akulov[1].

we have displacement of the 180° walls, while in strong fields we have transverse inversion. Of course, in an actual crystal these two processes may be superimposed and where the polarization curve is concerned it is not always feasible to separate the sections corresponding to each process in its pure form. In the case of several forms of longitudinal and transverse inversion, the polarization process will obviously be even more complex; insofar as we know it has never been studied in detail.

The effect observed by Rzhanov[2] in 1949 is explained by the difference in the processes of displacement of the 180° and 90° domain walls in tetragonal $BaTiO_3$ (triaxial). Rzhanov found that the hysteresis loop in a weak field became much more pronounced in the case of a specimen to which a strong field was applied and removed beforehand (i.e., the preliminary application of a strong field increased the polarization). This effect is explained by the fact that in the case of the direct application of a weak field the domains with spontaneous polarization axes at an angle of 90° to the field do not participate in the polarization process. On the other hand, after application of a strong field, which produces transverse inversion, all the domains participate in the polarization process in a weak field.

Recently Little[3] investigated in detail the difference in the formation (nucleation) and motion of 180° and 90° walls in tetragonal $BaTiO_3$. Subsequently McQuarrie[4], on the basis of Little's results and the difference in the energies associated with the motion of the 180° and 90° walls, suggested that the aging of $BaTiO_3$ ceramics and crystals consists of the return of the 90° domains to their initial positions, which appears to be a plausible hypothesis.

The above described more or less complex processes as well as a number of others occur only in multiaxial crystals; they do not occur in uniaxial ones. Thus it may be asserted that the domain structure, its behavior and the number of important properties of ferroelectric single crystals depend on the number of axes of spontaneous polarization present in the given crystal type. The number of axes present, in turn, is determined by the symmetry of the initial, nonferroelectric state, or more precisely the number of equivalent axes transforming one to the other by means of the elements of symmetry of the initial, nonferroelectric phase.

In the case of a number of ferroelectric crystals, in the nonferroelectric phase there may be several groups of equivalent, potential ferroelectric axes (a group, in this sense, may consist of a single axis it if it is a singular one). Accordingly, in such crystals (for example, $BaTiO_3$) there may be several ferroelectric phases. Naturally, the domain structure in each phase will depend upon along which group of axes spontaneous polarization develops in the given phase.

Thus we come to the conclusion that the orientation of the domains and, consequently, the general character of the domain structure are determined by the symmetry of the crystal in the initial, nonferroelectric phase and the direction (axis in the initial phase) along which spontaneous polarization arises in the given ferroelectric phase.

Macrosymmetry in multidomain crystals

Ordered orientation of the domains along one or several axes of spontaneous polarization (in the case of uniaxial or multiaxial crystals, respectively) leads to a multidomain crystal becoming essentially a polysynthetic twin (or the formation of a unique texture with axes of finite order) whose components

are domains. The twinning elements here are the symmetry elements present in the crystal in the initial, nonferroelectric phase eliminated in the transition to the ferroelectric phase. This is characteristic of the class of reversible phase transitions to which ferroelectric transitions belong.

As a result the multidomain crystal as regards its statistically averaged macrosymmetry returns to the symmetry of the initial nonferroelectric phase*. This is understandable inasmuch as in the absence of an artificially imposed (for example, by application of an electric field) preferred direction, the crystal in the transition to the ferroelectric phase, breaking up into domains, tends to retain its initial shape (minimal expenditure of energy).

Fig.1

a b

Fig.2.

Fig.1. Model of statistical conjunction of the domains of Rochelle salt.
Fig.2. Model of the statistical conjunction of the domains of $BaTiO_3$: a) tetragonal modification, b) rhombohedral modification. (Shaded faces - areas of emergence of the positive ends of the P_s vectors.)

The tendency of a multidomain crystal to return to the symmetry of the initial nonferroelectric phase is particularly clearly evident if we examine formal twins comprised of equal domains (unit cells) having all possible orientations for the given ferroelectric phase of the crystal (Figs.1 & 2).

We note that in twinning of domains there must obtain at their point or area of contact not only the geometric condition of matching of the elements of symmetry of the initial phase but also the electric condition of neutrality of the common domain walls. Hence, for example, twinning of the 90° domains in $BaTiO_3$ occurs so that the positive end of the axis of polarization of one domain is matched with the negative end of the polarization of the next domain. Analysis of possible twinning on the basis only of electric neutrality of the common domain boundaries, however, can lead to errors. Thus it would appear that in tetragonal $BaTiO_3$, in addition to the (110) twinning plane (domain wall), there could be twinning about the (111) plane inasmuch as all intersections of it with the (001) plane yield a 45° non-charged boundary. Actually, however, there is no (111) symmetry plane in the initial cubic crystal and hence twinning about it is impossible.

The above observation regarding the return of a multidomain crystal as regards its macrosymmetry to the symmetry of the initial nonferroelectric

---

*For crystals of Rochelle salt this fact, noted by Chernysheva[5], was recently examined in detail by the present authors[6].

phase pertains not only to polarization and external form but also to all the physical properties of the crystal taken as a whole. Consequently, if the crystal in its initial nonferroelectric phase does not have piezoelectric properties, for example, the polydomain crystal will not exhibit piezoelectric properties either (example: $BaTiO_3$). And, on the contrary, if the crystal in its initial phase possesses piezoelectric properties, it will have them in the ferroelectric phase as well (example: Rochelle salt). In fact, the piezoelectric properties of Rochelle salt can be utilized in practice only because Rochelle salt, which is a "soft" ferroelectric, does not retain the polarized state and readily returns to the multidomain state so that it possesses piezoelectric properties both in the initial nonferroelectric and in the multidomain ferroelectric states.

The return of a multidomain crystal as regards symmetry of its physical properties to the symmetry of the initial nonferroelectric phase has been rigorously demonstrated by the writers on the example of a crystal of Rochelle salt[6]; an analogous proof can readily be carried through for any ferroelectric crystal.

It must be emphasized that the above assertions pertain to the macroscopic properties of crystals, i.e., to the properties of the crystal as a whole. The microscopic properties, specifically the properties commonly observed in optical and x-ray investigations of crystals, will naturally correspond to the symmetry of the crystal in the ferroelectric phase. It is obvious, too, that the above conclusion is valid statistically, that is, applies to the averaged attributes. Deviations in the case of some preferred orientation of the domains will be evinced by the effect of unipolarity, lowering of the symmetry, the appearance of specific piezoelectric coefficients, etc. This applies particularly to the case when we are dealing not with a complete crystal but with a specimen cut from a particular growth pyramid.

Thus it may be asserted not only that the orientation of the domains and a number of other important properties of multidomain crystals are determined by the symmetry of the initial non-ferroelectric phase and the directions in which spontaneous polarization occurs, but also that through twinning of the domains multidomain crystals tend to return to the symmetry of the initial nonferroelectric phase as regards macrosymmetry of the shape and physical properties of the crystal. Hence from an analysis of a formal twin comprised of equal domains in conformity with the possible axes of spontaneous polarization and the symmetry elements present in the crystal in the initial nonferroelectric phase we can determine all the possible orientations of the domains and directions of their walls, i.e., deduce all the general regularities concerning the domain structure of any ferroelectric crystal and the symmetry of its macroscopic properties in the multidomain state. To do this, however, we must know the symmetry of the initial nonferroelectric phase and the direction of the axis (or one of the group of possible axes) of spontaneous polarization. In the case of $BaTiO_3$ crystals both are known and, consequently, from an examination of formal twins we can readily predict the presence of $70^\circ32'$, $109^\circ28'$ and 180° domain walls in rhombohedral $BaTiO_3$ (see Fig.2,b) and the presence of 60°, 90°, 120° and 180° walls in rhombic $BaTiO_3$ and therefore give the orientation of these boundaries relative to the edges of a crystal plate of any arbitrary cut.

Series of possible ferroelectric phase transitions

In the light of what we have just deduced regarding the decisive role played by the symmetry of the initial nonferroelectric phase as regards the orientation of the domains in the multidomain crystal in the ferroelectric phase, we can attempt to establish all the possible ferroelectric phase transitions for all classes of crystals; this would be of undoubted interest inasmuch as it should enable us to make certain predictions in addition to foretelling the possible orientation of the domains.

Despite the fact that the number of known ferroelectric crystals exceeds thirty, the number of known different ferroelectric phase transitions is not great. They are all accompanied by a change in the symmetry of the crystal and its transition to a different crystallographic class as indicated in Table 1.

Table 1

Changes of symmetry in different series of crystals incident to ferroelectric phase transitions

KH_2PO_4 & ferroelectrics isomorphic with it	Rochelle salt & ferroelectrics isomorphic with it	$BaTiO_3$ & other perovskite-type ferroelectrics	Ilmenite type ferroelectrics	Guanidine aluminum sulfate & similar electrics
$\bar{4}\cdot m$	2:2	$\bar{6}/4$	$\bar{6}$	
↑↓	↑↓	↑↓		
$2\cdot m$	2	$4\cdot m$		$3\cdot m$
		↑↓		
		$2\cdot m$		
		↑↓		
		$3\cdot m$		

From an examination of the table it will be evident that the change in symmetry of all the crystals can be interpreted in the same way: at the boundary of the ferroelectric region, due to the rise of spontaneous polarization, the unit cell undergoes spontaneous electrostrictional deformation, if in the nonferroelectric phase the crystal did not possess piezoelectric properties, or spontaneous piezoelectric deformation, if in the initial nonferroelectric phase the crystal was not piezoelectric. Obviously, in the latter case the effect of the electrostriction can be neglected inasmuch as it is always much smaller than the piezoeffect; in addition, as can readily be shown, electrostrictional deformation would lead to the same change in symmetry as the piezoelectric deformation.

The spontaneously deformed cell changes its symmetry to that of a lower order. The individual domains and the entire crystal, if it is a single-domain crystal, will have the same symmetry. Although the spontaneous deformation is always comparatively small, it is important in principle inasmuch as it determines the class into which the crystal is transformed in the ferroelectric region. It may be noted that a single domain crystal in view of the presence in it of a singular polar axis (axis of spontaneous polarization) must always belong to one of ten so-called pyroelectric classes inasmuch as only these classes have a singular polar axis.

We must emphasize here one important point which is evident from the example of the phase transitions in $BaTiO_3$. In the case of several ferro-

electric transitions occurring in the same type of crystal, in each transition the spontaneous deformation, just as the regularities of the domain structure examined above, is determined not by the symmetry of the preceding higher temperature phase but by the symmetry of the initial nonferroelectric phase. This is characteristic of all ferroelectric crystals exhibiting several ferroelectric phases. This conclusion is understandable inasmuch as the sequence of the ferroelectric phases is not rigorously constant. Thus, for example, $BaTiO_3$ undergoes the transitions $\bar{6}/4 \leftrightarrow 4 \cdot m \leftrightarrow 2 \cdot m \leftrightarrow 3 \cdot m$; it is known, however, that $BaTiO_3$ in a mixed solution with other perovskite-type crystals can give the transitions $\bar{6}/4 \leftrightarrow 4 \cdot m \leftrightarrow 3 \cdot m$ and $6/\bar{4} \leftrightarrow 3 \cdot m \leftrightarrow 2m$. It is clear, therefore, that the modification $4 \cdot m$ cannot determine the attributes of modification $2 \cdot m$ and that the modification $2 \cdot m$ cannot determine the properties of the $3 \cdot m$ phase. In other words, the properties of all the ferroelectric phases must be determined by the initial nonferroelectric phase.

Let us take up a few illustrative examples. In Rochelle salt the spontaneous polarization arises along the rhombic x axis. In connection with a change in the only piezoelectric coefficient (d_{14}) associated with the spontaneous polarization, there occurs a shift of the unit cell about the x axis and the cell (and with it the single-domain crystal) becomes monoclinic. In tetragonal $BaTiO_3$ the spontaneous polarization arises along the edge of the cube, for example, in the [001] direction (z axis). The initial cubic crystal does not have piezoelectric properties. Hence, through alteration of the electrostriction coefficients $Q_{33} = Q_{11}$, $Q_{23} = Q_{13}$ and Q_{13}, the unit cell undergoes spontaneous elongation along the z axis and an equal transverse contraction along the x and y axes and becomes tetragonal. In rhombic $BaTiO_3$ the spontaneous polarization is directed along a diagonal of a cubic face (for example, in the [011] direction). Resolving the spontaneous polarization vector P_s into components along the z and y axes, we find that the cubic cell will undergo compression along the x axis, characterized by the coefficient $0.5\ (Q_{12} + Q_{13})$, and an equal elongation along the y and z axes, described by the modulus $0.5\ (Q_{22} + Q_{23}) = 0.5\ (Q_{11} + Q_{13})$ and the modulus $0.5\ (Q_{33} + Q_{32}) = 0.5\ (Q_{11} + Q_{13})$ and, finally, a rotation about the x axis characterized by the coefficient $0.5\ Q_{44}$ (evinced due to $0.5\ P_{sy} \cdot P_{sz}$). As a result the cell becomes rhombic. In the rhombohedral modification of $BaTiO_3$ the spontaneous polarization arises along a volume diagonal of the cube (for example, the [111] direction.

Resolving P_s into components along the x, y and z axes, we find that the unit cell will undergo equal longitudinal deformations along all three axes, characterized by the modulus $0.33\ (Q_{11} + Q_{12} + Q_{13})$ in view of the equality of the coefficients $Q_{11} = Q_{22} = Q_{33}$ and $Q_{12} = Q_{13} = Q_{23}$ and equal rotations about all three axes in view of the equality $Q_{44} = Q_{55} = Q_{66}$. Thus, the cubic cell becomes rhombohedral and with it the single-domain crystal. The spontaneous deformations in real crystals in all the examined examples are consistent with this picture.

Thus it may be asserted that every ferroelectric phase transition is accompanied by spontaneous deformation leading to a change in the symmetry of the crystal; this deformation is due to the piezoelectric effect and/or electrostriction associated with the spontaneous polarization arising in the crystal with the initial nonferroelectric symmetry. In view of this we can determine all the ferroelectric transformations of ferroelectric crystals from one class to another. To do this we must examine all thirty-two classes in turn and establish into what class or classes they may be transformed with a given direction of the axis of spontaneous polarization.

By way of example, let us examine the class $m \cdot 4 : m$. Since the crystals of this class do not exhibit a piezoeffect, their spontaneous deformation can occur only through electrostriction. If the spontaneous polarization in the crystal is directed along the fourth order axis (the z axis), the cell will undergo longitudinal elongation and an equal transverse contraction at the expense of the coefficients Q_{13}, $Q_{23} = Q_{13}$ and Q_{33}, i.e., the cell will remain tetragonal, but in view of the fact that the z axis is a polar one all the transverse axes and planes of symmetry will vanish. As a result the single-domain crystal will be transformed from class $m \cdot 4 : m$ to class $4 \cdot m$. If the spontaneous polarization is directed along the x axis (second order axis), then due to a change in the coefficients Q_{11}, Q_{21} and Q_{31} the unit cell will elongate along the x axis and undergo different degrees of contraction along the y and z axes. The crystal will go over from class $m \cdot 4 : m$ to $2 \cdot m$. The same result is obtained if the spontaneous polarization is directed either along the y axis or the diagonal xy. If the spontaneous polarization is directed along one of the planes of symmetry but does not coincide with any of the symmetry axes, the deformation will be such that the crystal will be transformed to class m. Finally, if the spontaneous polarization is in an arbitrary direction not coinciding with any of the axes or planes of symmetry, the crystal will go over from class $m \cdot 4 : m$ to class 1. We will not hereinafter consider the transitions to classes m and 1, inasmuch as such transitions are not encountered in practice and furthermore are associated with an excessively high uncertainty as regards the direction of spontaneous polarization; however, one should bear in mind the hypothetical possibility of transition of crystals of all classes to class 1 and of transitions of crystals from classes having planes of symmetry to class m (see Ref.7).

Thus disregarding transitions to classes 1 and m, we find that for the initial class $m \cdot 4 : m$ only the following transitions are possible:

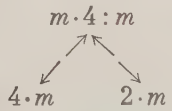

If we carry out the same operations for class $4 \cdot m$, we find that with the spontaneous polarization directed along the z axis the cell undergoes elongation along the z axis and equal transverse contraction along the x and y axes, i.e., the crystal does not change its symmetry and, consequently, does not undergo a ferroelectric transition. If the spontaneous polarization arises in other directions, the crystal will go over into class m or 1, which we have agreed not to consider. Consequently, class $4 \cdot m$ is not an "initial" class for ferroelectric transformations.

Through analogous analysis of the other crystallographic classes we can make up a table giving all the possible ferroelectric phase transitions from one crystal class to another. This has been done in Table 2. No other ferroelectric phase transitions are possible.

At this point we would like to make two remarks.

First, Table 2 can be arrived at by a more simple but formal method by means of the familiar Curie symmetry principle. As enunciated by Shubnikov[8] according to this principle the "effect" symmetry group is the highest subgroup of the "cause" symmetry groups with the given arrangement of the symmetry elements of these groups. In our case the "cause" symmetry group will be the symmetry group of the habit of the crystal in nonferroelectric phase and the symmetry group of the vector P_s (symmetry group of the stationary

cone). The "effect" group will be the symmetry group of the class into which the crystal is transformed as a result of appearance of spontaneous polarization. This group is obtained as the concomitance of all the common elements of the symmetry obtaining as a result of surposition on the polyhedron corresponding to the crystal habit group of the cone in the direction of the axis of spontaneous polarization. By means of this formal geometric procedure we can readily arrive at Table 2.

Table 2

Possible ferroelectric phase transitions and the accompanying changes in symmetry

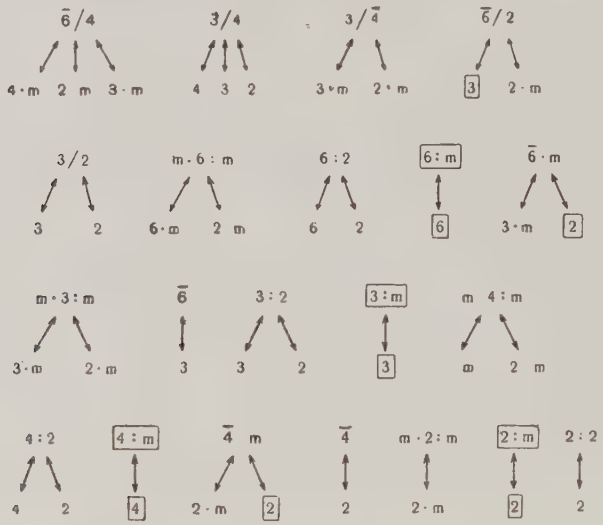

Second, generally speaking Table 2 pertains not only to ferroelectric transitions but can be employed for determining the change in the symmetry of a crystal under the influence of any polar vector acting in any direction. Thus, by means of the table one can readily determine how the symmetry of a crystal will change when an electret is made of it, or from a crystal of what symmetry and under the action of what influences one can obtain a Kerr cell, etc.

Crystals of the same classes encountered in the different series of Table 2 differ from each other as regards domain structure, primarily due to differences in the number of axes of spontaneous polarization. Even if the number of axes of spontaneous polarization is the same, the domain structure of these crystals will still be different inasmuch as the domains will be twinned in conformity with the elements of symmetry obtaining in the initial classes. The difference in the domain structure of ferroelectric crystals of the same class but belonging in different rows (series) makes it possible to explain purely formally why, for example, a KH_2PO_4 class $2 \cdot m$ crystal transforms to class $\bar{4} \cdot m$ rather than to class $\bar{6}/4$ (through class $4 \cdot m$), as do perovskite-type crystals.

In the transitions $m \cdot 3 : m \leftrightarrow 2 \cdot m$, $3 : 2 \leftrightarrow 2$ and $3/2 \leftrightarrow 3$ the ferroelectric axes proved to be the polar axes of the initial nonferroelectric phase. In such cases, as was noted above, spontaneous polarization can arise only in one direction along each of the ferroelectric axes and not in opposite directions as in the great majority of cases. Hence, although as a rule the number of

directions of spontaneous polarization is equal to twice the number of axes of spontaneous polarization, in three cases (which are rarely or never encountered in practice) the number of directions is equal to the number of axes.

A few of the transitions in Table 2 (the ones in boxes) are such that by means of twins of the resultant class one can return to the symmetry of the initial nonferroelectric class provided only that in the ferroelectric phase the crystals contain an equal number of components of twin right and left enantiomorphous forms. The actual existence of such transitions is highly doubtful.

In crystals of the middle systems, a ferroelectric phase transition with polarization directed along a higher order axis appears to be more favored than transitions with spontaneous polarization in any other direction. We note further that Table 2 comprises transitions from classes of crystals having piezoelectric properties and hence associated with spontaneous electrostrictional deformation and not only with spontaneous piezoelectric deformation. This will obtain in the case when the vector P_S is directed along the z axis for crystals of initial piezoelectric classes in which there are no piezoelectric properties along the z axis. No transition of this type has yet been detected experimentally.

All the known actual transitions are fully consistent with Table 2; in fact, if we leave aside the unlikely transitions with the appearance of two enantiomorphous forms, it may be noted that the table does not show any transitions that are now known to be nonexistent. True, the table cannot predict the sequence of transitions in a given series of ferroelectric transformations but this sequence, as has been noted, is not invariable and hence is not a matter of principle. The table also does not allow of predicting the existence of a lower Curie point (such as exists in Rochelle salt) or the nonexistence of such a point (as in KH_2PO_4), but on the basis of the table we can affirm that if there is, for example, a second ferroelectric transition in the series $2:2 \leftrightarrow 2$, it will be at a lower Curie temperature and will be a transition back to class 2:2, inasmuch as no other ferroelectric phases except this one are possible in this series. Hence the table makes it possible to indicate uniquely the number of all possible ferroelectric phases.

The table also enables us to make a number of other deductions and predictions. We see from the table, for example, that none of the ferroelectric classes is an initial class for a series of ferroelectric transformations. Consequently, there must necessarily be an upper Curie point with a transition into the nonferroelectric phase in each and every ferroelectric crystal (provided, of course, it does not decompose at a lower temperature).

From the table we can predict the certain absence or possible existence of a new (further) ferroelectric transition. Actually the table enables us to predict not simply the possibility of a transition but the possibility of a transition to a given specific class, if the series of the ferroelectric transition is known; or where the series is not known, we can at least determine the limited number of possible variants of this transition.

In a number of cases we can make a number of certain precise assertions regarding transitions on the basis of the table. Thus, concerning ilmenite-type ferroelectrics ($LiNbO_3$ and $LiTaO_3$) we only know that they belong to class $\bar{6}$ (Schweinler[9]). Consequently, for them only one ferroelectric phase with the transition $\bar{6} \leftrightarrow 3$ is possible. Regarding the newly discovered ferroelectric guanidine aluminum sulfate we know only that in its ferroelectric phase it belongs to class $3 \cdot m$. No phase transitions in it have been detected[10]. In our table class $3 \cdot m$ appears in several series. Inasmuch as it is known that

the shape of guanidine aluminum sulfate crystals is a hexagonal prism, it is clear that this crystal cannot belong in the series where the initial class is cubic; hence the crystal must belong in the series with the initial class $m \cdot 3 : m$ or the series with the initial class $\bar{6} \cdot m$ (which is more probable) and in this case it will have only one ferroelectric phase.

When the series to which a given crystal belongs is known unambiguously, the table enables us to predict the orientation of the domains and their walls and the symmetry of the macroscopic properties of the crystal on the basis of the above mentioned determining role of the symmetry of the initial nonferroelectric phase. Thus a guanidine aluminum sulfate crystal should have only an antiparallel arrangement of the domains and in the plane parallel to the z axis only 180° domain walls. Hence for optical detection of domains apparently one must proceed in the manner employed by Merz[10] in observing the 180° domains in $BaTiO_3$. A multidomain guanidine aluminum sulfate crystal, provided it is not unipolar, cannot be piezoelectric in general if this crystal belongs in the series with the initial class $\bar{6} \cdot m$, or should be piezoelectric only along the z axis if it belongs in the series with the initial class $m \cdot 3 : m$.

Conclusions

Motion picture photography of the phase transitions in $BaTiO_3$ single crystals[12] and investigation of their properties have substantiated the above formulated regularities concerning the orientation of domains and domain walls in multidomain ferroelectric single crystals, as well as our deductions regarding the macrosymmetry of their physical properties, despite the great diversity and complexity of actual domain structures.

Institute of Crystallography of the
Academy of Sciences of the USSR

References

1. N.S.Akulov, Doklady AN SSSR, 106, 31 (1956).
2. A.V.Rzhanov, Zhur.eksp.i teor.fiz., 19, 335 (1949).
3. E.A.Little, Phys.Rev., 98, 978 (1955).
4. M.McQuarrie, J.Amer.Cer.Soc., 39, No.2, 54 (1956).
5. M.A.Chernysheva, Dissertation, Institute of Crystallography, USSR, Academy of Sciences, M.1955.
6. I.S.Zheludev & L.A.Shuvalov, Transactions, Institute of Crystallography, USSR Academy of Sciences, No.12, 59 (1956).
7. I.S.Zheludev & L.A.Shuvalov, Kristallografiia, 1, 681 (1956).
8. A.V.Shubnikov, Usp.fiz.nauk., 59, 591 (1956).
9. H.C.Schweinler, Phys.Rev., 87, 5 (1952).
10. A.N.Holden, W.J.Merz, J.P.Remeika & B.T.Matthias, Phys.Rev., 101, 962 (1956).
11. W.J.Merz, Phys.Rev., 88, 421 (1952).
12. I.S.Zheludev & V.F.Parvov, Kristallografiia (Crystallography), 1, 484 (1956).

CRYSTALLOCHEMISTRY OF FERROELECTRICS WITH THE PEROVSKITE STRUCTURE

- Iu.N.Venevtsev & G.S.Zhdanov

Introduction

As we know ferroelectric transformations are associated with structural changes. Hence crystallochemical investigation of ferroelectrics should be of particular interest: we have in mind specifically study of the spatial arrangement of atoms in ferroelectric crystals and determination of the regularities governing such arrangements and the correlation between the structure and the ferroelectric and other properties of crystals.

At present, where most ferroelectrics and antiferroelectrics of the barium titanate type are concerned, we know the lattice symmetry and the temperature dependence of the phase transitions in these compounds and have available a wealth of data on the solid solutions formed by these compounds. Despite the fact that the nature of the atomic displacements has been studied in only a few ferro- and antiferroelectric materials, we can already fairly reliably classify these compounds according to structural indices and at least obtain some indication of the relationship between the structure and the character of the spontaneous polarization. The present report is devoted to the results of investigations carried out by the writers in this field. In the report we shall also draw on the data of Ref.1

1. Perovskite type structures

Ferroelectrics having the composition ABO_3 and the perovskite type structure are characterized by the presence of BO_6 octahedra sharing corners with the vacancies between them occupied by A ions. The coordination numbers of the B and O ions are 6, while the coordination number of the A ions is 12. The ideal cubic unit cell of the perovskite type (space group $O_h^1 - Pm3m$) is shown in two versions in Fig.1.

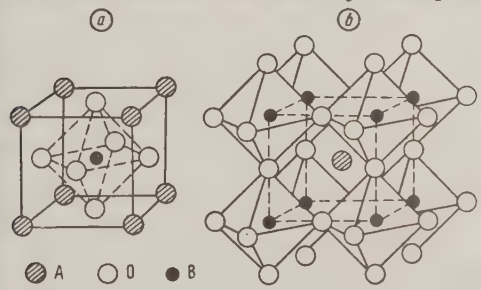

Fig.1. Ideal cubic perovskite type unit cell: a) origin of coordinates at an A ion, b) origin at a B ion.

In the very first investigations of ABO_3 compounds[2-5] it was established that realization of the perovskite type structure depends mainly on the ratio of the radii of the component ions. The valence of the A ions may be 1, 2 or 3, while that of the B ions must be 5, 4 or 3, respectively, inasmuch as it is essential that in compounds of this type the sum of the negative valences (-2.3 = -6) be numerically equal to the sum of the positive valences (m + n = 6).

Let us first consider the size of the ions. To this end let us examine a perovskite type unit cell in which each ion is symmetrically surrounded by ions of the opposite charge. With good approximation the ions may be regarded as spheres whose size is characterized by the ionic radius. If the radii of the A and oxygen ions are equal, these ions will form a closely packed cubic structure. Without displacing the oxygen ions, there can be incorporated in the oxygen octahedra B ions with a radius not exceeding 0.414 the radius of the oxygen ion (1.36 A)*, i.e., with a maximum radius of 0.56 A.

---

*The values of the atomic radii used herein are taken from Refs.6 & 7.

Thus in the case when the radii of the A and O ions are equal ($r_A = r_O$) and the radius (r_B) of the B ion is 0.56 A we have the situation of ideal contact of every ion with its neighbors. This ideal contact of the spherical ions will obtain when $r_A > r_O$ and $r_B > 0.56$ A provided the ratio $(r_A - r_O)/\sqrt{2}\,(r_B - r_O)$ (hereinafter designated by t) equals 1.

Available experimental data on ABO_3 compounds crystallizing with the perovskite structure indicate, however, that the condition for ideal contact does not have to be rigorously fulfilled for the crystal to have the perovskite type structure. In other words, t may be either somewhat greater or smaller than unity. When $r_B > 0.56$ A, in the first case the B ions will have "room" (extra space about them) in the lattice, and in the second case the A ions will have "room". Some investigators[8-10] regard deviation of the factor t from unity as one of the reasons for the distortions of the perovskite ideal lattice in observed certain compounds.

According to Megaw[8], Naray-Szabo[9] and some other authors it is sufficient to take into account only the difference between the coordination numbers of the ions, while according to Zachariasen[4] one must also take into account certain other factors. According to the former the factor t can be characterized by the formula

$$t = \frac{R_{A(\text{c.n.}\,12)} + R_O}{\sqrt{2}\,(R_B + R_O)}, \qquad (1)$$

while according to Zachariasen the formula should be

$$t = \frac{1{,}06\,(R_A + R_O)}{0{,}95\sqrt{2}\,(R_B + R_O)}. \qquad (2)$$

In these expressions R_A, R_B and R_O are the tabular values of the radii of the A, B and O ions, while $R_{A(c.n.12)}$ is the tabular value of the radius of the A ion corrected for the case of the coordination number 12.

As calculated by means of both these formulas t for the ferroelectric $BaTiO_3$ is greater than unity, while the factor for the antiferroelectric $PbZrO_3$ comes out as less than unity. In the case of the ferroelectric $PbTiO_3$ the value of t turns out to be less than unity (0.98) if we use Eq.(1) but greater than unity (1.01) if evaluated according to Eq.(2). In view of the degree of accuracy of the respective calculations (the values of the ionic radii used in the calculations are known only to within 0.02 A) the value of t for $PbTiO_3$ could be taken as unity; in other words, in this case evaluation of the factor t is not conclusive. The question of which cation has "room" in the $PbTiO_3$ lattice can therefore not be solved by geometric analysis; to answer this question one must turn to experiment.

Some investigators (Smolenskii[12] and Megaw[13]) are of the opinion that it is impossible to use ionic radii for geometric analysis of the structure of ferroelectrics and antiferroelectrics. We are inclined to agree that crystallochemical analyses should be based primarily on experimental data on the structure and properties of $PbTiO_3$, $PbZrO_3$ and other ferro- and antiferroelectric compounds of the $BaTiO_3$ group.

2. Classification of ferro- and antiferroelectrics of the $BaTiO_3$ group according to the type of ferroactive cation (A or B)

Even in their earliest publications Vul[14] and his coworkers note that the distinctive properties of $BaTiO_3$, the properties that distinguish this compound for most other titanates, are connected with the fact that the titanium

ion has "room" or, in the words of other investigators, is loosely held in the $BaTiO_3$ crystal cell. Undoubtedly the large size of the octahedral vacancy occupied by the titanium ion in the $BaTiO_3$ cell is one of the reasons why below the Curie point the Ti ion is displaced from the center of the oxygen octahedron and gives rise to electric polarization. In view of this the Ti cation may be regarded as the "trigger" of the polarization mechanism or, in other words, as ferroactive. In our opinion the primary condition for ferroactivity is that the ion in question must have "room" in the cell.

In studying the ferroelectric $KNbO_3$, Shirane, Pepinsky et al[15,16] found that the ferroelectric properties of this compound are fully similar to those of $BaTiO_3$. In particular, $KNbO_3$ undergoes similar polymorphous transitions, i.e., with decreasing temperature the cubic modification changes to the tetragonal, the tetragonal goes over into the pseudomonoclinic (orthorhombic) and the last goes over into the rhombohedral, the difference between $KNbO_3$ and $BaTiO_3$ being that in the former the transition points are shifted to the side of higher temperatures. Hence by analogy with what obtains in the case of $BaTiO_3$ one must conclude that the niobium ion in $KNbO_3$ has "room", i.e., that the Nb ion is ferroactive.

Until recently it has been assumed that the ferroelectrics $BaTiO_3$ and $PbTiO_3$ are complete analogs. However, the difference between the phase diagrams of the solid solutions $Ba(Ti,Sn)O_3$ and $Pb(Ti,Sn)O_3$ and of the solid solutions $Ba(Ti,Zr)O_3$ and $Pb(Ti,Zr)O_3$ established in our earlier investigations[1,17 & 18] indicates that the mechanism of polarization in $BaTiO_3$ differs from the mechanism in $PbTiO_3$. This difference between the properties of barium and lead titanate was explained by the fact that the ferroactive cation in the case of $PbTiO_3$ is not the B-type titanium ion, as in $BaTiO_3$, but the A-type lead ion. In other words, whereas in barium titanate the Ti ion has "room", in the lead titanate crystal the ion with free space about it is the Pb ion.

Where the antiferroelectric compound $PbZrO_3$ is concerned, the results of x-ray studies[19] indicate that the ions having "room" in the unit cell of $PbZrO_3$, as well as in the cell of the pseudoclinic and rhombohedral modifications of $Pb(Zr,Ti)O_3$ solid solution, are the Pb cations, i.e., that in the given case the lead cation is ferroactive.

The experimental data indicating that the Pb cation in the $PbZrO_3$ cell has "room" to shift are consistent with results of evaluation of the factor t for this compound according to either of the above formulas. This indicates the possibility of carrying out geometric analysis by means of the criterion t (when this differs appreciably from unity) for the purpose of establishing the type of ferroactive cation in the sense defined above.

In the antiferroelectric $PbHfO_3$ the radius of the Hf^{4+} ion (0.78 A) is close to the radius of the Zr^{4+} ion (0.82 A) and appreciably greater than the radius of the Ti^{4+} ion (0.64 A). Consequently, in the $PbHfO_3$ cell, as in the cells of $PbTiO_3$ and $PbZrO_3$, the loosely held and hence ferroactive ion is the Pb ion.

In the group of compounds characterized by anomalous dielectric properties, namely, $NaNbO_3$, $NaTaO_3$ and $CdTiO_3$, in contrast to $PbTiO_3$, the A type ions are appreciably smaller. The radius of the Pb^{2+} ion is 1.26 A, while the radii of the Na^+ and Cd^{2+} ions are identical and equal to 0.98 A. Consequently, in these compounds the A ions have "room".

The results of our classification of ferro- and antiferroelectrics of the $BaTiO_3$ group according to the type (A or B) of the ferroactive cation are shown in Table 1. (The table also includes the compounds $KTaO_3$, $CeAlO_3$ and $CeCrO_3$

which will be discussed below.) The table lists the Curie points, the radii of the A and B ions and the value of t computed according to Eq.(1). This equation appears to give better agreement with the experimental data. It must be noted that until now most investigators[11,20] have used the less satisfactory formula (2) for geometric analysis of the structure of ferro- and antiferroelectric compounds in the $BaTiO_3$ group. Thus, when calculated by means of formula (2) the value of t for $PbTiO_3$ proves to be greater than unity (1.04). On the basis of this value $PbTiO_3$ should be classed among compounds with a ferroactive B cation which is contrary to the experimental evidence. The correction for the different coordination number of the A ion was made (as indicated by Bokii[6]) by increasing the tabular value for the radius of the ion by 12%.

Table 1

Classification of ferro- and antiferroelectrics of the $BaTiO_3$ group according to type of ferroactive cation (A or B)

Character of polarization	Ferroactive cation	ABO_3	R_A, Å	R_B, Å	t*	θ, °K	symmetry above θ
Ferroelectric	B	$BaTiO_3$	1,38	0,64	1,03	393	cubic
		$KNbO_3$	1,33	0,66	1,00	708	
	A	$KTaO_3$	1,33	0,66	1,00	13	
		$PbTiO_3$	1,26	0,64	0,98	773	
Antiferroelectric		$PbHfO_3$	1,26	0,78	0,92	488	
		$PbZrO_3$	1,26	0,82	0,90	503	
		$CeAlO_3$	1,02	0,57	0,92	549?	
		$CeCrO_3$	1,02	0,64	0,89	438?	
		$NaNbO_3$	0,98	0,66	0,86	693	pseudo-cubic
		$NaTaO_3$	0,99	0,66	0,86	748?	
----?--		$CdTiO_3$	0,99	0,64	0,87	55—60	

*t computed according to Eq.1 taking R_O=1.36 A

It will be seen that we have classified $NaTaO_3$, $CeAlO_3$ and $CeCrO_3$ among the compounds with antiferroelectric properties. This assignment was based on the following considerations: first, $NaTaO_3$, according to Matthias[21], and $CeAlO_3$ and $CeCrO_3$, according to Keith & Roy[22], are characterized by high dielectric constants; second, the structural properties of $NaTaO_3$, $CeAlO_3$ and, apparently, $CeCrO_3$ are similar to those of the well-known antiferroelectrics $NaNbO_3$, $PbZrO_3$ and $PbHfO_3$. Thus these antiferroelectric compounds have packet structures composed of subcells of monoclinic symmetry[1] and a value of t - as calculated according to Eq.(1) - appreciably smaller than unity. For $NaTaO_3$, $CeAlO_3$ and $CeCrO_3$ the values of t are also smaller than unity; furthermore it is known that $NaTaO_3$ has a monoclinically distorted subcell[23], while that the subcell of $CeAlO_3$ is also monoclinically distorted follows from the report of Keith & Roy[22]. In the case of $CeCrO_3$ the dimensions of the Cr^{3+} ion (0.64 A) are close to those of the Al^{3+} ion (0.57 A), hence there is every reason to assume that $CeCrO_3$ will have the same antiferroelectric properties as $CeAlO_3$.

Returning to the compounds $NaNbO_3$, $NaTaO_3$ and $CdTiO_3$, we note that the cells of these compounds, in contrast to the cells of other ferro- and antiferroelectric compounds are pseudocubic rather than cubic at temperatures above the Curie point. Thus $CdTiO_3$ above its Curie point (-210° according to Smolenskii[12]), i.e., at room temperature, has a rhombic packet structure

comprised of monoclinically distorted subcells[8].

It has hitherto been assumed that $NaTaO_3$ has a Curie point at 475° (Matthias[24]). According to the latest data (Ref. 25), however, the transition at 475° results only in distortion of the lattice but is not accompanied by the appearance of ferroelectric or antiferroelectric properties. Apparently, the true Curie point for $NaTaO_3$ lies at some temperature below 475°. For this reason we have put a question mark in Table 1 next to this old, doubtful value of the Curie point for sodium tantalate.

X-ray and optical studies[26-30] have disclosed several polymorphous transformation in $NaNbO_3$ in the temperature range below 640°. At the same time it has proved impossible to detect any anomaly in the temperature dependence of the dielectric constant of $NaNbO_3$ in the range of high temperatures (above 400°) by dielectric measurements owing to the high losses. Hence we cannot positively associate the Curie point with 640°.* Structural changes apparently do occur in $NaNbO_3$ at 640°, but they need not necessarily be connected with the appearance of ferro- or antiferroelectric properties. It is known, for example, that in the $CaTiO_3$-$SrTiO_3$ system there occur polymorphous transformations not accompanied by the appearance of anomalous dielectric properties[32,33].

The fact that the Curie point in the system $KNbO_3$-$NaNbO_3$ remains virtually constant in the range from 0 to 90 mole % $NaNbO_3$, established by Shirane, Newnham & Pepinsky[27], may be taken as an indication that the Curie point of $NaNbO_3$ is approximately equal to the Curie point of $KNbO_3$. According to Matthias & Remeika[26] and Wood[28], the Curie temperature of $KNbO_3$ is 435°. According to x-ray studies[30] small but detectable changes are observed in $NaNbO_3$ at 420°. In view of this it may be assumed that the Curie point of $NaNbO_3$ lies at about 420°.

As may be noted from Table 1, there appears to be a definite correlation between the value of t and the character of the electric polarization: when the value of t is appreciably smaller than unity the compound exhibits antiferroelectric properties. In view of this the reported[12] indications that $CdTiO_3$ has ferroelectric properties calls for further verification inasmuch as the value of t for $CdTiO_3$ is 0.87. We note, incidentally, that the compounds $NaNbO_3$, $NaTaO_3$ and $CdTiO_3$ have the lowest values of t among those listed in Table 1.

Finally, let us turn to the ferroelectric $KTaO_3$. The calculated value of t for this compound is 1.00 and as such gives us no direct indication regarding the type of the ferroactive cation. Let us, therefore, analyze this case further. Let us see how the value of t for $KTaO_3$ can change with decreasing temperature (the Curie temperature of $KTaO_3$ is 13° K[34]). With decreasing temperature the ionic radii will decrease due to reduction of the amplitude of the thermal vibrations of the ions; the greatest reduction in amplitude will occur in the case of the potassium ion inasmuch as potassium is lighter than tantalum and has a lower valence.

Thus, if we assume that at room temperature the tantalum ion has a certain geometric possibility for displacement (i.e., actually the calculated value of t was some 0.01-0.02 greater than 1.00), with decreasing temperature this possibility will vanish. In other words, if this assumption is correct $KTaO_3$ should have no ferroelectric properties. Actually, however, it has been found that $KTaO_3$ does become ferroelectric at low temperatures. Hence it is most probable that t for $KTaO_3$ is in fact equal to 1.00 at room temperature. With decreasing temperature t decreases slightly for the above

---

*The inference that the Curie point of $NaNbO_3$ is not connected with the transition at 640° has also been made by Smolenskii & Krainik[31].

indicated reasons and as a result the K ions gain "room", i.e., acquire some possibility for displacement. In the case of $KTaO_3$, consequently, the ferroactive cation is presumably the K ion.

Thus it may be concluded that if t at room temperature equals unity, then with a change in temperature one should expect a change in the value of t to the side of greater or lower values.

In the case when the calculated value of t differs from unity by at least 0.02-0.03 it may be assumed that at temperatures differing from room temperature the ratio of the size of the ions will remain qualitatively unchanged. That is, for example, if t is appreciably greater than unity at room temperature, it will also be greater than unity at other temperatures.

Despite the contrary opinion of some investigators[12,13] what has been said above shows that it is expedient and feasible to make use of the ionic radii for general geometric analysis of the possible atomic displacements in the crystal structures of the ferro- and antiferroelectric components of the $BaTiO_3$ group. As may be seen from Table 1, for ferroelectrics we have values $t \geqslant 1$ while for antiferroelectrics we observe only $t < 1$. The values of t for ferro- and antiferroelectrics lie between the limits of 0.86 and 1.03; the values of t for antiferroelectrics all fall within the range from 0.86 to 0.92.

As has been noted, the ferroactive cations (A or B) are displaced at a certain temperature (below the Curie point) from the symmetric position occupied by them in the cubic modification cell and thereby produce a polar rearrangement of the entire cell. Up to this point we have considered only the matter of determining the type (A or B) of the ferroactive cation in different compounds. Let us now turn to the geometry of the displacement of the ferroactive cations.

3. Displacements of the ferroactive cations

According to x-ray and neutron diffraction studies[35-40], in the tetragonal modification of barium titanate, the ferroactive titanium cation and the oxygen ions are displaced different amounts along a fourth order axis from the symmetric positions occupied by them in the cubic unit cell. The displacements in the pseudomonoclinic (orthorhombic) and rhombohedral modifications of $BaTiO_3$ have not been investigated. Kay & Vousden[41], however, have advanced certain assumptions regarding the character of these displacements. In particular, they assumed that the titanium cation is displaced along the second order axis in the pseudomonoclinic modification and along the third order axis in the rhombohedral modification. The displacements of the titanium cation in the oxygen octahedron are shown schematically in Fig.2. For the sake of simplicity in the pseudocubic modifications only the oxygen ions (shown in their undisplaced positions) towards which the titanium ion is displaced are indicated.

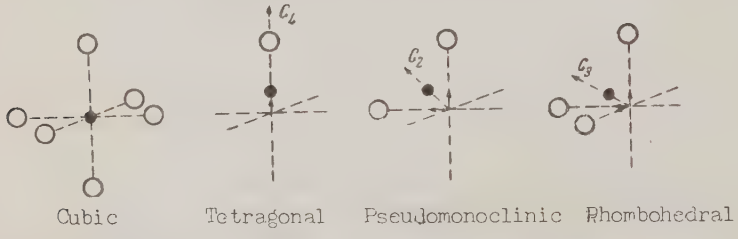

Fig.2. Possible displacements of a ferroactive B cation from its position in the cubic perovskite type lattice.

The character of the ionic displacements in $KNbO_3$ is the same as in $BaTiO_3$ inasmuch as for both $t > 1$. Among the compounds with a ferroactive A cation listed in Table 1 we have data on the atomic displacements only for $PbTiO_3$,

$PbZrO_3$ and $NaNbO_3$. According to the results of a recently published combined x-ray and neutron diffraction study[42], in the tetragonal modification of $PbTiO_3$ the ferroactive Pb cations are displaced along the fourth order axis (c-axis). In an investigation of the antiferroelectric $PbZrO_3$, it was established[43] that the Pb ions are displaced antiparallel along the second order (a) axes of the initial cubic cells. We note, incidentally, that in such displacements of the Pb ions the symmetry of the subcells comprising the packet structure of the antiferroelectric is monoclinic. The results of an interpretation[44] of the structure of the antiferroelectric $NaNbO_3$ indicate that just as in the case of $PbZrO_3$ there is an antiparallel displacement of the Pb cations along the second order axes of the initial cubic cells.

The ferroactive A cation can also be displaced along the third order axes. Unfortunately, such displacements have not been observed in any of the compounds listed in Table 1. They have, however, been detected in the cells of the rhombohedral modification of the $Pb(Ti,Zr)O_3$ solid solution[19].

Thus displacement of ferroactive B and A cations has been observed along the second, third and fourth order axes, as a result of which the cells undergo monoclinic, rhombohedral and tetragonal distortion, respectively. We want to emphasize that the shift observed in antiferroelectrics is an antiparallel displacement of the ferroactive A cation along the second order (*a*) axis of the initial cell.

For illustration of the observed displacements of the ferroactive A cation in Fig.3 we show an appropriate view of the perovskite type cubic cell and separate "detail" views of the groups of oxygen ions towards which the A cation is displaced when shifted along the C_4, C_2 and C_3 axes. As may be seen from the figure when displaced along the C_4 axis the A cation comes closer to four oxygen ions, when displaced along the C_3 axis it comes closer to three oxygen ions and finally when displaced along the C_2 axis it approaches five oxygen ions, the approach to one being particularly close in the last case.

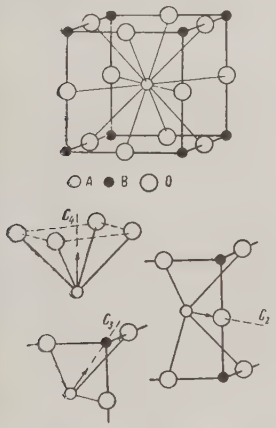

Fig.3. Unit cell of the perovskite type and possible displacement of the ferroactive A cations along the axes of symmetry from its initial central position in the cubic cell.

The coordination numbers of the ferroactive A and B cations when shifted along the different axes of symmetry of the initial cubic cell are listed in Table 2. In order to emphasize the fact that there is no radical change in the coordination numbers incident to these shifts, the coordination numbers of the cations are given in the form of sums. The addends not in parentheses give the number of oxygen ions the cation comes closer to as a result of the displacement. In each case the addend in parentheses indicates the number of oxygen ions the cation moves further away from (this number includes oxygen ions at different initial distances from the ferroactive cation.

Before concluding this section on the geometry of the displacement of ferroactive cations we must touch upon one more point.

Ferroelectrics with a value of $t > 1$ generally exhibit three phase transitions. With decreasing temperature the B cation is successively displaced along the C_4 axis, then the C_2 axis and finally the C_3 axis.

At the same time the ferroelectric $PbTiO_3$ for which $t < 1$ exhibits only one phase transition in which the lead cation is displaced along the fourth

order axis. In the case of the antiferroelectric $PbZrO_3$ for which $t < 1$, there is also observed only one phase transition in which the lead ion is displaced along the second order axis as the temperature is reduced. As is known, in the solid solutions $(Pb,Ba)ZrO_3$, $Pb(Zr,Ti)O_3$ and $Pb(Zr,Sn)O_3$ a specimen of the same composition, for example, a composition close to $PbZrO_3$, may be characterized at different temperatures by either rhombohedral or monoclinic distortion of the unit cells. In other words, shifts of the ferroactive A ion may occur along the third and fourth order axes in the same specimen. So far, however, no one has detected successive displacements of a ferroactive A cation in all the three possible directions in any ferro- or antiferroelectric with $t < 1$. Yet this sort of triple displacement is apparently theoretically possible.

Table 2

Coordination numbers of the ferroactive A and B ions before and after different displacements

Direction of shift	Symmetry	Coordination number of the cation	
		A	B
-	Cubic	12	6
C_2	Pseudomonoclinic	1 + 4 + (7)	2 + (4)
C_3	Rhombohedral	3 + (9)	3 + (3)
C_4	Tetragonal	4 + (8)	1 + (5)

4. Character of the chemical bonds in ferro- and antiferroelectrics with the perovskite type structure

Let us now turn to one of the fundamental questions in the field of ferroelectricity, the question of the chemical bonds in ferroelectrics.

The reasons for the displacements of the ions and the accompanying deformations of the unit cells must obviously be sought in the interaction between the particles forming the crystal.

Most of the ferro- and antiferroelectrics we have considered here consists of ions having the electronic configuration of a noble gas. The predominant form of interaction of such particles is ionic; however, inasmuch as the polarizabilities of the ions are not zero, there must also be some covalent interaction with the fraction of covalent bonds being the larger, the higher the polarizability of the ions involved.

The lead ion, however, does not have the noble gas configuration. In view of this and the fact that the polarizability of the lead ion is relatively high, the covalent character of the bonds in this ion is appreciably more pronounced than in others.

Most investigators[12,13,44 & 45] justifiably consider ferro- and antiferroelectric compounds with the structure of perovskite as being essentially ionic compounds with a small fraction or admixture of covalent bonds. A number of investigators, however, attribute a very important role to this fraction of covalent bonds where the origin of ferroelectricity is concerned. Thus, Megaw[13] and Vousden[44] suggest that the spontaneous polarization arises due to a sharp enhancement of the covalent character of the bonds at the Curie point. Megaw argues as follows regarding the increased covalent character of the bonds in $BaTiO_3$. As is known, one can judge of the nature of the

chemical bonds in compounds on the basis of the interatomic distances. In $BaTiO_3$ the Ti—O separation is reduced. The reason for these ions being held in this close position may be either an appreciable covalent coupling between them or the influence of a strong internal field. Megaw considers the latter to be improbable and ascribes the principal role to covalent interaction between the titanium and oxygen ions. At the same time Skanavi[46], Känzig[38] and other investigators have shown that strong internal fields do have an influence on the approach of the titanium oxygen ions to each other. Hence Megaw's conclusion regarding the appreciable covalent interaction between titanium and oxygen is not entirely well-founded.

Above we have noted that the covalent character of the bonds in the case of lead ions is more pronounced than in the case of ions of the noble gas electron configuration. However, the observed isomorphism of $PbTiO_3$ with $BaTiO_3$, $SrTiO_3$ and other compounds with the perovskite type structure in which the A ion is an alkali earth metal ion indicates that the character of the lead ion bonds is similar to that of alkali earth metal ions. Furthermore, it is known that the lead ion in the case of the $Pb(Ti,Zr)O_3$ solid solution changes its direction of displacement and hence its coordination number several times as the $PbZrO_3$ content is increased: at first it shifts along the fourth order axis and has the coordination number 4 + (8), it is then displaced along the third order axis and has the coordination number 3 + + (9) and finally it shifts along the second order axis and its coordination number becomes 1 + 4 + (7). This "mobility" of the lead atom characterizes it in this case as a particle with predominantly ionic bonds. In view of what has been said above it may be concluded that ferroelectrics with the perovskite structure have bonds of a predominantly ionic character.

Conclusions

Ferroelectrics and antiferroelectrics having the composition ABO_3 and crystallizing with the perovskite type lattice have loose structures with predominantly ionic bonds. In the cells of the ferroelectric compounds $BaTiO_3$ and $KNbO_3$ the ions with "room",i.e., the loosely held ions, are the B type ions. In the cells of the antiferroelectrics $KTaO_3$ (at low temperatures) and $PbTiO_3$ and in the cells of the antiferroelectrics $PbHfO_3$, $PbZrO_3$, $NaNbO_3$, $NaTaO_3$, $CeAlO_3$ and $CeCrO_3$ the type A cations are loosely held. The cations that have "extra space" in the cell are ferroactive. Displacements of the ferroactive A cation as well as of the ferroactive B cations may occur along the second, third and fourth order axes, producing respectively, monoclinic, rhombohedral and tetragonal distortions of the unit cells. The geometric criterion $t = \frac{R_{A(C.\,\#\,12)} - R_O}{\sqrt{2}(R_B + R_O)}$ is most effective for determining the type (A or B) of the cation that has "room" in the cell. When $t > 1$, the B cation is loosely held, while when $t < 1$, the A cation has "room". For ferroelectrics there are observed values of t both larger and smaller than unity. For antiferroelectrics the observed values of t are always smaller than unity and the cells of these compounds always exhibit monoclinic distortion.

"L.Ia.Karpov" Physical-Chemical Institute

References

1. Iu.N.Venevtsev, Dissertation, Moscow Physics and Engineering Institute, M., 1955.
2. V.M.Goldsmidt, T.Barth & G.Lunde, Skrifter Norske Videnskaps Adak., Oslo, J. Mat. Naturv. Klasse, 7, 21 (1945).
3. V.M.Goldsmidt, Geochem. Vert. d. Elem., VII, VIII (1927).
4. W.H.Zachariasen, Skrifter Norske Videnskaps Akad., Oslo, J.Mat. Naturv. Klasse, 4 (1928).
5. A.Hoffman, ZS. Phys. Chem., B28, 65 (1935).
6. G.B.Bokii, Vvedenie v kristallokhimiiu (Introduction to crystallochemistry), M. 1954.
7. N.V.Belov & G.B.Bokii, Referaty dokladov na I Soveshchanii po kristallokhimi (Abstracts of reports presented at the First Conference on Crystallochemistry), M.-L., 1954.
8. H.D.Megaw, Proc.Phys.Soc., 58, 133 (1946).
9. J.Naray-Szabo, Müegyetemi Közlemenyek, Budapest, No.1, 30, (1947).
10. G..H.Jonker, J.H.vanSanten,Chem. Weekblad, 43, 672 (1947).
11. S.Nomura, J.Phys.Soc.Japan, 10, 2, 112 (1955).
12. G.A.Smolenskii, Zhur.tekh.fiz., 20, No.2, 137 (1950); Doklady AN SSSR, 70, No.3, 405 (1950); Thesis, Institute of the Chemistry of Silicates, AN SSSR, L., 1954.
13. H.D.Megaw, Acta crystallogr., 5, 739 (1952).
14. B.M.Vul, Elektrichestvo (Electricity), 3, 12 (1946).
15. G.Shirane, H.Danner, A.Pavlovic & R.Pepinsky, Phys.Rev., 93, 672 (1954).
16. G.Shirane, R.Newnham & R.Pepinsky, Phys.Rev., 96, 581 (1954).
17. Iu.N.Venevtsev & G.S.Zhdanov, Izv. AN SSSR, Ser. fiz., 20, 178 (1956). (Trans. in Bulletin, V.20, No.2, p. 161).
18. Iu.N.Venevtsev, G.S.Zhdanov & T.N.Shendrik, Kristallografiia (Crystallography), 1, 657 (1956).
19. E.Sawaguchi, J.Phys.Soc.Japan, 8, 5, 615 (1953).
20. E.Wainer & C.Wentworth, J.Am.Ceram.Soc., 35, 8, 207 (1952).
21. B.T.Matthias, Phys.Rev., 75, 117 (1949).
22. M.L.Keith & R.Roy, Amer.Mineralog., 39, 1-2, 1 (1954).
23. P.Vousden, Acta Crystallogr., 4, 373 (1951).
24. B.T.Matthias, Phys.Rev., 75, 1771 (1949).
25. G.A.Smolenskii, Present issue of the Bulletin, p. 235.
26. B.T.Matthias &. J.P.Remeika, Phys.Rev., 82, 727 (1951).
27. G.Shirane, R.Newnham & R.Pepinsky, Phys.Rev., 96, 581 (1954).
28. E.A.Wood, Acta Cryst., 4, 353 (1951).
29. L.E.Cross & B.J.Nicholson, Phil. Mag., 46, 453 (1955).
30. M.H.Francombe, Acta Cryst., 9, 256 (1956).
31. N.N.Krainik, Izv. AN SSSR, Ser.fiz., 21, No.3 (1957). (For translation see next issue of the Bulletin.)
32. H.Graenicher & O.Jakits, Supplemento Nuovo Cimento, 11, 480 (1954).

33. M.McQuarrie, J.Am.Cer.Soc., 38, 12, 444 (1955).
34. I.K.Hulm, B.T.Matthias & E.A.Long, Phys.Rev., 79, 885 (1950).
35. G.C.Danielson, B.T.Matthias & I.M.Richardson, Phys.Rev., 74, 986 (1948).
36. G.C.Danielson, R.E.Rundle, Phys.Rev., 75, 1630 (1949); Bull. Am. Phys. Soc., 24, 3, 45 (1949).
37. H.F.Kay, H.I.Wellard & P.Vousden, Nature, 163, 636 (1949).
38. W.Känzig, Phys.Rev., 80, 94 (1950); Helv.Phys.Acta, 24, 175 (1951).
39. H.T.Evans, Acta Cryst., 4, 377 (1951); Phys.Rev., 83, 879 (1951); Bull. Am. Phys.Soc., 26, 4, 15 (1951); Tech. Report, No.58, Lab. for Insulation Research, M.I.T., 1953.
40. B.C.Frazer, H.R.Danner & R.Pepinsky, Phys. Rev., 100, 745 (1954).
41. H.F.Kay & P.Vousden, Phil. Mag., 40, 1019 (1949).
42. G.Shirane, R.Pepinsky & B.C.Frazer, Acta Cryst., 9, 131 (1956); Phys.Rev., 97, 1179 (1954).
43. E.Sawaguchi, H.Maniwa & S.Hoshino, Phys.Rev., 83, 1078 (1951).
44. P.Vousden, Acta Cryst., 4, 545 (1951).
45. H.D.Megaw, Acta Cryst., 7, 187 (1954).
46. G.I.Skanavi, Zhur.eksp.i teor.fiz., 27, 399 (1947); Fizika dielektrikov (Physics of Dielectrics), M.-L., 1949.

CHARACTER OF THE CHANGES IN THE DOMAIN STRUCTURE OF ROCHELLE SALT IN ALTERNATING ELECTRIC FIELDS

- I.S.Zheludev & R.Ia.Sit'ko

In order to clarify the role of domains in the process of repolarization of ferroelectrics we undertook[1] a motion picture study of the domain structure of Rochelle salt in 32 and 1000 cps alternating fields of different strengths. The cinematography was carried out in a microscopic set-up especially adapted for this purpose. By way of specimens we used X-cut plates measuring 20 x 20 x 1 mm. The electrodes were made of silver foil, but in the area of observation (about 1 mm^2), instead of silver, the specimen was covered with a transparent conducting coating. The specimens were maintained at a temperature of 11.5° by means of a thermostat.

For cinematographic recording of even relatively slow processes in alternating electric fields one should in principle use high-speed photography. We used a different method, however, namely, motion picture photography at the usual rate (about 32 frames per second) but with stroboscopic illumination. By means of stroboscopic illumination one can "extend in time" the observation of rapid processes. That employment of this procedure is practical is evinced by the fact that the observed domain motion was reproducable in cycle after cycle with the field intensities and frequencies used in our experiments.

In the case of 32 cps fields the stroboscopic effect was obtained through the difference between the frequency of the motion picture camera shutter and the frequency of the electric field, i.e., the field and shutter were slightly desynchronized. The resultant approximately 40-fold slowing down of the observed process made it possible to follow the repolarization through a complete cycle of the electric field. In the case of the 1000 cps field we used a mechanical stroboscope to interrupt the illumination; the resultant slowing down was approximately 4000-fold.

Fig.1a shows the changes in the domain structure in an electric field having a frequency of 32 cps and a strength of 36 v/cm. Concurrently with observation and photography of the domain structure we followed the character of the polarization by recording the hysteresis loops on an oscillograph. It was found that the polarization curve is far from saturation at the given field strength, nevertheless the hysteresis character of the field dependence of the polarization was clearly evident in the observed curve.

Accordingly, in the figures the frames corresponding to equal field strengths, attained as the field increased and decreased are arranged in vertical columns; the frames corresponding to the maximum field intensities are mounted at the extreme right and left of the figure. The points marked by Roman numerals on the field sinusoid at the bottom of the figure correspond to the frames identified with the same Arabic numerals. This arrangement reflects the difference in the values of the polarization for the frames mounted over each other (for example, frames 2 and 8); it does not, however, graphically reflect the differences in the value of the polarization in going from frame to frame (for example, from frame 2 to frame 3).

At the top of the figure we have a frame showing the domain structure of the photographed section of the specimen with no field. As may be seen from this photograph the domains of opposite orientations within the photographed section do not occupy equal areas: the part corresponding to the light component occupies a major part of the area, while the part corresponding to the dark component takes up only a minor portion of the area. Thus, the domain

structure in this section is unipolar. We note that the unipolarity of the domain structure within the limits of the photographed section does not necessarily indicate that the specimen is unipolar as a whole.

The other frames correspond to fields differing 45° in phase (0, 45, 90, 135°, etc.). Frame 1 corresponds to the crest value of the field. It will be evident that in it the light domain component occupies virtually the entire field whereas the dark (antiparallel to the field) component is virtually absent. Reduction of the field strength from the crest value to zero (frames 2 and 3) leads to the appearance of a dark component, although the portion of the total area occupied by it still remains minor.

As the field builds up to the inverse crest, the portion of the area occupied by the dark component increases sharply (frames 4 and 5). The fact that at the V crest value of the field (frame 5) the dark component does not occupy the entire field of view (in contrast to the case of the light component in frame 1) is understandable inasmuch as in the initial state (frame at the top of the figure) the dark component was only weakly evident. Reduction of the field (going from frame 5 to frame 7) does not lead to any substantial change in the domain structure: as before the crystal seems to "remember" the domain structure it attained in the extreme position (frame 5). The increase in the field strength to the I crest (frames 7, 8 and 1) is accompanied by a more pronounced change in the domain structure. In this respect the section illustrated by frames 7 → 1 is analogous to the section characterized by frames 3 → 5.

In addition to the above traits characterizing the changes in the domain structure in an alternating field, two interesting facts emerge from a careful examination of the photographs. The first and more important is that the domain structure differs in appearance at equal field strengths depending on whether the given intensity is reached in an increasing or decreasing field. This will be evident from a comparison of frames 2 and 8 or 3 and 7. This is essentially hysteresis of the domain structure in an applied electric field.

The second interesting fact is that the domain structure of the initial specimen in the absence of a field (frame at top of the figure) does not occupy an intermediate position with respect to the structures obtained in passing through the zero values of the field (frames 3 and 7). This can readily be understood if we bear in mind that in the initial state the domain structure in the field of view was unipolar. Apparently, under the influence of the alternating field this unipolarity is reduced during the first cycles and there occurs a certain averaging of the light and dark components; that is to say the specimen in the field of view acquires a new "initial state". It must be noted, however, that after removal of the field this pseudoinitial state fades out rather quickly and the domain structure again acquires the appearance shown in the frame at the top of the figure.

Fig.1b shows the variation in domain structure at the same frequency but in a field having a crest strength of 56 v/cm. It will readily be seen that the general characteristics of the reorientation of the domains in this case are similar to those observed with the weaker field (Fig.1a). At the same time it may be noted that in the stronger field a greater fraction of the domains participates in the repolarization. Thus it will be seen from frame 5 (Fig.1b) that in this case an appreciably greater portion of the area is occupied by the dark component of the domains and that in fact at this crest value of the field the specimen is close to saturation.

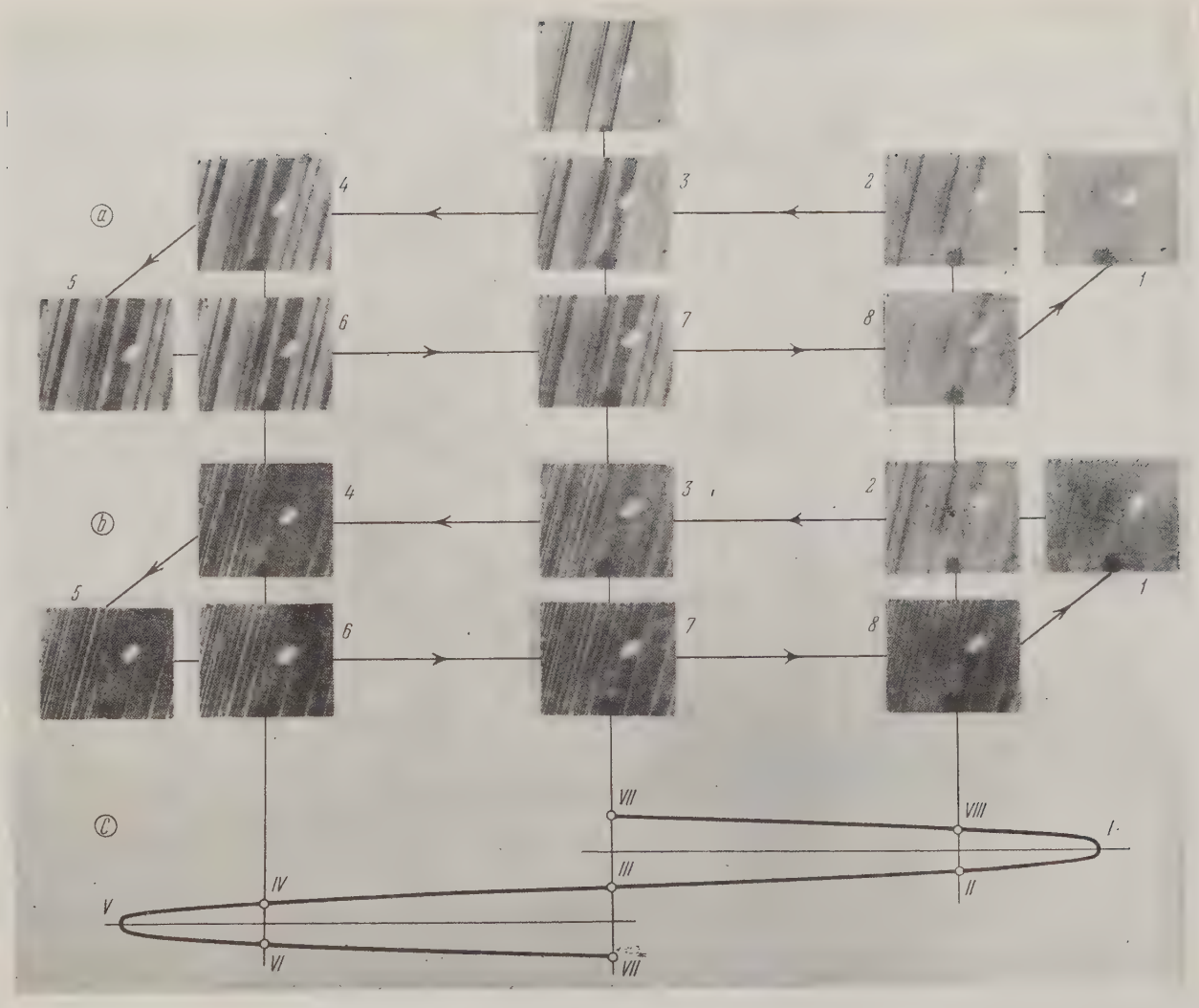

Fig.1. Changes in the domain structure through a voltage cycle at a frequency of 32 cps. Crest value of the field: a - 36 v/cm, b - 56 v/cm. The Roman figures at the field sinusoid correspond to the Arabic numerals at the frames.

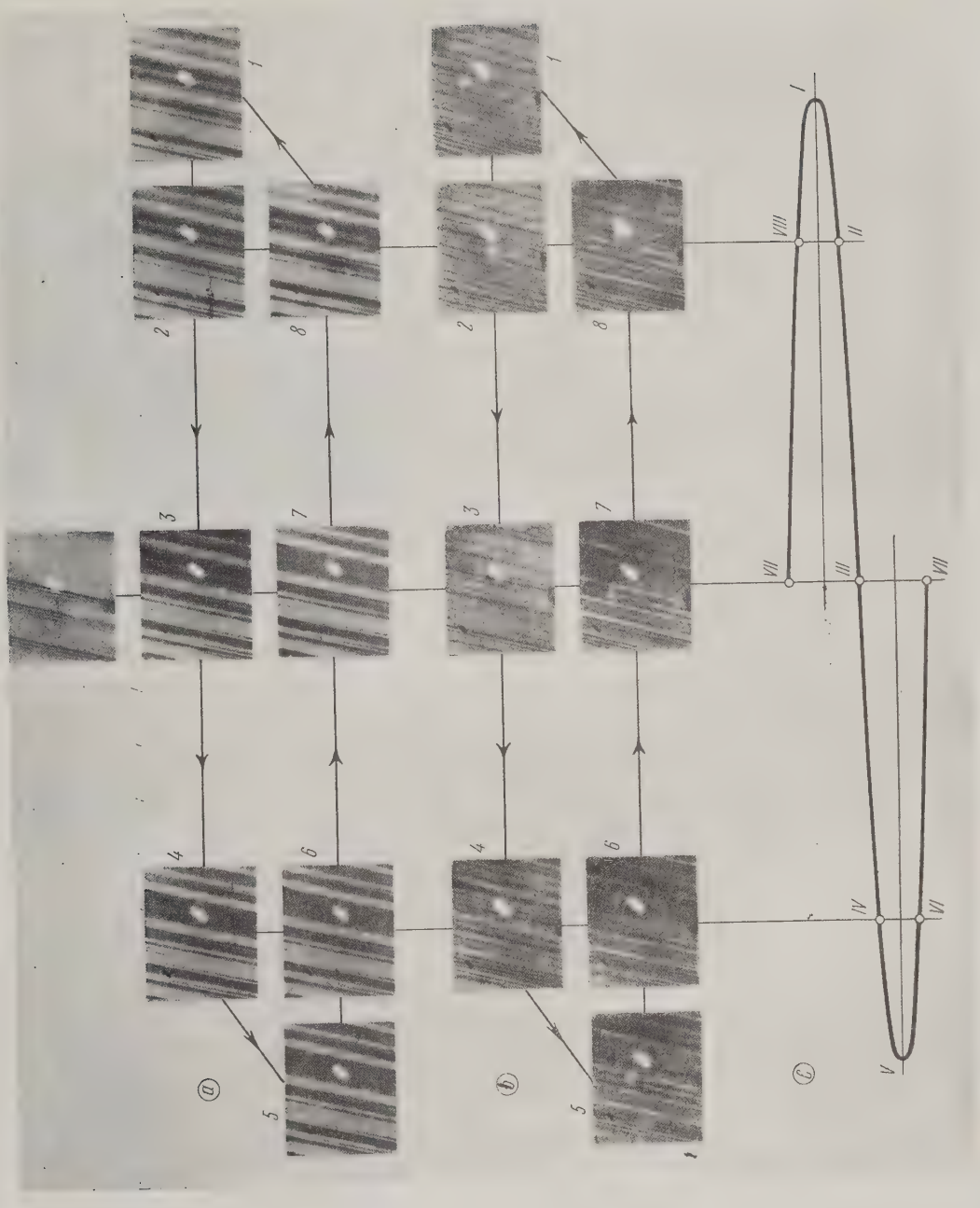

Fig.2. Same as Fig.1 but at a frequency of 1000 cps. Crest field: a - 56 v/cm, b - 76 v/cm.

It will also be evident from Fig.1b that at high field strengths the increase in the fraction of the area occupied by one of the components occurs not so much through expansion of the existing domains as through formation of new domains within the boundaries of the broad domains of the opposite orientation (compare, for example, frames 5 with frames 7 in Figs.1a and 1b). Thus, apparently, under the influence of strong fields the domains structure breaks up or disintegrates and at the same time the unipolarity of the observed section of the specimen virtually disappears.

The changes in the domain structure at a frequency of 1000 cps are shown in Fig.2. Fig.2a pertains to a field strength of 56 v/cm, while Fig.2b is for a field of 76 v/cm. As a whole the observations regarding the variations of domain structure made above in connection with Fig.1 remain in force. However, from a comparison of the frames obtained with the same field strength but at frequencies of 32 cps (Fig.1b) and 1000 cps (Fig.2a) it may be noted that at the higher frequency the unipolarity of the domain structure is far less pronounced while the mean size of the domains is noticeably greater. In other words, increasing the frequency tends to reduce the unipolarity of the domain structure through enlargement of the domains, while the breaking up of the individual large domains into smaller ones at higher frequencies occurs only at higher field intensities.

In addition to the above it may be noted that with increasing field strength hysteresis of the reorientation of the domains is more pronounced. Thus in the series of photographs of Fig.2b the dark component is barely discernible against the background of the light component in frame 3, while in frame 7 the dark component clearly predominates. In this respect frames 3 and 7 are virtually "negative" images of each other. In weak fields, on the other hand, hysteresis of the variation in domain structure although still evident is much less strongly pronounced (Fig.2a, frames 3 and 7).

Further experimental studies will obviously be necessary before any definitive deductions regarding the role of domains in the processes of polarization can be drawn. In concluding we would like to note that such investigations may help establish the relaxation time for domains and determine the dependence of this time on the electric field strength.

The authors desire to thank V.F.Parvov for his aid in the work.

Institute of Crystallography of the
Academy of Sciences of the USSR

References

1. I.S.Zheludev & R.Ia.Sit'ko, Kristallografiia (Crystallography), 1, 689 (1956).

SOME DETAILS OF THE DOMAIN STRUCTURE OF ROCHELLE SALT CRYSTALS AS DETERMINED BY OPTICAL OBSERVATION

- M.A.Chernysheva

As was shown in earlier contributions[1-4] the optical procedure can be successfully used for observing the domain structure in Rochelle salt crystals and investigating the changes occurring under the influence of an external mechanical or electric field.

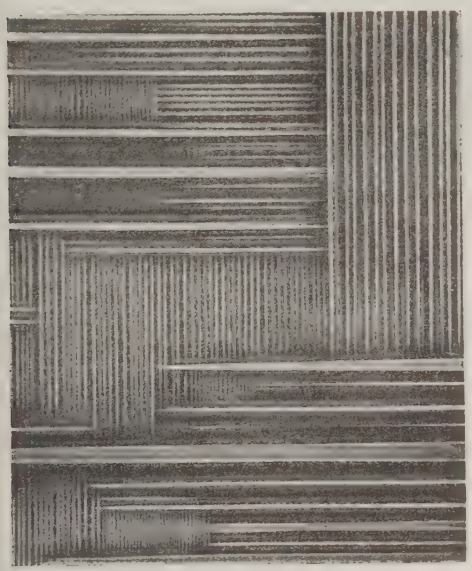

Fig.1. Domain structure of an X-cut plate of Rochelle salt. Crossed Nicols. Magnif. 45 X.

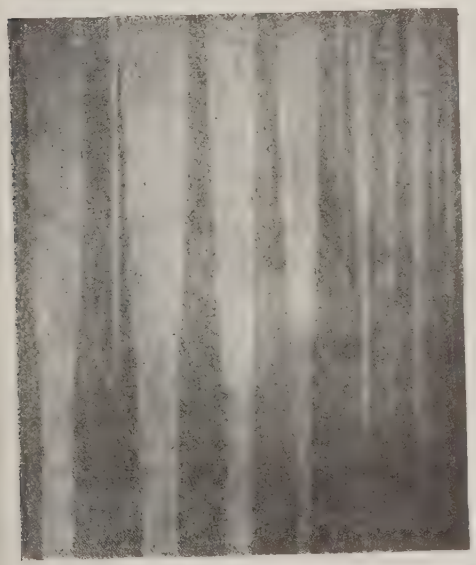

Fig.2. Domain structure of a crystal plate the normal to which lies in the *ac* plane and makes an angle of about 40° with the *a* axis. Crossed Nicols. Magnif. 100 X.

The transformation of the Rochelle crystal from the rhombic to the monoclinic modification is accompanied by spontaneous shear deformation and the formation of domains (twinning). The shear deformation causes rotation of the optical indicatrix about an axis that coincides with the axis. The optical indicatrices of neighboring antiparallel domains are rotated in opposite directions which leads to unequal extinction of the domains of opposite "sign". If the axis of the indicatrix of the domains of one sign is aligned with the plane of polarization, then as a result of the difference between the positions of extinction for the different domains the domain structure will appear in the form of dark and light areas when the crystal is viewed through crossed Nicols.

With the optical method the domain structure of Rochelle salt crystals can be clearly observed in X-cuts. As may be seen from Fig.1, in an X-cut plate the domains have the appearance of bands or wedges extending either along the *c* axis (*c*-domains) or along the *b* axis (*b*-domains).

An obvious question is what form do the domains have in the *a* direction?

In oblique cuts one can clearly observe only one system of domains, the *b*- or *c*-domains, depending on the orientation of the cut plate relative to the crystal axes. Thus, for example, in plates the normal to which lies in the *ac* plane, one can distinguish the *c*-domains (Fig.2), although not as clearly as in X-cuts. In studying such oblique cuts one can establish that the wedging-in of domains also occurs in planes at an angle to the *a* axis. In such cuts domains of different "signs", comprising the second system (for example, ±*b*-domains in plates the normal to which lies in the *ac* plane) cannot be distinguished inasmuch as in this case there will be several domains of

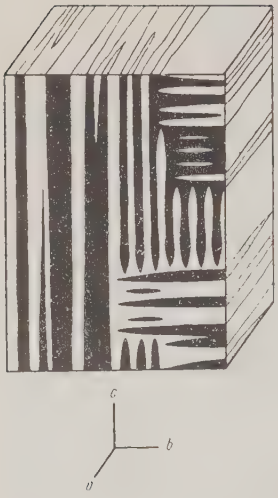

Fig.3. Model of domain structure of Rochelle salt crystals. The drawing corresponds to the X-cut. In cuts perpendicular to the b and c axes the domains cannot be detected optically.

opposite "sign" in the path of the light beam. In this case the areas of emergence of the domain boundaries to the surface of the specimen can be observed from the interference bands of different widths.

A direct proof of the formation of domains along the a axis is furnished by observation of ordinary X-cuts with the polarizing microscope focused on the upper and lower surfaces of the crystal plate. In such observations one can note not only changes in the thickness of the domain laminae along the a axis but also the nucleation or wedging-in of thinner domains inside the plate.

Fig.3 shows a volume model of the domain structure of Rochelle salt crystals. (This model is given without taking into account the segmental structure of the crystals.[4]) The drawing pertains to the X-cut. The domains, in general, are not plane-parallel laminae but rather are layers of variable thickness whose surfaces are approximately parallel to the b and c planes. Wedging-in of the domains occurs in the direction of all the principal axes.

The results of observation by the optical procedure also allow us to draw an important conclusion regarding the changes in domain structure of Rochelle salt crystals in the temperature interval between the Curie points.

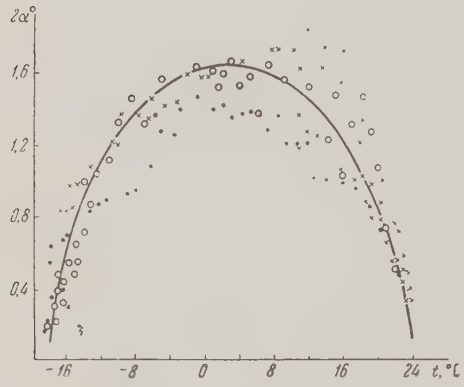

Fig.4. Curve characterizing the variation in the monoclinicity of Rochelle salt crystals in the temperature range between the Curie points. Vertical axis scaled in values of the angle 2α between the extinction directions for the components of a twin (neighboring antiparallel domains).

Ubbelohde & Woodward[5] on the basis of x-ray studies established that the change in symmetry of Rochelle salt crystals from the rhombic to the monoclinic occurs due to a change in the angle between the b and c axes; this angle (monoclinic) has a maximum value at a temperature of about 0° ($90^{\circ} \pm 1'48''$); at -15° it differs from 90° by no more than 12", while at $+15^{\circ}$ it differs from 90° by no more than 50". With these data one can juxtapose the results of investigations of the temperature dependences of the spontaneous polarization[6] and the spontaneous deformation[7] of Rochelle salt crystals; the curves characterizing the variation of these quantities have a typical dome-shape in the temperature interval between the Curie points. However, neither the spontaneous deformation nor the spontaneous polarization averaged over the entire specimen consisting of a large number of antiparallel domains can serve as a characteristic of the degree of monoclinicity of the crystals inasmuch as during the measurement of these quantities there may occur both rearrangement

inside the domains and displacement of the domain walls.

The individual characteristics of the domains can be obtained by the optical method. Owing to the opposite "signs" of the spontaneous deformation of neighboring antiparallel domains, the corresponding optical indicatrices are shifted a certain angle relative to each other about the *a* axis. To determine this angle we need only measure the angle 2α between the directions of extinction of the two components of a twin (i.e., neighboring antiparallel domains) in an X-cut plate. This angle may serve as a parameter of the monoclinicity of the crystal in the same way as the monoclinic angle determined by the x-ray procedure.

We carried out measurements of the angle between the directions of extinction for the components of a twin (neighboring domains) by means of an appropriate double-crystal microscope. In view of the observed statistical spread of the extinction positions the measurements were made with a 540 mμ filter with a 10 mμ passband.

The results of these measurements are shown in Fig.4. The differently identified points pertain to different measurement cycles. Each point corresponds to the arithmetic mean of not less than five individual measurements.

It will be seen that the degree of monoclinicity of Rochelle salt crystals changes continuously with changing temperature and attains a maximum at a temperature approximately half-way between the Curie points (at about $+3^{\circ}$). As the Curie points are approached the monoclinicity parameter rapidly falls off to zero. A noteworthy feature is the somewhat greater scattering of points in the temperature range from $+10$ to $+18^{\circ}$, which, we feel, is not accidental. It should also be noted that repeated variation of the temperature of the same specimen over the range between the Curie points (going only slightly above and below the respective Curie points) leads to a noticeable general lowering of the curve (solid dots). We feel it would be premature at this time to attempt an interpretation of this effect.

It may be assumed that the results shown in Fig.4 may be of interest not only for the theory of ferroelectricity but also for the theory of second order phase transitions.

The optical method also makes it possible to carry out an analysis of the mechanical stresses in Rochelle salt crystals. Under the influence of external loads[2] or internal stresses[4,8] there occurs a rearrangement of the domain structure consistent with a transformation to an energetically more advantageous state.

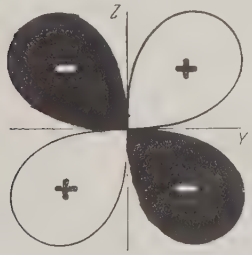

Fig.5. Rosette of equal tangential stresses corresponding to the distribution of stresses in an X-cut plate of Rochelle salt under local loading along the *a* axis.

Recently, Indenbom succeeded in establishing a quantitative relationship between the distribution of stresses and the distribution of domains[9]. He found that the thickness of the domains is determined by the magnitude of the tangential stresses acting on the twinning plane in the direction of twinning. If an X-cut plate is observed through crossed Nicols along the second order axis (*a* axis) and the plane of polarization is aligned with the axis of the indicatrix of one of the domains, a general lightening of the field of view due to an increase in the proportion of "light" domains will correspond to stresses of one "sign", while a general darkening will correspond to stresses of opposite "sign". Lines of equal tangential stresses will be manifested as lines of equal ratios between the thicknesses of the neighboring domains, i.e., as lines of equal

Fig.6. Distribution of stresses about two edge dislocations of opposite "sign". X-cut plate of Rochelle salt. Crossed Nicols. Magnif. 340 X.

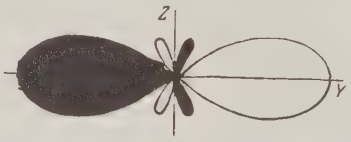

Fig.7. Rosette of equal tangential stresses corresponding to stress distribution about an edge dislocation.

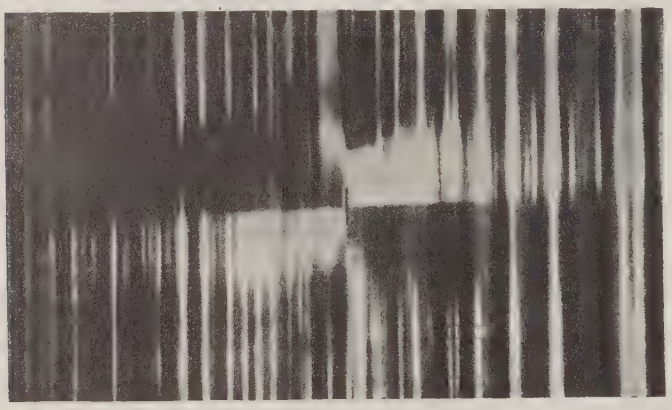

Fig.8. Distribution of domains about an elongated inclusion parallel to the z axis (at the center of the photograph) in an X-cut crystal of Rochelle salt. Crossed Nicols. Magnification 340 X.

lightenings (or darkenings). Thus, for example, the distribution of tangential stresses with local loading of a Rochelle salt plate is described in polar coordinates by the formula $\rho = \sin 2\theta \cdot r^{-2}$. The corresponding curve (rosette) of equal tangential stresses is shown in Fig.5. An analogous picture of the stress distribution was actually obtained by us for an X-cut plate loaded by means of a small glass ball[2].

The above described characteristics of Rochelle salt crystals can advantageously be used in studying the character of defects in real crystals from the stress field produced by such defects. In particular, in processing the experimental material described in Ref.8, we called attention to the correspondence of the domain (twin) structure, such as that shown in Fig.6, to the familiar distribution of stresses about an edge dislocation[10], characteristic of the distortion of the crystal lattice along the line of an extra atomic plane. Mathematically the distribution of stresses about an edge dislocation is characterized by the expression $\cos\theta \cdot \cos 2\theta \cdot r^{-1}$ describing the rosette pictured in Fig.7. From a comparison of Figs.6 and 7 it will immediately be evident that there are present in the crystal two edge dislocations of opposite sign. From a careful study of Fig.7 it may also be concluded that these two dislocations are not independent but are associated with a common "extra plane" which in the present case is simply a thin elongated inclusion. The dislocations themselves in this case are undoubtedly macroscopic dislocations of Stepanov's elasticity theory[11]. This is substantiated by a comparison of Fig.6 with Fig.8 in which one can distinctly see at the center an elongated

inclusion parallel to the Z axis; this inclusion gives rise to a rearrangement of the domain structure analogous to that pictured in Fig.6 only with the difference that here the rosettes corresponding to the ends of the inclusion are shifted and partially overlap.

In conclusion it may be noted that the optical method may also be employed for analysis of different transient processes associated with rearrangements of the domain structure of Rochelle salt crystals (for example, hysteresis, relaxation effects, etc.).

Institute of Crystallography of the
Academy of Sciences of the USSR

References

1. M.V.Klassen-Nekliudova, M.A.Chernysheva & A.A.Shternberg, Doklady AN SSSR, 63, 527 (1948).
2. M.A.Chernysheva, Doklady AN SSSR, 74, 247 (1950).
3. M.A.Chernysheva, Doklady AN SSSR, 81, 1065 (1951).
4. M.A.Chernysheva, Doklady AN SSSR, 91, 87 (1953).
5. A.R.Ubbelohde & I.Woodward, Proc.Roy.Soc., A185, 448 (1946).
6. H.Mueller, Ann.N.Y.Acad.Sci., 40, 34, 321 (1940); J.Hablützel, Helv. Phys. Acta, 12, 489 (1939).
7. W.P.Mason, Piezoelectric crystals and their application in ultrasonics (In Russian trans. M. 1952).
8. M.A.Chernysheva, Thesis, Institute of Crystallography, USSR Ac. of Sci., M., 1955.
9. V.L. Indebom & M.A.Chernysheva, Doklady AN SSSR, 111, 596 (1956).
10. G.Taylor, Proc.Roy.Soc., A145, 362 (1934).
11. A.V.Stepanov, Izv. AN SSSR, Otd. tekh. nauk., 9, 90 (1954).

BULLETIN of the Academy of Sciences of the USSR - Physical Series
Volume 21, Number 2, 1957

Table of Contents

	Page Orig.	Trans.
Transactions of the Eighth All-Union Conference on Semiconductors (Continued from Vol.20,No.12b and Vol.21,No.1)		
Section on Semiconductor Catalysis		
Some problems in the field of semiconductor catalysis - S.Z.Roginskii	163	163
On problems arising in the theory of semiconductors as catalytic agents - F.F.Vol'kenshtein	176	177
On some questions of semiconductor analysis - F.F.Vol'kenshtein	179	180
Investigation of the catalytic properties of NiO-base solid solutions - N.P.Keier, S.Z.Roginskii & I.S.Sazonova	183	184
Relation between the catalytic activity and electric conductivity of zinc oxide and the influence of optical radiation of these properties - I.A.Miasnikov	192	192
Summary of results of investigations of the relation between the electronic surface states in a semiconductor and catalytic effects - V.I.Liashenko & I.I.Stepko	201	201
Investigation of adsorption of gases on manganese dioxide by the electric conductivity method - S.Iu.Elovich & L.Ia.Margolis	206	206
Influence of adsorption on the conductivity and work function of semiconductors - V.B.Sandormirskii	211	211
Section on the Optical Properties of Semiconductors		
Absorption of light in mercury halide crystals - E.F.Gross & A.A.Kaplianskii	220	220
Transactions of the Fifth Conference on the Application of X-Rays to the Investigation of Materials (Concl. from Vol.20, Nos. 6 & 7)		
Experimental verification of the influence of anisotropy of the crystallites on the shape of the Debye ring in the x-ray pattern of stressed specimens - G.I.Aksenov & V.A.Moshchanskii	226	229

	Page Orig.	Trans.
Transactions of the First Conference on Ferroelectricity		
Survey of some of the results of recent investigations of ferroelectric materials - G.A.Smolenskii	233	235
Orientation of the domains and macrosymmetry of the properties of ferroelectric single crystals - I.S.Zheludev & L.A.Shuvalov	264	266
Crystallochemistry of ferroelectrics with the perovskite structure - Iu.N.Venevtsev & G.S.Zhdanov	275	277
Character of the changes in the domain structure of Rochelle salt in alternating electric fields - I.S.Zheludev & R.Ia.Sit'ko	286	288
Some details of the domain structure of Rochelle salt crystals as determined by optical observation - M.A.Chernysheva	289	293

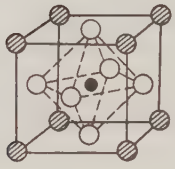

Translated in 1958 by
Columbia Technical Translations
5 Vermont Avenue, White Plains, N.Y.

TRANSACTIONS OF THE FIRST CONFERENCE ON FERROELECTRICITY

Leningrad, 19-24 June, 1956

(Continued from Vol. 21, No.2)

GROWTH AND INVESTIGATION OF FERROELECTRIC SINGLE CRYSTALS

- N.S.Novosil'tsev, A.L.Khodakov, M.L.Sholokhovich, E.G.Fesenko & O.P.Kramarov

The first published reports[1-3] on successful preparation of small barium titanate crystals from a solution in molten salts date back to 1947. Subsequently, many investigators here and abroad have given their attention to growing and studying crystals of similar substances, substances that are of ever greater importance in modern technology[4-11].

At our institute we have grown and investigated the properties of crystals of barium, strontium and lead titanate, lead zirconate and single crystals of the solid solutions $(Ba,Sr)TiO_3$ and $(Ba,Pb)TiO_3$. This research, which was preceded by extensive investigation of ceramic ferroelectrics continues to this day[12-27]. However, the preparation of these substances in the form of large crystals still remains a difficult and not fully solved problem. Unfortunately, these materials cannot be crystallized by the well developed techniques of growing crystals from aqueous solutions inasmuch as they are virtually insoluble in water. In general two procedures are available for preparing crystals of the listed substances: 1) crystallization from solutions in melts of other lower-melting point materials that do not interact chemically with the dissolved substances and 2) crystallization from a melt of the substance itself.

The formation of crystals through hardening of melts of compounds of the $BaTiO_3$ type is hampered by difficulties in finding a suitable crucible material inasmuch as at high temperatures the titanates and allied compounds tend to interact with most refractory materials. In the case of lead titanate and lead zirconate the possibility of obtaining crystals from the melt is entirely excluded inasmuch as these compounds tend to decompose in fusing.

In 1952 von Hippel[4] reported successful preparation of fairly large crystals of $BaTiO_3$ and magnetite. Details on the technique for growing barium titanate crystals have also been published by Kay[28]. At present the most advanced technique for growing $BaTiO_3$ and similar crystals is crystallization from solutions in fused salts. Most of the crystals studied by different investigators have been prepared by this procedure.

A number of investigations carried out in our Institute have been devoted to the interaction of barium, strontium and lead titanate and lead zirconate with a number of different substances in melts[29-36]. On the basis of these studies we have been able to find several suitable fused-salt solvents for these compounds and to establish the best conditions for their crystallization.

Some of the more interesting deductions drawn from the results of this research are the following. Barium and strontium titanate and to a lesser extent lead titanate are substances that are poorly soluble in most fused-salt solvents. Lead zirconate is characterized by the poorest solubility. However, most of the investigated binary systems as well as the systems representing a diagonal section through the diagram of ternary solutions proved to be eutectic systems. This makes it possible to utilize a whole series of substances as fluxes for the crystallization of barium, strontium and lead titanate.

A characteristic of most stable diagonal cross sections of systems with $BaTiO_3$, $SrTiO_3$ and $PbTiO_3$ is the very low content of these substances in the eutectic compositions. Thus the exchange reaction in these sections is sharply displaced to the side of these titanates. This is clearly illustrated by the results of a series of investigations of a number of mutual systems (see Refs.33,34 & 35) having a singular character.

The crystallization curves of the listed titanates in the investigated stable cross sections rise very steeply which indicates the possibility of

stratification of the melt at high temperatures. This fact must be borne in mind in specifying the procedure and conditions for crystallization of these titanates from the different melts which fuse at very high temperatures. In selecting the crystallization procedure one should also bear in mind the fact, known from metallurgy and obvious from general considerations, that crystals formed near the eutectic point tend to be the smallest. Consequently, in growing crystals one should try to use melts the composition of which is reasonably remote from the composition of the eutectic mixture.

Methods of Growing Crystals from a Solution of Polycrystalline Ferroelectrics in Melts of Other Substances

In growing $BaTiO_3$ and $SrTiO_3$ crystals from a melt consisting of a mixture of sodium and potassium carbonates we used hermetically sealed Armco iron crucibles of two types:

1) the crucibles of the first type were simple cylinders with screw covers; these were loaded with an appropriate mixture of the solvent salts and polycrystalline barium or strontium titanate;

2) the crucibles of the second gype were double; part of the reagents was placed on the bottom of the main large crucible, while the other part was loaded into a small crucible of the same iron which was suspended in the upper part of the large crucible. The remaining space was filled with substances serving as a medium for the diffusion of Ba and TiO_3 ions towards the point of crystal growth. The crucibles were held for several days at different temperatures ranging from 750 to 1200°.

Research carried out in the Institute on the chemical affinity in the systems consisting of potassium fluoride and barium or strontium titanate made it possible to develop a procedure for growing barium titanate and strontium titanate crystals and, subsequently, crystals of their solid solutions from a melt of potassium fluoride. The crystals were grown in a platinum cup. The crystallization procedure varied depending upon whether an open or closed cup was used; in the case of crystallization in an open cup the melt was held for a long time at a constant temperature and then slowly cooled to complete solidification of the mixture; in the case of a closed cup the melt was simply slowly cooled to the solidification point.

So far as we know there is no information in the literature on the preparation of crystals of solid solutions of substances with the perovskite structure. The technique developed in the Institute for growing crystals of $(Ba,Sr)TiO_3$ and $(Ba,Pb)TiO_3$ solid solutions was based on a series of investigations of the surface of crystallization in the systems K_2F_2—$BaTiO_3$—$SrTiO_3$ and K_2F_2—$BaTiO_3$—$PbTiO_3$ with subsequent x-ray diffraction studies of the solid phases.

The growth of single crystals of lead salts from a melt of potassium fluoride is fraught with a number of difficulties. In view of this we undertook a search for other solvents. Obviously, the desirable attributes for the flux were the following: it should have a low melting point, it should melt without decomposition of the lead salt, it should be rather viscous in the fused state and it should crystallize with supercooling. One solvent meeting these requirements is lead metaborate. The melting point diagram of the $Pb(BO_2)_2$—$PbTiO_3$ system is shown in Fig.1. It will be seen from the diagram that the solubility of lead titanate in lead metaborate is appreciable at relatively moderate temperatures.

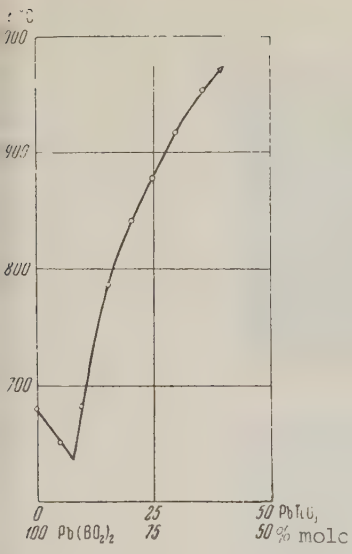

Fig.1. Variation of the melting point of $Pb(BO_2)_2$-$PbTiO_3$ mixtures with the composition.

Unfortunately, crystals of lead zirconate cannot be obtained from this solvent. We did succeed, however, in obtaining lead zirconate single crystals by crystallization from a solution of polycrystalline lead zirconate in molten potassium fluoride. The crystals obtained were very small, transparent, light green in color and had the form of regularly bounded hexahedral plates.

Investigation of Ferroelectric Single Crystals

Forms and transformations of barium titanate single crystals

We grew a number of different lots of barium titanate crystals differing as regards the value of the c/a ratio at room temperature. The Curie point of such crystals lies at temperatures well above room temperature[7,8], for example, at 50, 80 or 110°. The crystals with Curie points at 50° and 80° were grown from a solution of previously prepared barium titanate in a melt of fused salts. The crystals with Curie points at 50° and 80° were grown from a solution of previously prepared barium titanate in a melt of fused salts. The crystals with the Curie point at 110° were grown by a procedure involving an exchange reaction. For the crystals of all three lots the transition at the Curie point is clearly evident in the curve characterizing the temperature dependence of the dielectric constant (Fig.2). A second transition near 0°C was also unmistakable in all cases. A third transition at negative temperatures was less clearly evident. A domain structure was observed in all these single crystal forms by the usual optical procedure.

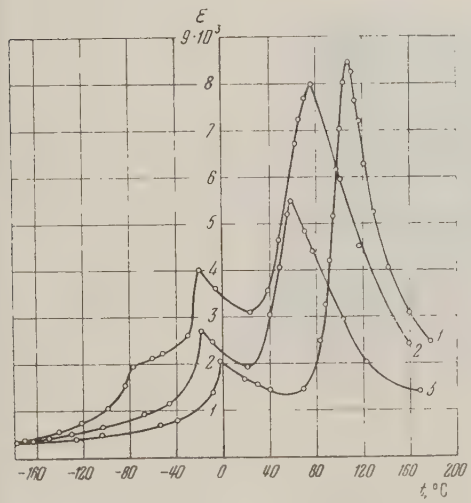

Fig.2. Influence of the conditions of crystallization on the temperature dependence of the dielectric constant of $BaTiO_3$: 1) θ = 110°, 2) θ = 80° and 3) θ = 50°.

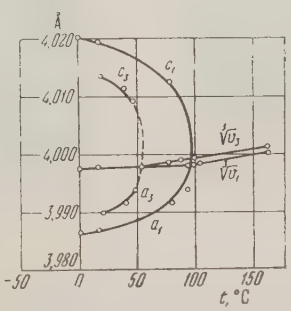

Fig.3. Dependence of the lattice constants on the temperature for $BaTiO_3$ crystals (according to x-ray data). The subscripts correspond to the numbers at the curves in Fig.2.

X-ray studies substantiated the fact that phase transitions occur at the temperatures indicated by the dielectric constant vs temperature curves[7,8] (Fig.3). In addition to a domain structure, laminarity and a segmented texture were observed in the barium titanate crystals (Fig.4). These structural

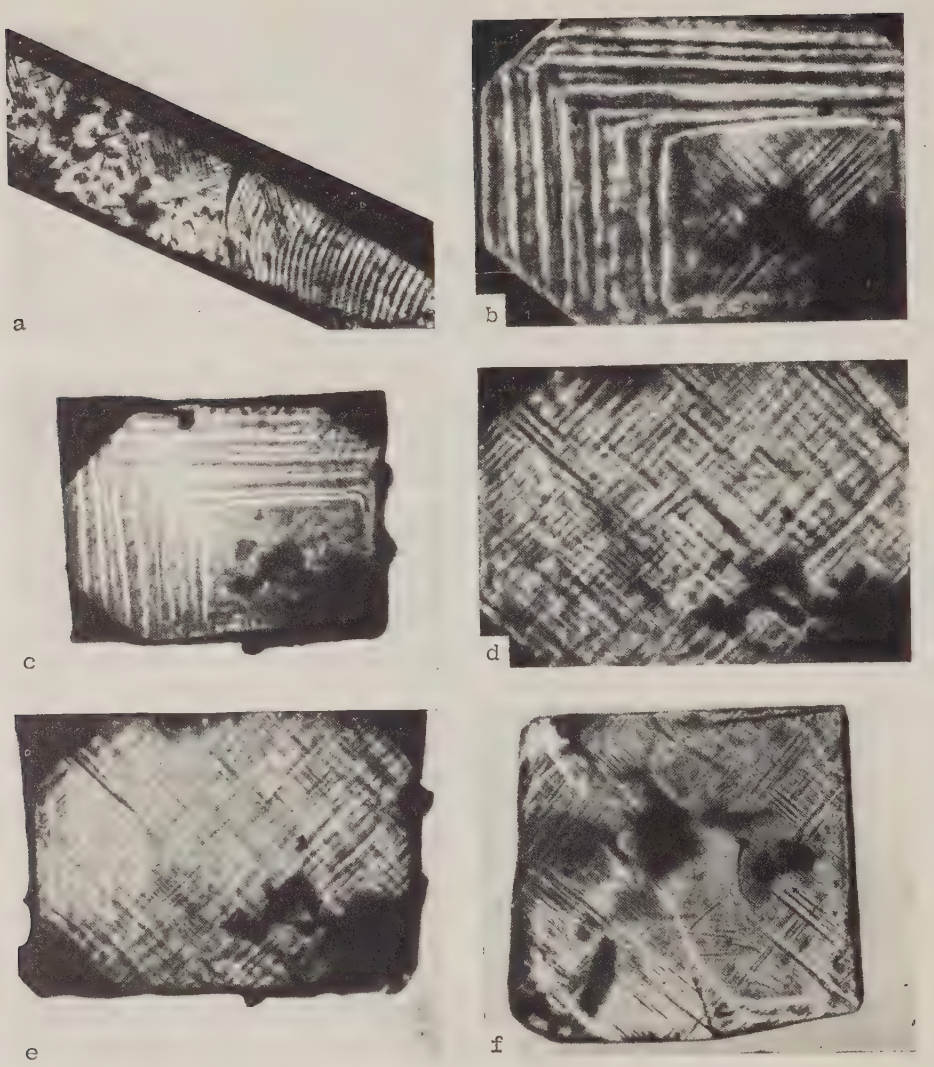

Fig.4. Domain structure of $BaTiO_3$ crystals at different temperatures: a) laminar and domain structure of crystals at 26° (the Curie point for these crystals was 110°); b) laminar and domain structure at 63° (slightly below the Curie point for the given crystal); c) same crystal as in (b) but at 70°; the domain structure has vanished, while the laminar structure is unchanged; d) mixed structure of the same crystal heated above the Curie point to complete disappearance of the domain structure and then cooled to 30°; e) same crystal at 26°; f) segmented texture and domain structure of crystals of a different lot at 20°.

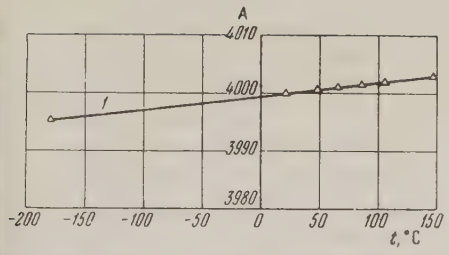

Fig.5. Temperature dependence of the lattice constants (x 10^8 cm) for the cubic modification of $BaTiO_3$.

features developed in the process of growth and, unlike the domain structure, did not disappear with heating[8]. It is interesting to note that we observed temperature hysteresis of the variations in domain structure. Careful studies showed that single crystals, like titanate ceramics, may change many of their properties under the influence of a number of different factors. Some crystals after intense heating and rapid cooling exhibited a decrease of their dielectric constant from 2750 to 1900 over a period of three days. Barium titanate ceramics change color to a certain extent under the influence of daylight; by heating under vacuum, cathode bombardment or other procedures one can enhance the darkening to the point of obtaining entirely black specimens of the ceramic or single crystals. It has been established by x-ray studies that this blackening is not accompanied by structural changes; however, the blackening is accompanied by a transformation of the specimens into a semiconductor with so high an electric conductivity that measurement of the dielectric parameters becomes impossible. After appropriate heat treatment the darkened specimens regain their initial properties.

In the process of crystallization of $BaTiO_3$ from fused-salt solutions one can obtain different modifications of $BaTiO_3$ crystals with anomalous ferroelectric properties. Chiefly by varying the temperature conditions one can grow crystals with different values of the ratio c/a, including nonferroelectric crystals. There can be obtained crystals having a cubic cell even at room temperature (Fig.5). Through appropriate control of thermal conditions we succeeded in growing crystals with a maximum dielectric constant at -50° (Fig.6, curve 1). The curve characterizing the temperature dependence of the dielectric constant for such crystals has a comparatively low, very broad maximum similar to that observed for $BaTiO_3$ solid solutions with a high concentration of the second component.

In subsequent experiments we found that such crystals can be smoothly carried through a series of states by suitable heat treatment (Fig.6, curves II-V). As a result of appropriate heat treatment the crystals develop normal ferroelectric properties and exhibit clearly pronounced phase transitions. This effect was detected not only in crystals of ABO_3 type substances but, subsequently, also in solid solutions of such substances (Fig.7). At present heat treatment is being widely used in this Institute for correcting anomalies, i.e., for obtaining crystals with the desired normal properties.

We give this information on the lability of the ferroelectric properties of crystals because we feel it should be useful in setting up the procedure for growing crystals both commercially and in the laboratory; we feel that an understanding of this lability can prove highly important when it comes to developing new and more promising methods of preparing large crystals by solidification of melts of ferroelectric substances. For example, our experiments with crystallization by the method of passing the ingredients through a flame shows that the crystals obtained by this procedure are always characterized by large anomalies. By appropriate heat treatment, however, they can always be transformed to normal crystals (Fig.8). As we know, a serious interfering factor in the process of growing ferroelectric crystals by solidification of melts is the existence of a high temperature hexagonal

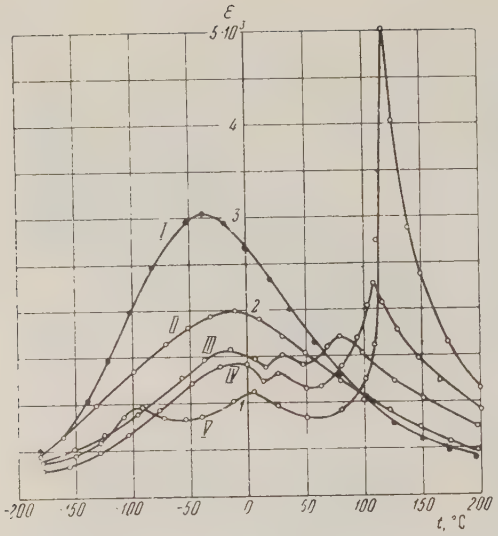

Fig.6. Influence of heat treatment on the character of the temperature dependence of the dielectric constant of $BaTiO_3$: I) before heat treatment, II,II,IV & V) after heating to 1000, 1100, 1200 and 1300°, respectively.

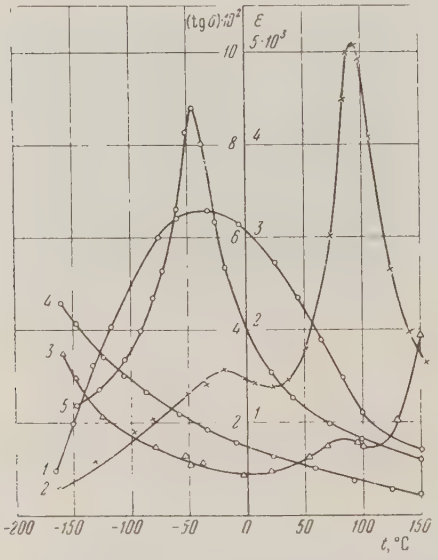

Fig.7. Temperature dependences of ϵ and tan δ for single crystals of (Ba,Sr)TiO_3 solid solutions: 1) ϵ for 10% $SrTiO_3$ + + 90% $BaTiO_3$ solution before heat treatment, 2) ϵ for the same crystal after heat treatment, 3) tan δ for the same crystal after heat treatment, 4 & 5) ϵ for 50% $SrTiO_3$ + 50% $BaTiO_3$ solid solution before and after heat treatment, respectively.

nonferroelectric modification of $BaTiO_3$. The transformation of hexagonal barium titanate into titanate with the perovskite structure is also accompanied by gradual development of ferroelectric properties. This last, however, is not accompanied by displacement of the Curie peak as in the case of the specimen characterized by the curves of Fig.6.

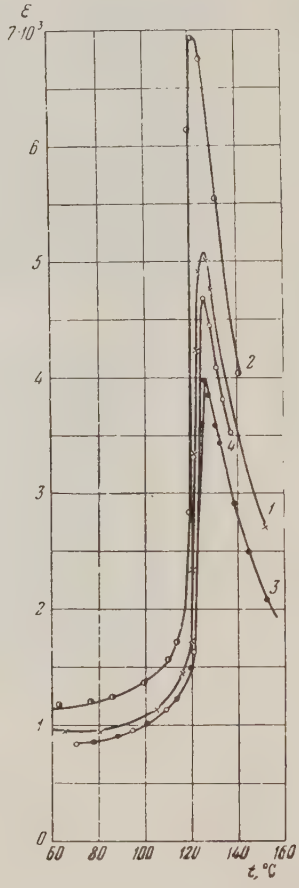

Fig.8. Temperature dependence of the dielectric constant of specimens of $BaTiO_3$ with different thermal histories: 1) well fused specimen, 2) same specimen after firing (annealing), 3) blackened fused specimen, 4) same specimen bleached by annealing.

$SrTiO_3$ single crystals

Two methods were used in preparing $SrTiO_3$ crystals:

1) from a solution of polycrystalline $SrTiO_3$ in a melt of potassium fluoride;

2) from a solution of polycrystalline $SrTiO_3$ in a flux of 50% sodium carbonate plus 50% potassium carbonate.

Crystals obtained by the first procedure are entirely transparent, light green in color and only of the form {100}. Analysis of these crystals showed 47.6% strontium, 25.9% titanium, the remainder being oxygen and impurities. Crystals grown by the second procedure are less transparent with the {100} and {111} forms predominating. These crystals are somewhat contaminated with iron (iron content 0.7%). The dielectric constant and loss tangent of these crystals were measured in a wide range of temperatures (-180 to +160°) at frequencies from $2 \cdot 10^7$ to 10^5 cps; the field dependences of these parameters were investigated at audiofrequencies and hysteresis loops were recorded.

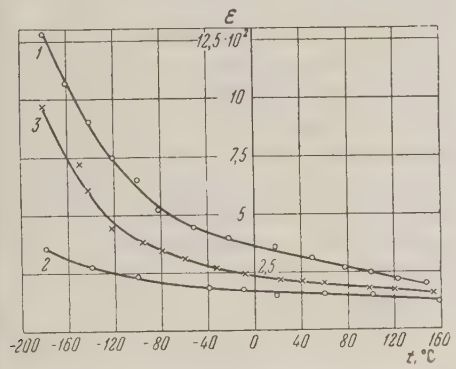

Fig.9. Temperature dependence of the dielectric constant of $SrTiO_3$: 1) for crystals grown from a solution in sodium and and potassium carbonates, 2) for crystals grown from potassium fluoride, 3) for a polycrystalline specimen.

The $SrTiO_3$ single crystals obtained by the two procedures differ somewhat as regards dielectric properties. The temperature dependences of the dielectric constant for crystals of both lots are shown in Fig.9. Curve 1 shows the dependence for strontium titanate obtained from the carbonate melt, curve 2 the dependence for a crystal obtained from the potassium fluoride melt and curve 3 the dependence for a polycrystalline strontium titanate specimen. It will be seen that an increase of the dielectric constant at low temperatures is observed for all the specimens, which indicates the probability of a maximum in the curve at very low temperatures. The value of ϵ at room temperature for the strontium titanate obtained from the carbonate melt is 340, while $\tan \delta = (3\text{-}5) \cdot 10^{-4}$. According to Merker[6], $\epsilon = 310$ and $\tan \delta = 3 \cdot 10^{-4}$. The crystals grown from molten potassium fluoride have consistently lower values of the dielectric constant (Fig.9, curve 2). After heating the temperature dependence and the magnitude of the dielectric constant of these crystals approach those for crystals grown from the carbonate solution.

Single crystals of $(Ba,Sr)TiO_3$ solid solutions

Single crystals were grown from solutions of mixtures of barium titanate and strontium titanate in a melt of potassium fluoride. The dielectric parameters of such single crystals change markedly as a result of heat treatment. After annealing at 1350° for 3 hours the crystals noticeably darkened but at the same time acquired normal ferroelectric properties. The temperature dependences of the dielectric constant of crystals containing 10 and 50% strontium titanate before and after annealing are shown in Fig.7. It will be seen that after treatment the crystals exhibit a well pronounced dielectric constant peak at temperatures approximately corresponding to the Curie points of polycrystalline solid solutions having the same composition. Heat treatment

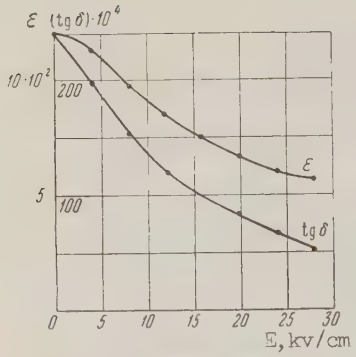

Fig.10. Variation of the reversible dielectric constant and loss tangent (at 10^6 cps) for a 10% $SrTiO_3$-90% $BaTiO_3$ crystal with the biasing dc field strength.

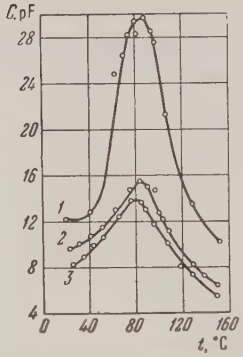

Fig.11. Influence of a biasing field E on the temperature dependence of the capacitance of a 10% $SrTiO_3$+90% $BaTiO_3$ crystal. Measurements made a frequency of 10^6 cps. 1) E = 0, 2) E = 8, 3) E = 16.9 kv/cm.

has an analogous effect on $(Ba,Sr)TiO_3$ single crystals of intermediate compositions. The temperature dependence of the loss tangent of a single crystal with 10% strontium titanate after annealing is shown by curve 3 in Fig.7. Oscillographic studies showed that before annealing the hysteresis loops are similar to Raleigh loops, while after annealing the hysteresis loops assume the shape common to ferroelectrics. The nonlinear properties of heat treated crystals are also manifested in the dependence of the reversible dielectric constant on the biasing dc field strength. The field dependence of the capacitance in the presence of a biasing field for a crystal of the same composition is shown in Fig.11. At the Curie point the capacitance is more than halved in a 16 kv/cm field. The influence of an applied dc field makes itself felt far beyond the Curie point. Specimens not subjected to heat treatment exhibit a noticeably weaker field dependence of ϵ and $\tan \delta$.

Crystallization during solidification of molten barium titanate

Statton[37] in 1951 made an attempt to establish the phase diagram of the $BaO-TiO_2$ system; his measurements were made under vacuum. Since in heating under vacuum the properties of titanates change and these compounds readily go over into metastable states, Statton's results can only be regarded as approximate. In 1954, Trzebiatowski, Drus & Berak[38] investigated the same phase diagram using more reliable methods. Recently, Rose & Roy[39] published new data on this system.

According to the data of different authors the melting point of barium metatitanate lies in the 1610-1700° interval. At these temperatures the use of platinum and quartz containers is precluded. Corundum and zirconium crucibles are also unsuitable. Although chromemagnesite dishes proved to be stable, they show a strong tendency to absorb barium titanate. Hence it is expedient to utilize methods not involving the use of a crucible, such as the method developed by Verneil for growing corundum crystals. At the request of B.M.Vul, S.K.Popov attempted to prepare barium titanate crystals by the method of sprinkling through a flame. In view of the fact that barium titanate has metastable states and a high temperature phase transition Popov failed to achieve satisfactory results. As noted above, in connection with our study of the metastable states of titanates, we found a procedure for transforming them to the normal state. Hence we feel it would be worthwhile to repeat these flame experiments.

In order to obtain single crystals from a melt under conditions precluding contact of the molten material with the walls of a crucible, we experimented

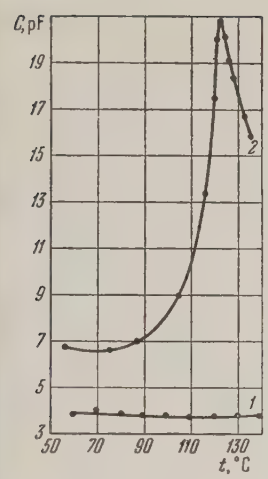

Fig.12. Effect of annealing on the ferroelectric properties of hexagonal barium titanate: 1) initial nonferroelectric hexagonal crystal, 2) same crystal after annealing (perovskite type structure).

with a procedure based on the poor heat conductivity and high viscosity of barium titanate. If a sufficiently massive specimen of barium titanate is used its central portion can be brought to the melting point while the outside remains solid and serves as the container. In this case under the solidifying crust there form cavities which are filled with crystals. In most cases these crystals are small thin plates.

Investigation of the dielectric parameters of polycrystalline specimens cut from remelted barium titanate showed that after appropriate aging the dielectric characteristics of such specimens are virtually identical with those of the polycrystalline ceramic produced by the conventional technique. X-ray studies showed that the perovskite type structure is retained after remelting. However, individual single crystals extracted from the remelted mass were nonferroelectric and belonged to the hexagonal modification.

In a number of cases, in solidified melts we observed sizeable transparent vitreous sections. They did not have the external faceting of crystals but as regards structure were monocrystalline masses. Kinetoscopic investigation in polarized light showed the typical pattern for uniaxial crystals. We investigated the birefringence and index of refraction in the visible region of the spectrum of such specimens. Initially such specimens are not ferroelectric, but after prolonged heating ferroelectric properties gradually appear (Fig.12): before annealing the dielectric constant is small and virtually temperature independent over a wide interval, while after annealing a sharp peak appears at about 120°. Thus the initial hexagonal structure disappears and is replaced by the perovskite structure. Unfortunately, heat treatment also results in a certain degree of turbidity. In view of the closeness of the two modifications as regards density and energy of the lattice, the readiness with which one form is transformed into the other and certain other considerations, we feel that it would be worthwhile to continue these experiments with a view to developing a

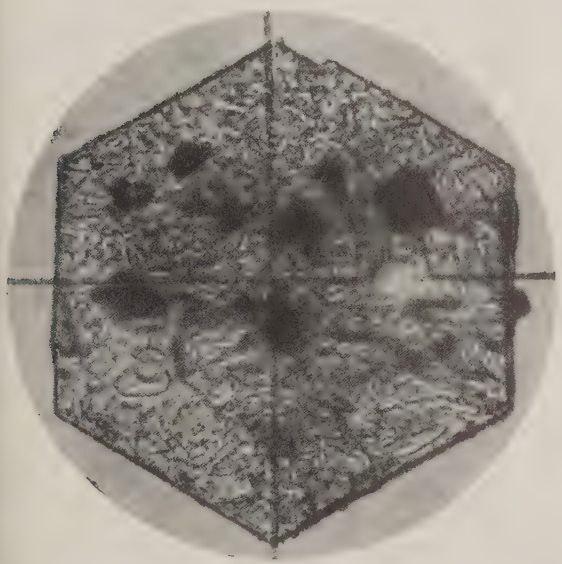

Fig.13. Hexagonal plate-like crystal formed in a cavity.

a procedure that would effect the transformation without involving the appearance of turbidity.

Numerous individual well-defined hexagonal crystals are encountered in solidified melts. Many such crystals are formed in hollows and cavities (Fig.13). We also found that many fine crystals are formed inside solidified drops of molten barium titanate poured through air from a sufficient height. The minute crystals formed inside such drops are optically homogeneous (transparent). It is interesting to note that inside such solidified drops there are encountered side by side hexagonal plates and cubes; these crystal forms also differ as regards color: light green and black. According to a recently published report, Merker[6] succeeded in obtaining large and good crystals (true of strontium titanate rather than barium titanate) by the flame method. The crystals obtained by Merker were also characterized by anomalies similar to those described above. Such anomalies can readily be eliminated by supplementary heat treatment. Apparently, the technique for obtaining large crystals described by von Hippel[4] also requires additional heat treatment of the crystals to obtain normal ferroelectric properties.

The results of our work at the Institute on the preparation of ferroelectric crystals show that the conditions of crystallization have a strong influence on the ferroelectric properties of the specimens. Ferroelectric materials have a strong tendency to form in metastable states which after solidification may persist for a long time. In view of this the importance of heat treatment and aging in the preparation of ferroelectric crystals are understandable. These distinctive characteristics of ferroelectrics should be borne in mind in developing techniques for growing ferroelectric crystals.

Scientific Research Physical-Mathematical Institute
at Rostov-on-the-Don University

References

1. H.Blattner, W.Känzing & W.Merz, Helv.Phys.Acta, 22, 35 (1949).
2. H.F.Kay & R.G.Rhodes, Nature, 160, 126 (1947).
3. B.Matthias, Phys.Rev., 73, 808 (1948).
4. A.von Hippel, ZS. f. Phys., 133, 158 (1952).
5. S.P.Remeika, J.Amer.Chem.Soc., 76, 940 (1954).
6. L.Merker, Trans.Amer.Inst.Mining Eng., 7, 645 (1955).
7. I.N.Beliaev, N.S.Novosil'tsev, A.L.Khodakov & E.G.Fesenko, Doklady AN SSSR, 78, 875 (1952).
8. I.N.Beliaev, N.S.Novosil'tsev, E.G.Fesenko & A.L.Khodakov, Zhur.eksp. teor.fiz., 23, 211 (1952).
9. I.N.Beliaev, N.S.Novosil'tsev, E.G.Fesenko & A.L.Khodakov, Doklady AN SSSR, 83, 875 (1952).
10. I.N.Beliaev & A.L.Khodakov, Zhur.eksp.i teor.fiz., 22, 376 (1952).
11. E.G.Fesenko, Doklady AN SSSR, 88, 785 (1953).
12. N.S.Novosil'tsev & A.L.Khodakov, Zhur.tekh.fiz., 17, 651 (1947).
13. A.L.Khodakov, Zhur.tekh.fiz., 20, 529 (1950).
14. N.S.Novosil'tsev, Zhur.tekh.fiz., 20, 809 (1950).
15. I.N.Beliaev, Uchenye zapiski (Scientific Notes), Rostov State University, 16, 77 (1951).
16. N.S.Novosil'tsev, A.L.Khodakov & M.S.Shul'man, Doklady AN SSSR, 83, 829 (1952).

17. N.S.Novosil'tsev, A.L.Khodakov & M.S.Shul'man, Zhur.tekh.fiz., 22, 336 (1952).
18. E.G.Fesenko & A.G.Slabchenko, Zhur.tekh.fiz., 24, 1288 (1954).
19. I.N.Beliaev, A.L.Khodakov & M.L.Sholokhovich, Zhur.fiz.khim., 27, 376 (1953).
20. N.S.Novosil'tsev & A.L.Khodakov, Zhur.eksp.i teor.fiz., 27, 94 (1954).
21. I.N.Beliaev, N.S.Novosil'tsev & A.L.Khodakov, Trudy (Transactions) NIFMI (Scientific Research Physical-Mathematical Institute), 27, 67 (1955).
22. I.N.Beliaev, N.S.Novosil'tsev & A.L.Khodakov, Trudy NIFMI, 27, 63 (1955).
23. N.S.Novosil'tsev, A.L.Khodakov & M.S.Shul'man, Trudy NIFMI, 27, 9 (1955).
24. A.L.Khodakov & M.S.Shul'man, Trudy NIFMI, 27, 25 (1955).
25. N.S.Novosil'tsev & A.L.Khodakov, Uchenye zapiski (Scientific Notes), Rostov State University, 32, 147 (1955).
26. N.S.Novosil'tsev & A.L.Khodakov, Zhur.tekh.fiz., 26, 51 (1956).
27. N.S.Novosil'tsev & A.L.Khodakov, Zhur.tekh.fiz., 26, 310 (1956).
28. H.F.Kay, J.Phys.Soc., 18, 230 (1955).
29. I.N.Beliaev & M.L.Sholokhovich, Doklady AN SSSR, 77, 51 (1951).
30. M.L.Sholokhovich & I.N.Beliaev, Zhur.ob.khim. (J.Gen.Chemistry), 24, 216 (1954).
31. I.N.Beliaev, M.L.Sholokhovich & G.V.Barkova, Zhur.ob.khim., 24, 211 (1954).
32. I.N.Beliaev & M.L.Sholokhovich, Trudy NIFMI, 27, 43 (1955).
33. I.N.Beliaev & M.L.Sholokhovich, Trudy NIFMI, 27, 55 (1955).
34. M.L.Sholokhovich & I.N.Beliaev, Zhur.ob.khim., 24, 218 (1954).
35. M.L.Sholokhovich & G.V.Barkova, Zhur.ob.khim., 25, 1255 (1955).
36. I.N.Beliaev, M.L.Sholokhovich & G.V.Barkova, Zhur.neorg.khim. (J.Inorganic Chemistry), 1, 1026 (1956).
37. W.O.Statton, J.Chem.Physics, 19, 33 (1951).
38. W.Trzebiatowski, M.Drus & S.Berak, Roczniki chemii, 28, 21 (1954).
39. D.E.Rose & R.J.Roy, J.Amer.Cer.Soc., 38, 102 (1955).

SOME CHARACTERISTICS OF SINGLE CRYSTALS OF $PbTiO_3$ AND $(Ba,Pb)TiO_3$ SOLID SOLUTIONS

- E.G.Fesenko, O.P.Kramarov, A.L.Khodakov & M.L.Sholokhovich

Single crystals of lead titanate obtained by crystallization from the ternary mixture V_2O_5+PbO+TiO_2 have been described earlier[1,2]. Later reports[3,4] noted the possibility of using sodium silicate as the solvent for obtaining $BaTiO_3$ single crystals.

Recently we established that lead metaborate can also be used as the flux in preparing $PbTiO_3$ single crystals. This compound is highly suitable for this purpose inasmuch as lead titanate can be crystallized from it at relatively low temperatures (900-700°). Unfortunately, lead metaborate cannot be used as the fuse-salt solvent for preparing single crystals of $(Ba,Pb)TiO_3$ solid solutions at low temperatures, for an exchange reaction occurs as a result of which $PbTiO_3$ crystallizes out of the solution.

For this reason we used potassium fluoride as the fuse-salt solvent for preparing crystals of $(Ba,Pb)TiO_3$ solid solutions. By cooling melts of mixtures of KF, $PbTiO_3$ and $BaTiO_3$ taken in different proportions one can obtain a continuous series of $(Ba,Pb)TiO_3$ solid solutions. This follows from our study of the melting-point diagram of the system K_2F_2-$BaTiO_3$-$PbTiO_3$ in conjunction with x-ray analyses of the solid phases. $PbTiO_3$ crystals can be separated from the KF by dissolving the fluoride in water.

In the present report we shall describe the properties of $PbTiO_3$ crystals obtained by crystallization from melts of sodium silicate and lead metaborate and the properties of crystals of $(Ba,Pb)TiO_3$ solid solutions. In most cases the crystals were grown in a platinum cup heated in a nichrome resistance furnace, the temperature of which was controlled by means of an electronic regulator.

Hereinafter we shall use the following designations:

Crystals of lot I are crystals of $PbTiO_3$ grown and described earlier[1].

Crystals of lot II are single crystals of $PbTiO_3$ obtained by slow cooling of a melt consisting of 80% $Pb(BO_2)_2$ + 20% $PbTiO_3$* from 900 to 680°. The formed single crystals were separated by treating the solidified melt with concentrated nitric acid and then dissolving the reaction products with water. In contrast to the crystals described earlier and the crystals of $PbTiO_3$ grown from a melt of sodium silicate, the $PbTiO_3$ crystals obtained by crystallization from the $Pb(BO_2)_2$ melt are transparent, light green and have the forms {100}, {110} and {111}.

Crystals of lot III were grown from a melt consisting of 50% Na_2SiO_3 + + 50% $PbTiO_3$ in an open corundum crucible. The melt was held at a temperature of 1100° the time necessary for complete solution and then slowly cooled to 850°. The crystals are opaque and only of the {100} form.

Crystals of lot IV were grown from a melt of 88% KF + 12% of a mixture consisting of 60% $PbTiO_3$ + 40% $BaTiO_3$ by slow cooling of the melt from 940 to 780°. Unlike the other lots, the crystals of this lot were grown in a covered platinum cup. X-ray analysis showed that these single crystals had a composition corresponding to the original proportion of the components, i.e., 60% $PbTiO_3$ and 40% $BaTiO_3$.

Crystals of lot V were grown from a melt of 90% KF + 8% of a mixture consisting of 50% $PbTiO_3$ + 50% $BaTiO_3$ in an open platinum cup. In this case the melt was held for a long time at 860° and then slowly cooled to complete

---

*Here and below all percentages are molar percent.

solidification. The composition of the resultant single crystals differs appreciably from that of the initial mixture. These crystals are brown, poorly transparent and solely of the form {100}. Among the finer crystals, however, there are many entirely transparent hexahedral plates.

Structure and Optical Properties

Table 1

Lot No.	Lattice parameter, A		Spontaneous deformation
	c	a	
I	4,147	3,902	0,063
II	4,151	3,900	0,064
V	4,037	3,965	0,018

The structural type, symmetry and unit cell dimensions of these single crystals were determined by analysis of x-ray powder patterns. The powder patterns showed that the single crystals of the lots listed in Table 1 have the perovskite type structure with a tetragonal cell. The lattice parameters of these crystals and the variation of these parameters with temperature were found from x-ray patterns recorded in a RKE type camera[5] specially adapted[6] for work at different temperatures. The focused on lines were those for which $\Sigma h_i^2 = 24$, 25 or 26, depending on the magnitude and ratio of the parameters. Unfiltered Cu radiation was used in all the work.

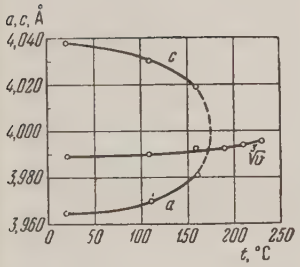

Fig.1. Lattice parameters of $(Ba,Pb)TiO_3$ solid solution crystals (lot IV) as a function of the temperature.

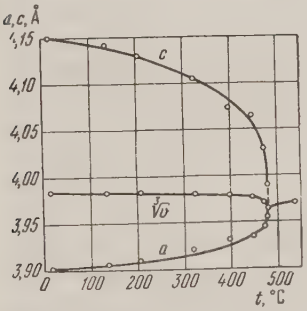

Fig.2. Same as Fig.1 but for $PbTiO_3$ single crystals (lot II).

It will be seen from the table that the spontaneous deformation increases with increasing lead content. Figs.1 and 2 show the variation of the lattice parameters of the solid solution crystals of lot IV and of pure lead titanate crystals of lot II, respectively, as a function of the temperature. The curve characterizing the temperature dependence of the parameters of the solid solution shows no anomalies and is very close to the curve described earlier[6] for polycrystalline specimens. In the case of the lead titanate crystals, however, there is an anomaly (Fig.2): over an appreciable temperature range the volume decreases linearly with increasing temperature but near the Curie point the linearity breaks down; the net decrease in volume in going from 20 to 490° is somewhat greater than 1% (0.75 A^3).

In the linear region the expansion coefficient is approximately $-2.8 \cdot 10^{-6}$/degree. It should be noted that the change in the values of the lattice parameters at the Curie point is more abrupt than in the case of polycrystalline $PbTiO_3$. The character of the changes at the Curie point indicate that this is a transition of the first order.

The optical properties of the crystals were studied by means of a polarizing microscope, the stage of which was equipped with a suitable heater to permit of observations at high temperatures. Domain structure was observed in the crystals of all lots of lead titanate and those of the lot V solid solution. Photographs of one of the $PbTiO_3$ crystals (0.4 mm) of lot II obtained below and above the Curie point are shown in Fig.3. The mean values of the indices of refraction

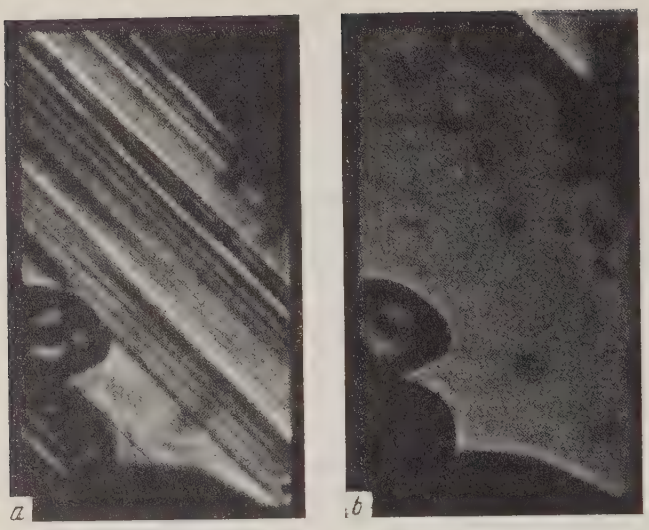

Fig.3. Domain structure of a $PbTiO_3$ crystal from lot II: a) heated up to Curie point; b) heating above the Curie point.

of the crystals of different lots as determined by the immersion method in S-Se alloy are listed in Table 2.

Table 2

Lot no.	Index of refraction
I	2.65
II	2.71
V	2.52

Dielectric Properties

The dielectric properties of the different $PbTiO_3$ and $(Ba,Pb)TiO_3$ crystals were investigated in the temperature range from room temperature to 400° with a KV-1 Q-meter. The electric conductivity was measured with a vacuum type MOM-2M megohmmeter. Insofar as was possible we selected crystals having two plane parallel faces for these measurements; the silver electrodes were fired on at 600-650°.

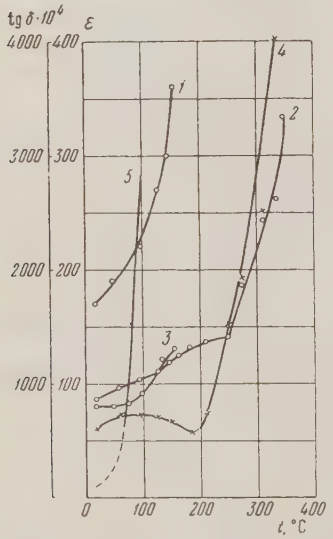

Fig.4. Temperature dependences of ε and tan δ for the $PbTiO_3$ single crystals of different lots: 1) ε for lot I, 2) ε for lot II, 3) ε for lot III, 4) tan δ for lot II, 5) tan δ for lot III.

$PbTiO_3$ single crystals

The data on the dielectric parameters of crystals of lot I are given in Ref.1. According to these data the dielectric constant ε of $PbTiO_3$ at room temperature and a frequency of 10^7 cps equals 150 and tan $\delta = 30 \cdot 10^{-2}$. These crystals were dark brown and apparently contained an appreciable amount of impurities which may explain their high conductivity and loss tangent. This is substantiated by the marked decrease in tan δ with increasing frequency.

Crystals of lot II, as noted above, are transparent and presumably contain less impurities. At a frequency of 10^6 cps and room temperature for most of them tan $\delta = 7 \cdot 10^{-2}$, while for some, the particularly transparent ones, the value was only of the order of $1\text{-}2 \cdot 10^{-2}$. The dielectric constant of the single crystals of lot II is smaller than that of the crystals of lot I and at room temperature averaged 85.

The lead titanate crystals of lot III had approximately the same dielectric constant as the crystals of lot II and an even lower loss tangent at room temperature.

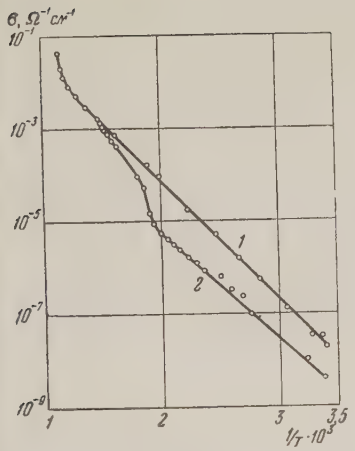

Fig.5. Temperature dependence of the conductivity of $PbTiO_3$ single crystals:
1) lot I,
2) lot II.

The temperature dependences of ϵ and tan δ for the lead titanate single crystals of all three lots are shown in Fig.4.

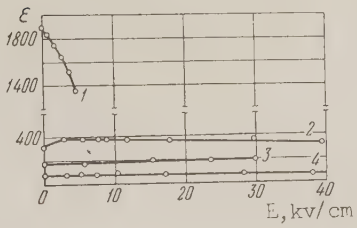

Fig.6. Dependence of the reversible dielectric constant at a frequency of 10^6 cps on the biasing dc field for different ferroelectric crystals: 1 - $BaTiO_3$, 2 - $(Ba,Pb)TiO_3$ (lot V), 3- $(Ba,Pb)TiO_3$ (lot IV), 4 - $PbTiO_3$.

Owing to the great increase in conductivity with temperature it proved impossible to determine the Curie point of these new crystals, just as it was for the crystals of lot I, although the conductivity of the new crystals is appreciably lower (Fig.5) than those of lot I.

Measurements in strong low-frequency fields on an oscillographic set-up showed that due to the strong internal field in lead titanate it is impossible to obtain saturation at room temperature: with E = 8 kv/cm the hysteresis-loop oscillograms are virtually Raleigh figures. The presence of a large internal field may also explain the virtually constant value of the dielectric constant in biasing dc fields up to 50 kv/cm (curve 4 in Fig.6).

Single crystals of $(Ba,Pb)TiO_3$ solid solutions

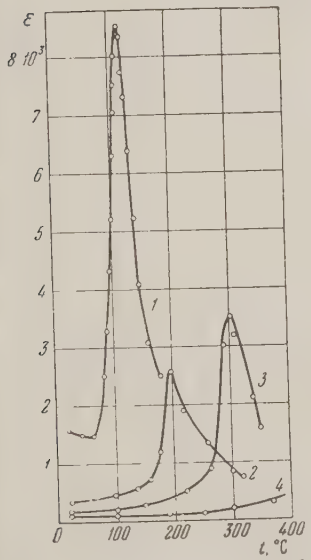

Fig.7. Temperature dependence of the dielectric constant for single crystals: 1- $BaTiO_3$, 2- $(Ba,Pb)TiO_3$ (lot IV), 3- $(Ba,Pb)TiO_3$ (lot V), 4- $PbTiO_3$ (lot II).

The most extensive investigation was made of the solid solution single crystals (lots IV and V). The temperature dependence of the dielectric constant of crystals of these lots is shown in Fig.7, where for purposes of comparison we also show the variation of ϵ as a function of the temperature of $BaTiO_3$ single crystals (curve 1) and $PbTiO_3$ single crystals of lot II (curve 4). It will be noted from the character of the temperature variation of ϵ that these solid solution single crystals have pronounced ferroelectric properties.

The dielectric constant at the Curie point of crystals of lot V rises to 17 times its value at room temperature and to 6 times its value for crystals of lot IV. The $\epsilon = f(t)$ curves fall off somewhat less steeply on the side of higher temperatures and the variation satisfies the Curie-Weiss law. The Curie-Weiss constant for lot V equals $1.7 \cdot 10^5$, while that for lot IV equals $1.4 \cdot 10^5$.

The variation of the reversible dielectric constant measured at a frequency of 10^6 cps is shown in Fig.6. The effect of a biasing field on the dielectric constant of solid solution single crystals differs, depending on the $PbTiO_3$ content. Whereas in the case of crystals of lot IV (curve 3) biasing

fields of up to 30 kv/cm tend to increase the constant at all values of the field, in the case of crystals of lot V (curve 2) an increase of ϵ is observed only in weak fields (up to 3 kv/cm), while at large values of E (up to 40 kv/cm) ϵ decreases, dropping approximately to its initial value. For purposes of comparison the dielectric curves for $BaTiO_3$ (curve 1) and the $PbTiO_3$ crystals of lot II (curve 4) are also shown in Fig.6.

As was shown in earlier reports[7,8] (Ba,Sr)TiO_3 solid solution single crystals prepared from fluoride melts acquire normal ferroelectric properties only after appropriate heat treatment (1 hour heating at 1300°). In contrast the (Ba,Pb)TiO_3 solid solutions discussed herein were not subjected to any heat treatment and exhibited pronounced ferroelectric characteristics in their initial "as prepared" state (Fig.7).

Conclusions

1. On the basis of earlier physical-chemical studies of a number of new systems we succeeded in preparing single crystals of (Ba,Pb)TiO_3 solid solutions with different proportions of components. We also grew $PbTiO_3$ single crystals from melts of sodium silicate and lead metaborate.

2. All the grown crystals are of the perovskite type with a tetragonal lattice. The spontaneous deformation of these crystals increases with increasing lead content. The character of the temperature dependence of the parameters of the $PbTiO_3$ and (Ba,Pb)TiO_3 specimens indicate that the transition observed in them is a first order transition.

3. The presence of domain structure in the $PbTiO_3$ and (Ba,Pb)TiO_3 solid solution crystals were established by optical studies. The mean index of refraction of the crystals increases with increasing lead concentration.

4. All the crystals exhibited the variation of the dielectric constant as a function of the temperature characteristic of ferroelectrics. In the case of some compositions the dielectric constant at the Curie point exceeds its value at room temperature by a factor of almost 20. The existence of hysteresis loops and the character of the field dependence of the reversible dielectric constant indicate that these ferroelectric materials are characterized by a strong internal field.

Scientific Research Physical-Mathematical Institute
at Rostov-on-the-Don State University

References

1. I.N.Beliaev & A.L.Khodakov, Zhur.eksp.i teor.fiz., 22,376 (1952).
2. I.N.Belizev & A.K.Nesterova, Zhur.ob.khim. (J.Gen.Chem.) 22,396 (1952).
3. I.N.Beliaev, M.L.Sholokhovich & G.V.Barkova, Zhur.ob.khim., 24,21 (1954).
4. M.L.Sholokhovich & G.V.Barkova, Zhur.ob.khim., 25,1255 (1955).
5. S.S.Kvitka & M.M.Umanskii, Izv.AN SSSR, Ser.fiz., 17, 271 (1951).
6. G.Shirane, S.Hoshino & K.Suzuki, Phys.Rev., 80, 1105 (1950).
7. N.S.Novosil'tsev & A.L.Khodakov, Doklady AN SSSR, 85,1263 (1952).
8. A.L.Khodakov, M.L.Sholokhovich, E.G.Fesenko & O.P.Kramarov, Doklady AN SSSR, 108, 825 (1956).

STRUCTURE OF THE OH BAND IN THE SPECTRA OF CRYSTALS CONTAINING HYDROGEN BONDS

- A. I. Stekhanov

Investigation of the vibrational spectra of crystals in which the hydrogen bond is present shows that the intensity distribution in the region of vibrations of the OH group is very complicated. Actually there have been very few experimental studies of the spectrum associated with the hydrogen bond and yet it would seem that such investigations may be important when it comes to clarifying a number of questions in solid state physics and may yield additional insight into the nature of the hydrogen bond.

In our earlier works[1,2] we investigated the Raman spectra of a gypsum crystal ($CaSO_4 \cdot 2H_2O$). In the region extending from 3200 to 3750 cm^{-1} we detected a wide band attributable to the valence vibration of the water of crystallization molecules. Experiments with polarized light showed that this band consists of a surposition of two bands, identical in appearance and shifted 90 cm^{-1} relative to each other. When the crystal was cooled to the temperature of liquid nitrogen the intensity of these OH bands was noticeably reduced and a series of fairly sharp lines could be distinguished against the faint background.

We are inclined to interpret the appearance of the double OH band in the Raman spectrum of gypsum as a result of splitting of the symmetric frequency of the water of crystallization molecules in consequence of the tunnel effect for protons, while the characteristic fine structure of the OH band, we feel, is due to coupling between the intramolecular vibrations of the OH group and the intermolecular vibrations.

In view of the results obtained we thought it would be of interest to extend the investigation to include a more detailed study of the Raman spectrum as well as the infrared absorption spectrum of gypsum crystals and a general investigation of the structure of the OH band in the spectra of other crystals containing hydrogen bonds. In particular, it would be desirable to investigate ferroelectric crystals containing hydrogen bonds. According to present-day theory the ferroelectric properties of such crystals are connected with displacements of the protons along the lines of the hydrogen bonds. Hence, in the study that is the subject of the present report, we undertook a careful investigation of the Raman spectra of gypsum, Rochelle salt, ammonium di-H phosphate and sodium di-H phosphate in the high-frequency region and of the infrared absorption spectrum of gypsum in the region of the first overtone of the OH vibrations. $NaH_2PO_4 \cdot 2H_2O$ crystals are not ferroelectric, nevertheless investigation of their spectrum is of interest inasmuch as they contain the hydrogen bond.

In investigating the Raman spectra of the crystals we used the set-up described in Ref.3 which allows of obtaining sharp scattering spectra from the 2537 A resonance line of mercury. The spectra were photographed by means of a Zeiss Q-24 quartz spectrograph having a dispersion of 10.6 A/mm in the 3500 cm^{-1} region. The crystal spectra were studied with different orientations of the crystal axes relative to the directions of the exciting and scattered beams. The infrared absorption spectrum of gypsum was investigated on a double quartz prism Müller-Hilger monochromator which has a plate factor of 55 A/mm in the 6500 cm^{-1} region. A PbS photocell was used for detecting the infrared radiation.

The Raman spectra of gypsum in the high-frequency region obtained at 100 and -196°C are shown in Fig.1. Both spectra were photographed with an exposure of about 20 min. It will be seen from these spectrograms that the

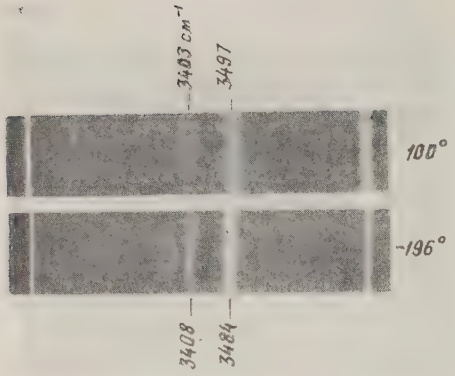

Fig.1. Principal lines of the OH band in the Raman spectrum of gypsum with the crystal at 100 and -196°C.

Raman spectrum of gypsum in the region of the OH group vibrations consists of two intense Raman lines*. The frequencies of these lines with the crystal at -196° are ν_1 = 3408 and ν_2 = 3484 cm^{-1}, while at room temperature the respective frequencies are 3405 and 3495 cm^{-1}. Heating of the crystal to 100° leads to displacement of the lines in the opposite directions: the ν_1 line is displaced to the side of lower frequencies by 5 cm^{-1}. while the ν_2 line is shifted to the side of higher frequencies by 13 cm^{-1}. As a result of this radically different temperature dependence of the lines, the width of the doublet varies appreciably with temperature. Thus when the temperature of the crystal is increased from -196 to 100° the separation of the doublet increases from 76 to 94 cm^{-1}. This change is clearly evident in the spectrograms of Fig.1.

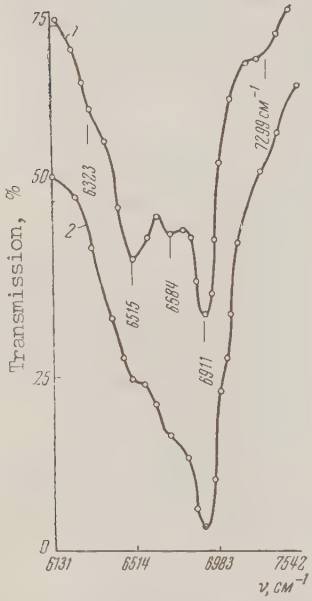

Fig.2. Infrared absorption spectra of gypsum in the region of the first overtone of the OH vibrations recorded for two orientations of the crystal: 1) b axis aligned with the direction of the incident beam; 2) b axis perpendicular to the incident light.

The infrared absorption spectra of gypsum in the region of the first overtone of the valence vibrations of the OH group are shown in Fig.2**. Spectrum 1 was obtained with the crystal oriented so that the b axis was aligned with the direction of the incident light, while spectrum 2 is for the case when the b axis was perpendicular to the direction of the incident beam. The thickness of the specimen in both cases was 1.2 mm.

It will be seen that the infrared spectrum of gypsum is rather complicated. Spectrum 1 comprises two clear absorption maxima at 6515 and 6911 cm^{-1} and one relatively weak maximum at 6684 cm^{-1}. In addition a certain rise in absorption is evident near 7299 and 6323 cm^{-1}. Spectrum 2 differs noticeably from spectrum 1: the absorption band at 6515 cm^{-1}, clearly evident in spectrum 1, becomes much weaker in spectrum 2, while the intensity of the band at 6911 cm^{-1} increases appreciably. On the other hand, the 6684 cm^{-1} band undergoes no noticeable change in going from one orientation of the crystal to the other.

Microphotograms of the Raman spectra of crystals of Rochelle salt, ammonium di-H phosphate and sodium di-H phosphate in the region of vibrations of the OH groups are reproduced in Figs.3 through 6.

---

*By increasing the exposure to 7 hours we were able to detect a broad band having a complex structure in this spectral region.

**I. I. Novakov participated in the study of the infrared absorption spectra of gypsum.

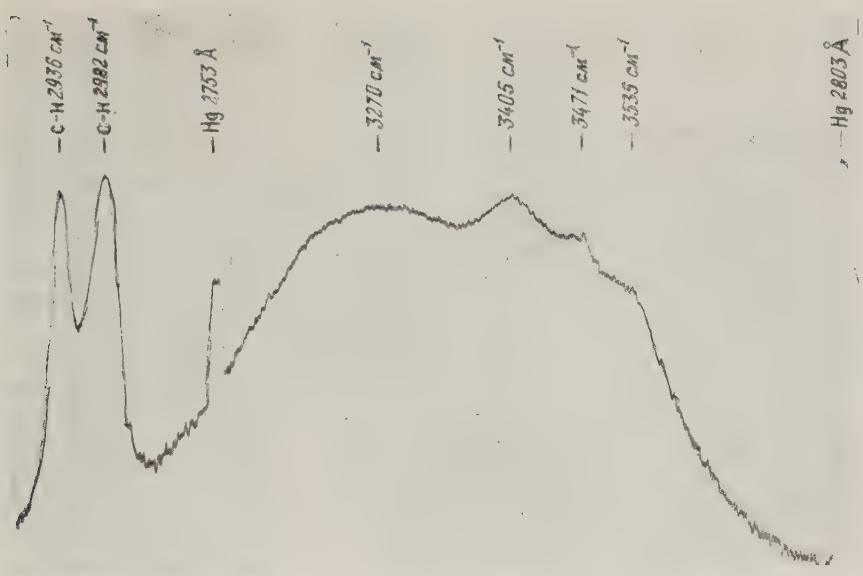

Fig.3. Microphotogram of the Raman spectrum of Rochelle salt.

The Rochelle salt spectrum shown in Fig.3 corresponds to the orientation in which the b axis of the crystal is parallel to the direction of the incident beam. The scattered light was observed in the direction of the c axis. It will be evident from this photogram that the OH band in Rochelle salt is very broad and has a complicated structure. The band begins on the short wave side at the 2936 and 2982 cm^{-1} Raman lines, which are associated with CH vibrations, and extends to 3740 cm^{-1}, i.e., has a width of about 800 cm^{-1}. Against the continuous background one can distinguish four intensity maxima at 3270, 3405, 3471 and 3535 cm^{-1}; the first of these is appreciably wider than the other three.

Heating the Rochelle salt crystal from 20 to 38° leads to only minor changes in the intensity distribution in the OH band. The broad peak at 3270 cm^{-1} is reduced somewhat in intensity and smoothed out; the other three peaks become less sharp. This will be evident from a comparison of the photometric curves a and b in Fig.4. A much greater change in the spectrum of Rochelle salt is observed when the crystal is cooled to -196°. Photogram c in Fig.4 shows that in this case instead of the three intensity maxima at 3405, 3471 and 3535 cm^{-1} there appear separate, sharp and very intense Raman lines, while at the location of the broad maximum at 3270 cm^{-1} there persists a continuous spectrum section extending over a range of about 300 cm^{-1}. Careful study of this continuous spectrum section discloses a weak doublet at 3280 and 3345 cm^{-1} which we have marked by the two left-hand arrows in the microphotogram.

The Raman spectrum of an $NH_4H_2PO_4$ single crystal shown in Fig.5 was obtained with the crystal oriented so that its c axis was aligned with the incident light beam. It will be seen that in the wave number range from 2400 to 3400 cm^{-1} there is a continuous spectrum with three very broad but clearly pronounced peaks at about 2650, 2840 and 3150 cm^{-1}.

The Raman spectrum of sodium di-H phosphate in the region of the vibrations of the OH group is shown in Fig.6. It comprises a broad band extending

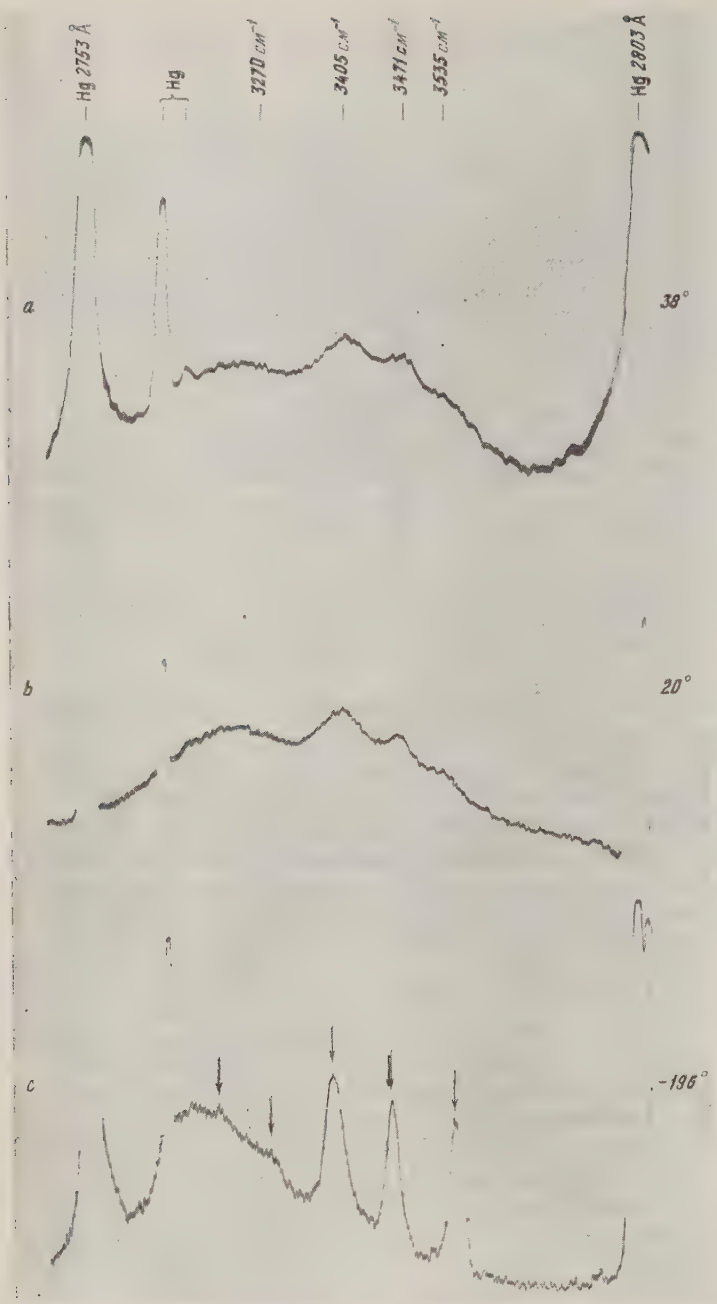

Fig.4. Microphotograms of the Raman spectra of Rochelle salt at 38, 20 and -196°.

from 3230 to 3500 cm^{-1} and one sharp line at 3559 cm^{-1}. It will be seen from the photogram that this band consists of two doublets situated at 3263 & 3322 and 3396 & 3454 cm^{-1}. The first doublet is hard to distinguish in the microphotogram but is clearly noticeable in photographs of the spectrum.

In studying the high-frequency part of the Raman spectrum of the $NaH_2PO_4 \cdot 2H_2O$ crystal, we obtained very clear photographs of the spectrum in the region of low frequencies as well. Near the exciting line in these spectrograms we detected sharp lines having the wave numbers 58, 86, 113 and 146 cm^{-1} as well as two groups of lines situated in the intervals 400 to 550 and 900 to 1000 cm^{-1}; the first group consists of five lines at 420, 454, 481, 523 and 544 cm^{-1}, while the second group is comprised of four lines at 912, 945, 994 and 1007 cm^{-1}.

Thus the study of the spectra of crystals of gypsum, Rochelle salt, ammonium di-H phosphate and sodium di-H phosphate shows that a highly complex distribution of intensities obtains in the spectral region associated with the vibrations of the OH group. Let us see how these complicated spectra may be interpreted.

The Raman spectrum of gypsum has been studied by many investigators. The most detailed investigation in the region of the vibrations of the OH group is that of Cabbannes & Aynard[4] who studied the dependence of the intensity of the 3405 and 3495 cm^{-1} lines on the orientation of the crystal as well as the

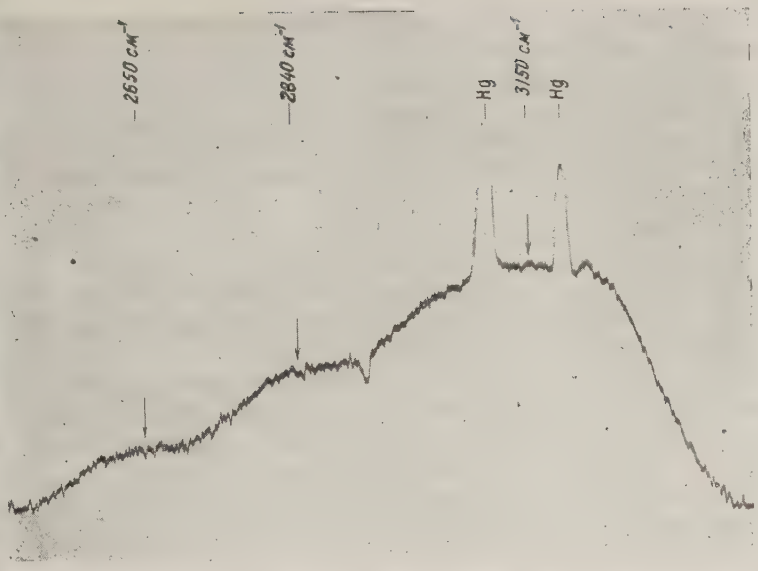

Fig.5. Microphotogram of the Raman spectrum of ammonium di-H phosphate.

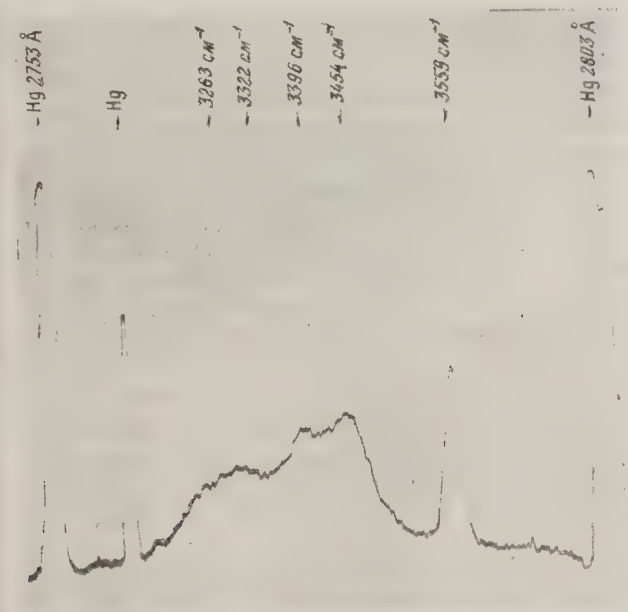

Fig.6. Microphotogram of the Raman spectrum of sodium di-H phosphate.

polarization of these lines. On the basis of their results Cabbannes & Aynard attribute the $\nu_1 = 3405$ and $\nu_2 = 3495$ cm^{-1} lines to the symmetric and antisymmetric, respectively, vibrations of the crystallization water molecule. We feel there is reason to question this interpretation. If the line 2 is associated with the antisymmetric vibrations of the crystallization water molecule, it should be very weak in the Raman spectrum. Hence we feel that in all probability the frequency actually associated with the antisymmetric vibrations of the water molecules has not yet been observed in the Raman spectrum of water vapor. Assuming the ν_2 line to be very weak, only the ν_1 line corresponding to the symmetric vibrations of the water molecule should be clearly discernable in the Raman spectrum.

Our investigation of the shift of the fundamental frequencies of the OH band as a function of the temperature (Fig.1) shows that the ν_1 and ν_2 lines are displaced in opposite directions: with increasing temperature the frequency ν_1 decreases, while the frequency ν_2 increases. If we turn to the results of investigations of the temperature dependence of the position of the OH bands, we find that in both Raman spectra and infrared absorption spectra the frequency of the valence vibrations of the OH group in both crystals and liquids is always displaced to the side of higher frequencies with increasing temperature. This temperature dependence of the frequencies of the OH group is explained in the theory of the hydrogen bond. Consequently, from contrary temperature dependence of the $\nu_1 = 3405$ cm^{-1} line we deduce that its origin, too, is different from that inferred by Cabbannes & Aynard.

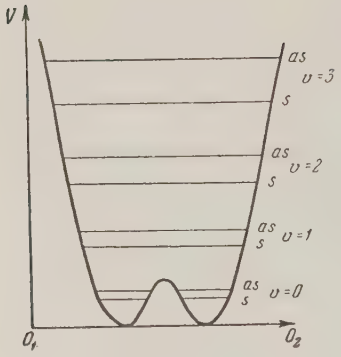

Fig.7. Potential field along the line of the hydrogen bond.

We feel that the appearance of these two intense lines in the gypsum spectrum in the region of the valence vibration of the OH group must be regarded as the result of splitting of the symmetric frequency of the crystallization water molecule due to the proton tunnel effect. As is known splitting on the vibrational levels due to the tunnel effect is associated with a characteristic two-minima form of the potential function. In some cases in the presence of the hydrogen bond the curve along which the proton moves has two minima corresponding to the two equilibrium positions of the proton (Fig.7). This was shown by Huggins[5] in investigating the hydrogen bond in water and in ice. The idea that the potential field along the line of the hydrogen bond has the form shown in Fig.7 was further developed by Mason[6] in the theory of ferroelectric crystals containing hydrogen bonds. More recently the question of the role of the hydrogen bond in the process of a proton passing through the potential barrier has been examined in the theoretical work of Sokolov[7]. Thus it may now be considered established that in some cases the potential curve along the hydrogen bond has two minima separated by a potential barrier. Hence we feel it logical to assume that in substances in which the hydrogen bond is present one may expect to observe splitting of the vibrational levels of the OH group and the appearance of two OH bands in the Raman and infrared spectra.

Let us now turn to the deductions that follow from the theory of the tunnel effect. As was noted above the presence of two minima in the potential curve leads to splitting of the vibrational levels of the molecule into two sublevels. The wave function associated with the upper sublevel as is always antisymmetric; the wave function corresponding to the lower sublevel s is always symmetric. In the Raman spectrum only the transitions $as \rightarrow as$ and $s \rightarrow s$ are active, while in the infrared spectrum the transitions $as \rightarrow s$ and $s \rightarrow as$ which should yield two spectral lines, are active. The magnitude of this splitting is directly related with the probability of transition of the proton from one potential well to the other; that is, the greater the splitting the higher the probability of finding the particle at either side of the potential barrier.

The results of our experiments with gypsum are consistent with these deductions from theory. In the spectrum of gypsum we did find that the OH band is split into two bands, the separation between which depends on the temperature. With increasing temperature the separation (splitting) increases because the two components are displaced in opposite directions (Fig.1). The increase in separation with temperature is, we feel, undoubtedly connected with the fact that the probability of transition of the proton from one potential well to the other increases with temperature due to lowering of the barrier. In other words, in the light of this interpretation we can expect increasingly greater splitting of the OH band at higher temperatures and this is exactly what we observed in our study.

As was noted above the double band in the region of the OH group vibrations is also observed in the infrared spectrum of gypsum. It will be clearly seen from Fig.2 that in the region of the first overtone of the OH vibrations there appear two characteristic bands at 6515 and 6911 cm^{-1}, the intensity of which changes in different ways in going from one orientation of

the crystal to the other. An analogous variation in intensity with changes in orientation is observed for the components of the 3403 & 3497 cm^{-1} doublet appearing in the Raman spectrum recorded at 100° (Fig.1). Consequently, we have reason to assume that the doublets observed in the infrared and Raman spectra of gypsum have the same origin. As for the band at 6684 cm^{-1}, it may be noted that this band was observed for the first time in the present investigation and its nature is still unclear. Possibly it is a combined frequency of the $2\nu + \nu_{1,2}$ type where 2ν is an octave of the deformation frequency of the crystallization water molecule and $\nu_{1,2}$ is one or the other component of the doublet. Combinations of this type in infrared absorption spectra have been observed rather frequently, given a sufficient thickness of the specimen. In our case the maximum thickness of the specimen attained 1.5 mm. The very weak bands at 7299 and 6323 cm^{-1} appear in the spectrum as a result of coupling between the intramolecular vibrations of the OH group and the intermolecular vibrations.

The doublet structure of the OH band in the infrared spectrum of gypsum is also observed in the region of the fundamental tone and of the second overtone. The data of different investigators[8-12] on the position of the two OH bands in the gypsum spectrum and the magnitude of the observed splitting are listed in Table 1. Comparing the results of investigations of the infrared spectrum obtained by different authors who studied the fundamental, we see that the width of the doublet Δ_i in the infrared spectrum is not less than 110-125 cm^{-1}. The width of the doublet Δ_R in the Raman spectrum, according to our measurements, is 90 cm^{-1} (see Fig.1). Juxtaposition of the data on the positions of the doublet in both regions, moreover, shows that the components of the doublet Δ_R lie within the doublet Δ_i in the infrared spectrum. The distinctive features of the doublet structure of the OH band in the Raman and infrared spectra can be understood if we consider the transitions between the split vibrational levels (see Fig.7). As we noted above, according to the applicable selection rules, $as \rightarrow as$ and $s \rightarrow s$ transitions are allowed; this leads to the appearance of a doublet with a separation of components equal to the difference in splitting of the upper and lower levels. In the infrared spectrum, in contrast, there may be manifested only the transitions $as \rightarrow s$ and $s \rightarrow as$; in this case again there is formed a doublet but the separation between the lines here must be equal to the sum of the splittings of the upper and lower levels. Thus in the light of this interpretation the width of the doublet in the Raman spectrum must be smaller than the distance between the corresponding components of the OH band in the infrared spectrum.

Table 1

Infrared spectrum of gypsum

Author	Ref.	Observed frequencies cm^{-1}	Splitting
Duval & Lecomte	8	3400 3510	110
Faint	9	3400 3525	125
Zaitsev & Neporent	10	3410 3510	110
Ellis	11	3390 3510	120
		6670 6900	230
		9800 10200	400
Louisfer	12	6667 7017	350
		9852 10695	843
Our data		6515 6911	386

From the experimentally determined values of the separation between the lines of the doublet in the Raman and infrared spectra one can calculate the

Table 2

v	$\Delta\nu$, cm^{-1}	$\frac{(\Delta\nu)_{v=0}}{(\Delta\nu)_{v=1,2,3}}$
0	15	1
1	105	7
2	215	14
3	385	26

magnitude of the splitting of the ground (zeroth) vibrational level of the OH group (v = 0) as well as of the first (v = 1), second (v = 2) and third (v = 3) levels. We carried out such calculations using our data on the Raman scattering as well as the data of Ellis (Table 1) based on his measurements of absorption in the region of the fundamental and first and second overtones. The results of our calculations are shown in Table 2. In the first column we list the quantum numbers of the vibrational levels of the valence vibrations of the OH group, in the second column the magnitude of the splitting of the vibrational levels and in the third the splitting of the first, second and third levels referred to the splitting of the v = 0 level.

It will be seen from the table that the calculated splitting of the vibrational levels of the OH group in gypsum increases very rapidly with increasing quantum number v. In actual fact the increase in splitting of the levels may occur even more rapidly inasmuch as the width of the doublet in the region of the first and second overtones reported by Ellis is probably much too low (compare his data with our data and those of Louisfert[12]). Nevertheless the results of our calculations of the splitting of the OH vibration levels in gypsum are in good agreement with the predictions of theory regarding the increase in the doublet splitting with increasing quantum number v in the case of the tunnel effect.

Let us now turn to the Raman spectra of crystals of Rochelle salt, ammonium di-H phosphate and sodium di-H phosphate. The Raman spectra of $NaKC_4H_4O_6 \cdot 4H_2O$ and $NH_4H_2PO_4$ crystals have been the subject of numerous studies; the spectrum of $NaH_2PO_4 \cdot 2H_2O$ on the other hand, was apparently obtained for the first time in the present investigation.

In the work of Nedungadi[13], devoted to the Raman spectrum of Rochelle salt, it was shown that in the high-frequency region of the spectrum there appear two broad and intense bands with peaks at 3262 and 3400 cm^{-1} and two weak bands at about 3468 and 3534 cm^{-1}.

The most detailed investigation of the Raman spectrum of Rochelle salt in the region of the vibrations of the OH group is that of Baryshanskaia, Landsberg & Matulevich[14] who studied the spectrum at different temperatures. These authors note that at the temperature of liquid helium the spectrum of the OH group in Rochelle salt consists of a band extending from 3180 to 3300 cm^{-1} and three lines having the wave numbers 3390, 3453 and 3538 cm^{-1}. They also investigated the spectrum of Rochelle salt above and below both Curie points and in the temperature interval between the Curie points both in the presence and in the absence of an electric field. They showed that in all cases the spectrum of Rochelle salt in the short wavelength region undergoes no noticeable changes.

A recent report by Chapelle, Champier & Delain[15] is also devoted to the Raman spectrum of Rochelle salt. One purpose of this investigation was to determine the temperature dependence of this spectrum. These investigators report that the spectrum of the $NaKC_4H_4O_6 \cdot 4H_2O$ in the region of the valence vibrations of the OH group at room temperature consists of two wide bands having distinct peaks at 3277, 3407, 3476 and 3535 cm^{-1}. According to their report, as the temperature is increased, the intensity of the maxima at 3277 and 3407 cm^{-1} remains virtually constant, while the intensity of the maxima at 3476 and 3535 cm^{-1} decreases; at 33° the 3535 cm^{-1} peak fades out completely.

On the basis of their results, these authors infer that the 3277 and 3407 cm^{-1} peaks are associated with vibrations of the tartrate hydroxyl ion, while the 3476 and 3535 cm^{-1} peaks are attributable to the hydration water. From the fact that when the crystal is heated above the Curie point, the 3535 cm^{-1} band disappears, they conclude that the ferroelectric properties of Rochelle salt are due to the presence of the crystallization water molecules.

In our experiments with Rochelle salt crystals we obtained clear Raman spectra in the region of the valence vibrations of the OH group. As was shown above (Fig.4), heating of the crystal from 20 to 38° leads only to a minor redistribution of intensities in the OH band. Further, no substantial changes in the spectrum were observed when the temperature was reduced to -18°. These results of ours are in agreement with the observations of Baryshanskaia, Landsburg & Matulevich. As may be seen from Fig.4, we did not observe the substantial changes in the Rochelle salt spectrum reported by Chapelle, Champier & Delain. We noted a substantial change in the appearance of the spectrum only when the Rochelle salt crystal was cooled to the temperature of liquid nitrogen (Fig.4c): in this case instead of the three broad maxima at 3407, 3476 and 3535 cm^{-1} there appear individual sharp and intense Raman lines, while at the location of the broad 3270 cm^{-1} intensity maximum there persists a section of continuous spectrum, against which as a background one can distinguish a weak doublet.

We feel that our results cast doubt on the interpretation of the OH group spectrum in Rochelle salt advanced by Chapelle, Champier & Delain.

In our opinion the complicated structure of the OH vibration band in the Raman spectrum of Rochelle salt is due to the presence of hydrogen bonds of different lengths. Bearing this in mind one can interpret the observed Raman spectra on the assumption that the tunnel effect for protons may obtain in Rochelle salt crystals.

As is known[6] the Rochelle salt crystal contains three hydrogen bonds whose lengths are 2.59, 2.86 and 3.02 Å. It is reasonable to assume that the 2.59 Å hydrogen bond is responsible for the appearance of the 3270 cm^{-1} broad maximum in the Raman spectrum of Rochelle salt. At low temperatures this maximum is replaced by the 3280 & 3345 cm^{-1} doublet. If these assignments are correct, then the 3535 cm^{-1} line should be ascribed to the "free" vibrations of the OH group when the separation between the oxygens is 3.02 Å and, consequently, there is no effective hydrogen bond between them. Thus, in consequence of the tunnel effect for the proton, there apparently obtains in the Rochelle salt crystal splitting of the two vibrational frequencies corresponding to the 2.59 and 2.86 Å hydrogen bonds.

The problem of the proton tunnel effect can be clarified by investigating crystals containing hydrogen bonds of the same length; in this case, obviously, one should expect the appearance of only one doublet in the Raman spectrum. Such equal hydrogen bond crystals include, for example, the ferroelectric crystals KH_2PO_4 and $NH_4H_2PO_4$.

The Raman spectra of potassium di-H phosphate and ammonium di-H phosphate have been investigated by Landsberg & Baryshanskaia[16]. In their report they indicate that the spectrum of $NH_4H_2PO_4$ comprises two OH vibration bands and a strong band associated with vibrations of the NH group. As regards their appearance and position in the spectrum, the detected bands are remininscent of the corresponding band in the spectrum of KH_2PO_4.

Later, Narayanan[17], investigating the spectrum of $NH_4H_2PO_4$ detected, in addition to the intense NH group band, two bands at 2600 and 2800 cm^{-1} in the high-frequency part of the spectrum.

In our experiments with an $NH_4H_2PO_4$ crystal we also observed in the high-frequency region of the Raman spectrum a section of continuous spectrum (Fig.5) with three very broad intensity peaks located at about 2650, 2840 and 3150 cm^{-1}. The 3150 cm^{-1} band is associated with the NH vibrations, while the 2650 and 2840 cm^{-1} bands are due to vibrations of the OH group and may well be the components of a doublet.

In the region of the vibrations of the OH group in the Raman spectrum of sodium di-H phosphate (Fig.6) we detected two doublets at 3263 and 3322 cm^{-1} and 3396 and 3454 cm^{-1} and a single line at 3559 cm^{-1}. It is impossible at present to interpret the spectrum of $NaH_2PO_4 \cdot 2H_2O$ due to lack of adequate information on the crystal structure of this substance.

Thus in studying the Raman spectra of gypsum, Rochelle salt, ammonium di-H phosphate and sodium di-H phosphate we observed the characteristic doublet structure of the OH band in the spectra of all these crystals, a structure which we feel can be interpreted from the point of view of the proton tunnel effect. Further investigation of vibrational spectra, however, are necessary before any definitive conclusions regarding the role of the tunnel effect can be reached.

In conclusion the writer desires to thank E.F.Gross for his interest in the work and discussion of the results.

Leningrad Physical-Technical Institute of the
Academy of Sciences of the USSR

References

1. A.I.Stekhanov, Doklady AN SSSR, 92, 281 (1953).
2. A.I.Stekhanov, Doklady AN SSSR, 106, 433 (1956).
3. A.I.Stekhanov, Zhur.eksp.i teor.fiz., 20, 330 (1950).
4. J.Cabbannes & R.Aynard, J.de Phys., 3, 137 (1942).
5. M.L.Huggins, J.Phys.Chem., 40, 723 (1936).
6. W.P.Mason, Piezoelectric Crystals, (In Russ. trans., M,1952).
7. N.D.Sokolov, Doklady AN SSSR, 60, 825 (1948).
8. C.Duval & J.Lecomte, C.R., 227, 1154 (1948).
9. C.Paint, J.Chim.phys.et Phys.-chim.biol., 50, 8 (1953).
10. G.A.Zaitsev & B.S.Neporent, Zhur.eksp.i teor.fiz., 29, 857 (1955).
11. I.W.Ellis, Phys.Rev., 38, 698 (1931).
12. I.Louisfer, J.Phys.et Rad., 8, 21 (1947).
13. T.M.K.Nedungadi, Proc.Ind.Acad.Sci., A11, 413 (1940).
14. F.S.Baryshanskaia, G.S.Landsberg & G.P.Matulevich, Izv.AN SSSR, Ser. fiz., 12, 573 (1948).
15. J.Chapelle, G.Champier & C.Delain, J.Chim.phys.et Phys.-chim.biol., 50, 96 (1953).
16. G.S.Landsberg & F.S.Baryshanskaia, Doklady AN SSSR, 61, 1027 (1948).
17. P.S.Narayanan, Proc.Ind.Acad.Sci., A28, 469 (1948).

ON THE SHAPE OF THE POTENTIAL CURVE OF THE HYDROGEN BOND IN CERTAIN CRYSTALS

- A.N. Lazarev

The shape of the potential curve associated with the hydrogen bond is a significant factor that must be taken into account in explaining the physical properties of many crystals and in particular in interpreting the nature of ferroelectricity in KH_2PO_4, Rochelle salt and other crystals.

The probable forms of the potential curve in the complex A—H...B for different strengths of the hydrogen bond (H...B) are shown in Fig.1 (Magat[1]). In the case of a very weak hydrogen bond the interaction which is primarily electrostatic in character, leads to an increase in the anharmonicity (Fig.1,b) as compared with the isolated A—H bond (Fig.1,a).

With further increase in the strength of the hydrogen bond transition of the proton becomes possible, i.e., it becomes necessary to take into account the interaction of the A—H bond with the virtual H—B bond (Fig.1,c). Further decrease of the separation A...B and strengthening of the hydrogen bond lead to decrease in the energy of activation for the proton transition, to "delocalization"

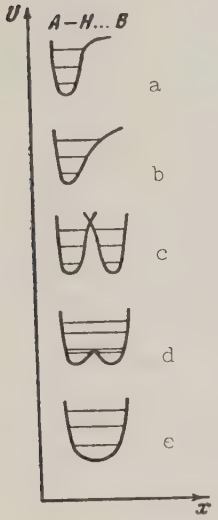

Fig.1. Suggested shape of the potential curve for the proton in the complex A—H...B as a function of the strength of the hydrogen bond[1] (x - coordinate of the H atom along the line A...B): a) isolated A—H bond; b) weak, primarily electrostatic AH...B interaction; c) somewhat stronger hydrogen bond; transition of the proton to the B atom possible: A...HB; d) strong hydrogen bond with "delocalization" of the proton; e) case of particularly strong hydrogen bond - "symmetric" AHB bond.

of the proton (Fig.1,d). Finally, in exceptional cases[2] with a particularly short hydrogen bond the potential barrier may disappear completely (Fig.1,e).

According to present day concepts the ferroelectric effect in Rochelle salt and KH_2PO_4 crystals is connected with the ability of the protons to shift along the direction of the hydrogen bonds. In such crystals there exist short hydrogen bonds (the O—H...O distance is of the order of 2.5-2.6 Å) which are presumably characterized by potential curves of the form shown in Fig.1,e. Below the Curie point the proton is "frozen" in one of the two potential wells; application of an external electric field, however, enables the proton to overcome the moderately high potential barrier. At higher temperatures the thermal energy exceeds the height of the barrier and the probabilities of finding the proton in either of the two potential wells become equal.

According to neutron diffraction data, at temperatures below the Curie point the proton in KH_2PO_4 is displaced 0.21 Å from the midpoint of the O...O separation; the direction of this displacement can be changed by the application of an electric field. At room temperature the protons are symmetrically distributed along the O—H...O bonds up to 0.18 Å to both sides of the midpoint.

It may be assumed that the shape of the potential curve will be evinced in the appearance of the vibrational spectra. The spectroscopic properties of a symmetric double potential well have been analyzed in detail for the

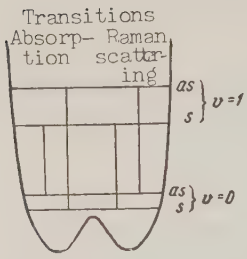

Fig.2. Selection rules for transitions in the case of a symmetric potential curve with two minima.

ammonium molecule[4] and can be extended to other cases of potential curves of the same type. All the vibrational levels corresponding to vibrations in the direction of the tunnel effect split into two sublevels. The magnitude of the splitting is proportional to the probability of the tunnel effect and, consequently, the levels situated considerably below the potential barrier virtually do not split. In contrast, the splitting is appreciable for high-lying vibrational levels. In the case of splitting the wave function associated with the upper sublevel is always antisymmetric, while that associated with the lower level is symmetric. Thus all the frequencies of the vibrational spectrum split with the magnitude of the splitting increasing in overtones. Inasmuch as the active transitions in absorption are $s - as$ and $as - s$, while the transitions active in the Raman effect are $as - as$ and $s - s$, the splitting in the Raman spectrum must be smaller than in the absorption spectrum (Fig.2). In the low frequency region of the absorption spectrum there should be observed the transition $v = 0(s) \rightarrow v = 0(as)$.

Thus in the case of short hydrogen bonds when the potential barrier is not high one may hope to detect splitting in the vibrational spectrum. Kovner & Kapshtal'[5] hypothesized that the appearance of two frequencies in the valence vibrations of the OH group in the Raman spectrum of KH_2PO_4 crystals[6,7] is due to the tunnel effect. To check this hypothesis one must compare the Raman spectrum with the absorption spectrum. The absorption spectrum of KH_2PO_4 has been investigated a number of times; it comprises a wide band with a maximum located, according to different authors, either at 2800 cm^{-1} (Ketelaar[8]) or at 2400 cm^{-1} (Pease & Bacon[3] and Lord & Merrifield[9]). Murphy[10] found very weak bands at 2400 and 2200 cm^{-1} in the reflection spectrum.

In view of the divergence of the data in the literature we felt it expedient to reinvestigate the infrared spectrum of KH_2PO_4 in the region of the valence frequencies of the OH group. Inasmuch as the investigation of the absorption spectrum of a KH_2PO_4 single crystal is difficult due to the necessity of preparing extremely thin cuts, we employed the procedure of compressing transparent discs from a mixture of the compound with powdered potassium bromide[11]. This procedure allows of obtaining sharper spectra than can be observed with the aid of other powder methods. A shortcoming of this procedure is the appearance in the spectrum of an absorption band associated with water contained in the KBr. Obviously this method is applicable only in cases when the investigated compound does not react or form mixed crystals with potassium bromide.

The absorption spectrum of KH_2PO_4 obtained on an ISP-14-b spectrometer with an LiF prism is shown in Fig.3. It will be seen that it comprises two diffused bands at 2825 and 2445 cm^{-1}; the narrower absorption band (at the left) is associated with the adsorbed water.

In their investigation of the Raman spectrum of KH_2PO_4 Landsberg & Baryshanskaia[6] report observing two bands* at 2800 and 2500 cm^{-1}, while Narayanan[7] gives the band frequencies as 2700 and 2500 cm^{-1}. Thus, the splitting in the absorption spectrum is somewhat greater than in the Raman spectrum. The splitting of the levels can readily be calculated; taking 2750 and 2500 cm^{-1}

---

*Both bands are polarized in the same direction as might be expected if their appearance is attributed to the tunnel effect.

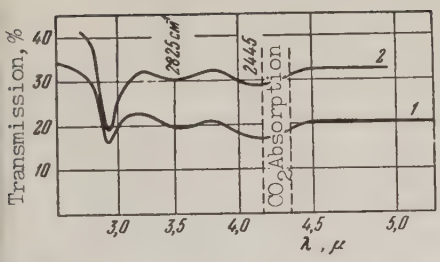

Fig.3. Absorption spectrum of KH_2PO_4 obtained on an ISP-14-b spectrometer with an LiF prism. 25 mm diameter specimen compressed of a mixture of KH_2PO_4 with KBr: 1) 10 mg KH_2PO_4 per 2g KBr; 2) 5 mg KH_2PO_4 per 2g KBr.

for the Raman frequencies, we obtain 55-75 cm^{-1} for the zeroth level and 305-325 cm^{-1} for the first vibrational level. In view of the uncertainty in determining the position of the bands in the spectrum, these evaluations are obviously only approximate. There can be no doubt, however, that the splitting of the vibrational levels in KH_2PO_4 is at least one order of magnitude lower than evaluated by Kovner & Pakshtal'. Possibly the difference is connected with the fact that in their calculation these authors assumed a very low value for the height of the potential barrier (under 1 Kcal)*. Inasmuch as it was found that the splitting of the vibrational levels is minor, it may be concluded that the zeroth (and possibly the first) level lies below the peak of the barrier, i.e., that the height of the barrier is appreciably greater than 3.5 Kcal ($h\nu_{OH}/2$).

It may be noted that the height of the potential barrier should not exceed 1 Kcal if it is assumed that it is of the same order of magnitude as kT at the Curie point. This evaluation, however, is too rough, for under the above assumption no account is taken of the fact that in the ferroelectric effect the proton transfer process is a cooperative one, i.e., the activation energy of simultaneous transfer of the protons in n bonds is appreciably lower than the sum of the activation energies for transfer of the protons in n isolated bonds[12,13]. The above may explain why according to spectroscopic data the potential barrier in each separate bond appears to be rather high.

It must be noted that replacement of the hydrogen by deuterium should appreciably reduce the probability of the tunnel effect and, consequently, sharply decrease the splitting of the levels. Actually only one valence vibration band (at 1750 cm^{-1}) associated with the O—D group has been detected[9] in the absorption spectrum of KD_2PO_4 even though satisfactory resolution is readily obtainable in this region of the spectrum by conventional procedures for powdered specimens. The fact that there is no splitting of the O—D band in the KD_2PO_4 spectrum can thus be explained by the lesser splitting of the levels as compared with KH_2PO_4.

The suggested interpretation of the spectrum of KH_2PO_4 in the region of the OH vibrations is not the only possible one. For example, Narayanan[7] investigating the Raman spectrum of the compound attributed both the bands observed by him (2500 and 2700 cm^{-1}) to the fundamental frequencies of the H_2PO_4 ion. We feel, however, that the difference in frequencies observed in the Raman spectrum as against the absorption spectrum and the fact that the two bands in the absorption spectrum are appreciably further apart than the two bands in the Raman spectrum are evidence in favor of the tunnel effect hypothesis. The same considerations render the suggestion that the two OH frequencies are due to the presence of several molecules in the unit cell rather unlikely. Moreover, according to the theory of Davydov[14] in this case the bands should be polarized in mutually perpendicular directions.

---

*According to the evaluation of Magat[1] the height of the potential barrier in KH_2PO_4 is greater than 7.8 Kcal but appreciably below 20 Kcal.

The tunnel effect hypothesis can be further verified by investigating the infrared spectrum of KH_2PO_4 in the region of the overtones and in the far infrared, i.e., by seeking evidence of the $v = 0(s) \rightarrow v = 0(as)$ transition.

Recently attempts have been made to explain the structure of the bands associated with the valence OH vibrations in a number of compounds[15,16], including substances with comparatively long hydrogen bonds, by means of the tunnel effect. There are a number of experimental facts, however, that indicate that in the case of long hydrogen bonds (2.7 Å and greater) the transition of the proton is realized only by classical transfer over the barrier[12]. Consequently, the splitting of the vibrational levels in such cases can hardly be great.

Stekhanov[16,17] detected in the Raman spectrum of gypsum in the region of the OH group vibrations two intense lines and groups of three weak lines (clearly distinguishable at low temperatures) to both sides of these. Stekhanov ascribes the appearance of the two intense lines to the tunnel effect and attributes the weak lines to combinations of the valence OH vibrations with the intermolecular vibrations of the hydrogen bonds.

As was noted above in attempting to verify the hypothesis that the splitting of the bands is due to the tunnel effect it is particularly important to compare the Raman spectrum with the infrared absorption spectrum and also to investigate the overtones. The band in the gypsum spectrum associated with the valence vibrations of the OH group has been investigated by many authors working with both powdered specimens and single crystals. Most detailed investigation of the infrared spectrum of gypsum have been carried out by Zaitsev & Neporent[18]; they observed a doublet structure of the bands with a separation between the components somewhat greater than in the Raman spectrum. A doublet has also been observed in the overtones[19].

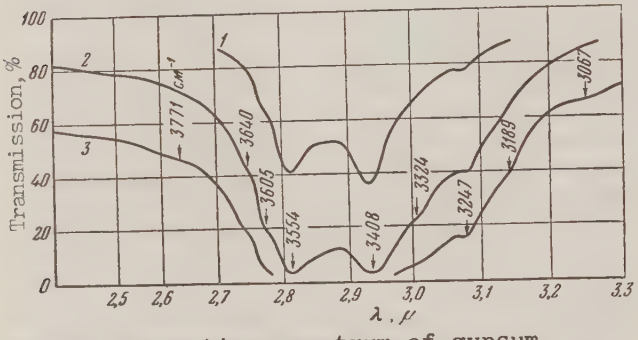

Fig.4. Absorption spectrum of gypsum ($CaSO_4 \cdot 2H_2O$) obtained on the same instrument as the spectrum shown in Fig.3. Specimen 25 mm in diameter compressed of a mixture of gypsum with potassium bromide. $CaSO_4 \cdot 2H_2O$ content per 2 g KBr: 1) 1 mg, 2) 5 mg, 3) 10 mg.

We felt it would be desirable to carry out a supplementary investigation of the absorption spectrum of gypsum for the purpose of making an accurate determination of the OH-vibration frequencies. Inasmuch as the high absorption coefficient hampers investigation of the OH bands in the spectra of single crystals, while powdered specimens yield a very diffused band, we again had recourse to the method of compressing a mixture of powdered gypsum with potassium bromide, in this case taking special measures to insure elimination of the water adsorbed by the gypsum and KBr. In the absorption spectrum as obtained with an ISP-14-b spectroscope with an LiF prism the OH band has a complicated structure (Fig.4): series of weaker bands appear to either side of the intense double maximum. Investigation of the absorption spectrum on an instrument with a higher dispersion (Fig.5)* shows that in the region of intense absorp-

---

*The author desires to thank V.M.Chulanovskii for making available an IKS-6 spectrometer for these measurements.

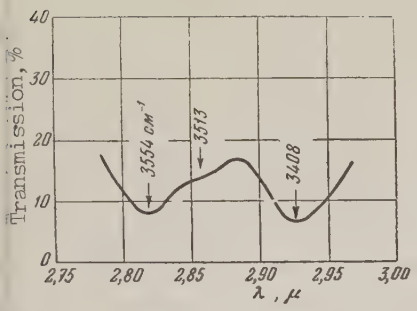

Fig.5. Absorption spectrum of gypsum obtained on a high dispersion instrument (IKS-6 spectroscope). Specimen 25 mm in diameter compressed of a mixture of 4 mg $CaSO_4 \cdot 2H_2O$ per 2 g KBr.

tion there are three bands located at 3408, 3513 and 3554 cm^{-1}; the 3513 cm^{-1} band is somewhat less intense than the others and the frequency of this band was determined with a somewhat lower accuracy than for the other two bands. The observed frequencies in the absorption spectrum and the Raman frequencies reported by Stekhanov are listed in the accompanying table.

If we take the two most intense bands in the Raman spectrum and the 3408 and 3554 cm^{-1} bands in the absorption spectrum, we find that the ratio of the frequencies in the two spectra is not inconsistent with the tunnel effect hypothesis. The fact that the band near 3400 cm^{-1} in both the absorption and the Raman spectra has virtually the same frequency can be explained by the very small splitting of the zeroth vibrational level.

Comparison of the absorption and Raman spectra of gypsum

Frequencies in the absorption spectrum, cm^{-1} (at. +20°)	Frequencies in the Raman spectrum, cm^{-1}	
	at -200°	at +100°
3067		
3189	3230	
3247	3273	
3324	3349	
3408	3408	3403
3513	3484	3497
3554	3564	
3605	3626	
3640	3673	
3771		

On the other hand, the presence in the absorption spectrum of three intense bands and the different polarizations of the two lines in the Raman spectrum allow, we feel, of a different interpretation of the OH frequencies in the gypsum spectrum.

The two intense lines near 3400 and 3500 cm^{-1} in the Raman spectrum can be set against the bands at 3408 and 3513 cm^{-1} in the absorption spectrum; it will be noted that the separations between them are virtually equal (within the limits of the possible experimental error). The only line in the Raman spectrum matching the intense absorption band at 3554 cm^{-1} is the weak line at 3565 cm^{-1}. Thus we can postulate the presence of at least three fundamental frequencies in the gypsum spectrum in the OH vibration region.

The numerous satellites appearing to both sides of the three principal absorption maxima can apparently be juxtaposed with the lines detected by Stekhanov in the Raman spectrum and ascribed by him to combinations (coupling) of the OH vibrations with the intermolecular vibrations of the hydrogen bonds.

Inasmuch as the use of the method of compressing specimens with potassium bromide requires a certain degree of caution (in some cases some distortion of the spectrum may occur), we recorded the absorption spectrum of a specimen of gypsum in the region from 2 to 15μ. The results obtained agree to within 5-10 cm^{-1} with the results of investigation of the gypsum spectrum by other methods[18]. It may be assumed therefore that there is no appreciable distortion in the OH frequency region of the spectrum obtained from our compressed specimen.

We also investigated (on a diffraction grating instrument) the absorption spectrum in the region from 1.3 to 1.6 μ of a plate of gypsum (selenite) cut parallel to the perfect cleavage plane. Four bands - at 7280, 6925, 6720 and 6520 cm^{-1} - appear in this spectrum (Fig.6). The first of these can hardly

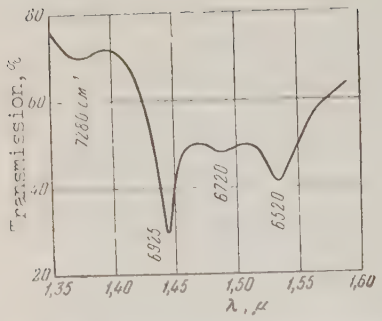

Fig.6. Absorption spectrum of gypsum in the region of the OH vibration overtones obtained on a diffraction grating instrument. Thickness of the layer 0.8 mm; illumination perpendicular to the perfect cleavage plane.

be an overtone of the valence OH vibrations. The other three bands can be interpreted as the first overtones of the three most intense fundamental frequencies - 3554, 3513 and 3408 cm^{-1}. The ratios of the overtone frequencies to twice the frequencies of the fundamentals are 0.97, 0.96 and 0.96, respectively. Thus if we take all three frequencies to be simple overtones of the OH vibrations, we find that in the region of the first overtone there is no increase in separation between the bands as compared with the fundamental tone, something which should be observed if the splitting were due to the tunnel effect.

If we accept that all the three intense absorption bands are associated with fundamental frequencies, we are faced with the question of why there should be three frequencies of the valence OH vibrations in gypsum. It might be suggested that the 3554 cm^{-1} band, which is intense in the absorption and relatively weak in the Raman spectrum, corresponds to antisymmetric valence vibrations of the water molecules (3580 cm^{-1} in the spectrum of liquid water). The frequencies 3513 and 3408 cm^{-1}, evinced by intense bands in both the absorption and Raman spectra, can be attributed to symmetric vibrations of the water molecules (3450 cm^{-1} in water). The presence of the two frequencies can then be explained by splitting of the symmetric vibration in the spectrum of the crystal in conformity with the theory of Davydov[14]. According to the data of Stekhanov[16,17], these two bands in the Raman spectrum are polarized in mutually perpendicular directions which again is in agreement with the theory. Analogous splitting of the deformation vibration of water in the absorption spectrum of gypsum has been observed and interpreted by Zaitsev & Neporent[18]. The reason for the absence of splitting of the asymmetric vibration of the water molecules remains unclear; it might tentatively be suggested that the band at 3605 cm^{-1} in the absorption spectrum is the second component.

A more conclusive interpretation of the frequencies of the OH vibrations in the spectrum of gypsum must await further investigations. It would be desirable, too, to explore further the possible role of the tunnel effect for the proton in hydrogen bonds by investigating a number of other suitable substances.

The writer desires to thank E.F.Gross who supervised the work and Ia.I. Ryskin who participated in discussions of the results.

Institute of the Chemistry of Silicates of the
Academy of Sciences of the USSR

References

1. M.Magat, J.Chim.phys.et Phys.-chim.biol., 52, 272 (1955).
2. R.E.Rundle & M.Parasol, J.Chem.Phys., 20, 1487 (1952).
3. R.S.Pease & G.E.Bacon, Nature (London), 173, 443 (1954).
4. M.V.Vol'kenshtein, M.A.El'iashevich & B.I.Stepanov, Kolebaniia molekul, (Molecular vibrations), Vol.1, M.-L., 1949.
5. M.A.Kovner & V.N.Kapshtal', Izv.AN SSSR, Ser.fiz., 17, 561 (1953).
6. G.S.Landsberg & F.S.Baryshanskaia, Doklady AN SSSR, 61, 1027 (1948).
7. P.S.Narayanan, Proc.Ind.Acad.Sci., A33, 240 (1951).
8. J.A.A.Ketelaar, Disc.Faraday Soc., 9, 211 (1950).
9. R.C.Lord & R.F.Merrifield, J.Chem.Phys., 21, 166 (1953).
10. G.M.Murphy, G.Weiner & J.J.Oberly, J.Chem.Phys., 22, 1322 (1954).
11. M.M.Stimson & M.J.O'Donnell, J.Amer.Chem.Soc., 74, 1805 (1952).
12. N.D.Sokolov, Usp.fiz.nauk., 57, 177 (1955).
13. A.R.Ubbelohde & K.J.Gallagher, Acta Crystallogr., 8,71 (1955).
14. A.S.Davydov, Transactions, Institute of Physics Ukrainian SSR Ac. of Sci., No.1 (1951).
15. I.Oshida, I.Ooshika & R.Miyasaka, J.Phys.Soc.Japan, 10, 849 (1955).
16. A.I.Stakhanov, Doklady AN SSSR, 106, 433 (1956).
17. A.I.Stekhanov, Doklady AN SSSR, 92, 281 (1953).
18. G.A.Zaitsev & B.S.Neporent, Zhur.eksp.i teor.fiz., 29, 857 (1955).
19. J.Louisfert, J.Phys.et Radium, 8, 22 (1947).

FERROELECTRIC CHARACTERISTICS OF ROCHELLE SALT CRYSTALS SUBJECTED TO RADIOACTIVE RADIATION

- V.A. Iurin

Historically Rochelle salt is the first member of the class of substances known as ferroelectrics, crystalline substances that exhibit spontaneous electric polarization in a certain temperature interval. One of the distinctive characteristics of ferroelectrics is the nonlinear dependence of the polarization on the external electric field. The polarization curves of X-cut plates of Rochelle salt in an alternating field, which have the shape of electromagnetic hysteresis loops (Fig.1,a), are generally familiar. Such curves are commonly called normal hysteresis loops in the literature.

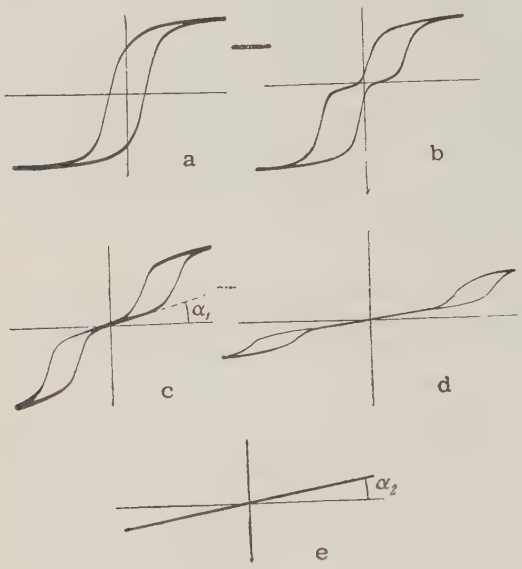

Fig.1. Hysteresis loops of Rochelle salt at 18° in a 50 cps field. Crystals irradiated with γ-rays from Co^{60}; dosage rate 10 r/hr: a) no irradiation (maximum field strength E_{max} = 800 v/cm, maximum polarization $P_{max} = 18 \cdot 10^{-8}$ cm^{-2}), b) after 1 hour irradiation (E_{max} = 1100 v/cm), c) after 2 hrs. irradiation (E_{max} = 1100 v/cm), d) after 5 hrs. irradiation (E_{max} = 1330 v/cm), e) after 11 hrs. irradiation (E_{max} = 1330 v/cm).

As was noted in an earlier communication[1], irradiation of Rochelle salt crystals with γ-rays alters the character of their polarization. X-cut specimens of Rochelle salt measuring 20 x 10 x 1.5 mm, after application of silver foil electrodes, were exposed to a Co^{60} source; the dosage rate received by the crystal was about 10^5 roentgen per hour.

The hysteresis loops of specimens exposed to different periods of irradiation are shown in Fig.1. It will be seen that even after a short irradiation time (Fig.1,b) the hysteresis loop begins to differ from the normal, tending to narrow at the middle. Increasing the irradiation time leads to enhancement of this narrowing to the point where a linear section appears (Fig.1,c). Such loops, which are reminiscent of the polarization curves of antiferroelectrics near the Curie point, are commonly called double loops in the literature. With further irradiation the length of the linear section increases, while the terminal loops become smaller (Fig.1,d), and finally disappear altogether (Fig.1,e).

Careful study of the anomalous polarization of Rochelle salt at room temperature showed that the slope of the saturation branch in a double hysteresis loop (angle β - see Fig.2) is appreciably less than the slope of the linear section of the loop (angle α). This difference in the slopes (angles) is conveniently observed on an oscilloscope screen by applying a biasing dc field to the specimen. This shifts the "working point", i.e., the section of the anomalous loop displayed on the screen and thus makes it possible to examine individual sections of the loop in detail. The intensity of the alternating

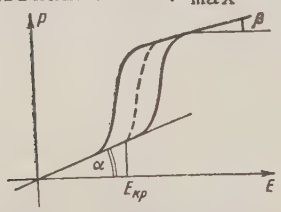

Fig.2. Diagram of one half of a double hysteresis loop of Rochelle salt.

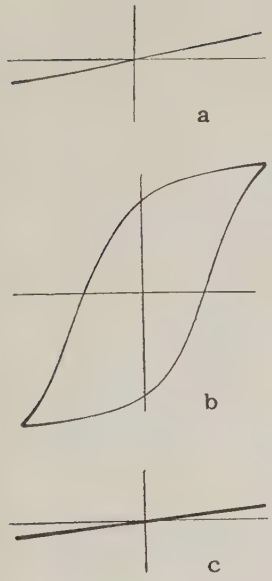

Fig.3. Different sections of the double hysteresis loop of Rochelle salt obtained by applying biasing dc fields of different strengths ($t = 18.6^{\circ}$, frequency 50 cps, specimen irradiated 2 hrs., maximum intensity of the ac field in all cases $E_{max} = 330$ v/cm): a) $E_{dc} = 0$, b) $E_{dc} = 450$ v/cm and c) $E_{dc} = 2000$ v/cm.

field must be less than the critical value E_c (E_c is the field strength at which the field dependence of the polarization becomes nonlinear).

The results of applying a biasing dc field are shown in Fig.3 (the amplification of the oscilloscope here is appreciably greater than in the case of Fig.1). Fig.3,a is recorded with no dc field; only the central linear section of the double loop is visible. In the case of Fig.3,b the strength of the dc field is approximately equal to the critical value; in this case the right-hand section of the double hysteresis loop appears on the screen. In Fig.3,c, corresponding to a biasing field considerably exceeding the saturation field value, we have only the saturation branch of the double loop. The difference between the angles in Fig.3,a and Fig.3,b is obvious.

This difference in slopes indicates that in a γ-irradiated crystal the mechanism of polarization in fields corresponding to the linear section of the loop ($E \lesssim E_c$) apparently differs from the mechanism of polarization in strong saturation-value fields. It is interesting to note that in the extreme case, too, when after prolonged irradiation the double loops no longer appear (Fig.1,e), the slope of the $P = f(E)$ curve does not remain constant: at a certain, rather high field value the slope of the line characterizing the field dependence of the polarization begins to change (Fig.4,a). This effect can also be conveniently observed by applying a biasing dc field. In Fig.4,b we show the section of the $P = f(E)$ curve in the region of the inflection; here E_{dc} equals the field intensity at which the slope begins to change.

The process of polarization of ferroelectrics is closely associated with rearrangement and reorientation of the domain structure[2]. As is known[3], domain structure is present not only in lightly irradiated specimens but also in specimens subjected to prolonged irradiation, i.e., in specimens for which anonymous (or no) hysteresis loops are obtained.

We observed the behavior of the domain structure in specimens exhibiting double hysteresis loops under the influence of biasing dc and alternating electric fields by means of a polarization microscope and stroboscopic illumination. The specimen holder electrodes of the thermostatic stage of the microscope were connected to a Sawyer & Tower circuit which made it possible to observe simultaneously the

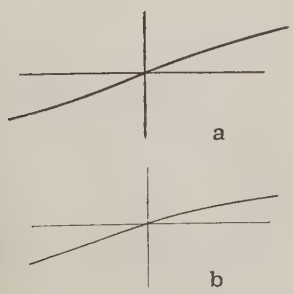

Fig.4. Polarization of Rochelle salt after prolonged irradiation with γ-rays ($t = 18^{\circ}$, frequency 50 cps, irradiation period 11 hrs.): a) maximum intensity of ac field $E_{max} = 2660$ v/cm, biasing dc field $E_{dc} = 0$; b) $E_{max} = 1800$ v/cm, $E_{dc} = 1400$ v/cm.

the character of the polarization (from the hysteresis loop) and the domain structure of the specimen. These qualitative observations showed that reorientation of the domains begins only in fields equal to the critical value on the hysteresis loop; in subcritic fields no noticeable change in the domain structure is apparent. In other words, active reorientation of the domains corresponds to the appearance of terminal hysteresis loops at the ends of the linear section: the right-hand branch of the double loop appears incident to reorientation of the domains of one polarity, while the left-hand branch corresponds to reorientation of the domains of opposite polarity. The size of the end hysteresis loops depends on the "fraction of participation" of the domains in the polarization of the specimen. After a short period of irradiation with γ-rays when one part of the double loop amounts to about half the initial hysteresis loop (Fig.1, a & b), there is complete reorientation of the domains. After more prolonged irradiation leading to an appreciable reduction of the double loop branches there occurs only partial rearrangement of the domain structure. Finally, after sufficiently prolonged irradiation (attainment of the state of Fig.1,e) no changes in the domain structure under the influence of an electric field are observed.

With a view to a fuller determination the change in the ferroelectric properties of γ-irradiated Rochelle salt crystals, we investigated the temperature dependences of the anomalous polarization of specimens subjected to increasing doses of irradiation. The electrodes of the thermostatic specimen holder were alternately connected to a capacitance bridge and to the Sawyer & Tower circuit which made it possible to follow the variation in the dielectric constant and simultaneously record the hysteresis loops.

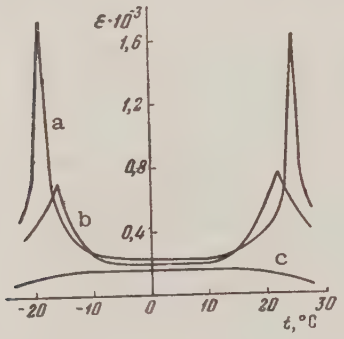

Fig.5. Temperature dependence of the dielectric constant of irradiated Rochelle salt as measured on a capacitance bridge at a field strength of 8 v/cm: a) not irradiated, b) after 2 hours irradiation, c) after 11 hours 10 min. irradiation.

The temperature dependence of the dielectric constant in weak fields obtained for one of our specimens prior to irradiation had the appearance of the familiar curve for Rochelle salt with two sharp peaks at the Curie points (curve a in Fig.5). Under the influence of irradiation the peaks become flatter and move closer to each other (curve b in Fig.5) and finally at the limit go over into a curve with a broad plateau (curve c in Fig.5). It will be noted that curve b was obtained for a specimen irradiated for a period (2 hours) yielding a double hysteresis loop in strong fields (Fig.1,c), while curve c was obtained for a specimen irradiated for a period (over 11 hours) leading to disappearance of the double loops (Fig.1,e).

It may be of interest to compare the results of measurements of the dielectric constant in weak and in strong fields. Determinations made from photographs of the hysteresis loops showed that the curves characterizing the temperature dependences of the dielectric constant as evaluated from the slopes of the linear sections in Fig.1,c & e (i.e., the angles α_1 and α_2) virtually coincide with the curves b & c in Fig.5 obtained from capacitance bridge measurements in weak fields. As for the branches of the anomalous hysteresis loops, it may be noted that they change with temperature in a manner similar to normal hysteresis loops.

Investigation of the piezoelectric effect in Rochelle salt specimens subjected to radioactive irradiation is also not without interest. We carried out approximate determinations of the piezoelectric constant g_{14} of irradiated specimens by the static method using an electrometer. We found that within the limits of the experimental error irradiated specimens having an anomalous polarization including a linear P = f(E) dependence (Fig.1,d) exhibit a piezoeffect and have almost the same value of the piezoelectric constant g_{14} as non-irradiated specimens.

In addition to the above cited experimental data on the properties of Rochelle salt crystals subjected to radioactive irradiation, we note that, as was shown earlier[1], Rochelle salt decomposes to a noticeable extent under the influence of γ-radiation: gases (H_2, CO, CO_2, CH_4) are evolved in amounts of about 5 molecules per 100 ev and the crystal becomes colored yellow. The total number of $C_4H_4O_6^{-2}$ anions decomposing is not great. Even in the case of irradiation leading to a complete loss of ferroelectric properties only one out of several thousand molecules decomposes. As a result, the charge of an ion pair is neutralized which apparently gives rise to stresses in the crystal lattice.

In view of what has been said above it may be hypothesized that the linear part of the double hysteresis loop is essentially an elongated initial section of the polarization curve (initial dielectric constant section). Such an elongation of the initial section may be produced by the decomposition products of Rochelle salt forming in the process of irradiation; being caught in the crystal lattice and producing stresses in it they "clamp" or "wedge in" the domains. Thus in the case of irradiated crystals appreciably greater field strengths are necessary to produce reorientation of the domains; in the case of prolonged irradiation the reorientation is completely suppressed.

It is interesting to note that the introduction of impurities into the crystal lattice in the process of growing Rochelle salt crystals, as has been shown by Eisner[4], sometimes also leads to the appearance of anomalous polarization. According to our experiments anomalous polarization also arises when Rochelle salt crystals are irradiated with x-rays, however, the double loops obtained in this case are less distinct (see Fig.6).

Fig.6. Hysteresis loop of Rochelle salt irradiated with x-rays. Irradiation time 1 hour; Mo radiation, tube voltage 56 kv, current 10 ma.

The process of polarization characterized by anomalous hysteresis loops (Fig.1,c) is commonly associated with the polarization of antiferroelectric crystals (theoretically predicted by Kittel and investigated by other authors[5-7]) in which the electric dipoles in neighboring unit cells are arranged antiparallel.

The stresses arising in the crystal lattice of Rochelle salt as the result of introduction of impurities either by irradiation or in the process of growth apparently transform the crystal to a new and different energy state. In this state the antiparallel arrangement of the domains leads to linear polarization in subcritical fields analogous to that obtaining in antiferroelectric crystals.

From the standpoint of a superficial analogy with antiferroelectrics, investigation of the temperature dependence of the critical field is of particular interest. Evaluations made on the basis of measurements of the double hysteresis loop indicate that the critical field in general increases with decreasing temperature. Determinations based on the hysteresis loops are necessarily approximate and some other, more accurate procedure must be employed for determining the quantitative variation of E_c as a function of the temperature.

Investigation of the anomalous polarization of Rochelle salt analogous to the polarization of antiferroelectrics may open the way to a better understanding of the characteristics of polarization both in ferroelectrics and antiferroelectrics and thus help establish the similarities and differences inherent in these effects. Rochelle salt is a particularly suitable material for such investigations inasmuch as by varying the period of irradiation one can alter the character of polarization from purely ferroelectric polarization to a polarization analogous to that of antiferroelectrics.

In conclusion the writer desires to thank I.S.Zheludev for guidance in the work and A.S.Baberkin for help in irradiation of the crystals.

Institute of Crystallography of the
Academy of Sciences of the USSR

References

1. I.S.Zheludev, M.A.Proskurnin, V.A.Iurin & A.S.Baberkin, Doklady AN SSSR, 103, 207 (1955).
2. M.A.Chernusheva, Dissertation, Institute of Crystallography, Ac. of Sci. USSR, M., 1955.
3. I.S.Zheludev & V.A.Iurin, Izv.AN SSSR, Ser.fiz., 20, 211 (1956). (Trans. in Bulletin, Vol.20, No.2, p. 193.)
4. I.Ia.Eisner, Present issue of the Bulletin, p. 341.
5. C.Kittel, Phys.Rev., 82, 729 (1951).
6. G.Shirane, E.Sawaguchi & Y.Takagi, Phys.Rev., 84, 476 (1951).
7. L.E.Gross & B.J.Nicholson, Phil.Mag., 46, 376 (1955).

ON CERTAIN CHARACTERISTICS OF DIELECTRIC HYSTERESIS IN ROCHELLE SALT

- I. Ia. Eisner

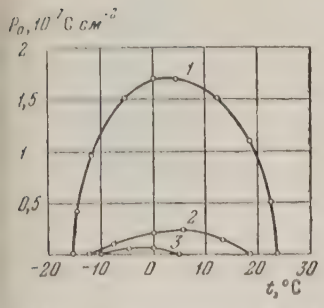

Fig. 1. Temperature dependence of the residual polarization: 1) pure Rochelle salt, 2) Rochelle salt with boron, 3) Rochelle salt with molybdenum.

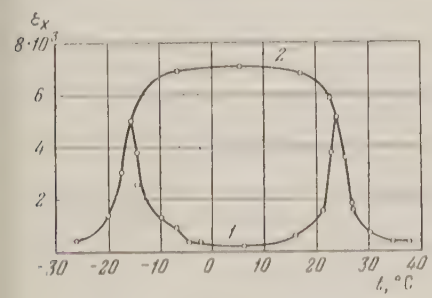

Fig. 2. Temperature dependences of the dielectric constant of an X-cut of pure Rochelle salt at field intensities of 1) 20 v/cm and 2) 350 v/cm.

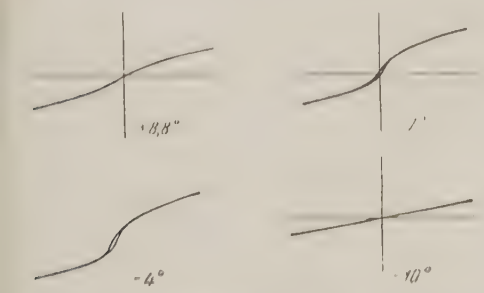

Fig. 3. Influence of temperature on the hysteresis loops of Rochelle salt containing Mo (f = 50 cps, E_{max} = 700 v/cm, $P_{max} = 6.9 \cdot 10^{-8}$ coulomb/cm^2).

Variation of the polarization with the intensity of the electric field along the X axis has been detected and investigated in ordinary Rochelle salt crystals and in Rochelle salt crystals containing deuterium in the crystallization water[1-3]. Dielectric hysteresis in isomorphous crystals of $NaKC_4H_4O_6 \cdot 4H_2O$ and $NaNH_4C_4H_4O_6 \cdot 4H_2O$ has been detected by Eremeev & Kurchatov.[4] Earlier the present author studied the properties of Rochelle salt in the presence of non-isomorphous impurities. Measurements[5] in 50 cps alternating fields showed that Mo, B and Cu impurities alter the electric properties of Rochelle salt: the phase transition points are shifted, the ferroelectric properties are changed and the loss tangent is reduced.

Continuing our investigation of Rochelle salt with impurity elements, we observed a relation between the instantaneous value of the polarization and the applied voltage, primarily for X-cut plates, in the temperature range from -20 to +40°. Dielectric hysteresis was studied by means of an oscilloscope connected to the familiar circuit developed by Sawyer & Tower[1] and other investigators[2,3 & 6]. The displays were photographed full-scale and the resultant photographic records used for quantitative analysis. The oscillographic studies were carried out with the temperature of the specimen either held constant or varied very slowly.

First we investigated the dielectric hysteresis of Rochelle salt not containing artificially introduced impurities. The results obtained from analysis of the oscilloscope photographs are the following: the coercive force increases with temperature from zero at the Curie points to a maximum value of ~150 v/cm in the 10-20° interval; the residual polarization (Fig. 1) increases with temperature from zero at the Curie points to a maximum value at 4°; according to our evaluation, this maximum value is 500 coulomb/cm^2, i.e., appreciably lower than the value reported by Hablützel[2]. We were also able to determine from the oscillograms the variation with temperature of the normal dielectric constant which attains a maximum value of 7000 in the interval between the Curie points at a field intensity of 350 v/cm (Fig. 2, curve 2).

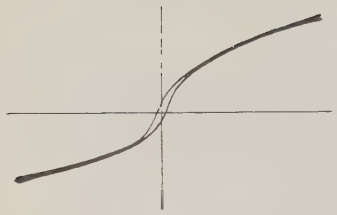

Fig.4. Typical hysteresis loop oscillogram for Rochelle salt containing Mo.

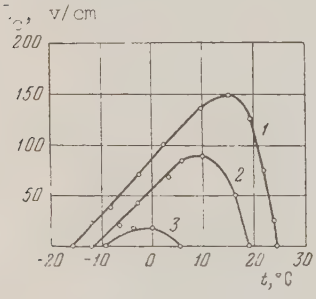

Fig.5. Temperature dependence of the coercive field E_c for: 1) pure Rochelle salt, 2) Rochelle salt with B, and 3) Rochelle salt with Mo.

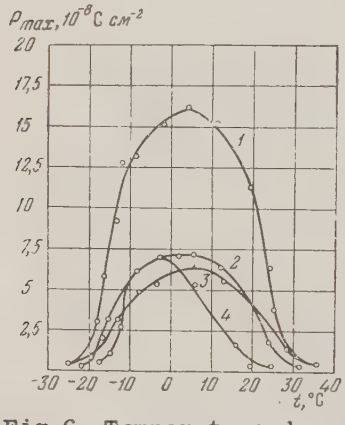

Fig.6. Temperature dependence of the maximum polarization for 1) pure Rochelle salt, 2) Rochelle salt containing B, 3) Rochelle salt containing Cu, and 4) Rochelle salt containing Mo as an impurity.

Fig.3 shows a series of oscillograms obtained for Rochelle salt containing Mo as an impurity. In the temperature interval between the Curie points (-9.5 to +5°) the polarization varies nonlinearly with the temperature; outside this temperature interval it is a linear function of the temperature and hysteresis disappears. As compared with the hysteresis loops of pure Rochelle salt the area of the loops for Rochelle salt containing Mo as an impurity (Fig.4) is much smaller and is much less sensitive to changes in temperature. The coercive force equals zero at the Curie points, rises to 20 v/cm between these points and remains virtually constant in the interval between the Curie points (Fig.5, curve 3), whereas the coercive force in pure Rochelle salt and in Rochelle salt with boron shows appreciable variation in this temperature range (Fig.5, curves 1 & 2).

The temperature dependence of the maximum polarization P_{max} for the boron containing salt is analogous to the dependence for pure Rochelle salt (Fig.6, curves 4 & 1).

Fig.7 shows a series of oscillograms obtained for an X-cut specimen of Rochelle salt containing boron. A distinctive feature of these loops is a certain deformation: they are noticeably narrowed in the middle (low field values). This obviously affects the values of both the residual polarization and coercive force. The coercive force is equal to zero at the Curie points and increases to 90 v/cm at a temperature of about 10°. The residual polarization attains a maximum value of 75 coulomb/cm^2 at 6°. The widest hysteresis loops are obtained in the temperature interval from 0 to 10°, just as for pure Rochelle salt.

Further we analyzed a series of oscillograms obtained for Rochelle salt containing Cu. Here it is pertinent to note that in crystals grown from a solution of a complex compound of Rochelle salt and copper there occurs selective absorption of the copper, clearly evinced by the color distribution in the crystals (see Fig.8). In view of this we felt it would be of interest to study the dielectric properties not only of X-cuts but of

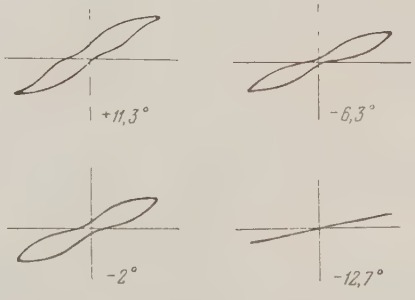

Fig.7. Influence of temperature on the hysteresis loops of an X-cut Rochelle salt containing B (f = 50 cps, E_{max} = 720 v/cm, P_{max} = = $6.9 \cdot 10^{-8}$ coulomb/cm^2.)

other cuts of Rochelle salt crystals containing Cu.

Oscillograms of an X-cut plate of Rochelle salt containing Cu are shown in Fig.9. Dielectric hysteresis is observed in the interval between the Curie points; outside this interval the field dependence of the polarization is linear. As before we determined the dielectric constant from the oscillograms; its temperature dependence is shown in Fig.10 in fields of 20 and 600 v/cm.

Between the Curie points the dielectric constant attains an average value of 750. In the oscillograms (Fig.11) obtained for a plate cut parallel to the (210) face for the same crystal there appears in every case a linear interval (the field was perpendicular to the (210) face). At the ends of this interval we have the nonlinear variation typical of ferroelectrics.

Analogous oscillograms were also obtained for a plate cut parallel to the (210) face of a crystal grown from a

Fig.8. Crystal of Rochelle salt containing Cu and showing selective absorption of Cu.

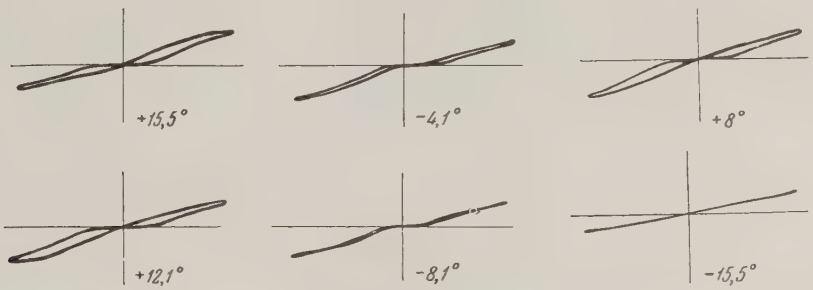

Fig.9. Same as Fig.7 but for Rochelle salt containing Cu (f = 50 cps, E_{max} = 600 v/cm, $P_{max} = 6 \cdot 10^{-8}$ coulomb/cm^2).

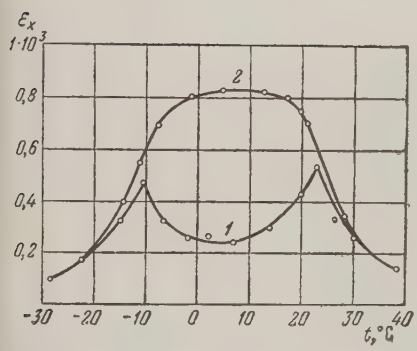

Fig.10. Temperature dependences of the dielectric constant of Rochelle salt containing Cu at different field intensities: 1) 10 v/cm and 2) 600 v/cm.

mixture of Rochelle salt and copper acetate (Fig.12). Within the range of the field strengths used in our experiments the polarization of these crystals as a function of the field at -12.7° is linear. Anomalous loops of the type shown have been observed for some antiferroelectrics[7-9] at higher temperatures.

Finally in Fig.13 we show one oscillogram obtained for an X-cut of a Rochelle salt crystal subjected to irradiation with x-rays. The hysteresis loop is anomalous and similar to the loop obtained for Rochelle crystals exposed to radioactive radiation[10]. It exhibits obvious similarities with the hysteresis loops we obtained for Rochelle salt containing B and Cu impurities. From an analysis of the hysteresis loops of specimens exposed to fairly large x-ray dosages it may be concluded that irradiation with x-rays does not increase the dielectric losses

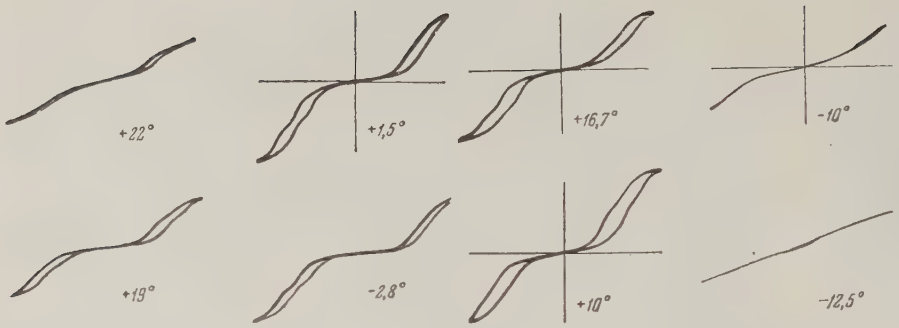

Fig. 11. Same as Fig.9 but for a cut of Rochelle salt with Cu parallel to the (210) face (f = 50 cps, E_{max} = 860 v/cm, $P_{max} = 8.6 \cdot 10^{-8}$ coulomb/cm^2).

Fig.12. Same as Fig.11 but for a crystal grown from a solution of Rochelle salt and copper acetate.

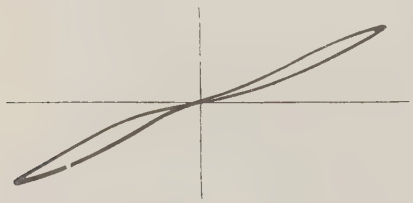

Fig.13. Typical oscillogram of a Rochelle salt crystal exposed to x-rays.

as reportedly occurs in the case of rock salt crystals[11]. In contrast to some of the cases examined above, exposure to x-rays does not result in any noticeable displacement of the Curie points.

Conclusions

1. Crystals of Rochelle salt containing Mo, B or Cu as impurities when investigated in a 50 cycle alternating field of about 700 v/cm exhibit dielectric hysteresis in the temperature interval between Curie points, but the hysteresis loops differ in appearance from the loops characteristic of pure Rochelle salt crystals.

2. Rochelle salt crystals grown from a solution of the salt containing ammonium molybdenum show only negligibly small dielectric losses in strong electric fields. In the temperature range between the Curie points the variation of the polarization as a function of the electric field is nonlinear.

3. Crystals of Rochelle salt containing boron, grown from a solution under conditions of mutual saturation, yield anomalous hysteresis loops narrowed in the region of low field intensities. This deformation of the loops may be interpreted as a result of retardation

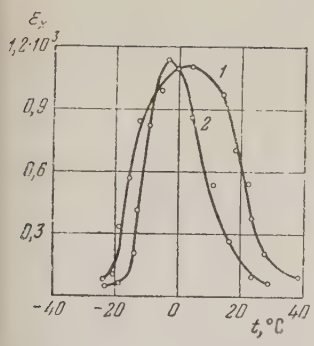

Fig.14. Temperature dependence of the dielectric constant: 1) Rochelle salt with B at a field strength of 720 v/cm, 2) Rochelle salt containing Mo at a field strength of 700 v/cm.

of reorientation of the domains[12] by the impurity inclusions.

4. Crystals of Rochelle salt containing copper are characterized by pronounced anomaly of the dielectric hysteresis loops. Specifically, in a certain rather wide field intensity interval - this pertains to cuts parallel to the (210) face - the polarization is a linear function of the field and hysteresis loops appear only in fields above a certain rather high value. Clearly, the conditions for the appearance of polarization in the presence of impurity ions change with increasing intensity of the external electric field.

The question of whether in this case there occurs a phase transition at the Curie points from the paraelectric to the antiferroelectric state requires further experimental study.

5. Through analysis of the hysteresis loops obtained for Rochelle salt crystals containing Mo, B and Cu,we determined the temperature dependence of the dielectric constant of these crystals in strong electric fields. The results are shown in Fig.14.

L'vov State Pedagogical Institute

References

1. C.B.Sawyer & C.H.Tower, Phys.Rev., 35, 269 (1930).
2. I.Hablützel, Helv.Phys.Acta, 12, 489 (1939).
3. R.David, Helv.Phys.Acta, 12, 489 (1939).
4. M.Eremeev & B.Kurchatov, Zhur.eksp.i teor.fiz., 2, 329 (1932).
5. I.Ia.Eisner, Izv. AN SSSR, Ser.fiz., 20, 215 (1956). (Trans. Bulletin, Vol.20, No.2, p. 197).
6. B.M.Vul & I.M.Gol'dman, Doklady AN SSSR, 57, 21 (1946).
7. E.Sawaguchi, J.Phys.Soc. of Japan, 8, 615 (1953).
8. Gen Shirane, Phys.Rev., 86, 219 (1952).
9. E.Sawaguchi, H.Maniwa & S.Hashino, Phys.Rev., 83, 1078 (1951).
10. I.S.Zheludev & V.A.Iurin, Izv. AN SSSR, Ser.fiz., 20, 211 (1956). (Trans. Bulletin, Vol. 20, No.2, p. 193.)
11. Iu.A.Sikorskii, Doklady AN SSSR, 40, 47 (1948).
12. M.A.Chernysheva, Doklady AN SSSR, 81, 1065 (1951).

ON MICROSCOPIC THEORIES OF THE FERROELECTRIC PROPERTIES OF BARIUM TITANATE

- R.E.Pasynkov

The molecular nature of the ferroelectric properties of $BaTiO_3$ is at present explained by two essentially different mechanisms, leading to variants of the "ionic displacement theory" and the "electronic theory". The authors of the existing ionic displacement theories[1-4] proceed from the assumption that the spontaneous polarization in ferroelectric substances results from inelastic ionic displacements which, under the influence of the acting effective fields, are accompanied by electron polarization.

In the electronic theory[5], on the contrary, it is assumed that the electron shells of the ions are spontaneously deformed with subsequent elastic displacement of the ions from their equilibrium positions. In spite of their essential differences, both of these mechanisms yield qualitative, and in some cases even quantitative, explanations of some experimental data. Some of the physical premises involved, however, are contradictory. Hence, we feel that the time has arrived to examine the various concepts underlying these theories.

On the Further Development of the Ionic Displacement Theories

According to these theories the displacements of the ions from their symmetric positions cause large effective fields which tend to hold the ions in their new positions. The spontaneous polarization that develops in the process is also due to the electronic dipole moments resulting from the action of the effective fields on the electron shells of the ions. The interaction of the ions is accounted for in two ways. The interaction of nearest neighbors is given by a function U_k of the coordinates x, y, z which describes the potential energy distribution in which the ions of the k-th sublattice "move". Long-range forces, i.e., electrostatic forces, are introduced by adding to $U_k(x, y, z)$ a term $q'_k(\mathrm{F}_k\mathrm{r}_k)$ which is equal to the potential energy of an ion with charge q_k, displaced a distance r_k in the effective field F_k.* The effective field depends not on the instantaneous coordinates, but on the mean coordinates of all the other ions, and, therefore, on the statistical properties of the crystal lattice as a whole.

Accordingly, the theoretical treatments of the various authors reduce to the solution of two, in a sense independent, problems:

1) calculation of the effective fields acting on the different ions and of the total polarization as a function of the applied field and average ionic displacements;

2) formulation and solution of equations which determine the electric and thermal states of the crystal under conditions of thermodynamic equilibrium. From these equations one can determine the phase transition points, the temperature dependences of the spontaneous polarization and dielectric constant, the entropy anomaly, etc.

The familiar Lorentz method is commonly used in calculating the effective fields acting on the different ions. The most important part of the problem involves calculating the fields due to the displaced charges and dipoles within the Lorentz sphere. The crystal lattice is divided into m simple monatomic

---

*Using the terminology of Kozlovskii,[6] we denote by q'_k the "dynamic charge" which accounts for the change in the electrostatic force acting on the displaced ion due to the presence of the electronic dipole moment.

cubic sublattices (for $BaTiO_3$ $m = 5$); the result obtained is[6]

$$F_{kx} = \gamma_k E_x + \sum_{k'=1}^{m} \beta_{kk'} P_{gk'x} \tag{1a}$$

and

$$P_x = \gamma_p E_x + \sum_{k=1}^{m} \varrho_{k'} P_{gk'x}, \tag{1b}$$

where P_x is the x component of the total polarization of the crystal. P_{gkx} is the electric moment per unit volume, resulting from the displacement of the ions of the k-th sublattice from their symmetric positions ($P_{gkx} = Nq_k\bar{x}_k$, where N is the number of cells per unit volume, and x_k is the mean ionic displacement), E_x is the x component of the external field, and γ_k, γ_p, $\beta_{kk'}$ and $\varrho_{k'}$ are coefficients depending on the ionic polarizabilities, the ion charges, and the lattice structure.

It is important to emphasize that all these coefficients are calculated for point ions, assuming that the polarizabilities and charges of the ions are the same as those of free ions, and disregarding both possible overlapping of the electron shells and thermal vibration of the ions. In view of these assumptions and simplifications it is doubtful that even the most careful calculations of the coefficients are reliable.[1] It is thus also doubtful that one can obtain good quantitative agreement between experiment and a theory whose coefficients are calculated in this way. Therefore the most significant result in the solution of the effective-field problem is the establishment of a functional relationship between F_{kx}, P_x, E_x and P_{gkx} and finding the order of magnitude of the coefficients in Eqs.(1). These are the determining factors in obtaining those most important qualitative characteristics of ferroelectric substances which, in the present state of the theory, can be most meaningfully compared with the experimental data.

If we assume that the rise of spontaneous polarization is due to displacement of the ions belonging to a single sublattice (for instance the titanium ions), then the sums in Eqs.(1) will contain only one term and can be written

$$F_{kx} = \gamma_k E_x + \beta_k P_{gkx} \tag{2a}$$

and

$$P_{kx} = \gamma_p E_x + \varrho_k P_{gkx}. \tag{2b}$$

In this form these equations are essentially the same as the semi-empirical formulas of Mason and Matthias[1] which in somewhat modified form have been used in the electron theory. The difference lies only in the fact that in the equations corresponding to (2a) and (2b) the Jaynes[5] replaces the electric moment P_{gkx} by the polarization P_{ex} associated with the deformation of the electron shells.

The equations of state for the crystal lattice are obtained with the aid of the free energy of the system

$$A = -NkT \ln Z, \tag{3}$$

where Z is the sum-over-states.

In the existing ionic theories Z is calculated without taking into account quantum mechanical effects; the calculations are based on the following assumptions.

1) The potential energy of an ion is given by the function $U_k(x,y,z) - -q'_k(\mathbf{F}_k \mathbf{r}_k)$, and the integrals which give the states of the separate ions are multiplicative. This is equivalent to neglecting correlations between the instantaneous ion positions.

2) The appearance of spontaneous polarization is due to the ions of a single sublattice (i.e. commonly the Ti^{+4} ions), which we shall henceforth call the ferroactive ions. The statistical distribution of only these ions is considered, while temperature effects related to vibrations of other elements of the crystal structure are ignored.

Accordingly, Z is written

$$Z = \frac{1}{N!}\left\{\frac{(2\pi kTm_k)^{3/2}}{h^3}\int\limits_{V_k}\exp\left[-\frac{U_k(x,y,z) - q'_k(\mathbf{F}_k \mathbf{r}_k)}{kT}\right]dV_k\right\}^N, \qquad (4)$$

where m_k is the ion mass, and h is Planck's constant.

Inserting (4) into (3) and differentiating with respect to P_{gkx}, we obtain the relation

$$P_{gkx} = \frac{\partial \Lambda}{\partial F_{kx}}.$$

If we now use (2a) to write F_{kx} in terms of P_{gkx} and E_x, we obtain an equation whose solution gives the temperature dependence of the spontaneous polarization (at $E_x = 0$) and dielectric constant.

These are the methods and fundamental approximations of present day ionic displacement theories. They differ from each other in the definition and form of the function $U_k(x,y,z)$. Thus in the Mason-Matthias theory[1] $U_k(x,y,z)$ is defined in terms of six local minima displaced relative to the center of the cell. Devonshire[3] and Slater[2] write $U_k(x,y,z)$ in a form characteristic for anharmonic oscillators. Detailed analysis and comparison of these theories has led some authors[5,7,8] to favor the anharmonic oscillator model.

The purpose of the present article is not to compare these theories, but to investigate the above-mentioned assumption common to both that the thermal vibrations of only the ferroactive ions, or more accurately of the ions belonging to a single sublattice, are significant. At present, when x-ray and neutron diffraction studies have established[8,9] that the ions of all the sublattices in $BaTiO_3$ are displaced, this assumption seems highly questionable even in the light of the general approximations described above.

Let us thus consider a more general case in which all the ions of the crystal lattice are assumed to undergo vibrations. We shall maintain the assumptions made in deriving the formulas for the effective fields, as well as the assumption that there is no correlation between the instantaneous positions of the separate ions. A more rigorous calculation of the effective fields (taking account of quantum mechanical effects) and the question of correlation are larger problems of solid state physics. Kliachkin[10] and Kozlovskii[11] have attempted to account for correlation in connection with the ferroelectric problem. Klichkin, however, applies Bogoliubov's method to a lattice consisting of rotating dipoles, and Kozlovskii treats one-dimensional bound vibrations of a single ferroelectrically active sublattice, assuming all the other ions to be rigidly fixed.

In accordance with the foregoing, we write the sum-over-states in the form

$$Z = \frac{1}{N!}\prod_{k=1}^{m}\left\{\left[\frac{(2\pi kTm_k)^{3/2}}{h^3}\int\limits_{V_k}\exp\left(-\frac{U_k(x,y,z) - q'_k(F_k r_k)}{kT}\right)dV_k\right]\right\}^N, \qquad (5)$$

where m is the number of sublattices.

For the particular case (for instance, the model of local minima in the Mason-Matthias theory) when $U_k(x, y, z)$ can assume only discrete values, the integral in (5) should be written as the sum

$$\sum_{j=1}^{n} \exp\left[-\frac{U_{jk} - q'_k \mathbf{F}_k \mathbf{r}_k)}{kT}\right] V_j,$$

where n is the number of discrete states with energy U_{jk}, the V_j are volumes determined by the statistical weights of these states and r_k is the average coordinate of an ion in such a state.

We shall further restrict the considerations by assuming that U_k is symmetric with respect to reflection and that the integrand decreases so rapidly with r_k that the integration over the volume of an elementary cell may be replaced by integration to infinity without significant sacrifice of accuracy.

The free energy is

$$A = -NkT \ln\left(\frac{e}{N} \prod_{k=1}^{m} \frac{(2\pi k T m_k)^{3/2}}{h^3}\right) - NkT \sum_{k=1}^{m} \ln\left[\int \exp\left(-\frac{U_k - q'_k (\mathbf{F}_k \mathbf{r}_k)}{kT}\right) dV_k\right]. \quad (6)$$

Further,

$$Pq_{kx} = Nq_k \bar{x}_k = \frac{Nq_k \int x_k \exp\left[-\frac{U_k - q'_k (\mathbf{F}_k \mathbf{r}_k)}{kT}\right] dV_k}{\int \exp\left[-\frac{U_k - q'_k (\mathbf{F}_k \mathbf{r}_k)}{kT}\right] dV_k} = \frac{q_k}{q'_k} \cdot \frac{\partial A}{\partial F_{kx}}. \quad (7)$$

Differentiating with respect to all the F_{kx} and inserting (1a), we obtain a set of $3m$ equations of the form

$$Pq_{kx} - \varphi_{kx}(T; E_x, E_y, E_z; P_{gix}, \ldots, P_{gkx}, \ldots, P_{gmz}) = 0, \quad (8)$$

where

$$\varphi_{kx}(T; E_x, \ldots; P_{gmz}) = \frac{1}{\nu_k} \left(\frac{\partial A}{\partial F_{kx}}\right)_{(F_{ki} = \nu_k E_i + \sum_{k=1}^{m} \beta_{kk'} P_{gki})}; \quad \nu_k = \frac{q'_k}{q_k}.$$

If all the E_i are set equal to zero, we obtain the equation of state for the ferroelectric that defines the temperature dependence of the spontaneous polarization. This equation is

$$P^0_{gkx} - \varphi^0_{kx}(T; P^0_{g1x}, \ldots, P^0_{gkx}, \ldots, P^0_{gmz}) = 0. \quad (9)$$

Let us first consider an important special case. We shall assume that all the ions undergo pure harmonic vibrations, i.e., that for all k's

$$U_k(x, y, z) = a_k (x^2 + y^2 + z^2).$$

In this case the integration in (7) is readily performed and hence (9) can be rewritten as

$$P^0_{gkx} - \alpha^i_k F_{kx} = 0,$$

$\frac{N\vartheta_k q_k}{2qk}$ is the polarizability of the ionic displacements.

Inserting (1a) into the foregoing expressions, we obtain a set of linear equations of the form

$$\sum_{k'=1}^{m} (\alpha_k^i \beta_{kk'} + \delta_{kk'}) P_{gk'x}^0 = 0,$$

where $\delta_{kk'}$ is the Kronecker delta.

In general such a set of equations has only trivial solutions, which would mean that the crystal is paraelectric. In the particular case, however, when the determinant whose elements are $\alpha_k^i \beta_{kk'} + \delta_{kk'}$ vanishes, there exist nontrivial solutions of the form

$$P_{gkx}^0 = \tau A_k,$$

where the A_k are the minors of the k-th row, and τ is an arbitrary constant. These solutions, however, are unstable, as can readily be shown by a direct calculation of the free energy, which is found to be a quadratic function of the P_{gkx}^0 that decreases without limit as the P_{ox} increase.

A stable ferroelectric configuration can obtain only when the free energy of the crystal is given by an expression which contains both terms proportional to the $(P_{gkx}^0)^2$, whose sum is negative, and terms of higher powers of the P_{gkx}^0, whose sum is positive. The terms containing the higher powers of the P_{gkx}^0, provide for saturation of the spontaneous polarization and may appear in the expression for the free energy if the ions of at least one sublattice move under the influence of nonlinear forces. This may occur, in other words, if at least one of the $U_k(x, y, z)$ contains terms of higher power than x^2, y^2 or z^2.

It is just these terms that lead to the temperature and nonlinear effects characteristic of ferroelectrics. As for the condition, namely, the requirement that the sum of the terms proportional to $(P_{gkx}^0)^2$ be negative, it has been shown[12] that this is equivalent to requiring that the electric forces acting on the ions predominate over the elastic restoring forces. This condition, which was derived for a single ferroactive lattice, should remain also in effect, although in a somewhat altered form, when the ions of all the sublattices are displaced.

Thus the ions which undergo harmonic vibrations do not affect the temperature characteristics of a ferroelectric, although it can be shown that if they are taken into account in calculating the effective fields and total polarization a significant correction to the expression for the coefficients of (2a) and (2b) is obtained.

The theory based on the assumption that the ions of only one sublattice undergo anharmonic vibrations while those of all the other sublattices undergo harmonic oscillations is undoubtedly an advance over the previous theories. To the writer, however, this assumption seems somewhat unlikely. At present, when it has been shown that all the ions are displaced, there is good reason to assume that they all also undergo anharmonic vibrations. Calculations by Devonshire[3] and Syrkin[13] have shown that the ferroelectricity is more likely due to the oxygen rather than to the titanium ions, so that it would seem that the oxygen ions together with the barium with which they are directly bound may undergo vibrations that are strongly anharmonic.*

This case wherein all the sublattices determine the temperature characteristics of the ferroelectric leads to Eqs.(9).

According to a theorem on implicit functions[14] the existence of a unique nontrivial set of solutions of equations of the form of (9) is determined by those values of the P_{gkx}^0, which satisfy (9) and for which the functional determinant

---

*Jaynes[5] considers the model in which the ferroelectrically active ions are those of oxygen, rather than titanium, to be the more representative one.

$$\begin{vmatrix} 1-\frac{\partial\varphi^0_{1x}}{\partial P^0_{g1x}} & -\frac{\partial\varphi^0_{1x}}{\partial P^0_{g1y}}\cdots & -\frac{\partial\varphi^0_{1x}}{\partial P^0_{gki}}\cdots & -\frac{\partial\varphi^0_{1x}}{\partial P^0_{gmz}} \\ -\frac{\partial\varphi^0_{1y}}{\partial P^0_{g1x}} & 1-\frac{\partial\varphi^0_{1y}}{\partial P^0_{g1y}}\cdots & -\frac{\partial\varphi^0_{1y}}{\partial P^0_{gki}}\cdots & -\frac{\partial\varphi^0_{1y}}{\partial P^0_{gmz}} \\ \cdots\cdots & \cdots\cdots & \cdots\cdots & \cdots\cdots \\ -\frac{\partial\varphi^0_{ki}}{\partial P^0_{g1x}} & -\frac{\partial\varphi^0_{ki}}{\partial P^0_{g1y}}\cdots & 1-\frac{\partial\varphi^0_{ki}}{\partial P^0_{gki}}\cdots & -\frac{\partial\varphi^0_{ki}}{\partial P^0_{gmz}} \\ \cdots\cdots & \cdots\cdots & \cdots\cdots & \cdots\cdots \\ -\frac{\partial\varphi^0_{mz}}{\partial P^0_{g1x}} & -\frac{\partial\varphi^0_{mz}}{\partial P^0_{g1y}}\cdots & -\frac{\partial\varphi^0_{mz}}{\partial P^0_{gki}}\cdots & 1-\frac{\partial\varphi^0_{mz}}{\partial P^0_{gmz}} \end{vmatrix} \qquad (10)$$

fails to vanish.

When the determinant of Eq.(10) vanishes, this indicates that the set of equations (9) is no longer "stable" and is the necessary and sufficient condition for a phase transition. The equations thus obtained can be used to calculate the phase transition temperatures. In particular, the transition temperature to the paraelectric state is found by inserting the trivial solutions

$$P^0_{g1x} = P^0_{g1y} = \ldots = P^0_{gki} = \ldots = P^0_{gmz} \equiv 0\ ^*.$$

of (9) into the determinant of (10).

In connection with this assertion, we shall show that solutions of the form

$$P^0_{glx} \equiv 0 \quad \text{with } P^0_{g1x},\ P^0_{g2x},\ldots,\ P_{gmz} \neq 0$$

cannot exist in a certain finite temperature range or in other words that a phase transition associated with the vanishing of some of the P^0_{glx} or a set of the $P^0_{g2x},\ldots,P^0_{glx}$ cannot occur. The only case which is possible is that in which the full component P_{0x} vanishes, which means that the spontaneous displacements of all the sublattices go to zero simultaneously.

Let us consider the auxiliary set of equations obtained from (9) by multiplying each of the equations by ρ_k from (1b) and then summing, namely,

$$\left.\begin{aligned} P_{0x} - \sum_{k=1}^{m}\rho_k\varphi^0_{kx} &= 0, \\ P_{0y} - \sum_{k=1}^{m}\rho_k\varphi^0_{ky} &= 0, \\ P_{0z} - \sum_{k=1}^{m}\rho_k\varphi^0_{kz} &= 0. \end{aligned}\right\} \qquad (11)$$

It can readily be shown that this set of equations is satisfied by solutions of the form

$$P_{0x} \equiv 0; \quad P^0_{g1x} = P^0_{g2x} = \ldots = P^0_{gmx} \equiv 0; \quad P_{0y} \neq 0; \quad P_{0z} \neq 0.$$

---

*In the case of a first order phase transition this assertion is valid for the transition from a paraelectric to a ferroelectric state.

Indeed, setting $F_{lx} = 0$ and inserting the result into (7), we obtain

$$\sum_{k=1}^{m} \rho_k \varphi_{kx}^0 = N \sum_{k=1}^{m} \rho_k q_k \frac{\int\limits_{V_k} x_k \exp\left[-\frac{U_k - q_k'(F_{ky} \cdot y + F_{kz} \cdot z)}{kT}\right] dV_k}{\int\limits_{V_k} \exp\left[-\frac{U_k - q_k'(F_{ky} \cdot y + F_{kz} \cdot z)}{kT}\right] dV_k} \equiv 0.$$

Since $U_k(x, y, z)$ must be an even function of the coordinates, this identity holds true.

Analogously one can prove the existence of all combinations of solutions describing rotations of the spontaneous polarization vector, i.e., the low-temperature transitions.

Let us now assume that $P_{0x} \neq 0$, but $P_{g1x}^0 \equiv 0$ for $P_{g1x}^0, \ldots, P_{gmz}^0 \neq 0$.

For simplicity let us also set $P_{0y} = P_{0z} \equiv 0$, which in view of the fact that P_{0x}, P_{0y} and P_{0z} vanish independently represents no further restriction.

According to (7) and (9) we obtain

$$\varphi_{lx}^0 = \frac{Nq_l \int\limits_{v_l} x_l \exp\left[-\frac{U_l - q_l' F_{lx} x_l}{kT}\right] dv_l}{\int\limits_{v_l} \exp\left[-\frac{U_l - q_l' F_{lx} x_l}{kT}\right] dv_l} \equiv 0.$$

This is possible in the case of the identity

$$F_{lx} = \sum_{k'=1}^{m} \beta_{lk'} (1 - \delta_{lk'}) P_{gk'x}^0 \equiv 0. \tag{12}$$

The identity (12) can obtain over a certain temperature range provided all the P_{gkx}^0 (except, of course, P_{glx}^0) are proportional to each other, i.e., if there exists a relation of the form

$$\frac{P_{g1x}^0}{\varkappa_1} = \frac{P_{g2x}^0}{\varkappa_2} = \cdots = \frac{P_{gmx}^0}{\varkappa_m} = f(T), \tag{13}$$

where the $\varkappa_k$ are constants depending on the sublattice number.

In this case we have

$$\sum_{k=1}^{m} \beta_{lk} (1 - \delta_{lk}) \varkappa_k = 0.$$

As a special case of (13) we have $f(T) = \text{const}$.

Let us consider the expression

$$\frac{P_{glx}^0}{P_{gkx}^0} = \frac{\varkappa_l}{\varkappa_k} = \frac{Nq_l \int\limits_{v_l} x_l \exp\left[-\frac{U_l - q_l' F_{lx} x_l}{kT}\right] dv_l}{\int\limits_{v_l} \exp\left[-\frac{U_l - q_l' F_{lx} x_l}{kT}\right] dv_l} \cdot \frac{\int \exp\left[-\frac{U_k - q_k' F_{kx} x_k}{kT}\right] dv_k}{Nq_k \int x_k \exp\left[-\frac{U_k - q_k' \cdot F_{kx} x_k}{kT}\right] dv_k}$$

or

$$\frac{\partial \left\{\frac{kT}{\nu_l} \ln\left[\int\limits_{v_l} \exp\left(-\frac{U_l - q_l' F_{lx} x_l}{kT}\right) dv_l\right]\right\}}{\partial F_{lx}} = \frac{\varkappa_l}{\varkappa_k} \cdot \frac{\partial \left\{\frac{kT}{\nu_l} \ln\left[\int\limits_{v_k} \exp\left(-\frac{U_k - q_k' F_k x_k}{kT}\right) dv_k\right]\right\}}{\partial F_{kx}}.$$

This identity holds true if both derivatives vanish or if the integrands are equal up to a constant factor. The first of these alternatives is possible only if $F_{lx} = F_{kx} \equiv 0$, which contradicts the original assumptions. The second holds for ferroactive lattices if

$$U_l(x, y, z) = U_k(x, y, z) \quad \text{and} \quad F_{lx} q'_x = F_{kx} q'_k,$$

which is also excluded.

Thus a system consisting of several active sublattices has only a single transition point at which the spontaneous displacements of these sublattices from their symmetric positions vanish.

There is another question that merits consideration. If there are several ferroelectrically active sublattices one might hypothesize the possible existence of antiferroelectricity, that is, hypothesize the existence of solutions of (9) such that over some temperature range the spontaneous displacements of different ions compensate each other, i.e.,

$$P_{0x} \equiv 0, \text{ and } P^0_{g1x}, \ldots, P^0_{gkx}, \ldots, P^0_{gmx} \neq 0.$$

We shall show that this is also impossible.

From (11), we have

$$\sum_{k=1}^{m} \rho_k \varphi^0_{kx} = \sum_{k=1}^{m} \rho_k P^0_{gkx} \equiv 0.$$

This identity holds true if a relation such as (13) obtains and in addition

$$\sum_{k=1}^{m} \rho_k \varkappa_k = 0.$$

The rest of the proof is entirely analogous to the preceding one. Thus an antiferroelectric configuration can occur only as a result of "opposite" displacements of ions belonging to the same sublattice. From the point of view of the microscopic theories under consideration here this assumption reduces to the purely formal separation of the sum-over-states for the k-th sublattice into two multiplicative groups:

$$Z_k = \left\{ \frac{1}{(N/2)!} \int_{v_k} \exp\left[-\frac{U_k - q'_k (\mathbf{F}'_k \mathbf{r}_k)}{kT} \right] dv \right\}^{\frac{N}{2}} \cdot \left\{ \frac{1}{(N/2)!} \int_{v_k} \exp\left[-\frac{U_k - q'_k (\mathbf{F}''_k \mathbf{r}_k)}{kT} \right] dv \right\}^{\frac{N}{2}},$$

for which $F'_k = -F''_k$.

The number of equations of state of the form $P'_{gkx} = -\frac{1}{v_k} \cdot \frac{\partial A}{\partial F_k}$ will then be doubled. Such an approach,* however, leads to no more profound (atomic) an interpretation of the appearance of antiferroelectricity than does the thermodynamic theory of Kittel[15].

The conclusions we have reached, apparently remain valid even for the strongest possible correlation between the instantaneous positions of the separate ions, inasmuch as even in this case the ions of different sublattices move under very different conditions.

---

*We note that proceding in this way we can postulate the existence of highly complicated ionic displacement configurations, for instance "fan-shaped", displacements with a period much greater than the normal period of the lattice.

Let us return to Eqs.(9). It is not possible to solve these equations in general for arbitrary $U_k(x, y, z)$. It is therefore expedient to seek an approximate method for each specific form of $U_k(x, y, z)$, i.e., for each of the suggested theoretical models.

In all methods of defining $U_k(x, y, z)$ the Curie point must be determined from the fact that a functional determinant vanishes.

As an illustration, let us consider this rule as applied to the theories in which it is assumed that there is one ferroactive lattice. The equations of state are written

$$\frac{P_{0x}}{\rho} - \varphi_x^0(T, P_{0x}, P_{0y}, P_{0z}) = 0,$$

$$\frac{P_{0y}}{\rho} - \varphi_y^0(T, P_{0x}, P_{0y}, P_{0z}) = 0,$$

$$\frac{P_{0z}}{\rho} - \varphi_z^0(T, P_{0x}, P_{0y}, P_{0z}) = 0.$$

Since $F_{0x} = \beta P_{gx}^0$ and $P_{0x} = \rho P_{gx}^0$, we can readily express the equations in terms of the components of the total spontaneous polarization. The meaning of these equations should be the same as that of the equations of state obtained by differentiating the free energy $A_T(T, P_{0x}, P_{0y}, P_{0z})$, obtained in the thermodynamic theory of ferroelectricity.[16,17] We can therefore write

$$\tau\left[\frac{P_{0x}}{\rho} - \varphi_x^0(T, P_{0x}, P_{0y}, P_{0z})\right] = \frac{\partial A_T(T, P_{0x}, P_{0y}, P_{0z})}{\partial P_{0x}},$$

where τ is a dimensionless factor.

Further, we have

$$\tau^3 \begin{vmatrix} \frac{1}{\rho} - \frac{\partial \varphi_x^0}{\partial P_{0x}} & -\frac{\partial \varphi_x^0}{\partial P_{0y}} & -\frac{\partial \varphi_x}{\partial P_{0z}} \\ -\frac{\partial \varphi_y^0}{\partial P_{0x}} & \frac{1}{\rho} - \frac{\partial \varphi_y}{\partial P_{0y}} & -\frac{\partial \varphi_y}{\partial P_{0z}} \\ -\frac{\partial \varphi_z^0}{\partial P_{0x}} & -\frac{\partial \varphi_z}{\partial P_{0y}} & \frac{1}{\rho} - \frac{\partial \varphi_z^0}{\partial P_{0z}} \end{vmatrix} = \begin{vmatrix} \frac{\partial^2 A_T}{\partial P_{0x}^2} & \frac{\partial^2 A_T}{\partial P_{0y}\partial P_{0x}} & \frac{\partial^2 A_T}{\partial P_{0z}\partial P_{0x}} \\ \frac{\partial^2 A_T}{\partial P_{0x}\partial P_{0y}} & \frac{\partial^2 A_T}{\partial P_{0y}^2} & \frac{\partial^2 A_T}{\partial P_{0z}\partial P_{0y}} \\ \frac{\partial^2 A_T}{\partial P_{0x}\partial P_{0z}} & \frac{\partial^2 A_T}{\partial P_{0y}\partial P_{0z}} & \frac{\partial^2 A_T}{\partial P_{0z}^2} \end{vmatrix}. \qquad (14)$$

It follows from this that the functional determinant vanishes when the right side of (14) vanishes, which, according to the thermodynamic theory of ferroelectricity, is an indication of lack of stability, i.e., absence of an absolute minimum of the free energy.

In the region of tetragonal symmetry and above the Curie point the determinant has only diagonal terms:

$$\begin{vmatrix} \frac{1}{\rho} - \frac{\partial \varphi_x^0}{\partial P_{0x}} & 0 & 0 \\ 0 & \frac{1}{\rho} - \frac{\partial \varphi_y^0}{\partial P_{0y}} & 0 \\ 0 & 0 & \frac{1}{\rho} - \frac{\partial \varphi_z^0}{\partial P_{0z}} \end{vmatrix}$$

Hence one of the conditions that this determinant vanish is

$$\frac{1}{\rho} - \frac{\partial \varphi_x^0}{\partial P_{0x}} = 0.$$

Making use of (7), we obtain

$$k\vartheta = \beta N q' q \overline{(x - \bar{x})^2}$$

or since $x = 0$ at the Curie point,

$$k\vartheta = \beta N q' q \bar{x}^2.$$

Inasmuch as $\beta N q x$ is the effective field when all the ions are displaced a distance x, this relation establishes the connection between the mean kinetic energy of an oscillating ion at the Curie point and its mean potential energy, if there is full correlation between the displacements of all the ions. Calculation of the expansion coefficients of the free energy in terms of fluctuations of the mean ionic displacements should lead to further deductions regarding the relation between the ferroelectric effects and fluctuations.

The method of calculation discussed here can be applied in evaluating the different theoretical models. Noting, however, the shortcomings of the Mason-Matthias model, it would be more expedient to obtain the temperature dependences of the spontaneous polarization, dielectric constant and entropy from the standpoint of the Devonshire-Slater anharmonic-oscillator theory. Such calculations, carried through taking into account the anharmonicity of the vibrations of all the ions, should help further refine this theory.

Remarks on the Electronic Theory of Ferroelectricity

Jaynes[5], the proponent of the electronic theory of ferroelectricity, casts doubt upon the basic assumptions of the ionic displacement theory.*

The present writer feels, however, that the arguments advanced by Jaynes to prove the inconsistency of the ion theories and the advantages of the electronic theory are not entirely convincing.

1. Jaynes calls attention to the fact that the properties of $BaTiO_3$ and ferroelectrics in general are significantly different from those of pyroelectric substances, such as tourmaline. Inasmuch as there can be no doubt that the genesis of the pyroelectric properties of tourmaline is "ionic", Jaynes concludes that interpretation of the properties of $BaTiO_3$ requires a qualitatively different mechanism.

Admitting that the pyroelectric properties of tourmaline are due to ionic displacements, it is still necessary to explain why it is impossible to apply one of the theoretical models, such as Slater's, to the description of these properties. A possible explanation may be that the tourmaline ions are rigidly fixed to their displaced positions. It would seem that these ions undergo small oscillations with little anharmonicity. In other words, the ions move in a narrow potential well with steep walls, whereas the ions of ferroelectrics undergo large-amplitude strongly anharmonic vibrations.

In the light of these concepts one can also explain the difference between the properties of pyroelectric and ferroelectric substances.

2. Initially electronic theory was based on x-ray diffraction studies which failed to disclose displacements of all the ions in barium titanate.

---

*The principal concepts of Jaynes' theory were described in survey presented by Smolenskii[8] at this Conference.

Now, however, as the author of the electronic theory himself has noted, there is little doubt that all $BaTiO_3$ ions do undergo displacements. Jaynes does not consider this fact alone sufficient to invalidate the electronic theory, since according to the theory these displacements are caused by the field produced by the initial electronic processes.

Admitting the existence of ionic displacements, one cannot avoid considering the statistical interactions of these ions. This should introduce significant corrections to the conditions for the occurrence of spontaneous polarization and to the temperature characteristics obtained from the electronic theory.

The question of which come first, the deformations of the electron shells or the ionic displacements, is one involving the kinetics of the rise of spontaneous polarization.

3. According to Matthias[18] and Smolenskii[19] ferroelectricity occurs in crystals which contain positive ions with the noble gas electron shell configuration at the center of the oxygen octahedrons. Jaynes considers this an evidence in favor of the electronic theory. Actually, this also indicates that the formation of covalent bonds tends to cause the positive ions and the oxygen ions in the octahedra to move closer together.

4. Jaynes points to the high index of refraction of ferroelectric substances as an indication of the high electronic polarizability, which is due to exchange of electrons between the oxygen and titanium ions. In addition, the occurrence of a maximum of the index of refraction in the neighborhood of the Curie point indicates a rearrangement of the electron structure of the crystal. These facts, however, do not disprove the ionic theories. Undoubtedly a certain rearrangement of the electron shells must take place at the Curie point (even according to the ionic theories). It should be noted, however, that the maximum rise of the index of refraction is very small, amounting to only 3% of its normal value. The existence of a frequency relaxation effect, in connection with which ϵ falls off by a factor of several hundred, in itself indicates the enormous role played by ionic displacements.

Thus Jaynes' assertion that the ionic theories are inconsistent is not well founded. Nevertheless, Jaynes' work is of great interest in that it is the first attempt to treat an oxygen octahedron as a single quantum mechanical ensemble. The problem of finding the quantum states of an octahedron is extremely important where clarifying the nature of the bonds between different ions is concerned.

Jaynes' proof that it is possible in principle for spontaneous polarization to arise as a result of purely electron effects is an important result. The further development of these concepts, taking into account ionic effects and their related temperature effects, is one of the most important and pressing problems in the theory of ferroelectricity.

In conclusion I desire to express my gratitude to G.A.Smolenskii for his attention to the work.

Institute of Semiconductors of the
Academy of Sciences of the USSR

References

1. W.P.Mason & B.T.Matthias, Phys.Rev., 74, 1662 (1948).
2. J.S.Slater, Phys.Rev., 78, 748 (1950).
3. A.F.Devonshire, Phil.Mag., 40, 1040 (1949).
4. A.Hagedorn, ZS.f.Phys., 133, 394 (1952).
5. E.Jaynes, Ferroelectricity. - Princeton University Press, 1953.
6. V.Kh.Kozlovskii, Zhur.tekh.fiz., 21, 1388 (1951).
7. G.A.Smolenskii & R.E.Pasynkov, Zhur.eksp.i teor.fiz., 25, 1 (1953).
8. G.A.Smolenskii, Izv. AN SSSR, Ser.fiz., 21, 233 (1957). (Trans. in Bulletin, Vol.21, No.2, p. 235.)
9. J.Shirane, F.Jona & R.Pepinsky, Proc.IRE, 12, 1738 (1955).
10. V.I.Kliachkin, Present issue of the Bulletin, p.364.
11. V.Kh.Kozlovskii, Zhur.tekh.fiz., 26, 5 (1956).
12. G.A.Smolenskii & V.Kh.Kozlovskii, Zhur.tekh.fiz., 23, 3 (1956).
13. L.N.Syrkin, Kristallografiia (Crystallography), 1, 3 (1956).
14. V.I.Smirnov, Kurs matematiki (Course in mathematics) Vol.III, M.-L. 1953.
15. C.Kittel, Phys.Rev., 82, 723 (1951).
16. V.L.Ginzburg, Usp.fiz.nauk., 38, 4 (1949).
17. M.L.Shirobokov & L.I.Kholodenko, Zhur.eksp.i teor.fiz., 21, 1239 (1951).
18. B.T.Mattias, Phys.Rev., 35, 1771 (1949).
19. G.A.Smolenskii & N.V.Kozhevnikova, Doklady AN SSSR, 76, 519 (1951).

ION DYNAMICS AND ELECTROSTATIC ENERGY OF FERROELECTRICS

- V.Kh.Kozlovskii

In the molecular theories of ferroelectricity, one must consider the motion of ferroelectrically active (hereinafter "ferroactive") vibrators in some type of anharmonic force field. Statistical methods have been used by several authors (other than Ginzburg[1]) by computing the appropriate phase integrals, free energy and polarization.[1-4] This is a complicated procedure and the results are predicated on the assumption that the anharmonic forces can be regarded as perturbations. In the case of ferroelectricity this assumption is a serious restriction.

We have made use of dynamic principles by means of which the anharmonic forces can be correctly taken into account. Let us use Hamilton's variational principle $\delta\overline{L} = 0$, extended over an infinite time interval, and write the displacements of the ferroactive ions in the form

$$\xi = s + u\theta(t),$$

where $\theta(t)$ is an almost sinusoidal function satisfying the conditions $\overline{\theta} = 0$ and $\overline{\theta^2} = 1$ so that s and u have the meaning of the average displacement and mean square deviation (dispersion), respectively; they are determined from the variational principle. The temperature is introduced into the equations by the condition

$$m\overline{\dot{\xi}^2} = mu^2\overline{\dot{\theta}^2} = kT.$$

This method was used to treat a ferroelectric with a single movable rigid lattice whose potential energy is given in terms of the lattice displacement by a function of the form

$$U = \frac{c'}{2}\xi^2 + \frac{b}{4}\xi^4. \qquad (1)$$

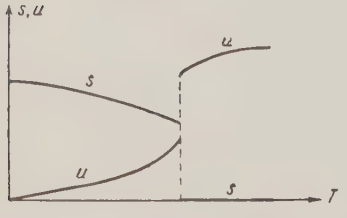

Fig.1. Temperature dependences of the displacement and dispersion in a ferroelectric substance with a movable rigid lattice.

The temperature dependences of the displacement and dispersion are found on analysis to be of the form shown in Fig.1. The phase transition temperature is related to the height of potential barrier by $kT \approx 0{,}60\ U_m$. Roughly speaking, kT' is the total energy of the vibrator at the transition point. From this one may conclude that below the transition temperature the ion undergoes relaxation from one potential well to the other and that above the transition temperature it vibrates above the barrier.

Further, we investigated a ferroelectric with two movable rigid lattices. In this case the potential energy is given by

$$U = \frac{1}{2}c_1'\xi_1^2 + \frac{1}{2}c_2'\xi_2^2 + c_{12}'\xi_1\xi_2 + \frac{1}{4}b_1\xi_1^4 + \frac{1}{4}b_2\xi_2^4. \qquad (2)$$

For a ferroactive lattice the coefficients c_k' are negative. If neither lattice is ferroactive, then in the case of weak interaction $(c_{12}'^2 < c_1'c_2')$ the crystal is not ferroelectric. On the contrary, there exists a second order ferroelectric phase transition. In the case of a single ferroactive lattice, we have one first order phase transition if the interaction is weak and a second order phase transition if the interaction is strong. The inequality

which now determines the strength of the interaction, however, is not the same as the previous one. In the case of two ferroactive lattices, we have two first order transitions with weak interaction $(c_{12}'^2 < c_1' c_2')$ and one second order phase transition with strong interaction.

We have also refined the theory whose model is a vibrator with the potential energy given by

$$U = \frac{c}{2}\xi^2 + \frac{b}{4}\xi^4 - \frac{1}{2}e^* Ass\xi. \tag{3}$$

Depending on the sign of c the potential well may have one or two minima. The energy of the vibrator is given as the sum of terms corresponding to its energy in the absence of polarization and the energy in the effective field. Analysis shows that in the two-minimum model there occurs a first order phase transition and in the one-minimum model a second order phase transition in most cases. Below we shall generalize the theory of this model to include the case of diatomic ferroactive molecules.

When these molecules are sufficiently far apart and separated by a grid of non-ferroactive ions, the crystal structure corresponds to that of Rochelle salt. Each cell of Rochelle salt contains two ferroactive protons which are located close to each other and whose vibrations are coupled. There is no correlation between the motion of the protons in different cells. The potential energy is given by

$$U = \frac{c_1'}{2}\xi_1^2 + c_{12}'\xi_1\xi_2 + \frac{c_2'}{2}\xi_2^2 - \frac{1}{2}e_1^*(A_{11}'s_1 + A_{12}'s_2)\xi_1 - \frac{1}{2}e_2^*(A_{21}'s_1 + A_{22}'s_2)\xi_2. \tag{4}$$

This energy is comprised of the energy in the absence of polarization and the energy in the effective field due to polarization. Here a fairly large number of different cases is possible. Thus there may be cases of vibration when the potential well has one or two minima with various relations between the elastic forces and the effective-field forces. As a result there may occur one first or second order phase transition, two second order phase transitions or two first order phase transitions.

We next consider the very general case of a nonrigid ferroactive lattice whose potential energy is given in the form of a power series in terms of the displacements of all the ions, i.e.,

$$U = \frac{1}{2}\sum_{ll'} c^{ll'}\xi^l\xi^{l'} + \frac{1}{4}\sum_{ll'\bar{l}\bar{l}'} b^{ll'\bar{l}\bar{l}'}\xi^l\xi^{l'}\xi^{\bar{l}}\xi^{\bar{l}'}. \tag{5}$$

Here the quadratic form is negative and the fourth-order form is positive.

The properties of a ferroelectric substance depend strongly on how rapidly the temperature correlation factor decreases:

$$\rho^{|l-l'|} = \overline{\theta_l\theta_{l'}}.$$

When it falls off slowly, we have "rigid" (strong) correlation. Then the temperature dependence of the dispersion is that shown in Fig.2a. As the temperature is increased the dispersion increases, following the curve for the polar state, until at certain temperature there occurs an abrupt transition (dashed line) to the curve of the nonpolar state. On cooling there takes place a sudden transition back to the polarized state, but in this case the jump occurs at a lower temperature, where the two curves intersect. Thus the first order phase transition is accompanied by temperature hysteresis. In the case of "soft" (weak) correlation, when the correlation factor varies greatly with temperature, the phase transition becomes a continuous one, as

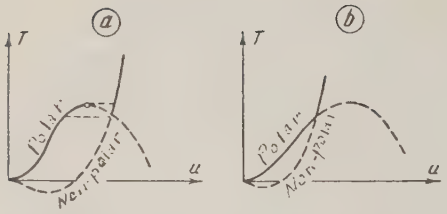

Fig.2. Temperature dependence of the dispersion: a) for a ferroelectric with strong correlation, b) for a ferroelectric substance with weak correlation. The dash sections of the curves represent unstable states.

is shown in Fig.2b.

The temperature dependence of ϵ in a weak electric field is shown, for the case of strong correlation in Fig.3. As the temperature decreases ϵ varies along a hyperbola, followed by a discontinuity. The same kind of discontinuity occurs on heating. In the case of weak correlation ϵ varies along a hyperbola on both sides of the Curie point, following Ginzburg's[1] "twin" or pair law.

Further, we have investigated the behavior of a ferroelectric substance with strong correlation in a strong electric field. Fig.4 shows how the hysteresis loop of such a substance changes as it is heated. At temperatures far below the phase transition point, the loop has the usual shape (Fig.4a). As the temperature is increased, a wave appears in the loop, and above the transition point it separates into two loops which finally disappear. Figures 4b-d illustrate this phenomenon. The hysteresis loop has the ordinary shape when the correlation is weak.

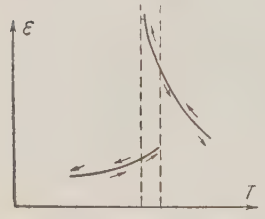

Fig.3. Temperature dependence of the dielectric constant of a ferroelectric with strong correlation.

The theory described is essentially phenomenological. We shall now attempt to determine the force constants on the basis of ionic interactions. First let us consider the electrostatic energy of the polarized crystal. We shall use the Born notation to describe the ions. The cell number is designated by l; the basic ions and the translational sublattices they form are denoted by the index k. Surrounding the k, l ion by a Lorentz sphere, we will have the following expressions for the effective values of the field intensity and potential:

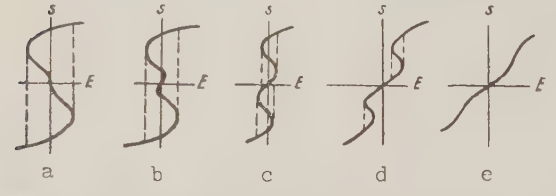

Fig.4. Temperature variation of the hysteresis loops of a ferroelectric with strong correlation in strong electric fields: a) at a temperature well below the phase transition point, b & c) at temperatures just below the transition point, d & e) at a temperature above the transition point. States for which $ds/dE < 0$ are unstable.

$$\mathbf{E}_{k'} = \mathbf{E} + \frac{4\pi}{3}\mathbf{P} + \sum_k S_l \left[3\,\frac{\mathbf{r}^l_{k'k}(\mathbf{p}_k \mathbf{r}^l_{k'k})}{(r^l_{k'k})^5} - \frac{\mathbf{p}_k}{(r^l_{k'k})^3} - q_k \frac{\mathbf{r}^l_{k'k}}{(r^l_{k'k})^3} \right] \tag{6}$$

and

$$\varphi^{l'}_{k'} = -\left(\mathbf{E} + \frac{4\pi}{3}\mathbf{P}\right)\mathbf{R}^{l'}_{k'} + \sum_k S_l \frac{q_k}{\mathbf{r}^l_{k'k}} - \sum_k S_l \frac{\mathbf{p}_k \mathbf{r}^l_{k'k}}{(\mathbf{r}^l_{k'k})^3}. \tag{7}$$

The energy of the (k', l') ion in the effective field is given by $q_{k'}\varphi^{l'}_{k'} - \mathbf{p}_{k'}\mathbf{E}_{k'}$; the energy of the crystal is obtained by summing over k' and l' and dividing the sum by 2 if there is no external field. Since the energy

due to the external field should not be divided by 2, the correct expression for the crystal energy in an external field is given by

$$U_e = \frac{1}{2}\sum_{k'} S_{l'} (q_{k'}\varphi^{l'}_{k'} - \mathbf{p}_{k'}\mathbf{E}_{k'}) - \frac{1}{2}\sum_{k'} S_{l'} (q_{k'}\mathbf{R}^{l'}_{k'} + \mathbf{p}_{k'})\mathbf{E}_0. \tag{8}$$

wherein account is taken of the fact that the external field is already contained in $\mathbf{E}_{k'}$.

Denoting the energy per unit cell by U_{1e} and making use of (6) and (7), we obtain

$$U_{1e} = -\frac{1}{2}\left(\mathbf{E} + \frac{4\pi}{3}\mathbf{P} + \mathbf{E}_0\right)\sum_{k'}(q_{k'}\mathbf{R}^{l'}_{k'} + \mathbf{p}_{k'}) + \frac{1}{2}\sum_{k'k} S_l \frac{q_{k'}q_k}{r^l_{k'k}} -$$

$$-\frac{1}{2}\sum_{k'k} S_l q_{k'}\frac{\mathbf{r}_k\mathbf{r}^l_{k'k}}{(r^l_{k'k})^3} + \frac{1}{2}\sum_{k'k} S_l q_k \frac{\mathbf{p}_{k'}\mathbf{r}^l_{k'k}}{(r^l_{k'k})^3} - \frac{1}{2}\sum_{k'k} S_l \left[3\frac{(\mathbf{p}_{k'}\mathbf{r}^l_{k'k})(\mathbf{p}_k\mathbf{r}^l_{k'k})}{(r^l_{k'k})^5} - \frac{\mathbf{p}_{k'}\mathbf{p}_k}{(r^l_{k'k})^3}\right]. \tag{9}$$

The quantity $\sum_{k'}(q_{k'}\mathbf{R}^{l'}_{k'} + \mathbf{p}_{k'})$ is the dipole moment of a unit cell and is equal to P/N, where N is the number of cells.

Introducing structure coefficients, we can write the sums in the form

$$S_l \frac{\mathbf{p}_{k'}\mathbf{r}^l_{k'k}}{(r^l_{k'k})^3} = \sum_x p_{k'x}\Omega^{k'}_{kx}; \quad S_l\left[3\frac{(\mathbf{p}_{k'}\mathbf{r}^l_{k'k})(\mathbf{p}_k\mathbf{r}^l_{k'k})}{(r^l_{k'k})^5} - \frac{\mathbf{p}_{k'}\mathbf{p}_k}{(r^l_{k'k})^3}\right] = \sum_{xy} p_{k'x}p_{ky}Q^{k'}_{kxy}. \tag{10}$$

Eq. (9) can then be rewritten as

$$U_{1e} = -\frac{1}{2N}(\mathbf{E}_0 + \mathbf{E})\mathbf{P} - \frac{2\pi}{3N}P^2 + \frac{1}{2}\sum_{k'k} q_{k'}q_k S_l \frac{1}{r^l_{k'k}} +$$

$$+\sum_{k'k} q_k \sum_x p_{k'x}\Omega^{k'}_{kx} - \frac{1}{2}\sum_{k'k}\sum_{xy} p_{k'x}p_{ky}Q^{k'}_{kxy}. \tag{11}$$

We now add the elastic dipole energy $\frac{1}{2}\sum_k \frac{p_k^2}{\alpha_k}$ to (11), calling the result also the electrostatic energy since it is written entirely in terms of quantities characterizing electrostatic fields.

Expanding in Taylor's series in the relative displacements

$$S_l \frac{1}{r^l_{k'k}} = S_l \frac{1}{\overset{0}{r}{}^l_{k'k}} + \sum_x \overset{0}{\Omega}{}^{k'}_{kx} s_{k'kx} + \frac{1}{2}\sum_{xy}\overset{0}{Q}{}^{k'}_{kxy} s_{k'kx}s_{k'ky} + \cdots \tag{12}$$

and

$$\Omega^{k'}_{kx} = \overset{0}{\Omega}{}^{k'}_{kx} + \sum_y \overset{0}{Q}{}^{k'}_{kxy} s_{k'ky} + \cdots, \tag{13}$$

we write the energy in the form

$$U_{1e} + U_{1d} = -\frac{1}{2}(\mathbf{E} + \mathbf{E}_0)\frac{\mathbf{P}}{N} - \frac{2\pi}{3}\cdot\frac{\mathbf{P}^2}{N} + \frac{1}{4}\sum_{k'k} q_{k'}q_k \sum_{xy}\overset{0}{Q}{}^{k'}_{kxy} s_{k'kx}s_{k'ky} +$$

$$+\sum_{k'k} q_k \sum_{xy}\overset{0}{Q}{}^{k'}_{kxy} p_{k'x}s_{k'ky} - \frac{1}{2}\sum_{k'k}\sum_{xy}\overset{0}{Q}{}^{k'}_{kxy} p_{k'x}p_{ky} + \frac{1}{2}\sum_k \frac{p_k^2}{\alpha_k}. \tag{14}$$

Account is here taken of the lattice symmetry by virtue of which the linear terms are eliminated. The relation between E and $\mathbf{E}_0$ is determined by the shape of the sample and in some simple cases is of the form $\mathbf{E} = \mathbf{E}_0 - k_f\mathbf{P}$ where k_f is a form factor. It can be shown that the perovskite lattice symmetry leads to the relation

$$Q^{k'}_{kxy} = Q^{k'}_{kx}\,\delta_{xy}. \tag{15}$$

If only the j-th lattice is displaced along the x axis, then setting $Q^j_{kx} = Q^j_k$ and $p_{kx} = p_k$ and assuming that $E = 0$, (14) and (15) lead to

$$\overset{j}{U}_{1e} + \overset{j}{U}_{1d} = -\frac{1}{2}\left(k_f + \frac{4\pi}{3}\right)\frac{P^2}{N} + \frac{1}{2}\,q_j\,s_j^2 \sum_{k\neq j} q_k \overset{0}{Q}{}^j_k + p_j\,s_j \sum_{k\neq j} q_k \overset{0}{Q}{}^j_k -$$

$$- q_j\,s_j \sum_{k\neq j} p_k \overset{0}{Q}{}^j_k - \frac{1}{2}\sum_{k'k} \overset{0}{Q}{}^{k'}_k\,p_{k'}\,p_k + \frac{1}{2}\sum_k \frac{p_k^2}{\alpha_k}. \tag{16}$$

We are here treating the equilibrium state, so that the polarizations, moments p_k (or effective fields E_k), and ion displacements are interdependent. If the displacements are given, their relations are conveniently written in the form[5]

$$\left.\begin{aligned} E_k &= \gamma_k E + \sum_j A_{kj}\,s_j \\ \text{and} \qquad P &= \gamma_p E + \sum_j A_{pj}\,s_j. \end{aligned}\right\} \tag{17}$$

Assuming that only one lattice is displaced and that there is no field E, (16) and (17) lead to

$$U_{1e} + U_{1d} = -\frac{1}{2}\,c_{ej}\,s_j^2,$$

where

$$c_{ej} = \left(k_f + \frac{4\pi}{3}\right)\frac{A^2_{pj}}{N} - q_j \sum_{k\neq j} q_k \overset{0}{Q}{}^j_k - 2\alpha_j A_{jj} \sum_k q_k \overset{0}{Q}{}^j_k + 2q_j \sum_k \alpha_k A_{kj} \overset{0}{Q}{}^j_k +$$

$$+ \sum_{k'k} \alpha_{k'}\,\alpha_k \overset{0}{Q}{}^{k'}_k A_{k'j} A_{kj} - \sum \alpha_k A_{kj}. \tag{18}$$

The coefficient c_{ej} may be called the electrostatic coefficient of the astaticism of the sublattice.

Inasmuch as there are also nonelectrostatic forces acting between the ions, the potential energy of spontaneous polarization per unit cell can be written

$$U_1 = \frac{1}{2}(c - c_e)\,s^2 + \frac{1}{4}\,b s^4. \tag{19}$$

when a single lattice is displaced.

In Eq.(19) c is due to nonelectrostatic forces, whereas b is due primarily to the electrostatic ones. These constants cannot at present be calculated with the necessary accuracy, since there does not exist sufficient information on the interaction of ions in partially homeopolar crystals, the type to which ferroelectrics belong. It might be tentatively assumed that c is of the same order as c_e and b can be calculated from the measured value of the transition heat. In a discontinuous transition this latent heat is equal to the change in potential energy:

$$Q_1 = \frac{\gamma^2}{2}\left(1 - \frac{\gamma^2}{2}\right)\frac{(c_e - c)^2}{b}. \tag{20}$$

Here $\gamma = \frac{s_T}{s} = \frac{P_T}{P}$ where s_T and P_T refer to a temperature in the immediate neighborhood of the phase transition point. The values of the force constants

can be verified by means of the following formula for the spontaneous displacement, obtained from (19):

$$s = \sqrt{\frac{c_e - c}{b}}. \qquad (21)$$

Calculations have been performed using numerical values found previously by the author.[5] The following values were obtained for the titanium ions in $BaTiO_3$: $c_e = 6 \cdot 10^{-5}$ cgs units, $Q_1 = 3 \cdot 10^{-15}$ erg per molecule,[6] and $\gamma = 0.5$.[7] Assuming that $c_e - c$ is of the order of 10^5, we find that $b = 3 \cdot 10^{23}$. From (21) we then get $s = 0.05$A. The directly measured ionic displacements are of the same order of magnitude.

Ionic displacements (in A) in $BaTiO_3$, according to the data of different investigators[8]

Ions	Känzig	Evans I	Evans II	Neutron diffr. data
O_1	—0,13	—0,1	—0,02	—0,04
Ti	—0,06	0,05	0,14	0,12
Ba	0	0	0,08	0,06

It is of interest to analyze the available experimental data (see accompanying table) on ionic displacements in $BaTiO_3$. The displacements are referred to the network of the oxygen ions located in planes perpendicular to the polar axis. It should be noted that neutron diffraction data give the displacement of the ionic nuclei, whereas x-ray diffraction data give the displacements of the centers of the electron shells. The latter are obtained from the former with the aid of the correction factor

$$\delta = \frac{\alpha E_{ef}}{Ze}. \qquad (22)$$

Calculations show that this correction is appreciable only for oxygen. If one uses Känzig's data, the displacement of the oxygen nucleus is $s_O = 0.01$ A. Evaluating the effective field according to the formulas deduced earlier in Ref.5, we obtain $E_O = 1.7 \cdot 10^6$; then from (22) we get $\delta = 0.11$ A. Thus the larger part of the displacement observed by Känzig is due to polarization of the ions. Taking this correction into account, we calculated the spontaneous polarization of $BaTiO_3$ by means of the equation derived in Ref.5 and find $P = 26 \cdot 10^{-6}$ coulomb/cm^2. This value is in agreement with the experimentally determined value reported by Cross[7].

Neutron diffraction data lead to value of $P = 70 \cdot 10^{-6}$ coulomb/cm^2 for the spontaneous polarization. Clearly more accurate determination of the spontaneous polarization may help clarify the picture of the ionic displacements in barium titanate.

Institute of Semiconductors of the
Academy of Sciences of the USSR

References

1. V.Ginzburg, Usp.fiz.nauk., 38, 490 (1949).
2. S.Boguslawsky, Phys.ZS., 15, 283 (1914).
3. A.Devonshire, Phil.Mag., 40, 1040 (1949).
4. J.Slater, Phys.Rev., 78, 748 (1950).
5. V.Kozlovskii, Zhur.tekh.fiz., 21, 1388 (1951).
6. W.Merz, Helv.Phys.Acta, 21, 210 (1948).
7. L.Cross, Phil.Mag., 44, 1161 (1953).
8. G.Shirane, R.Pepinsky & B.Frazer, Acta Crystallogr., 9, 131 (1956).

TOWARDS A THEORY OF ORIENTATION ORDERING IN MOLECULAR CRYSTALS

- V. I. Kliachkin

The present article represents an attempt to formulate the general statistical mechanical equations for a system of molecules with rotational degrees of freedom. We use the method of particle distribution functions proposed by Bogoliubov[1].

Since Bogoliubov's method is based on the most general considerations of Gibbs statistics, the physical content of approximations used in several theoretical developments can be immediately understood. We are speaking here of theories[2,3] of order-disorder transitions in the crystal (solid) phase. As is known, Bogoliubov's method has so far been used to solve problems related to the liquid state.

The fact that we shall be dealing with the crystal state will be reflected to some extent in the final relationships deduced. Nevertheless from the purely formal point of view the approach is essentially the same as Bogoliubov's, although of course, the fundamental expression for the probability of a given configuration state in the system takes on a somewhat different physical meaning.

The ordinary dynamic theory[4] leading to orientation waves is hardly adequate when it comes to investigation of phase transitions associated with the breakdown of long-range ordering. This follows from the fact that at temperatures in the neighborhood of the transition point one may no longer assume that the angular deviations of the molecular axes with their equilibrium positions are small. The small-angle condition, however, is one of the basic premises of the dynamic theory.

Fundamental Relations

Let us consider a crystal consisting of N interacting molecules randomly oriented. We shall assume that the centroids of these molecules form a rigid spatial crystal structure which can be represented in terms of a set of n interpenetrating simple sublattices. Let us denote the number of molecules in the sublattices $1,\ldots,n$ by $N_1,\ldots,N_n$. We then have

$$N = \sum_{k=1}^{n} N_k. \tag{1}$$

The spatial orientation of the molecule at the i-th site of the k-th sublattice will be given by the angle coordinates $(\theta_i^k,\ \varphi_i^k) \equiv \omega_i^k$, where $i = 1, \ldots, N_l;\ k = 1, \ldots, n$.

Proceeding according to Bogoliubov, we shall start from the general theory of equilibrium states based on the Gibbs canonical distribution

$$D_N = D_N(\omega_1^1, \ldots, \omega_{N_1}^1; \ldots; \omega_1^k, \ldots, \omega_{N_k}^k; \ldots; \omega_1^n, \ldots, \omega_{N_n}^n) = Q_N^{-1} \exp - \frac{U_N}{kT}, \tag{2}$$

where D_N is the probability distribution function for the orientations of the N molecules and Q_N is usual the configuration integral

$$Q_N = \underbrace{\int \cdots \int}_{N} \exp - \frac{U_N}{kT} \prod_{k=1}^{n} \prod_{i=1}^{N_k} d\omega^k. \tag{2a}$$

In the following development we shall not take account of translational waves of the lattice, inasmuch as the center-of-mass coordinates of the molecules, which determine the separations between them, will appear in U_N, and

therefore in D_N, only as parameters, whereas the angle coordinates ω_i^k are the dynamic variables for which we must find probability distribution functions at the given temperature.

The neglect of thermal vibrations means that we are not taking into account the influence of translational waves on the character of the orientational disordering. In the first approximation this would seem to be justifiable, since the orientational "melting" temperatures and ferroelectric Curie points lie far below the ordinary melting point of the crystal, i.e., orientational disordering occurs in a temperature region in which the long-range order of the centers of mass of the molecules is stable.

If the potential energy of the system is defined, as by Bogoliubov,[1] in terms of two-particle interactions, U_N is given by

$$U_N = \frac{1}{2} \sum_{k=1}^{n} \sum_{l=1}^{n} \sum_{i=1}^{N_k} \sum_{j=1}^{N_l} U_{ij}^{kl} (\omega_i^k, \omega_j^l) \tag{3}$$

with $U_{ii}^{kk} = 0$.

In the special case, which we shall treat separately, when the molecules interact directly only with their nearest neighbors, the expression for U_N becomes

$$U_N = \frac{1}{2} \sum_{k=1}^{n} \sum_{i=1}^{n} \sum_{\substack{l=1 \\ l \neq k}}^{N_k} \sum_{j=1}^{m_k^l} U_{ij}^{kl} (\omega_i^k, \omega_j^l) \tag{3a}$$

where again $U_{ii}^{kk} = 0$.

In this equation m_k^l is the number of nearest neighbors of the molecule at the k-th site of the l-th sublattice.

The total number of nearest neighbors of a molecule in the l-th sublattice will obviously be

$$Z_k = \sum_{\substack{l=1 \\ l \neq k}}^{n} m_k^l . \tag{3b}$$

The two-body interaction energy depends both on the orientation of the molecules and on the positions of their centers of mass, a fact which appears analytically in (3) in the different indices for molecules at different lattice sites, that is

$$U_{ij}^{kl} (\omega_i^k, \omega_j^l) \equiv U (R_{ij}^{kl}, \omega_i^k, \omega_j^l) = U_{ji}^{lk} (\omega_j^l, \omega_i^k), \tag{3c}$$

where R_{ij}^{kl} is the distance between the centers of mass of molecule i, k and molecule j, l.

We now introduce Bogoliubov's distribution functions

$$F_{s_1, \ldots, s_n} (\omega_1^1, \ldots, \omega_{s_1}^1; \ldots; \omega_1^k, \ldots, \omega_{s_k}^k; \ldots; \omega_1^n, \ldots, \omega_{s_n}^n) = (4\pi)^s \underbrace{\int \ldots \int}_{(N-s)} D_N \cdot \prod_{k=1}^{n} \prod_{i=s_k+1}^{N_k} d\omega_i^k . \tag{4}$$

Eq. (4) gives the probability of an orientational configuration of a group of s molecules, where

$$s = \sum_{k=1}^{n} s_k . \tag{4a}$$

From the general identity

$$\nabla_{\omega_i^k} D_N + \frac{D_N}{kT} \nabla_{\omega_i^k} U_N = 0. \tag{5}$$

(here the operator $\nabla_{\omega_i^k}$ acts on the coordinates of any molecule i, k of the chosen group of s molecules), we then obtain in complete analogy with Bogoliubov the following integro-differential equations for the function $F_{s_1,\ldots s_n}$:

$$\nabla_{\omega_i^k} F_{s_1,\ldots,\, s_n} + \frac{1}{kT} F_{s_1,\ldots,\, s_n} \cdot \nabla_{\omega_i^k} U_{s_1,\ldots,\, s_n} +$$

$$+ \frac{1}{4\pi kT} \sum_{l=1}^{n} \sum_{j=s_l+1}^{N_l} \int F_{s_1,\ldots,\, s_l+1,\ldots,\, s_n} \cdot \nabla_{\omega_i^k} U_{ij}^{kl}\,(\omega_i^k, \omega_j^l)\, d\omega_j^l = 0, \tag{6}$$

where

$$U_{s_1,\ldots,\, s_n} = \frac{1}{2} \sum_{l=1}^{n} \sum_{k=1}^{n} \sum_{j=1}^{s_l} \sum_{i=1}^{s_k} U_{ij}^{kl}\,(\omega_i^k, \omega_j^l) \tag{6a}$$

with $U_{ii}^{kk} = 0$.

In Eq.(6) the function $F_{s_1,\ldots,s_l+1,\ldots,s_n}$ gives the probability of an orientational configuration of a group of $s+1$ molecules, i.e.,

$$F_{s_1,\ldots,\, s_k+1,\ldots,\, s_n} = F_{s_1,\ldots,\, s_l+1,\ldots,\, s_n}(\omega_1^1, \ldots, \omega_{s_1}^1, \ldots, \omega_1^l, \ldots, \omega_{s_k}^l;\ \omega_{s_k+1}^l, \ldots, \omega_1^n, \ldots, \omega_{s_n}^n). \tag{6b}$$

Since the different terms in the sum under the integral in (6) pertain to molecules at different distances from the chosen i-th molecule of the k-th lattice, Eq.(6) cannot be further simplified.

Similarly, in the special case of when the direct two-body interaction noticeably affects only the immediate neighbors, i.e., when U_N is given by (3a), we obtain

$$\nabla_{\omega_i^k} F_{s_1,\ldots,\, s_n} + \frac{1}{kT} F_{s_1,\ldots,\, s_n} \cdot \nabla_{\omega_i^k} U_{s_1,\ldots,\, s_n} +$$

$$+ \frac{1}{4\pi kT} \sum_{\substack{l=1 \\ l \neq k}}^{n} \sum_{j=p_{il}^k+1}^{m_k^l} \int F_{s_1,\ldots,\, s_k+1,\ldots,\, s_n} \cdot \nabla_{\omega_i^k} U_{ij}^{kl}\,(\omega_i^k, \omega_j^l)\, d\omega_j^l = 0. \tag{7}$$

Here

$$U_{s_1,\ldots,\, s_n} = \frac{1}{2} \sum_{k=1}^{n} \sum_{i=1}^{s_k} \sum_{\substack{l=1 \\ l \neq k}}^{n} \sum_{j=1}^{p_{il}^k} U_{ij}^{kl}\,(\omega_i^k, \omega_j^l). \tag{7a}$$

In the above p_{il}^k gives the number of molecules of the l-th lattice which are neighbors of the i-th site of the k-th lattice and are in the chosen group of s molecules for which the probability density $F_{s_1,\ldots,\, s_n}$ is determined. Since, however, the integral of (7) summation is carried out over all molecules that do not enter into this group of s molecules but are nearest neighbors of the i-th site of the k-th lattice, the two-body interaction energy can in this case be considered independent of the indices i and j. This makes it possible to simplify Eq.(7). Specifically,

$$\nabla_{\omega_i^k} F_{s_1,\ldots,\, s_n} + \frac{1}{kT} F_{s_1,\ldots,\, s_n} \cdot \nabla_{\omega_i^k} U_{s_1,\ldots,\, s_n} +$$

$$+ \frac{1}{4\pi kT} \sum_{\substack{l=1 \\ l \neq k}}^{n} \sum_{j=p_{il}^k+1}^{m_k^l} \int F_{s_1,\ldots,\, s_k+1,\ldots,\, s_n} \cdot \nabla_{\omega_i^k} U^{kl}\,(\omega_i^k, \omega_j^l)\, d\omega_j^l = 0. \tag{8}$$

It is important to note that the integration in Eqs.(7) and (8) is taken over the coordinates of the molecules which are nearest neighbors of the i-th site (i.e., of the center of a coordination group). The form of Eq.(8) depends strongly on the way one chooses the s molecules whose distribution function is sought.

In particular, if the i-th molecule of the k-th sublattice enters into this group together with all its nearest neighbors, then $p_{il}^k = m_k^l$, and Eq.(8) becomes

$$\nabla_{\omega_i^k} F_{s_1,\ldots,s_n} + \frac{1}{kT} F_{s_1,\ldots,s_n} \cdot \nabla_{\omega_i^k} U_{s_1,\ldots,s_n} = 0, \tag{8a}$$

$$U_{s_1,\ldots,s_n} = \frac{1}{2} \sum_{k=1}^{n} \sum_{i=1}^{s_k} \sum_{\substack{l=1 \\ l\neq k}}^{n} \sum_{j=1}^{m_k^l} U^{lk}(\omega_i^k, \omega_j^l) \tag{8b}$$

with $U_{ii}^{kk} = 0$.

Similarly, in the special case when none of the nearest neighbors of the i-th molecule of the k-th sublattice are comprised in the group of s molecules, we have $p_{il}^k = 0$, and (8) becomes

$$\nabla_{\omega_i^k} F_{s_1,\ldots,s_n} + \frac{1}{4\pi kT} \sum_{\substack{l=1 \\ l\neq k}}^{n} \sum_{j=1}^{m_k^l} \int F_{s_1,\ldots,s_n} \cdot \nabla_{\omega_i^k} U^{kl}(\omega_i^k, \omega_j^l)\, d\omega_j^l = 0. \tag{8c}$$

Eqs.(8c) show most clearly the "cooperative effect", i.e., the existence of correlation in the long-range order, which is, however, the effect of the forces whose range is less than the dimensions of a coordination group.

Thus Eqs.(6) and (8) make it possible, in principle, to calculate the orientation probability density for a group of s molecules coupled by long-range or short-range forces, respectively.

Analysis of the Distribution Function

Kirkwood and Takagi[2,3] begin their theoretical attempts to explain the physical conditions leading to a stable ordered configuration by trying to find the probability distribution function for the orientation of a single molecule in a crystal.

We shall show that the results of these works are contained in the solutions of Eqs.(6) and (8). For a group consisting of a single molecule these equations become

$$\nabla_{\omega_i^k} F_k(\omega_i^k) + \frac{1}{4\pi kT} \sum_{l=1}^{n} \sum_{j=1}^{N_l} \int F_{kl}(\omega_i^k, \omega_j^l) \cdot \nabla_{\omega_i^k} U_{ij}^{kl}(\omega_i^k, \omega_j^l)\, d\omega_j^l = 0 \tag{9}$$

in the case of long-range forces, and

$$\nabla_{\omega_i^k} F_k(\omega_i^k) + \frac{1}{4\pi kT} \sum_{\substack{l=1 \\ l\neq k}}^{n} m_k^l \int F_{kl}(\omega_i^k, \omega_j^l) \cdot \nabla_{\omega_i^k} U^{kl}(\omega_i^k, \omega_j^l)\, d\omega_j^l = 0 \tag{9a}$$

in the case of short-range forces (in (9) and (9a) the index 1_k, 1_l is replaced by k, l). In the present work we shall restrict our considerations to the simplest case, in which one may write

$$F_{kl}(\omega_i^k, \omega_j^l) = F_k(\omega_i^k) \cdot F_l(\omega_j^l) \equiv F_k(\omega) F_l(\omega'). \tag{10}$$

The approximation of Eq.(10) for the binary distribution function immediately transforms (9) and (9a) to a form which makes it possible to obtain the results of Kirkwood[2] and Takagi[3].

Indeed, from (9) and (10) we obtain

$$\left.\begin{aligned} F_k(\omega) &= \lambda_k \exp -\frac{W_k(\omega)}{kT} \\ \lambda_k^{-1} &= \frac{1}{4\pi}\int \exp -\frac{W_k(\omega)}{kT}\, d\omega \end{aligned}\right\} \tag{11}$$

(we have dropped the indices i, k on ω, since (11) is valid for all possible indices; further, we shall write k, l as a subscript, so that $U^{kl} \equiv U_{kl}$). For the energy $W_k(\omega)$ we then obtain

$$W_k(\omega) = \frac{1}{4\pi}\sum_{l=1}^{n}\sum_{j=1}^{N_l}\int F_l(\omega')\, U_{ij}^{kl}(\omega, \omega')\, d\omega' \tag{12}$$

in the case of long-range forces, and

$$W_k(\omega) = \frac{1}{4\pi}\sum_{\substack{l=1\\ l\neq k}}^{n} m_k^l \int F_l(\omega')\, U_{kl}(\omega, \omega')\, d\omega'. \tag{12a}$$

in the case of short-range forces.

Thus the difference in the character of the interaction changes only the kernel of the set of nonlinear integral Eqs.(12) and (12a).

The set (12a) leads to Kirkwood's[2] result for the special case of body-centered and face-centered cubic lattices.

In this case we have

$$m_k^l \equiv Z_l = Z = \begin{cases} 8 - \text{for a body-centered cube,} \\ 4 - \text{for a face-centered cube.} \end{cases}$$

If we now assume that the character of the interaction forces does not depend on which of the simple sublattices the neighboring molecule belongs to, (12a) leads directly to

$$\ln \frac{F_k(\omega)}{\lambda_k} = -\frac{Z}{4\pi kT}\sum_{\substack{l=1\\ l\neq k}}^{n}\int F_l(\omega')\, U(\omega, \omega')\, d\omega'. \tag{13}$$

Eqs.(13) are the basic equations of Kirkwood's work[2] devoted to second order phase transitions in molecular crystals.

In the same way, assuming the long-range forces to give a pure dipole interaction, i.e., assuming that the energy U_{ij}^{kl} in Eqs.(12) is given by

$$U_{ij}^{kl}(\omega, \omega') = (R_{ij}^{kl})^{-3}\left\{\mathbf{p}_k\mathbf{p}_l' - 3\mathbf{p}_k\frac{\mathbf{R}_{ij}^{kl}}{R_{ij}^{kl}}\cdot p_l'\frac{\mathbf{R}_{ij}^{kl}}{R_{ij}^{kl}}\right\}, \tag{14}$$

we obtain

$$W_k(\omega) = -\mathbf{p}_k\sum_{l=1}^{n}\mathbf{E}_l^k = -\sum_{\alpha}\sum_{l=1}^{n} p_{k\alpha}E_{l\alpha}^k, \tag{15}$$

where $\alpha = 1, 2, 3$.

In these equations $\mathbf{p}_k$ and $\mathbf{p}_l'$ are the dipole moment vectors of the molecules with orientations ω and ω' located at the i-th and j-th sites of the k-th and l-th sublattices, respectively.

The quantities E_l^k can be interpreted as the internal field due to the l-th lattice acting on an arbitrary molecule of the k-th lattice and given by

$$\mathrm{E}_l^k = \sum_{j=1}^{N_l} (R_{ij}^{kl})^{-5} \left\{ 3\mathrm{R}_{ij}^{kl} (\overline{\mathrm{p}_l'} \mathrm{R}_{ji}^{lk}) - \overline{\mathrm{p}_l'} (\mathrm{R}_{ij}^{kl})^2 \right\} = \sum_{\alpha} \mathrm{e}_\alpha \left\{ \sum_{j=1}^{N_l} \sum_{\beta} \Delta_{ij\alpha\beta} \overline{p_{l\beta}'} \right\}, \tag{16}$$

where the e_α are the unit vectors along the axes of an orthogonal coordinate system.

The $\Delta_{ij\alpha\beta}^{kl}$ are given by

$$\Delta_{ij\alpha\beta}^{kl} = (R_{ij}^{kl})^{-5} \{ 3R_{ij\alpha}^{ki} R_{ji\beta}^{lk} - \delta_{\alpha\beta} (R_{ij}^{kl})^2 \}, \tag{17}$$

where $\delta_{\alpha,\beta}$ is the Kronecker delta.

The quantity $\overline{\mathrm{p}_l}$, which is interpreted as the mean dipole moment of a molecule in the l-th lattice, is given by

$$\overline{\mathrm{p}_l} = \frac{1}{4\pi} \int \mathrm{p}_l (\omega) F_l (\omega) \, d\omega. \tag{18}$$

The components of p_l are of the usual form:

$$\left.\begin{matrix} p_{lx} \\ p_{ly} \\ p_{lz} \end{matrix}\right\} = p \cdot \begin{cases} \sin\theta_l \cos\varphi_l, \\ \sin\theta_l \sin\varphi_l, \\ \cos\theta_l. \end{cases}$$

Noting that the mean dipole moment of the l-th sublattice is determined by (18), and bearing in mind Eqs.(11) and (15), one can readily obtain an expression for $\overline{p}_{k\alpha}$ as a function of the temperature T. This is

$$\overline{p}_{l\alpha} = p \frac{E_{l\alpha}}{E_l} L\left(\frac{p}{kT} E_l \right), \tag{19}$$

where $L(x)$ is the ordinary Langevin function and

$$E_l = \left(\sum_{\alpha} E_{l\alpha}^2 \right)^{1/2}.$$

From Eq.(16) we can write (19) in the form

$$\frac{X_k \cos\theta_{k\beta}}{\sigma} = \sum_{\alpha} \sum_{l=1}^{n} \varepsilon_{\alpha\beta}^{kl} \cdot \cos\theta_{l\alpha} \cdot L(X_l), \tag{20}$$

where $\cos\theta_{k\beta}$ is the direction cosine of E_k along the β axis (it is obvious from (19) that the vector $\mathrm{E}_k = \sum_{l=1}^{n} \mathrm{E}_l^k$ is in the same direction as $\overline{\mathrm{p}_k}$), i.e.,

$$\cos\theta_{k\alpha} = \frac{E_{k\alpha}}{E_k}. \tag{20a}$$

In Eq.(20) we have set

and

$$\left.\begin{aligned} \varepsilon_{\alpha\beta}^{kl} &= \sum_{j=1}^{N_l} \Delta_{ij\alpha\beta}^{kl} \\ \sigma &= \frac{p^2}{kT}. \end{aligned}\right\} \tag{20b}$$

In the special case of face-centered and body-centered lattices,

$$\varepsilon_{\alpha\beta}^{kl} = 0 \quad \text{with} \quad \alpha \neq \beta,$$

so that the general expression (20) coincides with the condition

$$\frac{X_k \cos\theta_{k\beta}}{\sigma} = \sum_{l=1}^{n} \varepsilon_{\beta\beta}^{kl} \cos\theta_{\beta}^{l} \cdot L(X_l). \tag{21}$$

given by Takagi[3].

In an analogous fashion one can introduce the polarization, obtain the matrix of Lorentz factors, determine the Curie point in Eq.(21), and determine the phase transition to the disordered state, that is, investigate the ferroelectric and antiferroelectric states as was done by Takagi[3].

Conclusions

An investigation of the probability distribution function for the molecular orientation shows that the results of Kirkwood and Takagi can be obtained by solving the exact Eqs.(9) and (9a) with the approximation of Eq.(10).

In this approach to the problem no physical phenomena associated with taking into account correlations in the orientations of different molecules need be considered.

It follows from (10) that in the present case the ordered-disordered transition is equivalent to orientational "evaporation", rather than "melting," with the characteristic retention of the short-range order in the orientations above the transition point. In view of this, it would appear that (10) cannot be considered a good approximation for the molecular binary distribution function and particularly for molecules belonging to the same coordination group.

In those crystals in which the molecular interaction can be described in terms of dipole forces, the use of (10) precludes any relation between the orientation of a molecule and the internal field acting on it. The direction of the internal field in this case is determined entirely by the direction of the mean dipole moment in the given lattice. For this reason we do not consider here the effects of reactive self-interaction due to correlation between the internal field and the direction of the molecular axis.

We note in addition the following. From the formally mathematical point of view the rigorous Eqs.(9) and (9a), which pertain to short-range and long-range forces, respectively, differ only as regards their kernels. The solution of these equations in the no-correlation approximation leads to phase transitions which can be identified with orientational "melting"[2] and disordering of the ferroelectric or antiferroelectric structure.[3]

It now becomes possible to describe both phenomena in the framework of a single statistical model. This approach is logically valid, since experiment shows the qualitative resemblance of orientational "melting" to the disordering of the ferroelectric phase. This applies particularly to the temperature dependence of the dielectric constant, the structure changes at the transition point, the behavior of the specific heat, etc.[5-8]

This is especially noticeable in the temperature dependence of ϵ in crystals of the HCl type and in antiferroelectric substances such as $PbZrO_3$ and $ND_4D_2PO_4$. In both cases the transition to the ordered state is accompanied by a sharp drop in the dielectric constant.

The existing physical differences between ferroelectricity and orientation

"melting" may be due to the different nature of the forces responsible for the stable ordered structure. As may be seen from (9a) and has already been mentioned by Kirkwood[2], orientational order in HCl-type crystals is due to short-range forces, whereas the stability of the ferroelectric phase in ionic crystals is a result of the ordering influence of an internal field, the magnitude of which is determined primarily by long-range dipole forces. This obviously leads to the quantitative difference between the corresponding physical quantities.

We note that the rotating-molecule model cannot be considered satisfactory for describing ferroelectric effects in ionic crystals. The characteristics deduced from this model, however, do not restrict the generality of our conclusions, since an appropriate theory can be constructed also to describe disordering of ionic displacements.

In our opinion further work should be devoted to an investigation of Eqs.(8) and (8b) or their simpler forms (9) and (9b), in which the approximation of Eq.(10) is replaced by another expression which takes into account explicitly the correlation in molecular orientations. This will lead both to a clarification of the role of reactive self-interaction and possibly to a theoretical explanation of the short-range order persists at temperatures above the transition point.

In conclusion, I desire to thank G.A.Smolenskii and A.I.Ansel'm for many helpful remarks and valuable discussions.

Note added in proof:

After presentation of this report we became acquainted with the results obtained by A.E.Glauberman (L'vov University) and published in Doklady AN SSSR 108, 49 (1956).

The method proposed by Glauberman for solving the set of equations seems to us hardly applicable to the problem of a molecular crystal. The choice of a dipole gas model as the zeroth approximation, with the subsequent treatment of the intermolecular dipole forces as small perturbations in the first approximation, would presumably lead to results in the form of corrections to real "orientational" gases. This kind of approximation, of course, which describes the system at a temperature much above the Curie point, cannot lead to phase transitions such as occur in actual crystals. In addition, the condition that the orientational part of the internal energy be small compared with the energy of the dipole gas in the external field still requires physical proof. Therefore the choice of the multiplicative law for the distribution function in the zeroth approximation, which makes it possible to describe the intermolecular interaction in terms of an average self-consistent internal field, would seem to us to be more logical.

Institute of Semiconductors
of the Academy of Sciences of the USSR

References

1. N.N.Bogoliubov, Problemy dinamicheskoi teorii v statisticheskoi fizike (Dynamic theory problems in statistical physics) M.-L. 1946.
2. I.Kirkwood, J.Chem.Phys., 8,205 (1940).
3. Y.Takagi, Phys.Rev., 85, 315 (1952).
4. Ia.I.Frenkel', Statisticheskaia fizika (Statistical physics)M.-L. 1948.
5. G.Shirane, E.Sawaguchi & Y.Takagi, Phys.Rev., 84,476 (1951).
6. W.P.Mason & B.T.Matthias, Phys.Rev., 88,477 (1952).
7. N.Brown & R.Cale, J.Chem.Phys., 21,1383 (1953).
8. R.Swenson & R.Cole, J.Chem.Phys., 22, 284 (1954).

TOWARDS A THEORY OF HYSTERESIS IN $BaTiO_3$

- L.P.Kholodenko

In the present communication we shall consider hysteresis phenomena in an ideal single-domain crystal not subject to elastic stresses. Only experiment can tell whether the equations obtained are applicable to a real crystal.

The usual treatment of phase transitions is based on the idea that the transition from a phase A to a phase B takes place at a temperature such that $\Phi_A(p, T) = \Phi_B(p, T)$. This refers to the usual assertion that the experimentally observed phases of a crystal are states in which the thermodynamic potential Φ has an absolute minimum at certain values of p and T.

This can be illustrated by considering the variation of Φ as a function of an internal parameter ξ. Then if for given values of p and T the $\Phi(\xi)$ curve is of the form shown in Fig.1, the experimentally observed crystal state will be that corresponding to ξ_B. Let us now assume that as p and T are varied, the $\Phi(\xi)$ curve is deformed so that the minimum ξ_A becomes the deeper one. Under these conditions the experimentally observed state will be that corresponding to ξ_A. The transition takes place when $\Phi(\xi_A) = \Phi(\xi_B)$. This treatment is valid provided the relaxation time is short. If, however, the relaxation time is long then the system may remain for an appreciable time in a metastable state corresponding to a relative minimum.

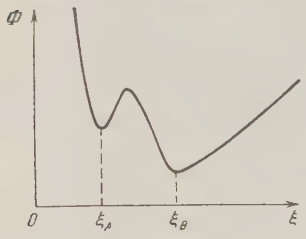

Fig.1. The thermodynamic potential Φ of a crystal as a function of an internal parameter ξ.

An evaluation of the relaxation time τ (which we shall not perform in the present paper) shows that it may indeed be quite large compared to the time of experimental observation of crystals. In other words, metastable states may play a significant role in $BaTiO_3$. Indeed, this is convincingly evinced by the presence of thermal hysteresis itself. In the usual treatment, however, thermal hysteresis is assumed not to occur.

In view of this, we have made an assumption which to some extent contradicts the usual one. We have assumed, namely, that the transition from phase B to phase A takes place only under those p, T conditions at which the minimum at ξ_B vanishes. In other words, the relaxation time τ is assumed to be infinitely large.

We must preface our calculations with a remark concerning the form of the thermodynamic potential Φ as a function of P_x, P_y, and P_z. It is known that terms up to the sixth order must be considered. Some authors, without giving any justification, take into account only one sixth order term (see, for instance, Devonshire[1]). There exist, however, three independent invariants in the case of cubic symmetry. When they are all included, the thermodynamic potential is written in the form

$$\Phi = \Phi_0 + \alpha P^2 + \frac{1}{2}\beta_1 P^4 + \beta_2 (P_x^2 P_y^2 + P_z^2 P_y^2 + P_z^2 P_x^2) + \frac{1}{3}\gamma_1 P^6 + \\ + \gamma_2 [P_x^4 (P_y^2 + P_z^2) + P_y^4 (P_z^2 + P_x^2) + P_z^4 (P_x^2 + P_y^2)] + \gamma_3 P_x^2 P_y^2 P_z^2. \qquad (1)$$

The minima of Φ are then given by the following conditions:

I. $$P_x^2 = P_y^2 = P_z^2 = 0 \qquad (2)$$

with the subsidiary condition

$$\alpha > 0. \tag{2a}$$

II. $$P_x^2 = P_y^2 = 0, \quad P_z^2 = P^2 \neq 0 \text{ and } \beta_1 P^2 + \gamma_1 P^4 + \alpha = 0 \tag{3}$$

with the subsidiary conditions

$$\beta_1 + 2\gamma_1 P^2 > 0 \tag{4}$$

$$\beta_2 + \gamma_2 P^2 > 0. \tag{5}$$

III. $$P_x^2 = P_y^2 \neq 0, \quad P_z^2 = 0 \text{ and } (\beta_1 + {}^1/_2 \beta_2) P^2 + (\gamma_1 + {}^3/_4 \gamma_2) P^4 + \alpha = 0 \tag{6}$$

with the subsidiary conditions

$$(\beta_1 + {}^1/_2 \beta_2) + 2(\gamma_1 + {}^3/_4 \gamma_2) P^2 > 0, \tag{7}$$

$$2\beta_2 + (\gamma_3 - \gamma_2) P^2 > 0, \tag{8}$$

$$\beta_2 + \gamma_2 P^2 < 0. \tag{9}$$

IV. $$P_x^2 = P_y^2 = P_z^2 \neq 0 \text{ and } (\beta_1 + {}^2/_3 \beta_2) P^2 + (\gamma_1 + {}^2/_3 \gamma_2 + {}^1/_9 \gamma_3) P^4 + \alpha = 0 \tag{10}$$

with the subsidiary conditions

$$(\beta_1 + {}^2/_3 \beta_2) + 2(\gamma_1 + {}^2/_3 \gamma_2 + {}^1/_9 \gamma_3) P^2 > 0, \tag{11}$$

$$3\beta_2 + \gamma_3 P^2 < 0. \tag{12}$$

From the point of view we are here developing (i.e., that $\tau = \infty$) the transition from phase I to phase II takes place when condition (2a) is no longer satisfied, i.e., when $\alpha = 0$. The reverse transition from II to I takes place either when $\beta_1 + 2\gamma_1 P^2 = 0$ or when $\beta_2 + \gamma_2 P^2 = 0$. Likewise the transitions between the other phases take place when one of the necessary and sufficient conditions for a minimum breaks down.

In order to determine uniquely which of the subsidiary conditions determines the temperature of a particular phase transition, we must know something about the temperature dependence of the coefficients α, β_1, β_2, γ_1, γ_2, and γ_3.

Ordinarily α is considered a linear function of the temperature, while the other coefficients are regarded as constants, although there seems to be no particular reason for this. In the present work β_1 and β_2 shall not be considered constants, but rather linear functions of the temperature. The coefficients γ_1, γ_2 and γ_3, however, will be considered constant. It should be noted that there is no a priori reason for this assumption. Since, however, one cannot assume that β_1 and β_2 are constants, the assumption made is the simplest. The inadmissibility of assuming all the coefficients other than α to be constants can be seen merely from the fact that the spontaneous polarization in phases III and IV is experimentally found to be virtually the same, whereas theory predicts an increase with decreasing temperature.

In order to explain the general pattern of the phase transitions, it is sufficient to assume that $\beta_1(T)$ monotonically falls off with rising temperature, and that $\beta_2(T)$ at the same time monotonically increases (with p = = const). The assumed linear temperature dependence of β_1 and β_2 makes it possible to deduce relatively simple expressions for finding the phase transition temperatures. Whether or not this is a sufficiently good approximation only experiments can show.

The derivatives $d\beta_1/dT$ and $d\beta_2/dT$, which are assumed to be constant, can be found from experiment in the following manner. As is known, P^2_{III} and P^2_{IV} are very weakly dependent on the temperature. Neglecting this dependence, i.e., assuming these quantities to be temperature independent, by differentiation of the second equations of (9) and (10) with respect to T we arrive at

$$\left(\frac{d\beta_1}{dT}+\frac{1}{2}\frac{d\beta_2}{dT}\right)P_{\mathrm{III}}^2+\frac{d\alpha}{dT}=0$$

and

$$\left(\frac{d\beta_1}{dT}+\frac{2}{3}\frac{d\beta_2}{dT}\right)P_{\mathrm{IV}}^2+\frac{d\alpha}{dT}=0.$$

These equations can be solved for $d\beta_1/dT$ and $d\beta_2/dT$. It is found that the former <0, while the latter >0. Their magnitudes can be easily found from experimental data.

In order to make use of the subsidiary conditions for the minima, we must know the signs of γ_1, γ_2, and γ_3.

The coefficient γ_1 must be considered positive. This is seen from the fact that if $\gamma_1<0$, then Φ would decrease without bound with increasing P (in the case of phase II) and this would mean that there exists a condition under which the crystal breaks up or disintegrates spontaneously. Since this is not observed experimentally, we must assume that $\gamma_1>0$. The coefficient γ_2 is also positive. This is evident from a comparison of the inequalities (5) and (9), which must be simultaneously fulfilled in the temperature range wherein both phase II and phase III can exist. One need only take account of the fact, known from experiment, that $P_{\mathrm{III}}^2>P_{\mathrm{II}}^2$.

Further, for consistence with the character of experimentally observed phase transitions, one must assume that $\gamma_3<0$.

Under these conditions we obtain the succession of phases shown in Fig.2. Let us assume that T decreases from a high value. Then at the temperature T_{12} at which $\alpha = 0$ there occurs the first high-temperature transition to phase II. As the temperature is further decreased the transition to phase III takes place at T_{23} given by $\beta_2(T_{23})+\gamma_2P_{\mathrm{II}}^2(T_{23})=0$. Still lower, we arrive at T_{34}, given by $2\beta_2(T_{34})+(\gamma_3-\gamma_2)P_{\mathrm{III}}^2(T_{34})=0$, at which there is a transition to phase IV. With rising temperature, the transition from phase IV to phase III takes place at T_{43}, the temperature satisfying the equation

$$3\beta_2(T_{43})+\gamma_3P_{\mathrm{IV}}^2(T_{43})=0.$$

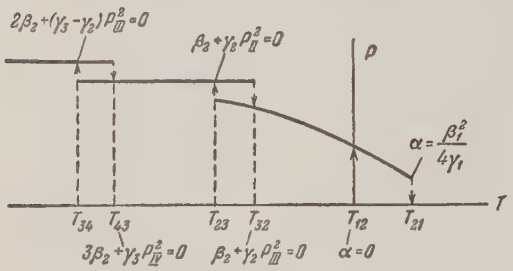

Fig.2. The temperature dependence of the spontaneous polarization of a barium titanate single crystal in all successive phases.

Continuing the temperature increase, we arrive at the transition point T_{32}, given by $\beta_2(T_{32})+\gamma_2P_{\mathrm{III}}^2(T_{32})=0$.

A further increase of the temperature brings us to the transition to phase I at T_{21}, which satisfies the equation $\beta_1P_{\mathrm{II}}^2+2\gamma_1P_{\mathrm{II}}^4=0$.

If this is a second order phase transition, then P = 0 and the temperature T_{21} obtained from this last equation is the same as T_{12}. If it is a first order phase transition, we have

$$\alpha(T_{21})=\frac{\beta_1^2(T_{21})}{4\gamma_1}.$$

Assuming the linear dependence of α, β_1 and β_2, the above equations can be used in conjunction with the experimental values of the transition point temperatures and polarizations at these points to find the values of γ_1, γ_2, and γ_3 as well as β_1 and β_2 at some of these points. Since the values of $d\beta_1/dT$ and $d\beta_2/dT$ can also be found (as has already been mentioned above),

$\beta_1(T)$ and $\beta_2(T)$ are known for arbitrary temperatures (the number of unknowns is six, which is equal to the number of transition points).

One can calculate the temperature dependence of the dielectric constant in the vicinity of the phase transition points. Since the temperature dependence near the Curie point is well known for the case of second order phase transitions, we shall mention only some results obtained for a first order transition. It is found that on approaching T_{12} from above (i.e., from the high-temperature side), the usual Curie-Weiss law

$$\varepsilon = \frac{C_{12}}{T - T_{12}} .$$

holds.

On approaching T_{21} from the low temperature side, there is a singularity only in the longitudinal component $\varepsilon_{\parallel}$. This is given by

$$\varepsilon_{\parallel} = \frac{C_{21}}{(T_{21} - T)^{1/2}} .$$

We also find that this singularity obtains only in the case of isothermal polarization and vanishes in the case of adiabatic polarization. Separate components of the ε_{ik} tensor have singularities also at other transition points. Thus, on approaching T_{23} from above, we find that $\varepsilon_{\perp}$ satisfies the Curie-Weiss law. On approaching T_{32} from below, the principal component of the ε'_{ik} tensor which has a singularity is that corresponding to the Y' direction (see Fig.3). This component ε'_{yy} satisfies the Curie-Weiss law (with its own constant). On approaching T_{34} from above, on the other hand, ε'_{zz} and ε'_{yy} have no singularities, but ε'_{xx} obeys the Curie-Weiss law. Finally, on approaching T_{43} from below, it is found that both the principal transverse components ε'_{xx} and ε'_{yy} conform to the Curie-Weiss law. The longitudinal component ε'_{zz} has no singularities (see Fig.4).

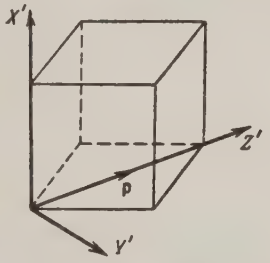

Fig.3. Directions of the X', Y' and Z' axes in the orthorhombic phase.

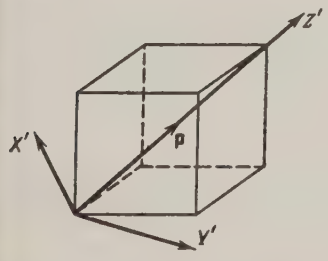

Fig.4. The directions of the X', Y' and Z' axes in the rhombohedral phase.

Having concluded our consideration of thermal hysteresis, let us now turn to ordinary dielectric hysteresis. In these calculations, too, we did not take into account domain structure. As opposed to what happens in the case of thermal hysteresis, however, the domain structure should be of great importance in this case. Nevertheless it is found that a qualitatively correct description of the experimentally observed facts can be obtained theoretically even without considering the domain structure. We are speaking here of the way the hysteresis loops change with temperature, an effect that has been experimentally investigated by Merz.[2]

Restricting ourselves to the temperature region above T_{32}, the thermodynamic potential can be written

$$\Phi = \Phi_0 + \alpha P^2 + \frac{1}{2}\beta_1 P^4 + \frac{1}{3}\gamma_1 P^6 - PE;$$

where, as previously, it is understood that we are dealing with an ideal crystal not subject to elastic stresses.

Inasmuch as analysis of second order transitions leads to results that are already given in the literature, we shall limit our examination here to the case of a first order transition. We assume, therefore, that $\beta_1 < 0$ and $\gamma_1 > 0$. Let us introduce the dimensionless variables

$$p = \sqrt{\frac{-\gamma_1}{\beta_1}}\, P \quad \text{and} \quad e = \frac{1}{2} \cdot \frac{\gamma_1^{3/2}}{(-\beta_1)^{5/2}} E$$

and write $\alpha\gamma_1 / \beta_1^2 = \xi$ and $\frac{\Phi - \Phi_0}{\beta_1^3}\gamma_1^2 \equiv \varphi$. In these variables the dimensionless potential φ is of the form

$$\varphi = \frac{1}{3} p^6 - \frac{1}{2} p^4 + \xi p^2 - 2pe.$$

The condition for thermodynamic equilibrium in the crystal is

$$\frac{\partial \varphi}{\partial p} = 0 \quad \text{or} \quad p^5 - p^3 + p\xi = e$$

with the subsidiary condition $\frac{\partial^2 \varphi}{\partial p^2} > 0$.

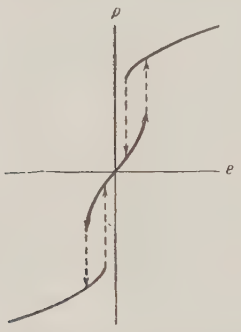

Fig.5. Double hysteresis loop.

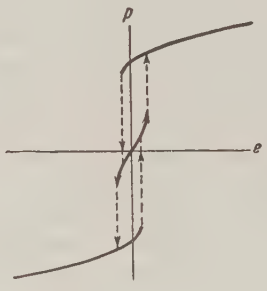

Fig.6. Hysteresis loop of the transitional type $(0{,}2 < \xi < 0{,}25)$

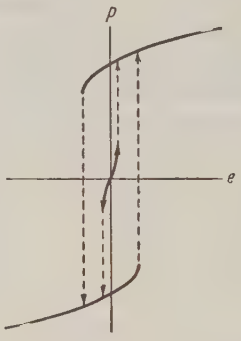

Fig.7. Normal hysteresis loop $(0 < \xi < 0{,}2)$

An investigation of the expression for φ by a combination of graphic and analytic methods leads to the following conclusions.

1) For $\xi > 9/20$, there is no hysteresis and $p(e)$ is nonlinear.

2) In the interval $0.25 < \xi < 0.45$, i.e., in an interval approximately equal to the interval of temperature hysteresis, the hysteresis loops are double (see Fig.5). It is interesting that there exists a region of small values of e in which the variation is reversible (in this region p is a nonlinear function of e, although the nonlinearity is minor).

3) In the narrow interval $0.2 < \xi < 0.25$ the hysteresis loops are of a transitional form - see Fig.6 (a region of reversible small values of p persists).

4) In the interval $0 < \xi < 0.2$ the hysteresis loops have the conventional form, but the reversible region of small values of p still remains (Fig.7). When $\xi < 0$, the hysteresis loop is qualitatively similar to that shown in Fig.6, but has no reversible region.

References

1. A.F.Devonshire, Adv. in Phys., 3, 85 (1954).
2. W.Merz, Phys. Rev., 91, 513 (1953).

RELATION BETWEEN THE DIELECTRIC, PIEZOELECTRIC AND ELASTIC PROPERTIES OF POLYCRYSTALLINE CERAMIC AND THOSE OF A SINGLE CRYSTAL

- S.V.Bogdanov, B.M.Vul and A.M.Timonin

1. Most ferroelectric substances of practical importance are now prepared, both for research and for engineering applications, in the form of polycrstalline specimens (or components) whose properties represent in some sort the averaged properties of the microcrystals composing the polycrystalline aggregate. It is therefore of interest to have expressions relating the parameters of polycrystalline ceramics with the corresponding parameters of the constituent single crystals. Shirobokov, Adirovich, and the authors of the present article[1] have treated this problem as it applies to ferroelectric ceramics. At the First All-Soviet Conference on Piezoelectricity in 1952 we presented certain conclusions based on our results to that date.

The different authors cited above, however, approached this problem in somewhat different ways, although they used approximately the same premises and assumptions. In addition, each property was treated and calculated separately. In the present article we propose a general method for calculating the dielectric constant tensor, the piezoelectric modulus tensor and the elastic constant tensor of the polycrystalline material in terms of the corresponding characteristics of the single crystal. This is done by averaging the piezoelectric transducer equations, and is thus a generalization of earlier contributions referred to above. The expressions obtained can be used to evaluate the properties both of "polarized" and unpolarized ceramics.

2. The equations relating the elastic, dielectric and piezoelectric properties of a piezoelectric substance can be written in tensor notation in the form

$$\xi_{ij} = S^E_{ijkl}\sigma_{kl} - d_{mij}E_m \tag{1}$$

and

$$D_n = \varepsilon^\sigma_{mn}E_m - 4\pi d_{nkl}\,\sigma_{kl}, \tag{2}$$

where $i, j, k, l, m,$ and n take on the values 1, 2, and 3, and the summation convention is used. In these equations ξ_{ij} is the strain tensor, S^E_{ijkl} is the compliance coefficient tensor at zero field, σ_{kl} is the mechanical stress tensor, d_{mij} is the piezoelectric coefficient tensor, E_m is the electric field, D_n is the electric induction, and ε^σ_{mn} is the dielectric constant tensor in the absence of mechanical stress.

These equations are applicable both to each individual single crystal making up the polycrystalline sample and to the ceramic as a whole. At the same time the macroscopic quantities characterizing the ceramic will be averages, taken over the whole ceramic, of their values for the separate single crystals.

Let $\xi'_{ij}(\vartheta, \varphi, \psi)$ denote the deformation tensor of a single crystal, where $\vartheta, \varphi,$ and ψ are the Euler angles giving the orientation of the single-crystal principal coordinate system with respect to a coordinate system fixed in the ceramic. Then the deformation of the ceramic is given by

$$\xi_{ij} = \frac{\iiint \xi'_{ij}(\vartheta, \varphi, \psi)\, f(\vartheta, \varphi, \psi) \sin\vartheta \, d\vartheta d\varphi d\psi}{\iiint \sin\vartheta \, d\vartheta d\varphi d\psi}, \tag{3}$$

where $f(\vartheta, \varphi, \psi)$ is the Euler-angle distribution function of ξ'_{ij}.

The polycrystalline sample consists of randomly oriented single crystals, so that $f(\vartheta, \varphi, \psi) = 1$, and the Euler angles of the single crystals lie in the

intervals

$$0 \leqslant \vartheta \leqslant \pi; \quad 0 \leqslant \varphi \leqslant 2\pi; \quad 0 \leqslant \psi \leqslant 2\pi.$$

To be specific let us deal with barium titanate. If $BaTiO_3$ ceramic is subjected to a dc electric field of sufficient strength, it is "polarized", which means that the polar axes of the single crystals take on a certain orientation.* Then these axes will lie within a certain solid angle Ω whose magnitude is determined by the polarization mechanism. The maximum Euler angle ϑ will then no longer be π, but some smaller angle θ. If in the process of polarization a polar axis of a single crystal can be rotated only through a certain limited angle, the angular distribution within the solid angle Ω will be homogeneous after polarization as well, i.e., with $\vartheta > \theta$, we have $f(\vartheta, \varphi, \psi) = 0$, and with $\vartheta < \theta$, $f(\vartheta, \varphi, \psi) = 1$.

With the above considerations in mind, Eq. (3) for a polarized ceramic becomes

$$\xi_{ij} = \frac{1}{4\pi^2 (1-\cos\theta)} \iiint \xi'_{ij}(\vartheta, \varphi, \psi) \sin\vartheta \, d\vartheta d\varphi d\psi. \tag{4}$$

Let us express the deformation $\xi'_{ij}(\vartheta, \varphi, \psi)$ of a single crystal in terms of the mechanical stress σ'_{kl} and electric field E'_m applied to it. According to (1) we have

$$\xi'_{ij} = S'^{E}_{ijkl} \sigma'_{kl} - d'_{mij} E'_m,$$

Then the deformation of the ceramic is given by

$$\xi_{ij} = \frac{1}{4\pi^2 (1-\cos\theta)} \left[\iiint S'^{E}_{ijkl} \sigma'_{kl} \sin\vartheta \, d\vartheta d\varphi d\psi - \iiint d'_{mij} E'_m \sin\vartheta \, d\vartheta d\varphi d\psi \right]. \tag{5}$$

The compliance coefficient S'^{E}_{ijkl} and the piezoelectric coefficient d'_{mij} are written in the coordinate system fixed in the ceramic. For our purposes it is more convenient to write them in terms of their components in the principal coordinate system of the single crystal. If these components are S^{*E}_{pqrs} and d^{*}_{npq}, then

$$S'^{E}_{ijkl} = \alpha_{ip}\alpha_{jq}\alpha_{kr}\alpha_{ls} S^{*E}_{pqrs}$$

and (6)

$$d'_{mij} = \alpha_{mn}\alpha_{ip}\alpha_{jq} d^{*}_{npq},$$

where the α's are the elements of the transformation matrix from the single-crystal principal coordinate system to the coordinate system fixed in the ceramic. These matrix elements are the cosines of the angles between the axes of these systems, according to

	x_1	x_2	x_3
x_1'	α_{11}	α_{12}	α_{13}
x_2'	α_{21}	α_{22}	α_{23}
x_3'	α_{31}	α_{32}	α_{33}

---

*To be more accurate, one should speak of the polar axes of the crystal domains. This refinement would not, however, affect the following argument.

where the primed axes are those fixed in the ceramic, and the unprimed ones are the principal axes of the single crystal.

Inserting (6) into (5), we obtain

$$\xi_{ij} = \frac{1}{4\pi^2(1-\cos\theta)}\left[\iiint \alpha_{ip}\alpha_{jq}\alpha_{kr}\alpha_{ls}S^{*E}_{pqrs}\sigma'_{kl}\sin\vartheta\, d\vartheta d\varphi d\psi - \iiint \alpha_{mn}\alpha_{ip}\alpha_{jq}d^{*}_{npq}E'_m\sin\vartheta\, d\vartheta d\varphi d\psi\right], \quad (7)$$

where the direction cosines α_{ij} are related to the Euler angles by the familiar expressions

$$\left.\begin{aligned}
\alpha_{11} &= \cos\vartheta\cos\varphi\cos\psi - \sin\varphi\sin\psi,\\
\alpha_{21} &= -(\cos\vartheta\cos\varphi\sin\psi + \sin\varphi\cos\psi),\\
\alpha_{31} &= \sin\vartheta\cos\varphi,\\
\alpha_{12} &= \cos\vartheta\sin\varphi\cos\psi + \cos\varphi\sin\psi,\\
\alpha_{22} &= -\cos\vartheta\sin\varphi\sin\psi + \cos\varphi\cos\psi,\\
\alpha_{32} &= \sin\vartheta\sin\psi,\\
\alpha_{13} &= -\sin\vartheta\cos\psi,\\
\alpha_{23} &= \sin\vartheta\sin\psi,\\
\alpha_{33} &= \cos\vartheta.
\end{aligned}\right\} \quad (8)$$

Thus in order to find how an external mechanical stress σ_{kl} and electric field E_m deform the ceramic, we must use them to describe the stress σ'_{kl} and field E'_m acting on each microcrystal. This, however, involves certain difficulties. In fact, in the preparation of a ceramic there may arise local internal stresses σ^{in}_{kl} which, in turn, cause local internal electric fields E^{in}_m due to the piezoelectric effect in the single crystals. It is true, of course, that in time the electric conductivity of the ceramic causes these fields to vanish, but the internal stresses will remain. Therefore the mechanical stress acting on each single crystal will be the sum of the external and internal stresses, so that we may write

$$\sigma'_{kl} = \sigma_{kl} + \sigma^{in}_{kl}.$$

If, however, the internal stresses do not change when an external stress is applied, then up to the elastic limit they may be neglected, for they produce only a certain initial deformation to the ceramic. In addition, the field acting on a given microcrystal may not be equal to the mean field, i.e., to the field acting on the ceramic as a whole. Nevertheless, if the internal stresses do not change when an external field is applied, and the dimensions of the individual microcrystals are much greater than of the molecular order, then in the first approximation one may assume that the field acting on a given microcrystal is equal to the applied field, i.e., that $E_m = E'_m$.

Under these assumptions Eq.(7) becomes

$$\xi_{ij} = \left[\frac{1}{4\pi^2(1-\cos\theta)}\iiint \alpha_{ip}\alpha_{jq}\alpha_{kr}\alpha_{ls}S^{*E}_{pqrs}\sin\vartheta\, d\vartheta d\varphi d\psi\right]\sigma_{kl} - \left[\frac{1}{4\pi^2(1-\cos\theta)}\iiint \alpha_{mn}\alpha_{ip}\alpha_{jq}d^{*}_{npq}\sin\vartheta\, d\vartheta d\varphi d\psi\right]E_m. \quad (9)$$

If we now compare (1) and (9), we obtain the following equations for the compliance and piezoelectric coefficients of the ceramic:

$$S^{E}_{ijkl} = \frac{1}{4\pi^2(1-\cos\theta)}\iiint \alpha_{ip}\alpha_{jq}\alpha_{kr}\alpha_{ls}S^{*E}_{pqrs}\sin\vartheta\, d\vartheta d\varphi d\psi \quad (10)$$

and

$$d_{mij} = \frac{1}{4\pi^2(1-\cos\theta)} \iiint \alpha_{mn}\alpha_{ip}\alpha_{jq} d^*_{npq} \sin\vartheta \, d\vartheta d\varphi d\psi. \tag{11}$$

Eq.(2) can be used in an analogous fashion to obtain the dielectric constant of the ceramic:

$$\varepsilon^{\sigma}_{mn} = \frac{1}{4\pi^2(1-\cos\theta)} \iiint \alpha_{mp}\alpha_{nq}\varepsilon^{*\sigma}_{pq} \sin\vartheta \, d\vartheta d\varphi d\psi. \tag{12}$$

Utilizing Eq.(8), we can now perform the simple integrations necessary for each specific type of microcrystal composing the given ceramic. In particular, for barium titanate Eqs.(10), (11), and (12) give

$$\begin{aligned} S^E_{11} = \frac{1}{1-\cos\theta} \Big\{ & S^{*E}_{11}(0{,}4 - 0{,}056\cos^5\theta - 0{,}062\cos^3\theta - 0{,}28\cos\theta) + \\ & + (2S^{*E}_{12} + S^{*E}_{66})\left(\frac{1}{15} 0{,}0125\cos^5\theta - 0{,}01\cos^3\theta - 0{,}047\cos\theta\right) + \\ & + 2(2S^{*E}_{13} + S^{*E}_{44})\left(\frac{1}{15} + 0{,}0375\cos^5\theta - 0{,}042\cos^3\theta - 0{,}0625\cos\theta\right) + \\ & + S^{*E}_{33}(0{,}2 - 0{,}075\cos^5\theta + 0{,}25\cos^3\theta - 0{,}375\cos\theta)\Big\}, \end{aligned} \tag{13}$$

$$\begin{aligned} S^E_{33} = \frac{1}{1-\cos\theta} \Big\{ & S^{*E}_{11}(0{,}4 - 0{,}15\cos^5\theta + 0{,}5\cos^3\theta - 0{,}75\cos\theta) + \\ & + (2S^{*E}_{12} + S^{*E}_{66})\left(\frac{1}{15} - 0{,}025\cos^5\theta + 0{,}083\cos^3\theta - 0{,}125\cos\theta\right) + \\ & + 2(2S^{*E}_{13} + S^{*E}_{44})\left(\frac{1}{15} + 0{,}1\cos^5\theta - 0{,}167\cos^3\theta\right) + S^{*E}_{33}(0{,}2 - 0{,}2\cos^5\theta)\Big\}, \end{aligned} \tag{14}$$

$$d_{33} = \frac{1}{4}(1+\cos\theta)\{(1+\cos^2\theta)d^*_{33} + \sin^2\theta(d^*_{31} + d^*_{15})\}, \tag{15}$$

$$d_{31} = d_{32} = \frac{1}{8}(1+\cos\theta)\{\sin^2\theta(d^*_{33} - d^*_{15}) + (4 - \sin^2\theta)d^*_{31}\}, \tag{16}$$

$$d_{15} = d_{24} = \frac{1}{4}(1+\cos\theta)\{\sin^2\theta(d^*_{33} - d^*_{31}) + (1+\cos^2\theta)d^*_{15}\}, \tag{17}$$

$$\varepsilon^{\sigma}_{11} = \varepsilon^{\sigma}_{22} = \frac{1}{6}[(4 + \cos\theta + \cos^2\theta)\varepsilon^{*\sigma}_{11} + (2 - \cos\theta - \cos^2\theta)\varepsilon^{*\sigma}_{33}], \tag{18}$$

$$\varepsilon^{\sigma}_{33} = \frac{1}{3}[(2 - \cos\theta - \cos^2\theta)\varepsilon^{*\sigma}_{11} + (1 + \cos\theta + \cos^2\theta)\varepsilon^{*\sigma}_{33}]. \tag{19}$$

From the equations obtained it is seen that in the case of a nonpolarized ceramic ($\theta = \pi$)

$$\left.\begin{aligned} & d_{33} = d_{31} = d_{32} = d_{15} = d_{24} = 0, \qquad \varepsilon^{\sigma}_{11} = \varepsilon^{\sigma}_{22} = \varepsilon^{\sigma}_{33} = \frac{1}{3}(2\varepsilon^{*\sigma}_{11} + \varepsilon^{*\sigma}_{33}), \\ & S^E_{11} = S^E_{33} = \frac{1}{15}[6S^{*E}_{11} + 3S^{*E}_{33} + 2(2S^{*E}_{13} + S^{*E}_{44}) + (2S^{*E}_{12} + S^{*E}_{66})]. \end{aligned}\right\} \tag{20}$$

As has already been mentioned, θ is determined by the polarization mechanism. If in the polarization process the polar axis of a microcrystal can change by 90°, then $\theta = 55°$. If its orientation can change only by 180°, then $\theta = 90°$. From an examination of Eqs.(13), (14), (18) and (19) it will be evident that if $\theta = 90°$, then in the polarized ceramic we will have $S^E_{11} = S^E_{33}$ and $\varepsilon^{\sigma}_{11} = \varepsilon^{\sigma}_{33}$, that is there should be no anisotropy of either the compliance coefficients or the dielectric constant.

On the other hand, if $\theta = 55°$, anisotropy of the elastic and dielectric properties should be evident.

For these two values of θ, Eqs. (15), (16) and (17) become

$$\left.\begin{aligned} d_{33} &= 0{,}25\,(d^*_{33} + d^*_{31} + d^*_{15}),\\ d_{31} &= 0{,}125\,(d^*_{33} + 3\,d^*_{31} - d^*_{15}),\\ d_{15} &= 0{,}25\,(d^*_{33} - d^*_{31} + d^*_{15}), \end{aligned}\right\} \quad (21) \qquad \left.\begin{aligned} d_{33} &= 0{,}26\,(2\,d^*_{33} + d^*_{31} + d^*_{15})\\ d_{31} &= 0{,}13\,(d^*_{33} + 5\,d^*_{31} - d^*_{15}),\\ d_{15} &= 0{,}26\,(d^*_{33} - d^*_{31} + 2d^*_{15}). \end{aligned}\right\} \quad (22)$$

($\theta = 90°$ for (21); $\theta = 55°$ for (22))

These equations can be used to determine the piezoelectric coefficients of a single crystal when the piezoelectric coefficients of the ceramic are known.

According to our data, the coefficients of barium titanate ceramic are

$$d_{33} \approx 4{,}0\cdot 10^{-6}, \quad d_{31} \approx -1{,}5\cdot 10^{-6}, \quad d_{15} \approx 5{,}5\cdot 10^{-6}.$$

Then (21) gives

$$d^*_{33} \approx 8{,}0\cdot 10^{-6}, \quad d^*_{31} \approx -3{,}0\cdot 10^{-6}, \quad d^*_{15} \approx 11{,}0\cdot 10^{-6};$$

and (22) gives

$$d^*_{33} \approx 5{,}1\cdot 10^{-6}, \quad d^*_{31} \approx -1{,}9\cdot 10^{-6}, \quad d^*_{15} \approx 7{,}0\cdot 10^{-6}.$$

According to data in the literature[2], the piezoelectric coefficients of barium titanate single crystals are

$$d^*_{33} = 9{,}5\cdot 10^{-6} \quad \text{and} \quad d^*_{31} = -3{,}1\cdot 10^{-6}. \qquad (23)$$

It is thus seen that Eqs. (21) give much better agreement with experiment than do (22). From this one may conclude that the polar axes of the single crystals primarily flip 180° in the polarization process.

In conclusion, it should be noted that Eqs. (10)-(12) may lead one to believe that the number of independent constants among S^E_{ijkl}, d_{mij} and ε^σ_{mn} of a ceramic is determined by the symmetry of the microcrystals comprising it, i.e., by the number of independent constants among S^{*E}_{ijkl}, d^*_{mij} and $\varepsilon^{*\sigma}_{mn}$. This, however, is incorrect, since the number of these independent constants for the ceramic is determined by the macroscopic symmetries of the ceramic itself.

Thus, in particular, an unpolarized ceramic is an isotropic body, but a polarized ceramic belongs to the point symmetry group $\infty\cdot m$. This will determine the number of independent constants among S^E_{ijkl}, d_{mij} and ε^σ_{mn} of a ceramic, regardless of the symmetry of the constituent microcrystals.

"P.N.Lebedev" Physical Institute of the
Academy of Sciences of the USSR

References

1. B.M.Vul, Vestnik informatsii (Information bulletin) BNT MV, 3, 15 (1951); M.Ia.Shirobokov, Otchet (Report) GFTI, 1951; E.I.Adirovich, Otchet (Report) FIAN 1951.

2. W.L.Bond, W.P.Mason & H.J.McSkimin, Phys.Rev., 82, 442 (1951).

NONLINEAR PROPERTIES OF FERROELECTRICS

- B.M.Vul

Introduction

The dielectric constant of a substance is given by the expression

$$\varepsilon = 1 + 4\pi \frac{P}{E}, \tag{1}$$

where P is the polarization per unit volume and E is the electric field strength.

In ordinary dielectrics, as has been shown by experiment, the polarization is proportional to the field intensity up to values close to the breakthrough field. Inasmuch as the electrostriction in such dielectrics is small, the capacitance of capacitors in which they are used is independent of the voltage.

In contrast, in ferroelectric materials E and P are not linearly related (which is why spontaneous polarization may arise in ferroelectrics[1]). Usually as the first approximation the relation between E and P in the region close to the Curie point is taken as

$$E = 2\alpha P + 2\beta P^3, \tag{2}$$

where α and β are coefficients dependent on the temperature and pressure.[2]

For the purpose of determining the coefficient β, which is quantitative measure of the nonlinearity, we carried out measurements of the equivalent and reversible values of the dielectric constant above Curie point.

The measurements of the former quality were made on a Schering bridge at a frequency of 50 cps. In the case of an applied ac voltage, the current flowing through a nonlinear capacitor comprises, in addition to the fundamental, a number of higher harmonics. The measuring set-up, i.e., the bridge or resonant circuit, separates out the fundamental. Hence the results obtained in this case give the capacitance value that is equivalent to that measurable at the fundamental frequency and the given voltage. The value of ϵ determined in this manner is termed the equivalent dielectric constant for the given method of measurement.

The reversible dielectric constant was measured at a low amplitude of an ac signal superposed on a biasing dc voltage.

Measurement of the equivalent dielectric constant

Since $\epsilon \gg 1$, it follows from (1) and (2) that

$$\frac{E}{2P} = \frac{2\pi}{\varepsilon} = \alpha + \beta P^2. \tag{3}$$

The results for one of the samples, obtained at 9° above the Curie point, are shown in Fig.1 in the form of curves of $2\pi/\epsilon = f(P^2)$. The Curie point of this specimen was $\theta = 111°$; the measurements were made at 120°.

The polarization P was determined on the basis of the measured values of the capacitance C at different voltages V, according to the expression

$$P = CV/S$$

where S is the cross sectional area of the specimen.

It is evident from the results shown in Fig.1 that under the given conditions Eq.(1) is a sufficiently good approximation. Field strengths of up to 30 kv/cm were used in the tests.

As may be seen from the data, the nonlinearity coefficient for polycrystalline barium titanate ($\theta = 111^{\circ}$) at 120° is $2.3 \cdot 10^{-12}$ cgse units.

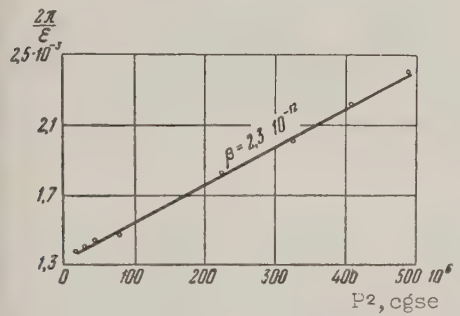

Fig.1. Variation of $2\pi/\epsilon$ with P^2 as determined by measurements at a frequency of 50 cps (ϵ is the equivalent dielectric constant).

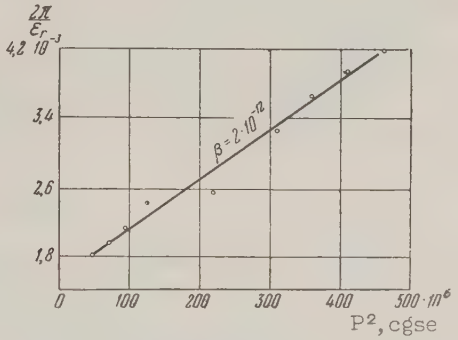

Fig.2. Same as Fig.1, but for the reversible dielectric constant ϵ_r.

Measurements at different temperatures showed that the coefficient β decreases with rising temperature above the Curie point. At temperatures appreciably higher than the Curie point, β tends to zero and the nonlinearity vanishes.

Measurement of the reversible dielectric constant

Above the Curie point, the reversible dielectric constant ϵ_r by definition is

$$\varepsilon_r = 1 + 4\pi \frac{dP}{dE} \approx 4\pi \frac{dP}{dE}. \tag{4}$$

Utilizing (2), we find

$$\frac{4\pi}{\varepsilon_r} = 2\alpha + 6\beta P^2. \tag{5}$$

Let us denote the dielectric constant at minimal fields, i.e., when $E \to 0$, by ϵ_0. Inasmuch as above the Curie point, when $E = 0$, the polarization P is also zero, we have

$$\alpha = \frac{2\pi}{\varepsilon_0}. \tag{6}$$

Substituting (6) in (5), we get

$$\frac{2\pi}{\varepsilon_r} = \frac{2\pi}{\varepsilon_0} + 3\beta P^2. \tag{7}$$

Through measurements of the reversible constant ϵ_r when the amplitude of the signal is very low compared with the biasing dc voltage one can obtain the value of the polarization P from (2).

Invoking (2) and (7), we find

$$P = \frac{3E}{4\pi\left(\frac{1}{\varepsilon_r} + \frac{2}{\varepsilon_0}\right)}.$$

Thus, knowing ϵ_r and having measured ϵ_o, we can readily calculate P. The results of our measurements of ϵ_r in the form of the functional dependence of $2\pi/\epsilon_r$ on P^2 are shown in Fig.2.

The nonlinearity coefficient β can also be evaluated from these data. On the basis of our measurements, for the same sample and temperature (120^o), we found $\beta = 2.10^{12}$ cgse units. This value differs by about 15% from that obtained on the basis of the equivalent dielectric constant measurements.

Conclusions

The nonlinear properties of ferroelectric ceramics above the Curie point can be quantitatively characterized by the coefficient β, i.e., the factor at P^3 in an expansion of the field strength E in powers of the polarization P. The numerical value of this coefficient can be found by measuring the equivalent or reversible dielectric constant.

I.M.Gol'dman participated in the work.

"P.N.Lebedev" Physical Institute of the
Academy of Sciences of the USSR

References

1. I.V.Kurchatov, Segnetoelektriki (Ferroelectrics), M.-L. 1933.
2. V.L.Ginzburg, Usp.fiz.nauk, 38, 490 (1948).

BEHAVIOR OF CERTAIN FERROELECTRICS IN STRONG ELECTRIC FIELDS

- V.A.Bokov

Sometime after Vul and Gol'dman established that barium titanate is ferroelectric, they also showed that its dielectric constant depends on the intensity of the applied electric field. Nonlinear capacitors of barium titanate and its solid solutions are already coming into use in the electronic industry for dielectric amplifiers, frequency multipliers and frequency modulators. Hence investigations of the behavior of these ferroelectrics in strong electric fields are of practical as well as of purely scientific interest.

The present work is a continuation of the extensive investigation of $(Ba,Sr)TiO_3$, $Ba(Ti,Sn)O_3$ and $Ba(Ti,Zr)O_3$ solid solutions initiated some time ago in the laboratory of G.A.Smolenskii.

The solid solution specimens were prepared by the usual procedure from the carbonates and oxides of the corresponding elements and were virtually free of surface porosity. «Ч» ("Pure") and «ЧДА» ("Pure for Analysis") grade reagents were used. We determined the temperature dependences of the total polarization, coercive force and hysteresis loss per cycle for a number of solid solution specimens. These quantities were evaluated from the hysteresis loops recorded at a frequency of 50 cps and a field strength of 25 kv/cm (here and below the voltages given are RMS values).

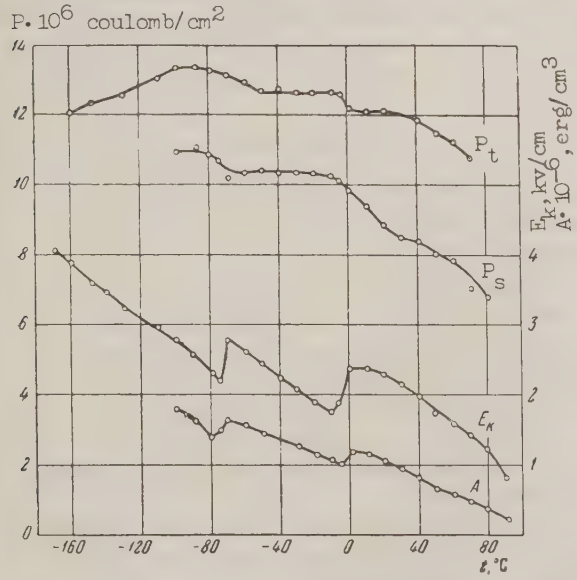

Fig.1. Temperature dependences of the coercive force (E_k), hysteresis loss per cycle (A), total polarization (P_t) and spontaneous polarization (P_s) for the $(Ba_{0.9},Sr_{0.1})TiO_3$ solid solution.

By way of illustration the dependences obtained for the $(Ba_{0.9},Sr_{0.1})TiO_3$ solid solution are reproduced in Fig.1.

The coercivity and the hysteresis loss decrease at the transitions from the tetragonal to the orthorhombic phase and from the orthorhombic to the rhombohedral; within each phase they increase with decreasing temperature. These results are in quantitative agreement with those obtained by Wieder[1] in analogous experiments with barium titanate single crystals and with the theory of Devonshire[2] which, according to the calculations of Wieder, leads to an analogous dependence for the coercive force. The decrease in coercive force and hysteresis loss in going from a phase of higher to a phase of lower symmetry may be connected with a decrease in the value of the elastic coefficients incident to the phase transitions and the associated decrease in energy (part of the energy is expended on mechanical deformations connected with reorientation of the domains).

The total polarization, as may be seen from Fig.1, increases in going from the tetragonal to the orthorhombic and from the orthorhombic to the rhombohedral modifications. The spontaneous polarization, as determined from the hysteresis loops, shows an analogous dependence. It is known from the

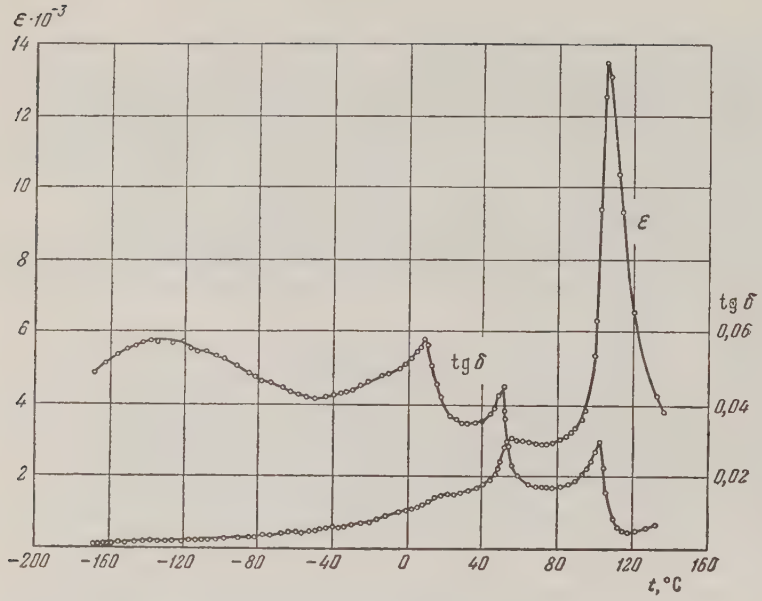

Fig.2. Temperature dependences of ϵ and tan δ of $Ba(Ti_{0.95},Zr_{0.05})O_3$ solid solution at E = 20 v/cm and f = 1 kc.

work of Merz[3] and Wieder[4] that the value of the spontaneous polarization of barium titanate single crystals does not change in going through the phase transitions. Hence the increase in the spontaneous polarization of polycrystalline specimens at the low temperature transitions is apparently connected with the fact that in the orthorhombic phase the domains can be oriented to a greater extent by an equal field than in the tetragonal phase, and in the rhombohedral phase to a greater extent than in the orthorhombic (naturally the comparison applies to temperatures not too far from the transition point).

By virtue of the fact that at the phase transitions there is observed a sharp change in the coercive force and, according to the data of Wieder[4], also a change in the mobility of the domains, in polycrystalline specimens in weak fields as the phase transition points are approached from the side of low temperatures the number of orienting domains increases and then with the transition to a phase of higher symmetry sharply falls off. This leads to the appearance of maxima in the loss tangent curve at the phase transitions and to the absence of abrupt changes in the value of the dielectric constant (Fig.2), although such changes might be expected from the temperature dependence of the dielectric constant of single domain crystals.

In addition to investigating the hysteresis loops of the above mentioned solid solutions we determined the variation of the dielectric constant with the field strength at room temperature as well as the temperature dependence of the dielectric constant in different ac fields for a number of specimens having different compositions.

Before proceeding to a description of the results, it may be worth recalling that in the case of ferroelectrics it is common to distinguish between three types of dielectric constants: the differential, the normal or total and the reversible. Both the total and the differential constants can be determined from the hysteresis loops. In measurements with a bridge, however, one cannot obtain the value of the total capacitance inasmuch as due to the nonlinearity of a capacitor with a ferroelectric it is impossible to balance the bridge fully; one can obtain compensation only with respect to the first harmonic. In doing this we obtain the value of the linear capaci-

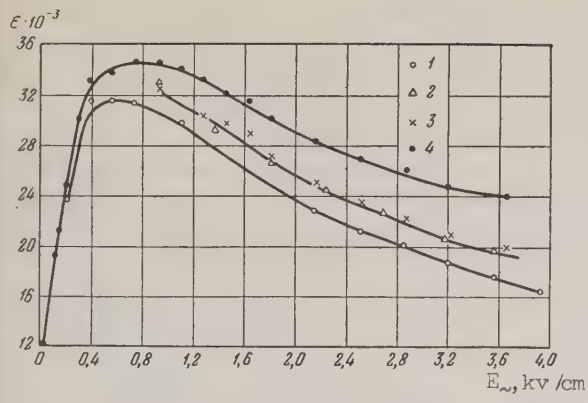

Fig.3. Dependences of the dielectric constant of specimens of $Ba(Ti_{0.9},Sn_{0.1})O_3$ solid solution on the ac field strength as determined: 1) from hysteresis loops at a frequency of 70 cps (ϵ_t), 2) from capacitance bridge measurements at a frequency of 50 cps, 3) from the first harmonic current at 70 cps and 4) from the effective current at 70 cps.

tance through which there would pass the same current of the fundamental frequency as through the nonlinear capacitance with the same voltage. This capacitance and the corresponding dielectric constant may be termed the capacitance and dielectric constant for the fundamental frequency.

In Fig.3 we show the variations of the dielectric constant with the ac field intensity for a $Ba(Ti_{0.9},Sn_{0.1})O_3$ solid solution specimen measured at room temperature by three different methods. As may be seen from the curves, the highest value of the dielectric constant is that obtained from the effective current (ϵ_{eff}); the dielectric constant obtained from measurements with a capacitance bridge is somewhat smaller. Finally, the curve for the dielectric constant determined from the hysteresis loop lies still lower. It may be recalled that ϵ_t for the fundamental hysteresis loop is determined from the maximum value of the first harmonic.

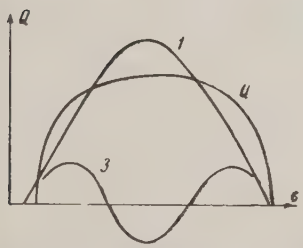

Fig.4. Variation of the total charge (Q) and of its first (1) and third (3) harmonics during a half cycle.

As may be seen from Fig.4, the third harmonic of the charge, which is the next in magnitude after the first, has a polarity opposite to that of the first harmonic just when the latter passes through a maximum. Consequently, the amplitude of the first harmonic is greater than the maximum value of the total charge and $\epsilon_1 > \epsilon_t$.

In the present investigation the dielectric constant ϵ_1 was determined from the capacitance of the specimen as calculated on the basis of the first harmonic of the current. The current was measured by means of a wave analyzer at a frequency of 70 cps. In addition to the first harmonic, we measured the effective values of all the current harmonics having values greater than 5% of the first harmonic. This gave us the spectral (harmonic) composition of the current and made it feasible to determine the coefficient of nonlinear distortion. The measurements showed that the values of the higher current harmonics are appreciable even in not particularly strong fields. Thus, for example, for specimens of the $Ba(Ti_{0.9},Sn_{0.1})O_3$ and $Ba(Ti_{0.9},Zr_{0.1})O_3$ solid solutions at field intensities of 3 kv/cm, the third harmonic amounts to 50% and the fifth harmonic to 30% of the magnitude of the first harmonic. The coefficient of nonlinear distortion for these specimens attains 100% in fields of the order of 8 kv/cm.

Investigation of the temperature dependences of ϵ_1 at different values of the ac field showed that in fields from 1 to 3 kv/cm these dependences are characterized by appreciable maxima of ϵ_1 at the points of the low temperature

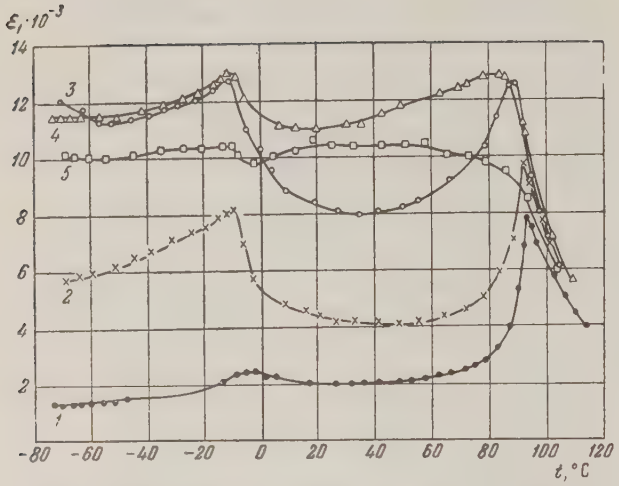

Fig.5. Temperature dependences of the dielectric constant ϵ_1 of the $(Ba_{0.9},Sr_{0.1})TiO_3$ solid solution at different intensities of the ac field: 1) 71 v/cm, 2) 1, 3) 3, 4) 6 and 5) 10 kv/cm.

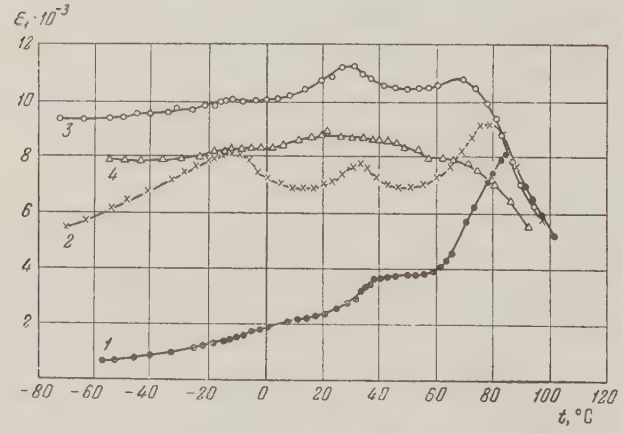

Fig.6. Temperature dependences of the dielectric constant ϵ_1 of the $Ba(Ti_{0.95},Sn_{0.05})O_3$ solid solution at different intensities of the ac field: 1) 53 v/cm, 2) 1, 3) 5 and 4) 10 kv/cm.

phase transitions (Figs.5 & 6). With further increase in the ac field strength, the height of the ϵ_1 peak increases and at the same time the peak is shifted to the side of lower temperatures. In still stronger fields the temperature dependence of ϵ_1 curve is smoothed out.

We believe that this variation in the temperature dependence of ϵ_1 in different fields can be explained as follows.

In a weak field the dielectric constant falls off sharply below the Curie point inasmuch as with the appearance of spontaneous polarization the induced polarization, which predominates in a weak field, decreases. In the case of stronger fields the dielectric constant continues to increase as the temperature is reduced below the Curie point. This is explained by the fact that near the Curie point the domains can "switch" relatively easily, hence here the role of orientational polarization is great even in not very strong fields. As the temperature is reduced, on the one hand, spontaneous polarization increases which should lead to an increase of the dielectric constant and, on the other hand, the orientation (switching) of the domains will be reoriented. The first process predominates immediately below the Curie point and, consequently, the dielectric constant increases at first, but with further decrease of temperature the second process becomes increasingly important (fewer domains are oriented by the field) which leads to a decrease of the dielectric constant. Obviously, the stronger the applied field the lower will be the temperature of the dielectric constant maximum and the slower its rate of decrease as the temperature is reduced below that corresponding to the peak value of ϵ_1. It should be noted that in this qualitative examination we have not taken into account the nonlinear character of the dependence of the induced polarization on the intensity of the electric field inasmuch as in strong fields the dielectric constant in the ferroelectric

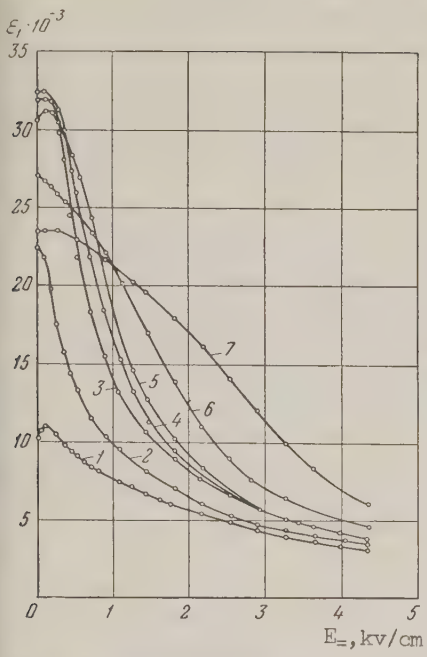

Fig.7. Variation of ϵ_1 of a $Ba(Ti_{0.9},Sn_{0.1})O_3$ specimen with the biasing dc field in different ac fields: 1) 36 v/cm, 2) 0.18, 3) 0.45, 4) 0.75, 5) 1.0, 6) 1.97, 7) 3 kv/cm.

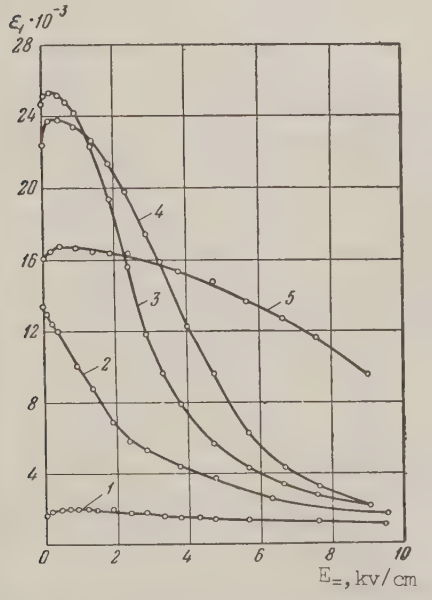

Fig.8. Variation of ϵ_1 of a $Ba(Ti_{0.9},Zr_{0.1})O_3$ specimen with the biasing dc field in different ac fields: 1) 95 v/cm, 2) 0.95, 3) 2.85, 4) 4.8, 5) 9 kv/cm.

region is determined primarily by the orientational polarization.

The decrease of the coercive force at the transition from the tetragonal to the orthorhombic phase and from the orthorhombic to the rhombohedral phase leads to an increase in the number of reorienting domains. In fields from 1 to 3 kv/cm increase in the number of switching domains may be so appreciable as to lead to an increase of the dielectric constant incident to these transitions. Then with further decrease of the temperature, by virtue of the gradual increase of the coercive force the number of orienting domains decreases and the dielectric constant falls off. In sufficiently strong fields and at not very low temperatures the number of domains oriented by the field varies little with the temperature; consequently the temperature dependence of the dielectric constant is smoothed out.

When ferroelectric ceramics are used in dielectric amplifiers their nonlinear characteristics are significant; particularly important in such applications are the dependences of the dielectric constant ϵ_1 and the nonlinearity $N = (1/\epsilon_1)(d\epsilon_1/dE)$ on the biasing dc field in different ac fields. The dc biasing field dependences of ϵ_1 in different ac fields for specimens of $Ba(Ti_{0.9},Sn_{0.1})O_3$ and $Ba(Ti_{0.9},Zr_{0.1})O_3$ solid solutions are shown in Figs. 7 & 8. All the curves were recorded for increasing values of the biasing field. Prior to recording each curve the specimens were heated to above the Curie point. As may be seen from the figures the rate of falling off of the dielectric constant with increasing ac field strength at first increases and then decreases. The steepest curve is obtained at an ac field strength approximately corresponding to the maximum dielectric constant on the curves for $\epsilon_1 = f(E)$, which is in agreement with the results obtained by Verbitskaia[5] for Varikond. The dc field dependences of the nonlinearity observed for a specimen of $Ba(Ti_{0.9},Sn_{0.1})O_3$ solid solution are shown in Fig.9. Of the investigated solid solutions those with a $BaSnO_3$ or $BaZrO_3$ content of 5-10% exhibited the most pronounced nonlinear properties.

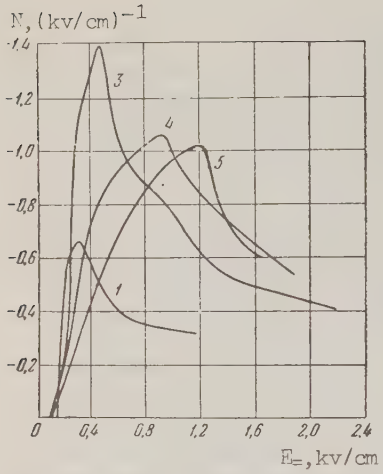

Fig.9. Variation of the nonlinearity N of a $Ba(Ti_{0.9},Sn_{0.1})O_3$ solid solution specimen with the biasing dc field in different ac fields: 1) 36 v/cm, 2) 0.18, 3) 0.45, 4) 0.75, 5) 1.0, 6) 1.97, 7) 3 kv/cm.

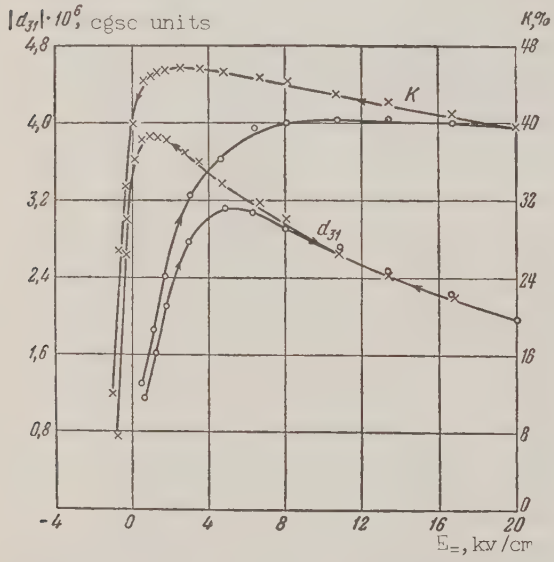

Fig.10. Variation of the absolute value of the piezoelectric coefficient $|d_{31}|$ and the electromechanical coupling coefficient K of $Ba(Ti_{0.95},Sn_{0.05})O_3$ with the intensity of the polarizing field.

The ease with which the domains switch depends to a considerable extent on the spontaneous deformations of the unit cell. The closer the unit cell to the cubic, the less energy is expended on the mechanical deformations incident to reorientation of the domains. Consequently, as was first noted by Smolenskii[9], in ferroelectrics with low electrostriction there should be observed high values of the initial and total dielectric constant and, naturally, the nonlinear properties must be more pronounced. Dilatometric investigations carried out by Smolenskii and his colleagues[6-8] have shown that in solid solutions of the $(Ba,Sr)TiO_3$, $Ba(Ti,Sn)O_3$ and $Ba(Ti,Zr)O_3$ systems the electrostriction decreases with increasing content of the second component. Hence the pronounced nonlinear characteristics of our specimens of solid solutions with 5-10% $BaSnO_3$ or $BaZrO_3$ can be largely explained by the low electrostriction. In addition, it may be noted that the solid solutions containing less than 10% $BaSnO_3$ or $BaZrO_3$ are characterized by the presence of three phase transitions separated by relatively small temperature intervals. This close grouping of the transition points should obviously be manifested in the nonlinear characteristics in the temperature range comprising the phase transitions since, as we have noted above, the coercive force decreases and the mobility of the domains increases incident to a transition from a phase of higher to a phase of lower symmetry.

A very high value of ϵ is obtained for the solid solutions enumerated above as well as for solid solutions containing from 60 to 80% $SrTiO_3$ in case of measurements in weak fields in the vicinity of the Curie point. This can apparently be explained by the appreciable orientational polarization obtaining near the Curie point even in weak fields.

Investigations at room temperature of the dependence of the piezoelectric coefficient d_{31} on the intensity of the polarizing field showed that in the case of solid solutions possessing pronounced nonlinear characteristics $|d_{31}|$ passes through a maximum (Fig.10). Analogous varia-

tions but with less pronounced peaks were first obtained by Roi[9] for the piezoelectric coefficient d_{33} and explained by him as being due to changes of the domain structure. This explanation appears plausible.

Institute of Semiconductors of the
Academy of Sciences of the USSR

References

1. H.H.Wieder, J.Appl.Phys., 26, 1479 (1955).
2. A.F.Devonshire, Phil.Mag., 40, 1040 (1949).
3. W.J.Merz, Phys.Rev., 76, 1221 (1949).
4. H.H.Wieder, Phys.Rev., 99, 1161 (1955).
5. T.N.Verbitskaia, Doklady AN SSSR, 100, 29 (1955).
6. G.A.Smolenskii & V.A.Isupov, Zhur.tekh.fiz., 24, 1375 (1954).
7. G.A.Smolenskii & K.I.Rozgachev, Zhur.tekh.fiz., 24, 1753 (1954).
8. G.A.Smolenskii, N.P.Tarutin & N.P.Grudtsin, Zhur.tekh.fiz., 24, 1584 (1954).
9. N.A.Roi, Akusticheskii zhurnal (Acoustic Journal), 2, 62 (1956).

PIEZOELECTRIC PROPERTIES OF BARIUM TITANATE CERAMIC WITH CERTAIN ADDITIVES

- S.V.Bogdanov

Introduction

In studying the piezoelectric properties of barium titanate under static conditions we established that the pressure dependence of the piezoelectric charge appearing on the boundaries of a polarized specimen is not linear. The results of these studies were presented in a report by Vul and the present writer at the First All-Union Conference on Piezoelectricity called by the Institute of Crystallography of the USSR Academy of Sciences in 1952. The deviation from linearity in barium titanate begins under mechanical loads of the order of 30-50 kg/cm^2. The character of the observed dependences was explained with the aid of certain concepts regarding changes in the domain structure of the microcrystals of which polycrystalline specimens are composed under the influence of mechanical loads. Briefly our argument was the following.

After the application of a strong dc field, the residual polarization of each individual microcrystal has a positive projection on the direction of this field and this produces a general residual polarization of the specimen that determines the piezoeffect in it.

Deformation of the microcrystal under the influence of the external mechanical stress produces a change in its domain structure (or fragmentation of it into domains if the crystal was initially a single-domain one). This change occurs so that the specific weight of the domains oriented in the direction of the microcrystal axis that lengthens under deformation increases, which leads to a decrease of the general residual polarization of the specimen. This type of change in the domain structure is connected with the positive electrostriction of barium titanate. The change in the domain structure may be of a reversible or irreversible character, depending on the magnitude and duration of the applied mechanical stress.

It is logical to assume that the change in domain structure under a given mechanical stress will be the greater, the smaller the coercive force and the greater the deformation of the crystal, i.e., the larger the flexibility modulus (compliance coefficient) and Poisson's ratio. Barium titanate with some additives such as SnO_2 and $BaTiO_3$-$BaSnO_3$ type solid solutions have a loose lattice and a low coercive force. Hence it may reasonably be expected that in such materials the above mentioned effects will be more pronounced. And in fact, investigation of the variation of the piezoelectric charge as a function of the mechanical stress in a number of solid solutions containing $BaSnO_3$ as well as of barium titanate with SnO_3 added has shown that changes in the domain structure play a predominant role in these materials. In the present report we shall speak of some of the dielectric and piezoelectric properties of barium titanate containing 3% SnO_2 and hence designated T-3 in our laboratory.

All the tests were carried out on samples prepared by our technological group under the supervision of Cherepanov; the measurements were performed by Razbash.

Dielectric and piezoelectric properties of the T-3 ceramic

The addition of SnO_2 to barium titanate leads to lowering of the Curie point, increase in the dielectric constant, decrease of the spontaneous polarization, residual magnetization and coercive force, and an increase in the modulus of flexibility and the Poisson ratio.

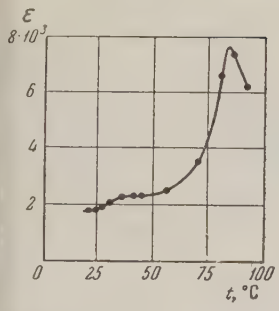

Fig.1. Temperature dependence of the dielectric constant of T-3.

The product T-3 is characterized by the following parameters: the dielectric constant at room temperature measured in a weak ac field ($E_{\sim} \approx 2.5$ v/cm) at a frequency of 190 kc equals $(1.7\text{-}1.8)\cdot 10^3$; the Curie point θ lies at 82-87°; in the vicinity of 30-35° there is observed a certain increase of the dielectric constant presumably connected with a low temperature phase transition.

The temperature dependence of the dielectric constant for a T-3 specimen is shown in Fig.1.

According to the data of Kovalenko the spontaneous polarization P_s of the T-3 material is $3.35\cdot 10^{-6}$ coulomb/cm^2, the residual polarization $P_{res} \approx 2.0\cdot 10^{-6}$ coulomb/cm^2; the coercive force $E_c \approx 1.2$ kv/cm. From dynamic measurements on polarized discs it follows that $S^E_{11} \approx 1.0\cdot 10^{-12}$ cm^2/dyne and $\sigma_{12} \approx 0.32$.

For purposes of comparison we give the same parameters for ceramic specimens of barium titanate:

$\epsilon_{20°C} \approx 1000$, $T_o \approx 120°$	$P_s \approx 6.0\cdot 10^{-6}$ coulomb/cm^2
$P_{res} \approx 4.5\cdot 10^{-6}$ coulomb/cm^2	$E_c \approx 2.25$ kv/cm
$S^E_{11} \approx (0.8\text{-}0.9)\cdot 10^{-12}$ cm^2/dyne	$\sigma_{12} \approx 0.21\text{-}0.28$

Thus for T-3 the dielectric constant has about twice the value, while the spontaneous polarization, residual polarization and coercive force have about half the value characteristic of barium titanate; the flexibility modulus and Poisson's ratio are somewhat higher than for barium titanate. On the basis of these data one can make a tentative comparison of the probable piezoelectric constant d_{33} of T-3 with the corresponding constant of barium titanate by making use of the theoretical expression for a single crystal, namely

$$d_{33} = \frac{\gamma_1 \varepsilon_{33} P_s}{2\pi}.$$

In such comparisons it is assumed that both ceramics are polarized to saturation, that the values of ϵ and P_s of the ceramics are proportional to the corresponding quantities for single crystals and that the coefficients γ_1 for the two ceramics are nearly equal. Then we have

$$\frac{[d_{33}]_{BaTiO_3}}{[d_{33}]_{T\text{-}3}} \approx \frac{[\varepsilon P_s]_{BaTiO_3}}{[\varepsilon P_s]_{T\text{-}3}} \approx 1.$$

Measurements of the piezoelectric coefficient d_{33} of T-3 under very small loads ($\sigma_{33} \approx 4$ kg/cm^2) showed that it is actually of the same order of magnitude as the coefficient of barium titanate and equals approximately $4.8\cdot 10^{-6}$ cgse units (Fig.2) (the coefficient d_{33} is numerically equal to the slope of the curve $Q_3 = f(\sigma_{33})$ where Q_3 is the piezoelectric charge per unit area of the face perpendicular to the X_3 axis and σ_{33} is the mechanical stress acting along the normal to this face). Under heavy mechanical loads the linearity of $Q_3 = f(\sigma_{33})$ breaks down (Fig.2), i.e., under high stresses the piezoelectric coefficient is no longer a constant. However, in the range of loads from approximately 40-50 kg/cm^2 to 125-150 kg/cm^2 a second linear interval appears in the curve characterizing the variation of Q_3 as a function of

σ_{33} (Fig.3); the corresponding value of the piezoelectric coefficient is $(14\text{-}19)\cdot10^{-6}$ cgse units. At higher mechanical loads the functional dependence of Q_3 on σ_{33} again becomes nonlinear (Fig.4).

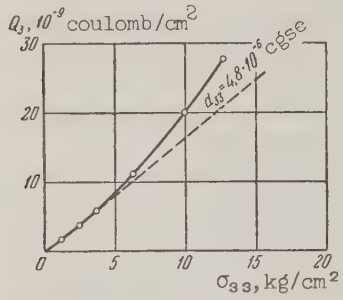

Fig.2. Variation of the piezoelectric charge with the mechanical stress for a T-3 specimen.

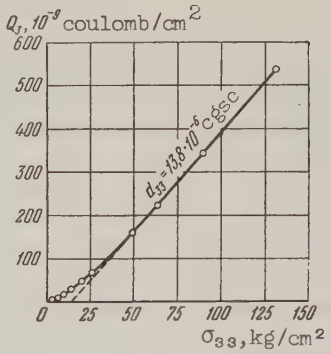

Fig.3. Variation of the piezoelectric charge with the mechanical stress for a T-3 specimen.

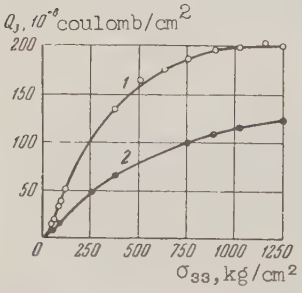

Fig.4. Variation of the piezoelectric charge with the mechanical stress for T-3 specimens before (1) and after (2) aging.

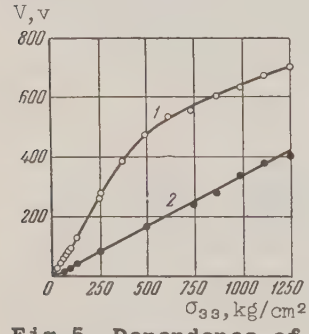

Fig.5. Dependence of the voltage produced by a piezoelectric cell of T-3 on the mechanical stress before (1) and and after (2) aging with a constant shunting capacitance C_s = 1600 μμf.

The 3-4 fold increase of the piezoelectric constant at the second linear section, we believe, can be explained by reversible changes of the domain structure of the microcrystals under the influence of the heavier loads. This hypothesis is substantiated by the fact that after artificial aging, consisting of holding the specimen for a long time under a very heavy load which produces a reversible reorientation of the domains (in our case a load of ~1450 kb/cm^2 applied for ~46 hours), the magnitude of the piezoelectric constant for the second linear section is appreciably reduced, in our case from $15\cdot10^{-6}$ to $6\cdot10^{-6}$, i.e., by more than a factor of 2, while the initial-section piezoelectric constant decreases relatively little (from $4.8\cdot10^{-6}$ to $4.3\cdot10^{-6}$); the latter minor decrease is due to the general reduction of the residual polarization (Fig. 4).

The fact that these ceramics are characterized by an appreciable nonlinearity of the dielectric constant[1] gives reason to assume that the variation of the voltage developed by a piezoelectric cell of the T-3 product as a function of the mechanical stress $V_3 = f(\sigma_{33})$ will be appreciably more linear than the variation of the piezoelectric charge inasmuch as the change in the piezoelectric coefficient will to some extent compensate the change in the dielectric constant ($V_3 = 4\pi \cdot h \frac{d_{33}}{\varepsilon} \sigma_{33}$, where h is the thickness of the specimen). And in fact an experimental determination of the variation of V_3 as a function of σ_{33} for a 4 mm thick specimen and a constant shunting capacitance C_s = 1600 μμf (see Fig.5) substantiated this hypothesis.

Conclusions

1. Barium titanate with certain additives such as SnO_2 and barium titanate solid solutions with barium stanate, as compared with $BaTiO_3$, have a lower Curie point, a reduced spontaneous polarization and a smaller coercive force and at the same time a larger modulus of flexibility (compliance coefficient) and higher Poisson's ratio and these factors in turn facilitate reorientation of the domains under mechanical stresses.

2. Reversible changes in the domain structure under the action of mechanical stresses lead to an appreciable increase of the piezoelectric constant d_{33}.

3. It may be assumed that at sufficiently high frequencies no changes of the domain structure will occur and that consequently the effects associated with such changes will not be manifest.

"P.N.Lebedev" Physical Institute of the
Academy of Sciences of the USSR

References

1. G.A.Smolenskii, M.A.Karamyshev & K.I.Rozgachev, Doklady AN SSSR, 79, 53 (1951).

INVERSE PIEZOEFFECT IN POLYCRYSTALLINE $BaTiO_3$ UNDER STATIC CONDITIONS

- G.M.Kovalenko

Introduction

We know from the literature[1] that Vul, Roberts, Rzhanov, Bogdanov and a number of other investigators have studied the piezoelectric properties of polycrystalline barium titanate in addition to its other characteristics. The results of work on the piezoeffect in polycrystalline $BaTiO_3$ carried out at the Physical Institute of the Academy of Sciences of the USSR have been described in the reports of Vul & Bogdanov at the present Conference.

A report on an investigation of the inverse piezoeffect in ferroelectric crystals of potassium phosphate (KH_2PO_4) was published some years ago by Arx & Bantle[2].

We felt it would be of interest to investigate experimentally the inverse piezoelectric effect in polarized polycrystalline barium titanate.

The purpose of the present investigation was a) to establish the character of the dependence of the resulting deformation on the intensity of the applied dc field and b) to determine the dependence of the amplitude of oscillation of polarized polycrystalline specimens of $BaTiO_3$ prepared by the standard technology on the intensity of a 50 cps alternating field.

Specimens

The measurements were carried out on 12 specimens taken from four lots prepared by the usual procedure employed in this laboratory. Technical grade raw materials were used throughout. The mixture was ground in a powder mill for 50 hours then dried and compressed into discs. The specimens were fired at 1380° in a Silit resistance furnace. After firing the samples were ground down to a thickness of 0.65 cm. The diameter of all the samples was 1 cm. The electrodes were applied by firing on silver and were then polished to a mirror surface. The specimens were polarized in a dc field of 14 kv/cm for a period of 2 hours at room temperature (20°). After polarization and prior to measurement the samples were stored shorted for three to five days.

Measurement Procedure

The interferometric method was used for measuring the magnitude of the deformation resulting from the application of a potential to the specimens. The procedure for such measurements in a dc field is described by Romanov[3]; the procedure for the case of an ac field by Thomas & Warren, Osterberg, Kotliarevskii & Pumper and Smith[4]. All the measurements were made on a Zeiss comparator. The principle of operation in working with a comparator is the same as with a Michelson interferometer. One mirror was the polished (electrode) surface of the specimen mounted on the comparator stage. The interference pattern was obtained in an air wedge realized by means of special micrometric adjustment screws. With the wedge (screws) appropriately adjusted, the expansion or contraction of the specimen under the influence of a dc field could be evaluated from the displacement of the interference bands. The maximum value of the amplitude of oscillation of the specimens in the case of an ac field was evaluated from the darkening of the interference picture. All the measurements were made using the yellow line of helium, the wavelength of which is 5875.649 Å at 20° and 760 mm Hg.

Experimental Results

Dc electric field

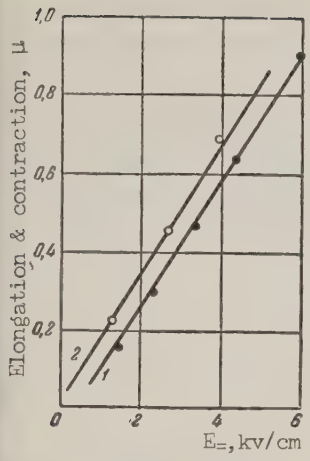

Fig.1. Deformation of $BaTiO_3$ ceramic as a function of the dc field strength: 1) elongation and 2) contraction.

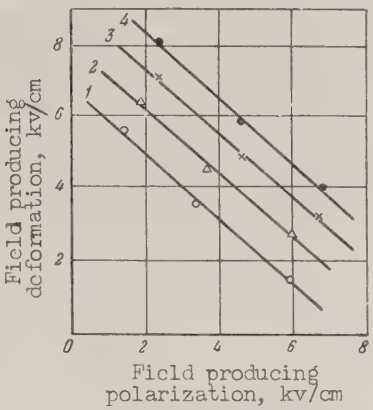

Fig.2. Dependence of the field strength producing a given deformation on the strength of the initial polarizing field: 1) deformation $0.15 \cdot 10^{-4}$ cm, 2) $0.3 \cdot 10^{-4}$ cm, 3) $0.45 \cdot 10^{-4}$ cm, 4) $0.60 \cdot 10^{-4}$ cm.

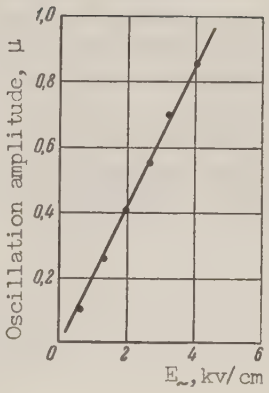

Fig. 3. Dependence of the amplitude of oscillation of $BaTiO_3$ on the ac field strength.

The magnitude of the inverse piezoeffect was measured in applying an increasing dc potential to the specimens, first with a polarity identical with that used in polarizing of the specimen and then with a reverse polarity. The former resulted in expansion of the specimen; the latter in contraction. The resultant variations are shown in Fig.1.

It was established for all specimens that in the case of reverse polarity of the applied field the contraction continues only to a certain value of the potential; at a certain field strength there occurs what might be termed complete depolarization of the specimens and with further increase in the field intensity the specimen begins to elongate, i.e., it is polarized in the direction opposite to that of the initial polarization. The mean value of the field intensity at which repolarization begins is always higher than the mean value of the field intensity at which the beginning of polarization of "fresh" specimens is observed.

Dependence of the piezoelectric coefficient on the electric field intensity for barium titanate (Sample No. 11)

V, v		$d_{33} \cdot 10^6$, cgse units	
++*	+−	++	+−
1600	700	3,00	6,30
2500	1500	3,70	6,00
3200	2300	4,00	5,85
3850	2900	4,60	6,50

*++ means that the polarity of the applied field is the same as that of the polarization field; +− indicates opposite polarity.

From the experimental data we calculated the values of the piezoelectric coefficient d_{33} both for the case of elongation and for the case of contraction. The values of the piezoelectric coefficient for one of the samples (No. 11) are listed in the accompanying table. The values of the piezoelectric coefficient obtained from measurements on a ballistic galvanometer under loads of 1 and 5 kg were 5.2 and $5.7 \cdot 10^{-6}$ cgse units, respectively.

It must be noted that in elongating the samples contract noticeably along the diameter.

In the course of the measurements it was noted that the value of the field producing a given deformation does not remain constant, but depends on the strength of the initial polarizing field (Fig.2).

Ac field

The dependence of the amplitude of oscillation of the samples on the ac field strength is shown in Fig.3.

Conclusions

1. The magnitude of the deformation of the investigated barium titanate specimens is linearly dependent on the intensity of the applied dc field.
2. In the case of application of an ac field the amplitude of oscillation increases in direct proportion to the applied field.

"P.N.Lebedev" Physical Institute of the
Academy of Sciences of the USSR

References

1. A.V.Rzhanov, Zhur.eksp.i teor.fiz., 19, 502 (1949); S.Roberts, Phys. Rev., 71, 890 (1947); B.M.Vul, Elektrichestvo, 3 (1946); S.V.Bogdanov, Present issue of the Bulletin, p. 392.
2. A.Arx & N.Bantle, Helv.Phys.Acta, 17, 298 (1944).
3. M.F.Romanova, Interferentsiia sveta i ee primenenie (Interference of light and its applications), M.-L., 1937.
4. H.A.Thomas & G.W.Warren, Phil.Mag., 5,32,1125 (1928); H.Osterberg, J.Opt.Soc.Am., 23, 30 (1933); N.L.Kotliarevskii & E.Ia.Pumper, Zhur.tekh. fiz., 11, 843 (1941); D.H.Smith, Proc.Phys.Soc., 57, 534 (1945).

A METHOD OF DETERMINING THE PIEZOELECTRIC COEFFICIENT FROM THE RADIAL VIBRATIONS OF A DISC

- S.V.Bogdanov & A.M.Timonin

The piezoelectric coefficient d_{31} can be determined from the radial vibrations of a disc by the method of resonance and antiresonance. This method is based on the fact that when one solves simultaneously the equation of a piezoelectric transducer and the equation of motion of a flat disc undergoing radial vibrations, it is feasible to relate experimentally observable quantities (the dimensions and density of the sample, the resonance and antiresonance frequencies and the dielectric constant of the material) with its piezoelectric and elastic constants (see, for instance, Mason[1]). These relations are

$$k_R^2 \approx \frac{f_{1a}-f_{1r}}{f_{1r}}\left[\frac{k_1^2-(1-\sigma_{12})}{1+\sigma_{12}}\right]=\frac{8\pi^2 d_{31}^2}{\varepsilon_{33}^T S_{11}^E (1-\sigma_{12})} \tag{1}$$

and

$$v=\frac{1}{\sqrt{S_{11}^E \rho (1-\sigma_{12}^2)}}=\frac{2\pi R f_{1r}}{k_1}, \tag{2}$$

where k_1 is the first (lowest) root of the transcendental equation

$$\frac{\left(\frac{\omega R}{v}\right)\cdot J_0\left(\frac{\omega R}{v}\right)}{J_1\left(\frac{\omega R}{v}\right)}=1-\sigma_{12}, \tag{3}$$

which determines the resonance frequency J_0 and J_1 are the zeroth and first order Bessel functions of the argument $(\omega R/v)$, ω is the angular frequency, R is the radius of the sample, k_R is the electromechanical coupling coefficient for radial vibrations, v is the velocity of sound in the sample, S_{11}^E is the compliance coefficient at zero field, σ_{12} is Poisson's ratio, ε_{33}^T is the dielectric constant of the free crystal, f_{1r} and f_{1a} are the first resonance and antiresonance frequencies for radial vibrations, respectively, and ρ is the density.

From Eqs.(1), (2) and (3) one can find d_{31}, S_{11}^E and v if σ_{12} is known.

Inasmuch as Poisson's ratio is usually not known, and it is impossible to solve Eq.(3) for k_1. In practice one can, however, use some mean value of σ_{12} for the given substance (Mason, for example, uses $\sigma_{12} = 0.27$ and obtains $k_1 = 2.03$). It is clear that this method can make no claim to accuracy, and therefore exact measurements require finding Poisson's ratio by some independent means.

This difficulty is easily avoided if one measures the second resonant frequency f_{2r} of radial vibrations of the disc. This frequency corresponds to the second root

$$k_2=\frac{2\pi f_{2r}}{v},$$

of Eq.(3), so that

$$\frac{1}{v}=\frac{k_1}{2\pi R f_{1r}}=\frac{k_2}{2\pi R f_{2r}}, \tag{4}$$

can be used for a graphical determination of Poisson's ratio and the velocity of sound in the specimen. Let us write

$$\varphi_1(\sigma_{12}) = \frac{k_1(\sigma_{12})}{2\pi R f_{1r}} \quad \text{and} \quad \varphi_2(\sigma_{12}) = \frac{k_2(\sigma_{12})}{2\pi R f_{2r}}.$$

At some value $\sigma_{12} = \sigma_{12}^{act}$ of Poisson's ratio (that of the material being investigated) there will obtain the equality

$$\varphi_1(\sigma_{12}^{act}) = \varphi_2(\sigma_{12}^{act}) = \frac{1}{v}.$$

For finding σ_{12}^{act} we proceed as follows. Assuming different values of k_1 and k_2, we use Eq.(3) to find the values of σ_{12} corresponding to them. We then construct the functions $\varphi_1 = \varphi_1(\sigma_{12})$ and $\varphi_2 = \varphi_2(\sigma_{12})$ and find their point of intersection, which determines $1/v$ and σ_{12} for the material.

In actually using this method, we found that in the interval $0{,}2 \leqslant \sigma_{12} \leqslant 0{,}35$ the variations of k_1 and k_2 with σ_{12} are practically linear:

$$\left.\begin{aligned} k_1 &= 1{,}86 + 0{,}633\,\sigma_{12}, \\ k_2 &= 5{,}33 + 0{,}2\,\sigma_{12}. \end{aligned}\right\} \tag{5}$$

Using (4), we find from (5) that

$$\sigma_{12} = \frac{5{,}33 f_{1r} - 1{,}86 f_{2r}}{0{,}633 f_{2r} - 0{,}2 f_{1r}}. \tag{6}$$

Having σ_{12}, we find k_1, and then v, S_{11}^E, k_R and d_{31}. Thus by performing a single additional measurement (i.e., determining f_{2r}) one can determine Poisson's ratio and then d_{31} with an accuracy sufficient for all practical purposes.

"P.N.Lebedev" Physical Institute of the
Academy of Sciences of the USSR

References

1. W.P.Mason, Piezoelectric crystals and their applications in ultrasonics. (In Russian translation, M. 1952.)

PYROELECTRIC AND PIEZOELECTRIC EFFECTS IN POLYCRYSTALLINE BARIUM TITANATE

- M.S.Kosman & Z.A.Shamro

The present study was devoted to an investigation of the pyroeffect in polycrystalline samples of barium titanate and the correlation between this effect and the piezoelectric effect. As we know, nonpolarized specimens of barium titanate exhibit no piezoelectric effect; when such specimens are heated no difference of potential develops between the opposite faces of the specimen. After polarization, however, specimens exhibit both a piezoeffect and a pyroeffect. This is, when a polarized specimen is heated a difference of potential appears on the electrodes attached to its faces and if these electrodes are connected to a galvanometer a measurable current flows through the circuit.

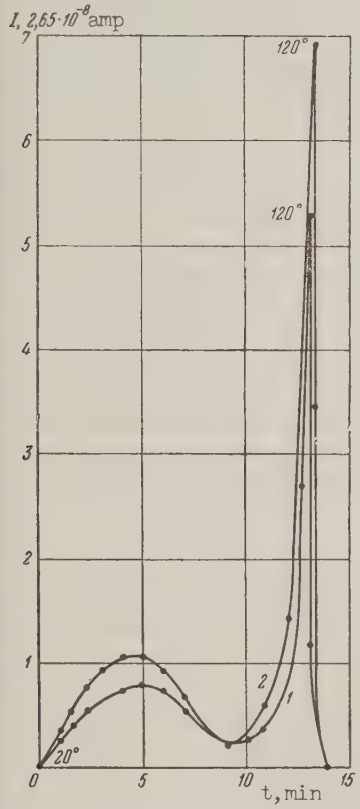

Fig.1. Variation with time (temperature) of the current obtained in heating a barium titanate specimen prepolarized at 20° and E_{pol} = 1600 v/mm: 1) t_{pol} = 5 min, 2) t_{pol} = 30 min.

The results of one such experiment are shown in Fig.1. The specimen characterized by curve 1 was polarized for 5 min in a field of 1600 v/mm at 20° and then shorted through a galvanometer. Immediately after polarization there was a measurable current in the circuit even with the specimen remaining at constant temperature, but this current soon (after about 30 min) fell off to below the sensitivity of our instrument. After this we measured the static piezoelectric constant of the specimen; in the given case it proved to be $1.2 \cdot 10^{-6}$ cgse units. Next the specimen was heated in an appropriate furnace. The horizontal scale in Fig.1 could be graduated in terms of temperature or heating time (since the rate of heating was virtually constant) but for the purpose of calculating the total charge it is more convenient to use the time scale. The corresponding temperatures are indicated at a number of points. As may be seen the current vs heating time curves exhibit two maxima. The first is rather broad but still appreciably sharper than the peak in the dielectric constant vs temperature curve associated with the transition of the barium titanate from the orthorhombic to the tetragonal modification. The second maximum is very sharp and occurs at 120°, i.e., the Curie point associated with the transition to cubic modification. No current appeared in the circuit during cooling of the specimen back to room temperature and the piezoelectric coefficient measured at room temperature proved to be zero. After this the specimen was again subjected to polarization in the same field and at the same temperature but this time for 30 min (curve 2) instead of 5 min. After this the piezoelectric coefficient of the specimen was found to be $1.56 \cdot 10^{-6}$ cgse units. The quantity of electricity taken off after the first polarization was $1.52 \cdot 10^{-5}$ coulomb, that after the second polarization was $2.0 \cdot 10^{-5}$ coulomb, i.e., was proportional

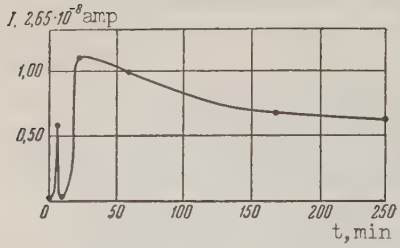

Fig.2. Pyrocurrent curve for barium titanate polarized at 110° and E_{pol} = = 1000 v/mm for 180 min.

to the initial piezoelectric coefficient. If the polarized specimen is heated to a temperature slightly below the Curie point and then cooled, a measurable current flows through the circuit both during heating and during cooling; the quantities of electricity flowing through the circuit during cooling and heating are equal but, of course, the directions of the current are opposed. This reversibility is observed for all heating-cooling cycles beginning with the second. During the first heating there is observed a certain energy loss incident to the transition to the orthorhombic modification.

Most of the investigated specimens were polarized at temperatures only slightly below the Curie point. The primary advantage of such "hot" polarization is the marked reduction in time necessary to attain the maximum value of the piezoelectric coefficient: instead of the hours necessary for polarization at room temperature, the time required is reduced to 3-5 min and the applied field can be weaker. More prolonged polarization does not increase the value of the coefficient but leads to certain qualitative changes in its behavior and to the accumulation of large absorption charges not connected with the ferroelectric properties.

Fig.2 shows the magnitude such absorption charges may attain. The figure gives the depolarization curve for a specimen polarized at 110° (Curie point 120°) in a field of 1000 v/mm for 3 hours. As will be seen from the figure the quantity of electricity given up in passing through the Curie point (first sharp maximum) is much less than the quantity obtained at higher temperatures and associated only with absorption processes.

One of the qualitative changes occurring during prolonged hot polarization is illustrated in the accompanying table and Fig.3. This specimen contained an admixture of lead and its Curie

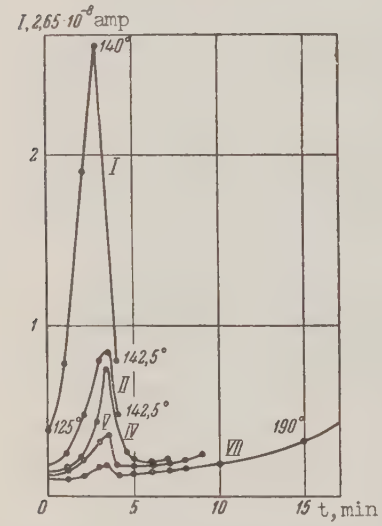

Fig.3. Pyrocurrent curves obtained for successive cycles of temperature depolarization of a barium titanate specimen initially polarized at 120° in a field E_{pol} = 1000 v/mm for 30 min. The depolarization conditions for the different curves are listed in the accompanying table.

Values of the residual piezoelectric coefficient of a barium titanate specimen subject to hot polarization after repeated heating and cooling cycles

No. of heating cycle	Time sample was held at t above Curie point, min	t_{max}, C°	d_{res}, 10^{-6} cgse
1	4	143	1,2
2	4	143	0,9
3	4	143	0,85
4	7	152	0,52
5	9	161	0,35
6	11	165	0,30
7	23	190	0,22
8	33	190	0,22

point was 140°. It was polarized by a 1000 v/mm field for 30 min at a temperature of 125°. The piezoelectric coefficient measured immediately after polarization at room temperature was $3.5 \cdot 10^{-6}$. The specimen was heated to a temperature above the Curie point and then cooled to room temperature; in the process the pyrocurves shown in Fig.3 were recorded. After cooling the residual piezoelectric coefficient was determined. In contrast to the case of specimens polarized under "soft" conditions, the residual coefficient in this case was not equal to zero. The specimen was then again heated above the Curie point and cooled, the process being repeated a number of times. The data characterizing these cycles are listed in the accompanying table.

The pyrocurrent curves for the first, second, fourth, fifth and seventh cycles are given in Fig.3. It will be seen that even prolonged heating at 190° after such comparatively "hard" polarization did not completely depolarize the specimen.

A longer polarization period would have resulted in a more firmly "fixed" piezoelectric coefficient components, but the heavy absorption currents that would appear in this case would make the pyrocurrent curves less characteristic.

The qualitative changes of the piezoelectric properties with increasing "hardness" of the polarization conditions also affect the temperature dependence of the piezoelectric coefficient. For example, for one of the specimens after polarization by a 1000 v/mm field for 5 minutes at 130° (Curie point 140°) the coefficient at room temperature was $3.3 \cdot 10^{-6}$ and that at 130° was $3.6 \cdot 10^{-6}$ cgse units; after additional polarization under the same conditions for 90 minutes the piezoelectric coefficient at room temperature was found to be $3.2 \cdot 10^{-6}$, but the coefficient at 130° fell off to $1.2 \cdot 10^{-6}$ cgse units. So great a change in the value of the coefficient and its anomalous temperature dependence are connected with changes in the properties of the barium titanate, produced by the action of strong fields at high temperatures. These changes are described in more detail in the thesis of N.I.Shefer.

"A.I.Gertsen" Leningrad State Pedagogical Institute

DIELECTRIC PROPERTIES OF THE NIOBATES AND TANTALATES OF BIVALENT METALS

- V.A. Isupov

The dielectric properties of the niobates and tantalates of bivalent metals have been studied to a far lesser extent than those of their titanates, zirconates and stanates. Yet the very first studies of these compounds (Wainer & Wentworth[1], Jaffe & Cook[2,3], Goodman[4], Shirane & Pepinsky[5] and Smolenskii & Agranovskaia[6]) showed that some of the niobates and tantalates are distinguished by a high dielectric constant and that $PbNb_2O_6$, $PbTa_2O_6$ and $Cd_2Nb_2O_7$ are ferroelectrics. Hence we felt it would be of interest to investigate further the dielectric properties of the niobates and tantalates of bivalent metals.

For preparing the specimens we used niobium pentoxide and tantalum pentoxide obtained by oxidation of the respective metals, the acetates of calcium, strontium, barium and cadmium and PbO. The niobium pentoxide contained up to 1% impurities; the tantalum pentoxide up to 2%. The Nb_2O_5, $CaCO_3$ and $CdCO_3$ were «Ч» ("Pure") grade reagents; the PbO, $BaCO_3$ and $SrCO_3$ were «ЧДА» ("Pure for Analysis") grade products.

The specimens were prepared by the ceramic procedure: the finely ground raw materials were briquetted and fired, then again powdered and compressed to the form of the specimens which were then subjected to the final sintering. Specimens containing the volatile oxides PbO and CdO were sintered in closed crucibles with a quantity of powdered PbO or $CdCO_3$ on the bottom. Most of the specimens had a superficial porosity of less than 0.5%.

In Tables 1 & 2 we list the dielectric constant and loss tangent measured at room temperature at a frequency of 1 kc and the temperature coefficient of the dielectric constant at a frequency of 1 Mc in the temperature range from 30 to 70°. The structure data given in the table are taken from the literature.

The curves characterizing the temperature dependence of the dielectric constant were recorded at a frequency of 500 kc in weak fields except for the solid solutions of the second kind; for these the temperature dependence was determined at a frequency of 150 kc.

It will be seen from Tables 1 & 2 that the niobates and tantalates of the bivalent metals are characterized by a high dielectric constant and a negative temperature coefficient of the constant. The only noteworthy exceptions are calcium metaniobate, metatantalate and pyroniobate.

The niobates having the highest dielectric constant are the following: lead metaniobate (ferroelectric, discovered by Goodman, $\epsilon = 280$, $\theta = 570°$), cadmium pyroniobate (ferroelectric, discovered by Cook & Jaffe, $\epsilon = 500\text{-}580$, $\theta = -90°$), cadmium metaniobate ($\epsilon = 90$) and lead pyroniobate ($\epsilon = 144$).

Among the tantalates the ones having the highest dielectric constant are strontium metatantalate ($\epsilon = 100\text{-}115$), barium tantalate sintered at temperatures above 1500° ($\epsilon = 132$), lead metatantalate (ferroelectric, discovered by Smolenskii & Agranovskaia, $\epsilon = 310$) and the pyrotantalates of cadmium ($\epsilon = 72\text{-}82$), strontium ($\epsilon = 110\text{-}120$) and lead ($\epsilon = 100\text{-}114$).

The dielectric constant of strontium pyrotantalate (Fig.2) increases with decreasing temperature; the curves for different specimens exhibit a maximum in the interval from -55 to -84°. Hysteresis loops are observed in the temperature range below this; hence strontium tantalate is also ferroelectric. The variation of ϵ exhibits another maximum in the temperature interval from -150 to -190°; this presumably corresponds to a low temperature phase transition.

The dielectric constants of strontium and barium metatantalate, strontium pyroniobate and calcium phyrotantalate all increase continuously with decreasin

Table 1

Dielectric properties and structure of niobates

Formula	Structure & lattice parameters	ε (t = 20°, f = 1 kc)	TC_ε (30–70°, $\alpha \cdot 10^6$ deg^{-1})	tg δ (1 kc, 20°)
$CaNb_2O_6$		20	100÷160	0,002
$CdNb_2O_6$		90	—2000	0,011
$SrNb_2O_6$		44	—	0,08
$PbNb_2O_6$	Orthorhombic unit cell containing 20 molecules	280 (Goodman)	Large positive (ferroelectric region) θ=570°	
$BaNb_2O_6$		40	—90	0,0023
$Ca_2Nb_2O_7$	Complicated structure, not of the perovskite type	31	270	0,009
$Cd_2Nb_2O_7$	Pyrochlore structure a = 10.372 A	500÷580	Large negative θ= —90°	0,014
$Sr_2Nb_2O_7$		60	—360	0,010
$Pb_2Nb_2O_7$	Rhombohedral distortion of pyrochlore structure a = 10.675 A, α = 88°50'	144	—1500	0,0003
$Ba_2Nb_2O_7$		45	—160	0,0018

Table 2

Dielectric properties and structure of tantalates

Formula	Structure & lattice parameters	ε (t = 20°, f = 1 kc)	TC_ε (30–70°, $\alpha \cdot 10^6$ deg^{-1})	tg δ (1 kc, 20°)
$CaTa_2O_6$		24÷25	10÷180	0,03
$CdTa_2O_6$		60	—510	0,16
$SrTa_2O_6$		100÷115	—1100	0,007
$PbTa_2O_6$		310÷400	Large positive (ferroelectric region) θ=240°	0,022
$BaTa_2O_7$		132	—1600	0,003
$Ca_2Ta_2O_7$	Pyrochlore type	45	—430	0,0009
$Cd_2Ta_2O_7$	Pyrochlore type a = 10.376 A	72÷82	—1000	0,07
$Sr_2Ta_2O_7$		120	Large negative	0,0007
$Pb_2Ta_2O_7$	Rhombohedral distortion of pyrochlore structure a = 10.700 A, α = 88°25'	100÷114	—340	0,006
$Ba_2Ta_2O_7$		46÷50	—460	0,0007

Table 3

Dielectric properties of composite materials

Composition	ε	tg δ	Composition	ε	tg δ
$La_2O_3.2TiO_2$	46÷55	0,012÷0,014	$Nb_2O_5.TiO_2$	132	0,036
$La_2O_3.2ZrO_2$	25	0,18	$Nb_2O_5.ZrO_2$	100	0,032
$La_2O_3.2SnO_2$	16,6	0,13	$Nb_2O_5.SnO_2$	280	0,27
$La_2O_3.Nb_2O_5$	23,6	0,04	$3CaO.Al_2O_3.3TiO_2$	112	0,001

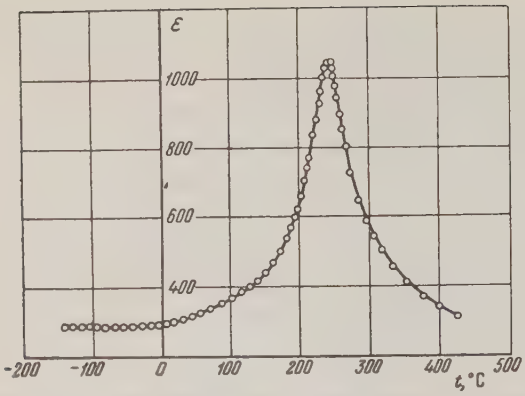

Fig.1. Temperature dependence of the dielectric constant of lead metatantalate.

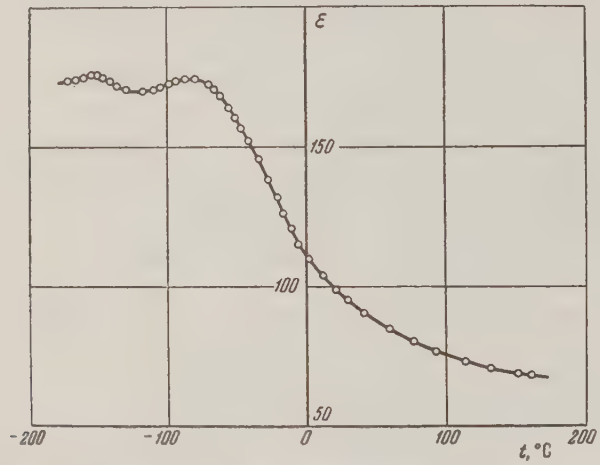

Fig.2. Temperature dependence of the dielectric constant of strontium pyrotantalate.

temperature down to the temperature of liquid nitrogen and exhibit no obvious anomalies. In the case of cadmium metaniobate there is a flat maximum for ϵ at about -155° and a rather sharp peak in the value of tan δ at about the same temperature; the exact temperature position of this peak depends on the frequency, which indicates that relaxation processes are involved in the effect.

Thus there are four known ferroelectrics among the niobates and tantalates of the bivalent metals: lead metaniobate and metatantalate, cadmium pyroniobate and strontium pyrotantalate. Only cadmium pyroniobate has been studied in any detail. This compound crystallizes with the pyrochlore structure in which the oxygen octahedra with the niobate ions inside them share corners. Lead pyroniobate and the pyrotantalates of cadmium, lead and calcium crystallize with the same structure. The crystal structure of calcium pyroniobate is different and more complicated. It is interesting to note that although lead pyroniobate has the pyrochlore structure it does not appear to be ferroelectric, while lead titanate having the perovskite structure has a very high Curie point. Although the dielectric constant of lead pyroniobate does pass through a flat maximum at 14°K (according to Hulm[7] and Shirane & Pepinsky[5]), no hysteresis loops at temperatures below this have been observed. As Jona, Shirane & Pepinsky[8] have shown that replacement of the cadmium ions by lead ions in cadmium pyroniobate leads to a downward shift of the Curie point. Similarly the Curie point is lowered when the niobium ions are replaced by tantalum ions or the cadmium ions by calcium ions.

We felt it would be of interest to investigate the effect of ionic replacements in strontium pyrotantalate. To this end we investigated the solid solutions: $Sr_2Ta_2O_7$-$Sr_2Nb_2O_7$, $Sr_2Ta_2O_7$-$Ba_2Ta_2O_7$ and $Sr_2Ta_2O_7$-$Ca_2Ta_2O_7$.

No x-ray diffraction studies on the formation of solid solutions in these systems have yet been made, but the observed appreciable shift of the Curie points indicates that solid solutions do form in a certain limited range of concentrations.

Inasmuch as the Curie point in the case of cadmium pyroniobate is lowered when the niobium ions are replaced by tantalum, one might expect that in the case of strontium pyrotantalate the Curie point will be raised as a result of replacement of the tantalum ions by niobium ions. As may be seen from

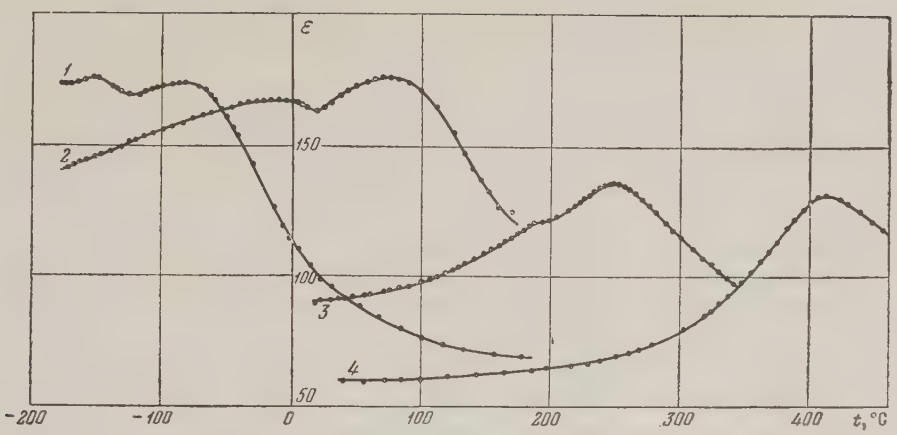

Fig.3. Temperature dependence of the dielectric constant of solid solutions of strontium pyroniobate in strontium pyrotantalate: 1) $Sr_2Ta_2O_7$, 2) $Sr_2(Ta_{0.95},Nb_{0.05})_2O_7$, 3) $Sr_2(Ta_{0.9},Nb_{0.1})_2O_7$, 4) $Sr_2(Ta_{0.8},Nb_{0.2})_2O_7$.

Fig.3, showing the temperature dependence of the dielectric constant of $Sr_2Ta_2O_7$-$Sr_2Nb_2O_7$ solid solutions, this expectation is fulfilled.

The Curie point rises approximately 32° for each mole percent $Sr_2Nb_2O_7$ (see Fig.6). The radii of the Nb^{5+} and Ta^{5+} ions being nearly equal, this shift of the Curie point to the side of higher temperatures can be explained by a change in the character of the bonds and the greater polarizability of Nb^{5+} as compared with the Ta^{5+} ion. At 20 mole percent $Sr_2Nb_2O_7$ the variation of the Curie point deviates from the linear which may be due to the fact that solid solutions no longer form at the higher concentrations. The low temperature phase transition is also shifted to the side of higher temperatures with increasing $Sr_2Nb_2O_7$ content.

It may be noted that according to the results of our measurements, in ceramic specimens of $(Cd,Sr)_2Nb_2O_7$ the Curie point goes down with increasing strontium pyroniobate concentration (in the 5 to 25 mole % $Sr_2Nb_2O_7$ interval).

Thus the addition of strontium pyroniobate to strontium pyrotantalate and cadmium pyroniobate displaces the Curie points of these compounds in opposite directions.

As is known the Curie point of the solid solutions $(Ba,Sr)TiO_3$ and $(Ba,Ca)TiO_3$ increases with increasing concentration of barium and decreases with increasing content of strontium and calcium. By analogy it might have been assumed that the same effects would be observed in the case of strontium pyrotantalate solid solutions. Measurements showed, however, that the Curie point θ_1 of $(Sr,Ba)_2Ta_2O_7$ solid solutions goes down with increasing $Ba_2Ta_2O_7$ content Figs.4 & 6. An inflection becomes evident at about 165° in the $\epsilon = f(t)$ curve for solutions with even a low $Ba_2Ta_2O_7$ content. With increasing barium pyrotantalate concentration this inflection turns into a maximum and grows more pronounced and at the same time is displaced to the side of lower temperatures, the shift being approximately proportional to the $Ba_2Ta_2O_7$ content. This linear variation breaks down, however, at barium tantalate concentrations above 20 mole %. This is apparently connected with the fact that the limit of the solubility range lies at about 20 mole %, so that with greater amounts of barium pyrotantalate present, a heterogeneous mixture is

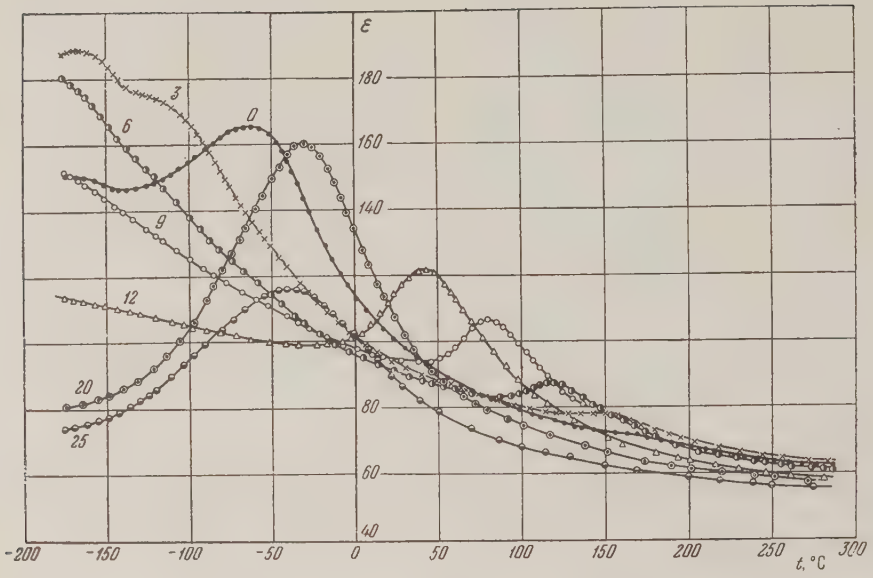

Fig.4. Temperature dependence of the dielectric constant of solid solutions of barium pyrotantalate in strontium pyrotantalate. The numbers at the curves indicate the barium pyrotantalate content in mole %.

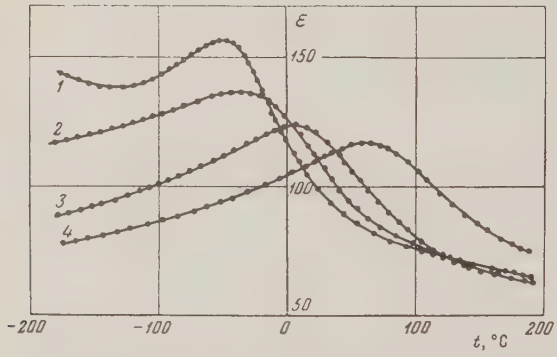

Fig.5. Temperature dependence of the dielectric constant of solid solutions of calcium pyrotantalate: 1) $Sr_2Ta_2O_7$, 2) $(Sr_{0.97},Ca_{0.03})_2Ta_2O_7$, 3) $(Sr_{0.94},Ca_{0.06})_2Ta_2O_7$, 4) $(Sr_{0.91},Ca_{0.09})_2Ta_2O_7$.

obtained. At temperatures below this maximum but above θ_1 hysteresis loops are not observed. Apparently these maxima correspond to points of nonferroelectric phase transitions which lead to distortion of the structure due to the large size of the barium ions. These phase transitions are probably similar to the transitions in $CaTiO_3$-$SrTiO_3$ solid solutions. It must be noted, however, that the observed dielectric constant maxima in the $(Sr,Ba)_2Ta_2O_7$ system may be due to relaxation effects.

Jona, Shirane & Pepinsky[8] showed that when the cadmium ions in cadmium pyroniobate are replaced by calcium ions the Curie point is displaced to the side of lower temperatures. As may be seen from Figs.5 & 6 in the case of strontium pyrotantalate replacement of strontium ions by calcium ions results in an increase of the Curie temperature.

Thus in strontium pyrotantalate solid solutions, when the strontium ions are replaced by larger barium ions with a higher electronic polarizability or by smaller calcium ions with a lower polarizability, the transition temperatures

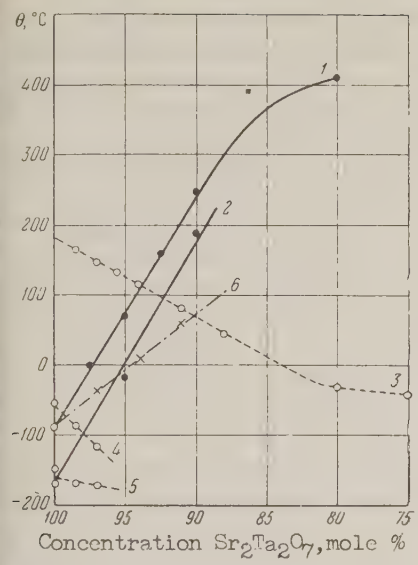

Fig.6. Variation of the temperature of the phase transitions in strontium pyrotantalate solid solutions as a function of the concentration of $Sr_2Ta_2O_7$: 1 & 2) the system $Sr_2(Ta,Nb)_2O_7$, 3,4 & 5) the system $(Sr,Ba)_2Ta_2O_7$, 6) the system $(Sr,Ca)_2Ta_2O_7$.

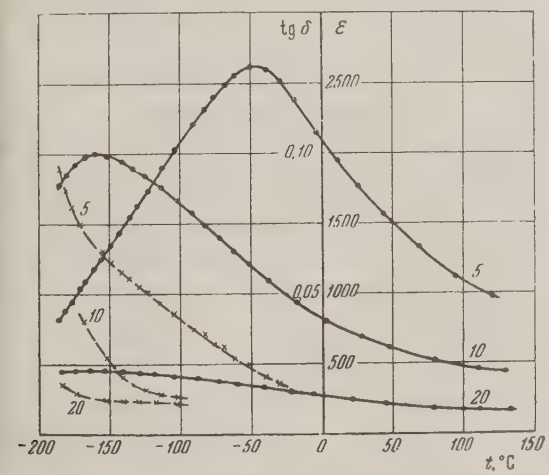

Fig.7. Temperature dependences of the dielectric constant (solid lines) and tan δ (dash lines) of $BaTiO_3$-$Ba_{0.5}TaO_3$ solid solutions. The numbers at the curves indicate the content of the second component in mole %.

are shifted in an entirely different manner than in the case of ferroelectric solid solutions with the perovskite structure. We feel that it would be of value and interest to investigate further strontium pyrotantalate base solid solutions, particularly their structure and the changes in structure occurring at the phase transition points.

In addition to investigating binary solid solutions of the types listed above, we are currently studying the changes in the dielectric properties produced by the addition of the niobates and tantalates of bivalent metals to barium titanate. In this case there may form solid solutions of the second kind: deficiency or defect-containing solid solutions. We can give some preliminary data on the $BaTiO_3$-$Ba_{0.5}TaO_3$ and $BaTiO_3$-$BaTaO_{3.5}$ systems. In these systems as a result of formation of solid solutions there results a defective perovskite type structure. As may be seen from Fig.7 the temperature of the dielectric constant maximum is displaced to the side of lower temperatures with increasing $Ba_{0.5}TaO_3$ content. At the same time the value of ϵ_{max} decreases. Apparently in the case of introduction of $Ba_{0.5}TaO_3$ into barium titanate the oxygen ions remain in their initial positions, but tantalum ions replace some of the titanium ions and two barium ions give way to one vacancy and one barium ion. It may be assumed that the formation of the solid solution in this case is analogous to that in the case of $NaNbO_3$-$CdNb_2O_6$ which was investigated by Lewis & White[9].

The addition of $BaTaO_{3.5}$ to barium tantalate also lowers the ϵ peak temperature and reduces the value of ϵ (Fig.8).

In view of their interesting properties solid solutions of barium niobates and tantalates may find practical application in engineering and industry.

In addition to the various solid solutions and compounds mentioned above we also investigated polycrystalline specimens of $Na(Nb,Ta)O_3$ solid solutions. For their preparation we used Nb_2O_5 and Ta_2O_5 prepared as outlined above and grade «Ч» ("Pure") Na_2CO_3. As may be seen from Fig.9, $NaTaO_3$ exhibits no dielectric anomalies in the temperature range from

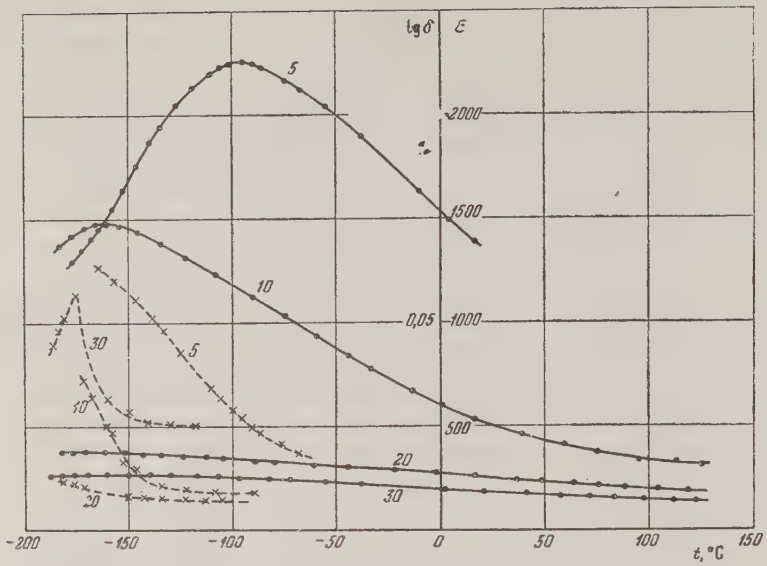

Fig.8. Same as Fig.7 but for $BaTiO_3$-$BaTaO_{3.5}$. The numbers at the curves indicate the content of the second component in mole %.

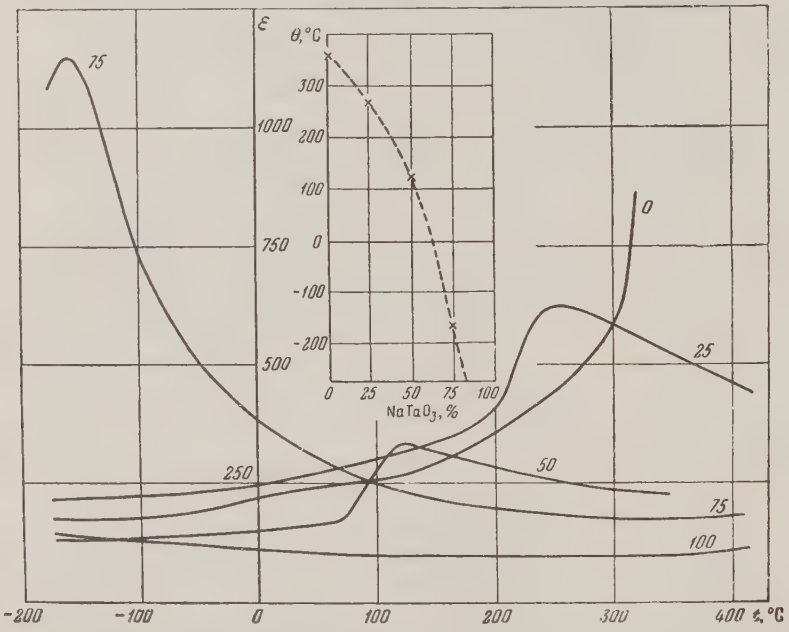

Fig.9. Temperature dependence of the dielectric constant of $Na(Nb,Ta)O_3$ solid solutions as measured at a frequency of 500 kc. The numbers at the curves give the concentration of $NaTaO_3$ in mole %. The insert diagram gives the dependence of the Curie point on the $NaTaO_3$ concentration.

-180 to +420°; the value of its dielectric constant increases continuously with decreasing temperature. The noticeable rise of ε at high temperatures is apparently connected with a marked increase in the electronic conductivity. Further, no anomalies in the temperature dependence of $\Delta l/l$ in the range from -180 to +510° were observed for $NaTaO_3$.

No real peak of the dielectric constant in $NaNbO_3$ was attained due to the strong increase in conductivity. With replacement of Nb by Ta the ε peak observed in $NaNbO_3$ at 360° is displaced to the side of lower temperatures. No hysteresis loops were observed at room temperature for $NaNb_{0.75}Ta_{0.25}O_3$ and $NaNb_{0.5}Ta_{0.5}O_3$; hysteresis loops in $NaNb_{0.25}Ta_{0.75}O_3$ were observed, however, at the temperature of liquid nitrogen.

Cross & Nicholson[10] investigated the temperature dependence of the dielectric constant of $NaNbO_3$ single crystals in a wide temperature range. As may

be seen from the $\epsilon = f(t)$ curves given in their report no dielectric constant peak is observed at the upper transition temperature ($\sim 640^{\circ}$), but the temperature coefficient of ϵ changes abruptly at this point. During subsequent cooling the dielectric constant increases, then drops suddenly at the temperature of the second transition ($\sim 480^{\circ}$); after this it starts rising anew and a sharp peak, similar to that exhibited by ϵ in $PbZrO_3$ at 230°, is observed only at the temperature of the lowest phase transition ($\sim 360^{\circ}$).

The anomalies of ϵ and the temperature coefficient of ϵ at the two upper transition points of $NaNbO_3$ are analogous to the anomalies characteristic of $(Ca,Sr)TiO_3$ solid solutions. This gives reason to assume that the higher temperature transitions of $NaNbO_3$ are "crystallochemical". If this is true $NaNbO_3$ is antiferroelectric only below 360°.

If this point of view is correct, then, as follows from Fig.9, $NaTaO_3$ is neither a ferroelectric nor antiferroelectric and the transition at 475° is a "crystallochemical" one.

In conclusion it may be said that investigation of the niobates and tantalates of bivalent metals and their solid solutions is of interest not only from the purely scientific but also from the engineering-technological viewpoint. In particular lead metaniobate and metatantalate and solid solutions based on these compounds, in view of their high Curie points, may find application in piezoelectric transducers intended for operation at elevated temperatures.

In conclusion I desire to thank G.A.Smolenskii for his guidance in the work.

Institute of Semiconductors of the
Academy of Sciences of the USSR

References

1. E.Wainer & Ch.Wentworth, J.Am.Cer.Soc., 35, 207 (1952); 35, 207 (1952).
2. W.R.Cook, H.Jaffe, Phys.Rev., 88, 1426 (1952).
3. W.R.Cook & H.Jaffe, Phys.Rev., 89, 129 (1953).
4. G.Goodman, J.Am.Cer.Soc., 36, 368 (1953).
5. G.Shirane & R.Pepinsky, Phys.Rev., 92, 504 (1953).
6. G.A.Smolenskii, Doklady AN SSSR, 97, 237 (1954).
7. J.K.Hulm, Phys.Rev., 92, 504 (1953).
8. F.Jona, G.Shirane & R.Pepinsky, Phys.Rev., 98, 903 (1955).
9. B.Lewis & E.A.D.White, Acta Cryst., 8, 849 (1955).
10. L.E.Cross & B.J.Nicholson, Phil.Mag., 46, 453 (1955).

INVESTIGATION OF THE ANTIFERROELECTRIC PROPERTIES OF SOME SOLID SOLUTIONS CONTAINING LEAD ZIRCONATE

- N.N.Krainik

At present we know of a number of compounds with the perovskite structure that are classed at antiferroelectrics: $PbZrO_3$, $NaNbO_3$, $PbHfO_3$ and some of their solid solutions. The hypothesis that $PbZrO_3$ is ferroelectric has been advanced by several Japanese scientists[1] and at present may be regarded as a working hypothesis which can serve to explain the anomalous properties of such compounds. The fact that the macroscopic net spontaneous polarization of antiferroelectrics even within the boundaries of a single domain is zero is explained by the antiparallel displacement of the ions. For a complete description of the antiferroelectric state, however, it is not sufficient to take into account the displacements of the ions of any one type, it is important to know and take account of the positions of all the ions, which is admittedly a difficult problem.

According to the data of Sawaguchi, Maniwa & Hoshino[2] lead zirconate has an orthorhombic structure. The main superstructure lines observed in x-ray diffraction patterns can be explained by an antiparallel displacement of the lead ions in the (001) plane along the face diagonal (Fig.1). There may also be a very small shift of the lead ions along the c axis, which is consistent with the small piezoeffect observed in lead zirconate by Roberts[3]. When the Zr^{4+} ion in $PbZrO_3$ is replaced by the smaller Ti^{4+} or Sn^{4+} ions and the Pb^{2+} ion by the larger Ba^{2+} ion there appears an intermediate ferroelectric phase (with a rhombohedral structure) between the low temperature antiferroelectric phase (analogous to that of pure $PbZrO_3$) and the paraelectric phase obtaining at high temperatures[4-9]. The temperature of the transition from the antiferroelectric to the ferroelectric phase decreases with increasing concentration of these ions.

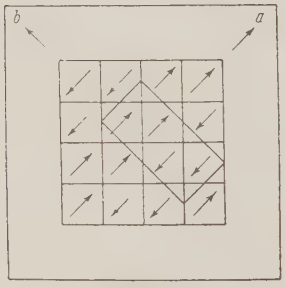

Fig.1. Projection of the packet structure of $PbZrO_3$ on the (001) plane (after Sawaguchi's model).

When the Pb^{2+} ion in $PbZrO_3$ is replaced by the smaller Sr^{2+} ion there appears an intermediate nonpolar, possibly antiferroelectric phase having a tetragonal structure with an axial ratio c/a = 0.9995 and an arrangement of superstructure lines differing from that observed for $PbZrO_3$ and clearly in conflict with the hypothesis of simple paired antiparallel shifts of the Pb^{2+} ions. The temperature of the transition from the lowest antiferroelectric phase to the intermediate phase decreases with increasing $SrZrO_3$ content, while at the same time the temperature of the transition from the intermediate to the paraelectric state first rises and then falls off at higher $SrZrO_3$ concentrations.

In order to gain a better understanding of the antiferroelectric state we felt it would be of interest to investigate a series of lead zirconate solid solutions. Accordingly, we synthesized a number of solid solution specimens in the systems $PbZrO_3$-$CaZrO_3$, $PbZrO_3$-"$PbCeO_3$" and $PbZrO_3$-"$CdZrO_3$" and investigated the temperature dependences of the dielectric constant, loss tangent and relative elongation as well as the field dependence of the polarization. We also made an attempt to synthesize the following solid solutions of lead zirconate with a small concentration of the second component: $PbZrO_3$-"$MgZrO_3$", $PbZrO_3$-"$ZnZrO_3$" and $PbZrO_3$-"$PbThO_3$".

Raw materials used in the preparation of ceramic specimens, composition of specimens, sintering temperature and losses of lead oxide and cadmium oxide during firing

Composition	Initial materials	Prelim. firing		Final firing		Reduction in weight during firing, %	
		t, °C	hours at t_{max}	t, °C	hours at t_{max}	PbO	CdO
$PbZrO_3$	PbO «ЧДА», ZrO_2 tech. (ZrO_2 content 98.4%)	—	—	900	1		—
Ca—n (n=2÷40)	PbO «ЧДА», ZrO_2 tech., $CaZrO_3$ (Ca—100)	950	1	1280÷1320	1	Samples for electric measurements to 3%; for dilat. measurements 10%	—
Ca—100	$CaCO_3$ «Ч», ZrO_2 tech.	—	—	1400	2		
Cd—n (n=1÷30)	1) $CdCO_3$ «Ч», ZrO_2 tech., PbO «ЧДА»	800	0	1100	1	To 3	To 25
	2) $CdCO_3$ «Ч», ZrO_2 tech., $PbZrO_3$	800	0	1100	1	To 2	To 20
Ce—n (n=1÷20)	ZrO_2 tech., PbO «ЧДА», CeO_2 (5% other rare earth oxides	950	2	1300	1	To 10	—
Mg—n (n=2,5÷10)	$MgCO_3$ «Ч», ZrO_2 tech., PbO «ЧДА»	1050*	1	1320	1	To 5	
Zn—n (n=1÷30)	$ZnCO_3$ «Ч», ZrO_2 tech., PbO «ЧДА»	950	2	1300	1	To 2	—
Th—n (n=1÷20)	ThO_2 «Ч», ZrO_2 tech., PbO «ЧДА»	950	2	1320	1	To 10	—

*The preliminary firing was carried out twice with subsequent grinding up of the material each time.

«Ч»= "Pure", «ЧДА»= "Pure for Analysis".

The conventional ceramic procedure was employed in preparing the specimens. Except for the $PbZrO_3$-"$CdZrO_3$" specimens, the compressed ceramics were fired in an atmosphere of PbO vapor; the specimens of the $PbZrO_3$-"$CdZrO_3$" system were fired in an atmosphere of CdO and PbO vapor.

The specimens were designated according to the calculated content of the second component: Ca-n, Cd-n, Ce-n and so on, where n is the concentration of the second component in mole percent. For example, Ca-10 stands for the composition 90% $PbZrO_3$ + 10% $CaZrO_3$, Ce-10 identifies the composition 90% $PbZrO_3$ + 10% "$PbCeO_3$". The loss of lead and cadmium oxide was checked by weighing the specimens before and after firing.

For preparing specimens of the system $PbZrO_3$-$CaZrO_3$ we used a $CaZrO_3$ product synthesized beforehand at 1400°. Specimens of the $PbZrO_3$-"$CdZrO_3$" system were prepared by two procedures: 1) directly from the appropriate oxides and carbonates and 2) by the addition of the appropriate compounds to previously synthesized $PbZrO_3$.

In the case of all the other systems the synthesis was effected directly from the corresponding oxides or carbonates.

$PbZrO_3$-$CaZrO_3$ system

In the $PbZrO_3$-$CaZrO_3$ system the Pb^{2+} (ionic radius r = 1.41 Å - Ref.10) is replaced by the smaller Ca^{2+} ion (r = 1.17 Å). According to x-ray data made available to us by Iu. N.Venev, a continuous series of solid solutions up to a $CaZrO_3$ content of 40% form in this system.

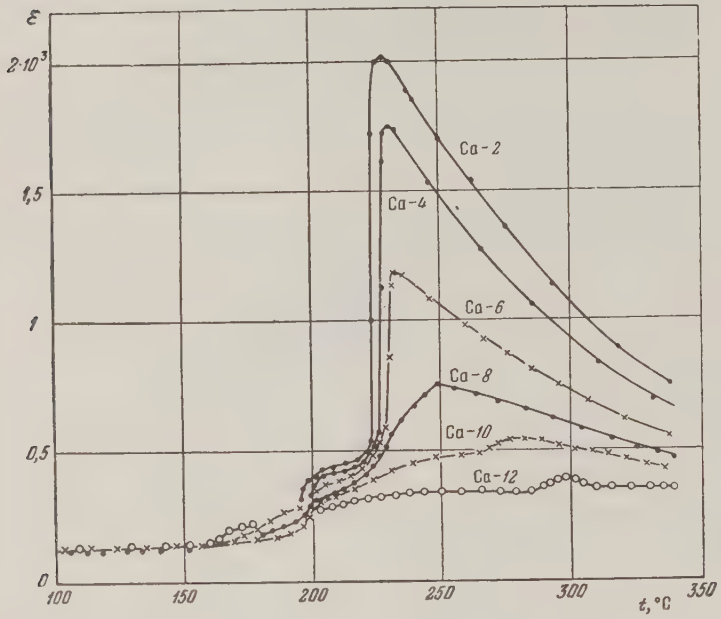

Fig.2. Temperature dependences of the dielectric constant of $PbZrO_3$-$CaZrO_3$ specimens.

The temperature dependences of solid solutions containing up to 12% $CaZrO_3$ are shown in Fig.2. It will be seen that in the case of solutions containing less than 8% $CaZrO_3$, there are two phase transitions and the appearance of the ε curves is analogous to that of the corresponding curves for the (Pb,Sr)ZrO_3 system[4]. The solutions containing from 8 to 12% $CaZrO_3$ exhibit three phase transitions. At higher concentrations of $CaZrO_3$ it becomes impossible to determine the temperature of these transitions from the variation of ε inasmuch as 1) the magnitude of the change in ε at the transition decreases, just as reported by Shirane[4] for (Pb,Sr)ZrO_3 solutions, 2) the temperature interval over which the transition occurs broadens, 3) the conductivity rises in the vicinity of the high temperature (third) transition due to the fact that the transition temperature becomes higher. The numeration of the transitions here and below is that indicated in Fig.3.

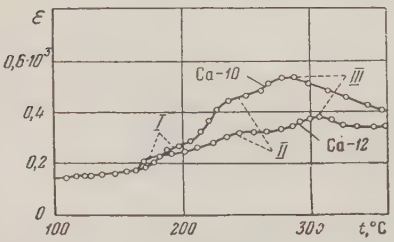

Fig.3. Temperature dependences of the dielectric constant of specimens Ca-10 and Ca-12 of the $PbZrO_3$-$CaZrO_3$ system (this figure represents part of Fig.2 plotted to a different scale).

The temperature dependences of the relative elongation of specimens containing up to 17% $CaZrO_3$ is shown in Fig.4.

In the case of specimens containing less than 10% $CaZrO_3$ the volume spontaneous change in both transitions is negative; the change in $\Delta l/l$ corresponding to the first transition decreases with increasing $CaZrO_3$ content, while that corresponding to the second transition increases. In the case of the Ca-10 specimen the second transition is diffuse; the reason for this may be that for it the second and third transitions are close. At a concentration of $CaZrO_3$ above 12% the striction at the first transition changes sign and becomes positive.

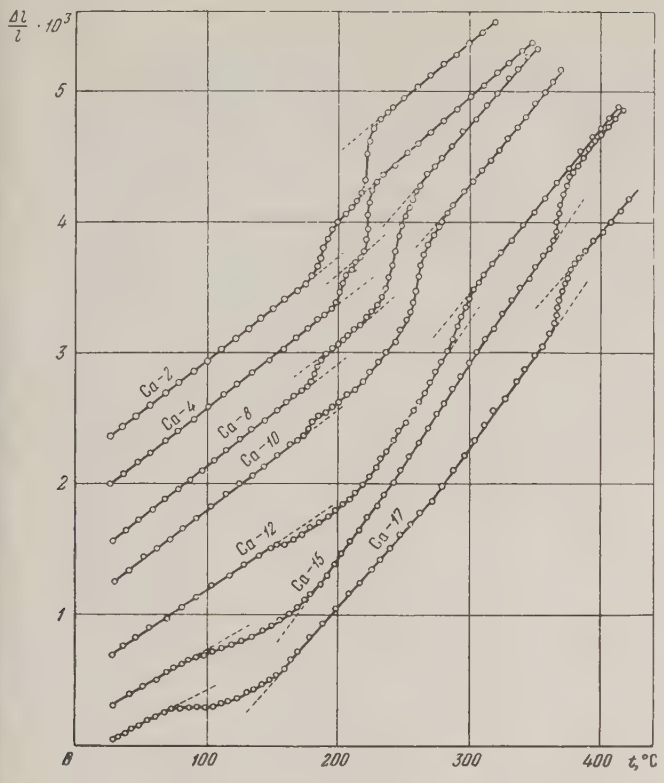

Fig.4. Temperature dependence of the elongation per unit length of specimens in the $PbZrO_3$-$CaZrO_3$ system.

An abrupt change in $\Delta l/l$ corresponding to negative striction is observed in the region of the third phase transition; no anomalies are observed in the temperature interval between the first and third phase transitions, but the thermal expansion coefficient of specimens Ca-12, Ca-15 and Ca-17 is characterized by a somewhat elevated value in this interval. This may lead to the diffuse character of the second phase transition and some decrease of the volume change occurring incident to this transition. In general, as the $CaZrO_3$ content is increased above 10% the $\Delta l/l$ vs t curves are smoothed and anomalies tend to decrease.

The variation of the polarization with the electric field intensity for the specimens of this system is linear in the temperature range from room temperature to 245°; no hysteresis loops were detected. The diagram of the phase transitions in the investigated $(Pb,Ca)ZrO_3$ solid solutions, based on the experimental temperature dependences of ϵ and $\Delta l/l$, is shown in Fig.5. The low temperature phase I is identical with the antiferroelectric phase of pure $PbZrO_3$; phase II is apparently similar to the intermediate phase in $(Pb,Sr)ZrO_3$ solid solutions; the probable character of phase III will be discussed below.

We observed no anomalies in the temperature dependence of the loss tangent in the region of the phase transitions.

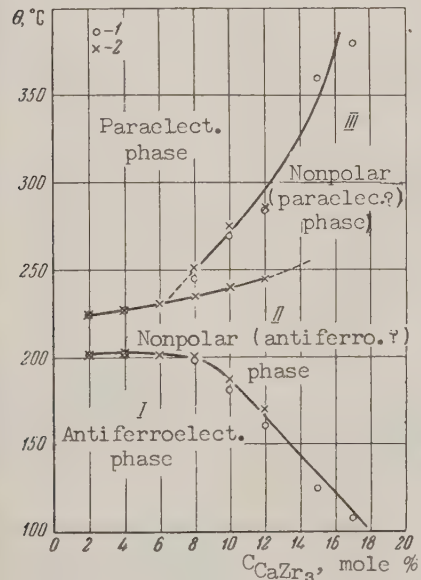

Fig.5. Phase transition diagram for the $PbZrO_3$-$CaZrO_3$ system: 1) data from dilatometric measurements, 2) data from measurements of the dielectric constant.

$PbZrO_3$-"$PbCeO_3$" system

In this system the Zr^{4+} ion (r = 0.82 Å) is replaced by the larger Ce^{4+} ion (r = 0.88 Å). According to the data of Smolenskii & Agranovskaia the compound "$PbCeO_3$" as such does not exist, but just as in the case of $PbZrO_3$-"$PbSnO_3$" solid solutions, $Pb(Zr,Ce)O_3$ solid solutions can apparently exist in a certain range of concentrations.

The temperature dependences of the dielectric constant of compositions containing up to 20% "$PbCeO_3$" are shown in Fig.6. With increasing "$PbCeO_3$" concentration, the height of the dielectric constant maximum decreases, while the temperature of the transition to the paraelectric state is slowly displaced to the side of higher temperatures. Two phase transitions are observed. The shape of the ϵ vs t curves is analogous to that of the curves for $(Pb,Sr)ZrO_3$ solid solutions.

Curve 1 in Fig.7 characterizes the temperature dependence of the relative elongation for specimen Ce-10. Both the phase transitions are associated with negative volume striction.

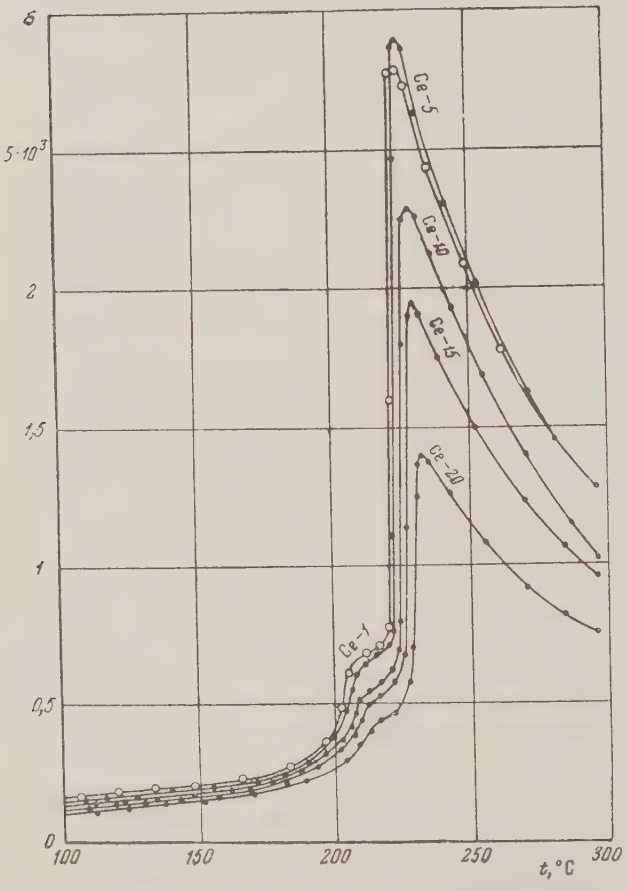

Fig.6. Temperature dependences of the dielectric constant of specimens of the $PbZrO_3$-"$PbCeO_3$" system.

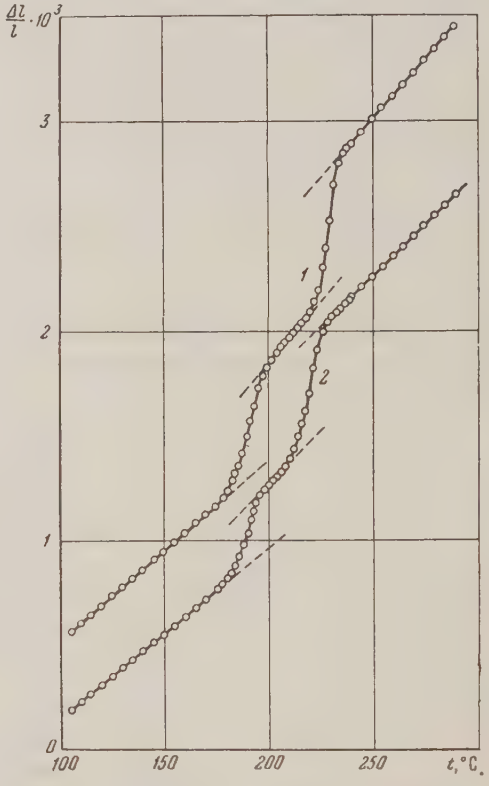

Fig.7. Variation with temperature of the elongation per unit length of specimens Ce-10 (curve 1) and Cd-10 (curve 2).

The electric field dependence of the polarization is linear up to 215°. In the vicinity of 220° there appear double hysteresis loops which disappear in the paraelectric region. This indicates, on the one hand, that the intermediate phase is nonpolar and, on the other hand,

that the free energies of this phase and of the ferroelectric phase are nearly equal.

The low temperature phase is identical with the antiferroelectric phase of pure $PbZrO_3$; the intermediate phase is apparently of the same nature as the intermediate phase in $(Pb,Sr)ZrO_3$ solid solutions.

No anomalies were observed in the temperature dependence of tan δ in the vicinity of the phase transitions.

$PbZrO_3$-"$CdZrO_3$" system*

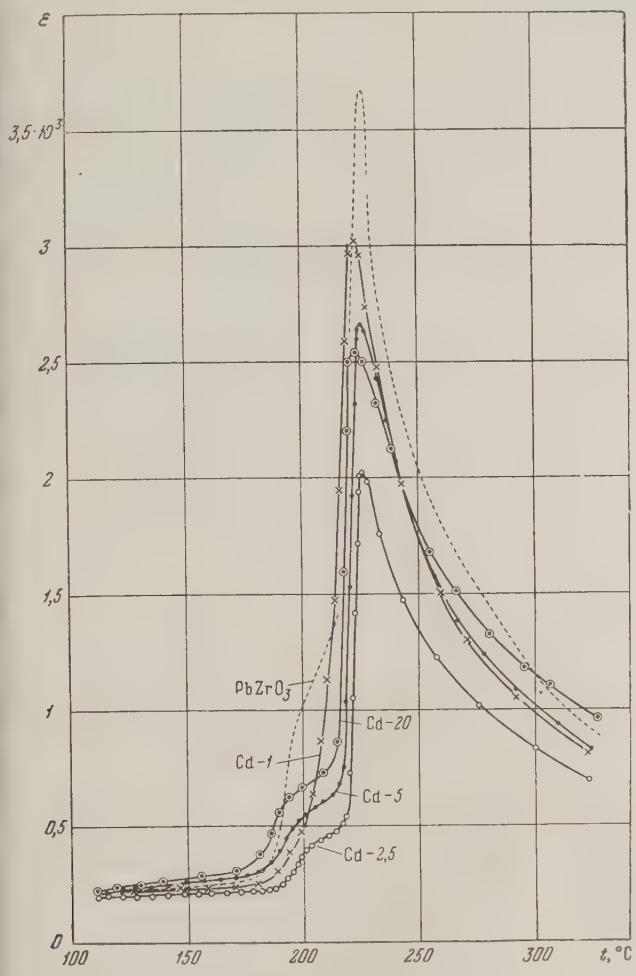

Fig.8. Temperature dependence of the dielectric constant of $PbZrO_3$-"$CdZrO_3$" specimens (prepared according to the first procedure).

In this system the Pb^{2+} ion (r = 1.41 Å) is replaced by the smaller Cd^{2+} ion (r = 1.11 Å). Naray-Szabo[11] reports that the compound $CdZrO_3$ does form, but so far this has not been confirmed by other investigators.

Fig.8 shows the variation of the dielectric constant of the specimens as a function of the temperature. Two phase transitions are observed at $CdZrO_3$ concentrations above 2.5%; the shape of the ε vs t curves is analogous to that of the curves for $(Pb,Sr)ZrO_3$ solid solutions. In the case of the Cd-1 specimen the low temperature transition is absent and the ε vs t curve in this region is intermediate between the corresponding curves for the technical grade $PbZrO_3$ used in preparing the specimens and the Cd-2.5 specimen.

Curve 2 in Fig.7 shows the temperature variation of the relative elongation of specimen Cd-10. Both phase transitions are associated with negative volume striction.

The electric field dependence of the polarization is linear; no hysteresis loops were detected in the temperature interval from room temperature to 230° and fields ranging up to the breakthrough value.

An x-ray study, carried out by A.M.Kalinina, of a number of specimens of this system prepared by both procedures failed to disclose any changes in the lattice parameters with increasing "$CdZrO_3$" content. Despite the fact that the x-ray studies give no

---

*The specimens were prepared according to the first described procedure.

indication of the formation of solid solutions in this system, the dielectric and dilatometric investigations of the specimens prepared by the first procedure furnish evidence that the Cd^{2+} ions enter the crystal lattice in amounts sufficient for the ferroelectric phase to disappear and for an intermediate nonpolar phase to form. The low temperature phase in the investigated specimens is identical with the antiferroelectric phase of pure $PbZrO_3$.

No anomalies were detected in the temperature dependence of tan δ of the specimens in the region of the phase transitions.

The systems $PbZrO_3$-"$MgZrO_3$", $PbZrO_3$-"$ZnZrO_3$", $PbZrO_3$-"$PbThO_3$" and $PbZrO_3$-"$CdZrO_3$"*

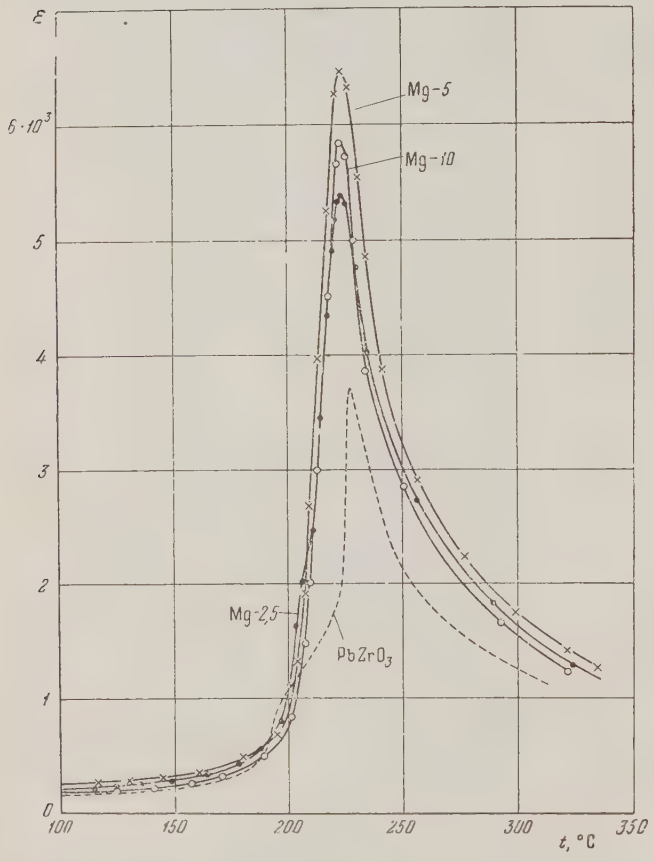

Fig.9. Temperature dependences of the dielectric constant of specimens of the $PbZrO_3$-"$MgZrO_3$" system.

The temperature dependences of the dielectric constant of the specimens of the $PbZrO_3$-"$MgZrO_3$" system is shown in Fig.9. The curves are generally similar to the curve for specimen Cd-1 (Fig. 8); no low temperature transition is observed.

It may be assumed that in spite of the large difference between the ionic radii of Pb^{2+} (r = 1.41 Å) and Mg^{2+} (r = 0.83 Å), a very small amount of magnesium does get incorporated into the crystal lattice and solid solutions are formed.

The results of the electric and dilatometric measurements on specimens of the PbZrO-"$ZnZrO_3$", $PbZrO_3$-"$PbThO_3$" and $PbZrO_3$-"$CdZrO_3$" systems (the specimens of the last system were prepared by the second procedure) are highly similar both to each other and to the results obtained for $PbZrO_3$. In all cases there is evident an intermediate ferroelectric phase, the temperature range for which coincides roughly with the corresponding range for the technical grade $PbZrO_3$ used in the preparation of the samples. X-ray studies of a number of specimens of the $PbZrO_3$-"$ZnZrO_3$" and $PbZrO_3$-"$PbThO_3$" systems carried out by Kalinina showed no changes in the lattice parameters with increasing concentration of the second component. Apparently solid solutions are not formed in these

---

*The specimens of the last system were prepared by the second procedure.

systems even at low concentrations of the second component. The reason for this is apparently the different character of the bonds peculiar to the different ions in question.

Discussion

The nature of antiferroelectricity in general and in particular the mechanism responsible for the transitions from the antiferroelectric to the ferroelectric state with increasing temperature observed in some solid solutions are obscure. Apparently, a significant role here is played by short-range forces. Among the factors whose influence should be taken into account is the electrostatic energy of the crystal lattice. Let us consider the problem from this viewpoint. Obviously, the treatment will not be complete or exhaustive inasmuch as there may be other forms of energy which we fail to take into account. We will also not take into account distortions of the ideal cubic lattice and possible changes in the influence of the oxygen ions in different solid solutions based on lead zirconate. The last is justified to some extent in view of the fact that we shall consider only solid solutions of $PbZrO_3$ with small concentrations of the second component.

Sauer[12] showed that the electrostatic energy of a simple cubic lattice with equal dipole moments at the lattice points has a minimum value with an antiparallel arrangement of the dipole moments; in the case of a body-centered and a face-centered cubic lattice the minimum energy corresponds to a parallel arrangement of the dipole moments. The electrostatic energy of body-centered and face-centered cubic lattices with an antiparallel arrangement of the dipole moments has a lower value if the dipoles are directed along a diagonal of the cube or a face than if they are directed along an edge. Takagi[13] analyzed a body-centered lattice of the CsCl type and showed that with a sufficiently small central dipole moment the antiparallel arrangement of the dipole moments may still be energetically advantageous, but that as the value of the central dipole moment increases the parallel arrangement becomes more advantageous. It must be noted that the designations "central" and "corner" moments are somewhat arbitrary and that which particular dipole moment is called the "central" one depends on the choice of the origin of the coordinates. Actually, here it is a question of the relative strength of the dipole moments situated at the points of each of the simple cubic lattices fitting one inside the other.

In the lead zirconate lattice there is a large corner dipole moment and a rather small central dipole moment due to the large size of the Zr^{4+} ion. (Here and below we assume the origin of the coordinates to be at the position of the bivalent cation so that the bivalent cation will be termed a corner one, while the quadrivalent ion at the center of the oxygen octahedron will be regarded as the central cation).

One must also take into account the character of the bonds. The results obtained by Shirane, Pepinsky and Frazer[14] in their x-ray and neutron diffraction studies of $PbTiO_3$ may be regarded as a confirmation of the hypothesis advanced by Megaw[15] and Blokhin[16] that the bonds between the lead and oxygen ions are partially covalent. In $PbTiO_3$ these bonds are realized between the Pb and O_{II} ions (O_{II} designates the oxygen ion in the position $x = 0$, $y = 1/2$ and $z = 1/2$; the tetragonal c axis is in the z direction). We assume that in $PbZrO_3$ there is partially covalent bonding between the Pb and O_I ions (O_I is the oxygen ion in the position $x = 1/2$, $y = 1/2$ and $z = 0$). This bond tends to increase the corner dipole moment directed along the face

diagonal which, in view of the limited freedom for displacement of the large Zr ion, favors the antiparallel arrangement of the dipole moments formed by the ions.

Replacement of the Zr ions (r = 0.82 Å) by the smaller Ti ions (r = 0.64 Å) and replacement of the Pb ions (r = 1.41 Å) by the larger Ba ions (r = 1.55 Å) which occurs in solutions of $PbZrO_3$ with substances having a large geometric factor t*, enhances the possibility of displacement of the central ions; this favors a parallel arrangement of the ions.

Replacement of the Pb ions by the smaller ions of Sr (r = 1.34 Å), Ca (r = 1.17 Å), or Cd (r = 1.11 Å) which occurs in solutions of $PbZrO_3$ with substances having a smaller geometric t factor, reduces the freedom for displacement of the central ions and hence furthers the antiparallel arrangement of the dipole moments.

The role of the geometric factor t in compounds with the perovskite type structure where the appearance of ferroelectricity and antiferroelectricity is concerned has been touched upon by Shirane[4] and analyzed in some detail by Venevtsev[17].

Our experimental work with a number of solid solutions based on $PbZrO_3$ showed that a relative increase in the free energy of the ferroelectric state and the appearance of an intermediate nonpolarized, possibly antiferroelectric phase when the t factor is reduced is a common trait for the solid solutions in this group. The results of our work show that analysis of this problem from the viewpoint of the electrostatic energy of the lattice helps throw some light on the regularities involved.

In our qualitative examination of the relative stability of the ferroelectric and antiferroelectric phases in $PbZrO_3$ solid solutions, we took into account only changes in the ionic polarizability of the central ions, which is to a degree justified by the low content of the second component in the solutions. It is obvious that for a more rigorous treatment of this problem one must take into account both the ionic and electronic polarizabilities of all the ions comprising the lattice as well as in the internal fields, the character of the bonds and the possible distortions of the ideal perovskite type lattice.

Let us examine the specific case of $CdTiO_3$. Despite the low value of the geometric factor (in $CdTiO_3$ t = 0.87, in $PbZrO_3$ t = 0.90 and in $PbHfO_3$ t = = 0.92 — Venevtsev & Zhdanov[9]), cadmium titanate has ferroelectric rather than antiferroelectric properties. From the values of the ionic radii and the t factor one might assume that the Cd^{2+} ion has "room" in the lattice, while the Ti^{4-} ion is "squeezed in" or tightly held, i.e., that the corner dipole moment should be large, while the central moment should be small, which should favor the appearance of antiferroelectricity. In view of the fact, however, that the electronic polarizability of Cd^{2+} is lower than that of Pb^{2+} and the homeopolar character of the Cd-O bond is less pronounced than that of the Pb-O bond, the magnitude of the corner dipole moment as compared with the central moment is not sufficient for the appearance of antiferroelectricity. Here one can hardly assume that the small corner ion, in this case the Cd ion, has "room" (is loosely held) in the perovskite lattice. As a result of the small size of the corner ion, the ideal lattice structure is distorted, for example, in the case of $CaTiO_3$ due to alternate tilting of the

---

*The geometric factor t, called the tolerance factor, is described by $t = (A - O)/\sqrt{2}(B - O)$, where (A -O) is the distance between the corner ion and oxygen ion and (B -O) is the separation between the central ion and the oxygen ion.

oxygen octahedra and as a result the corner ion is "squeezed in", i.e., is limited as regards possible displacement.

The reason for the appearance of the intermediate nonpolar phase in some of the $PbZrO_3$ solid solutions and the nature of this phase is obscure; no data on the character of the ionic displacements are available.

The observed change of the striction (volume change) from negative to positive at the first transition in the $(Pb,Ca)ZrO_3$ system is very interesting, particularly inasmuch as all the hitherto known transitions to the antiferroelectric state are associated with negative striction. It would be interesting to know whether this is not connected with an appreciable decrease of the volume of the unit cell due to increased concentration of $CaZrO_3$ in the solid solution and partially with the homeopolar character of the Pb-O bonds in the antiferroelectric state (a homeopolar bond would keep the Pb and O ions further apart).

In this connection it may be noted that the Pb-O distance in lead zirconate is apparently a predominant factor in determining the volume of the unit cell.

As for the third phase transition in the $(Pb,Ca)ZrO_3$ system, we suggest that this transition is analogous to the structural transitions observed by Gränicher & Jakits[18] in the $(Ca,Sr)TiO_3$ system and is a transition from one paraelectric state to another. The transition is apparently due to the small size of the Ca ion. Apparently the transition in $NaNbO_3$ in the 600-470° interval is of the same nature. Clearly with increasing content of the small ion in the solution the distortion will vanish at higher temperatures. This explains the shift to the side of higher temperatures observed for the third phase transition with increasing $CaZrO_3$ content.

Conclusions

1. We have made an attempt to interpret the relative stability of the ferroelectric and antiferroelectric states in solid solutions of lead zirconate with low concentrations of the second component from the point of view of the electrostatic energy of the crystal lattice. In doing so we have taken account only of the changes in the ionic polarizability of the central ions. It is obvious that for a more rigorous treatment one must take into account the ionic and electronic polarizabilities of all the ions comprising the lattice as well as of the internal fields, the character of the bonds and the distortions of the ideal perovskite type structure.

2. We synthesized specimens of a number of different compositions in the following systems: $PbZrO_3$-$CaZrO_3$, $PbZrO_3$-"$PbCeO_3$", $PbZrO_3$-"$CdZrO_3$", $PbZrO_3$-"$MgZrO_3$", $PbZrO_3$-"$PbThO_3$" and $PbZrO_3$-"$ZnZrO_3$" and investigated the temperature dependence of the dielectric constant, the loss tangent and the elongation per unit length as well as the dependence of the polarization on the intensity of the applied electric field.

3. On the basis of x-ray studies and the results of our measurements we conclude that solid solutions do not form in the $PbZrO_3$-"$PbThO_3$" and $PbZrO_3$-"$ZnZrO_3$" systems and in the $PbZrO_3$-"$CdZrO_3$" system in the case of specimens synthesized using presintered $PbZrO_3$.

In the $PbZrO_3$-"$MgZrO_3$" system and in the $PbZrO_3$-"$CdZrO_3$" system when the specimens are synthesized directly from the oxides and carbonates solid solutions apparently do form in the range of low concentrations of the respective second components.

4. In the $PbZrO_3$-$CaZrO_3$ system in the range of $CaZrO_3$ concentrations under

8 mole %, in the $PbZrO_3$-"$PbCeO_3$" system in general and in the $PbZrO_3$-"$CdZrO_3$" system prepared directly from the appropriate oxides and carbonates two phase transitions are observed: the low temperature transition corresponds to a transition from the antiferroelectric phase, analogous to the antiferroelectric phase in pure $PbZrO_3$, to an intermediate nonpolar, possibly antiferroelectric phase; the high temperature transition corresponds to a transition to the paraelectric state. Both phase transitions are associated with negative volume spontaneous striction.

5. A third high temperature phase transition occurs in the $PbZrO_3$-$CaZrO_3$ system; this transition is apparently a transition from a paraelectric state to another paraelectric state and is apparently due to the small size of the Ca ion. The temperature of this transition is displaced to the side of higher temperatures with increasing $CaZrO_3$ concentration.

6. In the $PbZrO_3$-$CaZrO_3$ system the volume spontaneous striction associated with the transition from the antiferroelectric to the intermediate nonpolar phase changes sign from negative to positive as the concentration of $CaZrO_3$ is increased.

7. No anomalies were detected in the temperature dependence of tan δ for specimens of the $PbZrO_3$-$CaZrO_3$, $PbZrO_3$-"$PbCeO_3$" and $PbZrO_3$-"$CdZrO_3$" systems in the region of the phase transitions.

In conclusion I wish to express my deep gratitude to G.A.Smolenskii for his constant interest in the work and discussion of the results.

Institute of Semiconductors of the
Academy of Sciences of the USSR

References

1. G.Shirane, G.Sawaguchi & A.Takeda, Phys.Rev., 84, 476 (1951).
2. E.Sawaguchi, H.Maniwa & S.Hoshino, Phys.Rev., 83, 1078 (1951).
3. S.Roberts, Phys.Rev., 83, 1078 (1951).
4. G.Shirane, Phys.Rev., 86, 219 (1952).
5. G.Shirane, K.Suzuki & A.Takeda, J. Phys.Soc.Japan, 7, 12 (1952).
6. E.Sawaguchi, J.Phys.Soc.Japan, 8, 6151 (1953).
7. L.Nomura, J.Phys.Soc.Japan, 10, 112 (1955).
8. G.A.Smolenskii, A.I.Agranovskaia, A.M.Kalinina & T.M.Fedotova, Zhur. tekh.fiz., 25, 2134 (1955).
9. Iu.N.Venevtsev & G.S.Zhdanov, Izv.AN SSSR, Ser.fiz., 20, 178 (1956). (Trans. in Bulletin, Vol.20, No.2, p.161).
10. G.B.Bokii, Vvedenie v kristallokhimiiu (Introduction to Crystallochemistry) M., 1954.
11. I.Narai-Szabo, Muegeutami Közlemenyck, 1, 30 (1947).
12. Sauer, Phys.Rev., 57, 142 (1940).
13. Y.Takagi, Phys.Rev., 85, 315 (1952).
14. G.Shirane, R.Pepinsky & B.Frazer, Acta Cryst., 9, 131 (1956).
15. H.D.Megaw, Proc.Phys.Soc. London, 58, 133 (1946); Acta Cryst., 7, 187 (1954).
16. M.A.Blokhin, Doklady AN SSSR, 95, 965 (1954); Doklady AN SSSR, 95, 1165 (1954).
17. Iu.N.Venevtsev, Dissertation, Moscow Mechanical Institute, M., 1955.
18. H.Gränicher & O.Jakits, Nuovo Cim., Suppl., 11, 480 (1954).

INVESTIGATION OF (Ba,Pb)(Ti,Sn)O_3 SOLID SOLUTIONS WITH FERROELECTRIC PROPERTIES

- I.E.Myl'nikova

Introduction

$BaTiO_3$ base solid solutions possessing ferroelectric properties are finding increasing application in the field of electronics. Investigation of such ferroelectric solid solutions is not only of practical but also of theoretical interest and can help give a clearer insight into the nature of ferroelectric effects.

Most studies to date have been devoted to solid solutions of $BaTiO_3$ with substances isomorphic with it, such as, strontium titanate, barium stanate and barium zirconate. There is little as yet known regarding the ferroelectric properties of multiple component systems.

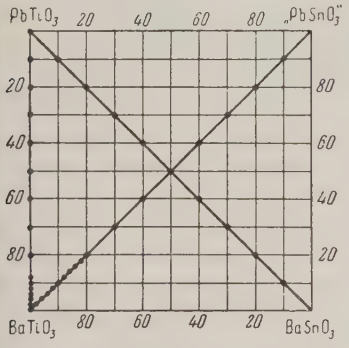

Fig.1. Compositions of the investigated solid solutions (mole %).

As the subject of our investigation we chose the system (Ba,Pb)(Ti,Sn)O_3. We investigated this system along two diagonal sections of the constitution diagram and in addition carried out a study of the ferroelectric properties of the binary system $BaTiO_3$-$PbTiO_3$. Detailed study of this binary system was prompted by the valuable technological properties of the solid solutions formed in it[1]. The $BaTiO_3$-$BaSnO_3$, $BaSnO_3$-"$PbSnO_3$" and $PbTiO_3$-"$PbSnO_3$" systems have been fairly thoroughly studied by other investigators[2,3] and hence were not taken up in the present work. The specific compositions investigated by us are indicated by the dots in Fig.1. The content of the initial components is given in molecular percent. Hereinafter specimens of the systems $BaTiO_3$-$PbTiO_3$, $BaTiO_3$-"$PbSnO_3$" and $PbTiO_3$-$BaSnO_3$ will be designated by the letters P, PN and BN respectively. The figures after these letters give the content of the second component. Thus P-10 stands for 90 mole % $BaTiO_3$ + 10 mole % $PbTiO_3$.

Synthesis and preparation of the specimens

In both laboratory and industrial practice barium titanate and its solid solutions with ferroelectric properties are prepared by reaction in the solid phase. In all cases it is important to insure not only completion of the reaction in the solid phase but also to obtain a well-sintered ceramic.

As is known, lead compounds are subject to thermal dissociation, hence particular attention must be paid in synthesis to assuring a stable composition. To this end, in addition to firing in air, we employed the procedure of firing the specimens in an atmosphere of lead oxide. The specimens on suitable stands were placed in a corundum curcible together with a smaller crucible filled with lead oxide. The large crucible was covered and sealed with a ceramic mass. In the process of heating the lead oxide in the small crucible is evaporated producing an atmosphere rich in PbO vapor inside the large crucible. At a certain temperature there was attained a dynamic balance at which the amount of lead oxide volatilizing from the specimen was approximately equal to the amount of lead oxide diffusing into it from the surrounding atmosphere. To facilitate determination of the loss of lead oxide during

synthesis we used previously prepared barium titanate. Thus the loss of lead oxide due to thermal dissociation could readily be determined by weighing the specimens before and after firing.

The sintering temperature for the solid solution specimens was increased with increasing barium titanate content. Obviously, with increasing temperature the partial vapor pressure of the lead oxide increases and at a certain point the specimens absorb excess lead oxide. For this reason solid solutions containing more than 90% $BaTiO_3$ were sintered in air, even though this involved some loss of zinc oxide (Table 1).

Table 1

Composition of specimens (mole %) and losses of lead oxide during sintering in air

System $BaTiO_3$ — $PbTiO_3$		System $BaTiO_3$ — «$PbSnO_3$»		Loss of lead oxide, % by weight
$BaTiO_3$	$PbTiO_3$	$BaTiO_3$	«$PbSnO_3$»	
98	2	98	2	~1
96	4	96	4	~2
94	6	94	6	~3
92	8	92	8	

In sintering $BaTiO_3$-$PbTiO_3$ specimens with a $BaTiO_3$ content under 90% in an atmosphere of lead oxide vapor the loss of PbO did not exceed 2%; the loss increased from 0.5 to 2% as the $PbTiO_3$ content in the specimen was raised from 10 to 90%.

Solid solutions containing "$PbSnO_3$" dissociate more readily: at "lead stanate" concentrations above 30% thermal dissociation starts before a sufficient amount of lead oxide vapor is formed to prevent it. Consequently, $BaTiO_3$-"$PbSnO_3$" samples fired in an atmosphere of PbO vapor, as a rule, undergo an appreciable loss of lead oxide. At a "$PbSnO_3$" content of 60% the PbO loss increases to about 5%.

The lead oxide losses in the case of specimens of the $PbTiO_3$-$BaSnO_3$ system amounted to 3-5% with sintering in an atmosphere of lead oxide vapor.

The sintering temperature for the different specimens was varied between 1250 and 1430° depending on the composition. The water absorption of specimens containing from 100 to 90% barium titanate was virtually nil. With an increase of the lead titanate content to above 60% the water absorption of the specimen attained about 5%.

Experimental results and discussion

The experimental procedures as regards measurement of the dielectric constant, the piezoelectric coefficient, the hysteresis loops and the linear expansion coefficient were identical with those used in the investigations of Refs.2-5 and hence will not be described here.

$BaTiO_3$-$PbTiO_3$ system

The temperature dependences of the dielectric constant were determined for specimens containing up to 50% lead titanate (Fig.2). In the case of specimens containing more than 50% lead titanate it proved impossible to study the variation of the dielectric constant as a function of the temperature because of the high conductivity of the specimens at elevated temperatures. As the amount of lead titanate is increased, the point corresponding to the phase transition from the cubic to the tetragonal modification is shifted to the side of higher temperatures. The low temperature phase transition points, on the contrary, are displaced towards lower temperatures. Thus in $BaTiO_3$-$PbTiO_3$ solid solutions the region characterized by the tetragonal structure is widened

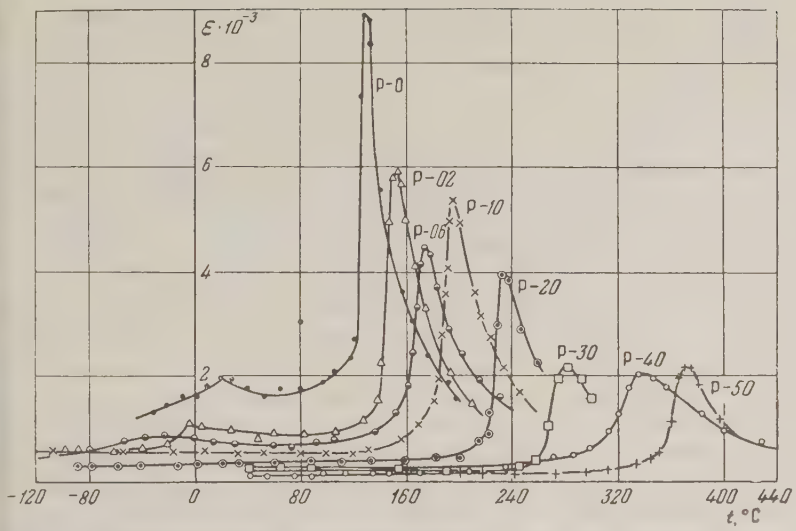

Fig.2. Temperature dependences of the dielectric constant of specimens of $BaTiO_3$-$PbTiO_3$ solid solutions.

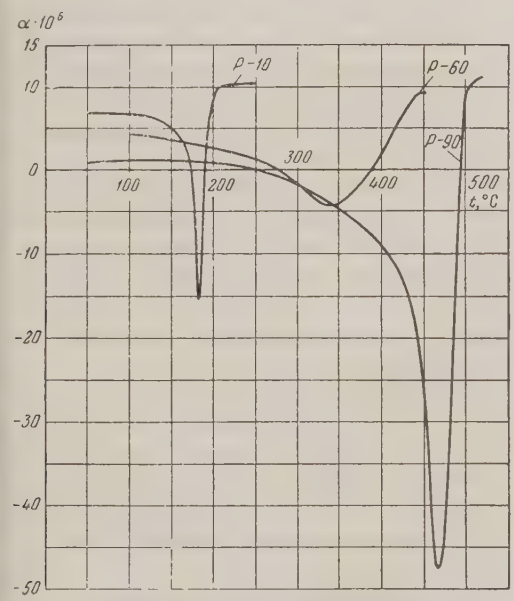

Fig.3. Temperature dependence of the coefficient of linear expansion of solid solution specimens of the $BaTiO_3$-$PbTiO_3$ system.

as compared with pure barium titanate. The value of the dielectric constant at the peak decreases with increasing lead titanate content. Also with increasing $PbTiO_3$ content there is observed a decrease of the temperature coefficient of the dielectric constant in the range from -60 to +60°, which is important for many electronic applications. In general our results are in agreement with the data of other investigators[6,7]

We calculated the values of the Curie-Weiss constant from the $1/\epsilon = f(t)$ curves. The Curie-Weiss constant for the tetragonal phase is smaller than for the cubic. There is no significant decrease in the value of the Curie-Weiss constant upon going over to either the cubic or the tetragonal phase.

Investigation of the temperature dependences of the elongation per unit length and the coefficient of linear expansion makes it possible to determine the temperatures of the phase transitions for specimens containing over 50% lead titanate, i.e., of specimens for which measurements of the dielectric constant in this region are impossible.

The linear expansion coefficient vs temperature curves for the solid solutions exhibit minima at the phase transition points (Fig.3). It will be seen that with increasing lead titanate content the position of the minimum is displaced to the side of higher temperatures. "Medium compositions" are distinguished by a broader minimum. This, apparently, is not connected with the quality of the synthesis but is due to microheterogeneity, a trait characteristic of many "medium composition" solid solutions.

The anomalous character of the linear expansion coefficient curves (i.e., the presence of a minimum) is connected with an increase in the volume of the unit cell incident to the transition from the cubic to the tetragonal structure (positive electrostriction). The electrostriction in the specimens increases with increasing lead titanate content. The specimens exhibit a higher

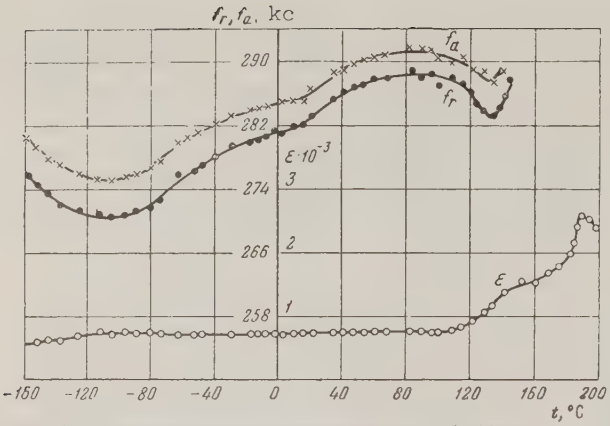

Fig.4. Temperature dependence of the resonance and antiresonance frequencies and the dielectric constant of a prepolarized specimen having the composition 90% $BaTiO_3$ + 10% $PbTiO_3$.

value of the linear expansion coefficient in the cubic phase as compared with the tetragonal one.

The piezoelectric properties of the ferroelectric materials were investigated under dynamic conditions using specimens in the form of discs 10 mm in diameter and 1-2 mm thick. Prior to the piezoelectric measurements the specimens were prepolarized in a 25 kv/cm field at room temperature for 24 hours.

The curves characterizing the variation of the resonance and antiresonance frequencies (and the dielectric constant) as a function of the temperature for a specimen containing 90% $BaTiO_3$ and 10% $PbTiO_3$ are shown in Fig.4.

Investigation of the temperature dependence of the resonance and antiresonance frequencies showed that both these grequencies exhibit a minimum in the temperature region of the high temperature phase transition; in the same temperature region there is a marked change in the value of the dielectric constant. This effect can be explained by depolarization of the sample as a whole inasmuch as the application of a polarizing field (E = 5 kv/cm) produced no observable change in the dielectric constant.

An analogous effect was observed in investigating barium titanate single crystals having appreciable internal stresses. The spontaneous polarization of the specimen remains unchanged in the process. As the lead titanate content is increased the difference between the transition temperature and the temperature of depolarization of the specimen increases. A minimum in the resonance and antiresonance frequency curves is also observed in the region of the low temperature phase transitions; this is undoubtedly associated with the decrease of the modulus of elasticity common to such phase transitions.

Table 2

Values of the piezoelectric coefficient and the electromechanical coupling coefficient for solid solutions of the $PbTiO_3$-$BaTiO_3$ system

Composition, molc %		$\lvert d_{31}\rvert \cdot 10^9$, cgse units		k, %	
$PbTiO_3$	$BaTiO_3$	t=20°	t=60°	t=20°	t=60°
2	98	2,5	1,9	26	22
6	94	2,4	2,0	28	26
8	92	2,1	1,8	27	25
12	88	1,3	1,2	16,5	16

The values of the piezoelectric modulus $|d_{31}|$ and the electromechanical coupling coefficient k at 20° and 60° for a number of $PbTiO_3$-$BaTiO_3$ solid solutions are listed in Table 2.

As may be seen from the table the values of these coefficients decrease only slightly with increasing lead titanate concentration up to 12%.

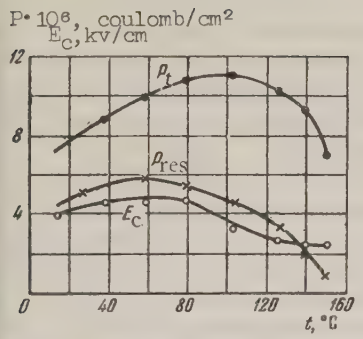

Fig.5. Temperature dependence of the total (P_t) and residual (P_{res}) polarization and the coercive force (E_c) for a specimen having the composition 94% $BaTiO_3$ + 6% $PbTiO_3$ at E = 15 kv/cm.

It will be noted that these binary solid solutions are characterized by a larger value of the ratio of the piezoelectric coefficient to the dielectric constant as compared with pure barium titanate, which is an important consideration where a number of technical applications are concerned. According to our results, solid solutions containing from 8 to 12% lead titanate are distinguished by low values of the temperature coefficients of the piezoelectric coefficient and the resonance frequency in the temperature range from -60 to +80°; this is in agreement with the data of Mason[1] and Roi[8]. The temperature coefficient of the resonance frequency in the range from -60 to +60° is $\sim 3 \cdot 10^{-4}$ degree^{-1}. A number of specimens containing 90% $BaTiO_3$ + 8% $PbTiO_3$ prepolarized in a 25 kv/cm field at room temperatures were allowed to age for several months; 270 days after polarization the piezoelectric coefficient $|d_{31}|$ amounted to 85% of its initial value.

Investigation of dielectric hysteresis in the temperature range above 20° showed that in the case of solid solutions containing more than 4 mole % lead titanate the curves characterizing the temperature dependences of the total polarization and the coercive force pass through a maximum (Fig.5). It must be noted that as the lead titanate content is increased the maxima shift to the side of higher temperatures. This effect can be explained by enhanced ferroelectric "hardness" of solid solutions containing lead titanate. In heating of ferroelectrically "hard" materials in a certain temperature interval the number of domains oriented by the field increases; in view of this one can expect a maximum to appear in the polarization vs temperature curves. At higher temperatures the total polarization decreases due to a decrease of the spontaneous polarization.

$BaTiO_3$-"$PbSnO_3$" system

Investigation of the $BaTiO_3$-"$PbSnO_3$" system is of considerable interest, first, because with the introduction of "lead stanate" both bivalent and tetravalent cations are replaced and, second, because one of its components, namely, "lead stanate" is a "fictitious" compound in the sense that it does not exist independently.

It may be concluded from the results of x-ray studies that solid solutions with a perovskite structure are formed at "lead stanate" concentrations of up to 70%. With a "$PbSnO_3$" content over 70% there appear in the x-ray diffraction patterns lines associated with lead dioxide and a crystal phase whose nature has not yet been established. In all probability this phase is a compound having the composition $2PbO.SnO_2$ found by Urazov[9] in investigating the phase diagram of PbO-SnO_2 and detected by Venevtsev[10] in his x-ray investigation of samples prepared from an initial mixture having the composition corresponding to "lead stanate".

Curves characterizing the temperature dependence of the dielectric constant for a number of solid solutions of the $BaTiO_3$-"$PbSnO_3$" system are shown in Fig.6.

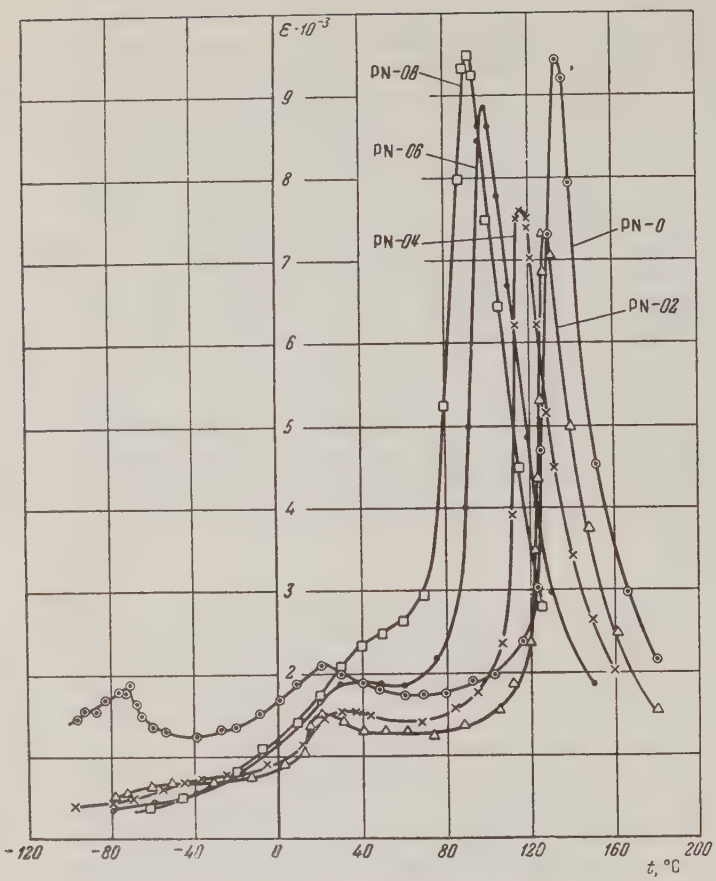

Fig.6. Temperature dependence of the dielectric constant of $BaTiO_3$-"$PbSnO_3$" solid solutions.

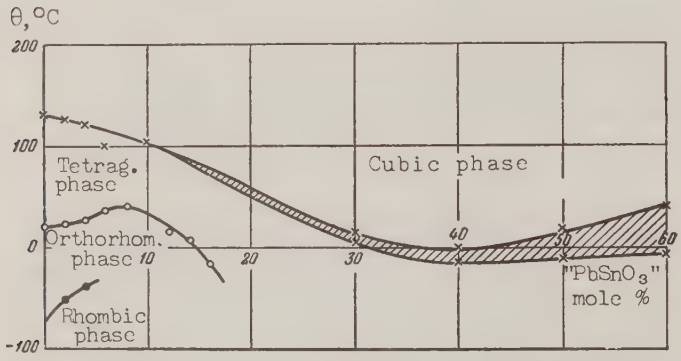

Fig.7. Approximate diagram of phase transitions in the $BaTiO_3$-"$PbSnO_3$" system.

Investigation of the temperature dependence of the dielectric constant and the resonance frequencies showed that with increasing "lead stanate" content the temperature of the transition from the cubic to the tetragonal structure is shifted first to the side of lower temperatures and then, beginning with a "lead stanate" content over 40%, to the side of higher temperatures. In the case of a high "lead stanate" content it is no longer justifiable to speak of a transition point, one must refer rather to a region of phase transformation.

The rise in the temperature of the phase transition as the "lead stanate" content is increased above 40% indicates that the ferroelectric properties of the solid solutions are determined by the presence of the "lead stanate" just as in the case of the $BaSnO_3$-"$PbSnO_3$" system[3].

The point of the low temperature phase transition, corresponding to the transformation from the tetragonal to the orthorhombic structure, with increasing "lead stanate" concentration is shifted first towards higher temperatures and then at a "lead stanate" concentration above 8% back to the side of lower temperatures. This interesting behavior is apparently explained by the fact that at first the influence of the tin ions predominates (the temperature of the transition rises) and then the influence of the lead ions begins to predominate (the transition temperature decreases). An analogous influence of the tin and lead ions is observed for the $BaTiO_3$-$BaSnO_3$ and $BaTiO_3$-$PbTiO_3$ systems. It is known

that in the former system the point of the low temperature phase transitions is shifted towards lower temperatures as the content of barium stanate (i.e., tin ions) is increased. In the latter system the temperature of the low temperature transitions is appreciably lowered with increasing concentration of lead titanate (i.e., lead ions).

A tentative phase transition diagram for the $BaTiO_3$-"$PbSnO_3$" system is shown in Fig.7.

Dilatometric measurements made for a number of specimens containing up to 20% "$PbSnO_3$" showed that the curves characterizing the temperature dependence of the linear expansion coefficient have minima; this is indicative of positive volume electrostriction. The magnitude of the electrostriction of the solid solutions is appreciably smaller than that of pure barium titanate.

Investigation of the dielectric hysteresis in specimens of the $BaTiO_3$-"$PbSnO_3$" system showed that, in contrast to $BaTiO_3$-$PbTiO_3$ solid solutions, specimens with a small content of "lead stanate" are ferroelectrically "soft"; saturation polarization in most specimens (at room temperature occurs in applied fields of only 15 kv/cm.

The $BaTiO_3$-"$PbSnO_3$" system has been partially investigated by Coffeen[11] who measured the variation of the dielectric constant and the loss angle in the temperature range from -60 to +80° for a number of samples of different composition; in contrast to our findings, according to Coffeen's data, specimens with a low "lead stanate" content have a flat temperature dependence of the dielectric constant.

$PbTiO_3$-$BaSnO_3$ system

In the case of the $PbTiO_3$-$BaSnO_3$ system, we studied the variation of the dielectric constant and the linear expansion coefficient as a function of the temperature. Temperature of the phase transition from the cubic to the tetragonal modification decreases with increasing barium stanate content.

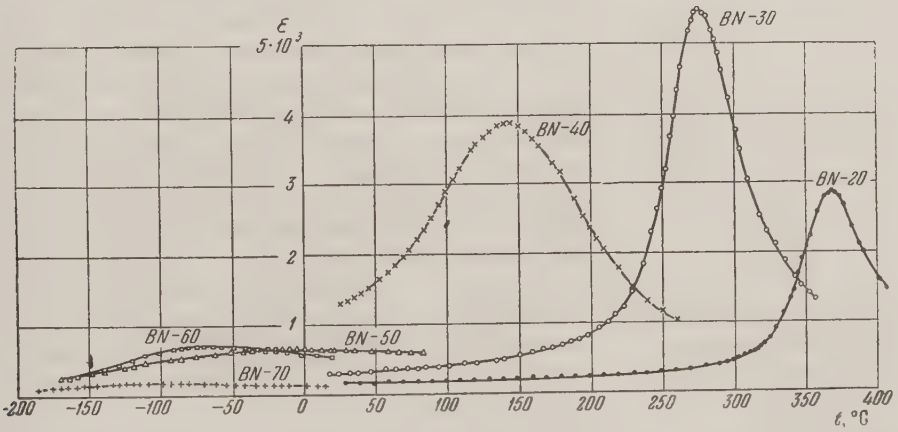

Fig.8. Temperature dependence of the dielectric constant of $PbTiO_3$-$BaSnO_3$ solid solution specimens.

With increasing $BaSnO_3$ content the peak dielectric constant (Fig.8) first increases (up to 30% $BaSnO_3$) and then decreases. This effect is probably connected with a decrease of the strictional stresses as evinced by the decrease of the jump of the linear expansion coefficient. An analogous variation is observed in the $BaTiO_3$-$BaSnO_3$ system[2].

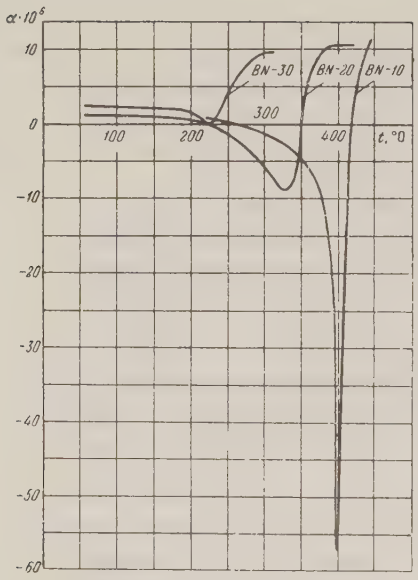

Fig.9. Temperature dependence of the linear expansion coefficient of $PbTiO_3$-$BaSnO_3$ solid solutions.

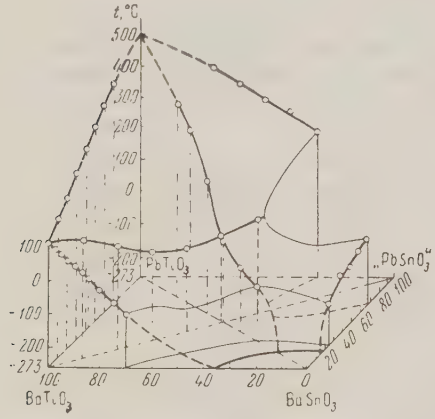

Fig.10. Tentative diagram of the transformations from the paraelectric to the ferroelectric phase in the $(Ba,Pb)(Ti,Sn)O_3$ system.

As the $BaSnO_3$ content is increased above 30%, the dielectric constant peak becomes less pronounced and finally degenerates completely. This behavior is typical of solid solutions obtained by adding a nonferroelectric substance to a ferroelectric material.

A distinct minimum appears in the curves characterizing the variation of the linear expansion coefficient with temperature (Fig.9). Hence here again we have positive volume electrostriction. As the barium stanate content is increased the minimum in the curves becomes lower and is shifted to the side of lower temperatures and, finally, at a sufficiently high $BaSnO_3$ content flattens out and disappears.

Conclusions

From the results of our investigations of the $BaTiO_3$-$PbTiO_3$, $BaTiO_3$-"$PbSnO_3$" and $PbTiO_3$-$BaSnO_3$ systems, as well as studies of the $BaTiO_3$-$BaSnO_3$, $BaSnO_3$-"$PbSnO_3$" and "$PbSnO_3$"-$PbTiO_3$ systems carried out by others in our laboratory, we were able to construct an approximate diagram of the phase transitions in the $(Ba,Pb)(Ti,Sn)O_3$ system. The variation of the transition temperature of solid solutions in this system from the paraelectric to the ferroelectric phase with the composition is shown in Fig.10.

It will be seen from the diagram that, as may have been expected, solid solutions with a large lead titanate content have the highest Curie points. The Curie point of the solid solutions goes down rapidly as the concentration of barium stanate, which is not ferroelectric, is increased. Solid solutions containing a large amount of barium stanate will presumably exhibit no ferroelectric properties. It must be borne in mind, of course, that this part of the diagram was obtained by linear extrapolation of the experimental data into the region of extremely low temperatures.

It will be noted that the surface characterizing the composition dependence of the transition temperature has a tilted concavity in the region of "medium" compositions.

As was pointed out above solid solutions are not formed in this system at "lead stanate" concentration above 70%; hence the corresponding part of the diagram is cut out in Fig.10.

In conclusion the writer desires to thank G.A.Smolenskii for valuable advice and discussion of the results.

Institute of Semiconductors of the
Academy of Sciences of the USSR

References

1. W.P.Mason, Piezoelectric crystals and their applications in ultrasonics, M., 1953.
2. G.A.Smolenskii & V.A.Isupov, Zhur.tekh.fiz., 24, 1375 (1954).
3. G.A.Smolenskii, A.I.Agranovskaia, A.M.Kalinina & T.A.Fedotova, Zhur. tekh.fiz., 25, 2134 (1955).
4. G.A.Smolenskii & K.I.Rozgachev, Zhur.tekh.fiz., 24, 1751 (1954).
5. G.A.Smolenskii, N.P.Tarutin & N.P.Grudtsin, Zhur.tekh.fiz., 24, 1584 (1954).
6. S.Nomura & S.Sawada, J.Phys.Soc.Japan, 6, 36 (1951).
7. J.Shirane & K.Suzuki, J.Phys.Soc.Japan, 6, 274 (1951).
8. N.A.Roi, Thesis, Physical Institute, USSR Ac. of Sci., 1953.
9. G.G.Urazov, E.M.Speranskaia & Z.F.Gulianitskaia, Tezisy dokladov i vystuplenii na III Vsesoiuznom soveshchanii po fiziko-khimicheskomu analizy (Abstracts of reports and speeches at the Third All-Union Conference on Physical-Chemical Analysis), M.-L., 1955.
10. Iu.N.Venevtsev, Thesis, Moscow Mechanical Institute, 1955.
11. W.W.Coffeen, J.Am.Cer.Soc., 37, 480 (1954).

ADDITIONAL DATA ON SOLID SOLUTIONS OF THE $PbTiO_3$-$SrTiO_3$ SYSTEM

- A.G.Boganov & R.A.Khomutetskaia

The aim of the present work was a more detailed and complete investigation of the ferroelectric solid solutions of the $PbTiO_3$-$SrTiO_3$ system. In all earlier investigations[1-6] the measurements of the electric characteristics were made on inadequately or incompletely synthesized samples. Smolenskii's investigation concerned only the temperature dependence of the dielectric constant of a few solid solutions, while the studies made by the Japanese scientists did not extend to investigation of dielectric hysteresis, the piezoelectric properties and determination of the spontaneous polarization.

Sintering temperatures, lead oxide losses and porosity of the solid solution samples

Designation of samples based on % $SrTiO_3$	Sintering temperature °C	Loss of PbO, % by weight	Gain in weight after 24 hours immersion in water
PS-10	1200	1,47	0,70
PS-20	1200	1,24	0,64
PS-30	1220	0,57	0,58
PS-40	1220	0,70	0,50
PS-50	1240	—0,35	0,16
PS-60	1250	—0,135	0,134
PS-70	1300	—0,15	0,00
PS-80	1300	—0,35	0,00
PS-90	1350	—0,53	0,67

In the present investigation we were able to realize a higher quality sytnesis than was achieved in earlier investigations; the concentration of the components was varied in steps of 10%. The investigation included a detailed determination of the temperature dependence of the dielectric constant, the loss tangent, the linear expansion coefficient and the piezoelectric modulus. Further we observed the dielectric hysteresis loops and computed the values of the polarization and coercive force on the basis of these loops.

The synthesis was carried out in an atmosphere of lead oxide vapor for all samples except those of pure $SrTiO_3$. Under these conditions the lead oxide losses were kept low and we succeeded in obtaining samples with minimal open porosity. The data on the lead oxide losses, the porosity and the firing temperature for the different specimens are listed in the accompanying table.

As may be seen from the table the porosity of the PS-70 and PS-80 (70 and 80% $SrTiO_3$) specimens was virtually nil. The maximum lead oxide loss, amounting to 1.5% occurred in synthesizing the

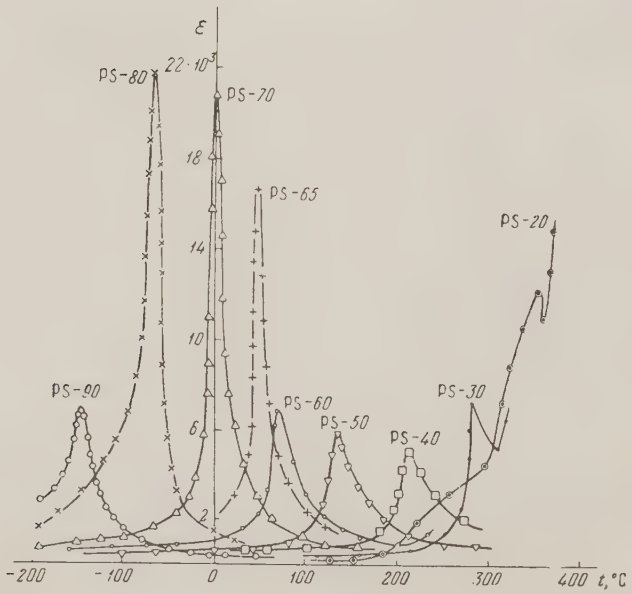

Fig.1. Temperature dependence of the dielectric constant ε of different solid solutions of the $PbTiO_3$-$SrTiO_3$ system.

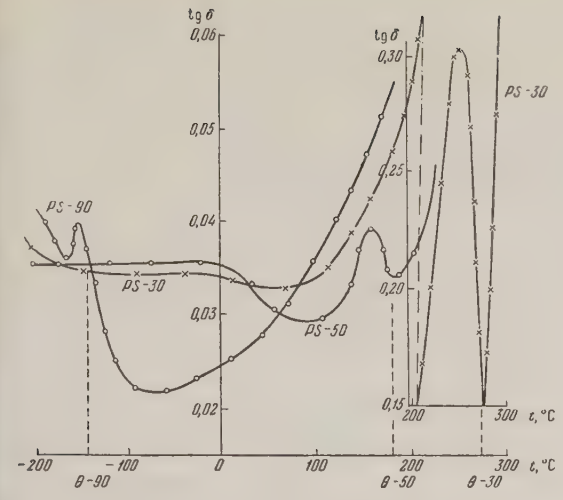

Fig.2. Temperature dependence of the dielectric loss tangent for PS-90, PS-50 and PS-30 specimens.

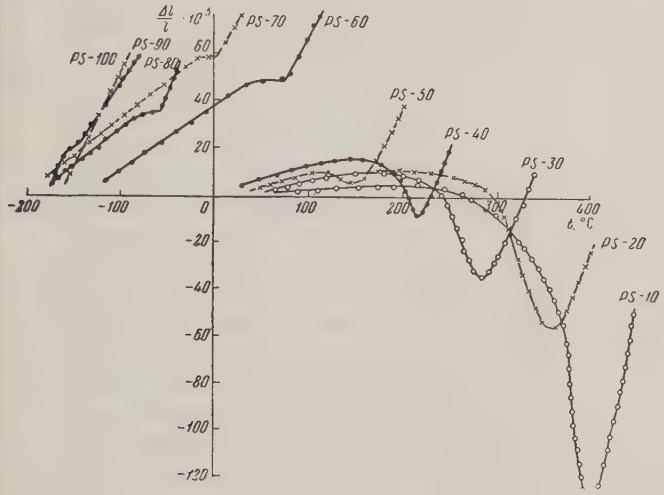

Fig.3. Temperature dependence of the elongation per unit length for specimens of different composition.

PS-10 specimens. It is worth noting that for the PS-60 and PS-70 solid solutions, which are of the greatest interest where practical technological applications are concerned, the sintering temperature did not exceed 1300°. The samples for the dilatometric measurements were prepared in the same manner.

The measurements of the dielectric constant ϵ and the loss tangent were carried out at a frequency of 5 kc in a special vacuum set-up developed for this purpose. This set-up allowed of carrying out parallel measurements on up to ten samples all maintained under identical temperature conditions. The results of the dielectric constant measurements are shown in Fig.1.

It will be seen from the figure that solid solutions containing 65, 70 and 80% $SrTiO_3$ have a very high value of the dielectric constant: of the order of $2 \cdot 10^4$ at the peak.

The high values of ϵ at the Curie point and temperatures above the Curie point for the PS-30 and PS-20 specimens can be explained by the appreciable increase in conductivity at the high (as compared with the other specimens) phase transition temperatures (300-400°). We did not succeed in detecting any additional phase transitions for either of these solid solutions despite repeated careful measurements of the temperature dependence of ϵ.

The temperature dependence of tan δ for a number of representative samples is shown in Fig.2. It will be seen that the tan δ = f(t) curves show a characteristic rise before the Curie point.

The elongation per unit length of the samples was determined by means of a mechanical-optical dilatometer having an indicating ratio of 1:4600. The $\Delta l/l = f(t)$ curves are shown in Fig.3. As will be evident from the curves, all the solid solutions are characterized by positive volume electrostriction, consistently increasing with increasing lead titanate content.

The value of the coefficient of linear expansion (Fig.4) of the solid solutions in the tetragonal modification falls off with increasing lead titanate content from $9 \cdot 10^{-6}$ to $1 \cdot 10^{-6}$ and remains within the range from $7 \cdot 10^{-6}$ to $1 \cdot 10^{-6}$ for the cubic modification.

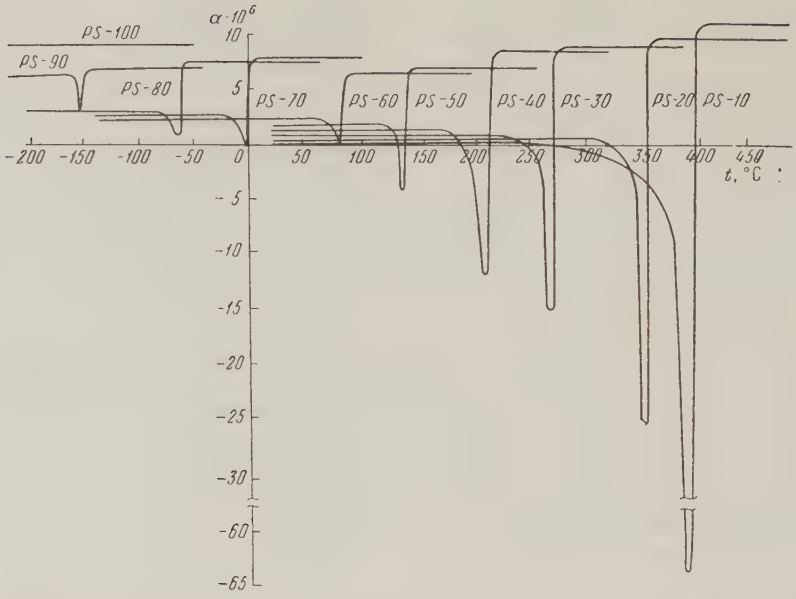

Fig.4. Temperature dependence of the coefficient of elongation for specimens of all compositions investigated in the $PbTiO_3$-$SrTiO_3$ system.

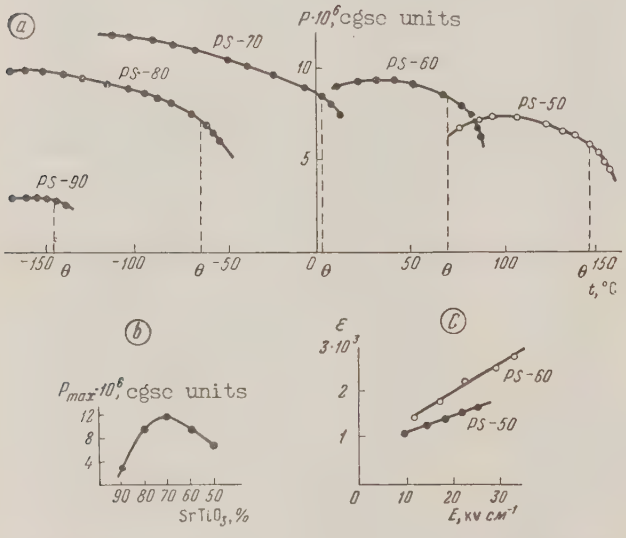

Fig.5. Dependences of: a) the total polarization P on the temperature, b) value of P_{max} on the concentration of the second component and c) dielectric constant on the field intensity at constant temperature.

The variation of the total polarization as a function of the temperature is shown in Fig.5. It will be seen that the ferroelectric "rigidity" or "hardness" increases with increasing concentration of $PbTiO_3$. Thus it proved to be impossible to obtain hysteresis loops for solid solutions containing more than 50% $PbTiO_3$ even at the highest intensities of the applied fields (up to 37 kv/cm). The decrease of the total polarization with decreasing temperature observed for the PS-50 specimen (Fig.5,a) is also explained by the appreciable ferroelectric "rigidity". As is evident from the dependence of ε on the field intensity measured at constant temperature (Fig.5,c) saturation of polarization is not observed even at field strengths of the order of 30-35 kv/cm, i.e., values that approach the breakthrough potential for the specimens.

The curve characterizing the dependence of the total polarization on the concentration of the second component (Fig.5,b) has a distinct maximum corresponding to the PS-70 composition; the value at the maximum is $12 \cdot 10^{-6}$ cgse units.

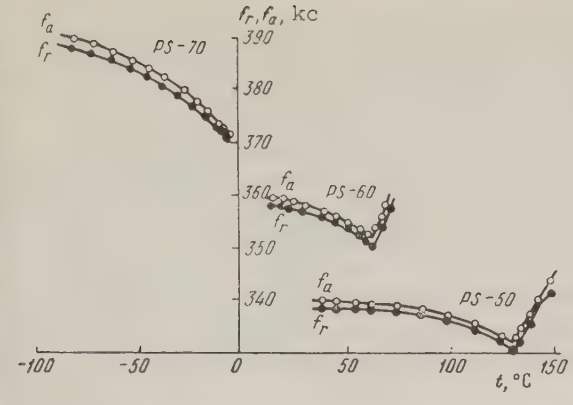

Fig.6. Temperature dependences of the resonance and antiresonance frequencies f_r and f_a for PS-70, PS-60 and PS-50 solid solution specimens.

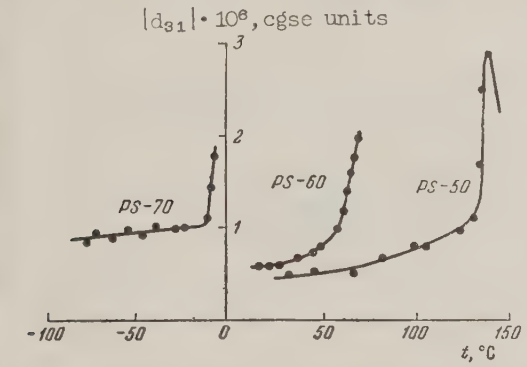

Fig.7. Temperature dependence of the piezoelectric coefficient $|d_{31}|$ for the PS-70, PS-60 and PS-50 solid solutions.

The temperature dependences of the piezoelectric coefficients for the PS-50, PS-60 and PS-70 solid solutions were obtained by recording the corresponding temperature dependences of the resonance and antiresonance frequencies for prepolarized specimens (Fig.6).

As may be seen from Fig.7, the magnitude of the piezoelectric coefficient decreases with increasing $PbTiO_3$ content from $1 \cdot 10^{-6}$ to $0.5 \cdot 10^{-6}$ cgse units.

Lastly, we would like to suggest that $PbTiO_3$-$SrTiO_3$ solid solutions containing 60-70% $SrTiO_3$, which are characterized by a high dielectric constant, have definite potentialities for use as sensing elements in infrared detecting equipment.

The sensing element in the form of a very thin wafer (0.1 mm) should be mounted in an evacuated envelope of material transparent to the desired spectral range and maintained by external thermostatic equipment at a temperature close to the Curie point of the material. Incidence of infrared radiation, as in the case of conventional bolometers and thermoelements would heat the sensing element and the resultant change in capacitance would alter the frequency of oscillation of the associated circuit. Then using the method of beats or some other resonance technique one could with appropriate amplification obtain an appreciable electric signal as a result of even a weak flux of radiation incident on the element.

Preliminary calculations indicate that for an element having the 60-70% $SrTiO_3$ composition one might attain a sensitivity of the order of 10^{-10}-$5 \cdot 10^{-11}$ w. In the calculations it was assumed that the sensitivity of the associated amplifying circuit as regards changes in capacitance is about 10^{-4}%. Obviously, a very compact (miniature) amplifier having this sensitivity for frequencies in the 10^6-10^7 range can readily be realized.

As is known the value of the dielectric constant of ferroelectric materials is not stable particularly near the Curie point. Hence a unit of this kind, in addition to temperature control, will require stabilization of the sensing element as regards dark capacitance; such stabilization for the proposed ferroelectric radiometer can be effected either mechanically by automatic retuning of the capacitor in the circuit during periods of shading of the element or electrically by compensation or correction of an additional constant field applied to the element (also during periods of artificial shading). Such correction or retuning can be made automatic with reference to the output signal during intervals of shading or covering of the element.

In closing we would like to list some of the probable advantages of such a capacitance ferroelectric radiometer using solid solutions of 60-70% $SrTiO_3$ and 40-30% $PbTiO_3$ as compared with present radiometric units:

1. A high sensitivity comparable or superior to the sensitivity of the best present infrared radiometers, semiconductor bolometers and thermoelements as well as superconducting bolometers at a more easily maintained temperature, i.e., at about room temperature (very sensitive superconducting bolometers, for example, have to be thermostatically maintained at 250-270°);

2. A high resistivity (10^{11}-10^{12} ohm cm) and very low losses at high frequencies; this makes it possible to reduce the size and weight of the amplifying equipment as compared with the equivalent equipment needed in conjunction with other radiometers where dc or pulsating low frequency amplification is required;

3. Simplicity of the technological preparation of the sensing element.

Institute of the Chemistry of Silicates of the
Academy of Sciences of the USSR

References

1. G.A.Smolenskii & K.I.Rozgachev, Zhur.tekh.fiz., 24, 1751 (1954).
2. E.N.Bunting, G.R.Shelton & A.S.Creamer, J.Am.Cer.Soc., 30,114 (1947).
3. G.A.Smolenskii, Zhur.tekh.fiz., 23, 3 (1952).
4. G.A.Smolenskii, Zhur.tekh.fiz., 20, 137 (1950).
5. S.Nomura & S.Sawada, J.Phys.Soc.Japan, 10, 108 (1955).
6. G.Shirane, S.Hoshino & K.Suzuki, Phys.Rev., 80, 1105 (1956).

VARIATION OF THE DIELECTRIC CONSTANT OF POLYCRYSTALLINE FERROELECTRICS WITH TIME UNDER THE INFLUENCE OF A MECHANICAL LOAD AND A DC ELECTRIC FIELD

- M.S.Lur'e

Investigations of the influence of a unilateral mechanical load and a dc field on the dielectric constant of polycrystalline ferroelectrics, carried out in electric fields of different intensities, have made it possible to bring out certain new regularities in the behavior of ferroelectrics. The load was applied in the direction of the field.

It was established that the variation of the dielectric constant with the time of application of the mechanical load for nonpolarized ceramic specimens in weak fields at temperatures below the Curie point has a distinctly transient character.

Fig.1 shows the variation of the relative change in the dielectric constant per unit load $\left(\frac{1}{\Delta P}\cdot\frac{\Delta\varepsilon}{\varepsilon}\right)$ as a function of the time for barium titanate. The load of about 10 kg/cm^2 was applied at the zero instant and removed at τ = 1800 sec.

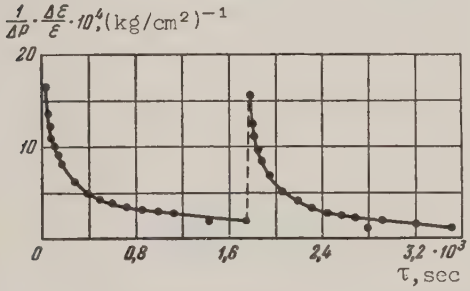

Fig.1. Variation of $\frac{1}{\Delta P}\cdot\frac{\Delta\varepsilon}{\varepsilon}$ with the time of application of the load for a $BaTiO_3$ specimen in a weak electric field at t = 20°.

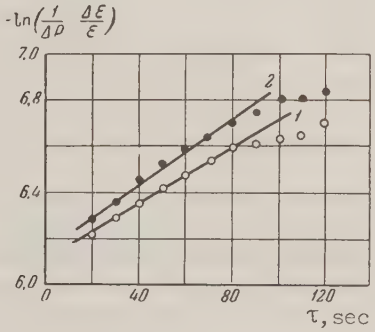

Fig.2. Variation of $-\ln\left(\frac{1}{\Delta P}\cdot\frac{\Delta\varepsilon}{\varepsilon}\right)$ with the time of application of the load: 1) load applied; 2) load removed.

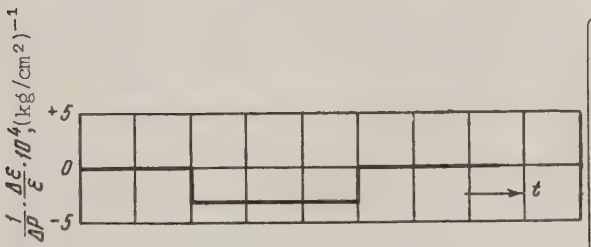

Fig.3. Same as Fig.1 but at t = 150°.

As may be seen from the curve the dielectric constant increases abruptly at the instants of application and removal of the load and then falls off to a value close to the initial one. The variation of $-\ln\left(\frac{1}{\Delta P}\cdot\frac{\Delta\varepsilon}{\varepsilon}\right)$ as a function of the time is shown in Fig.2. It will be seen that for short intervals the observed values fit a straight line. Thus the observed dependence is approximately characterized by the exponential law

$$\left| \frac{1}{\Delta P} \cdot \frac{\Delta \varepsilon}{\varepsilon} \right| = A_0 e^{-\alpha \tau},$$

where A_0 is the maximum value of $\frac{1}{\Delta P} \cdot \frac{\Delta \varepsilon}{\varepsilon}$, obtained by extrapolation of the logarithmic curve to $\tau = 0$.

At large values of τ there is a noticeable deviation from the exponential law. The coefficients α and α' characterizing the rate of decrease of $\frac{1}{\Delta P} \cdot \frac{\Delta \varepsilon}{\varepsilon}$ after application and removal of the load differ from each other and vary with the temperature. As the temperature increases the difference between α and α' becomes greater (Table 1).

Table 1

Dependence of the relative change in dielectric constant per unit load and of the coefficients characterizing the rate of this change on the temperature

t, °C	Load applied		Load removed	
	$A_0 \cdot 10^4$, $(kg/cm^2)^{-1}$	$\alpha \cdot 10^{-4}$, sec^{-1}	$A_0' \cdot 10^4$, $(kg/cm^2)^{-1}$	$\alpha' \cdot 10^4$, sec^{-1}
−195	8,4	110	8,4	110
+20	9,0	41	8,6	63
+60	6,7	43	5,8	103
+100	6,1	32	2,2	220
+200	−2,2	—	—	—

At temperatures above the Curie point the usual steady dependence of the dielectric constant on the time of application of the load obtains: i.e., $\frac{1}{\Delta P} \cdot \frac{\Delta \varepsilon}{\varepsilon} < 0$ and does not change with time (Fig.3). The above described effect is observed both for pure barium titanate and for its different solid solutions.

Investigation of the dependence of $\frac{1}{\Delta P} \cdot \frac{\Delta \varepsilon}{\varepsilon}$ on the strength of the applied alternating field shows that as the field strength is increased there occurs a transition from the transient process to the stable one characterized by $\frac{1}{\Delta P} \cdot \frac{\Delta \varepsilon}{\varepsilon} < 0$ at $t \gtrless \theta$. This transition occurs in a narrow ac field intensity interval; thus one can determine a certain mean value of the critical field E_c at which the transition from the unstable or transient process to the stable variation occurs. The factor $\frac{1}{\Delta P} \cdot \frac{\Delta \varepsilon}{\varepsilon}$ in the case of the steady process has a weak maximum in the region of the peak value of $\epsilon = f(E_\sim)$. The values of E_c and the maximum values of the factor $\frac{1}{\Delta P} \cdot \frac{\Delta \varepsilon}{\varepsilon}$ for different ferroelectrics are listed in Table 2. These values are based on measurements carried out at 20°.

Table 2

Values of the alternating electric field at which the unsteady process becomes steady and the maximum values of the relative change of ε per unit load for different dielectrics containing barium titanate

Composition, mole %	E_c, v/cm	$\frac{1}{\Delta P}\cdot\frac{\Delta\varepsilon}{\varepsilon}\cdot 10^4$, $(kg/cm^2)^{-1}$
$BaTiO_3$	2000	4
95% $BaTiO_3$+ 5% Pb_3O_4*	2800	—(small)
80% $BaTiO_3$+20% $SrTiO_3$	2500	— "
85% $BaTiO_3$+15% $BaZrO_3$	1100	6
95% $BaTiO_3$+ 5% $BaSnO_3$	1000	18
92% $BaTiO_3$+ 8% $BaSnO_3$	900	25
91% $BaTiO_3$+ 9% $BaSnO_3$	450	32
90% $BaTiO_3$+10% $BaSnO_3$	500	50
89% $BaTiO_3$+11% $BaSnO_3$	950	23

*Composition of initial components by weight; for the other specimens the composition is given in molar percent.

E_c generally decreases with increasing temperature. The critical field value decreases appreciably after aging of the specimen in a strong electric field ($E_\sim > E_c$); however, this after effect is short-lived.

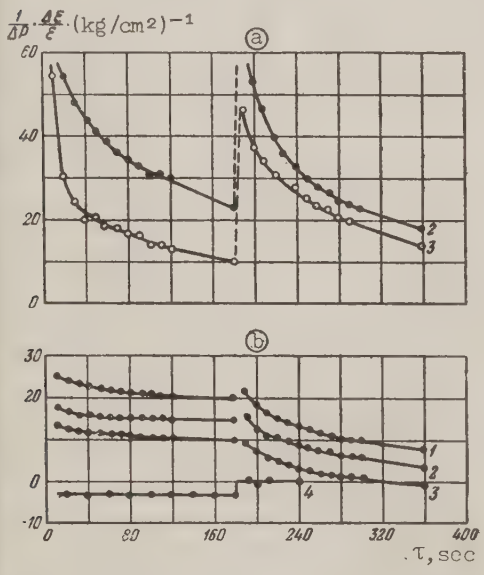

Fig.4. Variation of $\frac{1}{\Delta P}\cdot\frac{\Delta\varepsilon}{\varepsilon}$ with the time of application of the load and the temperature for a polarized 90% $BaTiO_3$ + 10% $BaSnO_3$ specimen: a) with no dc field, b) with a dc field of 11 kv/cm; 1) t = 20°, 2) t = 30°, 3) t = = 40°, 4) t = 90°.

The results of investigation of the variation of the dielectric constant with the time under load for prepolarized specimens shows that for such specimens, too, in weak fields and at $t < \theta$ the unsteady or transient variation of the dielectric constant obtains (curves 2 & 3 in Fig.4,a). The application of a strong polarizing field to the specimen leads to an appreciable stabilization of the process (curves 1-3 in Fig.4,b). In contrast to the steady process in strong alternating fields, however, in this case

$$\frac{1}{\Delta P}\cdot\frac{\Delta\varepsilon}{\varepsilon}\begin{cases} >0 & \text{for } t<\theta, \\ <0 & \text{for } t>\theta. \end{cases}$$

We also investigated the effect of a pulsed dc field on the dielectric constant of ferroelectrics. We used square pulses of considerable duration (up to several minutes). The effects observed are fully analogous to those occurring in the case of mechanical compression. In weak alternating fields and at temperatures below the Curie point there is an abrupt increase in the dielectric constant at the instants of application and removal of the dc field; the dielectric constant then falls off with time according to the

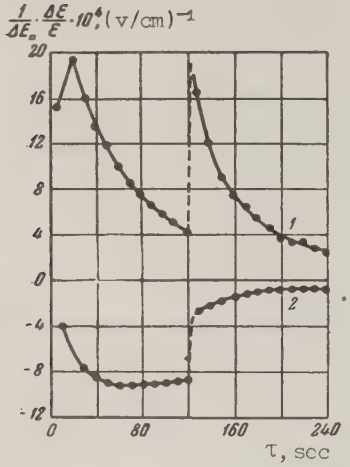

Fig.5. Variation of $\frac{1}{\Delta E_-}\cdot\frac{\Delta\varepsilon}{\varepsilon}$ with the time of application of a dc field and the temperature for a 90% $BaTiO_3$ + + 10% $BaSnO_3$ specimen: 1) t = 20° and 2) t = 60°.

$$\left|\frac{1}{\Delta E_-}\cdot\frac{\Delta\varepsilon}{\varepsilon}\right| = B_0 e^{-\beta\tau}.$$

law (curve 1 in Fig.5). At temperatures above the Curie point a steady dependence obtains with $\frac{1}{\Delta E_-}\cdot\frac{\Delta\varepsilon}{\varepsilon}<0$ (curve 2 in Fig.5).

It must be noted that in the case of a gradual variation of the dc field strength at a rate not exceeding 20-30 v/cm per sec no transient effect is observed, i.e., a steadily rising or falling curve is obtained.

As in the case of mechanical loading, with increasing alternating field strength there occurs a transition from the unstable or transient process to the stable one for which $\frac{1}{\Delta E_-}\cdot\frac{\Delta\varepsilon}{\varepsilon}<0$ at $t \gtrsim \theta$. As compared with the case of mechanical loading, the critical field strength in this case is much more strongly dependent on the previous history of the specimen; because of this it proved to be impossible to make an accurate evaluation of E_c for the case of applied dc fields.

The results cited above can be qualitatively interpreted from the standpoint of the domain structure of ferroelectrics. It is known that a weak alternating field produces only a partial reorientation of the spontaneous regions (180° domains) and that an appreciable fraction of the total number of domains is not reoriented by weak alternating fields. It may be hypothesized that the mechanical or electrical pulse, added to (i.e., acting in the same sense) as the corresponding phase of the ac voltage, induces displacement of some part of these domains which leads to an increase of the orientation polarization and, consequently, to an increase of the dielectric constant. The effect obviously should not depend on the sign of the change in the mechanical load or dc field. The subsequent exponential decrease of ϵ occurs as the result of the gradual return to the initial energetically advantageous initial structure. At the same time there acts on the crystal lattice of ferroelectrics a constant deforming force which hinders reorientation of the domains and leads to a constant, time independent decrease of the dielectric constant (the steady effect). It is evident that the relative contributions or ratio of these two effects will vary with changes in the intensity of the alternating field due to changes in the number of domains oriented by the field; in strong fields the steady effect will naturally predominate. The presence of these two effects explains the deviation from the exponential curve at large values of τ. The critical field value must be the lower, the greater the electric nonlinearity of the specimen; this is substantiated by the experimental data. The decrease in the value of E_c with increasing temperature occurs due to increasing ferroelectric "softness" of the specimen as the Curie point is approached. The observed reduction of the critical field strength as a result of subjection of the specimen to a strong alternating field is a consequence of the increase in the 180° reorientations (switching) of the domains. The influence of a mechanical load in the case of ap-

plication of a strong polarizing field can be explained as a result of disordering of the domains. Inasmuch as prior to the application of a load the domains are always rigidly oriented by the polarizing field such disordering must always lead to an increase of the dielectric constant. A certain decrease in the sensitivity of ferroelectric ceramics to loads with increasing temperature can be explained by an increase in the polarizing effect of dc fields.

Thus all the experimental results support the hypothesis that a domain orientation mechanism is involved in the observed effects.

All-Union Scientific Research Institute
for Exploratory Methods and Techniques

INVESTIGATION OF ULTRASONIC PROJECTORS EMPLOYING ROCHELLE SALT CRYSTALS

- K.A.Minaeva

One of the principal requirements set in acoustics for sound projectors or radiators is that they must have a certain directional characteristic. For most practical applications it is desirable to have a so-called piston radiator, all points of which vibrate in phase so that the sound is emitted in the direction perpendicular to the plane of the vibrating plate (piston). Actual projectors, as we know, fall short of the ideal.

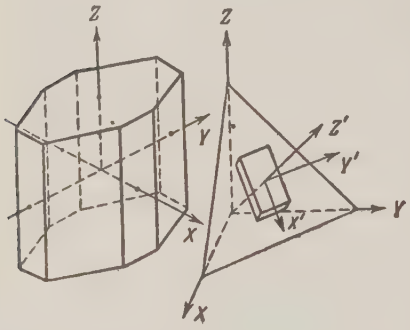

Fig.1. Orientation of an L-cut in a Rochelle salt crystal.

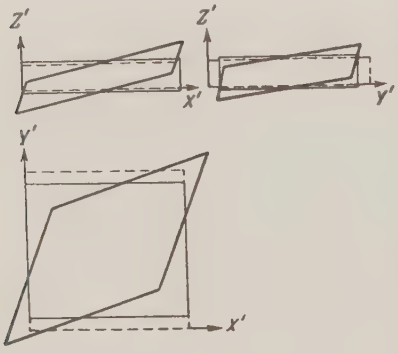

Fig.2. Deformation of an L-cut plate under static loads (general case).

The present investigation was concerned with ultrasonic projectors employing Rochelle salt crystals. In practice so-called L-cut plates (Fig.1) are commonly used for radiating (and receiving) ultrasound.

This cut was theoretically discovered by Cady[1] reasoning from the following considerations: the piezoelectric coefficient d'_{33}, characterizing the longitudinal piezoelectric effect (induced by the application of an electric field $E_{z'}$), has a maximum value for the orientation of the cut for which the normal z' to the plane of the cut makes equal angles with the crystallographic axes:

$$d'_{33} = \alpha_{31}\alpha_{32}\alpha_{33}(d_{14} + d_{25} + d_{36}),$$

where α_{31}, α_{32}, and α_{33} are the direction cosines of the normal and d_{14}, d_{25}, and d_{36} are the piezoelectric coefficients of Rochelle salt. Thus d'_{33} has a maximum value when

$$\alpha_{31} = \alpha_{32} = \alpha_{33} = \frac{1}{\sqrt{3}}.$$

Inasmuch as the L-cut has a maximum longitudinal piezoelectric effect (i.e., upon the application of an alternating electric field the L-cut plate is deformed in thickness) such cuts came to be used for ultrasonic projectors (receivers). It was soon noted, however, that the radiation does not always occur in the direction perpendicular to the plane of the plate: at some frequencies the projectors yield oblique directional characteristics, i.e., radiate to the side. This, it was found, is due to the fact that an L-cut plate under the influence of an applied alternating electric field $E_{z'}$ undergoes not only thickness vibrations but other types of oscillations, both simple and complex. The theoretically computed deformations of an L-cut plate are shown in Fig.2: the dash lines show the initial undeformed plate; the light solid lines show the deformations in thickness, length and width and the heavy solid lines show the resulting deformations. As a result of coupling and combination of the simple simultaneously occurring vibrations the different points of the radiating surface no longer vibrate in phase and this obviously affects the character of the radiated sound field.

Our primary aim, accordingly, was to find a cut possessing a longitudinal piezoeffect but as free as possible of interfering vibrations.

Proceeding from the general piezoelectric equations for rotated cuts and assuming that the piezoelectric coefficients responsible for thickness-shear deformations of the plate are zero ($d'_{34} = 0$ and $d'_{35} = 0$), we arrive at a cut whose orientation is determined by the following direction cosines for the normal to the cut:

$$\alpha_{31} = \sqrt{\frac{d_{25} + d_{36}}{2(d_{14} + d_{25} + d_{36})}},$$

$$\alpha_{32} = \sqrt{\frac{d_{14} + d_{36}}{2(d_{14} + d_{25} + d_{36})}},$$

$$\alpha_{33} = \sqrt{\frac{d_{14} + d_{25}}{2(d_{14} + d_{25} + d_{36})}}.$$

In practice, however, it is impossible to make such a cut in the case of Rochelle salt inasmuch as one of the direction cosines, namely, α_{31} as calculated is imaginary. Nonetheless, the possibility is not excluded that other crystals of class 2:2 having a different combination of "signs" of the piezoelectric coefficients can be used for the preparation of such cuts.

Thus, we have shown theoretically that in the case of Rochelle salt it is impossible to attain a cut possessing only a longitudinal piezoeffect and entirely free of shear strains. Hence our further research has been directed at investigating L-cut plates for the purpose of improving the directional characteristics of such cuts. Below we shall describe the part of the work concerned with establishing a correlation between the forms of oscillation of the radiating surfaces and the sound field. The method consists of establishing for each resonance frequency of the radiator and, hence, for each configuration of the vibrating surface peculiar to this frequency, the corresponding directional characteristic of the L-cut plate projector. The character of the oscillations of the emitting surfaces was established by obtaining and recording the Chladni sand-pattern figures.

Below we give one such correlation. At low frequencies (up to 20 kc) the circular L-cut plate in question (6.8 cm in diameter and 0.9 cm thick) undergoes flexural vibrations as evinced by the Chladni figures shown in Fig.3. Owing to the anisotropy of the investigated plates the resonance frequencies of the flexural vibrations naturally differ from the theoretically calculated frequencies for an isotropic plate; although, in actual fact, the Chladni figures and the sequence of the Chladni patterns with increasing frequency are in general agreement with the theoretical predictions for isotropic plates. In the table below we have juxtaposed the ratios of the experimentally determined frequencies to the fundamental resonance frequency with the theoretically calculated ratios for isotropic plates.

It will be seen from the table that the resonance frequencies of actual crystal plates are shifted to the side of lower frequencies as compared with the theoretical values. An interesting factor is that for crystal plates there is not just one resonance frequency corresponding to a given configuration of the vibrating surface, i.e., to a given Chladni figure, as in the case of isotropic plates, but actually several frequencies. With increasing or decreasing frequency the Chladni figure rotates about an axis perpendicular to the plane of the plate; for example, the resonance frequency f_{30} = 13 kc (three diametral lines) is preceded (or followed) by the frequency f'_{30} = 12 kc with an analogous Chladni figure but rotated through a certain angle relative to the first (see Fig.3,c & d). This can be explained by the fact that the given type of vibration, the resonance frequency of which f_{ij}

Comparison of the ratios of the experimentally determined resonance frequencies to the fundamental resonance frequency with the theoretically calculated ratios for isotropic plates.

Frequency ratio*	f_{20}/f_{20}	f_{01}/f_{20}	f_{30}/f_{20}	f_{11}/f_{20}	f_{40}/f_{20}
For isotropic plates	1	1,61	2,31	3,7	4,04
For L-cut plates	1	1,56	1,88	2,81	3,3

*Here f_{ij} are the resonance frequencies where i is the number of nodal diameters (diametric lines) and j is the number of nodal circles (circular line); i takes the values 0,1,2,3 and 4; j takes on the values of 0 and 1.

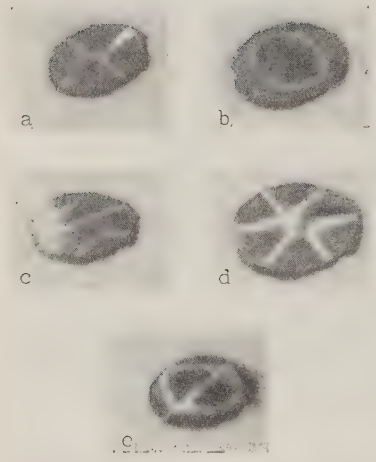

Fig.3. Chladni figures obtained on the surface of an L-cut plate at flexural vibration frequencies of a) f_{20} = 6.9, b) f_{01} = 10.8, c) f'_{30} = 12, d) f_{30} = 13, e) f'_{11} = 19.5 kc.

is proportional to $\sqrt{C_{kl}}$ (where C_{kl} is the corresponding modulus of elasticity) is determined not by a constant modulus of elasticity but by a modulus whose magnitude depends on the direction. In the case of the plate in question, at a resonance frequency corresponding to four nodal diameters the Chladni figure becomes very diffused since there is superimposed a strong shear node; there appear "regions of rotation" distorting the Chladni figure. The appearance of "regions of rotation" (i.e., churning or circular movement of the quartz sand at some points) can be explained either by shear oscillations or by the closeness of two neighboring resonances.

In the course of our experiments we investigated a large number (about 25) square and circular plates varying in thickness from 0.1 to 1 cm. Approximately the same frequency ratios (see table) were obtained for all the specimens and the sequence in which the different Chladni figures follow each other with increasing or decreasing frequency was found to be similar. We were able to investigate the character of the vibrations of plates by means of the Chladni figures in a frequency range from 3 to 30 kc. We also investigated the sound fields at frequencies for which the character of vibration of the radiating surface was known, i.e., for which Chladni figures were obtained. A block diagram of the experimental set-up is shown in Fig.4.

The radiating plate is placed on a thin rubber diaphragm which makes it possible to investigate the free vibrations of the plate. The sound receiver is rigidly mounted above the radiator. The set-up has provision for rotating the radiator about a horizontal axis. By tilting the radiating plate and at the same time recording the indications of the indicator (a vacuum tube voltmeter or an oscilloscope) one can plot the directional characteristic in the given plane. Furthermore the radiator can be rotated about a vertical axis passing through the center of the radiator and the receiver, so that by successive tilting in different orientations one can obtain the spatial characteristic. The distance between the radiator and receiver in our set-up was 1.12

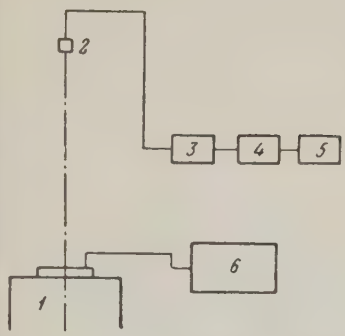

Fig.4. Block diagram of the set-up used for investigating the sound fields of L-cut plates: 1) radiator, 2) receiver, 3) amplifier, 4) filter, 5) indicator, 6) oscillator.

meters. The radiator in the experiments was, of course, the investigated L-cut plate.

The first fundamental resonance vibration frequency, corresponding to two diametral nodal lines, for the particular circular plate mentioned above is f_{20} = 6.9 kc (Fig.3,a). The second resonance frequency, corresponding to one nodal circle (Fig.3,b) is f_{01} = 10.8 kc; the directional characteristic obtained in this case is shown in Fig.5. The applied potential was 60 v. The spatial directional characteristic is essentially the corresponding surface of revolution.

The sound field corresponding to the next resonance frequency, f_{30} = 13 kc (three diametral nodal lines - see Fig.3,d) is shown in Fig.6. Here again the applied voltage was 60 v. To give an idea of the spatial directional characteristic, we note that when the plate is oriented so that one of the nodal diameters is in the plane in

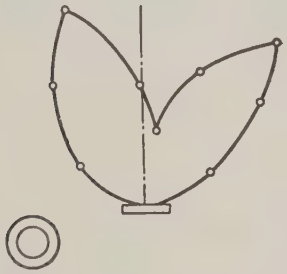

Fig.5. Directional characteristic of one of the investigated L-cut plates at a frequency of f_{01} = 10.8 kc; the corresponding Chladni figure (one nodal circle) is shown at the left.

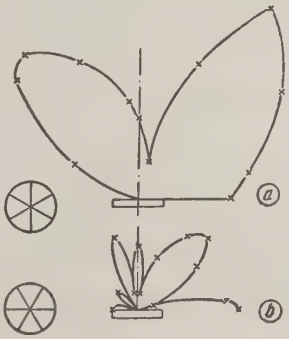

Fig.6. Same as Fig. 5 but at the frequency f_{30} = 13 kc.

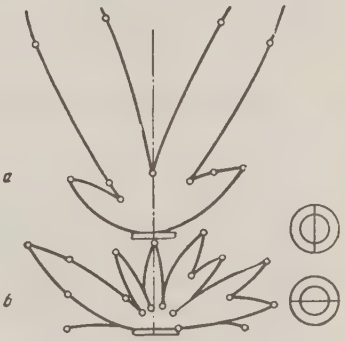

Fig.7. Same as Fig. 5 but at the frequency f_{11} = 19.5 kc.

which the characteristic is being recorded, the two-dimensional characteristic has the appearance shown in Fig.6,b, while when one of the diametral nodal lines is perpendicular to the plane of the characteristic, the two-dimensional characteristic is analogous to that shown in Fig.6,a (see the corresponding Chladni figures at the right of the respective characteristics). The radiation intensities in cases a and b differ by a factor of 3-4.

The sound field corresponding to the fourth resonance frequency, f_{11} = = 19.5 kc, (one nodal diameter and one nodal circle - see Fig.3,e) is shown in Fig.5. In this case the applied voltage was 40 v. As in the previous case the directional characteristic varies with the angle of rotation of the plate about the vertical axis, but in this case the angular period equals $360^\circ/4$ instead of $360^\circ/12$. When the nodal diameter is in the same plane as the characteristic, the latter has the appearance shown in Fig.7,b, while when

the diametral line is perpendicular to the plane of the characteristic, the directional characteristic is that shown in Fig.7,a. In going from a to b the intensity falls off by a factor of 3-4. The crosses and circles in Figs.5,6 & 7 indicate the experimental points.

No radiation resonances were observed at frequencies intermediate between those listed above.

Conclusions

1. Theoretical calculations show that in the case of Rochelle salt one cannot prepare a cut having a longitudinal piezoelectric effect and at the same time free of thickness-shear deformations. It may, however, be possible to make such cuts from other crystals of the 2:2 symmetry class, characterized by a different combination of the "signs" of the piezoelectric moduli d_{14}, d_{25}, and d_{36}.

2. The above described experiments showed that it is feasible to relate uniquely the sound field of a given radiator (receiver) with the amplitude distribution of its vibrating surface.

3. The experimental results indicate that through appropriate variation of the plate geometry it should be possible to improve the directional characteristics of L-cut Rochelle salt plates.

The writer desires to express her deep gratitude to A.V.Shubnikov, S.N.Rzhevkin and V.A.Koptsik for valuable suggestions and the interest shown in the work.

"M.V.Lomonosov" Moscow State University

References

1. W.G.Cady, Proc.Phys.Soc., 49, 646 (1937).
2. W.P.Mason, Piezoelectric crystals and their application in ultrasonics, (In Russian trans., M., 1952.)
3. L.Ia.Gutin, Izv.elektroprom. slabykh tokov (Bulletin of the Weak-Current Electric Industry), No.1, 46; No.2, 50 (1941).
4. N.W.McLachlan, Loudspeakers. Oxford, 1934.
5. Ivan Solc, Ceskoslov, J.Phys., 5, 2 (1955).

STABILIZED PIEZOCERAMIC MATERIALS

- R.E.Pasynkov & V.V.Vinogradov

One of the most important engineering uses of ferroelectric materials is in the fabrication of different electroacoustic transducers.

Piezoceramics (polycrystalline $BaTiO_3$ and some of its solid solutions) are characterized by a high efficiency both as emitters and receivers, for transducers employing these materials, unlike converters of nickel, do not require expenditure of an appreciable amount of power for polarization. Moreover, the technology of preparation of piezoceramics is relatively simple and one can readily obtain mechanically strong and generally stable elements of different shapes (prisms, cylinders, spheres, etc.).

Despite the fact, however, that the first attempts to use barium titanate in electroacoustics both here and abroad yielded positive results, there persisted a number of problems and difficulties connected with the characteristics of piezoceramics as ferroelectric materials. These problems and difficulties that have stood in the way of wider application of piezoceramics in electroacoustic transducers are the following.

1. Barium titanate has three transition points one of which lies at about 12°, i.e., in the range of operating temperatures of conventional transducers. The influence of this low temperature transition on the piezoelectric properties of the material has until recently been little studied; specifically, there has been virtually no detailed investigation of the effect of this transition on the parameters of electroacoustic transducers incorporating barium titanate ceramics. It is known, however, that these parameters are unstable in the vicinity of the phase transition. Thus there is obvious need for studying the problem and for finding methods of stabilizing the parameters.

2. The piezoelectric parameters of barium titanate are known to depend on the residual polarization. Inasmuch as the polarized state of barium titanate ceramics is energetically less stable than the nonpolarized state there is some question as regards the stability of these parameters under the influence of external factors such as shocks, vibration, temperature changes, electric fields, etc.

3. Until now no one has determined the region of linearity of piezoceramic transducers or the magnitude of the hysteresis losses of different piezoceramic materials, which to an appreciable degree determine the operating efficiency and the maximum realizable specific power of transducers.

The present investigation was undertaken with a view to finding the answers to these problems. Specifically, we investigated the properties of barium titanate and some of its solid solutions chosen on the basis of the following considerations.

Polycrystalline barium titanate has maxima in the temperature variation of dielectric constant and piezoelectric modulus and minima in the temperature dependence of the resonance frequency, the velocity of sound and modulus of elasticity at the low temperature transition point ($+12^{\circ}$). At the same time, where transducers are concerned, a necessary requirement is temperature stability of the parameters in a wide range (sometimes from -40 to $+40^{\circ}$). An effective method of stabilization is displacement of the second transition point to outside the range of the design operating temperatures. This is usually realized by the addition of appropriate components forming solid solutions with the $BaTiO_3$. It follows from the data in the literature[1] that the most interesting additives as regards stabilization are lead titanate and calcium titanate. For example, in the solid solution of barium titanate

with 6% calcium titanate, the temperature of the second phase transition is shifted some 60° to -50°. In view of this we decided to investigate some of the solid solutions having different concentrations of lead and calcium as well as mixtures containing 10% $SrTiO_3$ and 6% $BaSnO_3$; in all we investigated about 20 different compositions.

The temperature characteristics of the different materials were determined by recording the temperature dependences of the resonance and antiresonance frequencies and the dielectric constant for specimens of uniform size (the most convenient dimensions for experimental purposes proved to be 21 x 5 x 2 mm and 13 x 7 x 5 mm). The measurements were made by means of a specially designed set-up. For enhanced experimental accuracy the temperature dependences of all the parameters were determined at the same time. According to our evaluation the experimental error did not exceed 0.1%. The values of Young's modulus E_Y, the velocity of sound in the material c and the piezoelectric moduli d_{33} and d_{31} were then computed from the experimental data.

In order to be able to compare the absolute values in the temperature dependences of the electroacoustic parameters of transducers employing ceramics of different composition with a view to determining which type of solid solution is best suited for use in transducers, it is not sufficient to know the value and variation with temperature of the dielectric constant, the piezoelectric coefficients, the resonance frequencies, etc. taken singly. Such an evaluation is possible only by taking into account the entire complex of the measured parameters, in other words, one must on the basis of these parameters compute and plot the temperature dependence of the quantities actually characterizing the electroacoustical characteristics of transducers, namely, the specific acoustic power and the response. It is obviously more convenient and expedient to plot the characteristics of quantities containing parameters which depend only on the temperature and composition of the ceramic and are independent of the geometric dimensions and specific design of the transducer.

It must be noted that the characteristics of the specific acoustic power and response obtained in this manner characterize only the temperature-induced changes which would occur if the resonance frequency were entirely temperature independent. Inasmuch as in reality the resonance frequency drifts, the actual temperature-produced changes prove to be appreciably greater than the plots indicate. The actual magnitude of these changes depends on the attenuation ratio, i.e., on the geometry of the transducer, and at present it does not appear feasible to allow or correct for them accurately in the general case. An indirect characterization of these changes is given by the variation of the resonance frequency with temperature. This is shown in Fig.1 for the three ceramic compositions that on the basis of our experiments appear to be most promising, namely, $BaTiO_3$, 94% $BaTiO_3$ + 6% $CaTiO_3$ and 88% $BaTiO_3$ + 8% $CaTiO_3$ + 4% $PbTiO_3$; in addition, for purposes of comparison we give the curve for a magnetostrictional transducer of nickel. The dependences

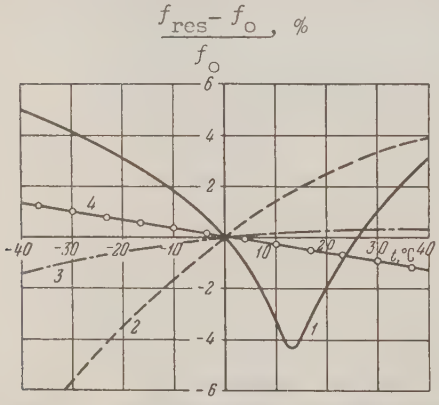

Fig.1. Temperature dependences of the resonance frequency of ferroelectrics: 1) $BaTiO_3$, 2) 94% $BaTiO_3$ + 6% $CaTiO_3$, 3) 88% $BaTiO_3$ + 8% $CaTiO_3$ + 4% $PbTiO_3$, 4) nickel transducer.

Table 1

Comparitive changes in the value of the ratio $(f_{res} - f_o)/f_o$ (in %) produced by different changes in temperature for three piezoelectric ceramics

Temperature interval, °C	$BaTiO_3$	$BaTiO_3$+ +6 % $CaTiO_3$	$BaTiO_3$+ +8 % $CaTiO_3$+4 % $PbTiO_3$
−40÷+40	9	11,5	1,9
0÷+30	5,5	2,8	0,4
0÷+10	0,40	0,10	0,01

plotted in the form of the percent change in f_{res} relative to the resonance frequency f_o at t = 0°.

In Fig.2 we give the temperature dependence of the parameter characterizing the response of the ferroelectric (for the same ceramics as characterized in Fig.1) a) when the longitudinal piezoeffect (d_{33}/ϵ) and b) when the transverse

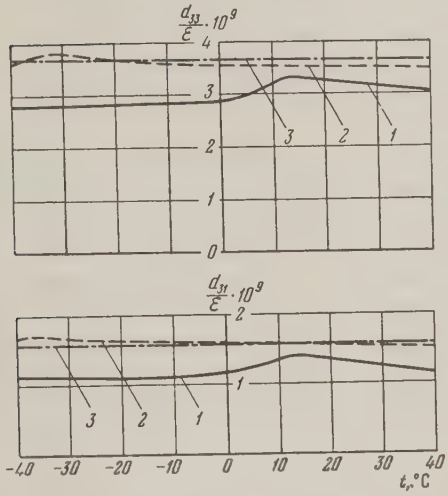

Fig.2. Temperature dependence of the parameter characterizing the response of ferroelectrics (the curve numbers correspond to those in Fig.1).

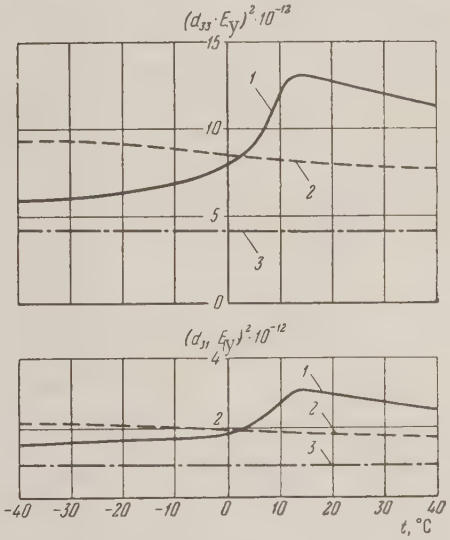

Fig.3. Temperature dependence of the parameter characterizing the specific acoustic power (curve numbers corresponding to those in Fig.1).

piezoeffect (d_{31}/ϵ) is used. It will readily be seen that the stabilized compositions insure a better response of the transducer than pure $BaTiO_3$.

The temperature dependences of the parameters characterizing the specific acoustic power ($d_{33}^2 \cdot E_y^2$ for the longitudinal and $d_{31}^2 \cdot E_y^2$ for the transverse piezoeffect) are given in Fig.3. The pronounced instability of the specific acoustic power for $BaTiO_3$ is clearly evident (in practice the instability is more pronounced due to the frequency drift). The stability of the other two ceramics is good, but it must be noted that it is obtained with a considerable sacrifice of the absolute value of the power radiated at a given potential.

For a full and complete comparison of the different types of ceramics as radiators one must take into account the hysteresis losses as well. The magnitude of these losses was determined on a hysteresigraph by observing the variation of the charge as a function of the applied ac voltage: $q = f(V_\sim)$. With the correct prephasing, the area of the figure on the screen of the hysterisigraph gives the energy loss per cycle. This quantity depends on the volume of the specimen and on the intensity of the applied field. Hence for characterizing the ceramics we introduced the "specific loss energy" A_o

described by

$$A_o = \frac{A}{vE^2} \quad (I\ V^{-2}\ cm^{-1}),$$

where A is the energy loss per cycle, v is the volume of the specimen and E is the applied electric field. A_o is independent of the size ofthe specimen and its shape and of the intensity of the applied field and characterizes the total effective loss of the given material.

By measuring the value of A for a large number of specimens of different lots we determined the mean value of this parameter for each composition. On the basis of this data one can calculate the hysteresis loss (or the equivalent resistance) for a ceramic unit of any composition and size at any field strength below the critical value for loss of linearity (2-3 kv/cm). The specific energy losses for a number of ceramic compositions are listed in Table 2.

Table 2

Specific energy loss for ceramics of different composition

Composition	A_s, $10^{-10} V^{-2} cm^{-1}$
$BaTiO_3$	0,8
$BaTiO_3$+6 % $CaTiO_3$	0,3
$BaTiO_3$+8 % $CaTiO_3$+ +4 % $PbTiO_3$	0,15
$BaTiO_3$+10 % $SrTiO_3$	4,5
$BaTiO_3$+ 6% $BaSnO_3$	3,0

Measurements carried out directly in a sound field showed that the region of linearity of piezoelectric ceramic transducers extends at least to a field value of about 4 kv/cm. Numerous tests have shown that the piezoelectric properties of the described ceramics are stable under the influence of mechanical factors and sharp changes in temperature. We also recorded the dependences of the piezoelectric coefficient of the ceramics on the intensity of the prepolarization field both for conditions of cold polarization (specimens held in the polarizing field at room temperature for 2 hours) and for conditions of hot polarization when the specimen was heated to a temperature above the Curie point (130-140°), placed into the polarizing dc field and cooled while in the applied field. The curves for $BaTiO_3$ are shown in Fig.4.

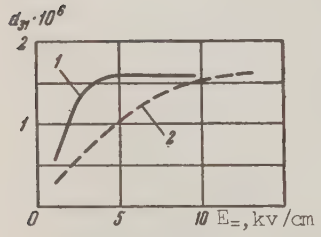

Fig.4. Variation of the piezoelectric constant d_{31} of $BaTiO_3$ on the prepolarization field: 1) hot polarization, 2) cold polarization.

Conclusions

1. Barium titanate is characterized in the temperature range from -40 to +40° by an appreciable instability of its electroacoustic parameters.

2. The stability can be improved by use of appropriate additives. The best ceramics from the point of view of their stability are ternary compositions containing both calcium titanate and lead titanate. These ceramics also yield a certain gain in sensitivity as compared with $BaTiO_3$. Hence it is expedient to use such ceramics for fabricating electroacoustic receivers. On the other hand, the specific acoustic power of transducers employing such ceramics is appreciably lower than that of transducers with $BaTiO_3$ which makes it inadvisable to use these solid solution ceramics for acoustic projectors.

3. The composition containing 6% $BaTiO_3$ may be recommended as a suitable material for both projectors and receivers inasmuch as it assures good stability while reducing the specific acoustic power by a factor of only about two.

4. Ceramics of barium titanate with barium stanate and strontium titanate, which have an enhanced value of the dielectric constant but are not particularly stable and have large hysteresis losses, are not suitable in general for electroacoustic transducers.

In closing we desire to thank V.I.Zaitseva, I.A.Serova and I.V.Ignat'eva for their help in preparing the specimens and carrying out the measurements.

Institute of Semiconductors of the
Academy of Sciences of the USSR

References

1. W.P.Mason, Acustica, 1, 200 (1954).

USE OF FERROELECTRICS IN FREQUENCY MULTIPLIERS

- D.M.Kazarnovskii & V.P.Sidorenko

Introduction

The shape of the curve characterizing the alternating current in a circuit incorporating a ferroelectric capacitor is distorted due to the nonlinear polarization of the ferroelectric. One can readily separate any of the odd harmonics by making use of current or voltage resonance. In the presence of a dc voltage there appear even harmonics in the current curve; this makes it possible to obtain even harmonics of the voltage. The first frequency multiplication circuit for alternating current utilizing the nonlinear characteristics of ferroelectrics was proposed by Volodin[1] who based his design on Rochelle salt. After the discovery of ceramic ferroelectrics, these also came to be used for frequency multipliers; a multiplier employing barium titanate was constructed soon after development of a successful procedure for synthesizing barium titanate[2]. Subsequently it was found, however, that certain solid solutions of barium titanate in which saturation of polarization was attained in relatively weak fields are better suited for use in multipliers. In 1952 Demichev[3] developed a frequency multiplier designed about water cooled flat-plate capacitors of a ceramic consisting of a solid solution of 10% $BaSnO_3$ + 90% $BaTiO_3$.

The early ferroelectric frequency multipliers were essentially static frequency converters for single-phase voltage. Yet in many cases it is desirable to obtain a high frequency three-phase voltage. Such high frequency three-phase sources are needed for supplying high speed three-phase motors such as those used in gyro devices and similar equipment.

Although the present investigation was undertaken primarily for the purpose of determining the principal characteristics of ferroelectric three-phase frequency multipliers, we feel that some of the results may be of general interest and perhaps may serve as the point of departure for the development of new applications.

While we had at our disposal a number of different solid solutions having ferroelectric properties, in view of the fact that the electronic industry at present produces only ferroelectric capacitors employing Varikond VK1 (barium titanate with a certain amount of tin oxide)[4], we decided to use a capacitor of this type for our main nonlinear element.

2. Behavior of ferroelectric capacitors in the presence of a sinusoidal voltage

The parameters commonly given in the literature are far from adequate for evaluating the characteristics of a ferroelectric capacitor when it is to be used in a multiplier circuit. Knowing the value of the effective capacitance makes it possible to find the reactive component of the current (which differs little from the full current) but does not offer a clue to the magnitude of the harmonic components. The loss tangent measured in weak fields cannot characterize the loss in a ferroelectric capacitor in the strong fields that obtains when it is employed in a multiplier. Even determining the coefficient of nonlinear distortion is not sufficient, inasmuch as even with the same value of the coefficient, the relative values of the current of the individual harmonics may be different.

The ratio of the capacitance C_2 of a ferroelectric capacitor at a voltage V_2 to the capacitance C_1 at voltage V_1 (the so-called capacitive nonlinearity) cannot serve as a criterion for evaluating the "multiplier" character-

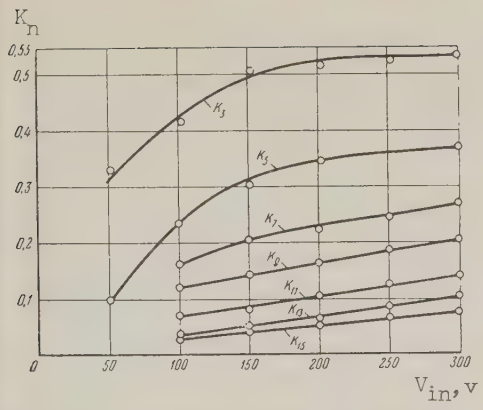

Fig.1. Variation of the current harmonic coefficients K_n as a function of the sinusoidal voltage ($L_o = 0$, $t = 25^o$).

istics of a ferroelectric capacitor inasmuch as this ratio is not related in explicit form with the magnitudes of the harmonic components of the current at the voltage V_2.

Comparison of ferroelectric capacitors of different types can be based on the values of the current of the n-th harmonic and the harmonic coefficient or factor $K_n = I_n/I_1$ as a function of the voltage and temperature at the same initial capacitance C_i of the ferroelectric capacitor. In an earlier communication[5] we gave the dependence of the factor of the third harmonic of the current of a VK1 ferroelectric capacitor on the voltage at different temperatures. The VK1-4 Varikond capacitor (operated in air) was connected to a 500 cps sinusoidal voltage source. Investigation of the influence of the voltage and temperature on the magnitude of the currents not only of the third but other higher harmonics showed that with increasing voltage the higher harmonic currents at first increase rapidly and that, subsequently, the rate of increase slows down (Fig.1). As the temperature approaches the phase transition point, the effect of the voltage becomes weaker, while the shape of the current curve approaches the sinusoidal. We note that even at temperatures above the Curie point the higher harmonics persist and there is observed a weak but definite dependence of the harmonic factors on the voltage. Even under favorable operating conditions for the ferroelectric capacitor, the value of the harmonic coefficients is fairly low: thus at 20^o and $V_{in} = 200$ v, the coefficient of the third harmonic $K_3 \leqslant 0.55$.

We will show below that a marked increase of the harmonic coefficients can be attained by connecting inductances into the circuit series with the ferroelectric capacitor. This makes it possible to increase appreciably the power at the multiplier output.

3. Losses in ferroelectric capacitors

In the case of a nonlinear capacitor, losses affect not only the efficiency of the multiplier but other characteristics as well. The introduction into the circuit of a resistance equivalent to the losses produces an increase in attenuation and a decrease of the current harmonic coefficients, particularly in the resonance regions. These losses depend greatly on the temperature of the capacitor, the applied voltage and the frequency. In view of this it is essential to determine the loss under conditions duplicating the operating conditions of the ferroelectric capacitor and to utilize in so far as possible procedures allowing of direct measurement of the losses under the given conditions. Such suitable procedures are the calorimetric and that based on the use of a wattmeter. In the present investigation the losses in the VK1 capacitors were measured by the wattmeter method*. The losses were measured at a frequency of 500 cps under conditions of natural cooling of the VK1-4

---

*We used the electrostatic wattmeter developed by A.N.Dmitriev at the Leningrad Electrotechnical Institute.

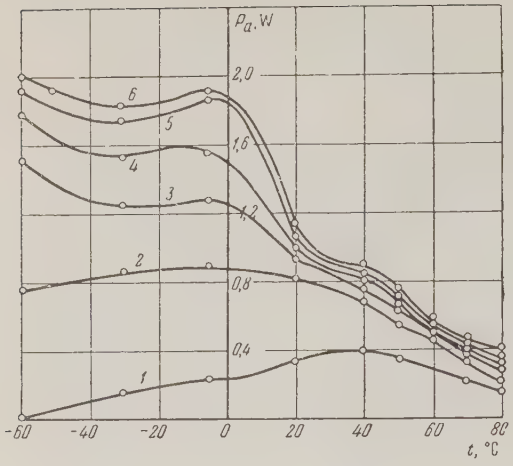

Fig.2. Variation of the loss in a VK1-4 ferroelectric capacitor as a function of the ambient air temperature at different input voltages: 1) V_{in} = 50 v, 2) 100 v, 3) 150 v, 4) 200 v, 5) 250 v, 6) 300 v.

capacitor. The losses change little with increasing ambient temperature (at the same voltage) up to about 0° after which they begin to decrease (Fig.2). This character of the dependence is due to the fact that, owing to the high value of the losses and inadequate cooling, the capacitor tends to heat up and its temperature may rise to 25-30° above that of the surrounding medium. The equivalent resistance introduced into the circuit due to the loss at a voltage of 200 v and an air temperature of 25° is of the order of 500 ohm. The effective loss tangent, calculated according to the formula

$$\tan \delta_{eff} = \frac{P_a}{V\sqrt{I_1^2 + I_3^2 + I_5^2 + \ldots}},$$

is fairly large - of the order of 0.2. The presence of the appreciable resistance introduced by the VK1 ferroelectric capacitor seriously limits the output power of the multiplier. Hence it is desirable to take measures to reduce the loss in ferroelectric capacitors intended for use in multipliers.

4. Ferroelectric capacitors in circuits with inductance

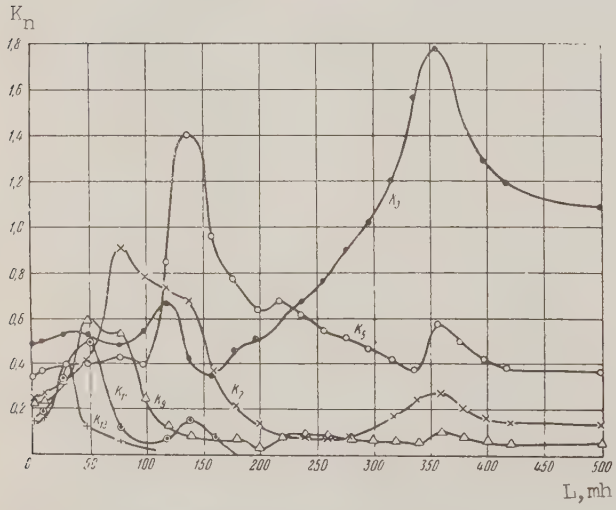

Fig.3. Dependence of the harmonic coefficients on the inductance (capacitor naturally cooled in air, V_{in} = 200 v, t = 25°).

We connected an inductance box, a resistance box and a standard 1 ohm resistance in series with the VK1-4 Varikond capacitor. The voltage taken off the standard resistance was applied to the harmonic analyzer by means of which we determined the odd current harmonics under different conditions.

It may be seen from Fig.3 that at a certain value of the inductance the coefficient of the third harmonic may exceed the coefficient of the first harmonic by a factor of 1.8 and that of the fifth harmonic by a factor of 1.4. In view of the appreciable loss in ferroelectric capacitors of the VK1 type the temperature in strong fields may rise appreciably above the ambient temperature. Hence in the case

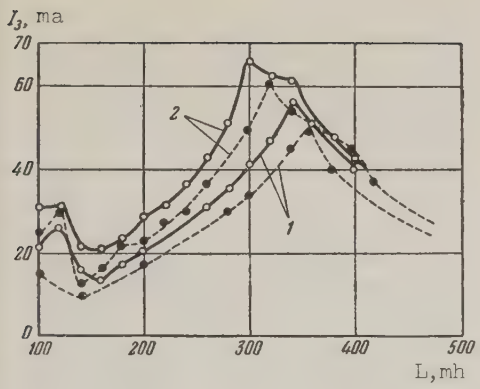

Fig.4. Dependence of the third harmonic current on the inductance and the medium surrounding the capacitor (V_{in} = 200 v): 1) capacitor in air, 2) capacitor in oil. Solid curves recorded at 25°; dash curves recorded at 50°.

of oil cooling, by virtue of the lower temperature obtaining in this case, the current of the harmonics increases (Fig.4). At certain values of the inductance there may be obtained third harmonic currents very much greater than the corresponding values with no inductance in the capacitor circuit (Fig.5).

The appearance of maxima in the curves characterizing the inductance dependence of the harmonic currents indicates the presence of resonance effects in the circuit; these explain the very appreciable magnitude of the harmonic currents at certain inductance values. The voltage on the ferroelectric capacitor is characterized by a distorted wave form; the magnitude of the voltage of the third harmonic may approach the value of the voltage of the first; the amplitudes of the other voltage harmonics may also be appreciable.

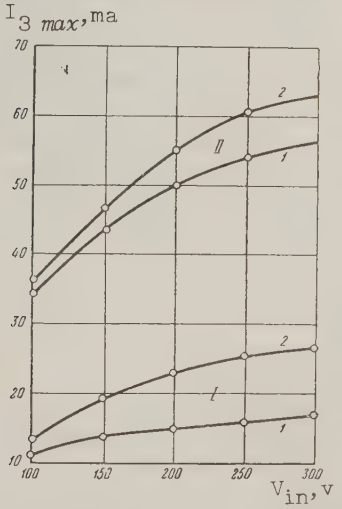

Fig.5. Dependence of the maximum third harmonic current $I_{3\ max}$ on the voltage on the circuit terminals (capacitor in air, R_o = 0): I) no inductance in the circuit, II) with an inductance L_o = = 0.2-0.4 h; 1) t = 50°, 2) t = 25°.

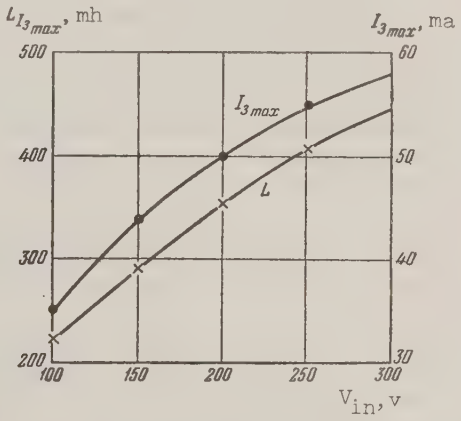

Fig.6. Dependence of the maximum current of the third harmonic $I_{3\ max}$ and the corresponding inductance $L_{I_{3\ max}}$ on the applied voltage (capacitor in air, t = = 25°).

As the applied voltage is increased, there is an increase not only in the value of the current maximum of the harmonics ($I_{n\ max}$) but also the value of the inductance ($L_{I_{n\ max}}$) corresponding to this maximum (Fig.6).

This effect is apparently connected with the fact that with increasing applied voltage the capacitance of the ferroelectric capacitor at first increases and then begins to decrease; consequently, to obtain a particular resonance at the frequency $3f_1$ at higher voltages it is necessary to increase

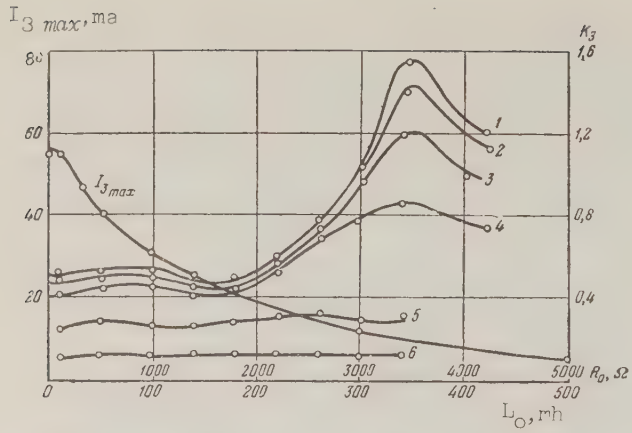

Fig.7. Dependence of the peak current of the third harmonic $I_{3\,max}$ on the additional resistance R_o and dependence of the coefficient of the third harmonic K_3 on the inductance L_o at different values of R_o: 1) 0, 2) 300, 3) 500, 4) 1000, 5) 3000, 6) 5000 ohm.

the inductance. In cases when the voltage component is small (higher harmonics) obviously displacement of the maximum of the current harmonic along the inductance scale is also possible but in this case it occurs at higher voltages.

Connecting an additional resistance R_o into the circuit leads to a reduction of the coefficients of the current harmonics owing to increased damping (Fig.7). Oscillograms show that with R_o = 3000 ohm the current curve comprises virtually no higher harmonics, while with R_o = 0 and the same inductance the third harmonic predominates in the current curve. It might be noted, however, that tests indicate that changes in the inductance with R_o = 3000 ohm have almost no noticeable effect on the shape of the current curve, while with R_o = 0 the shape of the curve is strongly dependent on the inductance in series with the ferroelectric capacitor. It follows from our results that at a certain inductance one can obtain a third harmonic current approximately 2.4 times greater than in the circuit of a ferroelectric capacitor with no inductance. The introduction of a resistance (including the resistance equivalent to the loss in the ferroelectric capacitor) results in a reduction of the third and higher current harmonics.

5. On use of ferroelectrics in frequency triplers for three-phase voltage supplies

One can obtain a tripled frequency three-phase voltage at the output of the frequency multiplier where there is available for the initial feed a nine-phase symmetrical system in which the neighboring voltage vectors are shifted 40° relative to each other. Such a system may be regarded as consisting of three three-phase systems rotated 40° relative to each other.

The voltages of the first, fourth and seventh phases are displaced 120°; consequently, the third harmonics in these phases will be in phase. In the same way we will have coincidence of the third harmonics of the second, fifth and eighth phases and of the third, sixth and ninth phases.

At the same time the third harmonics in one of these three-phase systems will be shifted 40° relative to the third harmonics in the other system, i.e., by 1/3 the period of the tripled frequency. Hence, if three ferroelectric capacitors, each in series with a primary winding, are connected into a delta network which in turn is connected to the first, fourth and seventh phases of the nine-phase system, the third harmonic (and others that are multiples of three) will be induced in the secondary windings (Fig.8). The fundamental frequency currents in this delta network will be 120° apart and hence their sum will be zero (just as the sum of the currents of the other harmonics that

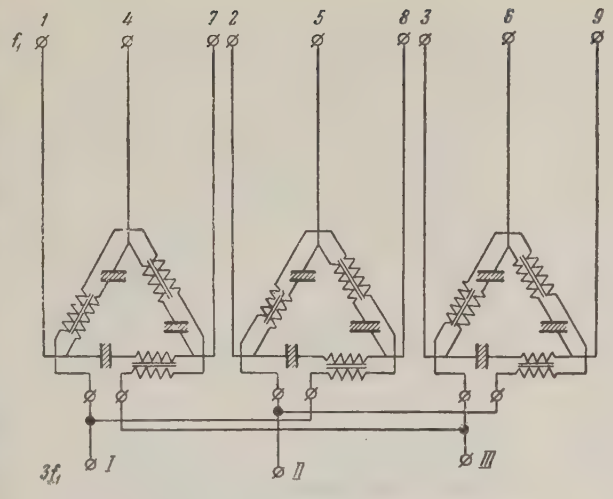

Fig.8. Diagram of three phase voltage supply frequency tripler.

are not multiples of three). Another similar delta network is connected to the second, fifth and eighth phases and a third network to the third, sixth and ninth phases. The secondary windings in each delta network are connected in series and as a result we obtain three voltages shifted relative to each other by 1/3 the period of the tripled frequency[6].

We note that if the secondary windings are connected in delta, the curve characterizing the tripled frequency line voltage will not contain the ninth harmonic nor will there be present components of the fundamental frequency or of the fifth, seventh, eleventh and higher non-multiple of three harmonics. It is also possible to use a circuit with the transformer in the zero (neutral) conductor.

In the case of a symmetrical system of voltages and the uniform loading it is sufficient to consider the operation of one phase (frequency $3f_1$). Hence for investigating the principal characteristics of a three-phase frequency multiplier we used a circuit consisting of three capacitor units comprised of four VK1-4 nonlinear capacitors each, which together with the primary windings of the transformer were connected into a delta network. An appropriate load was connected to the secondary winding (Fig.9). The current was measured by means of hot-wire ammeters, the output voltages by means of a vacuum tube voltmeter and the power by a low power factor wattmeter. The current harmonics were determined with the aid of an electric harmonic analyzer.

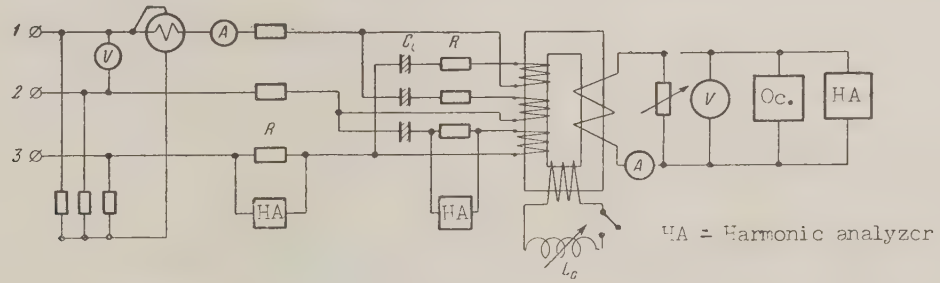

Fig.9. Experimental frequency tripler circuit.

6. Voltage and power at the output of the frequency multiplier in the case of a variable load

As the resistive load current is increased the voltage drop across the output transformer increases and in consequence the voltage V_3 at the frequency multiplier output decreases. In the case of variation of the inductive load the character of the dependence of V_3 on the load current I_3 may differ

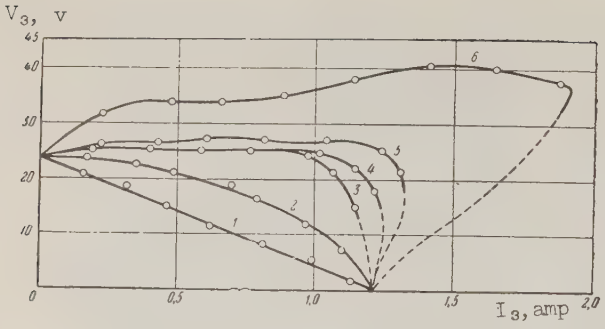

Fig.10. Variation of the voltage V_3 of the tripled frequency with the load current (capacitor in air, V_{in} = 200 v, t = 25°): 1) capacitive load, cos φ_3 = 0.1; 2) resistive load, 3) inductive load, cos φ_3 = = 0.7, 4) inductive load cos φ_3 = 0.6, 5) inductive load cos φ_3 = 0.5, 6) inductive load cos φ_3 = 0.1.

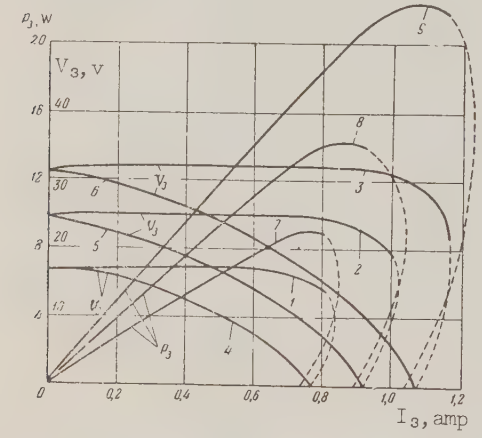

Fig.11. Dependences of the voltage V_3 and the active power P_3 of the tripled frequency on the load current (capacitor in air, t = 25°): 1,2,3,7,8,& 9 - inductive loads, cos φ_3 = 0.7; 4,5 & 6 - reactive loads; voltage on input 150 v for curves 1,4 & 7; 200 v for curves 2,5 & 8; 250 v for curves 3,6 & 9.

inasmuch as this involves a change in the value of the equivalent inductance connected in series with the capacitor. If the inductance of the output transformer is selected so that it will correspond to a point on the $I_3 = f(L_o)$ curve (see Fig.4) beyond the maximum (i.e., approximately $L_o > 0.5$ h), then the current of the third harmonic will increase with increasing inductive load due to reduction of the equivalent inductance in the circuit. Consequently, the emf of the transformer will rise, which will have a stabilizing influence on the third harmonic voltage. Thus one can obviously choose circuit parameters such that the voltage of the tripled frequency will virtually remain constant over a certain range of load currents.

We were able to provide such conditions in the experimental circuit. To this end we prepared a special toroidal output transformer with a Permalloy core having an appreciable inductance.

This made it possible to obtain a virtually horizontal external characteristic for load factors in the 0.6 to 0.8 range; this of course is a very desirable feature for such frequency converters (see Fig.10). It may be noted that the tripled frequency voltage is sinusoidal almost to the inflection point on the curve. The higher harmonic content of the current curve is strongly dependent on the character of the load. We separated the third harmonic of the primary current curve. Its magnitude is very small in the case of a capacitive load, but increase sharply in the case of inductive loads.

Variation of the applied voltage has a marked effect on the output (tripled frequency) voltage and the effective output power (Fig.11).

The maximum active power with cos φ_3 = 0.7 rises by more than 50% when the input voltage is increased from 200 to 250 v. It must be noted, however, that at a voltage of 250 v (and a frequency of 500 cps) the capacitors in a circuit with inductance cannot be operated for a prolonged period due to thermal breakdown.

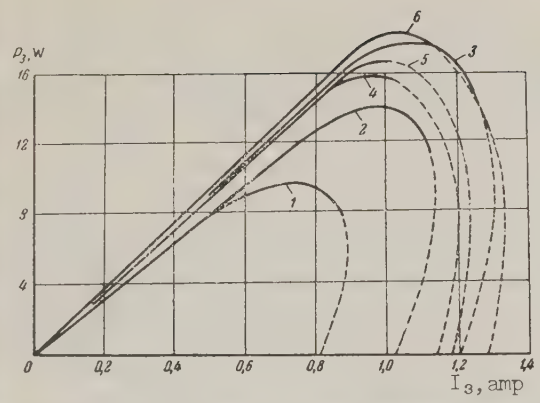

Fig.12. Variation of the active power P_3 with the load current (V_{in} = 200 v, $\cos \varphi_3 = 0.7$) for capacitors in air: 1) t = 50°, 2) t = 25°, 3) t = -60°; for capacitors in oil 4) t = 50°, 5) t = 25° and 6) t = -60°.

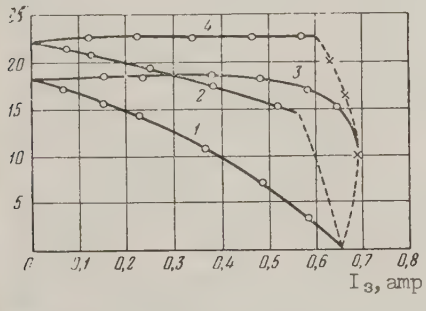

Fig.13. Dependence of the voltage V_3 on the load current (V_{in} = 200 v, t = 60°) with and without an inductive shunt. No shunt: 1) $\cos \varphi_3$ = 1, 2) $\cos \varphi_3 = 0.7$. With an inductive shunt: 2) $\cos \varphi_3$ = = 1, 4) $\cos \varphi_3 = 0.7$.

An increase of the ambient temperature affects not so much the output voltage as the maximum power. Thus, referred to the voltage at 25°, the voltage with $\cos \varphi_3 = 0.7$ increases by 15% at t = 60° and falls off by 4% at t = 50°. The maximum power, however, is reduced by a factor of almost one and a half when the temperature is increased to 50° due to overheating of the capacitors (Fig.12). By improving the cooling (immersing the capacitors in oil) one can reduce the effect of temperature changes and at the same time increase the maximum power at 25°.

Decreasing the rated capacitance of the ferroelectric capacitor unit leads to almost proportional reduction of the maximum power although at the same time the voltage at the multiplier output remains virtually unchanged (within the range of the horizontal section of the characteristics with $\cos \varphi_3 = 0.7$). When the rated capacitance is increased, the maximum power with the same output voltage and the given parameters of the output transformer will at first increase and then begin to fall off. This follows from the following considerations. The maximum current of the third harmonic is obtained with a certain relation between the rated capacitance of the ferroelectric capacitors and the inductance of the circuit (see Fig.4). An increase in capacitance is equivalent to a reduction of the inductance; hence when the capacitance increases to the point where the equivalent inductance in the circuit becomes less than $L_{I_3\ max}$, the external characteristic loses its horizontal section and becomes a falling one. Naturally at this point the maximum power begins to decrease.

7. Control of the voltage and power of the multiplier by means of a reactive shunt

The data given above show that the characteristics of a frequency multiplier of the given type depend to an appreciable extent on the applied voltage, the ambient temperature and the nature of the load. It is therefore feasible to utilize the dependence of the higher harmonic content in the current curve of a ferroelectric capacitor on the inductance for the purpose of stabilizing the multiplier characteristics. To this end an inductive shunt may be connected into the circuit. In the case of our experimental circuit we connected an inductance L_o = 7.3 mh to the auxiliary transformer winding (see Fig.9).

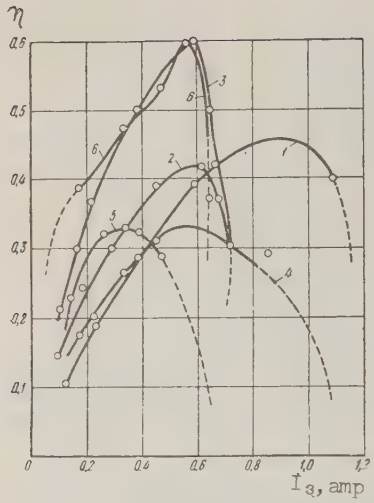

Fig.14. Dependence of the efficiency of the frequency multiplier on the load current for two values of the inductance L_o of the shunt (ferroelectric capacitors in air): 1,2 & 3) inductive load, $\cos \varphi_3 = 0.7$; 4,5 & 6) inductive load; 1 & 4) $t = 25^\circ$, no shunt, 2 & 5) $t = 60^\circ$, no shunt; 3 & 6) $t = 60^\circ$, $L_o = 7.3$ and 10.4 mh, respectively.

This specific value was chosen in order to obtain the maximum no-load voltage. By connecting in the inductance it is possible to obtain a voltage at 60° equal to that normally obtained at a temperature of 25°. Actually effective voltage control is obtainable not over the entire load range but only over the section from 0 to approximately the maximum power load (see Fig.13). In practice this is sufficient inasmuch as the rated power of the frequency tripler must necessarily be somewhat lower than the maximum limiting power. The given results pertain to the case when the equivalent inductance always remains greater than $L_{I_{3m}}$. If it is lower than $L_{I_{3m}}$ the voltage can obviously be regulated by means of a capacitive shunt. An inductive shunt can also be used for reducing the output voltage where this is desirable.

8. Efficiency of the multiplier

The efficiency of the multiplier was determined with reference to the active power: $\eta = P_3/P_{in}$, where P_3 is the output power of the multiplier and P_{in} is the input power. As may be seen from Fig.14, with increasing load current the efficiency at first rises and then falls off sharply. At a temperature of 60° the maximum efficiency corresponds to a lower load current than in the case of normal temperature (25°). It will be noted that far higher efficiency values are obtainable with an inductive shunt. This is due to the fact that connecting in the inductive shunt increases the tripled frequency voltage and, consequently, the useful power P_3. The highest efficiency obtained does not exceed 0.6. The relatively low efficiency values are due to the high losses in the VK1-4 ferroelectric capacitors employed. It may be assumed that given lower loss ferroelectric capacitors and improved transformer design it should be possible to realize frequency multipliers having higher efficiency values.

Power factors of the frequency multiplier at maximum efficiency

Power factor of load	t°	Power factor of multiplier-cos φ_{in}	
		without reactive shunt	with reactive shunt
0,7	25	0,17	—
	60	0,12	0,11
1	25	0,14	—
	60	0,08	0,10

9. Power factors

Where the ac supply is concerned a ferroelectric frequency multiplier is essentially a capacitive load with a low power factor. This makes it possible partially to compensate the phase shift and raise the power factor of the supply circuit. In order to determine the power factor, in addition to the active power P_{in},

we also measured the full (apparent) power S_{in}. The highest values of cos φ_{in} was obtained at the maximum efficiency (see table).

It will be seen from these results that the power factor goes down somewhat with increasing temperature. Connecting in a reactive shunt has little influence on the value of cos φ_{in}.

Conclusions

1. Among the principal characteristics of ferroelectric capacitors used for frequency multiplication are the voltage and temperature dependence (at a given fundamental frequency) of the current I_n of the desired harmonic, the current harmonic coefficient K_n and the loss P_a in the capacitor measured by the direct method.

For one particular VK1-4 Varikond capacitor operated in air with a sine voltage V = 200 v and a frequency of 500 cps, the determined values of the above parameters were $I_3 \leqslant 22$ ma, $K_3 \leqslant 0.55$ and $P_a \leqslant 1.7$ watt (tan δ_{eff} = = 0.2).

2. In a circuit with inductance, by virtue of particular resonances, the content of higher harmonic currents may be very appreciable. Under the conditions described above $I_3 \leqslant 55$ ma and $K_3 \leqslant 1.78$; with the same voltage and frequency but the VK1-4 capacitor operated in oil $I_3 \leqslant 65$ ma and $K_3 \leqslant 1.74$. The value of the inductance $L_{I_3\ max}$, corresponding to the maximum third harmonic current $I_{3\ max}$, increases almost linearly with the voltage. When a pure resistance is introduced into the circuit the magnitude of the current harmonics falls off and the influence of any inductance coupled into the circuit on these harmonics is reduced.

3. In the proposed three-phase voltage supply frequency tripler one can realize conditions where with increasing inductive load (within certain limits) with cos φ_3 = 0.6-0.8, the equivalent inductance decreases (but remains greater than $L_{I_3\ max}$). Under these conditions the tripled frequency voltage remains constant despite variation of the load. The maximum limiting triple frequency output power increases with increasing voltage and decreases with rising temperature. The maximum available power can be increased by using oil cooling. Under the conditions of our experiment the maximum power of one phase in the case of three delta-connected VK1-4 capacitors at 25° and 200 v is about 3.5 watts when the "ferro-capacitors" are operated in air and about 4.3 watts when they are immersed in oil. The tripled frequency voltage is sinusoidal at all loads below that corresponding to the maximum power.

4. Control of the voltage and power in the load range below the maximum power can be realized by means of a reactive shunt. At the same time by means of a reactive shunt it is possible to compensate to an appreciable extent for the influence of the ambient temperature on the voltage and delivered power.

5. The curve characterizing the variation of the efficiency with the load current has a maximum that shifts with changes in temperatures. When a reactive shunt is connected into the circuit the efficiency increases; the best efficiency obtained under the conditions of our experiment was 0.6.

6. The power factor of the frequency multiplier depends on the character and magnitude of the load and the applied voltage. The multiplier represents a capacitive load with cos φ_{in} = 0.17; connecting it to the supply line results in compensation of the inductive current and increase of the power factor of the supply line.

7. It should be possible to increase both the maximum output power and efficiency of multipliers of this type by the use of ferroelectric capacitors with an enhanced Q factor and higher electric strength.

8. Among the important steps to be taken in this field is initiation of production of oil-cooled ferroelectric capacitors having a capacitance of several microfarads, characterized by lower losses and higher electric strength when operated in frequency multiplier circuits of the described type.

The writers desire to thank S.F.Farmakovskii as well as A.A.Gerasimov, I.N.Chudinov and G.K.Merenishcheva for assistance in setting up the experiments.

References

1. V.P.Vologdin, ZS.techn.Phys., 13, 82 (1932).

2. V.P.Vologdin, Elektrichestvo (Electricity), No.8, 28 (1946).

3. A.D.Demichev, Report NIITVCh (Scientific Research Inst. of High Frequency Engineering), No.10, 1952.

4. T.N.Verbitskaia, Doklady AN SSSR, 100, 29 (1955).

5. D.M.Kazarnovskii & V.P.Sidorenko, Trudy (Transactions) "A.F.Mozhaiskii" LK VVIA, No.167, 1956.

6. D.M.Kazarnovskii, Informatsionnyi sbornik (Information Bulletin), "A.F.Mozhaiskii" LK VVIA, No.15, 1956.

ON EQUIPMENT FOR RESEARCH IN THE FIELD OF FERROELECTRICS USING SMALL SPECIMENS (Progress Report)

- I.S.Rez

Despite the marked upsurge of research in the field of ferroelectrics, we still have only a limited number of thoroughly investigated materials possessing ferroelectric properties in conjunction with the physical and chemical characteristics indispensable for engineering applications. In fact, only Rochelle salt and certain barium titanate systems are used to any extent in electronic equipment. The continuing advances in technology and engineering obviously call for an expanded list of piezoelectric and ferroelectric materials suitable for different special applications; accordingly there is urgent need for a program of research aimed at finding new piezoelectric and ferroelectric materials with the requisite physical and chemical characteristics.

In setting up such a research program one should be guided by the available data on the correlation between the chemical structure of substances and their piezoelectric and ferroelectric properties. On the basis of experimental data one can determine the potentially active structural elements and plot tentative genetic series.

Of considerable assistance in such preliminary research may be the concepts developed by Koptsik[1] regarding the sufficient (but not always necessary) condition for the existence of a piezoelectric effect in dielectric crystals, namely, the presence in the crystal structure of permanent dipoles arranged in accordance with space group regularities favorable for the appearance of a piezoeffect. Practical utilization of this semistatistical criterion is hampered by the necessity of knowing beforehand (primarily from investigations of the piezoelectric properties) of the Fedorov space group in which the material belongs. This, of course, is rarely known in the case of substances that have not already been studied from the piezoelectric standpoint.

Another promising line of search is opened by the theories[2-4] interpreting the presence of ferroelectric attributes to the displacement of the protons along the lines of hydrogen bonds. Hence it may be worthwhile to look for new ferroelectrics among substances forming low order of symmetry crystals containing hydrogen bonds.

It is also obviously expedient to search for new ferroelectrics among substances crystallizing with the perovskite and ilmenite structures in the light of the ideas and theories developed by Smolenskii and his co-workers[5], whose work has led to the discovery of a number of new ferroelectrics of the oxy-octahedral type.

From analysis of the known cases of detection of the piezoelectric effect[6] one can establish clear genetic series of piezoelectrically active substances: tartrates, dihydrogen phosphates, dihydrogen arsenates and so on, where inorganic materials are concerned. In the case of organic materials for which x-ray data are not available, analysis of the available data indicates that such piezoelectric materials are characterized by the presence of polar groups and, in some cases, by the presence of crystallization water in the constituent molecules.

Thus on the basis of the above and similar considerations, one can preselect likely piezoelectric materials for actual testing, thereby effecting a considerable economy of time and experimental effort. No less important than the preselection process, however, is development of a systematic and reliable procedure applicable to small amounts of the subject substance which need not necessarily be in the form of clearly defined crystals. This is a very important consideration inasmuch as in the early stages of exploratory

investigation it is often impossible to obtain large specimens of new or rarely synthesized materials. Moreover, the chances of obtaining more or less perfect crystals of such substances are altogether remote.

Accordingly, we proposed and put into effect the following program of investigation of diverse materials preselected on the basis of the "piezochemical" considerations set forth above:

1) Detection of piezoelectric activity in powdered or granular material, followed in the case of positive results by

2) investigation of the temperature dependence of the dielectric constant and resistance using standard pellet or tablet specimens;

3) check for the presence of dielectric hysteresis;

4) investigation of the temperature dependence of the loss in weight;

5) thermographic detection of possible phase transitions in the desirable operating temperature range;

6) dilatometric studies.

All the above tests and studies are designed to be carried out on the standard pellets or tablets.

Finally, the most promising materials are chosen for further more detailed investigation in the form of single crystals (if these can be grown), polycrystalline samples or ceramics.

While the tests under 3 through 6 above were carried out according to conventional procedures with only slight appropriate modifications, the investigations under points 1 and 2 required the development of some special equipment. The remainder of this report will be devoted to a description of this special equipment.

The piezoelectric activity of the pellet specimens was determined on the PT-2 type piezotester developed in our laboratory on the basis of the set-ups originated by Bergmann[7], Shein & Zheludev[8] and Kptsik[9]. This equipment is intended for evaluating the piezoelectric activity of specimens by the method of measuring the relative magnitude of the piezoelectric effect as compared with that of a standard, in our case a Curie cut quartz plate.

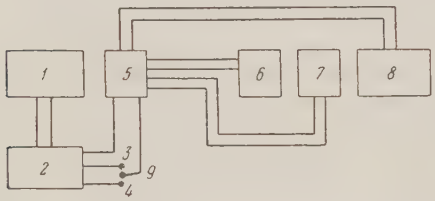

Fig.1. Diagram of set-up for determining the piezoelectric activity of small specimens: 1) ZG-2A audio generator, 2) piezotester, 3) output from specimen, 4) amplifying-matching unit, 6) EO-6M oscillograph, 7) noise meter, 8) EPP-09 vacuum tube potentiometer, 9) switch.

A block diagram of the set-up is shown in Fig.1. The complete set-up consists of a ZG-2A audio-frequency oscillator, the piezotester proper, an amplifying-matching unit, an EPP-09 vacuum tube potentiometer, an EO-6M oscillograph and a Sh-1 measuring amplifier (noise meter).

The piezotester proper is diagrammed in Fig.2. The specimen in the form of a powder, grains, a pellet or a cut plate is placed on the lower electrode which is permanently affixed to the porcelain rod which, in turn, is rigidly connected to the piezoelectric oscillator. The last consists of a stack of polarized barium titanate ceramic plates designed to vibrate axially when subjected to the voltage from the audio generator. The piezoelectric standard, i.e., the X-cut quartz disc reference vibrator, is mounted between the porcelain rod and the barium titanate ceramic stack. The second electrode presses down on the specimen and forms part of an assembly comprising an interchangeable weight and a set of guides.

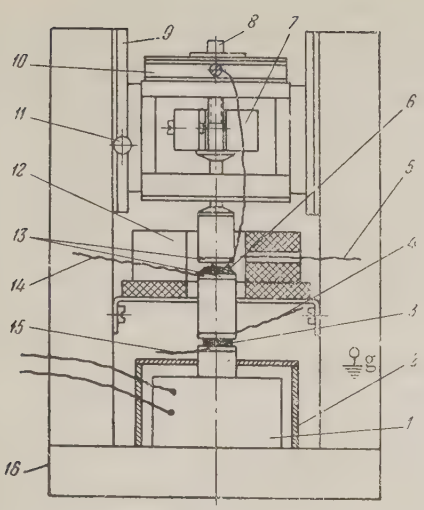

Fig.2. Diagram of piezotester. 1) piezoelectric vibrator, 2) shielding, 3) X-cut quartz plate standard, 4) lead from standard, 5) thermocouple leads, 6) specimen, 7) interchangeable weight, 8) movable electrode assembly, 9) guides for movable electrode assembly, 10) frame for electrode assembly guides, 11) clamping screw, 12) demountable heater, 13) specimen plates (electrodes), 14) lead from specimen, 15) lead, 16) tester frame.

To permit investigating the temperature dependence of the piezoelectric activity the set-up is provided with a demountable electric heater that can be set to surround the specimen. The piezoceramic vibrator and quartz standard are shielded from the heater by a thermal insulation plate. The temperature of the specimen is monitored and regulated by means of a thermocouple which is connected to an EPP-09 vacuum tube voltmeter equipped with a programming attachment.

The measurements are made at a frequency of 1000 cps which is sufficiently remote from the resonance frequencies of the specimen and vibrating components of the tester. The charge generated on the grains of the piezoelectric specimen under the influence of the mechanical vibrations produced by the ceramic stack and transmitted to the specimen by the porcelain rod and the standard quartz disc is taken off by the electrodes and applied to the input of the amplifying-matching unit.

The amplifying-matching unit (see Fig. 3) is essentially an amplifier with a 1000 cps tuned filter. The first and second stages of the amplifier are designed about 6Zh8 tubes and yield a gain of 10,000. The third stage employs a 6N8 double triode; the first triode operates as a signal voltage amplifier (amplification factor 10), while the second triode serves as a feedback voltage amplifier.

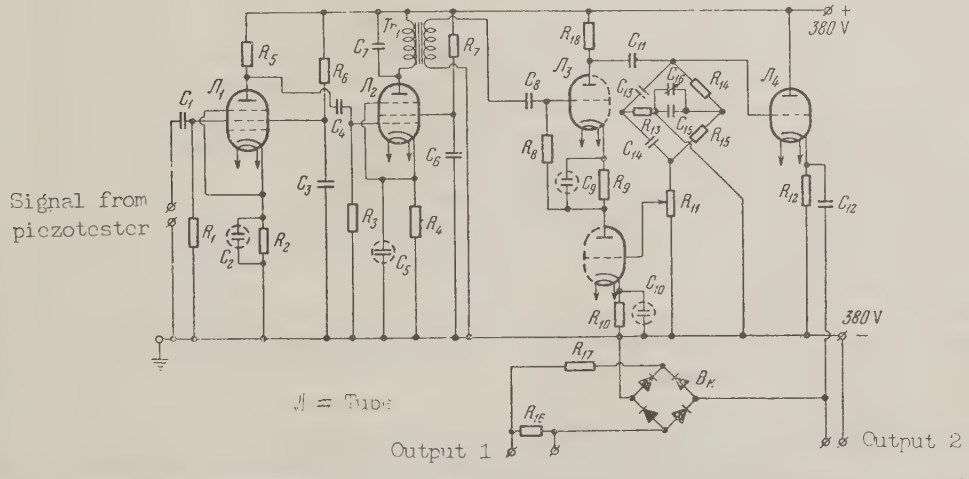

Fig.3. Circuit diagram of the amplifying-matching unit used in conjunction with the piezotester. Output 1 connects to the EPP-09 potentiometer; output 2 connects to the oscillograph and measuring amplifier (noise meter).

The filter operates as follows. The signal voltage, after amplification in the first two stages, is applied to the first triode of the 6N8 tube; the resonant filter is connected into the plate circuit of this triode. The filtered 1000 cps signal is applied to the grid-plate section of a cathode follower assembled about a 6S5 tube. Finally, the signal voltage is fed through an appropriate coupling capacitor to the Sh-1 noise meter which serves as the measuring amplifier (factor 100,000); the meter has a voltage divider at the input and an indicator graduated in decibels across the output. The vacuum tube potentiometer and the EO-6M oscillograph are connected in parallel with the noise meter. The voltage for the EPP-09 potentiometer is taken off a cuprous oxide rectifier. The amplifier is supplied from a separate 380 volt rectifier.

The pass-band of the filter is 30 cycles. The selectivity of the filter is regulated by means of the potentiometer R_{11} (Fig.3); the filter is tuned by means of the variable capacitor C_{16}.

With this set-up the piezoelectric activity can be evaluated with reference to the standard in three ways: a) from the display on the oscillograph, b) from the indications of the noise meter or c) from the indications or record of the EPP-09 potentiometer.

Exhaustive tests of the set-up using known piezoelectric substances successively in the form of single crystal plates, fragments of such crystals, fine grain specimens and pellets compressed of the powdered material showed that the set-up can be used for semi-quantitative evaluation of piezoelectric activity. The calibration test data are listed in the accompanying table.

In evaluating the test results obtained for new, not previously studied substances it is important to bear in mind the following. In our experiments we found that a number of substances with a centrosymmetric structure, that are definitely known not to be piezoelectric, when tested in the form of single-crystal or large grain specimens exhibit activity under heavy loads; this activity is accompanied by fracturing of the fragments or crystal grains. It is possible that in this case our highly sensitive equipment detects electrons emitted during mechanical destruction of the specimen. An analogous effect has been described by Krotova & Karasev[10] and its possibility must naturally be borne in mind in testing for piezoelectricity. In addition, in testing a powdered specimen of a dielectric with a high resistivity, such as polyvinyl chloride, for example, a certain accumulation of charge may occur due to the triboelectric effect; obviously, this too can mask or simulate an actual piezo-effect. Lastly, in the case of application of a load to specimens consisting of chaotically oriented fragments of centrosymmetric crystals there may occur mechanical distortion of the lattice symmetry of individual fragments which may also be accompanied by a false piezoelectric effect.

Nevertheless, it may in general be safely concluded that an investigated substance is piezoelectric if the measuring instrument indicates an activity of approximately the same order of magnitude as that of the standard crystal and a more or less undistorted sine wave is observed on the oscillograph screen. In the case of crystalline grains 1 mm^2 or larger in cross section the indications of the PT-2 piezotester may be regarded as reliable when there is no noticeable crumbling of the grains.

Investigation of the temperature dependence of the dielectric constant using standard tablets

One can determine whether a piezoelectric material possesses ferroelectric properties by investigating the temperature dependence of its dielectric constant. Where no high-quality single crystals of the material are available,

Dependence of the piezoelectric activity of materials as determined on the PT-2 piezotester on the state of the specimens

Material	Condition of specimen	Piezoactivity referred to X-cut quartz plate, db
Lithium sulfate, monohydrate	a) Y-cut plate cut from single crystal	+16, pure sine v.
	b) three flat chips from the same plate	+16, pure sine
	c) fine crystal power prepared from the same plate	-12, distorted sine
	d) tablet compressed of fragments from same plate	-14, distorted sine
Ethylene diamine tartrate	a) Y-cut plate from single crystal	+11, pure sine
	b) three flat chips from the same plate	+11, pure sine
	c) fine crystal powder prepared from the same plate	-4, pure sine
	d) tablet compressed of fragments of the same plate	-15, distorted sine
Potassium tartrate	a) Z-cut plate from a single crystal	+7, pure sine
	b) three flat chips from the same plate	+7, pure sine
	c) fine crystal powder prepared from the same plate	+7, pure sine
	d) tablet compressed of fragments of the same plate	-12, distorted sine

it is expedient to make the measurements on standard tablets compressed at the highest pressure available in the laboratory to insure the maximum effective density of the specimen. In our work we first determined the density of the material using the conventional density bottle procedure and then formed tablets under pressures of up to 100 kg/mm^2 in a tool steel die.

The compacted tablets were weighed and carefully measured. Next the capacitance and resistivity were measured by conventional methods. Finally, the individual tablets were placed in the thermodielecograph (see below) which automatically recorded the temperature variation of the dielectric constant.

The operating principle of the instrument is based on the fact that the capacitive reactance of a capacitor filled with the tested dielectric depends only on its dielectric constant ϵ (at constant frequency). A stabilized voltage is applied to the input of the circuit consisting of the specimen and a low value resistor in series. The voltage drop across the resistor is proportional to the current through the specimen which in turn depends on ϵ. The resistor is connected into the grid circuit of a tube; the associated circuitry amplifies and rectifies the grid signal which is fed to an automatic recording EPP-09 potentiometer.

Description of the thermodielecograph

The TDG-1 thermodielecograph is an instrument that yields an output voltage proportional to the value of ϵ of the connected specimen. The instrument is essentially a resistor coupled amplifier designed about two 6S5 tubes (see Fig.4). At the input the instrument has a voltage divider assembled of resistors and capacitors by means of which its output can be calibrated. The overall voltage amplification factor is 8. The amplifier output signal is matched with the low input resistance of the EPP-09 potentiometer which, as noted above, serves as the recording section of the set-up. The instrument is built on a metal chassis together with its supply rectifier.

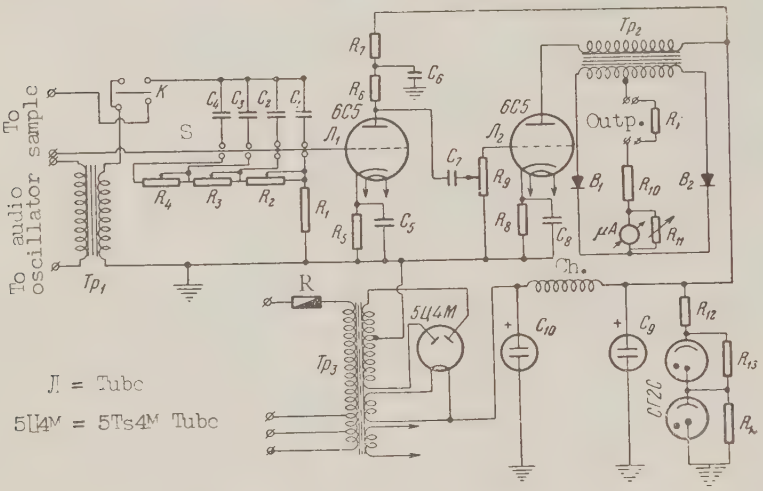

Fig.4. Circuit of the TDG-1 thermodielecograph.

The thermodielecograph circuit consists of an input transformer Tp_1 (see Fig.4), the above-mentioned calibrating voltage divider and two stages of amplification. The voltage divider is made up of the capacitors C_1, C_2, C_3 and C_4 and the resistors R_1, R_2, R_3 and R_4 and the range selector switch S. The double switch K serves to shift the instrument from "Operation" to "Calibration". In addition to the 6S5 (6C5 in the diagram) tubes, the resistor-coupled amplifier comprises the plate circuit resistor R_6 of the first tube, the cathode biasing network R_5C_5 of the first tube, the biasing network R_8C_8 of the second tube, the coupling capacitor C_7, the variable resistor R_9 regulating the output voltage and the output transformer Tp_2. B_1 and B_2 are copper oxide units rectifying the output voltage; μA is a microammeter and R_{11} is a variable ammeter shunt.

Tests showed that with the instrument set for range I, a change of 1 μμf of the capacitance in the test circuit produces a 1 mm displacement on the EPP-09 potentiometer scale (corresponding readings are obtained for the other range settings). In the case of a standard tablet 11.5 mm in diameter (1 cm^2 area) and 2 mm thick having a value of ϵ = 20 at room temperature, the measurement accuracy is 5-7%, which is adequate for the purpose in question, i.e.,

for determining the character of the temperature dependence of the dielectric constant.

The reproducibility of the results is satisfactory. The accuracy of the instrument can be enhanced by increasing the accuracy of calibration of the input voltage divider. The great merit of the thermodielecograph is that it yields a continuous and direct record of the variation of the dielectric constant of the specimen on the potentiometer chart (tape), whereas in photographic recording various intermediate steps or stages are generally involved.

The principal shortcoming of the instrument stems from the fact that its operation is based on the premise that the current through the specimen and grid-resistor is proportional to the dielectric constant of the specimen. This is true only as long as the losses are not great. Actually as the admittance increases, the curve recorded by the instrument gradually changes from a "thermodielecogram" to a curve of the temperature dependence of the resistance. Hence in selecting the operating range and interpreting the results, it is essential to spot check the values of the resistance and capacitance of the specimen at an appropriate high frequency on conventional instruments. We plan to eliminate this shortcoming and improve the instrument further by making provision for recording (on the same potentiometer tape) the thermodielecogram at an audio frequency and a dc resistance curve. This will make it easy to differentiate a true ferroelectric dielectric constant peak from a conductivity jump.

We note that some time after the design and construction of the TDG-1 thermodielecograph we received the report by Triebwasser[11] describing a similar instrument used by said author for investigating the ferroelectric properties of potassium niobate.

In conclusion I wish to express my obligation to L.Z.Rusakov, A.S.Sonin and A.A.Filimonov as well as to S.P.Nedachin and V.A.Verkhovtsev, students of Kiev Polytechnic Institute and Leningrad State University, for their help in the work.

References

1. V.A.Koptsik, Thesis, Moscow State University, 1952.
2. A.R.Ubbelohde & J.Woodward, Proc.Roy.Soc., 185, 448 (1946).
3. W.P.Mason, Phys.Rev., 72, 854 & 976 (1947).
4. J.C.Slater, Chem.Phys. 9, 1633 (1941).
5. G.A.Smolenskii, Dissertation, Academy of Sciences), 1954; Izv. AN SSSR, Ser. fiz., 20, 163 (1956), (Trans. Bulletin, Vol. 20, No.2, p. 149.)
6. W.L.Bond, BSTJ, 22, 145 (1949); K.Egli, Am.Miner., 33, 622 (1948); V.A.Koptsik, Izv. AN SSSR, Ser.fiz., 20, 219 (1956). (Trans. in Bulletin, Vol. 20, No.2, p. 201.)
7. L.Bergmann, Phys.ZS., 36, 31 (1935).
8. A.V.Shubnikov, I.S.Zheludev, V.P.Konstantinova & I.M.Sil'vestrova, Issledovanie p'ezoelektricheskikh tekstur (Investigation of piezoelectric textures) M.-L. 1955.
9. V.A.Koptsik, Izv. AN SSSR, Ser.fiz., 20, 219 (1956). (Trans. in Bulletin Vol.20, No.2, p.201.)
10. N.A.Krotova & V.A.Karasev, Doklady AN SSSR, 92, 607 (1953).
11. S.Triebwasser, Phys.Rev., 101, 993 (1956).

BULLETIN of the Academy of Sciences of the USSR - Physical Series
Vol.21, No.3 - Transactions of the First Conference on Ferroelectricity
(Continued from Vol.21, No.2)

TABLE OF CONTENTS

	Page Orig.	Trans.
Growth and investigation of ferroelectric single crystals - N.S.Novosil'tsev, A.L.Khodakov, M.L.Sholokhovich, E.G.Fesenko & O.P.Kramarov	295	303
Some characteristics of single crystals of $PbTiO_3$ and $(Ba,Pb)TiO_3$ solid solutions - E.G.Fesenko, O.P.Kramarov, A.L.Khodakov & M.L.Sholokhovich	305	314
Structure of the OH band in the spectra of crystals containing hydrogen bonds - A.I.Stekhanov	311	319
On the shape of the potential curve of the hydrogen bond in certain crystals - A.N.Lazarev	322	329
Ferroelectric characteristics of Rochelle salt crystals subjected to radioactive radiation - V.A.Iurin	329	336
On certain characteristics of dielectric hysteresis in Rochelle salt - I.Ia.Eisner	334	341
On microscopic theories of the ferroelectric properties of barium titanate - R.E.Pasynkov	340	346
Ion dynamics and electrostatic energy of ferroelectrics - V.Kh.Kozlovskii	352	358
Towards a theory of orientation ordering in molecular crystals - V.I.Kliachkin	359	364
Towards a theory of hysteresis in $BaTiO_3$ - L.P.Kholodenko	368	372
Relation between the dielectric, piezoelectric and elastic properties of polycrystalline ceramic and those of a single crystal - S.V.Bogdanov, B.M.Vul & A.M.Timonin	374	377
Nonlinear properties of ferroelectrics - B.M.Vul	379	382
Behavior of certain ferroelectrics in strong electric fields - V.A.Bokov	382	385
Piezoelectric properties of barium titanate ceramic with certain additives - S.V.Bogdanov	390	392

Inverse piezoeffect in polycrystalline $BaTiO_3$ under static conditions - G.M.Kovalenko	394	396
A method of determining the piezoelectric coefficient from the radial vibrations of a disc - S.V.Bogdanov & A.M.Timonin	397	399
Pyroelectric and piezoelectric effects in polycrystalline barium titanate - M.S.Kosman & Z.A.Shamro	399	401
Dielectric properties of the niobates and tantalates of bivalent metals - V.A.Isupov	402	404
Investigation of the antiferroelectric properties of some solid solutions containing lead zirconate - N.N.Krainik	411	412
Investigation of $(Ba,Pb)(Ti,Sn)O_3$ solid solutions with ferroelectric properties - I.E.Myl'nikova	423	423
Additional data on solid solutions of the $PbTiO_3$-$SrTiO_3$ system - A.G.Bogdanov & R.A.Khomutetskaia	433	432
Variation of the dielectric constant of polycrystalline ferroelectrics with time under the influence of a mechanical load and a dc electric field - M.S.Lur'e	439	437
Investigation of ultrasonic projectors employing Rochelle salt crystals - K.A.Minaeva	444	442
Stabilized piezoceramic materials - R.E.Pasynkov & V.V.Vinogradov	450	447
Use of ferroelectrics in frequency multipliers - D.M.Kazarnovskii & V.P.Sidorenko	455	452
On equipment for research in the field of ferroelectrics using small specimens - I.S.Rez	466	463

Translated in 1958 by
Columbia Technical Translations
5 Vermont Avenue, White Plains, N.Y.

TRANSACTIONS OF THE FIFTH CONFERENCE ON LUMINESCENCE

(CRYSTAL PHOSPHORS)

Tartu, 25-30 June 1956

(To be continued in Vol. 21, No. 5)

OPENING ADDRESS

- V.L.Levshin

Comrades!

The Fifth Conference on Luminescence convening today is, as you know, devoted to the luminescence of solid crystalline substances. At the Third All-Union Conference in 1951 this branch of luminescence was grouped with that of molecules. Now, however, the greatly increased scope of investigations of the emission processes of crystal phosphors and their technical applications has made it necessary to devote a special conference to the luminescence of crystal phosphors. In fact, in preparing this conference it became clear that the number of reports to be presented was so great that the conference would have to be subdivided into two parallel sections.

In this introductory address I shall merely briefly note some of the more significant advances in the field of crystal phosphors made during the five years that have elapsed since the last conference.

In preparing phosphors with desired properties it is essential to have raw materials of the highest purity; in recent years new methods for obtaining such high purity materials have been developed. Paramount in this respect are chromatographic methods which are capable of yielding very pure reagents. In particular it has now become possible to prepare extremely pure rare-earth elements for use as activators.

Until very recently the chemical composition of crystal phosphors was characterized by giving the composition of the initial batch and the temperature and time of heating. Yet we know that the properties of phosphors are also greatly dependent on a number of other factors involved in their preparation.

Thus numerous studies in recent years have demonstrated the great influence of the atmosphere in which the phosphor is synthesized. It was found that the sintering atmosphere affects the composition of the electron localization levels, the duration of phosphorescence and the maximum light sum of the phosphor. Procedures have been developed for rigorously controlling the ambient atmosphere in synthesis. Synthesis in air has virtually been abandoned in favor of heating under vacuum, in an atmosphere of neutral gases (nitrogen or argon), in a reducing atmosphere (hydrogen or ammonium), in an oxidizing atmosphere (oxygen) leading to the formation of oxides in the lattice, in an atmosphere of hydrogen sulfide capable of eliminating all traces of excess metals and oxidation products, etc.

Recent years have also seen marked development of sublimation techniques, thanks primarily to the work of F.E.Klement and his co-workers. Crystal phosphors obtained by sublimation are characterized by a number of distinctive features that are both of practical value and of interest from the viewpoint of phosphor research.

We now also have interesting new data on the processes occurring in the initial batches during the preparation of crystal phosphors. In this field significant work has been done by Prof.M.A.Konstantinova, who initiated the investigation of the processes of crystal formation by the methods of thermographic analysis, long used in metallurgy. Thermographic procedures make it possible to determine the temperature of the chemical and physico-chemical transformations occurring during heating of the initial mixture. In this manner, M.A.Konstantinova and her co-workers were able to investigate the formation of crystal phosphors, detect transformations of polymorphous compounds from one modification to another and establish the reasons for the instability of some types of crystal phosphors.

In his work, F.D.Klement treats crystal phosphors as mixed crystals in which the activator is one of the components. Phosphors activated by small amounts of activator are therefore regarded as poorly mixed crystals. This approach has enabled Klement to explain certain cases of triboquenching.

The last half decade has also seen the development of new methods of analysis of phosphor products. Worthy of particular note among these is the method of radioactive tracers by means of which one can determine the changes in the proportion of individual components during the process of preparation. This method was used, for example, in the Physical Institute Laboratory of the Academy to study the decrease in the amount of activator during heating of phosphor batches; it was found that in the case of phosphors with heavy metal activators, the change in the amount of activator during heating in most cases does not exceed 5%. In contrast, where volatile compounds are involved the losses may exceed 90% (for example, the loss of antimony in apatite in the presence of an excess of chlorine). The method of radioactive tracers has been used by the French physicists Edmond and Grillot for determining the contamination of phosphor raw materials with copper. The procedure proved to be 1000 times more sensitive than conventional chemical analysis.

Polarographic analysis, employed previously in other fields of analytic chemistry, has proved useful for determining the concentration of activators.

In recent years physical chemists have given special attention to the investigation of the state of luminescence centers and the formation of electron localization levels (electron traps).

The principle of charge compensation has proved of great help in gaining an insight into the mechanism of crystal phosphor formation; according to this principle, the introduced activator ion should not change the neutrality of the crystals. For example, in the case of activation of zinc sulfide by substitution of a monovalent copper or silver ion for a bivalent zinc ion, there must at the same time be introduced either an additional trivalent cation, for example, Al^{3+}, Ga^{3+} or In^{3+} or an ion of one of the rare-earth elements; this additional ion replaces a second zinc cation; or instead a monovalent halide anion may replace a bivalent sulfur ion.

The element introduced for charge compensation does not change the emission spectrum of the main activator but in some cases can play the role of an auxiliary activator yielding a specific additional glow. According to the concepts of the American physicist Williams the activator and coactivator form a pair, the two ions acting together in the quality of a luminescence center.

It follows from the above concepts that the activator ions lodge in most cases at the lattice sites, replacing ions of the host lattice; the difference in charge between the substituting and substituted for ion is compensated for by the introduction of the coactivator.

Part of the activator ions may also be located at the interstital sites. In the case of large interstital distances it is reasonable to assume that activator atoms having small atomic radii can readily penetrate to such sites. In such cases diffusion of the atomic activator into the crystal phosphor may occur at relatively moderate temperatures (400-500°) according to Real and Cherepnev.

Recently A.A.Bundel' obtained interesting results relative to the activating effect of different elements and regarding the role of different fluxes in the preparation of ZnS-type phosphors. Bundel' established that many nonmetals - oxygen, selenium, sulfur and tellurium - can serve as activators of ZnS phosphors. McKeag detected activation by phosphorus; Prener detected the analogous effect of arsenic.

The role of fluxes, while very important, reduces primarily to facilitating crystallization and to shifting the transition point from one crystal modification to another. For example, Bundel' showed that a Cu activated ZnS phosphor can be obtained without any flux by prolonged (64 hour) heating. In addition to facilitating penetration of the activator, the flux has a strong influence on the ratio of the wurzite to sphalerite structures in ZnS crystals.

Bundel' also developed an interesting procedure for introducing activators from the vapor phase; the procedure is suitable both for the introduction of metals and nonmetals. According to the above described concepts a center of luminescence or emission in a crystal phosphor consists of an activator located at the regular or interstital lattice sites with the neighboring cationic or anionic sites modified so as to compensate for the charge of the extraneous activator.

The experimental results obtained by Z.A.Trapeznikova, who studied zinc sulfide luminophors activated by rare-earth ions, lead to an analogous picture of the structure of emitting centers. These phosphors give emission spectra consisting of discrete narrow bands. Despite the fact that the rare-earth elements have a well-shielded electron shell, their emission spectra are highly subject to the influence of the crystal field. Trapeznikova found that the introduction of a second rare-earth element results in a pronounced change in the relative intensity of the band components in the spectra of these phosphors. It follows that the ions of two different rare-earth elements lodge at neighboring lattice sites.

In his recently published theoretical investigations of luminescence centers in crystal phosphors, Williams succeeded in interpreting the structure of the spectrum of thallium employed as an activator in alkali halide crystals.

It must be noted that the above views regarding the structure and location of emitting centers are not shared by all physicists. L.M.Shamovskii, for example, holds to the theory of surface distribution of activators. According to the views of Shamoskii all phosphor crystals fragment into minute blocks, the surfaces of which serve as the locations for the activator. That is, according to Shamovskii, only the activator ions lodging in surface sites are active, while the ions lodged in sites inside the crystal become inactive.

Significant results regarding the structure and location of emitting centers have been obtained by P.P.Feofilov on the basis of polarization studies. He investigated the polarization diagrams of the emission of cubic CaF_2 crystals activated by rare-earth elements and established that the emitters of individual Eu^{3+} ions are oscillators of different types and that the Eu^{3+} ions are oriented along the third order axes of the crystal.

Much attention has been given in recent years to investigation of the kinetics and energy relationships of the luminescence of crystal phosphors, the nature and mechanism of formation of localization levels, the motion of electrons and holes in crystal phosphors, the transfer of energy in the crystal lattice and the transformation of the absorbed energy. Different new techniques and procedures have been developed for studying these problems.

The method of thermal de-excitation or thermostimulated phosphorescence, proposed by Soviet scientists, has proved highly fruitful. As is known, this procedure consists in determining the temperatures corresponding to emission maxima of the previously excited phosphor, i.e., recording the so-called glow curves. Under conditions of uniform heating of the phosphor the emission intensity passes through successive maxima; this effect is connected with thermal release of electrons located at successively deeper energy levels (emptying of deeper traps).

Recently Ch.B.Lushchik and I.A.Perfianovich made significant contributions to the theory relating the emission-maxima temperatures with the energetic depths of the electron localization levels.

Thus the method of thermostimulation provided an effective means for determining the energy positions of the localization levels in different phosphors and the degree of their filling by electrons. Analyses of the thermostiumlated phosphorescence curves for phosphors of different composition, carried out by Soviet and foreign scientists, showed that the presence of individual groups of local levels is connected with the introduction of definite ingredients into the initial batch.

At first very high hopes were placed on the thermal de-excitation method. More careful studies showed, however, that by means of this procedure one cannot obtain a complete characteristic of the state of the phosphor and establish the depth of the localization levels and the degree of their occupation. It was found that very deep levels may not be evinced in the glow curves as a result of thermoquenching. Radiationless transitions occur from these deep traps. They can, however, be investigated in other ways. They can, for example, be detected by flashing of the phosphor under the influence of infrared light after complete decay of the normal phosphorescence. Energetically deeper levels are de-excited by rays of shorter wavelengths.

In addition to direct detection of these levels by infrared stimulated flashing, their existence can be noted by studying the absorption of the phosphors inasmuch as the electrons localized at the deep levels absorb infrared and sometimes shorter rays. Thus the additional absorption spectra yielded by excited phosphors make it possible to judge the depth of the localization levels and their degree of occupation by electrons.

Another way of investigating the state of crystal phosphors is through measurements of their electric properties. The presence of localized electrons in a crystal phosphor changes its dielectric constant. In the case of optical release of the electrons from local levels, the electric conductivity of the phosphor increases. Thus measurement of the electric properties of phosphors under illumination can be used for determining magnitude and distribution of the light sums stored by the phosphor.

It is usually expedient to use different experimental methods and procedures, for often they are not equivalent, but on the contrary complement each other. Thus the methods of investigating the absorption and the dielectric constant are connected with the presence of electrons on localization levels. The brightness of the infrared stimulated flashing and the increase in electric conductivity are also connected with the total number of localized electrons; these effects, however, are produced by electrons which have already left the localization levels as a result of the influence of the stimulating light on the phosphor. Finally, the thermal de-excitation (glow) curves indicate the number of electrons present in the excited phosphor at different localization levels but do not fully give the total number of these electrons inasmuch as part of the least electrons may undergo radiationless recombination. Thus the state of the excited phosphor can be fully investigated only by means of all these different procedures in conjunction.

As is known an important characteristic of phosphors is the shape of the luminescence growth and decay curve. Until recently accurate measurements in the 10^{-6} to 10^{-7} sec range presented great experimental difficulties. N.A. Tolstoi and his co-workers have now developed instruments which make it relatively easy to investigate this hitherto inaccessible time range. The characteristics of cuprous oxide, some platinocyanides and other compounds have already been investigated. By means of these new instruments it is possible to investigate not only the luminescence but also the photoconductivity. It

should also be noted that A.M.Bonch-Bruevich and his colleagues built a new very advanced type of fluorometer for investigating emission with a persistance of 10^{-9}-10^{-10} sec.

I will now go on to a description of the results obtained in the field of investigation of crystal phosphors.

In recent years there have been a great many studies devoted to clarifying the nature of individual localization levels (Bube, Hoogenstraten, Zhukova, Tunitskaia and others). Thus, for example, in investigating Cu and Co activated zinc sulfide phosphors there were detected individual levels associated with the zinc, copper and cobalt activators. These levels are distinguished from each other by increasing depth. In addition, there were identified levels associated with the anions: oxygen, sulfur and combinations of these with the activator atoms.

Usually each newly introduced activator forms a separate system of levels. In some cases, however, it may be hypothesized that the second activator lodges near the first and produces a marked change in the position of the initial localization level and sometimes in the storage capacity of the phosphor.

The fact that the electron localization levels depend on the introduction of an activator shows that an activator-emission center can at the same time give rise to an electron localization center or trap.

There have been observed cases when in two-activator phosphors the electrons localized at local levels produced by one of the activators recombine only with this activator. It is difficult to see what role is played by the conduction band in these cases. For example, the emission of Mn in the case of de-excitation of the third deep system of Mn levels in ZnS:Mn phosphors apparently belongs in this category.

Recently it was discovered that there is a difference between the behavior of electrons freed optically, i.e., due to absorption of light, and the behavior of thermal electrons freed as the result of thermal collisions. The former have a much higher energy than the latter. Experiments show that the optical electrons not infrequently undergo localization (retrapping), whereas the thermal electrons, on the contrary, after being released from the trapping levels, immediately recombine. Analogous results for a number of different phosphors, proving the low capacity of thermal electrons for repeated localization, have been obtained by N.V.Zhukova and, subsequently, by V.F.Tunitskaia and myself. An extensive investigation by V.V.Antonov-Romanovskii was devoted to this problem. Siui Siui-iun in the Luminescence Laboratory of the Physical Institute of the USSR Academy of Sciences carried out determinations of the ratio of the cross sections of trapping levels and recombination levels in ZnS:Cu:Co phosphor prepared by heating in an atmosphere of nitrogen. He found that in this phosphor which has only two systems of localization levels the probability of retrapping for the thermal electrons is very much lower (1:10 to 1:100) than the probability of recombination.

Our earlier concepts regarding the motion of electrons in the conduction band have recently been supplemented and amplified by analysis of the motion of holes in the valence band.

V.V.Antonov-Romanovskii, L.A.Vinokurov, M.V.Fok and others have recently developed new theoretical concepts for interpreting quenching effects in ZnS:Cu:Co phosphors.

Much attention has also been devoted to the problem of energy transfer in the crystal lattice. Recent years have seen a number of investigations indicating strong interaction of activators jointly introduced into the lattice. Such for example are europium and samarium, manganese and bismuth and a number of other pairs of interacting elements. The incident light energy

is absorbed by one of the centers (activators) and then transferred in some manner to the other. As a result of this energy transfer, the spectrum of the main activator is intensified. The coefficient of transfer apparently depends on the properties of the activator elements and their separation.

Of particular interest is the transfer of energy in scintillator crystals under excitation by fast particles. Here the absorption occurs in the host lattice. Nevertheless, as Bediaev, Galanin and Morgenshtern have shown, energy transfer to the centers occurs with high efficiency over distances of several tens of lattice constants.

Recently so-called exciton energy transfer has aroused considerable interest. Ia.I.Frenkel' showed that the crystal lattice having absorbed energy may go over into an excited state without releasing electrons into the conduction band. Inasmuch as in exciton excitation the electrons do not go over into the conduction band, exciton excitation is not accompanied by the appearance of photoconductivity. However, the excitation points can move in the crystal phosphor. When a migrating exciton approaches an emission center, it may transfer its energy to the center. The absorption leading to the appearance of the excitons is discrete; the associated absorption spectra recorded at liquid hydrogen and helium temperatures consist of series of discrete narrow bands. Similar absorption spectra have been observed by E.F.Gross and a number of scientists abroad.

Earlier similar narrow absorption bands were detected by A.N.Kokhanenko in the spectra of sublimated halide salts; at the time, however, they were attributed a different origin.

The luminescence efficiency of crystal phosphors, as we know, in most cases is appreciably less than unity. The reduced yield or loss is due to a number of different quenching processes such as inactive absorption by the crystal lattice, absorption of localized electrons (frequently leading to radiationless transitions), different forms of thermoquenching, etc. Recently a considerable amount of research on problems having to do with efficiency of phosphors has been made by M.N.Alentsev who showed that in principle Vavilov's law regarding the relation between the luminescence yield and the wavelength of the exciting light is valid for crystal phosphors as well. There are, however, certain complications in the case of crystal phosphors. For one thing, the character of absorption in crystal phosphors may be different for different frequencies of the exciting light, that is, there may be absorption by the regular lattice, absorption by lattice defects, absorption by the activator, exciton absorption and so on. Surely, the kinetics of the excitation-emission process are different for each of these different types of absorption which would naturally affect the efficiency.

In some cases, too, the efficiency is reduced by de-excitation under the influence of the exciting light. In such cases the efficiency should be investigated at low incident light intensities, i.e., at intensities not producing any noticeable de-excitation. V.V.Antonov-Romanovskii showed that in the case of optical de-excitation the efficiency must be reduced inasmuch as the release of each electron requires the expenditure of at least two energy quanta, namely, one photon for the initial excitation and one photon for releasing the electron from the localization level (trap).

It is usually assumed that the emission of crystal phosphors under conditions of constant excitation and in the absence of chemical changes of the phosphor is independent of the medium surrounding the phosphor. Actually, this is not always so. A.N.Terenin and K.V.Tagantsev have shown that in the case of zinc oxide and certain other luminophors the adsorption on the crystal surface of electronegative molecules from the surrounding medium leads to reversible changes in the luminescent ability of the crystal. The effect is

explained by a reduction in the rate of recombination due to capture of electrons by the adsorbed electronegative molecules. These experiments are interesting not only from the theoretical viewpoint but also from the standpoint of practical applications.

Before concluding I would like to sketch a picture of the process of luminescence decay that emerges from a juxtaposition of the decay curves for crystal phosphors with the thermal glow curves.

Initially when the phosphor is exposed to exciting light electrons are detached from the crystal lattice or from the activator atoms; these electrons move to the conduction band and from there are localized on trapping levels of different depths. We are omitting here from consideration the case of exciton excitation which has its own distinctive characteristics. The filling of the different levels is generally not uniform. Filling of the shallower levels is hampered by their rapid emptying due to thermal release of the electrons. Hence in most cases the deeper levels are filled first and an appreciable degree of filling of the shallower levels is attained only at high intensities of the exciting light.

In the case of pulsed excitation, however, one can sometimes observe the opposite picture: at low temperatures precluding thermal release of the trapped electrons, the shallower levels may fill before the deeper ones. Thus the rate and order of filling of the levels depends both on the character of the levels and on the conditions of excitation.

After cessation of excitation there occurs a rapid release of all the electrons whose levels correspond to the maxima in the thermal de-excitation (glow) curves lying below the temperature of the experiment. Hence at the beginning of phosphorescence there is an extremely rapid decay of luminance associated with the release of electrons from the several systems of shallowest levels; following this we have the emptying of the deeper levels which in principle occurs according to the exponential law for each system of levels inasmuch as retrapping of thermal electrons is relatively rare. Due to the wide dispersal of the trapping levels in depth, however, a number of levels in a fairly wide energy range are emptied more or less simultaneously, which accounts for the nonexponential decay observed in many cases. As the luminescence decays the role of the deeper levels becomes increasingly more important and the rate of decay falls off sharply inasmuch as thermal emptying of the deep levels proceeds very slowly at room temperature.

Next I would like to mention briefly a number of new types of phosphors developed in recent years.

First, it may be noted that during the last two years much attention has been given to electroluminescence. Electroluminescence, of course, is not new. Different forms of electroluminescence have been discovered and reported by Losev, Gudden, Pohl and Destriau. The last has engaged in investigations of the process over the past twenty years. However, only within the last two years have there been found possibilities for practical utilization of electroluminescence with the result that the number of investigations devoted to the subject has greatly increased.

A special meeting will be devoted to electroluminescence. Here I shall only mention that phosphors yielding electroluminescence, as well as electrophotoluminescence, must possess certain specific attributes. Several types of such crystal phosphors have been developed both abroad and here in the Soviet Union.

A number of new luminophors for "fluorescent" lamps have been developed within the past few years. Among them are luminophors "correcting" the red part of the spectrum of "fluorescent" lamps, for example, a two-activator

potassium phosphate phosphor. There have also been developed some new phosphors with better spectral characteristics for street lamps; these include arsenates, germanates and lithium-strontium-barium silicate with cerium and manganese, characterized by strong emission in the red region.

Finally there has been a significant advance in preparing constant luminance self-exciting coatings. Until recently primarily α-emitters (radium, radiothorium and mesothorium) were used as the radioactive exciting agents for phosphors. Recently here in the USSR and abroad active β-emitters have come into use for this purpose. These have a number of advantages. For one thing β-radiation does not produce disruptions of the ZnS lattice so that the new preparations have a long service life and can be made very bright. There have also been developed new scintillating phosphors for purposes of detecting and measuring hard radiation and the emission of radioactive sources.

Despite the great progress made in the field of crystal phorphors, there still remain many unsolved problems calling for intensified research. It is to be hoped that the present Conference will make some contribution towards the eventual solution of these problems.

CERTAIN CHARACTERISTICS OF SUBLIMATE PHOSPHORS AND METHODS OF PREPARING THEM (Abstract*)

- F.D.Klement

The report summarizes the results of the research carried out in the laboratory headed by the writer on sublimate phosphors. The report gives certain new data both on the methods of preparation and regarding the properties of phosphor sublimates as well as a general characterization of this class of crystal phosphors.

The report comprises an historical sketch of research in the field, a description of the structural and technical characteristics of sublimate phosphors (extreme thinness of the sublimated layers, high resolving power of the phosphors, low dispersion) and the technical applications based on these properties (determination of absorption coefficients and spectra, preparation of multiple layer and multiple color screens, control of crystal structure) and evaluation of the sublimation procedure for investigating processes involved in the formation and preparation of crystal phosphors in general (a correlation is established between the temperature conditions of formation and the crystallochemical parameters of the phosphor components; the diffusion mechanism involved in the formation of phosphors is considered in detail), an exposition of the influence of the gaseous medium on the processes of formation of sublimate phosphors and an attempt to interpret the mechanism of this effect.

Tartu State University

*Complete report in Optika i spektroskopiia, 1, 571 (1956).

NEW RESULTS IN THE FIELD OF PHOSPHORESCENCE RESEARCH

- V.V.Antonov-Romanovskii

Research in the field of the luminescence of crystal phosphors over the five years elapsed since the Third All-Union Conference on Luminescence is characterized by a number of significant achievements in the realms of both experiment and theory.

We shall review here the more important results obtained both abroad and here in the Soviet Union. From the standpoint of better insight into the nature of the processes occurring in crystal phosphors one may distinguish three principal directions of investigation: clarification of the nature of emission and trapping centers, study of the kinetics of luminescence and investigation of the energy balance.

Where the nature of luminescence centers is concerned one should first note the achievements of Williams[1]. Williams was the first to carry out a theoretical calculation of the activator absorption and emission band spectra for the case of KCl:Tl. His results proved to be in good agreement with experiment. It may therefore be asserted that the luminescence centers in KCl:Tl are Tl^+ ions located at the cation sites and perturbed by the field of the neighboring ions. Similar work is now being carried out in the Soviet Union by Adamov, Petrashen' and Potekhina at Leningrad University and by Krivoglaz in Kiev. Pekar, and subsequently Krivoglaz[2], carried out a general theoretical analysis of the shape and temperature dependence of the absorption and luminescence bands of impurity centers. The theoretical results are in agreement with experimental data.

As for experimental investigations of luminescence centers one might mention the following among the more important recent results.

It is known that the introduction of an activator into the host lattice frequently also leads to the formation of electron traps. These traps can apparently be identified with luminescence centers as recently shown in a joint contribution by Levshina, Morgenshtern, Trapeznikov and the writer[3] for SrS:Ce:Sm and SrS:Eu:Sm, and later by Lushchik[4] for KCl:Tl phosphor. On the other hand, there are known to be cases[5] when the capture centers trapping electrons can themselves become luminescence centers. Thus the former distinction between luminescence centers and trapping centers disappears.

The very fact that the additional absorption that arises as the result of excitation commonly exhibits structure indicates that the electron and hole traps as well as luminescence centers possess excitation levels. In alkali halide crystals (details of the work carried out in this field in Tartu will be reported on later at this Conference), we can evaluate the energy gap from the lower edge of the free band to the excitation level of the trap capturing electrons by a very interesting procedure which differs from that employed sometime ago in Pohl's laboratory in the case of F-centers.

Another interesting approach towards an understanding of the nature of luminescence centers is typified by investigations devoted to determining the valence state of the activator and the structure of luminescence centers. This approach is based essentially on investigating the chemical nature of centers of luminescence and capture. A distinctive feature of the chemical reactions leading to the formation of phosphors is that such reactions usually take place at a high temperature when both anionic and cationic vacancies can take part in the process. In interpreting the experimental results many authors have successfully made use of the principle of compensation[6,7] or even of microcompensation of charges and to a lesser extent of the principle of microcompensation of volumes[7].

In this respect the work of Kröger's[7] school is significant; in the contribution of Kröger and his associates the chemical state of the luminescence and trapping centers is related with the optical and electrical properties of the phosphor. Calculations of the number of different donor and acceptor levels are based on thermodynamic considerations and have yielded satisfactory agreement with experimental data (in their calculations it was assumed that the equilibrium state of the phosphor obtaining at the high synthesis temperature was frozen in by rapid cooling).

Recently, a new and highly promising method has been applied to the investigation of luminescence centers; this is the method of paramagnetic resonance and measurements of the magnetic susceptibility by means of which one can in a number of cases determine the valence state of the activator, coactivator, etc. (reports on this subject will be presented to the Conference by other speakers).

One might note another approach which appears to be very promising, namely, the use of high energy particles and artificial radioactivity for investigating the nature of luminescence centers. This, of course, should not be confused with conventional radioactive tracer procedures. Thus, for example, fast neutrons can shift luminophor ions from the regular sites to interstital sites; hence on the basis of properly designed experiments it should be possible to draw certain definite conclusions regarding the nature of luminescence centers in pure, i.e., impurity free, crystalline substances[9].

Another possibility - the creation of extraneous luminescence centers - follows from the comments of Williams[10] on the report presented by Grillot at the International Conference on Luminescence in Bristol (April 1954). Williams reported that Prener in order to determine the controversial nature of the activator in ZnS:Cu phosphor prepared pure ZnS containing 10^{-30} mole percent radioactive Zn^{65}. This isotope, as a result of 240 day K-capture, transforms to Cu. Inasmuch as in this nuclear reaction the recoil energy is insufficient to displace the Cu^{+} ion, it remains at the cationic site. Unfortunately, we have no further details on these promising experiments at present and do not know whether they have been continued to the point of yielding definitive information on the nature of the luminescence centers involved.

We might also note two approaches to the investigation of luminescence centers that have been developed primarily in the Soviet Union. The first, initiated by Vavilov, is based on the fact that the luminescence of elementary emitter is polarized and that from the polarization one can draw certain conclusions regarding the character of the emitters (electric or magnetic dipoles, quadrupoles or the like) and that in the case of cubic crystals one can form an idea of the orientation in them of anisotropic centers as was shown by Feofilov in an interesting report presented at the Fourth Conference on Luminescence. The second approach is based on the use of rare-earth elements as activators; the line spectrum of the luminescence of these elements is highly sensitive to the "environment" of the activator (a report by Trapeznikov, Trofimov and Feofilov on the subject will be presented at this Conference).

Each of the above mentioned methods of studying the nature of luminescence centers has its advantages and disadvantages.

The method of theoretical calculation of the centers of luminescence or capture, in view of the complexity of the calculations, is at present applicable only to simple systems, for example, to luminescence centers in KCl:Tl type phosphors and F-centers in alkali halide crystals. Nevertheless, if the theoretical results are found to agree well with the experimental data, it may be concluded that the assumptions regarding the character of luminescence centers upon which the calculations are founded are valid.

In more complicated cases, when theoretical calculations are difficult, one can legitimately speak only of the structure of luminescence or trapping centers, i.e., of the elementary formations of which the centers are composed. A complicated center may be formed, for example, when the valence state of the activator is such that it disturbs the neutrality of the lattice. Then in accord with the principle of charge compensation (or more accurately of microcompensation of charge), next to the activator there is incorporated into the lattice a coactivator ion, or, in some cases, a vacant lattice site may play the role of coactivator. The method of paramagnetic resonance particularly when used at low temperatures may in certain cases make it possible to determine the valence state of the introduced impurities. If the center is asymmetric its orientation can be determined by the polarization method.

Doubtless other methods can also contribute to the solution of our problem. Doubtless only through skillful use of various procedures in proper conjunction can we arrive at a definitive and unambiguous picture of the structure of any given type of center. So far there have been no such comprehensive investigations and this may explain why we still have such heated discussions regarding the nature of luminescence centers even in such a classical phosphor as ZnS:Cu.

Before going on to a different topic I would like to make a few remarks on the problem of the nature of luminescence centers.

It is known[3] that in alkaline earth phosphors with two rare earth activators, for example, Ce and Sm, these lodge next to each other in the crystal lattice. This may be explained as follows. The Ce and Sm enter into the bivalent lattice in the trivalent state. In accordance with the principle of charge compensation, in the absence of a coactivator there must be formed a monovalent cationic site for each two rare earth ions introduced into the lattice. In view of the principle of microcompensation of charge this vacant site should be located in the immediate proximity of the two rare earth ions.

Sometime ago Pringsheim[11] suggested that in the case of excitation of phosphors (for example, alkaline earth phosphors) with a trivalent rare earth activator - let us designate this by A^{3+} - the latter cannot be further ionized, for the ionization energy of a trivalent rare earth ion is too high. Instead, only a neighboring (perturbed) sulphur ion is ionized. Hence recombination occurs next to but not in the luminescence centers which only fluoresce at the expense of the energy released by this recombination. The paramagnetic method, being a quantitative one, could throw light on the problem. If the rare earth element is capable of additional ionization, then as a result of excitation the concentration of A^{3+} ions should decrease and at the same time there should appear a certain number of A^{4+} centers, which should be detectable by paramagnetic resonance. If, in addition, the A^{3+} ions are capable of capturing electrons there should also be formed detectable A^{2+} ions.

Although the method of determining the nature of elementary emitters and their orientation in the case of anisotropy of luminescence centers has been successfully used only for fluorescence so far, it can also undoubtedly be utilized for recombination luminescence in cases when the excitation energy is absorbed directly by the center and there is no energy transfer from one center to another (via a lower band or by resonance).

One last remark, while I am on the subject of centers: we still know next to nothing regarding the nature of so-called "edge emission" evinced by pure host materials and appearing at low temperatures (Arkhangel'skaia and Feofilov will present a report on the subject).

Thus it may be noted that research on the nature of luminescence centers has now only reached the stage where we are beginning to obtain conclusive

results. It may be hoped therefore that in the near future we will see significant developments in this field which might be called central to the luminescence of crystal phosphors inasmuch as in it we are concerned with the very formations in which the processes of fluorescence and phosphorescence occur.

Let us now turn to the kinetics of phosphorescence.

It may be noted that the first quantitative investigations of fluorescence began precisely with the kinetics of the process when in the latter half of the nineteenth century Becquerel invented the phosphoroscope and began to use photometry for investigating decay curves.

The kinetics of recombination, as we know, is determined by concentration factors, the depth of the electron and hole traps, and the cross sections for capture and recombination. Whereas the concentration factors - N the activator concentration, n the concentration of ionized centers or localized electrons and in some cases ν the concentration of traps - can be evaluated at least roughly and the depth ϵ of the electron traps can be determined by the method of thermostimulated emission, we have had until recently little reliable quantitative data on the cross sections for recombination σ and capture σ or their ratio σ_o/σ, which is the important factor in kinetics.

Investigations carried out by Siui-Siui-iun[12] at the Physics Institute of the Academy of Sciences on ZnS:Cu:Co phosphor showed that for thermal electrons at room temperature the ratio $\sigma_o/\sigma \approx 100$, while for optical electrons $\sigma_o/\sigma \approx 1$, which is in accord with the diffusion theory of phosphorescence[13], assuming that the ionized luminescence centers carry an excess positive charge while the traps are neutral. Anikina[14], working by another procedure on the phosphor SrS:Eu:Sm also found that for optical electrons $\sigma_o/\sigma \approx 1$. Shchukin[15], however, obtained a much lower value of the ratio σ_o/σ for thermal electrons in KCl:Tl, namely, ~ 10. This divergence was explained by the fact that the electrons are localized not at a vacant anionic site (excess positive charge) but on a pair of neighboring vacancies (cationic and anionic) which has the attributes of a dipole and which proved to be a more stable formation than a simple vacancy (theoretical calculations in this case yield $\sigma_o/\sigma \approx 10$). After trapping an electron, the pair quickly dissociates into a cationic vacancy and an ordinary DeBoer F-center. The effective cross sections were also determined by Lushchik and others by the method of thermal bleaching (the procedure will be described in another report at this Conference). These investigations have provided a basis for moving forward from phenomenological kinetics to a quantitative theory and where theoretical analyses are concerned have placed definite limits on the arbitrary choice of values of σ_o/σ.[16]

We note that in the kinetics of phosphorescence of significant quantities are not only σ_o and σ but also the product $\sigma_o n$ and $\sigma\nu$ which have the meaning of quantities proportional to the total probability of recombination and trapping, respectively. The disputed question of which probability, that of recombination or that of retrapping (or in other words whether the ratio $\sigma_o n/\sigma$ is greater or smaller than unity) can now be resolved by direct measurements of the ratio $\sigma_o n/\sigma\nu$. Experimental data[17] for thermal electrons show, for example, that as a rule for ZnS phosphors $\sigma_o n/\sigma\nu < 1$, while for alkali halide phosphors (provided the excitation is not very weak) $\sigma_o n/\sigma\nu > 1$.

It may be noted that whereas in the field of semiconductors the positive hole has long been recognized as a useful entity, in the kinetics of phosphorescence the hole became "an equal partner" of the electron comparatively recently. In fact, some "inequality" in this sense still persists in that usually emission is associated with recombination of free electrons with ionized centers, while recombination of free holes with localized electrons is generally assumed to lead to radiationless transitions or at most to ionization of

luminescence centers. There have, however, recently appeared experimental proofs of the fact that recombination of free holes with the electrons at the ground level of the activator may lead to emission (theoretically the probability appears trivial). Trapeznikov and the writer showed for the case of ZnS:Sm:Cu phosphor that the emission spectrum of Sm^{3+} consists of two groups of lines one of which, like the green band of Cu, is probably associated with recombination of thermal electrons and the other with recombination of holes[18] (see abstract in the next issue of the Bulletin).

There have also recently been obtained interesting results as regards techniques of determining the energy of localization of electrons and holes. Not long ago Lushchik (see article by Lushchik in the present issue of the Bulletin) developed a thermal bleaching procedure which is no less effective than the thermal de-excitation method and in some cases may be superior to the latter. Particularly interesting results may be obtained by simultaneous application of both these techniques. By means of these procedures one can not only determine the depth of electron traps but gain certain information regarding the kinetics and nature of these traps. For example, it now appears possible to resolve the additional absorption spectrum appearing incident to excitation into two parts: one associated with electrons and the other associated with holes. These procedures can also be used to obtain information on retrapping, etc.

Recently Bohun and Lepper, working independently, discovered a new effect[19]: a close correlation between the curves characterizing the variation in thermal emission and the curves characterizing thermal de-excitation (glow curves)*. It was found that in the case of uniform heating of a phosphor the temperatures of the thermoemission peaks correspond to the temperatures of the thermal de-excitation peaks. This indicates that thermoemission is due to electrons located in the conduction band. This phenomenon, as Lushchik has noted, can be utilized in conjunction with the thermal bleaching method for determining the nature of the additional absorption peaks, i.e., for determining whether they are electron or hole peaks inasmuch as holes cannot produce thermoemission.

Some new results have also been obtained in the thoroughly explored, almost classical field of the kinetics of phosphorescence decay. Eliashberg[21] showed that quantitative calculations of the luminescence decay of a phosphor with two trapping levels leads to curves of attenuation of brightness in time whose shape, particularly at the beginning, differs radically from a second order hyperbola and in some cases is highly unique. For example the decay curves with an equal relative but a different absolute filling of the traps may at first converge, then diverge (!) and then finally again converge (these results will be described in a report to be presented at this Conference).

Let us now turn to the question of energy balance.

In the case of phosphorescence this question is very complex. The reason for this is that in the case of recombination luminescence the yield q does not, as a rule, depend solely on the intensity E of the exciting light, i.e., is no longer a constant of the material. Hence in the case of phosphorescence the spectral dependence of q is more complex than in the case of fluorescence.

Alentsev, Vinokurov and the writer[22] showed that for the phosphor ZnS:Cu the output q is constant over an appreciable range of medium values of E; that

---

*Just as some time ago Garlick[20] established a correlation between the thermostimulated emission curve and the curve characterizing the variation in electric conductivity during heating of an excited phosphor.

is, that there is an extensive plateau above and below which q falls off. The decrease of q on the side of small values of E is explained by external quenching, while the decrease on the side of large values of E is due to the bleaching influence of the exciting light. Analogous investigations carried out by Vinokurov and the writer[23] on ZnS:Cu at different temperatures led to the conclusion that the decrease in efficiency as a result of introduction of Co into ZnS:Cu is due to the fact that the presence of Co gives rise to deep electron traps. This in turn, due to reduction of the probability of thermal ejection of localized electrons, leads to a relative increase in number of radiationless recombinations of these electrons with free holes. It was shown that in the region of the plateau the kinetics of the holes and of the electrons obeys the simple bimolecular reaction scheme. As a result of the experiments it also proved feasible to evaluate the localization energy for electrons and holes.

The presence of the plateau indicates that in this region, in which there are no auxiliary factors depressing the yield, the efficiency $q = q_o$ may be regarded as a constant of the material. Alentsev used this circumstance to determine the dependence of q_o on the wavelength of the exciting light for the phosphor ZnS:Cu; he also determined this dependence by means of another procedure (extrapolation) for ZnS. He found that in this case the spectral dependence of q is relatively simple and susceptible of interpretation. In particular it may be concluded that here the law for the spectral dependence of the output established by Vavilov for fluorescence is valid. We feel that this result for phosphorescence is significant.

Very recently Vinokurov and Fok[25] succeeded in showing for the phosphors ZnS:Cu and ZnS:Cu:Co that some of the regularities of the decrease in efficiency with decrease in intensity of the exciting light can be explained on the basis of the mechanism of external quenching. This last differs from that usually postulated in that account is taken of the possibility of retrapping of holes. Quenching of the phosphorescence of ZnS:Cu:Co and ZnS:Cu:Ni by infrared light can also be interpreted with the aid of this mechanism (a report on this subject will be presented at this Conference).

Although the above results are not necessarily general inasmuch as only a few phosphors of one type (ZnS) were investigated so far, they are of undoubted interest in that at least they indicate a promising approach to the problem of energy balance in phosphors.

A question intimately related with yield is that of sensitization of luminescence when the energy absorbed outside the luminescence centers is still transferred to them. The most common case of sensitized luminescence is observed when the exciting energy is absorbed by the host material of the phosphor. In this connection it is worth mentioning the results obtained by Shchukin[26]. Although Shchukin carried out a comparison of the photoexcitation of KCl:Tl in the absorption band of the activator with the excitation by γ- and x-rays, it must be borne in mind that this hard excitation is essentially similar to excitation by short ultraviolet rays inasmuch as in both cases the exciting energy is absorbed by the host material.

The quantum efficiency q of recombination luminescence may be represented in the form of the product $\eta\rho$, where η is the efficiency of ionization of the phosphor material (ratio of the number of ionization events to the total number of absorbed photons) and ρ is the efficiency of emission of the Tl^+ ions in case of electron recombination, i.e., the ratio of the number n_p of emitted photons to the number $n_e = \Delta n_A + \Delta n_s$ of electrons entering (during the same interval) into recombination with both ionized luminescence centers (Δn_A) and with holes in the host material (Δn_s). Hence ρ characterizes the loss occurring in the phosphor after ionization.

Shchukin investigated the magnitude of ρ. In the absence of sensitization one can write

$$\rho = \frac{n_p}{n_e} = \frac{\alpha \Delta n_A}{\Delta n_A + \Delta n_S} = \frac{\alpha}{1 + \frac{\Delta n_S}{\Delta n_A}},$$

where α is the probability of radiative transitions in the luminescence centers. Inasmuch as the deepest lying trapping levels in KCl:Tl are the F-levels, after the phosphor has been kept in the dark for a prolonged period the problem of evaluating ρ reduces to finding the ratio of the number of emitted photons to the number of destroyed F-centers (the number of these can be determined from absorption measurements).

For the case of photoexcitation in the absorption band of the activator it was found that

$$\rho_{photo} \approx 0.4.$$

Inasmuch as here absorption in the host material can be neglected and the holes do not leave the activator level, $\Delta n_S/\Delta n_A \ll 1$ and we find that the probability of radiative transitions in a luminescence center is $\alpha \approx \rho_{photo} \approx 0.4$. Smaller values of ρ, namely $\rho^{\gamma} \approx 0.16$ and $\rho^{x} \approx 0.1$ are obtained for the cases of excitation by γ- and x-rays.

In view of the fact, however, that γ- and x-rays are not characterized by selective absorption and the fact that the activator concentration is small it may be assumed that $(\Delta n_S/\Delta n_A)_{theo}$ is of the order of 10^4 and then

$$\rho^{\gamma}_{theo} \approx \rho^{x}_{theo} \approx 4 \cdot 10^{-5}.$$

The divergence between the experimental and theoretical values of ρ indicates the presence of sensitization.

One can envision two cases of sensitization. The first encompasses processes that are connected with reduction of the ratio $\Delta n_S/\Delta n_A$ relative to its theoretical value ($\sim 10^4$), i.e., as a result of sensitization, the ionization of the luminescence centers is enhanced (Δn_A increases, while Δn_S decreases). The second case is not associated with changes in the ratio $\Delta n_S/\Delta n_A$. The transfer of energy to the activator occurs not at the instant of excitation of the phosphor but later when the energy, released by recombination of a freed F-electron with a hole, is transferred by resonance to the Tl^+ ion, which then fluoresces. It proved feasible to determine from experiment which of the two cases of sensitization predominates. It was possible to evaluate $\Delta n_S/\Delta n_A$ directly from the observed decrease in activator absorption as the result of excitation. It was found that $\Delta n_S/\Delta n_A \approx 0.4$. From the formula

$$\rho = \frac{\alpha}{1 + \frac{\Delta n_S}{\Delta n_A}},$$

which is valid for the first case of sensitization, we find that with $\rho^{\gamma} \approx 0.16$ and $\rho^{x} \approx 0.1$ on the average $\Delta n_S/\Delta n_A \approx 2$.

For the second case, as was noted above, the value of $\Delta n_S/\Delta n_A$ should be of the order of 10^4. It follows therefore that in reality the first case obtains.

The above outlined results are indicative of the great progress made in the field of phosphorescence kinetics and the allied field of luminescence efficiency. This can be attributed to a number of factors: the stimulating influence of the increased practical use of luminophors, concise formulation

of the problems involved, the fact that theory was not forced on experiment or invented merely to explain a given result but, on the contrary, was based on experimental data (the method of "cross examination") and the availability of improved techniques for quantitative measurement of absorption.

It may be recalled that in his time S.I.Vavilov frequently emphasized the necessity of such measurements. Now these have been realized particularly as regards phosphors that can be prepared in the form of large single crystals.

The experimental and theoretical results obtained so far do not solve all our problems: there is still much that is unclear and many questions still to be resolved. Let us mention a few of these.

One difficult question is that posed by the greater-than-linear (sometimes quadratic) dependence of the initial rise of photoconductivity of phosphors, an effect noted by Tolstoi. The inconsistency between this kind of rise in conductivity and the common concept concerning recombination kinetics led Tolstoi to propose a unique two-step excitation mechanism (this, too, will be discussed in a report to be presented at the present Conference).

There is much that still remains unclear regarding the nature of the additional absorption appearing incident to excitation of SrS·CoS:Ce:Sm phosphors[27]. If it be assumed that absorption is due directly to the localized electron or ionized centers there is obtained the absurd result that the oscillator strength is of the order of 100.

The experimentally observed (by Siui Siui-iun) temperature dependence of the recombination to capture cross section ratio σ_o/σ prove useful in analyzing the kinetics of electroluminescence inasmuch as application of an electric field leads to appreciable increase of the electron temperature.

As regards the effective cross section for trapping of an electron by a center that is essentially a dipole (this cross section, as Shchukin showed, is relatively large), it may be noted that the same cross section should obtain for capture of a hole by the same center-dipole. This follows from the complete symmetry of the system free electron-dipole-free hole. It follows that if trapping or luminescence centers are complex formations whose elementary components carry excess charges, both positive and negative, such formations will necessarily attract both electrons and holes. This concept or model of centers should be of interest both from the standpoint of fluorescence kinetics and from that of the theory of luminescence centers.

It must be noted that many investigators when writing about filling of traps and luminescence efficiency quite unjustifiably neglect the de-exciting influence of the exciting light, i.e., the effect of the exciting light on localized electrons (or holes). Inasmuch as the existence of this influence has been proved by direct experiment both as regards filling of traps[28] and the value of the luminescence yield[14,29] ignoring it obviously invalidates the conclusions reached by these investigators. By way of illustration of the significant role played by the de-exciting effect of exciting light it may be noted that in the above cited explanation of the character of the dependence of q on E, this influence of the exciting light was taken into account.

It is known that alkaline earth phosphors, in contrast to ZnS phosphors do not exhibit noticeable photoconductivity despite the general similarity of the luminescent properties of these two types of phosphors. This noncorrespondence of the optical and electrical properties of the two types of phosphors may appear to be contradictory from the viewpoint of recombination phosphorescence. Indeed if recombination is due the motion of electrons, the electric properties of the phosphors should also be close if the decay rate, concentration of ionized centers and other attributes of these phosphors are

similar. The reason for this discrepancy must be sought along the following lines.

Inasmuch as most of the time the electrons are in a bound state, then other conditions being equal the rate of decay is determined by the mean lifetime of the electrons in the traps and not in the conduction zone. The conductivity, on the other hand, will also depend on the behavior of the electrons in the free state, i.e., on the efficiency of their scattering, and also on the following factor which we feel deserves more detailed consideration.

In the conduction zone a free electron transforms into a polaron if its velocity is less than a certain critical value v_o which is determined by the relaxation rate of the lattice. If the velocity of the polaron is greater than v_o, it becomes an electron since the medium does not have time to polarize. It is not impossible that in a zinc sulfide material, in contrast to an alkaline earth phosphor, even a relatively moderate electric field can bring the electron out of the polaron state; this may result in a sharp increase of the magnitude of its displacement (range) prior to recombination and, consequently, of the conductivity, inasmuch as the properties of an electron differ appreciably from the properties of a polaron due to the much greater effective mass of the latter - approximately 100 times the electron mass (in addition, at the same energy the velocity of the electron will be much greater than the velocity of a polaron).

The above considerations regarding the character of electron motion in the conduction band may also prove useful in interpreting certain electroluminescence effects and may help explain why some phosphors do not electroluminesce.

Comparing the results obtained in recent years in investigations of luminescence centers and kinetics, we note that more significant results have been obtained in the field of kinetics. It may be assumed that in the future the lag in the field of investigation of luminescence centers will be liquidated, particularly since the study of kinetics is becoming ever more closely allied with that of luminescence and capture centers just as study of the nature of centers is becoming ever more closely associated with investigation of the semiconductor properties of phosphors.

"P.N.Lebedev" Physical Institute of the
Academy of Sciences of the USSR

References

1. F.E.Williams, J.Chem.Phys., 19, 457 (1951); Phys.Rev., 82, 281 (1951).

2. M.A.Krivoglaz, Optika i spektroskopiia (Optics and spectroscopy), 1, 54 (1956).

3. V.V.Antonov-Romanovskii, V.L.Levshin, Z.L.Morgenshtern & Z.A.Trapeznikova, Izv. AN SSSR, Ser.fiz., 13, 75 (1949).

4. Ch.B.Lushchik, Izv. AN SSSR, Ser.fiz., 18, 687, (Trans.in Bulletin, Vol. 18, No.6, p.370); Issledovanie tsentrov zakhvata v shchelochno-galoidnykh kristallofosforakh. (Investigation of trapping centers in alkali halide crystal phosphors) Trudy (Transactions) Institute of Physics and Astronomy, Ac. of Sci., Estonian SSR, 3 (1955).

5. C.C.Klick, Phys.Rev., 94, 1541 (1954); P.J.Bodten, C.Z.Van Doorn & Y.Haven, Phil.Res.Rep., 9, 469 (1954).

6. F.A.Kröger & J.A.Dikhoff, Physica, 16, 297 (1950); F.A.Kröger, J. Chem.Phys., 20, 345 (1952).

7. F.A.Kröger & J.A.Dikhoff, J.Electrochem.Soc., 99, 144 (1952).
8. F.A.Kröger, Brit.J.Appl.Phys.Suppl., 4,S58 (1955).
9. P.Prinsheim & R.C.Vorack, ZS.f.Phys., 133, 2 (1952).
10. F.E.Williams, Brit.J.Appl.Phys.Suppl., 4, S96 (1955).
11. P.Prinsheim, Lumines.Materials, Symposium, 279 (1948).
12. Siui Siui-iun, Doklady AN SSSR, 103, 585 (1955); 106, 818 (1956).
13. V.V.Antonov-Romanovskii, Trudy (Reports, Physical Institute, Ac. of Sci.), 2, No.2-3, 159 (1942); J.Phys. (USSR), 6, 120 (1942); 7, 153 (1943).
14. L.I.Anikina, Trudy (Reports, Physical Institute Ac. of Sci.), 7, 5, (1956).
15. I.P.Shchukin, Doklady AN SSSR, 104, 211 (1955).
16. E.I.Adirovich, Nekotorye voprosy teorii liuminestsentsii kristallov (Some problems of the theory of the luminescence of crystals), M.-L., 1951.
17. V.V.Antonov-Romanovskii, Izv. AN SSSR, Ser.fiz., 10, 477 (1946).
18. V.V.Antonov-Romanovskii & Z.A.Trapeznikova, Optika i spektroskopiia, 2, 204 (1956).
19. A.Bohun, Ceskoslov. Casop. fys., 5, 75 (1955); J.Lepper, ZS.f. Naturforsch, 10a, 47 (1955).
20. G.F.J.Garlick, Luminescent Materials, Symposium, N.-Y., L. (1948).
21. G.M.Eliashberg, Optika i spektroskopiia, 2, 230 (1956).
22. M.N.Alentsev, V.V.Antonov-Romanovskii & L.A.Vinokurov, Doklady AN SSSR, 94, 1133 (1954).
23. V.V.Antonov-Romanovskii & L.A.Vinokurov, Optika i spektroskopiia, 1, 66, 71 (1956).
24. M.N.Alentsev, Optika i spektroskopiia, 2, 240 (1956).
25. L.A.Vinokurov & M.V.Fok, Optika i spektroskopiia, 2, 248 (1956).
26. I.P.Shchukin, Zhur.ekps.i teor.fiz., 29, 834 (1955).
27. L.I.Anikina & V.V.Antonov-Romanovskii, Doklady AN SSSR, 68, 669 (1949).
28. V.V.Antonov-Romanovskii, Izv. AN SSSR, Ser.fiz., 13, 91 (1949); 15, 637 (1951).
29. L.I.Anikina, Doklady AN SSSR, 88, 41 (1953).

ON THE POSSIBILITY OF TWO-STAGE EXCITATION OF PHOTOSEMICONDUCTOR EFFECTS (Summary*)

- N.A.Tolstoi & A.V.Shatilov

A number of experimentally observed regularities in the field of luminescence and photoconductivity cannot be satisfactorily explained by extant theories. We refer specifically to the regularities in the behavior of temperature and concentration quenched phosphors and photoresistors.

Some of the facts defying theoretical interpretation where luminescence is concerned are the following.

1. The steady state luminance I_∞ depends on the intensity of excitation E superproportionally, sometimes quadratically: $I_\infty \approx E^p$, where $1 < p \leqslant 2$.

2. The growth of luminescence becomes more rapid with increasing E, whereas the shape of the decay curve is virtually independent of E.

3. The ratio L_g/L_d (L_g is the area over the growth curve and L_d is the area under the decay curve) may be very large ($\sim$10-30) and increases with decreasing E.

4. The initial part of the growth curve is parabolic ($I \sim t^2$).

In the case of photoconductivity theoretical difficulties arise in attempting to interpret the following facts.

5. The steady state photoconductivity $\Delta\sigma_\infty$ depends on the intensity of excitation E surlinearly; the variation is often quadratic.

6. The rate of rise of photoconductivity increases with increasing E, while the decay curve is virtually independent of E.

7. The ratio L_g/L_d attains very high values (> 100) and increases with decreasing E.

8. The initial section of the growth curve is parabolic ($\Delta\sigma \sim t^2$).

Both groups of regularities obtain for some phosphors such as CdS:Cu:Fe.

For explaining these regularities, we propose a model based on the concept of a mechanism of two-stage excitation of the electrons in conjunction with pseudomolecular recombination.

The usual bimolecular theory, based on single stage excitation, allows of explaining regularities 1 and 4; the two-stage theory in addition to providing an alternative interpretation as regards 1 and 4 is also consistent with the behavior characterized by regularities 2,3,5,6,7 & 8.

Under conditions of weak or no quenching the formulas of the two-stage theory assume a form assuring qualitative agreement with experiment. For explaining the regularities of "ordinary" photoconductivity in n-type photosemiconductors it is necessary to assume the possibility of motion of the electrons in the impurity zone (corresponding to the first stage of excitation). With a high probability of retrapping of the electrons from the conduction zone (second stage of excitation) in the impurity zone (first stage), the concentration of the electrons in the latter and, consequently, the photoconductivity are proportional to the $E^{1/2}$ in a wide range of excitation intensities. This corresponds to the familiar law $\Delta\sigma_\infty \sim E^{1/2}$ for "ordinary" photoconductivity.

---

*For the full reports on which this summary is based see Zhur.eksp.i teor. fiz. (JETP); "Optika i spektroskopiia", 1, 216 (1956); "Radiotekhnike i elektronike", 1, 1135 (1956).

FLASH LUMINESCENCE OF ZINC SULFIDE PHOSPHORS

- N.A.Tolstoi, A.M.Tkachuk, N.N.Tkachuk & Z.S.Mansurova

The effect of flash growth of the long wave emission of zinc sulfide phosphors is observed not only in the case of ZnS:Mn but also in ZnS:Ni, ZnS:Co and in "pure" ZnS. In the case of the last, iron impurities may play a certain part. The flashes may have a brightness of up to 6.5 times greater than the luminance of the steady state emission (ZnS:Ni).

The intensity of the flash depends on the interruption time t_o in the exciting illumination. There is an optimal time $t_{o\ max}$ ("the ripening time") corresponding to a maximum flash intensity; $t_{o\ max}$ depends on the composition of the phosphor and the temperature. As $t_o \rightarrow \infty$ the flashing disappears. The temperature dependence of $t_{o\ max}$ obeys the $1/t_{o\ max} \sim e^{-u/kT}$ law.

Supplementary illumination of the phosphor during the dark interval has a pronounced effect on the subsequent flashes. Supplementary illumination with infrared shortens the ripening time, while orange-green illumination weakens or liquidates the ability to flash.

With sufficiently strong preliminary excitation, the magnitude of the flash does not depend on the intensity of the exciting light but does depend on its wavelength. In the case of repeated flash-excitation, however, the flash intensity does depend to an appreciable extent on the brightness of the exciting light.

The process of flash ripening is interpreted as a process of thermal dark transfer of electrons from local "supply levels" to local "flash levels". After the lapse of a sufficient time the electrons also thermally leave the flash levels. This interpretation is consistent with the $1/t_{o\ max} \sim e^{-u/kT}$ law. Investigations of the effect of flash growth of luminescence may help throw light on the mechanism of the phosphorescence of zinc sulfide phosphors in general and in particular may explain the nonlinearity of the steady state luminescence in the long wave and short wave bands.

Discussion Following the Two Preceding Reports

Question: Why is there no transition of the electrons from the "flash levels" to deep centers and why is no blue flashing observed?

N.A.Tolstoi: One of the possible explanations is that the flash levels are in geometric proximity to two red emission centers. In this case ejection of electrons from the flash levels would lead to their predominant transition to red emission centers. This is reminiscent of the analogous effect in thermal luminescence when the color of the emission depends on the type of levels from which the electrons escape. It will be recalled that this effect gave rise to the hypothesis of the spatial proximity of trapping centers and emission centers.

A.N.Terenin: Would you say that the supply levels coincide with the double transition levels and that, consequently, the kinetics of the process are subject to the same regularity as in the report you presented yesterday?

N.A.Tolstoi: In my report yesterday I emphasized distinctive characteristics of the kinetics of strongly quenched phosphors and noted the correspondence with the regularities yielded by the two-stage excitation theory. If phosphors exhibiting flash growth of luminescence are studied under conditions of nearly steady state excitation the blue emission is almost linear. Since there is necessarily some quenching or decay, there is observed a certain shift to the side of superlinearity which is in agreement with the two-stage excitation theory. The slow growth and rapid decay of luminescence

in the blue band, characteristic of "two-stage" kinetics is clearly evident.

The kinetics of the red band in this phosphor makes it feasible to follow the kinetics of the blue band. There is evident interaction or competition between the behavior of the blue and red bands; the relationship between the blue and red emissions is not one of correlation but of anticorrelation; they are in a sense complementary. V.L.Levshin showed this in his experiments for steady state luminescence; the flash growth illustrates this competition as regards kinetics.

V.N.Favorin: Did you observe the effect of flash photoconductivity?

N.A.Tolstoi: Yes. Also, V.A.Arkhangel'skaia observed it in CdS. We plan to investigate the flash rise of photoconductivity further in the future.

A.N.Terenin: If in two-stage excitation the second photon is not at all connected with the position of the upper level, how does your scheme differ from the usual de-excitation process? As regards their kinetics do these flash phosphors belong in the two-stage category?

N.A.Tolstoi: According to the two-stage theory, in excitation on the first level - in the case of little or no quenching - the number of electrons on the supply levels must be limited; it is limited by the fact that light ejects electrons from these levels. Thus we have here a limitation of the concentration of electrons first noted many years ago by V.V.Antonov-Romanovskii in connection with the de-exciting influence of the exciting light. This is an essential point in the two-stage scheme. It is substantiated experimentally by the fact that the magnitude of the flash does not depend on the intensity of the pre-exciting light if light of the same strength is turned on after each dark interval. If the intensity of the light turned on after a standard de-excitation is varied the intensity of the flashes changes. Consequently, the supply levels always have the same store of electrons regardless of the strength of the pre-exciting light, i.e., the number of electrons on these levels is limited.

At the same time we carried out experiments similar to those of V.V. Antonov-Romanovskii and Z.L.Morgenshtern. We pre-excited the phosphor with light of different wavelengths and in this case found that although the flash does not depend on the intensity of excitation it does depend on the spectral composition of the exciting light. This shows that the limitation in the number of electrons on these levels is connected with the de-exciting influence of the exciting light rather than with the fact that the number of such levels is limited.

N.V.Zhukova: How does the transition from the flash levels to the supply levels occur; does it go through the conduction band?

N.A.Tolstoi: I cannot answer this question at present.

I would like to add that there are a number of factors that indicate that the kinetics of blue luminescence of phosphors exhibiting flash growth are associated with the two-stage excitation mechanism.

E.K.Putseiko: What results did you obtain with "flash phosphors" at low temperatures?

N.A.Tolstoi: All the processes are slowed down. The ripening time depends on the temperature according to Boltzmann's law in the first approximation.

V.V.Antonov-Romanovskii: In explaining the absence of flash growth of short wave (blue) luminescence in the investigated phosphors, it is apparently assumed that this is due to the low probability of recombination of localized electrons released by the exciting light with ionized blue center.

This assumption appears artificial since there is no theoretical justification for selective or preferred recombination of the electrons only with red centers. I think that the absence of flashing in the blue band can be explained

in the same manner as N.A.Gorbacheva explained the analogous effect in $Cd_2P_2O_7$:Mn:Pb. Gorbacheva hypothesized that the Pb sensitizes the Mn by transition of holes through a lower zone from the ground level of Pb to levels of Mn that are located further from the upper edge of the valence band. This is substantiated by the fact that the blue emission decays more rapidly (almost exponentially) than the red, whose decay is characterized by the hyperbolic law. In this case, while the excited phosphor is in the dark, the concentration of ionized blue centers falls off virtually to zero so that there is no blue flashing due to the absence of ionized blue centers at the instant of the repeat excitation.

M.V.Fok: I refer to the report of Tolstoi and Shatilov. It seems to me that some of the facts that the speaker claims can only be explained by the "two-stage" theory can be interpreted on the basis of the old theory. In particular, I refer to the quadratic photoconductivity and the large ratio of the light sums in growth and in decay.

In the case of strong first-order quenching, the concentration n of ionized centers and the equivalent concentration of localized electrons are proportional to the excitation intensity E. In this case, as the speaker observed, the luminance of the phosphor is proportional to the square of the intensity of the exciting light. If the principal light sum is concentrated on levels of sufficient depth for the release of electrons from them to occur primarily due to the exciting light, the concentration of conduction electrons will be proportional to the square of the intensity of the exciting light. Thus according to this theory the concentration of conduction electrons is

$$N^- = \frac{\alpha + w_1 n}{\delta},$$

where α is the number of ionizations of luminescence centers per unit time, δ is the probability of localization of electrons and w_1 is the probability of their release from local levels.

In the case of a high probability of retrapping $\alpha \ll w_1 n$, and if the de-exciting effect is sufficiently strong, then $w_1 = DE$ (or rigorously speaking $w_1 = w_{10} + DE$, where w_{10} is the probability of thermal release).

We then have that $N^- \sim E^2$.

The ratio of the light sums according to this theory is

$$S_{\text{growth}}/S_{\text{decay}} = 3\frac{w_1}{w_{10}} + 2\frac{w}{w_{10}},$$

where w is the probability of thermal release of holes from the ionized luminescence centers. In the case of strong quenching and strong stimulation under the influence of the exciting light this ratio can be infinitely large.

The results reported by these speakers can be satisfactorily described on the basis of migration of holes in the valence zone from one activator to the other. Thus the ripening of the flashes is apparently connected with the time necessary for all the holes to escape from the blue centers. The absence of blue flashes is explained by the fact that, although there may be some electrons in the conduction band, due to the absence of ionized blue centers these electrons cannot combine with them and yield luminescence.

My calculations of the interaction of blue and green luminescence centers in ZnS:Cu phosphors showed that, assuming such migration of holes, where there is absorption of the exciting light by the blue luminescence centers, the blue band must decay much more rapidly than the green one. This is in fact observed experimentally.

In view of what I have said regarding the first report I feel that there is not as yet sufficient basis for so radical a revision of the present theory of the kinetics of luminescence of crystal phosphors.

N.F.Vol'kenshtein: What is the reason for the quadratic dependence of the photoconductivity?

Let us assume that a photon is absorbed and that as a result an exciton is formed. What is the further state of this exciton?

The photon "lives" for some time and then dies. The "decease" can occur in two ways: 1) the electron and hole forming the exciton may recombine - this recombination may be described as exothermic death of the exciton - or 2) the electron and hole forming the exciton may go off in different directions, i.e., the exciton may dissociate - this may be described as endothermic death of the exciton.

If the exciton does not die a natural death, it will perish in an "accident". Such an "accident" may be collision of the exciton with an impurity center. In such a collision, the exciton is annihilated and the released energy is expended on ionization of the impurity center. This in brief is the mechanism of exciton photoconductivity proposed by Lashkarev and Zhuze.

The exciton may, however, encounter another type of "accident", also resulting in its death. The exciton may collide not with an impurity center but with another exciton. Both excitons may perish in the encounter: one of the excitons is annihilated and the energy released in the process is utilized for dissociation of the other exciton. This is how photoconductivity proportional to the square of the light intensity may develop.

No one has as yet examined the problem of the collision of two excitons. Exciton theory is primarily a theory of single excitons. A theoretical investigation of the problem of interaction of excitons presents undoubted interest and may lead to intriguing results. Non-interacting excitons do not lead to photoconductivity. Interaction between them, however, may lead to the appearance of photoconductivity.

N.A.Tolstoi: I would like to say the following regarding the remarks of V.A.Antonov-Romanovskii concerning the role of holes in the scheme I proposed. I said that electrons ejected from flash levels are localized primarily on red centers. This is not a hypothesis but an experimental fact. Antonov-Romanovskii discussed the question of why electrons may combine only with red centers. This is only an explanation of an observed fact,not a contradiction of what I have said.

In the brief space of the report I could not dwell on all the details of the process of flash growth of luminescence. It is perfectly obvious that the number of free and localized holes must equal the number of free and localized electrons; after cessation of excitation, the holes may be partially lodged at blue centers and partially on red ones or only on red ones. I know of the possibility of explaining the fact that flashing is observed only in the red band by means of the hole mechanism, however, I would like to point out something else. Flash growth is observed both in excitation in the principal band (313 mμ) and the band of the activator (zinc, 365 mμ). Hence in the excitation of the flash there are immediately formed holes at blue centers. Therein lies the difference between the flashes in our phosphors from the flash effect in ordinary "flashing" phosphors, where the flash of luminescence is produced by red light rather than by the light normally exciting the phosphor and, consequently, the excitation of the electrons is not accompanied by the formation of new ionized luminescence centers. These considerations are not to be construed as objections to the "hole" interpretation; I merely mention them to show that a number of diverse details must be taken into account in elaborating a theory.

Regarding the remarks of M.V.Fok concerning the square law photoconductivity, I would like to note that we do not now actually have a single, unified and generally accepted theory of the kinetics of luminescence of crystal phosphors. My criticism applied to most of the theories advanced during the last decades. Most of them do not take into account either hole mechanisms or de-excitation by the exciting light. It is entirely possible that taking these effects into account may lead to agreement of the "ordinary" theory with the experimentally observed characteristics of photosemiconductor processes (large values of L_g/L_d, the fact that the growth of luminescence does,while the decay of luminescence does not depend on the intensity of excitation, the quadratic rise of photoconductivity, etc.). So far we have no theory that can explain all these diverse effects. The two-step excitation theory does explain them in the first approximation. I would say that the two-stage excitation theory is no more (or less) a radical revision of the theory of luminescence of crystal phosphors than the theory involving holes and de-excitation by the exciting light proposed by M.V.Fok. As for the last,I would like to note that according to Fok's theory L_g/L_d should increase with intensity of excitation, whereas actually this ratio decreases. Moreover, the square law behavior of the photoconductivity, as Kallmann and Kramers have shown for a number of phosphors, begins in the region of weak excitation when the de-excitation by the exciting light should presumably be very small. Finally, the parabolic increase in photoconductivity with time (in the initial stages) follows directly from the two-stage mechanism, but cannot be obtained from the scheme described by Fok.

ON THE LUMINESCENCE ZnS:Mn PHOSPHORS UNDER EXCITATION (Abstract)

- V.L.Levshin, N.S.Borodin & G.P.Neronova

The investigation was concerned with the increase in the brightness of the manganese band of ZnS:Mn phosphor with increasing intensity of excitation. The phosphor was excited by light of 312, 366, 405 and 436 mμ at temperatures of 20, 50, 110, 130 and 150°.

Saturation of the emission was observed with excitation by the 312 and 360 mμ lines. The shape of the curves is well characterized by the formula

$$J = \frac{aI}{I + b},$$

where J is the luminance of the phosphor, I is the intensity of the exciting light and a and b are constants.

The value of the maximum brightness of luminescence a under excitation by 366 mμ light is 3.6 times greater than under excitation by 312 mμ photons.

In the case of excitation by the 405 and 436 mμ lines, the increase in luminance was virtually proportional to the intensity of the exciting light and a slight tendency to saturation was observed only at the highest excitation intensities. Calculations showed that at the maximum luminescence only an insignificant fraction of the manganese ions are emission centers.

Emission in the manganese band increases sharply with increasing temperature. Beginning with 70°, however, there is evidence of thermoquenching. The temperature at which the maximum luminance under excitation is attained increases with the excitation intensity.

The following tentative luminescence mechanism is proposed to explain the results obtained. Under excitation by the 436 and 405 mμ lines there occurs primarily direct excitation of luminescence centers. Due to the short persistence of the emission, saturation does not occur. Excitation by 366 mμ light produces ionization of the zinc at the lattice defects. The released electrons are first drawn into the conduction band and then captured in trapping levels of different depths. The positive hole left by the departure of the electron, utilizing thermal energy, passes through the valence band to a manganese ion whose levels are located higher above the valence band than the zinc levels. In the case of excitation by 312 mμ photons, there occurs a transfer of electrons from the valence band to the conduction band, followed by their localization in traps. The positive holes forming in the valence band rise to the manganese centers. The final stage of the luminescence process under the influence of 366 and 312 mμ light is qualitatively analogous: thermal energy releases the electrons from the localization levels (traps); these electrons, after passing through the conduction band, recombine with the holes located near the manganese ions, thereby producing luminescence of the manganese centers.

The study also comprised investigation of the emission spectra of the sphalerite and wurzite modifications of ZnS:Mn phosphors at different concentrations of Mn and different temperatures. It was established that the wurzite modification favors the development of manganese luminescence. The blue emission of zinc is observed only at low temperatures. In the case of the sphalerite modification (Mn concentration 1 part in 10^3) the zinc luminescence under strong excitation amounts to only 60% of the total emission at room temperature. With rising temperature there occurs a luminescence energy shift from the zinc to the manganese as a result of which the zinc emission is weakened even outside the temperature quenching region. Increasing the manganese

concentration enhances the transition probability and favors development of the manganese luminescence.

"M.V.Lomonosov" Moscow State University

Discussion

V.V.Antonov-Romanovskii: The authors explain the ever slower growth of the luminescence in the red band of manganese with the simultaneous faster-than-linear increase in intensity of the blue band by the effect of saturation, i.e., by the almost complete ionization of the manganese canters. I think this is erroneous. I feel that the limitation of the light sum stored is due not to saturation but to the de-exciting effect of the exciting light. This follows, for example, from the results reported by Tolstoi et al ("Flash Luminescence of the Zinc Sulfide Phosphors"). Thus the assumptions of Levshin, Borodin & Neronova are in conflict with the experimental results of Tolstoi et al.

Consequently, the reason for the different behavior of the red and blue bands of ZnS:Mn is different from that suggested by Levshin et al. It may be assumed that the actual reason is that there is sensitization through the lower zone, that is, transfer of holes from the ground level of the blue centers to the ground levels of the red ones. If the kinetics of recombination of electrons with the ionized blue centers differs from the kinetics of release of holes from them, we have a logical explanation of the different nonlinear dependence of the two bands of ZnS:Mn.

N.A.Tolstoi: I would like to explain how from our scheme one can obtain the experimental fact described in detail by Levshin and his co-workers in their reports on the steady state luminescence of ZnS:Mn phosphors. Let us assume that the electrons from the supply levels go to the flash level. This process requires an activation energy and proceeds at different rates at different temperatures. Let us assume that the excitation is steady. Obviously, with increasing temperature the number of electrons arriving per second from the supply levels to the flash level must increase. Consequently, more electrons per second can reach the long wave centers from the flash level per unit time. That is, the red emission will be brighter. It is well known that the red band of ZnS:Mn phosphor increases in brightness with rising temperature.

On the other hand, the reserve of electrons on the supply levels after the exciting light is turned off should not depend on the temperature and the total number of electrons arriving at the flash levels remains the same. Thus the absolute magnitude of the flashes should not change. This is exactly what is observed for the ZnS:Ni and ZnS:Mn phosphors: with increasing temperature the absolute intensity of the flashes does not change but the steady state luminance increases.

V.L.Levshin: I fail to understand the remarks of V.V.Antonov-Romanovskii regarding the necessity of taking into account the role of the lower band, inasmuch as in my report I emphasized the role of the lower band and in my scheme examined the motion of holes in it.

The de-exciting influence of the exciting light undoubtedly plays a certain part in the development of certain luminescence processes in ZnS:Mn phosphors as well. In the effects under consideration, however, the role of de-excitation by the exciting light is minor. This follows from the fact that there is saturation of the manganese luminescence with increasing intensity of the excitation and from the existence of thermostimulation of the phosphors

under excitation. Possibly the de-excitation is particularly strong for electrons localized on deep levels that are not manifested in the thermal de-excitation curves due to thermoquenching.

As for the remarks of N.A.Tolstoi that the effects described by us fit in with his theoretical concepts, I note that N.A.Tolstoi in his scheme did not take into account the experimental curves characterizing the thermal de-excitation of ZnS:Mn phosphor and at present is essentially presenting the scheme for a theoretical phosphor which should yield the luminescence effects he observed. I think it would be desirable for Tolstoi to review the results of investigations of actual ZnS:Mn phosphors taking into account all the levels known to exist in it. Then perhaps our theories of the luminescence process, supplementing each other, may come to agree.

NEW PROCEDURES FOR INVESTIGATING RELAXATION PROCESSES AND TRAPPING CENTERS IN CRYSTAL PHOSPHORS (Abstract*)

- Ch.B.Lushchik

The report is devoted to new methods of investigating relaxation processes and trapping centers in crystal phosphors, namely, 1) the method of thermal bleaching which consists of measuring the dependence of the coefficient α of absorption (diffusion reflection) of the trapping centers - or of the quantity $-d\alpha/dt$ - on the temperature as the excited phosphor is heated at a constant rate β; 2) the method of thermooptical stimulation or de-excitation which amounts to periodic measurement of the brightness of optical flashes or the intensity of emission of the trapping centers during heating of the excited phosphor with β = const; 3) a variant of the method of Bull and Mason which amounts to measuring the light sums accumulated by the phosphor after excitation and heating at a constant rate to different temperatures; 4) the method based on measuring the dependence of the "negative excited absorption" (i.e., the decrease in absorption after excitation) on the temperature with the phosphor heated at a constant rate β.

The report illustrates some applications of these procedures for the solution of specific problems: for establishing the relation between the excited absorption bands (stimulation of optical flashing) and the thermostimulation (glow curve) peaks, for determining the energy of thermal ionization of trapping centers in the ground and excited states, the probability of retrapping, the degree of filling of the trapping levels, and the ratio of the cross sections for recombination, for investigating relaxation processes in the region of thermal quenching and, finally, for determining the "sign" of the relaxation process.

Lastly, the report describes certain procedures for direct investigation of the distribution of electrons and holes among the trapping levels during the relaxation process (thermal bleaching and thermooptical de-excitation under conditions of pulse heating).

Institute of Physics and Astronomy of the
Academy of Sciences of the Estonian SSR

---

*Complete report in Optika i spektroskopiia, 2, 220 (1957).

ON THE PHOSPHORESCENCE DECAY LAW FOR CRYSTAL PHOSPHORS (Abstract*)

- G.M.Eliashberg

Various considerations set forth by V.V.Antonov-Romanovskii[1] and the author[2] show that it is impossible to explain a number of the principal regularities of phosphorescence and, in particular, the experimental shape of the decay curves within the framework of the simple band model theory.

In elaborating the decay theory it is essential to take into account the deviations of actual phosphors from the simple band model. One such deviation is the complexity of the spectrum associated with the trapping levels in most phosphors. The possibility that this factor may have an appreciable influence on the character of the processes occurring in phosphors has been discussed by many authors[3-5]. In the present contribution we developed a quantitative decay theory based on a band model with two types of trapping levels.

The general equation describing the decay process in this model is

$$\frac{dy}{dx} = 1 + (C_1 + C_2)\frac{C_3}{C_2 + C_3}\cdot\frac{1}{x} - \frac{C_2 \cdot C_3}{(C_2 + C_3)^2}\cdot(x + C_1 + C_3)\cdot\frac{1}{y}, \qquad (1)$$

where

$$C_1 = \frac{A_2\nu_2}{Bn_0}, \quad C_2 = \frac{A_1\nu_1}{Bn_0}\cdot\frac{P_2}{P_1}, \quad C_3 = \frac{A_1\nu_1}{Bn_0}, \quad x = \frac{n}{n_0}, \quad y = \frac{P_1 n_1 + P_2 n_2}{n_0(P_1 + P_2)}.$$

Here n, n_1 and n_2 are, respectively, the concentrations of ionized luminescence centers and electrons in the traps of both types, ν_1 and ν_2 are the concentrations of the two types of traps, n_0 is the initial concentration of ionized centers, B is the probability of recombination of an electron with an ionized center, A_1 and A_2 are the probabilities of capture of an electron by the traps of the first and second type, and P_1 and P_2 are the probabilities of release of the electron from these traps. If the solution of (1) is known, the expression giving the decay curve in parametric form is

$$I = (P_1 + P_2)\cdot n_0 \cdot \frac{xy}{x + C_1 + C_3}, \qquad t = -\frac{1}{P_1 + P_2}\int_{x_0}^{x} \frac{x + C_1 + C_3}{xy}\,dx. \qquad (2)$$

The results of calculations for the particular case where $C_3 \gg C_1, C_3 \gg 1$ and $P_1 \gg P_2$ (high probability of retrapping on the shallow levels and widely separated levels) are given in Ref.2. The decay curves in this case have a very complex shape and differ in general from the conventional Becquerel curves.

In the case of not too widely separated levels and a high probability of retrapping the curves have a more simple shape.

In the case of a low retrapping probability, the presence of two systems of trapping levels has a particularly strong influence on the shape of the decay curves.

All the distinctive features of the decay curve for the given model are connected with redistribution of electrons between the different trapping levels during the decay process.

"Krasnyi Khimik" ("Red Chemist") Plant

---

*The complete report is listed under Ref.2.

References

1. V.V.Antonov-Romanovskii, Sov.kniga (The Soviet Book),1935,No.1,16 (1953).
2. G.M.Elishberg, Optika i spektroskopiia, 1, 230 (1956).
3. V.L.Levshin, Fotoliuminestsentsiia zhidkikh i tverdykh veshchestv (Photoluminescence of liquids and solids) M.-L., 1951.
4. R.P.Johnson, JOSA, 29, 387 (1939).
5. Ch.B.Lushchik, Trudy (Transactions) IFA AN Estonian SSSR, No.3 (1955); No.4 (1956).

Discussion

N.A.Tolstoi: To what extent can your model be extended to the process of the growth of luminescence and what are the difficulties encountered in attempting to do so?

G.M.Eliashberg: There is one substantial difficulty connected with the appearance of current carriers of both polarities. Whereas in decay, one can limit the consideration to electrons (assuming, for example, that the temperature is low), in the process of growth, one can hardly disregard the fact that holes appear in the valence band. I did carry out a preliminary calculation for the case when both holes and electrons appear in the process of luminescence growth but for lack of time I could not mention it in my report.

In connection with this I would like to suggest that the appearance of holes in the process of excitation perhaps should be taken into account in interpreting flash effects. It is possible that the difference between flash spectra and steady state luminescence spectra is that in the latter case the emission is due to recombination of electrons whereas in the former case it is due to recombination of holes.

A.A.Shishlovskii: To what extent can experimental phosphorescence decay curves be approximated by your formulas?

G.M.Eliashberg: A detailed quantitative comparison of the theory with experiment is difficult at present in view of the fact that the model parameters entering into the equations are not known for any phosphors. One can, however, fit the theoretical curves to parabolic experimental decay curves through appropriate choice of the parameters. This cannot be taken as proof of the validity of the theory inasmuch as the actual parameters for real phosphors are not known.

AFTERGLOW OF THE Eu^{3+} ION IN THORIUM OXIDE PHOSPHORS (Abstract*)

- M.V.Fok

Phosphors activated with trivalent rare earth elements exhibit line emission spectra due to forbidden electron transitions inside the 4f shell. In order to interpret these spectra it is necessary to know the lifetimes τ of the excited state corresponding to each line. Knowing these, it is possible to divide the lines into groups corresponding to transitions from one common upper level. In the case of recombination luminescence, however, the influence of the finite duration of the excited state of the activator ion can be expected to be manifested only in the very early stages of the phosphorescence, i.e., over an interval comparable in duration to τ, inasmuch as thereafter this influence is masked by slower recombination processes.

For the purpose of investigating the influence of the finite lifetime of the excited state on the afterglow of individual lines of Eu^{3+}, we recorded the spectra of the phosphors ThO_2:Eu and $Th(SO_4)_2ThO_2$:Eu (it was found that they have virtually identical characteristics). By means of a specially designed spark phosphoroscopic set-up, it was possible to realize pulse excitation of $\sim 10^{-5}$ sec duration and observe the afterglow in the interval from $3 \cdot 10^{-4}$ to $4 \cdot 10^{-2}$ sec after cessation of excitation.

It was found that the individual lines of the phosphor decay in different ways. It was noted that the brightness of some lines increases (instead of decreasing) for some time after cessation of excitation. This anomaly is particularly pronounced in the case of the 590 mμ line, the brightness of which increases by as much as 50% up to $2 \cdot 10^{-3}$ sec after cessation of excitation and thereafter falls off rather rapidly. This anomalous behavior of the afterglow can be explained by the fact that by virtue of the strong short-term excitation, the concentration of excited Eu^{3+} ions is small at the beginning of the afterglow. For some time recombination proceeds more rapidly than de-excitation with a resultant increase in the number of excited ions. Subsequently, the rate of recombination decreases and, when it becomes lower than the rate of de-excitation (luminescence), the brightness begins to fall off. This makes it possible to find the value of τ for each line from the afterglow curve despite the recombination character of the effect and the absence of an exponential section in the decay curve.

"P.N.Lebedev" Physical Institute of the
Academy of Sciences of the USSR

DISCUSSION

A.N.Zaidel': Were you able to establish a relationship between the observed lifetime and the height of the upper level?

M.V.Fok: We were able to investigate six lines in detail: one line for which $\tau = 3 \cdot 10^{-3}$, four lines for which τ is less than 10^{-3}-$4 \cdot 10^{-4}$ and one line for which no peak was observed, which means that τ is even shorter.

There are many lines in the spectrum of europium and the systematics of the spectrum are only roughly known. Only groups of lines, which often overlap, rather than individual lines have been interpreted. Here one can only ask whether different values of τ have been obtained for lines associated with transitions from the same level. There are apparently no such contradictions, but I cannot positively assert this in view of the lack of adequate interpretation of the spectrum.

---

*Complete report in Optika i spektroskopiia, 2, 127 (1957).

A.N.Zaidel': Why were not direct measurements of τ made using resonance excitation of the phosphor with light in the discrete absorption bands of Eu^{3+}?

M.V.Fok: The thing is that the absorption is associated with forbidden transitions. I succeeded in observing the absorption of rare earth ions and even succeeded in exciting the phosphor by the yellow mercury line, the resultant emission was so weak that it was barely possible to obtain a somewhat underexposed photograph with an exposure extending over the entire decay interval.

A.N.Zaidel': Each of the upper levels of the Eu^{3+} ion from which the transitions responsible for the investigated luminescence occur are split in the field of the crystal lattice. The separation between the components is of the order of tens of cm^{-1}, i.e., is small compared with kT. Hence if τ for a given level is about 10^{-3} sec, then over this interval there should be established a Boltzmann distribution among the sublevels of the excited term. Consequently, the lines associated with transitions from different sublevels of the same term should lead to equal values of τ and the number of different observed values of τ cannot exceed the number of upper electronic levels from which the transitions occur. Apparently, the number of such levels is not greater than two or three.

M.V.Fok: From my point of view the value of τ need not be the same for all sublevels of the same level. Although the energy separation between them may be small, the transition probability from one sublevel to another is very low. For this there must occur an appreciable displacement of the surrounding ions that will produce a spreading of the sublevels, then the system will go from one level to another. The potential barrier between them is very high and redistribution between these sublevels may not occur. If the redistribution does not occur, then the forbiddance is removed.

DECAY LAW FOR ZINC SULFIDE PHOSPHORS IN AND NEAR THE THERMOQUENCHING REGION (Abstract*)

- F. I. Vergunas

The report offers an explanation of the regularities observed for the afterglow of zinc sulfide phosphors near and in the region of temperature quenching on the basis of the further development of the theory of Adirovich. This theory takes into account quenching of the bimolecular type and the necessity of activation of radiationless recombination processes. The deduced equations are reduced to the set derived by Adirovich and solved for the condition of short electron lifetimes in the conduction band. The decay law is obtained in the form of three equations. In contrast to the decay law given by Adirovich, the parameter γ, which is equal to the ratio of the probabilities of localization (trapping) to the sum of the probabilities of recombination accompanied and not accompanied by radiation, is a function of the temperature.

Thus the decay law in the quenching region changes due to the temperature dependence of γ. The parameter γ remains constant near the quenching region but decreases in the quenching region. Hence the afterglow decay law near quenching is approximated by a fractional-exponent hyperbola, the degree of which is temperature independent, while in the quenching region the order of the hyperbola increases to about 2.5, as γ decreases. With further increase in temperature, the decay curves are approximated by exponential curves, that eventually go over into fractional hyperbolas. The higher the temperature and consequently the smaller γ, the later this transition is realized. As the initial light sum is decreased, the exponential section becomes smaller and the hyperbola larger. Calculations show that the influence of temperature and the degree of excitation on the character of the decay law remains the same when the phosphor is excited to less than saturation.

The transition from a fractional hyperbola to the exponential curve in the region of quenching is due to a diminution of the role of retrapping and, vice versa, the change from an exponential curve to a hyperbola with decrease of the initial light sum is associated with enhancement of the role of retrapping.

Calculations showed that

1) the temperature dependence of the light sum ν in the quenching region changes; the activation energy determined from the dependence of ν on T near the quenching region equals E/2 where E is the depth of the localization levels (traps), while in the quenching region the activation energy equals $(E + \Omega)/2$, where Ω is the activation energy for radiationless transitions;

2) the displacements of the second degree hyperbolas along the log t axis obtained in the case of weak excitations correspond to the energy E near the quenching region and to the sum $E + \Omega$ in the quenching region;

3) one can determine the depth of the localization levels from the variation with temperature of the time constant exponents obtained in the quenching region.

Both the qualitative and quantitative regularities following from the deduced decay law are in general agreement with experimental data for zinc sulfide phosphors. This agreement of the decay law deduced for an ideal phosphor in which there are assumed to be localization levels and emission centers of only one type with the law for real phosphors in which there are usually several types of levels is explained by the fact that in an actual phosphor there can readily be realized conditions close to those of the examined ideal model.

Tomsk State University

---

*Complete report published in Optika i spektroskopiia, 1, 416 (1956).

LUMINESCENCE DECAY OF ZnS:Cu and ZnS:Cu:Co PHOSPHORS IN AND NEAR THE THERMOQUENCHING REGION (Abstract)

- N.L.Gasting

The work comprised a detailed experimental investigation of the afterglow of ZnS:Cu and ZnS:Cu:Co phosphors near and in the thermoquenching region. The temperature induced quenching of these phosphors was measured.

The observed regularities are compared with different decay theories for the purpose of elucidating the form of the decay law obtaining for these crystal phosphors. The temperature quenching of ZnS:Cu phosphors was measured in the range from 300 to 700°K and that for ZnS:Cu:Co in the range from 100 to 600°K. The luminescence decay was also determined for different excitation conditions.

It was found that for the ZnS:Cu phosphor with weak steady excitation in the 398 to 495°K temperature interval the afterglow decay curves are hyperbolas with constant slopes, while at higher temperatures (430-510°K) the curves are fractional hyperbolas whose slope increases with increasing temperature.

In the case of strong equilibrium excitation the decay curves are again hyperbolas with constant slopes in the temperature region from 397 to 430°K - the region near quenching - while at higher temperatures (459-477°K) there are obtained transitional curves with initial exponential sections whose extent increases with increasing temperature and intensity of the exciting light. At still higher temperatures (498-510°K) pure exponential decays are obtained.

In the case of instantaneous excitation in the same quenching region (481-512°K), second order hyperbolas are obtained.

The same qualitative regularities were obtained for the ZnS:Cu:Co phosphor except for the hyperbolas with constant slope; these were absent, inasmuch as for our ZnS:Cu:Co phosphor specimens we did not in general observe a constant luminescence intensity during the time of excitation.

The significant experimental fact is that for one and the same phosphor specimen we obtained all the principal forms of the luminescence decay law: exponential, second order hyperbola and fractional hyperbola in the same temperature interval.

From the luminescence decay and quenching curves we calculated the activation energy U necessary for temperature quenching, the depth of the effective localization levels ϵ and the energy $\epsilon + \Omega$ (where Ω is the activation energy of radiationless processes in the phosphor). The energy values were found from the temperature variation of the light sums, from the shift of the hyperbolas and from the temperature dependence of the decay time constant ("slope" of the exponentials).

The results obtained are in satisfactory qualitative and quantitative agreement with the theoretical law of Adirovich as modified by F.I.Vergunas, taking into account quenching of the bimolecular type.

The good agreement of the experimental regularities obtained by us for actual phosphors with the theoretical law deduced for an ideal phosphor, having localization levels of only one kind and luminescence centers of one type, is explained by the fact that in the investigated temperature regions in our phosphors there exist in effect localization levels of only one depth and emission centers of only one kind. This deduction is substantiated by our quantitative results.

It follows from our experiments that the fundamental decay law for the phosphors in question is neither the exponential nor that characterized by a

second order hyperbola; the basic decay law is the Adirovich-Vergunas law, approximated in the general case by a fractional hyperbola and yielding exponential curves and second degree hyperbolas as particular cases.

Tomsk State University

* * * * * * *

INVESTIGATION OF THE DECAY OF ZnS:Mn and ZnS:Cu:Fe PHOSPHORS IN THE REGION OF TEMPERATURE QUENCHING OF THE LUMINESCENCE (Abstract)

- V.V.Nuvar'eva

The investigation concerned the luminescence decay of two zinc sulfide phosphors in which traps of different depths participate in the afterglow. It was established that for the initial decay stages the curves for ZnS:Cu:Fe ($1:10^{-5}$) and ZnS:Mn ($1:10^{-3}$) phosphors after prolonged equilibrium excitation near and in the quenching region are comprised of at least three exponential components for the first phosphor and two for the second. In the late stages the decay is hyperbolic (power-law): $I = At^{-\alpha}(\alpha \leq 2)$.

Upon heating, the rate of decay increases: the slope of the exponential curve increases in the case of both phosphors, while in the case of ZnS:Cu:Fe the order α of the fractional hyperbolas also becomes larger. With decreasing intensity of the exciting light (at the same temperature), the relative fraction of the exponential decay decreases, while that of the hyperbolic increases, although the rate of the latter also goes down.

It is concluded that the general appearance of the experimental decay curves and their behavior with variations in temperature and intensity of the exciting light are in good agreement with the theoretical decay law of Adirovich as deduced taking into account temperature quenching.

The exponential decays are not due to the presence of dark conductivity or processes of monomolecular quenching in bimolecular luminescence model; the reason for the exponential decay is the absence of retrapping.

Exponential sections of the decay curves can be described by $I = I_o e^{-pt}$, where $p = p_o^{-\epsilon/kT}$ is the probability of thermal release of electrons from a trap of depth ϵ This is qualitatively substantiated by the equality of the number of exponential processes of which the decay is comprised (as indicated by the number of steps or breaks in the decay curve plotted in log I vs t coordinates) with the number of thermostimulated emission peaks each of which is due to electrons released from trapping levels of one depth. The activation energy determined from the temperature dependence of the time constant of the exponential decay curve agrees within 30% with the depth ϵ of the trapping levels as determined from the thermostimulation experiments.

It is known that for any zinc sulfide phosphor $p_o = 10^{8\pm1}\text{sec}^{-1}$; in most cases a given phosphor is characterized by a unique value of the "attempt frequency". We, on the other hand, found a unique value of p_o for each kind of trapping level from the decay experiments. A possible verification of the determined values of p_o is furnished by the frequency dependences of the dielectric loss tangent for zinc sulfide phosphors.

Tomsk State University

INVESTIGATION OF ELECTRON TRAPPING LEVELS IN ZnS:Cu PHOSPHOR

- Iu.L.Lukantsever & L.R.Krasovskaia*

Introduction

There have been numerous investigations devoted to the kinetics of luminescence in zinc sulfide phosphors. It is noteworthy however that the data in the literature concerning the same properties of phosphors having the same chemical composition frequently disagree. This can in part be explained by differences in condition of preparation, degrees of purity of the raw materials, use of different fluxes, etc. These variations in technique make it difficult if not impossible to compare the results obtained by different investigators.

In view of this we felt it would be of interest to carry out a complex investigation of the same phosphor under identical experimental conditions by different procedures and to compare the results obtained in this manner.

In this report we shall give the results of an investigation of the trapping levels in ZnS:Cu phosphor** (1:10^{-4}, heating temperature 1100°, flux - NaCl) by two different optical techniques: the thermostimulation method and the method based on investigating the variation of the decay near and in the temperature quenching region.

The luminescence of the phosphor was excited by filtered light from a PRK-4 mercury tube (365 mμ). The luminescence of the phosphor was directed through a filter, passing the green emission band, to a FEU-17 photomultiplier, connected to a recording device through an appropriate amplifier. In the case of obtaining the decay curves, the recording device was an electronic EO-7 oscillograph especially adapted for this purpose; for recording the glow curves we used a short-period mirror galvanometer. In the latter experiments the phosphor was heated at the rate of 0.87 degree/sec; our equipment insured constant maintenance of this heating rate in the temperature interval from 123 to 550°K.

Results obtained for the trap depth by analysis of the glow curves

The thermostimulated emission curve for the investigated phosphor excited at 125°K is shown in Fig.1 (curve a). It will be seen that the curve has three peaks (I, II and III) located at 155-158°, 218-222° and 295-298°. The presence of three peaks indicates that we are dealing here with a so-called oxygen dominated phosphor possessing three groups of electron localization levels[1].

Since we felt it would be desirable to investigate the occupation of each of these three groups of levels and also to determine the depths of these levels, it was necessary to find experimental conditions under which the thermostimulation peaks could be separated. It proved feasible to realize this in two ways:

1. The phosphor was excited at different temperatures and the glow curves recorded. The series of curves obtained in this manner is shown in Fig.1. It will be seen from these curves that at a temperature of 200°K the shallowest traps no longer remain filled (i.e., peak I vanishes). At a temperature of 270° the electrons formerly stored on the levels of the second group are no

*This report was presented by F.I.Vergunas.

**The phosphor was obtained from the Luminescence Laboratory of the Physical Institute of the USSR Academy of Sciences.

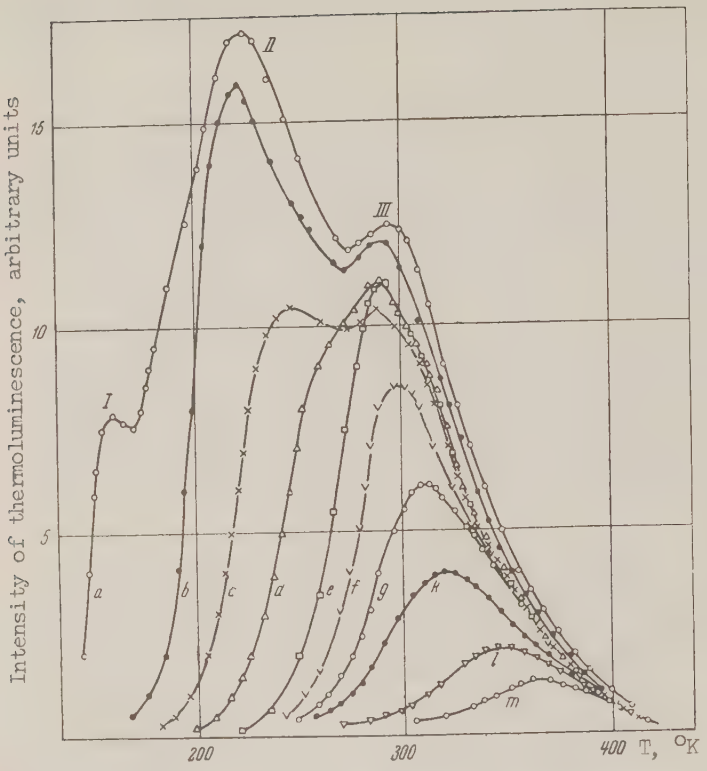

Fig.1. Glow curves for the ZnS:Cu phosphor obtained at different excitation temperatures (T_e): a) 125, b) 197, c) 231, d) 250, e) 269, f) 285.5, g) 297, k) 310, l) 332, and m) 353°K.

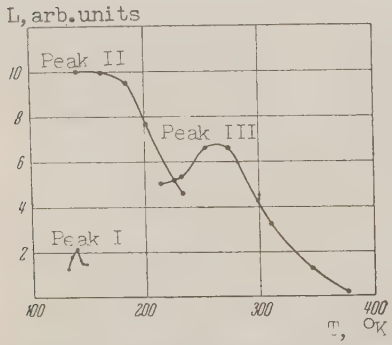

Fig.2. The variation of the light sums stored at the different groups of electron localization levels in ZnS:Cu phosphor with the temperature of excitation.

longer evident. As the temperature is increased above 270°, the light sum stored on the levels of the third group begins to decrease and the top of this peak (peak III) is gradually shifted to the side of higher temperatures.

2. The phosphor was excited at the lowest temperature obtainable under our conditions (123°K) and then warmed to different temperatures after which the thermostimulation curves were recorded. The results obtained in this manner were analogous to those shown in Fig.1, except that in this case displacement of the third peak was not observed. The separation of the thermostimulation peaks was effected by subtracting the curve having two maxima (curve b) from the curve having three maxima (curve a) and the curve having one maximum (curve e) from that having two maxima (curve b); that is, the light sums evinced in thermostimulation were determined planimetrically.

The dependence of the light sums stored on the localization levels of the three groups on the temperature of excitation of the phosphor is shown in Fig.2. It will be seen that at the temperatures at which the shallowest group of localization levels is virtually emptied, the deepest group is still filled. It also follows from Fig.2 that beginning with a temperature of about 280°K the thermoluminescence is due primarily to electrons released only from one, i.e., the deepest, group of traps.

We used different methods for determining the energy depth ϵ of the electron localization levels: the method of analysis of the glow curves proposed by V.V.Antonov-Romanovskii[2] and Urbach[3] and the method of evaluating ϵ from the temperature variation of the light sums evinced

Investigator	Formula	ξ, ev		
		Peak I	Peak II	Peak III
Antonov-Romanovskii (2)	$I = n^2 p_0 e^{-\varepsilon/kT}$	—	0,151	0,28
	$I = n_0^2 p_0 e^{-\varepsilon/kT}$	0,174	0,20	0,29
	$I = \frac{B}{p_0 c^2} e^{\varepsilon/kT}$	—	—	0,27
Urbach (3)	$\varepsilon = \frac{2kT_m^2 I_m}{L}$	0,12	0,16	0,28
Iastrebov (9)	$L = L_0 e^{\varepsilon/2kT}$	—	—	0,32

in thermostimulation[4].

The results of our evaluation of the trap depths by the three methods are summarized in the accompanying table.

It will be seen that there is satisfactory agreement of the values of ϵ for each of the three groups of localization levels.

Results of determination of the depths of the localization levels by analysis of the decay curves near and in the region of thermoquenching

According to the results of our measurements thermoquenching of the luminescence of our ZnS:Cu phosphor begins at a temperature of 400-415°K; the quenching activation energy equals 0.67 ev.

For determining the depths of the localization levels by the second method we utilized some of the regularities following from the Adirovich[5] decay law as developed in the work of F.E.Vergunas[6].

1. In the region of very small values of the parameter γ (γ is equal to the ratio of the probability of capture of electrons by localization levels of the given depth to the sum of the probabilities of recombination with and without radiation) the luminescence decay law is described by the formula

$$I = I_0 e^{-pt}, \tag{1}$$

where I_0 is the luminescence intensity at the instant t = 0 and p is the probability of thermal ejection of electrons from localization levels of a given kind. This probability is given by

$$p = p_0 e^{-\varepsilon/kT}. \tag{2}$$

Thus, using (2) one can determine the value of ϵ from the temperature variation of p.

2. Near the quenching region the variation of the light sum vs the temperature is characterized by the following law

$$L = L_0 e^{\varepsilon/2kT}, \tag{3}$$

where L_0 is a quantity not dependent on the temperature.

Thus utilizing (3) one can also determine the trap depth ϵ.

3. In the region of temperature quenching the light sum varies according to the law

$$L = L_{01} e^{\frac{\varepsilon+\Omega}{2kT}}, \tag{4}$$

where Ω is the activation energy for nonradiative recombinations and L_{01} is a quantity not dependent on the temperature.

Thus one can determine the quantity $\epsilon + \Omega$ from the temperature dependence of the light sum.

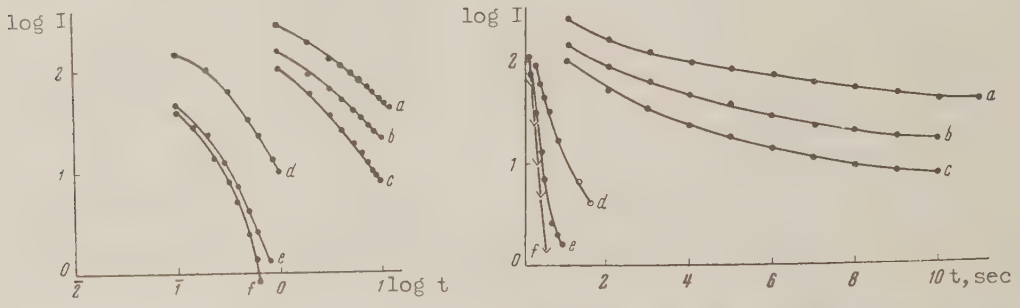

Fig.3. Decay curves for the ZnS:Cu phosphor at different temperatures (maximum - 100% - excitation intensity): a) 298, b) 360, c) 392, d) 463, e) 500, f) 508°K.

Some of the experimental decay curves for our phosphor recorded at different temperatures are shown in Fig.3. In these experiments the phosphor was excited by light of high intensity; this value being arbitrarily taken as 100%.

It will be obvious from an examination of the curves that in going over to the thermoquenching region the character of the decay changes. Whereas near the quenching region an appreciable fraction of the light sums is emitted according to the hyperbolic law (curves a,b and c), upon going into the quenching region the exponential beginning section of the decay curve increases in extent with increasing temperature (curves d and e). At sufficiently high temperatures the decay becomes wholly exponential (curve f).

We determined the values of p from the slope of the straight line plots (in log I vs t coordinates) characterizing the exponential sections of the decay curves; then from the variation of p as a function of the temperature, as determined from a series of measurements, we calculated ϵ. The value found was $\epsilon = 0.32$ ev. The light sums emitted in the decay were determined planimetrically. In the region near temperature quenching the plot of log L vs 1/T is virtually a straight line, i.e., the regularity (3) holds. The value of ϵ obtained from the slope of these straight line plots was 0.310 ev.

The temperature dependence of the light sums in the region of thermoquenching of luminescence (with appropriate correction for the role of quenching processes) is also characterized by a straight line in log L vs 1/T coordinates. From the slope of this plot we found $\epsilon + \Omega = 0.80$ ev.

In another series of experiments we recorded the decay curves with the intensity of the exciting light reduced to 7% of the initial intensity. The series of curves obtained in this case are reproduced in Fig.4. Comparison of these curves with those for the case of 100% intensity excitation shows that the slopes of the hyperbolic sections are reduced and that the exponential sections appear at higher temperatures. Decay at 508°K in the case of excitation by 100% intensity light occurs wholly according to the exponential law, while with excitation by 7% intensity light the decay is only partially

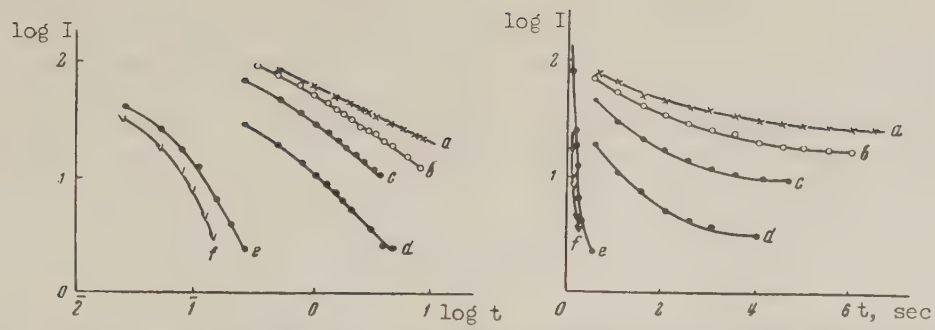

Fig.4. Decay curves for the ZnS:Cu phosphor at different temperatures (excitation at 0.07 E_{max}): a) 292, b) 360, c) 392, d) 460, e) 500, f) 508°K.

exponential while the tail of the curve is hyperbolic (curve f in Fig.4). We determined the values of ϵ and $\epsilon + \Omega$ from the data of Fig.4 in the same manner as previously. The respective values found were 0.34 and 0.75 ev.

The results of determination of the energy depths of the localization levels by the second method are summarized below.

	ϵ, ev
From the temperature dependence of the time constant of the exponentials	0.310
From the temperature dependence of the light sums near quenching:	
strong excitation	0.315
weak excitation	0.340
	$\epsilon + \Omega$ ev
From the temperature dependence of the light sums in the quenching region:	
strong excitation	0.80
weak excitation	0.75

From a comparison of the cited data it will be seen that the different methods of determining ϵ and $\epsilon + \Omega$ from the decay curves recorded at different intensities of the exciting light lead to results agreeing within 10%. Comparison of the results obtained for the electron localization energy with respect to the deepest group of levels by the methods of thermostimulation and from analysis of the decay curves shows that the determined values of ϵ agree within the limits of the experimental error.

Conclusions

1. We determined the energy required for releasing the electrons from the deepest localization levels (traps) by three independent methods: a) by analysis of the thermostimulation (glow) curves, b) by analysis of the luminescence decay of the phosphor in the region of temperature quenching and c) from the temperature dependence of the light sums in the region near that of thermoquenching of luminescence.

All three methods yield results agreeing within the limits of experimental error.

2. In the temperature interval in which the phosphor behaves as an ideal one (i.e., where the afterglow is due to release of electrons from localization levels of only one group) one can utilize the method of analysis of the decay curves for determining the energy depth of the given traps (see also Ref.7-8).

The writer desires to thank F.E.Vergunas for suggesting the subject of the investigation and aid in carrying it out.

Tomsk State University

References

1. W.Hoogenstraaten, J.Electroch.Soc., 100, 356 (1953).
2. V.V.Antonov-Romanovskii, Izv.AN SSSR, Ser.fiz., 10, 477 (1946).
3. Urbach Wien Ber. IIa, 139, 353 (1930).
4. I.V.Zhukova, Doklady AN SSSR, 103, 1001 (1955).
5. E.I.Adirovich, Nekotorye voprosy teorii liuminestsentsii kristallov (Some problems in the theory of luminescence of crystals) 1951.
6. F.I.Vergunas, Optika i spektroskopiia, 1, 416 (1956).
7. F.I.Vergunas & N.L.Gasting, Zhur.eksp.i teor.fiz., 28, 252 (1956).
8. V.V.Nuvar'eva, Dissertation, 1955.
9. V.A.Iastrebiv, Trudy (Transactions) FIAN, Physical Institute of the Academy of Sciences, 3, 123 (1946).

DISCUSSION FOLLOWING THE PRECEDING FOUR REPORTS

Ch.B.Lushchik: Do you consider that your treatment applies only to zinc sulfide phosphors or can the considerations be extended to other phosphors including alkali halide ones?

F.I.Vergunas: We did not investigate alkali halide phosphors. These may possibly have different characteristics. At present our deductions apply only to zinc sulfide phosphors.

M.V.Fok: According to your scheme where do radiationless transitions occur, in the luminescence center or outside it?

F.I.Vergunas: Nonradiative transitions do not occur in the luminescence centers inasmuch as in this case γ would not change with the temperature.

M.V.Fok: Perhaps this is recombination of a localized electron with a free hole?

F.I.Vergunas: I am not suggesting any definite mechanism for nonradiative transitions inasmuch as so far I have no experimental basis for this. I only assert that the kinetics of quenching is bimolecular.

M.V.Fok: You said that when the exciting light is turned on the bimolecular quenching mechanism begins to operate. Why does it cease operating when the exciting light is turned off? Does this occur abruptly?

F.I.Vergunas: Yes, apparently there is a jump. It is not clear at present why the kinetics of quenching change. In order to explain the experimentally observed regularities we were obliged to assume that the monomolecular type of quenching goes over into the bimolecular after cessation of excitation. We were forced to this conclusion by the experimental afterglow data. Perhaps further investigations will explain why this occurs.

V.V.Antonov-Romanovskii: For a nonradiative transition you write:

$$dn/dt = ANn - A_0Nn$$

where N is the electron concentration and n is the concentration of ionized luminescence centers.

You stated that you don't know where this occurs.

If you write A_0Nn for the number of recombinations with ionized luminescence centers without radiation, this means that the radiationless events occur in the luminescence center.

F.I.Vergunas: A possible picture is the following: a free electron may recombine with a center, settling on some level from which transitions with radiation occur; aside from that, the electron may recombine with a luminescence center, settling on some other energy level; from this second level it goes to the ground state without radiation. Recombination of the electron with the second level requires thermal activation.

Ch.B.Lushchik: How in your theory do you take into account hole processes in crystal phosphors? There can be no doubt that in a number of crystal phosohors hole processes play a substantial role. I understand that in your scheme you omit hole processes from consideration entirely. Why?

There are different possible methods for determining γ - not only from the decay, from which in fact it is difficult to do this. It seems to me that additional independent experimental evidence is necessary to support your principal argument that γ decreases with the temperature in the quenching region.

F.I.Vergunas: We have been measuring both the absolute values and the temperature dependence of γ, but these experiments have not yet been completed and hence we are not reporting on them. We determined the absolute values of γ from analysis of the decay curves. In order to determine γ, we had to know the probability of thermal release of localized electrons and the value of the light sums corresponding to different afterglow intensities. These quantities were determined experimentally. Near quenching γ proved to be greater than unity; in the quenching region γ decreased, approaching zero. We obtained this character of the temperature dependence of γ both with strong and weak excitation of the phosphor. We have not reported here on these results inasmuch as they still require further verification; that is, the experiments should be made not with just one phosphor but with several different ones.

We did not take hole processes into account. Possibly they do occur, but in ZnS phosphors they appear to have no significant influence on the decay regularities. The experimentally observed regularities are in agreement with the law deduced without taking hole processes into account.

N.A.Tolstoi: From what fraction of the steady excitation intensity did you start measuring the decay curves?

F.I.Vergunas: For all the phosphors except ZnS:Cu, the decay of which was recorded by means of an oscillograph, the measurements began 0.5-0.7 sec after cutting off the exciting light. In the case of ZnS:Cu:Co phosphors, the luminescence present in it remained constant for a brief interval after shutting off the exciting light and then began to decay. In the case of ZnS:Zn phosphor, we observed a jump in brightness, but at the moment I do not recall the magnitude of the change. For the ZnS:Cu phosphor prepared with NaCl flux the measurements were made by means of a multiplier tube and oscillograph. In this case the measurements of the decay began immediately after cutting off the excitation.

Ch.B.Lushchik: Have you any assurance that your thermostimulation peaks for ZnS:Cu are elementary ones? In the case of alkali halide crystal phosphors the glow curve peaks are so closely crowded together that they often overlap. Broad peaks have often been mistaken for elementary ones whereas

they are actually composite. Did you check to see whether the third peak is actually a single one?

F.I.Vergunas: The method proposed by V.V.Antonov-Romanovskii makes it possible to determine the depth of the electron localization levels. Analyzing the left and right parts of the curves we obtained values of 0.27-0.28 and 0.29 ev. From this it may be assumed that even if the peak is not an elementary one, the energies entering into its composition are close.

Ch.B.Lushchik: What do you think of the results of Bube, who for the same phosphors showed,at heating rates ten times slower than yours,that this peak develops structure, from which it follows that this peak is not an elementary one. It follows from the composite nature of the peak that in the process of emission, part of the trapping levels is not only displaced to the side of higher temperatures but also narrows.

F.I.Vergunas: We recorded the glow curves not only at a heating rate of 0.8 degree per sec but also at slower heating rates of the order of 0.2 degree per sec; at the slower rate we distinguished structure in the second peak but not in the third. The procedure employed in preparing the phosphor may be an important factor here. It may be that with one method of preparation this is a true elementary peak, while with another method structure may appear. It is possible that the phosphor used by Bube was prepared using a different procedure.

M.V.Fok: The last three reports we have heard are really three parts of a single report and my remarks shall apply to all of them as a whole.

I feel that the abrupt change of the quenching mechanism from monomolecular to bimolecular at the instant of cutting off the exciting light is altogether inexplicable. As is evident from the report, the exciting light does not act directly on the nonradiative transitions and hence there is no reason for the abrupt change in the quenching mechanism. On the other hand, the observed effect can possibly be explained by taking into account the presence of trapping levels of several different depths. As G.M.Eliashberg showed, in this case the decay must follow a complicated curve having an initial exponential section. That localization levels of different depths play a significant part is also evidenced by the different temperature dependence of the decay curves with different types of excitation (short-term and prolonged) even when the excitation intensity is the same. This shows that Adirovich's equation, used throughout by the authors of the reports, is not really applicable to the phosphors in question.

V.V.Antonov-Romanovskii: In addition to the remarks of M.V.Fok, I would like to note the following.

Adirovich's formula yields a curve differing from a second-order hyperbola only with an appreciable degree of filling of the trapping levels. Yet even at low temperatures the trapping levels are only partially occupied and at high temperatures the degree of filling will be even lower. Under these circumstances nothing but a second degree hyperbola can be obtained from Adirovich's formula.

I, too, feel that the abrupt change from one form of quenching to another at the instant of switching off the exciting light is strange and inexplicable. Further, the speakers assume that the quenching is internal, i.e., does not depend on the intensity of the exciting light. It must be recalled that in the region of temperature quenching nonlinear effects are extremely strong. Hence in the region of strong quenching one cannot ignore the motion of holes. For this reason I feel that the interpretation offered by the speakers is unacceptable.

G.M.Eliashberg: I would like to suggest that the agreement of the experimental decay curves demonstrated by the speakers with the theoretical decay law of Adirovich-Vergunas is only apparent. In the case of experimental curves the initial exponential decay goes over into a hyperbola of degree α, smaller than 2. The theoretical decay law yields exponential decay at the initial stages if γ, the ratio of the cross section for trapping to the cross section for recombination, is appreciably smaller than unity. Subsequently the exponential curve becomes a second order hyperbola. A fractional hyperbola with $\alpha < 2$ cannot be obtained with $\gamma < 1$. On the other hand, with $\gamma > 1$ there is no exponential section.

Another shortcoming of the theory is that the shape of the decay curve is determined only by the parameter γ and does not depend on the total trapping probability. The latter is proportional to the trapping cross section and the concentration of trapping levels.

F.I.Vergunas: Our concepts regarding the change in the kinetics of quenching at the instant of cessation of excitation appear to M.V.Fok to be ill-founded. This hypothesis was advanced in order to explain the observed experimental dependences. Further M.V.Fok considers that in our phosphors the intensity of the afterglow does not uniquely depend on the light sums and by the way of evidence cites the decay curves obtained with instantaneous or prolonged weak excitation. The decay curves were actually different but so were the initial light sums stored in the two cases. M.V.Fok and G.M.Eliashberg promised to explain the afterglow regularities observed by us on the basis of localization levels of two kinds, but in their remarks they have given no satisfactory explanation. Hence it is not clear to me whether one can explain both the qualitative and quantitative regularities observed by us from the viewpoint of localization levels of two kinds. Furthermore, we have no experimental basis for such an hypothesis: we observed only one peak in the thermostimulation curve when the phosphor was excited at room temperature or higher. M.V.Fok assumes that in recording our decay curves the intensity changed very little. This is not true for all the phosphors. In the case of ZnS:Cu:Co intensity changed by almost three orders of magnitude.

V.V.Antonov-Romanovskii considers that if one uses the concepts of Adirovich, then in the thermoquenching region, where the light sum is considerably smaller than the maximum possible light sum, one can obtain nothing but a second order hyperbola. As a matter of fact everything depends on γ; with γ close to zero, even with very small residual light sums an exponential section will be observed.

Ch.B.Lushchik considers that Adirovich's formula can be generalized to allow for the presence of hole processes and that this would give the elementary decay law. I feel that in determining the elementary decay low one must proceed from experiment. If the experimental results indicate that hole processes must be taken into account, then obviously they should be taken into account, but if there is no need to do this to explain the experimental regularities then obviously it is superfluous to allow for hole processes.

Ch.B.Lushchik infers that the increase in the parameter γ observed by him for alkali halide phosphors at temperatures below room temperature conflicts with our idea that γ decreases in the quenching region. The growth of γ observed by Lushchik can be explained by the necessity of activation of the localization process. This growth is not necessarily in conflict with the decrease of γ in the quenching region.

It can be asserted that in our phosphor there was no set of different localization levels. The depth of the levels proved to be the same as determined from analysis of the rising and from the falling parts of the thermo-

stimulation curves. Also, equal values for the depth of the localization levels were obtained from the variation of the light sums with strong and weak excitation. Consequently, the experimental evidence is that the decay is determined by levels of one depth.

In reply to G.M.Eliashberg I want to say that our plots of the theoretical dependences show that with $\gamma < 1$ the exponential curve at the far stages of decay goes over into a fractional hyperbola and not into a quadratic one. The decay law taking into account temperature quenching does not depend only on the parameter γ but also on the stored light sums. This is indicated by the transition of the exponential decay curve to a hyperbolic one as the intensity of the exciting light is reduced.

Ch.B.Lushchik: The method of determining γ at different temperatures to which I referred does not require knowing the number of trapping levels and the absolute value of the stored light sum. This is a direct absorption method that has nothing in common with the method of Siui Siui-iun (incidentally I feel that F.I.Vergunas' criticism of the latter method is partially justified).

Direct experiment yields a growth of γ with the temperature for alkali halide phosphors. In general, however, γ may either increase or decrease with temperature.

As Blokhintsev showed in 1945 the process of electron capture by a local level and the process of recombination may require an activation energy Q_c or Q_r. Hence we have $\gamma = \gamma_o e^{-(Q_c - Q_r)/kT}$. Consequently, whether γ increases or decreases with increasing temperature will depend on which of the activation energies is larger. In alkali halide phosphors Q_c is probably larger than Q_r. I feel that it is difficult to judge of the magnitude of γ from the decay laws. In general the basic premises of Vergunas' theory should be verified by more direct methods.

F.I.Vergunas: Ch.B.Lushchik observed that γ increases with the temperature in the case of alkali halide phosphors, but this does not conflict with our concepts inasmuch as his measurements pertain to low temperatures and not to the region of temperature quenching of luminescence, where according to our hypothesis γ should decrease with increasing temperature.

KINETICS OF THE INFRARED LUMINESCENCE OF CUPROUS OXIDE (Abstract*)

- N.A.Tolstoi, N.N.Tkachuk & R.K.Preobrazhenskii

Development of a new ultrataumeter procedure (a variant of the taumeter with electrooptical light modulation) made it possible to investigate for the first time the kinetics of luminescence of cuprous oxide. Investigation of the dependence of the luminescence relaxation time τ on the temperature and content of sur-stoichiometric oxygen showed the following. As the temperature is increased from -183° there occurs an anomalous rise of τ (from $5 \cdot 10^{-8}$ sec to $1\text{-}5 \cdot 10^{-6}$ sec). The growth of τ stops at about room temperature and with further heating τ tends to decrease (thermoquenching). Decreasing the oxygen content leads to a decrease in τ at all temperatures except the very lowest ones. In the case of some Cu_2O specimens there is observed at -130° a sharp maximum in the value of τ and the quantum yield of luminescence. The growth of τ with temperature can, in general, be explained from three points of view:

1) The mobility of the electrons decreases with increasing temperature; in consequence the time for recombination of electrons with luminescence centers is increased.

2) Electrons that have recombined with luminescence centers and formed excited centers are again ejected by the heat into the conduction band ("heat barrier"); the resultant delay in emission increases with the temperature.

3) The absorption mechanism is an exciton one (Zhuze, Ryvkin, Lashkarev and Karkhanin). Disintegration of the exciton on a charged acceptor leads to photoconductivity, while disintegration of the exciton on a noncharged acceptor leads to luminescence. If it be assumed that the exciton capture cross section is larger for a noncharged acceptor, then with increasing temperature the number of charged acceptors increases, the total exciton capture cross section for all centers decreases and τ increases.

Various considerations favor the last viewpoint. To obtain agreement with experiment, however, it must be assumed that luminescence occurs not as a direct result of disintegration of the exciton but after formation of an excited center with a lifetime of the order of $5 \cdot 10^{-8}$ sec. The energy required for excitation of the center is derived from the disintegration of the exciton.

DISCUSSION

Question: Did you observe changes in τ under different boundary conditions for the specimens in the sense of different impurities on the surface which are essentially boundary conditions for the exciton mechanism? If you apply the exciton mechanism, τ will depend not only on the interaction of the exciton with a center but also on the dynamics of the exciton. And how will this depend on the boundary conditions?

N.A.Tolstoi: Etching and grinding the surface of specimens sharply reduces τ. The influence of the state of the surface on the magnitude of τ comes down mainly to the influence of oxygen.

It is worth noting, however, that the oxygen has virtually no effect on the low temperature plateau in the variation of τ, consequently there is some factor that levels off τ; this plateau-producing factor is virtually independent of the composition of the specimens. Consequently, the luminescence relaxation time is connected not only with the "exciton" time but with some other "time" that appears to be the determining factor under most conditions.

---

*Complete report in Optika i spektroskopiia, 3, 116 & 210 (1957).

This is obviously the lifetime of the luminescence center formed after breaking up of the exciton.

B.P.Zakharchenia: The question of how the exciton interacts with a luminescence center recalls the more fundamental question: whether excitons exist in general? Doubts have been expressed whether the hydrogen-like series of absorption lines detected in cuprous oxide is associated with excitons. I would like to say a few words regarding some recently discovered properties of cuprous oxide and the possible existence of such quasiparticles (as excitons) in crystals.

G.F.Gross, N.M.Reinov and myself have recently obtained rather interesting information on excitons in cuprous oxide. The spectrum of cuprous oxide comprises a series of hydrogen-like absorption lines that appear near the absorption band of the crystal; these lines are extremely narrow at the temperature of liquid helium. It was found that in addition to the usual classical paramagnetic splitting of the exciton lines, there is observed a very interesting phenomenon characteristic of the exciton and in general peculiar to the absorption spectra of crystals. Namely, in addition to the ordinary Zeeman effect there is observed a shift of the Zeeman components to the short wave side of the spectrum, the shift being the greater the closer the lines to the short wave end of the spectrum. It was found that the displacement of the Zeeman components is proportional to the quantum number to the fourth power or the square of the exciton radius. This is a typical diamagnetic shift. Theoretically this effect is of a very small order of magnitude inasmuch as the speed of light enters into the denominator of the formula characterizing it; it must exist in isolated atoms. In the case of excitons this effect was observed for very large exciton radii. From the magnitude of the diamagnetic exciton shift we calculated the radius of the exciton for the level with the quantum number N = 5; it proved to be 200 A. According to Morse's model the radius of the exciton equals the dielectric constant multiplied by $h^2(\mu/r)$. Compared with an isolated atom the radius of the exciton is extremely large. In addition, the effective exciton mass which from our experiments proved to be 0.2 m_e, also has the effect of increasing the exciton radius.

Thus from these experiments on the Zeeman effects for the exciton it follows that in the exciton we are actually dealing with a system with two elementary charges - an electron and a hole - interacting according to Coulomb's law in a medium with a certain dielectric constant. Hence in the case of cuprous oxide one should seriously consider the exciton mechanism of luminescence; there can be no doubt that excitons play an important role in this mechanism.

N.A.Tolstoi: I would like to make a few remarks.

1. I would like to emphasize that the luminescence method of investigating photosorption has a number of advantages over other methods. Cuprous oxide is rather heterogeneous in the sense that different sections of specimens differ as regards their properties. By the luminescence technique it is possible to localize a very small spot or area and investigate the photosorption in different sections of the specimen.

2. Lashkarev cites as proof that the luminescence of cuprous oxide is of an exciton rather than electronic nature the fact that application of an electric field does not affect the luminescence efficiency. In collaboration with N.N.Tkachuk we carried out experiments by means of a more sensitive method, that is, by determinations of the relaxation time. We found that

even application of a 20,000 v/cm field has no influence on the relaxation time. Consequently, Lashkarev's hypothesis that in the excitation of cuprous oxide there are no free electrons and that excitons rather than electrons are responsible for the luminescence in this material is substantiated not only by luminescence efficiency measurements but also by relaxation experiments.

3. Investigation of the relaxation time, i.e., of the kinetics of luminescence, is of interest because luminescence, just as photoconductivity, occurs primarily in the thin layer near the surface. The state of the specimen in this superficial layer may be substantially different from the state in the depth of the specimen, that is, from the state that determines the electric conductivity and the Hall effect.

* * * * * *

SEMICONDUCTOR PROCESSES IN ORGANIC DYE LAYERS (Abstract*)

- A.T.Vartanian

Extensive studies of the electric and photoelectric properties of dye layers have shown that dyes should be regarded as a special class of organic semiconductors. The temperature dependence of the electric conductivity of many dyes can be described by the formula

$$\sigma = \sigma_o \exp (- \epsilon_c/2kT)$$

The values of the activation energy ϵ_c for trypaflavine, eosin, erythrosine, phloxin, pinacyanol and phthalocyanines are 2.28, 2.13, 2.15, 2.08, 1.8 and 1.6 ev, respectively. In all cases the energy is close to the corresponding long wave absorption limit. The conductivity of these layers is intrinsic. For a number of other dyes the activation energy ϵ_c is appreciably lower than that corresponding to the absorption edge. The conductivity of layers of these dyes is apparently extrinsic.

The temperature dependence of the photoconductivity also obeys the exponential law, but the corresponding activation energy ϵ_p is only a fraction of ϵ_c. For example, for trypaflavine $\epsilon_p = 0.53$; for pinacyanol 0.43; for erythrosine 0.5 ev, etc.

Under vacuum the variation of the photocurrent i_p with the intensity of illumination L is given by the formula

$$i_p = \alpha L^n,$$

where n is constant for any given layer. Depending on the state of the layer n may vary between 0.5 and 1.0. The spectral curves characterizing the relative photosensitivity, calculated per unit incident energy taking into account the dependence of the photocurrent on the illumination intensity ($i_p^{1/n}/L$) are in good agreement with the spectral absorption curves.

The photoconductivity of eosin, erythrosine, phloxin, phthalocyanines and some other dyes increases in the presence of oxygen. In the presence of oxygen the variation of the photocurrent with the illumination intensity still follows the law given above but the value of n is smaller.

---

*Complete report published in Trudy (Transactions) of the Physical Institute of the Academy of Sciences of the Estonian SSR, 1957.

The concept of the long-wave limit of photoconductivity has been introduced to characterize semiconductors. According to Moss the long-wave limit may be defined as the wavelength $\lambda_{1/2}$ for which the sensitivity is half the sensitivity at the maximum preceding the exponential falling off of the curve. In collaboration with I.A.Karpovich we have shown that the steep long wave side of the relative photosensitivity curve is described by the exponential law. The developed procedure was used for determining the optical activation energy $E_{\lambda_{1/2}}$ of a number of dyes. For example, for trypaflavine and erythrosine we obtained 2.3 and 2.1 ev, respectively, values that are consistent with those of the thermal activation energy. For determining the optical activation energy, we also used the method of "photoelectric straight line plots". In order to find the optical activation energy by this method it is essential to take into account the "nonlinearity" of the dependence of the photocurrent on the illumination intensity. Using the method of "photoelectric straight line plots" we obtained a value of 2.35 ev for trypaflavine ($n = 1$) and 2.14 ev for erythrosine ($n = 0.66$). These values are in good agreement with the above cited values of $E_{\lambda_{1/2}}$ for these dyes.

The determined regularities and activation energy values should serve as a reliable point of departure for further investigation of the photoelectric properties of dye activated organic phosphors.

DISCUSSION

V.A. Iastrebov: I do not agree with the speaker that the semiconductor mechanism is in no way involved in the processes occurring in the phosphors.

I have had occasion to measure the phosphorescence decay of about twenty organic substances. A distinctive feature of these measurements was that the decay was measured for a range of intensities varying by a factor of several million. I came to the conclusion that the decay law cannot be satisfactorily described in the framework of the monomolecular model. The results of these experiments have already been published. I proposed the following model: there obtains a recombination process followed by emission (de-excitation) from a metastable or excited state.

The unique character of the decay of organic substances as compared with the decay of ordinary semiconductors stems from the fact that the lifetime of the excited states formed after recombination is very short compared to their lifetime in ordinary crystal phosphors. Thus semiconductor concepts can safely be extended to phosphorescence phenomena.

A.T.Vartanian: I do not negate the semiconductor properties of organic dye layers. On the contrary, in all my work I have tried to show that organic dye layers are a class of organic semiconductors. I only feel that so far we do not have sufficient experimental justification for applying the concepts of the band theory of inorganic semiconductors to colored gelatin or colloidal films.

INFLUENCE OF ADSORPTION OF GASES ON THE LUMINESCENCE OF ZINC OXIDE (Abstract*)

- K.V.Tagantsev & A.N.Terenin

Our experiments showed that dry oxygen has a quenching influence on the luminescence of zinc oxide "aged" under vacuum at 200°. Admission of water vapor into the test chamber also produces quenching. Oxygen and water vapor together have a very strong quenching effect. The magnitude of the quenching depends on the duration of illumination. In the case of prolonged illumination there is observed reversible excitation of the quenched luminescence. Gaseous oxygen subjected to an electric discharge produces very strong quenching. Under continuous illumination there occurs reversible stimulation of the quenched luminescence. Quinone vapor at low pressure also quenches the luminescence of zinc oxide. Again under steady illumination reversible stimulation is observed.

The observed effects can be interpreted on the basis of electron capture by electrically negative adsorbed molecules.

"A.A.Zhdanov" Leningrad State University

DISCUSSION

V.L.Levshin: I would like to know to what extent the described effect can be expected to occur in other substances; I have in view oxides, including ZnO, with activators. If this effect is general, this may be very important where technical applications are concerned.

K.V.Tagantsev: I tried to work with ZnO activated with copper. Generally similar effects were observed, but I am reluctant to say anything definite inasmuch as they were very weak, in fact, within the limits of the experimental error.

F.F.Vol'kenshtein: It would appear that oxygen acts in different manners; you said that "activated" oxygen produces stronger quenching. What precisely is "activated" oxygen?

K.V.Tagantsev: In this case "activated" oxygen is apparently ozone.

Question: I understand you aged your specimens at temperatures from 200 to 400°. What was the effect of higher temperatures?

K.V.Tagantsev: In almost all the experiments we used 200°; only in a few cases was the temperature 400°. In these cases the quenching persisted, but was somewhat more pronounced.

V.I.Vergunas: The emission spectrum of ZnO contains two bands, a green and a yellow one. Were both bands equally quenched?

K.V.Tagantsev: We observed only the integral luminescence.

F.F.Vol'kenshtein: According to the report, adsorbed oxygen produces quenching of the luminescence; O_2 appears to be less active than O_3. Why? What must be done to a crystal to obtain luminescence? One must introduce an acceptor into the crystal, i.e., create electron traps. The electrons caught in these traps do not participate in the de-excitation. Any molecule localized on the surface and having electron affinity must rise to surface acceptor levels and thus plays the role of an electron trap. Electron traps arising on the surface as a result of adsorption perform the same functions as traps in the bulk of the crystal formed through the introduction of acceptor impurities into the crystal.

---

*Complete article in Optika i spektroskopiia, 2, 355 (1957)

Why does adsorption of ozone lead to a stronger effect than adsorption of oxygen? The O_3 molecule has a greater electron affinity than the O_2 molecule. This means that the O_3 levels lie below the O_2 levels and obviously the lower the acceptor levels, the greater the degree of occupation of these levels by electrons (other conditions being equal). Thus by replacing a given number of O_2 molecules by an equal number of O_3 molecules, we increase the number of electrons localized on these molecules. Consequently, replacement of oxygen by ozone must intensify the quenching. This is obviously the explanation for the difference in the quenching effects of oxygen and ozone.

I.A.Miasnikov: Regarding photosorption of oxygen. We found that in the case of prolonged illumination of zinc oxide in the presence of alcohol vapor stronger oxidation is observed than in the dark. Further, we found that the kinetics of adsorption of oxygen on zinc oxide differs in the presence as against the absence of light: in the presence of light the oxygen is adsorbed appreciably more rapidly and the process is to a certain extent irreversible. This indicates that the oxygen adsorbed on the surface under the influence of light is in an excited state. We determined that the oxygen enters into a reaction under the influence of light by means of a crystal pressure gage. Having constructed such a sensitive crystal analyzer, we measured the processes of photodesorption and not only detected the presence of photodesorption but also a decrease in the concentration of oxygen in the presence of alcohol vapor.

As regards the adsorption of ozone. Here one should perform a direct experiment: prepare pure ozone and investigate the luminescence or electroconductivity incident to the adsorption of ozone on the zinc oxide. This should help clarify the mechanism involved.

Now as for what F.F.Vol'kenshtein said. The same results can be interpreted by means of the laws of thermodynamic equilibrium between the excess zinc ions, which may be regarded as absorption centers, electrons and oxygen or ozone in the gaseous phase. We know that ozone decomposes readily at room temperature. Probably the ozone decomposes into oxygen in the adsorbed layer and obviously this should be evinced in measurements of the luminescence. If this process does not occur then this must be a reversible effect, but I did not observe any evidence of reversibility.

ON CANDOLUMINESCENCE OF CRYSTAL PHOSPHORS (Abstract*)

- V.A.Sokolov

V.M.Kudriavtseva, G.I.Siniapkina and the writer in a series of contributions have shown that so-called candoluminescence of a number of oxides can be satisfactorily explained on the basis of ordinary laws of thermal radiation. The success of these contributions has led certain authors to the premature conclusion that true candoluminescence does not exist under any circumstances.

There are, however, cases of thermal emission of substances, particularly under the influence of a flame (for example, erbium oxide and boron nitride activated with carbon) which cannot be satisfactorily explained by the laws of thermal radiation. It is interesting to note that most substances with which candoluminescence is associated are crystal phosphors containing activator centers (excess metal atoms or other) of some type. The writer believes that inasmuch as there does exist thermoluminescence, wherein electrons are thermally released from traps into the conduction zone as the first step in the luminescence process, there is no good reason to deny the possibility of direct excitation of luminescence centers in a phosphor by thermal vibrations of the lattice.

Evidence of the interaction of electron transitions with lattice vibrations is furnished by the vibrational structure of the photo- and candoluminescence spectra of certain crystalline substances (for example, ZnO and MgO) observed by a number of investigators including the writer.

As a result of the writer's experiments on thermal excitation of certain crystal phosphors (ZnS:Mn, ZnS:CdS:Cu and others) there were obtained thermal emission spectra containing secondary maxima corresponding to the region of photoluminescence of these substances. This is direct proof of the possibility of thermal excitation of activator centers. The emission component appearing in these cases, however, is apparently only the luminescence component of the equilibrium thermal radiation inasmuch as purely thermal excitation of true luminescence as an excess over the temperature radiation of the given body would be in conflict with the second law of thermodynamics.

In the cases of candoluminescence when the presence of this excess radiation has been definitely established, it must be assumed that in addition to the thermomechanism there exists another mechanism of excitation of the activator centers (possibly chemical processes, optical self-excitation or other).

Elucidation of the additional or other mechanism should be the primary problem in the investigation of true candoluminescence, individual cases of which appear to be experimentally established facts.

Note added in proof. New experiments carried out by the writer with the use of an isothermal box (suggested by M.V.Fok) definitely disproved the possibility of purely thermal excitation of candoluminescence. At the same time, recently the writer definitely established that luminescence of some crystal phosphors under the influence of a flame may actually occur. But this effect can be observed only till the phosphor is heated to the temperature of thermoquenching of luminescence. In order to avoid this quenching the writer used a slowly rotating brass cylinder filled with a cooling mixture. The luminophor applied to the outside of the cylinder was passed through the outer part of a colorless Bunsen burner flame; under these conditions the luminophor can be excited for a prolonged time, i.e., as long as the cooling is in effect. Visible thermal emission of the phosphor under these circumstances is precluded. The spectra of such luminescence are entirely similar

---

*The complete report is printed in the "Proceedings (Materialy) of the Fifth Conference on Luminescence", Tartu, 1957.

to the spectra of photo- and candoluminescence of the same substances. The true cause of this candoluminescence is apparently bombardment of the phosphors by the electrons and ions of the flame that have a sufficient energy to excite luminescence.

Tomsk Polytechnic Institute

DISCUSSION

M.N.Alentsev: I feel it necessary to make certain observations regarding candoluminescence. The importance of careful analysis of the experimental data stems from the fact that thermodynamically "pure" candoluminescence is impossible. If a body could, as a result of purely thermal processes, emit in some region of the spectrum more energy than the black-body radiation corresponding to the given temperature, then by placing this body in a closed mirrored box together with another absolutely black body at the same temperature, we would obtain heating of the black body which would, of course, be contrary to the second law of thermodynamics.

Hence the great importance of the work of V.N.Kudriavtseva and her coworkers who proved the thermal character of the radiation in the experiments where so-called "candoluminescence" was observed. The importance of Kudriavtseva's work was repeatedly emphasized by the late S.I.Vavilov. In this connection I would like to make a remark on the specific content of Sokolov's report. As proof of the existence of actual "candoluminescence" in individual cases he cites the approximate agreement of the "candoluminescence" spectrum with that of ordinary luminescence. This is not convincing inasmuch as in most cases luminescence spectra are located near the long-wave limit of the absorption band, while thermal radiation, according to Kirchoff's law, should also be concentrated in the vicinity of the long-wave absorption limit due to the sharp increase in the energy of black-body radiation with increasing wavelength.

M.V.Fok: In my opinion the experiments described by the speaker are not convincing and do not prove the existence of candoluminescence. Measurement of the temperature of the black substance and of the luminophor by means of thermocouples is not sufficiently accurate. The coincidence of the maxima in the spectra of photo- and candoluminescence in itself proves little, inasmuch as it may be fortuitous. If one subtracts the background of thermoluminescence against which candoluminescence is observed, the maximum will be displaced to the side of shorter wavelengths and will no longer coincide with the photoluminescence peak. Furthermore as M.A.Alentsev noted, purely thermal excitation of luminescence conflicts with the second law of thermodynamics.

One should attempt to observe candoluminescence by placing the luminophor in a cavity isothermal with it. Then the equality of temperatures will be maintained automatically and far more accurately. In this case it will be easier to observe the difference, if any, between the radiation of the absolute black body (box or cavity) and the luminophor.

V.A.Sokolov: I want to recall that my previous contributions were devoted to disproving the existence of candoluminescence and to explaining cases of presumably observed candoluminescence on the basis of the characteristics of thermal radiation. I would be highly pleased if all reported cases of candoluminescence without exception could be explained in this manner.

Unfortunately, there are facts that do not fit into the thermal radiation scheme. Hence it is possible that Nicolls' numerous investigations of cando-

luminescence are not all entirely erroneous and that they contain grains of verity that we have failed to take into account.

I am entirely in agreement with the remarks of M.A.Alentsev and M.V.Fok, particularly since in my report I noted that purely thermal excitation of candoluminescence is contrary to the laws of thermodynamics. It may be that some cases of violation of Kirchoff's law and, consequently, apparent violation of the second law of thermodynamics are connected with the presence of negative luminescence hypothesized by Stepanov and Fok. So far we have not made a search for negative radiation; apparently experiments along this line should be undertaken.

LUMINESCENCE OF SOME "PURE" SALTS

- V.A.Arkhangel'skaia & P.P.Feofilov

At the temperature of liquid air the luminescence spectra of some non-activated salts (HgI_2, PbI_2, AgI and CdS) consist of a series of bands, the width of which systematically increases towards the long wave side of the spectrum. The shortest wave narrow bands (half-width of the order of 1 mμ) are situated immediately next to the long wave narrow absorption bands characteristic of the salts.

The relative intensity of the individual bands in the luminescence spectrum of a given substance depends on the intensity of the exciting light. The intensity of the short wave bands (including the narrow ones) increases more rapidly than in direct proportion to the excitation intensity: i.e., $I \sim E^{\gamma}$, where $\gamma > 1$, while for the long wave bands, $\gamma \leqslant 1$.

The narrow luminescence bands of HgI_2 and CdS single crystals are fully polarized in the direction perpendicular to the optical axis of the crystals. The longer wave bands are also partially or fully polarized in the same direction.

The kinetics of luminescence of the investigated salts is typical of crystal phosphors. Luminescence processes systematically slow down in going to longer wavelengths. Persistence of luminescence in the narrow band does not exceed 10^{-6} sec, whereas in the long wave bands it may attain 10^{-4} sec.

Investigation of the spectra and the polarization of the narrow emission bands shows that they are associated with the same electron transitions as the narrow bands in the absorption spectra, i.e., that the emission is of a resonance nature.

Narrow bands in the absorption spectra of the investigated and similar "pure" salts are now commonly associated with the formation of excitons (Gross, Nikitin). In the light of this interpretation it must be assumed that the narrow bands in the emission spectra are due to break down of the exciton state. This interpretation, however, cannot be considered definitive inasmuch as a number of investigators (Kokhanenko, Shalimova and others) with some justification ascribed the narrow bands of "pure" salts to the sur-stoichiometric metal atoms.

DISCUSSION

A.A.Shishlovskii: What is the role of crystallization water and dissolved gases in these salts? Cannot the universal character of the effect be ascribed to either or both of these?

V.A.Arkhangel'skaia: These substances as chemical compounds do not contain bonded on crystallization water. As for dissolved gases, their influence was actually observed. In speaking of these salts as "pure" we mean that they contain no extraneous metal ions.

Question: To what extent may the luminescence be self-activated? In zinc and silver such luminescence is often pronounced.

V.A.Arkhangel'skaia: The concentration of whatever activators might have been present was not measured. The specimens were prepared by different procedures but in all cases the position of the bands was the same.

LINE LUMINESCENCE NEAR THE PRINCIPAL ABSORPTION EDGE OF CRYSTALS (Abstract*)

- A.A.Kaplianskii

The present communication is devoted to the work on luminescence of crystals carried out under the supervision of E.F.Gross in the Optical Laboratory of the Physical-Technical Institute. The excited (exciton) states of crystals were investigated by the spectroscopic method. The line structure of the absorption observed near the long wave absorption edge of a number of crystals is associated with the formation of excitons in the crystal lattice. Of interest, too, is the reverse process: the process of annihilation of an exciton with emission of a photon. In connection with this we investigated the luminescence of crystals possessing a discrete exciton structure at the absorption edge. Luminescence spectra of these crystals were studied primarily at 4.2°K and 77.3°K.

As a first step, an attempt was made to observe the luminescence of excitons in a Cu_2O crystal whose spectrum comprises a hydrogen-like series of absorption lines. In the case of Cu_2O, however, it proved possible to observe only the familiar infrared luminescence in the 1 μ region.

In the emission spectra of HgI_2 single crystals, however, there were detected at 4.2°K two narrow luminescence bands[1] which as regards their position (5324 A and 5352A), polarization ($E \perp c$) and relative intensity corresponded to the two absorption lines at 5296 A and 5321 A observed at 4.2°K at the principal absorption edge of HgI_2.[2] By means of a high dispersion spectrograph it proved possible to establish that the 5324 A line is a doublet ($\Delta\lambda$ = 3.5 A) and to detect an additional series of adjacent weak lines: λ = 5305, 5328 and 5339 A. It should be noted that the principal 5324 A line of HgI_2 is characterized by pronounced asymmetry (opposite for absorption and emission). Experimental data indicate that the line emission of HgI_2 appears as a result of transitions that are the reverse of the transitions responsible for the absorption of light in the lines, i.e., that we have here a resonance effect.

Investigation at 4.2°K of the luminescence of a $CuHgI_4$ crystal, the lattice of which contains the Hg group characteristic of HgI_2 centered in a tetrahedron of four I ions, disclosed the presence of line emission consisting of at least 11 lines (the most intense are the lines located at 5474, 5480, 5495 and 5520 A). Judging from the reflection spectra from Cu_2HgI_4, this emission is also of a resonance nature.

Investigation at 4.2°K of the luminescence of PbI_2 crystals (initially discovered at 77.3°K by Arkhangel'skaia and Feofilov[3]) enabled us to bring out new features of the emission spectrum. At 4.2° the luminescence spectrum of PbI_2 consists of several groups of lines. The highest frequency group comprises an intense line (triplet) at 4970 and two weak lines at 4962 and 4985 A. The 4970 A line corresponds apparently to the same electron transition as the strong absorption line at 4948 and is a resonance line. Next, moving to the long wave side, we have a group of emission bands (centered at about 5015 A) that has no counterpart in the absorption spectrum. Finally, we find a long wave group consisting of four equidistant bands in the region from 508 mμ. The frequency difference between these bands Δ = 67 cm^{-1}; the intensity of these bands decreases monotonically going towards the red side of the spectrum. Thus this equidistant emission of PbI_2 exhibits the distinctive features of so-called "edge emission" detected in a number of other crystals (CdS, ZnS and ZnO).

---

*Complete article in "Optika i spektroskopiia", 2, 107 (1957).

Observations of the absorption of CdS at 4.2°K disclosed the presence of a complex line structure in the absorption edge[4]. Comparison of the position of the familiar luminescence lines of CdS with the position of the absorption lines carried out by Gross & Iakobson[5] (analogous comparisons have also been made by Grillot[6] and Arkhangel'skaia & Feofilov[3]) showed that part of the short wave, blue luminescence lines can be matched with absorption lines, i.e., that in this case, too, we have resonance emission.

Gross & Sobolev[7] detected discrete structure in the 665-680 mμ interval in the adsorption edge of CdSe (at 4.2°K). They also investigated the luminescence of CdSe crystals and showed that there are present in it emission lines analogous to the blue luminescence of CdS; part of these lines correspond to absorption lines, i.e., are resonance lines. In addition, these investigators detected in the emission spectrum of CdSe an equally separated group of lines ($\Delta\nu$ = 182 cm^{-1}) in the 710-750 mμ interval; this emission group is analogous to the "green" luminescence of CdS.

Certain regularities may be deduced from the above results. The spectra of all the investigated crystals (HgI_2, CdS, PbI_2 and CdSe) are characterized by line structure at the absorption edge. The luminescence spectra of these crystals comprise narrow lines that may be identified as resonance lines with respect to absorption lines. As a rule these are distinguishable in the resonance emission lines corresponding only to the shorter wave absorption lines. It is also interesting to note the general similarity in the character of the luminescence spectra of PbI_2, CdS and CdSe crystals. In addition to the resonance lines these spectra include a group of emission lines, that have no or only very weak corresponding lines in the absorption spectra, and a long wave equidistant group of bands ("edge emission"). It would appear that the observed character of the luminescence spectrum, located near the absorption edge of crystals, is common to a number of materials. The experimental data indicate, too, that the spectral composition of this emission is very complicated and that the different components of the observed structure may have different origins.

If the line structure of the absorption edge is interpreted on the basis of the exciton model, it must be assumed that the resonance emission lines are due to exciton luminescence, i.e., to photons liberated in the annihilation of the excitons. As for the "edge" emission, its nature is as yet unclear.

It may be noted that we also observed resonance emission lines in the emission spectra of the crystals of a number of copper halides that exhibit narrow lines in their absorption spectra (these absorption lines have been attributed by Shalimova & Mendakov[8] to stoichiometrically excess copper atoms). Thus in the emission spectrum of CuCl, investigated primarily in the form of inclusions in NaCl crystals, we observed (in addition to the familiar luminescence band of Cu^+ in NaCl) two narrow bands at 3848 and 3765 A that coincide exactly with the corresponding absorption bands of CuCl (they are even self-reversed due to reabsorption)[9]. Similar resonance emission has been observed by B.S.Razbirin from CuBr and CuI crystals. These results are in conflict with the deductions of Shalimova & Mendakov[8], according to whom, the emission of copper halide crystals that is associated with electron transitions which are the inverse absorption transitions consists of wide bands in the visible region of the spectrum.

References

1. E.F.Gross, A.A.Kaplianskii & B.V.Novikov, Zhur.tekh.fiz., 26, 697 (1956); Doklady AN SSSR, 110, 761 (1956).
2. E.F.Gross & A.A.Kaplianskii, Zhur.tekh.fiz., 25, 2061 (1955).
3. V.A.Arkhangel'skaia & P.P.Feofilov, Doklady AN SSSR, 108, 803 (1956); Optika i spektroskopiia, 2, 107 (1957).
4. E.F.Gross & M.A.Iakobson, Doklady AN SSSR, 102, 485 (1955).
5. E.F.Gross & M.A.Iakobson, Zhur.tekh.fiz., 26, 6 (1956).
6. C.R.Grillot et. coll., 242, 1794 (1956).
7. E.F.Gross & V.V.Sobolev, Zhur.tekh.fiz., 26, 7 (1956).
8. K.V.Shalimova & N.S.Mendakov, Zhur.eksp.i teor.fiz., 26, 248 (1954).
9. E.F.Gross & A.A.Kaplianskii, Optika i spektroskopiia, 2, 204 (1957).

* * * * * *

LUMINESCENCE OF SILVER HALIDE SALTS

- S.I.Golub

Luminescence of pure silver halide or mixtures thereof can be observed in the case of powdered salts, single crystals and sublimates as well as of ordinary photographic emulsions on cooling to below -100°. The emission consists of more or less bright fluorescence and in some cases of a weak short-lived (of the order of one or a few seconds) phosphorescence.

In the luminescence excitation spectrum of silver chloride and bromide there is a maximum only at 375 mμ.

The emission spectrum of pure powdered silver chloride at -183° consists of one blue band peaking at 840 mμ. When the chloride is melted in air there appears a new band, a red one. If the melt is rapidly cooled, the blue band is suppressed. Consequently, it may be concluded that the blue band is associated with the crystal lattice, while the red band is due to a stoichiometric excess of silver.

Pure silver chloride crystals also have one blue luminescence band. Its intensity decreases as a result of plastic deformation of the crystal. This effect is slowly dissipated with time at ordinary temperatures and rapidly if the crystal is heated. These facts are also evidence that the blue band pertains to the crystal lattice.

Pure silver bromide has a green luminescence band which develops fully when the bromide is cooled to -250°. Brief heating of an AgBr specimen in air to a temperature close to the melting point, resulting in the formation of an excess of silver, leads to the appearance of an orange band that normally develops at -183°.

Mixed AgCl + AgBr and AgCl + AgI single crystals exhibit a gradual displacement of the luminescence bands to the side of longer wavelengths with increasing concentration of the second component. The addition of AgI to AgBr greatly stimulates the development of luminescence at -183°. The green band appearing in this case is also displaced to the side of longer wavelengths as compared with its position in the luminescence spectrum of pure AgBr.

Single crystals of AgCl + $MnCl_2$ (0.01 to 0.1 mole %) yield a bright red band which is excitable at a higher temperature than the blue band. There is redistribution of energy between the two bands with increasing temperature. This red band must be attributed to excess silver.

Silver chloride sublimates may simultaneously exhibit three luminescence bands: a blue, a green and a red. Treatment of the sublimate layers with $HgCl_2$ reduces the intensity of the red and green bands. It may therefore be concluded that the red and green luminescence centers are surface centers of metallic silver. Similarly, when photographic emulsions are treated with $HgBr_2$ their green luminescence band is greatly weakened. This indicates that the associated centers are also surface centers of metallic silver.

Inasmuch as the short wave bands are present in the luminescence of silver halide salts without a stoichiometric excess of silver, their centers are obviously more closely associated with the crystal lattice than the centers responsible for the long wave bands. It may reasonably be hypothesized that the short wave band centers are Frenkel type lattice defects.

The luminescence of AgCl and AgBr + AgI (~1 mole %) decays according to the hyperbolic law with a fractional exponent: $I = At^{-\alpha}$, where $\alpha = 0.25$. This indicates that the emission process is a recombination one and that silver halide salts should be classed with crystal phosphors activated with heavy metals.

The luminescence efficiency of silver halide salts may have a rather high value: 0.6 for AgCl and 0.8 for AgBr + AgI. The efficiency remains constant over the temperature range for -80 to -253°. This speaks in favor of the assumption that the absorption of the exciting light occurs primarily in the host material rather than in the activator.

"I.I.Mechnikov" Odessa State Institute

DISCUSSION

A.A.Shishlovskii: Could you not give a more convincing argument than references to the theory of Adirovich that the temperature independence of the efficiency substantiates the hypothesis that the absorption occurs primarily in the host material rather than in the activator?

S.I.Golub: We investigated the kinetics of this process in detail; I may note that there are other experimental investigations in which it is shown that in cases when the absorption occurs in the activator there is a decrease in efficiency at low temperatures and that when the exciting radiation is absorbed by the host material no such decrease of the output occurs.

A.A.Shishlovskii: Analysis of the results given in the report shows that crystal phosphors with an "internal" activator (i.e., a stoichiometric excess of the host lattice metal) and with an extraneous activator do not differ in any way in principle. One must approach the interpretation of spectral bands and the nature of luminescence centers with caution inasmuch as the same ions or atoms may yield different spectra, depending on the short-range order.

ON EFFECTS OBSERVED IN ALKALI HALIDE PHOSPHORS UNDER THE INFLUENCE OF INTERMITTENT LIGHT (Abstract*)

- I.A.Parfianovich

Under the influence of x-rays there form in the alkali halide phosphors KBr:Ni, KCl:Tl and NaCl:Ni at room temperature electron centers characterized by different degrees of thermal stability. The most stable among these centers are F-centers. In phosphors excited at elevated temperatures only F-centers are present. Under the influence of light in the F-band all the enumerated phosphors yield a light flash. In addition to recombination of the electrons released from the F-centers with the ionized luminescence centers, there also occurs a partial transition of the electrons to shallower trapping levels. The centers forming in this case are less stable than F-centers and are thermally ionized at room temperature. In KBr:Ni and KCl:Tl there are formed centers that completely disintegrate at room temperature within a few seconds, whereas the lifetime of the corresponding centers in NaCl:Ni at the same temperature is measured in hours.

In investigating the optical stimulation of these phosphors under intermittent light in the region of the F-band, we detected the effect of an increase of brightness of the flashes after a dark interval. This effect is observed in the case of KCl:Tl at room temperature. The magnitude of the effect varies with the temperature and increases if the phosphor is heated during the dark interval.

In NaCl:Ni the effect is observed only when the temperature is raised to about 100° after turning off the stimulating light.

In addition to this effect we observed another phenomenon in KBr:Ni and KCl:Tl, namely, an increase in the brightness of phosphorescence after cessation of the action of light in the F-band. In other words, after the stimulating light is cut off for some time, the brightness of the afterglow not only does not decrease, but on the contrary, increases. At constant temperature the afterglow goes through a maximum and then monotonically decreases.

We established that both effects are connected with the disintegration of relatively unstable electron centers forming as a result of the influence of light in the F-band region on the excited phosphor. The intensity of the flash varies with the concentration of the unstable electron centers. The rise in flash brightness is observed only after disintegration of the low stability centers. Thus it is evident that the two effects have a common cause. The luminescence intensity I can be described by the expression

$$I = AgN\eta,$$

where A is a quantity proportional to the effective cross section of an ionized luminescence center for electron capture, g is the relative probability of transition of an excited luminescence center to the ground state, N is the concentration of electrons in the conduction band and η is the concentration of ionized luminescence centers.

It follows from the above expression that I will change when any of the quantities in the right hand side of the equation change. One can hardly doubt the invariance of A and g under the conditions of our experiment. Thus we come to the conclusion that the increase in I is due to changes in η or N

---

*Complete report in "Optika i spectroskopiia" 2, 392 (1957).

or both. The question of which predominates and the kinetics of the rise in luminescence process in general will be considered in another report.

"A.A.Zhdanov" Irkutsk State University

DISCUSSION

Ch.B.Lushchik: The data cited by I.A.Parfianovich are of great interest. In connection with them I would like to make one comment.

Hitherto in work on the kinetics of crystal phosphors it has been implicitly assumed that the trapping levels in a phosphor are unchangeable and that all relaxation processes reduce to migration of electrons and holes. However, as has been directly shown for alkali halide phosphors, in addition to hole-electron processes, in phosphors even at room temperatures there may also occur ionic processes associated with displacements of microdefects of the crystal. The very interesting effect observed by I.A.Parfianovich, namely, the nonmonotonic variation of the brightness after stimulating light is cut off, may be connected with ionic processes. Microdefects from which the light has detached electrons may move through the crystal and associate with other trapping centers, increasing their number; this may be the cause of the flare-up of luminescence.

Certain other effects observed by V.Karkov in his work on the thermostimulation of crystal phosphors may also be connected with ionic processes. The role of ionic processes is probably important not only in alkali halide crystals but also in ZnS phosphors. I believe that these processes should be taken into account in interpreting experimental data.

ON THE QUENCHING OF ZnS:Cu:Co and ZnS:Cu:Ni PHOSPHORS BY INFRARED LIGHT (Abstract*)

- L.A.Vinokurov & M.V.Fok

Infrared light has both a stimulating and a quenching effect on ZnS:Cu:Co and ZnS:Cu:Ni phosphors. We found that at a constant intensity of the infrared light the dependence of the luminance I on the excitation intensity E is characterized by $I \sim E^{3/2}$. As regards the afterglow, the influence of red light leads to decay characterized by a second order hyperbola.

The usual external quenching scheme does not explain these regularities inasmuch as it gives exponential decay ("monomolecular" decay) and the relationship $I \sim E^2$. These regularities are obtained on the assumption that a hole having moved from the activator into the valence band cannot return and must necessarily enter into recombination with a localized electron.

We carried out a calculation of the steady brightness and the decay of the phosphor for the case when the hole in the valence band has a greater probability of returning to the luminescence center than of recombining with a localized electron. On this basis we obtained a formula explaining the experimentally observed dependence of the luminance on the excitation intensity and the hyperbolic rather than exponential character of the decay.

On the basis of the same calculations we were also able to explain the effect of Co and Ni as quenching agents and to show that in the case of not excessively strong quenching, when the efficiency is reduced by a moderate factor, a horizontal plateau should appear in the curve of the luminescence yield vs the excitation intensity, as is in fact the case when Co is introduced into the phosphor.

"P.N.Lebedev" Physical Institute of the
Academy of Sciences of the USSR

DISCUSSION

F.I.Vergunas: Why do you still obtain a hyperbolic decay law? According to your quenching scheme an electron from a lower band rises to the activator hole, while an electron from a local level descends to the hole remaining in the valence band. This "rise" characterizes the monomolecular process, while the "descent" is bimolecular. Quenching will occur only when the former process is more intense than the latter.

M.V.Fok: No. The thing is that here the kinetics of the holes is assumed to be fully analogous to that of the electrons. Where the motion of electrons is concerned we have the situation that an electron ejected from a local level has two possibilities: a) to return to some other local level or b) to recombine. The quadratic kinetics are obtained because the probability of recombination is not constant but depends on the number of ionized centers. Here we have not competing but successive processes. We postulate the same kinetics for the holes. That is, a hole freed from an ionization center can either recombine with a localized electron or return to another center and ionize it. As a result, the probability that a hole will recombine with a localized electron is not a constant quantity but one depending on the concentration of a localized electron. In our scheme it is assumed that the concentration of holes and conduction electrons is small; the concentration of ionized centers equals the concentration of localized electrons. Then the probability of such recombination is proportional to the square of the number of ionized centers and thus we obtain a second order hyperbola.

*Complete article in "Optika i spektroskopiia", 1, 248 (1956).

VARIATION OF THE LUMINESCENCE EFFICIENCY OF ZnS:Cu WITH THE WAVELENGTH OF THE EXCITING LIGHT (Abstract*)

- M.N.Alentsev

Measurements of the luminescence output of ZnS:Cu as a function of the wavelength of the exciting light made hitherto appear to be unsatisfactory for the following reasons: first, this phosphor has two emission bands (with maxima at about 460 and 580 mμ), and second, the output in both bands depends on the excitation intensity and hence the values of the efficiency for different wavelengths of exciting light, differing as regards intensity and absorption by the phosphor, are difficult to compare.

In order to investigate separately the efficiency of both bands we modified the preparation procedure so as to obtain samples whose emission comprised only one or the other of the two bands. As the blue band emitting phosphor we took ZnS:Zn heated at 600°; as a phosphor with virtually only green luminescence we chose ZnS:Cu (10^{-4} g/g) heated at 1200°.

The luminescence yield of ZnS:Zn increases with increasing excitation intensity due to internal quenching. Measurements of the efficiency for each wavelength of the exciting light were carried out at different excitation intensities. The resultant curves were extrapolated to infinitely high excitation intensities when internal quenching becomes nil. Thus we obtained the spectral dependence of the blue luminescence efficiency of ZnS:Zn under approximately equal conditions of excitation by light of different wavelengths.

It was found that the quantum efficiency with excitation in the absorption band of the activator (peak at about 340 mμ) is about one and a half times higher than in the case of excitation in the absorption band of the host material.

The luminescence output of ZnS:Cu decreases with increasing excitation intensity due to the de-exciting influence of the exciting light. Hence in this case we reduced the intensity of the exciting light to the point where the efficiency remained consant, i.e., to where the stimulating effect of the exciting light became nil.

The curve characterizing the variation of the quantum efficiency in the green band with the wavelength of the exciting light obtained in this manner has two maxima which coincide with the absorption maxima of the blue and green luminescence centers. The efficiency under excitation in the absorption band of the host material is again one and a half times smaller than at the maxima.

The experimental data show that there is appreciable loss in the transfer of excitation energy from the host material to the luminescence centers. On the other hand, the high efficiency in the green band under excitation by light in the absorption band of the blue luminescence centers indicates a high efficiency of energy transfer in this case.

"P.N.Lebedev" Physical Institute of the
Academy of Sciences of the USSR

---

*Complete article in "Optika i spektroskopiia", 1, 240 (1956).

SENSITIVITY OF "FLUORESCENT LAMP" LUMINOPHORS TO SHORT ULTRAVIOLET

- F.A.Butaeva & V.A.Fabrikant

In an earlier contribution[1] it was shown that the quantum luminescence efficiency of "fluorescent lamp" luminophors under excitation by the 1850 A line is appreciably greater than unity. This result, however, was obtained by means of an indirect method based on comparing the luminance of the investigated phosphors with the luminance of organic phosphors for which it was assumed that Vavilov's law holds.

In the present investigation we carried out direct measurements of the relative sensitivity of fluorescent lamp phosphors to the 1850 and 2537 A mercury lines. For the purpose of the experiments we designed and constructed the vacuum monochromator with a thermocouple shown in Fig.1. A very thin prism (base 10 mm) and lenses were used in order to minimize absorption. By virtue of the high dispersion of quartz in the short wave region of the spectrum, the 2537 and 1850 A lines were well resolved. The mount of the "Kipp" thermopile had provision for lateral and longitudinal displacement of the thermopile without disturbing the vacuum.[2]

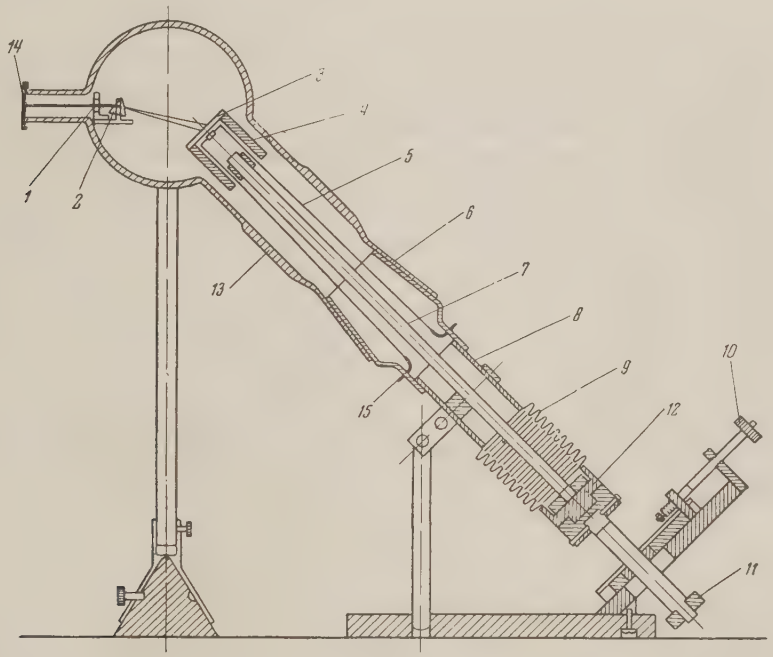

Fig.1. Diagram of vacuum monochromator set-up: 1) quartz lens, 2) quartz prism, 3) protective quartz plate, 4) thermopile housing, 5) leads, 6) joint, 7) support, 8) adapter (Kovar), 9) bellows, 10) screw for lateral positioning of thermopile, 11) screw for longitudinal positioning of thermopile, 12) coupling, 13) monochromator housing (glass), 14) quartz window, 15) thermopile lead terminals.

Inasmuch as the intensity of the 1850 A line emitted by the mercury-vapor discharge tube is appreciably lower than the intensity of the 2537 line, we designed a special combined light source which consisted of an aluminum electrode spark yielding the 1854.67 A line and a mercury tube yielding radiation concentrated in the 2537 A line. The spark was mounted in front of the tube. When using this combined source it proved feasible to work even without evacuating the monochromator. The thermopile served to determine the ratio of the intensities of the 1850 and 2537 A lines. Under our condition this ratio varied between 2 and 5 depending on the relative locations and operating regimes of the tube and spark gap. The luminance of the phosphor under excitation by the 1850 and 2537 A lines was measured by means of a cesium-bismuth photomultiplier. The investigated luminophor was placed in an optical cell in the form of a thick, virtually opaque layer. Measurements were made on a number of different both "fluorescent lamp" and other types of phosphors.

Table 1

Phosphor	$ZnSiO_3$		$ZnBeSiO_3$			$MgWO_4$		$CaWO_4$	$Cd_2B_2O_5$	Potassium gallophosphate
	217	1	P-91	L-27	L-28	P-37	L-29			
$\frac{\eta\ 1855\ A}{\eta\ 2537\ A}$	2,4	2,2	1,8	1,5	1,5	0,83	0,94	1,4	1,2	1,05

The data on the ratio of sensitivities to the 1850 and 2537 A lines are summarized in Table 1. These data are in agreement with the results of our earlier work. Using the data of Table 1 and the values of the quantum efficiency under excitation by the 2537 A line obtained by Shklover[2], one can readily calculate the quantum efficiency for excitation by the 1850 A line.

The results of such calculations are shown in Table 2. While the values listed in Table 2 may not be highly accurate, they do prove the existence of quantum efficiencies exceeding unity with excitation by the 1850 A line.

Table 2

Phosphor	Energetic efficiency		Quantum efficiency	
	η_e 1850	η_e 2537	η_q 1850	η_q 2537
Willemite 217	1,0	0,44	2,9	0,91
"	0,63	0,26	1,8	0,54
$ZnBeSiO_3$ (VEI)	0,5	0,28	1,6	0,67
$MgWO_4$ (VEI)	0,38	0,46	1,0	0,92
MWO_4 L-29	0,44	0,46	1,14	0,92
$Cd_2B_2O_5$	0,37	0,31	1,3	0,79
Potassium gallophosphate	0,46	0,54	1,4	0,98

Thus our earlier conclusion regarding the possibility of energy transfer of photons in the 1850 A region is substantiated. As may be seen from Table 1 the ratio of sensitivities depends on the type of luminophor. Hence one may expect the shape of the spectral curve for a given mixture of luminophors to vary with changes in the excitation conditions.

Fig.2 shows the curves obtained for a mixture of $ZnBeSiO_3$ and $MgWO_4$ obtained by excitation in a fluorescent lamp (2537 + 1850 A) and under excitation by the 2537 A line from a quartz tube equipped with a filter. It will be seen that the initial sections of the spectral curve diverge appreciably.

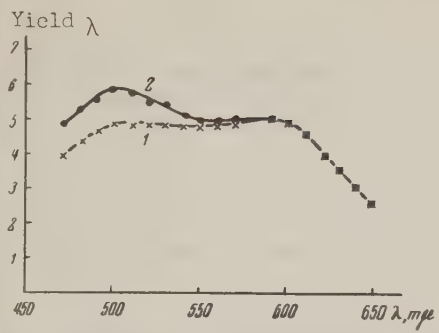

Fig.2. Spectral distribution in the emission band of a mixture of $ZnBeSiO_3$ and $MgWO_4$: 1) in a lamp (1850 + 2537 Å excitation), 2) not in lamp (2537 Å excitation).

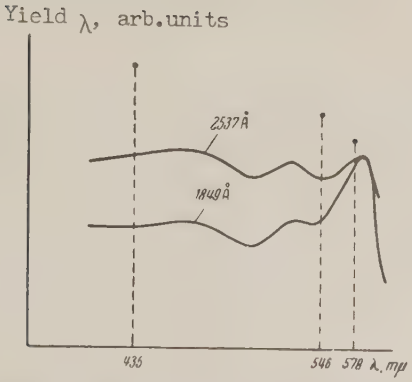

Fig.3. Spectral distribution in the emission band of a mixture of $ZnBeSiO_3$ + $MgWO_4$ excited by the 1850 and 2537 Å lines separately.

Fig. 3 shows the qualitative results obtained by the photographic method when the same $ZnBeSiO_3$ + $MgWO_4$ mixture was excited separately by the 1850 and 2537 Å lines. The significance of the role played by the 1850 Å line in the excitation of phosphors in fluorescent lamps will be evident from a comparison of Figs. 2 & 3.

All-Union Scientific Research Institute
for Light Technology

References

1. F.A.Butaeva & V.A.Fabrikant, Izv. AN SSSR, Ser.fiz., 18, 2 (1949).
2. D.A.Shklover, Zhur.tekh.fiz., No.II, 1239 (1949).
3. E.Morozova, Thesis, MEI (Moscow Power Institute), 1956.

SPECTRAL DISTRIBUTION AND ABSOLUTE VALUE OF THE PHOTOLUMINESCENCE OUTPUT OF THALLIUM-ACTIVATED ALKALI IODIDES (Abstract*)

- Z.L.Morgenshtern

Alkali iodides activated with thallium yield a high luminescence output under excitation by γ-rays; for this reason they are frequently used in scintillation counters. Available experimental data indicate that a transfer of excitation energy occurs from the host lattice to the activator. In order to elucidate the transfer mechanism, we felt it would be of interest to investigate the spectral dependence of the luminescence output under photoexcitation, particularly in the region of absorption of the host material, and to obtain the values of the absolute luminescence efficiency of these phosphors. We developed a procedure for measuring the absolute quantum efficiency of the luminescence of alkali halide phosphors and in the present investigation determined the spectral dependence of the luminescence output of Ki:Tl, NaI:Tl and CsI:Tl and measured the absolute photoluminescence efficiency of these phosphors by the developed procedure.

The quantum photoluminescence efficiency $\eta = F/E$, where F and E are, respectively, the emitted and absorbed energy expressed in terms of the number of photons. In order to obtain the absolute value of η it is sufficient to measure F and E in the same arbitrary units. Efficiency measurements were made in a photometric sphere (to take into account the full light flux); the detecting unit was a standard converter-luminophor (creamy yellow luminogen which is characterized by a constant quantum efficiency in the 240-500 mμ region) and an FEU-19 photomultiplier tube.

The absolute quantum efficiency of KI:Tl under excitation in the two absorption bands of the activator proved to be virtually the same: $\eta = 0.75 - 0.80$.

For NaI:Tl under excitation in the long wave absorption band of the activator we found $\eta = 0.61$, in the short wave absorption band - $\eta = 0.40$. The efficiency of CsI:Tl determined by the method of comparison with KI:Tl under excitation in the absorption band of the activator it was found to be 0.84.

The spectral distribution of the luminescence of the investigated crystals was measured by comparison with a luminophor having a constant quantum efficiency in the spectral region in question (anthracene and sodium salicylate). It was found that the output is virtually constant within the limits of the activator absorption band, that the output curve is shifted somewhat relative to the absorption curve in the long wave region of the spectrum and that the output falls off sharply in the region of the first absorption maximum of the host material. Upon going to shorter wavelengths the efficiency rises somewhat.

It may be concluded from the results obtained that in the absorption of light in the region of the first absorption maximum of alkali halide crystals (this maximum is commonly associated with excitons) energy is transferred from the host lattice to the activator with low efficiency.

"P.N.Lebedev" Physical Institute of the
Academy of Sciences of the USSR

---

*Complete reports published in Doklady AN SSSR, 105, 250 (1955) and Zhur.eksp.i teor.fiz., 29, 904 (1955).

ON CALCULATION OF THE LUMINESCENCE SPECTRA OF CRYSTAL PHOSPHORS (Abstract*)

- N.D.Potekhina

The absorption with a maximum at 210 mμ and emission with a peak at 250 mμ observed experimentally for NaCl:Ag phosphor are commonly associated with transitions in the silver ion: some authors identify these as forbidden $^3D_1 - {}^1S_0$ transitions, while others identify them as allowed $^3P_1 - {}^1S_0$ transitions.

We carried out a theoretical calculation of the emission and absorption bands for these transitions in the silver ion taking into account the influence of the field of the crystal lattice. In our calculations we used the method of Williams[1] based on the Born-Mayer electrostatic theory of crystal lattices. The luminescence center was assumed to be the silver ion replacing a positive sodium ion in the crystal lattice. The substitution of the silver ion results in displacement of the equilibrium positions of the neighboring six negative chlorine ions.

Considering the fully symmetric vibrations of the chlorine ions about the silver ion, we calculated the energy of the complex $Ag^+ + 6Cl^-$ as a function of the configuration coordinate Δa characterizing the radial displacements of the ions. For computing the energy of the luminescence center in the ground state we used the results of Mayer[2]. For calculating the excited states we determined the wave functions of the silver ion for the $4d^9 5s$ and $4d^9 5p$ configurations; these were then utilized to compute the polarizability, the repulsion constant and the Coulomb overlapping integral.

As a result we obtained configuration curves for the energy; on the basis of these we determined the theoretical emission and absorption bands on the assumption of a Boltzmann distribution in energy for the centers.

Comparison of the calculated bands with the experimentally observed ones shows that satisfactory agreement with experiment as regards position of the maxima and shape of the bands is obtained if the transition to the silver ion is considered to be $^3P_1 - {}^1S_0$.

This result cannot be considered as entirely rigorous and definitive in view of the semiempirical character of the method of calculation, which admittedly comprises a number of assumptions still in need of verification.

Physics Faculty of
Leningrad State University

References

1. F.E.Williams, J.Chem.Phys., 19, 457 (1951).
2. J.E.Mayer, J.Chem.Phys., 1, 270, 343 (1933).

DISCUSSION

Question: What reason is there to take into account only the fully symmetrical displacement of the chlorine atoms, so that you use only one configuration coordinate and assume that the fixed chlorine ions oscillate in unison? Why do you think it is unnecessary to take into account the type of vibrations when some of the ions approach each other, while the others recede?

N.D.Potekhina: There are a number of investigations that support this assumption; the main contribution is made by the symmetric vibrations. Recently there has been published a report showing that the introduction of an activator

---

*Complete report in "Optika i spektroskopiia", 2, 388 (1957).

ion leads to exactly such vibrations either about the Ag ion or about a vacancy. So we have indirect proof that our model is plausible.

Question: This pertains to local vibrations that arise about the activator. Do the fundamental vibrations of the lattice have appreciably less effect?

N.D.Potekhina: Yes, considerably less.

* * * * * *

INFLUENCE OF INFRARED RADIATION ON THE LUMINESCENCE OF ZINC SULFIDE PHOSPHORS (Abstract*)

- K.K.Rebane

The influence of infrared (hereinafter IR) on phosphors is of interest from two viewpoints: from that of investigation of the quantum efficiency (IR quenching) and from the standpoint of investigating trapping centers in phosphors. Herein we shall consider both aspects of the question since they are related.

We measured the sensitivity to IR quenching and IR flashing of ZnS:Cu($MgCl_2$) ZnS:ZnO:Cu(NaCl), ZnS:Cu(NaCl), ZnS:Cu(KCl), ZnS:Cu:Co(NaCl), ZnS:Cu:Ni(NaCl) and ZnS:Cu:Fe(NaCl) phosphors. We found that the IR sensitivity curves for these phosphors have two maxima, located at about 1250 and 740-800 mμ. The positions of the maxima of sensitivity to IR flashing correspond fairly closely to the positions of the peaks of sensitivity to IR quenching.

Through investigation of thermooptical stimulation[1-3], we determined the correlation between the thermostimulation maxima and the maxima in the curves characterizing the sensitivity to IR flashing for a number of phosphors. We found that the maximum of the sensitivity to IR light at about 1250 mμ corresponds to a thermostimulation maximum in the 40-60° temperature interval, while the maximum at 740-800 mμ corresponds to a thermal maximum at about 100-120°. The ratio of the optical ionization energy (E_λ) to the thermal ionization energy (E_t) is about 1.5.

On the basis of data on retrapping in the process of IR flashing and the data of Garlick & Gibson[4] on the polarity of the thermal current carriers, it can be concluded that the flash emission under the influence of 800 mμ light is associated with ejection of electrons from the trapping levels into the conduction band.

Inasmuch as in the investigated phosphors together with IR quenching there is always observed IR flashing at the beginning of the process, we have the choice between two different mechanisms to interpret the initial influence of the IR radiation: 1) the IR light releases only electrons or 2) the IR releases simultaneously both electrons and holes. Which of these alternatives obtains in reality can only be determined by further experiment.

The character of the temperature dependence of IR quenching and comparison of the dependence of the change in the width of the emission spectrum under the influence of IR and under the influence of temperature show that the effect of IR cannot be explained solely by local heating due to absorption of the IR radiation[5].

---

*The complete report is printed in the Proceedings (Materialy) of the Fifth Conference on Luminescence, Tartu, 1956.

Investigation of the influence of IR on the dependence of the intensity I of emission on the intensity E of excitation shows that under the influence of IR superlinearity appears or increases and that the dependence of I on E can be even greater than quadratic. The phenomenon of superlinearity in IR quenching is presumably analogous to the superlinearity evidenced in other forms of quenching[6-8]. This superlinearity can be explained on the assumption that the radiationless transitions occur outside the luminescence centers, i.e., that IR quenching is external quenching.

Our experimental data, particularly the data on the strong superlinearity under IR excitation and comparison of the processes of quenching with the processes of flashing in two activator phosphors give reason to assume that the radiationless transitions produced by IR light occur in separate quenching centers which compete with the luminescence centers in the recombination process.

Institute of Physics and Astronomy of the
Academy of Sciences of the Estonian SSR

References

1. Ch.B.Lushchik, Trudy (Transactions) IFA AN ESSR (Institute of Physics and Astronomy, Estonian SSSR Academy of Sciences), 4, 42 (1956).
2. Ch.B.Lushchik, Trudy IFA AN ESSR, 4, 53 (1956).
3. K.K.Rebane, Trudy IFA AN ESSR, 4, 82, (1956).
4. G.F.Garlick & A.F.Gibson, JOSA, 39, 935 (1949).
5. K.K.Rebane, Thesis, IFA AN ESSR, 1955.
6. N.A.Tolstoi, Doklady AN SSSR, 95, 249 (1954).
7. N.R.Nail, F.Urbach & D.Perlman, JOSA, 39, 690 (1949).
8. C.Duboc, Brit.J.Appl.Phys., Suppl., 4, 107 (1955).

EFFECT OF ACTIVATOR CONCENTRATION ON THE GAMMA- AND PHOTOLUMINESCENCE EFFICIENCIES OF THALLIUM-ACTIVATED ALKALI IODIDES (Abstract*)

- L.M.Beliaev, M.D.Galanin, Z.L.Morgenshtern & Z.A.Chizhikova

Alakli halide crystals activated with thallium are used in scintillation counters because of their high luminescence efficiency under excitation by high energy particles. At low activator concentrations, the energy is absorbed primarily in the host lattice and the high luminescence output of the activator indicates that there is efficient energy transfer from the lattice to the activator.

The purpose of the present investigation was to determine at what concentrations of the activator this transfer occurs with adequate efficiency and to establish the mean range of energy transfer in the lattice.

The experiments were carried out on NaI, KI and CsI single crystals activated with thallium, the concentration of which in the crystals was determined by the polariographic method. Measurements of the output under excitation by light in the region of the first absorption band of Tl showed that the efficiency is independent of the concentration, i.e., that there is no concentration quenching in the investigated range of concentrations (up to $\sim 1.6 \cdot 10^{-3}$ mole Tl/mole MeI).

The relative output with excitation by γ-rays as determined by measurements of both the scintillation amplitude and the intensity of the total emission, increases with increasing Tl concentration up to a point and then tends to a saturation value. (We were not able to observe the increase in luminescence intensity with concentration for CsI:Tl, since the only crystals available to us, although prepared without the introduction of thallium, contained traces of Tl in a sufficient amount to produce a high output; the traces were not determined analytically but were detected from the excitation and absorption spectra of thick crystals.) What might be termed the characteristic concentration, i.e., the concentration at which the output equals half the maximum value, is $5.9 \cdot 10^{-5}$ mole Tl/mole NaI for NaI:Tl, $24.4 \cdot 10^{-5}$ mole Tl/mole KI for KI:Tl and $< 3 \cdot 10^{-5}$ mole Tl/mole CsI for CsI:Tl. The corresponding mean distances between the activator ions are, respectively, 105, 72 and >178 A, or ~ 32, 20 and >40 lattice constants.

DISCUSSION

L.M.Beliaev: Regardless of by what conventional procedure the phosphor crystal is grown, the activator distribution in it is always inhomogeneous; this makes such crystals unsuitable for spectrometric purposes. Investigation of the dependence of the luminescence output on the activator concentration has made it possible to determine the range of concentrations at which the nonuniformity of the activator distribution has the least effect on the luminescence efficiency. Studies we carried out using radioactive tracers have shown the degree of homogeneity of activation and have made it possible to establish a correlation between the activator content in the mixture of the initial batch and the final crystal.

---

*Complete report in Doklady AN SSSR, 99, 691 (1954); 105, 57 (1955).

KINETICS OF γ-SCINTILLATION IN Tl-ACTIVATED SODIUM IODIDE CRYSTALS (Abstract*)

- I.K.Pliavin'

By oscillographic analysis of individual γ-scintillations in NaI(Tl) crystals, we showed that these scintillations have a very fast rise time ($\tau \leqslant 6 \cdot 10^{-8}$ sec) and an appreciably longer decay time ($\tau \approx 3 \cdot 10^{-7}$ sec), i.e., that the kinetics of γ-scintillation is analogous to that reported for scintillation excited by deuterons.

The γ-scintillation decay follows the exponential law (within the limits of the experimental error) and τ depends on the temperature, which is in agreement with the data obtained by other investigators by a different procedure. The scintillation decay time τ cannot be associated with the probability of the $^3P_1 - {}^1S_0$ radiative transition in Tl. This time apparently characterizes the depth of the electron or hole trapping levels in NaI(Tl). The plot of log τ vs the reciprocal of the temperature in the range from +80 to -175° consists of two straight lines corresponding to activation energies of 0.15 and 0.05 ev. At room temperature the decay is determined by the 0.15 ev levels; at lower temperatures the shallower levels begin to play a more important part.

At temperatures in the -140 to -175° range, the initial scintillation comprises a component with a persistence of the order of 10^{-7} sec.

The transition probability as evaluated from the area under the contour of the first absorption band of Tl in NaI (peak at $\sim$ 295 mμ) on the basis of measurements of absorption in crystals with a known Tl concentration leads to $\tau \approx 4 \cdot 10^{-8}$ sec. This value is in agreement with the scintillation growth time, which substantiates the hypothesis that the scintillation comprises a two-step process consisting of a nonradiative transition (freeing of electrons from the trapping levels) and a radiative transition in the activator.

"P.N.Lebedev" Physical Institute of the
Academy of Sciences of the USSR

DISCUSSION

M.D.Galanin: The results of I.K.Pliavin' indicate that some sort of intermediate metastable levels are involved in the process of scintillation as well as in that of photoluminescence. We still do not know, however, whether electrons or holes are trapped or the precise nature of the trapping levels involved. Apparently the trapping levels participating in these processes differ from localization levels situated in the forbidden band near the conduction band, inasmuch as it is commonly assumed that photoconduction should be absent in the case of excitation in the absorption bands of the activator.

---

*Complete report in "Optika i spektroskopiia", 2, 384 (1957).

ATOMIC ABSORPTION AND LUMINESCENCE CENTERS IN ALKALI HALIDE PHOSPHORS ACTIVATED WITH HEAVY METAL IONS AND THEIR FORMATION UNDER THE INFLUENCE OF HARD RADIATION (Abstract)

- M.L.Kats

As is known, the absorption spectra of alkali halide phosphors activated with heavy metals contain discrete bands characteristic of the activating impurity and situated near the long wave absorption edge of the host material.

The absorption spectra of alkali halide phosphors change markedly under the influence of x- and γ-rays; in addition to the familiar bands associated with F-centers there appears a series of new bands, primarily in the ultraviolet region, due to the activator centers but altered by the hard radiation. At the same time, in a number of cases (Ag, Cu, Sn, Pb and some other metals) there appear new luminescence bands associated with modified activator centers, while in individual cases the ability to luminesce in general develops only as a result of irradiation of the phosphor with x-rays. Thus, for example, in nonirradiated NaCl:Ni phosphors no discernible fluorescence is excited by light corresponding to the selective absorption band of the activator (246 mμ), but after irradiation of the phosphor with x-rays, producing new absorption bands at 216, 279, 350 and 465 mμ, NaCl:Ni crystals emit a characteristic orange-red fluorescence under the influence of long-wave ultraviolet.

Investigation of the absorption and luminescence spectra, thermostimulation, the bleaching influence of monochromatic light and other properties of absorption and luminescence spectra developing under the influence of hard radiation in the case of alkali halide crystal phosphors activated with heavy metal ions shows that the new centers arise as a result of capture of free electrons by the activator ions and the transformation of the ionic activator centers into atomic centers. This deduction is substantiated by the identity of the absorption bands appearing under the influence of x- and γ-rays and as a result of ordinary additive coloring by injection of electrons from the outside.

Analysis of the experimental data shows that in the case of alkali halide phosphors activated with silver, individual spectral bands, for example, the 288 mμ band in KCl:Ag, are associated with centers that are unique variants of F-centers in which one of the six cations surrounding the vacant halide site is a silver ion. Inasmuch as the ionization energy of Ag (7.54 ev) is greater than that of Na (5.12 ev), one may naturally expect 1) that the spectral band will be displaced relative to the usual F-band to the short wave side and 2) that the electron will be more tightly bound with the Ag^+ ion than with each Na^+ ion individually.

The hypothesis of L.M.Shamovskii that the 288 mμ band is due to absorption of light by thin films forming on the internal, intercrystalline surfaces of the mosaic substructure is not consistent with the experimental data. Specifically, the atomic 288 mμ band of KCl:Ag is not photoelectrically active and is not observed in the absorption spectra of thin and superthin silver coatings applied to different dielectrics, although the other longer wave absorption bands, i.e., those at 315, 340 and 440 mμ, appearing under the influence of hard radiation, are observed in the spectra of such coatings.

The 440 mμ band is due to colloidal silver particles; the 315 and 340 mμ bands, like the similar bands investigated by E.A.Kirillov in silver halide crystals exposed to light, may be due to particles intermediate in size between atomic and colloidal (probably small groups of atoms).

Having the ability to capture free electrons, the activator also performs the function of "sticking centers", as evinced by the appearance of local

acceptor levels characteristic of activating impurities in the electron energy spectrum. Nonactivating impurities as, for example, alkaline earth metal ions may also serve as trapping centers in alkali halide phosphors.

In both cases the trapping levels are manifested in the form of characteristic bands in the absorption spectra and peaks in the thermostimulation glow curves.

In addition to electronic absorption spectra, under the influence of hard radiation there appear in alkali halide phosphors centers of a different type. These different centers are responsible, for example, for the 216 mμ band in the absorption spectrum of NaCl:Ni.

Investigation of the changes produced in the absorption and emission spectra of alkali halide phosphors by hard radiation is not only important from the point of view of elucidating the nature of emission and trapping centers but also holds promise where development of new principles of x- and γ-ray dosimetry is concerned.

"N.G.Chernyshevskii" Saratov State University

* * * * * *

INFLUENCE OF X-RAYS ON THE ABSORPTION AND EMISSION OF Sn-ACTIVATED ALKALI HALIDE PHOSPHORS (Abstract)

- A.S.Andrianov & M.L.Kats

Investigation of the changes in the properties of absorption and luminescence centers under the influence of different factors can undoubtedly help elucidate the nature of these centers. In view of the distinctive structure of their absorption spectra, alkali halide phosphors with tin as the activator are of particular interest. Their spectra comprise six bands which in the case of KCl:Sn peak at 224, 232, 240, 252, 276 and 296 mμ.

After irradiation of the phosphor with x-rays the absorption falls off sharply at the short wave maxima (224, 232 & 240 mμ) and increases in the spectral region of the long wave maxima. In strongly irradiated phosphors the short wave group merges into a single band with a diffused maximum. These changes in the absorption spectrum are reversible: heating of the phosphor restores the absorption in the short wave bands and the absorption curve resumes its initial appearance.

Additive coloring of Sn-activated alkali halide phosphors leads, in general, to similar changes in their absorption spectra. As is known, in the case of additive coloring, extraneous electrons from the outside penetrate into the crystal and are localized at vacant halide ion sites and other lattice defects. Consequently, the changes in the absorption spectra in both cases - additive coloring and x-ray irradiation - are attributable to the same cause, namely, capture of additional electrons by some fraction of the activator ions. The increased absorption in the region in which the long wave absorption bands of non-irradiated crystal are located is also due to activator ions capturing excess electrons.

X-ray irradiated alkali halide phosphors activated with tin, in addition to fluorescing with a characteristic spectrum, also exhibit thermoluminescence, which, however, has a different spectral distribution. The difference between the spectra indicates that different mechanisms are involved in fluorescence and thermoluminescence. In the latter case the emission is apparently connected with the capture of excess electrons by the activator ions which, as a result, are transformed into singly ionized or quasineutral atomic Sn centers.

"N.G.Chernyshevskii" Saratov State University

ON THE MECHANISM OF SELECTIVE ABSORPTION OF THE ACTIVATOR IN KCl:Ag PHOSPHORS (Abstract*)

-M.L.Kats & V.K.Nikol'skii,

The absorption spectra of alkali halide phosphors activated with silver have been investigated by Smakula (1927), Forro (1929), Kato (1943) and Etzel & Schulman (1954). The results reported by the different investigators are conflicting: whereas Smakula and Kato detected only one activator band at the long wave absorption edge of the host material, according to the data of Forro and Etzel & Schulman the selective absorption of the activator consists of two or three bands. The absorption mechanism of these phosphors remains unclear.

According to our data the selective absorption spectrum of the activator in KCl:Ag consists of two intense bands with sharp peaks at 216 and 228 mμ and one very weak band with a peak of about 245 mμ.

By analogy with pure alkali halide crystals it might be assumed that the selective bands in the KCl:Ag spectrum are connected with excitation and subsequent transition of an electron from a halide ion to a neighboring cation, specifically the silver cation rather than the alkali metal one. Analysis of the experimental data, however, shows that this absorption mechanism is unlikely. The available data are also inconsistent with the hypothesis that the selective absorption centers in Ag-activated alkali halide phosphors are of a complex nature.

Very interesting changes occur in the absorption spectrum of KCl:Ag under the influence of x-rays. First, there appears a series of new strong absorption bands in the long wave region (270-500 mμ), in which the nonirradiated phosphor is entirely transparent. Then, in the short wave region there appear two strong absorption bands with peaks at 222 and 235 mμ and a weak band at about 260 mμ.

On the basis of a comparison of the 216, 228 and 245 mμ activator absorption bands in nonirradiated KCl:Ag phosphors and the 222, 235 and 260 mμ short wave bands appearing after irradiation with the absorption spectra of gaseous and hydrated Ag^+ ions these bands may be ascribed to specific electron transitions. Such comparison shows that the value of the separations $\Delta\nu$ between the components of the triplet associated with the Ag^+ ions in the gaseous state are virtually identical with the separations $\Delta\nu$ between the maxima of the bands observed in the spectra of hydrated silver ions and the KCl:Ag phosphor before and after irradiation with x-rays. It therefore follows that in all these cases the bands are due to the same electron transitions between the ground state $^1S_0$ and the components of the triplet $^3P_2$, $^3P_1$ and $^3P_0$. Interaction of the silver ions with the surrounding ions of the host material in liquid or solid solutions leads to broadening of the spectral lines of the free impurity into bands and their displacement to the long wave side of the spectrum.

From the fact that the 216, 228 and 245 mμ absorption bands in the spectra of nonirradiated phosphors and the 222, 235 and 260 mμ bands in the spectra of x-rayed KCl:Ag phosphor are attributable to the same respective electron transitions it follows that under the influence of x-rays the absorption bands of some fraction of the silver ions are simply displaced into the long wave region. Displacement may be due to the formation under the influence of x-rays of different defects (for example, anion and cation vacancies, positive holes, etc.) some of which are apparently localized close to the

---

*Complete report published in "Proceedings (Materialy) of the Fifth Conference on Luminescence", Tartu, 1957.

activator ions.

"N.G.Chernyshevskii" Saratov State University

DISCUSSION FOLLOWING THE PRECEDING THREE REPORTS

F.F.Vol'kenshtein: Regarding the A-center model. As is known, F-centers are electron acceptors. If the phosphor is illuminated by the F-band, the number of F-centers decreases and the number of F'-band centers increases. The same thing should occur in the case of A-centers; the A-center should capture a second electron, like an ordinary F-center, and hence if the crystal is illuminated with light in the A-band there must appear a longer wave A'-band corresponding to centers with not one but two electrons. If such were indeed the case this would be a weighty argument in favor of the proposed model.

M.L.Kats: The A-band (288 mμ) is very stable as regards the influence of light; we used a source of very low intensity, namely, a hydrogen tube. Hence here the difficulty is purely experimental: one must find a stronger source or possibly work at low temperatures.

L.I.Tarasova: In connection with the interpretation of the long wave emission bands of nonirradiated alkali halide phosphors activated with silver, proposed by M.L.Kats, I would like to mention some preliminary results kindly made available by P.P.Feofilov. It was found that emission in the violet luminescence band of NaCl:Ag phosphor is almost fully polarized. The character of the azimuthal dependence of the degree of polarization indicates that the oscillators responsible for the emission of the band are oriented along fourth order axes, i.e., in the Ag^+—Cl^- direction.

These results are in accord with the model proposed by M.L.Kats, but are in conflict with the views expressed by a number of authors (in particular, Schulman) according to which this violet band is described to pairs of Ag^+ ions located at neighboring lattice sites; in this case the oscillators would be oriented along second order axes.

* * * * * *

LUMINESCENCE OF DIFFERENT TYPES OF LUMINOPHORS UNDER EXCITATION BY SHORT PULSES (Abstract*)

- A.A.Bundel', M.F.Popov & Iu.A.Chizhunova

According to present-day concepts, in the case of pulse excitation the maximum brightness (attained at the end of the excitation interval) of luminophors with recombination luminescence should be proportional to the square of the energy of the exciting pulse, while the brightness of luminophors with luminescence due to discrete centers should be proportional directly to the energy of the exciting pulse. We checked this experimentally (oscillographically) on samples of $ZnS_{55}\cdot CdS_{45}$-Ag($2\cdot10^{-4}$), 1.7 $ZnO\cdot SiO_2$-Mn($3\cdot10^{-3}$) and $CaWO_4$ with excitation by x-ray pulses of from $2.6\cdot10^{-5}$ to $1.5\cdot10^{-3}$ sec duration. In each of the four series of experiments the total excitation energy transmitted to the luminophor during the period of the pulse remained constant, the energy from series to series being increased in the proportion 1:2.25:4:9.

---

*Complete report in Trudy Instituta rentgenologii i radiologii (Transactions of the Institute of Roentgenology and Radiology), 9, 44 (1955).

It was found that with a given pulse energy, the maximum luminance of all luminophors, regardless of their luminescence mechanism, first increases with decrease of the pulse duration. After a certain duration peculiar to each luminophor ($2.6 \cdot 10^{-5}$-$1 \cdot 10^{-4}$ sec for $CaWO_4$, $5 \cdot 10^{-5}$-$2 \cdot 10^{-4}$ for ZnS·CdS-Ag and 0.8-$1 \cdot 10^{-3}$ for 1.7 $ZnO \cdot SiO_2$-Mn) the maximum brightness no longer depends on the pulse duration and is determined solely by its total energy. Inasmuch as these results are in fundamental conflict with the usual concepts, the experiments were repeated by photographing the emission sweep on a one-disc phosphoroscope with excitation by single pulses. The results were virtually identical with those obtained by the oscilloscopic method.

The total amount of luminescent energy emitted by the luminophor with pulse excitation as the pulse duration was varied from $2 \cdot 10^{-2}$ to $2 \cdot 10^{-6}$ sec remained the same for $CaWO_4$ and ZnS·CdS-Ag and decreased somewhat for 1.7 $ZnO \cdot SiO_2$-Mn.

Thus with sufficiently brief excitation, when the maximum brightness is determined by the total energy of the exciting pulse, there apparently occurs intensified storage of the light sums.

"V.M.Molotov" Institute of Roentgenology and Radiology

DISCUSSION

G.M.Eliashberg: These curves correspond to the same exposure? If the intensity was lower, was the time longer?

A.A.Bundel: Our experimental procedure was the following. We had a capacitor discharging from the same potential. The pulse duration was regulated in two ways: we varied the temperature of the cathode and the length of the wire shorting the spark gap (the wire served in this case as the cut-off) and we changed the distance from the screen to the focus of the x-ray tube. On the basis of this we calculated the energy of the pulse according to the square of the distance. For each distance we carried out a series of measurements with different durations which we determined in an appropriate manner in separate experiments and thus constructed the curves I have shown you.

The ordinates at a given pulse duration had the value of the maximum brightness for different values of the total excitation energy. It was equal to the constant charge of the capacitor divided by the square of the distance. Thus the total energy is the same along each curve.

M.D.Galanin: The position of the quadratic section on the curve giving the dependence of the luminescence intensity on the intensity of the short-term excitation must depend on the excitation density. It is possible that the reason why the quadratic dependence is not observed with pulsed x-ray excitation is that in the ionization excitation channels, appearing under the influence of fast electrons produced as a result of the photoeffect, the excitation density is very high.

A.A.Bundel': Of greatest interest to me are the anomalies we observed for luminophors with the discrete-center luminescence mechanism. The distinctive features of emission under pulsed excitation by x-rays of zinc sulfide-cadmium sulfide phosphor can be explained more simply: by M.D.Galanin's point of view or the concepts of diffusion of excited electrons by V.V.Antonov-Romanovski.

I would like to point out that the maximum brightness attained at the end of the exciting pulse becomes independent of the pulse duration in the case of all the investigated phosphors when the pulse duration is made equal to or less than the mean lifetime of the centers in the excited state. Both recombination and monomolecular luminophors behave the same. Possibly because in the case of pulse excitation in recombination luminophors the electrons are ejected not into the conduction band but to the excited levels of the luminescence centers.

SURFACE-ACTIVATED PHOSPHORS

- L.M.Shamovskii & Iu.N.Zhvanko

Introduction

The absorption spectra of alkali halide phosphors consist, in the first approximation, of the sum of the absorption spectra of the compounds comprising the mixed crystals. (Usually the absorption bands of the activator become somewhat sharper.) In analyzing the optical properties of crystal phosphors it is almost always feasible to separate the bands associated with the host material from those associated with the activating impurity[1]. In both the host material and in the activator taken separately absorption of light in the fundamental bands is accompanied by an internal photoeffect. Owing to transition of electrons from the upper filled band to the conduction band, there appear free electrons and holes which give rise to a detectable photoconductivity. It was natural to assume that in any crystal phosphor the basic excitation process would be the same as in compounds of which it is comprised. This simple excitation scheme, however, had to be rejected when it came to interpretation of the actual optical properties of thallium phosphors[2,3]. In order to explain the experimental data, it proved necessary to assume that the crystal phosphor consists of two phases (the host salt and the activator). Yet it was also shown experimentally that in the synthesis of some phosphors there are formed solid substitution solutions that obey Vegard's law. Further, it was established that the intensity of the long wave absorption band, indubitably connected with the presence of activator impurities in the phosphor crystal, increases in direct proportion to the actual concentration of the impurity[4]. These facts would appear to substantiate the assumption of an atomically dispersed distribution of the activator in the phosphor crystal. Yet no photoactivity has been detected in thallium phosphors with excitation in the absorption bands of either the host material or the activator[5]. In view of this it was hypothesized that optical excitation of phosphors, particularly in the activator bands involves processes connected solely with internal electron transitions in the activator ions situated singly or in pairs at the lattice sites of the mixed crystal[3,6].

All the above experimental data can be interpreted in a somewhat different fashion if we assume that the crystal phosphor has a microheterogeneous structure determined by a dual (i.e., two different kinds) distribution of the activator.*

The linear variation of the intensity of the activator bands with the total impurity content cannot be taken as proof that the activator is atomically dispersed through the crystal. If the absorption spectrum is due only to the part of the activator located on the contact surfaces, this linear variation would still obtain provided the coefficient of dual distribution

---

*We arrived at the assumption of a dual distribution of the activator and the heterogeneous character of the microstructure on the basis of analysis of the characteristics of additive coloring and bleaching[7]; these assumptions were subsequently substantiated by x-ray (Laue diffraction) and ultramicroscopic studies[8,9]. The dual distribution of the activator in NaCl:Mn phosphor is also confirmed by paramagnetic resonance studies[10]. In these studies it has been shown that in this phosphor only one of the states of the activator is effective where luminescence is concerned. The activator in this state forms local aggregations and is not present in an atomically dispersed form.

of the activator remains constant; only the apparent value of the oscillator strength would change if calculated by the Smakula dispersion formula[11]. The observed deviations from Vegard's law where the variation of the lattice parameters of KCl:Ti phosphor with changes in the thallium concentration are concerned are large; they are greater than the possible experimental errors and do not conflict with the hypothesis of a dual (two-type) distribution of the activator[12].

Although in thallium phosphors no measureable photoconductivity has been detected, even here one must assume the possibility of excitation energy transfer from the host material to the luminescence centers by holes and electrons[5]. Thermostimulation and bleaching studies[13] of alkali halide phosphors prove that the persistent afterglow in these phosphors is connected with temporary localization of the electrons and holes on the structural defects of the crystal proper, defects that are independent of the activator. The photoelectric character of the fluorescence of excited phosphors is also substantiated, particularly, by investigations of scintillation under the influence of ionizing radioactive radiations*. Consequently, the luminescence processes must be considered as a result of recombination of electrons and holes in the activator[5] despite the absence of a measureable photoconductivity.

Intensity of the activator absorption bands in KI:Tl and KI:In phosphors as a function of the activator concentration and the type of activator compound.

As has been repeatedly noted by different investigators, the optimal proportion of different activators in crystal phosphors varies over a very wide range. In general the optimum dosage increases with increasing solubility of the given impurity in the host lattice. In particular, it has been noted that in ZnS:Mn and ZnS:Pb phosphors the Mn and Pb play a dual role, that is, appear as both a component of the host lattice and as the activator when they are located at special defective sites of the phosphor[15].

From the standpoint of gaining an insight into the correlation between the luminescence and the structural characteristics of crystal phosphors, investigations of the character of the distribution of the activator in them are particularly important. For purposes of such investigations, most suitable are alkali halide salts grown in the form of single crystals.

If the activator is distributed in the crystal phosphor in two ways (dual distribution), its coefficient of distribution in the two different states must be dependent on the character of the phase equilibrium in this two-component system. Hence if the same activator is introduced alternately in the form of different compounds, its coefficient of distribution at equal molecular concentrations would be different. Inasmuch as the introduced impurity can serve as an activator only in one of the states, the dual character of the distribution must obviously be manifested in the absorption spectrum of the activator.

For the purposes of our investigation we selected KI activated with thallium and indium. The activators were introduced in the metallic form and in the form of the respective iodide, oxide or sulfide. The single crystals were grown in sealed ampoules. The crystal plates for the absorption measurements were optically ground on both sides to a uniform thickness (within 0.008 cm). An SF-4 spectrophotometer was employed for making the spectral photographs. The activator concentration in the crystals was

---

*A 1 Mev β-particle gives rise to some 20,000-30,000 photons in the emission spectrum of NaI:Tl.

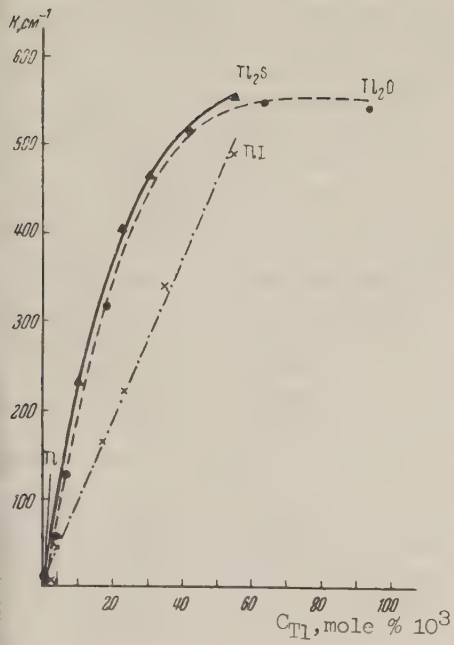

Fig.1. Variation of the absorption coefficient for λ = = 285 mμ light in KI:Tl phosphors with the thallium concentration as determined by analysis.

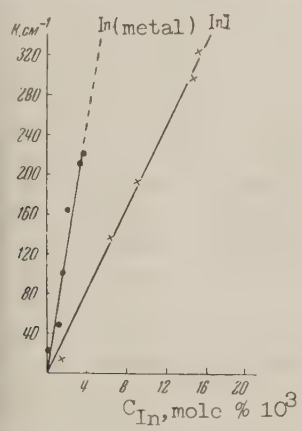

Fig.2. Variation of the coefficient of absorption at the maximum of the activator band at 262 mμ in KI:In phosphors with the indium concentration.

determined polarographically[16], colorimetrically[17] and by the method of fluorometric titrations. For purposes of analysis we took portions from the central part of large single crystals grown next to the crystals used for the absorption measurements.

The absorption and luminescence spectra of KI:Tl and KI:In phosphors proved to be identical in all details and independent of the type of activator compound at concentrations under 10^{-2} mole %. KI:Tl has two activator bands located at 285 and 236 mμ. The maximum in the luminescence spectrum of KI:Tl is situated at 410 mμ and only at high concentrations of Tl is there observed a second broad band with a maximum at 460-470 mμ. In KI:In the activator absorption had three peaks: at 310 (low intensity), 262 and 230 mμ. The maximum of the luminescence band was located at 560 mμ[18].

Crystal phosphors activated with the metal have the same properties as those in which the activator is added in the ionic form (i.e., in the form of a compound). In order to preclude oxidation of the metal the crystals were grown in an atmosphere of dry hydrogen; thallium and indium do not form heat stable hydrides[19].

The dependence of the coefficient of absorption in KI:Tl phosphor at the long wave band maximum (285 mμ) on the actual (molar) concentration of Tl in the crystals is shown in Fig.1. The data given in Fig.2 for the KI:In phosphor pertain to the band peaking at 262 mμ inasmuch as the longest wavelength activator band, situated at 310 mμ in the absorption spectrum of these crystals, is barely discernible.

The following deductions may be drawn from the cited experimental data.

1. At small concentrations of the activator the absorption and luminescence spectra of KI:Tl and KI:In phosphors are virtually independent of the form of the compound used for introducing the activator in the process of growing the single crystals. Consequently, it may be assumed that identical absorption and emission centers are formed in the phosphors in all cases.

2. At the same total content of the activator the intensity of the absorption bands associated with it in the spectrum of the crystal phosphor differs significantly where the different compounds and pure metal are concerned. It follows that only the part of the activator locating at particular sites (defects) of the mixed crystal is manifested in the activator absorption spectrum. These results

substantiate our hypothesis regarding the dual character of the activator distribution in crystal phosphors[20]. This deduction is at variance with the currently held concepts regarding the structure of alkali halide phosphors and the character of the luminescence processes therein.

3. The more soluble activator compounds (forming substitutional solid solutions with the host material) yield - at equal concentrations - less intense additional absorption bands. It follows therefor that the activator ions located at the lattice sites do not give rise to centers of additional absorption and luminescence centers. These properties (i.e., the formation of additional absorption and luminescence centers) are peculiar to the activator that lodges on the contact surfaces, producing the polyhedral structure of the phosphor. Obviously, in the case of weakly soluble forms of the activator a greater proportion of the activator material will be deposited on the contact surfaces.* Deposition of the activator on the intercrystalline contact surfaces is not a result of decomposition of supersaturated solid solutions. This is evinced by the fact that the relative value of the coefficient of dual distribution of the activator as determined from the slope of the curves in Figs.1 & 2 remains constant from the very lowest impurity concentrations. The relative distribution of the activator in the two different locations in the crystal phosphor (lattice sites and intercrystalline surfaces) obviously depends on the phase equilibrium for the given system and on the ability of the introduced impurities as a surface active material to produce a mosaic structure. In the case of introduction of large amounts of the activator impurity and at enhanced rates of crystallization, polymolecular activator layers may form on the intercrystalline surfaces.

4. In the range of low activator concentrations the intensity of the activator bands in the absorption spectrum of the phosphor increases in proportion to the impurity concentration.** This linear dependence, however, cannot be advanced as experimental evidence that structurally these phosphors are purely substitutional solid solutions inasmuch as at equal concentrations of the activator centers the intensity of the bands characterizing them differs for different activator compounds.

For weakly soluble activator compounds there is observed a deviation from the linear dependence (straight dash-dot line in Fig.1) indicative of a gradual approach to saturation. It is probable that the state of saturation is connected with activator concentrations sufficient for complete covering of the crystalline interfaces. The amount of activator on these contact surfaces is usually small and hence has little effect on the lattice parameters, so that any deviation from Vegard's law is virtually undetectable experimentally

---

*In the case of additive coloring of phosphors, when the activator ions locating on the contact surfaces are reduced to atoms and tend to aggregate into colloidal particles, the surface distribution of the activator can be observed under the ultramicroscope[9].

**The results obtained by us for the KI:TlI system agree with the data of Yuster & Delbecq[4]. These authors investigated the dependence of the intensity of the activator bands on the concentration of TlI (up to $2 \cdot 10^{-3}$ mole % Tl) at the temperatures of liquid nitrogen and helium. The strength of the oscillators as calculated by Smakula's equation proved to be 0.17. On the basis of our measurements at room temperature the corresponding value is 0.15. At low temperatures the band peaking at 285 mμ is displaced to 282 mμ and the absorption bands become more intense and narrower. The product of the absorption coefficient at the maximum by the half width remains virtually constant and is independent of the temperature.

Metallic thallium and indium give rise to more intense activator bands. In view of the low solubility of these metals in the fused salts, it is difficult to introduce them in sufficiently high concentrations. It must be emphasized that metallic thallium or indium yield the same activator bands and the same luminescence spectrum of the phosphor as their compounds, i.e., as when introduced in the form of ions. This may be explained by the character of the atomic bonds of the metal on the surface of the ionic lattice (see Vol'kenshtein & Roginskii[21]). One can scarcely admit the possibility of a double exchange reaction here, for this would be in conflict with the chemical nature of the compounds in question. Moreover double exchange reactions would lead to the formation of the iodides, in which case the curves for metallic activators in Figs.1 & 2 would coincide for the curves for TlI and InI as activators whereas actually there is an appreciable divergence between the curves.

Electron acceptor levels forming in crystals in the presence of an activator

Microdefects in alkali halide crystals form a system of electron acceptor levels commonly referred to as F-, F'- and M- centers[22]. In addition there may form in these crystals aggregations of F-centers or R'-centers[23] and colloidal centers of the alkali metal atoms; these are usually localized at the dislocations[9,23]. The color centers forming inside the lattice and on the contact surfaces are in equilibrium with each other[23,24]. Plastic deformation of the crystals increases the concentration of acceptor levels on the dislocations.* In additively colored KCl, after a certain amount of plastic deformation the F'-, R- and M-centers become unstable and upon irradiation of the crystals in the F-band there form colloidal aggregates[25].

In the presence of an activator there form in the crystals additional, still deeper electron acceptor levels. As the activator concentration is increased the stability of the F-centers decreases[9]; at the same time the shallower electron acceptor levels also become less stable.

Taking into account the microheterogeneous structure of alkali halide phosphors and the dual distribution of activator in them we can elucidate in which of its two states the activator forms electron acceptor levels. With this purpose in mind, we synthesized KCl and NaCl single crystals by the method of Kiropulos with additions of different amounts of AgCl as activator. The specimens were then colored in saturated vapor of the corresponding alkali metal at a temperature of 550° for 20 hours. Finally, the crystals were ground to form plane parallel plates and these were used to measure the absorption spectrum on an SF-4 spectrophotometer.

These particular materials were selected in view of the following considerations.

1. Sodium chloride and potassium chloride have the same structure. They differ, however, in that the solubility of AgCl in NaCl is unlimited whereas the solubility of this activator in KCl is limited and rather low[26]. Consequently, in the case of dual distribution of the activator the fraction of silver ions entering into the lattice isomorphically (i.e., located at substitutional sites) will be appreciably greater in NaCl:Ag than in KCl:Ag. Hence if in the process of additive coloring the electron localization centers are silver ions situated at lattice sites, then with an equal concentra-

---

*Approximately 10^{17} such traps per cm^3 form in KCl under 10% plastic deformation[25].

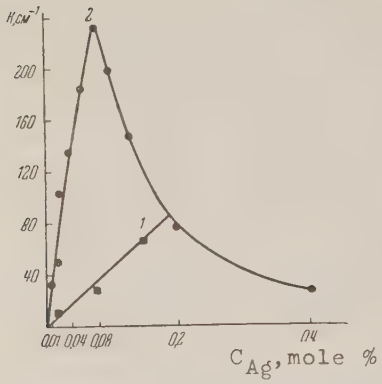

Fig.3. Variation of the coefficient of absorption at the maximum of the atomic band as a function of the silver concentration in the melt: 1) in NaCl:Ag and 2) in KCl:Ag phosphor.

tion of activator in both phosphors the intensity of the atomic bands in the absorption spectrum of NaCl:Ag will be appreciably greater than in the spectrum KCl:Ag. And, on the contrary, if the system of electron acceptor levels owes its existence to the activator lodged on the intercrystalline contact surfaces, then the atomic bands in the spectrum of KCl:Ag will be more intense than in NaCl:Ag. Silver atoms do not "mix" with alkali metal ions and hence interaction of the activator with electrons can be investigated without the interfering complications connected with the formation of large colloidal particles that often form, in addition to the other centers, in additively colored crystals.

Thallium activated phosphors are not suited for purposes of such investigation inasmuch as in the case of their additive coloring, even at low concentrations of the activator, there is formed a high concentration of colloidal particles of different size. As a result, there appear wide absorption bands, greatly exceeding the area of the activator bands in the non-colored phosphor.

Under the ultramicroscope one can readily observe spherical particles regularly distributed along the dislocations[9]. Rolleder[28] inferred that atomic thallium forms in additively colored KCl:Tl despite the fact that the bands observed by him had a half width greater than 1.5 ev with a peak at about 309 mμ. Rolleder used Smakula's formula for calculating the concentration of these centers, assuming for the oscillator strength the value found for F-centers in KCl. Actually, however, in KCl:Ag phosphor the peak of the absorption band for atomic centers is located at 285 mμ; the corresponding peak in NaCl:Ag is situated at 273 mμ.

The results of our measurements of the variation of the coefficient of absorption at the peaks of these bands with the concentration of the activator introduced into the melt in growing the crystals are shown in Fig.3.

In both cases at low concentrations of the activator the intensity of the atomic absorption bands of additively colored specimens increases in proportion to the AgCl content. At equal activator concentrations the atomic bands are more intense in KCl:Ag as compared with NaCl:Ag. This again substantiates our hypothesis of the dual nature of the distribution of activator and at the same time indicates that the atomic centers form only on the contact surfaces. In other words, the activator produces electron acceptor levels only on the block boundaries of the microheterogeneous structure of the phosphor. On the other hand, the activator ions lodging at the lattice sites do not localize electrons and are not reduced to atoms.*

The electron localization levels produced by the activator are so deep that they cannot be ionized thermally. This deduction follows directly from

---

*Kats[29] shares this point of view. He suggests that the atomic centers are electrons localized at vacant and anionic sites located next to the activator ions in the lattice.

the results of experiments on bleaching additively colored phosphors. When these are heated in cadmium vapor[7] or in an electric field the F-centers and the colloids in equilibrium with them (as well as the R- and M-centers) are eliminated from the colored crystals. In contrast, the atomic color centers remain unchanged. These can again transform into ions only when the colored crystals are heated in the vapor of the corresponding halide. In this respect the atomic centers differ substantially from other electron acceptor levels (traps) which are usually investigated by the method of thermostimulation (glow curves).

As may be seen from Fig.3 the intensity of the 285 mμ band associated with the atomic centers in KCl:Ag at first increases with increasing activator concentration and then falls off to the vanishing point.* At the same time there appear new bands in the long wave region of the absorption spectrum; these increase in intensity with increasing activator concentration. The crystals acquire a distinctive orange-red color and under the ultramicroscope one can observe colloidal metal particles. We believe that these colloidal particles form as a result of surface migration of the metal ions after a certain critical concentration is attained. This process is irreversible in contrast to the equilibrium characteristic of the formation of colloidal particles of the alkali metal in the case of thermal or optical transformation of F-centers. In the latter case the aggregation process is realized through ionization of the F-centers and localization of the released electrons on the contact surfaces with subsequent migration of cations to them.[30]

Investigation of the kinetics of phosphorescence of NaBr:InSe phosphor and the nature of the photoelectric conductivity

The ability of the activator to produce deep electron acceptor levels on the contact surfaces leads to the formation of barrier layers in the crystal phosphor. If the potential energy of the electrons on these contact surfaces is much less than the energy of the electrons at the lower edge of the conduction band of the host crystal a unique screening is produced in the barrier layers. We suggest the following interpretation of the character of this screening.

The electrons localized on the contact surfaces cannot be brought into the conduction band under the influence of the potential gradient of an external electric field applied to the crystal. This follows directly from the results of experiments on additive coloring of phosphors with an optimal propertion of activator[7]. Consequently, the entire potential gradient is distributed in the surface layers, while inside the crystal lattice there is no directed electric field. Under these conditions it is impossible to detect any photoconductivity despite the fact that free electrons and holes are produced in the crystal in the process of excitation. Their motion is determined by the contact potentials on the intercrystalline surfaces, particularly in cases when their mean free path is commensurable with the distance between two neighboring contact surfaces. When the crystal phosphor is excited in the activator bands, the electrons and holes appear only on the contact surfaces. The barrier layer prevents them from moving through the crystal.

---

*Analogous experiments with NaCl:Ag were not successful. Inasmuch as the rate of additive coloring falls off sharply at a relatively low concentration, it proved impossible to obtain plates of sufficient thickness for absorption measurements even by prolonged heating at high temperatures in sodium vapor.

This, we suggest, is a qualitative explanation of the absence of a measurable photoconductivity in thallium phosphors.

We feel, however, that this peculiarity of thallium phosphors is not a sufficient basis for segregating them into a special group, distinct from other typical phosphors. In connection with this we undertook a search for new activators for alkali halide salts, activators that would make it possible to obtain crystal phosphors with the same properties as those obtained by the introduction of thallium but that would at the same time possess photoconductivity such as that common to zinc sulfide phosphors.

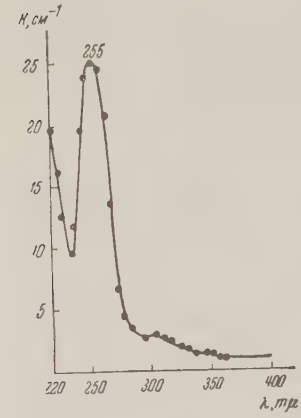

Fig.4. Absorption spectrum of the NaBr: InSe phosphor.

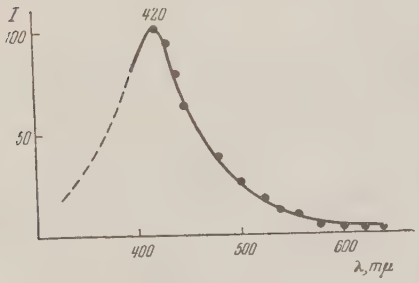

Fig.5. Luminescence spectrum of the NaBr: InSe phosphor.

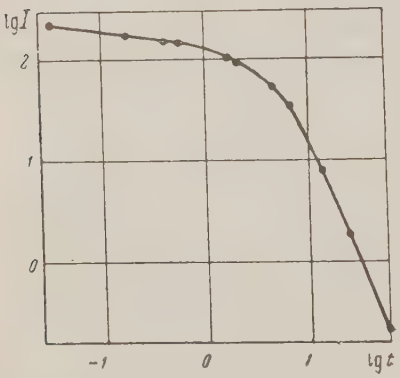

Fig.6. Luminescence decay of the NaBr: InSe phosphor.

Among the new phosphors prepared in these experiments, of greatest interest perhaps, are single crystals of sodium bromide activated with InSe. The absorption spectrum of this phosphor in the region of the activator bands is shown in Fig.4. At room temperature three bands are observed: a very weak one at 310 mμ and stronger ones at 255 and 220 mμ. The luminescence spectrum, shown in Fig.5, has a peak at 420 mμ and, as in the case of all typical phosphors, does not depend on the energy of the exciting radiation. In contrast to thallium phosphors, InSe activated NaBr single crystals when excited by light in the activator bands yield a bright and persistent afterglow of the same spectral composition as their fluorescence. Fig.6 shows the decay curve of the fluorescence excited by the 254 mμ mercury line. It has the usual shape of a second order hyperbola.

Excitation of the NaBr: InSe phosphor by light in the activator bands gives rise to pronounced and readily detectable photoconductivity. The "sign" of the photocurrent carriers was determined by the capacitor method. They proved to be negative, i.e., electrons. Photoconductivity in NaBr: InSe is appreciably lower than in ZnS phosphors or silver halide salts, inasmuch as in alkali halide crystals the electron displacement is 1-2 orders of magnitude lower than in zinc sulfide and approximately four orders of magnitude less than in well annealed AgCl single crystals.

Thus the absence of a measurable photoconductivity in some phosphors cannot be interpreted as experimental substantiation of the Seitz structural model and luminescence scheme.

From the cited experimental data it may be concluded that in the process of growth the activating impurities, acting as surface active materials, give rise to the polyhedral structure

observed in alkali phosphor crystals. The mosaic structure of alkali halide phosphors is one of their fundamental attributes. The character of the additional absorption spectrum is determined by the activator located on the intercrystalline contact surfaces. Deep electron localization levels form on these contact surfaces. Their recombination with holes corresponds to liberation of energy in the form of radiation. The luminescence spectrum is determined by the difference between the energies of the localized holes and electrons on the contact surfaces. Consequently, alkali halide phosphors are surface activated crystals and should be distinguished as such from the class of luminophors with discrete emission centers. Hence in the case of phosphors of this type in order to obtain a high efficiency, it is necessary to produce a well-branched network of contact surfaces with sufficiently deep electron or hole localization levels. The optimal proportion of the activator is determined by its coefficient of dual distribution in the crystal and depends on the portion of the introduced impurities capable of being adsorbed on the intercrystalline surfaces and producing barrier layers.

The writers desire to thank E.E.Bukke and Z.L.Morgenshtern for their aid in determining the electrical and luminescent properties of the NaBr:InSe phosphor.

All-Union Institute of Mineral Raw Materials.

References

1. F.D.Klement, Trudy (Transactions), Institute of Physics and Astronomy of the Estonian SSR Academy of Sciences, 1, 13 (1955).

2. N.F.Mott & R.W.Gurney, Electronic Processes in Ionic Crystals (In Russian trans., M.1950).

3. F.Seitz, J.Chem.Phys., 6, 454 (1938).

4. E.Koch, ZS.f.Phys., 57, 638 (1929); 59, 378 (1930); P.Yuster & C. Delbecq, J.Chem.Phys., 21, 892 (1953); J.Schulman, R.Ginter & C.Klick, J.Opt. Soc.Am., 40, 854 (1950); J.Etzel, J.Schulman, R.Ginter & J.Claffy, J.Phys.Rev., 85, 1063 (1952); L.Beliaev, M.Galanin, Z.Morgenshtern & Z.Chizhikova, Doklady, AN SSSR, 99, No.5, 691 (1954).

5. P.Prigsheim, Fluorescence and Phosphorescence (P.433, in Russian trans. M.-L.,1951); R.K.Swank, Usp.fiz.nauk., 58, No.3, 519 (1956).

6. F.E.Williams, J.Phys.Chem., 57, 780 (1953).

7. L.Shamovskii & L.Rodionova, Doklady AN SSSR, 92, 5, 939 (1953).

8. L.Shamovskii, L.Rodionova, G.Sidorenko & Iu.Zhvanko, Doklady AN SSSR, 99, 235 (1954).

9. L.Shamovskii & L.Rodionova, Doklady AN SSSR, 99, 381 (1954).

10. R.Oschima, H.Abe, H.Nagano & M.Nagusa, J.Chem.Phys., 23, 1721 (1955).

11. A.Smakula, ZS.f.Phys., 59, 603 (1930).

12. O.Stasow & E.Sauer, Gött.Nachr., 3, 77 (1928); W.Runciman & E.Steward, Proc.Phys.Soc., 66, 401, 5 (1953).

13. Ch.Lushchik, Trudy (Transactions), Institute of Physics and Astronomy of the Estonian SSR Academy of Sciences, 3 (1955).

14. G.A.Morton, Dosimetry of Ionizing Radiations (In Russian trans., M. 1956).

15. P.Prigsheim, Fluorescence and Phosphorescence, (P.415, in Russian trans., M.1951).

16. T.V.Aref'eva, A.A.Pozdniakova & R.G.Pats, Sb.khimichekikh, fiziko-khimicheskikh i spektral'nykh metodov opredeleniia redkikh i rasseiannykh elementov (Collected articles on chemical, physical-chemical and spectroscopic methods of determining rare and scattered elements), No.1, 98 (1955).

17. S.D.Gur'ev & E.P.Shkrobot, see Ref.16 above, No.1, 103 (1955).
18. Iu.Zhvanko, Z.Morgenshtern & L.Shamovskii, Izv.AN SSSR, Ser.fiz., 21, 5 (1957). (Translation in Bulletin, Vol.21, No.5).
19. D.Heard, Introduction to the Chemistry of Hydrides (In Russian trans., M., 1954).
20. L.Shamovskii, Optika i spektroskopiia, 1, 3, 407 (1956).
21. F.Vol'kenshtein & S.Roginskii, Zhur.fiz.khim., 29, 485 (1955).
22. F.Seitz, Rev.Mod.Phys., 26, 1 (1954).
23. A.Scott & W.Smith, Phys.Rev., 83, 982 (1951).
24. A.Scott, W.Smith & M.Thompson, J.Phys.Chem., 57, 757 (1953).
25. Werner, Känzig & Ueta, Phys.Rev., 98, 236 (1955).
26. Landolt-Börnstein, Phys.-Chem. Tabellen, 1 (1923).
27. M.Hansen, The Structure of Binary Alloys, Vol. (In Russian trans. M.1941).
28. I.Rolleder, Bulletin of the Polish Academy of Sciences, Section 3, No.9, 2 (1954).
29. M.L.Kats, Doklady AN SSSR, 58, 1637 (1947).
30. A.Scott & F.Theisen, J.Chem.Phys., 20, 529 (1952).

DISCUSSION

M.V.Fok: What do you think of the work of Williams* who calculated the theoretical spectrum of KCl:Tl and obtained good agreement with experiment? He assumed that the energy is absorbed by ions located at the lattice sites.

L.M.Shamovskii: I think it would be interesting to try to apply Williams' calculations to the model where the activator is located on the contact surfaces and also to carry out calculations for NaI:Tl, RbI:Tl and KI:Tl. The lattice parameters of these phosphors differ widely, while their absorption and luminescence spectra are virtually identical.

M.L.Kats: In speaking of the properties of crystal phosphors in the presence of activator ions you infer that your remarks apply not only to your particular case but to all activators in alkali halide phosphors including silver. Does it not seem strange to you that you take different lattices where the gap between the filled and upper bands differs, take different activators and in all cases assume that the activator levels lie in the filled band and hence are not manifested?

L.M.Shamovskii: The absorption spectra of many phosphors are made up of the sum of the absorption spectra of the activator and of the host material. Hence the long wave bands always belong to the activator. By virtue of the fact that the activator is located on the contact surfaces, the bands associated with it become narrower and sharper. I assume that the activator ions lodged at the lattice sites are not evinced in the absorption spectrum in the form of independent bands. Perhaps they do absorb but their bands are masked by the fundamental absorption of the host material.

Question: You introduce metallic thallium and assume that it exists in the form of atoms, then you introduce Tl^+ and assume that it exists in the form of ions, if not in the lattice at any rate on the surface. How do you explain that different centers yield identical spectra?

L.M.Shamovskii: This question will be considered in detail in the report of Vol'kenshtein and Roginskii on the adsorption of metal atoms on the surface of an ionic crystal. Regardless of whether the activator is introduced in the

---

*For criticism of Williams' work see: D.A.Petterson, C.C.Klik, Phys. Rev., 105, 401 (1957) and R.S.Knox, D.L.Dexter, Phys.Rev., 104, 1245 (1957).

form of ions or atoms, the bands of the additional absorption and the luminescence spectrum of the phosphor will remain unchanged. They greatly differ, however, as regards the absorption coefficient at the maximum of the activator band. This difference, we believe, is due to the difference in the values of the coefficient of dual distribution of the activator.

F.D.Klement: In every scientific argument we must approach the subject with utmost objectivity and renounce all preconceived ideas. If new data show that we must abandon a currently held view we must be prepared to do so, but the new hypothesis or premises must explain not only the new but also the old data.

In the present case I feel that the facts support the present, commonly held view that the particles present in the crystal in the solid solution form do actually participate in the process of luminescence. Our x-ray diffraction data, the necessity of heating the mixture to form a phosphor, the behavior of phosphor sublimates studied in our laboratory and numerous other facts are consistent with the concept of phosphors as a solid solution but may be difficult to explain from the viewpoint of contact surfaces advanced by Shamovskii. I want to emphasize that I do not deny the possibility of absorption of activator on the contact surfaces or the possible existence of a class of adsorbate phosphors; I am merely arguing against the view that everything in ordinary crystal phosphors depends on the contact surfaces and adsorption and that the activator ions lodging on the regular lattice sites and the intersites play no significant role in luminescence.

A.A.Shishlovskii: The assertion of the speaker that activator ions located at lattice sites play no role in crystal phosphors is in conflict with the spectral data for alkali halide phosphors wherein certain luminescence bands are excited in the absorption band of the activator located in the higher wavelength region as compared with the absorption of the host lattice. These bands have been calculated by Williams and have been also observed in aqueous solutions of halide salts of thallium, lead and other heavy metals. Very different conditions obtain for ions located at microdefects of the host lattice; these conditions are responsible for the different appearance of the spectra and are highly pronounced in phosphor sublimates.

Ch.B.Lushchik: All the facts cited by the speaker show that there is no difference between phosphors activated with Tl^+ and phosphors activated with In^+. The speaker simply compared the Tl^+ and In^+ bands corresponding to different electron transitions in the ions. Photoconductivity should also be observed in the short wave band of Tl^+. On the other hand, it should not be observed in the long wave band of In^+. The long wave band corresponds to the $^1S_o \rightarrow {}^3P_1$ transition which does not lead to ionization of the luminescence center, while the short wave band corresponds to the $^1S_o \rightarrow {}^1P_1$ transition for which ionization is more probable. The fact that photoconductivity was detected in NaBr:InSe is of great interest.

N.I.Ivanova: I feel that one should not go to extreme points of view as regards thallium phosphors. I would like to cite a few facts that indicate that not all but at least some of the emission bands may be attributed to activator located on the surface. The KCl:Tl phosphor has several luminescence bands: a band at 305 mμ, several intermediate bands and an orange band. These behave in different manners; the 305 mμ band is characteristic of single crystals and is present at low concentrations of the activator. At high concentrations (up to 16% Tl) the orange band becomes intense (I shall not speak of the intermediate bands here). It is difficult to attribute all these bands to the same thallium ions and explain the appearance of the orange band only by a change in the selection rules. At such high concentrations of

thallium there must be an appreciable distortion of the short-range order and something other than a change in the degree of forbiddenness of the transitions must be involved.

Further when we heat the phosphor the spectrum changes with increasing temperature. At low temperatures the ultraviolet band is intense although the others are also present, while at 300° the ultraviolet band vanishes and the intensity of the orange band is greatly enhanced. This is particularly noticeable in the case of specimens consisting of fragmented or ground up coarse grains; such fragmentation obviously bares initially internal layers of the crystal, i.e., brings to the surface thallium which initially defused into the lattice. We attempted to grow KCl:Tl single crystals with a high concentration of thallium in order to obtain a phosphor with an orange band. We succeeded in doing this only under conditions when the crystal became turbid; microscopic examination showed that the orange light emanated from chipped out portions or fragments of such crystals.

K.K.Rebane: Admittedly Williams' calculations are not as rigorous as they might be and the accuracy of his results is not high, but it must be noted that in order to bring Shamovskii's concepts into line with Williams' results it is not sufficient to modify or refine Williams' calculations. If Shamovskii's viewpoint were the correct one, then all of Williams' calculations and the deductions following therefrom, which as we know give fairly good agreement with a number of experiments, would be incorrect inasmuch as the model upon which Williams' calculations are based would be wholly erroneous. In view of the agreement with experiment, however, we feel that Williams' model is correct.

For the absorption bands of the Tl^+ ion in the KCl crystal lattice to be superposed on the fundamental absorption and not appear in the absorption spectrum of the activated crystal (as Shamovskii suggests is the case) the energy separation between the levels of the ion in the lattice should increase as compared with the separations for the free ion. It is known, however, that as a rule the distance between the energy levels of an ion decreases in the crystal. Williams, too, obtained a long wave shift of the absorption band of Tl^+ compared with the lines of the free Tl^+ ion. It is hardly conceivable that the error in Williams' calculations is so great that even the sign of the relative displacement of the terms is wrong.

I feel that the fact, cited by Shamovskii himself, that there obtains a virtually unchanged absorption band of the activator in the liquid phase is in itself convincing evidence that the ions located at the lattice sites absorb light.

L.M.Shamovskii: I do not at all deny the possibility of diffusion of the activator into the host lattice. On the contrary, this follows directly from our hypothesis of the dual character of the activator distribution.

The fact that the mixture has to be heated to "form" a phosphor is not proof that the luminescence centers must necessarily be located at the lattice sites of the substitutional solid solution. Heating is also necessary for surface distribution of the activator. It is no accident, I believe, that the temperature of "formation of phosphors" corresponds to that of sintering of the powder. The process of sintering is the result of surface migration of ions. In contrast, recrystallization is directly connected with diffusion into the bulk. Recrystallization processes, however, become noticeable only at appreciably higher temperatures than those of the beginning of sintering. The degree of isomorphism is important not only for the formation of solid solutions but also as regards the surface properties. This follows from the fact that the activator is distributed in the phosphor in a dual manner. The coefficient of distribution has a thermodynamic nature.

The available x-ray diffraction data regarding the fulfillment of Vegard's law do not preclude the possibility of distribution of the activator particles over the contact surfaces. This is substantiated by the results of a number of different investigations, even though admittedly in the case of the KCl:TlCl system, which is characterized by unlimited mutual solubility of the components, the predominant part of the Tl^+ ions may enter into the composition of the solid solution.

Contrary to Klement's assertions that the intensity of the absorption and luminescence bands falls off with decreasing solubility of the activator, according to our results at equal activator concentrations in KI:Tl and KI:In phosphors the most intense bands in the absorption and luminescence spectra are obtained with the least soluble activator compounds. This result is obviously not consistent with the concept of phosphors as substitutional solid solutions.

Quenching of luminescence incident to fragmentation of the phosphor may be interpreted from different standpoints. Not every surface is suitable or favorable for luminescence. It is known, for example, that plastic deformation of crystal phosphors sharply reduces the light output and the scintillation efficiency. Hence in the process of preparation crystal phosphors are subjected to prolonged heating in order to eliminate various structural dislocations (aside from contact surfaces produced by the activator) capable of localizing electrons and holes and thus obviating their participation in the processes of recombination on the activator. The hypothesis advanced by some investigators that fragmentation leads to an increase in the concentration of vacant sites in the lattice and acceleration of impurity diffusion into the crystal appears questionable to me.

As regards the remarks of Ch.B.Lushchik it should be noted that photoconductivity in thallium phosphors is not observed when the phosphor is irradiated in either the activator bands or in those of the host material. The photoelectric character of the excitation of thallium phosphors by hard radiation, on the other hand, cannot be doubted. We explain the absence of a measurable photoconductivity by the existence in these phosphors of contact surfaces with deep electron localization levels. They give rise to screening and have barrier properties. It is not only by chance, therefore, that phosphors with a sufficiently high proportion of activator are not colored by additive methods even with the application of a strong field. This is why we felt that the appearance of electron conductivity and a persistent afterglow associated with the recombination mechanism in NaBr:InSe phosphor was particularly significant.

We regard the redistribution of intensity in the emission spectrum of phosphors with changes in the activator concentration as a result of the formation of thicker than monomolecular activator layers on the contact surfaces.

Now regarding the remarks of K.K.Rebane. It is known that the absorption spectrum of crystal phosphors in the first approximation may be regarded as the sum of the absorption bands of the activator and the host material. For each material, excitation in the long wave bands is interpreted as a result of transition of electrons from the highest filled band to the lowest conduction band. The upper band of filled levels corresponds to the valence electrons of the halide and not of the metal or the thallium. The short wave bands of the activators which might be attributed to the transition of valence electrons from the filled cation levels are overlapped and masked by the long

wave absorption of the host lattice. For this reason one cannot observe independent absorption bands associated with the thallium in alkali halide phosphors. Consequently, the activator bands in phosphors may be interpreted as associated with electron transitions from the valence band of the halide to the conduction band within the bounds of the contact surfaces. According to our hypothesized band model the photoelectrons produced in this manner cannot penetrate into the conduction band of the host material (or its solid solution). The scheme proposed by us is consistent with the approximate additivity of the absorption spectra of phosphors. As for the analogy with the absorption spectra of aqueous solutions, it appears to us to be consistent with our model inasmuch as there may form groupings similar to the complexes in solutions on the contact surfaces of phosphors. On the other hand, the undoubted existence of complexes in aqueous solutions and the similarity of their optical properties with those of crystal phosphors cannot be satisfactorily explained on the basis of the model of isomorphous location of the activator in the crystal lattice.

LUMINESCENCE AND DISTRIBUTION OF TRAPPING LEVELS IN ALKALI HALIDE CRYSTALS WITH EXCESS HALIDE

- M.N.D'iachenko

Electron trapping levels in colored alkali halide layers are apparently due to impurities and inhomogeneities in the structure of the crystals, i.e., to F- and F'-centers and other lattice defects. Changes in the structure of real crystals are usually ascribed to the formation of anion and cation vacancies at the regular lattice sites and positively or negatively charged ions at the interstital sites, all of which together with surface cracks and atomic impurities may create conditions for the appearance of additional trapping levels.

Our experiments show that the number of trapping levels in NaCl crystals increases when the crystals are annealed at temperatures close to the melting point. Presumably as a result of the heat treatment there form cation and anion vacancies at the regular sites and positive and negative ions at the interstital ones. Introduction of excess halide into the crystals also results in an increase in the number of trapping levels; the increase is particularly great when iodine is introduced into the NaCl crystals. Heating of these crystals in sodium vapor leads to different results.

Introduction of other metals - Cu, Ni and Ag - as activators also has a peculiar effect on the trapping levels. Trapping levels in alkali halide crystals has been investigated by Kats[1], Parfianovich[2] and D'iachenko[3]. Significant results have also been obtained by Lushchik[4,5].

Our experimental data on trapping levels in alkali halide crystals, fluorite and quartz, taking into account the influence of annealing and the presence in the crystals of halides and metal activators, cannot be satisfactorily explained from the standpoint of present models and theories of elementary centers in crystal phosphors[6-14].

In the present report we give the results of our investigation of trapping levels in colored NaCl crystals activated with halides. The distribution in energy of the trapping levels was determined on the basis of the glow curves of the ultraviolet and visible luminescence after excitation of the crystals by x-rays. In some cases we also excited the halide activated crystals by β-particles from artificial radioactive sources. The ultraviolet radiation from the colored crystals was detected by means of a photon counter sensitive to radiation in the 1800 to 4000 A range[15]. The visible luminescence was measured by a FEU-19 photomultiplier. The thermostimulation of the crystals was realized by uniform heating at the rate of 1.75 degree per min over the entire investigated temperature range. The NaCl specimens used for determining the influence of halides were of the same size and were cut from the same piece as the control specimens. The halides were introduced into the crystals in sealed pyrex tubes held at a temperature of 650° for a period of 10 hours; the halide vapor pressure in the tubes was approximately atmospheric. The control specimens were subjected to a similar heat treatment in tubes with air.

The crystals were excited with x-rays in two steps: at room temperature and at the temperature of liquid air for 10 minutes (x-ray tube voltage 150 kv; current 10 milliamp).

NaCl crystals activated with halides become colored and luminesce in the ultraviolet and visible regions of the spectrum more intensely than natural crystals, both those subjected and not subjected to high temperature annealing.

The glow curves for the ultraviolet luminescence of NaCl crystals activated with Cl, Br and I are shown in Fig.1. As may be seen, the intensity of the

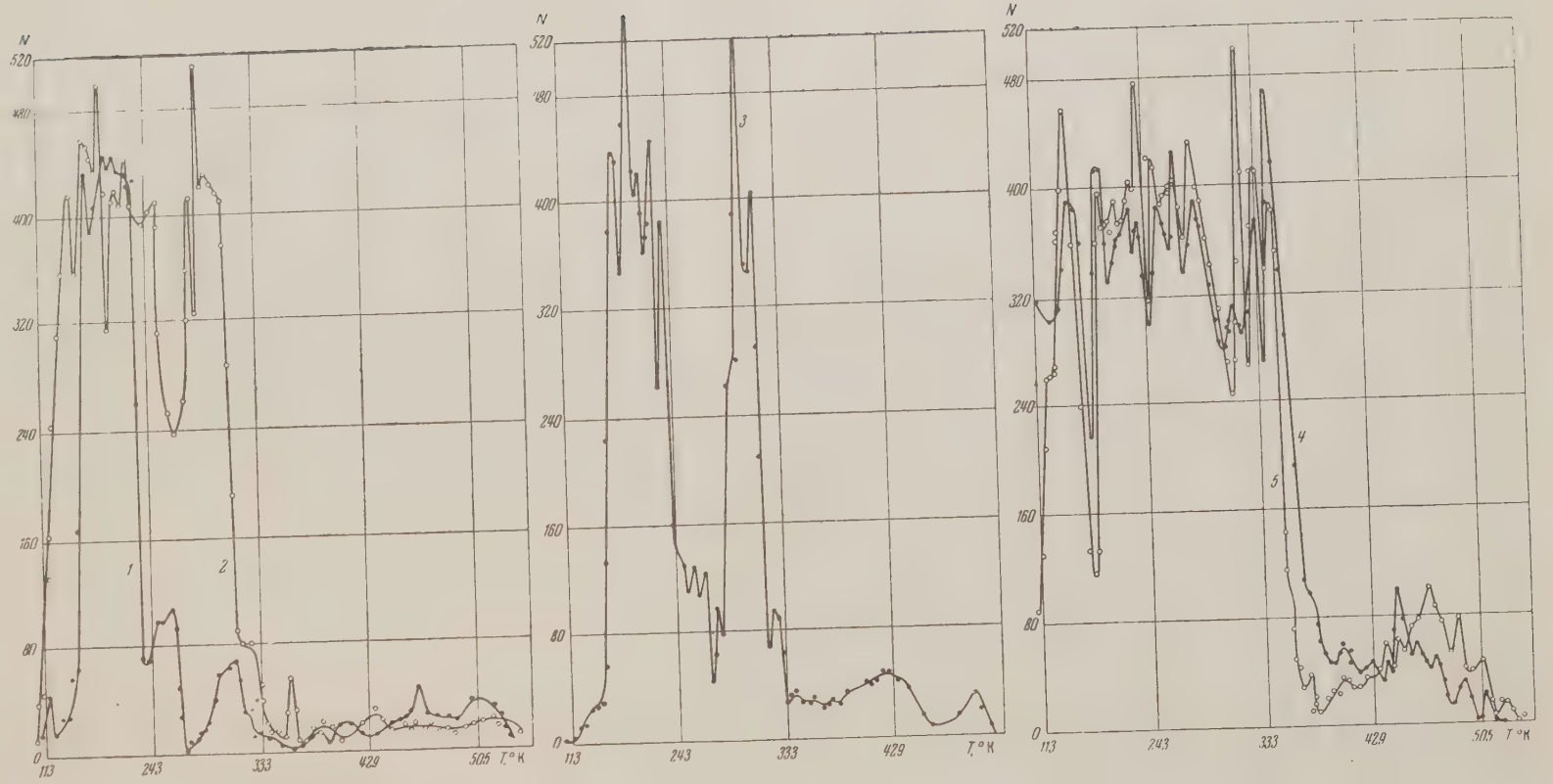

Fig.1. Thermostimulated ultraviolet luminescence of NaCl crystals excited by x-rays: 1) nonactivated (control) crystal, 2) crystal activated with Br, 3) crystal activated with Cl, 4 & 5) crystal activated with I (the curves pertain to two different specimens).

ultraviolet luminescence peaks in the temperature range from 113 to 330°K is somewhat greater in the case of Cl and Br activated crystals than in the case of the control. Bromine exerts a somewhat greater influence on the trapping level distribution than chlorine. In the temperature interval from 340 to 550°K an excess of Cl or Br produces no noticeable change in the intensity of the weak peaks.

The greatest effect, however, is produced by the presence of excess iodine. In this case there appears an appreciable number of new trapping levels. The ultraviolet peaks are pronounced over the entire investigated temperature range and are particularly intense in the interval from 113 to 350°K. The reproducibility where the temperature positions of the individual peaks in the emission of different specimens is concerned is satisfactory (see curves 4 & 5 in Fig.1).

Only one component is observed in the decay of the ultraviolet luminescence of x-ray excited NaCl crystals activated with Cl, Br and I (Fig.2). Crystals activated with iodine yield the most intense luminescence in the ultraviolet; the luminescence of Br activated crystals is less intense and that of Cl activated ones is still weaker.

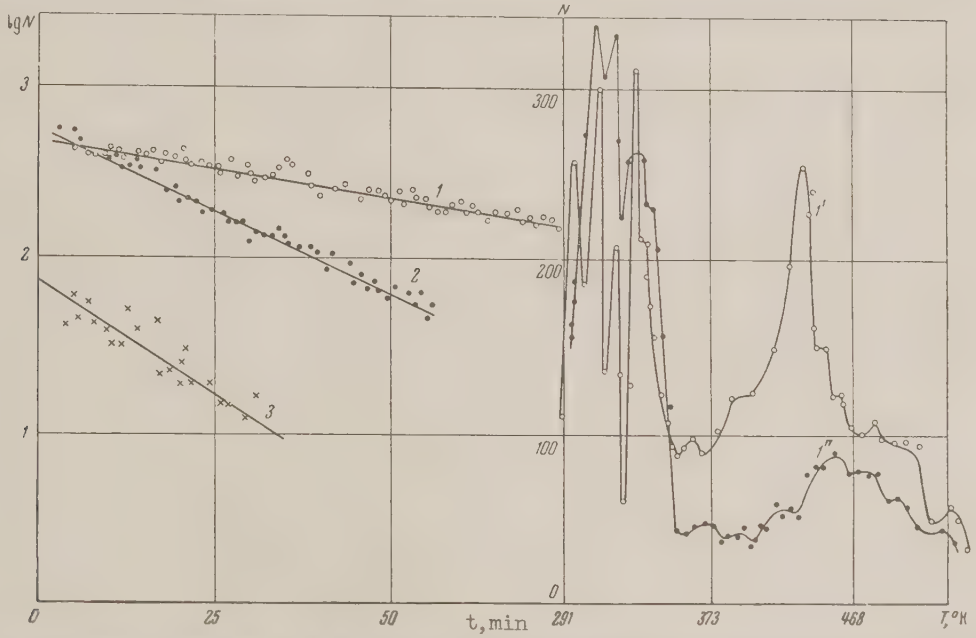

Fig.2. Decay (curves 1,2 & 3) and thermostimulated emission after complete natural decay (1' & 1'') of the ultraviolet luminescence of x-ray excited NaCl crystals: 1) activated with I, 2) activated with Br, 3) activated with Cl, 1' & 1'') activated with I (curve 1'' pertains to the same crystal after repeat excitation with x-rays following the first cycle of decay and thermostimulation).

After natural decay of the luminescence, we again recorded the thermostimulation curves for the same crystals. Curve 1' in Fig.2 shows a number of ultraviolet luminescence peaks for a NaCl:I crystal. Curve 1'' was obtained for the same crystal after repeat excitation with x-rays. The reduction of the intensity peaks in this curve in the temperature interval from 370 to 500°K can be explained by the partial elimination of iodine from the crystal during the first thermostimulation heating.

It is known that natural NaCl crystals can luminesce under excitation by light from a spark between aluminum electrodes. At the same time light from a cadmium electrode spark does not excite luminescence in such crystals. In the case of NaCl crystals annealed at a temperature close to the melting point, however, excitation by light from a cadmium electrode spark does produce both visible and ultraviolet luminescence. No discernible luminescence is excited in these crystals under excitation by ultraviolet rays from a mercury tube. Ultraviolet light from a quartz mercury discharge tube excites luminescence in NaCl crystals activated with iodine but not in NaCl crystals activated with either chlroine or bromine. This may be explained by the absence in such crystals of trapping levels having a depth of approximately 5 ev. Traps of approximately this depth are present in NaCl:I crystals. These levels are presumably associated with the V-band.

The thermostimulated luminescence of nonannealed NaCl crystals in the visible region of the spectrum is much less intense than that of annealed crystals; furthermore, the glow curves for nonannealed crystals comprise appreciably fewer peaks than the curves for annealed crystals, as may be seen by comparing the curves in Fig.3.

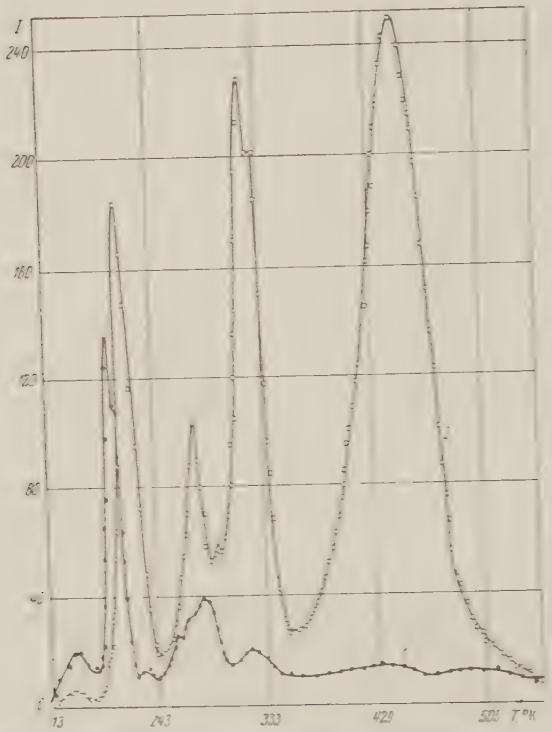

Fig.3. Thermostimulated luminescence of NaCl crystals in the visible region of the spectrum: 1) nonannealed crystal, 2) annealed crystal.

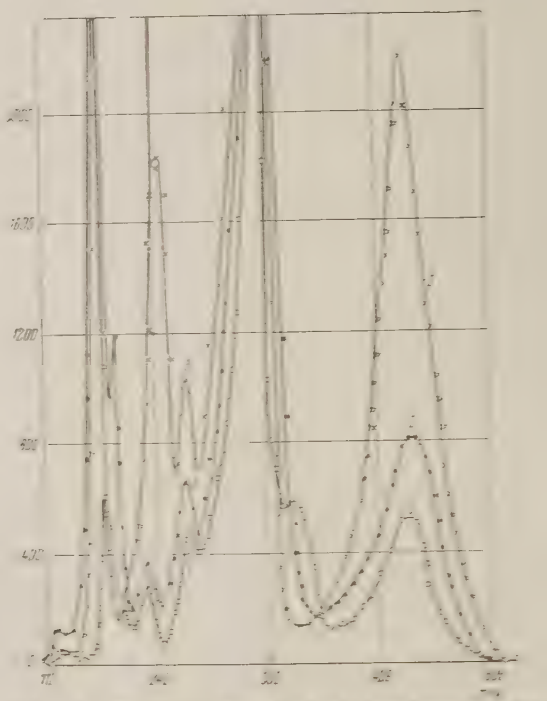

Fig.4. Thermostimulated luminescence in the visible region of the spectrum of NaCl crystals: 1) activated with Cl, 2) activated with Br, 3) activated with I.

The number of thermal peaks in the visible region is as a rule appreciably smaller than in the ultraviolet both for annealed crystals and for crystals activated with halides. Fig.4 shows the glow curves characterizing the

thermostimulated luminescence in the visible region (as recorded by means of a photomultiplier) for NaCl crystals activated with Cl, Br and I. As may be seen from the curves the temperatures corresponding to the luminescence maxima are virtually identical for all crystals. The luminescence intensity at all the thermal peaks increases in proportion to the atomic weight of the introduced activating halide.

Inasmuch as the size of the atoms is proportional to $A^{1/3}$, the introduction of larger atoms leads to greater disruptions of the crystal lattice, which in turn may lead to the appearance of new trapping levels and strengthening of the already present ones.

Through the use of appropriate light filters we established that the visible emission from natural annealed crystals and crystals activated with iodine occurs primarily in the blue-violet and green regions of the spectrum. For the I activated crystal a number of peaks of the blue-violet luminescence were observed in the temperature interval from 113 to 270°K (Fig.5); the intensity of the peaks differs: the greatest emission occurs at the maximum at 180°K, the intensity of the other peaks being appreciably weaker (curve 1). A weak maximum in the green luminescence was observed at 200°K (curve 2). In the temperature range from 270 to 500°K, we found two intense peaks of the blue-violet luminescence (at 320 and 455°K), and two relatively weak maxima of the green luminescence (at 345 and 436°K). Similar curves for the thermostimulated luminescence in the blue-green region were obtained for annealed crystals.

The blue-violet and green luminescence in these crystals was formerly attributed by us to electron transitions from the conduction band to the F-band and somewhat shallower trapping levels. It must be noted, however, that the green luminescence observed in colored crystals at the temperature of thermal dissociation of F-centers can apparently be explained by retrapping of electrons on shallow levels. On the other hand, the violet emission observed in some crystals cannot be explained by such transitions. It can be identified only with electron transitions to deeper levels.

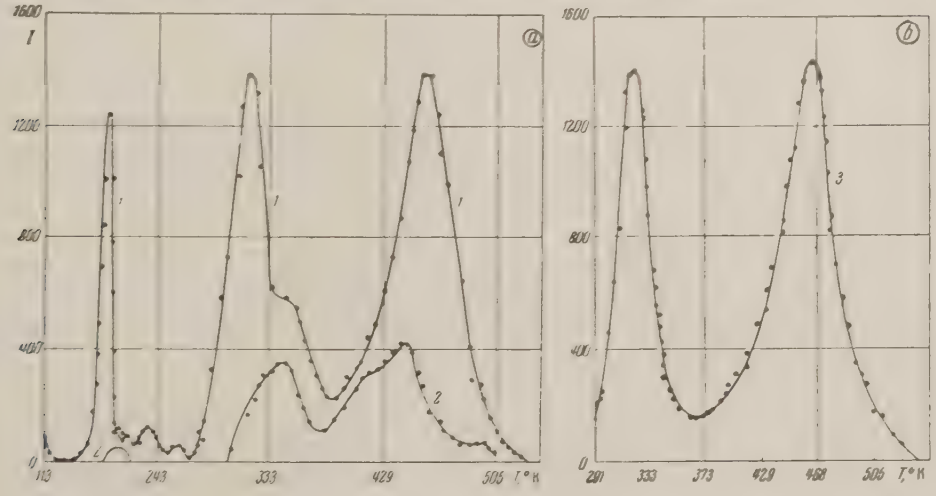

Fig.5. Curves of the thermostimulated luminescence of a NaCl:I crystal recorded through filters with maximum transmission at 1) 480 mμ, 2) 530 mμ, and 3) 720 mμ.

In the case of some annealed and I activated NaCl crystals we also observed red luminescence, the temperature maxima of which coincided with the temperature maxima for the blue-violet emission from the same crystals.

In experiments with crystals with F-centers excited by light in the F-band we observed thermal peaks of the infrared luminescence in NaCl at 77 and 220°K, in KBr at 98, 165 and 250°K and in KCl at 113, 220, 265, 305 and 370°K. Annealing the crystals enhanced the intensity of the infrared emission and accelerated the decay. The infrared radiation was detected by means of an FESS-U-10 tube equipped with a 0.5 mm thick ebonite cap.

To summarize, our experiments showed the following:

1. In the case of NaCl crystals activated with Cu, Ni and Ag there is observed an appreciable increase of both the intensity of the ultraviolet luminescence and the number of glow peaks in the 113 to 400°K temperature interval and a marked weakening of the glow peaks in the temperature interval from 400 to 500°K (Fig.6) as compared with nonactivated crystals. These activated crystals are also characterized by a number of very intense peaks of the visible luminescence in the temperature range from 113 to 500°K (Fig.7).

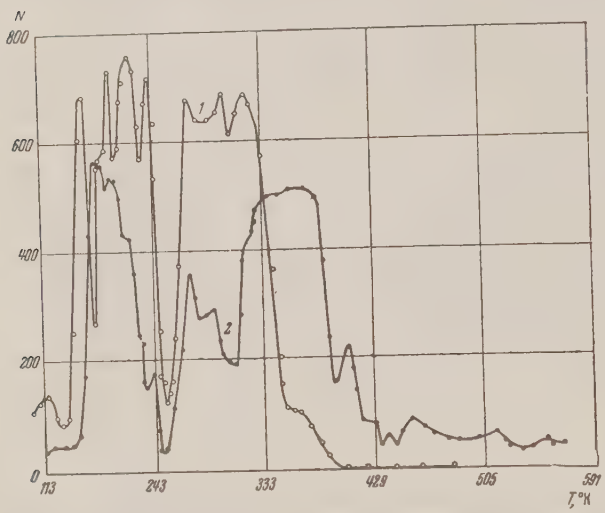

Fig.6. Thermostimulated ultraviolet luminescence of NaCl crystals: 1) activated with Cu, 2) activated with Ag.

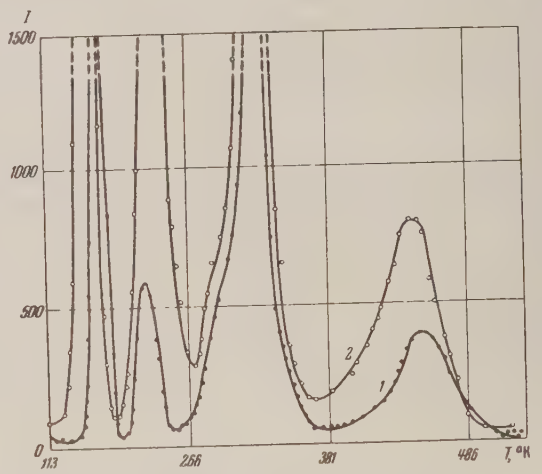

Fig.7. Thermostimulated visible luminescence of NaCl crystals: 1) activated with Cu, 2) activated with Ag.

2. NaCl crystals colored in sodium vapor are characterized by a relatively large number of comparatively low intensity peaks of the ultraviolet luminescence in the temperature range from 113 to 400°K and a complete absence of peaks in the 400 to 500°K temperature interval.

3. Natural NaCl crystals annealed at 750° are also characterized by a large number of ultraviolet luminescence peaks in the entire investigated temperature interval (113-500°K); moreover, the intensity of these peaks is appreciably greater than in the case of crystals colored in sodium vapor (Fig.8). The annealed natural crystals also exhibit a number of peaks in the visible region of the spectrum, but these are of somewhat lower intensity than in the case of the NaCl:Cu, NaCl:Ni and NaCl:Ag phosphors.

4. As compared with nonactivated NaCl crystals, an appreciable increase in the number and intensity of the peaks is observed in NaCl crystals activated with Cl, Br and particularly I. In the case of iodine activated crys-

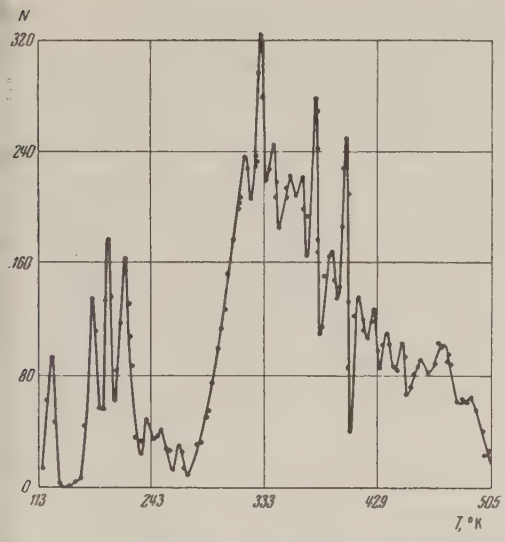

Fig.8. Thermostimulated ultraviolet luminescence of an NaCl crystal annealed at 750°.

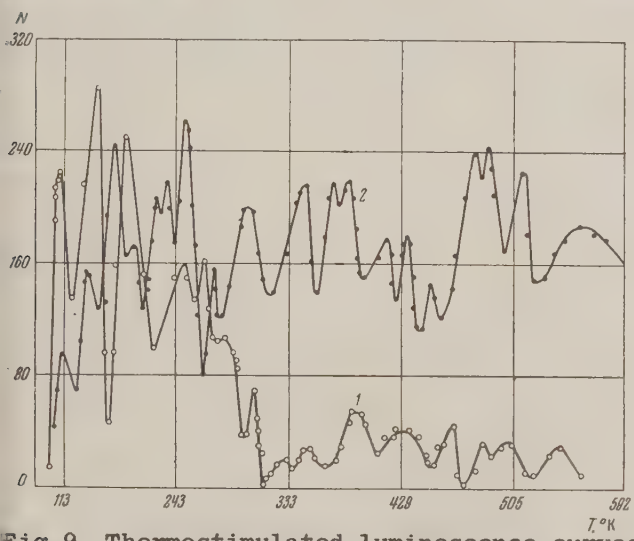

Fig.9. Thermostimulated luminescence curves for NaCl crystals excited by β-particles: 1) nonannealed crystal, 2) crystal annealed at 750°.

tals there is a noticeable increase in the number of trapping levels emptying over the entire temperature range from 113 to 500°K.

5. Excitation of both annealed and nonannealed NaCl crystals by β-particles does not lead to any appreciable increase in the number of visible luminescence peaks as compared with excitation by x-rays. In the ultraviolet region, on the other hand, β-particle excitation does result in a certain increase in the number of peaks (Fig.9).

6. Neutron bombardment of natural NaCl crystals results in the appearance of new trapping levels emptying in the 113 to 500°K temperature range. Fig.10 shows the glow curve for a nonannealed NaCl crystal subjected to neutron bombardment prior to excitation and thermostimulation. In our experiments the crystals were bombarded with both fast and slow neutrons, as a result of which there may have formed in the specimens both extraneous Mg and S atoms and holes.

The experimental results can be interpreted as follows.

1. In thermal de-excitation of trapping levels located between the conduction band and the F-band, the visible emission is due to electron transitions from the conduction band to the F and shallower levels, while the ultraviolet emission is associated with electron transitions from the conduction band to deeper levels lying above the ground state band (V-levels and others).

2. The absence of ultraviolet luminescence peaks in the 400-500° range in the case of crystals activated with Cu, Ag and Ni may be explained by the destruction of deep traps through electrolysis and in the case of crystals colored in sodium vapor by partial neutralization of the free vacancies by Na ions.

3. The increase in the intensity of the luminescence peaks in the 400 to 500°K temperature range in the case of annealed crystals is due to the appearance in the crystal of anion and cation vacancies and of ions at the interstital sites as the result of thermal diffusion. This is also apparently the reason for the increase in the intensity of luminescence in this temperature interval of iodine activated crystals.

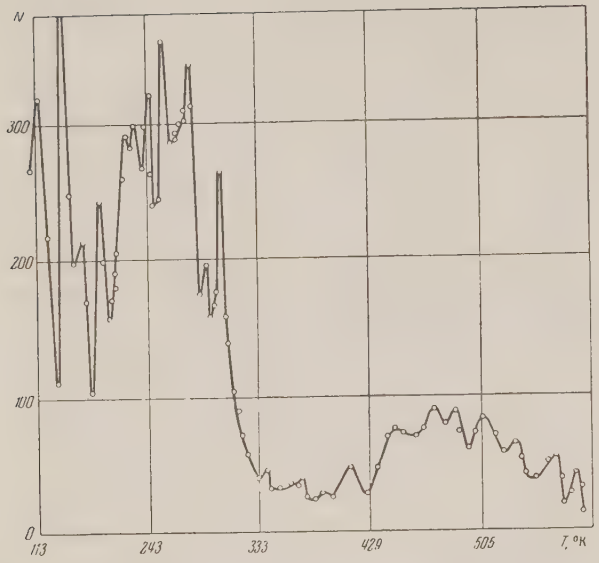

Fig.10. Glow curves for a nonannealed NaCl crystal subjected to neutron bombardment.

4. The noticeable increase in the number of ultraviolet luminescence peaks when the NaCl crystals are excited by β-particles (as compared with x-rays) may be explained by the formation of holes, i.e., anion and cation vacancies in the crystal. The formation of such holes may also explain the appearance of peaks in the 400-500°K range in all the above enumerated cases.

5. The existence of so great a number of levels in NaCl crystals, particularly the activated and annealed ones, cannot be fully explained only by the presence in them of elementary centers of the F, F', M and V types. Apparently, there also exist in such crystals more complicated trapping centers which if they are not combinations of simple centers may at any rate be more complex aggregations or molecular groups lodging on surface crevices and at other defects of the crystal structure.

Kharkov Institute of Medical Radiology and
Kharkov Institute of Railway Transport Engineers

DISCUSSION

A.A.Shishlovskii: M.N.D'iachenko showed us a number of thermostimulation curves with a large number of peaks obtained by means of counters; he noted that the entire band disappears simultaneously with all the peaks. I wonder whether these peaks are real; that is, do they have any real meaning or are they simply the result of unstable operation of the counters?

M.N.D'iachenko: Regarding the reliability of the peaks, I would like to point out that the experiment was carried out in the following manner. The crystal was heated at a uniform rate while two photon counters were directed at it, one with a sensitivity from 1800 to 4000 Å, the other with a range from 1800 to 3000 A. One curve was obtained by means of the more sensitive counter and the other by means of the other one. The peaks in the two curves coincide. If you take any pair of curves and superimpose them you will see at once that the peaks line up.

Ch.B.Lushchik: Did the counter circuits have independent power supplies?

M.N.D'iachenko: Yes, these were two entirely independent circuits. In investigating trapping centers one set-up yields sharp peaks, the other bell-shaped ones; the former is closer to the quantum process, while the latter is macroscopic, that is, averages the result. That is the only difference.

Ch.B.Lushchik: I am still doubtful about the real significance of the peaks. The peaks are too narrow; they are much narrower than the theoretical bands. In our measurements with a photomultiplier tube with the set-up properly adjusted we did not get such peaks.

VISIBLE LUMINESCENCE OF SUBTRACTIVELY COLORED ROCK SALT CRYSTALS AT DIFFERENT TEMPERATURES

- D.M.Eremin

As we know, colored alkali halide crystals luminesce both in the ultraviolet and in the visible regions of the spectrum. Whereas there have been many investigations devoted to the ultraviolet luminescence[1-4], there have been very few studies of the visible radiation. This can be explained by the experimental difficulties connected with the low intensity of the emission in the visible region.

We constructed photon counters with a very high sensitivity in a wide spectral range. By means of these new counters we were able to record the visible emission of alkali halide crystals through appropriate light filters. The luminescence of the crystals was excited by x-rays from an RUP-1 x-ray unit operated at a voltage of 140 kv and a current of 10 ma.

Photon counters

Photon counters constructed hitherto, mostly with cathodes made of a thick layer of metal, in most cases record only ultraviolet radiation and only in exceptional cases (and then with low sensitivity) the short wave part of the visible spectrum.

It was commonly assumed that the reason for the response of some photon counters to visible radiation is the presence of impurities that give rise to a long "tail" in the counter characteristic, extending to the red limit of the sensitivity of the given metal. This assumption is true for counters weakly sensitive to the short wave part of the visible spectrum, prepared according to the conventional technique, provided there are actually impurities giving rise to this sensitivity in the metal of which the photocathode is made. Our photon counters are characterized by a high sensitivity in the visible region of the spectrum. The maximum wavelength to which the counters respond is about 7300 Å; the operating potential is 600-680 v; the plateau extends about 80 v. The dark background of individual counters varies from 1 pulse per 2 min to 2 pulses per 1 min. The counters are very stable in operation and their voltage and spectral characteristics do not change appreciably with time. Several counters have been in operation for almost three years.

We carried out a careful spectroscopic analysis of the aluminum of which the photocathodes of our counters were made to determine the presence of possible impurities. No impurities whose work function might assure sensitivity to visible light were detected. Hence the response of our counters to visible radiation is not due to the presence of such impurities. The reason for the sensitivity of our counters to visible light is mechanical polishing of the cathode surface without subsequent heating under vacuum. It is known[5] that mechanical polishing leads to the formation of a surface layer whose structure and properties differ from those of the bulk metal. Heating the polished metal at a temperature above that of crystallization leads to re-establishment of the bulk metal structure and properties (recrystallization). Counters with aluminum cathodes, that initially responded to the entire visible spectrum, after heating under vacuum at 350-400° for 3 hours completely lost their sensitivity to visible radiation. The spectral response of such counters became approximately equivalent to that of conventional counters fabricated hitherto.

Temperature dependence of the visible emission intensity

There have been many investigations of trapping centers in alkali halide crystals by the method of thermostimulation of luminescence. Nevertheless the nature of the luminescence centers in these crystals still remains unclear[6].

When NaCl crystals are irradiated with x-rays, in addition to the ultraviolet emission there is also a weak blue-violet luminescence. In view of the fact that in alkali halide crystals there are a number of trapping levels of different depths, when the excited crystal is heated there must occur different electron transitions. The presence of these different electron transitions must produce changes in the spectral composition of the luminescence. Actually in investigating the visible luminescence of natural NaCl crystals excited by x-rays at room temperature with subsequent x-ray irradiation at the temperature of liquid oxygen, we established that the spectral distribution of the thermostimulated luminescence of the crystal differs at different peaks. Thus at -150° the maximum emission lies at 5900 Å (curve 1, Fig.1), at -63° the maximum is displaced to 4500 Å (curve 2), and at +60° to 4200 Å (curve 3). As may be seen from Fig.1 the intensity peak of the luminescence is displaced to the side of shorter wavelengths with increasing temperature.

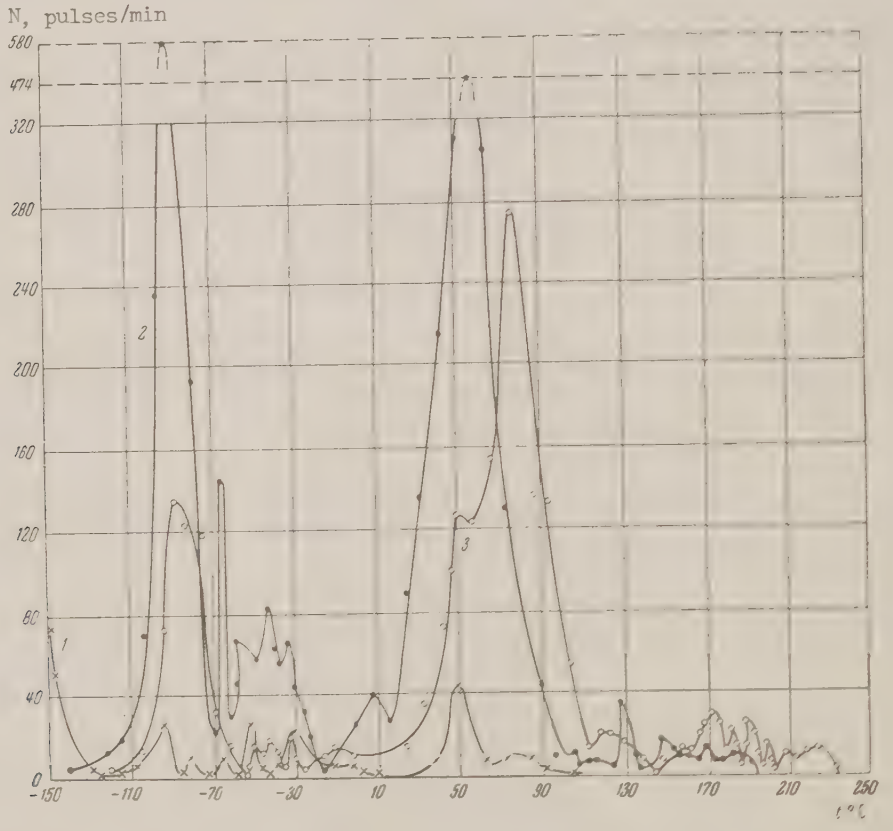

Fig.1. Glow curves of an NaCl crystal excited at room temperature and then at the temperature of liquid oxygen recorded through filters with maximum transmission at 1) 5900 Å, 2) 4500 Å, 3) 4200 Å.

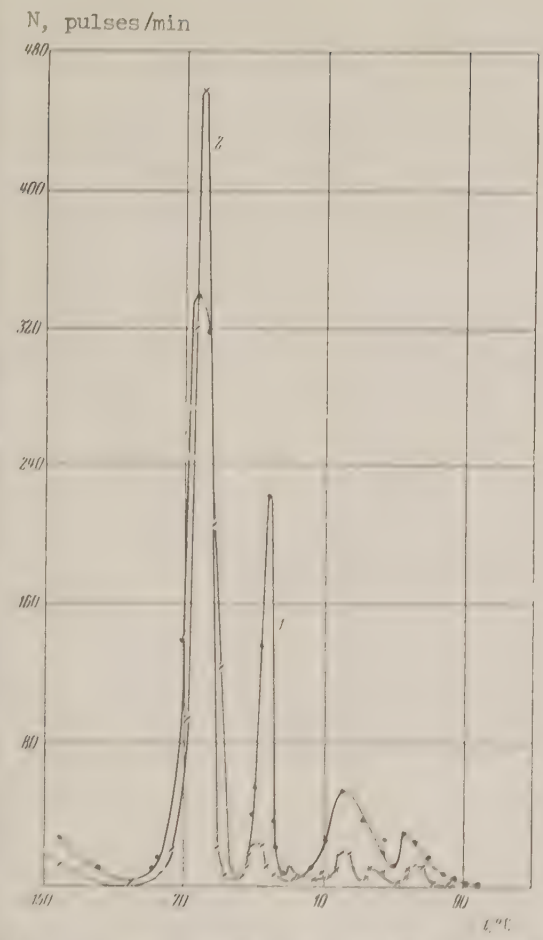

Fig.2. Glow curves for an NaCl crystal excited at the temperature of liquid oxygen recorded through filters with maximum transmission at 1) 4500 Å and 2) 4200 Å.

In order to obtain additional data on the visible luminescence of alkali halide phosphors we carried out experiments with natural NaCl crystals excited at different temperatures (the temperature of liquid oxygen, room temperature, the temperature of breakdown of F-centers and higher temperatures). The thermal de-excitation (glow) curves were recorded in the temperature interval from -170 to +220°.

The thermostimulation curves obtained for an NaCl crystal excited by x-rays at the temperature of liquid oxygen are shown in Fig.2. Curve 1 was recorded through a light filter passing blue radiation (~4500 Å). It will be seen that the curve comprises several peaks of different heights. The two highest peaks are located at -60 and -22°. There are also two noticeable luminescence maxima at +24 and +60°, the positions of which indicate the presence of electrons in the F-band. Curve 2 was recorded under the same conditions with a filter passing violet light (~4200 Å). This curve also comprises a number of peaks whose positions coincide roughly with those of the blue luminescence.

It should be noted that if before irradiation at the temperature of liquid oxygen the NaCl crystal is x-irradiated at room temperature, the maximum intensity of the emission at -60° occurs in the blue band (Fig.1, curves 2 & 3), while when the crystal is irradiated only at the temperature of liquid oxygen the violet luminescence at this temperature is the more intense (Fig.2, curves 1 & 2). This can be explained by the fact that when the crystal is x-irradiated only at the low temperature no electrons are localized in the F-band. Thus the F-levels remain unoccupied (the crystal does not become colored even after prolonged x-raying).

Some investigators assert that NaCl crystals irradiated at the temperature of liquid oxygen become colored lemon-yellow; this was not substantiated in our experiments. When the crystal is warmed the electrons released into the conduction band by thermal emptying of the shallower traps in part return to the normally filled levels and in part go to the F-levels where they are localized. When a sufficiently high temperature is reached the F-centers dissociate, it is assumed in this case the electrons released into the conduction band partly return to the F-band and partly go to deeper levels with emission in the visible region of the spectrum. If this is the case one may naturally ask whether visible emission will be observed if the possibility

of localization of electrons in the F-band is precluded? In order to answer this question we carried out experiments with highly colored crystals, including both naturally colored dark blue crystals and crystals artificially colored in sodium vapor.

As regards influence of temperature the color of such crystals is more stable than that of crystals colored by x-ray irradiation. Complete bleaching of naturally colored crystals occurs at a temperature of 380-400°, while crystals colored in sodium vapor require a still higher temperature (600-650°). Both naturally colored and Na colored crystals when excited by x-rays at room temperature fluoresce with a barely noticeable emission in the visible region. After cessation of excitation no visible phosphorescence is observed. When such crystals are irradiated at liquid oxygen temperature there is also discerned a very weak visible fluorescence. After cessation of excitation, in the process of being warmed to room temperature, these crystals yield barely noticeable flashes of luminescence in the visible region. With further heating up to 220° no visible phosphorescence is observed. The fact that the phosphorescence in the long wave visible region of the spectrum of naturally colored crystals and crystals colored in Na vapor is weak and of short persistence is due apparently first to the absence of electron transitions to deeper levels and second to a reduction in the number of trapping centers in such crystals. Trapping centers forming in such crystals are apparently relatively unstable as regards optical stimulation. Thus if two crystals, one uncolored and one colored in sodium vapor are irradiated at the temperature of liquid oxygen and then after excitation illuminated with visible light from an electric lamp for 1 minute, then while being warmed the colored crystal yields no visible luminescence whereas the uncolored crystal flashes noticeably in the visible region.

Experiments of this type with NaCl crystals colored by means of x-rays are rendered difficult by the de-exciting influence of this radiation. A number of investigators[7-11] have shown that the exciting light in addition to exciting the phosphor also has a de-exciting effect. The de-exciting influence of the exciting light in the case of alkali halide phosphors has hitherto not been established experimentally[6]. In order to determine whether the de-exciting effect occurs in alkali halide crystals and evaluate its influence on the visible luminescence, we carried out experiments with natural NaCl crystals. Two identical crystals chipped from the same specimen of rock salt were simultaneously irradiated with x-rays at room temperature in the dark; then one of these specimens was cooled to the temperature of liquid oxygen and exposed to x-rays for 5-10 minutes, while the other crystal was kept in the dark but not x-irradiated. After the additionally irradiated crystal had warmed to room temperature we could discern a noticeable difference in the color of the two crystals. The color of the crystal additionally irradiated in liquid oxygen was weaker than that of the crystal irradiated only at room temperature.

If such crystals are subjected to thermal bleaching it is found that the crystal additionally irradiated in liquid oxygen is fully bleached at 150° while the crystal irradiated only at room temperature retains some color up to 220°.

These experimental data substantiate the hypothesis regarding the existence of two or more types of color centers: relatively unstable ones and more stable centers[12,13]. Our experiments show that the more stable color centers (F-centers) in NaCl crystals are bleached or de-excited by x-rays at the temperature of liquid oxygen. The remaining color of the crystal neither increases nor decreases no matter how long irradiation is continued. Apparently

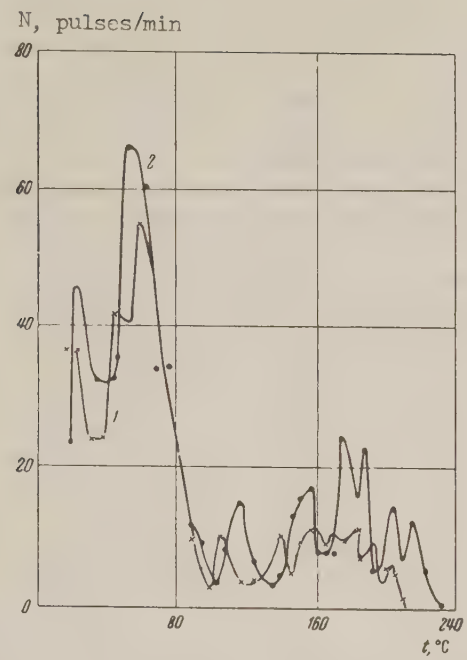

Fig.3. Glow curves for an NaCl crystal excited at room temperature recorded through filters with a transition maximum at 1) 4500 Å and 2) 4200 Å.

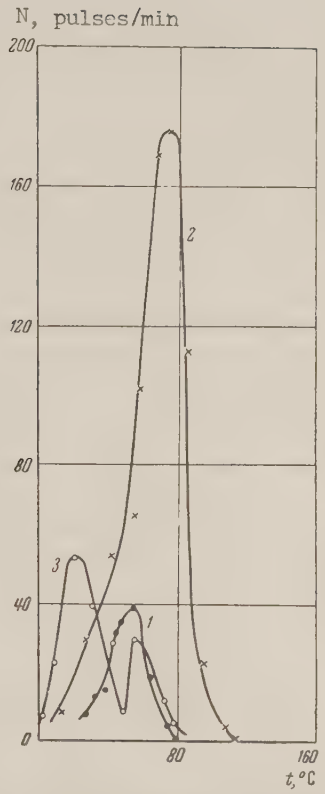

Fig.4. Glow curves for an NaCl crystal excited for 1) 3 min at room temperature, 2) 3 min at room temperature and then 3 min at liquid oxygen temperature and 3) 3 min at liquid oxygen temperature (violet ~4200 Å filter).

at some point there is established a dynamic equilibrium between formation of color centers and their dissociation by the exciting light. Some authors[14,15] assume that for the formation of color in x-irradiated NaCl crystals there must also be present a thermal effect stabilizing the F-centers. The absence of coloring at low temperatures is explained by the absence of this thermal stabilizing effect.

The thermostimulation curves recorded through filters with peak transmission at 4500 A (curve 1) and at 4200 A (curve 2) are shown in Fig.3. The crystal in this case was irradiated with x-rays at room temperature for 10 minutes. As may be seen, the curves consist of two groups of peaks associated with the break up of two different types of color centers: relatively unstable ones at 25 and 60° and more stable centers at 120, 150, 180 and 210°. The most intense radiation incident to the dissociation of these centers is the violet.

We established on the basis of a number of experiments that if the crystal is irradiated at room temperature and then again at the temperature of liquid oxygen the luminescence intensity at the temperature of break-up of the relatively unstable centers is more intense than when an identical crystal is irradiated only at room temperature.

This is illustrated by the curves in Fig.4. Curve 1 shows the maximum luminescence intensity observed in the case when the crystal was irradiated at room temperature for 3 min; curve 2 pertains to the case when the crystal

was irradiated for 3 min at room temperature and then again for 3 min at the temperature of liquid oxygen, while curve 3 is for a crystal that was irradiated only at the temperature of liquid oxygen for 3 min. All the curves were recorded through the violet filter. All the other experimental conditions were the same in the three cases. One might think that the sum of the areas under curves 1 & 3 (corresponding to the stored light energy) should equal the area under curve 2. It is obvious from the figure, however, that the area under curve 2 is several times greater than the sum of the areas under curves 1 & 3. Apparently in the case of re-irradiation of the crystal at low temperature, the x-rays have a de-exciting effect resulting in a redistribution of electrons; the electrons are transferred from the deeper levels (F-centers) to shallower levels (relatively unstable centers) and upon subsequent thermostimulation yield a greater light sum than in the case of excitation either only at room temperature or only at that of liquid oxygen.

Further evidence in support of the above interpretation of the kinetics of visible luminescence of nonactivated crystals is furnished by experiments in which the crystals were excited at or above the temperature of dissociation of F-centers. When alkali halide crystals (NaCl and KCl) are irradiated with x-rays at the temperature of break-up of F-centers, intense luminescence is observed but the crystals do not become colored. With further increase in temperature the visible emission becomes weaker and finally disappears entirely at $+250^{\circ}$.

Conclusions

1. As the result of our investigation of the visible luminescence of NaCl crystals excited by x-rays, we established that the spectral composition of the thermostimulated emission peaks changes with the temperature. As the crystal is warmed the maximum luminescence intensity is displaced to the side of shorter wavelengths. In addition we found that the spectral composition of the low temperature visible luminescence peaks changes depending on the method of excitation. Thus in the case of excitation of the crystal at room temperature with subsequent x-irradiation at the temperature of liquid oxygen the maximum intensity of the emission at -60° is in the blue band, while in the case of excitation of the crystal only at the temperature of liquid oxygen the maximum intensity of the thermostimulated luminescence at -60° is in the violet band.

2. We also established experimentally the existence of the de-exciting effect of the exciting x-rays in the case of alkali halide crystals.

Physics Faculty of the "C.M.Kirov"
Kharkov Institute of Railway Transport Engineers

References

1. V.Kudriavtseva, Zhur.eksp.i teor.fiz., 4, 709 (1934).
2. M.D'iachenko, Zhur.eksp.i teor.fiz., 8, 105 (1938); 9, 307 (1939).
3. M.Kats, Zhur.eksp.i teor.fiz., 8, 100 (1938); Doklady AN SSSR, 30, 78 (1941).
4. M.Podashevskii & A.Polonskii, Doklady AN SSSR, 21, 15 (1938).
5. Z.Pinsker, Diffraktsiia elektronov (Electron diffraction), M.-L., 1949

6. Ch.Lushchik, Trudy (Transactions) Institute of Physics and Astronomy of the Estonian SSR Academy of Sciences), 1955.

7. Z.Morgenshtern, Doklady AN SSSR, 58, 783 (1947).

8. Z.Trapeznikova, Doklady AN SSSR, 58, 791 (1947).

9. V.Antonov-Romanovskii, V.Levshin, Z.Morgenshtern & Z.Trapeznikova, Izv. AN SSSR, Ser.fiz., 13, 75 (1949).

10. V.Antonov-Romanovskii, Izv.AN SSSR, Ser.fiz., 13, 91 (1949); Izv. AN SSSR, Ser.fiz., 15, 637 (1951).

11. V.Antonov-Romanovskii & A.Vinokurov, Zhur.eksp.i teor.fiz., 29, 830 (1955).

12. N.Brilliantov & Z.Morgenshtern, Zhur.eksp.i teor.fiz., 8, 40 (1938).

13. M.Kats, Izv.AN SSSR, Ser.fiz., 13, 149 (1949).

14. P.Tarkavoskii, Vvutrennii fotoeffekt v dielektrikakh (The internal photoeffect in dielectrics)M.-L., 1940.

15. I.Parfianovich, Zhur.eksp.i teor.fiz., 19, 605 (1949); Izv.AN SSSR, Ser.fiz., 15, 669 (1951).

DISCUSSION

A.A.Shatalov: D.M.Eremin spoke of stable and unstable centers. Actually the centers that are produced by the x-irradiation coloring procedure are unstable (in such cases an electron is detached from the ground state, a hole forms and then quickly recombines with the electron); after illumination and slight warming such centers vanish, but all the other color centers are of the same type and should not be differentiated as regards degree of stability. In fact there can be no distinction or division except into subtractively and additively colored crystals. Naturally, the centers disappear with increasing temperature but this depends on the concentration of the centers, the nature of the crystal, the temperature and similar factors.

B.Z.Semenov: We have additively colored NaCl crystals, true, with Ni. We obtained an intense blue color and a very low peak associated with F-centers (in measuring the absorption spectrum on an SF-4 spectrometer). The colloidal "blue" Na particles masked the usual color due to F-centers.

I.A.Parfianovich: Regarding stable and unstable F-centers. When we speak of stable centers we generally have in mind additively colored crystals, although as Eremin's experiments show F-centers are not always stable. When it comes to subtractively colored crystals, then holes play an important role in the formation of centers, the process is actually more complicated than in the case of additive coloring since the centers are less stable.

PHOTOCHEMICAL TRANSFORMATIONS OF COLOR CENTERS IN HEATED ALKALI HALIDE CRYSTALS (Abstract)

- A. A. Shatalov

We measured the variation with time of the optical density of F-centers in the process of their reversible photochemical dissociation and thermal restoration in KCl crystals at temperatures of 270-300°. At the same time we also determined the associated curves pertaining to the appearance of the X-band under the influence of light and its thermal fading in the dark. We elucidated the character of the influence of the initial concentration of F-centers, the number of repeated exposures to light, the temperature and the intensity of white and monochromatic light on the rate of the photochemical process. By solving simple kinetic equations we found the time dependence of the concentration of F- and X-centers; these theoretical results were in good agreement with the experimental curves. From the exponential nature of the variation in concentration it may be concluded that the investigated photochemical reaction is monomolecular.

We also determined the time isotherms of the optical density of F-centers in KCl in the case of irreversible photochemical transformation. The temperature dependence of the rate of the photochemical process shows that the break-up of F-centers in the temperature interval from 20 to 250° is connected with ionic regrouping.

In NaCl crystals at temperatures from 200 to 400° thermal stability of the F-centers is possible only at very low initial concentrations of the centers. Even at a relatively low concentration there occurs rapid thermal coagulation of the colloids beginning with the formation of F-centers. The influence of monochromatic light in the region of the absorption maximum leads to a process which is the reverse of what occurs in KCl. The X-centers dissociate, transforming into F-centers. The rate of this process is the higher, the closer the wavelength of the incident light to the peak of the X-band. One can obtain against the background of the red color of the X-centers bright yellow areas of F-centers of any shape, i.e., identical to the geometric form of the light probe. We measured the variation of the absorption spectra as well as the time dependences of the optical density of the X-bands, from which one may evaluate the intensity and variation in rate of the process under different conditions. The blue colloidal color can also be transformed into the initial atomic one but this process proceeds much more slowly at the same light intensities.

The spectral absorption of the X-bands in different alkali halide crystals satisfies the familiar relationship $\nu_{max} d^2 = \text{const}$. This proves that the X-centers are all of the same type as regards structure and that they are formations related to the properties of the host crystal lattice.

In view of the stability of X-centers under the influence of light absorbed by them, it would be more expedient to use crystal plates colored with such centers for narrow band light filters in the visible and infrared regions than plates colored with F-centers, as suggested by Friedman & Clover[1]. The results obtained in the present investigation supplement our arguments advanced earlier[2,3] in favor of interpretation of X-centers as small aggregates of F-centers.

"T.G.Shevchenko" Kiev State University
Institute of Crystallography of the USSR Academy of Sciences

References

1. H.Friedman & C.P.Clover, J.of the Optical Soc.America, 39, 9 (1949).
2. A.A.Shatalov, Doklady AN SSSR, 92, 549 (1953).
3. A.A.Shatalov, Trudy (Transactions) Physics Faculty of Kiev State University, No.7, 47 (1955).

DISCUSSION

I.A.Parfianovich: Did you measure the quantum efficiency of the transformations?

A.A.Shatalov: Yes, It is very low - of the order of 1-2%. The low quantum efficiency is explained by the fact that far from every absorption of a photon leads to photochemical destruction of a color center. Only part of the excited electrons is further thermally excited into the conduction band. Only part of these are localized on F-centers to form F'-centers. Finally, only part of these, not having time to dissociate thermally, are stabilized by combining with a halide vacancy to form an F_2-center.

* * * * * *

INFLUENCE OF POLARIZED LIGHT ON COLOR CENTERS IN ALKALI HALIDE CRYSTALS (Abstract)

- O.A.Shmit

The present work was devoted to further investigation of color centers (trapping centers) in alkali halide crystals. The procedure was the following: a photochemical reaction was produced in a colored alkali halide crystal by means of plane polarized light; the reaction products were studied (for light absorption) also by means of plane polarized light. If the reaction products are anisotropic formations, dichroism is observed in the absorption. By measuring the magnitude of the dichroism as well as its angular dependence one can judge of the structure of the color centers. The observed dichroism in the M absorption band in KCl substantiates the M-center model proposed by Seitz. Dichroism is also observed in the F absorption band. This effect is connected with the polarizing influence of M-centers on F-centers. It would appear that by measurement of absorption of linearly polarized light one can investigate retrapping at levels on which electrons were detached in the process of excitation by light.

Latvian State University

DISCUSSION

I.A.Parfianovich: What role do F'-centers play?

O.A.Shmit: F'-centers do not exist in KCl at room temperature; they appear at low temperatures, beginning with -140°. In NaCl the F- and F'-bands greatly overlap and the effect is smeared out.

THERMAL IONIZATION ENERGY OF TRAPS IN ALKALI HALIDE PHOSPHORS (Abstract)

- I.A. Parfianovich

One of the important characteristics of electron trapping centers in semiconductors and crystal phosphors is their thermal ionization energy. In experimental investigations this quantity is usually determined from the relation

$$p = p_0 e^{-\epsilon/kT},$$

where p is the probability of thermal ionization of a center, p_0 is a frequency factor, ϵ is the thermal ionization energy, k is Boltzmann's constant and T is the temperature.

In the case of crystal phosphors ϵ may be determined from the experimental temperature dependence of the luminescence. Commonly the thermostimulation (glow curve) procedure is used for finding ϵ. Actually there is a considerable spread in the reported values due partly to the narrowness of the temperature interval in which it is feasible to study the variation in the ionization rate of the centers and partly to the fact that generally there is no rigorous theoretical basis for the thermal calculations, so that different investigators made different simplifying assumptions. This is particularly evident in the case of ZnS:Cu which has been the subject of many studies.

The question of thermal characteristics of F-centers in alkali halide crystals is particularly important. Until very recently there has been considerable uncertainty as to how well the results of theoretical calculations agree with experiment. Theorists have compared their results with experimental data of Smakula obtained in investigating the temperature dependence of electronic conductivity of alkali halide crystals, but even interpretations of Smakula's data have been a matter of controversy. Careful investigations of thermostimulation of NaCl:Ni phosphors, as well as NaCl crystals excited by x-rays, showed that the parameters of the highest-temperature peak, corresponding to the F band, depend both on the previous heat treatment of the crystals and on the activator concentration. It was also found that natural and artificial crystals differ from each other in this respect.

A detailed and comprehensive investigation of the kinetics of the process showed that in NaCl:Ni phosphors activated at 700°, it is possible to neglect electron retrapping in considering thermostimulation. This conclusion was substantiated by comparison of experimental glow curves with the theoretical curve calculated for a first order process. It was found that in NaCl:Ni phosphors for centers corresponding to the last peak: $\epsilon = 1.4$ ev and $p_0 = 6.3 \cdot 10^{-2}$ sec^{-1}.

Analogous investigations of the luminescence of natural NaCl crystals led to the following results for F-centers: $\epsilon = 1.72$ ev and $p_0 = 6.3 \cdot 10^{14}$ sec^{-1}. These results may, we feel, be regarded as closest to the true values for F-centers in NaCl.

The report concludes with an analysis of the theoretical results obtained by various authors and a juxtaposition of the experimental values of ϵ found by other investigators and the present writer. It is noted that the appreciabl divergence between theoretical and experimental data, characteristic of earlier investigations, has been minimized.

"A.A. Zhdanov" Irkutsk State University

LUMINESCENCE LIFETIME OF COLOR CENTERS IN IONIC CRYSTALS (Abstract*)

- A.M.Bonch-Bruevich, G.A.Tishchenko & P.P.Feofilov

The availability of a new GOI (State Optical Institute) fluoremeter, characterized by a high resolution and good sensitivity, enabled us to investigate the luminescence persistence τ of complex color centers in certain ionic crystals: LiF, NaF and CaF_2. The crystals were colored both photochemically by hard radiation and additively (by CaF_2).

In all cases the duration of luminescence at room temperature proved to be of the order of 10^{-8}-10^{-9} sec and was independent of the method of coloring as well as of the intensity and wavelength of the exciting light.

In x-rayed LiF crystals we observed two types of color centers, differing as regards their luminescence spectra and their orientation as indicated by polarization measurements. The luminescence lifetimes of these centers also differed and differences were also noted in the values of τ for two related types of luminescing color centers in CaF_2 crystals ("red" and "blue" centers).

The luminescence persistence of the color centers changed little when the temperature was reduced to 90°K but did fall when the crystals were heated. This decrease in τ is due to thermoquenching and is not connected with the accompanying irreversible thermal disintegration of the centers.

Knowing the value of τ and the characteristics of the absorption spectrum one can determine the concentration of color centers and their oscillator strengths.

---

*Complete report in "Optika i spektroskopiia" 2, 136 (1957).

ON THE STABILITY OF F-CENTERS IN NaCl:Ni PHOSPHORS (Abstract*)

- E. I. Shuraleva

The present study was devoted to an investigation of the optical and thermal stability of F-centers and the light sums stored in them in NaCl:Ni phosphor excited by x-rays. The x-irradiated crystals were illuminated with light in the region of the F absorption band or kept for a prolonged period in the dark at room temperature. We determined the influence on dissociation of F-centers and the reduction of the corresponding light sums of such factors as heat treatment of the crystals, the presence of an activator, the activator concentration and the temperature at which the given specimen was excited.

Comparison of the optical and thermal stability of the F-centers and the light sums stored in them in a pure NaCl crystal, in crystals subjected to heat and electric treatment and in NaCl:Ni phosphors containing different concentrations of the activator leads to the following conclusions:

1) The greatest stability of the F-centers and the largest corresponding light sums obtain in pure NaCl crystals.

2) Preliminary heat and electric treatment of the crystals reduces the stability of the F-centers.

3) Introduction of the activator accelerates the process of dissociation of F-centers; the stability of the F-centers and corresponding light sums decrease with increasing Ni concentration,

4) Raising the temperature at which the crystals are excited increases the stability of the F-centers and the corresponding light sums in the case of all specimens.

An attempt is made to explain the observed regularities from the viewpoint of presence in the crystal of lattice defects, electron and hole color centers as well as from the standpoint of concentration quenching which probably occurs in NaCl:Ni phosphors.

Physical-Chemical Scientific Research Institute
at "A. A. Zhdanov" Irkutsk State University

DISCUSSION OF THE REPORTS PRESENTED BY I. A. PARFIANOVICH & E. I. SHURALEV

Ch. B. Lushchik: The data presented by I. A. Parfianovich are of great interest. As a suggestion, I would like to call his attention to the necessity of investigating the thermal stability of V-centers of different types in NaCl crystals prepared by different procedures and including, of course, natural NaCl crystals. Without such data it is difficult to determine the reason for the divergence between the experimental results of different investigators. It is undoubtedly necessary to take into account hole processes in alkali halide phosphors.

B. Z. Semenov: I look askance at the exact agreement of the experimental and theoretical curves of the thermoluminescence for the second band because of the variation in the maximum in this band, the fact that it shifts for different nickel concentrations.

We carried out experiments on thermostimulation of NaCl:$NiCl_2$ ($NiCl_2$ concentration 0.7 mole %). We also observed a lower stability of the F-centers, but in our case there appeared a new band with a peak at 103° due to colloidal Ni particles. We observed peaks at 72, 103 and 157°. Under conditions of repeat x-ray irradiation and de-excitation we observed a sharp

---

*Complete report in "Optika i spektroskopiia", 2, 396 (1957).

drop in the F-peak and its displacement to the side of lower temperatures; this was also observed in the case of preliminary heating at the temperature of thermostimulation and subsequent x-raying and de-excitation. The effect can be explained by coagulation of the colloidal particles and their competition with F-centers, the trapping in such formations of halide vacancies. In successive x-irradiations and de-excitations no displacement of the maximum of the F-peak was observed.

M.L.Kats: The principal facts established in the investigation of E.I. Shuraleva are that in NaCl:Ni phosphors the stability of F-centers is lower than in nonactivated NaCl crystals and that it decreases with increasing concentration of the activator. E.I.Shuraleva infers that the decrease in the intensity of the F-centers is due to recombination of electrons with positive holes, i.e., with V-centers, and with ionized activator centers. In NaCl:Ni phosphors grown from a melt, the activator is incorporated in the lattice in the form of Ni^{2+} ions and it is hardly likely that in excitation there can occur additional ionization of these ions, in view of their high ionization potential compared with that of the host material ions. Hence there can be no recombination with triply ionized nickel. The decrease in the stability of the F-centers is due primarily to trapping of electrons by Ni^{2+} ions, as is evinced by a decrease of the absorption in the activator band at 248 mμ. Measurements show that even with complete bleaching of the F-band, the hole absorption band decreases little in intensity and, consequently, hole centers cannot play a predominant role in the reduction in stability of the F-centers in NaCl:Ni phosphors. On the contrary, our work shows that the primary role in the luminescence of NaCl:Ni phosphors is played by atomic nickel centers forming as a result of trapping by the activator ions of electrons released from different localization levels including the F-levels.

I.A.Parfianovich: Regarding investigation of hole centers, it is true that one cannot do without them. I fully agree on this point.

One of the commentators has questioned the close agreement of the experimental curves with the theoretical ones. The experiments were carried out very carefully. First I must note that the nickel luminescence has a definite spectral composition; the concentration undoubtedly influences both the structure and the position of the peaks, but at 700° the activated crystal is under conditions where we have the possibility of comparing the experimental data with the theoretical ones. At lower temperatures there may appear a luminescence band having a different spectral distribution and it will evidently affect the peaks, shifting them to the other side. At higher temperatures clearer results are obtained.

I.E.Shuraleva: In connection with the remarks of M.L.Kats I would like to remark that I explained the different stabilities of F-centers in NaCl crystals not only by the presence of V-bands, characterized by different stability. The decrease in the stability of F-centers with the introduction of an activator is also explained by another factor, namely, the predominance of the process of recombination of electrons released from the F-centers with ionized luminescence centers. I do not deny the role of Ni ions in trapping electrons, but experiment shows that in the investigated phosphors the principal cause for the reduction of the stability of F-centers is the process of recombination of F-electrons with luminescence centers.

LUMINESCENCE OF COLOR CENTERS IN CsI:Tl CRYSTALS (Abstract*)

- Z.L.Morgenshtern & I.P.Shchukin

It was found that, in the case of CsI crystals with a relatively high concentration of thallium, excitation in the region of the absorption band of the activator (300 mμ) and in the region of the long wave absorption edge of the activator (365 mμ) produces different effects. The former gives rise to yellow-green fluorescence (two close bands peaking at 540 and 580 mμ) with $\tau = 1 \cdot 10^{-6}$ sec, while the latter produces negligible fluorescence and an intense yellow phosphorescence (peak at 580 mμ) that gradually builds up under continuing excitation. At the same time the absorption spectrum of the crystal changes: additional absorption bands appear and the crystal becomes colored. X-rays and γ-rays also produce coloring. One can readily follow the development of the additional absorption bands with peaks at 385, 460, 520 and 840 mμ. The intensity of all these bands increases with increasing thallium concentration in the case of both optical and x-ray coloring.

When the colored crystal is excited in the region of the additional absorption bands (385 and 460 mμ) there is observed an intense red luminescence with $\lambda_{max} \approx 660$ mμ. It is interesting to note that excitation in the longer wave band ($\lambda_{ex} = 435$ mμ) produces only short-lived emission ($\tau = 6 \cdot 10^{-7}$ sec), while excitation in the short wave band ($\lambda_{ex} = 365$ mμ) gives rise to both red fluorescence and in intense yellow-orange afterglow.

When the colored crystals are heated, the color centers dissociate and the additional absorption disappears, i.e., the crystals are bleached. The thermoluminescence curve has two peaks, one at 63, the other at 125°. The depths of the corresponding trapping levels, as calculated from the glow curves, are 0.74 and 0.95 ev, respectively. It follows from the thermobleaching data and results of additional experiments that the deeper trapping level is associated with the two additional absorption bands at 385 and 460 mμ, while the shallower level corresponds to the band at 840 mμ.

On the basis of our experimental results one can draw certain conclusions regarding the structure of the luminescence and trapping centers in CsI:Tl crystals. We deduce that there are two types of centers in uncolored CsI:Tl crystals: the centers of the first type, according to commonly accepted concepts, are thallium ions replacing regular Cs^+ ions in the lattice, while centers of the second type consist of a thallium ion located next to a cation vacancy, i.e., are $Tl^+ + |\overline{+}|$ formations.

The centers of the first type are responsible for the absorption bands and the yellow-green fluorescence; the centers of the second type are the cause of the long wave absorption edge of the activator and the yellow phosphorescence. This yellow phosphorescence is due to the fact that the cation vacancy, acting as an additional negative charge, reduces the binding energy of the electron with the center. The escaping electrons, becoming localized, form color centers. Inasmuch as the concentration of color centers increases with increasing thallium concentration both in the case of optical and of x-ray excitation, it follows that the trapping centers are formations that comprise thallium. The deepest traps may be either a thallium ion situated next to an anion vacancy (such a formation will attract electrons) or two thallium ions located at neighboring cation sites.

Polarization experiments carried out by P.P.Feofilov have established that the red luminescence centers in these crystals are oriented along fourth order axes, i.e., are arranged along the cation sites. Thus, it is more

---

*Complete report in "Optika i spektroskopiia", 1, 190 (1956).

probable that the color centers are pairs of thallium ions, ledged at neighboring sites, that have captured an electron.

"P.N.Lebedev" Physical Institute of the
Academy of Sciences of the USSR

DISCUSSION

P.P.Feofilov described in detail his polarization measurements on a CsI:Tl crystal on the basis of which one can select the more likely of the two possible models of luminescence centers. (See Optika i spektroskopiia, 1, 952 (1956).)

Ch.B.Lushchik: As has been shown by Krivoglaz and myself, by analysis of the potential curves for local centers one can relate the values of E_{absorb} and E_T. If E_T is greater than $E_{absorb}/2$ the center can luminesce; but if $E_T < E_{absorb}/2$; i.e., the centers should not luminesce, but they do.

It must be assumed here, apparently, that the ionization of the activator trapping centers is effected by holes. In this case the value of E_T determined by the speaker does not actually correspond to the energy of thermal ionization of the activator trapping centers but is the energy of thermal ionization of some sort of hole trapping centers.

Z.L.Morgenshtern: The polarization measurements of P.P.Feofilov have played an important part in the interpretation we propose for luminescence centers. If the luminescence centers are oriented along fourth order axes, then, aside from the possibility we suggest, it may be that the thallium ion can be situated next to a vacant cation site. But in this case it cannot attract an electron. That is why we have rejected this alternative and hold to our model, namely, that a color and emission center consists of two thallium ions lodged at neighboring cation sites.

As for what Ch.B.Lushchik said, this question can be answered if one determines the polarity of the carriers.

M.L.Kats: Could not the color center in your case be a quasi F-center, that is, a thallium ion next to a halide vacancy?

Z.L.Morgenshtern: No, because in that case the centers would be oriented along third order axes. This would be in conflict with the results of Feofilov's polarization experiments.

ULTRATAUMETER

- N.A.Tolstoi, A.M.Tkachuk & N.N.Tkachuk

Introduction

The taumeter procedure developed by Tolstoi & Feofilov[1-4] made it possible to effect a number of investigations of different relaxation processes, including photoconduction and luminescence[5-15]. In the course of these investigations there have been established a number of regularities that have significantly furthered our understanding of the mechanism of photosemiconductor processes. The range of relaxation times susceptible of measurement by the taumeter procedure extends from 10^{-1} to 10^{-5} sec. Processes involving shorter times - 10^{-7}-10^{-8} sec and less - (primarily luminescence processes) are encompassed by the fluorometer method in its diverse variants (Tumerman[16], Galanin[17] and Bonch-Bruevich[18]). Thus until recently the relaxation time interval from 10^{-5} to 10^{-7} sec remained inaccessible to experiment. In his report to the Second All-Union Conference on Luminescence Vavilov[4] characterized this interval as the lacuna or "blank space" on the experimenters' map. Specifically, he said, "I would like to emphasize that all measures should be taken to adapt the taumeter for measurements in this interval as well. In principle this is possible. Every effort should be made in this direction because I am certain that a whole class of new effects is hidden in this blank space".

The ultrataumeter procedure which we shall describe in this report was developed by us to meet the challenge issued by the S.I.Vavilov. The full set of equipment designed and constructed in our laboratory (ultrataumeter with a mechanical light modulator, altrataumeter with electro-optical light modulation and ultrataumeter for photoluminescence) made it feasible to investigate the kinetics of a number of luminophors for the first time. The unique nature of some of their relaxation regularities, discovered by means of the ultrataumeter, fully validate the prophetic words of S.I.Vavilov.

The ultrataumeter procedure does not differ from the taumeter method in principle; it differs from the earlier procedure only as regards experimental technique. The idea of the taumeter (as a method of investigating relaxation processes in a variable asymptotic time scale) is in principle applicable to repeating processes of any duration, but its practical realization for processes in the 10^{-5} to 10^{-7} sec range is predicated upon the solution of the following experimental problems[19]:

1) obtaining square exciting pulses with leading and trailing edge times of the order of 10^{-7} sec; in the case of photosemiconductor processes (with which we are primarily dealing here) this means light pulses, while for such processes as cathodoluminescence, dielectric polarization and gas discharges the requirement applies to electric pulses;

2) design and construction of a photomultiplier circuit (for investigation of luminescence) or an appropriate electric circuit (for studying photoconductivity) with an inertia (lag) of the order of 10^{-7} sec or less;

3) practical realization of a wide band cathode-ray oscillograph with a settling time of the order of 10^{-7} sec and X and Y amplifiers having rigorously identical characteristics and capable of faithfully transmitting square pulses without distortion.

In sections I, II and III below we shall describe how we succeeded in solving these problems.

Before going on to this description, however, we would like to note some of the distinctive features of the taumeter procedure in general and show

that the question of the limits of the time interval susceptible of measurement by the taumeter procedure has a rather unexpected solution.

Even in the first experiments in 1947 (taumeter with a mechanical light modulator), it was noted that having measured the relaxation time τ (for example, in the cause of luminescence of a uranyl salt) under normal conditions of operation of the instrument, one could then reduce the rate of rotation of the modulator disc to a very low value (in other words greatly increase the leading edge time of the exciting square pulse) and still obtain virtually the same value of τ.[4] Theoretically it would seem that one of the essential conditions for correct measurement would be a short pulse rise time as compared with the duration of the investigated relaxation process. Tests showed, however, that the pulse edge time can be not only commensurate with the relaxation time but even appreciably greater than the latter with little distortion of the result. This unexpected and very valuable attribute of the taumeter method is connected with the fact that it is intrinsically a "null method". The ability of the taumeter to give correct results proved to be stable not only in the case of violation of the short pulse edge time requirement, but also in the case of violation of other ostensibly important requirements: inertialessness (zero response time) of the associated electronic equipment and oscillograph. Experiments show that the overall inertia* (lag) of the components of the taumeter set-up (source of square pulses, signal receiver and oscillograph) can be appreciably greater than the inertia of the investigated effect without appreciable diminution of the accuracy of measurement of τ.

S.M.Ryvkin, who was one of the first to use the taumeter procedure for studying photoconductivity, thoroughly investigated the above mentioned useful characteristic of the taumeter method and obtained a quantitative evaluation of the accuracy of the method as a function of the ratio of the inertia of the instrument components to that of the investigated process. It follows from his calculations[20], for example, that in the case of an inertia of the set-up 30 times greater than that of the investigated process the measurements still have an accuracy of 10% of the maximum possible. In view of the high accuracy of the taumeter under normal operating conditions, we can reasonably attempt to measure times of the order of 10^{-7} sec with an overall inertia of the set-up of the order of $3 \cdot 10^{-6}$ sec.

It must be noted, however, that rigorously speaking the above considerations pertain only to the case of investigation of exponential or nearly exponential relaxation processes. Where it is a question of precise investigation of the shape of the curve (for example, a hyperbolic or similar one) the above considerations begin to lose force. Hence, although one can utilize the above mentioned valuable property of the taumeter in appropriate cases, every attempt should be made to reduce the inertia of the set-up to the minimum, for this extends the range of applicability of the procedure not only quantitatively (making it feasible to measure briefer times) but also qualitatively (allowing accurate determination of the shape of the curves characterizing the investigated process). In addition, inasmuch as almost all the elements of the taumeter procedure are comprised in the method of electric differentiation[21], while the effectiveness of the latter, in contrast to the taumeter method, significantly depends on the inertialessness of all the components of the set-up, it is important to have available an ultrataumeter for these purposes as well.

---

*For lack of a better general term "inertia", a literal translation from the Russian, will be used below. Its meaning is obvious from the context. -- Translator.

Analysis of the technical aspects of realizing an ultrataumeter leads to the conclusion that the principal difficulty lies in the conflict between the "intensity" and the "inertialessness" (instantaneous response) requirements. Thus in designing the oscillograph the matter of obtaining a sufficiently high amplification factor is connected with the difficulties of assuring a sufficiently wide frequency pass-band (short settling time). Obtaining a sufficiently strong signal from the photomultiplier or photoresistor calls for the use of a sufficiently large load resistance, but increasing the load resistance (other conditions being equal) leads to a proportional increase in the inertia. Obtaining sufficiently steep pulse fronts in the case of mechanical modulation of the light pulses calls for the use of a small light source and this in turn is connected with reduction of the light flux.

It should not be inferred from the above that realization of the indicated technical requirements is impossible in principle. One should only bear in mind that each component of the ultrataumeter must be designed to more exacting technical specifications than the corresponding components of the taumeter, although, naturally, the use of new different approaches and procedures is not precluded.

I. Data Unit

In the ultrataumeter set-up designed for investigation of luminescence relaxation photomultipliers are used in both channels. Their photoelectric inertia is a fixed quantity but the inertia introduced by the associated circuit linking them with the oscillograph depends on the design of the specific circuits employed. In order to have the possibility of using a relatively large load resistance R at the photomultiplier output without introducing an excessive CR electric inertia (where C is the capacitance of the wiring connecting the photomultiplier with the oscillograph and the input capacitance of the oscillograph), it is essential to use a cathode follower mounted in the immediate proximity of the photomultiplier signal output. A cathode follower, being an impedance transformer, reduces the output resistance of the photomultiplier to a value approximately equal to 1/S, where S is the tube transconductance. We used either acorn type tubes (S $\approx$ 3 ma/v) or twin bantam 6N15 triodes (S $\approx$ 10 ma/v) which yielded values of the output resistance equal to $\sim$ 300 and 100 ohms, respectively. This made it possible to use comparatively long cables for transmitting the signal to the oscillograph without substantial increase of the inertia. The capacitance of the cable was of the order of 10 μμf; hence in this case RC $\approx 1\text{-}3\cdot10^{-8}$ sec. This inertia can be neglected compared with that associated with the load resistance of the photomultiplier and the output capacitance of the cathode follower. Taking a minimal load resistance of 10-20 kiloohm and evaluating the distributed capacitance as about 10 μμf, we obtain a value of $1\text{-}2\cdot10^{-7}$ sec for the total inertia introduced by the data unit.

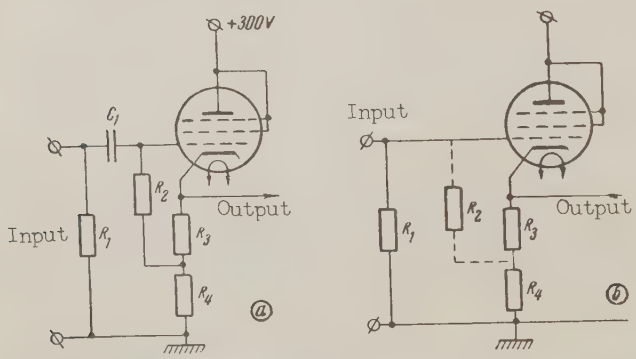

Fig.1. Cathode follower circuits.

In our experiments we used both domestic FEU-19 type photomultiplier tubes (cesium

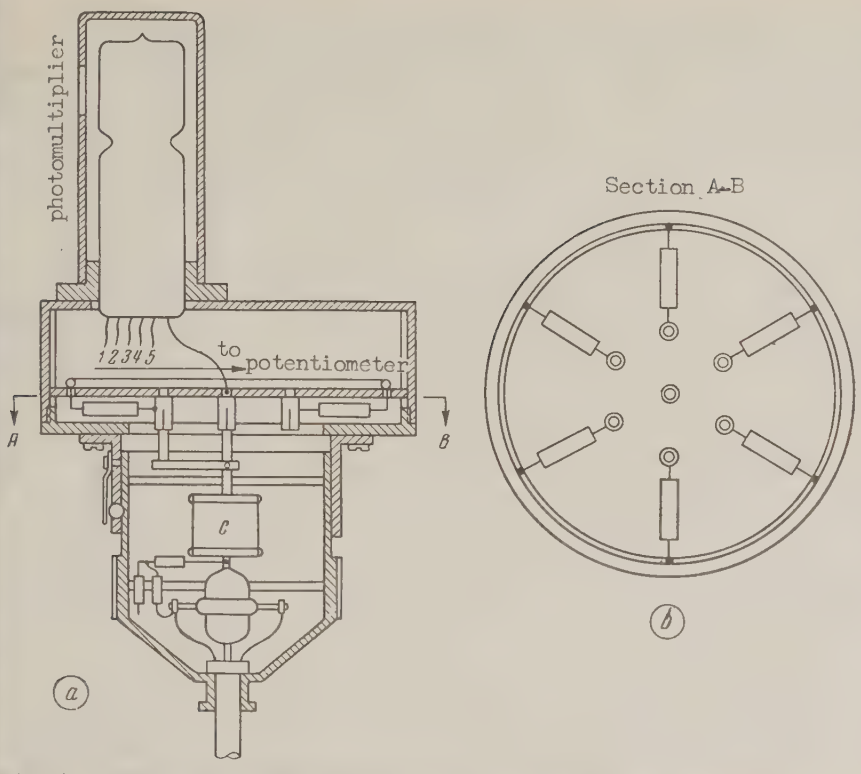

Fig.2. AEG photomultiplier mount assembly and resistor selector head.

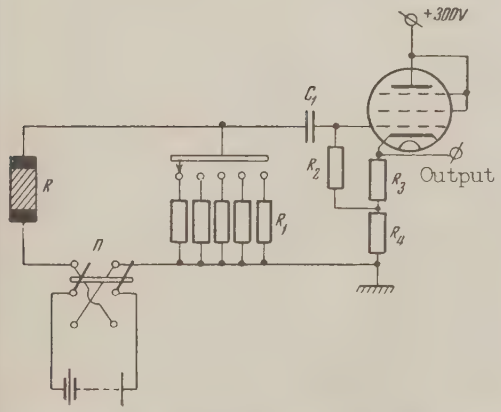

Fig.3. Photoresistor coupling circuit.

antimony photocathode) and imported AEG photomultipliers (cesium oxide). Our experiments showed that it is essential to use the same type of photomultiplier tube with the same load resistance both for detecting the emission of the luminophor and for sensing the sweep signal.

Either of the circuits shown in Fig.1 can be used for the cathode followers repeating the signal from the photomultipliers. Circuit a comprises a separating capacitor which limits the frequency passband from below. The divider R_3 & R_4 allows of selecting the quiescent point of the tube in the most advantageous manner, i.e., obtaining the maximum linear output range. Circuit b does not contain the separating capacitor and hence is suitable for repeating signals extending down to low frequencies. The absence of the separating capacitor, moreover, reduces the input capacitance relative to the ground, which widens the passband on the high side as well. These advantages, however, are nullified by the following shortcomings of this circuit: in the case of small values of R_1 (comparable to or smaller than $R_3 + R_4$) selection of the working range (quiescent point) by connecting in an appropriate resistor R_2 becomes impossible due to the "shorting" effect of R_1; the grid potential becomes too negative and the linearity range is sharply reduced. Increasing R makes it possible to avoid this shortcoming, but on the other hand, limits the frequency passband from above. Thus the circuit variant b can be recommended for use only in the case of weak, not excessively rapid relaxation signals with very long tails.

The design of the mount used for the AEG phototube together with the associated acorn tube cathode follower is shown in Fig.2,a. It is important to be able to vary the load resistance (R_1 in Fig.1) during the experiments.

Hence the design of the mounting assembly includes a load selector switch with a very small parasitic capacitance. The rotating head containing the cathode follower and the other circuit components can be pulled up and rotated to different positions. The connection is made by means of a double pin and mating miniature twin jack (Fig.2,b): one jack is connected with the shortest possible lead to the signal output of the photomultiplier tube, the other to one of the load resistors. A similar mounting assembly was developed for the FEU-19 tube.

In the ultrataumeter set-up intended for investigation of photoconductivity, a photomultiplier tube with a cathode follower (as described above) is employed in the sweep channel, while the investigated photoresistor is connected as shown in Fig.3 to the main channel cathode follower.

A necessary condition for the voltage drop over the load resistor R_1 to be proportional to the conductivity 1/R of the investigated specimen (photoresistor) is $R \gg R_1$. Inasmuch as the conductivity of the specimen varies not only with changes in illumination but also (and usually to a far greater extent) with changes in temperature one must have available a wide range of resistors R_1. It must be borne in mind that the electric inertia of the input depends (with a given input capacitance) not on the resistance of the specimen R but on the load resistance R_1, hence the inertia can be reduced by making R_1 small; at the same time, however, the amplitude of the useful signal is also reduced and, consequently, a high-resistance photoresistor requires the use of a high-resistance load resistor. This makes it essential to use a cathode follower in the data unit. Whenever the load resistor R_1 in the data unit is changed one should also change the load resistor R_1 in the sweep channel photomultiplier assembly so that the electric inertia of both channels will remain the same.

In making measurements by the ultrataumeter procedure it is important to minimize the ac noise in the entire set-up. Tests showed that alternating

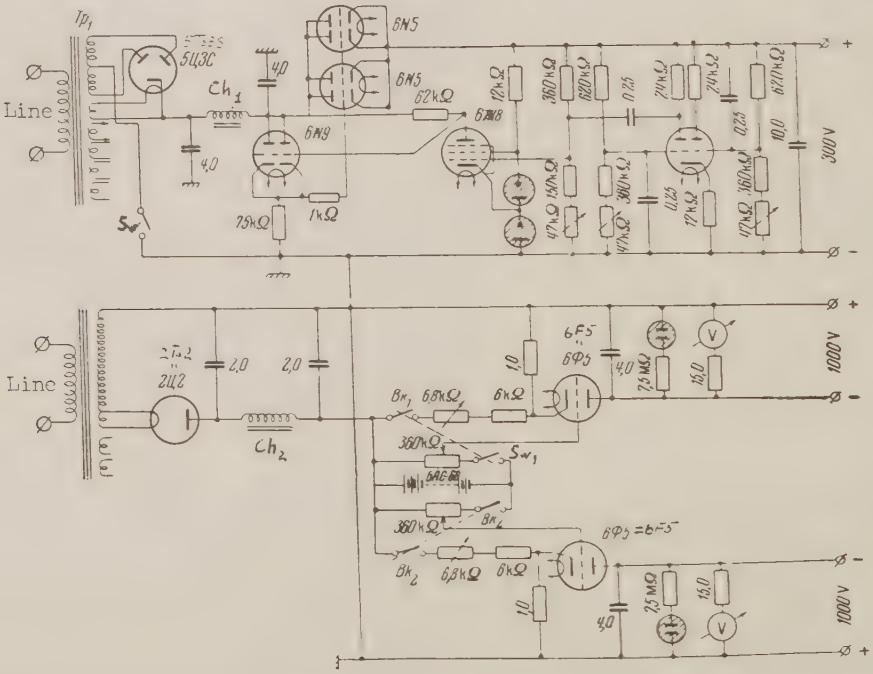

Fig.4. Combined power supply and voltage regulator for two photomultipliers and two cathode followers.

current can be used for the filaments of the cathode follower tubes in the data units (provided the filaments are well grounded), but that the plates must be supplied from a rectifier with electronic stabilization having a noise level of less than 0.01 v with a supply voltage of 300 v. The photomultiplier tubes can also be supplied from a rectifier with electronic stabilization with reference not to a stabilovolt but a dry cell inasmuch as the photomultiplier tubes are very sensitive to noise particularly when exposed to a certain amount of spurious light.

Fig.4 shows the diagram of the latest version of the power supply unit used by us for supplying two photomultiplier tubes and two cathode followers. The separate supply circuits assure complete absence of interference between the two channels. The background noise of the rectifiers shown in Fig.4 is less than 0.001 v.

II. Ultrataumeter Oscillograph

1. Auxiliary units

Inasmuch as no oscillographs suitable for use with the ultrataumeter are produced by the domestic electronic industry, we found it necessary to design and assemble our own instrument. Experience shows that the quality of operation of the oscillograph is decisive where the performance of the ultrataumeter as a whole is concerned; hence we will describe our oscillograph design in some detail.

The block diagram of our oscillograph is shown in Fig.5. Each pair of plates of the cathode ray tube can be connected either to one of the main amplifiers or to the linear sweep. Thus the oscillograph can be operated in any of the following modes:

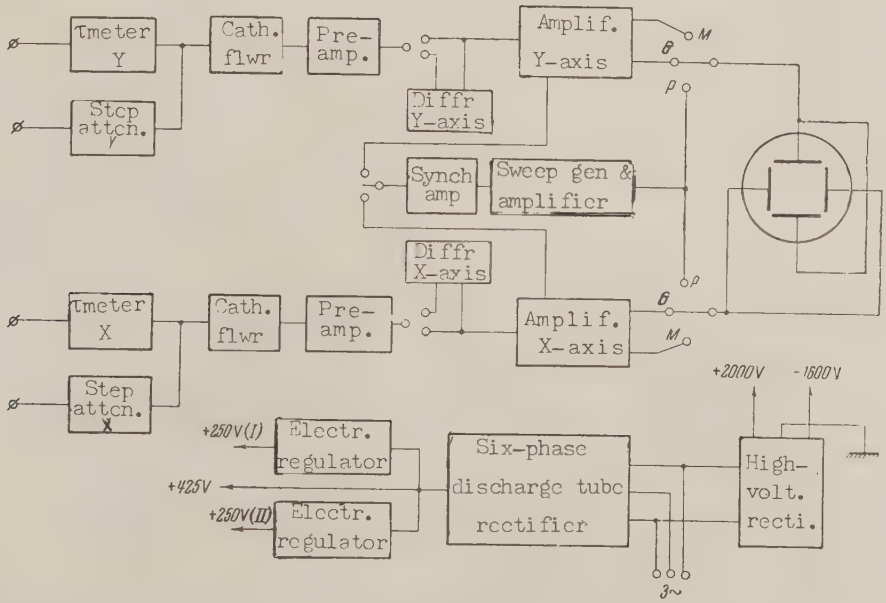

Fig.5. Block diagram of the oscillograph: +425 v - to final stages of all amplifiers, +250 v (I) - to Y amplifier, synchronization and sweep generator, +250 v (II) - to X amplifier.

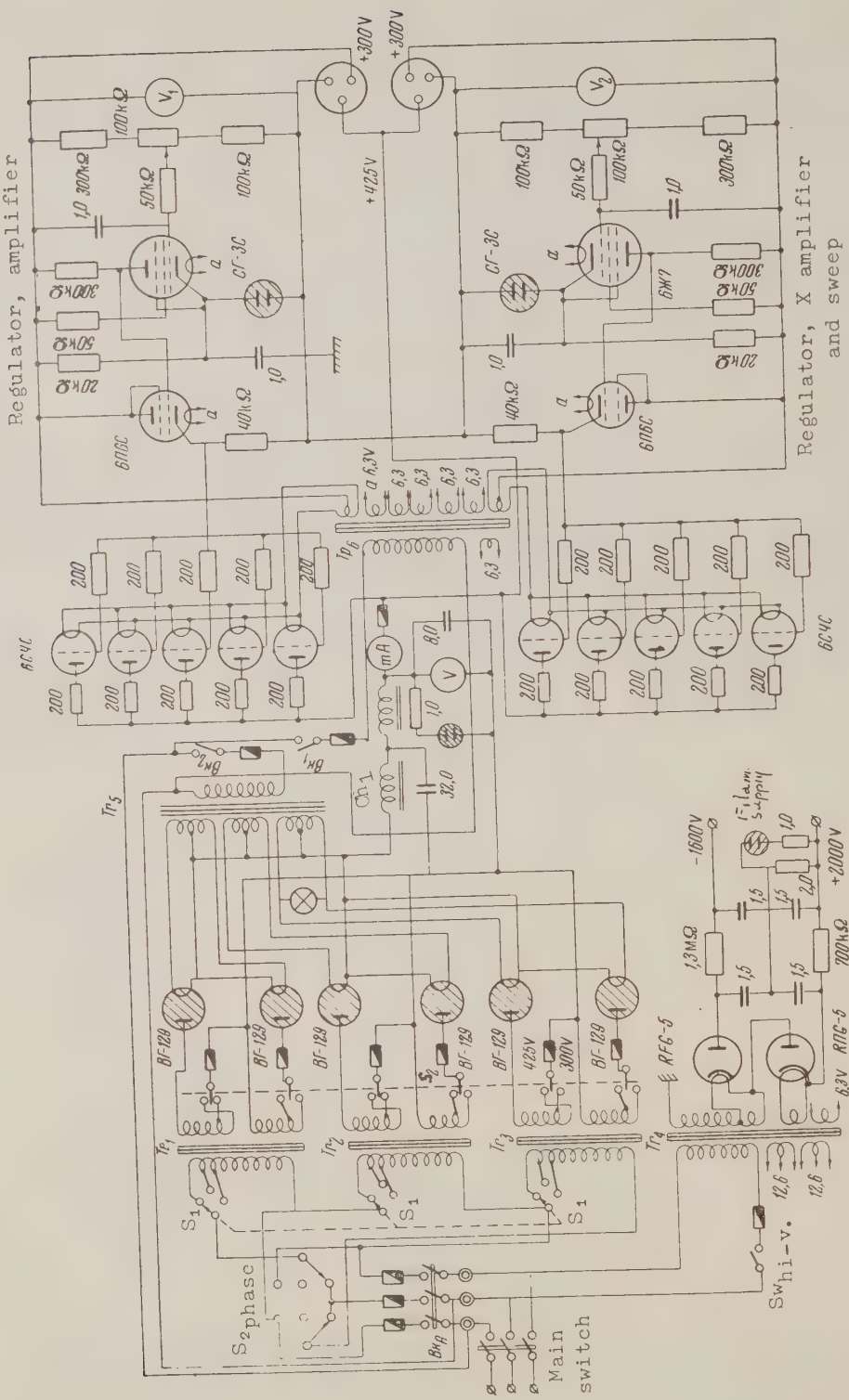

Fig.6. Oscillograph power supply.

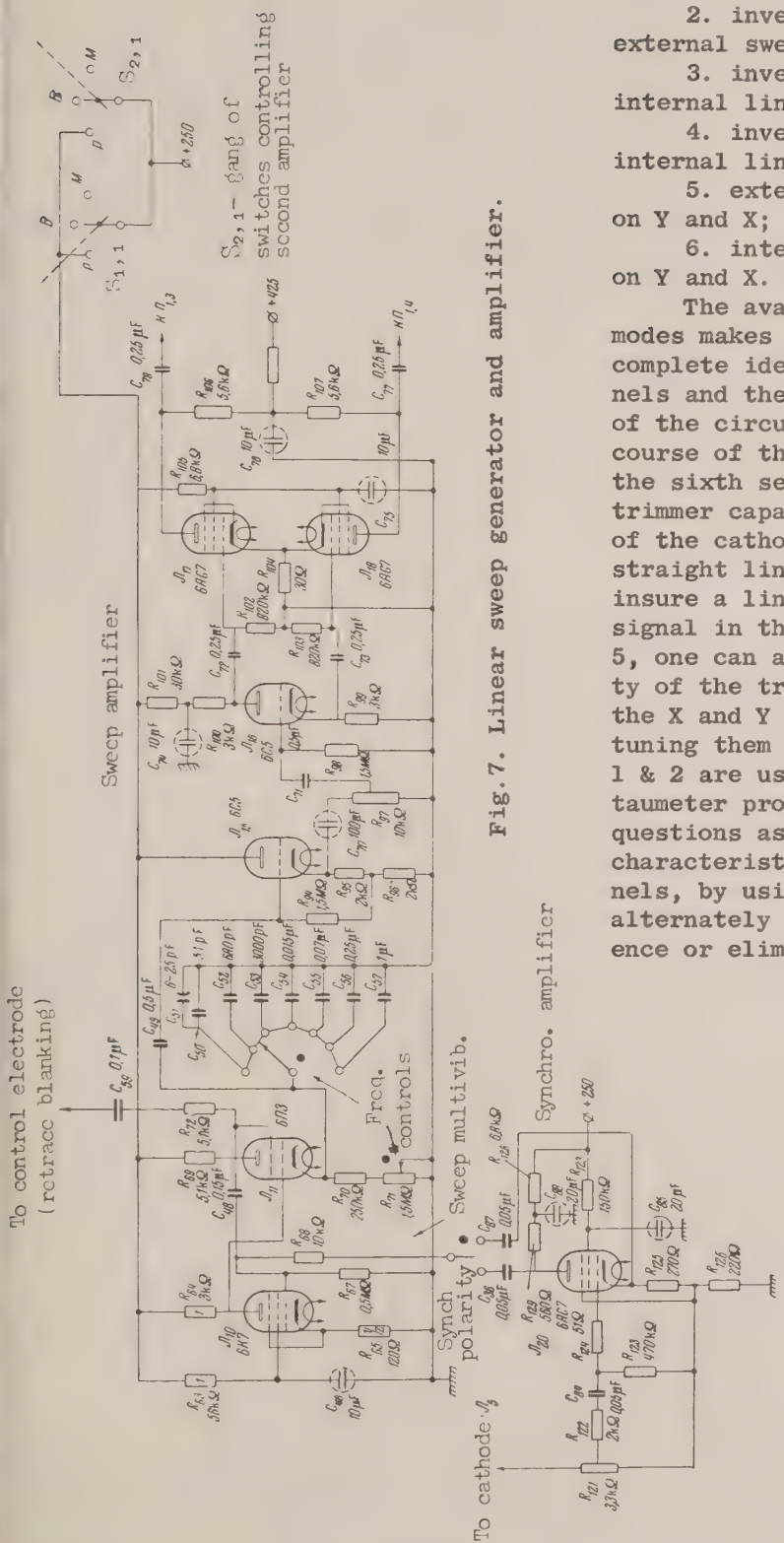

Fig.7. Linear sweep generator and amplifier.

1. investigated signal on Y; external signal on X;

2. investigated signal on X; external sweep signal on Y;

3. investigated signal on Y; internal linear sweep on X;

4. investigated signal on X; internal linear sweep on Y;

5. external signal simultaneously on Y and X;

6. internal sweep simultaneously on Y and X.

The availability of the different modes makes it possible to adjust for complete identity of the X and Y channels and the check on the operation of the circuitry as necessary in the course of the experiments. Thus with the sixth setting, by adjusting the trimmer capacitor between the plates of the cathode ray tube (to obtain a straight line on the screen) one can insure a linear "self-sweep" of the signal in the tube itself. With mode 5, one can adjust for complete identity of the transfer characteristics of the X and Y channel multipliers by tuning them as necessary. Settings 1 & 2 are used in working by the ultrataumeter procedure; in the case of any questions as to the identity of the characteristics of the X and Y channels, by using connections 1 and 2 alternately one can detect any difference or eliminate its effect by

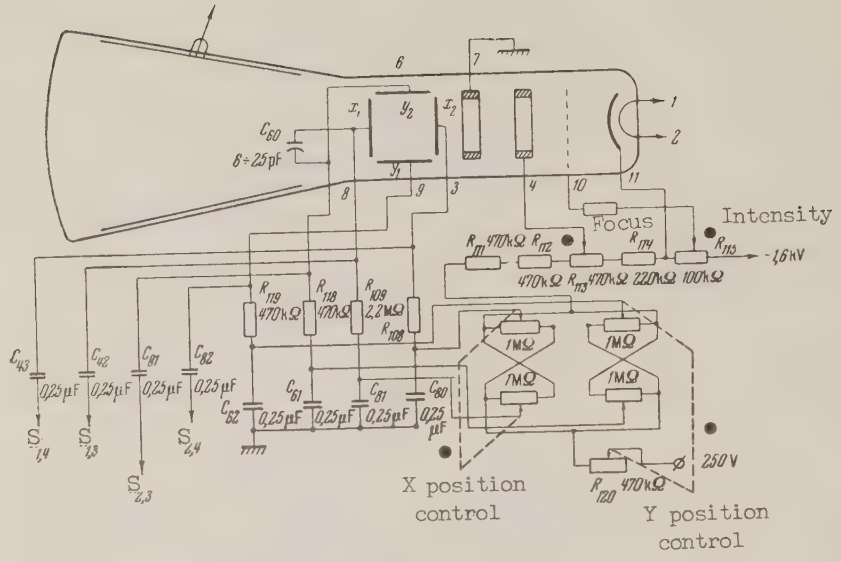

Fig.8. Cathode ray tube circuit.

averaging the results. Settings 3 & 4 are used to check the operation of each of the main amplifiers separately as well as the linearity of the internal sweep.

The oscillograph rectifier is designed to have sufficient reserve power to permit supplying the various auxiliary instruments used in conjunction with the oscillograph. The oscillograph power unit is diagrammed in Fig.6.

The main power rectifier is based on a six-phase circuit that provides a relatively smooth voltage even before the filter and stabilizer (about 6% background noise). The rectifiers proper are VG-129 gas discharge tubes. Each pair of phases has a separate step-up transformer. The transformation ratio can be regulated (285—300—315 or 405—425—445) by means of the switches S_1 and S_2 and makes it possible to use different types of output tubes in the oscillograph; by appropriate adjustment of the controls one can also take off voltages of 600 and 850 v (also ±5%). Switch 1 is used for going over from six-phase delta to operation from a single-phase current supply; the background noise of the rectifier in this case is somewhat higher.

In the case of normal six-phase operation the background noise of the rectifier (after the double LC filter) is ~1 v. The rated current of the rectifier is about 1.5 amp. The high voltage rectifier for supplying the tube gives +2 kv and -1.6 kv relative to the ground; this gives a total accelerating potential of 3.6 kv, which is sufficient to insure an adequate intensity of the spot on the screen even in the case of fast pulses with a low repetition rate.

The tubes of the X and Y amplifiers and the linear sweep circuit are supplied by two separate electronic regulators (also shown in Fig.6). The separate supply for the amplifiers fully eliminates crosstalk. The fact that the voltage to each of the amplifiers can be controlled separately makes for greater flexibility of tuning and adjustment. Each of the two stabilizers gives 300 ma at 200-300 v; the background noise is 0.01 v.

The linear sweep generator is of the conventional type (Fig.7). The range of repetition rates is from 10 cycles to 200 kc per sec. The cathode ray tube hook-up is shown in Fig.8.

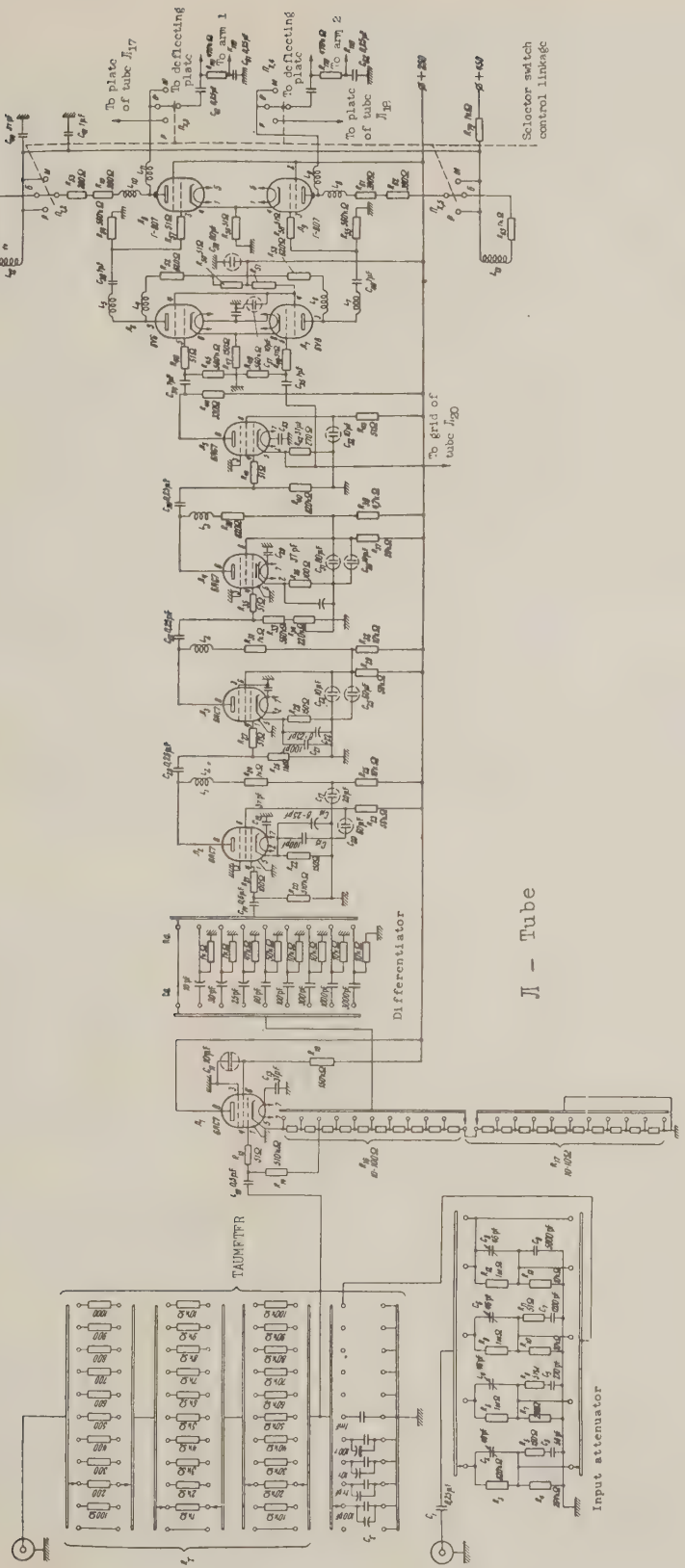

Fig.9. Amplifier circuit.

2. Main amplifiers

The X and Y channel amplifiers are identical. The amplifier circuit diagram is shown in Fig.9. Here $Л_1$ is the cathode amplifier tube, $Л_2$, $Л_3$ and $Л_4$ are amplifying tubes with high frequency compensation by the inductances L_1, L_2 and L_3 and low frequency correction by the capacitors C_{20}, C_{25} and C_{30}; $Л_5$ is the phase inverter; $Л_6$ and $Л_7$ are push-pull preamplifiers; $Л_8$ and $Л_9$ are the final push-pull amplifiers. As noted both amplifiers are identical as regards circuit, wiring, etc. Moreover all the corresponding pairs of tubes were carefully matched on the basis of special selective tests. The frequency characteristics of the amplifiers extend from two cycles to ~12 Mc with an amplification coefficient k = 500.

The circuit, incidentally, provides for changing k to about 1000 with simultaneous narrowing of the frequency band to 3 Mc. This change is effected by connecting in higher loads into the plate circuits of the terminal amplifier tubes (with simultaneous adjustment of the compensating inductances). The amplification factor is changed (independently for each amplifier) by means of knobs brought out to the front panel of the oscillograph. In order to minimize the effect of switching on the characteristics of the oscillograph the switches in question are located immediately next to the final tubes; the knobs are linked with the switches by appropriate hinged rods. These switches also shift the connection of the cathode-ray tube plates from the main amplifiers to the linear sweep. Thus each switch has three positions:

P - plates connected to the linear sweep amplifier;

B - deflecting plates connected with the higher plate loads (k = 500);

M - deflecting plates connected with the lighter plate loads (K = 1000).

It should be noted that for operating positions B and M one must provide automatic cutoff of the sweep inasmuch as otherwise the sweep signal is fed through the multicontact capacitance of the switch to the deflector plates.

3. Signal attenuation and the taumeter

The variations in the amplitude of the signals viewed on the oscillograph screen are inevitably limited from "above" by the dimensions of the central portion of the screen (area in which the cathode ray tube is "linear") and from "below" by readability of the trace. This, of course, makes it necessary to have the possibility of attenuating the input signal. Usually attenuation is accomplished by a step divider at the input and a continuously variable attenuator in the cathode circuit of the cathode follower. Our experiments showed, however, that the presence of the step RC-divider at the amplifier input introduces some distortion into the shape of the signal. Hence in our design of the oscillograph we provided for feeding in the signal to the grid of the first tube through a special coaxial jack, bypassing the input attenuator. In this case the input attenuator is entirely disconnected from the oscillograph circuit. This arrangement was found preferable for most of the work involving amplification of signals from photomultipliers.

Continuously variable attenuators for oscillographs of our type commonly employ a circuit such as that shown in Fig.10. The equivalent resistance $R_1 + R_2$ equals about 110 ohm (for a 6AC7 tube, $S \approx 9$ ma/v). The variable resistor (R in Fig.10) used in such circuits normally has a rating of 1-2 kiloohm, with $C \approx 100$ μf. Obviously, with the attenuator control in different positions the equivalent resistance in the grid input circuit of the following tube will differ but will always be greater than 110 ohm. Experience shows that with control by this type of attenuator the transfer characteristics of the amplifier vary.

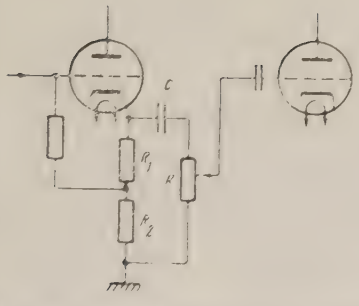

Fig.10. Continuously variable attenuator circuit.

Identical operation of both amplifiers can be attained in such cases only when the controls of the two variable attenuators are in exactly the same position. Obviously, in the case of ordinary variable resistors it is virtually impossible to match both attenuators without special control tuning. It follows from the above that this type of continuously variable attenuation is not satisfactory. Hence we designed a "fine-step" attenuator in which the voltage on the grid of the following tube is taken off an array of resistors, comprising the cathode resistance of the cathode follower. The cathode resistance consists of a set of fixed resistors mounted on two 10-position switches, which gives 100 steps of attenuation (Fig.11).

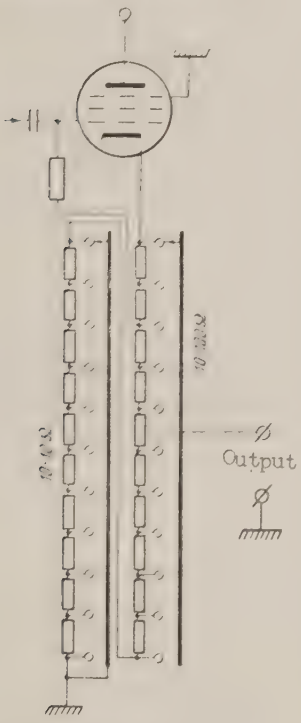

Fig.11. Fine-step attenuator circuit.

The advantages of this method of attenuation are the following: a) the exact settings of the attenuator can be recorded and reproduced at will to match the attenuation of both amplifiers; b) one can readily obtain the desired working range of the attenuator by connecting in a suitable grid leak (neither a nor b can be realized with a variable resistor which moreover is inclined to be noisy) and c) it expands the range of the amplitude linearity of the cathode follower (13 volts as compared with 8 volt range obtained with an attenuator of the type shown in Fig.10). A minor shortcoming of the attenuator is that it does not cover the entire attenuation range uniformly. In critical cases one can, of course, use the ideal form of attenuation, namely, reducing the amount of light incident on the photomultipliers in both amplification channels.

One should also exercise great care in selecting and designing the "taumeter" switching circuit, i.e., the switching arrangement for selecting the calibrated integrating RC networks, used in both amplifier channels of our oscillograph. The conventional switching circuit used earlier in connection with the original taumeter set-up (Fig.12) proved to be unsatisfactory for signals with very steep fronts: it proved impossible to obtain complete matching of the time constants obtained with different combinations of capacitors and resistors. For example, ten resistors of 100 ohms each are not equivalent to one resistor of 1000 ohms when both are connected with the same capacitors. This is due to the fact that the resistors themselves have a noticeable capacitance. Better results were obtained with the switching circuit shown in Fig.13 in which only one capacitor and one resistor are connected into the circuit at a given time, i.e., for each position of the double low-capacitance switches.

The presence of "taumeters" in both channels makes it possible, first to tune them accurately with respect to each other and, second, to use the cross measurement procedure, i.e., to use X as the signal channel and Y as the exponential sweep channel for one series of measurements and then Y as the signal channel and X as the sweep channel for the next series, thereby eliminating possible errors.

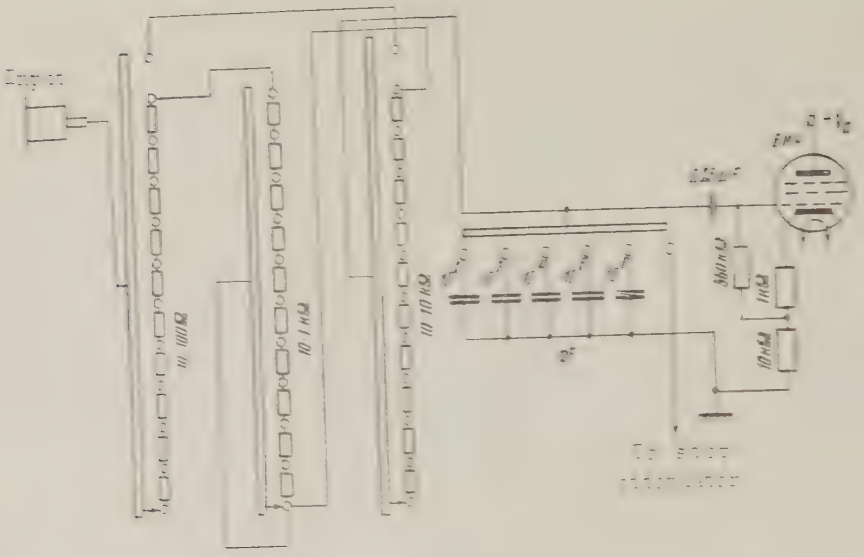

Fig. 12. Original taumeter switching circuit.

4. Electric differentiator

The accuracy of electric differentiation depends on the quality of the square pulse fronts and on the width of the oscillograph pass band. The wide band characteristics of our oscillograph make it particularly suitable for use of electric differentiation. Each of the amplifiers of our oscillo-

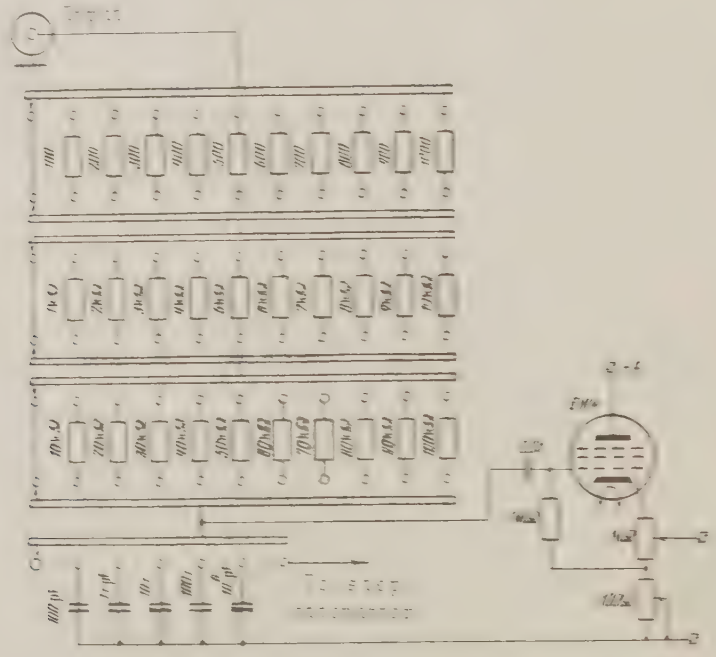

Fig.13. Improved ultrataumeter switching circuit

graph incorporates a switch, controlled from the front panel, by means of which one can connect in (between the cathode follower and the first preamplifier tube) one of eight differentiating networks with time constants of 10^{-8}, $3\cdot10^{-8}$, 10^{-7}, $3\cdot10^{-7}$, 10^{-6}, $3\cdot10^{-6}$, 10^{-5} and $3\cdot10^{-5}$ sec. The smallest possible miniature capacitors are used throughout.

Usually the differentiator determines the ratio of the signal amplitude to the amplitude of derivative of the signal (height of the "peak"). In the case of good differentiation ($\beta = \tau/RC \gg 1$), the amplitude of the signal is somewhat greater than that of the "peak"; hence for the signal and "peak" to be comparable on the oscillograph screen one must attenuate the signal by a certain factor.

Our fine-step attenuator can weaken the signal by a factor of 100. Thus, if on the screen the scales of the attenuated signal and the nonattenuated "peak" are equal, this means that the quality of differentiation allowed by the oscillograph is 100. A 1 inch scale of the signal and "peak" corresponds to a signal of $4\cdot10^{-2}$ RMS volts with an amplification factor k = 500. Consequently, the amplitude of the signal before the attenuator must be ~4 RMS volts or 11.2 crest volts. This lies within the range of the amplitude linearity of our cathode follower. It will be seen from this how important this linearity range is for insuring high quality differentiation.

5. Some characteristics of the oscillograph

To facilitate tuning the oscillograph and checking its transfer characteristics, we constructed a square pulse generator with a repetition rate of 100 kc, employing the "clipped sine" circuit shown in Fig.14. This generator gives very pure square pulses, thus allowing of tuning the oscillograph for the absence of "horns". The pulse edge time is $\sim10^{-7}$ sec. This generator was also used for investigating the relaxation of the cathodoluminescence of very fast cathodoluminophors by the ultrataumeter procedure.

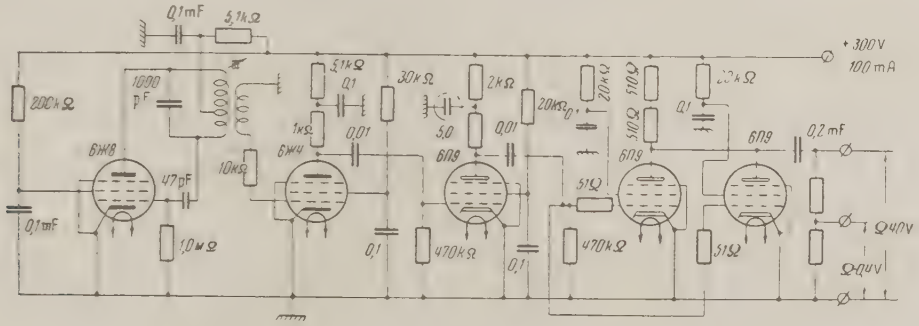

Fig. 14. Circuit of square pulse generator.

Fig.15, a shows the trace of these pulses as they appeared on the screen of our oscillograph. The pulse duration is 5 microsec. It will be seen that the pulse edges are steep. The virtual identity of the operating characteristics of the X and Y amplifiers is illustrated by the oscillogram of Fig. 15,b; here the square pulse was applied simultaneously to both amplifiers. The loop shown in Fig.15,c was obtained by introducing an "inertia" of 10^{-8} sec into the "taumeter" of one of the amplifiers. The difference between traces b and c clearly illustrates the sensitivity of the ultrataumeter method; it will be evident from the traces that an inertia of the order of

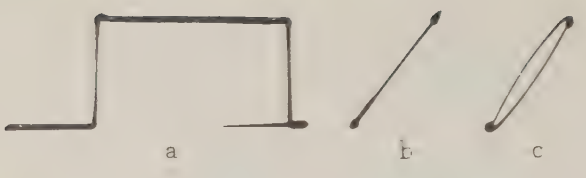

Fig.15. Traces of square pulses.

$2 \cdot 10^{-9}$ sec can be detected by means of our oscillograph. It should be noted, however, that so high a sensitivity to small inertias is fully evinced only in the case of very "pure" signals, i.e., signals not distorted by noise. The signals from photomultiplier tubes are actually never quite so pure. This reduces the sensitivity to $1\text{-}2 \cdot 10^{-8}$ sec. In order to check the operation of the oscillograph in the region of very low frequencies (i.e., the quality of rendition of the "top" of the square pulses), we constructed a square pulse generator with a very low repetition rate. On the whole the horizontal frequency characteristic of our instrument extends from ~5 cycles to ~10 Mc with k = 500 or to 3 Mc with k = 1000. The highest frequency still passed by the oscillograph amplifiers is about 14 Mc. The final fine tuning of the amplifiers is effected by adjustment of the correcting inductances.

We have described the oscillograph in considerable detail because experience shows that it is critical where the successful operation of the whole ultrataumeter set-up is concerned.

III. Mechanical Light Modulator

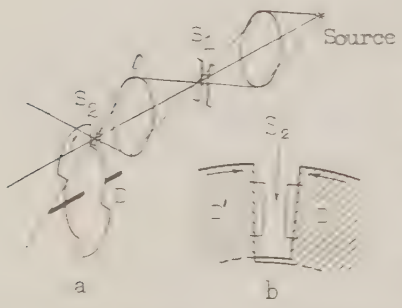

Fig.16. Diagram of mechanical light modulator.

The mechanical light modulator, constructed by us for one of the variants of the ultrataumeter, can be used to modulate light of any spectral composition within the range of transmission of the quartz lenses. The use of mirror optics throughout would extend this range even further and eliminate chromatic aberration. The design of the modulator (like the design of the modulator used in the original taumeter) is based on a rotating disc (shutter) with projections or tabs chopping the focused light beam at its narrowest point. In the design of the ultrataumeter modulator we used an original technique for cutting down the leading and trailing edge times[22].

Let us assume that we have a rectangular slit S_1 illuminated by light focused on it by the condensing lens (Fig.16,a). The quartz parabolic lens O forms a reduced image of the slit S_2 in the plane of the rotating disc D. As the disc rotates the projecting tabs chop the light beam. Obviously, the greater the peripheral speed of the disc and the greater the reduction produced by the lens O, the shorter will be the fronts of the square light pulses. A limit on the rate of rotation of the disc is imposed by mechanical considerations (essentially resistance to rupture under the influence of centrifugal force). The limit as regards reduction of the size of the slit image S_2 is imposed by the necessity of obtaining a sufficient amount of light (in the final analysis this depends on the aperture of the lens O). Let us assume that we have attained both limits for the given design. Then the edge time of the square light pulse can still be halved if we arrange to have the slit image S_2 chopped not by one disc D but also and simultaneously by a second

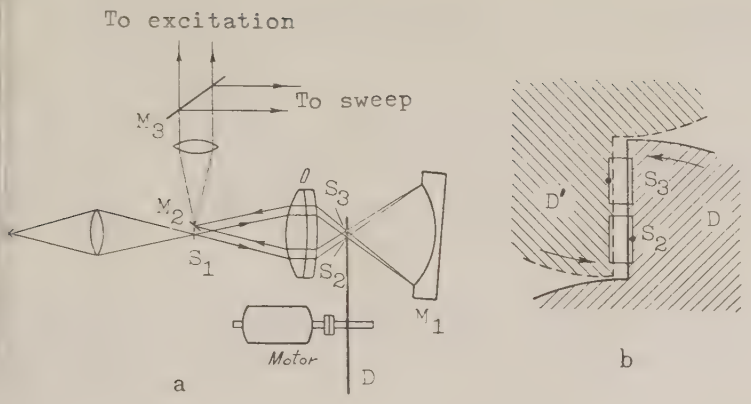

Fig.17. Optical design of the modulator.

disc D' rotating in the opposite sense (Fig.16,b) with the same speed. Obviously, the edges of the tabs of both discs must meet exactly at the center of the slit. Clearly, such precise synchronization of two very rapidly rotating discs is not realizable in practice. This difficulty can easily be obviated, however, if instead of a mechanical second disc, we use an inverted image of the first disc in a concave mirror. Thus we obtain the optical arrangement pictured in Fig.17,a.

The concave spherical mirror M_1 returns the light beam, producing a real inverted image S_3 of the "slit" S_2 (i.e., the reduced image of the actual slit S_1 formed by the lens O). The mirror is turned slightly about the horizontal axis so that S_3 does not quite coincide with S_2, but lies just above or below S_2. The returned light beam passes through the lens O in the reverse direction, either above or below the slit S_1, where it is intercepted by the small mirror M_2 and directed to the investigated luminophor (i.e., used for excitation). The quartz plate M_3 diverts a portion of the modulated light to the photomultiplier actuating the sweep.

Inasmuch as the spherical mirror M_1 forms an inverted image of the same size of everything in the plane of S_2 and S_3, the edge of the disc D will have its optical "twin" moving towards it and meeting it at the center of the images S_2 and S_3. Thus the returned light beam will be fully "chopped" when the real disc D covers only half of S_3 and the effective pulse edge time will be reduced by half (Fig.17,b).

For example, if the width of slit S_1 is 1 mm, the width of the slit image S_2 is 0.1 mm, the diameter of the disc D = 20 cm and the rate of rotation of the disc is 12,000 rpm, the effective edge time will be $8 \cdot 10^{-7}$ sec with ordinary modulation, but only $4 \cdot 10^{-7}$ sec when the above described optical technique of doubling the front steepness is employed.

Taking into account the distinctive characteristics of the taumeter procedure (see introduction), we can count on measuring much shorter times. Indeed, we found that with a version of the "mirror doubling" modulator in which $S_2 \approx 0.5$ mm and the pulse edge time was $\sim 2 \cdot 10^{-6}$ sec (the calculated front steepness was substantiated by measurements by the method of electric differentiation[21]) it was possible to detect inertias of the order of $5 \cdot 10^{-8}$ sec. Thus the practical limit of the potentialities of the ultrataumeter employing a mechanical light modulator with "mirror doubling" is about 10^{-8} sec. Unfortunately, attainment of this limit involves an appreciable sacrifice in the amount of available light.

The use of quartz and mirror optical components makes it possible to utilize the above described modulator for obtaining square light pulses in a wide spectral range. Unfortunately, chromatic aberration of the lens O makes it necessary to focus the image of slit S_1 on the plane of the disc separately for each wavelength. This inconvenience can be eliminated by using an appropriate condensing mirror instead of the lens O.

The results of measurements of the luminescence of platinocyanide compounds made by means of the ultrataumeter were presented at the Fourth Conference on Luminescence[23].

IV. Other Variants of the Ultrataumeter

In addition to the ultrataumeter with a mechanical light modulator described above, we realized two other ultrataumeters differing only as regards the character of the modulators employed.

1. Ultrataumeter with an electro-optical light modulator (Kerr cell). This instrument is designed for modulation of light only in the visible part of the spectrum. It has been successfully used for investigating the kinetics of infrared luminescence of cuprous oxide. The Kerr cell modulator has been described elsewhere[24,25].

2. Ultrataumeter for investigating the kinetics of cathodoluminescence. A number of different generators of square electric pulses (including the 100 kc generator described above) have been used in this version; the electric pulses control the electron beam exciting the investigated cathodoluminophor. Cathodoluminescence relaxation times of down to 10^{-7} sec can be measured by the instrument. Measurements made by means of this version of the ultrataumeter will be published in the near future.

References

1. N.A.Tolstoi & P.P.Feofilov, Doklady AN SSSR, 58, 389 (1947).
2. N.A.Tolstoi & P.P.Feofilov, Zhur.eksp.i teor.fiz., 19, 421 (1949).
3. N.A.Tolstoi & P.P.Feofilov, Usp.fiz.nauk., 41, 44 (1950).
4. N.A.Tolstoi & P.P.Feofilov, Izv.AN SSSR, Ser.fiz., 13, 211 (1949).
5. N.A.Tolstoi & P.P.Feofilov, Doklady AN SSSR, 59, 235 (1948).
6. V.A.Arkhangel'skaia, A.M.Bonch-Bruevich, N.A.Tolstoi & P.P.Feofilov, Doklady AN SSSR, 64, 187 (1949).
7. D.B.Gurevich, N.A.Tolstoi & P.P.Feofilov, Doklady AN SSSR, 66, 365 (1949).
8. N.A.Tolstoi & P.P.Feofilov, Doklady AN SSSR, 68, 285 (1949).
9. D.B.Gurevich, N.A.Tolstoi & P.P.Feofilov, Zhur.eksp.i teor.fiz., 20, 769 (1950); 20, 1039 (1950).
10. D.B.Gurevich, N.A.Tolstoi & P.P.Feofilov, Doklady AN SSSR, 71, 29 (1950)
11. V.A.Arkhangel'skaia, A.M.Bonch-Bruevich, N.A.Tolstoi & P.P.Feofilov, Zhur.eksp.i teor.fiz., 21, 290 (1951); 21, 297 (1951).
12. N.A.Tolstoi & P.P.Feofilov, Izv.AN SSSR, Ser.fiz., 16, 59 (1951).
13. V.A.Arkhangel'skaia, A.M.Bonch-Bruevich, N.A.Tolstoi, Izv.AN SSSR, Ser.fiz., 15, 695 (1951).
14. N.A.Tolstoi & P.P.Feofilov, Doklady AN SSSR, 85, 551 (1952).
15. N.A.Tolstoi, V.T.Kolomiets, O.N.Golikova & M.Ia.Tsenter, Zhur.eksp.i teor.fiz., 30, 575 (1956).
16. L.A.Tumerman, Usp.fiz.nauk., 33, 218 (1947).
17. M.D.Galanin, Trudy (Transactions), Physical Institute of the USSR Ac. of Sci., 5, 341 (1950).
18. A.M.Bonch-Bruevich, Izv.AN SSSR, Ser.fiz., 20, 5, 591 (1956). (Translation in Bulletin, 20, No.5, P.536.)
19. N.A.Tolstoi, Trudy sessii GOI, posviashch. pamiati S.I.Vavilov (Transactions of the meeting of the State Optical Institute devoted to the memory of S.I.Vavilov), 1953.

20. S.M.Ryvkin, Izv.AN SSSR, Ser.fiz., 15, 721 (1951).
21. N.A.Tolstoi, Izv.AN SSSR, Ser.fiz., 15, 712 (1951).
22. N.A.Tolstoi, Doklady AN SSSR, 102, 935 (1955).
23. N.A.Tolstoi, A.K.Trofimov, A.M.Tkachuk & N.N.Tkachuk, Izv.AN SSSR, Ser.fiz., 20, 583 (1956). (Translation in Bulletin, 20, No.5, p.529).
24. N.A.Tolstoi & N.N.Tkachuk, Doklady AN SSSR, 95, 65 (1954).
25. N.A.Tolstoi, N.N.Tkachuk & R.K.Preobrazhenskii, Optika i spektroskopiia, 2, 116 (1957).

DISCUSSION

Question: How is your ultrataumeter used for investigating cathodoluminophors and how does it compare with extant instruments?

N.A.Tolstoi: Part of the ultrataumeter is used for investigating cathodoluminescence, namely, the wide band oscillograph with the light modulator replaced by an electric generator producing square pulses. Two such electric modulators were constructed, one for 40 cycles, the other for 100 kc.

In the course of an investigation by means of the ultrataumeter, carried out by Arkhangel'skaia, Petoshina, Tkachuk and myself, we succeeded in measuring some cathodoluminophors with a relaxation time of $2 \cdot 10^{-7}$ sec. The range on the side of long relaxation times is limited only by flickering of the pattern on the oscillograph screen or by the low frequency cutoff of the oscillograph (about 3 cycles).

As for comparison with extant instruments, I know of no instruments capable of measuring relaxation times of the order of 10^{-7} sec with comparable precision. I understand that such measurements are being made abroad, but I am under the impression that the accuracy obtained in the range of such short relaxation times is appreciably lower.

PERSISTENT LUMINESCENT COATINGS ACTIVATED BY ARTIFICIAL β-ACTIVE ISOTOPES

- V.L.Levshin, E.I.Panasiuk & L.A.Pakhomycheva

Dials made of self-excited materials are used on many instruments. Such materials have also found application as signs and indicators in unlighted places and as special warning devices.

The materials now in use are primarily zinc sulfide phosphors excited by α-rays from natural radioactive sources, usually salts of radium or mixtures of radiothorium with mesothorium. The α-particles from these sources have a high energy and limited range; consequently, along their path through the crystal phosphor, aside from activating the luminescence centers, they produce strong disruptions in the crystal lattice and this in turn reduces the luminance of the phosphor. Hence no matter how long a lifetime an α-emitter has, the useful service life of the materials activated by it does not exceed two to three years.

The rate of deterioration of the crystal lattice is roughly proportional to the quantity of α-emitting material present which limits the amount of radio-active material that can be introduced, and this in turn places a bound on the possibility of increasing the brightness of the luminous coating.

The initial luminance of the "permanent" type "Z" («З») compound now commonly used is 0.2 asb. For many practical applications this is quite insufficient. Coatings having several times this intensity are required. Also, it would be desirable to have materials glowing not only in green, but in other colors as well. Blue, orange, and particularly red, luminescing materials have not hitherto been made due to their low subjective brightness. The human eye is relatively less sensitive to blue and red and it is impractical to introduce sufficiently large amounts of α-activator. Thus we have the need for prolonging the service life of self-luminescent materials together with the incompatible requirement of enhanced brightness.

This problem, unsolvable by means of α-emitters as activators, appears to be solvable by using β-emitters.

Since 1950, research at the "P.N.Lebedev" Physical Institute of the USSR Academy of Sciences has been underway with a view to developing self-luminescent materials with different radioisotopes as activators.* Many artificial radioisotopes, both short and long-lived, isolated and in isotopic mixtures, have been tested.

As phosphor activators, the most suitable artificial isotopes are those emitting β-rays only and having a long lifetime. It is desirable to avoid isotopes emitting γ-rays as well as β-particles, for protection against γ-radiation is rather difficult.

After extensive investigation of a number of phosphors, it has been found that the ZnS:Cu phosphor, generally used with α-emitters, has the greatest luminance under β-excitation.

In the experiments described below it was shown that β-emitters incorporated into ZnS in quantities high enough to produce brighter coatings than the standard "Z" type produce virtually no disruptions of the crystal lattice. When the ZnS:Cu phosphor is activated by a separated isotope, the brightness of the luminophor decreases at the same rate as the isotope due to its radioactive decay. Examples of such preparations are phosphors activated with W^{185} and Cs^{137}.

Lately, a few notes on applications of phosphors activated by β-isotopes have appeared in foreign literature.

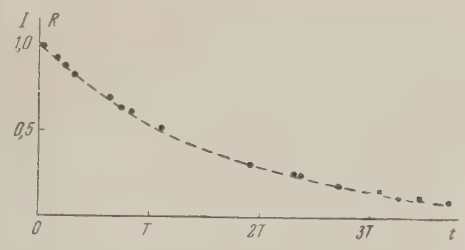

Fig.1. Dots - variation with time of the luminance of W^{185} activated ZnS:Cu phosphors; dashes - decay curve of W^{185}.

Tungsten W^{185} is a β-emitter with a period of 73.2 days and maximum energy E_β = 0.43 Mev. The results of measurements of the luminance of W^{185} containing phosphors are given in Fig.1. The comparison of the observed points with the decay curve (dash line) shows the proportionality of the brightness of the phosphor to the quantity of W^{185} remaining in it.

Data on the brightness of phosphors activated by Cs^{137} is given in Fig.2; the curves show that the brightness of the phosphors remains virtually constant over a period of two years.

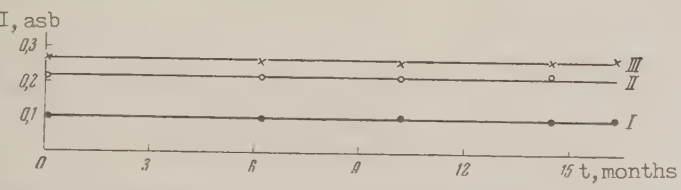

Fig.2. Variation of the luminance of three phosphors activated by Cs^{137} as a function of time.

This isotope can be obtained in a very pure state. It has a long half-life (T = = 33 years). Apart from β-emission (E_{β_1} = 0.521 Mev (95%) and E_{β_2} = 1.2 Mev (5%), it also emits γ-rays (E_γ = = 0.666 Mev). The presence of γ-rays prevents wider application of Cs^{137} as an activator. It can be recommended only in cases where an extremely high emission stability is indispensable.

For general use we recommend stable luminophors activated by Sr^{90} (T = = 19.9 years, E_{β_1} = 0.61 Mev and E_{β_2} = 2.3 Mev). Unfortunately, we did not have at our disposal enough pure Sr^{90} free of other radioactive admixtures, particularly of the short-lived Sr^{89} (T = 54.5 days, E_β = 1.5 Mev). For this reason we established the absence of deleterious effects of Sr^{90} on the ZnS:Cu phosphor indirectly: we measured the variation in brightness of samples containing different concentrations of Sr^{90} over a long period of time. Should the β-radiation cause destruction of the crystal lattice, the deterioration of the samples with higher concentrations of Sr^{90} should proceed faster than that of samples with low concentrations. No such differences in the intensity-time relationships was observed, as is evidenced by the results of the following tests.

A series of five samples (I-V) was prepared. The quantity of Sr^{90} in these ranged from 0.5 millicurie for sample I to 6 millicurie for sample V. The brightness of the weakest sample was taken as the arbitrary unit. The points in Fig.3 represent the relative initial luminances of the samples; the crosses, the relative intensities after 8 months. Throughout, the ratios remained the same. Due to the decay of short-lived radioactive impurities, the absolute brightness of all the samples decreased by approximately 15%.

The absence of damage to the ZnS was also confirmed by irradiating ZnS:Cu screens with β-particle sources of ~5 millicurie. Following irradiation of the screen with a very strong Sr^{90} source (100 millicurie) a slight darkening of the phosphor was observed; this cleared up a short time after cessation of irradiation.

The rates of change in brightness of the above described series of Sr^{90} activated phosphors are shown in Fig.4. As noted, our Sr^{90} material contained a considerable amount of Sr^{89}. This explains the decrease in brightness observed during the first 50 days; from then on the luminance remained virtually constant over the 300 day test period.

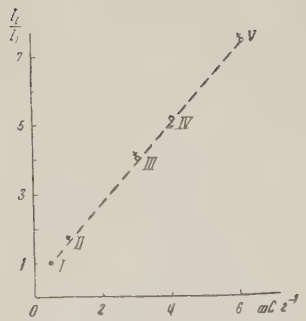

Fig.3.

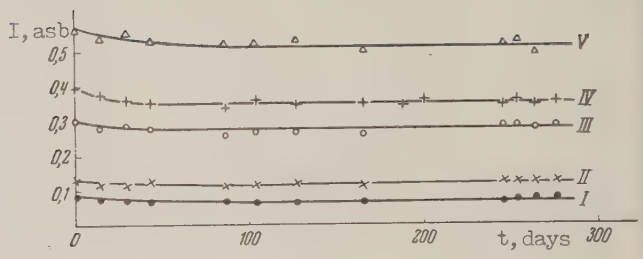

Fig.4.

Fig.3. Plot illustrating the independence of the relative luminance of specimens on the quantity of Sr^{90} present in the phosphor. Horizontal scale - activity; vertical scale - luminance of specimens referred to that of sample I. Circles - initial values; crosses - values after 8 months.

Fig.4. Luminance of samples I through V, activated by different quantities of Sr^{90} vs time in days.

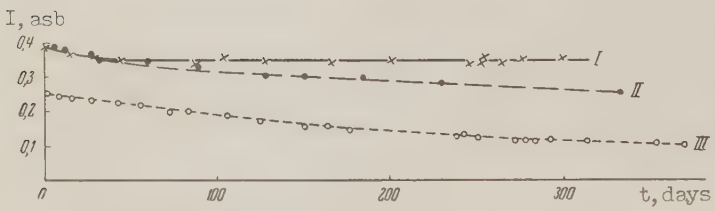

Fig.5. Comparison of the change in luminance with time for 3 samples: I) activated by Sr^{90}, II) activated by Sr^{90} with considerable quantity of short-lived isotopes, III) standard compound "Z" (α-excited preparation).

Fig.5 shows the comparative intensity-time curves for 3 samples: sample IV of the above series, a specimen activated by a radioactive mixture richer in Sr^{90} and having the same initial radiance (0.4 asb), and a sample of the standard α-activated "Z" type substance having an initial luminance of 0.25 asb. During the 300 day test period the brightness of the "Z" phosphor decreased to one-half of its initial value, while the brightness of the sample activated by Sr^{90} decreased only by 10-15%, with most of the decrease occurring during the first days when the short-lived Sr^{89} was disintegrating. In the case of "technical grade", poorly separated isotopes, the luminance stability is somewhat inferio (Fig.5).

All these experiments indicate that β-radiation does not cause destructio of the ZnS crystal lattice. This feature allows of the introduction of β-emitters in large quantities, which in turn makes it possible to realize (1) long-lived luminescent compositions of high intrinsic brightness and (2) phosphors having different luminescence colors.

In our tests, by introducing large quantities of Sr^{90} it was possible to obtain compositions with a very high brightness. Under laboratory conditions we succeeded in obtaining compositions with a luminance of 3 asb in the case of 1 mm thick layers. It is important to note that the variation of brightness with coating thickness in the case of the β-activated materials is different from that in the case of α-activated ones since the range of

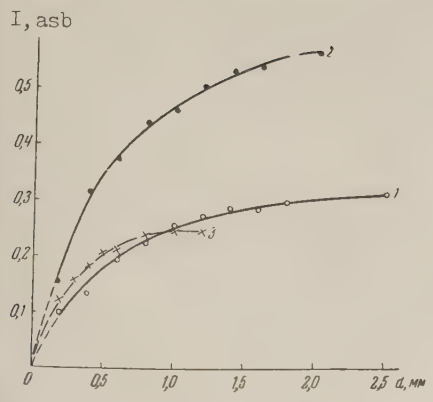

Fig.6. Dependence of the luminance on the thickness of the layer: 1 & 2) phosphors activated by different quantities of β-emitter, 3) standard "Z" type phosphor.

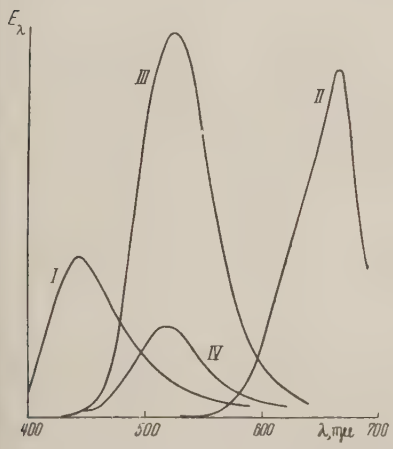

Fig.7. Spectral distribution of the emission of Sr^{90} activated phosphors: I) ZnS:Ag, II) ZnSCdS:Cu, III) ZnS:Cu, IV) type "Z" (for comparison).

β-particles is considerably greater. The variations in brightness with the layer thickness for two phosphors having different concentrations of Sr^{90} (1 & 2) and also for the "Z" type material are shown in Fig.6. For the "Z" compound peak brightness is virtually attained at a thickness of 1 mm. Compositions activated by Sr^{90} do not reach a maximum value even at thicknesses of 2-2.5 mm. In view of the energy dependence of the range of β-particles the optimum coating thickness must be determined separately for each activating isotope.

By increasing the content of β-emitters and the thickness of the layer, one can readily realize coatings with ten or more times the luminance of the standard "Z" type coating.

The intense luminance of the new products opens new avenues of application. Old compositions based on ZnS were only green emitting, whereas the possibility of using β-emitters in large quantities makes it feasible to prepare strong luminophors of different colors. This is extremely important, for instance, for differential signaling.

The spectral distribution of the emission of several special Sr^{90} activated phosphors is given in Fig.7: Curve 1 - ZnS:Ag phosphor yielding blue luminance ($\lambda_{max} \approx 450$ mμ), curve II - ZnS:CdS:Cu phosphor ($\lambda_{max} \approx 660$ mμ), curve III - ZnS:Cu phosphor ($\lambda_{max} \approx 520$ mμ) which had a luminance of 0.8 asb, and curve IV - the standard "Z" phosphor (α-excitation, ~ 0.2 asb). To determine the effective brightness, the curves of Fig.7 should be multiplied by the corresponding spectral sensitivity of the human eye; this leads to less favorable values for the blue and red phosphors. Nevertheless, the actual brightness of the blue and red phosphors is sufficient for most practical purposes.

It may be noted that the luminance of the new phosphors depends to some extent on the temperature. A rapid temperature rise from 20 to 70° produces an increase in brightness of 10-15%; cooling the phosphor leads to a corresponding decrease in emission.

β-radiation is more penetrating than α-radiation hence the use of β-emitters calls for better protection against radioactivity. The new luminophors should be covered with thick shields of plastic or silica glass. Not all kinds of silica glass are suitable for screens, for many types darken under irradiation. For this reason we tested a number of different types of glass made available by the MELZ plant. The change in the spectral transmission of several kinds of glass β-irradiated by 100 milicurie of Sr^{90} for 16 hours is shown in Fig.8. The upper curves show transmission before irradiation; the lower ones, after it. An introduction of 1% of CeO_2 into glass (Fig.8,b)

eliminates darkening. "Lead glass" (containing 30% PbO) shows a smaller decrease of transmission (Fig.8,d) than ordinary silica glass that does not contain CeO_2. Thus glass with 1% of CeO_2 can be recommended as a protective covering for β-activated luminophors when working conditions make it impossible to use plastic shields. The transmission of most plastics does not decrease under the action of β-radiation.

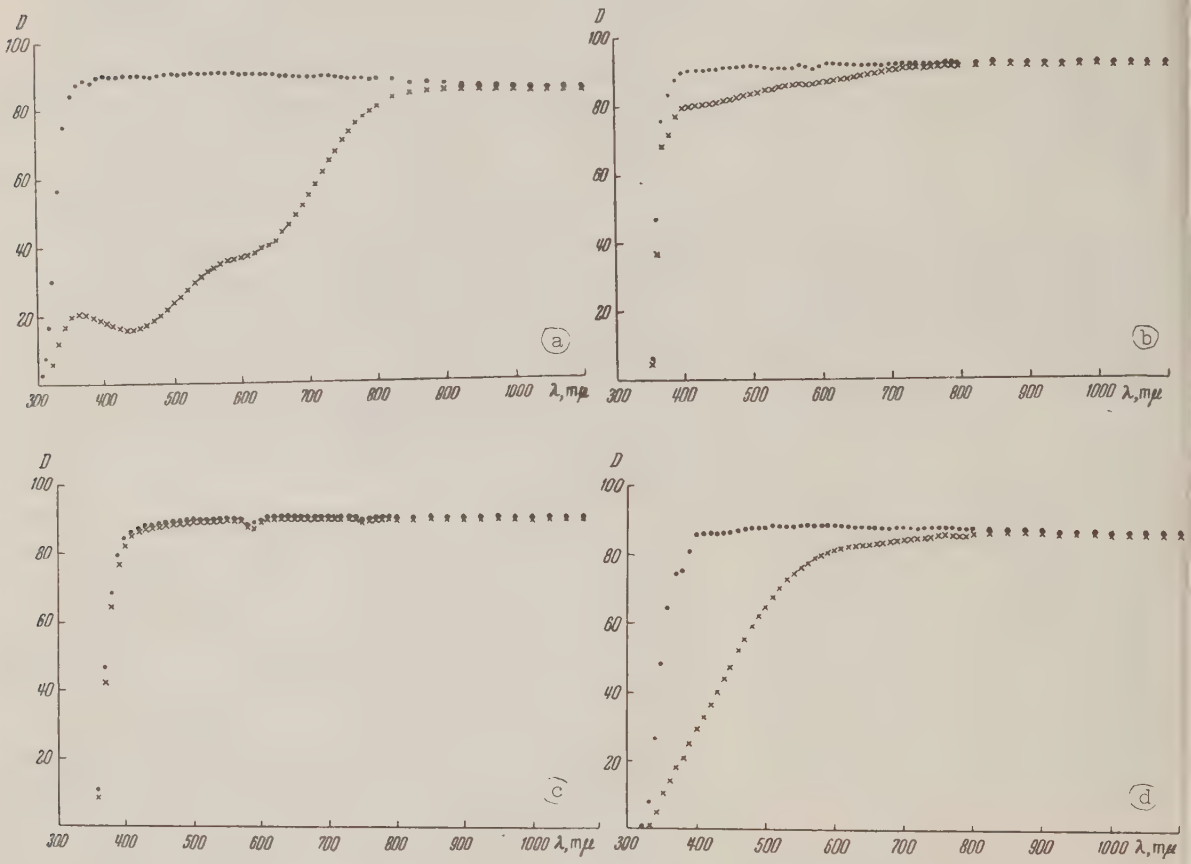

Fig.8. Spectral transmission in percent for different kinds of silica glass before (dots) and after (crosses) β-irradiation: a) electro-vacuum (barium glass without CeO_2), b) the same with 0.5% of CeO_2, c) with 1% of CeO_2 and d) lead glass (30% PbO) without CeO_2.

Conclusions

1. The isotopes Sr^{90} and, for special cases, Cs^{137} are recommended as exciters for persistent luminescent coatings.

2. Appropriate phosphors activated by Sr^{90} may - depending on operational conditions - have a service life of ten years or more.

3. The maximum luminance of the green luminophors with Sr^{90} can be ten times as high as that of present α-activated coatings.

4. Self-activated phosphors emitting different colors of light with a sufficient intensity for practical purposes have been prepared.

5. Transparent plastics and silica glass with 1% CeO_2 are recommended for protective shields.

Once they are in production, the new luminescent materials will be considerably cheaper than the ones produced today.

New applications of these long-lived phosphors are possible, due to superior features of β-activated luminescence. For example, they could be used as indicators and direction signs in coal mines and similar dark locations. The use of these phosphors in finished products is particularly expedient because in such cases it will be easier to provide appropriate radiation shielding. Thanks to their high stability, the new β-activated phosphors could serve as standard sources for calibration of low light intensities and thus prove of value in certain photometric and astronomical measurements.

"P.N.Lebedev" Physical Institute of the
Academy of Sciences of the USSR

References

1. Energeticheskie iadrenye reaktory i ispolzovanie produktov deleniia (Nuclear power reactors and the use of fission products) Collection of articles, M., 1955.

DISCUSSION

V.V.Antonov-Romanovskii: Please, tell us what is the size of the crystals? On the average - a few microns?

V.L.Levshin: I think about 10 μ.

V.V.Antonov-Romanovskii: Is it possible to increase the brightness of the phosphors by using larger crystals in order to minimize scattering?

V.L.Levshin: This may be possible. There may be other means of increasing brightness as well.

Question: Apart from phosphors with Sr^{90}, there have been some patents, published abroad, covering luminophors with tritium. Could you please indicate the possibilities of using such phosphors?

V.L.Levshin: Patents exist, but the phosphors are hard to make because tritium is a very noxious substance and such activation is inefficient at the present time due to the high price of tritium.

Question: What is the effect of β-activated phosphors on the human organism as compared with the effect of the "Z" type compound?

V.L.Levshin: It is more difficult to provide protection from β-emitters than from α-emitters, but β-radiation itself is not so dangerous because it penetrates tissues and its action is less localized. One should, however, be very cautious with these phosphors; special facilities should be designed for their production.

Question: What are the possibilities of manufacturing the new phosphors? When will it be possible to produce them industrially?

V.L.Levshin: That depends on the speed with which industry will respond to the demand, for industry now has all that is necessary for their production.

T.B.Shchenkina: The work of the Physical Institute on creating new phosphors is very interesting, due to their higher brightness, longer life and lower price. I consider it necessary to include in the recommendations of the conference that the Ministry of Chemical Industry should accept them for rapid mass production, and also organize the production of protective containers for the luminescent signs the design of which should be standardized.

In conclusion, we are grateful to Prof.Levshin and his associates for the rapid and effective solution of the problem of creating luminous signs with these new products.

L.A.Markovskii: Very interesting work on creating new long-lived luminophors was performed at the physical Institute under the leadership of V.L.Levshin. Luminescent materials have been made which exceed the brightness of type "Z" phosphors several times and which have different colors of emitted light. Certainly, these qualities will find an application on many types of special devices.

Still it is premature to speak of their general use in the national economy. The main objection is their high activity which exceeds that of phosphors employing radium several times. This makes them quite dangerous, especially if one takes into account the specific hazards of Sr^{90}. Consequently, a wide use of these luminophors should not be made until methods of handling them safely have been devised by the appropriate medical agencies.

V.L.Levshin: I think we should take note of the proposals of Comrade Shchekina and Markovskii, but it seems to me that the task of elaborating safety standards should be undertaken by the Ministry of Health and the Ministry of Chemical Industry as soon as possible and it would be particularly desirable to have Comrade Markovskii work on it himself.

PROCEDURES AND INSTRUMENTS FOR MEASURING LUMINESCENCE

- D.A. Shklover & R.S. Ioffe

The development of research in the field of luminescence and increasing fabrication of different products utilizing luminescence (fluorescent lamps, cathode-ray tubes, image converter tubes and the like) have brought to the fore the problem of measuring the optical characteristics of luminescence. Among the more important of these characteristics are the brightness, the light yield, the color and the spectral distribution of the emission. The distinctive features of luminescence - the diversity of the spectra and color of the emission and the generally low intensity - make it impossible to use ordinary photometric equipment, particularly for purposes of production control. Thus the increased use of phosphors brought the need for developing special measurement procedures and instruments.

In the present report we shall describe some of the instruments for measuring luminescence developed at the VNISI (All-Union Scientific Research Institute of Light Engineering). These instruments employ modern photoelectric measurement techniques that insure the necessary accuracy, reproducibility and rapidity in determining the optical characteristics of luminophors.

In order to obtain brightness and color data consistent with visual evaluation by means of photoelectric procedures one must have three radiation detectors with spectral sensitivity curves similar to the MKO "specific components of a standard observer" curves[1].

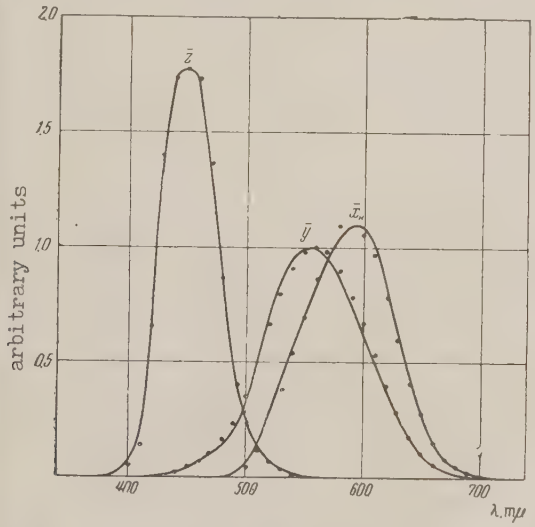

Fig.1. Spectral sensitivity curves of the colorimeter detectors: solid lines - the required "standard observer" sensitivity values; points - actual data obtained with a Bi-S cathode.

In order to facilitate selection of the correcting light filters for reproducing the requisite spectral curves in photoelectric colorimeters, the VNISI used the converted specific component curves shown in Fig.1. The radiation detectors used in the VNISI colorimeters are selenium photocells and photomultiplier tubes with cesium-bismuth cathodes equipped with specially designed combinations of correcting glass light filters. The UFK-1 and UFK-2 type VNISI photoelectric colorimeters have found extensive application in scientific research institutes and plant laboratories for measuring the brightness, light yield and chromatic characteristics of luminophors. For measuring the emission of cathodoluminophors and cathode-ray tube screens the colorimetric head is mounted immediately in front of the investigated object; the color and brightness of the emission are then found on the basis of the galvanometer readings for the three photocurrents by reference to a calibration nomogram.

For measuring the emission of photoluminophors the UFK type colorimeters can be used in conjunction with a special source[2] (Fig.2) consisting of three germicidal lamps emitting the 2537 Å resonance line. Separation of the luminescence emission from the visible light of the lamp is effected by the differ-

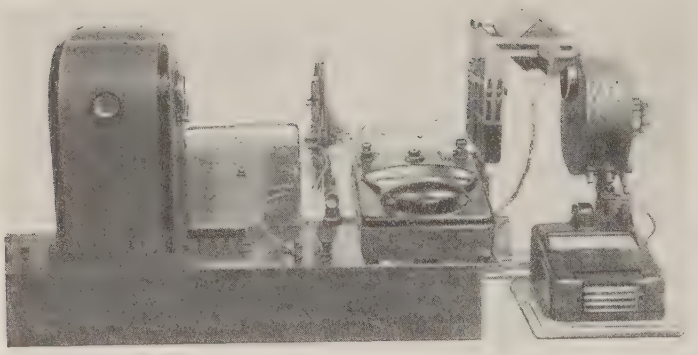

Fig.2. UFK-1 colorimeter with source for measuring the emission of photoluminophors.

ence method, using a light filter absorbing the resonance emission. The colorimeter is calibrated with reference to a standard incandescent lamp provided with the equipment.

Increasing production of fluorescent lamps made it necessary to develop a special colorimeter for checking the emission of such lamps in accordance with the set spectral tolerances[3]. Such a colorimeter must obviously have the requisite accuracy together with the necessary ease and speed of operation. A general view of the UFK-1 instrument is shown in Fig.3. The fluorescent tube chamber contains a turret holding six tubes; while one is being measured, the other five are in process of coming into operation. The emission of the checked tube is received by a colorimetric head consisting of three selenium photocells equipped with appropriate correcting light filters. The colorimetric head is mounted in a special light-proof chamber which also houses the standard incandescent bulb used for calibrating the instrument. The color of the emission is measured by the compensation-null method, the result of measurement being obtained directly in the form of a point on a viewing chart which carries the color tolerances for different types of fluorescent tubes. The luminance of the lamp is read on a separate scale. The inspection rate is 30 lamps per hour. The accuracy of determining the relative color components is 0.005; the accuracy as regards brightness is 2-3%.

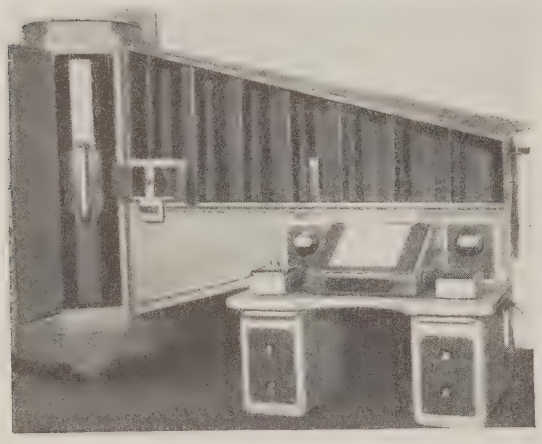

Fig.3. Equipment for checking the emission of fluorescent lamps.

In some cases of luminescence measurement it is necessary to check the color of emission of small areas of low brightness. This, for example, is the case in investigating the color and brightness distribution over the surface of cathode-ray tube screens, checking color rendition in color television, measuring the color and brightness of self-luminous coatings, etc. For such measurements the sensitivity of the colorimeters described above is insufficient.

In view of this, and particularly, to help solve the problems connected with the development of color television the VNISI developed a new instrument, namely the TK-1 television colorimeter which it is planned to put into small-scale production next year.

As is known, the principal difficulty in designing a photoelectric colorimeter is realizing three radiation detectors with spectral sensitivity curves similar to the MKO standard observer curves (i.e., the sensitivity curves of

the "standard" human eye). Until recently this problem was successfully solved only for selenium photocells. Selenium photocells, however, are relatively insensitive and do not allow of amplifying the photocurrent and, therefore, cannot be used in designing high-sensitivity instruments. The photocells and photomultipliers with cesium-bismuth and cesium oxide cathodes are not suitable for use in photoelectric colorimetry in view of the very unfavorable shape of their spectral sensitivity curves.

Recently the NII MRTP (Scientific Research Institute of the Ministry of the Radio Engineering Industry) and the VEI (All-Union Electrotechnical Institute) developed a new cesium-bismuth photocathode which has spectral characteristics suitable for application in highly sensitive light measuring instruments. The VEI-designed FEU-13 photomultiplier with a cesium-bismuth cathode is used in the TK-1 colorimeter. The spectral sensitivity of this photocathode encompasses the entire visible region of the spectrum and has a maximum at about 500-520 mμ.

A system of correction of the spectral sensitivity of the cesium-bismuth photocathode, based on a combination of glass light filters of different thickness, developed at the VNISI makes it feasible to realize three detectors with spectral sensitivity curves close to the requisite $\bar{x}$, $\bar{y}$ and $\bar{z}$ curves (Fig.1). The availability of a detector with a spectral sensitivity curve corresponding to the luminosity factor curve $\bar{y}$ makes it possible to use the TK-1 colorimeter as a nitometer.

The optical system of the instrument is designed so as to provide for the possibility of sighting small individual areas of the investigated surface. The measured emission is collected by a two-lens optical system, producing an illuminated circle of standard size on the photomultiplier cathode. A standard illuminated area is an important requirement where high accuracy is concerned in view of the fact that the sensitivity of photocathodes is not uniform over their entire surface.

Fig.4. The TK-1 television colorimeter.

A full internal reflection prism mounted in the path of the light beam is used for sighting. The observer sees an image of the investigated area on the frosted face of the prism through a sighting eyepiece. An iris diaphragm mounted in front of the prism serves to delimit the individual area it is desired to investigate. The maximum size of the area susceptible of measurements by the colorimeter is 50 x 50 mm, the minimal area is 5 x 5 mm.

The photomultipliers of the instrument are supplied from a built-in high voltage electronic regulator, stabilizing the voltage to within 0.1%. The output from the photomultiplier is fed into a one-stage amplifier which provides for a wide range of variation of the colorimeter sensitivity and makes it possible to use a pointer-type indicating instrument. The maximum sensitivity of the TK-1 colorimeter is 100 μA/asb and can be reduced by a factor of up to 1000.

A photograph of the TK-1 colorimeter is reproduced in Fig.4. The colorimeter consists of two units: the colorimetric head containing the detecting part of the instrument and a portable cabinet housing the power supply and the measuring instruments. The design of the colorimeter provides for

using the colorimetric head together with the photomultiplier supply unit separately from the rest of the instrument. This makes it possible to use the photomultiplier for spectral and similar measurements.

The described procedures and instruments are used in the VNISI and in a number of plants and scientific research institutes for measuring and studying luminescence for the purpose of production control of phosphors, the elaboration of standards and tolerances for luminophors, the solution of diverse technological problems and for monitoring the quality of television images.

All-Union Scientific Research Institute of Light Engineering

References

1. D.A.Shklover, Izv.AN SSSR, Ser.fiz., 13, 271 (1949).
2. Iu.P.Sidel'kovskii, Svetotekhnika (Light Engineering), No.5 (1956).
3. R.S.Ioffe & D.A.Shklover, Svetotekhnika (Light Engineering), No.2 (1955).

DISCUSSION

Question: Are there available commercial instruments for measuring the brightness (in absolute units) of luminescent coatings applied to dials and similar surfaces?

D.A.Shklover: The only instrument that could be used for this purpose is the television colorimeter I described. We have built six such colorimeters for different organizations, but so far there is no commercial production.

EQUIPMENT FOR INVESTIGATING THE LUMINESCENCE OF CRYSTAL PHOSPHORS

- Z.M. Sverdlov

The extensive development of luminescence analysis and its application in various branches of science and industry calls for the production of equipment suitable for investigating the properties of luminescent liquids and solids. The lack until recently of quantity production of simple equipment for qualitative determinations of luminescence, for measurement of luminescence intensities and for investigation of luminescence spectra has held back the practical application of luminescence analysis procedures.

The non-availability of commercial instruments for luminescence studies has been particularly acutely felt in geological organizations. Many natural minerals are essentially crystal phosphors; consequently, investigation of their luminescence may yield valuable information on the genesis of these minerals and prove useful in prospecting for them.

Hence the development, design and batch production of equipment for investigation of luminescence has been pursued since 1950 under the aegis of the Ministry of Geology and Preservation of Mineral Resources by the All-Union Scientific Research Geological Institute (VSEGEI) in collaboration with the "Geologorazvedka" (Geological Prospecting) Plant.

The developed luminescence equipment is based on the experimental and theoretical investigations of the luminescence of liquids and solids carried out by Academician S.I.Vavilov and his school. The prototypes of the instruments described below were the experimental models that have been under development since 1936 in the laboratory of S.I.Vavilov in the State Optical Institute[1-4].

As a result of the collaboration of the Luminescence Analysis Laboratory of the VSEGEI and the "Geologorazvedka" Plant the following instruments and equipment are now being produced in quantity.

A. Equipment for qualitative investigation of luminescence
   1. LIuM-1 (ЛЮМ-1) luminescent analytic lamp.
   2. LIuM-2 (ЛЮМ-2) luminescent mineraloscope.
   3. "Polius" (="Pole") field luminoscope.
   4. PLS-53 (ПЛС-53) universal field luminoscope.
   5. PLS-55 (ПЛС-55) field uranoscope.

B. Equipment for quantitative investigation of luminescence
   6. LIuKS-1 (ЛЮКС-1) luminescent colorimeter.
   7. LIuF-51 (ЛЮФ-51) luminescent photometer.
   8. LFS-54 (ЛФС-54) field luminescent photometer.
   9. FAS-1 (ФАС-1) photoelectric absorptiometer.

C. Equipment for investigating the luminescence spectra of minerals
   10. LMS-1 (ЛМС-1) luminescent microspectrometer.

A. Equipment for Qualitative Investigation of Luminescence

1. LIuM-1 luminescent analytic lamp

The LIuM-1 analytic lamp (Fig.1) is a source of near ultraviolet rays (λ = 366 mμ) exciting the luminescence of many natural materials both organic and inorganic. The LIuM-1 is used in geology for identifying and investigating bitumens, petroleums and other minerals, in biology for determining vitamin content, in agriculture for evaluating the germination of seed and the quality of vegetables, in machine building for detecting hair cracks in metal parts and in medicine for diagnosis of skin and other ailments.

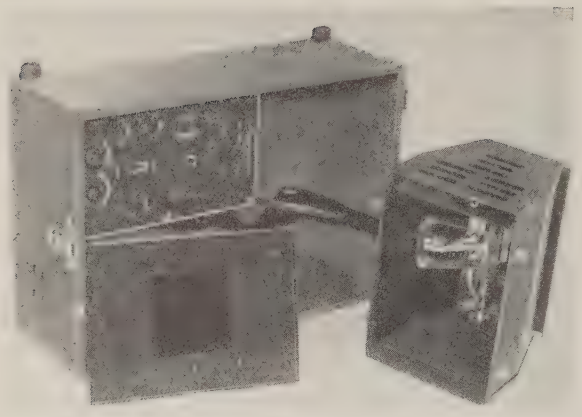

Fig.1. LIuM-1 luminescent analytic lamp.

The actual source of ultraviolet rays in the LIuM-1 is a PRK-4 (ПРК-4) quartz mercury vapor tube. The visible light emitted by the tube is absorbed by an UFS-3 (УФС-3) ultraviolet filter.

The lamp is designed for connecting to a 127 or 220 volt ac line and incorporates its own supply unit consisting of a coil and capacitor. The power consumption of the LIuM-1 is 220 ± 8 watts at 3.75 amp. The LIuM-1 luminescent lamp can also serve as an ultraviolet source for a luminescence microscope. Any biological or petrographic microscope with glass optics can be used in conjunction with this lamp for observing the luminescence of microspecimens.

2. LIuM-2 luminescent mineraloscope

The LIuM-2 luminescent mineraloscope (Fig.2) is intended for exciting the luminescence of minerals (scheelite, powellite, willemite, uranium minerals and others) by short wave ultraviolet (λ = 253.7 mμ).

Fig.2. LIuM-2 luminescent mineraloscope.

The ultraviolet source in the instrument is a PRK-4 quartz mercury tube operated in the glow discharge regime. Under glow discharge conditions this tube produces ultraviolet radiation rich in short wave ultraviolet. The 253.7 mμ resonance line of mercury accounts for 90% of the emitted radiation energy. The tube is supplied from an automobile ignition coil mounted inside the instrument case. The primary of the coil is connected to the 7 volt output of a step-down transformer supplied from the regular ac line (127 or 220 volt). The visible radiation of the PRK-4 lamp is absorbed by an UFS-1 light filter. This filter having a thickness of 2 mm passes approximately 50% of the radiation in the region of the 253.7 mμ mercury line.

The LIuM-2 instrument is suitable for mass luminescence analysis of minerals. It is particularly useful for luminescence analysis of concentrates, slimes and so on under a binocular magnifier. Grains of scheelite, zircon, willemite and other luminescent minerals can readily be detected and separated from the nonluminescent material.

3. "Polius" field luminoscope

The "Polius" field luminoscope (Fig.3) is intended for identification in the field of luminescent minerals (scheelite, powellite, zircon, uranium

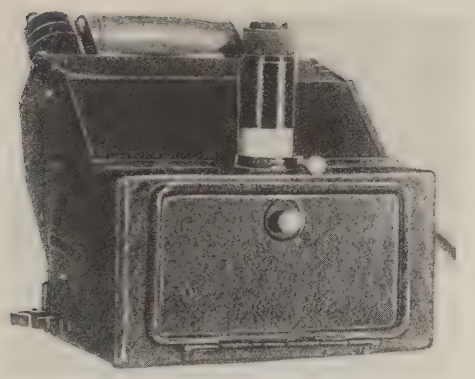

Fig.3. "Polius" field luminoscope.

minerals, etc.) that are excited by short wave ultraviolet (253.7 mμ) under field conditions. The ultraviolet source is a PRK-4 quartz mercury tube mounted at the focus of a parabolic aluminum reflector. The tube is operated at a voltage of about 10,000 v from an automobile ignition coil supplied from a 6 volt alkaline battery. An UFS-1 ultraviolet filter is used to absorb the visible radiation of the mercury tube. For the purpose of examination and determination of luminescent uranium minerals possessing characteristic line luminescence spectra the "Polius" instrument is equipped with a simple direct vision spectrometer. The "Polius" instrument is suitable for observing luminescing minerals in the dark, i.e., in underground workings or on the surface at night.

4. PLS-53 universal field luminoscope

The PLS-53 universal field luminoscope (Fig.4) is intended for quantitative determination of luminescent minerals excited by 360 mμ ultraviolet rays and 400-460 mμ visible light.

The sun is used as the source of ultraviolet (360 mμ) radiation, while the source of visible light (400-460 mμ) is the lamp of an MN-13 pocket flashlight supplied from a 4.6 v battery. Mainly uranium minerals luminesce under the influence of the visible blue radiation. A plate of blue FS-1 (ФС-1) glass is used as the light filter passing ultraviolet and blue rays.

The luminescent mineral is observed through an eyepiece. Two additional filters are provided for absorbing the visible rays passed by the FS-1 filter: one, an SZS-14 (СЗС-14) filter absorbing red rays, is mounted above the examined specimen while the other, a ZhS-16 (ЖС-16) filter absorbing violet light, is located in the eyepiece.

The availability of three light filters makes it possible to use the PLS-53 luminoscope for observing both strongly and weakly luminescing minerals with complete elimination of scattered visible light. The examined specimen is pressed against the base of the instrument.

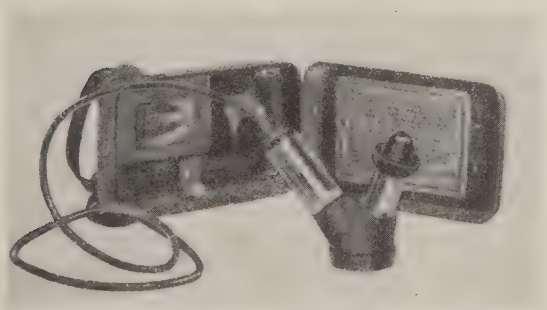

Fig.4. PLS-53 universal field luminoscope.

Fig.5. PLS-55 field uranoscope.

5. PLS-55 field uranoscope (experimental model)

The PLS-55 field uranoscope (Fig.5) is intended for qualitative determination of luminescent uranium minerals in the dark (i.e., underground or at night). The luminescence is excited by an MN-13 flashlight lamp supplied from a 4.6 v battery and mounted at the focus of a parabolic reflector or lens. A blue FS-1 filter is used to pass the 400-460 mμ blue rays exciting the luminescence of uranium minerals and cut off the other visible light. The luminescence is observed through special spectacles equipped with ZhS-16 light-filter lenses. The ZhS-16 filter absorbs the blue light scattered by the specimen and passes the yellow-green luminescence characteristic of uranium minerals.

B.Equipment for Quantitative Investigation of Luminescence

The LiuKS-1 luminescent colorimeter (Fig.6) is intended for quantitative determination of the content of luminescent material in solutions.

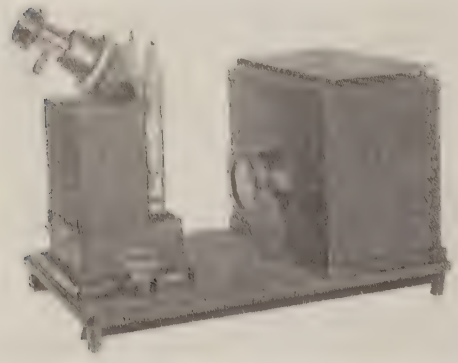

Fig.6. LIuKS-1 luminescent colorimeter.

The ultraviolet source in the instrument is a PRK-4 quartz mercury tube mounted in the housing of the instrument and operated in the arc discharge regime. The visible rays emitted by the tube are absorbed by an UFS-3 filter. The ultraviolet light (366 mμ) is concentrated by an uviol glass collector on the tubes containing the luminescent solutions: one tube contains the investigated solution, the other the reference or standard.

The luminescence is observed through the bottom of the tubes at right angles to the direction of the exciting ultraviolet rays. An image of the tube bottoms is formed in the field of view by an appropriate system of lenses and rectangular and rhomboidal prisms. The observer looking through the eyepiece sees a circle divided in half by the line of contact of the rhomboidal prisms. One half the field is illuminated by the investigated solution, the other half by the reference. The brightness of the half circles is equalized by means of three polaroid plates, one of which can be rotated. The position of the rotatable plate is indicated on a vernier dial.

The design of the instrument also provides for using a solid luminescent plate, approximating the luminescence of the investigated solution, instead of a standard solution as reference. This is desirable because often standard solutions deteriorate as a result of photochemical reactions. This allows of carrying out mass analyses without need for recalibrating the instrument.

The LIuKS-1 instrument should find wide application in the field of geological investigations, in prospecting for petroleum and natural gas, in quantitative determination of bitumens in solutions extracted from minerals, etc.

7. LIuF-51 luminescent photometer

The LIuF-51 luminescent photometer (Fig.7) is intended for qualitative determination of the uranium content in NaF beads under laboratory conditions by measuring the luminescence intensity of the beads.

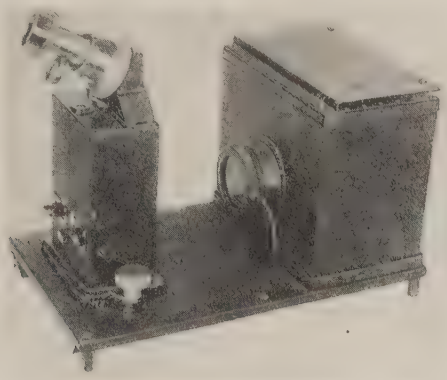

Fig.7. LIuF-51 luminescent photometer.

The ultraviolet source in the instrument is a PRK-4 quartz mercury tube supplied from the regular 127 or 220 v line through an appropriate coil and capacitor. The visible radiation emitted by the lamp is absorbed by an UFS-3 filter.

The ultraviolet rays passed by the UFS-3 filter are concentrated by a collecting lens and mirrors on the luminescent beads, one of which is the investigated bead, the other the reference one. An appropriate system of lenses and rhomboidal prisms forms an image of the beads in the field of the eyepiece. The optical axis of the instrument is deflected 60° by an equilateral prism. The observer looking through the eyepiece sees a circle divided in half by a line. One half the circle is illuminated by the investigated bead, the other by the comparison one. The brightness of the two half-fields of the photometer is equalized by means of three polaroid plates, one of which can be rotated about its axis. The angle of rotation of the polaroid at which the brightness of the field is equalized and the dividing line between the two half-fields disappears is indicated on a dial viewed through a magnifier. The instrument is calibrated by means of standard beads containing known amounts of uranium.

The sensitivity obtained with the LIuF-51 instrument is $5 \cdot 10^{-10}$ g uranium in a 5 mg bead. The accuracy of determination is about ±20%.

8. LFS-54 field luminescent photometer

Fig.8. LFS-54 field luminescent photometer.

The LFS-54 field luminescent photometer (Fig.8) is intended for qualitative determination of the uranium content in NaF beads under either laboratory or field conditions by measuring the luminescence intensity of the beads by visual photometry.

The UV source used for exciting the luminescence of the sodium fluoride beads is a miniature UFO-4A (УФО-4А) ultraviolet lamp. The lamp is supplied from a 24 v dc source and draws 0.35 amp current. The instrument can be operated either from a storage battery or from the regular ac line (127 or 220 v) through a step-down transformer and rectifier. The beads are illuminated by the UFO-4A lamp from below; they can also be illuminated by incident sunlight from above.

The LFS-54 photometer is equipped with an UFS-3 filter passing long ultraviolet (366 mμ)

and absorbing visible rays. The observer simultaneously views two beads: the standard and the investigated one. The investigated bead is placed in a recess in a dovetail slide. As in the LIuF-51 luminescent photometer the observer sees a circle, half of which pertains to the investigated bead and the other half to the reference bead. The brightness of the half-circles is equalized by means of three polaroid plates, one of which rotates about its axis with the angle of rotation being indicated on a vernier dial. The sensitivity and accuracy are equal to those of the LIuF-51 instrument.

9. FAS-1 photoelectric absorptiometer

The FAS-1 photoelectric absorptiometer (Fig.9) is intended for qualitative photometric determination of the content of metal ions in solutions on the basis of the luminescence and absorption in the ultraviolet and visible regions of the spectrum and for qualitative determination of the uranium content in NaF beads on the basis of the luminescence. The luminescence intensity and degree of absorption of solutions are measured by means of a FEU-19 photomultiplier equipped with an appropriate rectifier and voltage regulator.

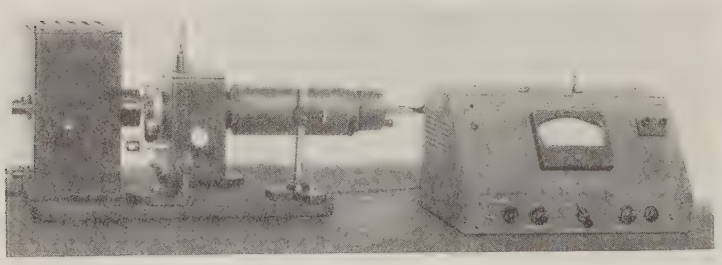

Fig.9. FAS-1 photoelectric absorptiometer.

The UV source in the instrument is an UFO-4A miniature lamp equipped with UFS-1 (250 mμ) and UFS-3 (366 mμ) ultraviolet filters. The long or short wave ultraviolet beam passes alternately through one of two cells; one cell is filled with the solvent, the other with the investigated solution. The instrument is calibrated beforehand with reference to standard solutions. The light passing through the cell (solution or solvent) falls on a luminescent screen made of silica glass containing uranium salts. The luminescence of the uranium glass is measured by the sensitive FEU-19 photomultiplier.

The FAS-1 instrument can be used for quantitative determinations of uranium, molybdenum, tantalum, niobium, titanium and other elements in solutions. An accesory unit is used in conjunction with the FAS-1 for qualitative determination of uranium in NaF beads.

C. Equipment for Investigating Luminescence Spectra of Minerals

10. LMS-1 luminescent microspectrometer (experimental model)

The LMS-1 luminescent microspectrometer (Fig.10) is intended for qualitative determinations of luminescent minerals in microscopic grains and comparison of their luminescence spectra with the spectra of standards.

The UV source in the LMS-1 instrument is a PRK-4 quartz mercury tube equipped with a collecting lens and UFS-3 filter. The instrument has two mirrors: the first directs the ultraviolet rays through a condenser to a standard, while the second illuminates the investigated microspecimen.

The optical system yields an image of the luminescent standard and the microspecimen at the dividing line of a Lummer cube. Half the hypotenuse of one of the prisms comprising the Lummer cube is silvered. A cylindrical lens together with the objective forms an image of the dividing line of the Lummer

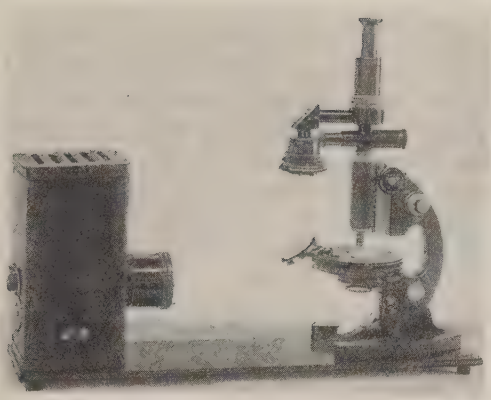

Fig.10. LMS-1 luminescent microspectrometer.

cube at infinity. The observer looking through the eyepiece of the direct vision spectroscope sees the two spectra, one above the other, separated by the fine dividing line. The upper spectrum pertains to the standard, the lower to the microspecimen.

If the investigated microcrystal has a mineralogical composition analogous to that of the standard, the two spectra seen in the field of view will be identical as regards the number and arrangement of the bands.

The LMS-1 instrument should prove useful in mineralogical laboratories for investigating uranium and other minerals.

All the described instruments are being employed in different scientific and industrial organizations for investigating the luminescence of both macroscopic and microscopic luminescent specimens. They are being used by geologists for qualitative and quantitative investigations of minerals and ores.

All-Union Scientific Research Geological Institute

References

1. E.M.Brumberg & Z.M.Sverdlov, Izv.AN SSSR, Ser.fiz., 4, 75 (1940).
2. V.G.Melkov & Z.M.Sverdlov, Doklady AN SSSR, 31, 4 (1941).
3. E.M.Brumberg, Z.M.Sverdlov & T.V.Timofeeva, Izv.AN SSSR, Ser.fiz., 13, 242 (1948).
4. Z.M.Sverdlov, Razvedka nedr (Mineral Prospecting), No.3, 33 (1952).

DISCUSSION

K.V.Tagantsev: Is the photoelectric absorptiometer being produced commercially?

E.M.Sverdlov: The "Geologorazvedka" Plant should bring out two production type models this year; batch production is planned for next year. The Ministry of Geology has agreed to provide a limited number of instruments to meet the current requirements of organizations and other ministries. In the future, if there is a greater demand for the instruments, they will have to be manufactured in the plants of the Ministry of Instrument Manufacture.

K.V.Tagantsev: What is the approximate cost of the absorptiometer?

Z.M.Sverdlov: I think it will be under 5000 rubles initially.

Question: Why can't a universal photometer be used for investigating luminescence?

Z.M.Sverdlov: The Pulfrich type photometer has a serious shortcoming that you are undoubtedly aware of: this photometer employs a cat's eye, in view of which the observer's eye must always be kept in exactly the same position. The accuracy provided by this instrument is insufficient particularly when used by an inexperienced observer. Moreover, Pulfrich photometers are not available. We are in the process of developing simple instruments for general use.

Question: What are the possibilities of using luminescence procedures for investigating microsections? To what extent are ultraviolet rays passed by the optical components of microscopes - lenses, nicols and polarizers - and of course mineral sections?

Z.M.Sverdlov: As for use of a luminescent microscope for investigating sections, here the limitations are connected with the technique used in preparing the sections. Generally microscope optics are transparent to long wave ultraviolet, but it is important to mount these sections by means of a nonluminescent cement. Canada balsam, which is usually used for mounting, luminesces. As for short wave ultraviolet, polarizing microscopes in their present form are unsuitable for this purpose because they do not transmit the far ultraviolet.

Question: Suppose the immersion technique is used instead of mounting the sections with Canada balsam?

Z.M.Sverdlov: Immersion microsections can be investigated in the long wave ultraviolet. At present the electric engineering industry at our request is putting into production an ultraviolet source, designated as the SVDSh-100 (СВДШ-100) lamp. This is a very small and bright point source yielding both long and short wave ultraviolet, including the mercury resonance line (the SVDSh-250 lamp has been in production for some time but it does not give the resonance line because of self-reversal). In the near future we plan to bring out an attachment unit based on this lamp by means of which it will be possible to investigate the luminescence excited by both long wave and short wave ultraviolet.

EQUIPMENT FOR ULTRAVIOLET IRRADIATION OF LUMINESCENT COATINGS AND MATERIALS

- N.V.Gorbachev

In recent years the All-Union Scientific Research Institute of Light Engineering (VNISI) developed and produced in limited quantities a number of new designs of ultraviolet sources employing quartz mercury tubes and fluorescent lamps of a special type*. These sources are intended for work with luminescent paints and materials and also for the purposes of luminescence materiology and analysis.

A photograph of the UV source designated PUF-2 (ПУФ-2) is reproduced in Fig.1. It employs a PRK-2 (ПРК-2) mercury tube rated at 375 watts. The unit has a metallic housing 155 mm in diameter and 400 mm in length, a cylindrical uviol glass UFS-3 (УФС-3) filter and a stand. The unit is supplied with a transformer coil for connection to a regular 220 v ac supply line. The design eliminates extraneous light leakage and provides for natural ventilation. The light opening of the source can be varied over a wide range by means of a metallic shutter. The tube housing can be positioned on the stand in either the vertical or horizontal position. The lamp unit weighs 2.5 kg, the stand 5 kg and the transformer unit 6.25 kg.

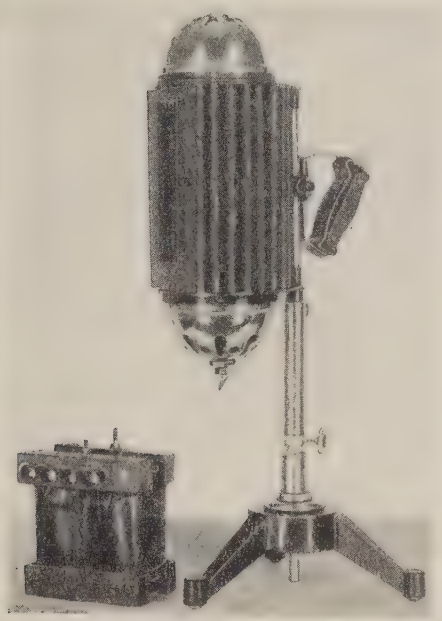

Fig.1. VNISI PUF-2 ultraviolet source with stand and power pack.

The intensity of the PUF-2 is 100-120 $\mu w\ cm^{-2}$; this intensity is sufficient to excite a luminance of 510 asb of the FK-112 crystal phosphor. The unit stands up well under continuous operation under different conditions and is used for "lighting" fluorescent pictures and signs of fairly large size.

In cases when a lower ultraviolet intensity is required, for example, in luminescence materiology and analysis, "lighting" relatively small fluorescent signs and so one, it is more expedient to use sources with 15 watt fluorescent tubes coated with the L-33 crystal phosphor[1]. The use of such fluorescent lamps instead of powerful mercury discharge lamps cuts down the power consumption, lowers the operating temperature and generally facilitates operation (for example, makes it possible to reignite the lamps without waiting for them to cool).

At the request of the USSR Academy of Sciences, the VNISI developed two new ultraviolet fluorescent lamp units: a table model and a suspended type.

The PUF-5 table unit (Fig.2) contains three 15 watt fluorescent lamps of the usual size coated with L-33 phosphor. The unit is operated from a 127 volt line. The overall height of the unit is 430 mm, the length of the lamp housing is 485 mm; the base measures 240 x 200 x 70 mm. The unit weighs 9.5 kg.

The starters, transformers and one common push-button switch controlling

---

*Engineers P.S.Evdokishkin, L.A.Bogoliubov and the late N.D.Fedotov participated in the development of the equipment.

Fig.2. A VNISI PUF-5 ultraviolet source; table model with three 15 watt fluorescent lamps.

all three lamps are mounted in the cast silicon-aluminum base. The lamp housing arms are double-hinged so that the housing can be raised or lowered and turned through an angle of 90°. The unit has a diffusing reflector; the light opening measures 385 x 140 mm and is covered with a pane of UFS-3 black uviol glass.

The intensity of the ultraviolet radiation at 300 mm from the lamps is 220 μw cm^{-2}; the lighting is fairly uniform, i.e., the ratio $I_{min}:I_{max}$ over an area 500 x 600 mm does not exceed 1:3.

The suspended unit - designated PUF-6 - also has three 15 watt fluorescent tubes, a black uviol glass filter and a reflector and in addition 3 starters. The transformer is housed in the ceiling fitting which can also be mounted on a wall by means of special brackets. The design of this suspended unit is shown in Fig.3.

The VNISI also developed for special work with fluorescent coatings and for luminescence analysis under field conditions a portable ultraviolet source - PUF-7 (ПУФ-7) - employing the special type UFO-4A (УФО-4А) fluorescent lamp[2]. This unit is designed for operation on 24 v direct current supplied

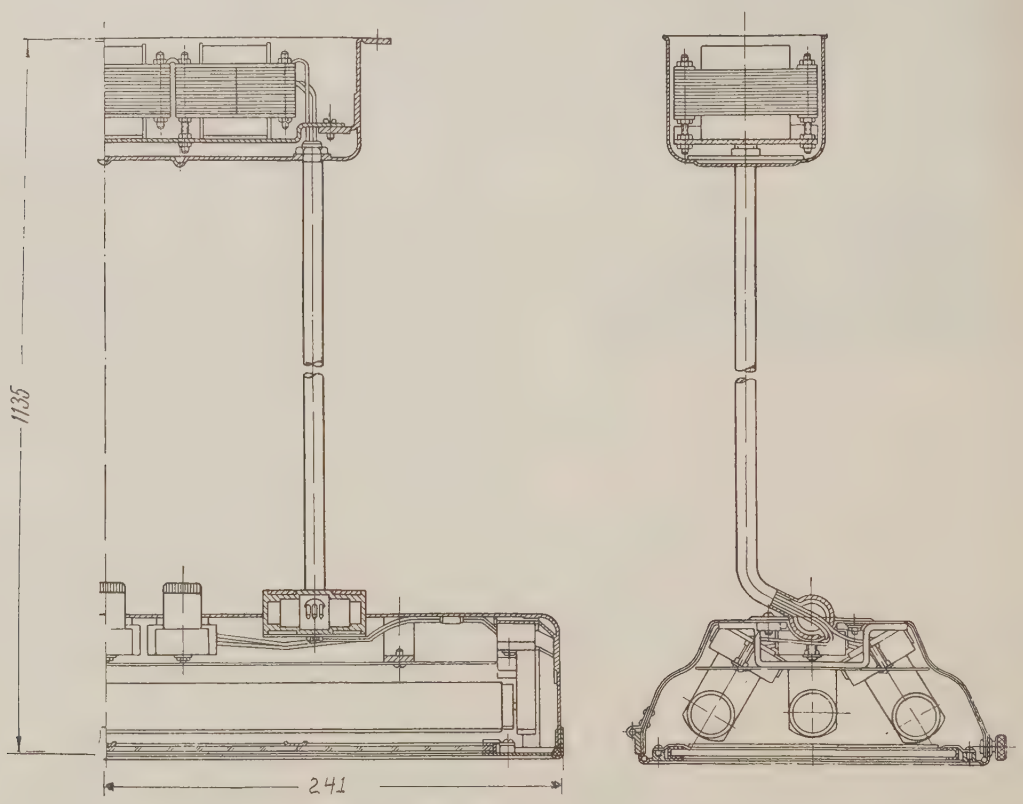

Fig.3. A VNISI PUF-6 ultraviolet source; ceiling or wall unit with three 15 watt fluorescent lamps.

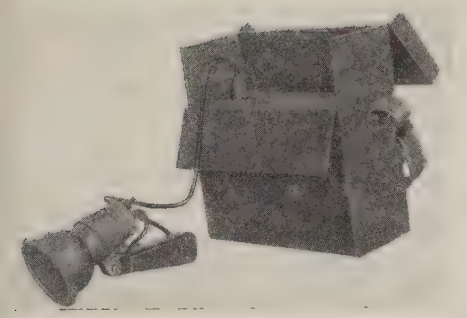

Fig.4. VNISI PUF-7 portable ultraviolet source with battery pack.

either from storage batteries or a pack of IKS-V-3 dry cells (1.6 v, 3 amp·hours). The rated current drawn by the UFO-4A lamp is 0.35 amp. The battery pack providing for rated operation of the lamp for 3 hours measures 80 x 180 x 150 mm and weighs 1.5 kg together with its case. A photograph of the source with the battery pack is shown in Fig.4. The dimensions of the unit are the following: length 126 mm, height together with handle 182 mm, diameter of reflector with rim 80 mm. The weight of the unit with cable is 0.4 kg.

The intensity of the ultraviolet radiation provided by the PUF-7 source at a distance of 30 cm in the axial direction is about 8 $\mu w\ cm^{-2}$; this is sufficient to provide a luminance of zinc sulfide luminous coatings of 10 asb. The unit has been used under field conditions by a Moscow State University prospecting expedition.

In conclusion it must be noted that the ultraviolet sources now being produced do not satisfy the varied requirements of different users working in diverse fields of technology; appropriate measures should be taken to stimulate the development and improvement of ultraviolet lighting equipment. Fluorescent paints and luminescent materials can come into general use in industry, decorative art, the motion pictures and the theatre only when we have organized production of relatively inexpensive and technically adequate ultraviolet radiation sources.

All-Union Scientific Research Institute of Light Engineering

References

1. N.V.Gorbachev, Izv.AN SSSR, Ser.fiz., 15, 846 (1951).
2. Sb.Samoletnye svetovye pribory i elektroustanovochnaia apparatura (Collection of articles on Aircraft Light Instruments and Electrical Equipment), TsBTI MEP, 1955.

DISCUSSION

F.I.Vergunas: What is the desk unit you described called and where can it be acquired?

N.V.Gorbachev: The source is called the PUF-5. It is being produced in small batches by the All-Union Institute of Light Engineering under the Ministry of the Electrical Engineering Industry. As I noted, similar units are being produced for ceiling or wall mounting. They differ from the desk source only as regards location of the transformers.

V.L.Levshin: I think that we can support the suggestion of N.V.Gorbachev that production of this equipment should be encouraged.

USE OF SCINTILLATION COUNTERS IN RADIOMETRIC EQUIPMENT FOR PROSPECTING FOR RADIOACTIVE ORE DEPOSITS

- A.L. Iakubovich

Among the great number of useful minerals that have drawn the attention of men during the past 15-20 years uranium occupies a prominent position. Geological exploration and prospecting for uranium ores, undertaken on a mass scale in different parts of the world, have led to the discovery of a large number of uranium deposits. It can safely be asserted that this stupendous task could not be accomplished without recourse to the procedures of radiometry, based on the detection of the radioactive emission of uranium and its decay products. For the purpose of search for radioactive ore deposits there have been developed and put into production in the Soviet Union in the post-war years various radiometric instruments. Until recently this equipment was based primarily on the ionization principle in the sense that the devices used in the equipment for detecting α-, β- and γ-radiations were either ionization chambers or charged particle and γ-counters.

The most extensive use in practice was made of γ-radiometers employing gas-filled counters with an independent discharge, commonly known as Geiger-Muller counters. It must be noted, however, that in view of a number of shortcomings inherent in counters of this type, γ-measuring equipment based on them does not satisfy the increasingly exacting requirements of prospecting and mineralogical exploration.

One of the principal shortcomings of ionization counters is their low efficiency as regards detection of γ-rays which does not exceed 1-1.5% for gammas in the energy range of interest (to 3 Mev). At the same time these counters have a high (virtually 100%) efficiency as regards detection of charged cosmic particles which, of course, makes for a high cosmic ray background in such counters. Another drawback of gas-filled counters is their relatively low resolving power due to the long dead time. Finally, these counters are not particularly suitable for evaluating the energy of the incident γ-rays.

The above considerations explain why in attempting to develop new radiometric equipment we turned to the principle of scintillation detection of radioactive radiations, a principle which after almost 20 years of neglect was revived on the basis of new techniques in post-war nuclear experimental physics.

Despite the paucity of suitable phosphors and the even more limited choice of photomultiplier tubes available at that time we succeeded in 1951 in constructing the first domestic prototype of a prospecting instrument with a scintillation counter in the form of a naphthalene-anthracene crystal, kindly grown for us by the Institute of Crystallography of the Academy of Sciences, and an FEU-19 photomultiplier.

In the course of modernizing the design and construction of this equipment, in 1952 we built a laboratory analyzing scintillation set-up (designated LAU-52) intended for rapid quantitative determinations of the radioactivity of powdered specimens by analysis of their α-, β- and γ-radiations.

The set-up consists of three alternately connected in detector-analyzer units for α-, β- and γ-radiation, a control cabinet housing the amplifier and recording circuits and a rectifier and power supply unit. The γ-radiation detector-analyzer in the set-up is a scintillation counter comprised of a NaI:Tl phosphor crystal, grown for us in the laboratory of L.M. Shamovskii, and a FEU-19 or S (C) type (the latter designed by N.S. Khlebnikov) photomultiplier.

The α-radiation detector-analyzer is designed about a scintillation counter with a zinc sulfide luminescent screen having a thickness of about 4-5 mg/cm^2.

Where analysis for β-rays is concerned, it proved expedient to use an independent discharge type ionization counter; counters of this type have virtually 100% efficiency as regards detecting β-particles of energies above 200 kev. An important consideration here is that by virtue of their low sensitivity to γ-rays these counters have a low background due to the accompanying γ-radiation.

In addition to the radiation detectors the set-up comprises a linear pulse amplifier with a wide dynamic range, a single channel pulse height analyzer with a variable level and gate, a decade scaling circuit with a 1:100 ratio and a registering device sunchronized with an electric time recording system.

At present a commercial model of this apparatus is in production under the designation LAS (JIAC). In designing this commercial unit we took into account the power supply conditions likely to be encountered in remote and rural areas: the allowable supply line variations are ±20% as regards voltage and ±5% as regards frequency.

In order to illustrate the potentialities of the apparatus I take the liberty of citing some of its metric characteristics.

1. The efficiency of detecting γ-radiation from a radium source is about 70%, i.e., almost two orders of magnitude higher than the efficiency in detecting γ-radiation by means of other extant measuring equipment based on gas-filled photon counters.

2. The minimal concentration of equilibrium uranium in a 100 g specimen that can be determined with certainty on the basis of the γ-radiation by means of the apparatus during a 3 minute period of observation is $15 \cdot 10^{-5}$% as compared with the concentration of $2\text{-}3 \cdot 10^{-2}$% detectable by equipment based on gas-filled counters.

3. By virtue of the high statistical accuracy of the observations it is feasible to reduce substantially the time necessary for each measurement; thus, for example, in radiometric analyses on the basis for γ-rays of ores containing some hundredths of a percent of uranium, i.e., with a uranium content that can already be measured by extant ionization γ-measuring equipment, requires only about one hundredth the time necessary for attaining an equal accuracy with conventional ionization equipment.

4. By combined measurement with reference to β- and γ-rays the apparatus can be used for analysis of uranium ores in which the radioactive equilibrium between the uranium and radium has been disturbed (this applies to ores with a uranium concentration from a few ten thousandths of a percent).

5. By taking advantage of the difference between the γ-spectra of the decay products of the uranium and thorium series one can make separate determinations of uranium and thorium in mixed specimens. Such determinations are based on analysis of the distribution in height of the output pulses of the scintillation γ-counter and are practical for specimens with concentrations from $5\text{-}7 \cdot 10^{-3}$% uranium (or thorium) without preliminary chemical treatment of the assay sample. The time required for analysis of a 100 g sample does not exceed 10-15 min.

6. Where measurements with reference to the α-emission are concerned the set-up insures a recording efficiency close to 100%.

7. For the purpose of determining the energy of the α-particles by measuring their range in air the α-unit has provision for stepless variation of the distance between the emitting surface of the sample and the luminescent

screen over a range from 1 to 110 mm.

The above metric characteristics of the LAU-52 apparatus were obtained in the course of the first investigations of the prototype set-up and obviously are not an exhaustive listing of its potentialities; we feel, however, that they convincingly demonstrate the necessity of wider use of the scintillation principle for detecting radioactive radiations, particularly γ-radiation, in prospecting equipment.

In 1953 we developed a highly sensitive quick-acting instrument with automatic recording, based on scintillation γ-counters and intended for searching for uranium deposits from an airplane. Aircraft reconnaissance based on continuous recording of the γ-field over the earth surface at the practicable flight altitude involves a number of specific difficulties connected with the measurement of low γ-radiation intensities at an appreciable distance from the emitting deposits and with the instrument in rapid motion. Aerial γ-measuring equipment based on gas-filled counters, used hitherto, having a relatively low sensitivity (frequently comparable to the cosmic ray background) and a relatively slow response limits the possibilities of accurate recording of minor variations in the intensity of the γ-field over the flight path. In designing aerial γ-measuring equipment employing scintillation counters, in addition to the usual requirements applicable to all scintillometers, we have the additional requirement of providing a large "sensing volume" of the γ-detector, i.e., a large effective crystal volume.

At the time we were limited as regards the availability of suitable phosphors and hence were forced to use NaI:Tl crystals of relatively small size; there were mounted in a mosaic assembly in a single light pipe. The light pipe was a truncated cone of optical plexiglass. Seven cylindrical NaI:Tl crystals each 40 mm in diameter and 50 mm long (the crystals were grown in the laboratory of L.M.Shamovskii) were mounted flush with the large base of the cone while the small base of the cone was viewed by a B type photomultiplier (designed by N.S.Khlebnikov). The detector analyzer unit of this aerial γ-radiometer comprises three similar scintillation counters connected in parallel. The pulses originating at different instants in the scintillation counters are amplified by a linear amplifier and their average number per unit time, characterizing the total γ-activity, is continuously recorded in the automatic registering unit of the first search channel of the instrument.

At the same time the recorder of the second, so-called separating channel of the instrument, makes a continuous record of the hard component of the γ-field due primarily to γ-radiation from the decay products of thorium. The magnitude of this component is determined by the average frequency of pulses at the output of the pulse height discriminator which has a high discrimination level. The ratio of the indications of the first and second channels characterizes the spectral composition of the γ-field and thus indicates the nature of the activity of the deposits in the surveyed area.

Equipment based on this design is now being produced by the "Geologorazvedka" Plant in the form of a four channel type ASG-38 (АСГ-38) aero-geophysical set. The additional two channels of the set measure and record the variation in the magnetic field of the earth and the absolute flight altitude of the aircraft.

Before concluding I would like to say a few words regarding the metric characteristics and operational possibilities of the ASG-38 aerial γ-radiometer.

1. As regards its overall sensitivity the equipment is 2.5 times as sensitive as the latest aerial γ-survey instruments based on 72 gas-filled photon counters. With a counting rate of 160 pulses/sec per 1 μ hour the

instrument has a threshold of reliable registration of 0.25 μ hour with the time constant of the integrating circuit equal to 1.8 sec.

2. In view of the high efficiency of the instrument as regards detection of γ-radiation from natural radioactive elements, the equipment is characterized by a very favorable ratio of the measured radiation to the cosmic ray background, which naturally enhances the accuracy of recording the γ-field as compared with earlier instruments.

3. In the case of an anomalous rise of the γ-activity of the emitting area in the amount of only 2-3 μ hour, one can evaluate the spectral composition of the γ-radiation which facilitates distinguishing the areas in question as regards their activity. It should be emphasized that the purpose is not to distinguish from the air deposits of uranium from desposits of thorium but primarily to eliminate the large number of areas characterized by an anomalously high γ-activity due to a high concentration of scattered thorium minerals.

The high sensitivity and low residual background of the instrument together with the directional sensitivity achieved in the design of the γ-radiation detectors materially increased the efficiency of aerial prospecting for uranium ores.

I will not describe here other scintillation prospecting equipment developed by us, such as the compact automatic recording field γ-radiometer for use in continuous motion (i.e., in moving vehicles) or the field scintillation analyzer for preliminary analysis of the radioactivity of minerals, particularly since they do not differ in principle from the equipment I have described.

A very important attribute of scintillation γ-detecting prospecting equipment is its spectral response, that is, the dependence of the efficiency on the energy of the incident γ-rays. The thing is that γ-radiometers employing gas-filled counters react primarily to the hard γ-radiation from the decay product of radium and virtually do not detect the soft γ-radiation from the decay products of uranium. Hence in surveying with such radiometers one can miss very interesting uranium deposits if the radioactive equilibrium in them is shifted to the side of radium deficiency. The enhanced sensitivity of scintillation counters to low energy gammas makes it possible to use scintillation equipment both in prospecting for nonequilibrium ores and for locating a uranium deposits from their scattered emanations.

It is impossible in the brief space of this report to give a complete picture of the work carried out by us in the field of utilization of the scintillation principle of detecting radioactive radiations for the purposes of prospecting radiometry. We hope that it will be clear, however, from what we have said to what an appreciable extent application of this principle makes it possible to enhance the efficiency of radiometric equipment and thus make prospecting for radioactive ores more effective.

To provide a basis for even wider use of scintillation counters in exploratory and prospecting geophysics we would like to call the attention of scientists concerned with the problem of scintillators to the following matters:

1) We are in need of phosphors in the form of activated alkali halide crystals having a high light output, a large volume and high spectroscopic qualities.

2) An important requirement for crystal phosphors, where we are concerned, is minimal thermoquenching of the luminescence.

3) For purposes of field operation we would like to have phosphors not impaired by contact with air.

4) To allow development of compact and convenient radiometric equipment we need phosphors characterized by an efficiency and emission spectrum that would make it feasible to utilize them in conjunction with gas-filled light photon counters.

5) We need high efficiency liquid and plastic scintillators that could be used in the design of reliable aerial γ-detecting prospecting equipment with a large "sensing volume" of the γ-radiation detector;

6) To permit wider utilization of the methods of α-spectroscopy, we need serviceable and high-efficiency phosphors characterized by a linear relationship between the light output and the absorbed energy for α-particles of energies from 0.5 Mev.

Solution of these problems, that is, development of such crystal phosphors will undoubtedly lead to even wider use of scintillation radiometric equipment and radiometric geophysical methods in prospecting for both radioactive ores and many other useful mineral deposits.

All-Union Institute of Mineral Raw Materials

BULLETIN of the Academy of Sciences of the USSR - Physical Series
Vol.21, No.4 - Transactions of the Fifth Conference on Luminescence
(Crystal Phosphors)

TABLE OF CONTENTS

	Page Orig.	Trans.
Opening address - V.L.Levshin	475	475
Certain characteristics of sublimate phosphors and methods of preparing them (A) - F.D.Klement	483	482
New results in the field of phosphorescence research - V.V.Antonov-Romanovskii	484	483
On the possibility of two-stage excitation of photosemiconductor effects - N.A.Tolstoi & A.V.Shatilov	494	493
Flash luminescence of zinc sulfide phosphors - N.A.Tolstoi, A.M.Tkachuk, N.N.Tkachuk & Z.S.Mansurova	495	494
On the luminescence of ZnS:Mn phosphors under excitation (A) - V.L.Levshin, N.S.Borodin & G.P.Neronova	499	499
On the phosphorescence decay law for crystal phosphors (A) - G.M.Eliashberg	502	501
New procedures for investigating relaxation processes and trapping centers in crystal phosphors (A) - Ch.B.Lushchik	504	502
Afterglow of the Eu^{3+} ion in thorium oxide phosphors (A) - M.V.Fok	505	504
Decay law for zinc sulfide phosphors in and near the thermoquenching region (A) - F.I.Vergunas	507	506
Luminescence decay of ZnS:Cu and ZnS:Cu:Co phosphors near and in the thermoquenching region (A) - N.L.Gasting	508	507
Investigation of the decay of ZnS:Mn and ZnS:Cu:Fe phosphors in the region of thermoquenching of the luminescence (A) - V.V.Nuvar'eva	510	508
Investigation of electron trapping levels in ZnS:Cu phosphor - Iu.L.Lukantsever & L.R.Krasovskaia	511	509
Kinetics of the infrared luminescence of cuprous oxide (A) - N.A.Tolstoi, N.N.Tkachuk & R.K.Preobrazhenskii	521	519
Semiconductor processes in organic dye layers (A) - A.T.Vartanian	523	521
Influence of adsorption of gases on the luminescence of zinc oxide (A) - K.V.Tagantsev & A.N.Terenin	525	523
On candoluminescence of crystal phosphors (A) - V.A.Sokolov	528	525

	Page Orig.	Trans.
Luminescence of some "pure" salts - V.A.Arkhangel'skaia & P.P.Feofilov	530	528
Line luminescence near the principal absorption edge of crystals (A) - A.A.Kaplianskii	531	529
Luminescence of silver halide salts - S.I.Golub	534	531
On effects observed in alkali halide phosphors under the influence of intermittent light (A) - I.A.Parfianovich	536	533
On the quenching of ZnS:Cu:CO and ZnS:Cu:Ni phosphors by infrared light (A) - L.A.Vinokurov & M.V.Fok	538	535
Variation of the luminescence efficiency of ZnS:Cu with the wavelength of the exciting light (A) - M.N.Alentsev	539	536
Sensitivity of "fluorescent lamp" luminophors to short ultraviolet - F.A.Butaeva & V.A.Fabrikant	541	537
Spectral distribution and absolute value of the photoluminescence output of thallium-activated alkali iodides (A) - Z.L.Morgenshtern	544	540
On calculation of the luminescence spectra of crystal phosphors (A) - N.D.Potekhina	545	541
Influence of infrared radiation on the luminescence of zinc sulfide phosphors (A) - K.K.Rebane	546	542
Effect of activator concentration on the γ- and photoluminescence efficiencies of thallium-activated alkali iodides (A) - L.M.Beliaev, M.D.Galanin, Z.L.Morgenshtern & Z.A.Chizhikova	548	544
Kinetics of γ-scintillation in Tl-activated sodium iodide crystals (A) - I.K.Pliavin'	549	545
Atomic absorption and luminescence centers in alkali halide phosphors activated with heavy metal ions and their formation under the influence of hard radiation (A) - M.L.Kats	550	546
Influence of x-rays on the absorption and emission of Sn-activated alkali halide phosphors (A) - A.S.Andrianov & M.L.Kats	552	547
On the mechanism of selective absorption of the activator in KCl:Ag phosphors (A) - M.L.Kats & V.K.Nikol'skii	553	548
Luminescence of different types of luminophors under excitation by short pulses (A) - A.A.Bundel', M.F.Popov & Iu.A.Chizhunova	555	549
Surface-activated phosphors - L.M.Shamovskii & Iu.N.Zhvanko	557	551
Luminescence and distribution of trapping levels in alkali halide crystals with excess halide - M.N.D'iachenko	570	565

	Page Orig.	Trans.
Visible luminescence of subtactively colored rock salt crystals at different temperatures - D.M.Eremin	580	573
Photochemical transformations of color centers in heated alkali halide crystals (A) - A.A.Shatalov	587	580
Influence of polarized light on color centers in alkali halide crystals (A) - O.A.Shmit	588	581
Thermal ionization energy of traps in alkali halide phosphors (A) - I.A.Parfianovich	589	582
Luminescence lifetime of color centers in ionic crystals (A) - A.M.Bonch-Bruevich, G.A.Tishchenko & P.P.Feofilov	590	583
On the stability of F-centers in NaCl:Ni phosphors (A) - E.I.Shuraleva	591	584
Luminescence of color centers in CsI:Tl crystals (A) - Z.L.Morgenshtern & I.P.Shchukin	593	586
Ultrataumeter - N.A.Tolstoi, A.M.Tkachuk & N.N.Tkachuk	595	588
Persistent luminescent coatings activated by artificial β-active isotopes - V.L.Levshin, E.I.Panasiuk & L.A.Pakhomycheva	612	606
Procedures and instruments for measuring luminescence - D.A.Shklover & R.S.Ioffe	619	613
Equipment for investigating the luminescence of crystal phosphors - Z.M.Sverdlov	623	617
Equipment for ultraviolet irradiation of luminescent coatings and materials - N.V.Gorbachev	632	625
Use of scintillation counters in radiometric equipment for prospecting for radioactive ore deposits - A.L.Iakubovich	636	628

A = Abstract. We give complete translations of the abstracts as they appear in the Russian journal. (Trans. Editor's Note)

Translated in 1958 by
Columbia Technical Translations
5 Vermont Ave., White Plains, N.Y.

Advertisement

The

Transactions of the Fourth Conference on Luminescence

(Molecular Luminescence and Luminescence Analysis)

appeared in Vol. 20, Nos. 4 and 5 of the Bulletin.

Copies of these issues are still available at $20 each.

5 VERMONT AVENUE
WHITE PLAINS, N. Y.

TRANSACTIONS OF THE FIFTH CONFERENCE ON LUMINESCENCE

(Crystal Phosphors)

(Continued from Vol.21, No.4)

STIMULATION AND QUENCHING OF PHOTOCONDUCTION IN CADMIUM SULFIDE

- B.T.Kolomiets

The fact that there is a phenomenological similarity between luminescence and photoconduction, first surmised years ago, is now finding increasing experimental verification. Thus, for example, the manifold investigation of the kinetics of photoconduction carried out on a large number of semiconductors by Tolstoi and Feofilov[1] showed the existence of undoubted correlation between the steady-state and relaxation attributes of photoconductivity, on the one hand, and luminescence, on the other.

Bearing in mind the phenomenological similarity of the effects of luminescence and photoconduction, we carried out research directed at elucidating the role of impurities in the photoconductivity of semiconductors. The first data on the participation of the impurities in the photoconduction mechanism, analogous to the role played by impurities in the emission of most crystal phosphors, were obtained for indium selenide[2]. Subsequently, we carried out similar investigations of the sulfides and selenides and tellurides of a number of metals. In these investigations it was established that the introduction of elements of group VI to the periodic table may yield diverse effects analogous to those observed incident to the introduction of impurities into crystal phosphors[3].

In the first part of this report we shall present data pertaining to an investigation of the photoelectric properties of cadmium sulfide powder carried out in 1951-2 as a continuation of our research into the role of impurities in the mechanism of photoconductivity.

Cadmium sulfide, long familiar as a crystal phosphor, is of particular interest from our standpoint in that its single crystals are known to evince photoconduction. At present this material is used for fabricating photoresistors for the visible and ultraviolet regions of the spectrum as well as for work with γ- and x-rays. To illustrate the pronounced photoelectric properties of cadmium sulfide we need only note that the sensitivity in the visible region of the spectrum of commercial photoresistors employing CdS is $3 \cdot 10^4$ times higher than the sensitivity of conventional cesium antimony phototubes.

Initially cadmium sulfide drew our interest as a subject for investigation because of the conflicting data reported by Goos[4] and Frerichs[5] for this material. Goos investigating the photoelectric properties of cadmium sulfide powder failed to detect any noticeable photoconductivity, while Frerichs working with the same substance in the form of single crystals reported that CdS has exceptionally high photoelectric attributes. We discovered the reason for this disagreement and found a way of imparting photoelectric properties, approximately equal to those of single crystals, to powdered cadmium sulfide[6]. Among the several differences between the two forms of CdS is the difference in the spectral distribution of the internal photoeffect illustrated in Fig.1. It was found, however, that this difference is due primarily to a difference in light scattering; this was determined by measuring the spectral sensitivity of specimens obtained by grinding up the cadmium sulfide single crystals.

The second stage of our work with cadmium sulfide was investigation of the effect of impurities on its photoelectric characteristics.

The fact that impurities play an active role in determining the character of the spectral distribution of photoconductivity in CdS was established by Goos, who discovered a supplementary sensitivity maximum in cadmium sulfide activated with copper[4]. Later the influence of copper and silver on the

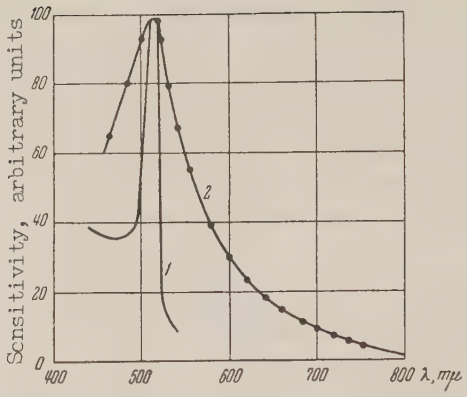

Fig.1. Spectral distribution of the internal photoeffect in cadmium sulfide: 1) single crystals, 2) powder.

photoconductivity of cadmium sulfide in the form of layers and single crystals was described by Goercke[7] and Veith[8].

Our investigations, which were apparently contemporary with those of Goercke and Veith, were carried out on powdery cadmium sulfide. In the present report we shall restrict ourselves to a brief description of the results obtained with copper as the impurity. We merely note that generally silver has an analogous effect.

Concentrations of copper (the activator) ranging from 10^{-6} to 10^{-3} g per gram cadmium sulfide were introduced in the conventional manner for crystal phosphors. The conductivity and photoconductivity measurements were made on discs compressed of the powder with appropriately applied electrodes.

Our experiments showed that the introduction of copper produces substantial changes in the spectral distribution of the internal photoelectric effect. Beginning with very low copper concentrations there is observed an increase in sensitivity in the long wave region and with increasing activator concentration a peak in the vicinity of 600 mμ develops in the spectral curve. At a copper concentration of the order of $7 \cdot 10^{-5}$ g/g the spectral curve has two equal maxima at 515 and 600 mμ. Further increase in the copper content leads to weakening of the principal (515 mμ) sensitivity peak and finally at a certain high copper concentration this peak disappears entirely. These results are illustrated in Fig.2.

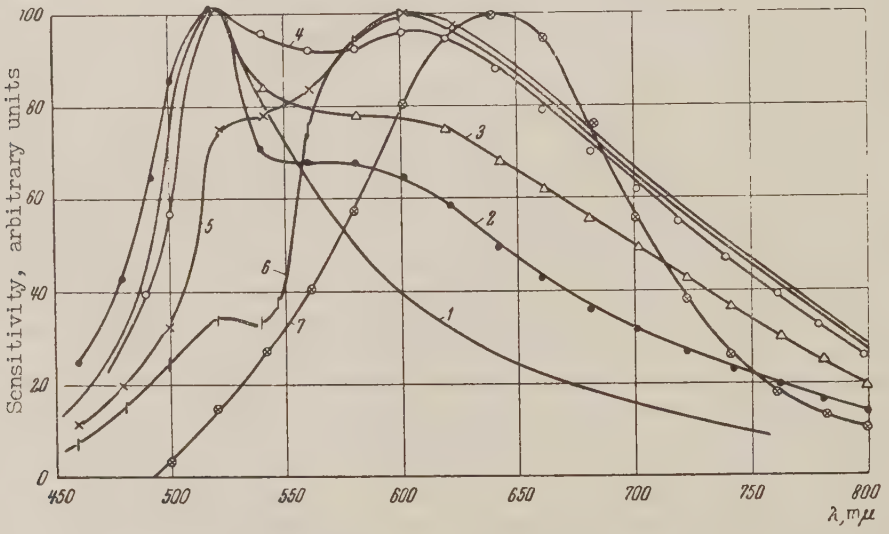

Fig.2. Spectral distribution of the internal photoeffect in cadmium sulfide with different concentrations of copper: 1) pure CdS, 2) $1.0 \cdot 10^{-5}$, 3) $2.5 \cdot 10^{-5}$, 4) $5.0 \cdot 10^{-5}$, 5) $1.0 \cdot 10^{-4}$, 6) $5.0 \cdot 10^{-4}$, 7) $1.0 \cdot 10^{-3}$g Cu per gram CdS.

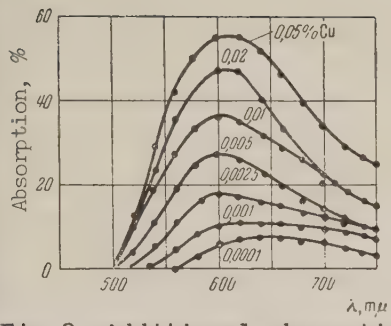

Fig.3. Additional absorption in CdS produced by the introduction of copper and its variation with the Cu concentration.

They are in qualitative agreement with the data of Goercke and Veith.

Investigation of the optical properties of cadmium sulfide activated with copper showed that simultaneously with the appearance of the new supplementary photoconductivity maximum, an additional band appears in the absorption spectrum with a peak at the same wavelength as the photoeffect maximum. The final results obtained by means of a GOI recording spectrophotometer are shown in Fig.3.* As may be seen from the figure the intensity of absorption in the band associated with copper increases with increasing Cu concentration, which is in accord with the variation of the spectral sensitivity.

Cadmium sulfide activated with copper luminesces intensely in the red and infrared regions of the spectrum (excitation by 365 and 546 mμ light). With increasing concentration the long wave luminescence tends to predominate.

Thus the above described strong dependence of the spectral distribution of the internal photoeffect on the amount of impurity (activator) present gives us another phenomenological similarity of photoconductivity with luminescence. Where photoconductivity is concerned, this result is of interest because in the described case we have obtained for the first time the possibility of controlling its spectral distribution, i.e., obtaining for photoconduction what has long been available for luminescence.

If there exists a similarity between luminescence and photoconduction a phenomenological similarity not only as regards the kinetics of electron transitions but also where other characteristic properties are concerned, one may also naturally expect qualitative agreement as regards quenching of luminescence and photoconduction. In the following paragraphs we shall briefly summarize the results of a number of experiments on quenching of photoconductivity in powdered cadmium sulfide carried out in 1955-6. By way of quenching agents we used the familiar killers, i.e., iron, cobalt and nickel, which were introduced in the usual manner.

Our experiments showed that the introduction of killers into pure cadmium sulfide does not noticeably change its spectral sensitivity. On the other hand, the introduction of iron into cadmium sulfide activated with copper, for example, leads to an appreciable change in the spectral distribution of the internal photoeffect. To illustrate this new experimental fact, in Fig.4 we show the results obtained when 0.1% iron was introduced into cadmium sulfate containing 0.005% copper, the copper concentration at which the supplementary photoconductivity band is equal to the principal one. In Fig.5 we give analogous data for CdS with 0.02% copper, the Cu concentration at which the "intrinsic" photoconductivity virtually vanishes.

Cobalt and nickel have an analogous but weaker effect on the spectral characteristics of cadmium sulfide.

The experimental data shown in Figs.4 & 5 show, first, that the effect of quenching of photoconduction actually does exist. They also show that the quenching primarily affects the photoconductivity produced by the copper impurity. It may be noted that the quenching occurs at appreciably higher

---

*I take this occasion to thank N.I.Berdnikov for carrying out the spectrometric measurements.

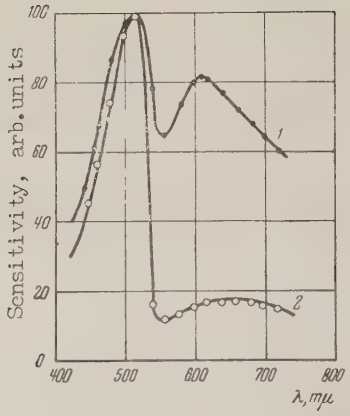

Fig.4. Quenching of photoconductivity in Cu activated cadmium sulfide by iron: 1) CdS + 0.005% Cu, 2) same phosphor but with 0.1% Fe added.

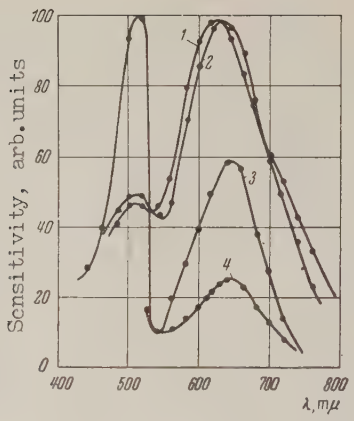

Fig.5. Quenching of photoconductivity in CdS activated with 0.02% copper by iron: 1) no iron, 2) 0.001% Fe, 3) 0.01% Fe, 4) 0.1% Fe.

concentrations of the killer than in the case of luminescence. It should also be noted, however, that the photoconductivity is also stimulated by higher concentrations of the activator than is luminescence.

The cited data, we feel, clearly prove that there is a qualitative similarity of the phenomena induced by the introduction of impurities in the luminescence of crystal phosphors and the photoconduction of semiconductors. Just as in the case of luminescence, however, investigation of only the spectral distribution of the internal photoeffect cannot yield an answer to the classical question of where the activator atoms are located in the lattice. One must obviously have recourse to certain other experimental facts to answer this question. In the case of cadmium sulfide we feel that such an auxiliary fact may be the character of the dependence of the conductivity on the copper content.

Our measurements of the dark conductivity showed that the effect of copper on this conductivity is unique. Contrary to what occurs in n-type semiconductors when a metal is introduced, in cadmium sulfide the conductivity decreases with increasing copper content. This is illustrated by the experimental curve shown in Fig.6. An analogous variation is observed when silver is introduced as the activator. These results, incidentally, are in agreement with the data of Goercke[7] and Veith[8].

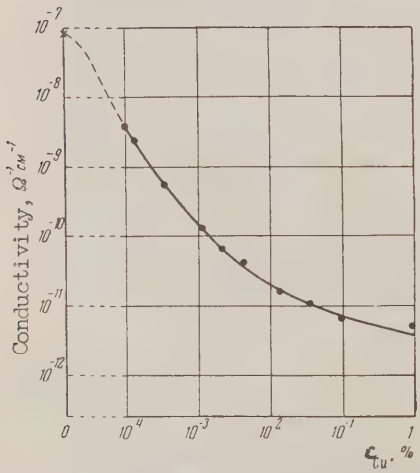

Fig.6. Variation of the conductivity of CdS with the copper concentration.

The decrease of the conductivity of cadmium sulfide with the introduction of copper or silver can, we believe, be explained simply on the assumption that the activator atoms are lodged at the regular (substitutional) lattice sites. During the heat treatment, employed to introduce the activator, the copper atoms replace cadmium atoms in the cadmium sulfide lattice. This hypothesis is entirely admissible particularly in view of

the fact that the atoms in question are close in size. Substitution of a monovalent copper atom for a bivalent cadmium atom leads to the formation of an acceptor level or trap, capturing a conduction electron. Increasing the copper content increases the concentration of acceptors which naturally leads to a decrease in the conductivity.

Thus in the course of our investigation of the role of impurities in the spectral distribution of the internal photoeffect in cadmium sulfide, we obtained new results substantiating the phenomenological similarity of luminescence and photoconductivity. The most interesting of these results are:

1) the appearance of a new copper impurity photoconductivity band with a corresponding absorption band and

2) the existence of quenching of photoconductivity by impurities, analogous to the quenching of luminescence.

The character of the variation of the conductivity of cadmium sulfide with changes in copper concentration finds a natural explanation if it is assumed that the activator atoms are located at substitutional sites.

Our experimental results relating to the steady-state and relaxation properties of CdS:Cu and CdS:Cu:Fe have been published in Ref.9.

The experimental data cited in the present report were obtained partly in the Leningrad Institute of Physics and Technology and partly in the Scientific Research Institute of the Ministry of the Radio Engineering Industry. N.P.Kolomiets and A.O.Olesk participated in the work.

References

1. N.A.Tolstoi & P.P.Feofilov, Izv. AN SSSR, Ser.fiz., 16, 59 (1952).
2. B.T.Kolomiets & S.M.Ryvkin, Zhur.tekh.fiz., 17, 987 (1947).
3. B.T.Kolomiets, Thesis,LFTI (Leningrad Institute of Physics and Technology), 1952.
4. F.Goos, Ann.Phys., 39, 281 (1941).
5. R.Frerichs, Naturwiss., 33, 281 (1946).
6. B.T.Kolomiets, Doklady AN SSSR, 83, 561 (1952).
7. P.Goercke, Ann.Telecomm., 6, 235 (1951).
8. W.Veith, C.R., 230, 947 (1950).
9. N.A.Tolstoi, B.T.Kolomiets et al, Zhur.eksp.i teor.fiz., 30, 575 (1956).

DETERMINATION OF THE POLARITY OF THE PHOTOCONDUCTIVITY CURRENT CARRIERS IN ZnS PHOSPHORS (Abstract*)

- E.E.Bukke

For determining the polarity of the current carriers responsible for photoconduction in ZnS phosphors the author utilized a method analogous to that proposed by Ryvkin for semiconductors. The original set-up was supplemented by an arrangement by means of which a constant dc field could be applied to the phosphor held in the test capacitor. The application of an external electric field in some cases facilitates elucidating the polarity of the current carriers responsible for the photoconductivity. On the basis of data obtained as the result of investigation of 20 phosphors, it was concluded that the photoconductivity in most ZnS type phosphors is mixed, i.e., is due both to free electrons and holes.

In the course of investigating the influence of the dc field on the phosphor held in the test capacitor, it was found that there is slowly (over a period of 3-10 min) accumulated in the luminophor grains a space charge that almost fully compensates the influence of the external field. This effect must be borne in mind in determining the polarity of photoconductivity current carriers by the capacitor procedure.

"P.N.Lebedev" Physical Institute of the
Academy of Sciences of the USSR

* * * * * *

ON THE CAPACITOR PROCEDURE FOR DETERMINING THE POLARITY OF THE PHOTOCURRENT CARRIERS IN CRYSTAL PHOSPHORS (Abstract**)

- U.Kh.Nymm & L.Ia.Uibo

Determination of the polarity of the photocurrent carriers is very important in investigating semiconductors and crystal phosphors. A very convenient method for investigating semiconductors is the capacitor procedure by means of which one can study fine-grained crystalline substances having a high sensitivity (the procedure was proposed by Bergman & Hensler and subsequently developed and extensively used by Putseiko and others).

We developed a procedure for determining the polarity of photoconduction current carriers based on the use of an amplifier with a narrow passband; in this procedure no additional voltage is applied to the capacitor. The phase or polarity of the voltage appearing on the capacitor plates when the specimen is illuminated uniquely depends on the polarity of the current carriers. The developed procedure is based on recording this phase by means of a phase-sensitive circuit, a synchronous detector. By our procedure one can simultaneously determine both the magnitude and polarity of the photo-emf.

The procedure was used to determine the polarity of the current carriers in a number of ZnS:Cu and ZnS·CdS:Cu phosphors. The results are listed in the accompanying table.

---

*Complete report in "Optika i spektroskopiia", 3, No.3 (1957).

** Complete report published in Trudy (Transactions) of the Institute of Physics and Astronomy of the Estonian SSR, 4, 124 (1956).

Maximum wavelengths of the modulated and constant light and the polarity of current carriers in different ZnS type phosphors

Phosphor	λ_{max}, mμ		Polarity of photocurrent carriers
	modulated light	steady illum.	
ZnS-Cu	330	*	—
(0,03% Cu)	850	300	+
ZnS-Cu,Co	330	*	—
(10^{-5} Co)	850	330	0**
ZnS.ZnO-Cu	330	*	—
(3% ZnO)	850	330	0**
ZnS-Cu,Fe	330	*	—
(10^{-5} Fe)	850	330	+
ZnS-Cu, Ni	330	*	—
(10^{-5} Ni)	850	330	+
ZnS.CdS-Cu	white	*	+
(10% CdS)	800	330	0**
ZnS.CdS-Cu	360	*	—
(25% CdS)	850	360	+
ZnS.CdS-Cu	390	*	—
(35% CdS)	800	390	+
ZnS.CdS-Cu	410	*	—
(45% CdS)	800	410	+

*No steady illumination
**No photoconduction detected

We were interested primarily in the character of the photosensitivity in the region of infrared stimulation. We found that the investigated phosphors in the excited state become photosensitive in the near infrared region (exceptions were ZnS:Cu:Co and ZnS·ZnO:Cu in which no noticeable photosensitivity in the infrared was detected).

It will be seen from the listed data that the majority of photocurrent carriers in the case of infrared excitation are holes. On the basis of the usual energy schemes it may be concluded that irradiation with infrared produces electron transitions in the phosphor from the filled band to the levels of the ionized luminescence centers.

Tartu State University

Discussion of the Reports of B.T.Kolomiets, E.E.Bukke and U.Kh.Nymm & L.Ia.Uibo

V.P.Poruchikov: How do Cu, Cl and O affect the inertial characteristics of CdS? How does Cl influence the electric conductivity and photosensitivity? What is the optimal value of the ratio of the "light" current to the dark current for CdS:Cu?

B.T.Kolomiets: The inertial characteristics of cadmium sulfide are only weakly dependent on the Cu concentration, namely, the inertia decreases with increasing Cu content; we did not investigate the influence of Cl and O. It is difficult to answer the question regarding the optimal value of the ratio of the "light" current to the dark current inasmuch as the electric and photoelectric properties depend to an appreciable extent on the previous heat treatment. For phosphors prepared by a certain procedure, the ratio may be in the tens of thousands, but at the same time the absolute value of the photoconductivity may be small.

V.P.Poruchikov: What can you say regarding the possibility of preparing photoconducting layers of CdS powder with an organic binder?

B.T.Kolomiets: I think this should be feasible.

Incidentally, regarding the dependence of the photoconductivity of CdS on the Cu content I wanted to suggest that this dependence may serve as a means of analyzing CdS for the Cu content.

L.M.Shamovskii: Is photoconduction observed with excitation by γ-rays? Is the photoconductivity linearly dependent on the energy of the photons?

B.T.Kolomiets: Photoconductivity is induced by γ-rays, however, it is characterized by an appreciable inertia (lag). We did not investigate its dependence on the energy of the γ-rays.

Question: What are the upper and lower bounds of the inertia of CdS?

B.T.Kolomiets: The values of the time constant found in our experiments varied from 5 to 30 millisec; the lag tends to decrease with increasing Cu content. Unfortunately, no clear cut dependence was observed.

N.A.Vlasenko: How do you explain the appearance of the second photoconductivity maximum?

B.T.Kolomiets: The first maximum of the fundamental photoconductivity of CdS appears when there is an excess of Cd atoms. In this case the photoconductivity is a result of photoelectron transitions from these atoms. Upon introduction of copper into the CdS, there are formed additional acceptor levels which are responsible for the appearance of the new photoconductivity band, displaced into the red region. This band can probably be ascribed to electron transitions from the Cd ground levels to the Cu acceptor levels. As the amount of activator is increased these centers will be destroyed or emptied; finally all the electrons will be captured and there will remain only one form of photoelectron transitions. With different contributions from the two types of transitions, the shape of the spectral curve will vary accordingly.

A.N.Terenin: You mentioned quenching by oxygen in passing. If you really observed this effect of oxygen, was it reversible, that is, was the photoconductivity reestablished when the oxygen was eliminated? Did this effect involve only the intrinsic or fundamental band or the copper band as well?

B.T.Kolomiets: The observation pertained only to the copper band. The effect was fully reversible and is readily observed at high copper concentrations. The influence of oxygen should probably be ascribed to surface processes. There are definite indications of chemoabsorption. Up to a certain temperature the oxygen is bound on the surface and temperature variations do not affect the electric and photoelectric properties of the specimen. However, above a certain threshold value, i.e., beginning from 150°, the effect becomes noticeable. If the specimen is initially in vacuum, the introduction of air leads to fading of the conductivity and photoconductivity.

G.M.Eliashberg: Did you observe any changes in the character of the photoconductivity in going from excitation to phosphorescence?

E.E.Bukke: The experimental procedure does not allow of determining the conductivity during phosphorescence. With the procedure used the action of intermittent light is essential.

E.K.Putseiko: Did you observe effects connected with space charge in pure ZnS?

E.E.Bukke: Only to a minor extent. The formation of space charge and its dissipation are readily observed in phosphors with two activators or in the case of flashing (scintillating) phosphors.

E.K.Putseiko: I would like to say a few words regarding the determination of the polarity of photocurrent carriers in semiconductors by the capacitor method described by Nymm & Uibo.

Eight years ago, at the 1948 Conference on Luminescence, it was first shown that the capacitor method allows of determining the polarity of photocurrent carriers in different powdery semiconductors, phosphors and organic dyes[1]. By virtue of its simplicity this procedure is now widely used in a number of laboratories. The purpose of a series of investigations undertaken earlier in our laboratory was to elucidate the behavior of the polarity of photocurrent carriers in a number of semiconductors under illumination by light in different regions of the spectrum. It was found that application of a constant electric potential to the capacitor plates allows of differentiating the polarity of the photocurrent carriers in semiconductors with mixed (n- and p-type) conductivity[2,3]. In addition there were obtained data that

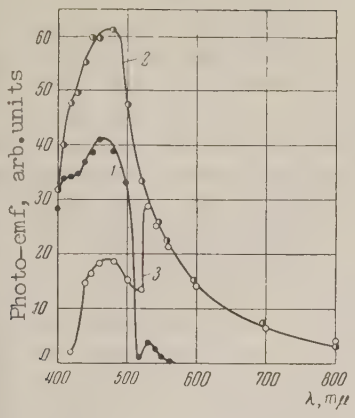

Fig.1. Photo-emf of a powdery CdS layer under illumination by intermittent light: 1) no applied potential, 2) -70 v on the semitransparent electrode, 3) +75 v on the semitransparent electrode.

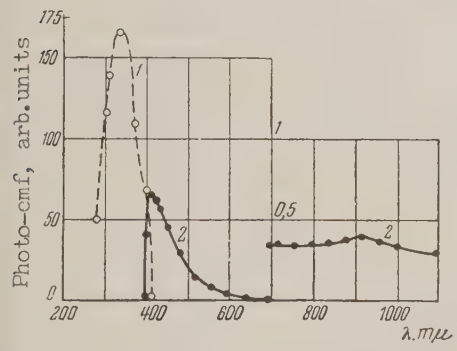

Fig.2. Photo-emf of ZnS:CdS:Cu phosphor under illumination: 1) by modulated ultraviolet light, 2) by modulated ultraviolet with simultaneous illumination by nonmodulated infrared light.

indicated that the polarity of the photocurrent carriers in a number of cases is connected with the surface state of the semiconductor. In later investigations we showed that absorption of iodine vapor changes the polarity of the photocurrent carriers in TlI and AgI.

It is relatively easy to determine the polarity of the photocurrent carriers by the method of Zhuze & Ryvkin in which the polarity is evaluated from the phase shift when the capacitor containing the semiconductor is illuminated with nonsymmetric light pulses. The situation is somewhat more complicated when a constant electric potential is applied to the capacitor plates. In this case there occurs accumulation of space charges in some semiconductors, which leads to unstable operation of the capacitor.

Some years ago the unstable effects in working by the capacitor method were virtually eliminated in our experiments by immersing the investigated powders in insulating media (vinylit varnish and others). The properties of many semiconductors (selenium, cadmium sulfide, diverse phosphors, etc.) undergo no noticeable changes as the result of such immersion. Under these conditions we succeeded not only in enhancing the sensitivity of the procedure but also in following the changes in the polarity of the photocurrent carriers in semiconductors with mixed conductivity. For example, Fig.1 shows the spectral curves measured by means of a narrow-band amplifier (amplification factor $3 \cdot 10^5$) for a powdery CdS layer. Curve 1 was obtained with no potential on the plates. It exhibits both the fundamental photoelectric sensitivity band and a weak, longer-wave photoeffect peak. Curve 2 was obtained with a negative voltage on the semitransparent electrode (plate) of the capacitor.

Under these conditions there is observed an increase in the intrinsic photoelectric sensitivity with its simultaneous extension into the long wave region of the spectrum. Curve 3 was obtained with a positive voltage on the semitransparent plate. In this case the photoelectric sensitivity of CdS exhibits two photo-emf maxima. The sensitivity of the region of the intrinsic photoeffect is sharply reduced, while the sensitivity in the region of the supplementary maximum is increased. In view of these data, it may be concluded that in the region of its intrinsic sensitivity the conductivity of CdS is of the n-type. As regards the supplementary photo-emf maximum, it may be assumed that the conductivity is mixed and apparently due to some additional photosensitivity centers with p-type conductivity.

It should also be noted that the presence of additional local levels in semiconductors can be detected not only in the case of application of an electric potential but also by the capacitor procedure with supplementary steady illumination with light of a certain wavelength. For example, in the case of ZnS·CdS:Cu phosphor only one photo-emf maximum is observed with the phosphor illuminated by ultraviolet. However, simultaneous illumination by modulated ultraviolet and steady infrared (or red) light leads to the appearance at the edge of the long wave photoeffect band of a new photo-emf maximum extending into the visible and infrared region to 1 μ or further (Fig.2). This additional photoeffect maximum can be detected even without steady illumination by the capacitor procedure with the application of an electric potential.

Thus we can draw the following conclusions. Determinations of the polarity of the photocurrent carriers by the capacitor method with nonsymmetric illumination bring out only the predominant type of conductivity in the photoconductor, i.e., the polarity of the majority current carriers. Use of the capacitor procedure with the application of an electric potential enhances the sensitivity of the procedure and allows of differentiating the type of conductivity in semiconductors in which both electron and hole carriers are present.

It would undoubtedly be of interest to carry out experiments in which a capacitor with an applied voltage is illuminated by nonsymmetric light pulses.

References

1. E.K.Putseiko, Doklady AN SSSR, 59, 471 (1948); Izv. AN SSSR, Ser. fiz., 13, 224 (1949).
2. E.K.Putseiko, Doklady AN SSSR, 67, 1009 (1949).
3. E.K.Putseiko, Izv.AN SSSR, Ser.fiz., 16, 34 (1952).

DETERMINATION OF THE DIELECTRIC CONSTANT OF EXCITED ZnS:Cu AND ZnS:Cu:Fe PHOSPHORS (Abstract*)

- O.V.Agashkin

An earlier investigation of Vergunas and the writer[1] was concerned with the regularities of the photodielectric effect (hereinafter PDE) in excited ZnS:Cu and ZnS:Cu:Fe phosphors. It was found with ZnS:Cu phosphor that the major part of the change in the dielectric constant under the influence of illumination is connected with an increase in the concentration of free current carriers, while in ZnS:Cu:Fe phosphor an appreciable part of the PDE is a result of an actual change in the dielectric constant of the powder grains. It was pointed out that these conclusions are susceptible of direct experimental check by obtaining data on the value of the real part of the complex dielectric constant of the phosphors in the excited and nonexcited states.

The purpose of the present investigation was to obtain these data.

Both these crystal phosphors are normally a fine-grain powder, i.e., a heterogeneous dielectric whose components are the phosphor grains and air. Determination of the dielectric constant ϵ of one of the components of the mixture from the measured value of ϵ of the mixture and the known value of ϵ of the second component is possible only when the volumetric concentration of the components is known. In the case of a mixture of phosphor powder with air it is impossible to determine the volumetric concentrations of the components. Consequently, in the present investigation the specimens were prepared in the form of weighed batches of the phosphor powder in transparent dielectrics, namely, polystyrene and plexiglass.

We measured the frequency dependences of the increments of capacitance produced by illumination of the specimens. From the frequency dependences obtained it followed that in the ZnS:Cu:Fe phosphor at a frequency of the applied field equal to 2 Mc polarization of the free charges on the grain boundaries is no longer established during the frequency period, while the change in capacity due to illumination is still great. At the same frequency the dielectric changes in the ZnS:Cu phosphor are still connected with the conductivity; this follows from the fact that at still higher frequencies a conductivity increment produced by illumination falls off to zero.

Vergunas and the writer[1] assumed that the quantity determined at 2 Mc for the ZnS:Cu:Fe phosphor was the capacitance of the specimen connected with the real part of the complex dielectric constant and that for the ZnS:Cu phosphor it was the complex capacitance. The values of the dielectric constant were calculated on the basis of the respective capacitance values by means of Lichtenecher's formula. The applicability of Lichtenecher's logarithmic formula to the given case was verified by means of standard mixtures.

As a result of the calculations it was found that the dielectric constant of ZnS:Cu:Fe and ZnS:Cu phosphors in the dark was close to 8 and was the same for measurements in both polystyrene and plexiglass. The value of ϵ for ZnS:Cu under illumination increased by 100% in the case of the measurements in polystyrene and by 200% in the measurements in plexiglass. At the same intensity of the exciting light the dielectric constant of the ZnS:Cu:Fe phosphor increased 80% in the case of measurements both in polystyrene and plexiglass. Inasmuch as the dielectric loss tangent in plexiglass is 10 times greater than in polystyrene, the conditions of polarization of the current carriers at the crystal phosphor grain boundaries (phosphor-plastic interfaces) are different in the two transparent dielectrics. Hence the

---

*Complete report in "Optika i spektroskopiia", 3, No.1 (1957).

observed increase in the dielectric constant of ZnS:Cu:Fe phosphor is a result of an increase in the real part of ϵ and can be connected only with an increase in the number of polarizing centers.

Determination at a frequency of 2 Mc of the dielectric constant of excited ZnS:Cu in polystyrene and in plexiglass leads to strongly divergent results. At higher frequencies the values of ϵ become the same and equal to the dark value. It follows therefore that the capacitance increment under illumination of a capacitor with ZnS:Cu is connected with changes in only the imaginary part of the complex dielectric constant.

Siberian Physical Technical Institute

References

1. F.I.Vergunas & O.V.Agashkin, Optika i spektroskopiia, 3, No.3 (1957). *(See abstract below.)*

* * * * * *

ELECTRIC AND OPTICAL PROPERTIES OF ZnS:Cu PHOSPHOR (Abstract*)

- F.I.Vergunas & O.V.Agashkin

The investigation was concerned with the variation of the dielectric properties of ZnS:Cu phosphor (Cu - 10^{-4} g/g; t = 1100°) under the influence of 365 mμ light. We determined the change in the dielectric loss tangent $\Delta(\tan\delta)$ and the capacitance $\Delta C/C_o$ of a capacitor containing the phosphor produced by this illumination. We recorded the dependences of $\Delta(\tan\delta)$ and $\Delta C/C_o$ on the frequency in the range from $3\cdot10^4$ to $6\cdot10^6$ cycles. In this frequency range we detected four maxima of $\Delta(\tan\delta)$ and an appreciable decrease from an initial high constant value of $\Delta C/C_o$. It was found that the position of the $\Delta(\tan\delta)$ maxima does not depend on the intensity E of the exciting light or on the nature of the substance binding the phosphor grains. The relative heights of the $\Delta(\tan\delta)$ peaks change with changes in E. We attribute the $\Delta(\tan\delta)$ maxima to electrons localized at "sticking" levels of different depths.

We investigated the regularities of the variation of $\Delta(\tan\delta)$ and $\Delta C/C_o$ with the intensity of the exciting light and obtained the relaxation curves characterizing the decay of $\Delta(\tan\delta)$ and $\Delta C/C_o$ after cutting off the exciting light. We obtained the following result for the low frequency maxima. During excitation $\Delta(\tan\delta)$ at first increases with increasing E, then falls off, tending to a constant value. After cessation of excitation $\Delta(\tan\delta)$ also at first increases and then decreases to the constant dark value. The capacitances, on the other hand, at all frequencies increase with increasing E during excitation tending finally to saturation, and decrease monotonically with time after cessation of excitation.

We investigated the temperature variations of $\Delta(\tan\delta)$ and $\Delta C/C_o$ during excitation and compared them with the temperature variation of the light sums stored at trapping levels at different depths; we also recorded temperature curves of $\Delta(\tan\delta)$ and compared them with the temperature curves for luminescence.

On the basis of analysis of the observed regularities for $\Delta(\tan\delta)$ and $\Delta C/C_o$ and comparison of them with the regularities characterizing the afterglow we conclude that frequency and temperature investigations of the dielectric loss tangent with changes of the capacitance can yield information of the parameters of the localization levels (depths of traps).

Siberian Physical-Technical Institute

*Complete report in "Optika i spektroskopiia" 3, No.3 (1957).

ON PROCEDURES FOR OBTAINING INORGANIC MATERIALS OF HIGH PURITY FOR LUMINOPHORS (Abstract*)

- I. I. Angelov

As a result of a research program carried out in the All-Union Scientific Research Institute of Chemical Reagents there have been developed procedures for obtaining salts of Zn, Cd, Ca, Mg, Na, K, Li, Sn, Si and ammonium for luminophor purposes containing less than $1 \cdot 10^{-5}$% Fe, Co, Ni and Mn and less than $1 \cdot 10^{-6}$% Cu.

One of the developed procedures amounts essentially to precipitation of the heavy metals and iron from solutions of "pure" grade salts with ammonium sulfide. As far as the heavy metals are concerned purification by this method is satisfactory, but the iron content in the products still remains between $5 \cdot 10^{-5}$ and $1 \cdot 10^{-4}$%. The remaining iron impurity is reduced by crystallization and absorption procedures; in the case of zinc and cadmium sulfates these are preceded by treatment with hydrogen peroxide or bromine water to oxidize the iron.

Tin dioxide of high purity was obtained by heating tin oxalate to 1100°; the oxalate was prepared by precipitation of "pure" grade tin dioxide with oxalic acid.

High purity silicic acid was obtained from doubly distilled ortho-ethyl silicic acid ester.

Another effective purification procedure is based on the ability of certain substances to form complex compounds with the impurity salts present in luminophor raw materials. As the complex forming agent we used sodium diethyl dithiocarbamate, which under certain conditions gives stable compounds with all the elements forming soluble sulfides. Activated charcoal was used to extract the complex compounds formed and the excess sodium diethyl dithiocarbamate. A number of very high purity luminophor materials were prepared by this procedure. In practice the necessary amount of an aqueous solution of sodium diethyl dithiocarbamate in the amount necessary to react with the impurities is added to a concentrated solution of the "pure" grade reagents at pH = 7-7.5 and room temperature. The resultant solution is then treated with activated charcoal and filtered. All the complex compounds of the impurity elements with the diethyl dithiocarbamate and the excess diethyl dithiocarbamate are absorbed by the charcoal. The products obtained after evaporation and crystallization of the solutions purified in this manner fully meet the requirements for luminophor raw materials.

Zinc and cadmium sulfate were prepared in the following manner. Appropriate amounts of 1% water-alkali solution of dimethyl glyoxime and aqueous solution of sodium diethyl dithiocarbamate were added to the concentrated solution of the desired sulfate (pH = 5.6-5.8). The solution mixture was thoroughly stirred and after 30 minutes treated with activated carbon and filtered. In order to get rid of the manganese impurities, a small amount of ammonia and ammonium persulfate are added to the solutions for oxidizing the manganese to the dioxide. The solution is heated to boiling in order to decompose the ammonium persulfate and filtered to remove precipitates. From such solutions, by precipitation with hydrogen sulfide one can readily obtain the corresponding sulfides of luminophor grade purity. Luminescence pure zinc oxide can be prepared by precipitating the hydroxide from a solution of zinc sulfate with ammonia; the precipitate is washed, dried, then heated to 1000-1100°.

The purification procedure based on the use of sodium diethyl dithio-

*Complete report published in "Proceedings (Materialy) of the Fifth Conference on Luminescence", Tartu, 1957.

carbamate as complexing agent assures products of a higher degree of purity than other purification procedures.

All-Union Scientific Research Institute of Chemical Reagents

* * * * * *

PURIFICATION OF CONCENTRATED SOLUTIONS OF SALTS TO LUMINOPHOR PURITY BY THE CHROMATOGRAPHIC METHOD (Abstract*)

- E.A.Bozhevol'nov & V.V.Trusov

1. The purpose of the present research was to develop chromatographic methods of purifying the chlorides and sulfates of zinc, cadmium, alkali and alkaline earth metals to the extent of reducing the Fe^{2+}, Fe^{3+}, Co^{2+} and Ni^{2+} content to under $1 \cdot 10^{-5}$% and the Cu^{2+} content to $1 \cdot 10^{-6}$%.

2. The problem of removing minute amounts of cationic impurities from concentrated solutions of strong electrolytes by the chromatographic method is a difficult one inasmuch as one has to take into account the presence of an anti-ionic effect tending to reduce the absorbing power of the absorbing agent; hence solution of this problem was not only of practical but of theoretical interest.

3. For the elimination of Fe^{2+}, Fe^{3+}, Co^{2+}, Ni^{2+} and Cu^{2+} from the alkali and alkaline earth metal sulfates and chlorides, we employed a procedure based on the ability of organic synthetic anionites (resins) to precipitate these impurities in the solid phase of the anionite. The character of the precipitate depends on the cations and anions present in the solution; in different cases oxides, hydroxides, subsalts of ammoniacal compounds may be precipitated. The different ions deposited in the column form chromatographic zones. The column yields a purified solution of the salt until these chromatographic zones extend to the full length of the column.

4. To remove these same impurities from solutions of cadmium and zinc sulfate, we developed a method involving depositing these impurities on the anionites in the form of negatively charged complex ions. The purification conditions here should be such that the complexing substance does not yield a complex with the cations of the purified salts but does form complexes with the impurities. In addition the complex forming agent must have the lowest possible exchange constant with the purified salt anions.

5. Both procedures allow of purifying concentrated (nearly saturated) solutions of the chlorides and sulfates in question with a large yield, which advantageously distinguishes our procedures from most other chromatographic methods. Both our procedures do away with the necessity of introducing extraneous substances (for example, NH_4^+, I^-, etc.) into the purified salts, which is also an advantageous feature.

6. The degree of purity afforded by our procedures is such that in analyzing for the remaining trace impurities it is necessary to work at the sensitivity limit of extant analytic methods ($1 \cdot 10^{-5}$% for Fe^{3+}, Co^{2+} and Ni^{2+} and $1 \cdot 10^{-6}$% for Cu^{2+}). A check on the efficacy of the procedure as regards elimination of cobalt, made using radioactive Co^{60}, showed that the cobalt content can be reduced to $3 \cdot 10^{-7}$%.

All-Union Scientific Research Institute of Chemical Reagents

*Complete report in "Proceedings (Materialy) of the Fifth Conference on Luminescence", Tartu, 1957.

CHROMATOGRAPHIC METHOD OF PURIFYING RAW MATERIALS FOR THE SYNTHESIS OF LUMINOPHORS (Abstract*)

- A.M.Gurvich, T.B.Gapon & M.S.Rabinovich

The chromatographic procedure provides a means of separating substances with similar chemical and physical properties. It can be used for purifying raw materials used for synthesis of luminophors.

Aluminum oxide gives good results as the chromatographic absorbent in purifying $CdSO_4$ and the salts of other cations characterized by less absorption in Al_2O_3 than Cd^{2+}. Contrary to the data in the literature, however, traces of Cu and Fe cannot be satisfactorily eliminated from zinc sulfate in Al_2O_3 chromatographic columns. We used both inorganic and organic sorbents for purifying zinc sulfate; the organic sorbents were used in conjunction with activated charcoal. One can obtain a high degree of purity of zinc sulfate not only as regards removal of Fe (final concentration in the filtrate $(2-3)\cdot10^{-5}$% referred to $ZnSO_4$) but also as regards elimination of Cu (concentration in filtrate under $1\cdot10^{-6}$%) and other heavy metals (Pb, Bi, etc.) with a column containing ZnO in mixture with Al_2O_3 (1:10 or 1:20). The enhanced effectiveness of ZnO, when used as a sorbent in a chromatographic column as compared with its action under ordinary conditions, is due to the multiplicity of the elementary separation events resulting from utilization of the counter current principle and the intimate contact between each bit of filtered solution with the chemosorbent. In the case of deposition of ZnS from an acidified solution under conditions when deposition of Ni and Co (as well as Fe^{2+}) is small, there is obtained a product of luminophor purity, provided the concentration of Ni and Co in the initial material is not high.

Virtually all traces of copper can be eliminated from zinc sulfate solutions by filtration through a column containing ZnS in mixture with Al_2O_3.

We obtained particularly good results when instead of the usual procedure of precipitating Ni with dimethyl glyoxime we employed filtration of the solution through a column containing dimethyl glyoxime. Departing from the procedure used by other investigators who have hitherto utilized dimethyl glyoxime and other organic reagents in inorganic chromatography, we used activated charcoal as the carrier agent, mixing it with dimethyl glyoxime and placing the mixture of the charcoal with the dimethyl glyoxime adsorbed on it above a layer of pure charcoal. This procedure not only eliminated all traces of dimethyl glyoxime, which is slightly soluble in water, from the filtrate but also made it possible to effect the removal not only of Ni but also Cu, Co and Fe impurities that form at $pH \geqslant 5.8$ stable complex salts with dimethyl glyoxime; these complex compounds as well as any dissolved dimethyl glyoxime are absorbed by the charcoal. The procedure can also be used for eliminating Cu, Fe, Ni and Co impurities from the salts of cadmium, alkali and alkaline earth metals. The degree of purity attained is virtually independent of the initial concentration of the impurities in the initial reagents. The specific characteristics of the sorbtion of the impurities in the described column assures a high productivity.

Analogous results were obtained with columns with activated charcoal and α-nitroso-β-naphthol.

All the developed purification procedures were checked by preparing luminophors - (Zn,Cd)S:Ag, ZnS:Ag, ZnS, and $CaWO_4$ - from the purified materials and then testing the products under excitation by x-rays and ultraviolet.

---

*Complete report in "Proceedings (Materialy) of the Fifth Conference on Luminescence", Tartu, 1957.

The purification procedure based on using coumns with activated charcoal and dimethyl glyoxime, as the simplest, most effective and least expensive, is now being utilized in the industrial production of luminophors.

"N.A.Semashko" Chemical Pharmaceutical Plant
and Institute of Physical Chemistry of the
Academy of Sciences of the USSR

Discussion of the Reports of I.I.Angelov, E.A.Bozhevol'nov & V.V.Trusov and A.M.Gurvich, T.B.Gapon & M.S.Rabinovich

Question (to I.I.Angelov): Which procedure do you recommend for industrial purification of $ZnSO_4$ and $CdSO_4$?

I.I.Angelov: For industrial work one should choose the method which gives the maximum purification of the products and which is the simplest, most rapid, safest and least expensive. Personally, I believe that the method based on sodium diethyl dithiocarbamate insures the highest degree of purity. The residual copper content when this procedure is used is less than $1 \cdot 10^{-7}$% which is very important in the production of phosphors.

Question: Do you think that the method proposed by you is sufficiently developed for industrial use?

I.I.Angelov: We have prepared several kilograms of products for the Physical Institute of the Academy of Sciences by this procedure. As far as I know the Institute was satisfied with the quality of the products.

Question: Is there sufficient production of diethyl dithiocarbamate to satisfy the increasing requirements?

I.I.Angelov: The amount required per ton of product is not great, hence I think that the supply is adequate.

Question: I would like to hear your views on the use of ionites for preparing pure substances.

I.I.Angelov: The ionite procedure involves a large expenditure of time for their purification and regeneration. Moreover, the procedure does not insure elimination of all impurity elements, particularly manganese.

Question: Is not the use of sodium diethyl dithiocarbamate for purifying solutions of zinc and cadmium sulfate hindered by the fact that these also form complexes with this reagent?

I.I.Angelov: Cadmium and zinc do form complex compounds with sodium diethyl dithiocarbamate, but these compounds are not stable.

Question: At what pH is purification of ammonium tungstate solutions carried out?

I.I.Angelov: At pH = 7.5.

Question: We carried out experiments on preparing tin dioxide according to your procedure. In all cases some metallic tin formed. Did this occur in your case?

I.I.Angelov: No. We did not observe the formation of metallic tin.

I.S.Rassonskaia: In what form did you deliver the cadmium sulfate to the Physical Institute of Academy of Sciences?

I.I.Angelov: In the form of a solution.

Question (to E.A.Bozhevol'nov): What is the productivity of your set-up?

E.A.Bozhevol'nov: The productivity of the set-up depends not only on its capacity as such but also on the amount of impurities present. The expenditure of materials (in kg) in purifying $ZnSO_4 \cdot 7H_2O$ is the following:

Substance	per cycle	per 10 kg yield	Substance	per cycle	per 10 kg yield
Zinc sulfate	24	10.2	Sulfuric acid (pure for analysis)	0.1	0.04
Sulfuric acid (tech.)	0.8	0.3	Nitroso-p-salt (pure)	0.005	0.002
Sodium hydroxide (pure for analysis)	0.15	0.06	Distilled water	50	21

The volume of anionite PE-9 in the swollen state in each column is 335 ml; the column diameter - 3.5 cm; cross section of column - 9.6 cm. Time for a complete cycle - 5.25 days; regeneration time - 1.25 days.

Question (to A.M.Gurvich): What is the content of Fe, Cu, Ni and Co in the reagents purified by the chromatographic procedure? What methods did you use of determining the impurities?

A.M.Gurvich: We used the same analytic methods that are employed in the "Krasnyi Khimik" (Red Chemist) Plant and in the IREA (Institute of Chemical Reagents).

The concentration of iron in the purified solutions was $2\text{-}4\cdot10^{-5}\%$; we could not detect the presence of nickel and cobalt by chemical methods; the concentration of cobalt is less than $1\cdot10^{-5}\%$. Actually, in the case of precipitation in an acid medium the concentration of cobalt is so low that it cannot be detected even by the radioactive tracer method.

Question: What is the content of anionic impurities in the luminophors prepared from the purified zinc sulfide?

A.M.Gurvich: This is not within the scope of my report and was not investigated in detail.

Question: Does the charcoal-dimethyl glyoxime column remove manganese impurities from zinc sulfate?

A.M.Gurvich: No, but the content of manganese in zinc sulfate is so insignificant that the manganese is wholly carried off by the mother liquor.

L.Ia.Markovskii: The described high purification methods are of considerable interest. All three methods were compared in the State Institute of Applied Chemistry. By the use of diethyl dithiocarbamate one can obtain $ZnSO_4$ and $CdSO_4$ solutions containing less than $1\cdot10^{-5}\%$ impurities. The procedure is very simple and given appropriate industrial equipment undoubtedly can be of practical interest. The use of the ionite method also yields a good degree of purification. However, the use of this method is hindered by the necessity of frequent regeneration of the ionite. Fairly satisfactory results were also obtained with the charcoal-dimethyl glyoxime column; however, the degree of purification, particularly with respect to iron, obtained by means of this procedure is inferior to that attainable with the diethyl dithiocarbamate method.

A.A.Bundel': The history of zinc sulfide luminophors has gone through two stages. The Lenard period with its inadequate techniques of purification came to a close in the early 30s. In view of the inadequate purity of the zinc sulfide employed the results of investigations carried out in this period are almost valueless. The second period began with the work of Schleede and is continuing to this day. The basis of all zinc sulfide luminophors used now is ZnS capable of self-activation. Development of methods of preparing pure ZnS formed the foundation of the present achievements of the chemistry of this class of luminophors. However, the obstacle to more profound understanding of the structure of luminescence centers even now is the inadequate purity

of the initial product: commercial zinc sulfate still contains several parts of iron and copper per 10 million parts ZnS.

Further progress as regards our knowledge of the structure of ZnS luminophors and improved quality of industrial phosphors can be attained only as ZnS of enhanced purity becomes available. The adsorption purification procedures now under development gives reason to hope that in the near future we will have available purer zinc sulfide.

Comparison of the results attained at the "N.A.Semashko" Plant with the data given us by E.A.Bozhevol'nov and I.I.Angelov show that the former procedure allows of obtaining a quality product only in combination with acid precipitation. This procedure is effective as regards metals of the iron group but cannot be used for reducing the copper content. The methods of E.A.Bozhevol'nov and I.I.Angelov allow of reducing the impurity content by a factor of at least 1.5. Hence they deserve the greatest attention and should be developed for industrial use.

Hitherto the attention of those working on the preparation of luminescent sulfides was turned only to the metallic impurities. This is insufficient, inasmuch as the presence of some anionic impurities in the final product also has a pronounced deleterious effect on the properties of the luminophors. In this respect it is sufficient to note that the metal-free "luminophor grade" ZnS produced by the "Krasnyi Khimik" Plant contain appreciable and variable amounts of sulfate ions and free sulfuric acid which makes them unsuitable for the preparation of certain types of luminophors. Chemists in the field should turn their attention to these harmful impurities as well.

Iu.S.Leonov: We checked the procedure for obtaining tin dioxide through tin oxalate, recommended by the Institute of Chemical Reagents. When the tin oxalate is heated at 1000-1100°, in addition to the dioxide, metallic tin is formed. There is no mention of this in the description issued by the Institute of Chemical Reagents. It seems to me that this procedure requires further development or revision.

G.V.Maksimova: At the Physical Institute of the Academy of Sciences I carried out work on cadmium sulfate purified by the procedures of Bozhevol'nov and Angelov: the heating curves for the two substances differ and in my opinion the product supplied by Bozhevol'nov is purer. Thus in the thermal curve of the cadmium sulfate from Bozhevol'nov there are five reversible endothermal effects corresponding to polymorphic transformations. Of these five effects, only two are observed in the case of the cadmium sulfate prepared by Angelov. Three polymorphic transformations are apparently suppressed by impurities. In addition in the thermocurve of cadmium sulfate, there is observed a large exothermal effect in the 350-400° interval, which is possible connected with oxidation of the organic impurities.

M.S.Rabinovich: Development of the chromatographic procedure for purifying ammonium tungstate solutions also led to a satisfactory procedure for obtaining calcium tungstate of high purity. The purification procedure consists of filtration of strongly alkaline solutions of $(NH_4)_2WO_4$ (pH ~ 12) through a column containing Al_2O_3 and ZnS in the ratio 10:1. The new method is now being used commercially in the "Semashko" Plant instead of the former method, which was based on purification of the ammonium tungstate by rubeanic acid and double precipitation of the $CaWO_4$.

M.A.Konstantinova-Shlezinger: In connection with the first two reports presented by representatives of the Institute of Chemical Reagents, I feel it necessary to note that in our work on the synthesis of crystal phosphors we still find it necessary to purify the reagents ourselves. This situation is abnormal and greatly slows down our work on synthesis of phosphors. Further-

more, most of the procedures recommended by the Institute of Chemical Reagents for obtaining high purity products that we have tried proved to be inadequate and we have had to spend a considerable amount of time on refining them and eliminating "bugs".

I.G.Shafran: In order to facilitate further improvement in the quality of crystal phosphors, we must establish the maximum allowable content of the individual impurity elements. For this one must naturally have raw materials of the utmost purity. The small amounts of such substances necessary for this purpose, however, need not be prepared by procedures suitable for industrial use or mass production. One can, for example, utilize the techniques for separating impurities utilized in chemical analysis.

The importance of establishing the maximum allowable amounts of impurities is illustrated by the case where the research chemists at our plant were required to develop an industrial procedure for preparing zinc salts containing less than $1 \cdot 10^{-5}$% lead. Later it was found that the presence of even $5 \cdot 10^{-4}$% lead had no appreciable effect on the quality of the luminophors prepared from the zinc sulfide.

A.M.Gurvich: From a comparison of the chemical analysis data given in our report and in the reports of Angelov and Bozhevol'nov, it is evident that the degree of purification of solutions of $ZnSO_4$, $CdSO_4$ and also of salts of alkali and alkaline earth metals attained with the charcoal-dimethyl glyoxime column procedure, at least as far as elimination of Cu, Co and Ni is concerned, is no whit inferior than that obtained by the procedures suggested by Angelov and Bozhevol'nov.

The inaccuracy of certain analytic data and the great divergence between the results obtained in different laboratories in evaluating the merits of the different purification procedures may be due to the influence of different extraneous impurities.*

In order to minimize these divergences it may be expedient to use the method of radioactive tracers.

In general, however, we feel that at present it is more correct to judge of the degree of purity on the basis of the quality of the luminophors prepared from the purified solutions, particularly since obtaining high quality luminophors is precisely the purpose of our work.

D.M.Korf: The procedure for purifying $ZnSO_4$ and $CdSO_4$ solutions for the production of luminophors employed in our plant is far from perfect; hence we would look with favor on any improvements in this stage of the production process. Due to the inadequacies of the technique the plant is forced to set very exacting requirements as regards the initial metallic zinc purchased and this of course is reflected in the final cost of the luminophors. Furthermore, the purification process now employed involves the expenditure of much time and labor. The main problem here is simplification of the procedure; cutting down the time required and increasing the efficiency. I am not convinced, however, that the purification procedure based on the use of columns filled with dimethyl glyoxime and activated charcoal is feasible industrially. The scales of production in the "Semashko" and "Krasnyi Khimik" Plants are

---

*Note added in proof. In comparing such analytic results it should be borne in mind that the impurity concentrations generally lie at or even beyond the limit of sensitivity of the analytic methods employed and consequently the conclusions drawn on the basis of the analytic data, particularly, when converted to the dry weight starting with different concentrations of the salts in the purified solutions, may prove misleading or erroneous.

different. We need a method by means of which one can purify an appreciable quantity of solutions per day without taking up a great deal of useful floor area. The procedure used at the "Semashko"Plant does not meet this requirement. The "Krasnyi Khimik" Plant uses this procedure only for the final stage of purification and only for a relatively small amount of solutions.

The method of purifying solutions with ammonium sulfide, proposed by the Institute of Chemical Reagents, is satisfactory but does not eliminate nickel, which, as we know, has a strong influence on the characteristics of the final luminophor. Research on developing better methods of purifying $ZnSO_4$ and $CdSO_4$ solutions must continue. There is also need for further work on development of faster analytic procedures.

I.I.Angelov: Comrade Markovskii of the State Institute of Applied Chemistry carried out a very important study. He checked all the extant procedures for obtaining the high purity substances necessary for the synthesis of luminophors and gave an objective evaluation. According to his conclusions the best results were obtained in the case of purification by means of the complexing agent sodium diethyl dithiocarbamate.

The "Krasnyi Khimik" Plant still does not use this procedure in production.

Comrade Konstantinov-Shlezinger for her thermographic investigations used $CdSO_4$ obtained by two different procedures. She states that the product obtained by the diethyl dithiocarbamate procedures gives some sort of thermal effect and from this concludes that the $CdSO_4$ obtained by this procedure is not suitable for the preparation of luminophors. She fails to take into account the fact that we purified the $CdSO_4$ solutions for obtaining CdS and not $CdSO_4$ crystal hydrate. The purified solution contained $(NH_4)_2SO_4$ which of course does not interfere with preparing pure CdS, but can affect the purity of the $CdSO_4$ crystal hydrate. Perhaps this impurity was responsible for the thermal effect observed by G.V.Maksimova.

Comrade Gurvich of the "Semashko" Plant stated that the carbon-dimethyl glyoxime procedure yields very satisfactory results but that the method of purification by means of sodium diethyl dithiocarbamate insures products with a higher degree of purity.

In sintering tin oxalate there is formed, in addition to SnO_2, some black SnO as well. In the case of an insufficient supply of air, metallic tin may also form. The problem of firing and oxidizing the product to SnO_2 requires further research.

E.A.Bozhevol'nov: It follows from all that has been said during this discussion that the chromatographic procedures open new possibilities and hold promise in the matter of purification of salts.

It must be borne in mind that there cannot be a universal procedure applicable to all cases. Each method is best for a certain purpose: where a particularly high purity of the salts is required one must give preference to chromatographic procedures; in cases where introduction of extraneous impurities (such as NH_4^+, I^- or Na^+) is inadmissable, the only possible procedure is that based on the use of anionites.

Manufacturing chemists must also bear in mind that if one starts with purer initial materials than employed in our experiments, one can greatly extend the inter-regeneration period. It is also obvious that in general anionite procedures are worthwhile and merit further development.

A.M.Gurvich: D.M.Korf informed us that the chromatographic purification procedure based on the use of carbon-dimethyl glyoxime columns is used for the preparation of materials for the fabrication of luminophors designed to meet particularly high quality standards. This emphatically shows that the

method we proposed does assure a high degree of purification. Comrade Korf considers, however, that the carbon-dimethyl glyoxime column procedure is not suitable for large-scale production in view of its low productivity. An investigation recently carried out by T.B.Gapon and myself, the results of which were only briefly mentioned in the report, shows that the rate of filtration through the carbon-dimethyl glyoxime columns can be appreciably increased over that currently employed. I want to emphasize that, in contrast to the procedures developed by Angelov and Bozhevol'nov who introduce the complexing agent into the solution, we introduced the complex forming agent into the column so that not only the absorption but also the chemical reaction occurs in the column and the complexes are adsorbed at the instant of their formation.

I.G.Shafran: In his remarks Comrade Gurvich said that analyses for iron impurity in the same batch of zinc sulfide carried out in different laboratories yielded different results. This might be explained by the use of HCl at different degrees of purity in the different laboratories.

Our analyses of samples of zinc sulfide prepared in the Laboratory of Inorganic Reagents of our Institute showed an iron content of about $10^{-5}\%$ with an experimental error not exceeding 25%. Analysis of samples of zinc sulfide previously produced by the "Krasnyi Khimik" Plant showed an iron content of approximately $10^{-4}\%$.

In my report I mentioned a rapid procedure developed by us for determining the nickel impurity in zinc sulfate, based on the standard sample principle. Analogous procedures could be developed for determining other impurity elements.

NEW CHEMICAL PROCEDURES FOR DETERMINING SMALL AMOUNTS OF IMPURITIES (Abstract*)

- I.G.Shafran

The writer in collaboration with the group under his supervision working at the All-Union Scientific Research Institute of Chemical Reagents developed procedures for determining trace amounts of impurities (Cu - $1 \cdot 10^{-6}$-$1 \cdot 10^{-5}$%, Fe - 10^{-5}%, Co - $1 \cdot 10^{-5}$%, Ni - $1 \cdot 10^{-5}$%, etc.) in high purity raw materials intended for the preparation of crystal phosphors. In a number of cases success was attained as a result of utilization of the following new methods of separation and analysis proposed by the writer.

1. Separation of iron and other impurities in the form of freshly precipitated hydroxides (or other relatively insoluble compounds) by passing a solution of the analyzed substance through a column with glass wool (serving as the adsorbent) with subsequent extraction of these impurities by means of appropriate solvents. Glass wool has a well-developed smooth surface which can readily be regenerated by washing with acid or some other appropriate reagent. The use of glass wool is limited, however, by the degree of solubility of the separated impurity compounds.

2. Method of cyclic concentration. The procedure is based on using an organic solvent and a number of reagents which cause transfer of the determined impurity at one pH value of the medium from the solution of the analyzed compound to the solvent layer and at another pH value from the solvent layer to a water layer; in this manner the impurities are concentrated from a large volume of the initial solution into a small final volume which is then utilized for conventional determination. Thus, for example, for the purpose of determination of iron it is extracted in the form of the rhodanide by several batches of isoamyl alcohol from an acidified solution of the analyzed compound. The organic layer is collected and treated with sulfosalicylic acid and ammonia; the iron rhodanide breaks down and the iron goes into the aqueous solution in the form of iron sulfosalicylate which is more stable in the ammoniacal medium. The water layer is acidified, then ammonium rhodanide is added to it and the iron rhodanide is again extracted; the presence of sulfosalicylic acid does not impede the process in view of the low stability of iron sulfosalicylate in this medium. This procedure is free of the limitations characterizing the foregoing adsorption procedure.

3. Method of removal of copper and other impurities. The procedure is based on passing a solution of the analyzed compound through a column with a resin (anionite) containing amino groups that form stable ammoniate type compounds with these impurities. By means of this procedure we succeeded in purifying a number of compounds, required for development of the analytic methods, to the extent of reducing the copper content to under $5 \cdot 10^{-7}$%.

In addition we propose a number of other techniques for enhancing the sensitivity and accuracy of determination of different impurities.

All-Union Scientific Research Institute of Chemical Reagents

---

*Complete report in "Proceedings (Materialy) of the Fifth Conference on Luminescence" Tartu, 1957.

SOME QUESTIONS OF THE CHEMISTRY OF SULFIDE LUMINOPHORS (Abstract*)

- A.A.Bundel' & A.I.Rusanova

Of the 22 elements known to be capable of activating ZnS, 15 produce luminescence in bands whose peaks are grouped in the narrow wavelength interval from 520 to 570 mμ. At the same time the chemical and other properties of these activators are highly different; it is sufficient to note that six of them are typical metalloids belonging in columns V and VI of the periodic table, while the other nine are metals from columns I through IV. This substantiates Klausens' hypothesis that the emission occurs not from the activator but from the sulfur ions belonging to the host lattice.

The fact that the chemical nature of the activator has little influence on the luminescence leads one to conclude that the phosphor forms as a result of interaction of the host material with the activator in the form of neutral atoms. This supposition is confirmed by the results of experiments on the preparation of luminophors by the introduction of O, S, P, Se, Fe, Zn, Cd and Hg in the elementary state from the vapor phase into ZnS crystals.

It has been shown experimentally that contrary to the oft-expressed opinion, fluxes do not participate in the formation of luminescence centers and are not the "suppliers" of the ions compensating the charge of the activator, purportedly penetrating into the ZnS lattice in the form of ions. The role of fluxes is limited to modifying the kinetics of the formation of the luminophor. The residual flux, not removed by washing or other treatment, is retained not in the phosphor crystals but in the intercrystalline voids.

Introduction of an elementary activator (with zero valence) into the ZnS lattice leads to disturbance of the stoichiometric proportion of the base material ions. Such derangements of the stoichiometric proportions are a common effect. Thermodynamically speaking, they are the result of thermal dissociation of the solid in the vapor or liquid phase and of the difference between the coefficients of distribution of the dissociation products in the solid as against the gaseous (or liquid) phases. In the case of expressly nonactivated ZnS and CdS luminophors, enrichment of the solid phase with surstoichiometric metal is attributable to the pronounced inequality of the partial pressures of the initial dissociation products (the metal and monatomic sulfur) developing as a result of the simultaneously occurring association of the atomic sulfur into diatomic molecules.

The nature of the dissociation mechanism of activation of ZnS and CdS helps explain the different stability of the metal-activated phosphors as regards sulfurization and the difference between the concentrations at which the activating effect of different activators becomes evident (for example, Ag and Cu, on the one hand, and Pb and Cd, on the other hand).

A tentative calculation, carried out for the ZnS-CdS system with a view to determining the CdS concentration at which the zinc band is suppressed yielded good agreement with experiment.

Activation of ZnS by the introduction of activators in the form of elements from the vapor phase brings out differences in the interrelationships of these elements with the host material that are in good agreement with the thermodynamic data and the data on the solubility of the activators and the products of their reaction with ZnS in zinc sulfide.

"V.M.Molotov" Institute of Roentgenology and Radiology

---

*Complete report in "Proceedings (Materialy) of the Fifth Conference on Luminescence", Tartu, 1957.

DISCUSSION

Question: You mentioned Wagner's method. Please characterize it briefly.

A.A.Bundel': It is described in ZS.phys.Chem., 22, 199 (1933). The basic idea is very simple. Wagner was interested in determining the nature of the current carriers in Cu_2O and Cu_2S and proposed the following approach. To subject Cu_2S specimens to heating in sulfur vapor and then investigate the change in electric conductivity, the polarity of the current carriers and the transfer number. From the experimental results Wagner drew certain logical conclusions regarding the structure of semiconductors. This method can be used for solving other problems.

Question: Did you measure the dissociation pressure or did you take the data from the literature?

A.A.Bundel': We took the data from the literature; the subject has been extensively investigated (Gerasimon, Kapustinskii, Britske and others). We used the data published by Pogorelov. At first I was suspicious regarding Pogorelov's data because the vapor pressure he gives is three order of magnitude higher than that reported by other authors. We found, however, that the discrepancy is readily explained. All the investigators who used the flow-through method took not ZnS alone but added metallic zinc to it and investigated the equilibrium in the ZnS-Zn system. Pogorelov, although he also used the flow-through method, condensed the zinc and determined the vapor pressure without introducing either zinc or cadmium. When you introduce zinc or cadmium the vapor pressure for pure zinc or cadmium is 10^3 times greater than for the atomic metal over ZnS.

B.M.Gugel': A recently published report by Bowers & Melamed (Phys.Ref., 99, 1781 (1955)) gives experimental proof of the fact that in the ZnS:Cu phosphor the activator cannot be in the atomic state inasmuch as in this case the phosphor would be paramagnetic, whereas actually ZnS:Cu phosphor is diamagnetic at all copper concentrations. Thus the concepts developed by the speaker regarding the state of the activator must be modified for the case of this phosphor. This, of course, does not prove that there cannot exist in ZnS excess Zn, S or other atoms, but at the same time it does show that the idea developed by the speaker cannot be regarded as universally applicable.

A.A.Bundel': I assert only that for the formation of a luminophor it is sufficient to bring into contact the ZnS crystal and an activator in the state of zero valence; I refrain from speculating on the further state of the activator in the crystal. As for the work of Bowers and Melamed, I feel that the results obtained by them are not sufficiently thorough to allow of drawing any categorical conclusions.

INVESTIGATION OF THE CORRELATION BETWEEN THE LUMINESCENCE AND THE CATALYTIC AND ADSORPTION PROPERTIES OF SELF-ACTIVATED ZnO AND ZnS CRYSTALS (Abstract*)

- L.N.Shekhter, I.A.Miasnikov & S.Ia.Pshezhetskii

We investigated the correlation between the luminescence, catalytic and adsorption properties of thin layers and highly dispersed powders of pure ZnO and ZnS.

Our investigations indicate that the catalytically active (as regards the utilized reaction - dehydrogenation of methanol) centers in pure ZnO may be regarded as a conjunction of a nonstoichiometric Zn^+ ion, located at the surface, and a conduction band electron. The process of catalytic dissociation of methanol in the presence of ZnO has a reducing effect on the catalyst, tending to increase the concentration of excess Zn on the surface and thereby altering both the luminescence spectrum and the catalytic activity accordingly. Experiments carried out with controlled introduction on radioactive zinc (Zn^{65}) substantiated the proposed catalytic and luminescence center model. Quenching of the luminescence bands of ZnO:Zn and ZnS:Zn by oxygen and sulfur vapor, respectively, also leads to a reduction of the catalytic activity.

With adsorption of oxygen on ZnO both the luminescence and electric conductivity are reduced. The oxygen is adsorbed on such a center with the capture of an electron from the conduction band, forming the temporary compound $Zn^+O^-_2$ which hinders repeat ionization of the excess ion and its recombination (the event giving rise to emission), thereby reducing the luminescence intensity. During adsorption of oxygen only the centers on the surface and at the "joints" between the crystals are blocked, so that the decrease in luminescence is appreciably less than the change in conductivity. The action of ultraviolet light in the fundamental absorption region causes photodesorption of the oxygen. Prolonged γ-irradiation in an atmosphere of oxygen leads to more durable occupation of such centers by oxygen (oxidation of the specimen). We also carried out experiments on neutron bombardment of catalyst-luminophor specimens.

Further we investigated the luminescence and catalytic properties of appropriately prepared specimens of the system ZnO-ZnS, which as regards catalytic activity and other characteristics differs from its constituent components.

"L.Ia.Karpov" Physical-Chemical Institute

DISCUSSION

Question: Catalytic activity is apparently a surface property of solids. On the other hand, the luminescence properties are supposed to be associated with emission centers in the bulk. What can you say regarding the relation between these two different phenomena?

L.N.Shekhter: Inasmuch as we have a certain concentration of zinc in the bulk it may be assumed that there is also a certain definite concentration on the surface. The radius of the electron shells of the activators - individual extraneous atoms disseminated through the crystal - is much greater than the radius of the shells of isolated atoms. Hence activators at a depth of several atomic radii from the surface may evince active properties. There are a number of investigations in which it has been shown that in a number of cases luminescence is due primarily to activators located at or near the surface.

---

*Complete report in "Proceedings (Materialy) of the Fifth Conference on Luminescence" Tartu, 1957.

Question: You investigated zinc oxide specimens, obtained by heating, which were not only the usual weak luminophors but also possessed catalytic activity. Did you also investigate the photocatalytic properties? What can you say regarding the fact that certain additives simultaneously quench luminescence and enhance the catalytic properties of semiconductors, i.e., act as promoters?

L.N.Shekhter: We investigated specimens obtained by precipitation of zinc in an atmosphere of oxygen. The specimens exhibit fairly good luminescence. We did not investigate the photocatalytic properties.

A.A.Krasnovskii: The idea that dislocations of the crystal lattice producing luminescence are also responsible for the catalytic and photocatalytic activity is very intriguing.

It must be said that in the case of phosphors the movement of electrons is evident in more explicit form. Hence for analytic chemists and photochemists phosphors are of extraordinary interest. Surely even now chemists have a very poor idea of the structure of the active centers responsible for catalysis and photosynthesis, while physicists appear to have a clearer picture of the nature of centers producing luminescence. Hence, phosphors should be a rewarding subject of study for chemists interested in the nature of photocatalytic reactions. Until now chemists have made relatively little use of the results obtained by investigators working in the field of phosphors. This is partly explained by the fact that phosphors are essentially a rather coarsely dispersed powder and, inasmuch as they have a relatively low specific surface, manifest only a relatively weak catalytic effect. A particularly interesting material that reunites the properties of luminophors and catalysts is zinc oxide, which explains the increasing attention given to this material in recent years.

It seems to me that the report we have just heard convincingly shows that the catalytic properties of some specimens of zinc oxide may actually be connected with the centers determining the luminescence. I feel, however, that these conclusions cannot be extended to all reactions of this type.

In this connection I would like to recall some observations we made nearly twenty years ago. We investigated the influence of ions adsorbed from a solution on the catalytic and photocatalytic activity of zinc oxide and titanium dioxide. Briefly the results were the following. In zinc oxide as well as in other oxides in the presence of which hydrogen peroxide is catalytically decomposed, this activity is relatively weakly evident; on the other hand, zinc oxide has the ability to promote photocatalytic formation of the hydroxide from water and oxygen. It was found that adsorption on the zinc oxide surface of some heavy metal ions enhances its catalytic properties. At the same time the luminescence of the zinc oxide is quenched. The same effects were not noticeable in the case of titanium dioxide which exhibits a very weak fluorescence.

E.K.Putseiko: The parallelism between the luminescence, catalytic and adsorption properties reported by the speaker does not always obtain. According to our experiments, zinc oxide with a very bright luminescence (some 2-3 orders of magnitude more intense than the ordinary) exhibits a low photoconductivity and weak adsorption properties.

F.F.Vol'kenshtein: The question has been asked: what is the origin of the connection between the catalytic activity, which is a typical surface property on the one hand, and the luminescence or electric conductivity, which is a typical bulk property, on the other hand. I would like to attempt to answer this question in the light of the electronic theory of catalysis.

There is always a certain concentration of free electrons and free holes on the surface of a semiconductor. It can be shown that these electrons and holes fulfill the functions of free valences, which so to say conduct the catalytic reaction on the semiconductor surface. The activity of the catalyst is determined by the concentration of these free valences on the surface. The surface, however, is in equilibrium with the volume. The concentration of electron (or hole) gas on the surface always depends on its concentration in the bulk. Hence the factors altering the concentration of the electron (hole) gas inside the crystal affect its catalytic activity as well. Thus the electron (hole) gas is the connecting link between the surface and the volume.

Another question I would like to say a few words about is that of the catalytically active centers on the surface of zinc oxide. The authors inferred that such centers are surstoichiometric or excess Zn^+ ions. According to the electronic theory such centers are free valences, either wandering over the surface or localized at defects. There is no contradiction here however. The Zn^{2+} or Zn^+ ions ejected to the surface are electron acceptors or, in other words, serve as centers of localization for free valences. The localization of a free valence transforms a Zn^{2+} ion into a Zn^+ ion or a Zn^+ ion into a neutral Zn atom. Thus from the standpoint of the electronic theory Zn^+ ions or Zn atoms distributed over the surface must fulfill the function of active centers inasmuch as they are essentially free superficial valences. The role of structural surface defects (with valence localized at them) as active centers was considered in the electronic theory of catalysis several years ago. Shekhter, Miasnikov and Pshezhetskii in interpreting their experimental data are in effect proceeding from the concepts of the electronic theory of catalysis.

I.A.Miasnikov: I would like to say a few words concerning the remarks made by Comrade Krasnovskii and Vol'kenshtein. We feel that it is natural and correct to seek a connection between the luminescence properties of oxide luminophors and their catalytic properties in cases when the luminophor-catalyst does not contain extraneous impurities, i.e., is a self-activated phosphor. Obviously, the presence of extraneous ions on the surface of the crystal (the example cited by Comrade Krasnovskii) may radically change the direction of the chemical process (for example, from dehydrogenation of alcohol to its hydrogenation), while the luminescent properties of such a catalyst may, at the same time, change in an entirely different manner. Thus in the case of ZnO with extraneous ions adsorbed on its surface we are dealing with a complex catalyst on which the chemical process may simultaneously proceed in different directions.

L.N.Shekhter: The character of the quantitative correlation between the luminescence and the catalytic activity depends to a substantial extent on the dimensions of the crystals, the contacts between them, the distribution of activators in them and the total area of the polycrystalline specimen. We record the luminescence emanating only from the external, exposed faces of the crystals, while the adsorption and catalytic process can occur not only on the surface but in the crevices and pores of the luminophor. Consequently, it is preferable to investigate to correlation between the luminescence and the catalytic activity using specimens in the form of thin layers or films, on which one can vary the amount of activator without changing the total surface of the specimen. This is what we did in the present investigation. In some cases strongly luminescing crystals may have a low catalytic activity. If under the given conditions one increases the concentration of the activators at the surface, the catalytic activity will increase together with the intensity of the luminescence up to the point of concentration quenching. Hence the anomaly noted by Comrade Putseiko in no way invalidates our interpretation of the character of the relationship between the optical and catalytic properties of self-activated ZnO crystals.

SOME DISTINCTIVE FEATURES OF THE LUMINESCENCE SPECTRA OF SULFIDE-SELENIDE LUMINOPHORS (Abstract*)

- A.A.Bundel' & Z.I.Guretskaia

We still lack adequate information on the spectra of sulfide-selenide luminophors. Most of the data in the literature were obtained with a high excitation intensity under conditions favoring predominance of the short wave bands. Yet the presence in the spectra of these luminophors of bands associated with the metalloid-activator in addition to the metal-activator bands lends particular interest to the spectra of such luminophors.

We investigated the emission of the ZnS-ZnSe system (up to 46% ZnSe content by weight) under excitation by 365 mμ light. Our results substantiated the earlier data of one of the writers and of Klasens on the existence of an independent Se band and an Se concentration interval in which the Se and Zn bands compete. We investigated the spectra of ZnS-ZnSe:As and ZnS-ZnSe:Mn prepared 1) by the introduction of increasing amounts of ZnSe into ZnS:Ag (10^{-4}g per gram ZnS) and into ZnS:Mn ($3\cdot10^{-3}$g per gram ZnS) - the spectra of ZnS:Ag and ZnS:Mn consist only of the bands of Ag and Mn, respectively - and 2) by the introduction of increasing amounts of Ag and Mn, respectively, into ZnS-ZnSe with a constant ZnSe content. It was established that the band of the metalloid-activator, selenium, behaves in the spectra in the same way as the metal-activator bands and competes with them just as they do with each other.

The stability of the Se band (as indicated by the concentration of the second competing activator at which the Se band is suppressed) is greater than the stability of the Zn band with respect to the same competing activator in a sulfide phosphor and increases with increasing Se concentration in the host material.

In contrast to the bands of the other activators (Zn, Ag, Cu and Se), the Mn band is not displaced to the side of longer wavelengths with increasing ZnSe content. The observed displacement of the spectral curve of ZnS-ZnSe:Mn to the side of shorter wavelengths at moderate concentrations of ZnSe and its reverse shift to the side of longer wavelengths with further increase in the ZnSe content is not due to displacement of the band specific to Mn as was inferred by Leverenz. These displacements are actually the result of surposition and competition of the Se and Mn bands: the shorter wavelength Se band at low ZnSe concentrations is displaced to the side of higher wavelengths with increasing ZnSe content, while the Mn band remains stationary throughout.

We found that ZnS-ZnSe can also be activated by a metalloid, namely, phosphorus. In view of the closeness of the Se and P bands, replacement of the Se band by the P band is evinced in a displacement of the peak by about 10 mμ to the side of longer wavelengths. The fact that an independent P band exists in ZnS-ZnSe is proved by behavior of specimens heated in air and H_2: when the luminophor is heated in H_2, the Se band is quenched while the P band appears only after such treatment; on the contrary, the heating in air leads to extinction of the P band and reestablishment of the Se band to its former intensity. ZnS:P reacts to changes in the vapor phase during heating in the same manner as ZnS-ZnSe:P. The P band appears only after heating in H_2 and is extinguished by subsequent heating in air, which brings out the Zn band. When such a specimen is again heated in H_2 the P band reappears, but with somewhat lower intensity due to loss of part of the phosphorus incident to heating.

The effects occurring due to competition between the bands of two

---

*Complete report in "Proceedings (Materialy) of the Fifth Conference on Luminescence" Tartu, 1957.

metalloid activators differ in no way from the effect associated with the competition between the bands of two metal activators.

"D.I.Mendeleev" Chemical Technological Institute

DISCUSSION

V.L.Levshin: It is not clear to me, when does the blue band associated with zinc disappear with the introduction of increasing amounts of selenium?

Z.I.Guretskaia: Inasmuch as our object was to investigate the interaction of the selenide bands we took compositions with a concentration at which the zinc bands are no longer evident in the spectrum of the luminophor. This occurs at a 20% selenide content.

A.V.Lavrov: Did you succeed in observing the Se band in the luminescence of the system activated with copper. If not, how do you explain this?

Z.I.Guretskaia: With the introduction of Cu in concentrations greater than the optimal, a short wave emission band is observed in the spectrum just as in the case of sulfides. The Cu and Se bands are not resolved due to their nearness.

A.V.Lavrov: What is the optimal concentration of Se at which the greatest increase in output is observed?

Z.I.Guretskaia: In the system with Mn the output begins to decrease at Se contents above 30%.

E.I.Blazhnova: I am surprised that you obtained luminophors with such a high concentration of ZnSe.

Z.I.Guretskaia: According to analyses the highest concentration of selenide in our samples was 46%. We did not work with higher concentrations of ZnSe.

ZINC SULFIDE-SELENIDE LUMINOPHORS AND THEIR TECHNICAL APPLICATIONS (Abstract*)

- E. I. Blazhnova

The report is devoted to the results of investigations of ZnS-ZnSe cathodoluminophors.

The first part of the report gives the results of an investigation of the spectral composition of the emission of ZnS-ZnSe, ZnS-ZnSe:Ag and ZnS-ZnSe: :Cu under excitation by an electron beam with voltages from 3 to 20 kv on the anode and beam current densities from 0.5 to 100 $\mu a/cm^2$ at the screen. It was found that the cathodoluminescence spectra of these luminophors exhibit a stron dependence both on the ZnSe content and on the excitation conditions. In most cases the spectra of these cathodoluminophors have, in addition to the fundamental emission band, a supplementary band which may either stand out separatel or be evinced by distortion of the shape of the fundamental band. This character of the spectra is explained by the influence on the activator ions of different (containing and not containing selenium) microregions of the crystal. Variation of the excitation conditions (anode voltage and current density) is accompanied by an appreciable redistribution of energy between the bands.

The second part of the report summarizes the results of an investigation of the afterglow of ZnS-ZnSe luminophors excited by a defocused electron beam. It was found that for these luminophors activated with Zn, Ag or Cu the afterglow (decay) in the region of variation of brightness from 0.5-1 to 20% relative to the brightness at the terminal instant of the exciting pulse is characterized by a hyperbola. Increasing the ZnSe content with any of the above listed activators produces a monotomic decrease of the afterglow time. Variation of the anode voltage over an appreciable range (3 to 10 kv) does not produce any noticeable change in the partial decay times. On the other hand, variation of the beam current density does have an appreciable effect on the partial decay times.

The third part of the report gives the results of an investigation of the light yield and brightness of screens prepared of the above luminophors under different electron excitation conditions.

Finally, conclusions are drawn on the basis of the experimental data regarding the expediency of utilizing luminophors of the ZnS-ZnSe system for a number of industrial and engineering purposes.

*Complete report in "Proceedings (Materialy) of the Fifth Conference on Luminescence" Tartu, 1957.

SOME REGULARITIES IN THE CATHODOLUMINESCENCE OF LUMINOPHORS (Abstract*)

- Z. I. Klabukova

1. Under intense excitation by an electron beam the spectra of (Zn,Cd)S and (Zn,Cd)S:Ag consist of a band with one maximum.

2. With the introduction of silver this maximum is smoothly displaced to the side of shorter wavelengths. The greatest shift obtains at a silver content of $1 \cdot 10^{-4}$g per gram of the base material, regardless of the CdS content.

3. With further increase in the Ag concentration the maximum begins to move to the side of longer wavelengths.

4. The magnitude of the displacement of the peak with the introduction of Ag in amounts up to $1 \cdot 10^{-4}$g per gram base material changes radically in going from a CdS content of 0-10% to 20% or higher. It may be assumed that different bands compete with the silver band in the two cases: in the former case only the zinc band, in the latter case the zinc and cadmium bands.

5. The shift into the long wave region with increasing Ag concentration above $1 \cdot 10^{-4}$g per gram base material is due, on the one hand, to decomposition of the homogeneous luminophor into mutually saturated sulfide phases and the formation, as a result of this, of Zn centers and, on the other hand, to the effect of self-absorption of luminescence, which is experimentally detectable in luminophors with a silver content exceeding the optimum Ag concentration.

6. From the experimentally observed variation of the spectra of (Zn,Cd)S:Ag luminophors one can draw certain inferences regarding both the interrelationship of the activators in the homogeneous medium and the influence of phase transitions in the host material.

* * * * * *

INVESTIGATION OF THE THERMAL STABILITY OF SULFIDE PHOSPHOR SCREENS (Abstract*)

- T. V. Korovkina

Despite the fact that luminophors of the ZnS and (Zn,Cd)S activated with silver are widely used in electronic engineering, there are no systematic data in the literature on the dependence of their emission spectra and brightness on the conditions of heat treatment in air and in vacuum. Yet the latter is particularly important when the luminophors are used in electron beam tubes.

Our experiments on thermal stability were carried out on specimens of the following luminophors: ZnS_{100}-$Ag_{0.01}$, $ZnS_{65} \cdot CdS_{35}$-$Ag_{0.01}$, $ZnS_{45} \cdot CdS_{55}$-$Ag_{0.01}$ and $ZnS_{25} \cdot CdS_{75}$-$Ag_{0.01}$. The specimens were prepared from raw materials supplied by the "Krasnyi khimik" (Red Chemist) Plant.

The luminophors were heat treated under conditions simulating those obtaining in the fabrication of cathode-ray tubes: heating in air at 350° for 3 hours and then under vacuum ($1 \cdot 10^{-5}$mmHg) at 400° for 4 hours. The brightness and emission spectra were measured under excitation with a divergent electron beam (anode voltage 8 kv; mean current density 1.5 $\mu a/cm^2$). The emission spectra were determined on an UM-2 monochromator equipped with a photomultiplier.

All the luminophors prepared with a ZnS or CdS base were characterized by a displacement of the emission spectra to the short wave side after heat treatment. The greater the proportion of CdS in the initial batch, the more appreciable was the displacement. The emission spectrum of ZnS:Ag did not change.

---

*Complete reports in "Proceedings (Materialy) of the Fifth Conference on Luminescence" Tartu, 1957.

In order to clarify the reason for the change in the emission spectra and brightness incident to heat treatment, we determined the temperature of the beginning of the change in the spectra characteristic for each of the luminophors. We investigated the influence of the activator (Ag) concentration on the thermal stability and the influence of the rate of cooling of the specimen both in the process of preparation and after heating in air. We also subjected activatorless (silver free) specimens with different proportions of ZnS and CdS to heat treatment. Our experiments showed that the emission spectrum of activatorless specimens does not change after heating in air or in vacuum. The magnitude of the short wave shift of the spectrum and the decrease in brightness due to heat treatment increase markedly with increasing silver concentration from 0.001% to 0.1%. It was established that the indicated dependence on the composition of the base material begins to be manifest when the luminophor is heated in air to 300-400° or higher and that it is strongly affected by the rate of cooling of the luminophor both in the process of preparation and after heat treatment of the luminophor.

The observed variations in the emission spectrum and brightness incident to heat treatment are reversible in character.

No change in the emission spectrum after heating in air or in vacuum is observed in the case of (Zn,Cd)S:Ag luminophors subject to sulfurization in sulfur vapor.

In view of the above it may be inferred that the variation of the spectra and brightness of luminophors incident to heat treatment is connected with diffusion of the activator (Ag), leading to a redistribution of the intensity of the Ag, Zn and possibly Cd bands; this obviously produces corresponding changes in the integral emission of the phosphor.

DISCUSSION

V.L.Levshin: First question - regarding the diffusion of silver. What silver remains on the surface? How great is the loss of activator during heatin

Second question - concerning graying of the phosphor due to formation of silver sulfide. To what extent do you think this reaction occurs? Did you carry out measurements of the intensity of emission during the heating of the phospho

T.V.Korovkina: We made all the measurements after heating of the luminopho specimens; that is, the measurements were made not during heating but when the specimen had cooled to room temperature. Where does the silver come from? I can say nothing definite on this point. There was a difference between the emis sion spectra of specimens subjected to rapid as against slow cooling. During the heating, we had the same amount of silver inasmuch as the conditions were identical. Specifically, we started with the same batch which was divided in half. Why should the slowly cooled specimen, which showed more graying, have a higher Ag concentration than the specimen that was cooled rapidly? If we accept that quenching generally freezes the initial structure of the specimen, it may be assumed that changes in solubility occur with variation in temperature.

A.A.Cherepnev: Did you obtain x-ray diffraction patterns?

T.V.Korovkina: No, we did not.

M.V.Grigor'ev: Could it be that after slow cooling the observed displacement of the spectral curve is due to a decrease in the amount of cadmium?

T.V.Korovkina: There was no loss of Cd. If you take a specimen heated in air and reheat it at 800° the initial spectrum is reestablished.

V.L.Levshin: I would like to recall that zinc sulfide and cadmium sulfide phosphors exhibit luminescence hysteresis when heated to several hundred degrees. This hysteresis effect was discovered by Iastrebov back in about 1940. In some cases the luminance depends on the instant of measurement. Possibly this factor influenced your results.

T.V.Korovkina: I measured variation of brightness as a function of the heat treatment. All the actual measurements were made at room temperature.

RADII AND CONCENTRATIONS OF ACTIVATOR IONS IN CRYSTAL PHOSPHORS (Abstract*)

- M.A.Konstantinova-Shlezinger

In recent years there have been evolved a number of new luminophors based on phosphates, silicates and other compounds. In the reports devoted to these luminophors, the synthesis is described so fully and accurately and at the same time the substances are so diverse that it would appear feasible and timely to try to distinguish those properties and regularities that are generally characteristic of crystallochemical phosphor systems and note the traits that are common to their synthesis.

If the premise that luminophors are crystallochemical systems in which part of the substitutional lattice sites are occupied by extraneous ions or atoms, then the possibility of formation of different specific crystal phosphors and the concentration of activator in them must depend on the degree of similarity of the activator ions and the lattice cations. In order to clarify this dependence we compared the activator concentrations in 53 crystal phosphors of different classes. We expressed the concentration in terms of the number of formular units per activator ion.

It was found that the luminophors in question could be divided into two groups: 1) luminophors in which the charges of the activator ion and of the replaced host cation are the same and the radii of these ions differ by less than 15% and 2) luminophors in which either the charges of the activator ions and host cations are different or the radius of the activator ion differs by more than 15% from the radius of the cation (or both). Within each group the activator concentration in luminophors with a simple homodesmic structure is lower than in phosphors formed of host materials with a heterodesmic structure.

In the first group the minimum activator concentration in luminophors with a heterodesmic structure is 100 formular units per activator ion, but in most cases the concentration is much higher (commonly between 50 and 10 formular units per ion). In homodesmic phosphors of this group the activator concentration generally lies in the range from 50 to 100 formular units per activator ion.

In the second group, in phosphors with a heterodesmic structure, the maximum concentration is 100 formular units per ion, while the minimum concentration is 1000 formular units per activator ion. In luminophors of the same group but with a homodesmic structure the activator concentration varies in the range from 1000 to several tens of thousands of formular units per activator ion.

We compared 40 ions of possible activators and 14 cations of host materials on the basis of both indications - the charges and radii - and found that of 560 possible pair combinations only 40 satisfy both conditions (equality of charges and less than 15% difference in radii). Of these 40 combinations, however, 13 are actually combinations of trivalent lanthanum with trivalent ions of the rare earth elements. If we leave out of consideration the still relatively little studied trivalent rare earth elements, there remain only 8 possible bivalent activators, among which manganese occupies a particularly favorable position inasmuch as its radius is of nearly the same size as the radii of most widely employed base material cations, namely, zinc, cadmium and calcium.

"P.N.Lebedev" Physical Institute of the
Academy of Sciences of the USSR

---

*Complete report in "Proceedings (Materialy) of the Fifth Conference on Luminescence" Tartu, 1957.

ROLE OF PHYSICAL-CHEMICAL SYSTEMS IN ZINC SULFIDE LUMINOPHORS (Abstract*)

- A.A.Cherepnev

The methods of physical-chemical analysis in the broadest sense of the term are applicable to investigation of the system of ZnS luminophors. In a prepared ZnS crystal phosphor we are dealing with a static physical-chemical system in which structure defects play a significant role.

ZnS luminophors are obtained as a result of processes of formation of physical-chemical systems. There obtain in the process the regularities of solid phase reactions (particularly solid-gas). The entry of the activator into the ZnS system, realized by "chemical means", is complicated by different kinds of interactions with surrounding substances. The physical-chemical processes in ZnS luminophors are topochemical.

Systems of mixed ZnS luminophors are considered by us primarily as molecular systems in which there form solutions and structures with macrorelationships corresponding to stoichiometric proportions.

However, the principal formations determining the luminophor system of ZnS composition are considered by us in the dispersed state. In the ZnS system there develop macro- and microdispersed structures and textures. Dispersed structures in ZnS luminophors are manifested in catalysis, electroluminescence and the behavior of such activators as Zn, Cu, Ag and Au. Separating out of phases produces changes in the luminescence; there is an obvious analogy between the formation of F-centers in alkali halides and the separation of aggregates in photographic emulsions and in light-sensitive glasses.

DISCUSSION FOLLOWING THE REPORTS OF M.A.KONSTANTINOVA-SHLEZINGER AND A.A.CHEREPNEV

I.S.Rassonskaia: M.A.Konstantinova-Shlezinger treats crystal phosphors as crystallochemical systems formed by the host and the activator. This approach made it possible to apply in the work done under her supervision methods and procedures which are usually utilized for investigating reactions occurring in the solid phase. Such methods are, for example, thermography, roentgenography and crystal optics. This approach appears to be very promising in phosphor chemistry for characterizing host materials and activators and understanding of the processes occurring during heat treatment.

It would be of undoubted interest to extend the extensive comparison of the size of host material and activator ions carried out by M.A.Konstantinova-Shlezinger along the lines of comparing the activating effect of different salts together with data on the phase diagrams of the corresponding binary systems. For gaining a deeper insight into the chemistry of luminophors, we undoubtedly should utilize physical-chemical analysis - investigation of the properties of systems as a function of their composition. A.A.Cherepnev in his report convincingly showed the expediency of applying physical-chemical analysis.

---

*Complete report in "Proceedings (Materialy) of the Fifth Conference on Luminescence", Tartu, 1957.

STRUCTURE OF ALKALI HALIDE PHOSPHORS AND THE MECHANISM OF LUMINESCENCE PROCESSES (Abstract*)

- L.M. Shamovskii, A.A. Dunina & Iu.N. Zhvanko

In modern luminescence theory the processes of excitation and emission in Tl-activated alkali halide phosphors are considered to be the result of electron transitions in the impurity ions situated at the lattice sites. It is assumed that excitation of typical phosphors by light in the long wave activator band leads directly to the formation of ionized luminescence centers. The luminescence occurs incident to the recombination of the centers with electrons. If the phosphor is excited by light in the fundamental absorption bands of the host material, the formation of these ionized luminescence centers occurs as a result of interaction of the activator with holes.

Our investigations of alkali halide phosphors showed the following:

1. In the presence of holes (and V-centers) the absorption and the shape and intensity of the activator bands in alkali halide phosphors remains unchanged. Consequently, the activator ions, regardless of their location in the phosphor, do not interact with holes, so that ionized luminescence centers cannot form in this manner.

2. On the contrary, the activator localizes electrons. As a result, the normally present supplementary absorption bands disappear and at the same time the crystal loses the ability to luminesce. We established that the electron localization (trapping) centers are located on the contact surfaces of the polyhedral structure of the phosphors.

3. The activator ions located at the lattice sites are neither electron donors nor acceptors and consequently do not participate directly in the luminescence.

4. We propose a new energetic model of alkali halide phosphors taking into account their microheterogeneous structure.

5. There is a correlation between the photochemical and luminescent properties of alkali halide crystals.

Pure salts at low temperatures even in the absence of an activator and with no deviations from rigorously stoichiometric proportions of the components are typical phosphors. In them the intensity of scintillation pulses increases in proportion to the energy of the ionizing radiation. Recombination of electrons and holes on the contact surfaces, just as in the crystals with an activator, is accompanied by luminescence.

At ordinary temperatures, however, the concentration of structural defects in the crystals attains an appreciable magnitude. The crystals acquire photochemical sensitivity. The free electrons and holes forming during photolysis can be trapped at vacant sites with the formation of F- or V-centers. At the same time atoms and aggregates of the alkali metal appear on the contact surfaces. This process is furthered by cationic conductivity, just as in photolysis of silver halide salts.

6. We investigated the variation of the electric conductivity of KI and KI:Tl as a function of the temperature and composition. We established that small amounts of activator sharply reduce the conductivity of the crystal, despite the development of polyhedral structure in the crystal. Introduction of an activator is equivalent to deep cooling of the crystal. In both cases the cationic conductivity decreases and the stability of the F- and V-centers and the photochemical sensitivity are reduced. In the case of deep cooling, too, electrons and holes are localized on the contact surfaces and their

---

*Complete report in "Optika i spektroskopiia", 3, No.2 (1957).

recombination, just as in crystals with an activator, is accompanied by luminescence. Finally, we showed that the maximum in the luminescence spectrum of pure NaI (band at 303 mμ) corresponds to the energy of interaction of localized electrons and holes on the contact surfaces.

All-Union Scientific Research Institute of Mineral Raw Materials

DISCUSSION

Question: What is your concept of the block structure forming in single crystals as a result of introduction of an activator?

L.M.Shamovskii: The activator with respect to alkali halide salts is a surface active substance. Consequently, the activator becomes distributed over the surfaces (dislocations) and gives rise to the polyhedral structure. The dual character of the activator distribution - on the contact surfaces and at the lattice sites of the host material - is determined by the ratio of the free energies of the two kinds of bonds involved. This is why, contrary to the case of pure crystals, prolonged heating of phosphors at high temperatures does not liquidate their mosaicity.

Ch.B.Lushchik: The views of L.M.Shamovskii concerning the role of interblock surfaces in luminescence and other phenomena are challenging and interesting. I feel however that the authors overevaluate the part played by contact surfaces. They assert that activator ions lodged at the lattice sites cannot absorb light and luminesce. This, at least in the case of the classical phosphor KCl:TlCl, is incorrect.

Let there be N activator particles in the crystal. Part of them, N_s, are located at the lattice sites and part, N_b, on the surfaces of the blocks. One can determine N_s by x-ray analysis. The experimental results for KCl:TlCl show that $N_s \approx N$, i.e., $N_s \gg N_b$. Koch's experiments with KCl:Tl show that the number of absorbers in this phosphor is $N_{abs} \approx N$. This means that $N_{abs} \approx N_s$. Thus, the ions lodged at the lattice sites undoubtedly can absorb. Experiments also show that the quantum luminescence efficiency of KCl:Tl is close to unity (100%). This means that $N_{lum} \approx N_{abs} \approx N_s$. Consequently, ions located at the lattice sites can also emit. Thus L.M.Shamovskii's assertion that the ions located at the lattice sites make no contribution to luminescence is ill-founded.

A.A.Shatalov: The conclusions regarding the distribution of the activator on the boundaries of individual crystal blocks, drawn by L.M.Shamovskii on the basis of splitting of the Laue spots, are doubtful. In collaboration with Zhmudskii and Gorodinskaia, I obtained Laue diffraction patterns of pure NaCl crystals colored electrolytically with F-centers and sodium colloids. The spots are clearly twinned. This indicates that the doubling of the spots is due either to atomically dispersed distribution of lattice defects or other factors (perhaps associated with the heat treatment). Shamovskii's assertion that the colloids are also distributed over the block boundaries is incorrect in view of their coagulational origin (combining of centers located in the lattice). Shamovskii's assertion is also contradicted by other experimenta. facts. Thus it is evident from an electron microscope photograph that we obtained of the colloids in NaCl that they are distributed both at the crevices and elsewhere. It is possible that the activator colloids are deposited to some extent at the cracks and microdefects, but it is obvious that there is an appreciable atomically dispersed distribution which is apparently responsible for the luminescence.

B.S.Aleksandrov: There have been doubts expressed here regarding the existence of a block structure. Its existence, however, is an experimentally established fact.

Back in 1952, Bernstein and Schardt, growing activated LiI crystals, discovered that all the activator emerges to the surface; no true solid solution is formed. Nevertheless, the crystal is activated. The only possible explanation is that the crystal has a heterogeneous structure. The reasons for this heterogeneity has been explained in numerous experimental investigations. There exists a certain distribution coefficient: during crystallization only part of the impurities present in the liquid phase are deposited in the solid phase. If the rate of growth is sufficiently high, the impurities in the liquid phase do not have time to diffuse and the activator accumulates in the liquid at the crystallization front. During the inevitable temperature fluctuations, the surface of crystallization moves in jumps and the activator separates out accordingly. In the case of limited solubility excess impurities are apparently deposited at the weakest points, i.e., at joints, cleavages and other defects.

L.M.Shamovskii: Our deduction that the activator is distributed in a dual manner does not conflict with the experimental data relative to the variation of the lattice parameters in the KCl:TlCl system with increasing thallium concentration. According to the experimental data, the increase in the lattice parameters is always smaller than would follow from Vegard's law. The amount of activator not entering into the composition of the substitutional solid solutions is fully sufficient for obtaining a phosphor with a microheterogeneous structure. The results obtained by Koch also do not contradict our dual distribution hypothesis. If the coefficient of dual distribution remains constant, the observed linear variation of the absorption with the activator concentration will persist even when the additional absorption bands of the phosphor correspond to only part of the introduced impurities. The oscillator strength is calculated according to the dispersion formula of Smakula, which, as we know, is applicable only for atomically dispersed distribution of the impurities. We assert that the long wave band of the phosphor is associated with the activator distributed over the contact surfaces. In this case Smakula's formula is not applicable (see for example, Smith, Chem.Phys., 57, 757 (1953)). Consequently, the apparent oscillator strength, calculated according to Smakula's formula, cannot be taken as proof of isomorphic distribution of the activator in phosphors.

It is true that the luminescence efficiency with excitation of the phosphor by light in the activator bands is close to unity and is virtually independent of the activator concentration. If the light is absorbed by the activator on the contact surfaces, then in this case, too, the number of absorbing centers will be equal to the number of luminescing centers. Our phosphor model is in accord with this fact. In the case of photoexcitation the absorption and emission are localized on the contact surfaces, hence there are no losses incident to energy transfer from the host lattice to the luminescence centers. Merely from the high luminescence efficiency one cannot conclude that the activator ions located at the lattice sites participate actively in the luminescence.

A.A.Shatalov asserts that a microheterogeneous structure is also observed in additively colored crystals when, in addition to F-centers, colloidal particles are present. There is nothing surprising in this. It has been definitively established by Scott and others that colloidal aggregates form outside the lattice, along the dislocations. A microheterogeneous structure in crystals may form upon addition of any surface active substance and is not

peculiar to phosphors. In contrast to other impurities, an activator in crystal phosphors produces a complex network of deep electron acceptor levels on the contact surfaces. These levels are what distinguishes crystal phosphors from other mixed crystals.

From B.S.Aleksandrov's remarks it would appear that he shares our view of the block structure of phosphors. We differ, however, as regards the causes of the microheterogeneity; Aleksandrov explains the block structure by the peculiarities of the growth of mixed crystals (i.e., by the kinetics of the process), while we interpret the mosaic as a result of the dual distribution of activator. At the same time we do not deny that the conditions of crystal growth may affect the activator distribution, although we feel that the growth factors are secondary.

ON THE NATURE OF LUMINESCENCE CENTERS IN ZINC SULFIDE LUMINOPHORS (Abstract*)

- Z. A. Trapeznikova

The principal results obtained in our extensive investigation of the properties of zinc sulfide phosphors activated with the rare earth elements are the following:

1. The line emission spectrum of samarium (Sm^{3+}) in the phosphor ZnS:Sm changes when small amounts of ZnO are introduced into the phosphor.

2. There is an absorption maximum at 332-333 mμ in the excitation spectrum of the ZnS:Sm phosphor. The corresponding luminescence spectrum consists of lines characteristic of the Sm^{3+} ion. When small amounts of zinc sulfide are added to the phosphor, in addition to the peak at 332 mμ, there appears a second excitation peak at 342 mμ. The emission spectrum at the maximum also consists of lines characteristic of luminescence of Sm^{3+}, but the relative intensities of the lines differ from those corresponding to the 332 mμ absorption peak.

3. Upon the introduction into the phosphor of other anions (Sl^{2-}, Cl^{-}, Br^{-} or I^{-}) instead of oxygen, there also appear new maxima in the excitation curve. At the same time the luminescence spectrum of the Sm^{3+} ion changes.

4. With the introduction, however, of other activators (rare earths, Cu^{+}, Ag^{+}, La^{2+} or Pb^{3+}) in place of Sm^{3+}, the same maximum at 332 mμ (as in the case of ZnS:Sm) appears in the excitation curve (we are not speaking here of the excitation peaks corresponding to absorption by the activators proper).

As in the case of ZnS:Sm the addition of zinc oxide to these phosphors leads to the appearance of a second excitation peak at 342 mμ.

The following conclusions may be drawn on the basis of the experimental data.

1. As a result of heating there form in zinc sulfide phosphors, regardless of the activator used, centers that absorb light in the 332-342 mμ region and that are capable of transferring the absorbed energy to luminescence centers formed by the activators. With absorption of light in this region the characteristic luminescence of the given activator is observed. Thus the luminescence of the activators in ZnS under excitation in the 332-342 mμ region is sensitized, just as in the case of absorption by the host material.

2. On the basis of analysis and comparison of the data of different authors we hypothesize that the excitation maxima in the 332-342 mμ region appear as the result of absorption of light by the pale blue luminescence centers of zinc sulfide phosphors.

3. It may be assumed that the absorbing centers are located at the cation sites inasmuch as the introduction of different activators does not alter the position of the absorption maximum, while the introduction of other anions does not change it. It is possible that the absorption centers appear as a result of formation of defects, namely, zinc vacancies.

4. The efficiency of transfer of the absorbed energy from the pale blue centers to the activator centers is higher than the efficiency of energy transfer from the host material.

5. Anions, introduced with the flux or zinc oxide, also participate in the formation of the luminescence centers inasmuch as they radically alter the structure of the line spectrum of samarium, present as the activator.

6. The question of whether the absorbing and emitting centers are integral

---

*Complete report in "Proceedings (Materialy) of the Fifth Conference on Luminescence" Tartu, 1957.

formations or exist separately in the ZnS lattice remains open. There are facts that appear to support either hypothesis.

"P.N.Lebedev" Physical Institute of the
Academy of Sciences of the USSR

DISCUSSION

F.M.Pekerman: There is the so-called sensitized Rothschild luminophor. Two activators are introduced into it to enhance the brightness. According to certain interpretations, the introduction of the second activator leads to the appearance of additional absorption. If this case is examined in the light of your concepts, it is difficult to understand why it was necessary to introduce a second activator if the sensitization occurs by virtue of the fact that the energy is transferred from the lattice.

Z.A.Trapeznikova: When the host lattice does not absorb or absorbs only weakly in the given wavelength interval, then it is necessary to introduce additional activators - sensitizers - absorbing light of the given wavelengths.

We found in our investigation that in zinc sulfide phosphors, in addition to energy transfer from the host material lattice, there is transfer of energy from centers absorbing in the 334 mμ region. These centers, apparently, are also responsible for the blue luminescence of activatorless zinc sulfide phosphor prepared with a halide flux. These centers are formed in different amounts in the process of preparation of all zinc sulfide phosphors. Hence in considering the properties of zinc sulfide luminophors it is essential to take into account the existence of these centers and their interrelation with the luminescence centers due to the activators.

A.A.Bundel': It is probable that in a number of cases the emission event occurs in the atoms or ions of the activator. This is particularly evident in the case of luminophors activated with rare earth elements. The line nature of the spectra of these elements makes such luminophors highly suitable subjects for investigation of the interrelationships between the host material and the activator. This was the view of Tomashek and Travinchek who almost 30 years ago undertook a detailed investigation of alkaline earth sulfides activated with different rare earths. Results of their investigations were unsatisfactory, however, owing to an unfortunate choice of the host material (sulfides prepared by the interaction of oxides with sulfur).

Hitherto attempts to activate zinc sulfide with rare earths have failed. Z.A.Trapeznikova was the first to develop procedures for preparing zinc sulfide phosphors activated with rare earth elements. This enabled her to gain a deeper insight into the relationship between the activator and the host material than Tomashek. I cannot wholly agree with the interpretation of the experimental results given by Z.A.Trapeznikova. I assume, however, that the work in this field is only beginning and that as new facts come to light the present hypotheses will be revised. At the present stage one can only wish Z.A.Trapeznikova luck in continuing her extensive investigation of rare earth-activated phosphors.

INFRARED PHOTOLUMINESCENCE OF LEAD SULFIDE (Abstract)

- L.N.Galkin

We investigated the photoluminescence of lead sulfide layers subjected to heat treatment in air. For investigating the luminescence we used special detectors and mirror optics; the dispersing component was a diffraction grating. The IR luminescence characteristic of lead sulfide is exhibited by specimens having a noticeable internal photoeffect and lies in the infrared range of the spectrum. The peak of the emission band was observed at about 2.8 μ at room temperature and shifted to the side of longer wavelengths with decreasing temperature. The energy luminescence efficiency with excitation by the green line of mercury is approximately 0.1% at 20°.

DISCUSSION

F.M.Pekerman: The work of L.N.Galkin is of great interest inasmuch as hitherto virtually nothing was known of the infrared luminescence of lead sulfide. A parallel investigation of the photoconductivity and the luminescence of PbS with a view to determining the energy distribution of the electrons participating in the two processes would undoubtedly be worthwhile.

B.T.Kolomiets: The described investigation is also of great interest because in the course of it L.N.Galkin developed new equipment that holds great potentialities for similar investigation of other substances. Let us hope that the report that we have heard today will be the first of a long series.

A few words regarding the contents of the report. I feel that L.N.Galkin is justified in his inference that the so-called "reversible" oxygen in lead sulfide is not responsible for the observed luminescence. I find it difficult, however, to accept L.N.Galkin's view that the centers responsible for the infrared luminescence are free surstoichiometric lead. U.L.Maslakov and D.A. Dunaev, for example, established that the electron levels of the excess Pb atoms in lead sulfide are in the conduction zone.

Further, the chemical reactions for the interaction of lead sulfide with oxygen given by the speaker are incomplete. Among the products of such reactions is the chemical compound $PbO \cdot PbSO_4$, which has been detected by electron diffraction studies.

LUMINESCENCE OF MICROPOROUS GLASS ACTIVATED WITH HEAVY METALS (Abstract*)

- E.V.Pershina & A.N.Terenin

By the introduction of Zn, Cd and Pb salts from aqueous and ammoniacal solutions into microporous sodium-boron-silicon glass and subsequent heating in air at 500° there are obtained phosphors exhibiting fluorescence and phosphorescence (several minutes) at room temperature. The optimal concentration of a given salt depends on its solubility and its capability of being adsorbed by the microporous glass.

Evacuation of air and the introduction or elimination of water have no discernible influence on the luminescence. The luminescence spectrum in all cases consists of a broad band in the visible region of the spectrum with principal peaks at about 460 and 540 mμ; the peaks are displaced to one side or the other and change somewhat as regards relative intensity when different salts are used. The peaks in the afterglow spectrum become narrower. The rates of decay of the blue and green bands differ.

The peak at 460 mμ is excited by light in the 310-330 mμ interval, while the peak at 549 mμ is excited by light in the 360 mμ region. The emission observed during illumination is excited by light in the entire interval from 310 to 360 mμ.

The peak at 460 mμ approximately coincides with the luminescence observed in silica and glasses, but has an appreciably lower intensity at room temperature and with optical excitation.

The intensity of the emission and afterglow of the specimens is very sensitive to changes in the surface structure of the microporous glass. The observed luminescence of microporous glass activated with the salts of heavy metals is obviously due to surface centers associated with distortions of the glass structure.

Department of Physics of
Leningrad State University

---

*Complete report in "Proceedings (Materialy) of the Fifth Conference on Luminescence" Tartu, 1957.

PHOSPHATE TYPE PHOTOLUMINOPHORS (Abstract*)

- N.A.Gorbacheva

In recent years there have been published many reports devoted to descriptions of phosphate luminophors (over 40 phosphate base luminophors have been prepared). Not only calcium halophosphate activated with antimony and manganese but also a number of other luminophors have been perfected by different investigators and recommended for use in fluorescent lamps. Nevertheless, even now the preparation of individual phosphates presents certain difficulties in view of the fact that a number of questions pertaining to the chemistry and crystallochemical structure of phosphates are still unsolved.

In the present investigation we determined the dependence of the character of the precipitates obtained on the precipitation conditions for the case of cadmium phosphates. The cadmium phosphates were precipitated from solutions of cadmium sulfate by ammonium di-H phosphate. It was established that different cadmium phosphates are obtained depending on the pH of the final solution and the precipitation temperature:

a) cadmium orthophosphate is obtained in precipitation of cadmium sulfate from a solution heated to boiling through pH values of the final solution not over 7;

b) cadmium phyrophosphate is obtained by precipitation at room temperature at pH values of the final solution equal to 7-8;

c) cadmium pyrophosphate with an admixture of the orthophosphate is obtained by precipitation from a solution heated to the boiling point up to a pH value of the final solution of 8;

d) a phosphate having the composition $Cd_5P_4O_{10}$ is obtained in the case of precipitation of the cadmium sulfate by ammonium di-H phosphate at room temperature up to a final solution pH value of 5.

The above findings were substantiated by the heating curves of the precipitates, Debye powder patterns and the characteristic shapes and dimensions of the crystals.

The luminophors synthesized from the cadmium phosphates obtained at different pH values of the final solution differ markedly from each other as regards brightness and have different decay times. It should be noted that the emission spectrum of luminophors synthesized from ortho- (peak at 615 mμ) and pyrophosphates (peak at 625 mμ) differ only insignificantly. The concentration of the activator, however, has a more pronounced effect on the luminescence spectrum: thus the peak in the emission spectrum of the luminophors synthesized from cadmium orthophosphate (pH = 5, "hot" precipitation) with a manganese concentration $C_{Mn} = 2.6 \cdot 10^{-3}$g per gram phosphate (peak at 610 mμ) is shifted to the side of longer wavelengths by 25 mμ compared with the position of the peak in the emission of the luminophor in which $C_{Mn} = 2.6 \cdot 10^{-2}$g per gram phosphate (peak at 635 mμ).

It was found that the brightest phosphors are obtained when cadmium phosphate obtained at room temperature and a pH of 5 of the final solution is used as the base material. On the basis of our study, through appropriate choice of the optimal precipitation conditions for the phosphates, we were able to enhance the luminance of a number of previously synthesized phosphors and to synthesize successfully the phosphate luminophor recommended for fluorescent lamps, namely, barium-titanate phosphate which has a luminescence spectrum virtually identical with that of magnesium tungstate, calcium ortho-

---

*Complete report in "Proceedings (Materialy) of the Fifth Conference on Luminescence" Tartu, 1957.

phosphate activated with cerium and manganese and calcium orthophosphate with tin and manganese, all of which are used to correct the emission of fluorescent lamps deficient in the infrared region.

In view of the ready availability of the raw materials and the possibility of preparing phosphate base luminophors emitting in almost any region of the visible spectrum, it may be assumed that in the future phosphate luminophors will occupy a very important place among fluorescent lamp phosphors.

"P.N.Lebedev" Physical Institute of the
Academy of Sciences of the USSR

DISCUSSION

Question: What were the x-raying conditions?

N.A.Gorbacheva: The x-ray patterns were recorded in an RKU-86 camera using an iron anticathode without a filter. The exposure times were 70-80 hours

Z.I.Klabukova: In what manner did you record the thermograms and what advantages do they have over Debye powder patterns for investigating the character of precipitates?

N.A.Gorbacheva: The thermograms were recorded in the usual manner, using a Kurnakov recording pyrometer. The thermographic procedure proved to be more sensitive than the Debye powder pattern one. Comparison of the thermal analysis data with the Debye patterns made it possible to separate the precipitates into the described types.

Z.I.Klabukova: Did you have occasion to record thermograms of zinc orthophosphate and, if you did, how did the heating curves for the β- and α-forms of $Zn_3(PO_4)_2$ differ?

N.A.Gorbacheva: We did record the thermocurves for the zinc orthophosphates. We only obtained the effect connected with the loss of water of crystallization. In order to obtain the α- and β-forms of zinc orthophosphate there must be activator present, while we worked with an activator free precipitate.

A.A.Bundel': Were your precipitation experiments reproducible?

N.A.Gorbacheva: Yes. In fact we repeatedly prepared and investigated the most interesting precipitates.

F.M.Pekerman: What advantages does barium-titanate phosphate have over $MgWO_4$? Did you compare the luminance of cadmium phosphate activated with Mn with the luminance of known luminophors? Is there a stimulation of luminescence when the cadmium phosphate is cooled?

N.A.Gorbacheva: The barium-titanate phosphate luminophor is cheaper to produce. We compared the brightness of a phosphate luminophor activated with manganese with zinc-beryllium silicate. The brightness of the former was 11.5% higher. In some cases we did observe some glow from phosphate luminophors cooled to the temperature of liquid air, but we did not particularly investigate this effect.

INVESTIGATION OF THE LUMINESCENT PROPERTIES OF SOME BOROPHOSPHATE COMPOUNDS (Abstract*)

- L.Ia.Markovskii & R.A.Shtrikhman

Boron phosphate (BPO_4) is a chemically stable and relatively high melting point substance having a white color and a crystal structure of the cristoballite type.

The purpose of the present study was to investigate the luminescent properties of boron phosphate and its possible complex salts bearing in mind that BPO_4 can be regarded as a mixed acid anhydride ($B_2O_3 \cdot P_2O_5$). There are only a few passing mentions in the literature of luminophors based on BPO_4 (Krieger - 1948, Rothschild - 1954).

1. We carried out experiments on the activation of BPO_4 with Mn, Ti, Ce and Nd. Only a weak luminescence under ultraviolet excitation was observed in the case of activation with Mn. We also investigated the activation of BPO_4 by Tl with different Tl concentrations and different heating temperatures. It was found that the optimal heating temperature is 700° and the optimal Tl concentration is 3.5%. Under these conditions there was obtained a luminophor with an emission peak at 410 mμ. We also established that interaction with Tl salts leads to disappearance of the BPO_4 phase and the formation of a new phase that is probably Tl_2BPO_5.

2. We investigated the products of the interaction of BPO_4 with the oxides of Zn, Be, Cd, Ca and Mg. The oxides of these metals decompose boron phosphate yielding different (depending on the conditions of heating) phosphate phases. Luminophors obtained by activating the different products with Mn possess luminescence characteristics (under ultraviolet excitation) different from those of pure phosphates activated with Mn under analogous conditions.

3. In order to explain the distinctive attributes of borophosphate luminophors, we carried out a study of luminophors synthesized of the phosphates of Zn, Be, Ca, Cd and Mg with additions of B_2O_3 and activated with Mn. The results brought out the distinctive influence of additions of B_2O_3 on the luminescent properties of the phosphates.

4. The experimental data indicate that the investigated phosphate luminophors can be divided into three groups differing appreciably as regards the effect on them of additions of B_2O_3.

Group I consists of zinc orthophosphate and cadmium pyrophosphate. This group of luminophors is characterized by a very strong influence of additions of B_2O_3. This influence is evinced in an increase in the intensity of emission under ultraviolet excitation, the existence of an optimum concentration of B_2O_3 and displacement of the spectral peak to the side of shorter wavelengths. The effect is particularly evident in the case of cadmium pyrophosphate which in the absence of manganese can be activated by B_2O_3 alone and yields luminescence with a maximum at about 575-580 mμ under excitation by 254 mμ light. Of the two luminophors in this group cadmium pyrophosphate activated with manganese and boron may be of practical value; its spectral characteristics are close to those of halophosphate.

Group II comprises beryllium phosphate and zinc pyrophosphate. With the addition of B_2O_3 the phosphates of this group undergo a change in phase composition together with a noticeable displacement of the spectral maximum to the short wave side and an increase in absorption in the region of 254 mμ.

Group III, consisting of Ca and Mg phosphates and Cd orthophosphate, is

---

*Complete report in "Proceedings (Materialy) of the Fifth Conference on Luminescence" Tartu, 1957.

immune to the influence of B_2O_3. Of practical importance in this group of luminophors may be the newly discovered phase of cadmium phosphate obtained by heating the initial materials at 750°. As regards brightness of emission this phosphate is somewhat superior to the commercial "halophosphatons" (crystal phosphors L-34 and L-35) and is characterized by a high intensity of emission in the red part of the spectrum.

State Institute of Applied Chemistry

DISCUSSION OF THE REPORTS PRESENTED BY N.A.GORBACHEVA AND L.Ia.MARKOVSKII & R.A.SHTRIKHMAN

I.S.Rassonskaia: How were your CdP_2O_7 and $Zn_3(PO_4)_2$ specimens prepared? Do you have analytic data on them?

L.Ia.Markovskii: The specimens were synthesized of purified phosphate salts with boric acid. According to analyses their compositions were stoichiometric.

I.S.Rassonskaia: What is the reason for the difference in the heating temperatures for the different mixtures? For example, you gave 900° for $ZnO-BPO_4$ and 800° for $2ZnO-BPO_4$.

L.Ia.Markovskii: The difference is due, first, to the fact that the temperature at which the oxide phase disappears differs for different systems and, second, to the appreciable fusing of the mixtures.

I.S.Rassonskaia: What percent PbO_4 did you add?

L.Ia.Markovskii: In all systems we took stoichiometric proportions.

I.S.Rassonskaia: What methods did you use for identifying the phases formed?

L.Ia.Markovskii: We did not carry out a complete identification. We obtained Debye diffraction patterns and compared them with powder patterns in the literature.

A.A.Bundel': You told us of a very interesting luminophor which is a completely vitrified product. With what sort of formations do you think its luminescent properties are associated? What is the fate of the boron anhydride in this luminophor? At what temperature does this glass being to soften?

L.Ia.Markovskii: I cannot say anything regarding the fate of the boron at this stage. Neither the borate phase nor BPO_4 is evinced in the diffraction patterns. Of course, up to 5-10% of these may not be detected by x-rays. Most of the boron oxide can be extracted from the heated product, so that the remainder is essentially the phosphate phase. The luminescent characteristics change little as the result of such extraction. Apparently, the formation of borate glass plays some part in the transition to the glass-like system. As you know borate glass exhibits luminescence. Here we have a surposition of two factors: on the one hand, the formation of a crystalline phase and, on the other hand, a glass-like phase. We did not determine the softening temperature.

I.S.Rassonskaia: I would like to say a few words regarding the significance of the thermography method or differential thermal analysis in studying reactions occurring during heating of substances in solid state. The resultant curves in temperature vs time coordinates bring out all the transformations associated with evolution or absorption of heat and give the temperature of the transition points. Obviously, in order to determine the nature of the transformations one must have recourse to other methods (thermogravimetry, x-ray analysis, etc.). The thermographic method is particularly important in

the investigation of finely dispersed materials that do not yield clear diffraction patterns.

Formation of substances in the amorphous state is often observed in precipitation of solutions and in dehydration of crystal hydrates and hydroxides in the process of heating, processes not uncommon in the preparation of luminophors. The thermography procedure can also be used for establishing the phase composition of mixtures, particularly of mixtures of salts, when the Debye powder patterns have very many lines due to the low degree symmetry of the salt crystals.

The report on borophosphate luminophors we have just heard is very interesting, but unfortunately the investigators did not determine the composition of the phases forming in the process of heating mixtures of BPO_4 with metal oxides. It might be useful in this connection to utilize the thermographic procedure in conjunction with the phase diagrams of the corresponding binary and ternary systems.

A.A.Bundel': The reports we have just heard are devoted to a very interesting problem in the field of luminescence. It must be said that phosphate luminophors may be of great practical value. Their synthesis and determining their structure, however, are very complicated matters. The physics and chemistry of precipitates in equilibrium with the salt solutions are very complicated and have been far from exhaustively studied.

Most reports on the subject of these phosphors published hitherto have been devoted merely to the preparation procedure and have not been concerned with the physical and chemical relationships involved. This is why the studies carried out by the speaker are so interesting. They represent the beginning of investigation of these systems and make use of different methods to this end.

L.A.Markovskii's report contains very interesting data on the sensitizing action of boron oxide, which we were told was in a glass-like state. Did it act as a flux or was it an inactive participant in the luminescing system? We cannot tell now because the investigation has not been completed. We hope that the work will be successfully continued.

MANGANESE-ACTIVATED LITHIUM-MAGNESIUM TUNGSTATE PHOSPHORS (Abstract*)

- Iu.S.Leonov

We investigated the process of formation of the bright red luminescing lithium-magnesium tungstate phosphor activated with manganese utilizing the methods of thermal and x-ray analysis. We established that the lithium is an integral part of the crystallochemical system and that the phosphor cannot be regarded as a mechanical mixture of the tungstates of lithium and magnesium. This is proved by 1) the appearance of an endothermal effect in the heating curves of the three component mixture, 2) the appearance of new lines in the Debye powder patterns and 3) the absence of the luminescence characteristic of magnesium tungstate. At the same time lithium-magnesium tungstate phosphors prepared under optimal conditions, i.e., luminophors characterized by the highest luminance, always contain a certain amount of lithium tungstate as a separate phase. The presence of this phase is evinced by the endothermal melting effect, the exothermal crystallization effect and the appearance of additional lines peculiar to lithium tungstate in the Debye powder patterns.

We found that the temperature of interaction of tungsten trioxide with a mixture of the carbonates of lithium and magnesium is lower than the temperature of interaction of the trioxide with separate carbonates. We assume that the carbonates of lithium and magnesium form an intermediate compound which facilitates the reaction with the tungsten trioxide.

Comparison of the effects evinced in the heating curves of batches of different composition and the data of luminescent and x-ray analyses shows that the crystal phosphor is formed only at a relatively high temperature (740°). It is evident from the powder patterns that the lithium tungstate separates out only at about this temperature. The appearance of lithium tungstate in the liquid phase in the batch facilitates penetration of the activator (the manganese) into the base material.

Beginning with 740° (the melting point of lithium tungstate), there is observed a sharp increase in the luminescence brightness. The effect of an admixture of lithium tungstate on the luminescent properties of the phosphor is appreciably weaker if the phosphor is activated with manganese chloride; this manganese salt fuses at only 650°.

The flash characteristic of lithium-magnesium tungstate phosphors, that is observed when the highly heated phosphor is cooled, is due to presence of lithium tungstate, i.e., specifically to the rapid crystallization of this compound from the supercooled state.

We investigated in detail the dependence of the luminescence intensity of lithium-magnesium tungstate phosphor on the concentration of manganese and on the type of salt (chloride, sulfate, nitrate or carbonate) in which the activator is introduced. We found that systems with high concentrations of Mn are unstable in the sense that during slow cooling the excess Mn separates out.

We found that the optimal concentration of Mn (the concentration corresponding to maximum luminance) depends to some extent on the type of Mn salt used; in the case of the sulfate and nitrate the optimal concentration is lower than when the Mn is introduced in the form of manganese chloride. Furthermore, if manganese sulfate is introduced into the prepared base material, the optimal concentration is even lower. The observed difference between the optimal concentrations of Mn is due, we believe, to the fact that

---

*Complete report in "Proceedings (Materialy) of the Fifth Conference on Luminescence" Tartu, 1957.

if melting of the manganese salt does not occur, penetration of the activator into the depth of the host lattice is hindered and the interaction reaction occurs only in the surface layer. For this reason the surface concentration of ions becomes greater than in the case of introduction of the manganese in the form of the chloride. In the case of activation of the previously prepared base material with manganese sulfates penetration into the host lattice becomes even more difficult and hence the surface concentration is still greater. Thus the difference between the concentration of the activator in the initial batch and its actual concentration in the surface luminescing layer of the crystal is the greater, the more difficult the penetration of the activator into the depth of the crystal.

"P.N.Lebedev" Physical Institute of the
Academy of Sciences of the USSR

DISCUSSION

Question: What effect does the formation of Li_2WO_4 have on the luminescent characteristics of the crystal phosphor?

Iu.S.Leonov: Lithium tungstate has no noticeable influence on the properties of the crystal phosphor.

A.A.Bundel': Do you know the exact chemical and phase compositions of your luminophor?

Iu.S.Leonov: I cannot give the proportion of the oxides. Both lithium oxide and magnesium oxide are present. The composition of the batch was $2Li_2O \cdot MgO \cdot 1.26WO_3$ plus Mn.

A.A.Bundel': Your specimens consisted apparently not of a single chemical compound but of a mixture of two compounds. To which of them do you ascribe the luminescent properties?

Iu.S.Leonov: To lithium-magnesium tungstate activated with Mn.

A.A.Bundel': What were the excitation conditions and the spectral composition of the emission?

Iu.S.Leonov: The spectrum of the luminophor is a band peaking at 6680 Å. Without manganese the phosphor does not luminesce.

Question: What was the specific purpose of your work?

Iu.S.Leonov: Tungstate luminophors are activatorless phosphors. Our luminophor, on the other hand, was an activated one. The activator was manganese, hence this investigation from this viewpoint was of interest. Our main purpose was to clarify the character of the processes occurring during heating of the batch and the degree of participation of the different components in the formation of the luminophor lattice.

A.A.Bundel': How do you distinguish between the flash and thermostimulated luminescence?

Iu.S.Leonov: The flash is of a different color.

ON THE CAUSES RESPONSIBLE FOR THE DISTINCTIVE CHARACTERISTICS OF CADMIUM SULFATE CRYSTAL PHOSPHORS (Abstract*)

- G.V.Maksimova

We utilized the method of thermal analysis for investigating cadmium sulfate type crystal phosphors.

The heating curves of nonactivated cadmium sulfate, recorded on a Kurnakov pyrometer, showed five reversible endothermal effects at 500, 525, 730, 765 and 805°, corresponding to enantiotropic polymorphous transformations of the cadmium sulfate. In other words, cadmium sulfate can exist in several crystal modifications. After elimination of the crystallization water (200°) there form in turn an α-modification, a β-modification, which is stable in the temperature range from 500 to 730°, and a γ-modification. The latter is formed as a result of the first high temperature effect and in cooling readily goes over into the medium temperature β-modification.

We synthesized different luminophors on the basis of the different crystal modifications of cadmium sulfate. The data on the synthesis conditions and the properties of the different forms of $CdSO_4$:Mn are listed in the accompanying table.

In the synthesis of the high temperature γ-modification in the specimens must be cooled rapidly after heating to prevent transformation to the β-modification. In practice the cooling conditions are difficult to control and reproduce exactly, so that there is actually obtained a mixture of the two modifications with different colors of luminescence.

As a result of our thermal investigations, the cause of another distinctive feature of cadmium sulfate luminophors became clear. It was found that the β- and γ-modifications exist in an unstable state and even with minor heating undergo transformations, evinced in the thermograms in the form of exothermal effects: during heating the γ-modification gradually transforms into the β-form, the color of the emission becomes yellow-green, the brightness falls off and the luminophor darkens; with further increase of temperature the darkened specimen again becomes white and exhibits a rose luminescence. The β-modification during heating transforms into the α-modification.

Thus the changes in cadmium sulfate luminophors evinced by the instability and darkening of the luminophors during heating, the variability of the quantitative luminescent characteristics (non-reproducibility of the luminophor properties in repeat measurements) and the burning out of the phosphors under cathode excitation are due to internal transformations of the crystal lattice of the base material.

"P.N.Lebedev" Physical Institute of the
Academy of Sciences of the USSR

DISCUSSION

A.K.Trofimov: Did you photograph the luminescence spectra of the γ- and β-modifications of $CdSO_4$:Sm? If so what was the difference between them?

G.V.Maksimova: These spectra were not photographed. With visual observation they virtually do not differ as regards color.

A.K.Trofimov: And in the case of $CdSO_4$ activated with Pb?

G.V.Maksimova: We did not photograph the spectra of the Pb activated phosphor.

---

*Complete report in "Proceedings (Materialy) of the Fifth Conference on Luminescence" Tartu, 1957.

Conditions of synthesis and luminescence properties of $CdSO_4$:Mn crystal phosphors

Modification	Heating temperature, °C	Cooling procedure	Comparison of $t_{specimen}$ with the thermogram for $CdSO_4$ - $MnSO_4$	Luminescence under excitation by near ultraviolet	Afterglow after excitation by mercury tube	Afterglow persistence, hours	Appearance
$CdSO_4 \cdot H_2O$:Mn Single crystal hydrate	>150	Rate of cooling has no effect	After first water effect	Violet	----	--	Friable powder
α	210-550	----	After second water effect	White-yellow with violet hue	Whitish, weak	< 3	same
β	550-730	Rapid	After first medium-temp. endothermal effect	Yellow with violet undertone	Yellow-green	~ 3	same
γ	> 730	Fast (liquid nitrogen or water)	After first high-temp. endothermal effect	Rose, weak	Rose	~ 1	Hard sintered material

G.I.Guretskaia: What practical applications do these phosphors have?

G.V.Maksimova: These luminophors are of theoretical interest; they have no practical applications.

A.A.Bundel': You infer the existence of three different modifications of $CdSO_4$ only on the basis of the reversibility of the heating curve. Did you carry out x-ray studies and do you know anything regarding the phase structure?

G.V.Maksimova: The first stage of the investigation was thermal analysis. X-ray patterns were photographed, but their interpretation is very difficult in view of the large number of lines present. There are no data in the literature on the structure of $CdSO_4$.

A.A.Bundel': You stated that in each temperature interval there exists a given phase; in addition, each of them exists in two forms. How can this be?

G.V.Maksimova: Here there exist two stable forms. If we heat them gradually, then at a temperature of about 500° one of the forms is retained while the second will transform into one of the forms of the β-modification.

A.A.Bundel': Do you have any reason to assume that equilibrium is established under your conditions?

G.V.Maksimova: In the end equilibrium must be attained, but naturally one cannot be sure that it was established during such rapid heating.

A.A.Bundel': Did you carry out chemical analyses of your products? Isn't the darkening connected with decomposition of the cadmium sulfate?

G.V.Maksimova: The chemical composition was not checked; however, cadmium sulfate without an activator does not darken. All the basic salts of cadmium sulfate decompose at the temperatures under 500°.

A.M.Kalinina: Did you obtain all three modifications in the pure form at a given temperature with prolonged heating?

G.V.Maksimova: For obtaining a given modification the duration of heating is not important. Obtaining the γ-modification in pure form at room temperature is rendered difficult by the reverse transformation to the β-modification.

A.M.Kalinina: Please explain the nature of the endothermal effect in the region of high temperatures.

G.V.Maksimova: As a result of the first and second high temperature effects the two forms of the β-modification go over into the two forms of the γ-modification. The last at one and the same temperature (810°), go over into a new modification.

D.N.Korf: The diverse experimental techniques and procedures developed by the speaker are of great interest, but unfortunately until now I have never heard of phosphors based on $CdSO_4$. While I do not doubt the value of the investigations carried out by Comrade Maksimova, I feel that it would be better if an equal amount of attention were given to questions of investigating say cadmium sulfide; I'm sure that many of my colleagues at the Plant would be grateful to the author for such a study.

DISCUSSION OF THE REPORTS OF Iu.S.LEONOV and G.V.MAKSIMOVA

M.A.Konstantinova-Shlezinger: The work we are now doing is aimed at the solution of the problems, without an understanding of which we cannot be of real help to industrial chemists in the matter of synthesis of luminophors. This indirect way may still be the shortest one when it comes to a solution of practical problems.

M.V.Grigor'ev: Workers in industry attentively follow reports presented at different scientific and technical conferences for the purpose of utilizing new advances and discoveries in industry. This fact should be borne in mind

in organizing such scientific conferences. Recently even conferences on purely theoretical questions have been set up with a view to helping industry solve its practical problems. If we view our present conference from this standpoint, I feel, that it is not satisfactory.

Crystal phosphors are now widely used in industry, in the production of tubes for television and oscillography, in the production of fluorescent lamps and so on. The program of our conference, however, does not include a single report that summarizes the experience gained in industry, that gives the methods and procedures of measuring the basic parameters of industrial crystal phosphors and indicates the important avenues of research necessary for the solution of problems posed by the Sixth Five Year Plan as regards development of black-and-white and color television, fluorescent lamps, etc. I feel that this is a serious gap in our program. Although we have heard individual reports touching upon industrial problems, they have not given us the complete, over-all picture. I would also like to call attention to the absence in most reports of suggestions as regards practical utilization of the experimental or scientific results obtained. This may be explained by the insufficiently careful selection of crystal phosphors for investigation (i.e., selection of phosphors that have no value for practical applications) and the fact that many investigations are undertaken without a specific, utilitarian purpose in mind.

I hope that the organizing committee will take these observations into account in arranging future conferences and that organizations working on the development and investigation of crystal phosphors will be more cognizant of the needs of industry in planning their research work.

A.A.Bundel': Both investigations are of great interest as examples of consistent application of one of the methods of physical-chemical analysis to elucidation of the structure of luminophors. It should be noted, however, that the speakers concentrated their attention on reactions occurring in the initial batch during the irreversible formation of the luminophor and did not adequately investigate the final products. Some of the details reported by the speakers give reason to assume that in a number of cases the effects observed by them were due to the fact that the investigated systems were in an unstable state, which should be taken into account in further studies.

CALCIUM SULFATE PHOSPHORS (Abstract*)

- B.M.Nosenko, L.S.Revzin & V.Ia.Iaskolko

We investigated the properties of $CaSO_4$ phosphors under electron excitation and also under γ- and β-irradiation. The thermoluminescence of $CaSO_4$:Mn was investigated in particular detail.

Cadmium sulfide activated with Co, Fe, Mg, Tl and Ag yields a weak greenish emission with different undertones; activation with Pb results in blue, with Zn in light blue, with Ni in orange-red, and with Mn in bright light-green luminescence. Thus $CaSO_4$ base phosphors with emission in any part of the visible spectrum can be prepared.

There are very few crystal phosphors capable of storing light sums under cathodoexcitation. $CaSO_4$ with all activators exhibits thermoluminescence after electron, γ- and β-excitation. The greatest storage capacity is possessed by $CaSO_4$:Mn. We determined the optimum activator concentrations and heating conditions. We also investigated the dependence of the light sum storage on the energy of the electrons and the charge on the screen in the case of cathodoexcitation. We tested the phosphors for the time of storage of the light sums at different temperatures.

The shape of the thermostimulation curves indicates that the luminescence mechanism is a recombination one. We determined the depth of the storage levels and checked some of the deductions of the theory of thermal de-excitation (thermostimulation).

The $CaSO_4$:Mn phosphor has been used as a dosimeter.** The radiation dose was determined from the maximum brightness of the dosimeter screen under thermostimulation at a given heating rate. With the use of an appropriate photomultiplier and galvanometer one can determine doses from 0.005 to hundreds of roentgens with a dosimeter screen having an area of only 1.5 cm^2. One of the advantages of utilizing $CaSO_4$:Mn for radiation monitoring purposes is the insensitivity of the material to visible light.

"V.I.Lenin" Central Asian State University

DISCUSSION

D.M.Korf: What is the loss of the stored energy?

L.S.Revzin: At 20° the phosphor loses approximately 30% of the stored light sum over a period of 72 hours; at a temperature of 30° it loses approximately 50%, but after 3 days the rate of loss is much lower.

Kamenskaia: When you discuss the question of whether the luminescence is mono- or bimolecular, you took as one of the criteria the flatness of one of the branches of the thermoluminescence curve. This indication can be used if the peak is an elementary one; if this is not the case the criterion is not valid.

L.S.Revzin: We checked the elementary character of the peak. Before carrying out these thermal de-excitation measurements, we de-excited the specimen with the stored light sums at different rates of heating (from 0.05° per sec to 20° per sec). We found no evidence that this was not an elementary peak.

---

*Complete report in "Optika i spektroskopiia", 3, No.3 (1957).

**V.V.Antonov-Romanovskii et al, Session of the USSR Academy of Sciences on the Peaceful Uses of Atomic Energy, 1-5 July, 1955.

Kamenskaia: I have very reliable data indicating that this is not an elementary peak. You also said that one of the criteria is the rate of the rise or falling off of the curve. How, in the given case, did you excite the phosphor?

L.S.Revzin: In the given case, it was β-excitation.

Kamenskaia: Then the question does not apply. We tested this phosphor as regards its suitability for dosimetry and came to somewhat more modest conclusions. We found that its sensitivity changes by almost a whole order of magnitude, depending on the exciting radiation. Furthermore, it does not have very good thermal characteristics. This phosphor does have one advantage: it is simple to prepare and does not require the use of an expensive activator, namely, europium. Still its sensitivity is inferior to phosphors with europium.

Question: Did you check the aging of the phosphor after repeated heating?

L.S.Revzin: Yes, and no noticeable aging as such was observed. However, at a very high electron density the luminescence intensity was somewhat weakened.

INVESTIGATION OF TRAPPING CENTERS AND THE KINETICS OF RELAXATION PROCESSES IN ALKALI HALIDE CRYSTAL PHOSPHORS (Abstract*)

- Ch.B.Lushchik, F.N.Zaitov, V.Ia.Kark, L.A.Teiss & I.V.Iaek

In the present investigation we attempted to clarify the role of trapping center of different types in the recombination luminescence of alkali halide phosphors through a comprehensive study of excited absorption, the excitation spectra of optical flashing, thermostimulation, thermobleaching and thermo-optical stimulation.

The centers involved in thermostimulation and optical flashing are the trapping centers of the base material (F, F', M, O, P and similar centers) and the trapping centers produced by bivalent impurities (Ca^{2+} and Sr^{2+}). The number and characteristics of centers of this type can be substantially altered by plastic deformation and heat treatment of the crystals. In studying such centers it is essential to take into account the ionic processes occurring under certain conditions in crystal phosphors.

We investigated the influence of a number of activators (Ag^{+}, Cu^{+}, Tl^{+}, Pb^{2+} and Mn^{2+}) on the spectrum of excited absorption, the thermostimulated emission and the thermobleaching of NaCl and KCl base phosphors. A particularly large number of electrons is stored in phosphors with two activators (for example, NaCl:Ca:Ag). The activator trapping centers are also manifested in recombination luminescence, their contribution, however, is frequently masked by temperature quenching.

The details of the mechanism of recombination luminescence of alkali halide phosphors are still far from clear. The commonly hypothesized ionization mechanism cannot explain a number of experimental facts.

Investigation of the relaxation of excited absorption in alkali halide phosphors showed that the distribution of electrons and holes over the trapping levels changes substantially during the rise and decay of luminescence The principal factor here is the complicated character of the relaxation processes in crystal phosphors.

The equilibrium distribution of electrons and holes over the trapping levels that is established as a result of prolonged excitation with x-rays is temperature dependent. Investigation of the negative excited absorption made it possible to evaluate the degree of occupation of the trapping levels by electrons. The degree of filling of some levels is high ($\sim$30%) but is far from complete. By direct experiment we showed that the principal reason for the absence of complete filling of the trapping levels and for the temperature dependence of the equilibrium distribution of electrons and holes is the de-exciting effect of x-rays.

Under conditions of strong excitation, in alkali halide phosphors the probability of retrapping is lower than the probability of recombinations. It was found that the ratio of the cross sections for trapping and for recombination decreases with decreasing temperature. In some cases the decrease in the value of this ratio is more rapid than follows from the diffusion theory of phosphorescence.

Under certain conditions alkali halide phosphors become similar to an ideal phosphor with trapping levels of only one depth. Under these conditions the relaxation process may be regarded, at least approximately, as a first order reaction. The order of the reaction was determined by direct experiments

---

*Complete report in "Proceedings (Materialy) of the Fifth Conference on Luminescence" Tartu, 1957.

by independent recording of the curves characterizing the relaxation of the brightness of the luminescence and the number of stored electrons.

Institute of Physics and Astronomy
of the Estonian SSR Academy of Sciences
and Tartu State University

DISCUSSION

Question: What is the mechanism of migrational luminescence of phosphors?

Ch.B.Lushchik: Apparently, the energy that is released in the recombination of electrons with localized holes and of holes with localized electrons may be transferred to nearby activator ions. This mechanism does not require ionization of the activator as a result of excitation; the fact that such ionization does not always occur follows from the experiments with NaCl::Mn. The Mn here is bivalent. Could it possibly be further ionized during excitation? Nevertheless, when an x-irradiated specimen of NaCl:Mn phosphor is illuminated in the F-band, there is observed luminescence clearly due to the Mn ions. In view of this and other experiments we feel justified in advancing the proposed mechanism as one of the possible hypotheses.

F.I.Vergunas: The speaker inferred that there are contradictions between the results obtained by his group and those of the group of Tomsk physicists. Actually there are no contradictions. 1. We investigated the elementary decay law. To this end we chose phosphors in which the afterglow is determined by trapping levels of one type and the luminescence by emission centers, also, of one kind. In investigating the phosphorescence of such phosphors we show that the decay law even for such an "ideal" phosphor is determined by the value of the parameter γ and the stored light sum. The speaker and his coworkers investigated phosphors in which there were simultaneously operative a number of different kinds of trapping levels and showed that the decay law is integral and that in the process of luminescence the electrons are redistributed over trapping levels of different depths. 2. The speaker showed that γ increases with increasing temperature. According to our concepts γ decreases in the quenching region. The speaker and his colleagues did not measure γ in the quenching region; consequently, their results do not conflict with our concepts.

I would like an answer to the following question. You showed that for alkali halide phosphors $\gamma < 1$; consequently, the decay curves must be exponential. V.V.Antonov-Romanovskii's doctor's dissertation showed that the decay curves of these same phosphors can be interpreted from the viewpoint of a simple bimolecular reaction. How do you reconcile the absence of retrapping ($\gamma < 1$) and the simple bimolecular luminescence scheme?

Ch.B.Lushchik: In my report I indicated that the Tomsk group does not fully take into account the factors, examined by Jones, leading to complication of the relaxation processes. The discussion of the report of F.I.Vergunas and her coworkers showed that there is some question regarding the elementary nature of the decay laws observed by them. In particular, it is doubtful that in the region above 100° Gasting was dealing with release of electrons from trapping levels of only one kind.

The conflict between our results regarding the temperature dependence of γ and the results of the Tomsk group is only apparent. I feel that in principle γ can either increase or decrease with the temperature. Moreover, our results were obtained for different phosphors.

NATURE OF TRAPPING LEVELS IN ZnS:Cu:Co PHOSPHORS AND THEIR FILLING UNDER DIFFERENT EXCITATION CONDITIONS (Abstract*)

- V.L.Levshin & V.F.Tunitskaia

We utilized the thermostimulation procedure for investigating the variation of the magnitude and distribution of light sums in ZnS:Cu:Co phosphors among levels of different types and depths, as a function of the duration of excitation and the wavelength (312, 366 and 436 mμ) of the exciting light. The principal results were the following.

1. The probability of filling of the given group of trapping levels with excitation by light of a given wavelength depends not only on the depth of the levels but on their origin**.

Specifically, in ZnS:Cu:Co with excitation by the 366 mμ line the deepest levels (50 and 80°) associated with Co are filled first; in ZnS:Zn heated in air both the groups of levels present (the level emptying at -130°, due to Zn, and the -60° level, due to oxygen) are occupied at the same rate; in ZnS:Cu phosphor heated in H_2S the probability of filling of the shallowest group of levels (-130°), due to zinc, is appreciably greater than the probability of filling of the deeper (-100°) group, due to compounds of copper with sulfur.

2. The wavelength of the exciting light has a very strong influence on the distribution of electrons among the levels of different depths which, in our opinion, is explained by the stimulating (de-exciting) or quenching influence of the exciting light.

3. In the case of preferential filling of the shallow levels and the presence of a large number of unfilled deeper levels, we did not note transfer of electrons from the shallower to the deeper levels during thermostimulation.

4. Investigation of phosphors illuminated simultaneously with the exciting light by longer wavelength quenching light showed that the long wave radiation has a stronger effect on the electrons located at the shallower levels. In the process some part of the optically released electrons is transferred from the shallower to the deeper levels (i.e., under the influence of the longer wavelength light the electrons released from the shallower levels are retrapped in the deeper lying ones).

"P.N.Lebedev" Physical Institute of the
Academy of Sciences of the USSR

DISCUSSION

Question: In what way do your data differ from those of Hoogenstraaten who in 1953 investigated the same phosphor under similar conditions and by the same procedure?

V.F.Tunitskaia: Hoogenstraaten's experiments were carried out at a heating rate of 3° per sec (or 180° per min). Under these circumstances, as Lushchik showed, the "resolving power" of the method is greatly reduced. Hence instead of the actual very complicated curve, Hoogenstraaten obtained a glow curve with only one or two peaks. Moreover, Hoogenstraaten did not investigate the dependence of the thermal de-excitation on the wavelength and intensity of the exciting light, which precisely was one of the more important aspects of our investigation.

---

*Complete report in "Optika i spektroskopiia", 2, 350 (1957).

**A report by A.A.Cherepneva and the present authors, published in "Optika i spektroskopiia" 1, 255 (1956), is devoted to clarification of the nature of the trapping levels in the investigated ZnS:Cu:Co phosphors.

ON THE FORMATION OF TRAPPING LEVELS IN ZnS:Mn PHOSPHORS (Abstract*)

- V.L.Levshin & B.D.Ryzhikov

We investigated the localization levels in ZnS:Mn phosphors under different excitation conditions and with different activator concentrations by the method of glow curves.

The thermostimulation curves for the blue luminescence of the wurzite modification of ZnS:Mn furnished evidence of four systems of trapping levels. The position of the glow curve peaks for the shallower levels depends on the activator concentration: with increasing Mn concentration, the peaks are shifted to the side of lower temperatures. Where the deeper levels are concerned the effect of concentration is more difficult to bring out in view of the appreciable overlapping of the thermostimulation bands. The relative development of the thermostimulation bands is strongly dependent on the Mn concentration. The deepest levels attain their maximum development at an Mn concentration of $3 \cdot 10^{-5}$ g/g.

The glow curves for the orange luminescence have an additional peak at 265°K. The relative development (intensity) and position of the orange luminescence temperature bands is also strongly dependent on the Mn concentration.

The complex character of the dependence of the relative strength of the individual thermostimulation bands on the activator concentration is explained by the fact that, in addition to replacing the zinc in the crystal lattice, the manganese can lodge at lattice defects. In general, substitution for zinc occurs at high concentrations of Mn, while at low concentrations the Mn lodges primarily at the defects. This distribution of the manganese leads to ordering of the electric field inside the crystal; in consequence, the absorption of the crystal in the visible region should decrease. A study of the spectra of diffuse reflection confirmed the existence of this effect. With the introduction of Mn, the absorption decreases up to an Mn concentration of 10^{-4}; an increase in absorption due to manganese ions becomes apparent only at higher concentrations.

Department of Physics of Moscow State University and
"P.N.Lebedev" Physical Institute of the Academy of Sciences of the USSR

DISCUSSION

N.V.Zhukova: Does the position of the peak of the zinc band in your ZnS:Mn phosphor coincide with the position of the zinc band in ZnS:Cu?

B.D.Ryzhikov: We compared the position of the zinc band only with the data of other investigators; in general there was good agreement.

M.V.Fok: Cannot the difference in the magnitude of the light sum storage be explained by the different de-exciting effect of the exciting light?

B.D.Ryzhikov: It can hardly be explained by this factor alone.

F.M.Pekerman: Does what you term "sensitization" occur at a high manganese concentration?

B.D.Ryzhikov: No, the effect is observed at a low Mn concentration. I showed the curves obtained for the phosphor with an optimal concentration of Mn for the pale blue luminescence. At this concentration the manganese does not form luminescence centers. Or, in any case, no orange emission is observed.

V.V.Antonov-Romanovskii: The report presented by B.D.Ryzhikov is of

---

*Complete report in "Optika i spektroskopiia" 3, No.6 (1957).

interest, for this is apparently the first investigation in which there has been detected for ZnS:Mn a decrease of the absorption of the base material in the region of the long wave absorption edge as a result of introduction of the activator.

Inasmuch as the absorption is ascribed to lattice defects, the decrease in absorption indicates a decrease in the number of defects. The speaker explains this by the lodging of manganese at these defects. One can also hypothesize a different mechanism.

Inasmuch as the phosphors in question had a hexagonal structure, it may be assumed that in cooling, even rapid cooling, the hexagonal structure is not fully frozen. Inasmuch as Mn favors stability of the hexagonal form, the presence of Mn reduces the fraction of cubic structure, distorting the hexagonal one.

The speaker showed us a diagram with two glow curves - the blue and orange (manganese) bands of the ZnS:Mn phosphor. The curves are similar in the region of the first two peaks, while the third peak is present only in the orange emission, which can be explained by quenching of the blue band. The similar character of the curves (up to quenching) shows that the recombination cross sections for the blue and red luminescence spectra are equal. From this it follows that if the ionized manganese luminescence center is an excess positive charge in the phosphor lattice, there must also be present in the lattice an ionized blue luminescence center. This is an interesting point where understanding of the nature of blue luminescence centers is concerned.

Ch.B.Lushchik: The report we have just heard is of great interest. I would like to make one remark however. There have been numerous studies of the thermostimulation of ZnS phosphors. Many of them are characterized by conflicting interpretations of the results. I feel that this is not accidental.

Thermostimulation alone is not sufficient for obtaining unambiguous results. Glow curve data are often appreciably distorted by temperature quenching. The influence of temperature quenching must be taken into account, for example, in interpreting the "copper" thermostimulation peak. I feel that only comprehensive, all-round investigation of trapping centers can lead to a consistent, unambiguous interpretation of the data. One must make joint use of the methods of excited absorption, thermal bleaching and thermooptical stimulation. These methods are qualitatively applicable to powders as well. Highly suitable for working with powders is a variant of the Bull & Mason procedure with the use of "peak-like heating" which was earlier used by us for testing the elementary nature of thermostimulation peaks.

F.I.Vergunas: In phosphors in which the afterglow is determined by trapping levels of one depth the decay law is hyperbolic. You appear inclined to regard this hyperbola as a result of superposition of exponentials. Why do you think it is not possible to explain the hyperbola by the fact that the electrons undergo repeat localizations (retrapping) at levels of the same depth as those from which they were released? In this case the decay curves will be approximated by hyperbolas.

V.L.Levshin: Admittedly the explanation of the character of the decay as a superposition of exponentials is a hypothesis, but I see no other way of explaining the hyperbolic character of the decay. Phosphors containing only one system of levels have been investigated and still the decay curves were hyperbolic.

If we don't admit the possibility of retrapping of electrons at levels of other depths, it is hard to admit repeat localization at levels of the same depth. Return of electrons to the former level will slow down the decay, but the exponential character of the curve will persist.

Ch.B.Lushchik: ZnS phosphors differ from alkali halide phosphors in that the width of the forbidden energy band and the separation of all the other energy levels in them are smaller than in NaCl or KCl. The trapping levels in ZnS phosphors are also probably more closely spaced than in NaCl. This makes more probable the hypothesis that the thermostimulation peaks in these phosphors are not elementary ones. G.M.Eliashberg showed that for a phosphor with two groups of levels the decay law is very complicated. He proved that in the presence of several levels the inflexions and bends in the decay curve are smoothed out.

Apparently, by virtue of the complicated distribution in energy of the trapping levels in these phosphors, the decay law for them is relatively simple. In alkali halide phosphors with a more "rarified" system of trapping levels, the integral decay law proves to be more complicated than for ZnS phosphors with their close-lying trapping levels.

In my opinion Becquerel's experimental law is not an elementary but an integral law.

INVESTIGATION OF THERMOSTIMULATED EMISSION OF CRYSTALLINE QUARTZ EXCITED BY X-RAYS (Abstract*)

- L.G.Chentsova, B.N.Grechushnikov & E.N.Batrak

A correlation has been noted in recently published reports between thermal bleaching of the smoky coloration of x-rayed quartz and the thermoluminescence effects occurring in the same temperature interval.

So far the nature of the trapping centers responsible for these effects has not been definitively established. There is no doubt, however, that the formation of these trapping centers is associated with lattice defects due to the introduction of extraneous ions in extremely minute amounts. Investigation of the paramagnetic resonance spectra of smoky and noncolored quartz showed that such ions may be Al^{3+} replacing Si^{4+} The resultant charge defect or deficiency, according to O'Bryan, is compensated for by the alkali ions.

To check the various hypotheses where thermoluminescence is concerned, we investigated the temperature stimulated emission of x-irradiated specimens of natural quartz from different deposits (locations) and hence, presumably, having different compositions and amounts of impurities. Good reproducibility of the glow curves for specimens cut from the same crystal was obtained. The glow curves for specimens prepared from crystals from different locations differed both as regards intensity of luminescence and the number and temperature-positions of the peaks. This, in our opinion, indicates that impurity ions of different types are responsible for the formation of the trapping centers.

The alkali "compensating" ions have an undoubted influence on the thermostimulated emission. We have reason to assume that these alkali ions are found in the structural "channels" of the quartz. It is known that in an electric field at high temperature alkali ions readily migrate in quartz along these channels. As a result there presumably occurs a replacement of the ions initially present in the channels by ions arriving from the anode.

Our tests showed that after migration of Li^+ and Na^+ ions through the quartz, the quartz does not lose its ability to become colored under the influence of x-irradiation. The absorption spectra of specimens x-rayed after introduction of Li^+ and Na^+ are very similar, while their glow curves differ greatly. In the case of specimens yielding two thermostimulation peaks prior to the introduction of Li^+ or Na^+ ions, one at 175° and the other at 290°; after introduction of Li^+ the peak at 175° becomes appreciably higher, while the peak at 290° remains unchanged. After introduction of Na^+ into identical specimens and subsequent x-irradiation the peak at 175° vanishes, while the position of the high temperature peak remains the same.

Thus our investigation showed that impurity ions, producing charge defects in the crystal lattice, and ions, initially present in the structural channels of the quartz and compensating these charge defects, play a significant role in the formation of trapping centers in quartz under the influence of x-rays.

Institute of Crystallography of the
Academy of Sciences of the USSR

---

*Complete report in "Optika i spektroskopiia", 3, No.4 (1957).

DISCUSSION

V.L.Levshin: How do you picture the mechanism of the formation of two systems of levels? You have one maximum at 175°; this maximum is weakened, becomes lower. How do you explain the appearance of the second maximum? Do we have here a competition process, i.e., are the electrons released from the lattice first localized at the 175° level and then localized at deeper levels or do we have here a process of successive excitation?

L.G.Chentsova: I believe that there is competition here, because in the case of quartz from one particular location we have a sharply pronounced maximum at 175°, while in the case of quartz from another location (Volyn') we have a peak at 290°.

Ch.B.Lushchik: What are the luminescence centers? Do you associate all the trapping centers with the impurities or only part of them?

L.G.Chentsova: At present we cannot draw any definitive conclusions. As you know, analysis of quartz is very difficult. Attempts to analyze quartzes, both colored and not colored, gave a very diffuse picture. The principal impurity elements in natural quartz are aluminum, lithium, sodium, potassium, manganese and magnesium. I don't know to what extent the rare earths may be present.

V.L.Levshin: How do the quartzes from different locations, differing appreciably as regards impurities, behave optically? What is their transparency?

L.G.Chentsova: We investigated the optical transmission of quartz only to 250 mμ.

G.M.Komovskii: There are types of quartz that do color and other types that do not color under irradiation; it is difficult to distinguish between them a priori. There is also the time factor: possibly most quartzes will color under prolonged x-irradiation.

L.G.Chentsova: It is true that most quartzes do become colored, but there are some that do not; for example, Marmora "diamonds" do not become colored even after 300 hours irradiation.

Ch.B.Lushchik: What are the excited absorption spectra of these quartzes like?

L.G.Chentsova: The absorption spectra of the different specimens are virtually undistinguishable.

F.D.Klement: Physicists investigating trapping centers were (at least until now) interested primarily in the kinetics of the process, the energy characteristics, and payed little attention to the chemical nature of the centers. The investigation reported on by L.G.Chentsova is of interest because here we have the first approach on the part of crystallographers to determining the nature of trapping centers. This approach must be applauded and investigations in this direction continued because it is important to know what trapping centers are in each specific case, if only from the point of view of practical control, of knowing whether they can be artificially created or, on the contrary, liquidated.

V.L.Levshin: I feel that one aspect of this very interesting series of experiments has not been sufficiently developed, namely, investigation of the relation between the optical properties of the specimens and the shape of the glow curves. Quartz is of particular interest because it is optically transparent. It would be desirable to have quartzes from different locations, activated with different impurities, compared as regards their optical characteristics in order to establish how the transparency varies with the nature of the impurities and at the same time to see how these impurities can be detected on the basis of the thermostimulated emission curves.

LUMINESCENCE OF CRYSTAL PHOSPHORS UNDER EXCITATION BY IONS (Abstract*)

- B.M.Nosenko, N.A.Strukov & M.D.Iagudaev

There have been very few studies devoted to investigation of the luminescence of phosphors under excitation by low-energy (under 10-50 kev) ions. Aside from their intrinsic interest, such investigations may be of value as a method of studying the interaction of ions with matter.

Our study was concerned primarily with Zn_2SiO_4:Mn, but we also investigated ZnS:Ag, $CaSO_4$:Mn, CuS and CdS:Cu and the sublimate phosphors KI:Tl, NaI:Tl and $CdBr_2$ and CdI_2 activated with Mn and Pb. The excitation was effected with positive Li, Na, K, Pb and Cs ions of energies from 0.5 to 6 kev. The basic procedure was comparison of the ionoluminescence with the cathodoluminescence.

Results

The spectral composition of the ionoluminescence does not differ from the emission under electron excitation. Further, the spectra of a "fresh" phosphor and a phosphor subjected to prolonged ion bombardment are identical. The brightness is proportional to the density of the ionic current and is linearly dependent on the ion energy.

The yield of ionoluminescence depends on the mass of the bombarded ions. In the case of willemite it amounts to 4% relative to the cathodoluminescence output with excitation by Li^+ and approximately 0.5% of the cathodoluminescence yield with excitation by Cs^+. The efficiencies differ somewhat for different phosphors.

The rate of deterioration of the luminescence (aging of the phosphor) depends on the irradiation density. The rate of aging also differs for different phosphors but does not depend on the activator concentration. Zinc sulfide phosphors are most subject to aging; alkali halide sublimate phosphors are least subject.

We developed a method for determining the depth of the damaged layer, i.e., the depth of penetration of the ions into the crystal. The procedure is based on comparing the measured energy dependences of the luminance under electron excitation of the ion irradiated phosphor and of a "fresh" phosphor. It was found that the depth of penetration is proportional to the ion energy and that in Zn_2SiO_4:Mn it is approximately 3 Å/kev for Na^+, K^+ and Cs^+ and about 9 Å/kev for Li^+ ions. We evaluated the ionization produced in the phosphor on the basis of the range of the ions and the light yield of ionoluminescence. The thickness of the nonluminescing layer of a "fresh" phosphor was evaluated to be about 2.5 A.

The procedure allows of evaluating the value of the coefficient γ of cathode sputtering of the phosphor. At an ion energy of 1.2 kev $\gamma \approx 1.6$ molecules per ion with irradiation by Na^+ and $\gamma \approx 3$ molecules per ion with bombardment by Cs^+. Lastly, we suggest a scheme of the process of aging of the phosphor and propose a mechanism of the ionization produced by heavy particles in a solid.

"V.I.Lenin" Central Asian State University

---

*Complete report in "Optika i spektroskopiia", 3, No.3 (1957).

DISCUSSION

V.L.Levshin: Did you observe reversible effects, that is, fatigue of the phosphors? You spoke of destruction or damage, yet before we have actual destruction of the crystal there may be weaker alterations. How do the alterations occur over the depth? Are they the same throughout the thickness? Are deeper layers damaged less?

B.M.Nosenko: We observed no fatigue. There is, however, irreversible aging immediately after irradiation even with a small quantity of ions. The damage does not heal even after hours and days and in the case of some specimens even over a period of a year, except for the disruption produced by lithium ions. In the case of lithium bombardment there is observed partial healing, to the extent of about 30%.

The ions do not produce uniform damage. Hence I spoke of the effective depth of destruction. Disruptions may occur to a great depth; in the upper part of the affected layer the phosphor loses the ability to luminesce; in the lower part the damage may be only partial. The variation is approximation linear.

L.M.Shamovskii: Actually in the process of ionic bombardment under vacuum you apply a certain amount of extraneous material to your luminophor. What happens in this case? Is there formed a layer which makes the luminescence invisible? Do the particles penetrate into the luminophor? I think it would be helpful if you would describe the experimental setup.

B.M.Nosenko: The apparatus consisted of an ion source, a focusing system, a detecting section, a screen and a heater. After the ion measurements an electron beam was directed on the same spot. The pressure was of the order of 10^{-6} mm Hg. You say that since we are dealing with ions it may be assumed that a deposit is formed. A 90% loss in luminance is produced with an irradiation density appreciably lower than that required to obtain a monomolecular coating. Hence there can be no question of a deposit forming on the phosphor. Concurrently with any deposition with ions, we have cathode sputtering, in the process of which each ion disperses several molecules, according to our measurements. In fact, ion irradiation removes a surface layer from the phosphor.

L.Ia.Markovskii: How do you explain the loss of radiance?

B.M.Nosenko: Upon impact there occurs displacement of the ion sites and the crystal lattice is distorted. The ability to luminesce is closely associated with ordering of the crystal lattice. This is one mechanism. Another mechanism, proposed by Seitz, is that when an ion hits the screen its energy is transformed into that of local heating. Local melting or even vaporization may occur. The resultant effect is the same - the lattice structure is distorted.

L.M.Shamovskii: I don't quite see how the disruption occurs. You noted that not only do the ions strike the surface but at the same time the surface of the phosphor is renewed due to sputtering. Do the ions penetrate into the depth to any extent? Did you investigate how much material penetrates into your phosphor by chemical or other means?

B.M.Nosenko: It is a question here of such insignificant amounts that I doubt whether chemical analyses could yield any useful information. Do the ions penetrate into the crystal? That the ions excite the phosphor is a fact: the phosphor luminesces. That the ions cause disruption or damage is also a fact; if the exciting ion beam has a sufficient energy the irradiated area appears dark. Whether the ions remain on the surface or penetrate further into the bulk, our measurements so far do not indicate, and this is not parti-

cularly important. What is important is to know what effect the ions produce, how their energy is transferred to the crystal lattice.

L.M.Shamovskii: Did you eliminate the possibility of simultaneous influence of ions and electrons?

B.M.Nosenko: We have magnetic analysis: the electrons are deflected to one side, the ions to the other, so there can be no doubt regarding the results.

Question: Did you try heating the specimens after irradiation?

B.M.Nosenko: In the case of damage by lithium ions a partial healing occurred upon heating to 600°. There was no noticeable healing of the damage caused by sodium and potassium ions.

* * * * * *

IMPROVING THE QUALITY OF LUMINOUS COATINGS IN FLUORESCENT LAMPS (Abstract*)

- B.M.Gugel' & M.M.Shapochnik

The principal luminophors used for fluorescent lamps are a mixture of magnesium tungstate and zinc-beryllium silicate activated with Mn ("white mixture") and calcium halophosphate activated with Sb and Mn. Luminophor coatings of the white mixture have a lower efficiency and inferior operational stability. The decrease in efficiency is a result of a photolytic reaction in the zinc-beryllium silicate under the influence of 1850 Å ultraviolet radiation. Stability is higher with higher concentrations of Mn and is also higher in phosphors with a higher value of the ratio $(ZnO + BeO)/SiO_2$. This indicates that there are formed quenching centers, that compete with the luminescence centers, in the acid component of the luminophor under the influence of 1850 Å ultraviolet.

Phosphor coatings of calcium halophosphate are very stable under the influence of both 2357 A and 1850 Å light in an oxidizing atmosphere. In a reducing atmosphere, however, there occur chemical reactions leading to decomposition of the luminophor; hence the presence of H_2O and CO_2 which dissociate under the influence of 1850 Å irradiation with the formation of H_2 and CO, respectively, leads to an appreciable loss of efficiency of the calcium halophosphate coating.

We investigated the influence of different factors in the synthesis of calcium halophosphate on its stability. Composition of the luminophor batch and, particularly, the presence in it of hydroxylapatite have a strong effect on the stability of calcium halophosphate. The most stable are luminophors with a high value of the ratio R (the ratio of the sum of the basic oxides to the PO_4 content) and a sufficiently high content of antimony soluble in HCl. The best results were obtained with $R \approx 1.64$ and $Sb_{sol} \approx 0.8\%$. The amount of soluble Sb in the $R \approx 1.64$ phosphor depends on the amount of hydroxylapatite impurity present in the initial $CaHPO_4$ and is maximal when the last is absent.

The stability of luminophors with $R < 1.64$ decreases despite the good solubility of Sb in the more acid base, while with $R > 1.64$ the stability falls off due to the sharp decrease in the solubility of Sb, which in this case separates out in the form of calcium antimonate. When the content of soluble Sb in the luminophor is increased above 1%, the stability and brightness de-

---

*Complete report in "Proceedings (Materialy) of the Fifth Conference on Luminescence", Tartu, 1957.

crease due to concentration quenching. The temperature of formation of the phosphor has an appreciable influence on the amount of soluble Sb in the luminophor with R $\approx$ 1.64 and on its stability. The most stable phosphors are obtained at heating temperatures $\geqslant 1200^{\circ}$, although the luminance differs little for luminophors prepared at temperatures in the interval from 1050 to 1200°.

The Mn content and the ratio F:Cl in the luminophor determine the spectral composition of the luminescence of calcium halophosphate but have no appreciable effect on its stability. With F:Cl $\approx$ 3.5 there are obtained luminophors that, through appropriate variation of the Mn content, can be used for fabricating fluorescent tubes with any desired color temperature in the range from 6500 to 2800°K.

In the process of applying the phosphor layer to the glass envelope an important role is played by peptization of the luminophor particles in suspension.

* * * * * *

ON THE CHOICE OF LUMINOPHORS FOR TELEVISION SCREENS (Abstract*)

- B.M.Gugel' & I.S.Veksler

Generally pairs of luminophors with complimentary emission colors are used for black-and-white television screens. In view of the large number of different phosphors available, different combinations are possible and for effective choice of a pair it is necessary to check the components as regards chromacity, saturation with respect to current under raster excitation and stability. The selected pair of components must also assure a high luminescence efficiency, the possibility of uniform application to the substrate, and, in the case of projection kinescopes, must meet the requirement of low saturation with respect to current under raster excitation.

It follows from analysis of the operation of luminophors with excitation by a scanning electron beam that saturation with respect to current is associated with the character of the decay of the phosphor. It has been shown theoretically that for luminophors with exponential decay saturation does not occur provided the screen is not heated to the temperature at which quenching begins; for luminophors with hyperbolic decay saturation with respect to current does obtain.

Experimental data show that for the luminophors $(Ca,Mg)(SiO_3)_2$:Ti and $(Zn,Be)_2SiO_4$:Mn, that are characterized by exponential decays, saturation with respect to current is not observed over the current density interval from 0.02 to 10 $\mu a\ cm^{-2}$ (raster excitation), while for the luminophors ZnS:Ag, ZnS:(Ag,Ni), (Zn,Cd)S:Ag and Zn(S,Se):Ag saturation with respect to current may be noticeable at current densities as low as 1 $\mu a\ cm^{-2}$. The experimental data for hyperbolic decay phosphors are characterized by the expression $B/I = C/(1 + bI)^{1/m}$, where B is the light flux from the screen with raster excitation, I is the current density and C, b and m are constants. The constant m has the same value for ZnS:Ag and (Zn,Cd)S:Ag; hence these two phosphors may be regarded as a "matched pair" as regards saturation characteristics.

The actual color range for "white" screens is rather wide, but for screens that are to be used in locations illuminated with incandescent lamps a "warm" white ($\sim 5000^{\circ}$K) is most pleasant. This requirement is met by any one of the

---

*Complete report in "Proceedings (Materialy) of the Fifth Conference on Luminescence", Tartu, 1957.

phosphors $ZnS_{45}.CdS_{55}$:Ag, $ZnS_{61}.CdS_{39}$:Ag, $ZnS_{20}.ZnSe_{80}$:Ag or $ZnS_{50}.ZnSe_{50}$ used in conjunction with ZnS:Ag. The highest efficiency, however, is obtained with $ZnS_{45}.CdS_{55}$:Ag. At the same time this phosphor noticeably absorbs the emission of ZnS:Ag so that variations in the thickness of the phosphor coating over the screen result in a "spotty" picture. The luminescence of this pair has a color temperature of 5250°K with a surface density of 3 mg/cm^2, but with variations of the coating density from 1.5 to 6 mg/cm^2 the color temperature varies, accordingly, from 6750° to 3650°K. In order to insure a uniform coating fine-grain ZnS:Ag and (Zn,Cd)S:Ag phosphors are used in fabricating Tv screens. The effective cathodoluminescence efficiency of unaluminized kinescope screens with smoky glass absorbing about 1/3 of the emitted light flux attains 6 candles per watt; by aluminizing the screen one can obtain an adequate picture brightness with a smoky glass substrate absorbing about 3/4 the light flux.

For projection kinescopes one should use only the silicate pair characterized by exponential decays (no saturation with respect to current). An aluminized screen of $CaMg(SiO_3)_2$:Ti and $(Zn,Be)_2SiO_4$:Mn at 25 kv and 8.5 μa cm^{-2} has a luminescence efficiency of 3 candles per watt. The stability of these phosphors is very high; the efficiency falls by only 5% after 500 hours of operation.

PHYSICAL-CHEMICAL PRINCIPLES OF APPLICATION OF LUMINOPHORS TO SCREENS BY THE METHOD OF SETTLING (Abstract*)

- L.A.Saminskii

In the application of phosphors to screens by the method of settling, the structure of the screen and the resolving power associated with it depend on the dispersion attributes of the medium.

In the case of sulfide phosphors, which are hydrophobic by nature, it is virtually impossible to obtain a fine-structured coating by settling in pure water. The presence in the water of sulfides, phosphates, alkalis and some other electrolytes appreciably reduces flocculation. The most effective stabilizers of water suspensions of zinc sulfide phosphors are sodium sulfide and potassium silicate. With increasing aggergative stability of the suspension the adhesion of the phosphor to the glass worsens. This indicates that electrostatic effects play an important role in the adhesion process inasmuch as the glass surface in the case of the investigated solutions has an electric potential of the same polarity as the luminophor particles.

The adhesion to glass of luminophors settled from Na_2S solutions increases with time particularly during the first few hours after clarification of the liquid. The structure of the screen does not alter in the process. The increase in adhesion is due to decomposition of the peptizing agent as a result of oxidation of the Na_2S by atmospheric oxygen. To fix screens applied by settling in a potassium silicate solution, it is essential to introduce additional electrolytes into the solution. The highest rate of fixation is attained under the conditions that are most favorable for polymerization of silicic acid. Salts of alkaline earth metals that in very minor concentrations produce rapid turbidity of the silicate are at the same time the most effective accelerators of the fixing. The dependence of the rate of development of turbidity of the silicate solution on the cation of the added electrolyte is characterized by the following proportions:

$$Ba^{2+}:Sr^{2+}:Ca^{2+}:Mg^{2+} = 100 : 60 : 6 : 3.$$

Accordingly, the highest rate of settling of the screens is observed in silicate solutions with salts of barium and strontium. Polymerization and formation of SiO_2 structures are connected with the conditions of absorption equilibrium at the surface of the colloidal particles, which, naturally, depends on the colloidal properties of the potassium silicate. Inasmuch as with increasing concentration of potassium silicate solutions these acquire colloidal character, the polymerization of the SiO_2 and the conditions of fixing of the screen depend on the molar concentration ratio $SiO_2:K_2O$ and on the concentration of the solution.

For example, in a 1% solution of potassium silicate containing 0.001 mole per liter $Sr(NO_3)_2$, the process of settling of the screens has a maximum rate at a molar ratio $SiO_2:K_2O = 2.7$.

Thus in potassium silicate solutions electrostatic effects do not have a decisive influence on the adhesion of the phosphor to the glass; the adhesion is determined primarily by the degree and condition of polymerization of the silicic acid. Hence the latter have an appreciable influence on the mechanical strength and stability of the screen after drying, inasmuch as due to shrinkage of the silica gel there may develop severe and possibly destructive stresses in the coating.

---

*Complete report in "Proceedings (Materialy) of the Fifth Conference on Luminescence", Tartu, 1957.

INVESTIGATION OF THE LUMINESCENCE OF URANIUM ACTIVATED SODIUM FLUORIDE (Abstract*)

- Z.M.Sverdlov

1. Alloys of sodium fluoride with uranium have characteristic band luminescence spectra and diffuse absorption spectra.

2. The luminescence decay of the alloys follows a complex law. In a narrow time interval the decay is hyperbolic.

3. The luminescence spectrum of sodium fluoride with uranium does not remain constant during decay; it differs at different stages of decay.

4. The intensity of luminescence of the alloys increases in proportion to the uranium content in a wide range of concentrations (from $1 \cdot 10^{-4}$ to $1 \cdot 10^{-1}$%). With further increase of uranium concentration in the alloy the intensity begins to decrease due to the formation of uranium compounds that absorb light in the visible region.

5. The presence of light metal (K, Ca, Mg, Al, V, etc.) impurities has little influence on the luminescence intensity; on the other hand, heavy metals (Fe, Cu, Mn, etc.) greatly weaken the intensity.

6. A simple procedure for qualitative determination of the uranium content in minerals, ores and waters has been developed on the basis of the specific characteristics of the luminescence of alloys of sodium fluoride with uranium. This procedure is now widely used in geological practice.

All-Union Scientific Research Geological Institute

DISCUSSION

A.V.Moskvin: Why have you simplified the treatment of the mineral samples? Why instead of dissolving in aqua regia, when you do not extract the uranium, do you simply precipitate with sodium carbonate, when you do not take into account the adsorption of uranium? This type of treatment often leads to serious errors. Are the errors in your case constant or do you have calibration curves with appropriate corrections?

Z.N.Sverdlov: The chemical treatment I described pertains only to the simplest case when the investigated material can readily be brought into solution. Where extraction is necessary, in cases when aqua regia does not dissolve the material, hydrochloric or sulfuric acid is added. Inasmuch as my main purpose was to describe the fundamentals of the procedure I did not go into the chemical aspects. Here quite a few analyses have been made by chemists, who in different cases developed different procedures for pretreating the minerals and ores.

G.F.Komovskii: You probably used the optical procedure for comparison because it is simplest. Why didn't you use a photomultiplier and photometer in order to determine the emission intensities?

Z.M.Sverdlov: At the first stage when it was necessary to develop a "mass production" procedure of laboratory analysis we had recourse to the simple optical system with the use of visual photometry. Now we have developed a new instrument employing a photomultiplier (the photocurrent is measured by means of a microammeter). This instrument will be demonstrated at the conference exhibit.

---

*Complete report in "Optika i spektroskopiia" 3, No.3 (1957).

THERMOLUMINESCENCE OF MINERALS

- G.F.Komovskii, V.S.Nikol'skii & O.N.Lozhnikova

Recently there have appeared in foreign literature a number of contributions[1] connected with studies of the thermoluminescence of minerals as a new scientific procedure for investigating minerals and rocks. In connection with this we feel that it may be timely to report on research we have carried out in this field.

By the term thrmoluminescence we understand the direct emission of radiation during heating of the investigated specimen (phosphor, mineral, rock, etc.) to a temperature below incandescence, i.e., to under 300-400°. The effect may therefore be characterized as temperature-stimulated luminescence, which, of course, has been investigated by many authors in the case of phosphors subjected to preliminary irradiation of some type.

In the case of minerals which are not subjected to artificial excitation, it must be assumed that the storage of light sums in them and the thermoluminescence are due to irradiation by some radioactive source, located either in the mineral itself or in the surrounding rocks and formations. It may be asserted that all minerals and rocks have a certain natural radioactivity, the average value of which is of the order of $2 \cdot 10^{-12}$ curie. In many cases when the mineral contains such radioactive elements as Ra, U, Th, K or Sm the activity may be much higher.

The α-, β- and γ-radiations, acting on the mineral over a long geological period (i.e., from the time of formation of the mineral), lead to the accumulation of an appreciable light sum which is readily released when the mineral is heated.

The mechanism of accumulation of light sums in minerals under the influence of radioactive irradiation can be explained, according to the band theory, by the formation of local levels of different depths (in most cases so-called F-centers) that often result in characteristic coloring of the crystal. There are several types of local levels: defects and vacancies in the crystal lattice, defects due to thermal motion and, finally, distortions due to the presence of extraneous ionic impurities and ionic dislocations and holes produced by the radioactive radiation.

Often the local levels are unfilled sites in the crystal lattice. The filling of such a site by an electron gives rise to an F-center. Finally, the presence of a metallic atom at an interstital site may also be the cause of a formation of an F-center. Under the influence of heating an electron from an F-center goes over into the conduction zone and, recombining with a luminescence center, produces thermoluminescence with emission of a characteristic wavelength. The local levels or traps are located at different depths with respect to the conduction zone and hence the transition of electrons from them into the conduction zone requires a certain degree of heating of the specimen, which is why the character of the emission during progressive heating changes.

After cessation of thermoluminescence of a mineral under prolonged heating, in many cases it can again be induced by irradiating the mineral with a light or radioactive source. The thermoluminescence spectrum in the visible region depends on the chemical composition of the crystal and the character and amount of impurities present.

It must be emphasized that thermoluminescence is common to most natural minerals and rocks. According to Daniels et al[1,2] it may be assumed that at least 75% of all minerals and rocks have the ability to thermoluminesce. Most intense thermoluminescence is observed in fluorites, carbonates, zircons and field spars.

The few minerals that do not thermoluminesce to a detectable degree can be made thermoluminescent by irradiating them with γ-rays, x-rays or α- and β-particles. Apparently, there participate in the process trapping levels of the same type as are already present in the nonirradiated crystal, but their number increases under the influence of irradiation. For investigating thermoluminescence and recording the emission curves one must use instruments sensitive to very weak light pulses. Such an instrument, for example, is a photomultiplier by means of which one can detect emissions amounting to only a few score photons.

In our work we used a FEU-19 photomultiplier with an end window. Our setup comprised a metallic box which housed a miniature ceramic furnace with a nichrome coil. This was supplied from a controllable autotransformer. The furnace was in contact with an aluminum plate on which the specimen was placed. A copper-constantan thermocouple connected to a galvanometer was mounted in the proximity of the specimen. The temperature was raised at the rate of about 1° per second. The specimen was covered with a diaphragm having a 10 x 10 mm window. The entire box was mounted on the light-tight housing of the photomultiplier, the face of which was flush against an insulating glass window inserted between the heated specimen and the photomultiplier. The photomultiplier was supplied through a double (ferroresonance and neon-tube) voltage regulator, rated at 5 kv.

The photomultiplier current was recorded by means of a mirror galvanometer having a sensitivity of $1 \cdot 10^{-9}$ amp, equipped with a variable shunt. The deflections of the galvanometer spot were recorded on a strip of photographic paper mounted on a rotating drum. The specimens were prepared by grinding the mineral to a fine powder; a portion of the powder, moistened with a weak water glass solution, was placed in a recess in the above mentioned aluminum plate.

The curves characterizing the rise and fall of thermoluminescence usually comprise two or three peaks of different heights; the character of the peaks differs for different minerals and depends on the depth of the trapping levels. Each peak corresponds to a particular group of levels.

We recorded a large number of thermoluminescence curves for crystalline calcite specimens from different locations. The reproducibility of the curves for the same specimen was satisfactory.

Saunders[3] in his report on an investigation of carbonates suggests that the thermoluminescence curves reflect the composition and crystallographic history of the limestones, i.e., their genesis, and yield certain indications relative to their age. Hence it should be possible to use this procedure for stratigraphic studies.

In order to enhance the thermoluminescence, foreign investigators have used irradiation of the minerals with γ-rays from radioactive Co^{60}. We found it more convenient and wholly satisfactory to use x-rays. We employed an x-ray tube with a tungsten anode. The BSV-W tube operated at 50 kv and 10 ma yields 7000 r/min at the exit window.

According to the data in the literature[4] the number of photons corresponding to 1 r at the indicated operating conditions is approximately $26 \cdot 10^9$ cm^{-2} sec^{-1}. Thus our x-ray tube yielded approximately $3 \cdot 10^{12}$ photons sec^{-1}. γ-Radiation of 1.8 Mev energy gives only $1.3 \cdot 10^9$ photons $cm^{-2} sec^{-1}$. Thus our x-ray tube gave an appreciably higher energy. According to the same data 1 mg of Ra yields only 8.3 r/hour or $\sim$0.002 r/sec.

According to Daniels, 1 Curie Po yields an amount of α-radiation which in 1 sec is equivalent to irradiation of the mineral with natural uranium for 1 million years. It may be assumed therefore that irradiation of the mineral

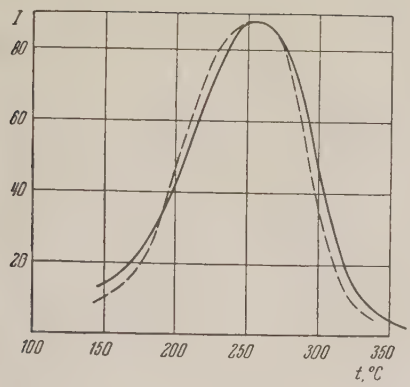

Fig.1. Thermoluminescence curves for a specimen of yellow calcite irradiated with x-rays (40 kv, 10 ma) for 2 min. (Curves recorded from the same specimen 15 min after irradiation.

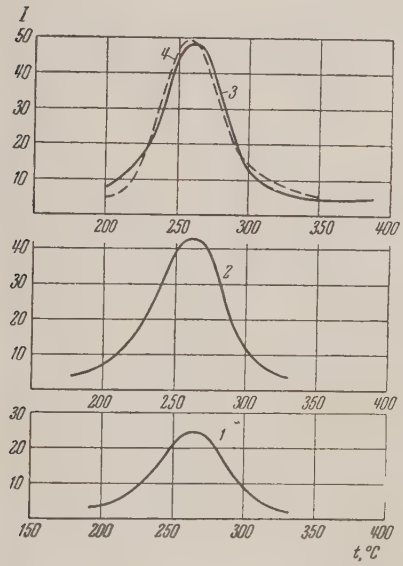

Fig.2. Thermoluminescence curves for a specimen of red-violet calcite irradiated with x-rays (tungsten anode, 35 kv, 10 ma) for 2-6 min (recorded 15 min after irradiation): 1) radiation time 2 min, 2) 4 min, 3 & 4) 6 min.

with even 1 r sec^{-1} is equivalent to very prolonged irradiation by a natural source with an activity of $1 \cdot 10^{-10}$ Curie.

The accompanying figures show the thermoluminescence curves obtained for two transparent calcites irradiated with x-rays under similar conditions.

Fig.1 shows the thermoluminescence curve for a yellow-orange calcite specimen. The two curves were recorded for the same specimen.

Fig.2 shows four thermoluminescence curves obtained for a red-violet calcite specimen. It will be evident from the curves that the height of the peaks depends on the time of x-irradiation. On the other hand, if we compare the height of the peaks in the curves of the yellow and red-violet calcites (curve 1, Fig.2), we see that the peak of the red-violet calcite is approximately four times higher than that of the yellow one. This indicates, apparently, that the red-violet calcite is appreciably younger than the yellow one. This conclusion was confirmed by the geologists who found these calcites.

In Figs.3 and 4 we give the thermoluminescence curves for two similar Belemnites fossils. Comparison of the heights of the peaks shows that the Belemnites absolutus, found in the Moscow region, is appreciably older; specifically, it dates to the Upper Jurassic period while the other fossil, Belemnites lateralis (Crimea) pertains to the Cretaceous period (the difference in ages is over 60 million years).

While many minerals thermoluminesce weakly, there are some capable of yielding a very strong emission, for example, fluorite, zircon and topaz. The thermoluminescence of these minerals can often be detected visually when they are heated to somewhat above 50°. The thermoluminescence spectrum depends, apparently, on the activators present in these minerals. As previously noted, the intensity of thermoluminescence can be increased by irradiating the mineral with x-rays, γ-rays or α- and β-particles. As a result of such irradiation the character of the thermoluminescence curves changes to some extent; some peaks become appreciably higher than those observed for the nonirradiated minerals. A mineral that no longer luminesces after prolonged heating can be made to thermoluminesce again by irradiation.

An obvious question is: in what manner can one utilize thermoluminescence as a new method of investigation? The answer to this question is given in the article of Daniels et al[1] where it is pointed out that the thermoluminescence procedure can be applied 1) in designing instruments for x-ray and γ-ray

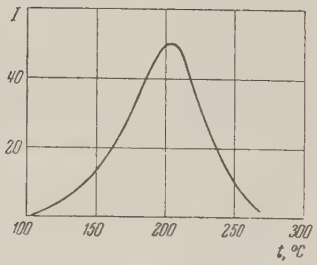

Fig.3. Thermoluminescence curves for Belemnites lateralis fossil specimen irradiated with x-rays (tungsten anode, 30 kev, 10 ma) for 20 min at 22 cm from the tube window (Cretaceous period).

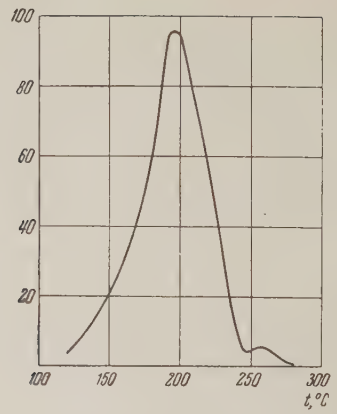

Fig.4. Same as Fig.3, but for Belemnites absolutus (Upper Jurassic).

dosimetry, 2) in identifying and checking minerals, 3) in investigating and preparing catalysts (particularly of aluminum oxide), 4) in investigating metamorphic minerals with a partially distorted lattice, 5) in stratigraphic studies of sedimentary deposits and 6) for determining the age of rocks and minerals. Furthermore, as we established, this procedure can be used for the control of enrichment processes in cases when the enriched mineral complex comprises a mineral luminescing more intensely than the others.

Giredmet (State Scientific Research Institute for Rare Metals)

References

1. F.Daniels, C.A.Boyd & D.F.Saunders, Usp.fiz.nauk, 51, 271 (1953).
2. F.Daniels, C.A.Boyd & D.F.Saunders, Science, 117, 343 (1953).
3. D.F.Saunders, Bull.Am.Assoc.Petrol.Geologists, 37, 114 (1953).
4. J.Parks, Bull.Am.Assoc.Petrol.Geologists, 37, 125 (1953).

INTRODUCTORY ADDRESS
(Section on Electroluminescence)

- V.V.Antonov-Romanovskii

The word "electroluminescence" is not new. In fact, in almost any book on luminescence one can find a classification of the different forms of luminescence according to the method of excitation and a definition to the effect that electroluminescence is emission under the influence of an electric discharge. Usually, however, this is understood to be a gas discharge.

Individual cases of emission of "condensed" materials have been detected and described at intervals over the past half century or more. In 1898 Braun[1] investigated the emission from electrodes in a galvanic bath. In 1923 Losev[2] detected emission from carborundum crystals at the point of contact with a needle point during passage of current. Destriau[3] working under Maurice Curie, beginning in 1936, investigated the luminescence of capacitors with crystal phosphor powder as the dielectric. The importance of clarifying the nature of these effects was noted long ago by S.I.Vavilov. A sharp break occurred in 1950 when Payne, Mager & Jerome (Ill.Eng. 45, 688 (1950)) published a report describing an electroluminescent lamp. This marked the beginning of rapid development of investigations of electroluminescence, prompted further by the new possibilities of its practical applications (light amplifiers and television screens). The work "electroluminescence" came to be applied virtually only to the luminescence of solid (sometimes liquid) materials.

A number of recent international conferences on luminescence have devoted an appreciable part of their programs to consideration of electroluminescence phenomena. More than 200 scientific reports have been published on the subject.

Nevertheless, even now we still do not know enough regarding the mechanism of electroluminescence. Most of the investigations in the field have been primarily experimental. I would like to mention one methodological and one theoretical feature distinguishing our debut in the field. The former is the use for investigation of the so-called luminescence brightness or radiance waves not only of sinusoidal voltage pulses but also of trapezoidal pulses. These have the advantage that they make it possible to separate the influence of the magnitude of the voltage from the influence of its derivative with respect to time. In the theoretical consideration of the question of the action of already present electrons and holes account is taken of the qualitative difference between the dependences of the probability of recombination and the probability of trapping of electrons (or holes) on their energy, which changes periodically with the field. This dependence follows directly from the diffusion theory of phosphorescence decay. The difference may be evinced more strongly in consequence of the fact that slow electrons accelerated by the field, i.e., polarons, can become electrons and, vice versa, while the properties of electrons and polarons differ appreciably (for example, their mass, mean free path, etc.). The next three reports will describe both theoretical investigations and practical achievements which, I feel, taking into account the relatively short time that has elapsed since the beginning of work in this field in the USSR, can serve as a guarantee that given sufficient effort and enthusiasm we can soon stand in the first rank of investigators in this field of luminescence.

References

1. F.Braun, Ann.d.Phys., 65, 361 (1898).
2. O.V.Losev, Telegrafiia i telefoniia (Telegraphy and Telephony),18,61 (1923).
3. G.J.Destriau, J.Chim.phys., 33, 620 (1936).

SOME RESULTS OF INVESTIGATIONS OF ELECTROLUMINESCENCE

- E.E.Bukke, L.A.Vinokurov, V.E.Oranovskii & Z.A.Trapeznikova

Electroluminescence is a relatively new but rapidly developing branch of luminescence.

In articles and reports that have appeared during the past 2-3 years one can find descriptions of many different phenomena which can be directly or indirectly related to electroluminescence. There are, in fact, a number of contradictory communications regarding the results of experiments; the contradictions are, presumably, connected with the difficulty of designing "pure" luminescence experiments. A number of different schemes or mechanisms of electroluminescence have been proposed, most of which satisfactorily explain part of the observed effects.

Our first electroluminescence experiments were aimed at familiarizing ourselves with the phenomenon, determining its distinctive characteristics and establishing the fundamental problems that require elucidation.

Numerous experiments with electroluminescing capacitors of different designs show that electroluminescence is observed at average field intensities of 10^4-10^5 v/cm and in individual cases at 10^3 v/cm, whereas theoretical calculations[1] indicate that average fields of the order of 10^6-10^7 v/cm are necessary to produce electroluminescence.

The appreciable divergence between the experimental and theoretical values may be explained if we assume that the field distribution inside the crystal is not uniform, that there are regions or layers with a high field concentration. There have been suggested mechanisms according to which the concentration of field occurs inside the crystal in the regions of contact of different parts of the crystal having different physical and chemical properties. Consideration of the effect of such regions led us to the conclusion that to obtain sufficiently high field concentrations it is sufficient to have surfaces through which charge carriers of a given polarity can pass only in one direction. Such a surface, for example, can be the interface between the crystal and the dielectric. Calculations show that this scheme is no less valid than a number of others that have been proposed for explaining field concentration. Regardless of how the field concentration occurs, luminescence apparently should not develop if the applied voltage is less than 4 v (the width of the band gap in ZnS is 4 ev). At lower potential differences neither breakthrough nor the pre-breakthrough state can be attained. We carried out experiments on determining the minimum voltage at which luminescence is still observed. A thin carefully prepared capacitor begins to glow at a voltage of 8.5 v. This experimental result is in agreement with the evaluations of many authors in which the minimal voltage per crystal was determined by computation on the basis of experimental results obtained with thick layers.

Zahlm et al[2] indicate that they observed electroluminescence at a voltage of about 10 v. This result is further confirmation of the fact that electroluminescence is not a consequence of electric discharge in air bubbles on the surface of the crystals inasmuch as for a discharge in air a potential of over 1000 v is necessary.

The radiance waves we obtained in applying a sinusoidal voltage to our experimental capacitor do not differ in shape from those obtained by other investigators[2,3]. Different luminophors and different bands of the same luminophor show some differences as regards shape and position of the radiance waves (this aspect of luminescence will be the subject of future investigations).

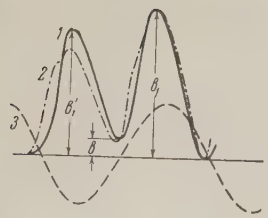

Fig.1. Radiance waves obtained with excitation by sinusoidal voltage pulses: 1) ZnS:Cu phosphor, 2) ZnS:Cu:Nd phosphor (green luminescence), 3) applied sinusoidal voltage.

As may be seen in Fig.1 the radiance waves for successive half-cycles of excitation differ in height. Inasmuch as there is no unanimity in the literature regarding the reason for this wave-difference[3], we decided to investigate this effect further. It must be noted that any asymmetry of the capacitor and associated circuit contributes strongly to the wave-difference and in some cases may be the cause of it. Nevertheless, having carefully eliminated all possible asymmetries, we still observed a wave-difference which we feel must be connected with the characteristics of this form of luminescence.

Having noted that the wave-difference increases in going over to a grayer powder and decreases in going to a more strongly scattering dielectric, we came to the same conclusion as Zahlm et al[2], namely, that the wave-difference is connected with the fact that each individual crystal emits primarily from the side or face turned in the direction of one of the electrodes. Inasmuch as investigations with a sinusoidal voltage do not allow of investigating separately the dependence of the electroluminescence on the field strength and on the rate of increase of the field, we carried out experiments with trapezoidal pulses (this pulse shape was suggested by M.V.Fok).

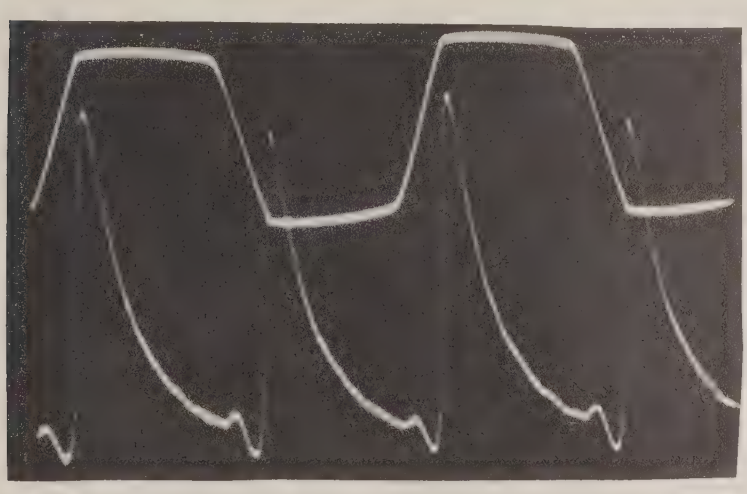

Fig.2. Radiance waves obtained with excitation of a phosphor by trapezoidal voltage pulses symmetric with respect to zero.

The radiance wave oscillograms obtained for one of the investigated phosphors with excitation by symmetrical (relative to zero) voltage pulses are shown in Fig.2. As may be seen from the figure, the emission maxima occur at the points of transition of the field from increase (or decrease) to a constant value. The position of the maxima does not change with either changes in amplitude or steepness of the pulse fronts. One of the possible explanations of these results is the following. As was shown in Ref.4 the recombination cross section for thermal electrons is greater than for "high-energy", optical electrons. Moreover, the ratio of the probability of recombination to the probability of trapping for optical electrons is appreciably smaller than for thermal electrons. Inasmuch as the electrons in the phosphor acquire an additional energy in the applied electric field, their role in the kinetics of luminescence may be assumed to be similar to the role of optical electrons in photoexcitation. In the light of these considerations, the rise of the radiance waves may be pictured as follows. As the external field increases, the electrons, acquiring

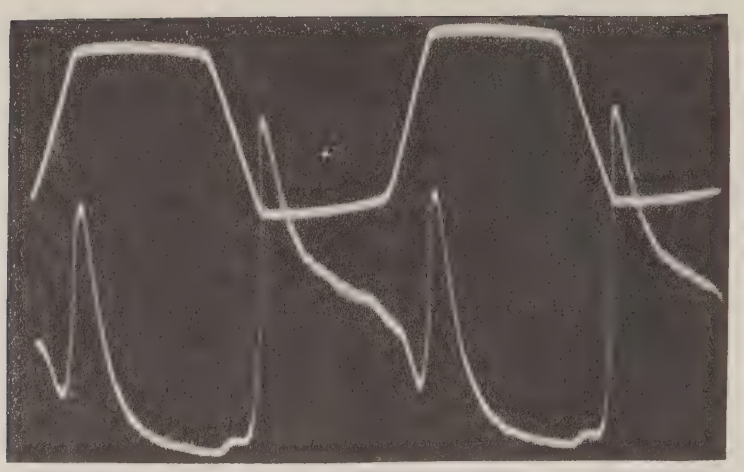

Fig.3. Radiance waves obtained with excitation of a phosphor by positive (nonsymmetric) voltage pulses.

energy, ionize the luminescence centers; at this stage the probability of their recombination with ionized luminescence centers is small. When the external field goes over to a constant value, the space charge in the crystal compensates the external field; the energy of the electrons decreases and the number of recombinations with luminescence centers increases accordingly with a resultant upsurge in luminescence. When the field again starts to change, i.e., departs from the "constant" value, the electrons that have formed a polarization charge, moving into the depths of the crystals, encounter ionized centers and yield a weaker secondary flash of luminescence. We felt that experiments with exciting voltage pulses nonsymmetric with respect to zero should help clarify the influence of the electric polarization of the crystal on the electroluminescence. Investigation of the radiance waves excited by such pulses showed that one of the peaks decreases in this case (Fig.3).

The fact that there is a difference between the ratio of the recombination and trapping cross sections for electrons accelerated by the field and the ratio for slow electrons is substantiated by the results of experiments in which the phosphor was simultaneously excited by an electric field and by light. The increase of the mean energy of the electrons under the influence of the field must lead to a decrease of the cross section for recombination of these electrons with luminescence centers as compared with the cross section for trapping; in consequence, the light sum stored in the phosphor must increase.

Experiments aimed at direct comparison of the light sum given by the decay after photoexcitation with the light sum evaluated from the decay after simultaneous photo and electroexcitation (the field was shut off during the decay time) did not yield positive results. The light sums agreed within the limits of the measurement error. By using a different procedure, however, it is possible to detect a small increase in the light sum stored under the influence of the applied field. To this end the field must be cut off before turning off the exciting light. In this case the luminance of the phosphor increases and for some time remains higher than the normal, steady excitation luminance of the phosphor without a field; after a certain period, the luminescence slowly falls off to the normal value.

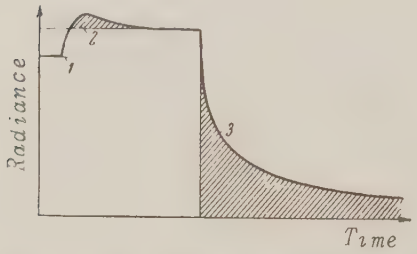

Fig.4. Variation of emission of a phosphor with optical and electric field excitation: 1) luminance with optical excitation and simultaneously applied electric field, 2) luminance with optical excitation only (field cut off), 3) decay.

The variation of the luminance in this experiment is shown in Fig.4. The experiment shows that under the influence of the electric field the phosphor stores up a light sum approximately 5% greater than stored under only optical excitation.

In order to investigate further the correlation between photoluminescence and electroluminescence we subjected the electroluminescing capacitor, excited simultaneously by an electric field and ultraviolet radiation, to the influence of infrared light. The experiments showed that the infrared radiation acts only on the optically excited part of the emission. This influence of infrared can be explained on the basis of either of the following hypotheses:

1) the volume of the crystal in which the processes associated with electroluminescence occur is appreciably smaller than the volume associated with photoluminescence, or

2) the electroluminescence centers are different as regards formation or structure from the photoluminescence centers.

In the latter case the electroluminescence spectra should differ from the photoluminescence spectra of the same phosphor. This was disproved by comparison of the electro- and photoluminescence spectra of a specially prepared ZnS:Cu:Nd phosphor. The line spectrum of Nd was the same with both photoexcitation and electroexcitation. Consequently, at least in this phosphor both electro- and photoluminescence occur in centers having the same structure and characteristics. Obviously, the volumes involved differ, which is in accord with the above mentioned concept regarding the necessity of concentration of the electric field.

The present experiments were carried out with electroluminophors prepared by two different procedures.

1. Zinc sulfide was activated by the introduction of copper, aluminum and manganese (yellow-orange luminescing phosphor) or copper and aluminum (blue and green luminescing phosphors). Ammonium chloride was used as the flux. Also small amounts of zinc oxide were added. The batches were heated in a stream of humid hydrogen sulfide at 1150°.

2. Copper and lead were introduced into the zinc sulfide as the activators and NaCl or $ZnCl_2$ employed as the flux. The batches were heated in a stream of nitrogen at 900°. The addition of small amounts of zinc oxide in this case did not lead to an increase in luminosity. On the other hand, the addition of large amounts (5-7 mole %) of zinc oxide resulted in the formation of electroluminophors in which surface breakthrough occurred upon the application of an electric field to the capacitor. Removal of the excess zinc oxide by washing with acetic acid eliminated the breakthrough but did not increase the brightness of the electroluminophor.

In investigating the conditions of synthesis of electroluminophors we succeeded in obtaining an electroluminescing ZnS:Cu luminophor at introduced copper concentrations of 10^{-6} gram-atom per mole ZnS. Such an electroluminophor is obtained if ZnS, free of zinc oxide, is heated with CuS in a stream of dry, oxygen-free nitrogen. This electroluminophor has a very faint gray color and a clearly visible electroluminescence. If a flux is added to the initial batch, the resultant luminophor is white but does not electroluminesce. In this case for electroluminescence to appear it is necessary to increase the amount of copper. This shows that for the appearance of electroluminescence what is important is not the amount of activator but the formation of a copper sulfide phase. Obviously, the brightness of the luminophor also depends on the number of luminescence centers and, consequently, on the amount of copper incorporated in the crystal. Hence increasing the solubility

of the CuS in the ZnS by means of different additives, provided there is segregation of the CuS in the form of a separate phase, leads to the formation of brighter electroluminophors. From this one can draw a second interesting conclusion, namely, that the solubility of copper sulfide in zinc sulfide is very low: even when the CuS is introduced in the amount of 10^{-6} gram-atom Cu per mole, part of the CuS remains in the form of a separate phase.

In connection with these results there arises the question of the nature of the luminescence centers responsible for the electroluminescence. Presumably if only the surface layer electroluminesced, the electroluminescence centers should be in different energy states from the photoluminescence centers distributed in the bulk of the crystal.

We reasoned that it would be helpful to investigate an electroluminophor activated with a rare earth element. As is known the rare earth elements have characteristic line spectra and the ratio between the intensities of the lines depends on the immediate surroundings of the rare earth ions. Therefore, rare earth ions located at the surface and inside the crystal should have different luminescence spectra. As noted above we prepared a ZnS:Cu:Nd luminophor Its electroluminescence is orange-yellow. We photographed the electroluminescence and photoluminescence spectra of this luminophor. They proved to be identical. This shows that the Nd^{3+} ions in both cases are in similar or identical energy states. Hence it cannot be assumed that only the centers at the surface electroluminesce. Apparently, electroluminescence is due primarily to centers located inside the crystal at or near the points or areas where copper sulfide is present in the form of a separate phase.

"P.N.Lebedev" Physical Institute of the
Academy of Sciences of the USSR

References

1. W.W.Piper, F.E.Williams, Phys.Rev., 98, 1809 (1955).
2. P.Zahlm, G.Diemer & H.A.Klasens, Phys.Res.Rep., 9, 81 (1954).
3. G.Destrau & Ivey, Proc.IRE, 43, 1911 (1955).
4. Siui Siui-iun, Doklady AN SSSR, 103, 585 (1955); 106, 818 (1956); Acta Physicochimica, 12, 58 (1956).

ZINC SULFIDE TYPE ELECTROLUMINOPHORS

- O.N.Kazankin, F.M.Pekerman & L.N.Petoshina

Introduction

The purpose of the present investigation was to determine the conditions for obtaining the most efficient electroluminophors. This problem is important inasmuch as the low radiance of present electroluminophors is an obstacle to their practical application. At the same time, in contrast to the voluminous literature on investigations of photoluminescence effects, there is little experimental data on the question except for the reports of Homer et al[1] and Frölich[2].

According to present-day theoretical concepts[3-6], electroluminescence effects occur at potential barriers arising at the interfaces of multiple component systems, both inside the crystal and on its surface. It is generally assumed that electroluminescence occurs due to collisions of electrons, supplied from donor levels, with luminescence centers.

The most favorable conditions for electroluminescence apparently obtain in the case of complete crystallization of the base material (thus according to Curie[3] no electroluminescence is observed in CaS:Bi phosphors with a low degree of crystallinity of the host).

Further, it also follows from experimental data that the introduction of large amounts of activator into ZnS:Cu phosphors leads to the formation of semiconductor layers on the zinc sulfide surface.[7]

According to certain theoretical considerations[3] the appearance in the conduction band of a certain number of electrons accelerated by the field and exciting the activator can be explained only by the presence of such a semiconductor layer.

It is known[7] that application of a layer of $CuSO_4$ to ZnS even without subsequent heating leads to the appearance of electroluminescence. Lastly, the addition of substances which are good semiconductors or which can form compounds that are semiconductors in the process of heating the phosphor also apparently tends to enhance the electroluminescence.

The presence of such semiconductor layers in the luminophor should lead to a particularly strong dependence of the intensity of luminescence on the atmosphere in which the phosphor is heated in the process of preparation. In view of this, as the first step we investigated the effect of different proportions of H_2S and HCl in the furnace atmosphere and the influence of an oxidizing atmosphere on the synthesis of electroluminophors.

Preparation of the Luminophors

We prepared phosphors with ZnS and ZnS.ZnSe as the base material, Cu as the activator and Al and Pb as the coactivators. The batches were heated in an atmosphere of H_2S and HCl in different proportions and in some cases with the addition of H_2O vapor to determine the effect of an oxidizing atmosphere. The ZnS:Cu phosphor batches were prepared by the usual wet procedure and carefully dried; batches were again dried immediately before heating to drive all traces of moisture away. In some cases in the preparation of phosphors with Pb we used the dry mixing procedure, wherein the other ingredients are added to the ZnS in dry form.

The heating was carried out in a long quartz tube plugged with a rubber stopper with holes for the tubes bringing in and carrying off the gas. The selected gas mixture was passed through the quartz tube containing the batch

for two hours before the actual heating. After this the quartz tube was placed into the furnace preheated to 1100° and the batch heated for 30 min. The same gas mixture was continually passed through the quartz tube during the cooling period.

Proportioning of the Gases

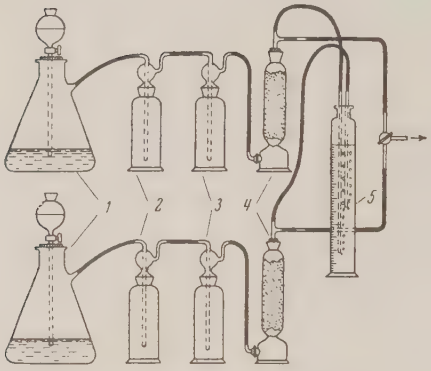

Fig.1. Set-up for preparing, cleaning and proportioning the gases (H_2S and HCl) used in heating the luminophors: 1) Bunsen flask, 2 & 3) splash bottles, 4) desiccating column, 5) pressure relief flask.

The H_2S and HCl gases were prepared, purified and proportioned by means of the set-up pictured in Fig.1. The hydrogen sulfide was prepared from sodium sulfide and sulfuric acid; the hydrogen chloride was prepared by dehydration of concentrated hydrochloric acid with strong H_2SO_4. The Bunsen flask 1 in the H_2S branch contains a concentrated sodium sulfide solution and in the HCl branch concentrated hydrochloric acid; the dropping funnels are filled with sulfuric acid.

The evolved gases, after passing through the two splash bottles 2 & 3, go through the desiccating column 4 filled with P_2O_5. The pressure flask 5 serves to assure a constant flow of the gases. From the desiccating column the gases go through capillaries to the three-way cock by means of which the gas mixture is proportioned. The vapor water content of the gases was less than 0.1%. The rate of gas flow through the system was about 100 ml/min.

The influence of an oxidizing atmosphere was investigated by introducing water vapor during heating of the phosphor; the amount of water vapor was regulated by varying the temperature of the water through which the H_2S was bubbled.

Measurement of the Luminescent Characteristics

The electroluminophors were investigated in both a solid dielectric - a mixture of melamine formaldehyde and rezyl resins - and in a liquid dielectric - castor oil.

In the first case a certain amount of the luminophor was mixed with a quantity of the resin (the suspension was thinned with benzene as necessary), flowed onto a sheet of conducting glass, which served as one of the electrodes, and dried to form a hard film. Next a coating of aluminum was sputtered on the film; this served as the second electrode. The thickness of the luminophor film could be varied from 100 to 60 microns.

In measuring the luminescent characteristics in such capacitors the data spread may be as great as 30%. Hence for accurate measurements we used a capacitor one electrode of which was an aluminum plate with a cemented on frame of lucite ~0.2 mm thick. The luminophor was mixed with castor oil and poured into the cell formed by the lucite frame and then covered with a sheet of conducting glass.

The reproducibility of the measurements with such a capacitor was within 10%. The capacitor assembly was mounted in a special holder over the slit of

the monochromator by means of which the emission spectrum was measured.

The excitation was produced by means of an audiofrequency oscillator in the frequency range from 50 to 20,000 cycles. The oscillator voltage was amplified to 1000 v.

For excitation of the luminophors with square pulses we used a Schmidt type circuit with an amplifier. The control pulses in this set-up were the sinusoidal pulses from the audio oscillator.

Experimental Results

Electroluminescence brightness and spectra

The relative luminosities of the ZnS:Cu and ZnS:Cu:Al luminophors with optimal concentrations of the activators and coactivator (Al) heated in different atmospheres are listed in Table 1.

Table 1

Influence of heating atmosphere on the luminance of the ZnS:Cu and ZnS:Cu:Al electroluminophors

Heating atmosphere	Relative luminance, %	
	ZnS-Cu (Cu=0,2%)	ZnS-Cu,Al (Cu=0,20%, Al=0,05%)
H_2S	100	1200
80% H_2S+20% HCl	900	1260
60% H_2S+40% HCl	1190	2280
40% H_2S+60% HCl	1430	2385
20% H_2S+80% HCl	2300	—
HCl	770	645

From a comparison of the data for the two systems, it will be evident that the ratio of the concentrations of H_2S and HCl plays a decisive role where the brightness of the resultant luminophors is concerned. For the ZnS:Cu system increasing the proportion of HCl from 0 to 80% results in a 23-fold increase in brightness. At the same time there is observed an appreciable increase in the size of the phosphors crystals (see Table 2). Yet, complete absence of H_2S (heating in HCl alone) leads to an appreciable reduction of the electroluminance.

The ZnS:Cu:Al system yields fairly bright electroluminophor specimens even with heating in H_2S alone. More strongly electroluminescing specimens, however, are obtained when HCl is also present in the heating atmosphere.

The ZnS:Cu:Al system[2] is characterized by a marked proclivity to recrystallization; in this respect it is similar to the ZnS.CdS system, which luminesces well when heated without a flux[8].

From the data listed in Table 1 it follows that by adding Al we simply enhance the ability of the ZnS:Cu system to recrystallize; the brightness of the ZnS:Cu:Al luminophors does not exceed the brightness of phosphors of the ZnS:Cu system heated in a mixture of 80% HCl + 20% H_2S. The emission spectra of these luminophors are shown in Fig.2.

Heating ZnS:Cu in H_2S results in a luminophor with a distinct red band.[2] Addition of HCl to the heating atmosphere shifts the luminescence peak into the green region.

The ZnS:Cu:Al (Al = 0.05%) phosphors have peak emission in the green region of the spectrum at optimal concentrations of Cu (about 0.2%).

The first electroluminophors prepared by Destriau contained a rather large amount of ZnO; Zalm[7] speaks of the beneficial effect of oxidation; Frölich[2] obtained results that indicate the favorable influence of oxygen on the electroluminescence of ZnS:Cu:Al phosphors heated in H_2S.

Table 2

Grain-size composition of the luminophors

Phosphor	Heating atmosphere	Granulometric composition of phosphor powder	
		∅, μ	%
ZnS-Cu	H_2S	To 3	20
		» 7	70
		» 14	100
	H_2S+HCl	To 3	2
		» 7	7
		» 14	36
		» 30	100
	HCl	To 3	10
		» 7	50
		» 14	80
		» 20	100
ZnS-Cu,Al	H_2S	To 3	26
		» 7	74
		» 14	100
	H_2S+HCl	To 7	2
		» 14	40
		» 30	100
	HCl	To 3	14
		» 7	47
		» 14	85
		» 20	100

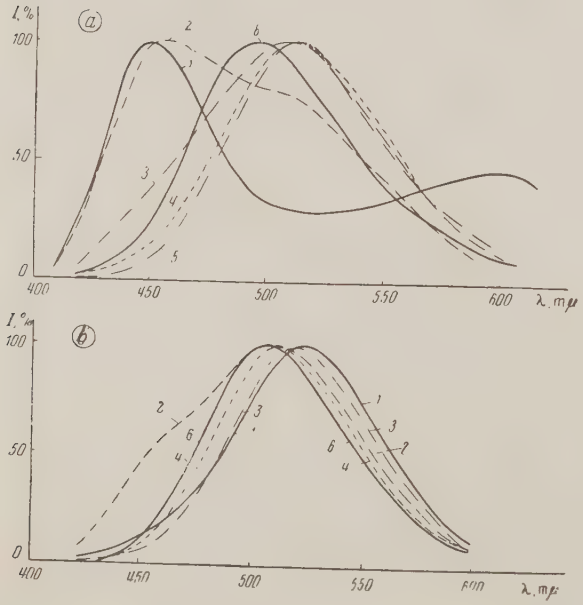

Fig.2. Effect of the heating atmosphere on the electroluminescence spectra of ZnS:Cu (a) and ZnS:Cu:Al (b) phosphors excited by an audio oscillator at a frequency of 5 kc and a voltage of 400 v: 1) 100% H_2S + 0% HCl, 2) 20% HCl, 3) 40% HCl, 4) 60% HCl, 5) 80% HCl, 6) 100% HCl.

As previously noted, we also investigated the influence of an oxidizing atmosphere by passing a certain amount of water vapor through the heating tube in addition to the H_2S or the H_2S + HCl mixture. The results are given in Tables 3 through 6. Thus by the addition of up to 3% water vapor one can appreciably increase the brightness of the ZnS:Cu phosphor obtained in heating in H_2S. As is evident from Fig.3,a, addition of water vapor reduces the intensity of the red band of Cu and shifts the emission maximum to the side of shorter wavelengths.

By heating with water vapor one can obtain rather brightly luminescing blue phosphors.

It also follows from Table 4 that H_2O vapor has a favorable effect on the brightness of electroluminophors heated in an atmosphere of H_2S + HCl up to a point. Increasing the amount of vapor to as much as 3% leads to a sharp decrease of the luminance. In contrast to the case of heating in H_2S alone, the addition of H_2O vapor in the case of heating in H_2S + + HCl has little effect on the electroluminescence spectrum (Fig.3,b).

Addition of H_2O vapor to the ZnS:Cu:Al system in the process of heating leads to the results shown in Tables 5 & 6 and Fig.4. Addition of H_2O vapor reduces the overall electroluminescence

Table 3

Brightness of ZnS:Cu phosphors heated in an atmosphere of H_2S with different amounts of H_2O vapor

Heating atmosphere	Relative luminance, %
H_2S without H_2O	100
$H_2S + 1\%$ H_2O	192
$H_2S + 3\%$ H_2O	133
$H_2S + 7\%$ H_2O	94

Table 4

Brightness of ZnS:Cu phosphors heated in an atmosphere of H_2S + HCl with different amounts of H_2O vapor

Heating atmosphere	Relative luminance %
$H_2S + HCl$ without H_2O	100
$(H_2S + HCl) + 1\%$ H_2O	158
$(H_2S + HCl) + 3\%$ H_2O	13
$(H_2S + HCl) + 7\%$ H_2O	1,5

Table 5

Brightness of ZnS:Cu:Al phosphors heated in an atmosphere of H_2S with different amounts of H_2O vapor

Heating atmosphere	Relative luminance, %
H_2S alone	100
$H_2S + 1\%$ H_2O	20
$H_2S + 3\%$ H_2O	28
$H_2S + 7\%$ H_2O	28

Table 6

Brightness of ZnS:Cu:Al phosphors heated in an atmosphere of H_2S + HCl with different amounts of H_2O vapor

Heating atmosphere	Relative luminance, %
$H_2S + HCl$ only	100
$H_2S + HCl + 1\%$ H_2O	82
$H_2S + HCl + 3\%$ H_2O	107
$H_2S + HCl + 7\%$ H_2O	156

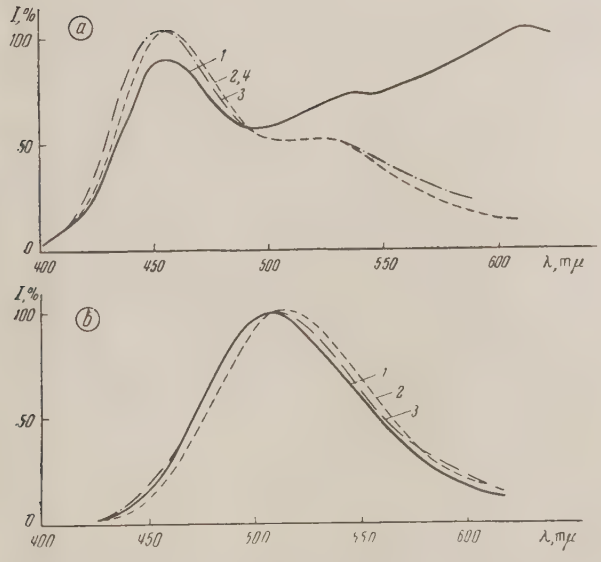

Fig.3. Dependence of the luminescence spectrum of ZnS:Cu heated in an atmosphere of H_2S (a) and in an atmosphere of 40% H_2S + 60% HCl (b) on the water vapor content of the heating atmosphere: 1) no H_2O, 2) 1% H_2O, 3) 3% H_2O, 4) 7% H_2O.

brightness and at the same time increases the relative intensity of the blue band. Apparently, in this case aluminum oxide is formed and the aluminum no longer participates in the formation of the phosphor.

The addition of H_2O vapor to ZnS:Cu:Al prepared by heating in an atmosphere of H_2S - HCl (Table 6) at first also reduces the electroluminescence brightness (again probably due to the formation of aluminum oxide), but then with further increase in the amount of H_2O vapor the electroluminescence brightness begins to increase.

It follows from the cited data that creation of favorable conditions for the formation of additional oxides (ZnO or Cu_2O) actually does increase the brightness of electroluminophors of the ZnS:Cu system.

More significant results are obtained by the introduction

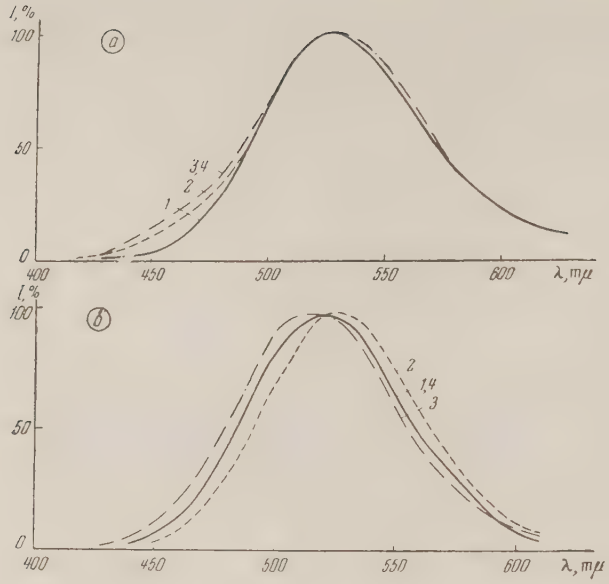

Fig.4. Same as Fig.3, but for ZnS:Cu:Al.

Table 7

Luminance of ZnS:Cu:Pb luminophors with and without the addition of Se, heated in an atmosphere of H_2S + HCl.

Phosphor	Heating atmosphere	Relative luminance %
ZnS-Cu,Pb	Air	100
ZnS-Cu,Pb	H_2S + HCl	250
ZnS-Cu,Pb + 20% Se		590
ZnS-Cu,Pb + 50% Se		340

of selenium and lead into the ZnS:Cu system. The addition of ZnSe to the ZnS:Cu system yields a series of bright electroluminophors with different spectral characteristics; as a rule, however, these have a brightness only one fourth that of the best ZnS:Cu specimens. An appreciable increase in brightness can be obtained by adding ZnSe to ZnS:Cu systems containing lead. In their report, Homer et al[1] describe bright electroluminophors obtained by adding Pb to the ZnS:Cu system.

The ZnS:Cu:Pb phosphors we prepared following the formulation and procedures given by Homer et al were heated in an atmosphere of nitrogen, air and H_2S + HCl. The results obtained in heating in nitrogen are better than those obtained in heating in air, but heating in H_2S + HCl increases the brightness by a factor of about 2.5. The further increase in brightness is observed with the addition of Se (see Table 7).

The actual content of lead and selenium in the phosphor product, naturally, differs from that in the initial batch. Thus, according to the data of chemical analysis, after heating in an atmosphere of H_2S + HCl, there remain in the phosphor approximately 1/10 the Pb and 1/5 the Se present in the initial batch. The appreciable increase of the electroluminescence produced by the addition of Se to the ZnS:Cu:Pb phosphors indicates that the introduction of additional semiconductors has a favorable effect on the electroluminescence intensity.

Dependence of the electroluminescence brightness on the applied voltage and frequency

Curves characterizing the variation of the electroluminance of ZnS:Cu and ZnS:Cu:Al electroluminophors with the applied voltage are shown in Fig.5; the corresponding curves for ZnS.ZnSe:Cu:Pb (λ_{max} = 510 mμ), reduced to the same scale, are given in Fig.6.

The voltage dependence in the investigated voltage range is satisfactorily described by the formula given by Destriau[9]:

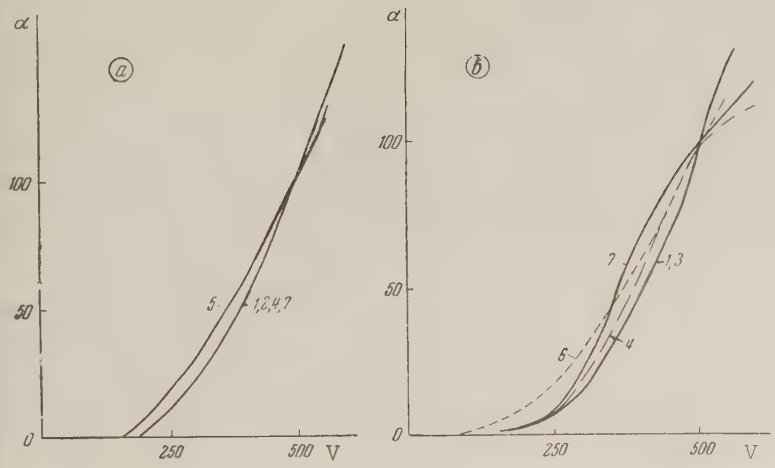

Fig.5. Variation of the brightness of ZnS:Cu (a) and ZnS:Cu:Al (b) phosphors, excited at a frequency of 5 kc, as a function of the applied voltage and the heating atmosphere: 1) H_2S, 2) H_2S + 3% H_2O, 3) H_2S + 6% H_2O, 4) 40% H_2S + 60% HCl, 5) 40% H_2S + + 60% HCl + 3% H_2O, 6) 40% H_2S + 60% HCl + 6% H_2O, 7) HCl.

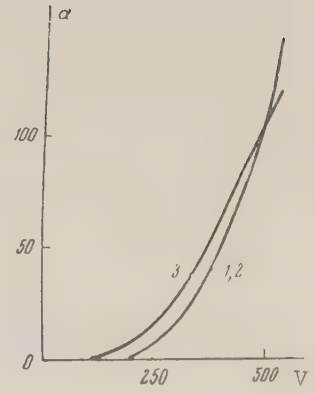

Fig.6. Variation of the brightness of ZnS:Cu:Pb (1,2) and ZnS.ZnSe:Cu:Pb (3) phosphors, excited at a frequency of 5 kc, as a function of the applied voltage and the heating atmosphere: 1) air, 2 & 3) H_2S + HCl.

$$B = f(E)e^{-b/E},$$

where B is the brightness of electroluminescence, f(E) is a function proportional to the number of accelerated electrons and $b = h\nu/e\omega_m$ (ω_m is the free path length).

The variation of B as a function of E is given with fair accuracy by the approximate formula:

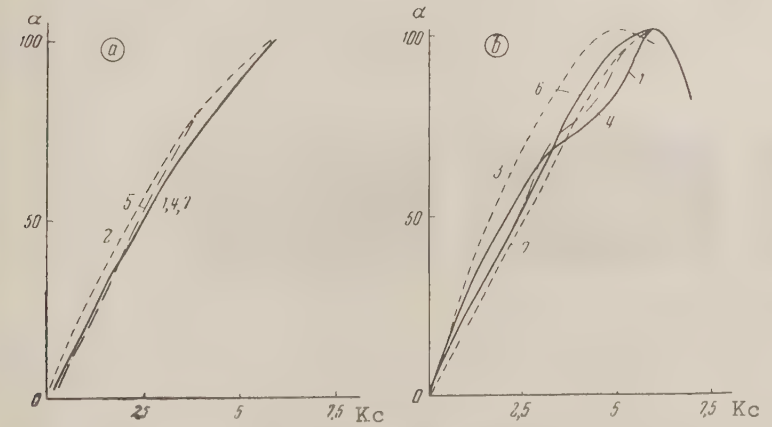

Fig.7. Variation of the brightness of ZnS:Cu (a) and ZnS:Cu:Al (b) phosphors with the frequency of the exciting oscillator and the heating atmosphere. See Fig.5 for curve designations.

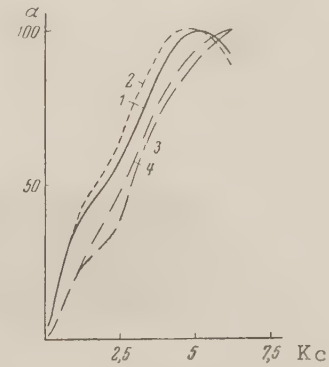

Fig.8. Variation of the brightness of electroluminophors with the frequency of the exciting voltage and the heating atmosphere (1 - air, 2-4 - H_2S + HCl): 1 & 2) ZnS:Cu:Pb, 3) ZnS.ZnSe: :Cu:Pb, 4) ZnS.ZnSe:Cu.

$$\log B = a/E,$$

inasmuch as f(E) varies much more slowly with the changes in voltage than the exponential term.

As will be evident from the curves shown in Figs.7 & 8, the electroluminescence brightness of the indicated phosphor systems increases with increasing frequency; the dependence is linear, however, only in a limited frequency interval. In some casesa maximum is observed in the curves at a frequency of about 5 kc. The effect has also been noted by Nudelmann & Matossi[10].

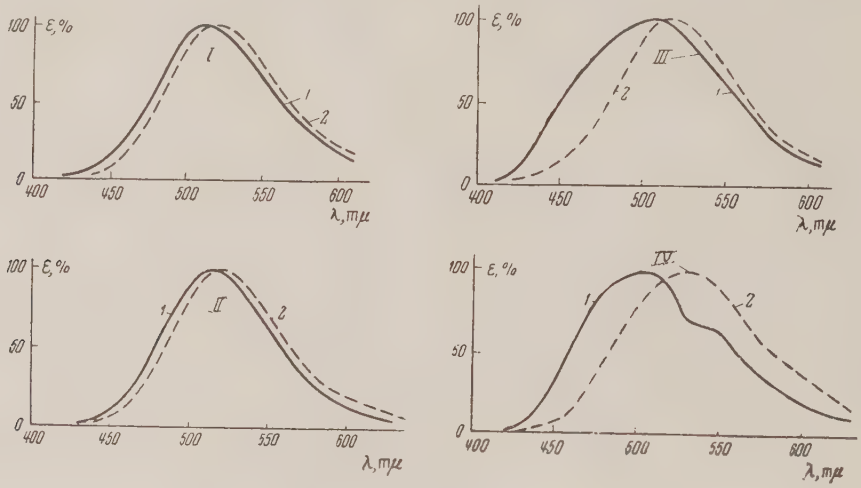

Fig.9. Dependence of the emission spectra of different luminophors on the frequency of the exciting oscillator (1 - 0.5 kc, 2 - 5 kc): I) ZnS:Cu, II) ZnS:Cu:Al, III) ZnS:Cu:Pb, IV) ZnS.ZnSe:Cu:Pb.

An appreciable change in the character of the spectrum with changes in frequency is observed only for the ZnS:Cu:Pb and ZnS.ZnSe:Cu:Pb phosphors (Fig.9). In the case of the ZnS:Cu and ZnS:Cu:Al phosphors, increasing the frequency by a factor of 10 results in a displacement of the electroluminescence peak by only about 5 mμ.

Radiance waves

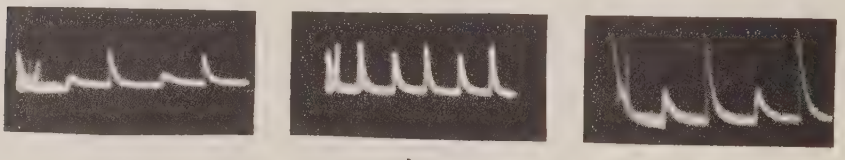

a b c

Fig.10. Radiance waves obtained with excitation by square pulses with a frequency of 0.5 kc for ZnS:Cu phosphors heated in different atmospheres: a) H_2S, b) 40% H_2S + 60% HCl, c) HCl.

It is known[7,9] that the curves characterizing the variation of the electroluminescence intensity when an alternating voltage is applied to the phosphor may have two maxima during a half-cycle. The first maximum is either in phase with the voltage or slightly shifted relative to it, while the second maximum appears when the voltage falls to zero. Many investigators have in-

ferred that the first maximum appears due to instantaneous recombination of the electrons with ionized centers, while the second is due to recombination of electrons initially remote from the centers. It may be assumed that the ratio of the heights of the first and second maxima is connected with changes in the number of electrons participating in the electroluminescence process[11] and, consequently, that the radiance waves for luminophors prepared in different ways should change accordingly.

Inasmuch as the shape of the radiance waves depends on the voltage and frequency[12], the different phosphors must be investigated under identical conditions; usually either a sinusoidal or square wave voltage pulses are applied to the capacitor.

The radiance waves we recorded for ZnS:Cu phosphor specimens heated in different atmospheres are shown in Fig.10. It will be seen from the traces that the ratio of the amplitude of the second maximum to the amplitude of the first increases as we approach the specimen characterized by the highest electroluminance.

Conclusions

1. Our systematic investigation of the influence of the synthesis atmosphere on the electroluminescent properties of zinc sulfide phosphors showed that the most favorable conditions for maximum luminescence brightness of the phosphors obtain at a certain ratio of the H_2S and HCl gas volumes.

2. In the case of the ZnS:Cu:Al system one can obtain rather bright electroluminophor specimens by heating in an atmosphere of H_2S alone, but the brightness of these specimens is still inferior to that obtained by heating in an atmosphere of H_2S + HCl.

3. The presence of conditions favoring oxidation enhances the electroluminescence brightness provided the oxygen containing compounds are introduced into the batch in very small amounts. Introduction of an excessive amount reduces the electroluminescence intensity. The fact that ZnO and Cu_2O, which are good semiconductors, form under these conditions shows that for obtaining efficient electroluminophors it is essential to have a system comprising several components that are semiconductors.

Apparently, this (i.e., the presence of semiconductor components) also accounts for the increase of brightness obtained by the addition of ZnSe to ZnS:Cu:Pb electroluminophors.

State Institute of Applied Chemistry

References

1. H.H.Homer, R.M.Rulon & K.H.Butler, J.Electrochem.Soc., 100,566 (1953).
2. H.C.Frölich, J.Electrochem.Soc., 100, 280 (1953).
3. D.Curie, J.Physique et Radium, 14, 510 (1953).
4. W.W.Piper & F.F.Williams, Phys.Rev., 81, 151 (1952); British J.Appl. Phys., Suppl., 4, 39 (1955).
5. D.R.Frankl, Phys.Rev., 100, 1104 (1955).
6. W.R.Watson, J.J.Dropkin & A.T.Halpin, Phys.Rev., 94, 477(A) (1954).
7. P.Zalm, G.Diemer & H.A.Klasens, Philips Res.Reports, 9, 81 (1954).
8. A.A.Bundel', Thesis, Moscow State University, 1956.
9. G.Destriau, Phil.Mag., 38, 700 (1947).
10. S.Nudelmann & F.Matossi, J.Electrochem.Soc., 103, 1, 34 (1956).
11. G.Destriau & J.Mattler, J.Physique et Radium, 1, 227 (1945).
12. G.Destriau, British J.Appl.Phys., Suppl., 4, 49 (1955).

ZINC SULFIDE BASE ELECTROLUMINOPHORS

- I.N.Orlov

Numerous reports on investigations of the electroluminescence of polycrystalline phosphors published during the past 5-6 years in scientific journals abroad are concerned for the most part with the properties of copper-activated zinc sulfide phosphors prepared by a special procedure. The distinctive characteristic of luminophors of this class is that the copper is introduced into the initial batch in amounts considerably exceeding the Cu content in ZnS:Cu phosphors intended for UV or CR excitation. The introduction of large amounts of Cu also proves necessary in the case when the luminescence band is produced in the zinc sulfide not by the copper itself but by other activators, i.e., the copper exerts a "sensitizing" effect on the electroluminescence of zinc sulfide phosphors with different other activators.[1]

There have been published a number of reports giving the details of preparation of electroluminescing hexagonal zinc sulfide phosphors[1,2]. According to the data in the literature, these electroluminophors are inferior as regards efficiency to zinc sulfide phosphors with a cubic structure, the preparation of which has been described by Homer et al[3]. The distinctive features of the synthesis of cubic luminophors are the following. In addition to the principal activator (copper or manganese) compounds of lead and zinc oxide are introduced into the batch; the batch is fired at 750-1050° in a nitrogen atmosphere. The addition of lead (up to $4 \cdot 10^{-3}$g per gram ZnS) led to the formation of brighter electroluminophors. The zinc oxide (up to 4%) was found necessary to obtain homogeneously luminescing products. The excess zinc oxide after heating was removed from the powdered phosphors by washing in hot acetic acid solutions. The luminescence color of the phosphors is controlled by varying the principal activator content: "Blue" electroluminophors contained $(2\text{-}4) \cdot 10^{-4}$g Cu per gram ZnS, "green" contained $2.5 \cdot 10^{-4}$ to $1 \cdot 10^{-3}$g Cu per gram ZnS, "yellow" - up to $1 \cdot 10^{-3}$g Cu per gram ZnS and up to $3 \cdot 10^{-3}$g Mn per gram ZnS. For the most part $ZnCl_2$ (about 3%) was used as the flux. According to the published data, such luminophors have an efficiency of up to 5 lumens per watt and are, apparently, more efficient than most other electroluminophors. They have found practical application in the production of electroluminescent lamps.

The present research was initiated for the purpose of developing a laboratory procedure for the synthesis of zinc sulfide luminophors. In the future it is proposed to determine the possibility of producing electroluminescent screens for various applications (low intensity light sources, television and other special purpose screens).

The investigation was concerned primarily with the synthesis of cubic ZnS:Cu:Pb and ZnS:Cu:Mn:Pb luminophors.

The batches were prepared by careful mixing of the components (ZnS,CuO, $2PbCO_3 \cdot Pb(OH)_2$, $ZnCl_2$, ZnO and $MnCl_2 \cdot 4H_2O$) without the addition of water. The batches were heated in a quartz tube in an electric furnace. Quartz crucibles having a capacity of about 70 g were placed uncovered inside the quartz tube through which was passed a stream of oxygen-free nitrogen. The heated powders were washed in a hot 10% acetic acid solution, then in hot distilled water, dried at 120-130° and finally after inspection and selection under UV (3650 A) excitation used for preparing the test suspensions in insulating lacquer.

The electroluminescence spectra were recorded by means of a VEI (All-Union Electrotechnical Institute) photomultiplier through an UM-2 universal monochromator. The set-up (monochromator-photomultiplier-mirror galvanometer) was graduated with reference to a standard VNIIM 2500°K lamp. The brightness

of the electroluminescence of the experimental capacitors was measured by means of a universal VEI UFK-1 photocolorimeter.

Electroluminescing capacitors

For investigating the electroluminescence of the synthesized phosphors we prepared special capacitors with one transparent electrode. In most cases the transparent electrode was a glass plate with a vaporized coating of tin dioxide. Tin dioxide coatings on glass have a resistivity of from 10^{-3} to 3 ohm/cm with a transmission of 80-90%.[4] These coatings are chemically stable (are not attacked by concentrated nitric and other acids and are only slowly etched by hydrochloric acid), mechanically strong and withstand heating in air to 450-500°. The SnO_2 coatings were prepared by placing hot (450°) glass plates in the stream of the products of thermal decomposition of $SnCl_2.2H_2O$, mixed with air.

In the case of capacitors of large area the use of transparent SnO_2 coated electrodes is disadvantageous in view of the appreciable voltage drop in the semiconductor layer. Moreover, it is difficult in practice to obtain a layer of uniform conductivity over the entire surface of a large plate.

Hence we also tried using metallic screens (brass or phosphor-bronze gauze) for the transparent electrodes. The use of special metallic screens, which appreciably simplifies the preparation of electroluminescent lamps, will apparently prove necessary in the fabrication of multiple unit capacitors for non-vacuum television and other special screens.

The second electrode of the capacitors used in most of our experiments was a thin vacuum evaporated aluminum coating covered with a layer of lacquer to protect the aluminum against oxidation.

Between the two electrodes was the layer of dielectric with the phosphor powder dispersed in it. In most cases the dielectric material was a mixture of malamine formaldehyde and alkyd rezyl resins. The K-421-02 and No.90 lacquers, put out by the chemical industry on the basis of these resins, are very convenient for preparing phosphor suspensions and yield an elastic, strong and relatively moisture resistant film when dried at 100-110°. Films about 100 microns thick are transparent and withstand a voltage of about 1500 v (RMS) without breakdown. The luminescing layers usually contained about 30% phosphor by weight. A lower degree of filling of the dielectric reduced the luminescence brightness, while a higher degree led to so-called "self-healing" breakthroughs of the layer along "bridges" of phosphor particles with the formation of nonluminescing spots in the layer.

Different designs of electroluminescing capacitors prepared in our laboratory in 1955 are shown in Fig.1.

ZnS:Cu:Pb and ZnS:Cu:Mn:Pb electroluminophors

The luminescence spectra of ZnS:Cu:Pb phosphors consist of two bands: a green band peaking at about 520 mμ and a blue peaking at about 460 mμ. The ratio of the intensities of these bands depends not only on the Cu content in the initial batch but also on the Pb content, the temperature and atmosphere of heating and the amount and type of flux used. In addition, this ratio depends on the frequency of the alternating field exciting the electroluminophor.

The brightest ZnS:Cu:Pb electroluminophors are obtained when about $8 \cdot 10^{-3}$g Pb per gram ZnS, 3% $ZnCl_2$ and 4.2% ZnO are incorporated in the batch; the heating must be carried out at 800-900° in an atmosphere of nitrogen.

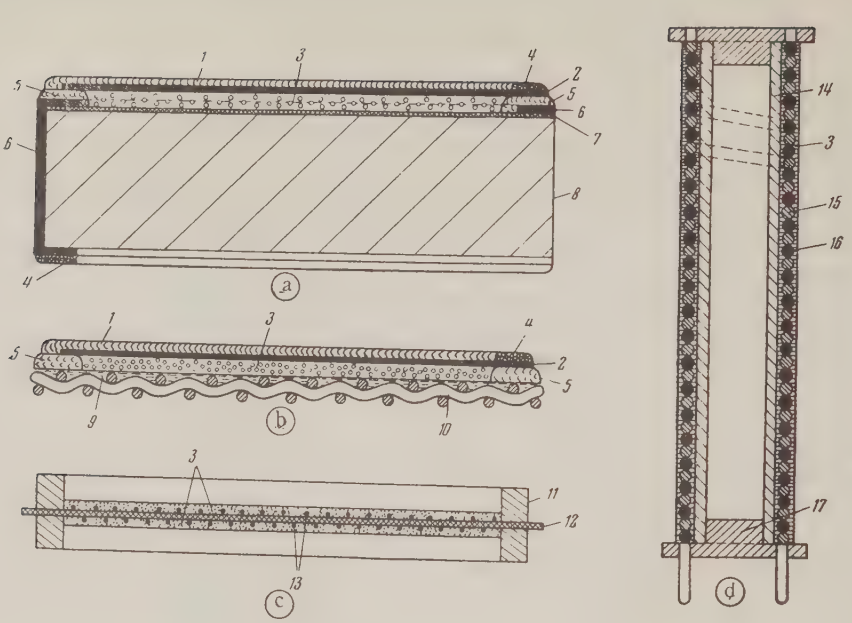

Fig.1. Electroluminescing capacitors: a) on glass, b) on a metallic screen, c) with two transparent electrodes, d) wire on a glass tube. 1) protective lacquer film, 2) aluminum coating, 3) layer of phosphor dispersed in the dielectric, 4) bronze powder contact, 5) frame of pure dielectric, 6) aquadag, 7) transparent conducting layer, 8) glass, 9) dielectric film, 10) metallic screen, 11) metallic frame, 12) mica, 13) metallic filaments, 14) glass tube, 15) enameled wire I, 16) enameled wire II, 17) base.

If these ingredients and the heating procedure are kept constant and only the amount of copper in the batches varied, it is found that below a certain threshold copper concentration the electroluminescence is very weak, with virtually only the blue band being discernible. Brighter "blue" electroluminophors are obtained when the copper content in the batch is about $3\cdot10^{-4}$g Cu per gram ZnS. In such luminophors, however, the green band is also fairly well developed, which can be noted from changes in the color of the luminescence with variation of the frequency of the exciting field. Gradual increase of the copper concentration leads to an increase of the relative intensity of the green band. The brightest "green" electroluminophors are obtained with a copper content in the batch of about $(1-2)\cdot10^{-3}$g Cu per gram ZnS. The color of these phosphors also changes with the frequency of the exciting alternating field. No such color variation is observed in the case of phosphors prepared with $5\cdot10^{-3}$g Cu or more per gram ZnS, but the brightness of these luminophors is relatively low: the decrease in brightness is apparently due not so much to concentration quenching as to a sharp increase in the conductivity of the phosphor grains: capacitors with such luminophors heat up appreciably during operation and breakdown often occurs even at relatively moderate field strengths The variation of the electroluminescence of ZnS:Cu:Pb phosphors as a function of the copper concentration in the batch is shown in Fig.2.

The effect of varying the Pb content in the batch, other conditions being equal, is the contrary of that obtained by varying the Cu content: small

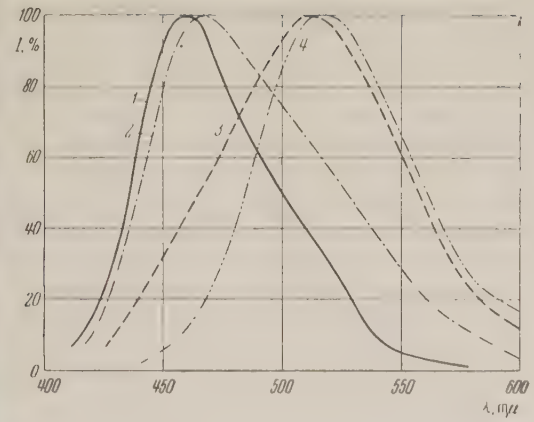

Fig.2. Variation of the electroluminescence spectrum of ZnS:Cu:Pb phosphors with the copper content of the batch. Batch composition: 100% ZnS+ + 3% $ZnCl_2$ + 4.2% ZnO + $8 \cdot 10^{-3}$g Pb per gram ZnS + (1) $3 \cdot 10^{-4}$g, (2) $2.7 \cdot 10^{-4}$g, (3) $2 \cdot 10^{-3}$g, (4) $5 \cdot 10^{-3}$g Cu per gram ZnS. Spectra obtained with excitation by a 5000 cps and 750 v field.

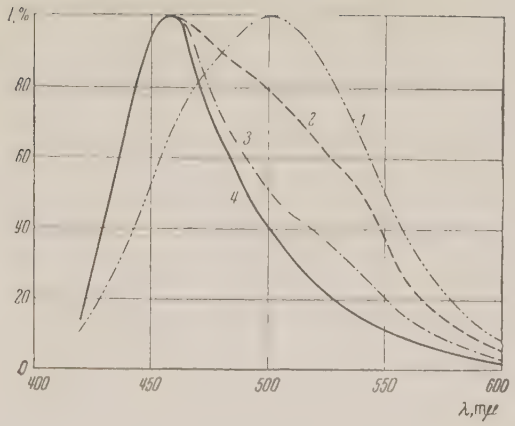

Fig.3. Variation of the electroluminescence spectrum of ZnS:Cu:Pb with the lead content in the batch. Batch composition: 100% ZnS + 3% $ZnCl_2$ + 4.2% ZnO + + $3 \cdot 10^{-4}$g Cu per gram ZnS + (1) $1.5 \cdot 10^{-3}$g, (2) $3.5 \cdot 10^{-3}$g, (3) $4.5 \cdot 10^{-3}$g, (4) $8.5 \cdot 10^{-3}$g Pb per gram ZnS. Spectra obtained with excitation by an 1850 cps, 450 v field. (All ac field values in these figures and below are RMS.)

additions of zinc favor development of the green luminescence band, while larger amounts tend to suppress it in favor of the blue.

The effect of different amounts of lead on the electroluminescence spectrum of phosphor containing $3 \cdot 10^{-4}$g Cu per gram ZnS is shown in Fig.3. Up to a concentration of $1 \cdot 10^{-3}$g Pb per gram ZnS, the green band predominates in the luminescence, but the brightness of the luminophor is low. Increasing the lead concentration to $9 \cdot 10^{-3}$g per gram ZnS together with an increase of the integral brightness leads to quenching of the green and stimulation of the blue band. Further increase in the Pb content reduces the integral brightness of the luminophor with no appreciable change in the spectrum.

Thus if we assume that the blue luminescence band of ZnS:Cu phosphors is connected with their decomposition into two phases and, consequently, attribute this band to activatorless ZnS, the role of lead may be characterized as that of a regulator of the amount of copper actually entering into the zinc sulfide lattice and activating it. As we shall show below, this influence is characteristic not only of lead.

ZnS:Mn phosphors do not exhibit electroluminescence. If, in addition to Mn, Cu is introduced, one can obtain a series of zinc sulfide electroluminophors whose luminescence color depends both on the concentration of Cu and that of Mn. Fig.4 shows the electroluminescence spectra of ZnS:Cu:Pb phosphors with different concentrations of manganese and a constant proportion of copper ($1 \cdot 10^{-3}$g per gram ZnS) and lead ($9 \cdot 10^{-3}$g per gram ZnS). In the Mn concentration interval from $2 \cdot 10^{-3}$ to $3 \cdot 10^{-3}$g Mn per gram ZnS there occurs a sharp change in the electroluminescence spectrum: the green copper band fades out and only the Mn band peaking at about 585 mμ remains. Further increase in the Mn content does not alter the luminescence spectrum, but does

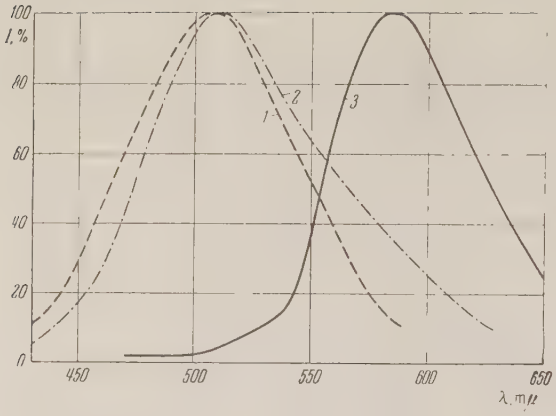

Fig.4. Variation of the electroluminescence spectrum of ZnS:Cu:Mn:Pb with the manganese content in the batch. Batch composition: 100% ZnS + + 3% $ZnCl_2$ + 4.2% ZnO + $1 \cdot 10^{-3}$g Cu per gram ZnS + $9 \cdot 10^{-3}$g Pb per gram ZnS + (1) $1\text{-}9 \cdot 10^{-4}$g, (2) $1\text{-}2 \cdot 10^{-3}$g, (3) $3 \cdot 10^{-3}$ - $5 \cdot 10^{-2}$g Mn per gram ZnS). Spectra obtained with excitation by an 1850 cps, 450 v field.

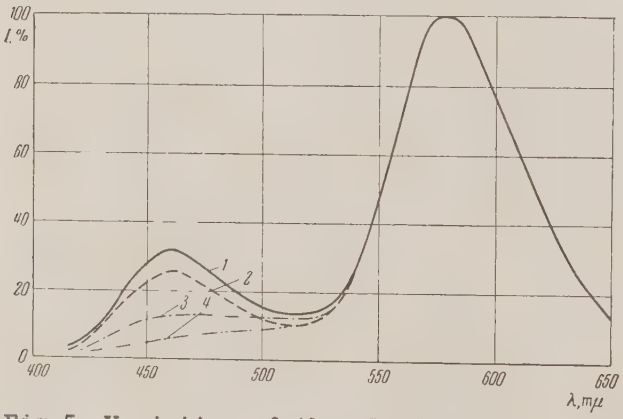

Fig.5. Variation of the electroluminescence spectrum of ZnS:Cu:Mn:Pb phosphors with the copper content in the batch. Batch composition: 100% ZnS + 3% $ZnCl_2$ + 4.2% ZnO + + $3 \cdot 10^{-3}$g Mn per gram ZnS + $9 \cdot 10^{-3}$g Pb per gram ZnS + (1) $3 \cdot 10^{-4}$g, (2) $6 \cdot 10^{-4}$g, (3) $8 \cdot 10^{-4}$g, (4) $1 \cdot 10^{-3}$g Cu per gram ZnS. Spectra obtained with excitation of the luminophors by an 1850 cps, 1500 v field.

lead to a decrease of the integral intensity. It should be noted that in the case of ZnS:Cu:Mn:Pb phosphors with an Mn content of $3 \cdot 10^{-3}$g per gram ZnS (green band entirely killed), increasing the copper content above $1 \cdot 10^{-3}$g per gram ZnS (the optimal content of copper for "green" ZnS:Cu:Pb phosphors) results only in a reduction of the brightness but does not change the spectrum, while decreasing the copper content intensifies the blue band associated with activatorless ZnS without appreciably altering the integral brightness. This last effect is shown in Fig.5. One can obtain "white" emission from luminophors with two luminescence bands - 460 and 585 mμ - under excitation with an electric field.

Influence of certain factors on the properties of zinc sulfide electroluminophors

We have already noted that by varying the amount of lead in the batch one can control the amount of copper actually lodging in the lattice and producing "green centers" in the phosphor. We found that the extent of incorporation of copper into the ZnS lattice can also be regulated by introducing compounds of antimony, bismuth and tin instead of lead into the batch. With the content of all the other components of the batch and the heating conditions being equal, the effectiveness of these additives as regards development of the blue luminescence band in ZnS:Cu phosphors (or what is equivalent as regards reduction of the amount of copper actually entering into the ZnS lattice) is characterized by the series

$$Sb > Bi. > Sn > Pb,$$

which agrees with the series characterizing the relative volatility of the corresponding chlorides:

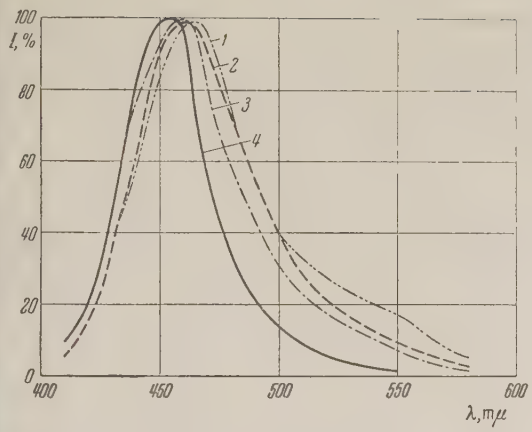

Fig.6. Influence on the spectrum of "blue" ZnS:Cu electroluminophor of different added impurities. Batch composition: 100% ZnS + 3% $ZnCl_2$ + + 4.2% ZnO + $3 \cdot 10^{-4}$g Cu per gram ZnS + (1) $1 \cdot 10^{-2}$g Sn, (2) $9 \cdot 10^{-3}$g Pb, (3) $8 \cdot 10^{-3}$g Bi, (4) $1.6 \cdot 10^{-1}$g Sb per gram ZnS. Spectra recorded with excitation by an 1850 cps 1000 v field.

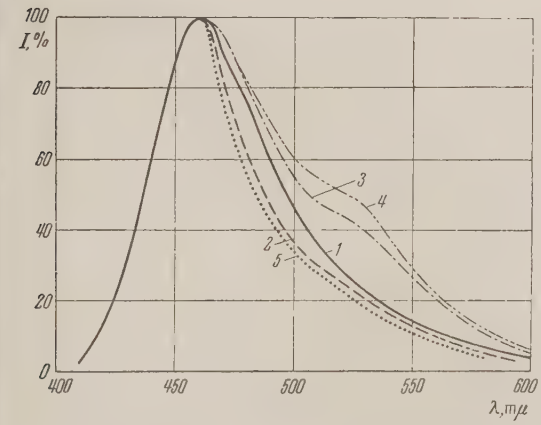

Fig.7. Influence on the spectrum of "blue" ZnS:Cu:Pb luminophor of different fluxes. Batch composition: 100% ZnS + 4.2% ZnO + $3 \cdot 10^{-4}$g Cu per gram ZnS + $8 \cdot 10^{-3}$g Pb per gram ZnS + + (1) 4% $ZnCl_2$, (2) 4% NaCl, (3) 4% $BaCl_2$, (4) 4% $MgCl_2$, (5) 2% NaCl + 2% NH_4Cl. Spectra recorded with excitation by an 1850 cps 1500 v field.

$$SbCl_3 > BiCl_3 > SnCl_2 > PbCl_2.$$

The luminescence spectra of the electroluminophors containing $3 \cdot 10^{-4}$g Cu per gram ZnS and different added impurities are shown in Fig.6.

Our investigation of the effect of these additives has not been completed. Some of the electroluminophors synthesized with such impurities may prove to be of practical value. For example, we obtained a rather bright electroluminophor with saturated blue luminescence in which the lead is replaced by bismuth in the amount of $3 \cdot 10^{-3}$g per gram ZnS. This luminophor in combination with the L-10 or L-15 phosphor might be used for the preparation of multiple unit capacitors capable of fulfilling the function of radar cascade screens. The results obtained with the introduction of various impurities in place of lead give reason to hope that by this means one can not only vary the color of zinc sulfide electroluminophors but also increase their efficiency.

Different fluxes have different effects on the emission spectrum and on the brightness of the electroluminophors. In addition to $ZnCl_2$, recommended in the literature, we also tested NaCl, NH_4Cl, $BaCl_2$ and $MgCl_2$. The electroluminescence spectra of phosphors prepared with $3 \cdot 10^{-4}$g Cu per gram ZnS and 4% of different fluxes in the batch are shown in Fig.7. The blue emission band is manifested most strongly when NaCl or a mixture of NaCl + NH_4Cl is used as the flux. Ammonium chloride alone yields specimens with a very low brightness. The influence of the listed fluxes on the spectral composition of the electroluminescence is similar at higher copper concentrations in the batch as well. As regards the brightness of the specimens, it may be noted that $ZnCl_2$ and NaCl give equivalent results, while the use of the other fluxes results in phosphors with a low electroluminescence intensity.

The addition of zinc oxide to the batch in amounts from 0.5 to 10% virtually has no influence on the emission spectrum of ZnS:Cu:Pb electroluminophors. As regards the brightness of these phosphors with excitation by an electric field, the addition of ZnO appreciably reduces the brightness of specimens heated in air as compared with specimens heated in nitrogen. With no ZnO in the batch, specimens heated in nitrogen and in air have virtually the same luminescence brightness. This factor allows of simplifying the synthesis procedure for ZnS:Cu:Pb electroluminophors.

Other conditions being equal, the heating temperature has an appreciable influence on both the emission spectrum and the brightness of the electroluminophors.

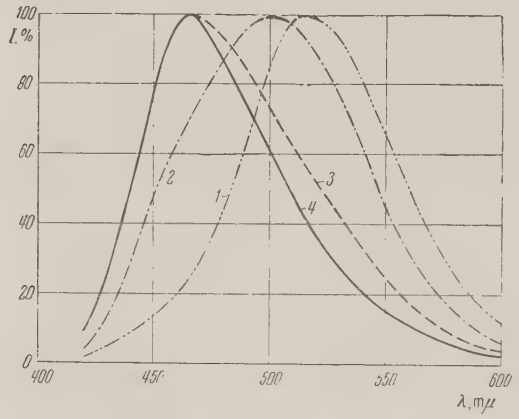

Fig. 8. Influence of the heating temperature on the electroluminescence spectrum of "green" ZnS:Cu:Pb phosphor. Batch composition: 100% ZnS + 3% $ZnCl_2$ + 4.2% ZnO + $2 \cdot 10^{-3}$g Cu per gram ZnS + $8 \cdot 10^{-3}$g Pb per gram ZnS). Heating temperatures: 1) 800°, 2) 1000°, 3) 1100°, 4) 1200°. Spectra recorded with excitation by a 1850 cps 1000 v field.

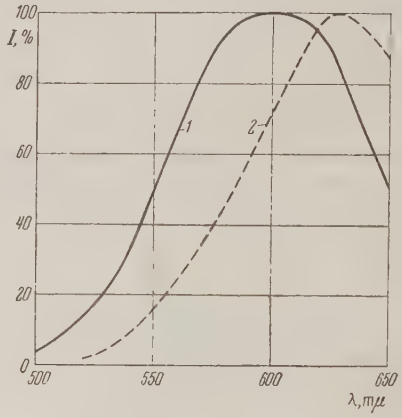

Fig. 9. Spectra of "yellow-orange" and "orange" ZnS.ZnSe electroluminophors. Spectra obtained with excitation by a 1850 cps 1000 v field. Batch composition: 5% ZnO + 2% $ZnCl_2$ + $3 \cdot 10^{-4}$g Cu + + $8 \cdot 10^{-3}$g Pb per gram base + (1) 30% ZnS + 70% ZnSe and (2) 15% ZnS + 85% ZnSe.

In Fig.8 we show the luminescence spectra of phosphors prepared from a batch containing $2 \cdot 10^{-3}$g Cu, $8 \cdot 10^{-3}$g Pb per gram ZnS, 4% ZnO and 3% $ZnCl_2$ by heating at different temperatures from 800 to 1200°. There is a noticeable shift of the luminescence to the short wave (blue) side with increasing temperature. The luminescence brightness decreases accordingly. The residual amount of lead in the prepared phosphor is equal to about $1 \cdot 10^{-4}$g per gram ZnS with heating at 800° and decreases to $1 \cdot 10^{-5}$g per gram ZnS when the heating temperature is raised to 1100°.

Partial replacement of the zinc with cadmium shifts the luminescence to the long wave side. Fairly bright ZnS.CdS:Cu:Pb electroluminophors are obtained, however, if the amount of cadmium sulfide in the batch does not exceed 15-20% ("yellow" electroluminophors). The addition of larger amounts of cadmium with the aim of obtaining "red" luminophors (up to 80% CdS) leads to a sharp increase in the conductivity of the phosphor grains and accordingly to a decrease of the efficiency. Under excitation by an electric field such luminophors yield thermal radiation rather than luminescence, although under

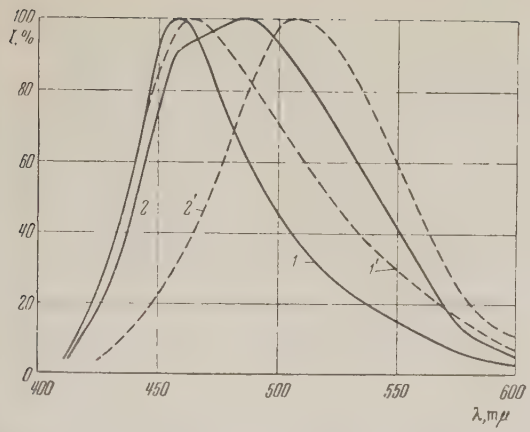

Fig.10. Variation of the spectra of "blue" and "green" electroluminophors with the frequency of the exciting electric field: 1) "blue" phosphor at 5000 cps (750 v), 1') "blue" at 370 cps (750 v), 2) "green" at 5000 cps (600 v), 2') "green" at 370 cps (600 v).

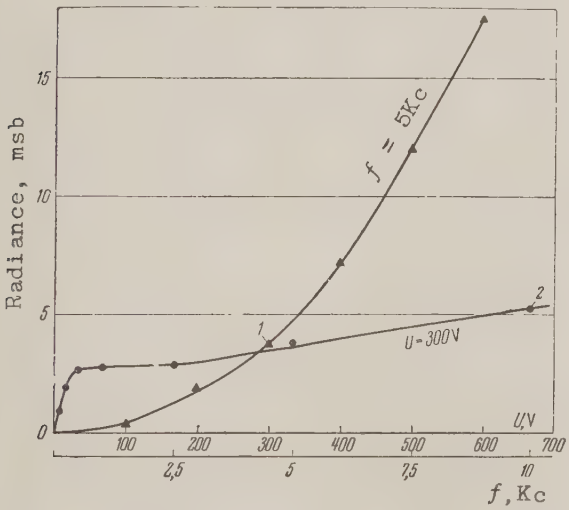

Fig.11. Dependence of the intensity of the electroluminescence on the frequency and voltage of the applied field for a "green" electroluminophor: 1) variation with RMS voltage, 2) variation with frequency.

ultraviolet excitation they are characterized by bright red luminescence.

By partial replacement of the sulfur with selenium one can obtain bright "yellow-orange" and "orange" ZnS.ZnSe:Cu: :Pb electroluminophors; their electroluminescence spectra are shown in Fig.9.

As was noted above, the color of the electroluminescence of the investigated phosphors also depends on the frequency of the exciting field. The change in color with variations in frequency is the greater, the more complex the emission spectrum of the electroluminophor. In the case of phosphors whose luminescence spectrum comprises only one band (blue, green or yellow), the color does not change with the field frequency.

The curves of Fig.10 show the variation of the luminescence spectrum with the frequency of the exciting electric field for two phosphor specimens: a "blue" and a "green" one. The brightness of the electroluminescence changes appreciably depending on the amplitude and frequency of the exciting voltage. This dependence for one of the "green" electroluminophors is shown in Fig.11.

It must be noted that the radiance values as measured with the capacitors of the type used in the present investigation depend not only on the properties of the electroluminophors but also on certain parameters of the capacitor (voltage drop in the conducting layer on the glass, degree of filling of the dielectric with the phosphor, thickness of the luminescing layer, amount of moisture present in the luminescent layer, etc.), parameters which we cannot as yet control in preparing the capacitors. Hence the results of luminance measurements cannot serve as an accurate index for comparing the characteristics of different luminophors and are deliberately omitted here. Furthermore, measurements of the small amounts of power dissipated in the electroluminescing capacitors presents certain experimental difficulties and until a reliable method for measuring the power has been found the detailed discussion of the efficiency of the electroluminophors is premature. According to a very rough evaluation, the efficiency of our best electroluminophor specimens (or more accurately of our electroluminescing capacitors) is about 4-5 lumens per watt.

Conclusions

It has been experimentally established by Waymouth & Bitter[5] that the luminescence of powdered electroluminophors is not uniform but is confined to small "spots"; the brightly luminescing "pinpoints" are located either at the tips of needle-shaped grains or at the areas of contact of two or more crystallites in the aggregates. The inhomogeneity of the luminescence of the particles, which indicates that electric field distribution in them is inhomogeneous, is a consequence of the different electric properties of the internal volume and surface layers of the phosphor grains[6], i.e., is apparently connected with the chemical inhomogeneity of the grains. We repeated the well-known experiments of Zalm et al[2] with $CuSO_4$ solutions. Ordinarily, the commercial phosphors K-10, K-50 and L-50 are not excited by an alternating field; however, after being moistened with a solution of $CuSO_4$ containing $1 \cdot 10^{-2}$g Cu per gram phosphor and dried at a temperature of 120-130°, they exhibit a weak electroluminescence with the color characteristic of their UV excited emission. These experiments and the above described effect of copper on the brightness of ZnS:Cu:Pb electroluminophors show that in order to obtain effective electroluminophors it is necessary to produce a phase rich in copper on the surface of the phosphor grains. Judging by the external appearance of the electroluminescing powders (the color ranges from gray to grayish cream depending on the copper content of the batch), it may be assumed that this phase comprises either CuS or CuO. So far we have not succeeded in detecting this phase in x-ray diffraction patterns, at least for specimens prepared from batches containing up to $3 \cdot 10^{-3}$g Cu per gram ZnS. The sharp drop in the brightness of the specimens and their sparking in the capacitors when more than $5 \cdot 10^{-3}$g Cu per gram ZnS is introduced into the batch shows that too large a quantity of the copper phase (which is a better conductor than ZnS) is undesirable, inasmuch as in this case the phosphor particles apparently become coated with a continuous layer of this phase, which effectively "short circuits" them.

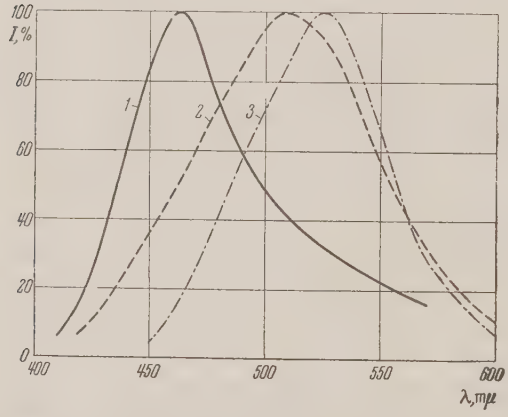

Fig.12. Influence of chlorine on the electroluminescence spectrum of ZnS:Cu phosphor. Spectra recorded with excitation by a 1850 cps 300 v field. Batch compositions: 1) ZnS + + CuO, 2) ZnS + $CuCl_2$, 3) ZnS + CuO + + 4% flux (NaCl + $MgCl_2$). In all cases the copper content in the batch was $8 \cdot 10^{-3}$g Cu per gram ZnS. All batches were heated in nitrogen at 900°.

Thus the introduction of relatively large amounts of copper into the batch is connected with the necessity of producing a phase rich in copper in the phosphors.

As regards the second function of copper - that of activator of the zinc sulfide electroluminophors - it may be concluded from the experimental data that chloride ions facilitate the penetration of the copper into the ZnS lattice. All the factors accelerating the elimination of chloride from the batch during heating (apparently after the flux has performed this essential role in recrystallization of the host material) reduce the relative intensity of the green copper band and the integral emission of the luminophor. This may explain the differences of the effects

produced by lead, tin, bismuth and antimony and the influence of increasing the heating temperature.

This view is further substantiated by the following data.

Electroluminophors can be obtained from a batch containing only ZnS and some copper compound. We prepared electroluminophors by adding copper in the form of CuO and $CuCl_2$. Moreover, we obtained an electroluminophor from a batch containing CuO and 4% flux ($NaCl + MgCl_2$). In all three cases the copper was introduced in the amount of $8 \cdot 10^{-3}$ g per gram ZnS and the batch heated at 900° in nitrogen. The luminescence spectra of all three electroluminophors are shown in Fig.12. When no chlorine was introduced into the batch (i.e., when CuO was used) the luminescence was blue. Introduction of the copper in the form of $CuCl_2$ shifted the electroluminescence to the long wave side; addition of a flux together with CuO yielded an electroluminophor with saturated blue luminescence.

It must be noted that the role of lead and other similar additives is apparently not limited to that of regulator of the residual chlorine in the phosphors. The brightest electroluminophors are obtained only in the presence of such impurities; it may be assumed that these substances also act to further the formation of phosphor grains possessing the requisite electric properties.

References

1. H.C.Froelich, J.Opt.Soc.Am., 43, 320 (1953).
2. P.Zalm, G.Diemer & H.A.Klasens, Philips Res.Rep., 9, 81 (1954).
3. H.H.Homer, R.M.Rulon & K.H.Butler, J.Electrochem.Soc., 100, 566 (1953).
4. R.Gomer, Rev.Sci.Instr., 24, 993 (1953).
5. J.F.Waymouth & F.Bitter, Phys.Rev., 95, 941 (1954).
6. W.W.Piper & F.E.Williams, Phys.Rev., 98, 1809 (1955).

DISCUSSION OF THE REPORTS OF BUKKE, VINOKUROV, ORANOVSKII, Z.A.TRAPEZNIKOVA & V.S.TROFIMOV, KAZANKIN, PEKERMAN & PETROSHINA and ORLOV

Question: What is, in your opinion, the mechanism of electroluminescence?

V.E.Oranovskii: According to all available data the mechanism of electroluminescence is essentially the same as in photoluminescence. So far no difference between the spectra has been detected. Obviously, the excitation is electronic. The electrons, having entered the conduction band, acquire a sufficient energy along their free path to excite centers by impact. According to the more widely held point of view, ionization occurs when the prebreakdown state of the luminophor is attained. There is multiplication of the electrons which excite centers along their paths, thus giving rise to luminescence.

As for where the electrons come from, whether they are ejected from the valence band or injected from without, there appear to be different points of view. It would appear to be impossible to choose between them at present due to lack of adequate experimental data. The theoretical interpretations from different viewpoints explain with equal success some part of the available experimental material, but so far no viewpoint can be definitively confirmed.

F.I.Vergunas: What was the composition of the dielectric resin, what solvent did you use and how were the phosphors applied?

V.E.Oranovskii: We used two dielectrics: silicone insulating oil (absolutely transparent) and a mixture of melamine formaldehyde and alkyd rezyl resins; the second is less transparent in a thick layer, but in a thin layer is completely transparent. In some cases we dried the suspension and obtained

a dry solid layer; in other cases we used liquid capacitors, that is, simply the resin with the phosphor suspended in it.

As for applying the liquid, the drops of the suspension are spread over the surface by the second electrode.

Question: How do you explain the wave-difference (for radiance waves) of opposite sign for trapezoidal pulse excitation as compared with sinusoidal excitation? I assume the duty factors were the same.

V.E.Oranovskii: The duty factor was the same, but the frquency was different. According to the data in the literature and, in particular, the results of Destriau it would appear that a wave-difference can be observed with both signs of the exciting field.

A.M.Bonch-Bruevich: What distinctive characteristics must a phosphor have for it to exhibit pronounced electroluminescence? Did you determine the dependence of the luminescence characteristics on the degree of dispersion of the powder, i.e., on the grain size? What is the frequency dependence of the electroluminescence?

V.E.Oranovskii: The most important trait of electroluminophors is a higher concentration of activator than in ordinary phosphors. We did carry out experiments on the influence of grain size; we took the same luminophor and screened it to separate the large and small grains. No difference was detected. Possibly this is due to the fact that so far we have not been able to prepare capacitors of the same thickness with the same ratio of dielectric to phosphor. With increasing frequency, the integral brightness increases, but the rate of increase is different for different bands. Thus ZnS:Cu has two bands: with increasing frequency, the intensity of the blue band increases without saturation, that of the green band with saturation.

F.M.Pekerman: What do you think of the views of Piper & Williams regarding the necessity of there being a potential barrier between the phosphor and the metallic electrodes? What in your opinion is the role of the polarization charge in the case of excitation by trapezoidal pulses?

V.E.Oranovskii: We proceed from the assumption that the electrons accelerated by the field, while accelerating,have a low probability of recombination since they have an energy exceeding the thermal energy. There is known to be a difference between the probabilities of recombination for optical and thermal electrons. Hence, while the field is rising there is no recombination, that is, we have a dark interval. When the field stops increasing and becomes constant, equilibrium between the applied external field and the field of the polarization charge is established. There is no field, or only a minimal field, inside the crystal. The electrons for which initially the probability of recombination was small, lose their energy and become capable of recombining. This explains the appearance of the radiance peak and is the way in which the polarization charge is evinced. With a symmetric pulse the polarization charge is fully compensated, while with a nonsymmetric pulse the polarization charge remains to some degree. Now as for the potential barrier. Apparently some field concentration is necessary for the appearance of electroluminescence. A potential barrier, however, can arise in different ways; it need not be assumed that the potential barrier must form only at the contact with metal. It can appear at any boundary that has rectifying characteristics.

L.N.Galkin: Are there different forms of electroluminescence?

V.E.Oranovskii: Two forms of electroluminescence are known: the Losev effect and the Destriau effect. The Losev effect is luminescence of a crystal, for example, carborundum, on the application of a dc voltage. The Destriau effect is electroluminescence under the influence of an alternating voltage. Where powders are concerned, a constant voltage does not give luminescence, but produces only a flash at the instants of application and removal of the

field. This can be explained by the polarization effect. In the case of the Losev effect, direct contact with metal apparently plays a certain role, but I am unable to go into the details of the matter because so far we have not worked with single crystals.

Z.I.Klabukova: Did you succeed in obtaining electroluminophors without zinc oxide in an atmosphere of nitrogen?

Z.A.Trapeznikova: If ZnS is purified to remove all impurity anions and then Cu_2S is added to it and the mixture heated in a stream of nitrogen with no traces of oxygen, then even at a Cu concentration of only 10^{-6}g per gram ZnS there is observed a very weak electroluminescence. If 10^{-4}g copper per gram ZnS are introduced, there is obtained a gray phosphor with a bright blue electroluminescence.

M.V.Fok: In liquid capacitors there is usually great vibration due to electrostatic attraction. How did you eliminate this?

F.M.Pekerman: Vibration was observed in the cases when the amount of phosphor was small and if we had a very thin layer. In most of our experiments with a layer thickness of about 200 microns no vibration was observed.

M.V.Fok: In our experiments we sometimes found that upon application of the field the brightness increased for a considerable time, for several minutes. Did you observe this?

F.M.Pekerman: Yes, we observed this effect. At first we though that it was the influence of heating, but this apparently is not the case. In view of this we began to wait about five minutes before starting measurements; after this delay reproducible results were obtained.

V.E.Oranovskii: How do you explain the maxima in the frequency characteristics?

F.M.Pekerman: We thought at first that it was due to some fault of our set-up, but their existence has been substantiated. Nudelmann in one of his reports states that on the basis of a communication from one of his co-workers it follows that the frequency characteristic is not linear, that in some cases there is observed a maximum near 4-5 kc.

Question: Do you have proofs that the semiconductor layer is located on the surface?

F.M.Pekerman: The proof is the gray color of the phosphor. This means that there is Cu_2S on the surface. Furthermore, we sprinkled a phosphor with a $CuSO_4$ solution and obtained an electroluminophor.

D.A.Shklover: I have a question for I.N.Orlov: What are the possibilities of practical utilization of electroluminophors?

I.N.Orlov: The practical possibilities, in my opinion, are extensive, just as the potentialities of utilization of semiconductor devices in general. Some of the possibilities have already been described in the literature. There is a detailed description of a light amplifier, realized by combining a photoresistor and an electroluminophor, yielding 50-fold amplification. Such amplifiers have great possibilities.

There are also published reports on amplifiers of a different type. These are sublimated films for amplification of ultraviolet and x-ray radiation. Such amplifiers are used for diverse x-ray screens.

Combination of an electroluminophor and a photoresistor with the use of optical feedback between them makes it possible to realize a data storage unit similar to a memory tube. Finally, one can use electroluminophors as sources of low intensity light for illuminating instruments and dials in aircraft and so on. Such luminaires already exist.

M.V.Fok: We do not as yet have sufficient reliable data on electroluminescence to elaborate a specific theory. I would however like to put forth a few considerations which, in my opinion, should be borne in mind in the future,

in elaborating a theory.

There appears to be general agreement that for the appearance of electroluminescence a field concentration in a small volume of crystal is necessary. I think, however, that the magnitude of this critical concentration is probably greatly overestimated. It is usually assumed that electroluminescence appears only when over the length of their mean free path the electrons can acquire an energy sufficient for ionization or excitation of luminescence centers. Nevertheless, it may be that experimentally observed electroluminescence occurs much earlier, when the necessary energy is accumulated only by a few electrons which happen to have at the given instant a free path somewhat longer than the mean one.

My second remark concerns the role of dark conductance. Apparently, a certain optimum dark conductance is necessary for electroluminescence. Some preliminary experiments carried out in our laboratory showed that electroluminescence can be frozen, that is, that it does not exist at the temperature of liquid air. This is probably connected with the sharp decrease of dark conductance. On the other hand, too great a dark conductance would lead to the situation where no space charge will form inside the crystal and, consequently, there will be no field concentration.

Lastly, I want to note that all poarlization processes and, particularly, field concentration have "inertia" which apparently should be taken into account in considering electroluminescence. Our tentative experiments on excitation of electroluminescence by a field having a frequency of about 10^{10} cps did not give a positive result, although the same phosphors luminesced brightly (to 300 asb) at audiofrequencies. Apparently, during so short an interval as 10^{-10} sec, field concentration cannot develop and the electrons do not have time to acquire the necessary energy.

F.F.Vol'kenshtein: Any attempt to develop a quantitative theory of electroluminescence is still premature. It is, however, possible to discuss the question of the possible mechanism of luminescence in qualitative form. I would like to say a few words regarding one possible and, I feel, plausible mechanism. Luminescence consists of two successive events. The first event is ionization of the activator (excitation), the second event is recombination of the electron with an ionized activator (luminescence).

Under ordinary conditions (i.e., in the absence of an external field - see Fig.1) the first event (excitation) may occur in only one way, that indicated by arrow 1 in Fig.1. The second event (luminescence) is shown in this figure by arrow 2.

Now let us assume that the phosphor is placed in a strong electric field. The energy bands in this case will be inclined as shown in Fig.2. The stronger the field, the greater will be the slope of the bands. Now the excitation event (removal of an electron from an activator atom) can occur in two ways: in addition to the transition shown by arrow 1 in Fig.2 (endothermal transition), the transition shown by arrow 2 (a transition which does not require the expenditure of energy) is possible. Transition 1 represents conventional photoexcitation; transition 2 may be termed electroexcitation. This transition is due to the field and has a tunnel mechanism. Electroluminescence differs from ordinary luminescence in that the excitation occurs not along path 1 but along path 2. The luminescence even is shown in Fig.2 by arrow 3.

What specifically follows from the proposed model?

1. It will be seen from Fig.2 that electroluminescence can occur only with a sufficiently strong and necessarily alternating electric field. A dc field can only yield a flash. This is confirmed by experiment. In the case of a constant field, luminescence will cease as soon as the local levels A shown in the left part of Fig.2 are denuded, while the levels shown in the

right part of the figure are filled, i.e., as soon as the space charge distribution in the crystal is stabilized. For the luminescence to endure, the conduction band in Fig.2 must "rock", that is, tilt first to one side and then the other.

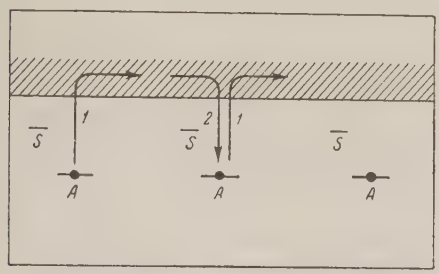

Fig.1

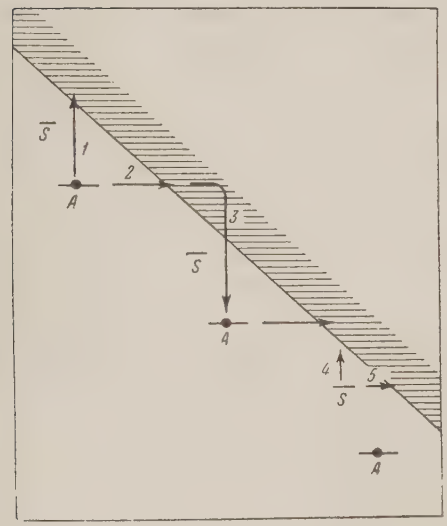

Fig.2

2. It is also clear that temperature should have no appreciable influence on the effect. This is also presumably in agreement with the experimental data.

3. In different phosphors electroluminescence must begin at different field intensities. According to the proposed mechanism, the deeper the activator levels are situated, the greater will be the field intensity necessary for electroluminescence. I don't know whether there are any experimental data on this point.

4. Electroluminescence must begin at fields at which Ohm's law no longer holds (in the case of semiconductors), i.e., in the prebreakdown region. The mechanism of electroluminescence is apparently closely connected with the prebreakthrough increase in conductivity. This increase in conductivity, immediately preceding breakthrough, occurs not according to the mechanism of impact ionization but according to the mechanism of field emission (tunnel effect).

5. Finally, we have the question of de-excitation of a crystal phosphor by an electric field. We have the following experimental fact: if a crystal phosphor in the absence of a field is excited by light and then placed into a strong field, the field will stimulate luminescence, i.e., the field will act in the same way as heating or illumination of the crystal with red or infrared light. This effect is also understandable from the standpoint of the proposed model. Thus the electrons stored on the trapping levels (levels S in Fig.2) can be released from them in two ways: by stimulation with heat or long wavelength light (arrow 4 in Fig.2) or by means of an electric field (arrow 5). It will be obvious that the de-exciting (stimulating) influence of the field must be observed at weaker field intensities than electroluminescence. Field strengths sufficient for electrostimulation, may not be sufficient for electroluminescence. Further, it is clear that while electroluminescence is possible only in an alternating field, electrostimulation can occur in a constant field. Only experiment can show whether these predictions are correct.

G.M.Eliashberg: In connection with the remarks of F.F.Vol'kenshtein it should be noted that the proposed mechanism of tunnel ionization of luminescence centers in an applied external field is not the sole agency responsible for the formation of ionized centers in electroluminescence. Rompe showed that electroluminescence of cadmium sulfide appears only after the field strength exceeds the breakdown value. Hence the ionization of centers in this case is apparently connected with loss of electric strength. As has

been shown by V.A.Chuenkov, loss of electric strength cannot be explained by tunnel ionization in view of the low probability of the tunnel effect at values of the field corresponding to the breakdown one. The mechanism of impact ionization is preferable. Consequently, this mechanism must also play an important role in electroluminescence. At the same time the tunnel mechanism can, of course, participate in the production of primary electrons.

F.F.Vol'kenshtein: The work of V.A.Chuenkov to which you refer is a new calculation (the accuracy of which I question by the way) based on the old mechanism (the mechanism of impact ionization). I agree with you that the mechanism of electroluminescence is certainly connected with the mechanism of breakdown. I am not convinced, however, that breakdown is due to the mechanism of impact ionization and not to the tunnel mechanism (the Zener mechanism).

A.N.Georgobiani: Investigation of brightness or radiance waves excited by trapezoidal pulses of one polarity (positive or negative - positive pulses are when the semiconducting glass is the positive electrode) brought out the two-component character of the waves. One component (see accompanying drawing) is connected with a rapidly decaying process (1), the other with a more slowly decaying one (2).

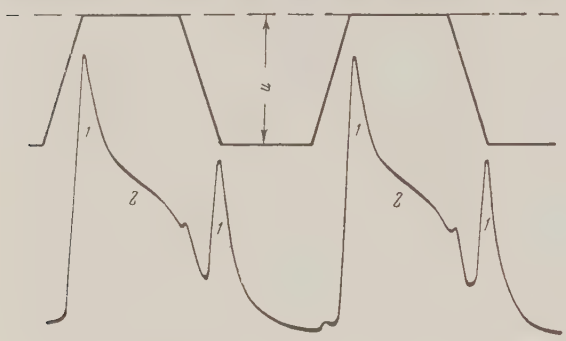

Whereas there are two components in the part of the radiance wave corresponding to the cut-off external field, the part of the radiance wave corresponding to the rising or applied electric field has only one, the first component. Analogously to the wave-difference observed in the case of symmetric pulses, in our experiments with unipolar pulses we observed a wave-difference between the two-component part of the radiance wave excited by positive pulses and the two-component part of the radiance wave excited by negative pulses. In the case of negative pulses the two-component part of the radiance wave is greater than in the case of positive pulses.

The wave-difference increases with increasing steepness of the trapezoidal pulse front. The first component is apparently due to recombination of electrons that participate in the process of impact ionization but do not have time to participate in the formation of a polarization charge (in other words, "optical" electrons), while the second component is due to recombination of a second group of electrons with ionized centers, namely, electrons participating in the formation of the polarization charge (in other words, the "thermal" electrons). The first group of electrons does not have time to move far from the ionization centers. These electrons rapidly slow down due to polarization when the field inside the crystal is removed and begin to recombine with the ionzation centers. The second group of electrons can recombine with ionization centers only by diffusing into the crystal when the external field is cut off. Consequently, the component of the radiance waves associated with this group of electrons rises and falls relatively slowly.

I would also like to say a few words regarding the remarks of F.F.Vol'kenshtein. It seems to me that despite the low probability of the tunnel effect, it can play a significant role, inasmuch as it is sufficient to have only one electron, that can serve as a "seed"; once initiated, the process of accumulation of electrons develops avalanche fashion from cycle to cycle due to ionization.

V.S.Trofimov: Some remarks regarding the theoretical views expressed by F.F.Vol'kenshtein. I think that for such ionization very strong fields (of the order of 10^7 v/cm) are necessary and, consequently, the field must be concentrated in a very small volume, that is, in a volume wherein there will be very few luminescence centers. That is why this mechanism appears implausible.

F.F.Vol'kenshtein: The mechanism of electrostatic ionization (the tunnel effect) according to certain extant theories produces breakdown of dielectrics. Consequently, this mechanism begins to operate in the range of breakdown field intensities. It is precisely in this region that electroluminescence is observed. If breakdown has an electrostatic origin, as many investigators assume, then one can also assume that electroluminescence has the same origin.

V.V.Antonov-Romanovskii: The following interesting effect is sometimes observed when a not very strong alternating field (i.e., a field not strong anough to produce electroluminescence) is applied to an excited phosphor. After a brief flare-up, the afterglow intensity falls off somewhat but the character of the decay remains the same as with no field. If the field is then removed, the afterglow intensity I is reestablished. With repeated application and removal of the field the pattern repeats, only the flash at the instant of application of the field is weaker. This is shown schematically in the accompanying drawing, where t_1 and t_2 are the instants of application of the field, and t_1' and t_2' are the instants of removal of the electric field. The brief flash or flare-up of phosphorescence at the instant of application of the field can be explained by assuming that the field "blows" the electrons from the shallower traps. The decrease in intensity under the influence of the field can be explained by an increase of the electron temperature, as a result of which the recombination cross section σ_o for electrons decreases relative to the trapping cross section σ, as follows from Siui Siui-iun's experiments (with ZnS:Cu:Co (Doklady AN SSSR, 103, 585 (1955) & 106, 818 (1956)). When the field is reapplied the intensity increases due to reduction of the electron temperature.

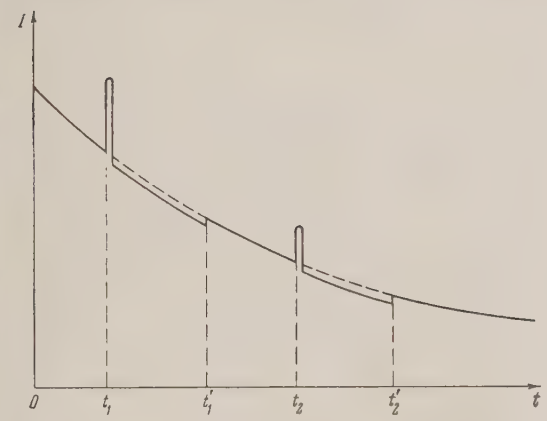

This inference regarding the influence of the electric field on the magnitude of the ratio σ_o/σ can in principle be checked by the following experiment. If the ratio σ_o/σ (both for electrons and for holes) decreases with application of a field, the storage of light sums under excitation in the presence of a field must be greater than with no field. Oranovskii in his report cited a case when this effect obtains. It is not great, however, and in some cases is not observed. It may be hypothesized that this is due to the fact that the field also exerts an opposite effect, hindering the storage of light sums and facilitates the release of electrons from the deeper traps.

The observed decrease in the steady-state luminescence intensity I_o with the application of a field can be explained on the assumption that the ratio σ_o/σ changes in a different way (to a greater degree) for electrons as compared with holes. Obviously, in the case of equal variation of σ_o/σ for electrons and for holes under the influence of an electric field, the light output (efficiency) will not change inasmuch as it is determined by the ratio of the number of radiative to the number of nonradiative transitions.

Taking into account the dependence of the ratio σ_o/σ on the value of the applied field may prove particularly useful in investigating radiance waves.

INFLUENCE OF CRUSHING ON THE PROPERTIES OF SOME CRYSTAL PHOSPHORS (Abstract*)

- F.D.Klement & R.I.Gindina

The purpose of the present investigation was to elucidate the nature of the quenching effect of mechanical fragmentation on the luminescence of some crystal phosphors. We assumed that in cases when the crystal phosphor is a supersaturated solid solution of the activator in the host material, fragmentation of the phosphor particles results in decomposition of the solid solution. Segregation of the excess activator leads to reduction of the effective activator concentration and to nonactive absorption of the exciting radiation (and in some cases absorption of part of the emitted light as well) in the separated out activator.

This assumption was checked experimentally on the following four phosphors: KCl.AgCl, NaCl.TlCl, KCl.TlCl and NaCl.AgCl. The first two are poorly miscible systems of components characterized by somewhat different crystal structures; the last two are characterized by a high degree of miscibility. The luminescence of all these phosphors comprises ultraviolet and visible bands; the ratios of their intensities depend on the activator concentration.

By measurement of the changes in the intensity ratios we determined that as a result of crushing the activator concentration is sharply reduced in the phosphors with a low degree of miscibility of the activator and host material, while in the phosphors characterized by high miscibility the activator concentration does not change.

The results were checked by "annealing" the respective phosphors (slow heating to a moderate temperature which also leads to decomposition of the supersaturated solution and reduction of the luminescence intensity). Crushing of such an "annealed" phosphor results in only a minor additional decrease in intensity.

We also found that at low activator concentrations, when absorption of the exciting radiation in the activator band is very weak, mechanical fragmentation leads to reduction of the luminescence intensity even without segregation of the activator. Apparently, the decrease is due to increased scattering in the more finely dispersed powder.

We examine the decomposition of supersaturated solid solutions incident to mechanical fragmentation both from the thermodynamic standpoint and from the viewpoint of processes of diffusion in the solid phase.

Tartu State University

* * * * * *

INFLUENCE OF THE ACTIVATOR-SALT ANION ON THE LUMINESCENCE OF ALKALI HALIDE PHOSPHORS (Abstract*)

- N. I. Ivanova

We investigated the influence of the activator-salt ion on the luminescence spectra of sodium and potassium halide phosphors activated with the halides of thallium and silver. We obtained the following results.

1. In the case of activation of the chlorides (or bromides) of alkali metals with the iodide of the activator metal a new band, i.e., a band not

---

*Complete report in Trudy (Transactions), Institute of Physics and Astronomy of the Estonian SSR, No.4, 3 (1956).

** Complete report in "Proceedings (Materialy) of the Fifth Conference on Luminescence" Tartu, 1957.

present in the spectrum of the phosphor activated with the chloride (or bromide) of the same activator, appears in the luminescence spectrum. The new band has its own excitation region. The intensity of this band increases with increasing concentration of the iodide.

2. The luminescence spectra of alkali metal iodide host phosphors are identical regardless of whether the activator is a chloride, bromide or iodide.

3. The luminescence spectra of alkali metal bromide host phosphors are indistinguishable with activation by the chloride or bromide of the activator.

4. In the case of activation of an alkali metal chloride by the bromide of the activator instead of the chloride there is observed a small displacement of the peak and broadening of the short wave band of the phosphor to the side of longer wavelengths. The shift increases upon addition of the bromide of the alkali metal to the phosphor.

It is hypothesized that the observed influence of iodine and bromine taken as the anions of the activator salt on the luminescence spectrum of the phosphors is due to the fact that the silver and thallium ions in the investigated phosphors join or group with iodine ions in preference to chlorine or bromine ions and with bromine ions in preference to chlorine ions.

"A.A.Zhdanov" Leningrad State University

* * * * * *

X-RAY STUDIES OF NH_4Cl:Tl AND NH_4Br:Tl PHOSPHORS (Abstract*)

- A.Ia.Pae

F.D.Klement has shown that in ammonium halide phosphors activated with thallium the activator concentration can be exceptionally high. Experiments show that these phosphors luminesce even when the amount of activator exceeds the amount of the base material.

Our specimens of NH_4Cl:Tl and NH_4Br:Tl phosphors were prepared by mixing the powdered initial materials and heating the mixture. Luminescence under UV excitation became evident immediately after mixing (i.e., even without heating). The x-ray analyses were carried out by the powder procedure.

It was found that heating of the NH_4Br:Tl phosphor for four hours at 160° did not suffice for the formation of a mixed crystal. Part of the TlBr retained its own crystal lattice.

Heating of the mixtures for 20 hours at 200° under vacuum insured the formation of a mixed crystal in the case of both NH_4Cl:Tl and NH_4Br:Tl with all proportions of the components. Higher temperatures and more prolonged heating promoted more complete diffusion. Specimens containing 70% and more Tl did not luminesce.

The lattice constants were determined at room temperature for the pure substances and for mixtures of NH_4Br and TlBr containing: 10, 30, 38, 50, 70 and 90% TlBr. The resultant data were in good agreement with Vegard's law.

In the case of the NH_4Cl + TlCl mixtures the lattice constants were determined for specimens containing 0.5, 1.0, 5.0, 10, 30, 50, 70 and 90% TlCl. In this case the lattice constant did not vary linearly with the concentration: the curve showed a downward bulge. Irregular changes in the lattice constant were also observed at low Tl concentrations. In the c-ray patterns of both series of mixed crystals, in addition to displacement of the interference lines, we observed changes in their relative intensity with changes in concentration, which substantiates replacement of NH_4^+ by Tl^+. Thus, for example, the interference lines from the faces the sum of whose indices $(h + k + l)$

---

*Complete report in Trudy (Transactions), Institute of Physics and Astronomy of the Estonian SSR, No.4 (1956).

is odd are absent in the chlorine phosphor series at a TlCl content of 10% and in the bromine series at a TlBr content of 38%, which is in good agreement with the theoretical concepts regarding substitution.

At room temperature the initial substances have the CsCl type lattice. At higher temperatures (for NH_4Br at temperatures above 138° and for NH_4Cl, above 184°) the ammonia salts have the NaCl type lattice, while the structural lattice of the thallium salts does not change with increasing temperature. Analysis of mixed NH_4Br + TlBr crystals at higher temperatures showed that in specimens containing 5% and more TlBr there occurs segregation of the TlBr and decomposition of the mixed crystals, which are stable at room temperature. There was no evidence in the x-ray patterns of decomposition of the mixed crystals of specimens containing less than 5% TlBr.

Tartu State University

DISCUSSION OF THE REPORTS OF KLEMENT & GINDINA, IVANOV AND PAE

L.M.Shamovskii: I would like to make a few remarks regarding the report of F.D.Klement and R.I.Gindina. On the basis of their experiments these authors came to the conclusion that mechanical fragmentation of phosphors leads to appreciable quenching of the luminescence as a result of decomposition of the supersaturated solutions. They infer that the quenching is connected with a decrease of the activator concentration in the crystal due to its removal from the lattice.

There is a different point of view, mentioned by the authors in their report. According to this view, mechanical crushing, as a result of plastic deformation, leads to the creation of an additional concentration of levels on which radiationless recombinations occur.

Obviously, to determine which of these views is correct, it would be expedient to carry out investigation of quenching of luminescence in the process of fragmentation of a crystal phosphor that is not a supersaturated solution.

In order to avoid possible errors connected with scattering of light one can recommend the procedure for obtaining optically transparent crystals by compacting phosphor powder, described in Phys.Rev., 97, 1714 (1955). The procedure consists of compacting the powder at a pressure of several tons; as a result there is obtained a transparent material.

A.A.Shishlovskii: The work of N.I.Ivanova is of considerable interest from the point of view of clarifying the nature of centers in phosphors. From the data presented it follows that in many cases the influence of anions in crystals is of the same character as in aqueous solutions. This means that in general one should not neglect the chemical, frequently homeopolar, bonds between the activator ions and the ions of the host material (medium).

INVESTIGATION OF THE PROPERTIES OF KI:In AND KI:Ga PHOSPHORS (Abstract*)

- Iu.N.Zhvanko, Z.L.Morgenshtern & L.M.Shamovskii

It is known that thallium is a good activator for alkali halide phosphors; the chemical analogs of thallium have hitherto not been investigated as activators. We prepared and investigated KI phosphors activated with In and Ga.

The phosphors KI:Tl, KI:In and KI:Ga were grown under identical conditions, specifically, in sealed quartz tubes in an atmosphere of hydrogen. The activator was introduced into the batch in metallic form.

Under optical excitation KI:In crystals yield a yellow-green luminescence ($\lambda_{max} \sim 50$ mμ), KI:Ga crystals yield orange luminescence ($\lambda_{max} \sim 600$ mμ). Thus, in the activator series Tl, In and Ga the emission maximum is displaced to the long wave side of the spectrum with decreasing atomic number of the activator.

Introduction of In or Ga, as of Tl, leads to the appearance of characteristic activator bands at the long wave absorption edge of the base material. In the case of KI:In there are observed bands peaking at about 230 and 262 mμ and at particularly high concentrations of In ($> 3 \cdot 10^{-4}$ mole %) another band at ~310 mμ appears. In the absorption spectrum of KI:Ga there are two intense bands with peaks at about 230 and 248-249 mμ.

In the excitation spectrum of the investigated crystals there are regions which can be matched with the absorption bands of the activators. As in the case of KI:Tl, the luminescence efficiency of these crystals falls off sharply with excitation in the region of the strong increase of absorption of the base material (at about 220 mμ) and the excitation bands are shifted to the long wave side relative to the absorption bands of the activator.

The quantum luminescence efficiencies of KI:In and KI:Ga were determined by comparison with KI:Tl and CsI:Tl for which the efficiency was measured earlier.** The determined values were 0.97 for KI:In and 0.65 for KI:Ga with excitation by 265 mμ radiation.

"P.N.Lebedev" Physical Institute of the USSR Academy of Sciences and
All-Union Scientific Research Institute of Mineral Raw Materials

* * * * * *

ON THE SPECTRAL CHARACTERISTICS OF SOME SUBLIMATE PHOSPHORS (Abstract***)

- A.F.Malysheva

Thin layers of material prepared by sublimation under vacuum are convenient for investigation of the spectral characteristics of both phosphors and pure nonluminescent materials. By comparing the absorption spectrum of the phosphor with the absorption spectra of the pure host and the pure activator one can elucidate the influence of the field of the host lattice on the energy levels of the activator and determine the influence of introduction of the activator on the absorption spectrum of the host.

---

*Complete report in Optika i spektroskopiia, 2 (1957).

**Z.L.Morgenshtern, Zhur.eksp.i teor.fiz., 29, 903 (1955); Izv.AN SSSR, Ser.fiz., 21, 544 (1957) - Trans. in Bulletin, 21, No.4, 540.

***Complete report in "Proceedings (Materialy) of the Fifth Conference on Luminescence" Tartu, 1957.

The present investigation was concerned with the absorption and excitation spectra of cesium halide base phosphors activated with thallium. The absorption spectra of the pure host and activator salts obtained in this study agree with the results of other investigators[1,2].

The absorption spectrum of the mixed "host + activator" system before heating is comprised of a surposition of the absorption spectra of the components. After heating assuring the greatest possible diffusion of the activator into the host lattice the spectrum of the system changes radically. Concurrently with the change in the absorption spectrum, luminescence appears. In the absorption spectrum of the CsCl.TlCl system there appears a narrow band peaking at 245-248 mμ and a band at about 210 mμ. Similarly in the absorption spectrum of the CsBr.TlBr system after heating there appear two bands with peaks at 215 and 263 mμ. In contrast to these two systems, in the absorption spectrum of the CsI.TlI phosphor there appear after heating three new bands with peaks at about 240, 270 and 299 mμ.

Changing the activator anion has little effect on the appearance and position of the absorption bands of these phosphors. With increasing activator concentration the position of the peaks in the absorption spectrum is shifted somewhat to the long wave side.

We also determined the excitation spectra of the investigated phosphors. In each case the excitation spectrum curve faithfully follows the curve of the absorption due to the activator incorporated into the host lattice.

We carried out a detailed comparison of the absorption spectra of the sublimate phosphors and of the corresponding single crystal phosphors; from the complete similarity of the spectra it may be concluded that the nature of the luminescence centers in the two forms is exactly the same.

Institute of Physics and Astronomy of the
Academy of Sciences of the Estonian SSR

References

1. R.Hilsch & R.Pohl, ZS.Phys., 57, 145 (1929); 59, 812 (1930); R.Pohl, Acta Physica Polonica, 5, 349 (1936); E.Schneider & H.O'Brian, Phys.Rev., 51, 293 (1937).

2. H.Fesefeldt, ZS.Phys., 64, 741 (1930); R.Hilsch & R.Pohl, ZS,Phys., 48, 384 (1928).

* * * * * *

EFFECT OF COMPRESSION ON THE LUMINESCENCE SPECTRA OF SOME CRYSTAL PHOSPHORS (Abstract*)

- Ia.Ia.Kirs

We investigated the influence of changes of the lattice constant produced by compression on the luminescence spectra of some crystal phosphors. For the purposes of the investigation we designed and assembled a set-up for investigating the spectral and radiance characteristics of crystal phosphors under the influence of hydrostatic pressures of up to 2000 atm. Compression produces a shift of the luminescence spectra of alkali halide phosphors activated

---

*Parts of the report are published in more detailed form in Trudy (Transactions), Institute of Physics and Astronomy of the Estonian SSR Academy of Sciences, No.4, 108 (1956).

with tin to the side of shorter wavelengths. The magnitude of the shift increases with increasing compressibility and lattice constant of the host material. Thus, for example, in the case of the NaBr:Sn phosphor the displacement equals 2 mμ, while for RbI:In it equals 7 mμ at an applied pressure of 2000 atm. We also investigated the effect of pressure on the spectra of KCl:Tl and (Zn,Cd)S:Ag. Further, we made an attempt to determine the influence of compression on the brightness of the KI:Sn phosphor in the region of temperature quenching.

We interpret the influence of pressure on the energy levels of the activator particles by means of the method of potential curves in configuration coordinates, employing the thermodynamic approximation first applied by Williams. We compare the pressure induced shift of the luminescence spectra of alkali halide phosphors activated with tin with the shifts of the spectral characteristics in the homologous series of the corresponding phosphors. It follows from the comparison that replacement of one type of particles by others in the homologous series of the phosphor bases and the change in the lattice constant in these series connected with this replacement act in opposite directions on the spectral characteristics of the activator (Sn) incorporated in the host lattice.

We also investigated the influence of temperature on the luminescence spectra of NaBr:Sn, KCl:Sn and KBr:Sn. Increasing the temperature leads to broadening of the emission bands and a noticeable shift of the bands to the short wave side. From the experiments on compression it would follow, however, that thermal expansion of the lattice should lead to a shift of the luminescence spectra to the side of longer wavelengths. In order to explain the observed effect, we hypothesize that the shift to the side of longer wavelengths incident to thermal expansion of the lattice is masked and countered by the appreciably greater shift to the short wave side due to interaction of the activator ions with the dynamic component of the intracrystalline field.

Institute of Physics and Astronomy of the
Academy of Sciences of the Estonian SSR

DISCUSSION OF THE REPORTS OF ZHVANKO, MORGENSHTERN & SHAMOVSKII, MALYSHEVA and KIRS

F.D.Klement: I would like to call attention to the significance of the results reported by Ia.Ia.Kirs from the standpoint of the two types of concentration in question: the activator is located at the lattice sites or on the interblock surfaces. It follows from the data of Kirs that there is a parallelism between the magnitude of the displacement of the luminescence spectrum and the coefficient of multilateral compression. In my opinion this parallelism can readily be explained by the fact that when the crystal is greatly compressed, the activators lodged in the host lattice will be subject to a stronger influence of the lattice field than in the normal (non-compressed) state. This parallelism cannot be as readily explained if it is assumed that the activator is located on the interblock surfaces.

N.R.Lushchik: I feel that the results given in the report of Zhvanko, Morgenshtern and Shamovskii are of great interest. All the cited data can readily be interpreted from the viewpoint of the Seitz phosphor model. I would like to note that our data on the absorption, excitation and emission spectra of KCl:In and KBr:In phosphors are also interpretable on the basis of this model.

The principal transitions should be ascribed to In ions located at the lattice sites. The band with a peak at 228 mμ corresponds to the $^1S_0 \rightarrow {}^3P_1$ transition in the KCl crystal; the band at about 282 mμ is associated with the recombination $^1S_0 \rightarrow {}^1P_1$ transition. The following table shows that in the free In^+ ion we have longer wavelength transitionsthan in Tl^+ ion. The same relative location of the bands persists with the introduction of ions into the KCl lattice. Analogous regularities are also observed for the ion pairs Sn^{2+} & Pb^{2+} and Cu^+ & Ag^+.

Transition	State of ion	Transition energy, ev			
		In^+	Sn^{2+}	Tl^+	Pb^{2+}
$^1S_0 - {}^3P_1$	Free ion	5,40	6,83	6,46	7,95
	Bound in KCl	4,30	4,31	5,10	4,54
$^1S_0 - {}^1P_1$	Free ion	6,82	9,86	9,35	11,76
	Bound in KCl	5,43	5,34	6,22	6,31

E.I.Blzhnova: The studies on sublimated films are of interest as regards helping to solve a number of problems in solid state physics and from the purely practical standpoint (preparation of high-resolution screens, etc.).

The phosphor laboratory of our Institute has been doing work on ZnS base films. We have prepared ZnS:Zn, ZnS:Mn, ZnS:P and ZnS:ZnSe coatings for screens 10 and 18 cm in diameter. The cathodoluminescence spectra, inertia, brightness and conditions of electron excitation have been investigated. The brightness of ZnS:Cu films is 3 msb at an anode voltage of 6 kv and a current of 1 $\mu a/cm^2$. We carried out a comparison of the luminescence spectra and the inertia and radiance characteristics of phosphor layers with the corresponding characteristics of powder phosphors. A close similarity of the cathodoluminescence spectra of layers and powders has been observed. The character of the decay of thin layers and powders is the same, but the partial decay times of layers are appreciably shorter. The thickness of the investigated layers was 0.1 to 2 microns.

A.A.Shishlovskii: The identity of the absorption spectra of sublimate phosphors and volume-activated single crystals reported by Malysheva is convincing proof of the fact that in sublimate phosphors the activator ions are located at the lattice sites. We know that the absorption spectra are also the same for aqueous solutions. It would be of interest to investigate luminescence spectra that are more sensitive to the short-range order of the activator cation.

Z.L.Morgenshtern: In our report we deliberately gave no interpretation of the results inasmuch as the opinions of the authors differ on this point. Personally, I believe that In and Ga, just as Tl when used as the activator, replace cations of the host material, i.e., are located at lattice sites. Apparently, here there also occur transitions similar to the transitions in the free In^+ or Ga^+ ions, just as obtains in KCl:In and KBr:In according to the data cited by N.E.Lushchik.

In the luminescence spectra of phosphors activated with In and Ga, as in phosphors activated with Tl, we observe one band; the absorption spectrum of In contains three bands, that of Ga two bands. Absorption bands in the case of In and Ga are not symmetrical; they are undoubtedly complicated, i.e., the levels associated with these bands undergo greater splitting than in the case of Tl, although from general considerations one might assume the contrary.

Iu.N.Zhvanko: The idea of activating alkali halide phosphors with metals originates from the hypothesis of Shamovskii regarding the dual distribution of the activator. It is known from the practice of synthesis of single

crystals that pure crystals grow best. We decided to find an effective activator which in small amounts would yield a high luminescence efficiency. This was done; we used substances that are very weakly soluble in the host lattice, namely, metals.

The dual distribution of the activator and the effectiveness as regards luminescence of only that part of it located on the blocks are proved by experiments on the introduction of In and InI: with equal molar concentrations of In the phosphor with metallic In has more intense absorption bands than the phosphor prepared with InI.

We are not alone in our views of a phosphor as a microheterogeneous system with dual distribution of the activator. Recently there has appeared a contribution by Oshima, Nagano & Nachuza (Chem.Phys., 23, 1721 (1955)). Investigating the KCl:Mn system by the method of paramagnetic resonance these authors found that the Mn is present in two states, but that only one state, that not atomically dispersed, is effective where luminescence is concerned.

A.F.Malysheva: Our comparison of the absorption spectra of single crystals and sublimate phosphors of the same composition was carried out in order to show that if in single crystals the absorption bands are due to activator ions lodged at the cation sites of the host lattice, then in sublimate phosphors the activator ions must be located in an analogous fashion, i.e., that sublimate phosphors are not purely surface activated phosphors.

INVESTIGATION OF THE REGULARITIES OF EMISSION OF FINELY DISPERSED LUMINESCENT MEDIA (Abstract*)

- A.P. Ivanov

Proceeding from available indications on the continuous variation of scattering, absorption and emission as a function of the layer thickness, we deduced formulas characterizing the intensity of luminescence as measured from the irradiated side as well as from the opposite side. The deduced expressions are applicable not only in the case of excitation of luminescence by UV but also for excitation by α- and β-particles.

In our study we have clarified the regularities governing the dependence of the luminescence on the degree of dispersion of the medium, the index of refraction, the coefficient of absorption, the thickness of the layer and other factors. It was also established that the use of different sources for exciting fragmented or ground up luminophor powders leads, in some cases, to an increase in intensity and in others to a decrease. We investigated the problem of finding the optimal conditions determining the maximum luminescence intensity. On the basis of our results one can judge of the true spectrum and luminescence efficiency of a material on the basis of measurements of the spectrum and efficiency under given conditions. Concurrently with calculations we carried out experimental work. The materials investigated were powders of ZnS-9 glass with particles ranging in size from 5 to 1000 microns. The monochromatic exciting radiation was separated by a double quartz monochromator in the interval from 230 to 365 mμ. The experimental data were in fairly good agreement with the predictions of theory and indicate that the proposed model can be used for calculations concerning powdered phosphors.

DISCUSSION

B.D.Ryzhikov: A.P.Ivanov correctly emphasized the importance of the problem, solution of which is of interest to a wide circle of investigators including those studying triboquenching. I would like to note that in the case of fragmentation of phosphors, the decrease of radiance occurs not only as a result of an increase of scattering and deformation but also for other reasons, for example, due to decomposition of the solid solution, the appearance of additional absorption and so on.

The report gives much data that will undoubtedly be of interest to experimenters. The method proposed by the author, however, cannot be applied in the cases important in practice, i.e., to particles smaller than 15 microns. For small particles it is essential to take into account diffraction effects, variations of scattering with wavelength. Moreover, for media with large absorption or strong scattering, one must take into account the variation of the luminescence efficiency with the intensity of the exciting light. I also want to note that the quantity used by the author to characterize the particle size does not take into account the degree of dispersion of actual powders. Hence it is not clear just what value should be substituted in the formula: the average particle size or some "effective" size and what is to be done in cases when the crystals are irregular and the dimensions in different directions are different.

---

*Detailed reports on the present investigation are published in Zhur. eksp.i teor.fiz., 26, 275 (1954); 30, 196 (1956), and Optika i spektroskopiia, 2, No.12 (1957).

A.P.Ivanov: I agree with the remarks of B.D.Ryzhikov that the given calculations are applicable to powders with a particle size not smaller than 1 micron (sic) in the case of investigations in the visible and near ultraviolet regions inasmuch as the effects of diffraction and interference are not taken into account in our model. Obviously, there must also be developed a theory applicable to scattering media with small particles.

We examined the question of finding the average particle size and found that it is necessary to take the arithmetic mean size. The problem of determining the scattering and absorption coefficients has been examined by a number of investigators. It has been established that it is possible to determine these parameters on the basis of measurements of the reflection and transmission of scattering layers.

INVESTIGATION OF THE DIFFUSION OF RARE EARTH ACTIVATORS IN DIFFERENT CRYSTALS ON THE BASIS OF LUMINESCENCE SPECTRA

- A.K.Trofimov

Diffusion in solids is obviously predicated on mobility of their particle When the amplitude of oscillation of a particle about some point of the crysta lattice becomes sufficiently great for rupture of its bonds, the particle can break away, i.e., leave its bound position. If at the given instant two parti cles of two different crystal phases are in the immediate proximity of each other (separated by a distance of a few angstroms), they can exchange places. Such exchange is facilitated by high temperatures and structural defects of the lattice.

The formation of crystal phosphors is also connected with the process of diffusion of activator ions in the crystal lattice of the host. This has been shown, for example, by Klement[1] and Ivanova[2] for sublimate alkali halide and alkaline earth metal phosphors activated with thallium. They also showed that the effective diffusion temperature is lower for smaller radii of the activator ion and lower melting points of the host crystal. These studies, as well as the work of Klement & Pribytkova[3], indicate the possibility of investigating the activator diffusion in crystals on the basis of the lumi- nescence spectra.

In an earlier contribution the author in collaboration with Tolkachev[4] showed the possibility of utilizing line luminescence spectra for qualitative observation of the kinetics of certain processes in solid phases, accompanied by alterations of crystal structure. In the process of crystallochemical transformations in the presence of several solid phases there obtain all the conditions necessary for diffusion of activator atoms into any of the phases of the system with the formation of a phosphor. The luminescence spectra will most accurately reflect the nature of the actual crystallochemical trans- formations when the activator concentrations in all the solid phases are equal It follows that in observing such transformations from the luminescence it is desirable to take into account the behavior of the activator in the given multiple component system in the sense of its relative ability to diffuse into the different crystal lattices. In addition the question of diffusion of activators is of intrinsic scientific interest.

In this connection it is of interest to know the "relative affinity" of the introduced activator for different crystalline host materials. Under the term "relative affinity" we mean here the ability to form a phosphor as deter- mined both by the nature of the activator and the properties of the host material. The possibility of formation of a phosphor depends primarily on the ability of the activator atoms to replace isomorphically cations or occupy vacant cation sites in the host lattice. This process will depend mainly on the ionic separations in the host crystal and on the ratio of the radii of the host and activator cations.

The present investigation was devoted to studying the diffusion of europium and samarium, inasmuch as these are the elements that are primarily used as activators in the luminescence method of observing crystallochemical transformations.[4]

The first observations of diffusion of europium in crystalline materials from the luminescence spectra were carried out by us on a heated mixture of the phosphor MgO:Eu with nonactivated ThO_2. A 1 to 1 (by weight) mixture of these materials was thoroughly ground and heated for 30 minutes at 1000°. Photographs of the luminescence spectra of the mixture showed that as a result of heating the spectrum of MgO:Eu disappears and in its place there appears

the spectrum of ThO_2:Eu. The transformation of the spectra can be explained only by diffusion of the atoms of the activator (Eu) from the MgO lattice to the ThO_2 lattice. In order to check this deduction we carried out a chemical separation of the heated mixture into the oxides and investigated the luminescence spectra of these. This separation was feasible by virtue of the fact that MgO is readily soluble in strong hydrochloric acid, while ThO_2 is insoluble in this acid. The separated oxides were reheated. Photographs of the luminescence spectra of the separated oxides showed all the europium, despite its good solubility in strong HCl, was concentrated in the ThO_2. The very possibility of chemical separation of the oxides by acid solution of their heated mixture shows that no chemical interaction occurs between them at temperatures up to 1000°.

The results of these experiments obviously raised a number of questions connected with the diffusion of rare earth activators in different crystals. We were primarily interested, however, in the direction and temperature of diffusion of these activators in binary mixtures of different crystals as an index to the "relative affinity" of the activators. To this end we investigated, by observation of the luminescence spectra, the diffusion at different temperatures of europium and samarium in different mechanical mixtures of crystalline phosphor powders and pure base materials. From among the large number of crystalline substances that could serve as phosphor hosts we chose the compounds listed in the accompanying table.

Crystallochemical characteristics of the compounds used in the investigation

Compound	Crystal structure	Radius cation	t_{melt}, C°	Ratio abs. temperatures formation of phosphor to fusion base
CaF_2	CaF_2 type cubic	1,04	1360	0,72
SrF_2	Same	1,20	1190	0,87
BaF_2	Same	1,38	1280	0,95
$CaSO_4$	Rhombohedral	1,04	1450	0,74
$Ca_3(PO_4)_2$	Same	1,04	1670	—
ThO_2	CaF_2 type cubic	0,95	2800	0,18
$CaMoO_4$	Tetragonal	1,04	1600	0,30
$CaWO_4$	Same	0,04	1600	—
LaF_3	Hexagonal	1,04	1400	0,57
La_2O_3	Same	1,04	2315	0,37
SnO_2	Tetragonal	0,67	1127	—

Our choice was based on the following requirements: 1) the substance must yield, when activated with Eu and Sm, phosphors with bright line spectra in order to facilitate observation; 2) the radius of the cation should be close to the radius of Eu^{3+}(0.97) and Sm^{3+}(0.97) in order to insure isomorphic incorporation of the activator into the host lattice; 3) the crystal structures of the various substances should be different in order to allow of determining the influence of crystal structure on the diffusion of the activator; 4) the selected substances should not enter into chemical reactions with each other inasmuch as this would hinder observation of the diffusion effect; 5) the melting point of the substance should be high so that the investigation could be carried out in a wide temperature range. The pertinent properties of the selected substances are shown in the table.

Using these compounds we prepared phosphors with Eu and Sm in each case using the optimal heating temperature for maximum luminance. The concentration of activator in all the phosphors was $5 \cdot 10^{-2}$%. All the phosphors had an

adequate brightness and line luminescence spectra. The nonactivated host materials were the same compounds heated at a temperature corresponding to the optimal temperature for the phosphor with the given compound as the host.

Next mechanical mixtures (in the molar ratio 1:1) were prepared of all the phosphors and nonactivated hosts in all possible phosphor + nonactivated host pair combinations. For the investigation of the diffusion of europium alone we prepared 110 different mechanical mixtures, among which each was repeated according to the principle

A:Eu + B,
B:Eu + A,

where A and B are different compounds (hosts). Separate batches of each mixture were heated for 30 minutes at temperatures differing by 100° in the range from 700 to 1300°.

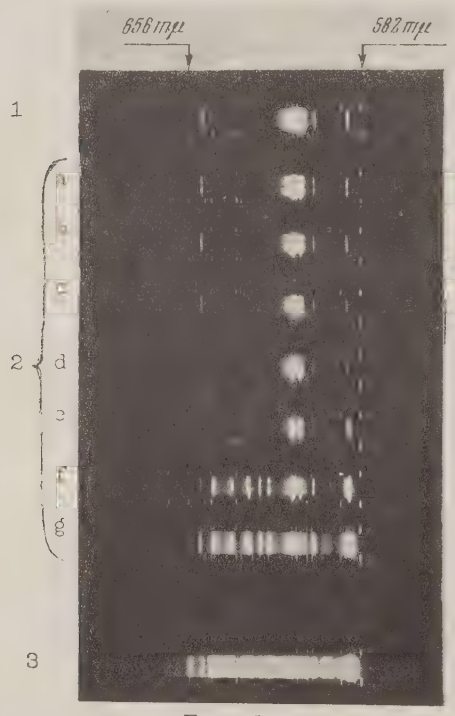

Fig. 1

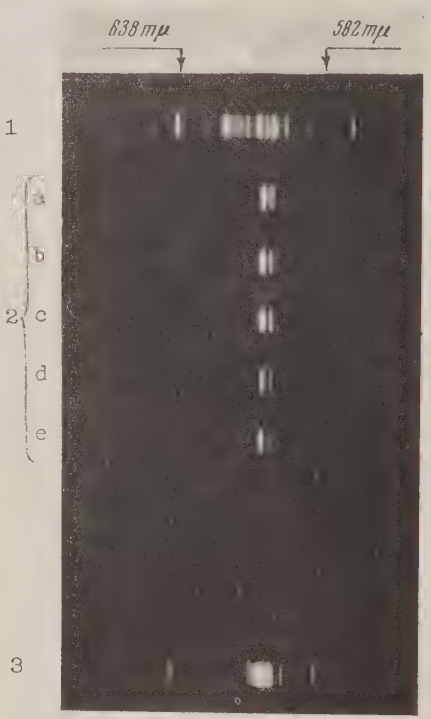

Fig. 2

Fig.1. Luminescence spectra of 1) $CaMoO_4$:Eu, 2) $CaMoO_4$:Eu + ThO_2 heated at a - 700°, b - 800°, c - 900°, d - 1000°, e - 1100°, f - 1200°, g - 1300°; 3) ThO_2:Eu.

Fig.2. Luminescence spectra of 1) CaF_2:Eu, 2) CaF_2:Eu + $CaMoO_4$, heated at a - 700°, b) 800°, c - 900°, d - 1000°, e - 1100°; 3) $CaMoO_4$:Eu.

It was evident from the photographs of the luminescence spectra that all the mixtures could be divided into two groups: mixtures for which the luminescence spectra did and mixtures for which the luminescence spectra did not change after heating. By way of illustration we show in Fig.1 photographs of the luminescence spectra of $CaMoO_4$:Eu (1), the mixture $CaMoO_4$:Eu + ThO_2 after

heating at different temperatures (2) and ThO_2:Eu (3). It will be seen from these spectra that Eu diffuses in the direction $CaMoO_4 \rightarrow ThO_2$ and that the process for the given crystal pair begins at a temperature of 1100°. Thus we conclude that the "relative affinity" of europium for the ThO_2 crystal lattice is greater than for the $CaMoO_4$ lattice. It should be noted that Eu has a greater affinity for some of the other investigated substances than for the $CaMoO_4$ lattice; for example, europium diffuses from CaF_2:Eu to $CaMoO_4$. In this case the process goes in the direction $CaF_2 \rightarrow CaMoO_4$ and begins at a lower temperature (700°), as may be inferred from the photographs of the luminescence spectra reproduced in Fig.2.

Thus from the character in the changes in the luminescence spectra of each pair one can establish whether diffusion occurs, and if it does, the direction and temperature at which it begins. The results of our investigation are shown in Fig.3 in which the arrows indicate the direction of diffusion of the activator in a mechanical mixture of the two given crystalline substances. In all cases the behavior of europium and samarium were identical as regards diffusion in the different crystals.

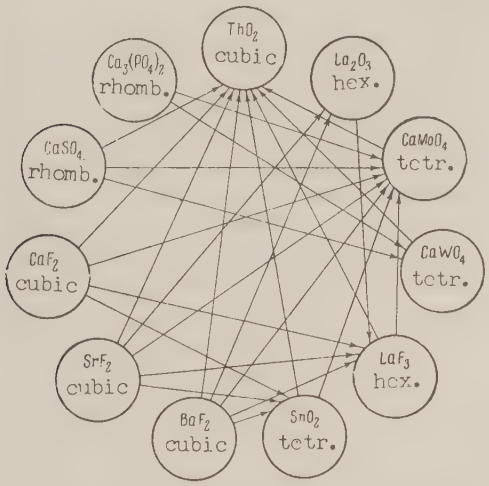

Fig.3. Direction of diffusion of the activator in mechanical mixtures of two crystalline materials during heating of the mixture.

It will be evident from Fig.3 that "acceptors" of rare earth activators are ThO_2, $CaMoO_4$, LaF_3, SnO_2, $CaWO_4$ and La_2O_3 crystals. The first two are particularly good "acceptors". Among the tested compounds, CaF_2, SrF_2, BaF_2, $CaSO_4$ and $Ca_3(PO_4)_2$ have no "acceptor" ability. It is possible, of course, that these compounds may act as "acceptors" with reference to other crystals, i.e., compounds not tested in our experiments. There is apparently no connection between the "acceptor ability" of a material and its crystal structure, for there are representatives of different crystal systems among both the materials having and those not having this ability. The reason for the difference between the acceptor properties of the investigated material must, apparently, be sought in the differences between their chemical properties.

It is noteworthy that in all the cases where diffusion of Eu and Sm did occur, it proceeded in only one direction for any given pair of crystals in the temperature range from 700 to 1300°. This gives reason to assume that the process of diffusion of the activator is determined by the thermodynamic state of the system crystal + activator. We believe that the ability of Eu and Sm to diffuse from one crystal lattice to another is connected with thermal "loosening" of the respective lattices. This is substantiated, first, by the fact that the temperature of beginning of diffusion for most "acceptors" is nearly the same regardless of the "donor" crystal (this temperature is about 1100° for ThO_2, 700° for $CaMoO_4$, 800° for La_2O_3 and 1200° for SnO_2) and second, by the fact that the ratio of the absolute temperature of formation of the phosphor to the melting temperature of the host is generally low (under 0.50) for the "acceptor" materials and comparatively high (over 0.50) for the other, "non-acceptor" materials (see table). In the case of many pairs of crystals

we detected no diffusion of Eu or Sm on the basis of the luminescence spectra in the entire range of heating temperatures (700-1300°). Such pairs are not connected by arrows in Fig.3.

The above facts alone do not allow of an unambiguous explanation of the reason for the different acceptor ability of different crystals. Nevertheless, there is good reason to associate this ability primarily with temperature factors since, as was noted above, the energy of "loosening" of the crystal lattice plays a significant role where the process of diffusion in solids is concerned.

The author desires to express his sincere thanks to P.P.Feofilov for his constant interest in the work and many valuable suggestions.

References

1. F.D.Klement, Doklady AN SSSR, 46, 295 (1945).

2. N.I.Ivanova, Dissertation, Leningrad State University, 1952.

3. F.D.Klement & N.N.Pribytkova, Vestnik (Review) Leningrad State University, 4-5, 38 (1946).

4. A.K.Trofimov & S.S.Tolkachev, Vestnik (Review) Leningrad State University, 4, No.1, 102 (1957).

A LUMINESCENCE METHOD OF OBSERVING CERTAIN CRYSTALLOCHEMICAL TRANSFORMATIONS IN SOLIDS (Abstract*)

- A.K.Trofimov & S.S.Tolkachev

A purpose of the present study was to determine the possibility of utilizing line luminescence spectra for qualitative observation of the kinetics of certain processes in solid phases, accompanied by changes in the crystal structure, namely, formation of mixed crystals in the CaF_2—SrF_2 system, the polymorphous transformation γ-$Al_2O_3 \rightarrow \alpha$-$Al_2O_3$ and chemical reactions. The last comprise three basic types of reactions: decomposition - thermal decomposition of $Al_2(SO_4)_3$, combination - formation of $MgAl_2O_4$, $BeAl_2O_4$, $ZnAl_2O_3$, and the aluminates of some alkali and alkaline earth metals and substitution - formation of $MgAl_2O_4$ from $BeAl_2O_4$ and MgO.

The method consists of photographing the luminescence spectra of phosphor specimens prepared of the investigated materials (as hosts) activated with a rare earth element (Eu or Sm) or chromium.

The results obtained by the luminescence spectrum procedure were substantiated by x-ray diffraction studies and are generally in agreement with the data in the literature.

The luminescence method has certain advantages over other methods, particularly over x-ray analysis: primarily the speed and simplicity of the technique. In some cases the luminescence method is the only one that can be used with any degree of success in view of the sensitivity of the luminescence spectra to local crystallochemical changes.

The applicability of the method is, however, limited by certain characteristics specific to crystal phosphors. For example, the procedure is suitable only for noncolored materials inasmuch as coloring of the phosphor leads to nonactive absorption of the exciting light. Another limitation is imposed by nonuniform distribution of the activator in the reacting solid-phase mixture. The question of distribution is connected with diffusion of activators in different crystalline materials (see preceding report by Trofimov - p. 754).

Our results are not to be construed as a fully developed luminescence procedure; they only serve to show that the luminescence method can in certain cases be utilized together with other methods for monitoring the phase composition of reacting solid crystalline materials.

---

*Complete report in Vestnik (Review), Leningrad State University, 4, No.1, 102 (1957).

DISCUSSION OF THE REPORTS OF A.K.TROFIMOV and A.K.TROFIMOV & S.S.TOLKACHEV

A.Z.Trapeznikova: The described method of studying reactions occurring in solid phases by observation of the changes occurring in the luminescence spectra of rare earth ions is original and very interesting. It would be desirable to determine more fully why when two materials are mixed the rare earth ions have a tendency to go over selectively into one of the materials - primarily the material with the higher melting point - instead of being equally distributed throughout the two materials. It would also be desirable to determine whether there is interaction between two rare earth substances when they are simultaneously introduced into a phosphor and if so, how this interaction depends on the nature of the anions.

S.V.Grum-Grzhimailo: It would be desirable to apply the interesting and valuable procedure developed by Trofimov to the synthesis of corundums and rubies. For determining the quality of the batch it is important to know the temperature of transition of the γ-modification of Al_2O_3 into the α-modification. The procedure may prove very valuable for determining the quality of the batch in synthesizing large spinal crystals.

A.K.Trofimov: In continuing our work we shall certainly bear in mind the suggestions made here.

PREPARATION OF LUMINOUS PAINTS AND THEIR USE IN MOTION PICTURE PRODUCTION

- M. I. Agranian and N.V.Gorbachev

The use of luminous paints and coatings in motion picture work has been held back by the lag in organizing production of such paints, suitable sources of ultraviolet illumination and special photographic light filters.

The luminous water colors and gouache paints developed by us* for painting, architectural and other art purposes were used in the first luminescent photography and motion pictures produced by the Leningrad and Moscow studios[1]. For efficient use of luminescent coatings in motion pictures it was necessary, however, to have available a special palette of luminescent paints and to develop a new technique of using them. Paints intended for drawing on celluloid must meet certain specific requirements.

The quality of animated films depends to an appreciable degree on the brilliance and purity of the colors; hence the matter of obtaining the pure saturated colors is particularly important. Luminescent paints make it possible to obtain in film productions a heightened intensity of individual details of the image without sacrifice of the background and surrounding color tones, which facilitates obtaining various special light and color effects.

The basic requirements set for luminescent paints in addition to high color and tone quality are good spreading, covering and adhesion when applied to celluloid, minimal peeling under high moisture conditions, rapid drying, elasticity and "reversibility" of the color layer.

Great difficulties were encountered in the initial attempts to use luminous paints in animation films due to the fact that ordinary paints burn out under the influence of ultraviolet, while the celluloid on which the drawings are usually made is not standard so that different batches exhibit different intensities of blue fluorescence.

In view of the above, at the request of the "Soiuzmul'tfil'm" (Union Animated Film) studio we carried out extensive research on the preparation of a palette of suitable luminous paints and developed methods of using them in the production of animated films.

The major difficulty in preparing the requisite palette of luminescent paints stems from the fact that the number of commercially available luminophors of different types is limited. The basic raw materials for preparation of luminescent paints are the zinc sulfide and cadmium sulfide phosphors put out by the "Krasnyi khimik" (Red Chemist) Plant and the "lumogen" produced by the Khar'kov Chemical Reagents Plant.

The adsorption organic pigments and paints based on them developed by us earlier** could not be included in the animated film palette due to their poor adhesion to celluloid, although they proved fully suitable for decorative purposes in ordinary motion picture productions. It may be noted that these organic pigments can be prepared in the form of luminescent silk or wool dust which, when applied in dry form to a sticky surface, gives the impression of glowing embroidery or applique in relief.

Paints prepared only from phosphors appear little saturated in mixed light (ultraviolet with some white) due to reflection by them of white light. With the addition of appropriate pigments one can increase the degree of saturation and even alter the color tone of paint. In this manner one can even obtain several color variants from the same phosphor.

---

*Inventors' certificate No.76789 of 30 July 1949. These paints are being produced by the "Krasnyi khudoznik" (Red Painter) Plant.

**Inventors' certificate No.102512 of 14 May 1956.

In selecting pigments for the animated film palette we had to exclude such pigments as chrome yellow, Mars yellow and the like, since these cannot be mixed with paints containing sulfur compounds. We also had to exclude pigments containing iron hydrates (for example, ochre and sienna) which appreciably quench the luminescence of crystal phosphors. In view of the above and taking into account the list of pigments put out by the domestic industry[2], we selected for test a number of possible mineral and organic pigments. We used these to prepare 100 sample paints. The best of these were then chosen to make up a palette of the requisite range on the basis of extensive tests and experiments. We also carried out a comprehensive testing program of various binders. The binding medium we recommend for water soluble paints is urea-formaldehyde resin stabilized with ammonia with the addition of 15-18% ethylene glycol. Bearing in mind that the "cells" for animated films are painted not only with gouache but sometimes with oil paints, while the luminescent paints are used only for individual details, we also developed a series of oil-varnish base luminescent paints intended for use in conjunction with oil paints. By way of binder for these we recommend acrylic mastic varnish consisting of polybutyl acrylate, mastic resin and turpentine with the addition of bleached linseed oil. This binder gives a light stable elastic film with good ultraviolet transmission. Both types of paints - the water soluble and the oil-varnish ones - can also be used for any other painting or decorative purposes.

As a result of our research there was obtained a palette of 24 basic luminescent paints that were satisfactorily recorded and reproduced by three layer color motion picture film. Ten of the paints (see Table 1), consisting of mixtures of phosphors and pigments, are intended for obtaining saturated colors with photography in mixed light. The next group of ten paints are of the same colors but are prepared without the addition of pigments and are intended primarily for photography with only ultraviolet illumination. The remaining four paints are white, gray and two browns. Two years' production experience have shown that these paints are fully satisfactory for animated film purposes.* These paints have good adhesion to celluloid, are sufficiently elastic, "reversible" and quick drying.

The palette of luminescent paints is composed so that under the same conditions of illumination one can obtain on the motion picture film with one and the same exposure all the fundamental colors simultaneously. The composition and color characteristics of the luminescent paints are listed in Table 1. The positions of the paint colors on the MKO (ICI) color diagram are shown in Fig.1.

Inasmuch as hitherto questions of color rendition of luminous paints in motion picture photography have not been adequately studied, we carried out a special investigation of the accuracy of rendition of the paint colors on different types of motion picture films exposed under different illumination conditions. To this end we prepared 12 test plates comprising 165 patches of different color tints. The color rendition was investigated both by visual evaluation of projections of the plates on a screen and by the method of colorimetric analysis.[3] The color characteristics of the patches were measured by means of a VNISI universal photoelectric colorimeter[4,5]. The colorimetric characteristics were supplemented by values of the luminosity determined as the ratio of the brightness of the given color patch to the brightness of a standard patch under the same illumination conditions. The standard patch was made of a mixture of phosphors and had the color of the emission of

---

*At present these paints are being produced by the "Soiuzmul'tfil'm" Studio.

Table 1

Composition and color characteristics of the luminous animated drawing paints

No.	Color	Luminophor	Pigment	Color coordinates X	Color coordinates Y	Dominant wave-length, mμ	Purity, %	Luminosity, %
1	Red	K-53	Rubin lake SK	0.678	0.305	624	94	14
2	Orange	FK-102	Cadmium orange	0.641	0.338	608	94	31
3	Yellow	Lumogen + L20	None	0.537	0.444	588	96	71
4	Greenish -yellow	Lumogen yellow	None	0.466	0.488	576	90	73
5	Green	Lumogen yellow + FK-106	"Fonal'" lake, basic green	0.315	0.639	552	96	65
6	Bluish -green	FK-106	Turquoise lake	0.160	0.454	501	66	64
7	Azure	K-10	Azure lake	0.160	0.259	486	54	41
8	Blue	K-10	Cobalt 255	0.136	0.159	478	65	19
9	Violet	FK-102 + K-5	"Fonal'" lake, violet	0.181	0.069	444	25	14
10	Purple	Same	Rubin lake SK	0.202	0.080	435	9	5
11	Red	FK-102	None	0.615	0.367	601	95	42
12	Orange	L-20	None	0.568	0.410	593	91	52
13	Yellow	K-50	None	0.497	0.461	582	92	75
14	Lemon-yellow	K-54	None	0.448	0.497	574	89	109
15	Yellow -green	FKP-03	None	0.212	0.688	533	83	78
16	Green	FK-106	None	0.212	0.490	510	58	79
17	Azure	K-10	Direct white	0.153	0.197	476	48	45
18	Blue	K-10	None	0.157	0.076	465	50	32
19	Violet	K-15	None	0.179	0.078	458	30	24
20	Purple	K-5 + FK-102	None	0.386	0.263	510	21	26

Table 1 (cont.)

No.	Color	Luminophor	Pigment	Color coordinates X	Color coordinates Y	Dominant wave-length, mμ	Purity, %	Luminosity %
21	White	FK-109 + K-50	None	0.333	0.333	---	--	100
22	Gray	Same	Carbon black	0.255	0.258	480	16	69
23	Reddish -brown	FK-102	" "	0.398	0.350	610	28	16
24	Yellowish -brown	FK-50	" "	0.390	0.370	565	27	18

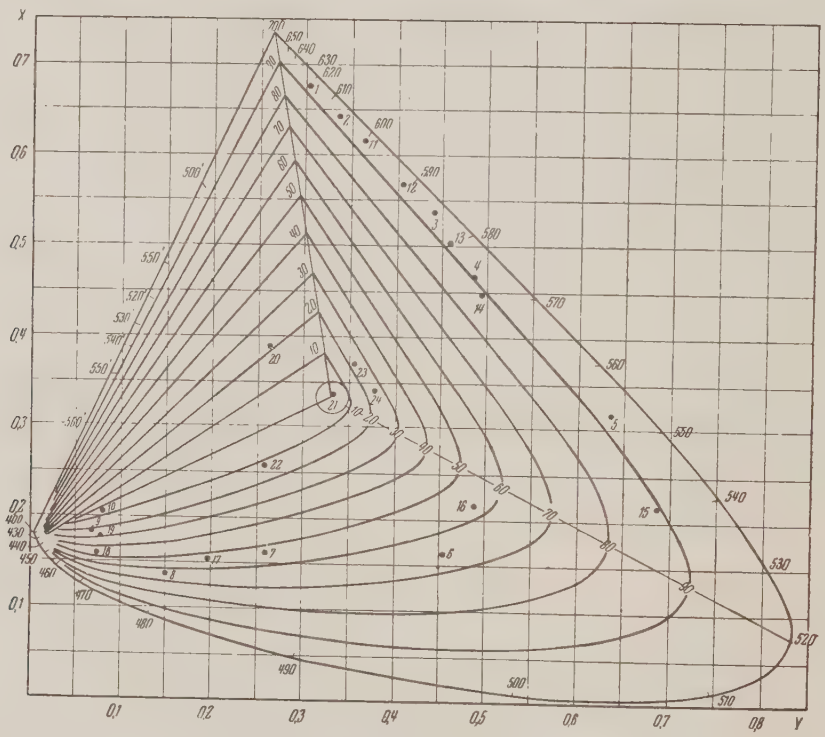

Fig.1. Positions of paint colors on color diagram.

an E light source with a color temperature of 5000°K and a radiance of 85 asb at an irradiation intensity of 80μw cm^{-2}. The photography was carried out on type B Agfa color and type DS-2 film at different levels of illumination.

The filters used in photographing the test plates were the WG-1 Shott filter 10 mm thick and the ZhS-4 filter 2 mm thick. The negatives were developed under the standard conditions employed in the "Soiuzmul'tfil'm" studio.

The positives were printed on the color positive film produced by Plant No.3. Both ultraviolet and mixed illumination were used in the tests. The ultraviolet illumination was provided by two "Gosteasvet" 100 watt PRK-7 mercury discharge lamps. The intensity of illumination at the surface of the animation cell varied from 540 to 1500 μw cm^{-2} depending on the position of the lamps. In the case of mixed illumination the above ultraviolet lamps were supplemented with 4 to 6 15-watt DS type fluorescent lamps, which produced an illumination of 210 to 300 lux.

To check on the possible influence of variations in processing, the series of test photographs were repeated at an interval of 75 days. Measurements showed virtually no variation as regards color reproduction of the patches. The color of the patches as reproduced on the film was measured by means of the VNISI photoelectric colorimeter. The film frames were projected directly on the photocell of the colorimeter by means of a slide projector. The light source in the projector was a 500 watt PZh-20 projection bulb with a compensating blue EG-3 Shott light filter mounted in front of it to bring the emission color of bulb closer to that of a high intensity arc. From a comparison of the results of measurements of the color of luminous and nonluminous (ordinary) animation paint patches and their reproduction on movie film (see Tables 2 & 3 and Fig.2) it follows that with the luminous paints it is possible to obtain on film colors of greater purity and hence of a higher degree of saturation with appreciably higher luminosity than with ordinary paints.

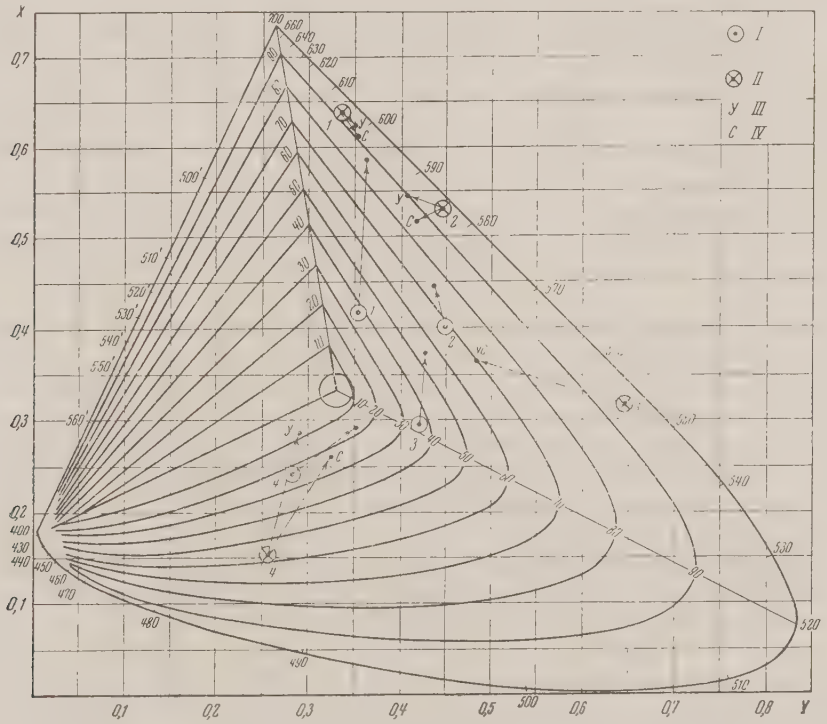

Fig.2. Color rendition on DS-2 motion picture film of ordinary and luminous animation paints: I) ordinary animation paints, II) luminous paints, III) under ultraviolet illumination, IV) under mixed illumination. The Arabic numerals in the diagram correspond to the color numeration in Tables 2 & 3.

Table 2

Color characteristics of the fundamental colors of the palette of luminous animation paints

№	Color	Color coordinates		Dominant wave-length, mμ	Purity, %	Luminosity %	Number of color thresholds
		X	Y				
	a) Original with ultraviolet illumination						
1	Red	0,641	0,338	608	94	31	
2	Yellow	0,537	0,444	586	96	71	
3	Green	0,315	0,639	552	94	65	
4	Azure	0,616	0,259	486	54	41	
	b) Reproduction on positive with photography on DS-2 film under ultraviolet illumination						
1	Red	0,630	0,352	605	95	8	1
2	Yellow	0,550	0,407	592	90	33	1
3	Green	0,367	0,488	568	70	13	5
4	Azure	0,288	0,292	479	8	9	9
	c) Reproduction on positive with photography on DS-2 film under mixed illumination						
1	Red	0,615	0,357	604	92	10	3
2	Yellow	0,521	0,421	587	87	40	1
3	Green	0,368	0,486	563	70	18	5
4	Azure	0,262	0,324	490	22	17	7
	d) Reproduction on positive with photography on Agfacolor film under ultraviolet illumination						
1	Red	0,583	0,376	598	90	12	7
2	Yellow	0,444	0,444	578	75	58	6
3	Green	0,318	0,480	546	58	35	3
4	Azure	0,200	0,300	489	42	22	3
	e) Reproduction on positive with photography on Agfacolor film under mixed illumination						
1	Red	0,618	0,362	602	95	15	5
2	Yellow	0,482	0,446	582	84	59	4
3	Green	0,428	0,485	572	82	70	8
4	Azure	0,264	0,346	494	25	22	6

We also carried out a series of experiments to determine the best type of light filter to use in front of the camera lens for absorption of the stray ultraviolet. On the basis of our tests of WG-1, GG-13 Shott, BS-9 and other filters having similar spectral transmission characteristics, we recommend the use of a 2 mm thick ZhS-4 filter for animation film work with luminous paints.

The developed luminous animation paints were used in 1954-1956 by the "Soiuzmul'tfil'm" studio for the production of "The Frog Princess", "Tagged Atoms", "Twelve Months", "The Snow Queen", "For the Good of Mankind", "A Northern Fairytale" and other films.

Table 3

Color characteristics of ordinary animation paints (best types as regards color reproduction)

№	Color	Color coordinates		Dominant wave-length, mμ	Purity, %	Luminosity %	Number of color thresholds
		X	Y				
a) Original with illumination by DS type "fluorescent" lamps (300 lux)							
1	Red	0,486	0,344	604	52	9	
2	Yellow	0,422	0,474	573	78	31	
3	Green	0,294	0,424	528	36	12	
4	Azure	0,212	0,256	483	32	12	
b) Reproduction on positive (photography on DS-2 film)							
1	Red	0,597	0,361	602	89	6	7
2	Yellow	0,451	0,441	580	77	23	2
3	Green	0,338	0,440	573	5	17	4
4	Azure	0,354	0,335	499	8	10	9

Summarizing the work carried out in collaboration with the collective of the "Soiuzmul'tfil'm" on the use of luminous films in animation work, we can indicate areas of particular utility of such paints: color correction, enhancing the color contrast, lending a glow to fairytale characters and obtaining special light effects.

In many cases when photographing backgrounds and scenery painted with ordinary animation paints it is impossible to obtain the desired pure color tone; it can, however, usually be achieved by means of luminous paints. For example, in the film "The Snow Maiden" the winter landscape in the prologue based on a "deep" blue color reproduced very poorly on film when painted with ordinary paints. By airbrushing luminous azure paint over the old background it proved possible to obtain a blue coloring that reproduced well on film.

It is difficult to obtain bright red tones by means of ordinary animation paints. In the film "The Brothers Liu", in one scene where it was necessary to separate the Chinese mandarin from the crowd, his costume was done in luminous paints and produced the effect of bright red silk. Ordinary yellow paints always come out darker on film than in the original. In "The Frog Princess" it proved feasible to render the color and sheen of the golden leaves in Kashei's kingdom only by using gold-yellow tone luminous paints. The bright pure colors of the "Magic Carpet" were also obtained by using the appropriate luminous paints.

One of the subjects in "Tagged Atoms" was the spectrum. Photographs of the spectrum painted with ordinary paints did not give the desired effect. Pure spectral colors were obtained only by photographing a spectrum painted with luminous paints.

Luminous paints are of great help in enhancing color contrast. The resultant images on film of shining and luminous objects (for example, the moon, stars, solar rays, flashing snowflakes, etc.) are considerably brighter if the painting is executed with luminous paints. If in a landscape painted with ordinary animation paints, the sky is painted with luminous paint a particularly pleasing effect of depth and transparency is obtained.

In the film "For the Good of Mankind" luminous paints were used to show radioactive emanations in the form of a large number of luminous arrows. Arrows done with ordinary paints photographed with a second exposure did not

produce the effect of emission. The desired radiant effect was readily obtained by the use of luminous paints, for they provided the necessary contrast between the background and the arrows.

Luminous paints are also highly useful in obtaining special light effects, for example, for showing Northern Lights, fireworks, rainbows, lightning fire, etc. In the film "A Northern Fairytale" interesting effects of the play of light on water and ice were obtained by photographing scenes done with luminous paints through corrugated lucite. By photographing the scene executed in light tones with luminous paints through different light filters one can create the illusion of changing illumination.

Luminous paints have proved useful in picturing different fairytale characters and objects. Thus, for example, pictures of the sun are frequently encountered in animation films. However, all attempts to show the shining of the sun on the screen with ordinary paints did not give the desired artistic effect inasmuch as the movement of the rays always appeared mechanical and all the rays had the same color. Only photography of paintings on celluloid with luminous paints could give the very interesting effect of diverging rays. Sparkling decorations and jewelry done with luminous paints enrich the costumes of the "Snow Maiden", "Uncle Frost", the "Snow Queen" and many other animated film personages.

Thus luminous paints improve the quality of animation films, greatly simplify their production and make it possible to obtain many artistic effects unattainable with ordinary techniques.

All-Union Light Engineering Institute

References

1. N.V.Gorbachev, Izv.AN SSSR, Ser.fiz., 13, 318 (1949).
2. N.V.Farmakovskii, Akvarel' (Watercolors), L, 1952.
3. S.O.Maizel' & E.S.Ratner, Tsvetovye raschety i izmereniia (Color calculations and measurements), M, 1941.
4. D.A.Shklover, Izv.AN SSSR, Ser.fiz., 15, 829 (1951).
5. D.A.Shklover, Svetotekhnika (Light Engineering), 4, No.1 (1956).

DISCUSSION

E.M.Mandel'berg: How do your paints behave on celluloid?

M.I.Agranian: Very well. We have observed their use in a number of studios for over a year. They appear to satisfy all requirements.

Question: What effect is obtained in mixing the paints?

M.I.Agranian: We developed special recommendations for work with these paints. Basically they obey the additive law.

Question: Will these paints be put on sale?

M.I.Agranian: Yes, the water soluble paints will shortly be put on the market by the "Krasnyi khudozhnik" plant.

Question: Do the colors change under ultraviolet?

M.I.Agranian: The color of the paints may or may not change depending on the pigment used.

USE OF LUMINOUS PAINTS IN THE THEATRE

- B.M.Baranov

I am not going to make a scientific statement; I want to tell you, as an artist, how luminescent painting of costumes and scenery is now being used in theatrical productions in our country.

Luminous paints were first used on the Soviet stage in 1925, but the significant development of luminescent painting dates back to 1939-1940, when our industry began to produce phosphors, lighting apparatus and mercury lamps.

In 1939-1940, several well-known painters, among them Bruni, Akimov and Dmitriev, made the scenery for several successful productions, using the results obtained by the Leningrad Theatrical Laboratory and the State Optical Institute.

Luminous make-up and luminous organic dyes were used for the first time in the play "Tale of Ivanushka", produced by the Leningrad Children's Theatre in February 1939.

Later, a laboratory of luminescent scenery painting was established in Moscow under the direction of the artist Mandel'berg; it has accomplished a great deal of useful work in the six years of its existence.

In Leningrad, the use of luminous paints was investigated by D.N.Lazarev, who published a number of papers on the subject.

At present, fruitful work is being done by the Laboratory of the Moscow Art Academic Theatre, which co-ordinates the efforts of artists, engineers, light technicians and individual laboratories as regards the utilization of luminous paints in the theatre.

In collaboration with this Laboratory, theatrical artists and stage managers create interesting productions where luminescence is an integral part of the show.

The All-Russian Theatrical Society is also doing a great deal to promote the use of luminescent paint, in particular, by offering courses and including special lectures on the proper uses of luminescent painting in the theatre in its seminars for artists and light technicians. It has also published a handbook on the subject.

In recent years, luminescent painting has become an indispensable part of staging, and is widely used in ballets, operas, children's entertainment, etc., not only in Moscow and Leningrad but in a number of other cities throughout our land. At the present stage of development, the artist's ability, his general culture and his technical skill are of the greatest importance.

Luminescent painting in the theatre should be used so as to enhance the artistic value of the production, and not as an end in itself, a piece of cheap trickery. Regrettably, there are theatrical painters whose unartistic, slap-dash work gives evidence of their bad taste, and this repels the audience and discourages producers from using luminous paints.

In addition to being employed simply for scenery and costumes, luminous paints can be used in more complex ways:

1. To heighten stage effects in a manner which cannot be achieved with ordinary paints, for example: in showing sunrise, sunset, moonlit landscapes, stars, lighted windows.

2. To introduce changes in the landscape.

3. To paint two different scenes on the same backdrop (thus, a winter landscape may be transformed into a summer one by a change of lighting).

Our techniques are, of course, far from perfect; but it is already clear that luminescent painting in the theatre has a great future.

I should like to take advantage of this opportunity to present our wishes, requests, and indeed our demands to scientists, laboratories and industry. While heretofore the quality of luminous paints and lighting equipment was more or less adequate for our needs, now that we have learned to achieve some of our most striking theatrical effects by means of luminescence, we need improved types of lighting which will enable us to illuminate luminescent scenery without darkening the stage, since the audience should be able to see what occurs on the stage at all times.

1. We need footlights and small lighting units which can be mounted in the scenery.

2. We also need special, beamed light sources permitting us to illuminate some one piece of scenery, some detail of staging or an actor's face.

3. A serious drawback of the PRK-7 mercury lamp is that it cools slowly, and that it must be allowed to cool before it can be lighted again; the interval is often too long for stage requirements.

4. A great defect of the mercury lamp is that the amount of light it gives cannot be controlled; if the technical problem of regulating the intensity of mercury lamps is too complex, thought might well be given to developing diaphragms and shutters for such light sources.

5. Although we should like very much to use luminescent paints in decorating streets, city squares, etc., for outdoor festivals, we have been forced to give up the idea, because the available light sources, paints and solvents are not adapted for outdoor use.

Imagine, my friends, what a riot of color we could provide for the World Youth Festival, which will be attended by tens of thousands of people from every corner of the world, people who will come not only to demonstrate their proficiency in sports and the arts, but also to take a look at Moscow in its holiday attire.

There is still time to give our country the possibility of providing a fitting background for this great historic event.

6. Scientists must develop optical equipment which would enable us to project a landscape, rain, snow, etc., on a flat surface covered with luminescent paint.

7. I'd like to say a few words about phosphors. In acting, the basic, the most important feature are the eyes. In the old days, before the Revolution, kerosene lamps were used to light the stage and the actors; now powerful floodlights are employed. Paradoxical as it may seem, kerosene lamps gave a warm, flickering, living light, which is more than can be said for modern lighting equipment.

This quality of modern lighting is especially pronounced when luminous paints are used. Luminous paints are dead; they are beautiful but cold; they are static - and it is up to you to breathe life into them.

8. In painting with oils, the artist uses white pigment to obtain the precise shade he wants. In water colors, the white paper performs the same function as the white pigment. There is nothing like this in the luminous paint palette, which a serious drawback; a white luminescent paint must be evolved.

9. The luminescent paint material must be finely ground, so that the different colors can be mixed, as is now done with oil paints, gouache and water colors.

10. I should also like to point out that some colors are more luminous, and others less so; it is desirable that they should all have the same high degree of brightness.

11. Incidentally, abroad in printing posters and advertisements they have been using luminous paints which shine by daylight without ultraviolet irradiation. It would be highly desirable for our science and industry to develop such paints.

12. Our theatres still have to procure lighting equipment, uviol glass and lamps from different plants and agencies. This is onerous. All the equipment required should be obtainable from a single agency.

If science and industry are able to meet these wishes, luminescent painting is sure to gain a firm foothold in our theatres.

ON LUMINESCENT DECORATIVE PAINTING

- E.M.Mandel'berg

Although luminescent painting is a relatively new art, it is no longer in its infancy, and the experience we have gained over the past few decades enables us today to aim at higher goals.

There was a time when we were happy to see even a few smears of luminous paint - applied by artisans, not artists - gleaming here and there on a stage or at an exhibition.

The paintings executed in our workshop by S.I.Vavilov, I.E.Grabar', B.V.Ioganson, K.F.Yuon and others bear witness to the fact that we have left behind those primitive daubs and are well on our way to the difficult and original form of decorative art known as luminescent painting.

The works which I shall mention later and the few sketches I am going to show you are no doubt far from perfect, but they do indicate that luminescent painting has an artistic content of its own and that it is progressing in the right direction.

In the last few years, luminescent painting was used with particular success in two productions: the ballet "Sleeping Beauty" given at the Gorky Opera and Ballet Theatre in 1953, and the opera "Ruslan and Ludmila", performed at the Kuibyshev Opera and Ballet Theatre in 1954.

In any examples I may cite I shall refrain from discussing artistic excellence or shortcomings, which are of no immediate interest to this Conference. I shall dwell only on technical matters which may directly influence the extent to which luminescent painting will be used in the theatre.

In the two productions I have mentioned, luminescent painting effects were obtained using ultraviolet irradiation from 12 - 16 PRK-7 lamps, equipped with parabolic reflectors, in combination with ordinary lighting of approximately the same intensity. This combination of two streams of light, complementing and correcting each other, enabled the audience to see the entire stage, up to the last backdrop, and also to see the faces of the actors - a matter of considerable importance. You see, for many years artists who, like myself, have long been deeply interested in these new luminous paints have been asked one and the same question by hundreds and thousands of people who have seen our exhibits at expositions and lectures: "Why aren't such methods being widely used in our theatres?"

The same question was put to us last year by nearly every one of the many thousands who visited the exhibition at the Izmailovskii Park of Culture and Rest in Moscow. I think that, in all fairness, we artists must not lay the entire blame on the inertia or conservatism of certain officials in the government departments concerned with the arts, but should accept a large share of it ourselves.

Our early experiments in the theatre, including the work I myself did for the fairytale "The Forest Song", produced in Moscow in 1944-6, and the examples cited by B.M.Baranov, discouraged many theatre workers from using luminous paints for a number of years. The reason for this is very simple.

As everyone knows, the central figure in the theatre is the actor. The actor produces an emotional effect on the audience not only by means of the spoken word, which conveys ideas and emotions, but also by projecting his entire personality, which he does mainly through changes in facial expression. But how is the audience to perceive these changes, which indicate the finest shadings of emotion, if the actor's face is invisible because the stage has been plunged into darkness or semi-darkness to make the luminous paints glow?

The character portrayed by the actor cannot be fully projected; worse still, even the words he speaks cannot be properly understood, so that the content of the play cannot be fully appreciated in the faint light. Only the luminescent effect - a mere technical trick - reaches the audience. The stage manager, too, feels hampered, for the darkness which hitherto has been mandatory on the stage and in the circus on such occasions prevents him from designing scenery in depth.

Thus we see that the success of the two productions - "The Sleeping Beauty" and "Ruslan and Ludmila" - where ultraviolet light was used in conjunction with visible light, is of signal importance. I should like to note that in "The Sleeping Beauty" the entire moving scenic panorama, measuring about 800 m^2, was executed with luminous paints. This is the first time that a single canvas of such large dimensions was painted with phosphor paints. It is further of interest that during three years' use it required no retouching whatever, whereas all the other backdrops in that ballet, painted with ordinary paints, had had to be redone several times during that period.

These phosphor paints owe their stability to the high quality of the water soluble binder which was evolved by the chemical section of our laboratory back in 1944 and on which I reported to the Second Conference on Luminescence in 1948. Now that the quality of this binder has been tested not only in the laboratory and on small and large stationary canvases, but also under the harsh conditions I have mentioned, I am ready to recommend it and to guarantee its stability in any and all circumstances.

The formula of this water soluble binder is as follows: to 1 liter boiled water, add 120 g casein, 30 g sodium carbonate or ammonium carbonate, 2 g phenol, and 20 cc formalin mixed with ammonia (in a ratio of 1 to 2).

This binder assures absolute stability of the luminous paints. If it is desired to use it as a fixing agent after the canvas has been painted, a heavy moist layer of the binder should be applied by means of an airbrush and the canvas should be laid out flat to dry for 8 to 10 hours. The experience with "Ruslan and Ludmila" shows that in large spectacular productions, where luminescent backdrops are combined with ordinary scenery and where visible light is used, it is extremely important to space out the use of luminsecent areas in such a way as to preserve a sense of rhythm and balance in the entire performance (to say nothing of a sense of measure).

I should like to stress that, as S.I.Vavilov pointed out, luminescent painting should be used to accent and heighten the general effect and should be employed only where it is indispensable and cannot be replaced or imitated by means of ordinary paints or the usual transparencies.

Such positive results as have been attained in the use of luminescent paints are due to the fact that we have developed a new technique of luminescent painting, based on a new palette combining phosphors with fillers, which I demonstrated at the Second Conference on Luminescence.

I must say, however, that the method of showing different images on the same canvas, a method which we worked out long ago, was used in only four productions between 1949 and 1953 and has still not been generally accepted. And yet this is the most interesting method we have, since it both enables the designer to achieve highly artistic effects and reduces the costs of production.

The reason why theatres are still not making sufficient use of luminescent painting is, I think, that most workers in the theatre are not acquainted with the latest achievements in this area; also, there is a shortage of artists, both designers and painters, familiar with the new technique of painting (and I mean painting and not merely coloring) with luminous paints used in conjunction with fillers.

On the other hand, I can report to the Conference on an interesting experiment in panoramic painting.

In December 1955, P.M.Tolkach, E.I.Shwarts and myself painted a large luminescent canvas, measuring 72 square meters, entitled "The Lights of the Five-Year Plans". It was mounted on an aluminum tubing frame and set up in the Georgii Hall of the Kremlin Palace.

Under electric light, the canvas showed a landscape, painted with ordinaar paints, representing a generalized image of one of our great rivers with hilly and wooded shores. When ultraviolet light was switched on, a luminescent painting sprang to life on the same canvas, showing a vast dam and power plant, gleaming with lights, built on the scene shown immediately before.

This large canvas was illuminated by means of only six PRK-7 lamps, in combination with a strong flood of visible light.

We have now painted a similar, but smaller, canvas (18 m^2) for the reopening of the exposition of my luminescent paintings, in the specially equipped hall in the Izmailovskii Park of Culture and Rest in Moscow (see photograph)

Fig.1. Self-transforming luminescent canvas "Lights of the Five-Year Plans". Above: picture under visible light. Below: picture under ultraviolet light.

The change from visible to ultraviolet light is effected by means of a remote-controlled electric clock and a system of relays.

[Note added in proof: By June 1957 we shall have completed a luminescent panorama entitled "The Bratsky Hydroelectric Plant". This canvas, painted for the celebration of the fortieth anniversary of the October Revolution, will be on exhibition in one of the halls of the Moscow Polytechnic Museum during the Sixth International Festival.]

In conclusion, I should like to draw attention to the following. For a number of years we, a small group of artists working in the field of luminescent painting, knew nothing of similar work being done abroad.

It would be desirable for us to establish contact with the best Western scientists and artists who are concerned with the uses of luminescent paints, in particular in the theatre, in architecture, in decorative painting, in printing, etc.

They could learn a great deal from us, but we, too, should learn from them.

In order to make progress and to put into practice the innovations and improvements we have evolved in our theoretical work, we must be able to rely on industry to produce cheaper and more varied luminescent paints and improved lighting equipment. In addition, we must begin forthwith to train designers and artists who will be fully familiar with the technique and technology of luminescent painting.

USE OF PARAMAGNETIC RESONANCE TECHNIQUES FOR INVESTIGATING THE STATE OF THE ACTIVATOR IN PHOSPHORS (Abstract*)

- A.A.Manenkov, A.M.Prokhorov, Z.A.Trapeznikova & M.V.Fok

We used the method of paramagnetic resonance for determining the valence of the activator in crystal phosphors and, also, for attempting to detect the change in valence during excitation of the phosphor. Measurements were made on SrS:Eu, CaF_2:Eu, SrS:Gd and SrS:Tb phosphors at room temperature by means of a superheterodyne radiospectroscope. It was established that Eu in the investigated phosphors is in the bivalent state, while Gd and Tb are in the trivalent state.

We were not able to detect a change of valence of the rare earth elements with excitation of the phosphor with an experimental accuracy of about 5%. At the same time, in the case of the phosphor SrS:Eu excited by light there is observed a decrease of about 10% of the optical absorption due to the introduction of europium. This divergence appreciably exceeds the limits of chance error of both methods and, possibly, indicates that another element in the luminescence centers, rather than europium, is ionized.

In view of the importance of possible ionization of the activator for the theory of luminescence centers, our experiments must be regarded as only preliminary. For definite solution of the problem one must enhance the sensitivity and accuracy of the procedure.

From the observed hyperfine structure of the Eu^{2+} and Gd^{3+} spectra we calculated the ratio of the magnetic moments of the Eu^{151} and Eu^{153} nuclei - $\mu_{151}/\mu_{153} = 2.24 \pm 0.03$ - and evaluated the magnitude of the magnetic moments of the Gd^{155} and Gd^{157} nuclei - $|\mu_{155}| \approx |\mu_{157}|$ 0.2 nuclear magnetons.

"P.N.Lebedev" Physical Institute of the
Academy of Sciences of the USSR

* * * * * *

NATURE OF LUMINESCENCE CENTERS IN ARTIFICIAL FLUORITE CRYSTALS ACTIVATED WITH RARE EARTHS AND URANIUM (Abstract**)

- P.P.Feofilov

1. In investigating the nature of luminescence centers in crystals it is necessary to bear in mind a) the possibility of isomorphic incorporation of the activator ions into the host lattice and b) the possibility of local compensation of disturbances of electric neutrality that may occur in the case of heterovalent isomorphism.

2. Investigation of the luminescence spectra of rare earth activators in artificial fluorite (CaF_2) single crystals shows that each rare earth element can yield two sharply differing luminescence spectra, depending on the conditions of preparation of the crystals. It is natural to attribute this difference between the spectra to differences in the structure of the immediate neighborhood of the rare earth ion (TR^{3+}), developing due to a difference in the manner of compensation of the excess positive charge.

3. In CaF_2:Tr crystals grown in an oxidizing atmosphere local compensation of the excess charge may be realized through isomorphic replacement of

---

*Complete report in Optika i spektroskopiia, 2, 470 (1957).

**Complete report in "Proceedings (Materialy) of the Fifth Conference on Luminescence" Tartu, 1957.

one of the fluorine ions in the immediate neighborhood of the TR^{3+} ion by an oxygen ion. This model of a luminescence center with stable charge compensation is in agreement with the results of polarization measurements indicating alignment of the centers along a third order symmetry axis and with data on the photochemical sensitivity of the crystals.

4. In CaF_2:TR crystals grown in a strongly reducing atmosphere there may form electron acceptor centers which inhibit the formation of color centers under the influence of hard radiations.

5. In the case of growth of the fluorite crystals under reducing conditions with rare earth elements capable of going into the bivalent state (samarium, europium and ytterbium) there may be incorporated in the CaF_2 crystal lattice bivalent rare earth ions with characteristic absorption and luminescence spectra.

6. In order to obtain luminescence centers in fluorite crystals activated with uranium one must provide strong oxidizing conditions to assure compensation of the excess charge by isomorphic replacement of four fluorine ions in the immediate neighborhood of the U^{6+} ion by four O^{2-} ions.

7. In view of the absence of vibrational frequencies associated with UO_2^{2+} in the luminescence spectra of CaF_2:U, we may conclude that in these crystals the luminescence centers are not formed about UO_2^{2+} ions but are U^{6+} ions with their neighboring ions.

DISCUSSION OF REPORTS OF MANENKOV, PROKHOROV, TRAPEZNIKOVA & FOK and FEOFILOV

Question (to A.A.Manenkov et al): Can one by means of your set-up obtain a paramagnetic resonance curve for pure alkali halide crystals with F-centers, having unpaired electrons?

A.A.Manenkov: It should be feasible; there are investigations of paramagnetic resonance for F-centers. The sensitivity of the procedure is sufficient; it is important that there be not less than 10^{13} F-centers in the crystal and then the absorption line can be detected.

Question: Can one determine the valence of Eu in alkaline earth silicate powders by the paramagnetic resonance procedure?

A.A.Manenkov: If the crystal structure of the silicate deviates little from the cubic it should be possible in the case when concentration is not very low. If the crystal structure differs greatly from the cubic, then it may not be possible to observe the paramagnetic resonance spectrum for a powder specimen; consequently, in this case it will be impossible to determine the valence of Eu.

A.N.Terenin: (to P.P.Feofilov) Did you actually observe diffusion of oxygen through the fluorite lattice with replacement of fluorine ions? At what temperatures did this occur?

P.P.Feofilov: Diffusion of oxygen was observed at relatively moderate temperatures, beginning from 800°. By continuing the heating for a reasonable time (an hour or more) one can assure diffusion of the oxygen into the bulk of a crystal having a volume of several cubic centimeters. The process begins from the surface. If a green crystal containing bivalent samarium is heated at 800°, it becomes bleached after a few hours. In the process there occurs not only oxidation of bivalent Sm to trivalent, but also formation of type 1 luminescence centers, that is, centers in which charge compensation, according to our hypothesis, is realized by oxygen.

CLOSING ADDRESS

- V.L.Levshin

Comrades! The Fifth Conference on Luminescence has completed its work. We can note with satisfaction that the work of the Conference was fruitful. We have heard a number of significant reports and have exchanged opinions on important problems in the luminescence of crystal phosphors. On some important questions there have been heated discussions which have helped establish the correct viewpoints and clarify the direction of further investigations.

There can be no doubt of the rapid and extensive development of the study of phosphor luminescence in the Soviet Union. One may note with particular pleasure the opening of several new centers of research. Among these one can point first to the recently organized large center in Tartu, headed by F.D. Klement. The work of F.D.Klement, Ch.B.Lushchik and their co-workers justly merited the attention of the Conference. Another fact we can note with satisfaction is the beginning of scientific studies of luminescence at so remote a site as the Central Asian University.

A distinctive feature of the Fifth Conference on Luminescence is the wide participation in it of chemists who have read us a number of important reports on new methods of purifying phosphor raw materials, the chemical properties of crystal phosphors and on the processes occurring in their formation.

Our Conference has noted with satisfaction the appreciable progress in the development of the phosphor industry and the appearance on the market of new types of phosphors.

Against the background of these successes one cannot but recall S.I. Vavilov who contributed so much to the science of luminescence and its applications in our country. This coming January will mark the fifth anniversary of his untimely death. I ask all present to honor the memory of Sergei Ivanovich by rising. (Everyone stands).

Despite the great advances in the field of luminescence in the USSR further progress in this field is essential. Our developing industry and the national economy set new demands that must be met by those working in all branches of luminescence. The fundamental, most important directions of our work and the means that will insure its successful accomplishment are noted in the resolution we have adopted.

I am sure that all those participating in the Conference, whatever their specific fields, will take all the necessary measures for realization in practice of the goals set, will work to spur further progress in the field of luminescence theory and insure that practical use will be made of new scientific achievements. Let us wish each other success in solving these important problems.

In concluding I want to express on the behalf of all those present our deep gratitude to the Soviet of Ministers of the Estonian Republic for their aid in organizing the Conference and providing the facilities for its fruitful work.

(In Estonian: The participants in the Fifth Conference on Luminescence are deeply grateful to the Soviet of Ministers of the Estonian Republic for help in organizing the Conference.

We leave with the warmest memories of the fraternal Estonian Republic.)

The participants in the Conference also express their heartfelt thanks to our dear hosts: Rector of Tartu University F.D.Klement, Pro-Rector A.V. Moskvin and Ch.B.Lushchik for their unstinting efforts in organizing the Conference. (Applause).

I declare the Fifth Conference on Luminescence closed.

RESOLUTION ADOPTED BY THE FIFTH CONFERENCE ON LUMINESCENCE (CRYSTAL PHOSPHORS) (Tartu, 25-30 June 1956)

The Fifth Conference on Luminescence is the second conference on luminescence devoted specifically to the topic of crystal phosphors.

The great number of participants (270) from nineteen cities of the USSR and the profusion of reports made it necessary to conduct the meetings of the Conference in two parallel sections.

The Conference heard over 100 reports devoted to different problems of luminescence of crystal phosphors in their physical, chemical and industrial aspects. Active participants in the Conference were both well-known scientists and young specialists. The Conference notes the great interest shown in the reports and the high level of the scientific discussions.

The exhibit of phosphors, phosphor products, instruments for investigating luminescence and examples of luminescent painting organized at the Conference was a great success and attracted the attention of numerous visitors. Particular interest was shown in the demonstrations of electroluminescent capacitors and the luminescent equipment produced by the VSEGEI ("Geologorazvedka" ("Geological Prospecting") Plant). Important, too, was the literature exhibit (journals, books, patents and scientific-historical publications) which enabled many of the conferees to familiarize themselves with sources of information otherwise difficult of access. The results of the Conference bear evidence of the further quantitative growth of the luminescence school founded by Academician S.I.Vavilov which has proved its ability to solve complex theoretical and practical problems in this field of physics.

The years since the Third Conference on Luminescence are characterized by a marked revival of scientific work on luminescence in institutions of higher learning and industrial institutes; scientists from industrial laboratories have presented a considerable number of reports. Since the Third Conference there have been significant advances in investigation of luminescence centers, the kinetics of phosphorescence and photoconductivity and photodielectric effects, and the development of physical and chemical methods and procedures for measuring the absolute efficiency, thermooptical stimulation, thermostimulation and studying of dark and ultra-short-term processes.

The Conference heard reports on new theoretical investigations of the kinetics of photosemiconductor phenomena and on the first investigations of electroluminescence. As at previous conferences, an appreciable number of reports was devoted to the topic of alkali halide phosphors. The Conference notes the importance of the reported on work in the field of preparation and analysis of high purity substances serving as the raw materials for scintillators and phosphors and of the studies of the potentialities of chromatographic procedures.

Research on the preparation and investigation of scintillation crystals and liquids has become particularly important now. The Conference notes with satisfaction that the domestic industry (Khar'kov Chemical Reagents Plant) is organizing the production of scintillation crystals.

The conference also notes that in the years since 1951 the Ministry of the Chemical Industry has carried out extensive work on the production of phosphors. The "Krasnyi khimik" Plant is now putting out 35 different types of luminophors and has organized the production of phosphors in the amounts necessary for industrial production of fluorescent lamps and cathode ray tubes. There have been organized scientific research groups at the GIPKh and at the "Krasnyi khimik" Plant carrying out studies on the purification of raw materials for phosphors and the synthesis of new luminophors.

The Conference calls attention to the inadequate development of scientific research work on such important problems as cathodo- and roentgenoluminescence and, particularly, electroluminescence. The Conference also considers it essential to point to the importance of comprehensive investigations of the luminescent and photoelectric properties of both typical crystal phosphors and typical semiconductors as part of a unified approach to elucidating the mechanism of photo-semiconductor phenomena.

The Conference considers it necessary that in addition to continuing research on the chemistry of luminophors, emphasis should be placed on the development of efficient procedures for purifying phosphor raw materials, including those used in conjunction with radioactive indicators, and to the practical utilization of these new procedures as they are developed in industry for enhancing the quality of phosphor production. Further research is also desirable as regards development of methods of determining and controlling the characteristics of luminophors and evaluating the dependence of these characteristics on the presence of extraneous impurities.

The Conference notes the need of improving the supply of modern equipment for basic and applied research in the field of luminescence. In connection with this the Conference deems it necessary to urge the appropriate ministries to spur production of the necessary equipment (large monochromators for the visible and ultraviolet regions, accessories for monochromators and the ISP-51 spectroscope, auxiliary equipment for the SF-4 instrument, fluorometers, taumeters, different sources with a continuous ultraviolet spectrum, standard lamps, various instruments with quartz optics, absorption and interference light filters, uviol glass, photocells, photomultipliers, voltage stabilizers, amplifiers, photoelectric absorption (FAS-1) and luminescent (LMS-2) microspectrometers of the type developed by the VSEGEI, the special ultraviolet lamps for luminescent analysis, developed by the GOI, special wide band oscillographs and paninfra photographic plates).

The Conference accordingly:

Requests the Ministry of the Electrotechnical Industry to include in the working plan of the VNISI the development of new ultraviolet sources including sources of medium intensity (100-500 watt), the Ministry of Geology and Preservation of Mineral Resources to instruct the VSEGEI and the Ministry of the Petroleum Industry to instruct the VNIGRI to expand their work on the development of equipment for luminescence analysis with a view to advancing the commercial production of such equipment.

Requests the Ministry of Geology and Preservation of Mineral Resources to include in the plan of the "Geologorazvedka" Plant for 1957 the production of LIuM-1, LIuM-2, FAS-1 and LMS-1 instruments.

Requests the Ministry of the Radio Engineering Industry to organize batch production of electronic voltage regulators, as designed by the GOI, for the supply of light sources, to set up production of the necessary standard mercury, krypton and special luminescent lamps together with the requisite starting and control devices, to set up batch production of demountable cathode ray tubes and to insure the production of the TK-1 television colorimeters developed by the VNISI.

Requests the Ministry of the Defense Industry to organize the production of UFK universal photoelectric colorimeters of the type developed by the VNISI.

Requests the Ministry of Electrotechnical Industry to organize the production of furnaces for growing single crystals.

Requests the Ministry of the Chemical Industry to take tne necessary measures to advance production of long-lived luminescent coatings with β-emitters and at the same time develop the appropriate protective and safety measures.

Requests the Ministry of the Chemical Industry to assure the production of small amounts of special luminophors as ordered by research institutes.

The Conference notes the deterioration of the situation as regards coordination of the work of different agencies since the time of liquidation of the Commission on Luminescence. In view of the opening of a number of new laboratories working in the field of luminescence, the Conference considers it essential to petition the Presidium of the USSR Academy of Sciences to reestablish a Commission on Luminescence in the appropriate department of the Academy with the participation of the interested ministries and institutions for the purpose of coordination of all scientific and applied research on luminescence. The lack of such a commission is significantly delaying the practical utilization of phosphors in the national economy of the USSR.

The Conference notes with satisfaction the new achievements in the field of publishing of literature on luminescence, specifically of the book by B. I. Stepanov and the appearance of the journal "Optika i spektroskopiia" and of the Trudy (Proceedings) of the Institute of Physics and Astronomy of the Academy of Sciences of the Estonian SSR. These journals, however, cannot provide for the publication of chemical reports. The publication of reports on the chemistry of luminophors should be concentrated in one of the chemical journals; in connection with this the Conference requests the Chemical Sciences Section of the Estonian SSR Academy of Sciences to appoint a chemist working in the field of luminescence to the editorial board of their journal.

The Conference recommends that the journals "Pribory i tekhnika eksperimenta" (Experimental Instruments and Techniques) and "Optika-mekhanicheskaia promyshlennost'" (The Optical-Mechanical Industry) periodically publish information on all new instruments applicable to the investigation of luminescence.

In line with the recommendations of the previous Conference regarding the publication of monographs on questions of luminescence, the present Conference considers it desirable to have compiled a large collective handbook comprising articles on the theoretical, experimental, methodological, chemical, technological and practical aspects of luminescence.

The Conference requests the Ministry of the Chemical Industry to issue as soon as possible a catalog of the phosphors produced under its aegis with indications of their luminescent characteristics.

The Conference considers it necessary to call a conference on molecular luminescence (including molecular spectroscopy) in 1957 in Kiev and a conference on crystal phosphors in 1958 in Moscow or Leningrad. It would be desirable at the latter conference to have an industrial section with the presentation of reports on the commercial production of phosphors and their uses.

It would be desirable to invite scientists from abroad to both conferences in order to establish contact between Soviet and foreign specialists in the field of luminescence.

The Conference thanks the personnel of the Institute of Physics and Astronomy of the Estonian Academy of Sciences and of Tartu State University for their work in preparing the Conference and for their excellent organization that has contributed so much to the success of the Conference.

The Conference expresses its deep appreciation to the Soviet of Ministers of Estonian SSR for making this Conference possible and for providing the exceptionally favorable conditions and facilities enjoyed by the Conference.

Bulletin of the Academy of Sciences of the USSR - Physical Series
Vol.21, No.5 - May 1957 - (Transactions of the Fifth Conference on Luminescence (Crystal Phosphors) - Continued from Vol.21, No.4)
Note: A = Abstract

TABLE OF CONTENTS

	Page Orig.	Trans.
Stimulation and quenching of photoconduction in cadmium sulfide - B.T.Kolomiets	643	639
Determination of the polarity of the photoconductivity current carriers in ZnS phosphors (A) - E.E.Bukke	648	644
On the capacitor procedure for determining the polarity of the photocurrent carriers in crystal phosphors (A) - U.Kh.Nymm and L.Ia.Uibo	648	644
Determination of dielectric constant of excited ZnS:Cu and ZnS:Cu:Fe phosphors (A) - O.V.Agashkin	652	649
Electric and optical properties of ZnS:Cu phosphor (A) - F.I.Vergunas and O.V.Agashkin	653	650
On procedures for obtaining inorganic materials of high purity for luminophors (A) - I.I.Angelov	654	651
Purification of concentrated solutions of salts to "luminophor purity" by the chromatographic method (A) - E.A.Bozhevol'nov and V.V.Trusov	655	652
Chromatographic method of purifying raw materials for the synthesis of luminophors (A) - A.M.Gurvich, T.B.Gapon and M.S. Rabinovich	656	653
New chemical procedures for determining small amounts of impurities (A) - I.G.Shafran	661	660
Some questions of the chemistry of sulfide luminophors (A) - A.A.Bundel' and A.I.Rusanova	662	661
Investigation of the correlation between the luminescence and the catalytic and adsorption properties of "self-activated" ZnO and ZnS crystals (A) - L.N.Shekhter, I.A.Miasnikov and S.Ia.Pshezhetskii	664	663
Some distinctive features of the luminescence spectra of sulfide--selenide luminophors (A) - A.A.Bundel' and Z.I.Guretskaia	667	666
Zinc sulfide-selenide luminophors and their technical applications (A) - E.I.Blazhnova	669	668
Some regularities in the cathodoluminescence of luminophors (A) Z.I.Klabukova	670	669

Investigation of the thermal stability of sulfide phosphor screens (A) - T.V.Korovkina 671 669

Radii and concentrations of activator ions in crystal phosphors (A) - M.A.Konstantinova-Shlezinger 673 671

Role of physical-chemical systems in zinc sulfide luminophors - A.A.Cherepnev 674 672

Structure of alkali halide phosphors and the mechanism of luminescence processes - L.M.Shamovskii, A.A.Dunina and Iu.N.Zhvanko 675 673

On the nature of luminescence centers in zinc sulfide luminophors (A) - Z.A.Trapeznikova 678 677

Infrared photoluminescence of lead sulfide (A) - L.N.Galkin 680 679

Luminescence of microporous glass activated with heavy metals (A) - E.V.Pershina and A.N.Terenin 681 680

Phosphate type photoluminophors - N.A.Gorbacheva 682 681

Investigation of the luminescent properties of some borophosphate compounds (A) - L.Ia.Markovskii and R.A.Shtrikhman 683 683

Manganese-activated lithium-magnesium tungstate phosphors (A) Iu.S.Leonov 686 686

On the causes responsible for the distinctive characteristics of cadmium sulfate crystal phosphors (A) - G.V.Maksimova 688 688

Cadmium sulfate phosphors (A) - B.M.Nosenko, L.S.Revzin and V.Ia.Iaskolko 691 692

Investigation of trapping centers and the kinetics of relaxation processes in alkali halide crystal phosphors (A) - Ch.B.Lushchik, F.N.Zaitov, V.Ia.Kark, L.A.Teiss & I.V.Iaek 693 694

Nature of trapping levels in ZnS:Cu:Co phosphors and their filling under different excitation conditions (A) - V.L.Levshin and V.F.Tunitskaia 695 696

On the formation of trapping levels in ZnSLMn phosphors (A) - V.L.Levshin and B.D.Ryzhikov 696 697

Investigation of thermostimulated emission of crystalline quartz excited by x-rays (A) - L.G.Chentsova, B.N.Grechushnikov and E.N.Batrak 699 700

Luminescence of crystal phosphors under excitation by ions (A) - B.N.Nosenko, N.A.Strukov and M.D.Iagudaev 701 702

On the choice of luminophors for television screens (A) - B.M.Gugel' and I.S.Vekeler 704 705

Improving the quality of luminous coatings in fluorescent lamps (A) - B.M.Gugel' and M.M.Shapochnik	705	704
Physical-chemical principles of application of luminophors to screens by the method of settling (A) - L.A.Saminskii	706	707
Investigation of the luminescence of uranium activated sodium fluoride (A) - Z.M.Sverdlov	710	708
Thermoluminescence of minerals - G.F.Komovskii, V.S.Nikol'skii and O.N.Lozhnikova	711	709
Introductory address (Section on electroluminescence) - V.V.Antonov-Romanovskii	715	713
Some results of investigations of electroluminescence - E.E.Bukke, L.A.Vinokurov, V.E.Oranovskii, Z.A.Trofimov	716	714
Zinc sulfide type electroluminophors - A.N.Kazankin, F.M.Pekerman and L.N.Petoshina	721	719
Zinc sulfide base electroluminophors - I.N.Orlov	731	728
Influence of crushing on the properties of some crystal phosphors (A) - F.D.Klement and R.I.Gindina	748	744
Influence of the activator-salt anion on the luminescence of alkali halide phosphors (A) - N.I.Ivanova	749	744
X-ray studies of NH_4Cl:Tl and NH_4Br:Tl phosphors (A) - A.Ia.Pae	749	745
Investigation of the properties of KI:In and KI:Ga phosphors (A) - Iu.N.Zhvanko, Z.L.Morgenshtern & L.M.Shamovskii	752	747
On the spectral characteristics of some sublimate phosphors (A) - A.F.Malysheva	753	747
Effect of compression on the luminescence spectra of some crystal phosphors (A) - Ia.Ia.Kirs	754	748
Investigation of the regularities of emission of finely dispersed luminescent media (A) - A.P.Ivanov	756	752
Investigation of the diffusion of rare earth activators in different crystals on the basis of luminescence spectra - A.K.Trofimov	757	754
A luminescence method of observing certain crystallochemical transformations in solids (A) - A.K.Trofimov and S.S.Tolkachev	761	759
Preparation of luminous paints and their use in motion picture production - M.N.Agranian and N.V.Gorbachev	763	761
Use of luminous paints in the theatre - B.M.Baranov	771	769

On luminescent decorative painting - A.M.Mandel'berg	774	772
Use of paramagnetic resonance techniques for investigating the state of the activator in phosphors - A.A.Manenkov, A.M. Prokhorov, Z.A.Trapeznikova and M.V.Fok	779	776
Nature of luminescence centers in artificial fluorite crystals activated with rare earths and uranium (A) - P.P.Feofilov	779	776
Closing address - V.L.Levshin	781	778
Resolution adopted by the Conference	783	779

Translated in 1958 by
Columbia Technical Translations
5 Vermont Ave., White Plains, N.Y.

Number 6 Volume 21 1957

BULLETIN

of the

Academy of Sciences of the USSR

- Physical Series -

(Izvestiia Akademii Nauk SSSR)
(Seriia fizicheskaia)

Reproduction rights reserved

by
Columbia Technical Translations
5 Vermont Avenue
White Plains, New York

Single Issues

$20

Annual Subscription

$215

Transactions of the Third Conference

on the

Physics of Magnetic Phenomena

*
* *

We take this opportunity to express our sincere appreciation to the authors whose reports were presented at the Conference in English for granting us permission to reproduce their contributions and for making available copies of their originals.

Columbia Technical Translations

Lithoprinted in U.S.A.
EDWARDS BROTHERS, INC.
Ann Arbor, Michigan

THE DE HAAS-VAN ALPHEN EFFECT

- D. Shoenberg

Recent work by Onsager[1] on the theory of the de Haas-van Alphen effect has shown that the effect may provide a powerful tool for elucidation of the electronic structure of metals. Onsager showed in fact that the period ($P = \Delta(1/H)$) of the oscillations is inversely proportional to the extreme area of cross section of the Fermi surface by planes perpendicular to the field.

From a knowledge of the extreme areas of a surface it is possible, as Lifshitz and Pogorelov[2] have shown, to construct the polar diagram of the surface (if the surface is centro-symmetrical and not too contorted). This method of investigating the Fermi surface has one important advantage over other possible methods; this is that if, as usually occurs for multivalent metals, the Fermi surface can be thought of as made up of a number of closed pieces (containing either electrons or holes), each individual piece contributes its own period and so, at least in principle, can be separately recognized. In other methods (such as a study of the anomalous skin effect) the quantity measured is a sum of the effects from all the various pieces and the separate contributions cannot ordinarily be recognized. Moreover, most other phenomena in metals involve more complicated quantities averaged over the Fermi surface, rather than such a simple feature as the extreme cross section area.

In principle, still more can be learned from the de Haas-van Alphen effect by studying how the amplitude of the oscillations varies with the field and temperature. According to a formula recently deduced by Lifshitz and Kosevich[3], based on a more thorough development of Onsager's idea, it is possible to find the value of $(dA/dE)_o$ at the Fermi surface, where A is the extreme area of cross section of the surface of constant energy E. From a knowledge of $(dA/dE)_o$ for all directions the electron velocity can be deduced. In practice such application of the theory is very difficult because of the difficulty of separating out the individual amplitudes of the several periodic terms which are usually simultaneously present in the observed oscillations.

Until fairly recently most of the experimental work has been done by the torque method in which the couple acting on a crystal suspended in a uniform magnetic field is measured. Owing to the limited fields which can be used in this method and the limitations of field stability and homogeneity, in practice it is impossible to measure periods much shorter than $P \approx 10^{-7}$ gauss^{-1} in this method; theory shows that this corresponds to only a very small area of cross-section of Fermi surface. In fact, the number n of electrons (or holes) contained within a closed piece of Fermi surface, which gives a period of this order of magnitude, is only about 10^{-3} per atom for a typical metal (for a spherical surface the simple relation $n = 0.95 \cdot 10^{-14}\, VP^{3/2}$ applies, where V is the atomic volume). For most metals other phenomena (specific heat, electrical conductivity, Hall effect, etc.) indicate that there should exist pieces of the Fermi surface containing a number of electrons or holes approaching one per atom; and it is likely, therefore, that the de Haas-van Alphen effect as observed by the torque method can show up only what might be called the "fine structure" of the Fermi surface: the small pockets of electrons and holes contained in very small parts of the Fermi surface where it intersects Brillouin zone boundaries. The larger pieces of the Fermi surface in multivalent metals and the whole of the Fermi surface in monovalent metals should yield de Haas-van Alphen oscillations with a period $P \approx 10^{-9}$ to 10^{-8} gauss^{-1} and, moreover, the amplitude of these oscillations should become appreciable only at fields of order 50 to 100 kilogauss which are not ordinarily available in an electromagnet.

To look for such oscillations I followed the example of my teacher Kapitsa and developed a new method of measurement in which the field is produced in pulses by discharging a capacitor and reaches a maximum value of about 100 kilogauss. The complete discharge lasts about 1/30 sec. The metal specimen has the form of a thin single crystal wire surrounded by a "pick-up" coil; during discharge of the capacitor an emf proportional to dM/dH and dH/dt is developed in the coil; this emf is amplified and displayed on an oscillograph. The amplitude of oscillation of dM/dH is proportional to the oscillation frequency, i.e., to $1/P$, and the method is therefore particularly sensitive to oscillations of very short period. By means of this method it has proved feasible to detect oscillations with values of P from about $6 \cdot 10^{-9}$ to $5 \cdot 10^{-8}$ gauss^{-1} in lead, tin and cadmium. So far, however, no very short period oscillations have been found in sodium, copper, silver, gold, mercury, gallium, bismuth, antimony, indium, zinc and aluminum, though for zinc, aluminum and beryllium, the fairly short period oscillations already known to exist at lower fields show up very prettily with this method.

An obvious possible cause of some of the negative results may be the complicating effect of eddy currents induced in the specimen by the varying field. These cause the field at the core of the specimen to lag behind the external field, and if the lag is large compared with the interval of one period, the amplitude of the oscillations will evidently be much reduced. For some metals the resistivity of the metal increases so much in the magnetic field as to make this effect negligible, but for sodium, copper, silver, gold, indium and perhaps others the eddy current effect may indeed be responsible for the apparent absence of de Haas-van Alphen oscillations. For zinc, alumium and beryllium the fact that the rather longer period oscillations ($\sim 10^{-7}$) show up well even at quite high values of dH/dt makes it improbable that eddy currents are responsible for masking oscillations having a shorter period.

I have recently tried a modification of the high field technique in the hope of eliminating the eddy current effect. This was to measure the magnetic behaviour in a very thin skin layer in a 10 Mc field. The output amplitude of a small mutual inductance, surrounding the specimen and fed by this RF current, oscillates as dM/dH oscillates with variation of the applied strong magnetic field; this output is rectified, amplified and the variations of dM/dH are displayed on an oscillograph. This RF method works quite well whenever the direct method works, but it still yields negative results with the metals for which the results were negative in the direct method tests, in spite of the fact that only the properties in the skin depth (of the order 10^{-4} cm thick) are measured. Possibly the trouble is that end effects cannot be avoided and the field variation near the ends of the specimen due to eddy currents may be serious enough to smear out the oscillations. It is, however, possible that the RF method does largely eliminate the eddy current effect, but that the amplitude of the de Haas-van Alphen effect is really too small to be detected. Another possibility is that an appreciable oscillation amplitude occurs only for certain rather narrow ranges of field directions relative to the crystal axes, and that the rather preliminary exploratory experiments carried out so far have not encompassed these ranges. The experimental data for lead and tin show that the shortest period oscillations ($P \sim 6 \cdot 10^{-9}$ gauss^{-1}) are observed only within 10° or so of certain crystal directions. Experiments to investigate these possibilities are being continued.

Although, in view of the above mentioned possibilities the negative results are not conclusive, my impression is that if the very short period oscillations characteristic of a large piece of Fermi surface occur at all in the metals mentioned, their amplitude is much smaller - by a factor of 100 or

or even 1000 - than predicted by the theoretical formula for free electrons. If this is so, it suggests that some important aspect of the effect of the lattice field on the electronic motion in a magnetic field has been ignored in the theory as it stands today. There is already evidence, based on the character of the field variation of the oscillation amplitude at low fields, that the energy levels are broadened more than might be expected from electron collisions; and other discrepancies, too, suggest that the theory needs improvement.

Returning to the problem of determination of the Fermi surfaces of metals from their de Haas-van Alphen periods, the position now is that for a few metals, particularly bismuth, antimony and arsenic, a quite reasonable agreement between experiment and theory can be obtained by assuming that the small pieces of Fermi surface involved are ellipsoids. For other metals an ellipsoidal representation clearly leads to inconsistencies, but little has so far been done to apply Onsager's idea systematically to determining the actual shape and size of Fermi surfaces from experimental data. A start in this direction has been made recently by Gunnersen[4], who has been able to show that the fairly short period oscillations in aluminum can be resolved into these periodic terms. From a systematic study of the variation of the periods of these terms with the field direction, he has shown, by applying Lifshitz and Pogorelov's theorem, that the relevant parts of the Fermi surface are equivalent to three cushion shaped surfaces with their principal axes mutually perpendicular. Theoretical considerations by Heine suggest that these surfaces are made up of pieces of the Fermi surface just inside the corners of the first Brillouin zone. A systematic study of lead, in which the observed oscillations are presumably due to much larger pieces of the Fermi surface has been started by Gold using the pulsed field method. Instead of rotating the magnetic field, as is usual in the torque method, the crystal and pick up coil are rotated within the solenoid. Thus all possible field directions relative to the crystal axes can be obtained by rotating in different planes. Gunnersen's and Gold's experiments should be regarded as "pilot" efforts, and in the light of the experience gained it is hoped to apply the procedure more widely.

Royal Society Mond Laboratory,
Cambridge, England.

References

1. L.Onsager, Phil. Mag., 43, 1006 (1952).
2. I.M.Lifshits & A.Pogorelov, Doklady AN SSSR, 96, 1143 (1954).
3. I.M.Lifshits & M.Kosevich, Zhur.eksp.i teor.fiz., 29, 730 (1955).
4. E.Gunnersen, Thesis, University of Cambridge, 1955.

INFLUENCE OF PRESSURE ON THE GALVANOMAGNETIC PROPERTIES OF BISMUTH

- N.E.Alekseevskii, N.B.Brandt & T.I.Kostina

In view of the results obtained in our investigations of the superconductivity of binary alloys based on bismuth[1,2] and the influence of pressure on their properties, we concluded that it would be desirable to investigate the influence of pressure on the galvanomagnetic properties of bismuth itself[3,4].

The extensive studies of the galvanomagnetic properties of a considerable number of pure metals carried out by E.S.Borovik served to establish a number of experimental regularities in this field[5].

In the present report we give the results of our investigation of the influence of compression on the temperature dependence of the electric resistance and on the galvanomagnetic properties of bismuth.

The bismuth specimens used in the investigation were single crystals either in the form of 2.5-3 mm diameter, 15 mm long rods or spheres 3 mm in diameter grown by the method of Kapitsa[6]. The principal impurities in the bismuth specimens were Pb, Sn, Te and Se; the concentrations of these impurities were varied from 0.0005 to 0.03%. The purest specimens were obtained by the zone purification procedure. The resistance of the specimens changed by a factor of more than 350 in the temperature range from room temperature to that of liquid helium, while the resistance in a 19,000 oersted field at 4.2°K changed more than 10^6 times.

The pressure was produced by the method of freezing water in a constant volume bomb, first utilized at low temperatures by Lazarev & Kan[7].

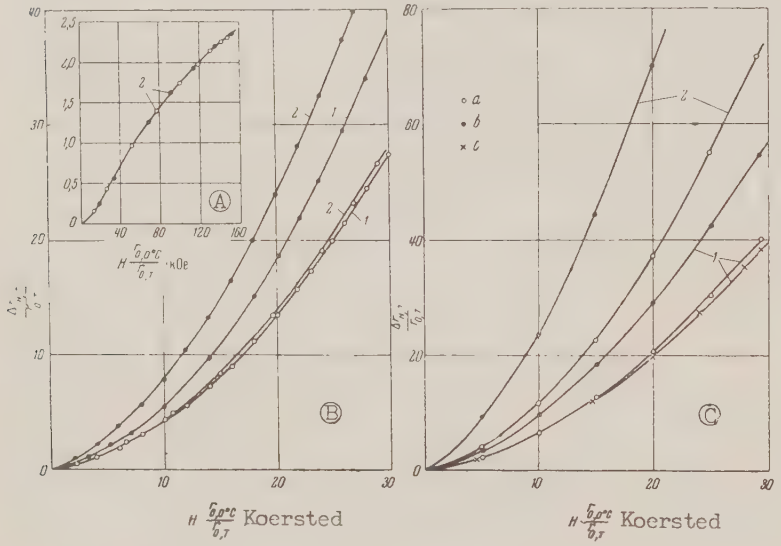

Fig.1. Dependences of $\frac{\Delta r_{H,T}}{r_{0,T}}$ on $H\cdot\frac{r_{0,0°C}}{r_{0,T}}$ averaged over the directions of maximum and minimum change of the resistance in the magnetic field for Bi specimens containing A - 0.032% Te (axis of specimen approximately perpendicular to principal axis), B - 0.0005% Te (axis of specimen approximately parallel to principal axis), C - 0.005% Sn (axis of specimen approximately parallel to principal axis); 1 - at 77°K, 2 - at 4.2°K; a - no pressure, b - p = 1750 kg/cm^2, c - pressure removed.

Fig.1 shows the dependence of the electric resistance of bismuth specimens with different Te and Sn contents on the "effective" magnetic field $H\frac{r_{0,0°C}}{r_{0,T}}$ at 77 and 4.2°K. Figs.2 & 3 show the dependence of the electric resistance of Bi containing 0.02% Pb on the magnetic field at 20.4 and 4.2°K. The dependences of the ratio of the Hall field E_y to the current field E_x on the magnetic field for the same Bi specimens are shown in Figs.4 & 5. As may be seen from the curves, the presence of Te and Pb in concentrations

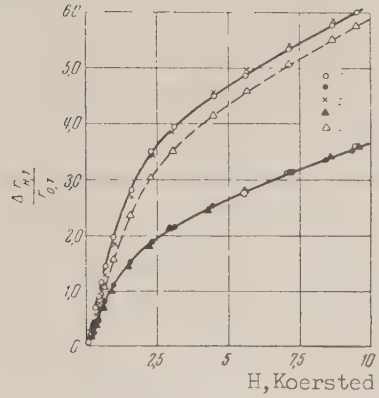

Fig.2

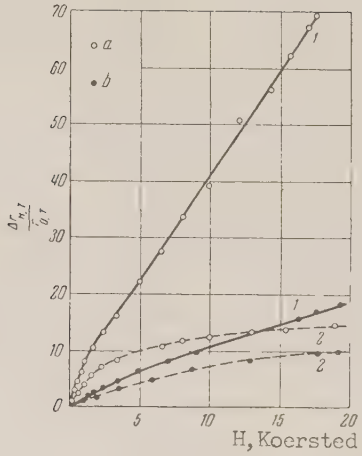

Fig.3

Fig.2. Variation of $\frac{\Delta r_{H,T}}{r_{0,T}}$ with H for Bi specimen with 0.02% Pb at 20.4°K; a - no pressure, b - p = 1750 kg/cm^2, c - pressure removed, d - 1750 kg/cm^2 pressure reapplied, e - repeat pressure removed.

Fig.3. Variation of $\frac{\Delta r_{H,T}}{r_{0,T}}$ with H for Bi specimens with 0.02% Pb at 4.2°K; a - no pressure, b - p = 1750 kg/cm^2; 1 - for direction of maximum change of r in field, 2 - for direction of minimum change of r in field.

of 0.02% and higher leads to a sharp deviation, even at relatively weak field values, from the square law variation of the resistance in the magnetic field characteristic of pure bismuth. As the impurity concentration is reduced the quadratic character of the dependence of r on H extends to increasingly higher field values. The magnetic field dependences of E_y/E_x are even more sensitive to the presence of impurities, for even at impurity concentrations less than 0.0005%, variation of E_y/E_x with H deviates sharply from the variation for pure Bi. The effect of Se on the galvanomagnetic properties of Bi is analogous to that of Te.

Compression produces a very appreciable change in the galvanomagnetic properties of Bi specimens. The influence of pressure continues to be appreciable through Pb and Sn impurity concentrations to 0.03%, whereas in the case of Te and Se there is no appreciable change of the galvanomagnetic properties as a result of pressure when the content of these impurities is greater than 0.005%.

Compression leads to a less sharply defined dependence of the resistance on the magnetic field and decreases the magnitude of the Hall constant in the entire range of investigated fields. The dependence of the change in resistance on the strength of the effective magnetic field, however, increases under compression. In the case of sufficiently pure specimens we observed a reversible decrease of the anisotropy of the change in resistance in the magnetic field, attaining 10% at a pressure of 1750 kg/cm^2. Here the anisotropy is understood to be the ratio of the maximum to the minimum change of resistance in the magnetic field.

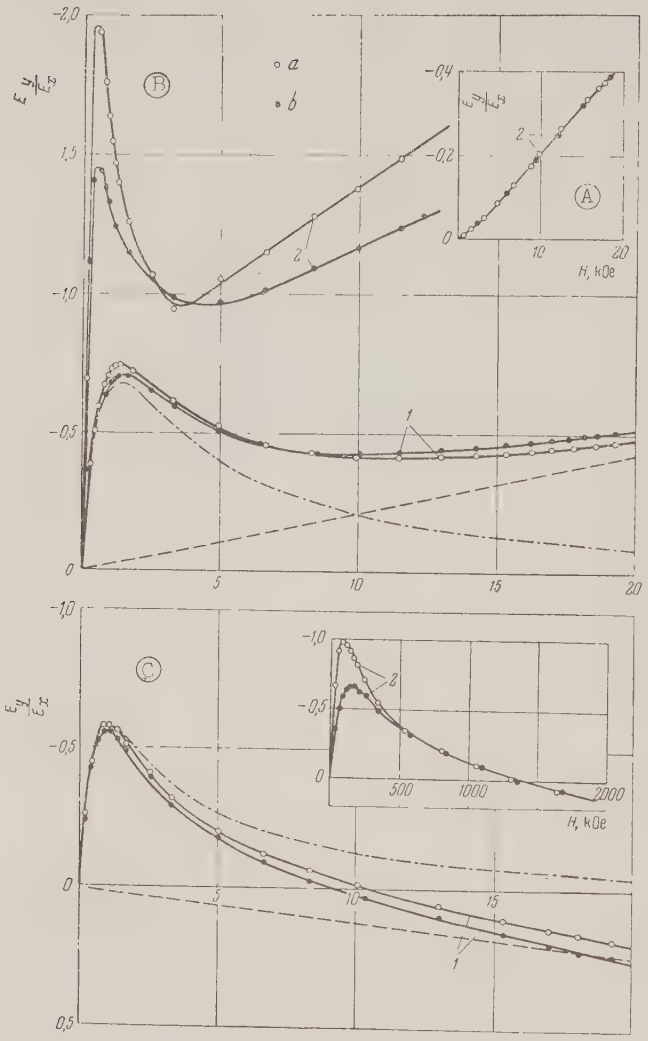

Fig.4. Variation of E_y/E_x with H for Bi specimens containing A - 0.032% Te, B - 0.0005% Te, C - 0.005% Sn; 1 - 77°K, 2 - 4.2°K; a - no pressure, b - p = 1750 kg/cm^2.

In investigating the temperature dependence of the electric resistance of bismuth specimens containing 0.02% Pb and specimens containing 0.015% Sn we found that compression up to a pressure of 1750 kg/cm^2 gives rise to a maximum in the r = (T) curve in the 30-40°K temperature region when the current is perpendicular to the principal axis (Figs.6 & 7). As the amount of impurity is increased, the maximum degenerates to a minor inflection in the curve. An analogous maximum was observed by Thompson & Wills[8] for bismuth specimens with an appreciably higher impurity content even in the absence of pressure.

We felt it would be of interest to compare the experimental results with the deductions of galvanomagnetic theory. We attempted to carry out such a comparison with the two-band theory developed by Blokhintsev & Nordheim[9], Sondheimer & Wilson[10] and Kohler[11], which despite its as yet primitive state has found quantitative substantiation in the work of Borovik[5], and with the recently published (Lifshits, Azbel' & Kaganov[12]) more rigorous theory of galvanomagnetic effects.

From the viewpoint of the two-band theory pure bismuth is regarded as a metal with equal numbers of current carriers in the conduction bands ($n_1 = n_2$). If we assume that low impurity concentrations (0.005%) do not appreciably disturb the equality $n_1 = n_2$, i.e., if taking $\Delta n/n$ to be small, we expand the expression E_y/E_x in terms of $\Delta n/n$, we get

$$\frac{E_y}{E_x} = \frac{\varphi_1 - \varphi_2}{1 + \varphi_1\varphi_2} + \frac{\Delta n}{2n}\varphi_{an},$$

where E_y is the Hall field, E_x is the current field, $\varphi_1 = \frac{e}{c} \cdot \frac{\tau_1}{m_1} H$, $\varphi_2 = \frac{e}{c} \cdot \frac{\tau_2}{m_2} H$; here e is the electron charge, c is the velocity of light, and τ_1/m_1 and τ_2/m_2 are the mobilities of the current carriers in the bands.

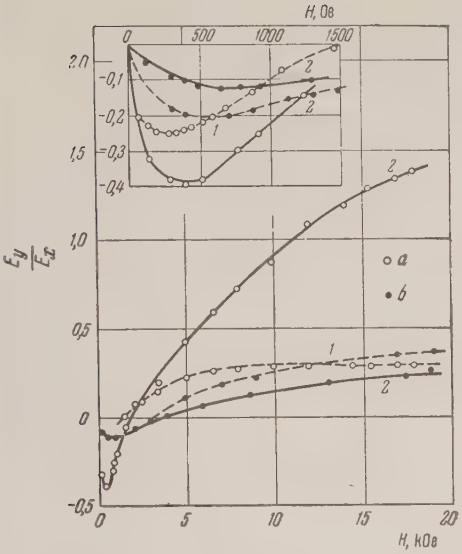

Fig.5. Variation of E_y/E_x with H for a Bi specimen with 0.02% Pb at 4.2°K; 1 - for direction of maximum change of r in field, 2 - for direction of minimum change of r in field.

For sufficiently strong fields this expression can be written in the form

$$\frac{E_y}{E_x} = a\frac{1}{H} + bH.$$

The value of $E_y/E_x \cdot H$ plotted as a function of H^2 yields a straight line with slope b. Having determined the slope one can separate the linear term from the dependence of E_y/E_x on H. The curves constructed in this manner are shown in Fig.4 (dash line curves). After subtracting bH from E_y/E_x, there is obtained a curve characteristic of a metal with $n_1 = n_2$.

Thus it may be inferred that the addition of a small amount of Sn, Pb, Te or Se to bismuth leads to the appearance in the variation of E_y/E_x as a function of H of a linear term described by a straight-line equation with a positive coefficient in the case of Te and Se and a negative coefficient in the case of Pb and Sn. Inasmuch as the sign of the Hall effect in pure Bi at low temperature is that associated with electron conduction, it

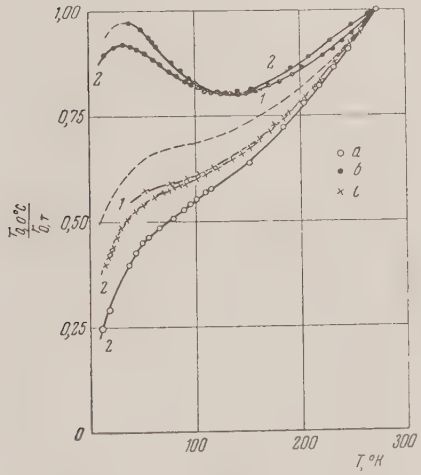

Fig.6

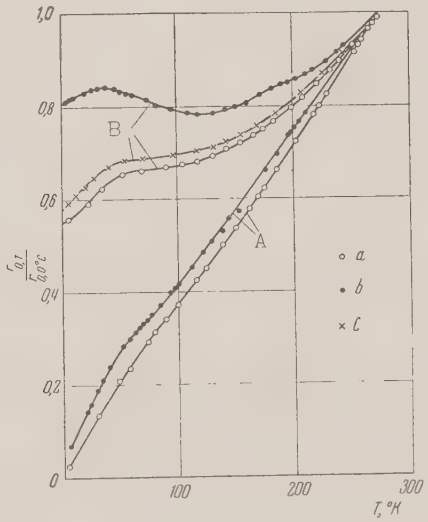

Fig.7

Fig.6. Temperature dependence of the resistance of two Bi specimens with approximately 0.02% Pb (in both specimens the second order axis was perpendicular to the direction of the current): 1 - specimen No.1, 2 - specimen No.2; a - no pressure, b - p = 1750 kg/cm^2, c - pressure removed.

Fig.7. Temperature dependence of the electric resistance of Bi specimens with A - 0.005% Sn, B - 0.015% Sn; a - no pressure, b - p = 1750 kg/cm^2, c - pressure removed.

may be assumed that the introduction of a small amount of Pb (or Sn) or Te (or Se) increases, respectively, the hole or electron component of the conduction in bismuth. The sign and magnitude of the slope of the linear term can, apparently, serve as a means of determining the amount and character of minor impurities in bismuth.

A rough evaluation of the change in concentration of current carriers in Bi under the influence of compression at 4.2°K, carried out on the basis of the two-band model, shows that a pressure of 1750 kg/cm^2 produces a 15-18% decrease of the electron concentration in Bi. A similar but more appreciable (3-4 times greater) reduction of the electron concentration occurs upon cooling from 77 to 4.2°K. It may be assumed that in both cases the changes occur as a result of changes in the lattice parameters. If there actually does occur a decrease of the electron concentration in bismuth under pressure, this may explain why superconductivity does not appear in bismuth when the material is compressed below the polymorphic transformation point.[1,2]

We made an attempt to compare our results with some of the deductions of the theory of Lifshits, Azbel' and Kaganov[12]. The preliminary calculations showed that the effective magnetic field attained in our experiments was probably not sufficiently strong for this theory to apply.

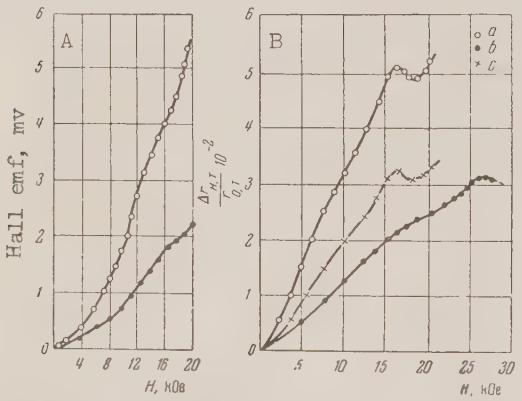

Fig.8. A - variation of the Hall emf with the magnetic field intensity for a Bi specimen with 0.002% Pb at 4.2°K, B - variation of $\frac{\Delta r_{H,T}}{r_{0,T}}$ with the magnetic field intensity for a Bi specimen with 0.0005% Te at 4.2°K; a - no pressure, b - p = 1750 kg/cm^2, c - pressure removed.

In the case of specimens of pure Bi, we also observed a fluctuating variation of r and the Hall emf with increasing magnetic field strength, which persisted under compression (Fig.8). This suggests the possibility of investigating the influence of compression on quantum effects in metals. Preliminary experiments on the influence of pressure on the de Haas-van Alphen effect in Bi indicate that the fluctuating character of the magnetic susceptibility persists under compression.

We believe that it may be possible to observe fluctuation of the variation in resistance with pressure in a constant magnetic field. Experiments along this line are in a preliminary stage.

Conclusions

Summarizing the results of our experiments, it must be noted that compression has a very strong influence on the galvanomagnetic properties of bismuth. Very minute amounts of Te (0.005% and over) fully eliminate the effects of pressure; in contrast, the influence of pressure persists to appreciably higher impurity concentrations (0.02%) when the impurities are Pb and Sn. The Hall constant and the ratio E_y/E_x change sign with the field for bismuth with Pb and Sn impurities; The ratio E_y/E_x in strong fields varies linearly with the field; the slope (angle and sign) of the plot characterizing the variation depends on the nature and amount of impurities present. This factor may be utilized for analytic purposes.

A maximum appears in the curve characterizing the temperature dependence of the resistance of Bi specimens containing 0.01-0.02% Pb or Sn under compression; the maximum disappears when the pressure is removed.

In the case of sufficiently pure Bi specimens there is observed fluctuation or oscillation of the variation of r and E_y/E_x with H; these persist under compression.

We suggest that it may be possible to observe fluctuations of r, E_y and the susceptibility with increasing compression in a constant magnetic field.

"S.I.Vavilov" Institute of Physical Problems

References

1. N.E.Alekseevskii, N.B.Brandt & T.I.Kostina, Izv.AN SSSR, Ser.fiz., 16, 233 (1952).
2. N.E.Alekseevskii & N.B.Brandt, Zhur.eksp.i teor.fiz., 28, 379 (1955).
3. N.E.Alekseevskii & N.B.Brandt, Zhur.eksp.i teor.fiz., 28, 379 (1955).
4. N.E.Alekseevskii, N.B.Brandt & T.I.Kostina, Doklady AN SSSR, 105, 46 (1955).
5. E.S.Borovik, Izv.AN SSSR, Ser.fiz., 19, 429 (1955). (Trans. in Bulletin, Vol.19, No.4, p.383.)
6. P.L.Kapitza, Proc.Roy.Soc., A 119, 358 (1928).
7. B.G.Lazarev & A.S.Kan, Zhur.eksp.i teor.fiz., 14, 470 (1944).
8. N.Thompson & H.Wills, Proc.Roy.Soc., A 155, 111 (1936).
9. D.Blokhintsev & D.Nordheim, Zs.f.Phys., 84, 168 (1933).
10. E.H.Sondheimer & A.H.Wilson, Proc.Roy.Soc., A 190, 435 (1947).
11. M.Kohler, Ann.d.Phys., 6, 186 (1949).
12. I.M.Lifshits, M.Ia.Azbel' & M.I.Kaganov, Zhur.eksp.i teor.fiz., 31, 1 (1957).

ON DETERMINATION OF THE INDIVIDUAL COMPONENTS OF THE MAGNETIC SUSCEPTIBILITY OF A SEMICONDUCTOR

- Ia.G.Dorfman

1. The magnetic susceptibility of an extrinsic semiconductor can be represented in the form of a sum:

$$\chi = \chi_a + \chi_e + \chi_i,$$

where χ_a is the susceptibility of the host material, χ_e is the susceptibility of the current carriers (i.e., electrons or holes) and χ_i is the susceptibility of the impurity atoms (or ions).

It is known that the introduction of a similar concept for the susceptibility of metals, namely,

$$\chi = \chi_j + \chi_e,$$

where χ_j is the susceptibility of the metal ions led in its time to the detection of paramagnetism of conduction electrons.[1] Since then there have appeared numerous contributions on the theory of paramagnetism and diamagnetism of conduction electrons in metals and semiconductors. Although these theories correctly picture the actual properties of materials in general, detailed verification of the theoretical concepts and, consequently, their refinement have been hindered by the fact that measurements of the individual components of the total susceptibility have not yet been realized. This also explains why little attention has been paid until very recently to the magnetic properties of semiconductors.

Attempts to determine χ_e for metals by calculating χ_j and experimental measurement of the total susceptibility χ could be of some value only at the early stages of investigation of the problem inasmuch as the accuracy of calculating χ_j does not exceed 10% at best.

The only method of determining the spin magnetic susceptibility of current carriers at present is the method based on measuring the absolute value of the paramagnetic resonance absorption as a function of the external magnetic field; the method was first applied by Hutchison & Pastor[2] to ammonia solutions of Na and by Schumacher & Slichter[3] to metallic Li and Na. This method yielded very interesting results, but it is onerous and complex.

Busch & Mooser[4] first attempted to determine the carrier susceptibility χ_e for semiconductors, using specimens of α tin. They measured the total susceptibility as a function of the temperature and extrapolated the value to absolute zero. They took this limiting value of χ to be that of χ_a. Assuming further that χ_a is temperature independent and that $\chi_i \approx 0$, Busch & Mooser ascribed the entire observed change of χ with increasing temperature to the appearance of current carriers, i.e., equated it to χ_e.

Stevens, Cleland, Crawford & Schweindler[5] used a somewhat different approach. They measured the total susceptibility of high purity germanium. Although the susceptibility of Ge changes with temperature, they assumed that the measured value at all temperatures gave χ_a. Then they measured the susceptibility of germanium doped with appreciable amounts of impurities at different temperatures. They subtracted the corresponding presumable value of χ_a from the measured total susceptibility of the doped specimens at each temperature.

Next, they evaluated theoretically the value of χ_i and finally obtained a certain residual susceptibility, which they ascribed to the current carriers, i.e., took as χ_e. In order to check the validity of their assumptions, Stevens et al calculated the carrier susceptibility χ_e theoretically. In

their calculations they took into account the specific shapes of the energy bands in Ge crystals and the effective mass values obtained from diamagnetic resonance and even introduced corrections for spin-orbit interaction.

These authors, however, did not give due attention to a significant fact, namely, that the measured diamagnetic susceptibility of high purity Ge, which they assumed to be equal to χ_a, exhibited a very strange temperature variation: it decreased rather rapidly with temperature. The authors were not able to determine the reason for this curious temperature variation of the susceptibility. They investigated a high purity silicon specimen and observed the same inexplicable effect. Having taken the measured susceptibility for high purity Ge as χ_a, Stevens et al tacitly assume that in the presence of appreciable amounts of impurities this susceptibility component varies with the temperature in exactly the same way as in pure germanium. They infer that the susceptibility χ_a should also presumably vary with the temperature in α-Sn and therefrom conclude that the assumption of Busch & Mooser regarding the invariance of χ_a is incorrect. Thus the assumptions of Stevens et al are irreconcilable with the results of Busch & Mooser.

In view of the above I feel that the values of χ_e reported by Busch & Mooser as well as those found by Stevens et al are open to question. Doubtful, too, are the data on the susceptibility of the impurity atoms and ions which in the work of both Busch & Mooser and of the American physicists is virtually equated to zero. Consequently, in my opinion, the values of χ_e found by these investigators cannot be regarded as sufficiently reliable to use them for refining the theory and introducing various small corrections of the type attempted by Stevens et al. In view of the rough character of the assumptions made, such corrections are not justified. Hence I thought it might be useful to examine the different other possibilities of experimental determination of the individual components of the magnetic susceptibility of a semiconductor with one type of current carrier.

In the present report I shall limit my consideration to matters of principle not going into the details of experimental techniques.

2. Let us first consider some possible approaches to measurement of the carrier susceptibility

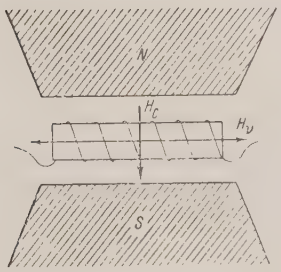

Fig.1.

Let us assume that we have a semiconductor rod in a strong constant magnetic field H_c (Fig.1). If at the same time there acts on the rod sufficiently strong alternating field H_ν directed perpendicularly to H_c, then, as we know, at a frequency $\nu_0 = g\frac{eH_e}{4\pi mch}$ of the alternating field, there should be observed spin paramagnetic resonance of the current carriers. The spins will precess in the plane perpendicular to the direction of H_c.

In this case the projection of the spins on the direction H_c will be zero and, consequently, the paramagnetic spin component of the carrier susceptibility can be excluded, i.e., $\chi_{e\,\mathrm{para}} = 0$.

If only half the semiconductor rod is subjected to the influence of the alternating field (Fig.2), a difference of potential should obviously appear at its ends:

$$V_1 = \frac{\chi_{e\,\mathrm{para}}}{2ne}[H_{2c}^2 - H_{1c}^2], \qquad (1)$$

where n is the number of current carriers per mole of the material.

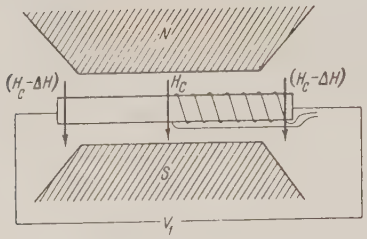

Fig.2.

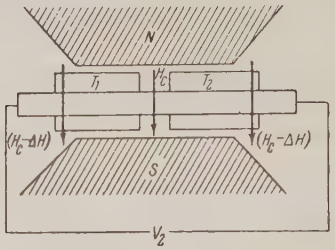

Fig.3.

Bearing in mind that $n = \frac{A}{\delta} n_0$, where n_0 is the number of current carriers per cm^3, A is the atomic weight and δ is the density of the material and that $1/n_0 e$ = R (the Hall constant), we obtain

$$V_1 = \frac{\delta}{A} R \chi_{e_{para}} H_c \Delta H, \tag{2}$$

where $H_{1c} = H_{2c} - \Delta H = H_c - \Delta H$.

So that elimination of $\chi_{e_{para}}$ will occur at the midpoint of the rod, the field gradient dH/dx must not be too great, i.e., must be taken consistent with the width of the resonance peak.

Now if the same rod is placed in only a constant magnetic field H_c and a temperature gradient is realized along it (Fig.3), then there should appear at the rod ends a difference of potential:

$$V_2 = \frac{1}{e}\left[\frac{\chi_{e_{T_1}}}{n_{T_1}} - \frac{\chi_{e_{T_2}}}{n_{T_1}}\right] H_c \Delta H, \tag{3}$$

where $\chi_{e_{T_1}}$ and $\chi_{e_{T_2}}$ are the magnetic susceptibilities of the current carriers at the temperatures T_1 and T_2, respectively. If $\chi_e = \frac{n_T c}{T}$, then obviously

$$V_2 = \frac{1}{e} C \left(\frac{1}{T_1} - \frac{1}{T_2}\right) H_c \Delta H. \tag{4}$$

It should be noted, however, that in a uniform magnetic field, i.e., in the absence of a field gradient but in the presence of a temperature gradient (Fig.4) there should be observed a longitudinal Nernst-Ettingshausen effect in the semiconductor, giving rise to a potential difference

$$V' \approx H_c^2.$$

The potential difference observed in the case illustrated in Fig.3 is the sum $V_1 = V_2 + V'$, i.e.,

$$V_1 = \frac{1}{e} C \left[\frac{1}{T_1} - \frac{1}{T_2}\right] H_c \Delta H + V'. \tag{5}$$

In order to determine the potential difference V_2 of interest to us, it is necessary to measure beforehand V' for the same specimen under the conditions characterized in Fig.4. Now, if a sufficiently strong alternating field H_ν is applied perpendicularly to H_c to the entire rod (Fig.5), then at paramagnetic resonance $\chi_{e_{para}}$ will be eliminated over the entire length of the rod and the observed potential difference will be

$$V_{II} = \frac{1}{e} C_{\text{dia}} \left[\frac{1}{T_1} - \frac{1}{T_2} \right] H_c \Delta H + V', \tag{6}$$

if the diamagnetic component of the carrier susceptibility

$$\chi_{e_{\text{dia}}} = \frac{n_T C_{\text{dia}}}{T}.$$

Thus the above described effects could serve as a source of information not only on χ_e as a whole but also regarding $\chi_{e_{\text{para}}}$ and $\chi_{e_{\text{dia}}}$

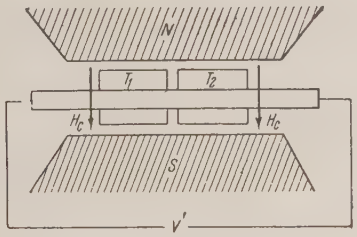

Fig. 4.

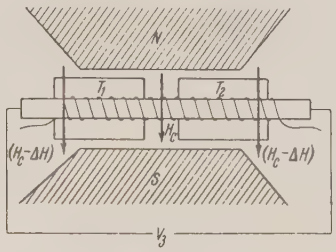

Fig. 5.

It may be noted that with reasonable values of the field H_c and of the field gradient, all these effects should presumably be of the order of 10^{-8}-10^{-9} v, but it should not be forgotten that they can be appreciably increased, first, by connecting a number of semiconductor rods in series and, second, by modulation of either H_c or H_ν and subsequent amplification of the signal.

3. Recently, Joussot-Dubien, Lemanceau & Pacault[6] succeeded in realizing a set-up by means of which they made direct measurement of the magnetic susceptibility of weakly magnetic materials of the order of 10^{-6} emu with an accuracy of 1% at a high frequency ($\sim 5 \cdot 10^6$ cps). This procedure opens new possibilities for measurement of the paramagnetic susceptibility of current carriers in semiconductors. The method developed by the French investigators actually allows of measuring the high frequency susceptibility χ'. In the diamagnetic dielectrics investigated by Joussot-Dubien et al, as might have been expected, χ' did not differ from the static susceptibility χ. This "equality" need not necessarily always obtain, particularly in working at higher frequencies.

If the coil with the investigated semiconductor specimen is placed in a constant field $H_c \perp H_\nu$, then at an appropriate value of H_c we would be able to observe paramagnetic resonance of current carriers in the specimen. With $H_c \gg H_\nu$, it may be assumed that the theory of paramagnetic resonance of Frenkel[7] will be applicable to the current carriers in the semiconductor; according to this theory, the high frequency paramagnetic susceptibility in the direction perpendicular to H_c is

$$\chi'_{e_{\text{para}}} \approx \chi_{e_{\text{para}}} \frac{\nu_0^2 (\nu_0^2 - \nu^2)}{(\nu_0^2 - \nu^2) + 4\nu\nu'}, \tag{7}$$

where ν_0 is the resonance frequency and $\nu' = 1/\tau$ (the reciprocal of the relaxation time τ). According to this expression, $\chi_{e_{\text{para}}}$ goes through zero at $\nu = \nu_0$. Consequently, in measuring the susceptibility of the specimen while varying H_c (or ν), we should note the instant when the carrier paramagnetism is virtually eliminated. Comparing the susceptibility measured at this instant with the susceptibility measured with $H_c = 0$, we can readily obtain $\chi_{e_{\text{para}}}$

In principle it may also be assumed that with the fields parallel we should (at an appropriate value of H_c) observe diamagnetic resonance of the current carriers.

Presumably Frenkel's theory should also be approximately applicable to this case inasmuch as for this theory it makes no difference whether the magnetization is due to spin orientation or to changes of the orbital motion of the current carriers, provided the attenuation is due to collisions with the lattice, which obtains in both cases.

Under these conditions one may expect $\chi'_{e_{dia}}$ to pass through zero at the instant of appearance of diamagnetic resonance. Consequently, this method should also allow of measuring $\chi_{e_{dia}}$ of the current carriers in semiconductors. It must be emphasized, however, that for this purpose it is essential to carry out the measurements of the high frequency susceptibility of weakly magnetic materials in the microwave region and at very low temperatures.

4. From the viewpoint of semiconductor theory, the measurement of the magnetic susceptibility χ_i of impurity atoms would present great interest.

Apparently this is feasible only in the case when the impurity atoms or ions have a magnetic moment, i.e., when the susceptibility of these atoms is paramagnetic.

As measurements of the spin resonance of impurity atoms carried out by Fletcher et al[8] showed, there are usually observed several resonance peaks due to interaction of the electron shell of the atom with its nuclear spin. Inasmuch as the above considerations regarding the dependence of χ' on H_c (or ν) apply to each of these peaks, obviously the above described method of determining the carrier magnetic susceptibility by measurement of the high frequency susceptibility χ' can be applied to impurity atoms as well. The presence of several peaks in the spin resonance of impurity atoms would make it possible, on the one hand, to separate the effect of these atoms from the current carrier effect and, on the other hand, to correlate it with the type of impurity atom.

5. Thus it will be seen that at present there are several approaches - feasible in principle - for direct measurement of the individual components of the magnetic susceptibility of semiconductors. Further analysis and experimentation will show which of them is the most promising and effective.

Leningrad Hydrometerological Institute

References

1. J.G.Dorfman, Zs.f.Phys., 17, 98 (1923).
2. C.Hutchison & R.Pastor, Rev.Mod.Phys., 25, 285 (1953).
3. R.Schumacher & C.Slichter, Phys.Rev., 101, 58 (1956).
4. G.Busch & E.Mooser, Helv.Phys.Acta, 26, 611 (1953).
5. D.Stevens, J.Cleland, J.Crawford & H.Schweindler, Phys.Rev., 100, 1084 (1955).
6. J.Joussot-Dubien, B.Lemanceau & A.Pacault, J.Chim.Phys., 53, 198 (1956).
7. Ia.I.Frenkel, Zhur.eksp.i teor.fiz., 15, 409 (1945).
8. R.Fletcher, W.Yager, G.Pearson, A.Holden, W.Read & F.Merritt, Phys. Rev., 94, 1392 (1954).

ON THE TRANSVERSE PHOTOMAGNETIC EFFECT IN n- AND p-TYPE GERMANIUM (Abstract)

- I.K.Kikoin & Iu.A.Bykovskii

The present investigation was concerned with the so-called transverse photomagnetic effect in germanium single crystals. This effect, which appears in semiconductors when they are illuminated in a magnetic field, is proportional to the square of the field and depends on the angle between the normal to the plane of the specimen and the direction of the magnetic field.

We determined the dependences of the transverse photomagnetic emf on the magnetic field and on the temperature.

The results show that for p-type germanium the photomagnetic emf changes sign at high field values. The field value at which the change of sign occurs depends on the intensity of the illumination and on the temperature.

At lower temperatures the change in sign is evinced in weaker fields.

* * * * * *

TOWARDS A THEORY OF FERROMAGNETISM IN A NONIDEAL LATTICE (Abstract*)

- V.L.Bonch-Bruevich

We consider the case of a ferromagnet whose lattice contains microdefects from the standpoint of the exchange model. Such microdefects of the structure may be vacancies, ions statically displaced from their equilibrium position, impurity atoms, etc. Under certain conditions the presence of such structure defects leads to the formation of local spin levels; the microdefects play the role of "demagnetization centers" reducing the spontaneous magnetization. In the report we give the results to which application of these concepts leads in the theory of ferrites, solid solutions of nonferromagnetic materials in ferromagnetic ones and small ferromagnets.

Moscow State University

---

*Complete article in FMM (Physics of Metals and Metallurgy), 2, 215 (1956).

PARAMAGNETIC BEHAVIOR OF SOME SALTS OF THE IRON GROUP OF ELEMENTS

- A.Bose

1. Introduction

The paramagnetic behavior of the salts of the different ions of the iron group has been explained in a general way by the crystalline electric field theory of Van Vleck[1] and others, which attributes the magnetic anisotropy and other thermal magnetic effects in these crystals mainly to the partial quenching of the orbital magnetic moments of the paramagnetic ions by the influence of the asymmetric electric fields of the neighboring charged particles in the crystal. As a wealth of experimental data on magnetic susceptibility and anisotropy of the crystals, mainly from the work of Krishnan and his collaborators[2-5], accumulated, many of the finer details of the theory were verified and considerable light was thrown upon the nature of these crystalline electric fields. Occasionally the new data necessitated modifications of the older ideas. In recent years advent of a powerful new tool, namely, the microwave absorption technique, has considerably extended the scope of investigations in this line and supplemented and overlapped the classical methods of measuring the susceptibilities. It is also well known that information from other sources, such as optical absorption, x-ray fine structure of the crystal, etc., is of immense help in deciphering the magnetic data.

Of the later refinements of the original field theory of the paramagnetic salts the main two are based on the considerations of 1) the influence of the field due to charges lying outside the primary Jahn-Teller cluster of charges immediately surrounding the paramagnetic ion, (Van Vleck[6]) and 2) the deviation of the crystalline fields from being purely of an electrostatic origin, depending upon the nature of binding between the paramagnetic ion and its neighbors (Van Vleck[7], Howard[8], Owen[9]).

The present paper contains a report of some of the work done in our laboratory during the last five years, basically connected with the idea of putting the above theoretical refinements to test. With this intention in view we had to refine considerably the techniques of magnetic susceptibility and anisotropy measurements of the single crystals of the paramagnetic salts, earlier developed in this laboratory by Krishnan and coworkers (Krishnan et al[2-5], Bose[10,11]) the details of which have been published from time to time (Datta[12-13], Dutta Roy[14-15]) and we do not propose to discuss them further. Suffice it to say that both susceptibility and anisotropy measurements have been brought to a reliability and accuracy ten times the previous ones.

2. Method of Measurement and Treatment of the Results

Our measurements cover a large number of single crystals of highly hydrated salts, either isomorphous or similarly constituted, of Cu^{++} and Ni^{++} for which the theoretical treatment is more or less complete and the experimental data are fairly straight forward. For these salts the anisotropies of single crystals between 90° and a temperature sufficiently above 300°K (i.e., to the point of transition to the polycrystalline state) have been measured by a modification of the well known method of Krishnan et al accurately to 0.1%, in which the "maximum couple" exerted by a homogeneous magnetic field on the crystal suspended with a fine quartz fibre is noted. The most troublesome source of uncertainty seems to us to be in the preparation of the samples. The results may differ by as much as 2 to 5% from crystal to crystal unless proper precautions are taken. By keeping a systematic painstaking

check on the chemical purity, stoichiometric composition, occlusions, distortions, twinning, etc., of the crystal, we succeeded in keeping this error below 0.1%.

Excepting the simple salts $NiSO_4\ 6H_2O$ and $NiSeO_4\ 6H_2O$, which are tetragonal and in which the principal magnetic axes are all uniquely determinned by the symmetry, the other salts studied by us are either triclinic, e.g., $CuSO_4.5H_2O$ and $CuSeO_4.5H_2O$, or monoclinic, e.g., the Tutton salts of Cu^{++} and Ni^{++}. In these latter, the angles of orientation of the principal magnetic axes of the crystal, where not fixed uniquely in the crystal, are, in general, found to change with temperature, sometimes considerably. In considering the principal anisotropy characteristics these changes have to be taken into account. Further, it is well known that all these crystals have more than one equivalent paramagnetic ionic cluster in their unit cell, inclined to each other, in a manner consistent with the symmetry elements of the unit cell. Hence the principal magnetic anisotropies or principal susceptibilities of the crystal are, in general, smaller than those of the paramagnetic ion itself. If the inclinations of the crystalline and ionic magnetic axes are known from the x-ray data or from the newer paramagnetic resonance data, it is possible to find the ionic anisotropies or susceptibilities from measurements on the crystal, using the relation:

$$\chi_i = \sum K_j \alpha_{ji}, \tag{1}$$

where i and j = 1, 2 or 3; the K's are the principal susceptibilities of the ion along the axes whose direction cosines are the α's and χ is the susceptibility of the lattice per gram·molecule. Unfortunately, however, such angular data are very scarce and therefore, not very suitable for our present discussion which extends over a large number of similar salts with slight differences in the structure. However, with some degree of approximation, which cannot be helped under the circumstances, regarding the structure of the ionic cluster, indicated by the approximate and restricted x-ray and resonance data, we can find the ionic anisotropy as well as the angle of inclination of the ions solely from the magnetic data on the crystal.

For example, if we assume that the paramagnetic ions have uniaxial symmetry, so that $K_1 = K_\parallel$ along the symmetry axis and $K_2 = K_3 = K_\perp$ perpendicular to that axis, $K_\parallel > K_\perp$, and the angle between the $K_\perp$ axes of the two equivalent ions in the unit cell is 2φ, then we have

$$\left.\begin{aligned} K_\parallel - K_\perp &= 2(\chi_1 - \chi_2) - (\chi_1 - \chi_3) \\ \text{and} \qquad \cos\varphi &= \frac{\chi_1 - \chi_3}{K_\parallel - K_\perp}. \end{aligned}\right\} \tag{2}$$

This is the case that occurs in all the Cu^{++} salts measured by us, as indicated by the x-ray and resonance data in a few cases and the similarity of the magnetic anisotropy behavior observed by us in all of them.

For the Ni^{++} salts on the other hand, resonance data cannot give a unique indication as to which two of the three values K_1, K_2 and K_3 are nearly equal, nor whether $K_\parallel > \text{or} < K_\perp$, because the method is not sensitive enough to find the anisotropy of the splitting factor g if it is smaller than about 3%, as happens in these Ni^{++} salts. However, combining our anisotropy measurements with the accurate x-ray data for one of the salts, namely, $NiSO_4 \cdot 6H_2O$, and the resonance data for the angles of orientation of ionic and crystalline magnetic axes in a few of the Tutton salts, we feel justified in saying that in all these cases either $K_1 \approx K_3$ or $K_1 \approx K_2 = K_\perp$ with K_2 or K_3, as the case

may be, $\approx K_{\parallel}$ and further, $K_{\perp} > K_{\parallel}$, since the magnetic behavior is very similar in all these salts. In this case, we have

$$\left.\begin{aligned} K_{\perp} - K_{\parallel} &= (\chi_1 - \chi_2) + (\chi_1 - \chi_3) \\ \text{and} \qquad \cos 2\varphi &= \frac{(\chi_1 - \chi_2) - (\chi_1 - \chi_3)}{K_{\perp} - K_{\parallel}} . \end{aligned}\right\} \qquad (3)$$

On these assumptions we have calculated the ionic anisotropies of the Cu^{++} and Ni^{++} ions in the different salts at different temperatures from the anisotropy measurements for single crystals. Though the resonance data indicate appreciable departures in some cases from the above tetragonal approximation, it is not possible to discuss the orthorhombic case until better data on the angular parameters are available. However, for our present purpose of comparison this approximation does not matter very much. The results are shown in the form of graphs of $\Delta K \cdot T$ vs T, where $\Delta K = |K_{\parallel} - K_{\perp}|$, in Figs.1 and 3.

3. Temperature Dependence of the Orientation of the Principal Magnetic Axes

We have mentioned that in triclinic and monoclinic crystals, the angle of orientation in the magnetic field of the magnetic axes (not uniquely fixed in the crystal by symmetry) changes appreciably with temperature. The variation is usually more pronounced above room temperature. For example, in the triclinic crystal $CuSO_4.5H_2O$ suspended in the magnetic field with the c axis vertical, the setting angle, say θ_1, which the $(\bar{1}00)$ plane makes with the field direction changes from 26.2° to only 26.4° between $90^{\circ}K$ and $200^{\circ}K$, but goes to 27.2° at $300^{\circ}K$ and to 29.3° at $336^{\circ}K$; above this temperature the crystal undergoes a transition: the orientation becomes indeterminate and the anisotropy zero, owing to the single crystal becoming polycrystalline. The change in the angle θ_2 ($\theta_2 = 8.7^{\circ}$ at $90^{\circ}K$) between $(\bar{1}11)$ plane and the field, when the crystal is suspended with the $(\bar{1}\bar{1}0)$ and $(\bar{1}11)$ planes vertical, is much smaller, being only about $+0.9^{\circ}$, as against the $+3.1^{\circ}$ change in θ_1, over the whole temperature range. For selenate pentahydrate similar changes in the angles are observed, namely, $\Delta\theta_1 = -2.4^{\circ}$ ($\theta_1 = 27.7^{\circ}$ at $90^{\circ}K$) and $\Delta\theta_2 = +1^{\circ}$ ($\theta_2 = 8.0^{\circ}$ at $90^{\circ}K$).

It is known from stereographic analysis of these salts (Krishnan & Mookherji[4] and Mookherji & Tin[16]) that each of the crystals has an axis of approximate tetragonal magnetic symmetry, which is nearly in the horizontal plane and sets normal to the field for the second mode of suspension. The small change in θ_2, therefore, shows that this axis does not appreciably change its direction in the crystal with temperature. But since for the first mode of suspension the approximate magnetic symmetry plane is at about 45° to the horizontal and the setting angle θ, for this case is found to change by a larger amount, the directions of the two nearly equal magnetic axes in the approximate symmetry plane must be altered appreciably, the projection of the axis directions on the horizontal plane being reflected in the change of θ_1; the smaller change in θ_2 is due to the fact that the tetragonal axis is not exactly in the horizontal plane in that case. The above also indicates that the angle φ between the χ_1 and $K_{\parallel}$ axis ($\approx 45^{\circ}$ at room temperature) may change somewhat at low temperatures.

For the two tetragonal crystals $NiSO_4.6H_2O$ and $NiSeO_4.6H_2O$, one of the magnetic axes is fixed along the c axis and the two others in the (001) plane are equal and less than the first. The $K_{\parallel}$ axis at room temperature is at about 45.7° to the $\chi_{\parallel}$ axis.

For the Tutton salts which are all monoclinic, the χ_1 and χ_2 axes (χ_1 being taken as greater than χ_2), in the (010) plane are arbitrarily placed at angles Ψ and θ to the c and a axes of the crystal. The χ_3 axis being fixed uniquely along b, cannot change direction with temperature. The χ_1 and also χ_2 directions are found to change with temperature; very little below about 140°K, but more or less rapidly as the temperature rises, up to the respective transition temperatures at which the same effect, as described above, occurs. With some exceptions, the change in the angle θ for most of the crystals is not more than a few degrees: for example, $\Delta\theta = +0.4^\circ$ between 90° and 120°K and -20.4° between 120° and 336°K for $Cu(NH_4)_2(SO_4)_2 \cdot 6H_2O$, 8.3° for $CuK_2(SO_4)_2$, $6H_2O$, 7.9° for $Ni(NH_4)_2(SO_4)_2\ 6H_2O$, 6.3° for $Ni(NH_4)_2(SeO_4)_2\ 6H_2O$ and 5° for $NiCs_2(SeO_4)_2 \cdot 6H_2O$, all these last being the change between 90°K and the respective transition temperature.

The corresponding changes in φ, i.e., the semiangle between the $K_{\parallel}$ axes in the unit cell are never very large; they range between 0.2 and 3.0° even for the salts in which $\Delta\theta$ is abnormally large.

It is obvious then that the observed changes in the orientations of the χ_2 axis, i.e., of the angle θ, are mainly due to a simultaneous rotation of the $K_{\parallel}$ axes of the two paramagnetic ions in the unit cell about the b axis of the crystal, whereas, the small relative rotations of the $K_{\parallel}$ axis in the plane $\chi_1\chi_3$ for the Cu^{++} salts, and in the plane $\chi_2\chi_3$ for the Ni^{++} salts, as indicated by the small changes in φ, are symmetric with reference to χ_1 and χ_2 and hence should not affect the positions of these to any appreciable extent.

In view of the approximate tetragonal symmetry of the electric field about the paramagnetic ion (with at most a small superposed orthorhombic component), the small diamagnetic anisotropy of the crystals, and the large separation between the ground orbital level and the next orbital level in the Stark pattern of both Cu^{++} and Ni^{++} salts (of the order of 10^3 and 10^4 cm^{-1}), the observed changes in the magnetic axes with temperature must be entirely due to the anisotropic thermal expansion of the crystals, which causes a rotation of the paramagnetic ionic groups in the crystal in a manner described above. The increasing rate of change in θ at high temperatures approaching the transition also points to the same conclusion. For, as the transition temperature is approached, the crystal becomes more and more unstable and the paramagnetic clusters change their relative orientations more or less quickly until at the transition point the arrangement becomes so distorted as to become altogether unstable, and reorientations and regroupings of the atoms to form more stable structures under the given conditions take place.

4. Temperature Dependence of the Anisotropy of the Cu^{++} ion

According to the crystalline electric field theory of Bethe[17], Van Vleck[1], Gorter[18], Polder[19], Abragam and Pryce[20], Bleaney et al[21], and others, the $^2D_{5/2}$-state of an octahedrally coordinated Cu^{++} ion, as found in the salts studied here, is split up by the predominant cubic part of the field into an orbital doublet, lying energetically below an orbital triplet by about 10^4 cm^{-1}. The tetragonal component of the field (according to our present approximation) splits each of these levels into two orbital sublevels. Each individual orbital level retains a two-fold Kramers spin degeneracy which the crystal field cannot remove. Then the anisotropy of the Cu^{++} ion in such crystals is given by

$$K_{\parallel} - K_{\perp} = \frac{N\beta^2}{4kT}(g_{\parallel}^2 - g_{\perp}^2) + 2N\beta^2\left(\frac{4}{E_{\parallel}} - \frac{1}{E_{\perp}}\right), \tag{4}$$

where the principal splitting factors

$$g_{\parallel} = 2 + 8w + 4uw + 3u^2$$

$$g_{\perp} = 2 + 2u - 4w^2,$$

here

$$u = -\frac{\lambda}{E_{\perp}}, \quad w = -\frac{\lambda}{E_{\parallel}},$$

λ = the spin-orbit coupling constant for Cu^{++} in these crystals and $E_{\parallel}$ and $E_{\perp}$ are the separations of the lower and upper split components of the triplet, respectively, from the lower component of the doublet.

Expression (4) may be reduced to the linear form:

$$(K_{\parallel} - K_{\perp}) \cdot T = AT + B, \qquad (5)$$

where

$$A = 2N\beta^2 (4/E_{\parallel} - 1/E_{\perp}),$$

$$B = \frac{N\beta^2}{4k}(g_{\parallel}^2 - g_{\perp}^2).$$

From the nature of our experimental graphs for $\Delta K.T$ vs T, it will be seen that in many of the salts a fairly good linearity of the curves obtains down to about 150°K, after which quite appreciable downward curvature occurs.

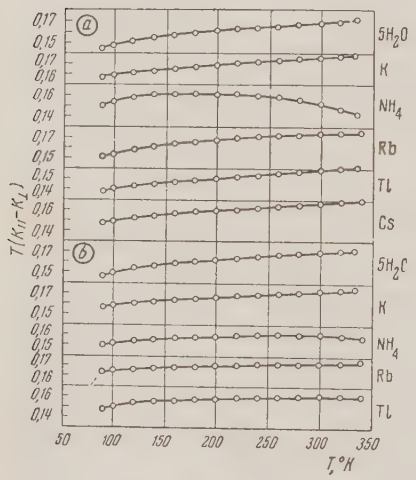

Fig.1. Curves showing the variation of $\Delta K \cdot T$ with T for different Cu^{++} salts between 90 and 300°K: a) sulfates, b) selenates. The ordinates of the curves for different salts have been shifted as necessary to avoid overlapping.

In the three specific cases of ammonium sulphate and selenate and thallium selenate, particularly the first, marked downward curvature is also observed in the high temperature region. On closer examination, the curves for the two pentahydrates and the two rubidium salts are also found to depart slightly from the linearity even above 150°K. In the two latter salts the linear portions at high temperatures are very nearly parallel to the T axis, so that the high frequency term in the anisotropy formula, namely, $A = 2N\beta^2 (4/E_{\parallel} - 1/E_{\perp})$, which should be given by the slope at high temperatures, is apparently abnormally small. It is remarkable that in the above named three salts this term is apparently negative and is actually abnormally high in the ammonium sulphate salt.

In most cases the departure from linearity in the low temperature region below 150°K seems to require as a first approximation a term like C/T in expression (5).

The values of $K_{\parallel} - K_{\perp}$ calculated from the observed crystal anisotropy at different temperatures of $CuSO_4,5H_2O$ by Krishnan and Mookherji[4] are given by the empirical formula:

$$K_{\parallel} - K_{\perp} = 0{,}572/(T + 4{,}5) - 0{,}379/(T - 2{,}0) = 0{,}173/T - 3{,}373/T^2.$$

This shows the departure from linearity at low temperatures, but apparently the temperature independent term is absent. Taking their actual measurement

values, it may be shown that the suppression of this latter term is due to their use of the mean susceptibility values derived from measurements on powder by de Haas and Gorter[22] in the form $\bar{\chi} = 0.457/(T + 0.7)$, while Bose & Mitra[23] established that the original Leiden data actually agree well with the formula: $\bar{\chi} = 67 \cdot 10^{-6} + 0.446/T - 0.098/T^2$ in the range from 280° to 14°K.

Hupse's[24] values of $K_{\parallel} - K_{\perp}$ for $CuK_2(SO_4)_2,6H_2O$ recalculated from her own experimental data may be represented by $K_{\parallel} - K_{\perp} = -44.1 + 0.158/T$, but the experimental scatter of the data (taken at room temperature and at hydrogen and helium temperatures) renders accurate calculation of the small slope and the departure from linearity, if any, quite uncertain.

In the several cases where our results show fairly good linearity of the curves above 150°K, the intercept of the linear portions with the $\Delta K.T$ axis, i.e., B in Eq.(5), gives the anisotropy of the Curie constants; the $g_{\parallel}^2 - g_{\perp}^2$ values may be calculated therefrom and compared with the direct evaluations of these from paramagnetic resonance data, where available. The agreement is fair, e.g., for the potassium, thallium and caesium double sulphates the values for the intercepts are 0.162, 0.137 and 0.155 from our anisotropy data as against 0.160, 0.138 and 0.158 from resonance data, respectively (Bleaney et al[25]).

In the Cu^{++} ion the basic orbital doublet is a "nonmagnetic" one (Bethe[17]), the components of which are separated a distance of the order of $10^3 cm^{-1}$ by the crystal electric field and the spin degeneracy of each level is only of a two-fold Kramers type, so that normally a departure from linearity is not expected theoretically, contrary to our present observations, an extreme example of which is the ammonium sulphate salt. Of course, the spin degeneracy might be removed to a minor extent by the magnetic dipole-dipole interaction and exchange coupling and thus cause a departure from linearity, but the effects of such interactions would be negligible in our temperature range, compared to the observed deviations, particularly for the Tutton salts which are magnetically highly diluted. That these interactions are indeed small has been shown by the fact that no anomaly in the specific heat curves in these salts is observed above 1°K.

The theory, however, neglects an important fact that the crystal electric fields may change with temperature in which case the orbital separations and hence the coefficients $(g^2_{\parallel} - g^2_{\perp})$ and $(4/E_{\parallel} - 1/E_{\perp})$ may vary with temperature and thus cause the observed departure from the theoretical linearity. These changes in the fields arise evidently from the usual anisotropic thermal expansion of the lattice. But as we know that the primary Jahn-Teller cluster of charges is very strongly bound to the Cu^{++} ion, it is the atoms, outside this cluster which are most affected by the thermal expansion directly. However, such changes in the relative positions of the outer atoms with temperature may induce sufficient corresponding thermal changes in the anisotropy of the Jahn-Teller cluster, which follows from the theory of Van Vleck[6] about the effect of the long range atoms upon the field of the short range cluster already mentioned. That there are such thermal changes in the electric field receives support from our earlier observations on the rotation of the principal magnetic axes in most crystals.

It is interesting to note in this connection that Benzie & Cooke[26] find no such deviation from the theory in the range 20° to 1°K in the results of their direct measurements are perhaps not so sensitive as the anisotropy measurements, since, by using the latter method Bose & Shoenberg[27] were able to detect a small departure from linearity in the helium range (4° to 1°K) in $CuK_2(SO_4)_2,6H_2O$, a departure about about 30 times smaller than that observed in the liquid air range. The reason for this is that the thermal

expansion being very small in the liquid helium range, the deviation from linearity due to the above cause is very small and the effect observed at helium temperatures perhaps mainly arises from the small spin splitting effects previously mentioned, which increase in importance at these low temperatures.

In view of the fact that the relationship between laws of thermal expansion in these crystals and the crystal fields may be quite complicated - little is known regarding this relationship at present - the apparent linearity in the upper parts of the curves observed for some of the salts may be quite misleading and the slopes and intercepts of these parts may not have the interpretation given by the simple theoretical formula (4), as is well exemplified by the two rubidium salts, in which the slopes are too small to make the high frequency terms of the theory compatible with the intercepts of the curve giving the values of $g_{\parallel}^2 - g_{\perp}^2$. The negative slopes of the high temperature portion of the curves for ammonium sulphate and selenate and thallium selenate also bring out this discrepancy in a more glaring manner. It would be interesting to see how the anisotropic electric fields vary with temperature and from salt to salt containing the same Cu^{++} ion. We shall discuss this variation in the following section.

5. Variation of the Crystal Field Constant with Temperature and from Salt to Salt.

With a slight obvious approximation the formula (4) may be written in the form

$$(K_{\parallel} - K_{\perp}) \cdot T = 2N\beta^2 (-\lambda/k + T) \cdot D, \tag{6}$$

where

$$D = 4/E_{\parallel} - 1/E_{\perp}.$$

It is interesting to note that if D is assumed independent of the temperature, we might calculate λ, the value of the spin orbit coupling, by eliminating D from Eq.(6) by using the anisotropy data at two temperatures. However, since the above assumption is not valid and the accuracy of the calculation depends only on the relative magnitude of the high frequency term, the value of λ may be quite misleading, as follows from our discussion in the preceding section. On the other hand, we have reasons to believe from our experiments on the Ni^{++} salts, dating back to 1939 and from recent more accurate calculations to be described later, that λ in crystals should not differ much from the free ion value. This goes against the findings of some paramagnetic resonance workers (Abragam & Pryce[20] and Griffiths & Owen[28]) who apparently detected a decrease of about 30% in the value of λ in crystals. An explanation of the apparent discrepancy has been suggested by Owen[9] in terms of a partial covalent binding between the central paramagnetic ion and the immediately surrounding atoms. The covalency factor apparently reduces the value of λ in the method of calculation of the resonance workers but this factor is eliminated in our method of calculation and so does not affect the results.

Thus, assuming with a fair degree of certainty that the free ion value of $\lambda = -829$ cm^{-1} (Shenstone & Wilets[29] – Laporte[30] gives -854 cm^{-1}) for the Cu^{++} ion to be valid in the present crystals and that $k = 0.698$ cm^{-1}, we have calculated the values of D in cm at different temperatures and for the different salts for comparison. It is to be noted that any value of D is its effective value at that temperature inclusive of the covalency factor,

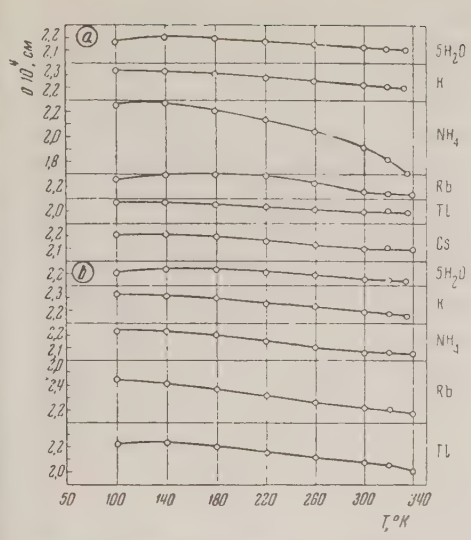

Fig.2. Variation of D with temperature for different Cu^{++} salts: a) sulfates, b) selenates.

which is a measure of the degree of overlap of the charge cloud of the Cu^{++} ion and the surrounding oxygen atoms. The values are represented in the form of plots of D vs T in Fig.2.

By comparing the calculated value of D at any given temperature with that obtained experimentally from observation of optical absorption levels, we may estimate the covalency factor. But the available absorption data do not at present show the existence of the anisotropic levels $E_{\parallel}$ and $E_{\perp}$.

The covalency factor may be assumed more or less isotropic, independent of temperature and the same for at least all the Tutton salts. The variation in D from salt to salt and with temperature is therefore due mainly to the variation in the direct and induced effects of the long range fields acting on the Cu^{++} ion, since the anisotropic field due to the primary distortion of the Jahn-Teller cluster is the same for all the salts. It will be seen that the type of variation from salt to salt does not seem to bear any simple relation to the changing radii of the alkali cation or the acid radical, although the type of variation with temperature is similar for many of the salts, their curves showing a definite negative slope above about 150°K. The curve for the ammonium sulphate salt is singular: in this case D rapidly falls with increasing temperature in the region 140° → 330°K and at the high temperatures has an abnormally low value compared to most of the other salts. The other ammonium and the two thallium salts also show somewhat abnormally low values at high temperatures, though the curvature is not so abnormal. The two potassium and rubidium salts have much higher values of D at high temperatures with the pentahydrates falling in between. Several of the curves show a flat maximum in the low temperature region.

In the absence of reliable detailed structural and thermal expansion data for the individual salts, it is not feasible at this stage to construct a theory correlating the magnetic and thermal behaviors of the crystals.

6. Temperature Variation of the Anisotropy in Ni^{++} Salts.

For the octahedrally coordinated Ni^{++} ion in the $3d^8\ ^3F_4$ ground state, the theory of Van Vleck[1], Schlapp & Penney[31] and Griffiths & Owen[28] gives the Stark pattern as consisting of a basic orbital singlet with two triplets above it, separated to the extent of some 10^4 cm^{-1} by the predominant cubic component of the crystal electric field. The components of the orbital triplet and the three-fold spin components of each orbital level are split up further by the rhombic component of the field and the spin-orbit coupling. On the assumption of approximate tetragonal symmetry, taking either K_2 or K_3 as $K_{\parallel}$, the remaining two approximately equal susceptibilities as $K_{\perp}$, and $K_{\perp} > K_{\parallel}$, according to the discussion above, we have for the anisotropy of the Ni^{++} ion,

$$K_\perp - K_\parallel = \frac{8N\beta^2}{3kT}\left[\frac{1}{4}(g_\perp^2 - g_\parallel^2) - \frac{\lambda^2}{6kT}(\alpha_\perp - \alpha_\parallel)\times\right.$$
$$\left.\times\{3g^2 - (g_\perp^2 - g_\parallel^2)\} - 3kT(\alpha_\perp - \alpha_\parallel)\right], \qquad (7)$$

in which $g_i = 2(1 + 4\lambda\alpha_i)\,(i = \parallel \text{ or } \perp)$ and $g^2 = \frac{1}{3}\left(g_\parallel^2 + 2g_\perp^2\right)$.

Here the α's are the field constants used by Penney & Schlapp[31], e.g., the mean α is numerically equal to the reciprocal of the separation between the lowest orbital singlet and the mean center of the next higher orbital triplet in the Stark pattern. The difference $(\alpha_\perp - \alpha_\parallel)$ is a measure of the relative separation of the tetragonal components of the triplet. The other symbols have their usual significance.

Expression (7) may be written in the form

$$(K_\perp - K_\parallel)\cdot T = AT + B + C/T, \qquad (8)$$

where

$$A = -8N\beta^2(\alpha_\perp - \alpha_\parallel),\ B = \frac{2N\beta^2}{3k}(g_\perp^2 - g_\parallel^2),$$
$$C = -\frac{4N\beta^2}{9k^2}\lambda^2(\alpha_\perp - \alpha_\parallel)\{3g^2 - (g_\perp^2 - g_\parallel^2)\}.$$

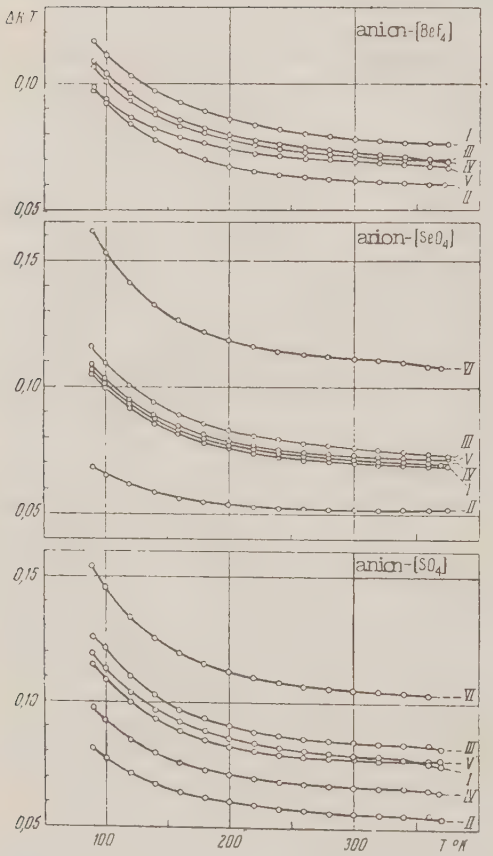

Fig.3 Curves showing the variation of $\Delta K\cdot T$ with T for different Ni^{++} salts in the temperature range from 90-370°K. The curves for each anion series are plotted to the same scale. I)K, II) NH_4, III) Pb, IV) Tl, V) CS and VI) $6H_2O$.

Obviously, the coefficients A, B and C represent, respectively, 1) the slope of the tangent to the $\Delta K\cdot T$ vs T curve at very high temperatures, 2) the intercept of this tangent with $\Delta K\cdot T$ axis and 3) the departure from linearity of the said curve with temperature, as an added term over and above AT + B. Further, A, B and C are related to each other through the field coefficients and spin-orbit coupling. It is to be remarked that a general fit of the experimental curves (Fig.3) with the theory is immediately noticeable and, unlike the Cu^{++} salts, the departure from linearity is a general feature of the Ni^{++} salts as required by the theory.

On closer examination of the experimental curves for the different salts we find 1) that the values obtained for the above coefficients are appreciably different from salt to salt, 2) that in many cases the three coefficients are not consistent with each other, as required by the relations (8) and 3) that in a few extreme cases the experimental curves seem to require other higher order terms for representation within experimental accuracy.

Since, just as for the Cu^{++} salts, spin-spin interaction, exchange interaction, exchange interaction, etc., may be neglected in our temperature ranges for these highly diluted Ni^{++} salts, the above departure from the theory

is obviously again the effect of the variations of the long range electric fields acting directly and indirectly upon the Ni^{++} ion. The nature of these departures indicates that the coefficients are really functions of the temperature and hence confirms the above conclusion. This conclusion is also supported by the already noted variations of the magnetic axes of the crystal with temperature, where they occur. It is worthy of note in this connection that since in Ni^{++} the lowest level in the Stark pattern is only three-fold degenerate in spin and the upper levels only have orbital degeneracy in a cubic field, the primary Jahn-Teller anisotropy of the $Ni^{++}.6H_2O$ cluster is very small, so that the major part of the anisotropy of the ion probably arises from the induced distortional effect of the long range fields. The temperature variation and salt to salt variation of the ionic anisotropy, therefore, should depend appreciably upon the corresponding relative changes in the long range structure, though the total anisotropy itself is fairly small. Our experiments lend full support to this view.

7. Calculation of the Spin-orbit Coupling Constant for the Ni^{++} Ion.

In contrast to the case of the Cu^{++} ion, the value of λ, characterizing the spin-orbit coupling, for the Ni^{++} ion may be calculated with a much higher degree of accuracy, which here depends mainly upon the accuracy of the $1/T^2$ term in the theory, constituting about 20 to 50% of the total anisotropy in our range of temperature. The method of calculation is to eliminate $\alpha_\perp - \alpha_\parallel$ inclusive of the "covalency factor", which is assumed constant for the purpose, from Eq.(7) rewritten as

$$K_\perp - K_\parallel = \frac{8N\beta^2}{3kT}\left\{8\lambda - 3kT - \frac{2\lambda^2}{kT} + 16\lambda^2\left[(\alpha_\perp + \alpha_\parallel) - \right.\right.$$
$$\left.\left. - \frac{2\lambda}{3kT}\left(\alpha_\parallel + \frac{\lambda}{3}(\alpha_\perp + 2\alpha_\parallel)^2\right)\right]\right\}(\alpha_\perp - \alpha_\parallel), \qquad (9)$$

using the experimental values for $K_\perp - K_\parallel$ at two temperatures. The terms within the brackets taken all together being small compared to the others (less than 10% of the total even at 100°K), it is enough for the present purpose to estimate them with a moderate degree of accuracy, taking $\alpha_\parallel$ and $\alpha_\perp$ to be $-6.4\cdot10^{-5}$cm. and $-8.8\cdot10^{-5}$cm from our latest unpublished susceptibility data on $NiSO_4.6H_2O$ at 300°K and neglecting the small variation with temperature and from salt to salt of the above field coefficients. It would be better to find by trial a value of λ which would most closely fit all the experimental values of $K_\perp - K_\parallel$ at the different temperatures, but in view of the approximations already made and for ease of demonstration, it would be enough if for the present we use for our calculations the ratios of the values of $K_\perp - K_\parallel$ at 300°K with those at 200° and 100°K. The values of λ fitting, to within 5 cm^{-1} (i.e., about 1.5%), the ratios of the anisotropies at those two temperatures are given in Table 1.

It will be seen that with the exception of the few cases marked with an asterisk in the table, the values of λ thus obtained for the different salts lie within a range of about 15 cm^{-1} (about 4.5%) on either side of the free ion value of -324 cm^{-1} (vide Owen[9]; Laporte's[30] 1928 value is -335 cm^{-1}). For the same salt the values for the two temperature ratios differ considerably in several cases and are more often greater than -324, but in the others the difference is still within about 15 cm^{-1}.

Since λ is very likely to be the same at all temperatures and in all the similar salts of the Ni^{++} ion and since the approximations involved in evaluating the terms within brackets in Eq.(9) would not affect the results to more

Table 1

Values of the spin-orbit interaction constant λ corresponding to the ratios of $\Delta K = K_{\perp} - K_{\parallel}$ at 100 & 300°K and 200 & 300°K for Ni^{++} ion salts

Crystal	$\frac{\Delta K_{100°K}}{\Delta K_{300°K}}$	λ, cm^{-1}	$\frac{\Delta K_{200°K}}{\Delta K_{300°K}}$	λ, cm^{-1}
$NiSO_4 \cdot 6H_2O$	4,17	—320	$1,60_5$	—320
$NiK_2(SO_4)_2 \cdot 6H_2O$	4,33	—350*	$1,63_8$	—350*
$Ni(NH_4)_2(SO_4)_2 \cdot 6H_2O$	4,19	—325	$1,62_5$	—335
$NiRb_2(SO_4)_2 \cdot 6H_2O$	4,33	—350*	$1,61_4$	—320
$NiTl_2(SO_4)_2 \cdot 6H_2O$	4,18	—320	$1,61_0$	—320
$NiCs_2(SO_4)_2 \cdot 6H_2O$	4,22	—330	$1,59_8$	—300*
$NiSeO_4 \cdot 6H_2O$	4,15	—315	$1,60_4$	—315
$NiK_2(SeO_4)_2 \cdot 6H_2O$	4,30	—345*	$1,62_0$	—335
$Ni(NH_4)_2(SeO_4)_2 \cdot 6H_2O$	3,82	—255*	$1,55_2$	—250*
$NiRb_2(SeO_4)_2 \cdot 6H_2O$	4,32	—350*	$1,63_5$	—350*
$NiTl_2(SeO_4)_2 \cdot 6H_2O$	4,24	—335	$1,61_7$	—330
$NiCs_2(SeO_4)_2 \cdot 6H_2O$	4,26	—335	$1,61_8$	—325
$NiK_2(BeF_4)_2 \cdot 6H_2O$	4,26	—335	$1,65_0$	—370*
$Ni(NH_4)_2(BeF_4)_2 \cdot 6H_2O$	4,47	—380*	$1,62_5$	—335
$NiRb_2(BeF_4)_2 \cdot 6H_2O$	4,25	—335	$1,63_2$	—345
$NiTl_2(BeF_4)_2 \cdot 6H_2O$	4,22	—330	$1,62_5$	—335
$NiCs_2(BeF_4)_2 \cdot 6H_2O$	4,01	—290*	$1,59_3$	—295*

than 1 or 2% at most, much of the far larger discrepancies appearing in the table must be entirely due to the assumption of the temperature independence of $(\alpha_{\perp} - \alpha_{\parallel})$. It should also be remembered that the scatter in the values would have been probably much less if we had considered all the temperatures in a series. The overall agreement of the value of within about ±5%, in most of the cases with the free ion value, with a more or less uniform scatter on either side due to small temperature effects is evidence in support of our earlier observation (1939) that the spin-orbit coupling in the crystal state is very nearly the same as in free ion, although at that time we used a more approximate formula.

8. Temperature Variation of the Anisotropic Crystal Electric Field.

It has been indicated in the previous sections that the crystal fields may vary with temperature. It has also been explained how the thermal expansion of the lattice affects indirectly the anisotropy of the strongly bound Jahn-Teller cluster and thereby causes mainly a change in the anisotropic part of the field. The field constant $(\alpha_{\perp} - \alpha_{\parallel})$ may now be calculated at different temperatures from Eq.(9) recalling that λ in crystals may be taken to be the same as that of the free ion, i.e., $\lambda = -234\ cm^{-1}$ and using the same approximations for evaluation of $\alpha_{\parallel}$ and $\alpha_{\perp}$ in the higher order terms as in the previous section. The values at different temperatures are represented graphically in Fig.4.

It will be found that the anisotropy of the electric field at 300°K varies considerably from salt to salt and is by far the largest in the two hexahydrated single salts and the smallest in all the ammonium double salts. The values for the different salts do not show any clear relationship to the radius of the alkali cationic or anionic radical as already seen for Cu^{++} salts. This is not surprising, since the anisotropies are probably complex functions of thermal expansion and values at any given temperature can hardly be compared, unless perhaps we proceed to very low temperatures,

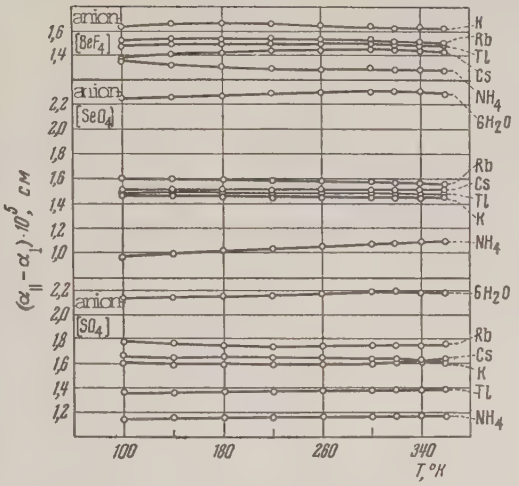

Fig.4. Variation of $\alpha_{\perp} - \alpha_{\parallel}$ with the temperature for different Ni^{++} ion salts.

where the fields might be independent of temperature, provided that in doing so no fundamental change in the structure has taken place in the crystal. The variations of the anisotropic field with temperature are mainly moderate and regular, although in a few cases more complicated variations do occur.

By comparing the effective value of $(\alpha_{\perp} - \alpha_{\parallel})$ with the optical absorption levels associated with transitions to the orbital triplet levels, the covalency factor might be determined, but the optical data are not refined enough to give any evidence for such levels.

We are now engaged in obtaining accurate values of the principal susceptibilities and accurate structural data for the salts at different temperatures in order to be able to analyze completely the variation of crystal fields from salt to salt and with temperature.

In conclusion I thank my student S.K.Dutta for developing the experimental techniques and for carrying out the accurate anisotropy measurements.

Indian Association for the Cultivation
of Science, Calcutta 32, India

References

1. J.H.Van Vleck, Phys.Rev., 41, 208 (1932).
2. K.S.Krishnan, N.C.Chakravarti & S.Banerjee, Phil.Trans.Roy.Soc., A232, 99 (1933).
3. K.S.Krishnan & A.Mookherji, Phil.Trans.Roy.Soc., A237, 135 (1938).
4. K.S.Krishnan & A.Mookherji, Phys.Rev., 54, 533, 841 (1938).
5. K.S.Krishnan, A.Mookherji & A.Bose, Phil.Trans.Roy.Soc., A238, 125 (1939).
6. J.H.Van Vleck, J.Chem.Phys., 7, 61, 72 (1939).
7. J.H.Van Vleck, J.Chem.Phys., 3, 813 (1935).
8. J.B.Howard, J.Chem.Phys., 3, 807 (1935).
9. J.Owen, Proc.Roy.Soc., A227, 183 (1955).
10. A.Bose, Indian J.Phys., 21, 275 (1947).
11. A.Bose, Indian J.Phys., 22, 74, 195, 276, 483 (1948).
12. S.K.Datta, Indian J.Phys., 27, 155 (1953).
13. S.K.Datta, Indian J.Phys., 28, 239 (1954).
14. Roy S.K.Dutta, Indian J.Phys., 28, 183 (1954).
15. Roy S.K.Dutta, Indian J.Phys., 29, 429 (1955).
16. A.Mookherji & M.T.Tin, ZS.Krist., A101, 412 (1939).
17. H.Bethe, Ann.d.Phys., 3, 133 (1929).
18. C.J.Gorter, Phys.Rev., 42, 437 (1932).
19. D.Polder, Physica, 9, 709 (1942).
20. A.Abragam, M.H.L.Pryce, Proc.Roy.Soc., A206, 164 (1951).

21. B.Bleaney, K.D.Bowers & M.H.L.Pryce, Proc.Roy.Soc., A228, 166 (1955).
22. W.J.DeHaas & C.J.Gorter, Proc.Roy.Soc.Acad.Amst., 33, 1101 (1930).
23. A.Bose & S.C.Mitra, Indian J.Phys., 26, 543 (1952).
24. J.Hupse, Physica, 9, 633 (1942).
25. B.Bleaney, P.Penrose & B.I.Plumpton, Proc.Roy.Soc., A198, 406 (1949).
26. R.J.Benzie & A.H.Cooke, Proc.Phys.Soc., A64, 124 (1951).
27. A.Bose & D.Shoenberg, Proc.Bose Res.Inst.Cal., 20, 1 (1955).
28. J.H.E.Griffiths & J.Owen, Proc.Roy.Soc., A213, 451 (1952).
29. A.G.Shenstone & L.Wilets, Phys.Rev., 83, 104 (1951).
30. O.Laporte, ZS.Phys., 47, 761 (1928).
31. R.Schlapp & W.G.Penney, Phys.Rev., 42, 666 (1932).

MAGNITOCHEMISTRY OF DIAMAGNETIC COMPOUNDS AND THE ROLE OF POLARIZING PARAMAGNETISM

- Ia.G.Dorfman

1. Magnitochemistry of materials with diamagnetic susceptibility encompasses a large number of compounds. Determining the correlation between the magnetic properties and the chemical structure, which is the basic problem of magnitochemistry, calls for careful elucidation of the role played by individual atoms, ions, radicals and so on comprising the investigated compound.

Initially, it seemed that the simplest subject from this viewpoint would be compounds containing ions with closed electron shells of the inert gas type. It was thought that the diamagnetic susceptibility of an ionic compound could be represented as the sum of the susceptibilities of the individual ions with an appropriate correction for deformation of the electron shells. A number of investigations were carried out on the basis of this assumption. Then attempts were made to compare the susceptibilities of individual ions as evaluated from the experimental data with the theoretically calculated values. These attempts were repeated as more refined methods of calculation were developed (Pauling[1], Van Vleck[2], Slater[3], Angus[4], Hartree[5], Stoner[6] and others); none of these attempts, however, succeeded in eliminating the divergences between theory and experiment which amounted to 10% or more. The matter has given rise to extensive discussion in recent years.

Comparison of "experimental" and theoretical values of ionic susceptibilities

Ion	χ_{ion}		
	"Experimental" value	Theoretical value	
		VanVleck[2]	Angus[4]
Na^+	6,1	4,2	3,7
K^+	14,6	16,7	13,1
Rb^+	22,0	35	27,0
F^-	9,4	8,1	7,2
Cl^-	24,2	29,0	22,9
Br^-	34,5	54,0	36,7

One group of investigators proceeds on the assumption that the additive law - $\chi_{salt} = \chi_{an} + \chi_{cat}$ - obtains precisely for simple salts inasmuch as optical data indicate that there is no serious deformation of the ionic shells in such salts. Hence these investigators strive to resolve χ_{salt} into two components χ_{an} and χ_{cat} in conformity with the additive law. The "experimental" values of the ionic susceptibilities deduced in this manner differ quite appreciably from the theoretically calculated values (see table). Another group of investigators, on the contrary, assumed that the theoretically calculated values of χ_{ion} are the true ones. They attempt to account for the deviation of the "experimental" values of the ionic susceptibilities from the theoretically calculated values by introducing various corrections. In fact, some of these investigators come to the conclusion that the divergence is due solely to the inaccuracy of the experimental data.[7]

We feel that both points of view are mistaken. First, the theoretically calculated values of the ionic susceptibilities can scarcely be accurate within 10% and, consequently, cannot be taken as the basis. Second, the additivity rule will not hold rigorously for salts if only because the susceptibility of a salt in addition to the purely diamagnetic term must also comprise a term χ_p, depending on the existence of polarization magnetism, discovered by Van Vleck. In other words

$$\chi_{salt} = \chi_{d.cat} + \chi_{d.an} + \chi_p.$$

As is known the polarization paramagnetic susceptibility χ_p equals zero only for atoms and ions having rigorously spherical symmetry. Hence it should not exist in isolated ions having the inert gas atomic structure. Polarization paramagnetism can, however, in principle be observed in salts wherein the spherical symmetry of the ion is distorted by the crystal field. Thus in the case of diamagnetic ionic salts one must introduce two corrections: one of them is associated with the necessity of taking into account the mutual alteration of the ionic radii leading to a certain diamagnetic effect; the other is connected with a change in the character of the ionic symmetry leading to the appearance of polarization paramagnetism. The first correction can be evaluated from the electric polarizability of ions by investigating the refraction of the salt; this correction is usually taken into account. The second correction has not hitherto been evaluated theoretically and is commonly ignored. Taking into account this correction may explain the anomalous magnetic properties of the isomorphic solid solutions investigated in detail by Bhatnagar & Kapur[8]. These authors investigated the susceptibility of a number of solid solution systems (KCl-KBr, NaCl-KCl and NaBr-KBr) and found that the variation of the diamagnetic susceptibility as a function of the component concentration is distinctly not linear. The concentration interval with the lowest melting point corresponds to the maximum diamagnetic susceptibility.

It might be assumed that this diamagnetic susceptibility maximum is due to variation of the effective radius of the ions. But in this case one should expect a certain parallelism between the variation of the diamagnetic susceptibility and the variation of the electronic polarizability α. Kirkwood's rule[9] indicates that $\chi_d \approx \alpha^{1/2}$.

Inasmuch as in the NaCl-KCl system, for example, the susceptibility at the maximum deviates by 10% from the linear variation, the refraction should exhibit a deviation of approximately 20% from linearity at the same point if the anomaly of the diamagnetic susceptibility is due to changes of the effective ionic radii. Experiment showed, however, that the variation of the refraction is almost exactly linear. This, in my opinion, indicates that the anomaly of the diamagnetic susceptibility in isomorphic solid solutions is due to the presence of the χ_p term, i.e., to the polarization paramagnetism of Van Vleck.

Actually the diamagnetic susceptibility maximum corresponds to precisely those component concentrations at which x-ray patterns show evidence of "maximum disordering" in the arrangement of the ions, i.e., the greatest isotropy of the ionic field.

Thus it may be assumed that even in simple ionic crystals the diamagnetism of the ions is suppressed by the crystal field and that this "suppression" attains a value of almost 10%. Until now this effect has received little or no attention.

2. The existence of the influence of polarization diamagnetism becomes even more evident when we turn to the magnitochemistry of diamagnetic nonpolar molecules. Pascal and his school have been developing over a period of many years a detailed magnitochemical system of organic compounds and have recently revised and brought their system up to date[11]. It must be noted, however, that polarization paramagnetism does not figure explicitly in either the old system or in the new one. The magnetic susceptibility χ_m of any compound, according to Pascal, is regarded as the sum of the atomic diamagnetic susceptibilities plus a certain sum of corrections determined by the characteristics of the chemical structure:

$$\chi_m = \sum_i n_i \chi_{A_i} + \sum_i \lambda_i.$$

It is obvious that polarization paramagnetism must enter implicitly in the second term which reunites all the so-called "constitutive" corrections. There is a case, however, when this representation of the susceptibility of the molecules may prove to be inadequate and a more profound analysis of polarization paramagnetism is indicated.

Let us, for example, consider the CCl_4 molecule. The experimental value of the susceptibility at room temperature (per mole) is

$$\chi_{CCl_4} = -67 \cdot 10^{-6}.$$

Yet calculation by the method of Pascal yields

$-83.52 \cdot 10^{-6}$ according to the old scheme or
$-81.4 \cdot 10^{-6}$ according to the new scheme.

If we make use of the above mentioned rule of Kirkwood, establishing the relationship between the diamagnetic susceptibility and the average electric molecular polarizability α, according to which

$$\chi_d = -3.11 \cdot 10^6 \sqrt{k\alpha},$$

where k is the total number of electrons in the molecule, we obtain

$$\chi_{d.CCl_4} \approx -86.4 \cdot 10^{-6};$$

consequently, in this case the "constitutive" corrections of Pascal fail to take into account a paramagnetic term $\chi_p \approx +19 \cdot 10^{-6}$.

In the case of such a relatively symmetric molecule as CCl_4, at first glance it is hard to imagine that deviation from spherical symmetry can give so appreciable a paramagnetic susceptibility component. It must be noted, however, that at room temperature the CCl_4 molecule is subject to vibrations that sharply distort its tetrahedral symmetry. An analogous situation obtains in the case of the CBr_4 and CI_4 molecules, the only difference being that in the bromide and iodide vibrations of the lattice are excited at lower temperatures. Consequently, the total diamagnetic susceptibility of these molecules should increase with decreasing temperature.

Unfortunately, there are as yet no experimental data in the literature on the magnetic susceptibility of these substances at low temperatures.

On the other hand, it is known that a number of purely chemical considerations have led chemists years ago to raise the question of possible distortion of the symmetry of CCl_4, CBr_4 and CI_4 molecules. These considerations have found an explanation in the results of studies of the vibrational spectra of these molecules.

In any case it is obvious that for molecules the "constitutive" correction of Pascal cannot always be regarded as independent of the temperature.

At the same time it follows from the above that in cases when there appears to be a change in the symmetry of the molecular field, it is desirable to give particular attention to polarization paramagnetism (see Ref.10).

Leningrad Hydrometeorological Institute

References

1. L.Pauling, Proc.Roy.Soc., London, A 114, 181 (1927).
2. J.H.Van Vleck, The Theory of Electric and Magnetic Susceptibilities, Oxford, 1932.
3. I.C.Slater, Phys.Rev., 36, 57 (1930).
4. W.R.Angus, Proc.Roy.Soc., London, A136, 569 (1932).
5. D.E.Hartree, Proc.Cambr.Phil.Soc., 24, 89 (1928).
6. E.C.Stoner, Proc.Leeds.Phil.Soc., 1, 484 (1929).
7. W.R.Myers, Rev.Mod.Phys., 24, 15 (1952).
8. S.S.Bhatnagar & P.L.Kapur, L.J.Ind.Chem.Soc., 9, 347 (1932).
9. I.G.Kirkwood, Phys.ZS., 33, 57 (1932).
10. Ia.G.Dorfman, Manitnye svoistva i stroenie veshchestva (Magnetic properties and the structure of matter) M., 1956.
11. P.Pascal, P.Pacault & J.Hoareau, C.R.Acad.Sci., 223, 1078 (1951).

CYCLOTRON AND PLASMA RESONANCE IN SOLIDS

- A.F.Kip

I shall discuss briefly three types of situation of practical importance which give rise to absorption of microwave energy by mobile charge carriers in solids. The first situation occurs in semiconductors in which the freely moving charge density is low. For the microwave frequency range from 9,000 to 60,000 Mc/s which is covered by our own experiments, the upper bound of charge density is $\sim 10^{13}/cm^3$. In this simple low charge density situation microwave absorption has been called cyclotron resonance absorption. In this case the only forces acting on the charge carriers are the externally applied magnetic field and the accelerating microwave electric field. The condition for maximum absorption is given by the usual cyclotron equation

$$\omega_c = \pm eH/m^* c_3,$$

where m^* is the effective mass of the charge carriers involved. The results for silicon and germanium as published earlier[1] are typical of this low carrier density situation.

For successful observations of cyclotron resonance to be feasible it is necessary to have long collision relaxation times for the charge carriers. If ω is the microwave angular frequency and τ is the relaxation time, the criterion for an observable resonance is that $\omega\tau \geqslant 1$. At the frequencies used, this requirement demands high purity samples (impurity content less than 1 part in 10^9) and low temperatures (in the region of liquid helium). The simple classical derivation of this relaxation time requirement and a plot of line widths for various values of $\omega\tau$ is given in Ref.1.

A rather surprising exception to the requirement for very high specimen purity occurs in the case of Ge-Si alloys. Experiments on samples containing up to 0.75% Ge in Si and 5.4% Si in Ge have given well resolved resonance absorption[2]. In contrast to this situation, 10^{-5}% of trivalent or pentavalent substitutional impurities makes resolution difficult.

Detailed results for the effective masses of electrons and holes in Si and Ge will not be given here since these results have already been published in detail.[1] It is enough to say here that, in general, there is anisotropy of the effective masses and that the experimental results can be well understood on the basis of band theory of energy surfaces.

The second situation of practical interest for the frequencies used occurs when the density of carriers is greater than about $10^{13}/cm^3$ and where the sample thickness is less than the skin depth. This situation we have termed plasma resonance. Both theoretical and experimental work have been done for the case where the effective mass is constant[3]. For this high carrier density we must take into account the depolarizing force resulting from the collection of charges at the ends of the sample. This charge separation results in an added force acting on the charge carriers and modifies the nature of the resonance condition.

As shown in Ref.3, this additional force may be taken into account by substituting ω', the effective frequency, for ω the microwave frequency as used in the low carrier density case. Here

$$\omega' = \omega - \omega_p^2/\omega;$$

Here $\omega_p = (L_i N e^2/m^*)^{1/2}$ is the plasma frequency, where L_i is the effective polarization factor (equal to $L/(1 + L\chi)$), χ is the dielectric susceptibility, N is the carrier density, e is the electron charge and m^* is the effective mass of the carriers.

If ω' is used in the integrated equations of motion in place of ω, the phenomena of magnetoplasma resonance are obtained from the cyclotron resonance equation.

Thus as the carrier concentration increases we go from a simple cyclotron resonance situation $(\omega' = \omega)$ to a magnetoresistance curve $(\omega' = 0)$ and finally to magnetoplasma resonance $(\omega' > \omega)$. A result which may at first seem surprising is that under conditions which give rise to magnetoplasma resonance, a reduction in the experimental frequency used gives rise to an increase in the magnetic field necessary for obtaining the magnetoplasma resonance peak. Another noteworthy result which distinguishes magnetoplasma resonance from simple cyclotron resonance is the absorption line shape which results from modulation of the carrier density in the sample, as obtained, for example, by modulating a light beam incident on the sample. In cyclotron resonance, modulation of the carrier density modulates the losses in the sample, and an absorption curve is obtained directly. In magnetoplasma resonance, the principal effect of carrier modulation is to shift the magnetic field position of the absorption curve. Consequently, in this case, carrier modulation gives the derivative of the absorption curve. Ref.3 shows both theoretical and experimental curves for plasma resonance absorption for the case of an n-type sample of InSb.

Recent work on InSb has shown that the effects of plasma resonance can be shorted out at least partially. In this experiment a thin slab of n-type InSb with a thickness less than the skin depth at 77°K, was studied at 24,000 Mc/sec. The external magnetic field was applied perpendicularly to the plane of the sample. It was shown that, when the sample was moved from the center of the cavity to a position very close to a cavity wall, the magnetic field for the resonance maximum was reduced by a factor of about 20%. This result was expected by virtue of the fact that the cavity wall provided a shorting path (partly capacitative) which partially prevented the building up of charges on the edges of the sample. More work must be done to investigate to what extent plasma effects can be avoided in this way.

Another result of the simple theory, as discussed in Ref.3, has to do with the behavior of a low concentration of a minority carrier in the presence of a high concentration of the majority carrier. This case is of practical importance in p-type InSb, in which we have observed cyclotron resonance of low concentration of electrons (approximately $10^8/cm^3$) against a background of relatively high concentration ($\sim 4 \cdot 10^{14}/cm^3$) of low mobility holes. The simple theory indicates that in the approximation that the motion of the majority carriers is not affected by the minority carriers, cyclotron resonance absorption by the minority carriers will be unaffected by majority carriers. Experimental evidence for this is that the electron cyclotron resonance peak in p-InSb is unaffected by sample geometry. This could not be the case if magnetoplasma resonance were involved.

The third case of practical interest we have considered is that in which the density of carriers is so large that a slab-shaped sample will have a thickness greater than the skin depth. We make the further provision that the mean free path of the charge carrier be less than the skin depth. These requirements are typical of metals in most cases. Two situations have been considered,[3] one with the external magnetic field perpendicular to the surface, the other with the field parallel to the surface. The important result in both cases is that as a result of the effect of eddy current losses no cyclotron resonance peak is expected as long as there is only one type of

charge carrier. These results then seem to rule out the observation of cyclotron resonance in simple metals, at least in cases which do not involve the anomalous skin depth.

Department of Physics,
University of California

References

1. G.Dresselhaus, A.F.Kip & C.Kittel, Phys.Rev., 98, 368 (1955); R.N. Dexter, H.J.Zeiger & B.Lax, Phys.Rev., 104, 637 (1956).

2. G.Dresselhaus, A.F.Kip, Han Ying Ku, G.Wagoner & M.C.Schyler, Phys. Rev., 100, 1218 (1955).

3. G.Dresselhaus, A.F.Kip & C.Kittel, Phys.Rev., 100, 618 (1955).

HYPERFINE STRUCTURE OF MAGNETIC RESONANCE IN SUPERCOOLED SOLUTIONS OF SALTS OF THE IRON GROUP

- N.S.Garif'ianov

The influence of nuclear spin on paramagnetic resonance absorption was discovered in 1948 by Al'tshuler, Kozyrev & Salikhov[1-3] in dilute aqueous solutions of Mn^{2+} at a frequency of the order of 100 Mc. Under these conditions the splittings produced by the moments of the ^{55}Mn nucleus become greater than the splittings produced by the constant magnetic field, i.e., there obtain conditions corresponding to the Zeeman effect in weak fields. The position of the hyperfine structure (hereinafter HFS) lines is well characterized by the expression

$$H^* = \frac{h\nu}{g_F \beta}, \tag{1}$$

where

$$g_F = g_e \frac{F(F+1) + J(J+1) - I(I+1)}{2F(F+1)}; \tag{2}$$

where g_e is the Lande factor, F is the resultant moment of the nucleus and shall, I is the nuclear spin and J is the resultant moment of the shell.

For the Mn^{2+} ion, whose ground state is $^6S_{5/2}$, J = I = 5/2 and g_e = 2. Hence for all values of F, (Eq.2) yields g_F = 1. This value for g_F was substantiated by experiment. Thus Eq.(2), which is valid for free or isolated atoms, proved to be applicable to aqueous solutions of Mn^{2+}.

Later the HFS of paramagnetic resonance in aqueous and supercooled solutions of Mn^{2+}, VO^{2+} and Cu^{2+} salts was studied at frequencies of ~10,000 Mc by a number of investigators.[4-8] In this frequency range, the resonance conditions for the elements of the iron group correspond to the case of strong magnetic fields. Below we give the results of our investigation of the HFS of paramagnetic resonance in supercooled solutions of $^{51}V^{2+}$, $^{51}VO^{2+}$, $^{53}Cr^{3+}$ and $^{55}Mn^{2+}$ and in mixtures of the isotopes $^{63}Cu^{2+}$ and $^{65}Cu^{2+}$ obtained in the frequency range from 58 to 600 Mc.

The purpose of the investigation was to check the applicability of Eq.(2) to solutions of salts of elements of the iron group in the supercooled state when averaging of the local electric fields due to thermal motion is hindered. The experimental procedure has been described earlier[9]. By way of solvents we used ethyl alcohol and glycerin. Supercooling of the salt solutions was realized by rapid chilling with liquid oxygen.

1. Mn^{2+}. Ground state $^6S_{5/2}$

In supercooled solutions containing bivalent Mn the value of g_F calculated according to Eq.(2), (i.e., 1) agrees well with the experimental value in the frequency range from 91 to 150 Mc) (see Table 1 and Fig. a). The divergence at 520 Mc may be explained by the

Table 1

Solution	Concentration, molc/liter	Values of g-factor calculated according to Eq.(1)			
		520 Mc	150 Mc	91 Mc	58 Mc
$MnCl_2$	0,5	1,2	1,0	1,0	—
$^{53}Cr(NO_3)_3$	0,05	—	1,7	1,5	1,2
VCl_2	0,05÷0,1	1,0	0,6	0,5	0,5

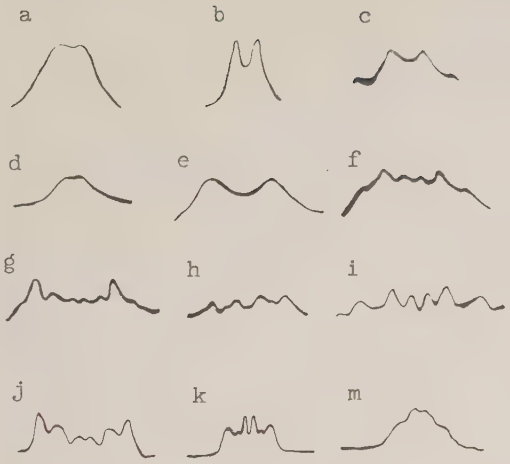

fact that here the Zeeman effect occurs in intermediate fields. Thus in supercooled solutions containing Mn^{2+} Eq.(2) agrees as well with experiment as in the case of the studies of water solutions (Fig.b)[1-3].

Figure

Paramagmetic absorption curves obtained with a 50 cps alternating magnetic field applied to the specimen in the absence of a constant magnetic field (all curves except b obtained at 90°K, curve b obtained at 300°K; solutions in: curve b, water; curves a,c,d & e, alcohol; curves g through m, glycerine): a & b - $MnCl_2$, C = 0.5 mole/liter, f = 150 Mc; c - $^{53}Cr(NO_3)_3$, C = = 0.50 mole/liter, f = 91 Mc; d - $Cr(NO_3)_3$, C = 0.05 mole/liter, f = 91 Mc; e - VCl_2, C = 0.5 mole/liter, f = 150 Mc; f - manganese glass, f = 252 Mc; g,h & i - $VOCl_2$, C = 0.5 mole/ /liter (g - 252 Mc, h - f = 150 Mc, i - 91 Mc); j,k & m - $Cu(NO_3)_2$, C = 0.1 mole/liter (j - f = 520 Mc, k - f = 260 Mc and m - f = 150 Mc).

2. $^{53}Cr^{3+}$. Ground state $^4F_{3/2}$

Eq.(2), deduced for free atoms and applicable to the HFS in water and supercooled solutions containing bivalent Mn ions in the $^6S_{5/2}$ state, is not suitable for describing the HFS of $^{53}Cr^{3+}$ inasmuch as local electric fields with nonspherical symmetry "freeze the orbit" in supercooled solutions. Hence, as experiment shows, in Eq.(2) one should substitute S instead of J and the spectroscopic splitting factor g instead of g_e, i.e., one must use the following expression for g_F:

$$g_F = g\frac{F(F+1)+S(S+1)-I(I+1)}{2F(F+1)}. \qquad (3)$$

For $^{53}Cr^{3+}$, S = J = 3/2 and $g \approx 2$, hence for all values of F expression (3) gives g_F = 1. As can be seen from Table 1, with decreasing frequency g_F for $^{53}Cr^{3+}$ actually does approach unity (Fig.c).* It may be concluded that the conditions for the Zeeman effect in weak fields for $^{53}Cr^{3+}$ are realized at a frequency f $\leqslant$ 58 Mc. For trivalent Cr (Fig.d) not enriched with $^{53}Cr^{3+}$ HFS lines are not observed.

3. V^{2+}. Ground state $^4F_{3/2}$

For V^{2+}, if we take S = 3/2, I = 7/2 and g = 2, Eq.(3) yields g_{F_1} = 0.6, g_{F_2} = 0.4, g_{F_3} = 0 and g_{F_4} = -1. In practice (Table 1) there is observed a single broad resonance curve with g_F approaching 0.5 as the frequency is reduced (Fig.e). We assume that this curve is a result of surposition of the two peaks with g_{F_1} = 0.6 and g_{F_2} = 0.4 and that the peak with g_{F_4} = -1 is

---

*The HFS in supercooled solutions containing $^{53}Cr^{3+}$ is not resolved at a frequency of 9500 Mc.[10]

not resolved. Thus for V^{2+} the conditions for the appearance of the Zeeman effect in weak fields are realized at a frequency of ~100 Mc.

4. Mn^{3+}. Ground state $^5D_0$

We investigated paramagnetic resonance in silica glass into which 1% Mn_2O_3 was introduced. At 90°K we succeeded in detecting at frequencies of 460, 252 and 92 Mc* several absorption maxima. The corresponding values of the g_F factor are listed in Table 2.

Table 2

Values of the g_F factor for manganese glass

Frequency, Mc	g_F factor		
	g_{F_1}**	g_{F_2}	g_{F_3}
400	4	1,5	—
252	4	1,3	0,66
98	4	0,73	—

As was already noted above the paramagnetic resonance absorption spectrum of aqueous and supercooled solutions of bivalent manganese salts in medium and weak fields has a single peak with $g_F \geqslant 1$. Regarding the glass as a supercooled solution[8], we assume that the HFS peak with $g_F < 1$ can be attributed only to compounds of manganese of different valence. To judge from the violet-purple color of the manganese glass it may be concluded that most of the manganese is the trivalent form.

Taking S = 2, I = 5/2 and $g = 2$ for Mn^{3+}, from Eq.(3) we find $g_{F_1} = 0.88$, $g_{F_2} = 0.82$, $g_{F_3} = 0.68$, $g_{F_4} = 0.26$ and $g_{F_5} = 2.6$. Hence we assume that the HFS peak with $g_F = 0.73$ observed for manganese glass is probably associated with compounds of trivalent manganese (Fig.f).

5. VO^{2+}. Ground state $^2D_{3/2}$

A very complicated paramagnetic resonance spectrum is observed for supercooled solutions containing VO^{2+} in the frequency range from 58 to 600 Mc; the number and position of the absorption peaks depends strongly on the frequency of the oscillating field (Figs. g,h & i). This dependence is shown in Table 3.

Table 3

Values of the g_F factor for a solution of $VOCl_2$ in glycerin (C = 0.5 mole/liter) at temperatures to 90°K

Frequency, Mc	g_F factor			
	g_{F_1}	g_{F_2}	g_{F_3}	g_{F_4}
600	1,0	1,8	2,4	
520	1,0	1,3	—	
252	0,7	0,8	1,7	8,0
150	0,5	0,8	1,3	2,0
91	0,1	0,26	0,6	—

As may be seen from Table 3 the dependence of the HFS lines in the paramagnetic absorption spectrum of VO^{2+} on the frequency of the oscillating field vanishes at frequencies under ~91 Mc (i.e., the Zeeman effect begins to obtain in weak fields at frequencies below this value). If we take S = 1/2, I = 7/2 and $g \approx 2$, Eq.(3) for VO^{2+} yields $g_F = 0.25$. Expression (3) yields agreement with experiment only for the $g_{F_2} = 0.26$ line at a frequency of 91 Mc; at present there is no satisfactory interpretation for the other HFS lines.

---

*The HFS at 9500 Mc is not resolved.

**The $g_{F_1} = 4$ peak is due to iron impurity in the glass.[11]

6. Cu^{2+}. Ground state $^2D_{5/2}$

In the case of supercooled solutions containing Cu^{2+} there also obtains a very strong dependence of the line positions on the frequency of the oscillating field (Figs. j,k & m). This dependence is summarized in Table 4.

Table 4

Values of the g_F factor for a solution of $Cu(NO_3)_2$ in glycerin (C = 0.1 mole/liter) at 90°K

Frequency, Mc	g_F factor		
	g_{F_1}	g_{F_2}	g_{F_3}
600	1,9	3,0	16
520	1,84	3,0	16
400	1,8	3,0	8,0
260	1,7	3,0	8,4
150	1,0	4,0	
92	0,8	2,0	
58	0,8	2,0	

As may be seen from the table, the conditions for the Zeeman effect in weak fields obtain at frequencies below ~92 Mc. For Cu^{2+}, Eq.(3) gives $g_F = 0.5$. Eq.(3) does not agree with the experimental results for supercooled solutions of Cu^{2+}. Thus in supercooled solutions of VO^{2+} and Cu^{2+}, in which the orbital moment is not fully frozen by the local electric fields of the solution; the position of the HFS paramagnetic resonance lines in weak fields is not described by expressions (2) and (3).

For a more exact check of these expressions one must have experimental data obtained at the temperature of liquid hydrogen.

Physical-Technical Institute of the
Kazan Branch of the USSR Academy of Sciences

References

1. S.A.Alt'shuler, B.M.Kozyrev & S.G.Salikhov, Doklady AN SSSR, 71, 855 (1950).
2. B.M.Kozyrev, Izv.AN SSSR, Ser.fiz., 16, 533 (1952).
3. B.M.Kozyrev, Discussions of the Faraday Society, 19, 135 (1955).
4. T.S.England & E.E.Shneider, Physica, 17, 221 (1951).
5. M.Tinkham, R.Weinstein & A.Kip, Phys.Rev., 84, 848 (1951).
6. N.S.Garif'ianov & B.M.Kozyrev, Doklady AN SSSR, 98, 829 (1954).
7. N.S.Garif'ianov & B.M.Kozyrev, Uchenye zapiski (Scientific Notes) Kazan State University, 114, 83 (1954).
8. N.S.Garif'ianov, Doklady AN SSSR, 103, 41 (1955).
9. N.S.Garif'ianov & B.M.Kozyrev, Zhur.eksp.i teor.fiz., 30, 272 (1956).
10. N.S.Garif'ianov, Doklady AN SSSR, 109, 725 (1956).
11. N.S.Garif'ianov, Doklady AN SSSR, 101, 503 (1955).

ELECTRON PARAMAGNETIC RESONANCE IN ELECTROLYTE SOLUTIONS

- B.M.Kozyrev

The line width ΔH of paramagnetic resonance absorption in solutions of salts is determined primarily by 1) magnetic dipole interactions between the ions (ΔH_{mag}), 2) electric interactions of the ions with the medium (ΔH_{el}), 3) hyperfine interactions of the electron spin of the ions with the spins of their atomic nuclei (ΔH_{hf}), and, finally, 4) in the case of very concentrated solutions, the line may be narrowed due to exchange interaction between the paramagnetic ions (ΔH_{exch}).

Thus the line width can be roughly characterized by the expression

$$\Delta H = \Delta H_{mag} + \Delta H_{el} + \Delta H_{hf} - \Delta H_{exch}.$$

One cannot, of course, consider the terms to be rigorously additive inasmuch as these factors may influence each other.

According to the theory of Bloembergen, Purcell & Pound[1] the magnetic dipole interactions in liquid solutions must be stronger the greater the concentration of the paramagnetic ions and the longer the mean correlation time $\tau_c = 4\pi a^2\eta/3kT$, where a is the ionic radius and η is the viscosity. Hence the magnetic interaction contribution to the line width ΔH_{mag} can be substantially reduced by reducing the concentration of the solution and raising the temperature (the latter is accompanied by decrease of the viscosity η). If the magnetic dipole interactions between the ions were primarily responsible for the total line width, we could obtain very narrow lines for a solution of any paramagnetic material. Experiments show, however, that this is not feasible in practice.

In a number of cases even with the greatest magnetic dilution the absorption line remains so wide that the effect cannot be observed at room or higher temperatures. This we know is the case for salts of Fe^{3+}, Fe^{2+}, V^{2+}, Cr^{2+} and Ni^{2+} in water, alcohol and glycerin and for nonaqueous solutions of Mn^{2+} salts. Even in the case of readily observed paramagnetic resonance (solutions of Cr^{3+}, VO^{2+} and Cu^{2+} salts and water solutions of Mn^{2+} salts) varrowing of the line virtually ceases at a concentration of 0.1-0.01 mole/ /liter. The limiting (minimal) line width is still appreciable: 10-100 gauss or more.

In most cases the great line width in solutions may be attributed to electric interactions. Thus if the fine splittings of the ground level of the paramagnetic ion produced by local electric fields are not too small (for example, of the order of 0.1 cm^{-1}) and the fine structure spectrum has no isotropic lines, then in consequence of the chaotic arrangement of the local fields relative to the external magnetic field, we should obtain a very wide (virtually unobservable) paramagnetic absorption curve. If among the fine structure lines there are some close to isotropic, the absorption curve may prove to be fairly narrow on condition that the relaxation time is not too short.

It might be assumed that increasing the temperature, i.e., shortening the mean correlation time τ_c should always lead to enhancement of the isotropicity, that is, to narrowing of the absorption lines. Experiments show, however, that heating of the solution is generally not nearly as effective as might be expected and in fact sometimes leads to broadening rather than narrowing of the absorption lines.

We believe that the reason for this lies in the existence of a rather stable short-range order in the arrangement of the solvent molecules (and

sometimes of the anions as well) about the paramagnetic ion. In other words, the microviscosity about the paramagnetic ion is much higher than the macroscopic viscosity of the liquid characterized by the coefficient η.

Hence the mean correlation time τ_c associated with the macroscopic viscosity η is not a satisfactory characteristic of the averaging effect of the motion on the local electric fields. As regards the last, solutions of salts of the iron group elements are closer to solids than to liquids.[2]

In the present report we shall be concerned mainly with determinations of the temperature dependence of the line width of paramagnetic resonance in solutions.

Most of the measurements in question were made at a magnetic field frequency of $1.27 \cdot 10^7$ cps in water solutions of Mn^{2+}, Cr^{3+}, Cu^{2+} and VO^{2+} by the Zavoiskii grid current method with modulation of the magnetic field. At so low an oscillation frequency the resonance peak as a rule is not resolved (except in the case of very dilute aqueous solutions of Mn^{2+} salts). Hence the line half-width ΔH was determined as double the value of the field H corresponding to half the absorption intensity observed with H = 0. The value of ΔH for solutions was determined by comparison with a standard material. In most cases this was $CrCl_3$ for which ΔH = 140 gauss at room temperature.

Among the investigated solutions the narrowest lines were yielded by water solutions of Mn^{2+} salts. This is connected with the extremely small value of the fine splitting constant for the Mn^{2+} ion: thus, in the cubic lattice of manganese sulfide the fine splitting constant $\Delta = 0.001$ cm^{-1}, i.e., is much smaller than the hyperfine splitting constant[3].

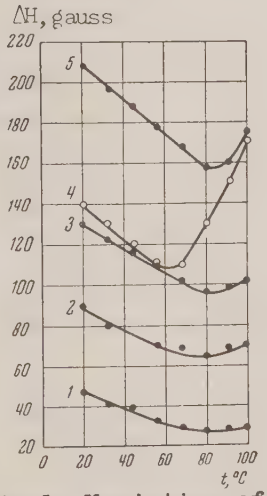

Fig.1. Variation of the line width ΔH with the temperature in water solutions of $MnCl_2$ of different concentration: 1 - 0.005, 2 - 0.5, 3 - 1 mole/liter $MnCl_2$, 4 - 0.5 mole/liter $MnCl_2$ + 4.3 mole/liter LiCl, 5 - 2 mole/liter MnCl; $f = 1.26 \cdot 10^7$ cps.

As a number of experiments have shown[4,5], in measurements at high frequencies, solutions containing Mn^{2+} yield six hyperfine structure peaks and at sufficiently low frequencies a single peak with a g-factor close to 1. The appearance of this single peak would at first glance indicate that we must assume that the thermal motion of the liquid leads to averaging of the local electric fields to spherical symmetry, i.e., would indicate that we must reject the concept of stable solvate shells inasmuch as calculations for the Mn^{2+} ion at low frequencies even in the case of a purely cubic field give a complicated spectrum[6].

On the other hand, experiments carried out in our laboratory by Kashaev[7] with polycrystals of the solid solution $(Mn,Zn)(NH_4)_2 \cdot (SO_4)_2 \cdot 6H_2O$ and the experiments of Garif'ianov[8] with supercooled solutions of Mn^{2+} salts in organic solvents showed that in both cases at frequencies of 10^7-10^8 cps an intense peak with $g = 1$ is observed. Hence the presence of this peak in itself does not mean that we must reject the concept of a stable solvate cell for the Mn^{2+} ion. Evidence that Mn^{2+} ions have such a stable shell is furnished by experimental measurements of ΔH in Mn^{2+} salt solutions at different temperatures. The results of such measurements for aqueous solutions of $MnCl_2$ are shown in Fig.1. We see that at all the investigated $MnCl_2$ concentrations the ΔH curves exhibit a minimum at approximately the same temperature,

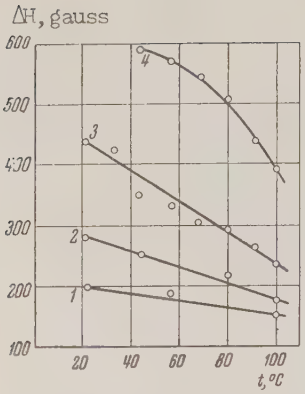

Fig.2. Variation of ΔH with the temperature in water solutions of trivalent chromium of different concentrations: 1 - 0.4 mole/liter $[Cr(H_2O)_6](NO_3)_3$, 2 - 1.5, 3 - 3, and 4 - 1 mole/liter $[Cr(H_2O)_4Cl_2]Cl$.

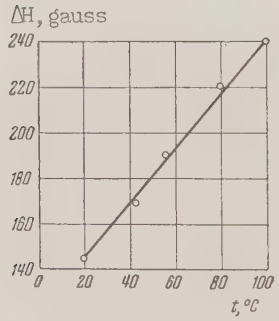

Fig.3. Variation of ΔH with temperature in a 1 mole/liter water solution of $Cu(NO_3)_2$ (points). Straight line: $\Delta H = aT^2$.

namely, at 80°. Analogous results were obtained at a frequency of 10^{10} cps by Tinkham, Weinstein & Kip[9].

If the narrowing of the line width in the temperature range from 20 to 80° is associated with the hypothesized averaging of the magnetic and electric local fields by molecular motion of the liquid, then the line broadening observed above 80° requires special explanation. We feel that it is most logical to ascribe this broadening to partial disintegration of the hydrate shell of the Mn^{2+} ions, leading to lowering of the symmetry of the local electric fields and, consequently, to increased electric splittings. Evidence in favor of this is the invariance of the temperature of the ΔH minimum and certain other facts. In particular, there is the fact that upon the introduction of a high concentration of Li^+ ions into the $MnCl_2$ solution the ΔH minimum is displaced to a lower temperature (~60°), while the broadening of the lines with further heating proves to be much greater, presumably because the Li^{2+} ions, having a much greater tendence to hydration, facilitate the partial disintegration of the Mn^{2+} ion hydrate shells.

On the other hand, in solutions of salts of trivalent chromium, whose hydrate shell, as is known, is characterized by exceptional stability, no ΔH minimum is observed in the temperature interval from 20 to 100°.

Fig.2 shows the temperature dependence of ΔH for a number of water solutions of $[Cr(H_2O)_6](NO_3)_3$ having different concentrations and a unimolar solution of $[Cr(H_2O)_4Cl_2]Cl$. In the solutions of the former salt the narrowing of the absorption lines with increasing temperature is approximately linear. The slope of the straight lines decreases with dilution.

Owing to the exceptional strength of the hydrate shell of chromium, its octahedral structure is not disrupted by thermal motion in the investigated temperature range. Hence raising the temperature can only lead to averaging of the deviations from the cubic field that are responsible for the fine structure of the line and are, presumably, associated with the more remote water molecules and with the anions. These deviations should be the greater, the higher the concentration of the solution; consequently, the averaging effect of the thermal motion is most strongly evinced at high concentrations.

In green chromium trichloride solutions the noncubic components of the field are relatively more important and here heating has a stronger influence on the line width. The difference as regards line width and its temperature dependence observed between green and violet solutions of chromium salts suggests the possibility of investigating complex formation in solutions by the method of paramagnetic resonance. We shall return to this question below in considering copper salt solutions.

Aqueous solutions of simple copper salts - for example, $(Cu(NO_3)_2$ and $CuSO_4$ - at room temperature yield paramagnetic resonance curves with a single peak for which $g = 2.184 \pm 0.005$. No hyperfine structure is discernible. Another remarkable characteristic of these copper compounds is the fact that the line width ($\Delta H = 140$ gauss) does not depend on either the concentration in the investigated range from 0.5 to 4 mole/liter or on the frequency in the range from 10^7 to 10^{10} cps. These attributes led the writer to hypothesize in an earlier contribution[2] that there exist in copper salt solutions in the indicated concentration range strong exchange interactions between the Cu^{2+} ions, leading to suppression or elimination of the hyperfine structure. Further measurements, however, make this hypothesis appear doubtful. In particular, it is contradicted by the observed temperature dependence of ΔH. The observed temperature dependence of ΔH for a unimolar water solution of $(Cu(NO_3)_2$ is shown in Fig.3. It will be seen from the figure that with increasing temperature the line width increases monotonically. Actually ΔH proves to be almost exactly proportional to the square of the absolute temperature.

Yet, in highly concentrated solutions of vanadium salt for which exchange narrowing is reliably established, increasing the temperature leads to narrowing of the lines. Thus for a 5.8 molar solution of $VOCl_2$, $\Delta H = 320$ gauss at 20° and only 260 gauss at 100°.

The attributes displayed by copper solutions can apparently be explained on the assumption that the symmetry of the local electric fields acting on the Cu^{2+} ions in solutions is cubic with an admixture of a trigonal rather than a rhombic component as is the case in most solid copper salts.

Bleaney, Bowers & Ingram[10] investigated solid Cu^{2+} salts with a trigonal component. In these the g factor proved to be virtually isotropic and the hyperfine structure constant A was found to be small and also isotropic. The small value of A explains the absence of a resolvable hyperfine structure in Cu^{2+} salt solutions; the line width observed in such solutions is due to spin-lattice interactions which must increase with increasing temperature if the Cu^{2+} ion solvate shell is sufficiently stable to be regarded as a solid formation at frequencies $\gg 10^7$ cps.

Values of the g factor and the line width ΔH in water solutions of copper halides

Concentration, mole/liter	$CuCl_2$ in water		$CuBr_2$ in water	
	g_{eff}*	ΔH, gauss**	g_{eff}*	ΔH, gauss**
4	2,167	225	2,162	320
3	2,171	185	2,174	170
2	2,175	160	2,174	160
1	2,184	140	2,175	150
0,5	~2,18	140	—	—

*Measured at $9.467 \cdot 10^9$ cps (sic) and 295°K.
**Measured at $2.97 \cdot 10^9$ cps (sic) and 295°K.

Before concluding let us turn to the question of complex formation in copper salt solutions. In solutions of simple Cu^{2+} salts, as noted above, the g factor and ΔH are independent of the concentration. This is not at all the case in complex salts as may be seen from the accompanying table.

At high concentrations, $CuCl_2$ and $CuBr_2$ solutions contain complex ions of the $(CuHal_x)^{2-x}$ type. As the solution is diluted with water the fraction of these complex ions decreases and, accordingly, the values of g and ΔH approach the respective values characteristic of the hydrated copper ion. In $CuCl_2$ solutions at a concentration of 1 mole/liter g and ΔH do not differ within the limits of experimental error from their "normal" values. The complex ions in $CuBr_2$ solutions are somewhat more stable, hence for these solutions g and ΔH still differ somewhat from the "normal"

values at the same concentration (1 mole/liter).

The greatest displacement of the absorption line was observed for solutions containing pyridine and ammonium complexes of copper. For the former $g = 2.04$; for the latter $g = 2.10$.

These data show that measurements of g or ΔH in solutions can serve as a method for investigating the processes of complex formation. The magnitude of the variation of these parameters is sufficiently great to allow of determining the instability constant and the coordination numbers in the case of sufficiently concentrated solutions.

Physical-Technical Institute of the
Kazan Branch of the Academy of Sciences of the USSR

References

1. N.Bloembergen, E.M.Purcell & R.V.Pound, Phys.Rev., 73, 678 (1948).
2. B.M.Kozyrev, Doklady AN SSSR, 103, 52 (1955); Faraday Soc.Discussions, 19, 135 (1955).
3. B.Bleaney & K.W.H.Stevens, Rep.Progr.Phys., 16, 108 (1953).
4. S.A.Alt'shuler, B.M.Kozyrev & S.G.Salikhov, Doklady AN SSSR, 71, 755 (1950).
5. N.S.Garif'ianov & B.M.Kozyrev, Doklady AN SSSR, 98, 923 (1954).
6. B.Bleaney, Faraday Soc.Discussions, 19, 175 (1955).
7. S.-Kh.G.Kashaev, Thesis, Molotov State University, 1954.
8. N.S.Garif'ianov, Doklady AN SSSR, 103, 41 (1955).
9. M.Tinkham, R.Weinstein & F.Kip, Phys.Rev., 84, 848 (1951).
10. B.Bleaney, K.D.Bowers & D.J.E.Ingram, Proc.Roy.Soc., A228, 147 (1955).

THERMODYNAMIC THEORY OF RELAXATION AND RESONANCE EFFECTS IN TWO-SPIN SYSTEMS

- G.V.Skrotskii and L.V.Kurbatov

The accepted equations for describing the time dependence of the magnetization of magnets are the semi-empirical ones of Bloch or of Landau - Lifshits or various modifications thereof. Even in modified form, however, the equations do not account for many behavioral properties of magnetic substances, so that their solutions often fail to agree with experiment. The concept of a magnetic substance as a "spin system" weakly interacting with the lattice makes it possible to use thermodynamic considerations to find the form of the differential equations characterizing the magnetization of a sample placed in a time-varying magnetic field.

I.G.Shaposhnikov[1] developed a thermodynamic method by means of which the thermodynamic potential of the magnetic system can be used to determine the susceptibility of a paramagnet as a function of the external alternating field frequency. Shaposhnikov's method, as we shall see below, can also be used to find the form of the differential equations describing the behavior of any magnetic substance in an external field. The constants entering these equations can always be expressed in terms of the relaxation times characterizing the subsystems of which the magnetic substance is comprised.

The "subdivision", introduced by Casimir and du Pre[2], of the magnet into two weakly interacting subsystems (the "spin system" and the lattice) is in many cases inadequate. Thus, for instance, paramagnetic solutions containing several kinds of ions and substances with uncompensated antiferromagnetism (ferrites), cannot be encompassed by such a simple scheme.

1. Let us consider substances with pure spin magnetism, which, from the magnetic point of view, can be thought of as a conjunction of two spin systems with different partial magnetizations M_1 and M_2 and different gyromagnetic ratios γ_1 and γ_2.

We shall assume that the spin systems that are responsible for the magnetic properties of the substance, and the lattice are quasi-independent of each other. In other words, we shall assume that in view of the weak interaction, equilibrium between the spin systems as well as between them and the lattice is attained at a much slower rate than within each of them per se. Hence, in this case there will be three temperatures, characterizing the state of the magnetic substance. These are T_0, the temperature of the lattice (which we shall consider constant*), and T_1 and T_2, the temperatures of the spin systems. The kinetics of the processes taking place within the magnetic substance are determined by the relaxation times τ_{11} and τ_{22} within each spin system, the relaxation times τ_{10} and τ_{20} between each spin system and the lattice, and the relaxation time τ between the spin systems.

We shall assume the homogeneous external magnetic field applied to the substance consists of a constant field H_0 and a weak periodic field h. These fields need not be parallel; thus we can write

$$\mathbf{H} = \mathbf{H}_0 + \mathbf{h}(t), \quad \mathbf{h} = \mathbf{h}_0 \exp(j\omega t), \quad h_0 \ll H_0 = H_{0z}. \tag{1}$$

The magnetization $M_i\,(i = 1, 2)$ of each of the spin systems is described by

$$\mathbf{M}_i = \mathbf{M}_{0i} + \mathbf{m}_i(t), \quad \mathbf{m}_i = \mathbf{m}_{0i} \exp(j\omega t), \quad m_{0i} \ll M_{0i}. \tag{2}$$

---

*As has been shown in Refs.1 & 2, the variation with time of the lattice temperature in paramagnets with pure spin magnetism is significant only at low temperatures and for low magnetic field frequencies.

The magnetic moments of the spin systems are acted upon, in general, not by the external field H, but by an effective field $\mathbf{H}_i$ comprised of the external field, the field due to exchange forces, the magnetic anisotropy field and the demagnetization field of the sample. Therefore

$$\mathbf{H}_i = \mathbf{H}_{0i} + \mathbf{h}_i. \tag{3}$$

For magnetically isotropic samples, we have

$$\left.\begin{aligned} \mathbf{H}_{0i} &= \mathbf{H}_0^* - \lambda_i \mathbf{M}_{0i} - \lambda \mathbf{M}_{0k}, \\ \mathbf{h}_i &= \mathbf{h}^* - \lambda_i \mathbf{m}_i - \lambda \mathbf{m}_k, \end{aligned}\right\} \tag{4}$$

where $i, k = 1, 2$ and $i \neq k$. The fields $\mathbf{H}_0^*$ and $\mathbf{h}^*$ differ from the external fields in that they allow for the demagnetizing effect of the sample. The coefficients λ_i and λ of the molecular field account for exchange interactions inside each of the spin systems and between them, and in different specific cases may have different signs.

If we assume that the temperature difference $\vartheta_{ik} = T_i - T_k$ between the spin systems and the differences $\vartheta_{i0} = T_i - T_0$ between each of the spin systems and the lattice are small compared to $\mathbf{T_0}$, $\mathbf{T_1}$ and $\mathbf{T_2}$, then the amount of heat transferred one spin system to the lattice and to the other spin system in a time dt can be written

$$\delta Q_i = \delta Q_{i0} + \delta Q_{ik} = \alpha_{i0}\vartheta_{i0}dt + \alpha_{ik}\vartheta_{ik}dt, \tag{5}$$

where α_{i0} and α_{ik} may be called the internal heat transfer coefficients between the corresponding subsystems. We shall assume that $\alpha_{ik} = \alpha_{ki}$.

Neglecting magnetostriction, the work done by the magnetic field on the i-th spin system may be written

$$\delta A = \mathbf{H}_i\, d\mathbf{M}_i. \tag{6}$$

Now for the i-th spin system the first law of thermodynamics can be written

$$dU_i = \mathbf{H}_i d\mathbf{M}_i - \alpha_{i0}\,\vartheta_{i0}dt - \alpha_{ik}\vartheta_{ik}dt, \tag{7}$$

where

$$U_i = \Phi_i - T_i \frac{\partial \Phi_i}{\partial T_i} + \mathbf{H}_i\mathbf{M}_i \tag{8}$$

is the internal energy of the spin system. Equ. (8) is valid for nonequilibrium processes provided Φ is understood to be the nonequilibrium thermodynamic potential.

2. When the variable field $h(t)$ is weak, in which case $m_i(t)$ and the temperature differences ϑ_{i0} and ϑ_{ik} are small, the spin systems may be assumed close to equilibrium (for which $\mathbf{H}_i = \mathbf{H}_{0i}$, $\mathbf{M}_i = \mathbf{M}_{0i}$ and $T_i = T_0$). We may then use series expansions of nonequilibrium functions of the variables h, ϑ_{i0}, ϑ_{ik} and $\mathbf{m}_i$, restricting ourselves to the linear approximations.

According to the method developed by Shaposhnikov[1], the time derivative $\dot{\mathbf{M}}_i = \dot{\mathbf{m}}_i$ of the magnetization is given by

$$\dot{m}_i^s = -f_i\,(\varkappa_i m_i^s - \xi_i h_i^s + \beta_i^s \vartheta_{i0}), \quad s \equiv (x, y, z), \tag{9}$$

where

$$\varkappa_i = \left[\frac{\partial^2\Phi_i}{(\partial M_i^z)^2}\right]_{M^z=M_{i0}}; \quad \xi_i = -\left[\frac{\partial^2\Phi_i}{\partial M_i^z \partial H_i^z}\right]_{\substack{M_i^z=M_{i0}\\ H_i^z=H_{i0}}}; \quad \beta_i^s = \left[\frac{\partial^2\Phi_i}{\partial M_i^s\,\partial T_i}\right]_{\substack{M_i^s=M_{i0}\\ T_i=T_0}}, \tag{10}$$

and $f_i = f_i(T_0, H_{0i})$ is a function which remains unknown in the thermodynamic theory. Invoking (4), we may rewrite (9) in the form

$$\dot{m}_i^s + f_i(\varkappa_i + \xi_i\lambda_i)\, m_i^s + f_i\xi_i\lambda m_k^s + f_i\beta_i^s\vartheta_{i0} = f_i\xi_i h^s. \tag{11}$$

In the linear approximation (7) may be written, using (8) and bearing in mind (4), as

$$\beta_i^s\dot{m}_i^s - \lambda_i q_i^s\dot{m}_i^s - \lambda q_i^s\dot{m}_i^s + q_i^s\dot{h}^s = \frac{\alpha_{i0}}{T_0}\vartheta_{i0} + \frac{\alpha_{ik}}{T_0}\vartheta_{ik} - \sigma_i\dot{\vartheta}_{i0}, \tag{12}$$

where

$$q_i^s = \left[\frac{\partial^2\Phi}{\partial H_i^s\,\partial T_i}\right]_{\substack{H_i^s=H_{i0}^s\\ T_i=T_0}}, \quad \sigma_i = \left[\frac{\partial^2\Phi_i}{\partial T_i^2}\right]_{T_i=T_0}, \tag{13}$$

and the twice occurring index s indicates summation.

We have so far not taken into account the gyroscopic properties of the magnetic moments, i.e., have regarded them as "free-swinging" magnetic needles. The gyroscopic nature of the moments may be accounted for by considering all of the calculations to have been performed in a coordinate system rotating about the direction of H_i with the Larmor frequency $\omega_i = |\gamma_i| \cdot H_i$. The transition to a stationary coordinate system, as is known, should be realized by the transformation

$$\dot{\mathbf{M}}_i^s \to \dot{\mathbf{M}}_i^s - \gamma_i[\mathbf{M}_i,\ \mathbf{H}_i]_s.$$

Eq. (11) can now be written

$$\dot{m}_i^s + f_i(\varkappa_i + \xi_i\lambda_i)\, m_i^s + f_i\xi_i\lambda m_k^s + f_i\beta_i^s\vartheta_{i0} = f_i\xi_i h^s + \gamma_i[\mathbf{M}_i,\ \mathbf{H}_i]_s. \tag{14}$$

As will be shown below, all the q_i^s vanish for paramagnets. It can be shown that they vanish also for ferromagnets.* Therefore Eq. (12) becomes

$$\beta\,\dot{m}_i^s = \frac{\alpha_{i0}}{T_0}\vartheta_{i0} + \frac{\alpha_{ik}}{T_0}\vartheta_{ik} - \sigma_i\dot{\vartheta}_{i0} + \gamma_i[M_i,\ H_i]_z\cdot\beta_i. \tag{15}$$

The eight equations contained in (14) and (15) together with the obvious relation $\vartheta_{ik} = \vartheta_{i0} - \vartheta_{k0}$ form a set which determines the time variation of spin-system magnetizations m_i^s and the temperatures ϑ_{i0}.

3. In order to determine the relaxation times characterizing the magnetic substance, let us investigate how the spin-system magnetizations m_i and the temperature differences ϑ_{i0} vary when the magnetic field is turned off. To bring out the different relaxation mechanisms, let us consider four particular cases.

A. If we neglect the interaction between the spin systems, i.e., set $\alpha_{ik} = 0$ and $\lambda = 0$, then according to (14) and (15) the approach to equilibrium after cutoff of the magnetic field is described by the equations

---

*From (10) it follows that $\beta_i^x = \beta_i^y = 0$ and $\beta_i^z = \beta_i$.

$$\dot{m}_i^s + f_i(\varkappa_i + \xi_i\lambda_i)\, m_i^s + f_i\beta_i^s\vartheta_{i0} = 0, \tag{16}$$

and

$$\beta_i\dot{m}_i^z = \frac{\alpha_{i0}}{T_0}\vartheta_{i0} - \sigma_i\dot{\vartheta}_{i0}. \tag{17}$$

In the case when the α_{i0} are so large that each of the spin systems is in equilibrium with the lattice, dividing (17) by α_{i0} and letting $\alpha_{i0}\to\infty$, we obtain $\vartheta_{i0} = 0$. It now follows from (16) that

$$\dot{m}_i^s + \frac{m_i^s}{\tau_{ii}} = 0,$$

where the quantity

$$\tau_{ii} = \frac{1}{f_i(\varkappa_i + \xi_i\lambda_i)} \tag{18}$$

may be defined as the "isothermal"intraspin relaxation time.

B. Let us now assume that the spin systems do not interact with the lattice, i.e., let $\alpha_{i0} = 0$. Then (17) becomes

$$\beta_i\dot{m}_i^z + \sigma_i\dot{\vartheta}_{i0} = 0. \tag{19}$$

Eliminating ϑ_{i0} from (16) and (19), we obtain

$$\dot{m}_i^s + f_i\left(\varkappa_i + \xi_i\lambda_i - \frac{\beta_i^2}{\sigma_i}\right) m_i^s = 0,$$

or

$$\dot{m}_i^s + \frac{m_i^s}{\tau_{ii}^Q} = 0,$$

where the quantity

$$\tau_{ii}^Q = \frac{1}{f_i\left(\varkappa_i + \xi_i\lambda_i - \frac{\beta_i^2}{\sigma_i}\right)} \tag{20}$$

may be defined as the "adiabatic" intraspin relaxation time. The relaxation times τ_{ii} and τ_{ii}^Q are defined in the thermodynamic method with an accuracy characterized by an undetermined factor f_i.

It follows from (18) and (20) that the "isothermal" and "adiabatic" intraspin relaxation times are related by

$$\tau_{ii} = \tau_{ii}^Q\left(1 - \frac{\beta_i^2}{\sigma_i(\varkappa_i + \xi_i\lambda_i)}\right), \tag{21}$$

a relation which does not contain f_i.

C. In order to determine the spin-lattice relaxation time, let us imagine that there is no intraspin relaxation, i.e., that $\tau_{ii} = 0$. Formally, this can be done by going to the limit $f_i\to\infty$. Then dividing (16) by f_i and going to this limit, we have

$$m_i^s = -\beta_i\vartheta_{i0} \,/\, (\varkappa_i + \xi_i\lambda_i).$$

Then from (17) we obtain the following expression describing the heat exchange between the i-th spin system and the lattice:

$$\dot{\vartheta}_{i0} + \frac{\vartheta_{i0}}{\tau_{i0}} = 0,$$

where the quantity

$$\tau_{i0} = \frac{T_0}{\alpha_{i0}} \cdot \frac{\beta_i^2 - \sigma_i(\varkappa_i + \xi_i\lambda_i)}{\varkappa_i + \xi_i\lambda_i} \tag{22}$$

may be defined as the spin-lattice relaxation time.

D. To find the relaxation times between the spin systems, that is, the spin-spin relaxation time, let us assume that the spin systems are isolated from the lattice, i.e., that $\alpha_{i0} = 0$. Heat exchange can now take place only between the spin systems, and, in the absence of an external field, Eqs.(15) for the spin systems become

$$\left.\begin{aligned} \beta_1 \dot{m}_1^z &= \frac{\alpha_{12}}{T_0}\vartheta_{12} - \sigma_1\dot{\vartheta}_{10}, \\ \beta_2 \dot{m}_2^z &= \frac{\alpha_{21}}{T_0}\vartheta_{21} - \sigma_2\dot{\vartheta}_{20}. \end{aligned}\right\} \tag{23}$$

We assume further that heat exchange between the spin systems does not disrupt the equilibrium within each system. Inasmuch as in this case there is no intraspin relaxation, (14) leads to

$$\left.\begin{aligned} (\varkappa_1 + \xi_1\lambda_1)\, m_1^z + \xi_1\lambda_1 m_2^z + \beta_1\vartheta_{10} = 0, \\ (\varkappa_2 + \xi_2\lambda_2)\, m_2^z + \xi_2\lambda_2 m_1^z + \beta_2\vartheta_{20} = 0. \end{aligned}\right\} \tag{24}$$

Eliminating m_1^z and m_2^z from (23) and (24), we arrive at a set of linear homogeneous differential equations of first order for ϑ_{10} and ϑ_{20}. We seek solutions in the form

$$\vartheta_{10} = \vartheta_{10}^0 \exp(-t/\tau) \text{ and } \vartheta_{20} = \vartheta_{20}^0 \exp(-t/\tau),$$

where τ is the spin-spin relaxation time. After appropriate elementary but cumbersome computations, we obtain the expression for τ from the solvability condition for the set.

In the case of paramagnets, when the exchange force fields may be neglected ($\lambda_1 = \lambda_2 = \lambda = 0$),

$$\tau = \Pi_{12}\frac{T_0}{\alpha_{12}} = \frac{K_1 \cdot K_2}{K_1 + K_2} \cdot \frac{T_0}{\alpha_{12}}, \tag{25}$$

where

$$K_i = \frac{\beta_i^2 - \sigma_i\varkappa_i}{\varkappa_i} \quad (i = 1,2). \tag{26}$$

Comparing (22) for $\lambda_i = 0$ with (25), we obtain the relation between the spin-lattice and spin-spin relaxation times, namely,

$$\tau_{i0} = \tau \cdot \frac{\alpha_{12}}{\alpha_{10}}\left(1 + \frac{K_1}{K_2}\right). \tag{27}$$

It is easily shown that K_1/K_2 is equal to the ratio of the specific heats of the spin systems in a constant field. As one may have expected, therefore, we find that in all cases $\tau_{10} > \tau$.

4. Let us apply the above results to paramagnets ($\lambda_1 = \lambda_2 = \lambda = 0$) in a magnetic field. In this case $H^* = H_0$ and $h^* = h$, since internal demagnetization effect can be neglected.

Proceeding according to Shaposhnikov[1], we shall write the nonequilibrium thermodynamic potential of the i-th spin system in the form

$$\Phi_i = -\frac{a_i}{2T} - \frac{TM_i^2}{2b_i} - (\mathbf{M}_i, \mathbf{H}_i + \mathcal{H}_{ik}), \tag{28}$$

where

$$\frac{a_i}{b_i} = \mathcal{H}_i^2, \quad \& \quad [c_i]_M = \frac{a_i}{T_0^2}. \tag{29}$$

Here $\mathcal{H}_i$ is the internal field due to magnetic interaction within the i-th spin system, $\mathcal{H}_{ik}$ is the magnetic field induced by k-th spin system in the i-th spin system, and $[c_i]_M$ is the specific heat of a spin system at constant magnetization. It follows from (28) that the q_i^s defined by (13), all vanish.

Bearing in mind (18), (22), and (25), Eqs.(14) and (15) now become

$$\left.\begin{aligned} \dot{m}_1^s + \frac{m_1^s}{\tau_{11}} + \frac{\beta_1^s}{\varkappa_1}\cdot\frac{\vartheta_{10}}{\tau_{11}} &= \frac{\xi_1}{\varkappa_1}\cdot\frac{h^s}{\tau_{11}} + \gamma_1 [\mathbf{M}_1, \mathbf{H}]_s, \\ \dot{m}_2^s + \frac{m_2^s}{\tau_{22}} + \frac{\beta_2^s}{\varkappa_2}\cdot\frac{\vartheta_{20}}{\tau_{22}} &= \frac{\xi_2}{\varkappa_2}\cdot\frac{h^s}{\tau_{22}} + \gamma_2 [\mathbf{M}_2, \mathbf{H}]_s, \end{aligned}\right\} \tag{30}$$

and

$$\left.\begin{aligned} \beta_1 \dot{m}_1^z &= \frac{K_1}{\tau_{10}}\vartheta_{10} + \frac{\Pi_{12}}{\tau}\vartheta_{12} - \sigma_1\dot{\vartheta}_{10}, \\ \beta_2 \dot{m}_2^z &= \frac{K_2}{\tau_{20}}\vartheta_{20} + \frac{\Pi_{12}}{\tau}\vartheta_{21} - \sigma_2\dot{\vartheta}_{20}, \end{aligned}\right\} \tag{31}$$

where we have taken into account the fact that in (31) $[\mathbf{M}, \mathbf{H}]_z \approx [\mathbf{m}, \mathbf{h}]_z \approx 0$.

Eliminating ϑ_{10}, ϑ_{20} and $\vartheta_{12} = \vartheta_{10} - \vartheta_{20}$ from (30) and (31), we obtain equations for the variable components m_1^z and m_2^z of the magnetizations of both spin systems, namely,

$$B_1\ddot{m}_1^z + A_1\dot{m}_1^z + D_1 m_1^z - \frac{\chi_{01}}{\chi_{02}}\cdot\frac{\Pi_{12}}{K_1}\cdot\frac{\tau_{22}}{\tau_{11}}\cdot\frac{\dot{m}_2^z}{\tau} - \frac{\chi_{01}}{\chi_{02}}\cdot\frac{\Pi_{12}}{K_1}\cdot\frac{m_2^z}{\tau_{11}\tau} = B_1\frac{\chi_{01}}{\tau_{11}}\dot{h}^z +$$

$$+ \frac{\chi_{01}}{\tau_{11}\tau_{10}}h^z + B_1\gamma_1[\dot{\mathbf{M}}_1, \mathbf{H}]_z + B_1\gamma_1[\mathbf{M}_1\dot{\mathbf{H}}]_z + D_1\tau_{11}\gamma_1[\mathbf{M}_1, \mathbf{H}]_z - \frac{\chi_{01}}{\chi_{02}}\cdot\frac{\Pi_{12}}{K_1}\cdot\frac{\tau_{22}}{\tau_{11}}\cdot\frac{\gamma_2}{\tau}[\mathbf{M}_2, \mathbf{H}]_z, \tag{32}$$

and

$$B_2\ddot{m}_2^z + A_2\dot{m}_2^z + D_2 m_2^z - \frac{\chi_{02}}{\chi_{01}}\cdot\frac{\Pi_{12}}{K_2}\cdot\frac{\tau_{11}}{\tau_{22}}\cdot\frac{\dot{m}_1^z}{\tau} - \frac{\chi_{02}}{\chi_{01}}\cdot\frac{\Pi_{12}}{K_2}\cdot\frac{m_1^z}{\tau_{22}\tau} = B_2\frac{\chi_{02}}{\tau_{22}}\dot{h}^z +$$

$$+ \frac{\chi_{02}}{\tau_{22}\tau_{20}}h^z + B_2\gamma_2[\dot{\mathbf{M}}_2, \mathbf{H}]_z + B_2\gamma_2[\mathbf{M}_2, \dot{\mathbf{H}}]_z + D_2\tau_{22}\gamma_2[\mathbf{M}_2, \mathbf{H}]_z - \frac{\chi_{02}}{\chi_{01}}\cdot\frac{\Pi_{12}}{K_2}\cdot\frac{\tau_{11}}{\tau_{22}}\cdot\frac{\gamma_1}{\tau}[\mathbf{M}_1, \mathbf{H}]_z, \tag{33}$$

where we have used the notation

$$B_i = -\frac{\sigma_i}{K_i} = \frac{1}{1 + \frac{H_0^2}{\mathcal{H}_i^2}}, \quad \chi_{0i} = \frac{1}{\varkappa_i} = \frac{b_i}{T_0} \qquad (i = 1,2). \tag{34}$$

$$A_i = \frac{1}{\tau_{ii}} + \frac{1}{\tau_{i0}} + \frac{\Pi_{ik}}{K_i}\cdot\frac{1}{\tau}, \quad D_i = \frac{1}{\tau_{ii}}\left(\frac{1}{\tau_{i0}} + \frac{\Pi_{ik}}{K_i}\cdot\frac{1}{\tau}\right). \tag{35}$$

It is easily shown that Eqs.(32) and (33) are valid also for the total magnetization of each of the spin systems.

In the case in question, the relaxation times of (18), (22), and (25) are, according to (28),

$$\tau_{ii} = \frac{\chi_{0i}}{f_i}; \quad \tau_{i0} = \frac{a_i + b_i H_0^2}{\alpha_{i0} T_0^2} = \frac{[C_i]_H}{\alpha_{i0}}; \quad \tau = \frac{[C_1]_H \cdot [C_2]_H}{[C_1]_H + [C_2]_H} \cdot \frac{1}{\alpha_{12}}. \tag{36}$$

We note that

$$\frac{\Pi_{12}}{K_1} = \frac{1}{1 + \dfrac{\chi_{01}(H_0^2 + \mathcal{H}_1^2)}{\chi_{02}(H_0^2 + \mathcal{H}_2^2)}} \quad \text{and} \quad \frac{\Pi_{12}}{K_2} = \frac{1}{1 + \dfrac{\chi_{02}(H_0^2 + \mathcal{H}_2^2)}{\chi_{01}(H_0^2 + \mathcal{H}_1^2)}}. \tag{37}$$

If II_0 and $\mathrm{h}(t)$ are parallel, Eqs.(32) and (33) become much simpler, since all vector product terms drop out.

5. Let us consider certain behavioral properties of paramagnets whose magnetization is due to a single spin system. In this case, setting $1/\tau = 0$ and dropping index i on B_i and χ_{0i}, we find from (32)

$$B\ddot{m} + \left(\frac{1}{\tau_{11}} + \frac{1}{\tau_{10}}\right)\dot{m} + \frac{m}{\tau_{11}\tau_{10}} = B\frac{\chi_0}{\tau_{11}}\dot{h} + \frac{\chi_0}{\tau_{11}\tau_{10}}h. \tag{38}$$

Recalling that $M = M_0 + m$ and that $H = H_0 + h$, we obtain

$$B\ddot{M} + \left(\frac{1}{\tau_{11}} + \frac{1}{\tau_{10}}\right)\dot{M} + \frac{M}{\tau_{11}\tau_{10}} = B\frac{\chi_0}{\tau_{11}}\dot{H} + \frac{\chi_0}{\tau_{11}\tau_{10}}H. \tag{39}$$

Let us investigate the process whereby equilibrium is established in such a system when the constant external field is cut off (i.e., when $(H = H_0 = 0$ for $t > 0$). We assume that $M = M_0$ at $t = 0$. Then

$$M = M_0 \exp(-t/T) \cdot \operatorname{ch} \Omega t, \tag{40}$$

where

$$\frac{2}{T} = \frac{1}{\tau_{11}} + \frac{1}{\tau_{10}}; \quad \Omega = \frac{1}{T}\sqrt{1 - \frac{\tau_{11}\tau_{10}}{\left(\frac{\tau_{11} + \tau_{10}}{2}\right)^2}}.$$

Eq.(40) describes the relaxation process leading to equilibrium in a "single-spin" paramagnet. For any given values of τ_{11} and τ_{10}, the quantity $\Omega^2 > 0$ and $\Omega T < 1$.

Eq.(40) can be written in the form

$$M = \frac{M_0}{2}(e^{-t/\tau_{11}} + e^{-t/\tau_{10}}).$$

In the presence of a constant magnetizing field H_0 and an alternating field $h = h_0 \exp(j\omega t)$ parallel to it, the solution of (38) is

$$m = \chi h \equiv (\chi' - j\chi'')h,$$

where

$$\frac{\chi'}{\chi_0} = \frac{1 + B\tau_{10}^2\omega^2}{(1 - B\tau_{10}\tau_{11}\omega^2)^2 + (\tau_{10} + \tau_{11})^2\omega^2}, \tag{41}$$

$$\frac{\chi''}{\chi_0} = -\frac{[\tau_{11} + (1 - B)\tau_{10}]\omega + B^2\tau_{11}\tau_{10}^2\omega^3}{(1 - B\tau_{10}\tau_{11}\omega^2)^2 + (\tau_{10} + \tau_{11})^2\omega^2}. \tag{42}$$

The notation F = 1 - B is often used in the literature on paramagnetic relaxation. Eqs. (41) and (42), as may have been expected, are identical with the expressions for χ' and χ'' deduced by Shaposhnikov in Ref. 1 where in a similar problem is considered.

6. Let us now turn to paramagnets, whose magnetic properties are due to two spin systems, subjected to parallel fields H_0 and $h_0 \exp(j\omega t)$. Setting

$$m_i = m_{0i} \exp(j\omega t),$$

in Eqs. (32) and (33), we obtain

$$(D_1 - B_1\omega^2 + j\omega A_1)\, m_{01} - \frac{\chi_{01}}{\chi_{02}} \cdot \frac{\Pi_{12}}{K_1}(1 + j\omega\tau_{22}) \frac{m_{02}}{\tau_{11}\tau} = \frac{\chi_{01}}{\tau_{11}\tau_{10}}(1 + jB_1\omega\tau_{10})\, h_0 -$$

$$- \frac{\chi_{02}}{\chi_{01}} \cdot \frac{\Pi_{12}}{K_2}(1 + j\omega\tau_{11}) \frac{m_{01}}{\tau_{22}\tau} + (D_2 - B_2\omega^2 + j\omega A_2)\, m_{02} = \frac{\chi_{02}}{\tau_{22}\tau_{20}}(1 + jB_2\omega\tau_{20}) h_0. \qquad (43)$$

Solving (43) for the magnetizations m_{01} and m_{02}, we obtain

$$m_{01} = \chi_1 h_0, \quad m_{02} = \chi_2 h_0,$$

where

$$\left.\begin{aligned} \chi_1 &= \frac{\frac{\chi_{01}}{\tau_{11}\tau_{10}}(1 + jB_1\omega\tau_{10})(D_2 - B_2\omega^2 + j\omega A_2) + \chi_{01}\frac{\Pi_{12}}{K_1}}{(D_1 - B_1\omega^2 + j\omega A_1)(D_2 - B_2\omega^2 + j\omega A_2) - \frac{\Pi_{12}^2}{K_1 K_2}} \times \frac{\frac{1}{\tau_{11}\tau_{22}\tau_{20}\tau}(1 + jB_2\omega\tau_{20})(1 + j\omega\tau_{22})}{\frac{1}{\tau_{11}\tau_{22}\tau^2}(1 + j\omega\tau_{11})(1 + j\omega\tau_{22})} \\ \chi_2 &= \frac{\frac{\chi_{02}}{\tau_{22}\tau_{20}}(1 + jB_2\omega\tau_{20})(D_1 - B_1\omega^2 + j\omega A_1) + \chi_{02}\frac{\Pi_{12}}{K_2}}{(D_1 - B_1\omega^2 + j\omega A_1)(D_2 - B_2\omega^2 + i\omega A_2) - \frac{\Pi_{12}^2}{K_1 K_2}} \times \frac{\frac{1}{\tau_{11}\tau_{22}\tau_{10}\tau}(1 + jB_1\omega\tau_{10})(1 + j\omega\tau_{11})}{\frac{1}{\tau_{11}\tau_{22}\tau^2}(1 + j\omega\tau_{11})(1 + j\omega\tau_{22})}. \end{aligned}\right\} \qquad (44)$$

Eqs. (44) can be simplified bearing in mind that $\tau_{ii} \ll \tau \ll \tau_{i0}$.

In strong constant fields, when $H_0 \gg \mathcal{H}_i$, the total susceptibility $\chi = \chi_1 + \chi_2$ of the paramagnet is given by

$$\frac{\chi}{\chi_0} = \frac{\frac{1}{\tau_{10}\tau_{20}} + \frac{1}{\tau\tau^*} + i\left(\frac{1}{\tau} + \frac{1}{\tau^*}\right)\omega}{\frac{1}{\tau_{10}\tau_{20}} + \frac{1}{\tau\tau^*} - \frac{\omega^2}{\tau_{11}\tau_{22}} + i\omega\left(\frac{1}{\tau_{10}} + \frac{1}{\tau_{20}} + \frac{1}{\tau}\right)}, \qquad (45)$$

where

$$\frac{\chi_{01}}{\tau_{10}} + \frac{\chi_{02}}{\tau_{20}} = \frac{\chi_0}{\tau^*}, \quad \frac{\chi_{01}}{\tau_{11}} + \frac{\chi_{02}}{\tau_{12}} = \frac{\chi_0}{\tau_{12}}, \qquad (46)$$

and $\chi_0 = \chi_{01} + \chi_{02}$ is the total static susceptibility of the paramagnet. If the constant field is so weak that $H_0 \ll \mathcal{H}_i$, then

$$\frac{\chi}{\chi_0} = \frac{\frac{1}{\tau_{11}\tau_{22}\tau_{10}\tau_{20}} + \frac{1}{\tau_{11}\tau_{22}T_{12}\tau} - \frac{\omega^2}{\tau_{12}}\left(\frac{1}{\tau_{10}} + \frac{1}{\tau_{20}} + \frac{1}{\tau}\right) - \frac{\omega^2}{\tau_{11}\tau_{22}} + i\frac{\omega}{\tau_{11}\tau_{22}}}{\frac{1}{\tau_{11}\tau_{22}\tau_{10}\tau_{20}} + \frac{1}{\tau_{11}\tau_{22}T_{12}\tau} - \frac{\omega^2}{\tau_{11}\tau_{22}} + i\frac{\omega}{\tau_{11}\tau_{22}}\left(\frac{1}{\tau} + \frac{1}{\tau_{10}} + \frac{1}{\tau_{20}}\right) - i\omega^3} \times$$

$$\times \frac{\left(\frac{1}{\tau_{10}} + \frac{1}{\tau_{20}} + \frac{1}{\tau}\right) + i\frac{\omega}{\tau_{12}}\left(\frac{1}{T_{12}\tau} - \omega^2\right)}{\left(\frac{1}{\tau_{11}} + \frac{1}{\tau_{22}} + \frac{1}{\tau}\right)}, \qquad (47)$$

where τ_{12} is given by (46), and

$$\frac{1}{T_{12}} = \frac{\Pi_{12}}{K_1} \cdot \frac{1}{\tau_{10}} + \frac{\Pi_{12}}{K_2} \cdot \frac{1}{\tau_{20}}. \qquad (48)$$

In the limit as $\tau \to \infty$, the solutions of (45) and (47) describe a paramagnet with two noninteracting spin systems which exchange heat only with the lattice.

7. Let us now assume that the alternating field $\mathbf{h} = \mathbf{h}_0 \exp(j\omega t)$ and the constant field $\mathbf{H}_0 \equiv \{0,0,H_z\}$ are mutually perpendicular. In the case of a paramagnetic system, the coefficients β_i^s from (10) and (28) are

$$\beta_i^x = 0, \quad \beta_i^y = 0, \quad \beta_i^z = \frac{H_0}{T_0}.$$

Eqs.(30) for the transverse components of the variable part of the magnetization now give

$$\begin{aligned} \dot{\mathbf{m}}_1 + \frac{\mathbf{m}_1}{\tau_{11}} &= \chi_{01}\,\mathbf{h} + \gamma_1 [\mathbf{M}_1, \mathbf{H}], \\ \dot{\mathbf{m}}_2 + \frac{\mathbf{m}_2}{\tau_{22}} &= \frac{\chi_{02}}{\tau_{22}}\,\mathbf{h} + \gamma_2 [\mathbf{M}_2, \mathbf{H}], \end{aligned} \tag{49}$$

where $\mathbf{m} \equiv (m_x, m_y)$ and $\mathbf{h} \equiv (h_x, h_y)$. The equations for the z components of $\mathbf{m}_1$ and $\mathbf{m}_2$ are obtained from (32) and (33).

It is remarkable that the spin-lattice and spin-spin relaxation times (τ_{i0} and τ) do not enter explicitly into Eqs.(49) for a paramagnet. Since the z components of $\mathbf{M}_1$ and $\mathbf{M}_2$ entering into (49) are given by equations which contain τ_{i0} and τ explicitly, the transverse components of $\mathbf{m}_1$ and $\mathbf{m}_2$ actually do depend on the τ_{i0} and τ, although only in the second approximation. The relaxation time τ will enter directly into (49) only if exchange force field is taken into account ($\lambda \neq 0$).

It can be shown that under certain assumptions Eqs.(49) retain the same form for ferromagnets as well.

Neglecting m_z as compared to M_0, Eq.(49) can be solved in the first approximation independently of the equations for the longitudinal components of the spin-system magnetizations. Then

$$\mathbf{m}_i = \chi_i \mathbf{h} + j [\mathbf{g}_i \mathbf{h}] \qquad (t = 1; 2) \tag{50}$$

where

$$\chi_i = \chi_0 \frac{1 + j\omega\tau_{ii} + \omega_i^2 \tau_{ii}^2}{(1 + j\omega\tau_{ii})^2 + \omega_i^2 \tau_{ii}^2}, \tag{51}$$

and

$$g_i = \chi_{0i} \frac{\gamma_i\, \omega\tau_{ii}^2}{(1 + j\omega\tau_{ii})^2 + \omega_i^2 \tau_{ii}^2} H_0; \tag{52}$$

here the χ_0 are complex susceptibilities and the g_i are the complex gyration vectors of the two spin systems.

The total susceptibility and gyration vector of the paramagnet are

$$\chi = \chi_1 + \chi_2 \text{ and } g = g_1 + g_2. \tag{53}$$

Separating the χ_i and g_i into their real and imaginary parts

$$\chi_i = \chi_i' - j\chi_i'' \text{ and } g_i = \rho_i' - j\rho_i'',$$

we obtain

$$\frac{\chi_i'}{\chi_0} = \frac{(1 + \tau_{ii}^2 \omega_i^2)^2 + (1 - \tau_{ii}^2 \omega^2)\, \tau_{ii}^2 \omega^2}{[1 + \tau_{ii}^2 (\omega_i^2 - \omega^2)]^2 + 4\tau_{ii}^2 \omega^2}, \tag{54}$$

$$\frac{\chi_i''}{\chi_0} = \frac{[1 + \tau_{ii}^2 (\omega_i^2 + \omega^2)]\, \tau_{ii}\, \omega}{[1 + \tau_{ii}^2 (\omega_i^2 - \omega^2)]^2 + 4\tau_{ii}^2\, \omega^2}, \tag{55}$$

$$\rho_i' = \chi_{0i} \frac{[1 + \tau_{ii}^2 (\omega_i^2 - \omega^2)]\, \gamma_i \tau_{ii}^2\, \omega}{[1 + \tau_{ii}^2 (\omega_i^2 - \omega^2)]^2 + 4\tau_{ii}^2\, \omega^2} H_0, \tag{56}$$

$$\rho_i'' = \chi_{0i} \frac{2\gamma_i\, \tau_{ii}^3\, \omega^2}{[1 + \tau_{ii}^2 (\omega_i^2 - \omega^2)]^2 + 4\tau_{ii}^2\, \omega^2} H_0. \tag{57}$$

The quantities χ_i', χ_i'', ρ_i' and ρ_i'' determine the magnetic and gyromagnetic properties of the paramagnet.

As is clear from the above, for the transverse components of the variable part of the magnetization in a single-spin system one should take one of Eqs. (49). The equation for the z component in this case is obtained from (32) in the limit as $\tau \to \infty$, namely

$$B\ddot{m}_z + \left(\frac{1}{\tau_{11}} + \frac{1}{\tau_{10}}\right)\dot{m}_z + \frac{1}{\tau_{11}\tau_{10}} m_z = B\gamma_1 [\dot{\mathbf{M}}, \mathbf{H}]_z + B\gamma_1 [\mathbf{M}, \dot{\mathbf{H}}]_z + \frac{1}{\tau_{10}} \gamma_1 [\mathbf{M}, \mathbf{H}]_z, \tag{58}$$

where B is given by (34). An approximate solution of (58) can be obtained by using one of Eqs. (50) for m_x and m_y. This gives

$$m_z = -\chi_0 \frac{\tau_{11}^4\, \omega^2 \omega_1^2}{[1 + \tau_{11}^2 (\omega_1^2 - \omega^2)]^2 + 4\tau_{11}^2\, \omega^2} \cdot \frac{h^2}{H_0}. \tag{59}$$

Let us compare Eqs. (49) for the transverse components of the magnetization with the Landau-Lifshits and Bloch equations. The Landau-Lifshits equation is

$$\dot{\mathbf{M}} = \gamma [\mathbf{M}, \mathbf{H}] - \frac{\lambda_0}{M^2} [\mathbf{M}, [\mathbf{M}, \mathbf{H}]];$$

for the case of a strong constant field $H_0 = H_z$, when one may assume that $M_z \approx M_0 = \chi_0 H_0$, inasmuch as $\mathbf{M} = \mathbf{M}_0 + \mathbf{m}$, we can, taking $\frac{1}{\tau_1} = \frac{\lambda_0}{\chi_0}$, rewrite the above equation in the form

$$\dot{\mathbf{m}} + \frac{\mathbf{m}}{\tau_1} = \frac{\chi_0}{\tau_1} \mathbf{h} + \gamma [\mathbf{M}, \mathbf{H}], \tag{60}$$

where $\mathbf{m} \equiv (m_x, m_y)$.

Comparing (60) with (49), we see that they agree if τ_1 is understood to mean the intraspin relaxation time. The Landau-Lifshits equation for the longitudinal component of the magnetization

$$\mathbf{m}_z = \gamma [\mathbf{M}, \mathbf{H}]_z$$

differs greatly from Eq. (58).

Eqs. (49) differ from the Bloch equations employed in the theory of nuclear induction. These equations are

$$\dot{M}_{x,y} = \gamma [\mathbf{M}, \mathbf{H}]_{x,y} - \frac{M_{xy}}{T_2} \text{ and } \dot{M}_z = \gamma [\mathbf{M}, \mathbf{H}]_z - \frac{M_z - M_0}{T_1}. \tag{61}$$

In contrast to Eqs. (49) and (60), the Bloch expressions for the transverse components of the magnetization contain no terms proportional to the alternating field strength. Eq. (58) for the longitudinal component

$M_z = M_0 + m_z$ goes over to an equation of a form analogous to that of the corresponding Bloch equation only for frequencies such that $\omega^2 \tau_{11} \tau_{10} \gg 1$.

We note that the longitudinal relaxation time in our case is not the spin-lattice relaxation time, but the time T which is obtained by combining τ_{11} and τ_{10}, according to the scheme

$$\frac{2}{T} = \frac{1}{\tau_{11}} + \frac{1}{\tau_{10}} .$$

An analysis of the application of the present theory to ferromagnets will be published elsewhere.

Ural Polytechnic Institute and
Sverdlovsk Medical Institute

References

1. I.G.Shaposhnikov, Zhur.eksp.i teor.fiz., 17, 824 (1947); 18, 533 (1948); 19, 225 & 577 (1949).
2. H.Casimir & F.duPre, Physica, 5, 507 (1938).
3. Sh.Z.Khlebopros, Doklady AN, Uzbek SSR, No.11, 8 (1953).

PARAMAGNETIC RESONANCE ABSORPTION OF ULTRASOUND IN SOME SALTS OF THE RARE EARTH ELEMENTS

- S.A.Al'tshuler, M.M.Zaripov & L.Ia.Shekun

1. The theory of ultrasonic paramagnetic resonance has been analyzed by one of the authors[1,2]. Whereas ordinary paramagnetic resonance is observed in two crossed magnetic fields (strong static and weak alternating fields), in ultrasonic resonance ultrasound is used instead of the alternating magnetic field. The nature of the mechanism by which ultrasound is absorbed is the same as that of the mechanism of paramagnetic lattice relaxation associated with single phonon processes. In both cases the energy exchange between the spin system and lattice vibrations occurs due to the spin-lattice interaction obtaining when the usual resonance condition is satisfied. This condition is that the energy separation of the magnetic sublevels be equal to the phonon energy. The magnitude of the acoustic paramagnetic resonance effect can be evaluated from the following formula for the ultrasonic absorption coefficient (see Eqs.(1), (4) and (5) in Ref.2):

$$\sigma = \frac{4\pi^2 N \nu^2}{\rho \nu_{1/2} v^3 kT} \left| F_{\alpha\beta} \right|^2; \qquad (1)$$

Here ρ is the density of the paramagnet, T is its temperature, v is the velocity of sound in it, N is the number of magnetic particles per unit volume, $\nu_{1/2}$ is the half-width of the absorption line, and ν is the ultrasonic frequency; α and β are the magnetic sublevels between which the transitions responsible for the effect occur. The matrix element $F_{\alpha\beta}$ of the operator entering into the expression for the spin-lattice interaction energy is given by

$$F_{\alpha\beta} = \sum r^2 \left(\frac{\partial U}{\partial x} \right)_{\alpha\beta}, \qquad (2)$$

where U is the interaction energy between the magnetic atom under consideration and the nearest particle, r is the distance between these particles, and x is the component of r along the sound propagation direction. The summation is carried out over nearest particles. In this way, the calculation of the absorption coefficient σ for various substances reduces to a computation of the matrix elements $F_{\alpha\beta}$. Such calculations have been given in Refs. 1 & 2 for typical salts of rare earth and iron group elements. It was assumed in these calculations that the spin-lattice interaction is caused by modulation of the electric field of the crystal by the lattice vibrations. The cases of magnetic and exchange interactions have also been analyzed. It was found that a very large effect could be expected in substances containing rare-earth ions with an even number of electrons. An evaluation was also made of nuclear acoustic magnetic resonance. It was found that in solid dielectrics the effect due to quadrupole interaction should be about 10^6 times greater than that caused by magnetic dipole interaction.

A number of interesting deductions follow from a comparison of the acoustical effect with ordinary magnetic resonance. It was established, in particular, that the ultrasonic paramagnetic absorption coefficient is usually much greater than the absorption coefficient for an rf field.

The lower sensitivity of ultrasonic equipment, however, and particularly, the difficulty of generating ultrasound of sufficiently high frequency seriously hamper observation of the acoustical effect. It is, therefore, expedient to apply indirect, as well as direct experimental methods to studying this effect. One such procedure is the saturation of ordinary paramagnetic resonance by means of ultrasound. This was the procedure recently used by Proctor and Tanttila[3] in an experimental study of quadrupole acoustic resonance

in $NaClO_3$ single crystals. The intensity of the rf absorption line was reduced very appreciably when the ultrasonic transducer was excited at the transition frequency.

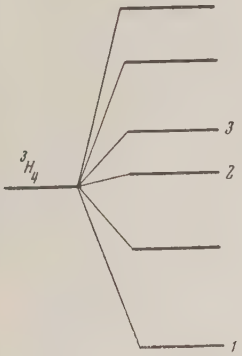

Fig.1. Splitting of the ground term of Pr^{3+} in ethyl sulfate.

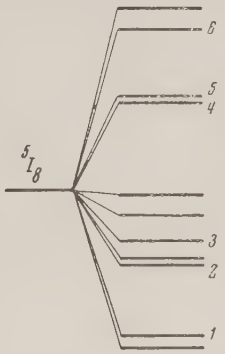

Fig.2. Splitting of the ground term of Ho^{3+} in ethyl sulfate.

In the present report we shall consider in detail the resonance absorption of ultrasound in some rare-earth salts. We chose rare-earth salts for three reasons. First, the acoustical effect in them is very large, so that an investigation of the relative magnitude of the effect for different elements is of definite interest. Second, no effective method has yet been found for studying spin-lattice interaction in rare-earth compounds; the acoustical resonance method may prove highly convenient in this regard. Third, in rare-earth salts one may expect a strong effect for transitions between hyperfine sublevels of the singlet electron states.

2. Thanks to the work of the Oxford group[4], we have considerable experimental and theoretical information on the rare-earth ethyl sulfates. We shall, therefore, first consider these substances. Let us begin with the elements whose triply charged ions contain an even number of electrons. The ground level of such an ion in ethyl sulfate splits into singlets and doublets.

We have determined the energy levels and wave functions in the usual manner[5].

By way of example, we present the splitting scheme of the ground levels of the Pr^{3+} and Ho^{3+} ions in Figs.1 and 2. The separation of the Stark sublevels is of the order of 10-100 cm^{-1}. The ground level of Eu^{3+} does not split, since the total angular momentum quantum number J = 0. We, therefore, calculated the splitting of the lowest excited state, namely $^7F_1$.

All the calculations pertain to an electric field with trigonal symmetry. In view of the Jahn-Teller effect, the actual symmetry of the field will be lower than that calculated and each of the doublets will split. This splitting, however, will be small compared to the Zeeman splitting in the magnetic fields usually used. Measurements have shown[6] that the Jahn-Teller splitting of the ground state doublet in Pr^{3+} in the ethyl sulfate is about 0.04 cm^{-1}.

The absorption coefficients σ_l for ultrasonic longitudinal waves as calculated by Eq.(1) are listed in arbitrary units in the accompanying table. The absorption coefficient σ_t for transverse sound waves is related to σ_l by the equation $4\sigma_l = 9\sigma_t$.

In calculating the $F_{\alpha\beta}$ we used the results of Shekun[7].

The coefficients σ were calculated for the case in which the sound is propagated perpendicularly to the crystal axis. When the propagation direction is along the crystal axis, $\sigma = 0$ for all of the doublets. In view of the initial (Jahn-Teller effect) doublet splitting, it is necessary to use ultrasonic frequencies not lower than 10^8-10^9 cps in practice. When the magnetic field is turned on, the splitting of the doublets increases.

Absorption coefficient for ultrasonic longitudinal waves in the ethyl sulfates of rare-earth elements, as calculated according to Eq.(1).

Ion	Doublet No.	Energy*, cm^{-1}	σ_l/ν^2	Ion	Doublet No.	Energy*, cm^{-1}	σ_l/ν^2
	1	0	1,0		1	4	4,3
Pr^{3+}	2	170	5,2		2	47	9,3
	3	212	1,0	Ho^{3+}	3	60	88,3
Eu^{3+}	1	270	471,0		4	139	0,0
					5	141	0,9
	1	7	2,2		6	197	88,3
Tb^{3+}	2	24	6,2				
	3	26	35,8		1	14	3,3
	4	50	6,2	Tm^{3+}	2	26	7,1
					3	98	29,1
					4	129	7,9

*The energy of the lowest level is taken as zero.

When the phonon energy is less than the Jahn-Teller splitting, although no resonance peak will be observed, σ will still depend on the field, i.e., will monotonically decrease with increasing H. It should be noted that a magnetic field perpendicular to the crystal axis shifts the doublet sublevels much less than a field parallel to the axis, since $g_\perp$ is zero for all doublets (quadratic Zeeman effect).

It will be seen from the table that the greatest absorption will be evinced by europium in the excited state.* Next in order of decreasing absorption are holmium, terbium and thulium (ground state).

Let us try to evaluate the absolute absorption for the specific case of the lowest lying doublet of Pr^{3+}, using Eq.(1). According to Shekun[7], $F_{\alpha\beta} \approx$ 2500 cm^{-1}. It may be assumed that in the undiluted rare-earth ethyl sulfate, the concentration of magnetic ions is $N = 3 \cdot 10^{21}$. At T = 20°K (the usual temperature in resonance experiments on rare-earth salts), $\nu_{1/2} = 8.4 \cdot 10^8$ sec^{-1}. Then assuming that $\rho = 3.5$ g-cm^{-3} and $v = 2.3 \cdot 10^5$ cm-sec^{-1}, we obtain $\sigma = 8.4 \cdot 10^{15} \nu^2$ cm^{-1}. We thus see that even at a frequency of about 10^7 cps the sound absorption shall be noticeable.

In addition to ethyl sulfate, the double nitrates of the rare-earths have been studied in some detail. The experiments have shown that the ground state in the double nitrate of praseodymium is a doublet. The eigenfunctions are similar to those of ethyl sulfate. Thus the coefficients σ will be of the same order of magnitude as in the latter salts.

We must turn briefly to rare-earth ions with odd numbers of electrons. In this case the matrix element of F becomes nonzero only in the second approximation in the magnetic field, since the doublets are of the Kramers type. The absorption probability will be multiplied by $(g\beta H/\Delta)^2$, where Δ is the splitting in the crystal field, β is the Bohr magneton, and g is the Lande g-factor. In this case the presence of a magnetic field is necessary for ultrasonic absorption, whereas in the case of ions with even numbers of electrons the function of the magnetic field is merely to modify the sublevel separation. If we take $\Delta = 170$ cm^{-1} (the distance between the low doublets in neodymium ethyl sulfate), then at T = 20°K we obtain $\sigma = 3 \cdot 10^{-39} \nu^4$ cm^{-1}, $h\nu = g\beta H$. We see that in this case the frequency dependence is much stronger than it is for even-electron ions. The absorption will increase greatly if there exist close-lying Stark sublevels. Thus, for instance, it is known that in cerium ethyl sulfate the two lowest doublets are separated by only 3 cm^{-1}, and, in this case, we obtain $\sigma = 10^{35} \nu^4$ cm^{-1} (at T = 20°K).

3. As has already been noted, the state of an ion characterized by an integral value of J splits into singlets and doublets in an electric field.

*It should be borne in mind that at the low temperatures required for paramagnetic resonance measurements (see Al'tschuler[1]) the population of the excited state is insignificant.

It is seen from the above that the Jahn-Teller splitting makes the experimental observation of ultrasonic resonance absorption at doublet levels difficult, since the required frequencies are of the order of 10^8-10^9 cps.

It is possible nevertheless to study ultrasonic absorption at lower frequencies. To show this, let us consider ultrasonic absorption at single electron energy levels. We shall bear in mind that every single-electron level is degenerate with respect to the nuclear spin. The magnetism of an atom in such a state will, in the first approximation, be purely nuclear. In the second approximation, the other electron energy levels may contribute to the magnetic moment of the atom (through interaction of the electrons with the nucleus and through the constant magnetic field) and the atomic magnetic moment will not be purely nuclear. Specifically, the magnitude magnetic moment μ will depend on the hyperfine structure constant and on the electron energy level separation. The order of magnitude of μ is given by

$$\mu \approx A\beta/\Delta.$$

It follows from this that the actual magnetic moment lies somewhere between the nuclear and electronic values.

Thus as regards both position and intensity of the absorption lines, the paramagnetic resonance effect associated with transitions between sublevels of the hyperfine structure will lie somewhere between the electronic and nuclear paramagnetic resonance effects. This question has been investigated in detail by Zaripov[5]; he showed that when the constant magnetic field is directed along the Z axis (i.e., the crystal axis), the hyperfine energy levels are described by the spin Hamiltonian

$$H_c = aI^2 + b\beta HI_z + P\left[I_z - \frac{1}{3}I(I+1)\right] - \gamma\beta_N HI_z, \qquad (3)$$

where a and b are constants dependent on A and Δ,P is the quadrupole coupling constant and I is the nuclear spin.

We note that the spin Hamiltonian used for calculating the hyperfine structure constants is derived in the same way as it is for ions of the iron group, whose lowest Stark level is a singlet. Determining the eigenvalues of (3) in the usual way, we obtain I + 1/2 doublets in the absence of a constant field, with an average separation between the doublets of about 0.001 cm^{-1}. It follows from this that if the ultrasound is absorbed due to transitions between the hyperfine structure levels, frequencies of the order of 10^7 cps may be used to observe the effect experimentally.

We have mentioned above that the calculation of ultrasonic resonance absorption necessitates computing the matrix elements $F_{\alpha\beta}$, where α and β now denote the wave functions of the hyperfine structure levels. We have performed this calculation for the lowest simple Pr^{3+} level and for the ground state of Ho^{3+}, using Zaripov's[5] wave functions. No absorption is obtained with zeroth approximation wave functions, since the nuclear parts of the wave functions are orthogonal. It is therefore necessary to use the wave functions of the next approximation. In this case the nonzero matrix elements $F_{\alpha\beta}$ are those between neighboring sublevels of the hyperfine structure. Thus the selection rules for the acoustical effect are the same as for ordinary paramagnetic resonance.

For Pr^{3+}, we obtained $F_{\alpha\beta} = 10^{-4}$ cm^{-1}. Unfortunately, the magnetic moment of the Ho nucleus is not known. If we assume it equal to that of the Pr nucleus, we obtain $F_{\alpha\beta} = 0.75$ cm^{-1} for the ground state of Ho^{3+}. We note

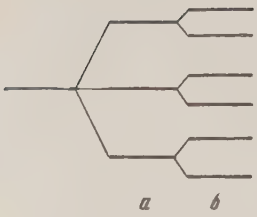

Fig.3. Splitting of the singlet electron level in Pr^{3+}: (a) due to interaction with the nuclear spin and (b) due to the external magnetic field.

that the magnitude of $F_{\alpha\beta}$ does not depend on the polarization of the sound wave.

In the present case the half-width of the absorption curves should be much less than in electron resonance. To estimate the absorption coefficient, we shall assume that $\nu_{1/2} = 10^5$ sec^{-1} at a temperature of 20°K in crystals magnetically diluted in the ratio 1:100. For Pr^{3+}, we then obtain $\sigma_l = \sigma_t = 2\cdot10^{-20}\nu^2$ cm^{-1}.

Absorption takes place only for sound propagating at right angles to the crystal axis. The low population of the simple level and the relatively small absorption coefficient make it unlikely that the effect can be detected experimentally in Pr^{3+}.

For Ho^{3+} we obtain $\sigma_l = \sigma_t = 1.5\cdot10^{-16}\nu^2$ cm^{-1}; in this case we note that the transverse polarized wave will be absorbed when the sound propagates parallel to the crystal axis, and the longitudinally polarized wave will be absorbed when the propagation is perpendicular to the crystal axis. Judging by the magnitude of σ one might expect to observe significant acoustic resonance absorption in Ho^{3+} at frequencies of the order of $3\cdot10^7$ cps. It is not possible, unfortunately, to indicate the resonance value of the constant magnetic field for the given frequency, since the nuclear magnetic moment of holmium is not known.

"V.I.Ul'ianov'Lenin Kazan" State University

References

1. S.A.Al'tshuler, Zhur.eksp.i teor.fiz., 28, 38 (1955).
2. S.A.Al'tshuler, Zhur.eksp.i teor.fiz., 28, 49 (1955).
3. W.G.Proctor & W.H.Tanttila, Phys.Rev., 98, 1854 (1955).
4. B.Bleaney & K.W.H.Stevens, Rep.Progr.Phys., 16, 108 (1953); K.D.Bowers & J.Owen, Rep.Progr.Phys., 18, 304 (1955).
5. M.M.Zaripov, Thesis, Kazan State University, 1955.
6. B.Bleaney & H.D.E.Scovil, Phil.Mag., 43, 999 (1952).
7. L.Ia.Shekun, Thesis, Kazan State University, 1956.

AN APPROXIMATE METHOD OF SECOND QUANTIZATION IN THE QUANTUM THEORY OF MAGNETISM

- N.N.Bogoliubov & S.Ia.Tiablikov

Investigations of equilibrium properties generally involves the problem of calculating the sum-over-states, and this requires knowledge of the corresponding energy spectrum. It is exceptionally difficult to calculate the energy spectrum of ferromagnets and it therefore becomes necessary to take recourse to a more or less simplified approach and approximate methods. In the present communication we wish to describe some research we have undertaken on this problem.

The evolution of approximate methods can be logically resolved into two stages. These are 1) the construction of a simplified "model" Hamiltonian which reproduces the characteristic features of the dynamic system being treated and 2) formulation of an approximate method for handling this simplified Hamiltonian.

The first problem is solved in the following way.[1] We begin with the exact second quantized Hamiltonian of the system. As a set of basis functions we choose "atomic" wave functions of the same type as in the "strongly bound electron" approximation in the single-electron treatment. Inasmuch as these atomic functions are initially not orthogonal, because of the partial overlap of the electron shells, we orthogonalize them by a special procedure. In this orthogonalization process "nonorthogonality integrals," whose values are significant primarily only for nearest neighbor atoms, appear in a natural way. If one deals with a complete set of functions, one obtains only a transformation from one form of the Hamiltonian to another, and the problem is no easier to solve. In actual calculations, therefore, we use only some of the atomic wave functions. We may argue the physical validity of this type of approximation (based on concepts such as those developed by Ritz) by remarking that the most important contribution to the lowest part of the energy spectrum of the whole system comes from the atomic wave functions in the lowest unfilled shells. In the above mentioned investigation,[1] for instance, we make the following approximations. We take into account only the wave functions of the d-electrons and assume that there is only one (additional) electron per atom, which electron is regarded as an s-electron. Such an obviously too restrictive assumption is not, however, needed in order to make use of the method described, and we have made it only from considerations of simplicity. With these assumptions the simplified Hamiltonian becomes

$$\mathcal{H} = \sum L(f\nu;\, f'\nu)\, a^{+}_{f\nu} a_{f'\nu} + \frac{1}{2} \sum F(f_1\nu_1,\, f_2\nu_2,\, f'_1\nu_1,\, f'_2\nu_2)\, a^{+}_{f_1\nu_1} a^{+}_{f_2\nu_2} a_{f_1'\nu_1} a_{f'_2\nu_2}, \qquad (1)$$

where f is the number of the lattice site and ν is the spin quantum number of the corresponding electron. If we were to make our model physically more meaningful by including several atomic wave functions, the index to ν would have to include not only the spin, but also the orbital angular momentum number.

We shall now apply the approximate method described in Ref.2 to the simplified Hamiltonian of Eq.(1). Let us imagine that we have the situation where the Fermi amplitudes $a_{f\nu}$ are replaced by classical quantities. Then, instead of determining the ground state of the $\mathcal{H}$ operator, we could treat the problem of minimizing the given classical form of E_o and then examine a second variation (the expression for which can be diagonalized) which will

give what might be called "small oscillations about the equilibrium position". We note that similar considerations are frequently invoked in quantum field theory in the adiabatic and strong coupling approximations. We advance this kind of fictitious assumption only in order to find some substitutions of variables, which are then later performed with the Fermi commutation rules of the quantum operators $a_{f\nu}$ taken into account. In this procedure the first problem that arises is that of finding the approximate ground state wave function corresponding to the formal replacement

$$a_{f,\nu} \to \theta_0(f, \nu), \quad \overset{+}{a}_{f,\nu} \to \overset{*}{\theta}_0(f, \nu). \tag{2}$$

It is easily seen, however, that if we perform the linear canonical transformation

$$a_{f,\nu} = \sum_{(\omega)} \theta_\omega(f, \nu)\, a_{f\omega}, \tag{3}$$

which gives the Hamiltonian in terms of the $a_{f\omega}$ instead of the $a_{f\nu}$, and then proceed by Fock's method taking an approximate wave function for which

$$n_{f\omega} = \begin{cases} 1, & \omega = 0, \\ 0, & \omega \neq 0; \end{cases} \tag{4}$$

then the $\theta_0(f, \nu)$ we are led to by the condition that the form be a minimum are given by just those equations which correspond to the formal replacement of Eq.(2). The functions $\theta_\omega(f, \nu)$ are constructed in a special way from the $\theta_0(f, \nu)$.

In order to evaluate the accuracy and establish a criterion for the applicability of this method, we shall operate with $\mathcal{H}$ in terms of the $a_{f,\omega}$.

In improving the zeroth approximation (4), let us assume that for the true wave functions of the ground state and weakly excited states these conditions are fulfilled approximately in the sense that the probability that $n_{f,0} \neq 1$ and $n_{f,\omega} \neq 0\ (\omega \neq 0)$ will be small. We then introduce the new operators

$$b_{f,\omega} = \overset{+}{a}_{f,0}\, a_{f,\omega}, \quad \overset{+}{b}_{f,\omega} = \overset{+}{a}_{f,\omega} a_{f,0}. \tag{5}$$

Here we have the question of the transformation of the Hamiltonian to the new variables and of the commutation rules of the new operators.

Simple calculations lead to the following commutation rules for the $b_{f,\omega}$:

$$\left.\begin{aligned} &b_{f_1,\omega_1} b_{f_2,\omega_2} - b_{f_2,\omega_2} b_{f_1,\omega_1} = 0; \\ &b_{f_1,\omega_1} \overset{+}{b}_{f_2,\omega_2} - b_{f_2,\omega_2} b_{f_1,\omega_1} = \delta_{f_1,f_2}\delta_{\omega_1,\omega_2} n_{f_1,0} - \delta_{f_1,f_2} \overset{+}{a}_{f_1,\omega_1} a_{f_2,\omega_2}. \end{aligned}\right\} \tag{6}$$

The basic approximation which we make in transforming the expression for $\mathcal{H}$ rests on the assumption that for any given site it is more probable that $n_{f,0} = 1$, than that $n_{f,\omega} = 1$ for $\omega \neq 0$. Examining the commutation relations, we see that the term $\overset{+}{a}_{f_1,\omega_1} a_{f_1,\omega_2}$ fails to vanish automatically when acting on a wave function only if the argument $n_{f,0}$ equals zero, but according to our assumption, the probability that $n_{f,0} = 0$ is small. Hence, in accord with our approximation we can replace the exact commutation relation (6) by the approximate one

$$b_{f_1,\omega_1} \overset{+}{b}_{f_2,\omega_2} - \overset{+}{b}_{f_2,\omega_2} b_{f_1,\omega_1} = \delta_{f_1,f_2}\delta_{\omega_1,\omega_2}. \tag{7}$$

An analogous approximation applied to the Hamiltonian gives

$$\mathcal{H} = E_0 + \sum (\lambda_\omega(f) - \lambda_0(f)) \overset{+}{b}_{f,\omega} b_{f,\omega} + \sum S(f_1, f_2; \omega_1, \omega_2) \overset{+}{b}_{f_1,\omega_1} b_{f_2,\omega_2} +$$

$$+ \frac{1}{2} \sum R(f_1, f_2; \omega_1, \omega_2) \overset{+}{b}_{f_1,\omega_1} \overset{+}{b}_{f_2,\omega_2} + \frac{1}{2} \sum \overset{*}{R}(f_1, f_2 \cdot \omega_1, \omega_2) b_{f_1,\omega_1} b_{f_2,\omega_2}, \qquad (8)$$

where λ_0, λ_ω are the eigenvalues of the equation for the θ_0, θ_ω which we have not written out explicitly due to lack of space, and S and R are certain functions of L, F, θ_0 and θ_ω; we note that in Eq. (8) $\omega \neq 0$.

It is interesting to note that Eq. (8) coincides with the form given by the second variation in the above-mentioned quasi-classical treatment.

Since in the given approximation the Hamiltonian $\mathcal{H}$ is a quadratic form of Bose operators, it is readily diagonalized.

The linear transformation

$$b_{f,\omega} = \sum \{u_k(f, \omega) \xi_k + \overset{+}{\xi}_k \overset{*}{v}_k(f, \omega)\} \qquad (9)$$

leads to the new Bose amplitudes ξ_k, $\overset{+}{\xi}_k$, in terms of which the Hamiltonian $\mathcal{H}$ takes on the diagonal form

$$\mathcal{H} = E_0 - \sum E(k) |v_k(f, \omega)|^2 + \sum E(k) \overset{+}{\xi}_k \xi_k, \qquad (10)$$

where $E(k)$ are the eigenvalues obtained in the diagonalization of the quadratic form of Eq. (8), and $u_k(f, \omega)$ and $v_k(f, \omega)$ are the corresponding eigenvectors.

The transition to the ξ_k, $\overset{+}{\xi}_k$ which diagonalizes the Hamiltonian also allows of a more rigorous formulation of the applicability of the approximation used to transform $\mathcal{H}$. In terms of the variables ξ we can consider the excited states of the system to be a set of elementary excitations or "quasi-particles" obeying Bose statistics. The number of such particles in the state k is $n_k = \overset{+}{\xi}_k \xi_k$ and the energy of each individual elementary excitation is $E(k)$. The average values of the occupation numbers $\bar{n}_k$ are given by the usual Bose distribution

$$\bar{n}_k = \left\{\exp\left(\frac{E(k)}{\vartheta}\right) - 1\right\}^{-1}.$$

The applicability of the method we have used to transform the Hamiltonian from an expression in Fermi amplitudes to one in Bose amplitudes rests on the assumption that the mathematical expectation value of $n_{f,\omega}$ (with $\omega \neq 0$) of the occupation number for the excited states at a given lattice site is much less than unity, so that the expressions

$$\overline{(1 - n_{f,0})}, \quad \overline{[(1 - n_{f_1,0})(1 - n_{f_2,0})]_{f_1 \neq f_2}}, \ldots$$

must be small quantities of increasing order of smallness. Noting that

$$\bar{n}_{f,\omega} = \sum_{(k)} \{|u_k(f, \omega)|^2 + |v_k(f, \omega)|^2\} \bar{n}_k + \sum_{(k)} |v_k(f, \omega)|^2,$$

we see that the mean numbers $\bar{n}_{f,\omega}$ may be considered small quantities only for weakly excited states ($\bar{n}_k \ll 1$) and only if the condition

$$\sum_{(k)} |v_k(f, \omega)|^2 \ll 1 \qquad (11)$$

is also fulfilled.

By calculating $\overline{n_{f_1,\omega_1} n_{f_2,\omega_2}}$, one can readily show that $\overline{[(1-n_{f_1,0})(1-n_{f_2,0})]_{f_1 \neq f_2}}$ will be of an order of smallness greater by one than $\overline{(1-n_{f,0})}$, etc. Therefore (11) is the applicability condition for the approximate second quantization method, since all the considerations apply to states close to the ground state.

We applied this method of calculating the energy spectrum of weakly excited states to the theory of ferromagnetism; in this case it led to the familiar results of Bloch's spin wave theory. When account is taken in the Hamiltonian of spin-spin and spin-orbit interactions[3], it becomes possible to calculate the temperature and field dependences of the magnetic anisotropy constants[4,5] and the magnetostriction[6].

We have also applied the method here described to the theory of antiferromagnetism[2]. The treatment was based on the well known model of Neel, according to which the sign of the exchange integral is negative for nearest neighbors in antiferromagnets, so that neighboring spins are antiparallel. It is found that the energy of the elementary excitations depends linearly on the wave vector. The results obtained for the magnetization and susceptibility of an isotropic antiferromagnet[7] in a weak field are similar to those obtained by the quasiclassical calculation of Hulten, namely,

$$M \approx H(1 - CT^2), \quad \chi \approx 1 - CT^2, \tag{12}$$

while for strong fields $M \approx M_0(1 - CT^{3/2})$. Calculations for uniaxial antiferromagnets, performed by Amatuni[8], gave results which are in qualitative agreement with the experimental data. In particular, it has been shown that in fields below a certain critical field value, $\chi_{11} \sim T^{1/2} e^{-\frac{a}{T}}$ in agreement with the results of Ziman, Tessman and Kubo. At fields above the critical value, the susceptibility χ_{11} is finite at T = 0 and passes through a minimum as a function of T, which agrees with the experiments of Paulis and Hardemann.

Above we have considered only an ideal lattice. Bonch-Bruevich[9] has carried out an interesting generalization of the spin wave method to the case of a lattice with defects.

Recently a promising new approach has been developed for investigating the case when the Hamiltonian is written as a scalar product of spin operators. For this case Dyson[10] developed a profound and interesting method which is based essentially on the introduction of collective variables. Dyson suggested that instead of the individual spins per se, the variables treated be their Fourier transforms, in terms of which the Hamiltonian is more easily diagonalized. In this method the most important problem is that of eliminating excess states. For its solution Dyson developed a method which is especially effective in the low temperature region. We feel that further investigation based on combination of Dyson's ideas with the described concepts of second quantization holds great promise.

Another interesting generalization of this type is the development of methods which would make it possible to obtain sufficiently accurate results for high and low temperatures and also allow of interpolation for intermediate temperatures. Some preliminary results in this direction have been obtained by one of the present authors and V.V.Tolmachev[11].

Physics Department of
Moscow State University

References

1. N.N.Bogoliubov & S.V.Tiablikov, Vestnik (Review) Moscow State University, No.3, 35 (1949).
2. N.N.Bogoliubov & S.V.Tiablikov, Zhur.eksp.i teor.fiz., 19, 256 (1949).
3. N.N.Bogoliubov & S.V.Tiablikov, Zhur.eksp.i teor.fiz., 19, 251 (1949).
4. S.V.Tiablikov, Zhur.eksp.i teor.fiz., 20, 661 (1950).
5. S.V.Tiablikov & A.A.Gusev, FMM (Physics of Metals and Metallography), 2, 385 (1956).
6. A.A.Gusev, Zhur.eksp.i teor.fiz., 29, 181 (1955).
7. S.V.Tiablikov, FMM (Physics of Metals and Metallography), 2, 193 (1956).
8. A.D.Amatuni, Thesis, Moscow State University, 1956.
9. V.L.Bonch-Bruevich, FMM (Physics of Metals and Metallography), 2, 215 (1956).
10. F.Dyson, Phys.Rev., 102, 1217 (1956).
11. V.V.Tolmachev & S.V.Tiablokov, Doklady AN SSSR, 108, 1029 (1956).

QUANTUM MECHANICAL TREATMENT OF FERROMAGNETISM IN METALS OF THE TRANSITION GROUPS

- S.V.Vonsovskii

1. The distinctive physical and chemical properties of metals, alloys and compounds of elements of the transition groups in the crystalline state are associated with the specific structure of the atomic electron shells of these elements, namely, with the presence of unfilled d- and f-shells in the isolated atoms. Analysis of the properties of atoms and ions in question shows that these are determined not only by the usual valence electrons but also by the electrons in the unfilled inner shells. Naturally, these inner shell electrons also play an active part in determining the different physical properties of molecules and crystals composed of these transition group elements.

The energy spectrum of a system of interacting valence and internal electrons in such crystals is characterized in the region close to the ground state by a far greater diversity of elementary excitations than in crystals devoid of such elements. It is, of course, true that the strong interaction between the former valence electrons in the crystal and the inner electrons makes it impossible to divide them arbitrarily into two strictly independent groups. From simple phenomenological considerations and analysis of the experimental data on the electric and magnetic properties of these crystals, however, one may assert that there exist two types of bands in the energy spectrum of elementary excitations in such crystals. One set of excitations is determined primarily by the active participation of the inner electrons. In the usual exchange theory of ferromagnetism these quasi-particles are Bose ferromagnons (spin waves). The other excitations, in contrast, are associated primarily with the valence electrons which are in the strong "field" due not only to the ions with filled electron shells but also to the inner electrons in the unfilled shells. In transition metals and alloys this part of the energy spectrum is constituted by "current excitations", i.e., conduction electrons, which form a gas of Fermi quasiparticles*; in semiconductors and semimetals a significant role is also played by exciton type excitations. In addition, there exists a phonon branch of Bose elementary excitations associated with the collective motion of the ionic lattice. Thus in the weak excitation region (low temperatures) macroscopic bodies containing elements of the transition groups behave, in the statistical thermodynamic sense, as a complex mixture of ideal gases of various types of quasiparticles (conduction electrons, excitons, phonons, ferromagnons, etc.). It is impossible, however, to associate each type of quasiparticle with the collective motion of any particular definite group of initial particles of the crystal; rather one should regard the quasiparticles as a result of the motion of the system as a whole.

2. Since it is practically impossible to find a rigorous solution to the complicated quantum mechanical problem of a crystal, quantitative results must always be obtained by developing some approximate model. As has been shown by Dirac,[1] the part of the Hamiltonian of a system of interacting

---

*It should be noted that there does not yet exist a rigorous multiple-electron treatment of metallic crystals whose ground state is not separated by an energy gap from the elementary "current" excitations. Usually these last are identified with thermally excited electrons and holes of the ideal Fermi gas with effective masses differing from those of the corresponding free particles.

electrons which depends on the spin (exchange energy) is of the form

$$\hat{H}_{ex} = -\frac{1}{2}\sum_{q,\,q'} I_{q,q'}(1 + \hat{S}_q \hat{S}_{q'}), \tag{1}$$

where $\hat{S}_q$ is the spin vector operator at the q-th lattice site and $I_{q,q'}$ is the matrix element of the energy operator (exchange integral), dependent on the specific properties of the electron system. The problem in approximate calculation is first to determine the form of the exchange integral. But precisely in the case of crystals containing ions of the transition groups it is highly incorrect to consider merely the "exchange" term in the operator of Eq.(1), since this does not take into account the properties of the electron system which are largely determined by the presence of conduction electrons, excitons, etc.

In his report at the Washington Conference on Magnetism, Slater[2] pointed out the inconsistency of the model which makes use of the Hamiltonian given in (1). He showed that this model cannot explain ferromagnetism even if one disregards the distinctive features of the electron structure of transition element atoms, since in taking account of the nonorthogonality of the atomic functions one must include the configuration interaction with polar states and this cannot be done by means of the operator of (1). Therefore when dealing with transition elements it is particularly important to start with a more accurate expression for the Hamiltonian of the system of interacting electrons. In its second quantized form, this operator may be written (see, for instance, Bogoliubov[3])

$$\hat{H} = \sum_{f,f'} L(f, f')\,\hat{a}_f^{+}\hat{a}_{f'} + \frac{1}{2}\sum_{f_2,f_2,f_1',f_2'} F(f_1, f_2; f_1', f_2')\,\hat{a}_{f_1}^{+}\hat{a}_{f_2}^{+}\hat{a}_{f_2}\hat{a}_{f_1}, \tag{2}$$

where f is the set of quantum numbers of individual-electron states in which the many-electron functions are expanded, L and F are, respectively, the matrix elements of the additive and binary parts of the energy operator, and $\hat{a}_f^{+}$ and $\hat{a}_f$ are the Fermi second quantization operators. To find the eigenvalues and eigenfunctions of this operator in general is, of course, a hopeless task, since it is, apparently, impossible to diagonalize the binary part of the operator generally.

There are at present two many-electron approximations which have received wide attention. These are, first, the Heitler-London-Heisenberg generalized model (HLHGM) which makes use of atomic (localized) single-particle functions to approximate the operator of (2), and second, the collective electron model which uses collective individual-electron Bloch functions. In the rigorous solution of the problem any choice of a complete set of individual-electron functions is entirely equivalent to any other choice. In view of unavoidable approximations related to the cut-off in the expansion of the many-electron wave function in the complete set of antisymmetrized products of the individual-electron wave functions, however, these models yield different results. Hence they cannot be applied indiscriminately: either one or the other can expediently be applied to crystals of a given type or even to a given energy band in a given crystal. The HLHGM model can be reasonably applied to those cases in which the ground state of a given band of the spectrum is not a conduction state and has a homogeneous distribution of the electron charge (semiconductors, ferromagnetic dielectrics, etc.), as well as to systems in which the current carriers in the ground state constitute a boson "gas" (semimetals and metals whose electric conductivity in the low temperature region departs from the T^5 law). The collective electron

model is applicable to typical metals in which the ground state corresponds to the presence of Fermi current carriers and is not separated by a finite energy gap from the elementary conduction excitations.

Mathematically speaking, the first effect of choosing one or another of the above types of approximation is to specify the meaning of the indices f and f' and to determine the matrix elements of L and F. After this the principal term of (2), which defines the ground state, is separated out, and the remaining part is diagonalized. The diagonal part gives the energy of the elementary excitations (dispersion relations), and the small non-diagonal elements describe the collision processes between quasiparticles. One must, of course, proceed carefully, since there always exists the danger that the results obtained will be strongly affected by the special features of the model chosen. It therefore becomes necessary to prove the universality of the different many-electron system properties under consideration and to show that these properties are not "sensitive" to the mathematical approximations. We believe that success can be achieved if one makes use of the currently developing method of the collective description of interactions, which was first introduced in describing the vibrations of electron plasma (see, for instance, Bohm and Pines[4]). According to this method different "overtones" of the complex motion of the many-electron and ion system are treated as collective and individual degrees of freedom of the electron and ion charge density. Since in quantum mechanics the electric charge density of particles is much richer in content than in classical electrodynamics, we are able to obtain many different kinds of quantum collective motions in a many-particle system. In addition to oscillations of the quasiclassical charge density, we must account also for oscillations of the exchange density (ferromagnons) and oscillations of the quantum transition density (nonconduction and conduction excitons).

3. For a first version of an approximate calculation it has been found helpful to use a "mixed" representation of (2) for crystals containing elements of the transition groups or their compounds. In this model the valence electrons are described by Bloch functions

$$\psi_{k,\sigma}(r, \sigma) = \alpha e^{ikr} u_k(r) c_\sigma(s), \quad (f \to k\sigma), \tag{3}$$

where k is the wave vector ("quasimomentum"), r is the radius vector, s is the spin coordinate, and σ is the spin quantum number. The inner electrons are described by localized atomic functions

$$\varphi(r - n) c_\sigma(s) \quad (f \to n, \sigma), \tag{4}$$

where n is the radius vector of the lattice site. This "hybrid" s-d model[5,6] makes it possible to obtain different bands of the electron-ion energy spectrum in crystals composed of transition atoms and to give a unified interpretation of all the static and kinetic "anomalies" of these substances.

If one neglects the biquadratic terms for conduction electrons (or assumes the self-consistent field approximation*), and introduces the homeopolar condition for the inner electrons (that is, assumes that at each lattice site there is always one and only one "internal" electron with a given

---

*A certain justification for this is furnished by the results of Bohm and Pines[4] and Kinoshita & Nambu[7].

spin projection*), which means that

$$\sum_{\sigma} \hat{a}^{+}_{n,\sigma} \hat{a}_{n,\sigma} = 1, \tag{5}$$

then for ferromagnets at low temperatures it is possible to go over from Fermi amplitudes $a_{n,\delta}$ to Bose amplitudes $\hat{b}_g$ for the inner electrons in (2), while retaining the Fermi amplitudes for the conduction electrons. As a result we obtain[6]

$$\hat{H} = U_0 + \sum_{k} \varepsilon_k \hat{N}^{+}_{k} + \sum_{k} \varepsilon_k \hat{N}^{-}_{k} - \sum_{k} I(k, k)\, \hat{N}_k + \sum_{q} \varepsilon_q \hat{N}_q + O, \tag{6}$$

where O is the highest order term containing three-, four-fold, etc., products of the operators

$$\sim \hat{a}^{+}_{k,\sigma} \hat{a}_{k',\sigma'}, \hat{b}_g,$$
$$\sim \hat{a}^{+}_{k,\sigma} \hat{a}_{k',\sigma'}, \hat{b}^{+}_{g},$$
$$\sim \hat{a}^{+}_{k,\sigma} \hat{a}_{k',\sigma'}, \hat{b}^{+}_{g} \hat{b}^{+}_{g}$$
$$\cdots\cdots\cdots$$

Here ε_k and ε_g are the energies of a conduction electron and a ferromagnon, respectively, g is the wave vector of a ferromagnon, $\hat{N}^{+}_{k}$, $\hat{N}^{-}_{k}$ and $\hat{N}_g = \hat{b}^{+}_{g} \hat{b}_g$ are occupation number operators for conduction electrons with right (+) and left (-) spin and ferromagnons, respectively, and $I(k, k)$ is the s-d exchange integral. The term with $I(k, k)$ and higher order terms which appear in (6) show mathematically how, within the framework of the model chosen, the ferromagnon "field" acts on the conduction electrons. If the diagonal part of (6) is separated out by unitary operators, the energy we obtain for states close to the ground state will be that of a mixture of two ideal gases, namely,

$$E_0 = U_0 + \sum_{k} \varepsilon^{+}_{k} N^{+}_{k} + \sum_{k} \varepsilon^{-}_{k} N^{-}_{k} + \sum_{g} \varepsilon^{*}_{g} N_g, \tag{7}$$

where ε^{+}_{k}, ε^{-}_{k} and ε^{*}_{g} are the renormalized quasiparticle energies. If we are interested in the case of complete saturation with $N_g = 0$, then

$$(\varepsilon^{+}_{k})_0 = \varepsilon_k \quad \text{and} \quad (\varepsilon^{-}_{k})_0 = \varepsilon_k - I(k, k).$$

The difference between these energies, which is equal to $I(k, k)$, defines the interaction of the conduction electrons with the "vacuum" of the ferromagnon "field". In the higher temperature region (close to the Curie point but still far from the temperature at which the Fermi gas becomes degenerate) one may use the energy centroid approximation for the ferromagnon subsystem, in which case the conduction electron energy becomes

$$\varepsilon^{\sigma}_{k} = \varepsilon_k - \frac{1}{2}(1 + \vec{\sigma}\vec{\mu})\, I(k, k), \tag{8}$$

where $\vec{\mu}$ is the mean magnetic moment of the inner electrons per lattice site and $\vec{\sigma}$ is the spin vector of the outer electron ($\sigma = \pm 1$). In the effective-mass approximation (8) becomes

$$\varepsilon^{\sigma}_{k} = -\alpha' \vec{\sigma}\vec{\mu} + (\beta + \beta' \vec{\sigma}\vec{\mu})(ak)^2, \tag{9}$$

---

*Actually there are several inner electrons at each site, but taking this into account would not appear to alter the qualitative results significantly - see Ref.8.

where α', β and β' are constants with the dimensions of energy (exchange and transfer integrals), and a is the lattice constant. According to (9), in the first approximation the effective mass of a conduction electron is

$$m^*(\sigma) = \frac{\hbar^2}{2a^2(\beta - \beta'\vec{\sigma}\vec{\mu})}. \quad (10)$$

It is most significant that this quantity is a function of the magnetic moment $\vec{\mu}$ of the inner electrons, so that close to the Curie point, where $d\mu/dT$ is large, there should occur a significant change in the velocity distribution of the conduction electrons with changes in temperature. This is the basic reason for the ferromagnetic anomalies of the static and kinetic properties of ferromagnets.

With the aid of this model, the present author and a group of Sverdlovsk theoretical physicists were able to explain many anomalous properties of ferromagnetic metals. Among these were the temperature dependence of the spontaneous magnetization of metals, alloys, and compounds near the Curie point,[5-9] the phenomenon of "fractionality" of the atomic magnetic moments,[5-10] the temperature dependence of the electric conductivity of ferromagnets close to the Curie point,[5] the anomalous optical,[11] magneto-optical,[12] photoelectric,[13] thermoelectric,[14] and galvanomagnetic[15] properties of ferromagnets, the thermal conductivity and the characteristics of sound absorption in ferromagnets,[16] and anomalies in the x-ray spectrum.[17] In addition, the magnetic interaction of electrons has been accounted for within the framework of this model.[18]

In the low-temperature region, the inclusion of higher order terms in (6) has made it possible to calculate kinetic effects in ferromagnets (electric conductivity,[19-20] thermal conductivity,[21] relaxation times,[22] the width of the ferromagnetic resonance absorption line,[23] etc.) and to find those parts of them which are due to the collision of ferromagnons with other quasiparticles.

Despite positive results achieved with its aid, the s-d exchange model (SDEM) has certain deficiencies. First, it incorrectly excludes interaction terms for conduction electrons, and second, it takes no account whatsoever of the point symmetry of the electron density in the crystal or of structural details of the electron shell of the initial atoms comprising the ferromagnet. In addition, as has been shown in recent neutron diffraction studies of ferromagnetic metals (see, for instance, Lowde[24] and Elliott[25]), the HLHGM is more valid for ferromagnets than the collective-electron model. In view of this it would seem desirable to continue trying to improve the SDEM with the aim of eliminating as many of the rough approximations as possible.

4. The SDEM can be used more effectively in carrying out calculations for ferromagnetic or antiferromagnetic semiconductors, since in this case it is easy to determine the ground state of the outer electrons and to take into account their elementary excitations. The first attempt at such generalization of the SDEM was undertaken by the author together with Seidov in giving a many-electron interpretation of the phenomenon of indirect exchange in ionic compounds.[26] This generalization has been further developed by Irkhin and Turov.[27] Essentially, this generalization consists of combining the SDEM with the generalized polar model of a semiconductor proposed earlier by the author.[28] It is assumed that at each lattice site there is in the ground state a single inner (d) electron and two outer electrons with antiparallel spins. In a closed outer electron shell excitation of the system may cause a transition of the electrons to an excited (for example, the p) state, whereas when the inner electrons are excited, ferromagnons are produced. The Hamiltonian of such a system can be written as a sum of separate terms in

the form

$$H = \hat{H}^d + \hat{H}^{sp} + \hat{H}^{spd}, \tag{11}$$

where, as in (6), $\hat{H}^d$ refers only to the inner electrons, $\hat{H}^{sp}$ only to the outer ones, and $\hat{H}^{spd}$ describes the interaction between the inner and outer electrons.

We consider only weakly excited states of the system and use the overlap integral of the wave functions from different sites as the small parameter in terms of which to expand the results. We then obtain two independent bands of elementary excitations for the outer electrons, namely, Bose quasiparticles which carry no current and Fermi current carriers. At low temperature the operator is of the form

$$\hat{H} = H_0 + \hat{H}^{\mathrm{M}} + \hat{H}^{\mathrm{B}} + \hat{H}^{\Phi} + \hat{H}^{\mathrm{MB}} + \hat{H}^{\mathrm{B}\Phi}(\varepsilon^3) + \hat{H}^{\mathrm{M}\Phi}(\varepsilon^3) + \ldots, \tag{12}$$

where H_0 is the ground state energy, $\hat{H}^{\mathrm{M}}$, $\hat{H}^{\mathrm{B}}$ and $\hat{H}^{\Phi}$ are the ferromagnon, Bose exciton and Fermi exciton energy operators of the outer electron system, and $\hat{H}^{\mathrm{MB}}$ is the ferromagnon-Bose exciton interaction operator. The operators which give the interaction of the ferromagnons with both types of excitons ($\hat{H}^{\mathrm{B}\Phi}$ and $\hat{H}^{\mathrm{M}\Phi}$) are of higher order in the small parameter (indicating a kind of "insulation" of the Bose and Fermi excitons). It now becomes possible to calculate all the kinetic processes in ferromagnetic semiconductors at low temperatures.

As has been pointed out above, however, at temperatures close to the Curie point the inner electrons can be approximated by the energy centroid method. Then (12) becomes

$$\hat{H} = H_0 + \hat{H}^{\mathrm{B}_0} + \hat{H}^{\mathrm{B}_1} + \hat{H}^{\Phi} + \hat{H}^{\mathrm{B}\Phi}(\varepsilon^3), \tag{13}$$

where $\hat{H}^{\mathrm{B}_0}$ and $\hat{H}^{\mathrm{B}_1}$ are operators which describe Bose quasiparticles with spin 0 and 1, respectively. As opposed to what occurs in the low-temperature case, these Bose energy bands of the spectrum are independent (up to second order terms). The coefficients which enter into the various terms of (13) depend on the magnetization of the crystal.

In solving the above problem, the following were the principal results obtained.

A. The spin-zero Bose exciton band of the energy spectrum is wider than the spin-one Bose exciton band. This is in agreement with the results of Merrifield[29], who used configuration-space methods to evaluate the singlet and triplet exciton energy band widths.

B. The magnetization effect of Bose excitons of the triplet band (with $\sigma = 1$) at temperatures $T \lesssim \theta$ (θ is the Curie point) is described by

$$\mu_{\mathrm{B}_1} \approx \mathrm{sh}\left(\frac{\Delta J_{sp}}{\varkappa T}\mu\right),$$

where $\Delta J_{sp} = J_s - J_p$ is the energy difference of the exchange integrals between the inner d electrons, on the one hand, and the outer s or p electrons, on the other, and $\varkappa$ is Boltzmann's constant. If $\Delta J_{sp}\,\mu \ll \varkappa T$, then $\mu_{\mathrm{B}_1} \sim \mu$.

C. The electric conductivity δ of the Fermi band of the energy spectrum ("holes" in the s shell and p electrons) is found to depend on the magnetization of the ferromagnet according to

$$\delta \sim e^{-\frac{\alpha}{\varkappa T}}\left[e^{\frac{\gamma}{\varkappa T}\mu}+e^{-\frac{\gamma}{\varkappa T}\mu}\right], \tag{14}$$

where α and γ are constants with the dimensions of energy and are dependent on the width of the energy "gap" between the s and p conduction bands. If $\gamma\mu \ll \varkappa T$, then

$$\frac{\delta(\mu)-\delta_0}{\delta_0} \sim \mu^2. \tag{15}$$

On the other hand, if $\gamma\mu > \varkappa T$ (in which case $e^{-\frac{\gamma\mu}{\varkappa T}} \ll e^{\frac{\gamma\mu}{\varkappa T}}$) then

$$\ln\delta(\mu) \sim \ln\delta_0 + \gamma\mu, \tag{16}$$

which means that in the neighborhood of θ the straight-line plot of ln δ as a function of 1/T should change slope. This would seem to be in qualitative agreement with the experimental results of Komar and Kliushin[30] for ferrites.

D. The magnetization of the Fermi excitons in the ferromagnon field is also found to be proportional to the magnetization of the inner electrons.

5. It is also of interest to consider the application of the SDEM to semimetals, i.e., to crystals which in the ground state are characterized by a low spontaneous polarization (ionization) of electrons from filled shells or from the impurities. It has often been hypothesized in the literature that such spontaneous polarization, since we are dealing with a metal, is either impossible or is so weak that it is pointless to speak of it. This point of view has been expounded most fully by Mott.[31] The arguments used, however, are based on classical considerations of the constant energy A necessary to form an electron-hole pair. It is forgotten, however, that in a system of interacting electrons we are dealing specifically with quantum laws ("widening" of energy bands) which can lead to partial spontaneous polarization in the ground state, characteristic of semimetals. Back in 1934-1936, the author in collaboration with Shubin[33] deduced the dependence of the ground state energy of a crystal on the "degree of polarization" s; specifically it was shown that an energy minimum (that is, a ground state energy) may be realized not only for s = 0 and s = s_{max}, but also for intermediate values of s.

6. The development of the SDEM in the last case is being pursued further. In conclusion it may be noted that the theoretical bases and concrete results of the SDEM can be improved and extended significantly if one makes use of the general theory of energy spectra of interacting systems of quantum particles (see, for instance, Bonch-Bruevich[33]) or of quantum field theory methods[7] and the collective description of interactions in many-electron systems.[4] In addition, the set of single-electron wave functions must be made more accurate, taking into account both the specific properties of the electron shells of isolated atoms and the point symmetry of the crystal. Finally, a more accurate diagonalization of the operator of Eq.(2) is necessary, as well as a more accurate allowance for the individual degrees of freedom of the electron-ion system.

Institute of the Physics of Metals of the
Ural Branch of the USSR Academy of Sciences

References

1. P.Dirac, The Principles of Quantum Mechanics (In Russ.Trans. M., 1957).
2. J.C.Slater, Rev.Mod.Phys., 25, 199 (1953).
3. N.N.Bogoliubov, Lektsii z kvantovoi statistiki (Lectures on quantum statistics) (Ukrainian) (Kiev, 1949).
4. D.Bohm & D.Pines, Phys.Rev., 82, 625 (1951); 85, 338 (1952); 92, 609 (1953).
5. S.V.Vonsovskii, Zhur.eksp.i teor.fiz., 16, 981 (1946).
6. S.V.Vonsovskii & E.A.Turov, Zhur.eksp.i teor.fiz., 24, 419 (1953).
7. T.Kinoshita & J.Nambu, Phys.Rev., 94, 498 (1954).
8. E.I.Kondorskii & A.Pakhomov, Doklady AN SSSR, 96, 1139 (1954).
9. K.B.Vlasov & S.V.Vonsovskii, FMM (Physics of Metals & Metallography), 2, 403 (1956).
10. S.V.Vonsovskii & K.B.Vlasov, Zhur.eksp.i teor.fiz., 25, 327 (1953).
11. S.V.Vonsovskii & A.V.Sokolov, Zhur.eksp.i teor.fiz., 19, 615 (1949).
12. S.V.Vonsovskii & A.V.Sokolov, Zhur.eksp.i teor.riz., 19, 703 (1949).
13. S.V.Vonsovskii & A.V.Sokolov, Doklady AN SSSR, 76, 197 (1950); S.V. Vonsovskii, A.V.Sokolov & A.Z.Veksler, Usp.fiz.nauk, 56, 477 (1955); A.Z.Veksler, Zhur.eksp.i teor.fiz., 29, 201 (1955).
14. A.V.Sokolov & A.Z.Veksler, Zhur.eksp.i teor.fiz., 25, 215 (1953).
15. S.V.Vonsovskii & K.P.Rodionov, Doklady AN SSSR, 75, 643 (1950); N.P. Patrakhin, Izv. AN SSSR, Ser.fiz., 16, 584 (1952); S.V.Vonsovskii, L.Ia.Kobelev & K.P.Rodionov, Izv. AN SSSR, Ser.fiz., 16, 569 (1952).
16. A.I.Rezanov, Izv. AN SSSR, Ser.fiz., 16, 581 (1952); Doklady AN SSSR, 82, 885 (1952); A.I.Rezanov, Symposium dedicated to the 70th anniversary of Academician A.F.Ioffe, Pub. AN SSSR, M.-L., 1950.
17. A.V.Sokolov, Zhur.eksp.i teor.fiz., 28, 326 (1955).
18. E.A.Turov, Doklady AN SSSR, 98, 945 (1954).
19. S.V.Vonsovskii, Zhur.eksp.i teor.fiz., 18, 190 (1948); A.I.Rezanov, Doklady AN SSSR, 92, 935 (1953).
20. E.A.Turov, Izv. AN SSSR, Ser.fiz., 19, 474 (1955). (Trans. in Bulletin, 19, No.4, 426.)
21. A.I.Rezanov & V.I.Cherepanov, Doklady AN SSSR, 93, 641 (1953).
22. E.A.Turov, Izv. AN SSSR, Ser.fiz., 19, 462 (1955). (Trans in Bulletin, 19, No.4, 414).
23. E.A.Turov & S.V.Vonsovskii, Zhur.eksp.i teor.fiz., 24, 501 (1953).
24. R.D.Lowde, Proc.Roy.Soc., 235, 305 (1956).
25. R.J.Elliott, Proc.Roy.Soc., 235, 289 (1956).
26. S.V.Vonsovskii & Iu.M.Seidov, Doklady AN SSSR, 107, 37 (1956).
27. Iu.P.Irkhin & E.A.Turov, FMM (Physics of Metals and Metallography), 4, 9 (1957).
28. S.V.Vonsovskii, Zhur.tekh.fiz., 25, 2022 (1955).
29. R.E.Merrifield, J.Chem.Phys., 23, 402 (1955).
30. A.P.Komar & V.V.Kliushin, Izv.AN SSSR, Ser.fiz., 18, 400 (1954). (Trans. Bulletin, 18, No.3, 96.)
31. N.F.Mott, Proc.Phys.Soc., A 62, 416 (1949).
32. S.P.Shubin & S.V.Vonsovskii, Sow.Phys., 7, 292 (1935).
33. V.L.Bonch-Bruevich, Zhur.eksp.i teor.fiz., 25, 417 (1953).

SOME REMARKS CONCERNING THE BLOCH SPIN WAVE THEORY

- Z. Semadeni

In 1930 Bloch* described a method for approximate solution of the problem of the exchange interaction between the electrons in an ideal crystal according to the Heitler-London-Heisenberg method. This made it possible to determine the energy eigenvalues $\varepsilon_p\,(p = 1, \ldots, N)$, the sum-over-states

$$Z = \sum_{r=0}^{N} \sum_{n_1+\ldots+n_N=r} \exp\left\{\frac{NH\mu - \sum_{p=1}^{N} n_p(\varepsilon_p + 2H\mu)}{kT}\right\} = \sum_{r=0}^{N} Z_r \tag{1}$$

(where N is the number of electrons, H is the magnetic field strength, and μ is the Bohr magneton) and the mean magnetization from the formula

$$\overline{M}(H_1 T) = kT\,\frac{\partial \ln Z}{\partial H}.$$

By further calculation and going to the limit $H \to 0$ Bloch obtained his well-known formula

$$\overline{M}(0, T) = N\mu\left[1 - \left(\frac{T}{\theta}\right)^{3/2}\right]. \tag{2}$$

These calculations are, however, of an approximate nature, and more accurate analysis shows that this approximate treatment involves two errors.

The first error lies in the fact that the first sum in Eq. (1) is changed from $\sum_{r=0}^{N}$ to $\sum_{r=0}^{\infty}$. Bloch justified this change of limits by noting that in view of the condition $\varepsilon_p + 2H\mu > 0$, the series

$$\sum_{r=0}^{\infty} \sum_{n_1+\ldots+n_N=r} \prod_{p=1}^{N} \exp\left\{-\frac{n_p}{kT}(\varepsilon_p + 2H\mu)\right\} = \prod_{p=1}^{N} \sum_{n_p=0}^{\infty} \left[e - \frac{\varepsilon_p + 2H\mu}{kT}\right]^{n_p} \tag{3}$$

converge and since N is a very large number, the difference between the sum to N and the limit $N = \infty$ should be very small. This argument is incorrect in view of the fact that for the ground state energy level $\varepsilon_0 = 0$, we have $\lim_{H \to 0} e^{-\frac{\varepsilon_0 + 2H\mu}{kT}} = 1$. Although the series of Eq. (3) converges, the residual sums $\sum_{r=N+1}^{\infty}$ increase without bound as $H \to 0$ (for lattices of all the types considered by Bloch).

The second error is easily evinced in the case of a linear chain. It consists of replacing the Riemann sum

$$\overline{M}(H, T) = N\mu - 2\mu \sum_{p=0}^{N-1} \frac{1}{\exp\left\{\frac{2J_1\left(1 - \cos\frac{2\pi_p}{N}\right) + 2H\mu}{kT}\right\} - 1} \tag{4}$$

by the integral

$$\overline{M}(H, T) \approx N\mu - 2\mu \int_0^{N-1} \frac{dp}{\exp\left\{23\left(1 - \cos\frac{2\pi p}{N}\right) + 2\alpha\right\} - 1}, \tag{5}$$

---

*F. Bloch, ZS.f.Phys., 61, 206 (1930).

where $\alpha = \frac{H\mu}{kT}$ and $\beta = \frac{I_1}{kT}$.

It is known that the difference between the integral $\int_a^b f(x)\,dx$ and the Riemann sum $\sum_{k=1}^{n} f(x_k)(x_k - x_{k-1})$ with the division $\pi = [a = x_0 < x_1 < \ldots < x_n = b]$ is at most equal to the mean oscillation

$$\Omega(\pi) = \sum_{k=1}^{n} (M_k - m_k)(x_k - x_{k-1}),$$

where $M_k = \max_{\langle x_{k-1},\, x_k\rangle} f(x)$ and $m_k = \min_{\langle x_{k-1} x_k\rangle} f(x)$.

In the case we are considering the function

$$f(p) = \frac{1}{\exp\left\{2\beta\left(1 - \cos\frac{2\pi p}{N}\right) + 2\alpha\right\} - 1}$$

decreases in the interval $\left\langle 0, \frac{N}{2}\right\rangle$ and increases in $\left\langle \frac{N}{2}, N\right\rangle$, so that an effective calculation of the mean oscillation is possible. In $\left\langle 0, \frac{N}{2}\right\rangle$ we have $M_i = m_{i-1}$, and in $\left\langle \frac{N}{2}, N\right\rangle$ we have $M_{i-1} = m_i$, so that for the division

$$\pi_0 = [p_0 = 0 < p_1 = 1 < \ldots < p_{4n-1} = 4n - 1]$$

we have

$$\Omega(\pi_0) = [f(0) - f(2n)] + [f(4n-1) - f(2n)] =$$

$$= \frac{e^{2\alpha}(e^{4\beta} - 1)}{(e^{2\alpha} - 1)(e^{4\beta + 2\alpha} - 1)} + \frac{e^{2\alpha} \cdot \left[e^{4\beta} - e^{2\beta\,(1 - \cos\frac{2\pi}{N})}\right]}{\left[e^{2\beta\,(1 - \cos\frac{2\pi}{N})} + 2\alpha - 1\right](e^{4\beta + 2\alpha} - 1)}.$$

If we take into account the fact that $\alpha = \frac{H\mu}{kT}$, we arrive at $\lim_{H \to 0} \Omega(\pi_0) = \infty$.

Thus the mean oscillation, which must be small if the sum of Eq. (4) is to be replaced by the integral of (5), becomes in fact unbounded as H → 0. A more accurate calculation which makes use of the concavity of $f(p)$ shows that

$$\lim_{H \to 0}\left[\sum_{k=0}^{N-1} f(p_k) - \int_0^{N-1} f(p)\,dp\right] = -\infty.$$

In order to obtain further information on the applicability of Eq. (2), let us return to (1) and determine the mean magnetization without making any approximations. We have

$$\overline{M}(H, T) = kT\frac{\partial \ln Z}{\partial H} = kT \cdot \frac{1}{Z} \sum_{r=0}^{N} \sum_{n_\mu} \exp\left\{\frac{NH\mu - \sum_{p=1}^{N} n_p(\varepsilon_p + 2H\mu)}{kT}\right\} \frac{N\mu - \sum_{p=1}^{N} n_p 2\mu}{kT}. \qquad (6)$$

In particular, if we go to the limit H → 0 for a linear chain, we obtain

$$\overline{M}(O, T) = N\mu - 2\mu \frac{\sum_{r=0}^{N} \sum_{n_\mu} \exp\left\{-\frac{1}{kT}\sum_{p=1}^{N} n_p \cdot 2J_1\left(1 - \cos\frac{2\pi p}{N}\right)\right\}}{\sum_{r=0}^{N} \sum_{n_\mu} \exp\left\{-\frac{1}{kT}\sum_{p=1}^{N} n_p \cdot 2J_1\left(1 - \cos\frac{2\pi p}{N}\right)\right\}}.$$

This equation, which gives the spontaneous magnetization, is finite because it is the sum of a finite number of finite terms. This deduction is valid also for other lattices.

In view of the above arguments, the following may be asserted.

1) A linear chain or plane lattice can be ferromagnetic, just as can a space lattice, since in all these cases the spontaneous magnetization is finite.

2) The simplifications used by Bloch are not correct. In particular, Bloch first added to (6) a quantity which increases without bound as H → 0, and then subtracted another such quantity, as a result of which for linear chains and plane lattices he obtained

$$\overline{M}(O, T) = \infty - \infty = \infty,$$

and for space lattices he obtained

$$\overline{M}(O, T) = \infty - \infty = N\mu\left[1 - \left(\frac{T}{\theta}\right)^{3/2}\right].$$

In other words, Eq.(2) is ill-founded. We shall show moreover that (2) is not even an approximation for (6) at low temperatures. To prove this, let $j_1 > 0$, then

$$\lim_{T \to 0} \exp\left\{-\frac{\sum_{p=0}^{N-1} n_p \cdot 2J_1\left(1 - \cos\frac{2\pi p}{N}\right)}{kT}\right\} = 1,$$

if $n_1 = n_2 = \ldots = n_{N-1} = 0$ and $n_N = 0$; in all other cases, however, this limit vanishes. It follows from this that

$$\lim_{T \to 0}\left[\lim_{H \to 0} \overline{M}(H, T)\right] = N\mu - 2\mu\,\frac{1 + 2 + \ldots + N}{N + 1} = 0.$$

This result differs from that of Bloch, who obtained

$$\lim_{T \to 0}\left[\lim_{H \to 0} \overline{M}(H, T)\right] = \lim_{T \to 0} N\mu\left[1 - \left(\frac{T}{\theta}\right)^{3/2}\right] = N\mu,$$

which is also in contradiction with experiment. It is easily seen, however, that the order of going to the limit is essential, since $\lim_{H \to 0}\left[\lim_{T \to 0} \overline{M}(H, T)\right] = -N\mu$ *.

Institute of Physics
Polish Academy of Sciences

---

*The Editors feel that the author's assertions regarding the erroneousness of Bloch's propositions and the conclusions he reaches on this basis are not entirely convincing. (Russian Editors' note.)

DISPERSION FORMULA FOR SPIN WAVES IN FERRIMAGNETS

- G. Czofta

1. Spin Precession Wave

To obtain a semiclassical description of spin waves we begin with the quantum mechanical equation for the m-th spin

$$t\hbar d\hat{\mathrm{S}}_m/dt = [\hat{\mathrm{S}}_m, \hat{H}], \tag{1}$$

where we express the energy operator $\hat{H}$ by means of Dirac's formula

$$\hat{H} = -\mu_0\gamma \sum_j \hat{\mathrm{S}}_j \mathrm{H}_0 - (1/\hbar^2) \sum_{j \neq j} \sum A_{ij} \hat{\mathrm{S}}_i \hat{\mathrm{S}}_j \tag{2}$$

(here we use MKS units; $\gamma = e/m$ is the gyromagnetic ratio for spin angular momentum and A_{ij} is the exchange integral for interaction between the i-th and j-th spins). If the right side of (1) is transformed with the aid of the commutation relations given in Ref.1 the following equation results:

$$\frac{d\hat{\mathrm{S}}_m}{dt} = \hat{\mathrm{S}}_m \cdot \left\{ \mu_0\gamma \mathrm{H}_0 + (2/\hbar^2) \sum_j A_{mj} \hat{\mathrm{S}}_j \right\}. \tag{3}$$

If the operators are now interpreted as their classical analogues and only nearest neighbor interactions considered, we obtain, for the case of a linear chain of atoms, the semiclassical equation:

$$\frac{d\mathrm{S}_m}{dt} = \mathrm{S}_m \cdot \left\{ \mu_0\gamma \mathrm{H}_0 + \frac{2A}{\hbar^2} (\mathrm{S}_{m+1} + \mathrm{S}_{m-1}) \right\}, \tag{4}$$

This has solutions of the form

$$\mathrm{S}_m = \mathrm{S}_{mz} + \mathrm{B} \cos(akm - \omega t) + \mathrm{C} \sin(akm - \omega t),$$

where $\mathrm{S}_{mz} \perp \mathrm{B} \perp \mathrm{C}$, $|\mathrm{B}| = |\mathrm{C}|$; a is the lattice constant and the magnitudes of k and ω, are related by

$$\omega = \mu_0\gamma H_0 + \frac{4A}{\hbar^2} (1 - \cos ak)\, S_{mz}. \tag{5}$$

Thus, in the semiclassical representation, without making any assumptions other than those stated, we obtain the wave of spin precession about the direction of H_0 (S_{mz} must be parallel to H_0) with angular frequency (5).

It is easily seen that neighboring spins are shifted in phase with respect to each other by an angle $\theta = ak$. For small wave number values $k \ll 1/a$, Eq.(5) takes the form

$$\omega = \mu_0\gamma H_0 + (2A/\hbar^2)\, a^2 k^2 S_{mz} \tag{6}$$

The same expression can be obtained by considering a continuous spin field.[2] Heller and Kramers[3] showed that in the ground state for any lattice site, the absolute magnitude of the component S_{mz} has a maximum, and that in an excited state its value is lower, since every excited spin wave reduces $|S_{mz}|$ by a factor of $1/n$, where n is the number of atoms in the chains.

2. Spin Waves in Ferro- and Antiferromagnets

Adopting a simple geometrical model based on the semiclassical representation of spin waves, Keffer, Kaplan and Yafet[4] by elementary calculations

arrived at the following approximate relationship

$$\omega = \mu_0 \gamma H_0 + (2A/\hbar^2)\, a^2 k^2 S, \tag{7}$$

which differs from (6) only in that it contains the absolute magnitude S of the spin vector rather than the coordinate S_{mz}; similarly these authors deduced the corresponding dependence

$$\omega = \mu_0 \gamma H_0 \pm (2A/\hbar^2)\, ak S. \tag{8}$$

for antiferromagnets.

From the last, which was known earlier[5,6] it follows that if neighboring spins are antiparallel (antiferromagnetic ordering), the precession wave can propagate in a normal mode (i.e., the same value of ω for each atom) only if the precession radii R_λ and R_ρ for left and right handed spins, respectively, are different. In this case the S_z components for the two sublattices will be unequal and we obtain a non-vanishing resultant component $\sum_i^n S_{zi}$ for the entire lattice. Keffer[7] has shown that the sign of this component depends on the type of wave ($R_\rho < R_\lambda$ or $R_\lambda > R_\rho$) and that its magnitude is increased by $\hbar$ for each spin wave of the same type excited. Hence we have the result that antiferromagnetism occurs only when both types of waves are present on an equal basis; in the presence of any circumstances which lead to the prevalence of one type of wave, we can expect the appearance of ferrimagnetism (according to Néel), even if all spin vectors have the same magnitude.

3. Spin Waves in Any Ferrimagnet

It is possible to generalize the results of Keffer, Kaplan & Yafet[4] for the case when neighboring atom spins do not have equal magnitudes, i.e., when $S_1 \neq S_2$. Here it is convenient to use Smart's[8] classification, according to which ferrimagnetism means parallel orientation of neighboring spins of unequal magnitudes and antiferrimagnetism means antiparallel alignment of neighboring spins of unequal magnitude. Thus from a formal standpoint at least ferromagnetism may be regarded as a special case of ferrimagnetism where $S_1 = S_2$, while antiferromagnetism may similarly be considered as a special case of antiferrimagnetism.

A. Generalization of results of Keffer, Kaplan & Yafet (KKY) for the case of ferrimagnetism.

We denote the sum of the spin vectors $S_{m-1}+S_{m+1}$ by Σ_1 if it pertains to sublattice I and by Σ_2 if it pertains to sublattice II. According to (4) the torque acting on the m-th vector is

$$\left.\begin{aligned} G_1 &= (2A/\hbar^2)\, S_1 \textstyle\sum_2 \sin\Phi_1 \quad \text{for sublattice I}, \\ G_2 &= (2A/\hbar^2)\, S_2 \textstyle\sum_1 \sin\Phi_2 \quad \text{for sublattice II.} \end{aligned}\right\} \tag{9}$$

Accepting KKY's approximation that the angles Φ_1, Φ_2 and θ are small, and requiring that the angular precession velocity $\omega = G/R$ (where R denotes the precession radius) satisfy the equation

$$\omega_1 = \omega_2 = \omega, \tag{10}$$

we obtain (see Fig.1):

$$x/R_1 = -y/R_2. \tag{11}$$

Taking the results of KKY's simple geometrical operations, we can write

$$\left.\begin{aligned} x &= R_2' - R_1 - (a^2k^2/2)\,R_2', \\ y &= R_2' - R_1 + (a^2k^2/2)\,R_1, \end{aligned}\right\} \tag{12}$$

whence

$$x/R_1 = -y/R_2 = \frac{x-y}{R_1+R_2} = -\frac{a^2k^2}{2}\cdot\frac{R_2'+R_1}{R_2+R_1}. \tag{13}$$

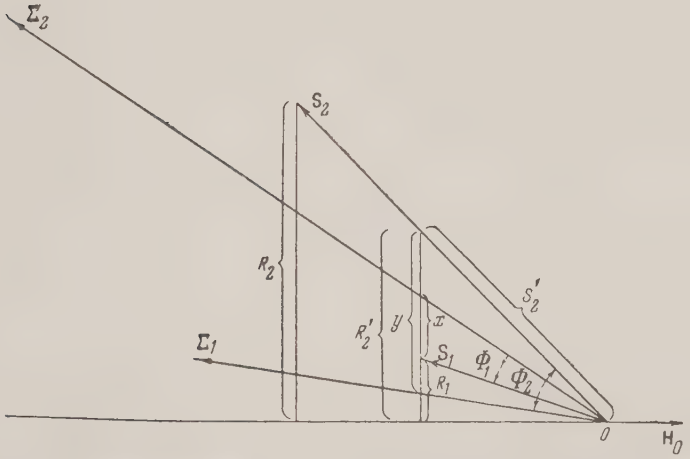

Fig.1. Case of ferrimagnetism. The spin vectors are plotted from a common origin 0 and in a single common plane.

In view of the assumed approximations (Fig.1),

$$R_1 \approx R_2' = S_2' R_2/S_2 \approx S_1 R_2/R_2, \tag{14}$$

and we finally obtain the dispersion formula

$$\omega = -(4A/\hbar^2)\frac{S_1 S_2}{S_1+S_2}\,a^2k^2. \tag{15}$$

B. Generalization of KKY's results for the case of antiferrimagnetic.

By referring to Fig.2, we can similarly write

$$G_1 = -(2A/\hbar^2)\,S_1 \sum\nolimits_2 \sin(\pi - \Phi_1); \quad G_2 = +(2A/\hbar^2)\,S_2 \sum\nolimits_1 \sin(\pi - \Phi_2), \tag{16}$$

whence, approximately,

$$G_1 = -(4A/\hbar^2)\,S_2 x; \quad G_2 = (4A/\hbar^2)\,S_2 y. \tag{17}$$

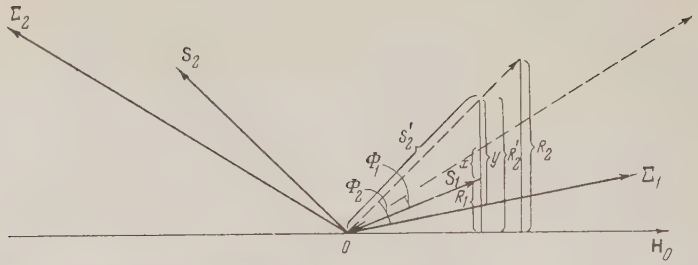

Fig.2. Case of antiferrimagnetism. The spin vectors are plotted from a common origin 0 and in a single common plane.

In the present case, we have

$$\omega_1 = G_1/R_1; \quad \omega_2 = -G_2/R_2. \tag{18}$$

Using relations analogous to (12), we get

$$R_2' - R_1 = \left(\frac{a^2k^2}{8}\right)(R_2R_2' + R_1^2)/(R_2 - R_1). \tag{19}$$

Thus for small values of k we obtain

$$x/R_1 = y/R_2 = \frac{x+y}{R_1+R_2} \approx 2\frac{R_2' - R_1}{R_2+R_1} = \frac{a^2k^2}{4} \cdot \frac{R_2R_2' + R_1^2}{R_2^2 - R_1^2}, \tag{20}$$

from which, taking into account the approximations of (14), we finally obtain the dispersion formula

$$\omega = \frac{A}{\hbar^2} \cdot \frac{S_1S_2}{S_1 - S_2} a^2k^2. \tag{21}$$

From the foregoing it is clear that (7) represents the special case of (15) when $S_1 \approx S_2$. It does not appear possible, however, to obtain (8) from (21) by setting $S_1 = S_2$ as might be expected. To obtain (8) it is necessary to return to (18) and follow the derivation indicated by KKY. It is clear from this that antiferromagnetism cannot be considered as a special case of antiferrimagnetism. Comparison of the two formulas obtained indicates antiferrimagnets are more likely to evince a similarity to ferrimagnets rather than antiferromagnets; this appears to be in agreement with experiment.*

Institute of Physics of the
Polish Academy of Science

References

1. C.Herring & Ch.Kittel, Phys.Rev., 81, 869 (1951).
2. W.Döring, ZS.f.Phys., 124, 501 (1948).
3. G.Heller & G.Kramers, Proc.Roy.AC.Sci.Amsterdam,37,378 (1934).
4. F.Keffer, H.Kaplan & Y.Yafet, Am.J.Phys., 21, 250 (1953).
5. L.Hulten, Proc.Roy.Ac.Sci.Amsterdam, 39, 190 (1936).
6. O.W.Anderson, Phys.Rev., 86, 694 (1952).
7. F.Keffer, Thesis. Univ.of California, Berkeley, 1952.
8. J.S.Smart, Am.Phys., 23, 356 (1953).

---

*The results here presented are in a sense a generalization of the work of Keffer, Kaplan & Yafet. These results pertain to a one-dimensional chain. It is not shown,however, that such a chain can be ferromagnetic (or antiferromagnetic); it is not clear just what meaning should be attributed to the cited dispersion formulas, particularly if it is borne in mind that the proof adduced in the preceding article by Semadeni is not convincing. (Russian Editors' Note).

FERROMAGNETISM OF CONDUCTION ELECTRONS

- G.S.Krinchik

1. Statement of the Problem

The criterion for ferromagnetism adopted by most modern authors is the Slater-Bethe criterion (see, for instance, Vonsovskii & Shur[1]), which is based on the premise that the exchange integral for the d electrons is positive in certain transition metals. This criterion was further developed in the s-d exchange model of Vonsovskii[1], who showed that the s-d exchange interaction leads to participation of the s electrons in the magnetization. When this model was compared with experiment,[2] it was found necessary to assume that the magnetic moments of the s and d electrons are antiparallel, i.e., that such uncompensated antiferromagnetism is a universal phenomenon.

Another possible point of view is that the s electrons make an important positive contribution to ferromagnetism, whereas the exchange interaction between the d electrons tends to suppress it. Dorfman and Kikoin[3] suggested in 1929 that ferromagnetism may be caused entirely by the s electrons and that the exchange interaction between the d electrons may be negative, leading to antiparallel orientation of their spins. Zener[4] used a model in which he also assumed that the exchange integral of the d electrons is negative, and that parallel orientation of their spins is established due to the positive s-d exchange interaction.

None of these points of view has as yet been given a rigorous theoretical foundation. As for the possibility that the s electrons may be ferromagnetic, it is highly unlikely. Although Bloch[5] asserted that the exchange interaction should cause a parallel spin orientation in the free-electron gas for certain definite electron separations, Wigner[6] and later Pines[7] showed, by including the correlation energy, that a free-electron gas can never become ferromagnetic no matter how low the density. It is evident, however, that the calculations of Wigner and Pines cannot be applied without restriction to the case of electrons in a transition metal. It is therefore still reasonable to discuss both points of view as to the role of electrons in ferromagnetism.

We shall discuss below the s electron model of ferromagnetism within the framework of the band theory, in a manner similar to that employed by Stoner, Mott and Pauling[1] in treating the magnetization of the d-band electrons on the basis of the Slater-Bethe criterion. It is assumed that above the Curie point the distribution of s and d electrons is given correctly by the ordinary individual-electron theory. As the temperature is reduced to absolute zero, the positive exchange interaction among the 4s electrons and between the 4s and 3d electrons leads to a maximum electron magnetization in the 3d and 4s bands in spite of the negative exchange interaction among the 3d electrons. Because the energy level density is so high in the d band, when the s electrons are magnetized half of them undergo transitions to the d band; as the temperature increases these electrons gradually return to the s band.

Figure 1 is a schematic diagram of the electron distribution in cobalt at absolute zero and above the Curie point. It should be noted that in this magnetization process the kinetic energy of the s electrons increases less than in the usual free electron gas model. It is seen from Fig.1 that this increase is found by taking not a parabolic band, but a band whose shape is such that half the s electrons lie in a parabolic band and all the others acquire the same energy, equal to the maximum energy of the electrons before

magnetization. Whereas for a free electron gas the kinetic energy difference between the magnetized and nonmagnetized states[8] is

$$\Delta E = E_M - E_N = \frac{3{,}51}{r_s^2} - \frac{2{,}21}{r_s^2} = \frac{1{,}3}{r_s^2},$$

it is easily seen that for an energy band of the above shape, in which the s electrons undergo transitions to the d band,

$$\Delta E = \frac{2{,}95}{r_s^2} - \frac{2{,}21}{r_s^2} = \frac{0{,}74}{r_s^2}$$

Here r_s is the radius of the sphere occupied by each electron expressed in Bohr orbits, and the energy is given in Rydbergs.

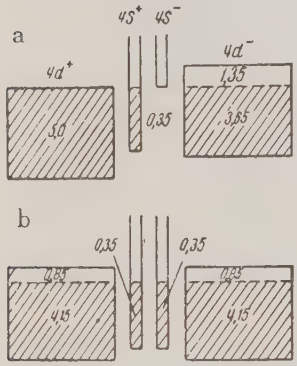

Fig.1. Electron structure of cobalt (a) at absolute zero, and (b) above the Curie point.

The above estimate is an argument in favor of the hypothesis of ferromagnetism of s electrons in metals, although we have not considered the exchange and correlation energies.

Thus the characteristics of the proposed model are, first, the distinctive mechanism of magnetization of the s electrons (leading to transition of the s electrons to the d band, temperature dependence of the number of s electrons and holes in the d band, etc.) and, second, a negative exchange integral for the d electron. In the next two sections we shall compare these inferences with available experimental data and in the last section we shall discuss possible additional experimental tests of the proposed model.

2. Magnetization of the s Electrons

A. Number of conduction electrons as determined from the Hall effect

Pugh and his co-workers[9] have systematically investigated the Hall effect in magnetic alloys in strong fields. They have arrived at the conclusion that it is possible to separate from the total Hall emf the so-called ordinary Hall effect which is proportional not to the magnetization of the sample, but to the external magnetic field. One can then proceed as with ordinary nonmagnetic metals and calculate, from the value of the Hall constant, the conduction electron concentration in the absence of hole conductivity. Their research was concerned with Fe-Ni, Ni-Co and Ni-Cu alloys and led, in particular, to the following conclusions which are easily explained by the proposed model:

(1) The number of s electrons is about half of the expected 0.5-0.6 electrons per atom.

(2) As the temperature is increased and the concentration of copper in Ni-Cu alloys is increased, the number of s electrons also increases, approaching the above mentioned expected value.

B. Atomic magnetic moments of pure metals

There are two fundamental difficulties in the study of the atomic magnetic moments of pure metals:

(1) Atomic magnetic moments occur in fractions of Bohr magnetons.

(2) Ferromagnetic and paramagnetic measurements give different numerical values for the atomic magnetic moments.

The values of ferromagnetic moments p_f are found by extrapolating the saturation magnetization to absolute zero. The results of measurements of the paramagnetic susceptibility above the Curie point are treated by the Curie-Weiss formula

$$\chi = \frac{C}{T - \theta_p}, \tag{1}$$

where

$$C = \frac{n\mu_B^2}{3k} n_p (n_p + 2); \quad p_p = \sqrt{n_p (n_p + 2)}; \tag{2}$$

here θ_p is the paramagnetic Curie point, n is the number of atoms, μ_B is the Bohr magneton, and n_p is the number of electrons per atom participating in the magnetization. It is found that the experimental values of n_p are not equal to p_f and there is no satisfactory explanation of this fact. As is seen from Fig.1, in the case of our model, in the first approximation we have

$$p_f = m + 2\sigma, \tag{3}$$

$$n_p = m + 4\sigma; \tag{4}$$

where m is the number of vacancies in the d band, if all the s and d electrons are assumed to be located in it, and σ is the number of electrons in the s band at absolute zero. If either Eq.(3) or (4) is used to obtain σ, the validity of the other one can be verified without recourse to additional constants. Table 1 shows comparative data for tha atomic magnetic moments of iron, cobalt, and nickel. The experimental values of p_p are taken from Sucksmith and Pearce.[10] The values of σ are taken to satisfy Eq.(3), but it must be emphasized that they are in good agreement with the Krutter, Slater and Manning[11] band structure calculations for nickel and iron.

Table 1

Atomic magnetic moments of Fe, Co and Ni

Metal	m	σ	p_f^{theo}	p_f^{exp}	n_p	p_p^{theo}	p_p^{exp}	Temp. range, °C
Fe	2	0,11	2,22	2,22	2,44	3,29	3,2	900 ÷ 1500
Co	1	0,35	1,7	1,71	2,4	3,25	3,15	1230 ÷ 1450
Ni	0	0,3	0,6	0,6	1,2	1,96	1,61 1,78	500 ÷ 850 925 ÷ 1200

C. Atomic magnetic moments of binary alloys of ferromagnetic components

Utilizing the collective electron model, we may justifiably apply Eqs. (3) and (4) to the calculation of the atomic magnetic moments of several binary alloys.

Fig.2 gives values of σ calculated by Eq.(3) for the Fe-Ni and Fe-Co systems. The experimental values of p_f for these alloys are those given by Bozorth.[12]

We have indicated at the curves which type of crystal lattice is stable at low temperatures for the given alloy, since there appears to be a correlation between the magnitude of σ and the type of lattice. The values of σ decrease for alloys with a tightly packed lattice. This may be due either to different degrees of overlap of the s and d bands in body- and face-centered lattices or to antiparallel orientation of some of the d-electron spins under the influence of negative exchange interaction (see the next section). The curve for the Ni-Co system is not shown, since the values of σ for these alloys hardly change, remaining between 0.3 and 0.35.

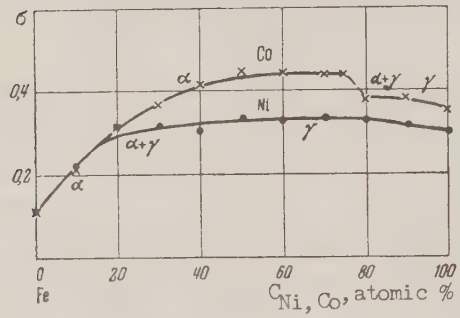

Fig.2. Concentration of s electrons in Fe-Co and Fe-Ni alloys.

In Fig.3 we give the theoretical and experimental values for atomic paramagnetic moments of alloys of Ni with Fe and Co. The data for Fe-Co alloys cannot be used, since this system undergoes a phase transition at the Curie point.

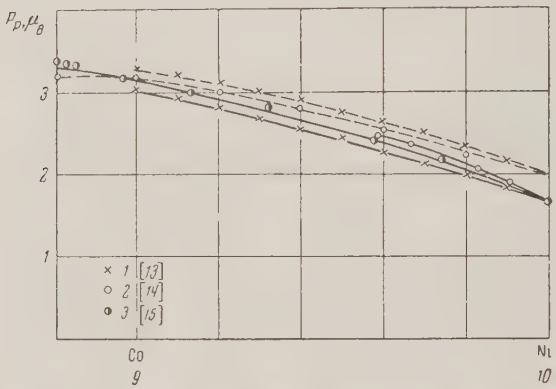

Fig.3. Atomic magnetic moments of binary alloys of nickel with iron and cobalt, as obtained from paramagnetic measurements: 1) Co-Ni alloys, 2 & 3) Fe-Ni alloys. Dash-line curves - theoretical values; the solid curves - experimental. The references pertain to the experimental points.

D. Atomic magnetic moments of Ni-base binary alloys

It will be seen from Table 1 that the calculated value of p_p for nickel is greater than the experimental one, particularly since it would seem that of the two experimental values listed, 1.61 is more trustworthy (see Section E). Now the assumption that the s electrons are not magnetized, leads to a value of p_p^{theo} that is too low, while the supposition that they are fully magnetized, leads to an overestimate. This disagreement can be explained with the aid of the additional assumption that the s electrons in nickel and its alloys are partially magnetized. This assumption would mean that the magnetic moments of m' electrons in the s band are compensated, and that m' remains constant as the temperature is increased from absolute zero to the Curie point. At the same time the number σ' of "magnetic" electrons doubles at high temperatures. Thus if we replace m and σ in Eqs.(3) and (4) by m' and σ', these equations can be used in the present case to determine m' and σ' for nickel. The value of n_p can be calculated from experimental data if the Curie constant is known. If $g = 2$ and $s = 1.2$, the Curie constant is given by

$$C_A = n_p \frac{N\mu_B^2}{k}. \qquad (5)$$

The experimental value of C_A per gram-atom of nickel is close to 0.323 (which corresponds to $p_p = 1.61$). Hence the number of electrons per atom that contribute to paramagnetism above the Curie point in nickel is 0.86, which differs from the value of 0.6 obtained from ferromagnetic measurements. Both these values are obtained from Eqs.(3) and (4) if we set $m' = 0.34$ and $\sigma' = 0.13$ electrons per atom.

We can use these values of m' and σ' for pure nickel to obtain the variation of the atomic magnetic moments in nickel alloys. Sardon's relation[12] for the decrease in the atomic ferromagnetic moment of nickel as a function of the number of valence electrons in the dissolved element is usually explained in the band model[1] by asserting that these electrons fill the d band. Every valence electron which is introduced with the alloying component reduces the saturation magnetization of nickel by one Bohr magneton, so that to eliminate ferromagnetism one must add 0.6 electrons per atom. A similar explanation of Sardon's law can be given in the framework of the ferromagnetic s electron model. In other words, 0.6 electrons per atom is a result which is independent of whether the s electrons are entirely or partially magnetized. Thus with the above values of m' and σ', the removal of ferromagnetism requires filling 0.47 vacancies in the 3d band and 0.13 in the 4s band, so that each "excess" electron added by the second, alloying element cancels one Bohr magneton.

The situation is quite different when we come to the reduction of the atomic magnetic moments obtained from paramagnetic measurements. Here the temperature dependent paramagnetism should also disappear when 0.6 electrons per atom are introduced, but now the magnetic moments of 0.86 electrons per atom cease contributing to paramagnetism. Therefore each added alloying-element electron compensates the magnetic moment of 0.86/06 = 1.43 electrons and if ΔC_A is extrapolated to 100% of the solute element, the change per valence electron will be $0.375 \cdot 1.43 = 0.536$. The data of Manders[17] processed by Néel[16] for alloys of nickel with copper, aluminum, titanium, tin, antimony, vanadium, tungsten and molybdenum give $\Delta C_A = 0.513$.

E. The temperature independent paramagnetism of nickel alloys

As has been shown by many experimenters (see, for instance, Fallot[14] and Manders[17]), the paramagnetic susceptibility of nickel and its alloys can be written

$$\chi = \chi_k + \frac{C}{T - \theta_p}, \qquad (6)$$

where χ_k is the temperature independent term and C is the Curie constant used in Eq.(5) to find n_p. It is natural to suppose that the temperature independent part of the paramagnetism is associated with those electrons which do not participate in the ferromagnetism. Since m' increases with decreasing σ', one should expect χ_k to increase when p_f or C are decreased. Indeed, Manders' measurements show that in all the alloys listed at the end of the previous section, wherein the magnetic moment falls off sharply with increasing concentration of alloying metal, χ_k increases. In the cases of a small decrease (Ni-Au, Ni-Pt), constancy (Ni-Pd) and increase (Ni-Mn) of the magnetic moment, Manders' accuracy of measurement allows only of inference that χ_k does not increase noticeably. Finally, Fallot[14] has established that in Fe-Ni alloys χ_k actually decreases with increasing Fe concentration.

It should be emphasized that the separation of the s electrons into electrons responsible for the temperature dependent paramagnetism and electrons responsible for the temperature independent part of the susceptibility is highly artificial. A consistent theory should yield a single formula for the complicated temperature dependence of the paramagnetic susceptibility of the whole electron gas, thus giving physical meaning to the concepts employed in constructing our model.

F. Spectroscopic splitting factor

The so-called spectroscopic splitting factor g, which is the ratio of the magnetic moment to the angular momentum as determined by experiments on ferromagnetic resonance, is usually greater than 2. This fact is explained by the presence of spin-orbit interaction[18]. The spin-orbit interaction should strongly influence the g value for the d electrons, but for the s electrons, which are weakly coupled with the lattice, g may be assumed equal to 2. In this case the magnitude of g will depend strongly on the relative concentrations of the s and d electrons participating in the ferromagnetism. This dependence is given by

$$g = (1 - x)\, g_d + x g_s, \tag{7}$$

where g is the experimentally measured value of the splitting factor, x is the relative concentration of s electrons, and g_d and g_s are the spectroscopic splitting factor values for the d and s electrons, respectively.

In a recently contribution Stanley and Reich[19] give experimentally measured values of g for nickel and its alloys with copper, aluminum, antimony and manganese. The first three alloys belong to the group in which the relative concentration of s and d electrons does not change with the concentration of alloying element (as follows from Section D). Indeed, experiment shows that in Ni and in the Ni-Cu, Ni-Al and Ni-Sb systems the value of g is constant and equal to 2.19 ± 0.02. Since x = 0.13/0.6 = 0.217 and g_s = 2.0 for nickel, Eq.(7) gives g_d = 2.24. In Ni-Mn alloys g decreases to 2.11 ± 0.02 for the alloy with a 13.5 atomic percent Mn concentration, the concentration at which the atomic magnetic moment of the alloy is approximately equal to that of nickel.[19] Assuming that all the s electrons are magnetized at this concentration, i.e., that $x \approx 0.5$, we obtain from Eq.(7) a value of 2.12, which agrees with experiment.

3. Negative Exchange Integral for d Electrons

A. α and γ-iron

The magnetic body-centered (α) and nonmagnetic face-centered (γ) modifications of iron have almost the same atomic separations, namely, 2.48 A for α-iron and 2.52 A for γ-iron at room temperature.[20] It has been pointed out by Zener[4] that this situation - inexplicable from the standpoint of the Slater-Bethe criterion - can be explained by an increase of the coordination number from 8 to 12, which, in turn, leads to an increase of the d exchange energy. However, in his approach to the matter from the atomic point of view, Zener was forced to postulate that α-iron has an ordered antiferromagnetic structure with uncompensated sublattice moments. In contrast, according to our band model, (as follows from Section 2B), α-iron may be considered a normal ferromagnet without the necessity of introducing this complicating assumption, and

γ-iron may be considered an antiferromagnet. This approach is particularly effective in considering the properties of binary magnetic alloys.

B. α-γ transition and the Curie point in Fe-Co system

In the Fe-Co binary system a unique phenomenon is observed in a wide range of cobalt concentrations (approximately from 15 to 70%): the temperature of the phase transition from the α to the γ modification coincides with the Curie point.[12] The explanation is the same as in the previous subsection, namely, that the increase in the number of nearest neighbors of each atom (the coordination number) incident to the phase transition leads to destruction of the ferromagnetism and transforms the alloy into an antiferromagnet.

C. The dependence of the Curie point on the Fe concentration in the Fe-Ni system

Binary Fe-Ni alloys crystalize in the face-centered cubic lattice at low temperatures in the Fe concentration range from 0 to 60%. Any increase in the number of iron atoms in the tightly packed solid solution lattice results in increased overlapping of the d shells of neighboring atoms. As the contribution to the molecular field from the d exchange term increases, the Curie point should go down. And in actual fact above an Fe concentration of 30%, the Curie point begins to decrease, approaching zero for the alloy with an Fe concentration of about 70%.[12] At still higher Fe concentrations, the Curie point again rises due to formation of the α modification.

We see that the drop in the Curie point in iron-nickel alloys in the "Invar" region can be explained by the influence of the negative d exchange interaction. The role of this interaction is particularly great in the Invar group of alloys near the point where ferromagnetism vanishes, and it is possible that this may explain not only the variation of the Curie point but many other physical anomalies of Invar alloys. The occurrence of strong negative exchange forces may, for instance, explain the enhanced susceptibility of the para-process, the volumetric magnetostriction of these alloys, etc. We shall consider the singular shift of the Curie point observed in Invar alloys under the influence of pressure in the next section.

D. Shift of Curie point under pressure

If the dependence of the exchange interaction on the interatomic distance is known, one can evaluate the displacement of the Curie point under compression. Néel[21] carried out such calculations, but recent measurements by Patrick[22] have failed to verify them.

Our model can be used to explain the shift of the Curie point in a different way. The molecular field is, roughly speaking, composed of two parts whose actions are opposite. When the contribution of the d exchange forces is large, the molecular field is weak and the Curie point is low; when the exchange contribution is negligibly small, the Curie point should reach its highest value. We shall assume that because the d electron eigenfunction contains the exponential of the radius, the d electron exchange integral depends more strongly on changes in interatomic distance of the metal than does the s electron exchange integral or that for the interaction between the s and d electrons. Then, all other conditions being equal, the following behavior should be observed. Pressure should cause less change of the Curie

point in metals with a high Curie point than in metals with a low Curie point. The applicability of this rule is restricted by the fact that the displacement of the Curie point should depend on the slope of the exchange integral, i.e., on its derivative with respect to the interatomic distance.

Nevertheless, this rule can be used to explain the change of magnitude and sign of the effect for various substances - see Table 2.

Table 2

Variation of the Curie point of metals and alloys under the influence of pressure

Metal	θ, °K	Change in θ, % per 1000 atmos.
Co	1393	$\leq 0{,}07$ *
Fe	1043	$\leq 0{,}01$ **
96 % Fe + 4 % Si	1003	$\leq 0{,}01$
90 % Fe + 10 % Si	888	$\leq 0{,}025$
32 % Fe + 68 % Ni	879	$\leq 0{,}015$
62 % Fe + 38 % Ni	~520	$-0{,}49$ ***
64 % Fe + 36 % Ni	483	$-0{,}74$ $-0{,}79$ ***
68 % Fe + 32 % Ni	~370	$-1{,}23$ ***
70 % Fe + 30 % Ni	353	$-1{,}64$

*Neel's theoretical value is -0.33.

**Neel's theoretical value is $+0.075$.

***Belov's data[23].

This rule cannot be applied to nickel and its alloys wherein the effect is positive, since the decrease in the Curie point is connected not with the increase in the contribution from the d exchange forces, but with the decrease in the atomic magnetic moment. One may therefore suppose that in the given case the rise in the Curie point is caused by the increase in the s-s and s-d exchange interaction under pressure.

4. Experiments to Verify the Model

A. Values of the g factor above and below the Curie point

As follows from Sections 2B and 2D, the relative s electron concentration x should be different in the ferromagnetic and paramagnetic states. Thus, for instance, below the Curie point in cobalt, $x = 0.35/1.7 = 0.2$, while above the Curie point $x = 0.7/2.4 = 0.3$. In nickel x also increases to 0.3. Therefore measurements of g by ferromagnetic resonance below the Curie point and paramagnetic resonance above the Curie point may serve as experimental verifications both of the hypothesis of s electron ferromagnetism and that of the partial magnetization of the s electrons in nickel and in its alloys. In both Co and Ni the g factor should decrease by about 0.02 above the Curie point.

B. Values of the g factor for Ni-Mn alloys

The decrease of the g factor with increase in Mn concentration in Ni-Mn alloys was explained in Section 2E by the increase of the relative concentration of s electrons. It is easily seen that if the proposed explanation is correct, further increase of the manganese concentration should result in a further growth of the g factor. For instance, in the ordered Ni_3Mn alloy the atomic magnetic moment is about one Bohr magneton.[12] The maximum proportion of magnetic s electrons and, therefore, of x, is 0.3, so that for this alloy g cannot be less than 2.17 if the spin-orbit coupling constant is to remain unchanged. The indicated method for verifying experimentally the contribution of the s electrons to ferromagnetism is particularly desirable, since

it involves application of a procedure, known to be reliable, to alloys with different manganese concentrations.

C. Paramagnetic susceptibility of Ni_3Mn alloy

It would be of interest to investigate the temperature dependence of the paramagnetic susceptibility of Ni_3Mn in the ordered and disordered states. In the former state, the Curie constant should be large. Its magnitude can be evaluated by means of Eqs.(3) and (4); χ_k should be zero. In the second case, C should be much less and χ_k should be appreciable.

D. The ferromagnetism of the γ-phase of Fe-Co alloys

At low Fe concentrations, the Curie point of Fe-Co alloys should increase with the Fe concentration.[12] One might expect that at higher iron concentrations in γ-phase alloys there will appear a region similar to the Invar region in Fe-Ni alloys. Starting with an iron concentration of some 20-25%, however, the γ-phase becomes unstable at low temperatures. It would be desirable by alloying and heat treatment to obtain a γ-modification of Fe-Co alloys with 30 to 80% Fe content that will be stable at low temperatures. In this interval one should be able to find "Invar" Fe-Co alloys whose Curie points can be evaluated by extrapolating the dependence of the Curie temperature to high Fe concentrations. The successful preparation of such alloys would verify the hypothesis that the d electron exchange integral is negative.

Thus the proposed model not only explains many experimental facts, but can also be used to design experiments aimed at verifying its basic postulates. This is particularly important since there already exist several more or less well developed models of the electronic structure of ferromagnets - those of Pauling, Stoner-Wolfarth[24], Vonsovskii, Zener, Bethe-Ganzhorn-Dehlinger[25] - (to say nothing of other special models invoked for explaining certain individual properties of ferromagnetic materials). Only special experiments designed to verify the particular premises of the different models can serve to indicate which of the models is worthy of further refinement and consistent theoretical development.

I take this opportunity to thank E.I.Kondorskii, S.V.Tiablikov and V.L. Bonch-Bruevich for many valuable remarks in discussions of the present work.

Department of Physics of Moscow State University

References

1. S.V.Vonsovskii & Ia.S.Shur, Ferromagnetizm (Ferromagnetism) M.-L., 1948.

2. S.V.Vonsovskii & K.B.Vlasov, Zhur.eksp.i teor.fiz., 25, 327 (1953).

3. Ia.G.Dorfman & I.K.Kikoin, ZhRFKhO (J.Russ.Phys.-Chem.Soc.), 51, 159 (1929); ZS.Phys., 54, 289 (1929).

4. C.Zener, Phys.Rev., 81, 440 (1951); 82, 403 (1951); 83, 299 (1951); 85, 324 (1952).

5. F.Bloch, ZS.Phys., 57, 545 (1929).

6. E.Wigner, Phys.Rev., 46, 1002 (1934); Trans.Far.Soc., 34, 678 (1938).
7. D.Pines, Phys.Rev., 92, 626 (1953).
8. G.Bethe & A.Sommerfeld, Electronic theory of metals (In Russ.trans., M.-L., 1938).
9. E.M.Pugh, Phys.Rev., 97, 647 (1955); S.Foners, Phys.Rev., 99, 1079 (1955).
10. W.Sucksmith & R.R.Pearce, Proc.Roy.Soc., A167, 189 (1938).
11. H.M.Krutter, Phys.Rev., 48, 664 (1935); J.C.Slater, Phys.Rev., 49, 537, 931 (1936); M.F.Manning, Phys.Rev., 43, 190 (1943).
12. R.M.Bozorth, Ferromagnetism (In Russ.trans., M. 1956).
13. O.Bloch, Ann.Chim.Phys., 26, 5 (1912).
14. M.Fallot, J.Phys.Radium, 5, 153 (1944).
15. M.Peschard, Revue de Met., 22, 490, 581, 663 (1925).
16. L.Neel, Ann.de Phys., 5, 232 (1936).
17. R.S.Manders, Ann.de Phys., 5, 167 (1936).
18. "Ferromagnitnyi rezonans" (Ferromagnetic resonance), Collected articles on, M., 1952.
19. K.J.Standley, K.H.Reich, Proc.Phys.Soc., B 68, 713 (1955).
20. Ch.S.Barrett, The Structure of Metals (In Russ.trans., M.-L., 1948).
21. L.Neel, Le Magnetisme, Vol.2, (1939).
22. L.Patrick, Phys.Rev., 93, 384 (1954).
23. Ia.G.Dorfman, Magnitnyi svoistva i stroenie veshchestva (Magnetic properties and the structure of matter), M.-L., 1955.
24. E.C.Stoner, Proc.Roy.Soc., A 165, 372 (1938); 169, 339 (1939); E.P.Wolfarth, Phil.Mag.,40, 708, 1095 (1949); 41, 534 (1950); 42, 374 (1951).
25. E.Bader, K.Ganzhorn & U.Dehlinger, ZS.f.Phys., 137, 190 (1954).

TOWARDS A THEORY OF SPONTANEOUS MAGNETIZATION OF THIN FILMS

- L.Valenta

Introduction

Of late increasing attention has been given to the magnetic properties of thin layers. The first theory of spontaneous magnetization of thin films was developed by Klein and Smith[1], who applied the Bloch spin-wave theory to the case of a simple lattice of spin 1/2 atoms with its (100) plane parallel to the film surfaces. Their calculations are based on the assumption that one may treat thin film as an unbounded medium satisfying Bloch's periodicity conditions, for which one of the periods is small and equal to the film thickness. The validity of such a theory is restricted not only by the spin-wave approximation itself, but also by the inconvenient fact that no known ferromagnet has such a lattice structure. Another shortcoming of the theory is that it can be applied only when the (100) lattice plane is parallel to the film surface and only in the case of spin 1/2. Thus the Klein-Smith theory can be used only to obtain approximate estimates at low temperatures. Experiment shows, however, that this theory gives a correct prediction of the general variation of spontaneous magnetization and the Curie point as a function of the film thickness. A more detailed comparison of the theory with experiment is handicapped not only by difficulties in the theory, but also by the lack of sufficient low-temperature experimental data.

Drigo[2] and Crittenden & Hoffmann[3] have attempted modifications of the Klein-Smith theory that would make it applicable in the range of higher temperatures. Without going into detail, one may say that such attempts to modify the spin-wave theory for higher temperatures are merely provisional, as is admitted by the authors themselves.

In the present work we have therefore attempted to develop a theory which would bear the same relation to the Klein-Smith spin-wave theory as Heisenberg's theory for bulk specimens bears to Bloch's spin-wave theory. Our approach is based on a generalization of the concept of magnetic sublattices.

Essentially, the magnetic sublattice concept, as introduced by Néel, consists of dividing all the atoms constituting the given sample into several groups of physically equivalent particles (i.e., identical particles existing under equal physical conditions); these groups Néel terms magnetic sublattices.

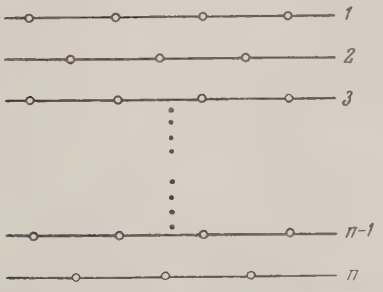

Fig.1. Schematic representation of the model of a homogeneous thin film consisting of n monatomic layers.

In the present work we shall regard the thin film as an unbounded homogeneous ideal plane layer composed of atoms of a single kind, situated in a vacuum. We shall consider physically equivalent the atoms in each monatomic plane at a constant distance from the surface of the film (Fig.1). The film consists of n such monatomic planes. We may therefore treat this film as a set of magnetic sublattices, where each sublattice is a separate monatomic layer parallel to the surface. As opposed to the interpretation of sublattices given for antiferromagnets and ferromagnets, in our thin-film model the sublattices are superposed one on top of another.

At higher temperatures such a system of

sublattices can be treated both by the Heisenberg theory and by the molecular field theory, and one may expect the results to be equivalent.

In this model a remarkable situation arises. If we go to thicker and thicker films, allowing the thickness to approach infinity, the individual monatomic layers (sublattices) become virtually equivalent and our treatment of the molecular fields becomes the same as Weiss' original treatment. For the case of very thin films, on the other hand, our theory is equivalent to Néel's, as can be seen from the simple example of an antiferromagnet with the NaCl type lattice. If we take a layer of such a substance whose surface is perpendicular to the (100) plane and then "pare" this layer down to two monatomic layers, the Néel sublattices become these two monatomic layers and thus sublattices in our sense of the word. One may therefore suppose that if the generalized theory is correct, it will agree with experiment to the same accuracy as does the Weiss-Néel theory.

Let us first consider this problem from the quantum mechanical point of view.

1. The Heisenberg Quantum Theory of Thin Films

In attempting to develop a quantum mechanical theory, one may start from Bloch's form[4] of the Heisenberg theory (see also Vlasov and Ishmukhametov[6]) which makes use of the energy centroid method. One can use the simple method of a film consisting of one-electron atoms and take into account only the exchange part of the energy operator. If it is then found that the results are analogous to those obtained by the molecular field method, it is more convenient to resort to the latter. The magnetic sublattice idea is utilized in the sense that we assume that the wave function of the entire system of all the electrons of the film can be expressed approximately as the wave function of the state in which the components of the magnetic moments of the individual sublattices in the direction of the magnetic field have definite values. This circumstance can then be employed in introducing the energy centroids. When we compare the theory derived in this way with the Vlasov-Ishmukhametov theory[6] of ferromagnets and antiferromagnets, we find that by identifying their (that is, Néel's) concept of a sublattice with our monatomic layers, our theory may be considered a generalization of theirs to the case of n sublattices. In this way we arrive at the result that the spontaneous magnetizations $y_i = J_i/J_{oi}$ (where $i = 1, 2, \ldots, n$ and where J_i is the magnetization at a given temperature and J_{oi} is the saturation magnetization per unit surface) of the separate sublattices are given by

$$y_i = \operatorname{th}\left\{1/kT\left[\left(A/2\sum_{k=1}^{n} s_{ik}y_k\right)+\beta H\right)\right]\right\} = B_{1/2}\left\{1/kT\left[\left(A/2\sum_{k=1}^{n} s_{ik}y_k\right)+\beta H\right]\right\} \quad (i=1,2,\ldots,n); \quad (1)$$

here k is Boltzmann's constant, A is the exchange integral for nearest neighbor atoms, s_{ik} is the number of nearest neighbors in the k-th plane of an atom situated in the i-th monatomic plane, β is the Bohr magneton and H is the magnetic field.

As is obvious from the form of Eq.(1), we would obtain the same results if we had used the concept of molecular fields whose strengths are proportional to the magnetizations of the separate monatomic layers. Henceforth, therefore, we shall make direct use of the molecular field method, and shall generalize Eq.(1) to the case of arbitrary values of J in the same way as is done for the theory of bulk specimens, that is, by introducing a general Brillouin function $B_j(x)$, where $x = \beta H/kT$.

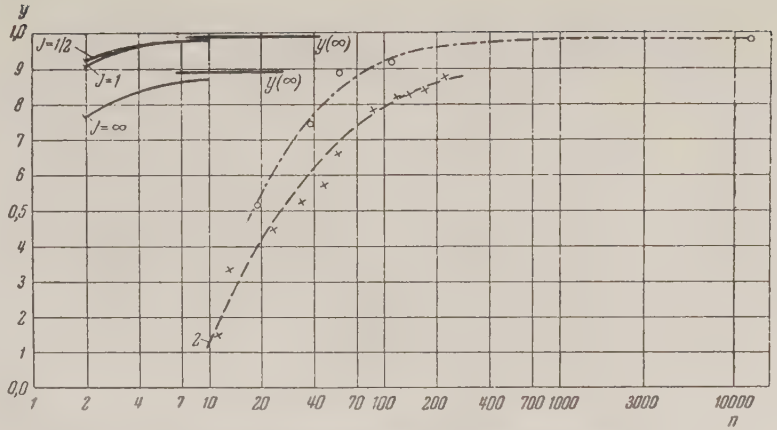

Fig.2. Calculated spontaneous magnetization of a thin film of Fe with the (100) lattice orientation as a function of the number n of monatomic planes, compared with the experimental data of Drigo (1) and Reincke (2).

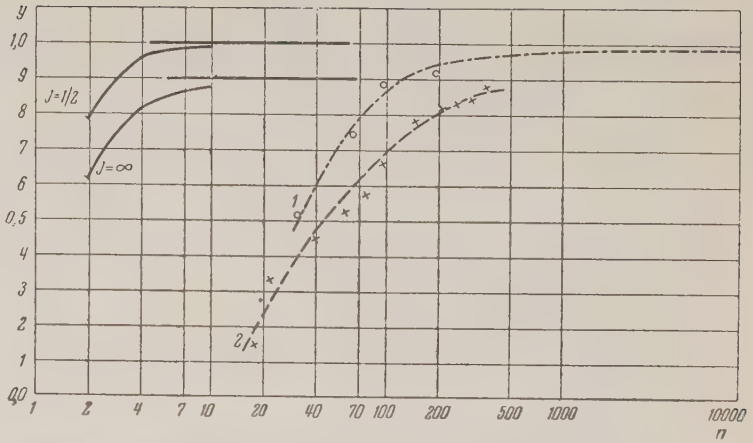

Fig.3. Same as Fig.2, but for the lattice orientation (111).

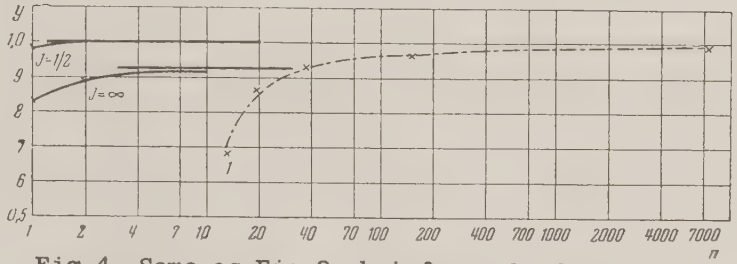

Fig.4. Same as Fig.2, but for a Co film with the lattice orientation (0001).

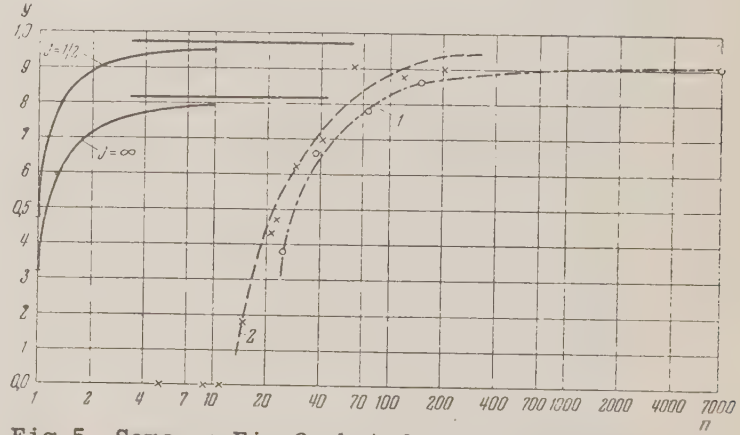

Fig.5. Same as Fig.2, but for an Ni film with the lattice orientation (111). The comparison is with the data of Drigo (1) and Crittenden & Hoffman (2).

2. The Theory of Molecular Fields of Thin Films

We used the molecular field method to calculate the spontaneous magnetization of thin films of the ferromagnetic elements Fe, Co and Ni as a function of the number n of monatomic layers (i.e., as a function of the film thickness). The calculated curves characterizing the dependence for different lattice orientations are shown in Figs.2 through 5. For comparison, some experimental points are plotted in the same figures (Drigo[2], Crittenden & Hoffman[3] and Reincke[7]). It will be evident from Fig.2 that the curves for J = 1/2 and J = 1 with the (100) orientation in Fe are almost the same; this is also true for the other cases investigated. We shall therefore restrict our further consideration to the two limiting cases J = 1/2 and J = ∞.

It will be seen from the figures that the theory is in qualitative agreement with experiment. Quantitatively, however, the agreement is not very good. We shall show that there are plausible explanations for this lack of agreement. The figures also indicate that according to our theory, spontaneous magnetization can exist in Ni and Co even in the case of a two-dimensional lattice.

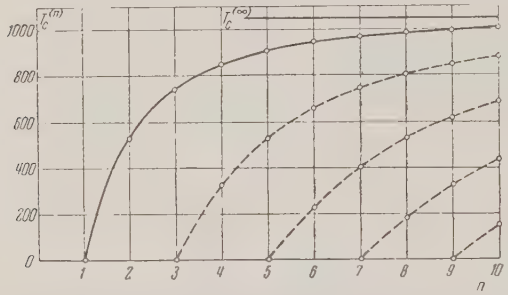

Fig.6. The theoretical Curie point of an Fe film with the lattice orientation (100) as a function of the number n of monatomic planes. The solid curve has physical significance.

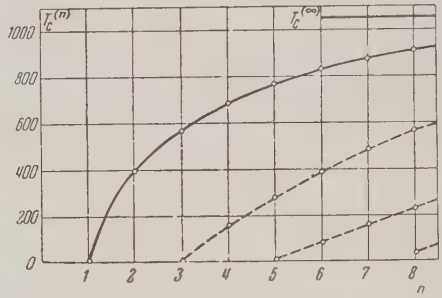

Fig.7. The same as Fig.6, but for the lattice orientation (111).

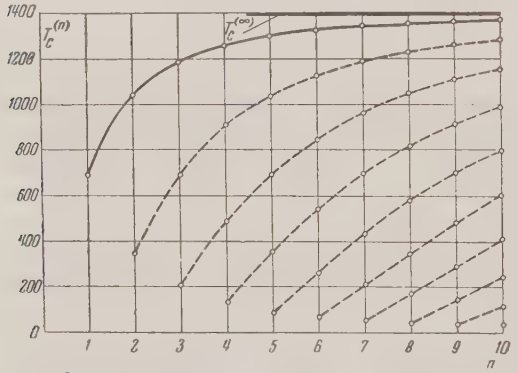

Fig.8. The same as Fig.6, but for a Co film with the lattice orientation (0001).

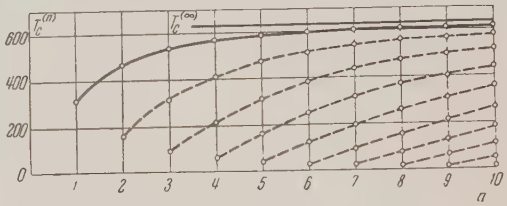

Fig.9. The same as Fig.6, but for an Ni film with the lattice orientation (111).

The proposed theory can also be used to calculate the Curie point $T_c^{(n)}$ as a function of the thickness of the film or number n of monatomic layers. The Curie point is found by solving the n-th order secular equation:

$$|s_{ik} - \lambda\delta_{ik}| = 0, \qquad (2)$$

where

$$\lambda(T) = \frac{3J}{J+1} \cdot \frac{1}{a} T,$$

$$\alpha = \frac{3J}{J+1} \cdot \frac{T_c^{(\infty)}}{s}, \qquad s = \sum_{k=-\infty}^{+\infty} s_{1k}.$$

All the roots of (2) are real. Not all, however, have physical meaning. The possible values of $T_c^{(n)}$ for Fe, Co and Ni films are given in Figs.6 through 9 for different values of n. The curves that have physical meaning are indicated by solid lines.

An interesting property of Eq.(2) is that it leads to simple relations independent of the film thickness between the roots for Fe, Co and Ni films having certain lattice orientations. Thus, for instance, for Ni (111) and Co (0001) we obtain the relation

$$\left(\frac{T_c^{(n)}}{T_c^{(\infty)}}\right)_{Co} = \left(\frac{T_c^{(n)}}{T_c^{(\infty)}}\right)_{Ni} \tag{3}$$

for n = 1,2,... . Similarly, for Fe (100) and Ni (111), and for Fe (100) and Co (0001), we obtain

$$2\left(\frac{T_c^{(n)}}{T_c^{(\infty)}}\right)_{Co} - \left(\frac{T_c^{(n)}}{T_c^{(\infty)}}\right)_{Fe} = 1, \tag{4a}$$

$$2\left(\frac{T_c^{(n)}}{T_c^{(\infty)}}\right)_{Ni} - \left(\frac{T_c^{(n)}}{T_c^{(\infty)}}\right)_{Fe} = 1 \tag{4b}$$

for n = 1,2,... . Unfortunately, it is impossible at present to compare these relations with experiment.

3. Discussion of the Results

In spite of the fact that there exist many experimental studies of thin films, we were able to compare our results only with the experimental data of the three investigations cited above (Refs. 2,3 and 7). Of these only Drigo[2] studied $T_c^{(n)}$ in addition to the spontaneous magnetization, and this only for some of his samples. In spite of this highly unsatisfactory basis for comparing our theory with experiment, we must make an attempt to draw some conclusions on the basis of the available material. It is remarkable that according to the experimental curves, which have essentially the same character as the theoretical ones, the spontaneous magnetization vanishes at thicker layers than is predicted by the theory. The measured values of $T_c^{(n)}$ as is seen from Fig.10, however, do not fall below the bound following from the theory.

Let us attempt to explain this discrepancy. One of the reasons for the divergences may be that the actual experimental layers were not in vacuum, but were formed on some solid substrate, such as glass[3,7] or copper[2]. Further, the measurements were mostly performed in air. In some cases the films were covered by a protective layer of SiO.[3] Contact with another medium may lead to different departures from ideal conditions. For one thing, the base surface is never an ideal plane; even in the case of their particularly careful experiments, Crittenden and Hoffman estimate that the deviation from an ideal plane was of the order of 6 Å, which would correspond to two or three monatomic layers.

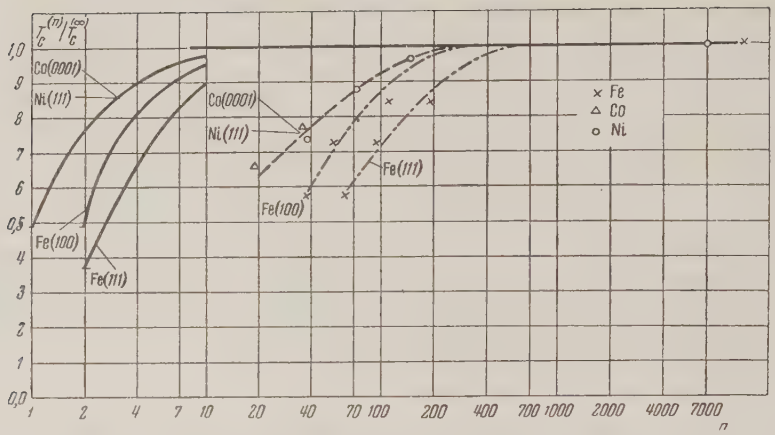

Fig.10. Variation of the theoretical relative Curie point as a function of the number of monatomic layers compared with the experimental data of Drigo[2] for Fe, Co and Ni.

Another complicating factor might be diffusion from one medium into the other. Unfortunately this question has still hardly been studied, but some indications can be obtained from Matano's measurements[8] of diffusion in Ni and Cu systems. From his measurements it would seem reasonable to conclude that such diffusion hardly plays any role in our case. The same may be said about glass supports. More important is a different type of diffusion, namely, oxidation, which is very difficult to eliminate. Thus, for instance, Crittenden and Hoffman attempted to protect their films by coatings of up to 200 Å in thickness, but found that when these protected films were brought into contact with air an oxide layer as much as 20 Å(!) thick was formed and that the oxide layer continued to grow with time. Other authors as well have observed such oxide layers. Thus one of the possible explanations for the vanishing of the spontaneous magnetization, which is observed even for thick samples, may be that the magnetic film may have accounted only for a small part of the total "measured" film thickness, comprised of the truly magnetic film and of a non-magnetic (or only weakly magnetic) oxide layer. Moreover, the structure of the oxide layer itself may play a significant role. Unfortunately, this question has not been adequately studied.

Another complication is the tendency of thin films to form grainy structures. This has been shown by several micrographs, particularly, some made with electron microscopes (see, for instance, Schopper[9]). It may even be true that graininess occurs more often than does a smooth, compact structure. It is clear that such graininess will alter the magnetic properties of the film. It is therefore necessary to study the actual structure of investigated films. Insufficient attention was paid to this point in the experimental studies which we have compared with our results. Only Crittenden and Hoffman attempted to show, using an indirect method, that their films were compact. It is clear that the extent of the deviations will depend whether the bulk or the surface plays the dominant role.

Further, it is quite difficult to measure the true thickness of thin films. All the methods commonly used, including those employed in the above

mentioned investigations, are more applicable to comparatively thick films. Each method appears to have an "optimal accuracy" thickness peculiar to itself (see, for example, Refs.9 and 10). It is therefore highly probable that in the case of very thin films the inaccuracy of thickness measurement distorts the results.

In view of these difficulties, it would be expedient in the future to give attention to those properties that do not depend directly on the thickness: for example, the relations predicted by Eqs.(3) and (4).

In conclusion, it may be said that the question of agreement between theory and experiment is still open. More experimental data is needed.

Physical Institute of the
Czechoslovak Academy of Sciences

References

1. M.J.Klein & R.S.Smith, Phys.Rev., 81, 378 (1951).
2. M.Drigo, Nuovo Cimento, 8, 498 (1951).
3. E.C.Crittenden & R.W.Hoffmann, Rev.Mod.Phys., 25, 310 (1953).
4. F.Bloch, ZS.f.Phys., 57, 545 (1929).
5. S.V.Vonsovskii & Ia.S.Shur, Ferromagnetizm (Ferromagnetism), M.1948).
6. K.B.Vlasov & B.Kh.Ishmukhametov, Zhur.eksp.i teor.fiz., 27, 75 (1954).
7. W.Reincke, ZS.f.Phys., 137, 169 (1954).
8. C.Matano, Jap.J.Phys., 8, 109 (1932-1933).
9. H.Schopper, Fortschr.d.Phys., 2, 275 (1954).
10. S.Melhfessel, Dünne Shichten. W.Knapp, Hall (Saale), 1953.

ON THE TEMPERATURE AND FIELD DEPENDENCE OF THE MAGNETIC ANISOTROPY CONSTANTS OF A CUBIC CRYSTAL (Abstract*)

- A. A. Gusev and S. V. Tiablikov

The Hamiltonian of the electron system which determines the ferromagnetism in the Heitler-London model can be written as a series of even powers of spin operators. Keeping terms only up to the fourth order and taking account of the cubic symmetry of the lattice, the approximate second quantization method can be used to determine the energy spectrum of the system, to calculate the free energy, and to obtain the temperature and magnetic field dependence of the magnetic anisotropy constants. The first magnetic anisotropy constant of a cubic ferromagnetic lattice is given by the approximate expression

$$K_1 \approx K_0^1 \left\{ 1 - 5 \left(\frac{\vartheta}{\vartheta_c} \right)^{3/2} \sum_{n=1}^{\infty} \frac{1}{n^{3/2}} \exp \left[- \frac{1}{\vartheta} 2\mu (H\sigma) n \right] \right\},$$

where $K_1^0 = \bar{J}_4/12v$ and $\vartheta_c = \frac{2\pi}{3} \bar{J}_2$ ($\bar{J}_2$ is the mean value of the exchange energy, $\bar{J}_4$ is the mean value of the magnetic interaction energy, and v is the volume per atom, given by $v = V/N$).

The expression obtained for K_1 is valid in the temperature interval $\bar{J}_4 < \vartheta \ll \bar{J}_2$, in accord with the conditions for the applicability of the theory.

Moscow State University

* * * * * *

CONCERNING THE SPECTRUM OF ELEMENTARY EXCITATIONS AND SOME KINETIC PROCESSES IN FERROMAGNETIC CRYSTALS (Abstract**)

- E. A. Turov

The report is devoted to a theoretical investigation of the energy spectrum of ferromagnetic metals and semiconductors, taking into account the inter-relation between the magnetic (spin), current (charge), and lattice (phonon) degrees of freedom of the system. The authors discuss the applications of the theory to certain kinetic phenomena in ferrmagnetic crystals: the electric conductivity, ferromagnetic resonance, etc.

---

* Complete report in FFM (Phys. Metals & Metallography) 2, 385 (1956).

** A complete account of the work is contained in E. A. Turov & Iu. P. Irkhin, FMM, 3, 15 (1956) and E. A. Turov Izv. (Bulletin) USSR Ac. of Sci., Phys. Ser., 19, 462 & 473 (Trans. pp. 414 & 426), (1955).

PHASE TRANSITIONS AND PHASE DIAGRAMS IN A RHOMBIC ANTIFERROMAGNETIC CRYSTAL (Abstract)

- C.J.Gorter & T.Van Peski-Tinbergen

The report is concerned with a theoretical investigation of the phase transitions that may occur in antiferromagnetic rhombic crystals. The calculations are carried out in the molecular field approximation although the general results, in the opinion of the authors, are not limited by this approximation.

The energy of the antiferromagnet is written as

$$U = -\frac{1}{2} N \sum_{x,y,z} \left\{ A_x \frac{M'_x M''_x}{\mu_x^2} - D_x \frac{M'^2_x + M''^2_x}{2\mu_x^2} \right\}, \qquad (1)$$

where M' and M'' are the mean magnetizations per ion of two equivalent sublattices, μ is the maximum value of the magnetic moment of the ion, A_x, A_y and A_z are the coefficients of antiferromagnetic interaction between the sublattices, D_x D_y and D_z are coefficients of the magnetic ferromagnetic or antiferromagnetic (<0) interaction inside one sublattice. The effective fields acting on the magnetization of the sublattices are given by

$$H' = H - \left(\frac{2}{N}\right)\left(\frac{\partial U}{\partial M'}\right); \quad H'' = H - \left(\frac{2}{N}\right)\left(\frac{\partial U}{\partial M''}\right),$$

where H is the intensity of the external magnetic field.

Assuming that the effective spin of the ions is 1/2 and neglecting its nondiagonal matrix elements, we obtain for the dependence of M' and M'' on H' and H'' the following relationship:

$$\left.\begin{aligned} \frac{M'_x}{\mu_x} &= \frac{\mu_x H'_x}{W'} \operatorname{tg} h \frac{W'}{kT}, \\ \frac{M''_x}{\mu_x} &= \frac{\mu_x H''_x}{W''} \operatorname{tg} h \frac{W''}{kT}, \end{aligned}\right\} \qquad (2)$$

where

$$W' = \left\{ \sum_{x,y,z} (\mu_x H'^2_x) \right\}^{1/2},$$

$$W'' = \left\{ \sum_{x,y,z} (\mu_x^2 H''^2_x) \right\}^{1/2}$$

and analogous expressions for the y and z components. Further, the authors consider the case when the external field is oriented in the direction of preferred (easy) antiferromagnetism. In this case

$$A_x + D_x > A_y + D_y > A_z + D_z \quad \text{and} \quad H_y = H_z = 0.$$

Three solutions are obtained for the dependence of the magnetization of the antiferromagnet on the strength of the external magnetic field: solutions a and b corresponding to the antiferromagnetic state (in solution a the magnetic moments of the sublattices are oriented parallel and antiparallel to the field, while in solution b the directions of the magnetic moments do not coincide with the directions of the field and the preferred antiferromagnetism) and solution p corresponding to the paramagnetic state.

Analyzing these states the authors conclude 1) that the transition from the antiferromagnetic (a or b) state to the paramagnetic (p) state is predominantly a second order transition (there may, however, be cases character-

ized by a certain relationship between the values of $A_x, A_y, A_z, D_x, D_y, D_z$, H and T when the a → p transition may be a first order one; there may also be phase transitions inside the a state) and 2) that the a → b transition is a first order transition. Near the first order transition line there may obtain metastable states and hysteresis effects.

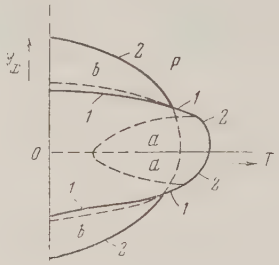

Example of H_x—T phase diagram: the a- and p-states are separated by a second order transition line which goes into a first order transition line; the a- and b-states are separated by a first order transition line which is a continuation of the above-mentioned line; the states b and p are separated by a second order transition line. The numbers at the lines indicate the order of the transitions.

By way of illustration one of the possible phase diagrams in the H_x—T plane for the case when $D_x = 2A_x$ and $A_y + D_y = 2\frac{2}{5}A_x$ is shown in the accompanying figure.

In conclusion the authors briefly discuss the case when the direction of the magnetic field is not aligned with the direction of preferred ferromagnetism.

Kamerlingh Onnes Laboratorium,
Leiden, Holland

METAMAGNETS OR ANTIFERROMAGNETIC SUBSTANCES WITH A THRESHOLD FIELD

- L.Neel

1. Introduction

Although the molecular field theory is not a rigorous one it is still our best guide in interpreting the magnetic properties of antiferromagnetic and ferromagnetic substances. In the present report we shall apply this theory to a particular category of antiferromagnetic substances possessing specific properties, substances which we shall group under the name of metamagnets, a term which has been applied earlier to some of these substances by J. Becquerel[1].

The theory of antiferromagnetism, proposed by us some time ago,[2] is based on dividing the lattice of the magnetic ions into two equivalent sublattices A and B, whose respective magnetizations we shall designate by M_a and M_b. We express the different exchange and superexchange interactions between the ions in terms of the two molecular fields H_a and H_b, acting, respectively, on the sublattices A and B and described by the expressions

$$H_a = n'M_a - nM_b \quad \text{and} \quad H_b = n'M_b - nM_a, \tag{1}$$

where n and n' are the two coefficients of the molecular field; the coefficient n is essentially positive. At high temperatures $M_a = M_b$ and the substance obeys the classical Curie-Weiss law; the magnetization J is given by

$$J = \frac{CH}{T-\theta_p}, \tag{2}$$

where C has the classical meaning of the Curie constant and where

$$\theta_p = \frac{1}{2} C(n'-n). \tag{3}$$

Below a certain temperature T_n order is established in the orientation of the magnetic moments and the two sublattices acquire spontaneous magnetizations equal in magnitude but opposite in direction; we designate the magnitude of the spontaneous magnetization of each sublattice by $\frac{1}{2}M$. This magnetization is a function of the temperature. Everything occurs as though each sublattice were ferromagnetic and acquired under the influence of the spontaneous molecular field $H_m = (n'+n)M/2$ a spontaneous magnetization $M/2$. The value of T_n is given by

$$T_n = \frac{1}{2} C(n+n'). \tag{4}$$

At the temperature $T = T_n$ the susceptibility is given by

$$\chi = \frac{1}{n}. \tag{5}$$

2. Different categories of antiferromagnetic substances

The value of n being given, that of n' cannot be arbitrary: obviously, if n' were negative and large as regards absolute magnitude compared with n there would obtain a different subdivision of the principal lattice into the two sublattices, corresponding to a lower free energy than that for the

subdivision initially adopted. We shall not go further here into this very complex question of the stability of the sublattices, which is connected with the structure of the crystal lattice and with the interactions between a given atom and its various neighbors.

The coefficients n and n' can be determined by means of expressions (3) and (4), if the values of the paramagnetic Curie temperature θ_p and the transition temperature T_n are known. When these coefficients are determined for several dozen not known and investigated antiferromagnetic substances, it becomes apparent that they may be conveniently divided into three principal groups. The first group, comprising such substances as FeO, MnO, etc., is characterized by negative values of n' in the range from $-0.51\,n$ to $-0.57\,n$; the arrangement of ions in substances of this group derives from that of the face-centered cubic lattice. The second group comprises substances like FeF_2, CoF_2, etc. and is characterized by negative values of n' in the range from $-0.16\,n$ to $-0.28\,n$; the arrangement of the ions derives from that of the body-centered cubic lattice: all the nearest neighbors of an atom of one sublattice belong to the other sublattice. Lastly, the third group comprising such substances as $NiCl_2$, $CoCl_2$, etc., is characterized by positive values of n' that are often very large compared with n. Herein we shall turn our attention primarily to the substances of the third group.

3. Magnitocrystalline coupling

To complete our description of the properties of antiferromagnets, it is necessary to take into account the magnitocrystalline coupling. This coupling leads to the appearance in the expression for the total energy of a term E_c which depends on the orientation of the antiferromagnetism direction with respect to the crystal axes. Let us assume, for example, that we are dealing with a uniaxial material in a zero magnetic field; the magnetization M_a and M_b of the two sublattices will be rigorously antiparallel and this term may, in the first approximation, be written in the form

$$E_c = -K' \cos^2 \theta, \tag{6}$$

where θ is the angle between the principal axis and the direction of antiferromagnetism, i.e., the direction parallel to M_a and M_b. If, for example, the constant K' is positive, the direction of antiferromagnetism coincides with the principal axis. We have very little information on the actual values of K', but we have reason to assume that they are of the same order of magnitude as the anisotropy constants of ferromagnetic materials, that is, of the order of 10^4-10^6 erg/g.

In the absence of external perturbations, the directions of antiferromagnetism will lie in the preferred directions corresponding to the minima of E_c. One can note a certain similarity between these preferred directions and the preferred directions of spontaneous magnetization in a ferromagnet, but there is actually a very important difference. Thus the application of a field H in the case of a ferromagnet gives rise to a couple of the order of MH; in contrast, in the case of an antiferromagnet, the couple acting in the direction of the antiferromagnetism is much smaller, being of the order of H^2/n. It follows that the directions of antiferromagnetism are probably much more difficult to alter than the directions of spontaneous magnetization in ferromagnets.

4. Parallel and perpendicular susceptibilities

In view of the fact that there exist preferred directions of antiferromagnetism, it is appropriate to distinguish between two cases of application of a magnetic field to an antiferromagnetic system: 1) the case when the field is applied at right angles to the preferred direction and 2) the case when the field is parallel to the preferred direction.

When the field is perpendicular to preferred direction, the system acquires a magnetization J parallel to H given by

$$J = \frac{H}{n}; \tag{7}$$

susceptibility J/H is independent of H and equal to $1/n$. This is termed the perpendicular susceptibility and designated by s_n.

When the applied field H is parallel to the preferred direction of antiferromagnetism, the parallel susceptibility s_p = J/H is always independent of the field, but its value is given by a more complicated expression:

$$\frac{1}{s_p} = n - \frac{1}{2}(n + n')\frac{M}{T}\frac{\mathrm{d}T}{\mathrm{d}M}, \tag{8}$$

where M/2 is the spontaneous magnetization of each of the sublattices mentioned above. At the transition temperature T_n, the factor $(M/T)\,\mathrm{d}T/\mathrm{d}M$ approaches zero, so that s_p approaches $1/n$, i.e., the value of s_n. On the contrary, when the temperature approaches absolute zero, $(M/T)\,\mathrm{d}T/\mathrm{d}M$ tends to infinity, so that s_p goes to zero.

Thus, when n' is of the same order of magnitude as n, the susceptibility s_p varies gradually from 0 to $1/n$ as T is increased from absolute zero to the transition temperature T_n. And, on the contrary, when n' is very large compared to n, the susceptibility s_p remains equal to zero up to a temperature close to T_n and then changes rapidly to reach the same value of $1/n$ at $T = T_n$.

When the magnetic field is parallel to the preferred direction of antiferromagnetism, the magnetization of the system is determined by the competition of two factors: 1) the increase of the magnetization M_a of the sublattice whose magnetization is directed in the same sense as H and 2) the decrease of M_b; the orientations of M_a and M_b however, remain constant just as the direction of antiferromagnetism. On the contrary, when the field is perpendicular to the direction of antiferromagnetism, M_a and M_b no longer remain antiparallel but tend to align themselves with the direction of the field. In this case one might conveniently define the direction of the antiferromagnetism as the external bisector of the angle between M_a and M_b; the direction of antiferromagnetism remains invariable regardless of H.

5. The decoupling effect and the threshold effect

A more detailed study of the effects obtaining in the case where the magnetic field is parallel to the direction of antiferromagnetism shows that there exists a critical field value that may be termed the threshold field, for which the direction of antiferromagnetism departs suddenly from the preferred direction and becomes perpendicular to it; at the same time there will be a discontinuity in the variation of the susceptibility which will jump suddenly from s_p to $1/n$, i.e., to s_n. The threshold field is given by

$$H_s^2 = 2K'n. \tag{9}$$

We inferred the existence of this effect back in 1936 (Ref.3) and it was rediscovered in 1952 by C.J.Gorter and his coworkers[4] during the course of a series of brilliant investigations of the magnetic properties of $CuCl_2 \cdot 2H_2O$. It may be noted here that in the case when K' equals zero, that is, in the case of absence of coupling between the crystal lattice and the direction of antiferromagnetism, the direction of antiferromagnetism is always oriented perpendicularly to the applied field and the susceptibility remains constant and equal to $1/n$.

In most ferromagnets the value of the threshold field H_s is probably very high so that the susceptibility remains independent of the field up to the highest values it is feasible to attain in practice, but this should not be the case when n is small, particularly, when the ratio n'/n is large.

6. Anisotropy constants K_0 and K_1 of an antiferromagnet

Let us now consider the influence of the magnitocrystalline energy on the existence of a threshold field. In order not to complicate the discussion unduly, we shall limit our consideration to a simple case: that of a uniaxial substance in which the ratio n'/n is large. In this case the modifications of the state of the system produced by the action of an external field reduce to simple changes in orientation of the spontaneous magnetizations M_a and M_b each of which retains a value equal to M/2 which depends only on the temperature T. The total energy of the system is equal to the sum of the Weiss-Heisenberg exchange energy, the energy of the system in the external field H and the magnitocrystalline energy. The part E_w of the exchange energy that does not depend on the angle between M_a and M_b is given by

$$E_w = n\mathbf{M}_a\mathbf{M}_b, \tag{10}$$

while the energy of the crystal in the external field is

$$E_h = -\mathbf{H}(\mathbf{M}_a + \mathbf{M}_b). \tag{11}$$

As for the magnitocrystalline energy E_c, the state of the system is defined by the angles θ and θ' between M_a and the axis and M_b and the axis and the angle φ between the meridian planes containing M_a and M_b. Bearing in mind that in the general expression for E_c there exist terms which do not depend on the angle between M_a and M_b and that these terms, therefore being isotropic, can be incorporated into the exchange terms by appropriate modification of the coefficient n, we can show that the general expression for the magnitocrystalline energy E_c of a uniaxial antiferromagnetic substance, restricted to terms of the second degree with respect to the direction cosines of M_b and M_a depends only on the constants K_0 and K_1 and may be written[5]

$$E = -\frac{1}{2}K_0(\cos^2\theta + \cos^2\theta') - K_1\cos\theta\cos\theta'. \tag{12}$$

7. Equilibrium states of the system

With no external field the equilibrium state of the system is obtained by determining the minimum of the sum $E_w + E_c$; from considerations of symmetry this minimum always corresponds to $\varphi = 0$. Three states are possible: two antiferromagnetic states and one ferromagnetic state. In the two antiferromagnetic states (Ap) and (An), the directions of antiferromagnetism are re-

spectively parallel and normal to the axis. In the ferromagnetic state (Fp), the preferred direction of spontaneous magnetization is parallel to the crystal axis.

In order to simplify writing of the results we introduce two auxiliary, dimensionless variables r and r' defined by the following expressions:

$$r = \frac{2(K_0 + K_1)}{nM^2} \text{ and } r' = \frac{2(K_0 - K_1)}{nM^2} . \qquad (13)$$

It is found[5] that with r' negative the system is in the (An) state when r is smaller than unity and in the (Fp) state when r is larger than unity. When r' is positive, the system is in the (Ap) state when $r-r'$ is smaller than unity and in the (Fp) state when $r-r'$ is larger than unity.

Plotting representative points in rectangular r and r' coordinates, one can divide the plane (r, r') into two regions by a broken line PQS: to the right of this line lies the ferromagnetic region; to the left the antiferromagnetic region (Fig.1).

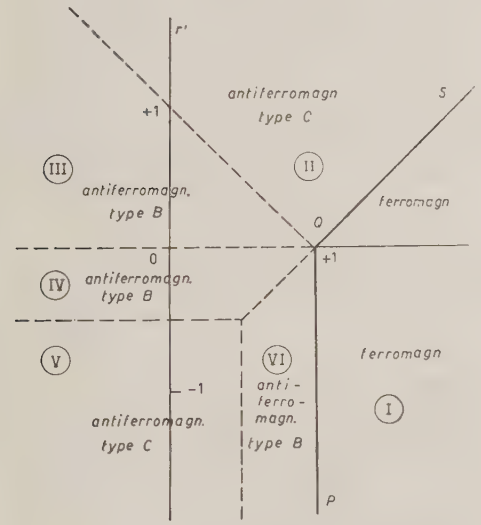

Fig.1. Antiferromagnetism-ferromagnetism state diagram in the (r,r') plane. When r' is positive, the crystal axis and the direction of antiferromagnetism are parallel; they are mutually perpendicular when r' is negative.

8. Effect of an external magnetic field

We must now complete our investigation of the antiferromagnetic region by determining the magnetization obtained in subjecting the system to an external field H. To this end we need only add to the energy of the system the term E_h given above by Eq.(11) and write the condition for minimum energy. The calculations are actually very simple and we will, therefore, merely give the results, which have already been published in part.[6] For the sake of brevity we shall express the magnetic field H in terms of the reduced variable

$$h = \frac{2H}{nM} . \qquad (14)$$

It is found, first, that with the applied magnetic field H perpendicular to the direction of antiferromagnetism, the magnetization remains proportional to H up to the saturation value M. The susceptibility s_n thus retains a constant value to the point where the reduced field h attains the value h_1 and one obtains a magnetization curve of the type A shown in Fig.2. The reciprocal of the perpendicular susceptibility $(1/s_n)$ is equal to $n(1 + r')$ when r' is positive and to $n(1-r)$ when r is negative (in the former case the direction of antiferromagnetism is parallel to the crystal axis; in the latter case it is perpendicular to the axis).

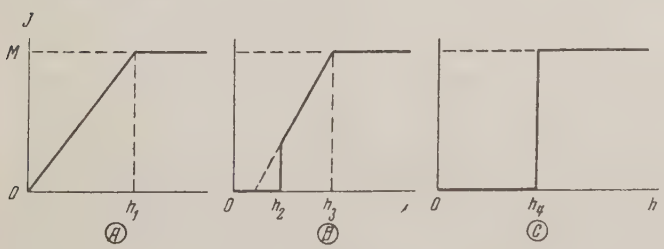

Fig.2.

Thus in the two cases we obtain values of the susceptibility s_n differing markedly from the conventional value $1/n$. This circumstance is of interest because, as will be shown below, the parameter r' may change with the temperature to a much greater extent than n. On the basis of this it may be possible to explain the abnormal variations of s_n sometimes observed.

The laws of magnetization of the system in a field parallel to the direction of antiferromagnetism are much more complicated than in the preceding case, inasmuch as here there must exist a threshold field. In the initial phase of magnetization the direction of the antiferromagnetism, defined as the external bisector of the angle between M_a and M_b is parallel to the direction of the field, while during the final phase, at the instant when M_a and M_b become parallel, it is perpendicular to the direction of the field; this means that there is a discontinuity or jump at a certain threshold field h_s. There are two types of magnetization curves (laws): type B in which the magnetization remains zero until the field attains the threshold value h_2 at which the magnetization jumps to a value below the saturation magnetization M. With further increase in the field strength the magnetization remains proportional to the field, with J/H = s_p constant, then attains saturation at $h = h_3$. In the case of type C magnetization, the discontinuity occurs at the field value h_4 and the magnetization jumps from zero directly to the saturation value M (see Fig. 2).

In this description we have assumed that the susceptibility is zero in the initial phase when the field is below the threshold value. As we pointed out above, (see Section 4) this hypothesis is valid to a temperature close to the transition temperature T_n, for we are limiting our consideration to the case where n' is large compared with n.

We have determined, as functions of r and r', the types of magnetization laws obtaining and the values of the corresponding critical fields h_2, h_3 and h_4. The plane (r, r') is divided, as may be seen in Fig.1, into six regions by the six straight lines $r' = 0$, $r = 1$, $r' = -1/2$, $r = 1/2$, $r - r' = 1$, $r + r' = 1$. The results of our calculations are summarized in Table 1.

If instead of a single crystal, one investigates a powder composed of randomly oriented crystallites, the mean susceptibility s_m is given in the first approximation by

$$s_m = 2s_n + s_p. \tag{15}$$

This formula is not rigorous for two reasons: it does not take into account the magnetic interactions between the crystallites and it also leaves out of account the rotation of the direction of antiferromagnetism which occurs when the field is applied to an oblique angle to the direction of antiferromagnetism (this rotation is of the order of h^2, while the rotation of M_a or of M_b is of the order of h). Nevertheless, because of its simplicity, we shall utilize Eq.(15); it shows that the presence of a threshold field is evinced in the case of a powder by a much more rapid variation of the magnetization as a function of h.

9. Paramagnetic hysteresis

The results that have been summarized in Table 1 were obtained on the assumption that the system always assumes the configuration corresponding to the lowest energy. Actually, false equilibrium states are possible; analysis of these effects relative to type B magnetization, for example, shows[6] that

Table 1

Values of the susceptibilities s_n and s_p and critical fields corresponding to the different regions of the (r, r') plane

Region in the (r,r') plane (Fig. 1)	Direction of antiferromagnetism	Value of s_n (type A magnet. law) and field h_1	Magnetization parallel to the axis		
			Type of magnetization	Value of s_p	Value of critical field
II	Parallel to crystal axis	$s_n = \frac{1}{n(1+r')}$ $h_1 = 2(1+r')$	C		$h_4 = 1+r'-r$
III	Same	$s_n = \frac{1}{n(1+r')}$ $h_1 = 2(1+r')$	B	$s_p = \frac{1}{n(1-r)}$	$h_2 = 2(1-r)^{1/2} r'^{1/2}$ $h_3 = 2(1-r)$
IV	Normal to crystal axis	$s_n = \frac{1}{n(1-r)}$ $h_1 = 2(1-r)$	B	$s_p = \frac{1}{n(1-r')}$	$h_2 = 2(-r')^{1/2}(1+r')^{1/2}$ $h_3 = 2(1+r')$
V	Same	$s_n = \frac{1}{n(1-r)}$ $h_1 = 2(1-r)$	C		$h_4 = 1$
VI	Same	$s_n = \frac{1}{n(1-r)}$ $h_1 = 2(1-r)$	B	$s_p = \frac{1}{nr}$	$h_2 = 2r^{1/2}(1-r)^{1/2}$ $h_3 = 2r$
I	The system is ferromagnetic; the direction of preferred spontaneous magnetization is normal to the axis.				

in an increasing magnetic field the decoupling effect or sudden shift in the direction of antiferromagnetism should occur only at a field h_2' greater than h_2 and, on the contrary, in a decreasing field the return of the direction of antiferromagnetism to its initial position occurs at a field value h_2'' lower than h_2. Thus there obtains a real hysteresis effect.

So far we have no precise experimental data on the subject and hence will not labor the point, particularly, since it is possible that there exists a mechanism that allows the system to assume automatically the minimal energy configuration. It is known that such a mechanism, namely, the displacement of the Bloch walls, allows in a ferromagnet of a choice between two oppositely magnetized phases, starting with the minimal energy phase for an almost zero applied field, whereas the reverse transition from one phase to the other should necessitate a very strong magnetic field. One might even hypothesize that in an antiferromagnetic substance there always exist, but in variable proportions, two phases one of which corresponds to a direction of antiferromagnetism parallel to the axis, the other to a direction perpendicular to the axis, and assume that the changes in the relative proportions between the phases are realized by displacement of the wall separating them.

10. Application to anhydrous chlorides

The considerations developed above are directly applicable to $NiCl_2$, $CoCl_2$ and $FeCl_2$ crystals as we have had occasion to show recently.[6]

The chlorides $NiCl_2$ and $CoCl_2$ very probably belong to type B; this is indicated by the fact that their susceptibility in fields of the order of

1000 oersted is much weaker (about two thirds) than their susceptibility in a 10,000 oersted field. This is what may be expected in the case of a powder, when there exists a threshold field of a medium value. Experimental data do not allow of determining the four constants n', n, r and r', for we have only two reliable quantities - the transition temperature T_n and the susceptibility in strong fields (virtually equal to s_n) - and one doubtful quantity - the value of the threshold field. If we assume arbitrarily that $r = r'$, we obtain the magnetization values (per gram) shown in Table 2.

Table 2

Substance	$NiCl_2$	$CoCl_2$	$FeCl_2$
n'	11 000	3 000	3 400
n	1 300	340	130
r	0.001 6	0.054	0.5

For $FeCl_2$, the amplitude of the discontinuity corresponding to the threshold field is very large, of the order of magnitude of the saturation magnetization. In this case we are obviously dealing with the type C magnetization law (Fig.2) and our representative point falls into region II in the (r, r') plane.

The value of the ratio n'/n is high - at least 10 - for all three chlorides. The initial susceptibility varies as the reciprocal of $n(1 + r)$; when r is small experiment shows that the susceptibility is virtually independent of the temperature, whence one may conclude that n is also practically temperature independent. This conclusion is logical inasmuch as n represents exchange interactions. On the contrary, the initial susceptibility of $FeCl_2$ is strongly dependent on the temperature; this is certainly due to the temperature variation of r, which cannot be neglected compared to unity inasmuch as it equals 0.5.

11. Application to $MnAu_2$.

Recently A.Meyer and P.Taglang have shown[7] that the magnetic susceptibility of the metallic compound $MnAu_2$ remains independent of the temperature from 100 to 300°K and of the magnetic field up to about 10,000 oersted. At this field value, the magnetization J begins to vary much more rapidly and then approaches the saturation value in conformity with the law

$$J = J_s\left(1 - \frac{b}{H^2}\right). \tag{16}$$

As we have shown in an earlier communication[5], this is exactly the behavior that may be expected in the case of an antiferromagnetic substance characterized by a magnetization law of type C and threshold field in the vicinity of 10,000 oersted. It may be assumed that in this case the representative point lies in region II in the (r, r') plane. From the value of the initial susceptibility $s_m = 3.76 \cdot 10^{-4}$ measured on a polycrystalline specimen, we find

$$n(1 + r') = 1770 \tag{17}$$

in the temperature interval from 100-300°K. From the values of the threshold field H_s and the saturation magnetization M, we deduce that in the same temperature interval H_s/M remains in the neighborhood of 270, whence

$$n(1 + r' - r) = 540, \tag{18}$$

but, unfortunately, this is still insufficient for determining n, r' and r.

It may be noted that in the case of iron and nickel, the two most thoroughly studied ferromagnetic substances, the ratio of the anisotropy constant to the square of the spontaneous magnetization (K/M^2) approaches zero at the Curie point. By analogy, it is logical to assume that in antiferromagnetic substances r and r' also both approach zero at the transition point T_n. It would follow that the susceptibility at $T = T_n$ is simply equal to $1/n$. The measurements of Meyer and Taglang indicate that the susceptibility of $MnAu_2$ passes at about $T_n = 370°K$ through a sharp maximum equal to $1.1 \cdot 10^{-3}$, which corresponds to $n = \sim 900$.

Assuming that n does not vary with T, we find on the basis of Eqs. (17) and (18) that in the 100-300°K temperature range r and r' are, respectively, about 1.4 and 1.0.

On the other hand, knowing the paramagnetic Curie point ($\theta_p = 451°K$) and the specific Curie constant ($C = 7.12 \cdot 10^{-3}$), we can by means of Eq. (3) find $n' - n$ and from it n'; this gives $n' = 128{,}000$. The ratio $n'/n = 142$ here is particularly large. This large value of n'/n and the fact that r and r' go from zero to 1.4 and 1.0, respectively, as the temperature is reduced from 370°K to 300°K, serve to explain why the maximum of the initial susceptibility at $T = T_n$ is so sharp. Another fact substantiates our interpretation: when the applied field is sufficiently strong [$h > 2(1 + r')$], the two spontaneous magnetizations M_a and M_b coincide in every one of the crystallites and the situation obtaining is entirely analogous to that in a uniaxial ferromagnetic substance with an anisotropy energy equal to $-(K_0 + K_1)\cos^2\theta$. The law of the approach to saturation in this case must be of the type given by (16) with

$$b = \frac{4K^2}{nM^2} = \frac{n^2r^2M^2}{15}. \tag{19}$$

According to the measurements of Meyer and Taglang, the value of b/M^2 remains in the vicinity of $0.64 \cdot 10^5$ in the temperature range from 100-300°K; whence we find $nr = 980$, whereas the value of nr deduced from earlier data was 1260; this result is highly satisfying in view of the extremely schematic character of the theory.

12. Temperature dependence of r and r'. Transition between ferromagnetism and antiferromagnetism.

We have already mentioned above the experimental indications that give reason to think that r and r' approach zero at the temperature T_n of disappearance of spontaneous magnetization. These results are supported by the deductions of the theory of Akulov[8], according to which the anisotropy constant of a cubic ferromagnet varies in the vicinity of the Curie point as the tenth power of the spontaneous magnetization. It follows therefore that r and r' vary as M^8 and go to zero at $T = T_n$. We shall assume therefore that this point is proved.

Far from the transition point, the anisotropy constants are sometimes proportional to the square of the spontaneous magnetization; in this case

r and r' are constant, as for example in $MnAu_2$ above 300°. But there are many other cases wherein the anisotropy constant varies to a far greater extent and in a more complicated manner: for example, in hexagonal substances such as Co and MnBi. Thus in cobalt K falls from $4.7 \cdot 10^7$ erg/mole to zero as the temperature is increased from -200 to +200°C, while the decrease of M^2 in the same temperature interval is only of the order of 5%. In MnBi the constant rises from zero to $3.5 \cdot 10^8$ erg/mole between 84 and 300°K, while M^2 decreases slightly.[9]

Finally, we come to the conclusion[10] that the representative point R of the state of the antiferromagnetic system shifts in the (r, r') plane as a function of the temperature to arrive at the origin at $T = T_n$. There may be cases when R, located initially at a low temperature in the region I where r' is positive (Fig.1), moves across the boundary QS between regions I and II at a certain temperature T_a and, continuing its displacement, crosses the boundary between regions II and III at a temperature T_b to arrive at the origin when $T = T_n$. In this case we would obviously be dealing with a substance which is ferromagnetic at low temperatures and which becomes antiferromagnetic at $T = T_a$; the antiferromagnetism is of type C for $T < T_b$ and of type B for $T_b < T < T_n$.

It follows from the considerations developed above that in region II ($T_a < T < T_b$) the relation between the threshold field H_s and the spontaneous magnetization M is given by

$$\frac{H_s}{M} = \frac{1}{2} n (1 + r' - r). \qquad (20)$$

It will be noted that the threshold field H_s approaches zero when T approaches T_a because the equation for the boundary QS between regions I and II is $1 + r' - r = 0$. Consequently, plotting H_s/M as a function of T, we obtain a curve which, on the one hand, goes to the origin as T approaches T_a and, on the other hand, extrapolated towards $T = T_n$ approaches $n/2$. It should be noted that this extrapolation must be carried out through the region II ($T_b < T < T_n$) in the interior of which there still exists a threshold field, but characterized by a different formula: $H_s/M = n(1 - r)^{\frac{1}{2}} r'^{\frac{1}{2}}$.

13. Another type of transition between ferromagnetism and antiferromagnetism

In the type of transition considered above, r' is positive. One can readily conceive of another type of transition corresponding to the case where r' is negative. In this case the representative point R', situated initially (at a low temperature) in the lower part of region I in the (r, r') plane, will move with increasing temperature, cross the boundary PQ between the regions I and IV at a certain temperature T_a, traverse the regions VI and IV and possibly the region V to arrive finally at the origin.

This second type of transition between ferromagnetism and antiferromagnetism is substantially different from the first type. Thus in region VI the magnetization law is of type B and the threshold field which is given by the relationship $H_s/M = n(1 - r)^{\frac{1}{2}} r'^{\frac{1}{2}}$, also approaches zero when $T = T_n$, because the equation for the boundary PQ is $r = 1$. There is, however, a fundamental difference: in the second type of transition the magnetization jump associated with the threshold field goes to zero when T approaches T_a, while in the first type the amplitude of the magnetization discontinuity remains equal to M. It should, therefore, be relatively easy to distinguish between the two cases experimentally.

14. Other transition mechanisms

An analysis of the role of magnitocrystalline coupling on the stability of the different possible configurations shows that the temperature variation of the anisotropy constant may give rise in some substances to a transition from a ferromagnetic to an antiferromagnetic state. This mechanism, naturally, is not the only one possible. Smart[11] has analyzed the different manners in which order can become established in magnetic substances with different crystal lattices as a function of the relative magnitudes of the exchange and superexchange interactions between neighboring atoms. If these interactions vary, i.e., if n and n' are functions of T, there may occur transitions from the ferromagnetic to the antiferromagnetic state. The theory of Smart, applied by him to the case of MnBi and MnAs, takes into account only the temperature variation of the isotropic exchange and superexchange interactions; it entirely disregards the role of the anisotropy constants and the existence of a threshold field. Obviously, it therefore does not lead to any relation between the value of the threshold field and the transition temperature. On the other hand, one cannot be certain that the temperature variation of n and n' in itself is sufficient to produce such effects; besides we have the means of determining whether the molecular field coefficients depend on the temperature. We have shown earlier[12] that in a substance possessing paramagnetism of the Langevin-Weiss type (this is the case of antiferromagnetic substances above their transition temperature T_n) the Curie constant is equal to its theoretical value for pure paramagnetism without a molecular field only in the case where the molecular field coefficients are independent of the temperature. In all other cases a correction factor must be introduced.

15. Application of the theory to interpretation of the magnetic properties of dysprosium

The magnetic properties of metallic dysprosium have been the subject in recent years of detailed studies by Trombe[13] and Elliott, Legvold & Spedding[14]. These properties are very complex and in many ways surprising. In region A, corresponding to temperatures below 90°, dysprosium behaved as a classical ferromagnet. In region B ($90^\circ K < T < 160^\circ K$) the magnetization isoterms present the following pattern: at first the magnetization varies more or less in proportion to the field up to a threshold field H_s, at which point there begins a much more rapid variation of the magnetization, leading finally to an approach to saturation according to the $1/H^2$ law. These isoterms show a striking analogy with those for $MnAu_2$, but whereas the threshold field of $MnAu_2$ varies little with the temperature, the temperature variation in the case of Dy is very pronounced: the field goes from 2500 oersted at 103°K to 10,000 oersted at 153°K.

Further, in the region C, situated above 160°, dysprosium becomes paramagnetic with a specific susceptibility which starts to rise with the temperature, passes through a sharp maximum (reaching a height of $4 \cdot 10^{-3}$) at 178°K and then falls off with further increase in temperature according to the Curie-Weiss law characterized by a Curie constant $C = 0.087$ and a paramagnetic Curie point $\theta_p = 157^\circ K$. In this C region we are undoubtedly dealing with antiferromagnetism with a transition point $T_n = 178^\circ K$. The value of n as determined from the relationship $n = 1/s$, where s is the susceptibility at $T = T_n$ (i.e., $4 \cdot 10^{-3}$) is 250. On the other hand, $n' - n = 2\theta_p C$, whence $n' - n = 3600$, so that $n' = 4100$. Thus, the ratio n'/n is rather large: ~ 16. Hence dysprosium

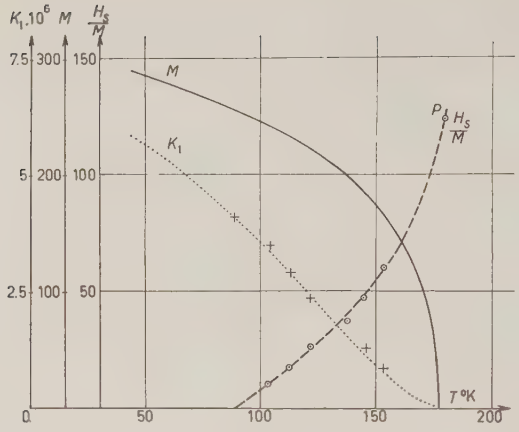

Fig.3.

apparently belongs to the same antiferromagnetic family as $FeCl_2$ and $MnAu_2$ and the existence of a threshold field in this case appears perfectly normal.

As for the transition to ferromagnetism that occurs when the temperature is reduced below 100°K, we suggest that it may be attributed to the temperature variation of the anisotropy constants K_0 and K_1. The fact that the magnetization jump remains very large in the vicinity of the transition point T_a shows that this transition is of the first order.

In order to verify this interpretation, we determined H_s and M from the experimental data and plotted H_s/M as a function of the temperature (Fig.3). It will be seen that we obtain a curve which intercepts the horizontal axis at 90°, i.e., in the immediate vicinity of T_a, estimated above as being about 100°. On the other hand, the same curve extrapolated to $T = T_n$ yields a value very close to 125 for $n/2$ in agreement with the prediction of theory that this is a first order transition. These facts are decisive evidence in favor of our interpretation.

On the other hand, an interpretation based on the assumption of temperature dependence of the molecular fields meets with two serious objections: 1) it does not explain the intimate relationship, disclosed by experiment, between the threshold field and the transition temperature T_a and 2) the fact that the Curie constant in the paramagnetic state has a value virtually equal to its theoretical value for Dy+++; this shows that the temperature dependence of the molecular field coefficients is very weak, as we have indicated above.

16. Value of the anisotropy constant K_1

Knowing n and M, one can from the value of the threshold field H_s find $r - r'$ and then K_1. The values of K_1 evaluated in this manner are plotted as a function of T in Fig.3. Thus we find that K_1 at 90°K equals about $4 \cdot 10^6$ erg/g or about $6.5 \cdot 10^8$ erg/mole. This value may be compared with the value of the anisotropy constant of the compound MnBi, namely, $3.5 \cdot 10^8$ erg/mole. Thus, the anisotropy constants that must be introduced in our interpretation are of the same order of magnitude as the anisotropy constants of known ferromagnetic substances.

The mean initial susceptibility s_m decreases from $4 \cdot 10^{-3}$ to $2.8 \cdot 10^{-3}$ as the temperature is reduced from 178 to 168°K. This decrease is attributable to the diminution of s_p and s_n. The parallel susceptibility s_p is given by Eq.(8); at 10° below T_n, $(M/T)\,dT/dM$ is approximately equal to -0.13, whence we have $s_p = 1.9 \cdot 10^{-3}$ or about half the susceptibility value corresponding to $T = T_n$. The increase in r' as we move away from T_n leads to a decrease of $s_n = 1/n(1 + r')$. Experiment yields only $r - r'$, which is equal to 0.30 at 10° below T_n. If we assume $r' = kr$, we must assign the reasonable value of 0.43 to k in order to obtain a value of s_m in agreement with the experimental data (neglecting the effect of an increase of r' on s_p).

Assuming now that k retains its value of 0.43 when the temperature varies, we deduce that $r + r'$ assumes the value of 1 at $T = T_b = 160$°K; this gives us

the temperature T_b at which the representative point moves across the boundary from region II to region III. The values of the threshold field that we have used correspond to lower temperatures, that is, to region II as we have implicitly assumed.

17. Application to erbium

The magnetic properties of erbium, although known less accurately[15], are analogous to those of dysprosium. Here again we can distinguish the same three regions A, B and C.

In the C Region there appears a susceptibility peak rising to $2.4 \cdot 10^{-3}$ at $T_n = 76^{\circ}K$; it corresponds to $n = 420$. Above T_n, we have Curie-Weiss paramagnetism characterized by a paramagnetic Curie point $\theta_p = +40^{\circ}$ and a Curie constant $C = 0.069$ (theoretical value). Thus we obtain $n' - n = 2\theta_p/C = 1160$, and, consequently, $n' = 1580$. The ratio $n'/n = 3.8$ is appreciably smaller than in the case of dysprosium.

In the B region there appears a threshold field which vanishes towards $30^{\circ}K$. The ratio H_s/M increases almost linearly as a function of the temperature; extrapolation of the curve to T_n yields a value of about 190, which in view of the appreciable experimental uncertainty is reasonably close to the theoretical value $n/2 = 210$. At $30^{\circ}K$ the anisotropy constant K_1 calculated by the same procedure as that for dysprosium is $\sim 6 \cdot 10^6$ erg/g or 10^9 erg/mole.

18. Conclusions

On the basis of experimental results one can distinguish among the general class of antiferromagnetic substances a particular group characterized by positive values of n', i.e., positive interactions inside each sublattice, and small values of n compared with n'. These conditions are favorable for observation of the threshold field ($FeCl_2$, $MnAu_2$, etc.) and possible transition from the antiferromagnetic to the ferromagnetic state in connection with the temperature variation of the anisotropy constants K_0 and K_1.

The same conditions also favor the presence of a permanent superficial magnetic moment associated with the Bloch walls separating the antiferromagnetic domains.[6]

Thus there is justification for putting these substances in a special category, that of metamagnetic substances, to return to a term coined by Becquerel[1] for some of them ($CoCl_2$, $NiCl_2$,...) even before the meaning of their singular magnetic properties had been fully elucidated.

It may well be that in the region of very low temperatures the theory proposed above will not suffice to account for all the magnetic properties of these substances, particularly when the magnetism carriers possess an orbital moment. One must, in this case, take into account the influence of the crystal electric field on the magnetic levels. If the displacement of these levels is of the order of nM^2 or $n'M^2$, the effects become extremely complicated and can no longer be interpreted in an intuitive manner.

Institute Fourier
Université de Grenoble

References

1. J.Becquerel, J.de Phys., 10, 10 (1939); Reunion Internationale de Magnétisme, Vol. I, p.97, Strasbourg, 1939.
2. L.Néel, Ann.de Phys., 17, 5 (1932); J.dePhys., 3, 160 (1932); Ann.de Phys., 5, 232 (1936); C.R.,203, 304 (1936).
3. L.Néel, Ann.de Phys., 5, 232 (1936).
4. C.J.Gorter & H.Haantjes, Physica, 17, 285 (1952); J.Ubbink, J.A.Poulis & C.J.Gorter, Physica, 17, 213 (1951); 18, 361 (1952).
5. L.Néel, C.R., 242, 1549 (1956).
6. L.Néel, X^{e} Conseil de Physique Solvay, Bruxelles, Septembre, 1954; Les electrons dans les métaux, p.251, Ed. by R.Stoops, Bruxelles, 1955.
7. A.Meyer & P.Taglang, C.R., 239, 961 & 1611 (1954); J.de Phys. Rad., 17 (1956).
8. N.Akulov, ZS.f.Physik, 100, 197 (1936).
9. C.Guillaud, Thesis, Strasbourg, 1943.
10. L.Néel, C.R., 242, 1549 & 1824 (1956).
11. J.S.Smart, Naval Res.Rep., No.2113 (July 1951); Phys.Rev., 90, 55 (1953).
12. L.Néel, Ann.de Phys. Series, II, 8, 237 (1937).
13. F.Trombe, J.Tech.CNRS, 23, 61 (June 1953).
14. F.J.Elliott, S.Legvold & F.H.Spedding, Phys.Rev., 94, 1143 (1954).
15. F.J.Elliott, S.Legvold & F.H.Spedding, Phys.Rev., 100, 1595 (1955).

- - - -

Translated from the French. We take this occasion to thank Prof. Néel for his kindness in supplying the French text. Trans.Editor - C.T.T.

A NEW FORM OF FERROMAGNETIC MATERIAL: RARE EARTH FERRITES OF THE GARNET TYPE

- L.Neel, F.Berteau, F.Forra & R.Pothene

Rare earth ferrites have very strange magnetic properties which may be interpreted in the following manner: a) the Fe ions are located in two sublattices forming a ferromagnetic system with a resultant magnetization R; b) the Gd ions produce magnetization in the direction opposite to R under the influence of the molecular field -nR. These properties have been attributed to the compound $FeMO_3$ (where M is the rare earth element) of the perovskite type. This interpretation was, however, doubtful inasmuch as in this structure all the sites occupied by the Fe ions are identical.

Recently, we determined that the properties in question are consonant with the general system $Fe'_2Fe''_3M_3O_{12}$ of the same type as garnet (group $O_h^{10} - Ia3d$, structure type H31). The Fe' ions are at 16a, the Fe'' at 24d and the Gd at 24c. The magnetic properties were also accurately determined in different cases, namely, with M = Y, Gd, Dy and Er.

The spontaneous magnetizations of the two Fe sublattices are directly opposed producing a resultant magnetization R equal at absolute zero to 5 μ_B (μ_B is the Bohr magneton) comprising the difference between three moments of 5 μ_B each, oriented positively and two moments oriented negatively. The M ions are magnetized by the molecular field -nR in the direction opposite to that of the ions located at 24d. For M = Gd with a moment equal to 7 μ_B, the 24c sublattice is noticeably saturated at absolute zero. The theoretical molecular moment equals $(3x7 - 3x5 + 2x5)\mu_B = 16\ \mu_B$, while extrapolation of the experimental data to absolute zero gives a value of 15 μ_B.

As for $FeMO_3$ with the perovskite structure, this is simply an antiferromagnet with a small residual moment similar to the moment in α-Fe_2O_3, due possibly to the not quite complete mutual compensation of the sublattices.

Institut Fourier,
Université de Grenoble

Translation editor's note:

The transactions of the Conference on the Physics of Magnetic Phenomena will be continued in Nos. 8 and 9 of Volume 21. No. 7 is devoted to the first part of the transactions of the Seventh Conference on Nuclear Spectroscopy.

BULLETIN OF THE ACADEMY OF SCIENCES OF THE USSR - Physical Series
Vol. 21, No. 6
Transactions of the Third Conference on the Physics of Magnetic Phenomena
(Moscow, 23-31 May 1956)

TABLE OF CONTENTS

	Page Orig.	Trans.
The de Haas-van Alphen effect - D.Shoenberg	787	789
Influence of pressure on the galvanomagnetic properties of bismuth - N.E.Alekseevskii, N.B.Brandt & T.I.Kostina	790	792
On determination of the individual components of the magnetic susceptibility of a semiconductor - Ia.G.Dorfman	796	798
On the transverse photomagnetic effect in n- and p-type germanium (Abstract) - I.K.Kikoin & Iu.A.Bykovskii	801	803
Towards a theory of ferromagnetism in a nonideal lattice (Abstract) - V.L.Bonch-Bruevich	801	803
Paramagnetic behavior of some salts of the iron group of elements - A.Bose	802	804
Magnetochemistry of diamagnetic compounds and the role of polarizing paramagnetism - Ia.G.Dorfman	817	817
Cyclotron and plasma resonance in solids - A.F.Kip	821	821
Hyperfine structure of paramagnetic resonance in supercooled solutions of salts of the iron group - N.S.Garif'ianov	824	824
Electron paramagnetic resonance in electrolyte solutions - B.M.Kozyrev	828	828
Thermodynamic theory of relaxation and resonance effects in two-spin systems - G.V.Skrotskii & L.V.Kurbatov	833	833
Resonance paramagnetic absorption of ultrasound in some salts of the rare earth elements - S.A.Al'tshuler, M.M.Zaripov & L.Ia.Shekun	844	844
An approximate method of second quantization in the quantum theory of magnetism - N.N.Bogoliubov & S.V.Tiablikov	849	849
Quantum mechanical treatment of ferromagnetism in metals of the transition groups - S.V.Vonsovskii	854	854
Some remarks concerning the Bloch spin wave theory - Z.Semadeni	862	862
Dispersion formula for spin waves in ferrimagnets - G.Czofta	865	865

Ferromagnetism of conduction electrons - G.S.Krinchik	869	869
Towards a theory of spontaneous magnetization of thin films - L.Valenta	879	879
On the temperature and field dependence of the magnetic anisotropy constants of a cubic crystal (Abstract) - A.A.Gusev & S.V.Tiablikov	887	886
Concerning the spectrum of elementary excitations and some kinetic processes in ferromagnetic crystals (Abstract) - E.A.Turov	887	886
Phase transitions and phase diagrams in a rhombic antiferromagnetic crystal - C.J.Gorter & T.van Peski-Tinbergen	888	887
Metamagnets or antiferromagnetic substances with a threshold field - L.Néel	890	889
A new form of ferromagnetic material: rare earth ferrites of the garnet type - L.Néel, F.Berteau, F.Forra & R.Pothené	904	903

Translated in 1958 by
Columbia Technical Translations
5 Vermont Ave., White Plains, N.Y.